VOLUME 23 / NUMBER 21
NOVEMBER 8, 1985
ACC. NOS. N85-32089 TO N85-33103

STAR
AN ABSTRACT JOURNAL

Scientific and Technical Aerospace Reports

PRODUCED BY THE
SCIENTIFIC AND TECHNICAL
INFORMATION
BRANCH

NASA

NATIONAL AERONAUTICS AND SPACE ADMINISTRATION

WHAT YOU CAN DO FOR *STAR*

All users of this abstract service are urged to forward reports to be considered for announcement in *STAR*. This will aid NASA in its efforts to provide the fullest possible coverage of all scientific and technical publications that might support aeronautics and space research and development. If you have prepared relevant reports (other than those that you will transmit to NASA, DoD, or DOE through the usual contract- or grant-reporting channels), please send them for consideration to the NASA Scientific and Technical Information Facility, P.O. Box 8757, B.W.I. Airport, Maryland 21240.

Reprints of journal articles, book chapters, and conference papers are also welcome. These will be considered for announcement in *STAR's* companion journal, *International Aerospace Abstracts*.

You may specify a particular source to be included in a report announcement if you wish; otherwise the report will be placed on public sale at the National Technical Information Service. Copyrighted publications will be announced but not distributed or sold.

PURCHASE OF *STAR*

The semimonthly issues are available for sale by the Superintendent of Documents, U.S. Government Printing Office, Washington, D.C. 20402.

PUBLISHED BY:

UNITED STATES GOVERNMENT
NATIONAL AERONAUTICS AND SPACE ADMINISTRATION
SCIENTIFIC AND TECHNICAL INFORMATION BRANCH
Scientific and Technical Aerospace Reports, Volume 23, is prepared by the NASA Scientific and Technical Information Facility operated for the National Aeronautics and Space Administration by RMS Associates.

The Administrator of the National Aeronautics and Space Administration has determined that the publication of this periodical is necessary in the transaction of the public business required by law of this Agency. Use of funds for printing this periodical has been approved by the Director of the Office of Management and Budget through March 22, 1988.

US ISSN 0036-8741

INTRODUCTION

Scientific and Technical Aerospace Reports (STAR) is a major component of a comprehensive National Aeronautics and Space Administration information system covering aeronautics, space, and supporting disciplines. *STAR* is issued on the 8th and 23rd of each month and announces current publications of the following types:

- NASA, NASA contractor, and NASA grantee reports
- Reports issued by other U.S. Government agencies, domestic and foreign institutions, universities, and private firms
- Translations in report form
- NASA-owned patents and patent applications
- Dissertations and theses

Cumulative index volumes are published annually.

Journal, book, and conference literature, cover-to-cover journal translations, and certain foreign dissertations are announced in a companion journal, *International Aerospace Abstracts (IAA)*, available on subscription from the American Institute of Aeronautics and Astronautics, Technical Information Service, 555 West 57th Street, 12th Floor, New York, New York 10019.

SUBJECT SCOPE

Subject scope of *STAR*, and *IAA* includes all aspects of aeronautics and space research and development, supporting basic and applied research, and applications. Aerospace aspects of earth resources, energy development, conservation, oceanography, environmental protection, urban transportation, and other topics of high national priority are also covered.

OTHER NASA PUBLICATIONS

Other NASA publications and information services are described in the publication, *The NASA Scientific and Technical Information System ... and How to Use It*, available without charge from the NASA Scientific and Technical Information Facility, P.O. Box 8757, B.W.I. Airport, Maryland 21240.

HOW TO USE *STAR* SUBJECT CATEGORIES

STAR is categorized by 10 major subject divisions divided into 74 specific subject categories and one general category/division. The major subject divisions are listed in the Table of Contents, together with a note for each that defines its scope and provides any cross-references. For example:

AERONAUTICS

Includes aeronautics (general); aerodynamics; air transportation and safety; aircraft communications and navigation; aircraft design, testing and performance; aircraft instrumentation; aircraft propulsion and power; aircraft stability and control; and research and support facilities (air).

For related information see also *Astronautics*.

Each major division is further divided into as many as nine specific categories, which are identified by category numbers.

Abstracts in *STAR* are grouped by specific category, the categories appearing in sequential order. Category breaks in the abstract section are identified by the category number and title, and a scope note. Cross-references to other categories are provided as appropriate. For example:

02 AERODYNAMICS

Includes aerodynamics of bodies, combinations, wings, rotors, and control surfaces; and internal flow in ducts and turbomachinery.

For related information see also *34 Fluid Mechanics and Heat Transfer*.

CROSS-REFERENCES

Individual *STAR* abstracts are not ordinarily cross-referenced, except for certain conference reports or book translations that have had separate abstracts written for their component papers or chapters. Citations and abstracts of the components follow immediately after those of the parent document. When the subject content of a component differs sufficiently from the general content of the parent, a cross-reference citation also is printed at the end of the category to which it normally would have been assigned if it were independent.

DOCUMENTS ON MICROFICHE

Documents on microfiche(1) are designated by a pound sign (#) following the accession number. The pound sign is used without regard to the source or quality of the microfiche.

AVAILABILITIES

One or more sources from which a document announced in *STAR* is available to the public is given in each citation. The most commonly indicated sources and their acronyms or abbreviations are listed below. If the publication is available from a source other than those listed, the publisher and his address will be displayed on the availability line or in combination with the corporate source line.

(1) A microfiche is a transparent sheet of film, 105 by 148 mm in size, containing as many as 60 to 98 pages of information reduced to micro images (not to exceed 26:1 reduction).

Avail: NTIS. Sold by the National Technical Information Service. Prices for hard copy (HC) and microfiche (MF) are indicated by a price code following the letters HC or MF in the *STAR* citation. Current values for the price codes are given in the tables on page vii.

Initially distributed microfiche under the NTIS SRIM (Selected Research in Microfiche) is available at greatly reduced unit prices. For this service and for information concerning subscription to NASA printed reports, consult the NTIS Subscription Section, Springfield, Va. 22161.

NOTE ON ORDERING DOCUMENTS: When ordering NASA publications (those followed by the * symbol), use the N accession number. NASA patent applications (only the specifications are offered) should be ordered by the US-Patent-Appl-SN number. Non-NASA publications (no asterisk) should be ordered by the AD, PB, or other *report* number shown on the last line of the citation, not by the N accession number. It is also advisable to cite the title and other bibliographic identification.

Avail: SOD (or GPO). Sold by the Superintendent of Documents, U.S. Government Printing Office, in hard copy. The current price and 'order number are given following the availability line. (NTIS will fill microfiche requests, as indicated above, for those documents identified by a # symbol.)

Avail: NASA Public Document Rooms. Documents so indicated may be examined at or purchased from the National Aeronautics and Space Adminstration, Public Documents Room (Room 126), 600 Independence Ave., S.W., Washington, D.C. 20546, or public document rooms located at each of the NASA research centers, the NASA Space Technology Laboratories, and the NASA Pasadena Office at the Jet Propulsion Laboratory.

Avail: DOE Depository Libraries. Organizations in U.S. cities and abroad that maintain collections of Department of Energy reports, usually in microfiche form, are listed in *Energy Research Abstracts*. Services available from the DOE and its depositories are described in a booklet, *DOE Technical Information Center - Its' Functions and Services* (TID-4660), which may be obtained without charge from the DOE Technical Information Center.

Avail: Univ. Microfilms. Documents so indicated are dissertations selected from *Dissertation Abstracts* and are sold by University Microfilms as xerographic copy (HC) and microfilm. All requests should cite the author and the Order Number as they appear in the citation.

Avail: USGS. Originals of many reports from the U.S. Geological Survey, which may contain color illustrations, or otherwise may not have the quality of illustrations preserved in the microfiche or facsimile reproduction, may be examined by the public at the libraries of the USGS field offices whose addresses are listed in this Introduction. The libraries may be queried concerning the availability of specific documents and the possible utilization of local copying services, such as color reproduction.

Avail: HMSO. Publications of Her Majesty's Stationery Office are sold in the U.S. by Pendragon House, Inc. (PHI), Redwood City, California. The U.S. price (including a service and mailing charge) is given, or a conversion table may be obtained from PHI.

Avail: BLL (formerly NLL): British Library Lending Division, Boston Spa, Wetherby, Yorkshire, England. Photocopies available from this organization at the price shown. (If none is given, inquiry should be addressed to the BLL.)

Avail: Fachinformationszentrum, Karlsruhe. Sold by the Fachinformationszentrum Energie, Physik, Mathematik GMBH, Eggenstein Leopoldshafen, Federal Republic of Germany, at the price shown in deutschmarks (DM).

Avail: Issuing Activity, or Corporate Author, or no indication of availability. Inquiries as to the availability of these documents should be addressed to the organization shown in the citation as the corporate author of the document.

Avail: U.S. Patent and Trademark Office. Sold by Commissioner of Patents and Trademarks, U.S. Patent and Trademark Office, at the standard price of 50 cents each, postage free. (See discussion of patents and patent applications below.)

Avail: ESDU. Pricing information on specific data, computer programs, and details on ESDU topic categories can be obtained from ESDU International Ltd. Requesters in North America should use the Virginia address while all other requesters should use the London address, both of which are on page vi.

NASA PATENTS AND PATENT APPLICATIONS

Patents and patent applications owned by NASA are announced in *STAR* under appropriate subject categories and are referenced in the *STAR* indexes. In the Report/Accession Number Index, patents are indexed by the NASA Case Number (which appears in lieu of the report number in other indexes), the U.S. Patent Number, the U.S. Patent Application Serial Number, and the U.S. Patent Class. Patent applications for which patents have not yet been issued are indexed by the NASA Case Number and the U.S. Patent Application Serial Number.

NASA *patent application specifications* are sold in paper copy by the National Technical Information Service at price code A02 ($7.00 domestic; $14.00 foreign). Microfiche are sold at price code A01 ($4.50 domestic; $9.00 foreign). The US-Patent-Appl-SN- number should be used in ordering either paper copy or microfiche from NTIS. Printed copies of *patents* (which are not microfiched) are available for purchase at 50 cents per copy from:

Commissioner of Patents and Trademarks
U.S. Patent and Trademark Office
Washington, D.C. 20231

When ordering patents, the U.S. Patent Number should be used, and payment must be remitted in advance, preferably by money order or check payable to the Commissioner of Patents and Trademarks. Prepaid purchase coupons for ordering are also available from the Patent and Trademark Office. The patents and patent applications announced in *STAR* are owned by NASA and are available for royalty-free licensing. Requests for licensing terms and further information should be addressed to:

Assistant General Counsel for Patent Matters/Code GP-1
National Aeronautics and Space Administration
Washington, D.C. 20546

ELIGIBILITY AND REGISTRATION FOR NASA INFORMATION PRODUCTS AND SERVICES

A variety of services is available to organizations of the following types that have registered with NASA to receive specific services or products:

1. NASA offices, research centers, contractors, subcontractors, grantees, and consultants;
2. Other U.S. Government agencies and their contractors;
3. Libraries in the United States that have arrangements with NASA to maintain collections of NASA documents for public reference;
4. Other organizations in the United States having a need for NASA documents in work related to aeronautics and space research;
5. Organizations abroad that have established reciprocal document exchange arrangements with NASA.

Only the central service points or central points of document acquisition and control within qualified organizations are eligible to register for NASA products and services. Domestic organizations that may be eligible to receive various classes of NASA publications and services should address their requests for registration or for further information to:

NASA Scientific and Technical Information Facility
ATTN: Registration Activity
P.O. Box 8757
B.W.I. Airport, Maryland 21240

Organizations abroad should direct requests to the same address, but to the attention of: International Exchange Program.

AVAILABILITY OF *STAR* ABSTRACTS ON MICROFICHE

Microfiche of the abstract sections of this issue and other issues of *STAR* are available on annual subscription from NTIS, Attn: Subscriptions, 5285 Port Royal Road, Springfield, Virginia 22161. Annual subscription rates are $60.00 North America; $120.00 foreign. Abstract sections for previous years retroactive to 1964 are available at the current rates. Microfiche for individual *STAR* issue abstract sections are not available.

PUBLIC COLLECTIONS OF NASA DOCUMENTS

DOMESTIC: NASA and NASA-sponsored documents and a large number of aerospace publications are available to the public for reference purposes at the library maintained by the American Institute of Aeronautics and Astronautics, Technical Information Service, 555 West 57th Street, 12th Floor, New York, New York 10019.

EUROPEAN: An extensive collection of NASA and NASA-sponsored publications is maintained by the British Library Lending Division, Boston Spa, Wetherby, Yorkshire, England for public access. The British Library Lending Division also has available many of the non-NASA publications cited in *Star*. European requesters may purchase facsimile copy or microfiche of NASA and NASA-sponsored documents, those identified by both the symbols # and * from ESA - Information Retrieval Service European Space Agency, 8-10 rue Mario-Nikis, 75738 Paris CEDEX 15, France.

FEDERAL DEPOSITORY LIBRARY PROGRAM

In order to provide the general public with greater access to U.S. Government publications, Congress established the Federal Depository Library Program under the Government Printing Office (GPO), with 50 regional depositories responsible for permanent retention of material, inter-library loan, and reference services. Over 1,300 other depositories also exist. A list of the regional GPO libraries appears on the inside back cover of *STAR*.

ADDRESSES OF ORGANIZATIONS

American Institute of Aeronautics and Astronautics
Technical Information Service
555 West 57th Street, 12th Floor
New York, New York 10019

British Library Lending Division,
Boston Spa, Wetherby, Yorkshire,
England

Commissioner of Patents and Trademarks
U.S. Patent and Trademark Office
Washington, D.C. 20231

Department of Energy
Technical Information Center
P.O. Box 62
Oak Ridge, Tennessee 37830

ESA-Information Retrieval Service
ESRIN
Via Galileo Galilei
00044 Frascati (Rome) Italy

ESDU International, Ltd.
1495 Chain Bridge Road
McLean, Virginia 22101

ESDU International, Ltd.
251-259 Regent Street
London, W1R 7AD, England

Fachinformationszentrum Energie, Physik, Mathematik GMBH
7514 Eggenstein Leopoldshafen
Federal Republic of Germany

Her Majesty's Stationery Office
P.O. Box 569, S.E. 1
London, England

NASA Scientific and Technical Information Facility
P.O. Box 8757
B.W.I. Airport, Maryland 21240

National Aeronautics and Space Administration
Scientific and Technical Information Branch (NIT-1)
Washington, D.C. 20546

National Technical Information Service
5285 Port Royal Road
Springfield, Virginia 22161

Pendragon House, Inc.
899 Broadway Avenue
Redwood City, California 94063

Superintendent of Documents
U.S. Government Printing Office
Washington, D.C. 20402

University Microfilms
A Xerox Company
300 North Zeeb Road
Ann Arbor, Michigan 48106

University Microfilms, Ltd.
Tylers Green
London, England

U.S. Geological Survey Library
National Center – MS 950
12201 Sunrise Valley Drive
Reston, Virginia 22092

U.S. Geological Survey Library
2255 North Gemini Drive
Flagstaff, Arizona 86001

U.S. Geological Survey
345 Middlefield Road
Menlo Park, California 94025

U.S. Geological Survey Library
Box 25046
Denver Federal Center, MS 914
Denver, Colorado 80225

NTIS PRICE SCHEDULES

Schedule A

STANDARD PAPER COPY PRICE SCHEDULE

(Effective January 1, 1983)

Price Code	Page Range	North American Price	Foreign Price
A01	Microfiche	$ 4.50	$ 9.00
A02	001-025	7.00	14.00
A03	026-050	8.50	17.00
A04	051-075	10.00	20.00
A05	076-100	11.50	23.00
A06	101-125	13.00	26.00
A07	126-150	14.50	29.00
A08	151-175	16.00	32.00
A09	176-200	17.50	35.00
A10	201-225	19.00	38.00
A11	226-250	20.50	41.00
A12	251-275	22.00	44.00
A13	276-300	23.50	47.00
A14	301-325	25.00	50.00
A15	326-350	26.50	53.00
A16	351-375	28.00	56.00
A17	376-400	29.50	59.00
A18	401-425	31.00	62.00
A19	426-450	32.50	65.00
A20	451-475	34.00	68.00
A21	476-500	35.50	71.00
A22	501-525	37.00	74.00
A23	526-550	38.50	77.00
A24	551-575	40.00	80.00
A25	576-600	41.50	83.00
A99	601-up	-- 1	-- 2

1. Add $1.50 for each additional 25 page increment or portion thereof for 601 pages up.

2. Add $3.00 for each additional 25 page increment or portion thereof for 601 pages and more.

Schedule E

EXCEPTION PRICE SCHEDULE

Paper Copy & Microfiche

Price Code	North American Price	Foreign Price
E01	$ 6.50	$ 13.50
E02	7.50	15.50
E03	9.50	19.50
E04	11.50	23.50
E05	13.50	27.50
E06	15.50	31.50
E07	17.50	35.50
E08	19.50	39.50
E09	21.50	43.50
E10	23.50	47.50
E11	25.50	51.50
E12	28.50	57.50
E13	31.50	63.50
E14	34.50	69.50
E15	37.50	75.50
E16	40.50	81.50
E17	43.50	88.50
E18	46.50	93.50
E19	51.50	102.50
E20	61.50	123.50
E-99 - Write for quote		
N01	35.00	45.00

VOLUME 23 NUMBER 21 / NOVEMBER 8, 1985

TABLE OF CONTENTS

AERONAUTICS

Includes aeronautics (general); aerodynamics; air transportation and safety; aircraft communications and navigation; aircraft design, testing and performance; aircraft instrumentation; aircraft propulsion and power; aircraft stability and control; and research and support facilities (air).

For related information see also *Astronautics*.

01 AERONAUTICS (GENERAL) **3551**

02 AERODYNAMICS **3551**

Includes aerodynamics of bodies, combinations, wings, rotors, and control surfaces; and internal flow in ducts and turbomachinery.

For related information see also *34 Fluid Mechanics and Heat Transfer*

03 AIR TRANSPORTATION AND SAFETY **3553**

Includes passenger and cargo air transport operations; and aircraft accidents.

For related information see also *16 Space Transportation* and *85 Urban Technology and Transportation*.

04 AIRCRAFT COMMUNICATIONS AND NAVIGATION **3554**

Includes digital and voice communication with aircraft; air navigation systems (satellite and ground based); and air traffic control.

For related information see also *17 Spacecraft Communications, Command and Tracking* and *32 Communications*.

05 AIRCRAFT DESIGN, TESTING AND PERFORMANCE **3554**

Includes aircraft simulation technology.

For related information see also *18 Spacecraft Design, Testing and Performance* and *39 Structural Mechanics*.

06 AIRCRAFT INSTRUMENTATION **N.A.**

Includes cockpit and cabin display devices; and flight instruments.

For related information see also *19 Spacecraft Instrumentation* and *35 Instrumentation and Photography*.

07 AIRCRAFT PROPULSION AND POWER **3556**

Includes prime propulsion systems and systems components, e.g., gas turbine engines and compressors; and on-board auxiliary power plants for aircraft.

For related information see also *20 Spacecraft Propulsion and Power, 28 Propellants and Fuels*, and *44 Energy Production and Conversion*.

08 AIRCRAFT STABILITY AND CONTROL **3556**

Includes aircraft handling qualities; piloting; flight controls; and autopilots.

09 RESEARCH AND SUPPORT FACILITIES (AIR) **3557**

Includes airports, hangars and runways; aircraft repair and overhaul facilities; wind tunnels; shock tube facilities; and engine test blocks.

For related information see also *14 Ground Support Systems and Facilities (Space)*.

ASTRONAUTICS

Includes astronautics (general); astrodynamics; ground support systems and facilities (space); launch vehicles and space vehicles; space transportation; spacecraft communications, command and tracking; spacecraft design, testing and performance; spacecraft instrumentation; and spacecraft propulsion and power.

For related information see also *Aeronautics*

12 ASTRONAUTICS (GENERAL) **3557**

For extraterrestrial exploration see *91 Lunar and Planetary Exploration*.

13 ASTRODYNAMICS **3558**

Includes powered and free-flight trajectories; and orbit and launching dynamics.

14 GROUND SUPPORT SYSTEMS AND FACILITIES (SPACE) **N.A.**

Includes launch complexes, research and production facilities; ground support equipment, e.g., mobile transporters; and simulators.

For related information see also *09 Research and Support Facilities (Air)*.

15 LAUNCH VEHICLES AND SPACE VEHICLES **3558**

Includes boosters; manned orbital laboratories; reusable vehicles; and space stations.

16 SPACE TRANSPORTATION **3558**

Includes passenger and cargo space transportation, e.g., shuttle operations; and rescue techniques.

For related information see also *03 Air Transportation and Safety* and *85 Urban Technology and Transportation*.

17 SPACECRAFT COMMUNICATION, COMMAND AND TRACKING **N.A.**

Includes telemetry; space communications networks; astronavigation; and radio blackout.

For related information see also *04 Aircraft Communications and Navigation* and *32 Communications*.

18 SPACECRAFT DESIGN, TESTING AND PERFORMANCE **3559**

Includes spacecraft thermal and environmental control; and attitude control.

For life support systems see *54 Man/System Technology and Life Support*. For related information see also *05 Aircraft Design, Testing and Performance* and *39 Structural Mechanics*.

19 SPACECRAFT INSTRUMENTATION **3560**

For related information see also *06 Aircraft Instrumentation* and *35 Instrumentation and Photography*.

20 SPACECRAFT PROPULSION AND POWER **3560**

Includes main propulsion systems and components, e.g., rocket engines; and spacecraft auxiliary power sources.

For related information see also *07 Aircraft Propulsion and Power, 28 Propellants and Fuels*, and *44 Energy Production and Conversion*.

CHEMISTRY AND MATERIALS

Includes chemistry and materials (general); composite materials; inorganic and physical chemistry; metallic materials; nonmetallic materials; and propellants and fuels.

23 CHEMISTRY AND MATERIALS (GENERAL) 3560
Includes biochemistry and organic chemistry.

24 COMPOSITE MATERIALS 3561
Includes laminates.

25 INORGANIC AND PHYSICAL CHEMISTRY 3562
Includes chemical analysis, e.g., chromatography; combustion theory; electrochemistry; and photochemistry.
For related information see also *77 Thermodynamics and Statistical Physics.*

26 METALLIC MATERIALS 3565
Includes physical, chemical, and mechanical properties of metals, e.g., corrosion; and metallurgy.

27 NONMETALLIC MATERIALS 3568
Includes physical, chemical, and mechanical properties of plastics, elastomers, lubricants, polymers, textiles, adhesives, and ceramic materials.

28 PROPELLANTS AND FUELS 3571
Includes rocket propellants, igniters, and oxidizers; storage and handling; and aircraft fuels.
For related information see also *07 Aircraft Propulsion and Power, 20 Spacecraft Propulsion and Power,* and *44 Energy Production and Conversion.*

ENGINEERING

Includes engineering (general); communications; electronics and electrical engineering; fluid mechanics and heat transfer; instrumentation and photography; lasers and masers; mechanical engineering; quality assurance and reliability; and structural mechanics.
For related information see also *Physics.*

31 ENGINEERING (GENERAL) 3572
Includes vacuum technology; control engineering; display engineering; and cryogenics.

32 COMMUNICATIONS 3573
Includes land and global communications; communications theory; and optical communications.
For related information see also *04 Aircraft Communications and Navigation* and *17 Spacecraft Communications, Command and Tracking.*

33 ELECTRONICS AND ELECTRICAL ENGINEERING 3579
Includes test equipment and maintainability; components, e.g., tunnel diodes and transistors; microminiaturization; and integrated circuitry.
For related information see also *60 Computer Operations and Hardware* and *76 Solid-State Physics.*

34 FLUID MECHANICS AND HEAT TRANSFER 3583
Includes boundary layers; hydrodynamics; fluidics; mass transfer; and ablation cooling.
For related information see also *02 Aerodynamics* and *77 Thermodynamics and Statistical Physics.*

35 INSTRUMENTATION AND PHOTOGRAPHY 3588
Includes remote sensors; measuring instruments and gages; detectors; cameras and photographic supplies; and holography.
For aerial photography see *43 Earth Resources.* For related information see also *06 Aircraft Instrumentation* and *19 Spacecraft Instrumentation.*

36 LASERS AND MASERS 3591
Includes parametric amplifiers.

37 MECHANICAL ENGINEERING 3595
Includes auxiliary systems (non-power); machine elements and processes; and mechanical equipment.

38 QUALITY ASSURANCE AND RELIABILITY 3597
Includes product sampling procedures and techniques; and quality control.

39 STRUCTURAL MECHANICS 3597
Includes structural element design and weight analysis; fatigue; and thermal stress.
For applications see *05 Aircraft Design, Testing and Performance* and *18 Spacecraft Design, Testing and Performance.*

GEOSCIENCES

Includes geosciences (general); earth resources; energy production and conversion; environment pollution; geophysics; meteorology and climatology; and oceanography.
For related information see also *Space Sciences.*

42 GEOSCIENCES (GENERAL) 3600

43 EARTH RESOURCES 3605
Includes remote sensing of earth resources by aircraft and spacecraft; photogrammetry; and aerial photography.
For instrumentation see *35 Instrumentation and Photography.*

44 ENERGY PRODUCTION AND CONVERSION 3607
Includes specific energy conversion systems, e.g., fuel cells and batteries; global sources of energy; fossil fuels; geophysical conversion; hydroelectric power; and wind power.
For related information see also *07 Aircraft Propulsion and Power, 20 Spacecraft Propulsion and Power, 28 Propellants and Fuels,* and *85 Urban Technology and Transportation.*

45 ENVIRONMENT POLLUTION 3613
Includes air, noise, thermal and water pollution; environment monitoring; and contamination control.

46 GEOPHYSICS 3615
Includes aeronomy; upper and lower atmosphere studies; ionospheric and magnetospheric physics; and geomagnetism.
For space radiation see *93 Space Radiation.*

47 METEOROLOGY AND CLIMATOLOGY 3634
Includes weather forecasting and modification.

48 OCEANOGRAPHY 3654
Includes biological, dynamic and physical oceanography; and marine resources.

LIFE SCIENCES

Includes sciences (general); aerospace medicine; behavioral sciences; man/system technology and life support; and planetary biology.

51 LIFE SCIENCES (GENERAL) **3656**
Includes genetics.

52 AEROSPACE MEDICINE **3663**
Includes physiological factors; biological effects of radiation; and weightlessness.

53 BEHAVIORAL SCIENCES **3665**
Includes psychological factors; individual and group behavior; crew training and evaluation; and psychiatric research.

54 MAN/SYSTEM TECHNOLOGY AND LIFE SUPPORT **3666**
Includes human engineering; biotechnology; and space suits and protective clothing.

55 PLANETARY BIOLOGY **3667**
Includes exobiology; and extraterrestrial life.

MATHEMATICAL AND COMPUTER SCIENCES

Includes mathematical and computer sciences (general); computer operations and hardware; computer programming and software; computer systems; cybernetics; numerical analysis; statistics and probability; systems analysis; and theoretical mathematics.

59 MATHEMATICAL AND COMPUTER SCIENCES (GENERAL) **N.A.**

60 COMPUTER OPERATIONS AND HARDWARE **3667**
Includes computer graphics and data processing.
For components see *33 Electronics and Electrical Engineering.*

61 COMPUTER PROGRAMMING AND SOFTWARE **3669**
Includes computer programs, routines, and algorithms.

62 COMPUTER SYSTEMS **3673**
Includes computer networks.

63 CYBERNETICS **N.A.**
Includes feedback and control theory.
For related information see also *54 Man/System Technology and Life Support.*

64 NUMERICAL ANALYSIS **3675**
Includes iteration, difference equations, and numerical approximation.

65 STATISTICS AND PROBABILITY **3678**
Includes data sampling and smoothing; Monte Carlo method; and stochastic processes.

66 SYSTEMS ANALYSIS **3678**
Includes mathematical modeling; network analysis; and operations research.

67 THEORETICAL MATHEMATICS **N.A.**
Includes topology and number theory.

PHYSICS

Includes physics (general); acoustics; atomic and molecular physics; nuclear and high-energy physics; optics; plasma physics; solid-state physics; and thermodynamics and statistical physics.
For related information see also *Engineering.*

70 PHYSICS (GENERAL) **3679**
For geophysics see *46 Geophysics.* For astrophysics see *90 Astrophysics.* For solar physics see *92 Solar Physics.*

71 ACOUSTICS **3698**
Includes sound generation, transmission, and attenuation.
For noise pollution see *45 Environment Pollution.*

72 ATOMIC AND MOLECULAR PHYSICS **3701**
Includes atomic structure and molecular spectra.

73 NUCLEAR AND HIGH-ENERGY PHYSICS **3703**
Includes elementary and nuclear particles; and reactor theory.
For space radiation see *93 Space Radiation.*

74 OPTICS **3704**
Includes light phenomena.

75 PLASMA PHYSICS **3707**
Includes magnetohydrodynamics and plasma fusion.
For ionospheric plasmas see *46 Geophysics.* For space plasmas see *90 Astrophysics.*

76 SOLID-STATE PHYSICS **3709**
Includes superconductivity.
For related information see also *33 Electronics and Electrical Engineering* and *36 Lasers and Masers.*

77 THERMODYNAMICS AND STATISTICAL PHYSICS **N.A.**
Includes quantum mechanics; and Bose and Fermi statistics.
For related information see also *25 Inorganic and Physical Chemistry* and *34 Fluid Mechanics and Heat Transfer.*

SOCIAL SCIENCES

Includes social sciences (general); administration and management; documentation and information science; economics and cost analysis; law and political science; and urban technology and transportation.

80 SOCIAL SCIENCES (GENERAL) **N.A.**
Includes educational matters.

81 ADMINISTRATION AND MANAGEMENT **3712**
Includes management planning and research.

82 DOCUMENTATION AND INFORMATION SCIENCE 3713
Includes information storage and retrieval technology; micrography; and library science.
For computer documentation see *61 Computer Programming and Software.*

83 ECONOMICS AND COST ANALYSIS N.A.
Includes cost effectiveness studies.

84 LAW AND POLITICAL SCIENCE N.A.
Includes space law; international law; international cooperation; and patent policy.

85 URBAN TECHNOLOGY AND TRANSPORTATION N.A.
Includes applications of space technology to urban problems; technology transfer; technology assessment; and surface and mass transportation.
For related information see *03 Air Transportation and Safety, 16 Space Transportation,* and *44 Energy Production and Conversion.*

SPACE SCIENCES

Includes space sciences (general); astronomy; astrophysics; lunar and planetary exploration; solar physics; and space radiation.
For related information see also *Geosciences.*

88 SPACE SCIENCES (GENERAL) 3714

89 ASTRONOMY 3716
Includes radio and gamma-ray astronomy; celestial mechanics; and astrometry.

90 ASTROPHYSICS 3716
Includes cosmology; and interstellar and interplanetary gases and dust.

91 LUNAR AND PLANETARY EXPLORATION 3717
Includes planetology; and manned and unmanned flights.
For spacecraft design see *18 Spacecraft Design, Testing and Performance.* For space stations see *15 Launch Vehicles and Space Vehicles.*

92 SOLAR PHYSICS 3722
Includes solar activity, solar flares, solar radiation and sunspots.

93 SPACE RADIATION 3724
Includes cosmic radiation; and inner and outer earth's radiation belts.
For biological effects of radiation see *52 Aerospace Medicine.* For theory see *73 Nuclear and High-Energy Physics.*

GENERAL

99 GENERAL N.A.

Note: N.A. means that no abstracts were assigned to this category for this issue.

SUBJECT INDEX I-1
PERSONAL AUTHOR INDEX I-61
CORPORATE SOURCE INDEX I-69
CONTRACT NUMBER INDEX I-81
REPORT / ACCESSION NUMBER INDEX I-83

TYPICAL CITATION AND ABSTRACT

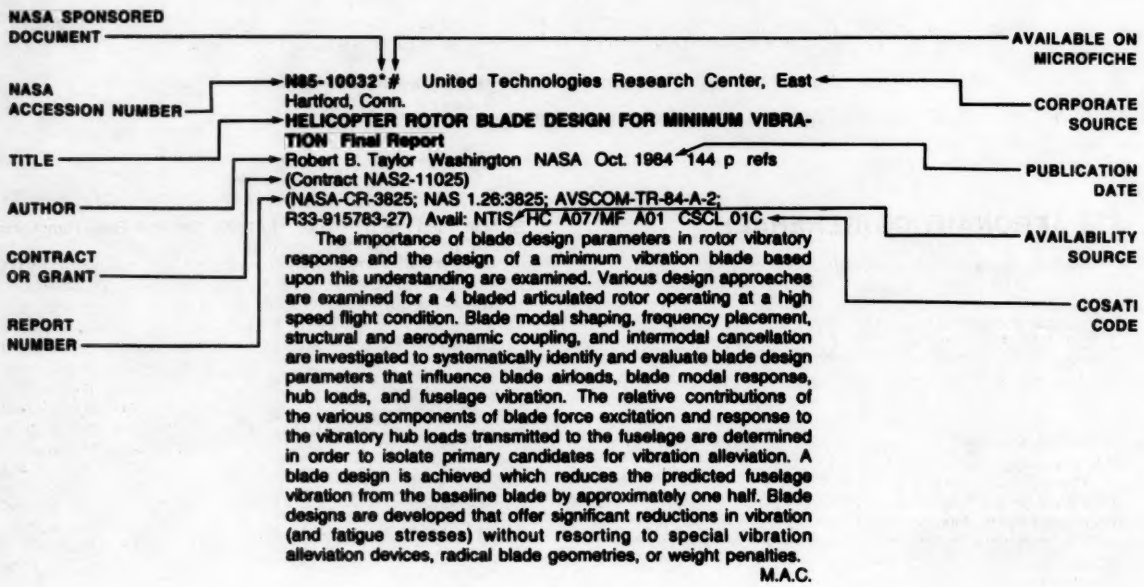
NASA SPONSORED DOCUMENT
AVAILABLE ON MICROFICHE
NASA ACCESSION NUMBER
N85-10032*# United Technologies Research Center, East Hartford, Conn.
CORPORATE SOURCE
TITLE
HELICOPTER ROTOR BLADE DESIGN FOR MINIMUM VIBRATION Final Report
PUBLICATION DATE
AUTHOR
Robert B. Taylor Washington NASA Oct. 1984 144 p refs
CONTRACT OR GRANT
(Contract NAS2-11025)
REPORT NUMBER
(NASA-CR-3825; NAS 1.26:3825; AVSCOM-TR-84-A-2; R33-915783-27) Avail: NTIS HC A07/MF A01 CSCL 01C
AVAILABILITY SOURCE
COSATI CODE
The importance of blade design parameters in rotor vibratory response and the design of a minimum vibration blade based upon this understanding are examined. Various design approaches are examined for a 4 bladed articulated rotor operating at a high speed flight condition. Blade modal shaping, frequency placement, structural and aerodynamic coupling, and intermodal cancellation are investigated to systematically identify and evaluate blade design parameters that influence blade airloads, blade modal response, hub loads, and fuselage vibration. The relative contributions of the various components of blade force excitation and response to the vibratory hub loads transmitted to the fuselage are determined in order to isolate primary candidates for vibration alleviation. A blade design is achieved which reduces the predicted fuselage vibration from the baseline blade by approximately one half. Blade designs are developed that offer significant reductions in vibration (and fatigue stresses) without resorting to special vibration alleviation devices, radical blade geometries, or weight penalties.
M.A.C.

VOLUME 23 NUMBER 21 / NOVEMBER 8, 1985

Scientific and Technical Aerospace Reports

A Semimonthly Publication of the National Aeronautics and Space Administration

01 AERONAUTICS (GENERAL)

N85-32089*# Loftin (Laurence K., Jr.), Newport News, Va.
QUEST FOR PERFORMANCE: THE EVOLUTION OF MODERN AIRCRAFT
Laurence K. Loftin, Jr. 1985 548 p refs Original contains color illustrations
(Contract NASw-3490)
(NASA-SP-468; NAS 1.21:468) Avail: NTIS HC A23/MF A01; SOD HC $26.00 as 033-000-00902-0 CSCL 01B

The technical evolution of the subsonic airplane is traced from a curiosity at the beginning of World War I to the highly useful machine of today. Included are descriptions of significant aircraft which incorporated important technical innovations and served to shape the future course of aeronautical development, as well as aircraft which represented the state-of-art in a particular time frame or were much used or liked. The discussion is related primarily to aircraft configuration evolution and associated aerodynamic characteristics and, to a lesser extent, to developments in aircraft construction and propulsion. The material is presented in a manner designed to appeal to the nontechnical reader who is interested in the evolution of the airplane, as well as to students of aeronautical engineering and others with an aeronautical background. Author

N85-32090*# National Aeronautics and Space Administration. Ames Research Center, Moffett Field, Calif.
RECENT DEVELOPMENTS IN ROTARY-BALANCE TESTING OF FIGHTER AIRCRAFT CONFIGURATIONS AT NASA AMES RESEARCH CENTER
Gerald N. Malcolm and Lewis B. Schiff Jul. 1985 28 p refs
(NASA-TM-86714; Rept-85211; NAS 1.15:86714) Avail: NTIS HC A03/MF A01 CSCL 01B

Two rotary balance apparatuses were developed for testing airplane models in a coning motion. A large scale apparatus, developed for use in the 12-Foot Pressure Wind tunnel primarily to permit testing at high Reynolds numbers, was recently used to investigate the aerodynamics of 0.05-scale model of the F-15 fighter aircraft. Effects of Reynolds number, spin rate parameter, model attitude, presence of a nose boom, and model/sting mounting angle were investigated. A smaller apparatus, which investigates the aerodynamics of bodies of revolution in a coning motion, was used in the 6-by-6 foot Supersonic Wind Tunnel to investigate the aerodynamic behavior of a simple representation of a modern fighter, the Standard Dynamic Model (SDM). Effects of spin rate parameter and model attitude were investigated. A description of the two rigs and a discussion of some of the results obtained in the respective test are presented. Author

N85-32091# Air Force Systems Command, Wright-Patterson AFB, Ohio. Foreign Technology Div.
ELECTRONIC RECONNAISSANCE AIRCRAFT OF THE SOVIET UNION NAVY
28 Mar. 1985 18 p Transl. into ENGLISH from Guoji Hangkong (China), no. 11, Nov. 1984 p 10-12
(AD-A154706; FTD-ID(RS)T-0045-85) Avail: NTIS HC A02/MF A01 CSCL 01/3

Gorshkov, the Deputy Minister of the Ministry of Defense and the Commander of the Navy of the Soviet Union pointed out The Fleet of the Soviet Union has been greatly developed since the 1960's. The Fleet, which was basically a seacoast defense force, now has become an ocean going fleet and is a tremendous striking force. In order to carry out combat operations efficiently, Soviet Naval theory pays no less attention to the security and reliability of communications and to extensive, continued reconnaissance activities than to the combat Navy itself. The Soviet Navy established a extensive ocean monitoring system to gather intelligence accurately and quickly. This system consists of reconnaissance satellites, warships, aircraft, large radio interception networks, and a great deal of equipment for collecting and appraising information. GRA

02 AERODYNAMICS

Includes aerodynamics of bodies, combinations, wings, rotors, and control surfaces; and internal flow in ducts and turbomachinery.

For related information see also *34 Fluid Mechanics and Heat Transfer.*

N85-32092*# National Aeronautics and Space Administration. Langley Research Center, Hampton, Va.
CALCULATION OF TRANSONIC STEADY AND OSCILLATORY PRESSURES ON A LOW ASPECT RATIO MODEL AND COMPARISON WITH EXPERIMENT
Robert M. Bennett, Eleanor C. Wynne, and Dennis G. Mabey Jun. 1985 18 p refs Presented at the 2nd Intern. Symp. on Aeroelasticity and Structural Dyn., Aachen, 1-3 Apr. 1985
(NASA-TM-86449; NAS 1.15:86449) Avail: NTIS HC A02/MF A01 CSCL 01A

Pressure data measured by the British Royal Aircraft Establishment for the AGARD SMP tailplane are compared with results calculated using the transonic small perturbation code XTRAN3S. A brief description of the analysis is given and a recently developed finite difference grid is described. Results are presented for five steady and nine harmonically oscillating cases near zero angle of attack and for a range of subsonic and transonic Mach numbers. Author

N85-32093*# Scientific Research Associates, Inc., Glastonbury, Conn.
TIP VORTEX COMPUTER CODE SRATIP. USER'S GUIDE Final Report
R. Levy and S. J. Lin Jul. 1985 70 p refs
(Contract NAS1-14904)
(NASA-CR-172603; NAS 1.26:172603) Avail: NTIS HC A04/MF A01 CSCL 01A

This User's Guide applies to the three dimensional viscous flow forward marching analysis, PEPSIG, as used for the calculation of the helicopter tip vortex flow field. The guide presents a discussion of the program flow and subroutines, as well as a list of sample input and output. Author

N85-32094*# National Aeronautics and Space Administration. Ames Research Center, Moffett Field, Calif.
AERODYNAMIC CHARACTERISTICS OF THE STANDARD DYNAMICS MODEL IN CONING MOTION AT MACH 0.6
Christopher Jermey and Lewis B. Schiff Jul. 1985 75 p refs
(NASA-TM-86717; Rept-85215; NAS 1.15:86717) Avail: NTIS HC A04/MF A01 CSCL 01A

A wind tunnel test was conducted on the Standard Dynamics Model (a simplified generic fighter aircraft shape) undergoing coning motion at Mach 0.6. Six component force and moment data are presented for a range of angle of attack, sideslip, and coning rates. At the relatively low non-dimensional coning rate employed (omega b/2V less than or equal to 0.04), the lateral aerodynamic characteristics generally show a linear variation with coning rate. Author

N85-32095*# Massachusetts Inst. of Tech., Cambridge. Fluid Dynamics Research Lab.
A PANEL METHOD STUDY OF VORTEX SHEETS WITH SPECIAL EMPHASIS ON SHEETS OF AXISYMMETRIC GEOMETRY M.S. Thesis
Ichiro Sugioka and Sheila E. Widnall Aug. 1985 115 p refs
(Grant NAG2-251)
(NASA-CR-177365; NAS 1.26:177365; FDRL-85-3) Avail: NTIS HC A06/MF A01 CSCL 01A

The self induced evolution of a vortex sheet was simulated by modeling the sheet using an integration of discrete elements of vorticity. Replacing small sections of a vortex sheet by flat panels of constant vorticity is found to reproduce more accurately the initial conditions for the Lagrangian simulation technique than replacement by point vortices. The flat panel method for the vortex sheet was then extended to model axisymmetric vortex sheets. The local and far field velocities induced by the axisymmetric panels were obtained using matched asymptotic analysis, and some of the uncertainties involved in other models of the axisymmetric vortex sheet have been eliminated. One important result of this analysis is the determination of the proper choice of core size for a circular vortex filament which may replace a section of an axisymmetric vortex sheet. Roll-up of both two dimensional and axisymmetric vortex sheets was computed using the panel methods developed in the report. Author

N85-32096# Nielsen Engineering and Research, Inc., Mountain View, Calif.
NOTES ON UNSTEADY TRANSONIC CASCADE FLOWS Technical Report, 12 Sep. 1983 - 28 Feb. 1985
D. Nixon and K. Tzuoo 8 May 1985 93 p
(Contract N00014-83-C-0435)
(AD-A154829; NEAR-TR-343) Avail: NTIS HC A05/MF A01 CSCL 20/4

Several topics concerned with the unsteady transonic flow through cascades are considered. The indicial theory developed in previous work for cascade flows is examined and certain shortcomings eliminated. A consequence of this work is that some questions regarding the appropriate far field boundary conditions to use are raised. The strong shock potential theory previously developed for isolated airfoil flows has been incorporated into the cascade code. A major topic in the present work is the examination of nonunique solutions for cascade flows. The variation of such solutions with cascade gap is studied with the conclusion that the nonunique solutions are unlikely to occur for practical gap/chord ratios. GRA

N85-32097# Naval Ship Research and Development Center, Bethesda, Md.
TRAILING EDGE FLOW AND AERODYNAMIC SOUND. PART 1: TONAL PRESSURE AND VELOCITY FLUCTUATIONS. PART 2: RANDOM PRESSURE AND VELOCITY FLUCTUATIONS Final Report
W. K. Blake Dec. 1984 106 p
(AD-A154947; DTNSRDC-83/113) Avail: NTIS HC A06/MF A01 CSCL 20/4

The turbulent field quantities at the trailing edges of lifting surfaces consist of two components. Locally-generated random fluctuations are generated by separation of the turbulent boundary layers and these fluctuations account for weakly correlated surface pressure fields. The second contribution is periodic, or nearly periodic, and is generated by the structured vortex pressure field. The aerodynamic properties of each of these contributions are examined for various trailing edge configurations, and the aeroacoustic qualities of each are explored. Rules are given for the prediction of the onset of either predominately tonal or predominantly random pressure fields. Relationships are given for estimating aerodynamic sound levels from the surface pressures for each class of aerodynamic excitation. GRA

N85-32098# Naval Ship Research and Development Center, Bethesda, Md. Ship Performance Dept.
AN EVALUATION OF FOUR METHODS OF NUMERICAL ANALYSIS FOR TWO-DIMENSIONAL AIRFOIL FLOWS Final Report
R. Burke Jul. 1984 31 p
(S12-66001)
(AD-A155202; DTNSRDC/SPD-1139-01) Avail: NTIS HC A03/MF A01 CSCL 20/4

This report compares four computer codes for predicting the inviscid and boundary layer flow over two dimensional airfoils. One of the codes obtains the inviscid flow using panel methods, and the boundary layer flow using integral methods. It is the only code considered here that includes both inviscid and boundary layer routines. Another code computes the inviscid flow, also using panel methods, but does not have a boundary layer routine. The remaining two codes calculate the vertical variation of flow variables within the boundary layer using finite differences; the external inviscid flow is not computed, and must be included in the program input. After a brief discussion of the solution method of each computer code, numerical predictions are compared against experimental data from two wind tunnel studies, involving four airfoil geometries. The airfoil shapes are described, and comparisons made between measured and predicted values of pressure distribution, turbulent separation point, and boundary layer parameters. GRA

N85-32099# Accumetrics Corp., Rockport, Miss.
APPLIED RESEARCH AND DEVELOPMENT FOR FALLING-SPHERE AIR DENSITY MEASURING SYSTEMS Final Technical Report, Jan. 1981 - Aug. 1984
D. H. Fryklund Aug. 1984 37 p
(Contract F19628-81-C-0050)
(AD-A155227; AFGL-TR-84-0192) Avail: NTIS HC A03/MF A01 CSCL 14/2

This contract involves the development, fabrication, testing, and calibration of four complete high altitude densitometer payloads, each comprised of a nose cone, an ejection system, and a ten-inch falling sphere. The sphere, in turn, is instrumented with a sensitive accelerometer, a TM system, a nutation sensor, and various ancillary power supply and control systems. Air density is determined by measuring the negative air-drag acceleration as experienced by the sphere as it falls through the atmosphere. By evaluating the air drag equation for a spherical shape having the same area and mass, with the measured fall velocity and negative acceleration the air density profile for the trajectory can be calculated. Air density measurement over the desired range of 50 to 150 KM requires the use of a sensitive accelerometer having a dynamic range of 0.01 to 0.0000001 g's. Four complete falling-sphere densitometer systems were designed, fabricated and launched at four locations: Wallops Island, VA; Kiruna, Sweden; Poker Flat, Alas.; and Andoya, Norway. The former back-up densitometer was upgraded and was flown during the Norway program. Three unique support units were designed and fabricated for use with the European payloads. A solar aspect system was

designed, fabricated and flown on the Alaskan payload. Additionally, several studies were performed to generally improve the ground and flight equipment. GRA

N85-32100# Naval Postgraduate School, Monterey, Calif.
WIND TUNNEL DRAG EVALUATIONS OF HELICOPTER NOSE SECTIONS M.S. Thesis
R. S. Mair Mar. 1985 106 p
(AD-A155489) Avail: NTIS HC A06/MF A01 CSCL 14/2

This thesis determines the aerodynamic drag parameters for three different generic helicopter nose fuselage sections at various angles of attack and velocities using a 3.5 x 5 foot wind tunnel and a locally constructed three component strain gage balance. A common center section is used with provisions for three different tail sections allowing for nine possible configurations to effect the overall shape of a fuselage. This allows a student in a basic conceptual helicopter design course a quantitative means of comparing general shapes in order to select the best configuration of the fuselage. However, the results are questionable due to problems with the strain gage balance used to determine the aerodynamic forces on the models. GRA

03 AIR TRANSPORTATION AND SAFETY

Includes passenger and cargo air transport operations; and aircraft accidents.

For related information see also *16 Space Transportation* and *85 Urban Technology and Transportation.*

N85-32101*# National Aeronautics and Space Administration. Ames Research Center, Moffett Field, Calif.
SIMULATION STUDIES OF TIME-CONTROL PROCEDURES FOR THE ADVANCED AIR TRAFFIC CONTROL SYSTEM
Leonard Tobias, Monica Alcabin, Heinz Erzberger, and Paul J. OBrien Jul. 1985 18 p refs
(NASA-TP-2493; T-3309; NAS 1.60:2493) Avail: NTIS HC A02/MF A01 CSCL 01C

The problem of mixing aircraft equipped with time-controlled guidance systems and unequipped aircraft in the terminal area has been investigated via a real-time air traffic control simulation. These four-dimensional (4D) guidance systems can predict and control the touchdown time of an aircraft to an accuracy of a few seconds throughout the descent. The objectives of this investigation were to (1) develop scheduling algorithms and operational procedures for various traffic mixes that ranged from 25% to 75% 4D-equipped aircraft; (2) examine the effect of time errors at 120 n. mi. from touchdown on touchdown time scheduling of the various mix conditions; and (3) develop efficient algorithms and procedures to null the initial time errors prior to reaching the final control sector, 30 n. mi. from touchdown. Results indicate substantial reduction in controller workload and an increase in orderliness when more than 25% of the aircraft are equipped with 4D guidance systems; initial random errors of up to + or - 2 min can be handled via a single speed advisory issued in the arrival control sector, thus avoiding disruption of the time schedule. Author

N85-32102# Committee on Appropriations (U. S. Senate).
AVIATION SYSTEM DELAYS
Washington GPO 1985 184 p refs Hearing before a Subcomm. of the Comm. on Appropriations, 98th Congr., 2nd Sess., 7 Sep. 1984
(S-Hrg-98-1241; GPO-39-723) Avail: Committee on Appropriations

The subcommittee on transportation discussed flight delays at many of the nations airports. The committee points out the delays may arise from many different points within the air transportation system including: the airport runway layout; the scheduling of airline flights; the noise rules imposed by certain communities; the weather forecast; the congested air traffic at major airports; and the airport terminal building design. J.W.G.

N85-32103# National Bureau of Standards, Gaithersburg, Md.
WALL FLAMES AND IMPLICATIONS FOR UPWARD FLAME SPREAD Final Report
J. G. Quintiere, M. Harkleroad, and Y. Hasemi (BRI, Japan) Atlantic City FAA Jun. 1985 56 p refs
(FAA-CT-85-2) Avail: NTIS HC A04/MF A01

New concepts for predicting the flame spread on materials from laboratory measurements are given. Heat transfer which precipitates and precedes upward flame spread on a vertical surface is studied. Six materials were featured. Their relevant flame spread measurements are presented. Heat transfer and flame height results are presented for wall samples burned at varying levels of external irradiance. Also complementary results are presented for methane line burner wall fires. An approximate theoretical analysis is included to serve as a guide to identifying the important variables and their relationship for correlation purposes. Experimental results yield flame height proportional to energy release rate, to the 2/3 power, and wall heat flux distributions are roughly correlated in terms of distance divided by flame height. Author

N85-32104# National Bureau of Standards, Gaithersburg, Md.
THE ROLE OF AIRCRAFT PANEL MATERIALS IN CABIN FIRES AND THEIR PROPERTIES Final Report
J. G. Quintiere, V. Babrauskas, L. Cooper, M. Harkleroad, K. Steckler, and A. Tewarson (Factory Mutual Research Corp.) Atlantic City FAA Jun. 1985 119 p refs
(FAA-CT-84-30) Avail: NTIS HC A06/MF A01

Analyses were performed on full-scale aircraft post-crash fire data. In particular the rate and involvement of aircraft wall and ceiling panels are examined. For two full-scale experiments the energy release rate of the interior cabin furnishings were estimated and an estimate of ceiling ignition computed. Also an extensive set of measurements, by several advanced state-of-the-art laboratory flammability devices, was conducted for fire aircraft panel materials. The measurements included piloted ignition by thermal radiation, energy release rate, combustion produce generation rates, lateral flame spread rates in a vertical orientation, flame heights and their heat transfer to a contiguous vertical surface, and for one devices results were obtained at conditions of oxygen concentrations lower than normal air. Comparison among the results for each device show good consistency of the ignition data, but only fair agreement or energy release rate data. Author

N85-32105# National Transportation Safety Board, Washington, D. C. Bureau of Safety Programs.
AIR CARRIER OVERWATER EMERGENCY EQUIPMENT AND PROCEDURES Safety Study, 1959 - 1984
12 Jun. 1985 26 p refs
(PB85-917006; NTSB/SS-85/02) Avail: NTIS HC A03/MF A01; SOD HC

The chances of surviving air carrier accidents into water would be increased if Federal Aviation Administration (FAA) emergency procedures and FAA approved survival equipment were improved. Current procedures assume that air carrier water contact accidents are primarily ditchings. In fact, a review of air carrier water contact accidents between 1959 and 1984 shows that such accidents are typically inadvertent, with no preparation time, substantial aircraft damage, and a high chance of occupant injury. Often the cabin floods quickly, followed by sinking of the aircraft within minutes. Typically, these accidents do not occur on extended overwater flight (the type of operation to which most FAA water survival regulations currently apply) but close to an airport, during approach or departure. At least 179 fully certificated airports in the United States are located within 5 miles of a significant body of water. The Board recommended the FAA require both life preservers and flotation seat cushions on all air carrier flights, and asked for improvements in life preserver design, packaging, accessibility, and ease of donning. Other recommendations deal with emergency evacuation slides, liferafts, flotation devices for infants, crew post crash survival training, and water rescue plans at airports near water. Author

N85-32106# RMS Technologies, Inc., Trevose, Pa.
SEAT EXPERIMENTS FOR THE FULL-SCALE TRANSPORT AIRCRAFT CONTROLLED IMPACT DEMONSTRATION Final Report
M. R. Cannon and R. E. Zimmermann Mar. 1985 247 p
(Contract DTFA03-81-C-00040)
(AD-A155024; FAA-CT-84-10) Avail: NTIS HC A11/MF A01 CSCL 01/3

As part of the FAA/NASA Controlled Impact Demonstration (CID) with a four-engine jet transport, 22 experimental seats have been placed on the aircraft by the contractor for the FAA. Four additional experimental seats have been directly installed by NASA and the FAA. Also, an originally installed pilot seat was included in the overall series of 27 seat experiments. Of the 22 seats installed by the contractor, 13 have been modified for the intent of improving their structural crashworthiness. These include 12 triple-occupant passenger seats and one flight attendant seat. The modification process was supported by extensive testing and analysis. Initially, identical seats were subjected to both static and dynamic destructive tests. From these tests, much was learned about the failure modes of the seat structure and the loads at which they would occur. Using these data, a design effort (supported by NASTRAN finite element models of the seats) produced methods for improving the capability of the seat structure to sustain crash loads. Prototypes of the designs were fabricated and subjected to identical static and dynamic testing sequences. Where necessary, design improvements were made and retested. Modified experimental seats were then fabricated for installation on the test aircraft. GRA

04 AIRCRAFT COMMUNICATIONS AND NAVIGATION

Includes digital and voice communication with aircraft; air navigation systems (satellite and ground based); and air traffic control.

For related information see also *17 Spacecraft Communications, Command, and Tracking* and *32 Communications.*

N85-32107# Committee on Public Works and Transportation (U.S. House).
STATUS OF THE AIR TRAFFIC CONTROL SYSTEM
Washington GPO 1984 1448 p refs Hearings before the Subcomm. on Invest. and Oversight of the Comm. on Public Works and Transportation, 98th Congr., 2nd Sess., 4 May, 7 Jun., 28 Oct., 20-22, 27-29 Mar., 4 Apr., and 26-27 Jun. 1984
(GPO-40-343) Avail: Subcommittee on Investigations and Oversight

The status of the air traffic control system is discussed. Emphasis is placed on the problems experienced by air traffic controllers as a result of inadequate staffing caused by firing striking controllers. R.J.F.

N85-32108# Coast Guard, Washington, D.C. Office of Navigation.
LORAN-C HARBOR AND HARBOR ENTRANCE SURVEY: CHARLESTON, SOUTH CAROLINA Final Report, Apr. - Jul. 1983
R. L. Gazlay Jan. 1985 91 p
(AD-A154875; USCG-N-1-85) Avail: NTIS HC A05/MF A01 CSCL 17/7

LORAN-C is being investigated as a possible aid to navigation in Harbor and Harbor Entrance areas, as outlined in the 1982 Federal Radio-navigation Plan. LORAN-C can be used in the repeatable mode for excellent repeatable accuracies using waypoints whose LORAN-C time difference (TD) values have been previously measured. The exact accuracy achievable in a given harbor area depends on many factors and is best determined by measurement. If the true geodetic position is measured with an independent reference positioning system in addition to measuring the LORAN-C TDs, one can use the resulting TDs in the repeatable mode to achieve geodetic accuracies better than + or - 80 meters in many areas. Responding to a U.S. Navy request, we measured LORAN-C TDs simultaneously with Miniranger III, Raydist, and GPS positions along two routes in the Charleston, SC area. The results show that LORAN-C can provide + or - 29 meters geodetic accuracy along the Charleston River route and the ocean route to 20 miles offshore when using surveyed waypoints in the repeatable mode. The accuracy achieved beyond 20 miles was + or - 36 meters due to using a less accurate reference positioning system for surveying that area. GRA

N85-32109# Army Engineer Topographic Labs., Fort Belvoir, Va.
THE POTENTIAL OF THE NAVSTAR GLOBAL POSITIONING SYSTEM FOR THE CORPS OF ENGINEERS, CIVIL WORKS
K. D. Robertson Feb. 1985 6 p
(AD-A154913; ETL-R-068) Avail: NTIS HC A02/MF A01 CSCL 17/7

The Department is in the process of deploying a new satellite system for the purpose of navigation and point positioning. While designed primarily for military applications, the system poses great potential for civilian use as well. In particular, the use of GPS in a geodetic mode may yield rapid, accurate survey positions in three dimensions. Thus, in the near future, GPS will become a valuable new tool to the Corps surveyor. GRA

05 AIRCRAFT DESIGN, TESTING AND PERFORMANCE

Includes aircraft simulation technology.

For related information see also *18 Spacecraft Design, Testing and Performance* and *39 Structural Mechanics.*

N85-32110*# National Aeronautics and Space Administration. Langley Research Center, Hampton, Va.
STUDY OF AN EFFICIENT LONG-RANGE MACH 2.7 SUPERSONIC TRANSPORT CONFIGURATION CONCEPT
Peter D. Gall Jul. 1985 53 p refs
(NASA-TM-86414; NAS 1.15:86414) Avail: NTIS HC A04/MF A01 CSCL 01C

A long range Mach 2.7 supersonic transport configuration concept was studied utilizing linear theory methods. The configuration was sized to carry 290 passengers 6,000 nautical miles nonstop. The final configuration has a maximum takeoff gross weight of 687,200 pounds, a wing loading of 69.8 lbf/sq.ft. and a thrust weight ratio of .278. The most significant result is that a significantly improved trimmed maximum lift drag ratio of 11.04 can be obtained for a supersonic transport at Mach 2.62 and 55, 000 feet. Author

N85-32111*# National Aeronautics and Space Administration. Langley Research Center, Hampton, Va.
PRELIMINARY SIZING AND PERFORMANCE OF AIRCRAFT
David E. Fetterman, Jr. Jul. 1985 115 p refs
(NASA-TM-86357; NAS 1.15:86357) Avail: NTIS HC A06/MF A01 CSCL 01C

The basic processes of a program that performs sizing operations on a baseline aircraft and determines their subsequent effects on aerodynamics, propulsion, weights, and mission performance are described. Input requirements are defined and output listings explained. Results obtained by applying the method to several types of aircraft are discussed. Author

N85-32112# Air Force Inst. of Tech., Wright-Patterson AFB, Ohio. School of Engineering.
USE OF MMLE3 TO DETERMINE LOWER ORDER EQUIVALENT SYSTEMS IN THE TIME DOMAIN M.S. Thesis
R. A. Schroeder Mar. 1985 69 p
(AD-A154700; AFIT/GAE/AA/85M-6) Avail: NTIS HC A04/MF A01 CSCL 09/2

This thesis explains the data reduction technique for determin-

ing lower order equivalent system (LOES) parameters using flight test maneuver time history data. This technique uses MMLE3, a modified NASA developed general program for maximum likelihood parameter estimation. The MMLE3 requires a state-space model relating input to output and a time history of the input and the output. From this information, accurate estimates of the components of the state-space model can be made. The LOES parameters determined by MMLE3 would be aircraft short period frequency, damping ratio, and time delay. Based on simulation testing, it was determined that this data reduction technique was feasible and accurate. The algorithm was further tested by using flight test data gathered in a T-38. The state-space model was modified to a modified second order model, to determine basic aircraft short period frequency and damping ratio. The flight test results effectively matched the published values of frequency and short period for the T-38. Based on the results of this testing, this technique of determining LOES parameters from time history data is effective. It should be incorporated into the USAF TPS curriculum for data reduction. GRA

N85-32113# Aeronautical Research Labs., Melbourne (Australia).
A PHASE-LOCKED FREQUENCY MULTIPLIER FOR THE SIGNAL AVERAGING OF THE VIBRATION OF THE WESSEX HELICOPTER INPUT SPIRAL BEVEL PINION
P. D. McFadden Jan. 1985 25 p
(AD-A154914; ARL/AERO-TM-423) Avail: NTIS HC A02/MF A01 CSCL 01/3

This Australian report provides details of the design of a phase-locked frequency multiplier for the conversion of a signal derived from the alternator of the Wessex helicopter into a pulse train suitable for controlling the sampling and signal averaging by a computer of the vibration of the input spiral bevel pinion in the Wessex main rotor gearbox. The frequency multiplier is implemented as a series of four phase-locked loops, and features an oscillator which maintains the loops at approximately the correct frequency in standby mode thereby reducing the time to lock when the input signal is applied. GRA

N85-32114# Aerospace Medical Research Labs., Wright-Patterson AFB, Ohio.
THE MEASUREMENT OF AIRCRAFT WINDSCREEN HAZE AND ITS EFFECT ON VISUAL PERFORMANCE Final Report
H. L. Task and L. V. Genco Feb. 1985 46 p
(AF Proj. 7184)
(AD-A154949; AFAMRL-TR-85-016) Avail: NTIS HC A03/MF A01 CSCL 06/16

A new method of measuring haze in installed aircraft transparencies is developed and explained. Using data obtained with the new method, equations were derived to help predict target detection performance as it is affected by windscreen haze, windscreen transmissivity, ambient illumination, mean target luminance, target contrast and target size. The equations may be applied to many transparency types and configurations. Graphs are provided to show the effects of another of typical visibility conditions. No similar relationships were found for older methods of measuring haze. GRA

N85-32115# Air Force Academy, Colo.
FLIGHT CONTROL SYSTEM FOR A COMPUTER CONTROLLED AIRCRAFT WITH LIMITED SENSORS
T. P. Webb 30 Apr. 1985 63 p
(AD-A155107; USAFA-TN-85-4) Avail: NTIS HC A04/MF A01 CSCL 01/4

The Department of Electrical Engineering at the United States Air Force Academy is attempting, through one of its senior design courses, to design, build, and fly a computer controlled aircraft. The Department of Aeronautics was asked to help design the flight control system to be implemented by the on-board digital computer. The project involved building and testing a wind tunnel model of the aircraft to determine its aerodynamic characteristics, performing mass tests on the actual aircraft to determine inertia characteristics, developing a 12 degree-of-freedom nonlinear aircraft simulation computer program, and designing the actual flight control system. This report describes only the last task. A complete flight control system for a small computer controlled aircraft was designed using only yaw rate, heading, lateral load factor, airspeed, altitude, and rate of climb feedback. This multi-input multi-output control problem was done using the classical root locus technique on a linearized system model. The simulation results revealed surprisingly good performance, considering the limitation on sensors. GRA

N85-32116# Army Aviation Engineering Flight Activity, Edwards AFB, Calif.
ARTIFICIAL AND NATURAL ICING TESTS YEH-60A QUICK FIX HELICOPTER Final Report, 5 Jan. - 21 Mar. 1984
E. J. Tavares, P. J. Sullivan, M. L. Hanks, and R. Woratschek Jun. 1984 88 p
(AD-A155147; AD-F630645; USAAEFA-83-21) Avail: NTIS HC A05/MF A01 CSCL 01/3

These tests were conducted to establish a moderate icing flight envelope for the helicopter with the AN/ALQ-151(V)2 countermeasures system installed. A total of 12.3 hours were flown in the icing environment. After damage to an unprotected direction finding (DF) dipole antenna during an icing encounter, the original DF dipole antennas were removed and a prototype thermoelectrically anti-iced DF dipole antenna was installed in position no. 3 (aft right side). During these tests 4 deficiencies and 16 shortcomings were noted. The two icing related deficiencies are: damage to the DF antenna element mounts and phenolic blocks caused by excessive element oscillations induced by ice accumulation; and erroneous readings on the Rosemount Icing Rate Indicator caused by electromagnetic interference from the electronic countermeasures system which prevents simultaneous safe operation of the ECM system and the blade deicing system. The two non-icing related deficiencies are: interference between the main rotor blades and the upper elements of the aft DF dipole antennas during rearward ground taxi and the inadequate cabin heat. The YEH-60A Quick Fix helicopter as originally configured (unheated DF antennas) was not suitable for flight in a moderate icing environment. GRA

N85-32117# Aeronautical Research Labs., Melbourne (Australia).
PROPOSAL FOR MODIFICATIONS TO THE WESSEX HELICOPTER MAIN ROTOR GEARBOX VIBRATION MONITORING PROGRAM
P. D. McFadden Jan. 1985 31 p
(AD-A155196; ARL/AERO-PROP-TM-422) Avail: NTIS HC A03/MF A01 CSCL 01/3

Modifications to the RAN Recorded Tape Vibration Analysis Program for the condition monitoring of the main rotor gearbox in the Wessex helicopter are proposed to take advantage of recent developments in the techniques of signal averaging and computer enhancement of vibration data. GRA

N85-32118# Air Force Systems Command, Wright-Patterson AFB, Ohio. Foreign Technology Div.
CHINA HAS DEVELOPED A NEW VERSION OF FIGHTER AIRCRAFT
17 Apr. 1985 15 p Transl. into ENGLISH from Conmilit. (China), v. 96, no. 11, Nov. 1984 p 10-11, 14-15
(AD-A155293; AD-F300613; FTD-ID(RS)T-0020-85) Avail: NTIS HC A02/MF A01 CSCL 01/3

This translation of a Chinese document describes the development of a new fighter aircraft. The contents of this note show that this aircraft has a delta main wing, two turbo jet engines and an excellent capacity of supersonic and high-altitude climb. From the synthesis of different documents, this is a new, modified MiG-21 attack plane. The nose air intake was expanded, and the aircraft has the feature of being able to fly under all weather conditions. The aircraft was fitted with a fire control system and more advanced electronic equipment. It has a single vertical tail and two all-flying tailplanes. According to the guesswork of some experts, this new fighter aircraft is perhaps the expanded version of the MiG-21. GRA

06 AIRCRAFT INSTRUMENTATION

Includes cockpit and cabin display devices; and flight instruments.

For related information see also *19 Spacecraft Instrumentation* and *35 Instrumentation and Photography.*

No abstracts in this category.

07 AIRCRAFT PROPULSION AND POWER

Includes prime propulsion systems and systems components, e.g., gas turbine engines and compressors; and on-board auxiliary power plants for aircraft.

For related information see also *20 Spacecraft Propulsion and Power, 28 Propellants and Fuels,* and *44 Energy Production and Conversion.*

N85-32119*# General Electric Co., Cincinnati, Ohio. Aircraft Engine Business Group.
COMPONENT-SPECIFIC MODELING Annual Status Report, 1 Jan. - 31 Dec. 1984
R. L. McKnight 1985 131 p
(Contract NAS3-23687)
(NASA-CR-174925; NAS 1.26:174925; ASR-2) Avail: NTIS HC A07/MF A01 CSCL 21E

Accomplishments are described for the second year effort of a 3-year program to develop methodology for component specific modeling of aircraft engine hot section components (turbine blades, turbine vanes, and burner liners). These accomplishments include: (1) engine thermodynamic and mission models; (2) geometry model generators; (3) remeshing; (4) specialty 3-D inelastic stuctural analysis; (5) computationally efficient solvers, (6) adaptive solution strategies; (7) engine performance parameters/component response variables decomposition and synthesis; (8) integrated software architecture and development, and (9) validation cases for software developed. Author

N85-32120*# National Aeronautics and Space Administration. Dryden (Hugh L.) Flight Research Center, Edwards, Calif.
PERFORMANCE IMPROVEMENTS OF A HIGHLY INTEGRATED DIGITAL ELECTRONIC CONTROL SYSTEM FOR AN F-15 AIRPLANE
Terrill W. Putnam, Frank W. Burcham, Jr., Mary G. Andries (Pratt and Whitney Aircraft, West Palm Beach, Fla.), and James B. Kelly (Pratt and Whitney Aircraft, West Palm Beach, Fla.) Aug. 1985 14 p refs Presented at the AIAA Guidance and Control Conf., Snowmass, Colo., 19-21 Aug. 1985
(NASA-TM-86748; H-1312; NAS 1.15:86748; AIAA-85-1876) Avail: NTIS HC A02/MF A01 CSCL 21E

The NASA highly integrated digital electronic control (HIDEC) program is structured to conduct flight research into the benefits of integrating an aircraft flight control system with the engine control system. A brief description of the HIDEC system installed on an F-15 aircraft is provided. The adaptive engine control system (ADECS) mode is described in detail, together with simulation results and analyses that show the significant excess thrust improvements achievable with the ADECS mode. It was found that this increased thrust capability is accompanied by reduced fan stall margin and can be realized during flight conditions where engine face distortion is low. The results of analyses and simulations also show that engine thrust response is improved and that fuel consumption can be reduced. Although the performance benefits that accrue because of airframe and engine control integration are being demonstrated on an F-15 aircraft, the principles are applicable to advanced aircraft such as the advanced tactical fighter and advanced tactical aircraft. Author

N85-32121# Air Force Inst. of Tech., Wright-Patterson AFB, Ohio. School of Engineering.
MICROPROCESSOR CONTROL DESIGN FOR A LOW-HEAD CROSSFLOW TURBINE M.S. Thesis
D. C. Ramsey Mar. 1985 343 p
(AD-A155477; AFIT/GE/ENG/85M-2) Avail: NTIS HC A15/MF A01 CSCL 09/2

A microprocessor based controller is designed for use on a low-head crossflow turbine, The design contains a model of the turbine, an algorithm for maximizing output power, software design, and software testing. Modelling of the turbine is performed using tabular data in order to avoid the complexity of deriving an equation model. Linear interpolation of the tabular data is used to obtain a continuous model of the turbine. Based upon turbine hardware, turbine characteristics, and economic feasibility, a search design is selected as most appropriate for the crossflow turbine. Specifically, a gradient search algorithm is chosen to maximum the turbine's output power. Software is designed for the gradient search and other modes of the controller. The software design contains flow diagrams, pseudo-code, and a data dictionary. Testing the software with the linear interpolation model shows the gradient search adequately maximizes the output power of the modelled crossflow turbine. GRA

08 AIRCRAFT STABILITY AND CONTROL

Includes aircraft handling qualities; piloting; flight controls; and autopilots.

N85-32122*# National Aeronautics and Space Administration. Dryden (Hugh L.) Flight Research Center, Edwards, Calif.
DEVELOPMENT AND VALIDATION OF A GENERAL PURPOSE LINEARIZATION PROGRAM FOR RIGID AIRCRAFT MODELS
Eugene L. Duke and Robert F. Antoniewicz Aug. 1985 14 p refs Presented at the AIAA Guidance, Navigation, and Control Conf., Snowmass, Colo., 19-21 Aug. 1985
(NASA-TM-86737; H-1295; NAS 1.15:86737; AIAA-85-1891) Avail: NTIS HC A02/MF A01 CSCL 01C

A FORTRAN program that provides the user with a powerful and flexible tool for the linearization of aircraft models is discussed. The program LINEAR numerically determines a linear systems model using nonlinear equations of motion and a user-supplied, nonlinear aerodynamic model. The system model determined by LINEAR consists of matrices for both the state and observation equations. The program has been designed to allow easy selection and definition of the state, control, and observation variables to be used in a particular model. Also, included in the report is a comparison of linear and nonlinear models for a high performance aircraft. Author

N85-32123*# National Aeronautics and Space Administration. Ames Research Center, Moffett Field, Calif.
IN-FLIGHT EVALUATION OF PURE TIME DELAYS IN PITCH AND ROLL
Donald T. Berry Aug. 1985 11 p refs Presented at the AIAA Conf., Snowmass, Colo., 19-21 Aug. 1985
(NASA-TM-86744; H-1308; NAS 1.15:86744) Avail: NTIS HC A02/MF A01 CSCL 01C

An in-flight investigation of the effect of pure time delays in pitch and roll was undertaken. The evaluation tasks consisted of low lift-to-drag-ratio landings of various levels of difficulty and formation flying. The results indicate that the effect of time delay is strongly dependent on the task. In the pitch axis, in calm air, spot landings from a lateral offset were most strongly influenced by time delay. In the roll axis, in calm air, formation flying was most strongly influenced by time delay. However, when landings were made in turbulence, flying qualities in pitch were only slightly degraded, whereas in roll they were severely degraded. Author

N85-32124# Naval Postgraduate School, Monterey, Calif.
DEVELOPMENT OF REDUCED ORDER MODELS FOR CONTROL SYSTEM DESIGN USING THE OPTSYSX PROGRAM M.S. Thesis
S. W. Nelson Dec. 1984 157 p
(AD-A154552) Avail: NTIS HC A08/MF A01 CSCL 09/2

The modern controls engineer is often faced with designing a system which is characterized by a large number of first order differential equations. It is highly desirable and sometimes necessary that such complex systems be reduced for analysis, synthesis and implementation into a physical control system. It is the intent of this thesis to present a mathematical procedure and computer software based upon this procedure which enable the control engineer to construct reduced order models. As examples, two large order systems are analyzed: a sixteenth order model of the F100 turbofan engine and a 98th order model of the X-29A aircraft control system. GRA

N85-32125# National Aeronautical Establishment, Ottawa (Ontario).
A PRELIMINARY INVESTIGATION OF HANDLING QUALITIES REQUIREMENTS FOR HELICOPTER INSTRUMENT FLIGHT DURING DECELERATING APPROACH MANEUVERS AND OVERSHOOT
S. Kereliuk and M. Morgan Feb. 1985 35 p
(AD-A154650; NAE-AN-26; NRC-24173) Avail: NTIS HC A03/MF A01 CSCL 01/2

This investigation was carried out to highlight deficiencies of helicopters handling qualities when performing low speed instrument approaches. Steep decelerating MLS (Microwave Landing System) approaches to a decision height of 50 feet, simultaneously decelerating to 20 knots, were performed in an airborne simulator —a variable-stability Bell 205A helicopter. Tracking performance, in terms of height, azimuth and speed errors was of an acceptable standard, but pilot workload was extremely high, especially during the overshoot phase. Benefits of different levels of control system augmentation were not readily apparent in this high workload environment. In view of the results of this investigation, a follow-on program is proposed where further attempts will be made to determine the effects of display and control sophistication on pilot workload during slow-speed helicopter instrument procedures. GRA

N85-32126# Aerospace Medical Research Labs., Wright-Patterson AFB, Ohio.
MYOELECTRIC CONTROL OF A COMPUTER BASED EXPERT SYSTEM FOR FLIGHT CONTROL
D. B. Rogers and P. B. Glaeser Apr. 1985 59 p
(AD-A154981; AFAMRL-TR-85-028) Avail: NTIS HC A04/MF A01 CSCL 05/8

The United States Air Force is constantly searching for new ways to transfer information between humans and machines. This goal becomes especially important in situations when conventional communication channels are overloaded or even inoperable. This document describes the results of a research effort to determine the possibility of using electromyographic signals to interface with a computer based expert system. The equipment described here is intended to demonstrate the feasibility of this type of control and facilitate future studies. This document describes a laboratory myoelectric control system which can detect activity in muscles and convert these signals into a digital format. The muscle inputs can then be used for computer control. The purpose of this thesis is to show that this type of control does work. GRA

09 RESEARCH AND SUPPORT FACILITIES (AIR)

Includes airports, hangars and runways; aircraft repair and overhaul facilities; wind tunnels; shock tube facilities; and engine test blocks.

For related information see also *14 Ground Support Systems and Facilities (Space).*

N85-32127# Naval Postgraduate School, Monterey, Calif.
THE NAVAL POSTGRADUATE SCHOOL FLIGHT MECHANICS LABORATORY: A FEASIBILITY STUDY M.S. Thesis
K. S. Reightler, Jr. Dec. 1984 47 p
(AD-A154578) Avail: NTIS HC A03/MF A01 CSCL 05/9

The Naval Postgraduate School (NPS) currently has no laboratory facilities to support the teaching of flight mechanics. This thesis concerns a feasibility study conducted to define the need for a flight mechanics laboratory at NPS, determine the methods used at other universities and availability of resources, develop a plan to integrate laboratory facilities into the NPS aeronautical engineering syllabus, and make recommendations concerning changes needed in the NPS Department of Aeronautics to enhance the teaching of flight mechanics. The general conclusion of the study is that a flight mechanics laboratory is essential to the study of flight mechanics at NPS. The proposed laboratory should include the selective use of flight simulators, computer instructional devices, a flight demonstration airplane, a fully instrumented flying laboratory, and a variable stability airplane. Extensive use should be made of contracted services. A flight mechanics laboratory used to support classroom instruction and research should be established at NPS as soon as possible. GRA

N85-32128# Missouri Univ., Rolla. Graduate Center for Cloud Physics.
CONSTRUCTION OF UNIVERSITY OF MISSOURI, ROLLA'S FULL SCALE CLOUD SIMULATION CHAMBER AND APPLIED RESEARCH Final Report
D. R. White 1 Mar. 1985 62 p
(Contracts F49620-80-C-0090; MIPR-138-84)
(AD-A154682; AFOSR-85-0409TR; ARO-1663.5-GS) Avail: NTIS HC A04/MF A01 CSCL 04/2

The purpose of this work is to construct two cooled wall cloud simulation chambers. The smaller 48-inch tall chamber capable of being cooled at 10 C/min and the larger 112-inch tall chamber capable of 15 C/min. Construction will include such support peripherals as secondary cooling, computer control, data acquisition, and other systems required for the operation of the chambers. The chambers will be incorporated into the existing Univ. of Mo., Rolla, cloud simulation facility. The construction and testing of these two cloud simulation chamber facilities, with precise wall temperature control, is described and discussed. GRA

12 ASTRONAUTICS (GENERAL)

For extraterrestrial exploration see *91 Lunar and Planetary Exploration.*

N85-32129* National Aeronautics and Space Administration. Johnson (Lyndon B.) Space Center,
MISSION OPERATIONS REQUIREMENTS DOCUMENT FOR D-1 EXPERIMENT 102, VESTIBULAR EXPERIMENTS IN SPACELAB
3 Jun. 1985 52 p
(NASA-TM-87495; JSC-LS-50110; NAS 1.15:87495) Avail: Issuing Activity CSCL 22A

The purpose of the Mission Operations Requirements Document (MORD) is to define the principal operations, functions, and modes required for each experiment. The MORD will be used as the basis for assessing compatibility between payload design at the Flight Operations Review. The MORD also contains essential

information for payload crew training, simulator development and support of other operations planning activities. An overview is presented of Experiment E102, Vestibular Experiments in Spacelab. The effects of O-g environment on the human vestibular system are investigated. This series of experiments uses the crew as subjects in the Spacelab to test the sensory-motor conflict theory of space sickness. B.W.

N85-32130*# University of Eastern Kentucky, Richmond. Dept. of Physics and Astronomy.
STUDY OF PROTON AND NEUTRON ACTIVATION OF METAL SAMPLES IN LOW EARTH ORBIT Final Technical Report
C. E. Laird Jul. 1985 156 p refs
(Contract NAS8-35180)
(NASA-CR-171596; NAS 1.26:171596) Avail: NTIS HC A08/MF A01 CSCL 22A

The anticipated nuclear activation of metal samples in low Earth orbit for the Spacelab and Long Duration Exposure Facility (LDEF) missions was studied. Compilations were made of scientific data needed in analyzing the samples. These compilations include reaction cross sections, half lives, reaction Q values, gamma ray energies, and competing reactions. Calculations were made of the expected activation given proton and neutron fluxes and target covering materials. Experiments were performed to determine reaction cross sections for protons of various energies from 60 to 200 MeV. A data analysis plan for studying the activation of the orbited samples was prepared. An analysis of the gamma ray spectra obtained from samples orbited on Spacelab 1 was completed. Author

13 ASTRODYNAMICS

Includes powered and free-flight trajectories; and orbit and launching dynamics.

N85-32131*# National Aeronautics and Space Administration. Goddard Space Flight Center, Greenbelt, Md.
EARTH ALBEDO AND THE ORBIT OF LAGEOS
David Parry Rubincam and Nelson R. Weiss Jun. 1985 73 p refs
(NASA-TM-86210; Rept-85B0381; NAS 1.15:86210) Avail: NTIS HC A04/MF A01 CSCL 22C

The long-period perturbations in the orbit of the Lageos satellite due to the Earth's albedo have been found using a new analytical formalism. The Earth is assumed to be a sphere whose surface diffusely reflects sunlight according to Lambert's law. Specular reflection is not considered. The formalism is based on spherical harmonics; it produces equations which hold regardless of whether the terminator is seen by the satellite or not. Specializing to the case of a realistic zonal albedo shows that Lageos' orbital semimajor axis changes periodically by only the a few millimeters and the eccentricity by one part in 100,000. The longitude of the node increases secularly. The effect considered here can explain neither the secular decay of 1.1 mm/day in the semimajor axis nor the observed along-track variations in acceleration of order 2 x 10 to the minus 12 power/sq ms. B.W.

N85-32132# Naval Surface Weapons Center, Dahlgren, Va.
A DERIVATION OF RELATIVISTIC EFFECTS IN SATELLITE TRACKING Final Report
L. R. Gibson Apr. 1983 26 p
(AD-A154620; NSWC/TR-83-55) Avail: NTIS HC A03/MF A01 CSCL 17/3

Starting with the Schwarzschild solution to Einstein's field equations, the equations for relativistic corrections to satellite tracking are derived. Included are corrections for range from satellite to Earth station, range from satellite to satellite, and Doppler range difference from satellite to Earth station. In addition, the classical and relativistic Doppler effects are derived in the appendixes. GRA

14 GROUND SUPPORT SYSTEMS AND FACILITIES (SPACE)

Includes launch complexes, research and production facilities; ground support equipment, e.g., mobile transporters; and simulators.

For related information see also *09 Research Support Facilities (Air).*

No abstracts in this category.

15 LAUNCH VEHICLES AND SPACE VEHICLES

Includes boosters; manned orbital laboratories; reusable vehicles; and space stations.

N85-32133*# Rockwell International Corp., Downey, Calif. Space Station Systems Div.
SPACE STATION CREW SAFETY ALTERNATIVES STUDY. VOLUME 2: THREAT DEVELOPMENT Final Report
R. F. Raasch, R. L. Peercy, Jr., and L. A. Rockoff Washington NASA Jun. 1985 239 p 5 Vol.
(Contract NAS1-17242)
(NASA-CR-3855; NAS 1.26:3855; SSD84-0053) Avail: NTIS HC A11/MF A01 CSCL 22B

The first 15 years of accumulated space station concepts for initial operational capability (IOC) during the early 1990's were considered. Twenty-five threats to the space station are identified and selected threats addressed as impacting safety criteria, escape and rescue, and human factors safety concerns. Of the 25 threats identified, eight are discussed including strategy options for threat control: fire, biological or toxic contamination, injury/illness, explosion, loss of pressurization, radiation, meteoroid penetration, and debris. E.A.K.

16 SPACE TRANSPORTATION

Includes passenger and cargo space transportation, e.g., shuttle operations; and rescue techniques.

For related information see also *03 Air Transportation and Safety* and *85 Urban Technology and Transportation.*

N85-32134*# SRI International Corp., Menlo Park, Calif. Artificial Intelligence Center.
NASA SPACE STATION AUTOMATION: AI-BASED TECHNOLOGY REVIEW
Oscar Firschein, Michael P. Georgeff, William park, Peter Neumann, William H. Kautz, Karl N. Levitt, Raphael J. Rom, and Andrew A. Poggio 1 Apr. 1985 325 p refs Revised
(Contract NAS2-11864; SRI Proj. 7268)
(NASA-CR-176094; NAS 1.26:176094) Avail: NTIS HC A14/MF A01 CSCL 22B

Research and Development projects in automation for the Space Station are discussed. Artificial Intelligence (AI) based automation technologies are planned to enhance crew safety through reduced need for EVA, increase crew productivity through the reduction of routine operations, increase space station autonomy, and augment space station capability through the use of teleoperation and robotics. AI technology will also be developed for the servicing of satellites at the Space Station, system monitoring and diagnosis, space manufacturing, and the assembly of large space structures. F.M.R.

N85-32135*# SRI International Corp., Menlo Park, Calif. Artificial Intelligence Center.

NASA SPACE STATION AUTOMATION: AI-BASED TECHNOLOGY REVIEW. EXECUTIVE SUMMARY
Oscar Firschein, Michael P. Georgeff, William Park, Peter C. Cheeseman, Jacob Goldberg, Peter Neumann, William H. Kautz, Karl N. Levitt, Raphael J. Rom, and Andrew A. Poggio 26 Mar. 1985 68 p Revised
(Contract NAS2-11864; SRI Proj. 7268)
(NASA-CR-176096; NAS 1.26:176096) Avail: NTIS HC A04/MF A01 CSCL 22B

Research and Development projects in automation technology for the Space Station are described. Artificial Intelligence (AI) based technologies are planned to enhance crew safety through reduced need for EVA, increase crew productivity through the reduction of routine operations, increase space station autonomy, and augment space station capability through the use of teleoperation and robotics. F.M.R.

N85-32136*# Hughes Aircraft Co., Culver City, Calif.
AUTOMATION STUDY FOR SPACE STATION SUBSYSTEMS AND MISSION GROUND SUPPORT Final Report
[1985] 82 p refs Sponsored by NASA. Johnson Spacecraft Center
(NASA-CR-176097; NAS 1.26:176097) Avail: NTIS HC A05/MF A01 CSCL 22B

An automation concept for the autonomous operation of space station subsystems, i.e., electric power, thermal control, and communications and tracking are discussed. To assure that functions essential for autonomous operations are not neglected, an operations function (systems monitoring and control) is included in the discussion. It is recommended that automated speech recognition and synthesis be considered a basic mode of man/machine interaction for space station command and control, and that the data management system (DMS) and other systems on the space station be designed to accommodate fully automated fault detection, isolation, and recovery within the system monitoring function of the DMS. F.M.R.

N85-32137*# National Aeronautics and Space Administration. Johnson (Lyndon B.) Space Center,
LIFE SCIENCES FLIGHT EXPERIMENTS PROGRAM MISSION SCIENCE REQUIREMENTS DOCUMENT. THE FIRST LIFE SCIENCES DEDICATED SPACELAB MISSION, PART 1
J. A. Rummel 1 Jun. 1982 92 p refs
(NASA-TM-87494; JSC-18295-Pt-1; NAS 1.15:87494) Avail: NTIS HC A05/MF A01 CSCL 22A

The Mission Science Requirements Document (MSRD) for the First Dedicated Life Sciences Mission (LS-1) represents the culmination of thousands of hours of experiment selection, and science requirement definition activities. NASA life sciences has never before attempted to integrate, both scientifically and operationally, a single mission dedicated to life sciences research, and the complexity of the planning required for such an endeavor should be apparent. This set of requirements completes the first phase of a continual process which will attempt to optimize (within available programmatic and mission resources) the science accomplished on this mission. Author

N85-32138# Congressional Budget Office, Washington, D. C.
PRICING OPTIONS FOR THE SPACE SHUTTLE. SPECIAL STUDY
Mar. 1985 58 p refs
Avail: NTIS HC A04/MF A01

The space shuttle is the most important means of placing satellites into orbit for scientific, commercial, and military purposes. The price which the National Aeronautics and Space Administration (NASA) charges foreign and commercial customers to use the shuttle's launch services has important implications for the development of space and for the future of the U.S. space program. Alternative shuttle prices, their relation to shuttle costs, and how alternative prices could affect the goals of the national space effort are analyzed. The costs of the shuttle system is analyzed, a set of pricing options is developed, the implications of these options for space policy objectives are explored. E.A.K.

N85-32139# Harvard Coll. Observatory, Cambridge, Mass.
THE SPACE SHUTTLE GLOW Final Report, 2 Nov. 1983 - 30 Sep. 1984
A. Dalgarno Hanscom AFB, Mass. AF Geophysics Lab. 17 Oct. 1984 40 p
(Contract F19628-84-K-0001)
(AD-A154937; AFGL-TR-84-0281) Avail: NTIS HC A03/MF A01 CSCL 22/2

Photographic pictures of the shuttle glow were analyzed. Radiative lifetime of the emitting species was found to be 0.7 msec by analyzing the spatial distribution of the glow intensity. The Atmospheric Explorer (AE) glow under daytime conditions has been examined. The glow was more intense in the daytime, but the production efficiency, measured in Rayleighs per oxygen atom, was found to be similar to the nighttime value. No dependence of the glow intensity on the ambient density was found. The production efficiency increased with time throughout the duration of the satellite in orbit. GRA

17 SPACECRAFT COMMUNICATIONS, COMMAND AND TRACKING

Includes telemetry; space communications networks; astronavigation; and radio blackout.

For related information see also *04 Aircraft Communications and Navigation* and *32 Communications.*

No abstracts in this category.

18 SPACECRAFT DESIGN, TESTING AND PERFORMANCE

Includes spacecraft thermal and environmental control; and attitude control.

For life support systems see *54 Man/System Technology and Life Support.* For related information see also *05 Aircraft Design, Testing and Performance* and *39 Structural Mechanics.*

N85-32140# Honeywell Systems and Research Center, Minneapolis, Minn.
ROBUST CONTROL OF MULTIVARIABLE AND LARGE SPACE SYSTEMS Final Report, 7 Jan. 1982 - 30 Jun. 1984
J. D. Doyle and T. B. Cunningham Mar. 1985 163 p
(Contract F49620-82-C-0090)
(AD-A155117; AFOSR-85-0473TR) Avail: NTIS HC A08/MF A01 CSCL 12/1

This report, in the form of a set of notes, details Honeywell's research results of the past year in Robust Multivariable Control Theory. These notes are made up of four major parts. Part 0 gives a review of the required notation and mathematical background. Part 1 reviews recent results on the problem of analyzing the performance and robustness properties of systems. Part 2 presents the results on synthesis which are the highlight of this report, and Part 3 outlines how the methods of the previous parts apply to control of large space structures. Author (GRA)

N85-32141# Naval Research Lab., Washington, D. C.
MAPPING WITH QUASAT (QUASAR SATELLITE) USING SHORT OBSERVATION TIMES
R. S. Simon, J. H. Spencer, and K. J. Johnston 22 May 1985 18 p
(Proj. RR0-3406)
(AD-A155155; NRL-MR-5539) Avail: NTIS HC A02/MF A01 CSCL 08/2

QUASAT (Quasar Satellite) is the name of a proposed satellite which will be an orbiting Very Long Baseline In-

terferometry (VLBI) observatory. As currently conceived, QUASAT would be a joint NASA-ESA mission to fly a 15 m diameter radio antenna, with multiple frequency capability up to 22 GHz, in an orbit with a semi-major axis of about 15000 km. The two primary motivations for QUASAT are (1) to increase the maximum angular resolution from the present VLBI network by a factor of 3, and (2) to increase the dynamic range present in VLBI maps by a factor of perhaps 10. For full details on both the scientific justification for QUASAT and the presently conceived QUASAT mission, the reader is referred to the 1984 European Space Agency's publication of the proceedings of the meeting Workshop on QUASAT, a VLBI Observatory in Space held in Austria, 18-22 June 1984. This report presents results of studies done to assess the imaging ability of QUASAT, with particular emphasis on QUASAT's capabilities with short observation times. GRA

19 SPACECRAFT INSTRUMENTATION

For related information see also *06 Aircraft Instrumentation* and *35 Instrumentation and Photography.*

N85-32142# Air Force Technical Applications Center, Patrick AFB, Fla.
RESULTS FROM RADIATION MONITORING EQUIPMENT EXPERIMENTS ON STS-41C, 41D, 41G AND 51A Final Report, 3 Feb. - 16 Nov. 1984
S. E. Cash, R. G. Madonna, M. R. McClellan, and M. E. Fields 18 Apr. 1985 98 p
(AD-A154676; AFTAC-TR-85-4) Avail: NTIS HC A05/MF A01 CSCL 18/4

The results from the Radiation Monitoring Equipment (RME) experiments, flown onboard STS-41C, 41D, 41G, and 51A are presented and discussed. The RME consists of the HRM-III gamma-ray counter and PRM neutron/proton dosimeter. The gamma-ray data agree with data from previous flights with somewhat higher readings on STS-41G. Large increases in count rates are observed when the Orbiter is in the South Atlantic and Southeast Asian Anomalies. Increases in count rate are also observed at higher latitudes. Neutron/proton dosage is consistent with NASA predictions. GRA

N85-32143# Air Force Geophysics Lab., Hanscom AFB, Mass.
FLUXGATE MAGNETOMETER (SSM) FOR THE DEFENSE METEOROLOGICAL SATELLITE PROGRAM (DMSP) BLOCK 5D-2, FLIGHT 7 Instrumentation Papers
F. J. Rich 25 Jul. 1984 30 p
(DA Proj. 231-1)
(AD-A155229; AFGL-TR-84-0225; AFGL-IP-326) Avail: NTIS HC A03/MF A01 CSCL 22/2

A triaxial fluxgate magnometer has been successfully flown on a satellite of the Defense Meteorological Satellite Program. This instrument is sensitive enough to be used for scientific studies as well as for spacecraft operations. Unlike previous scientific-quality magnetometers in space, the sensor for this instrument is not mounted on a long boom but is mounted on the outer skin of the satellite, under the thermal blanket. While magnetic signals from the spacecraft are noticeable in the data, they do not significantly degrade the quality of the data. Algorithms are now available to process the magnetic field data in a quick format. This enables a researcher to locate in the data the signature of disturbances in the Earth's magnetic field due to geophysical events. In particular, the signature of field-aligned currents associated with high-latitude phenomena such as aurora can be found in the data. Author (GRA)

20 SPACECRAFT PROPULSION AND POWER

Includes main propulsion systems and components, e.g., rocket engines; and spacecraft auxiliary power sources.

For related information see also *07 Aircraft Propulsion, 28 Propellants and Fuels,* and *44 Energy Production and Conversion.*

N85-32144 Pennsylvania State Univ., University Park.
RECESSION OF GRAPHITIC NOZZLES IN ROCKET MOTORS Ph.D. Thesis
Santoshi Tirthdas Keswani 1984 201 p
Avail: Univ. Microfilms Order No. DA8506637

A study has been conducted to develop a capability to predict recession of graphitic nozzles rocket motors. In the theoretical investigation, a model was developed based on the aerothermochemistry of the recession process. The problem was modeled as a quasi-steady, turbulent boundary-layer flow coupled through boundary conditions to the transient heat conduction process in the nozzle material. In the experimental investigation, a test rig has been designed and constructed to study the recession phenomenon of two different nozzle materials under identical flow conditions. Attempts to film the recession process were not successful since no transparent window material could withstand the high temperatures of the combustion products of aluminized propellants. The theoretical model was used to predict recession and heat transfer in different motors, for different nozzle geometries and materials. Dissert. Abstr.

N85-32145# Los Alamos National Lab., N. Mex.
CLARKE STATIONS AND MERCURIAN MASS-DRIVERS: ENERGY FOR LARGE-SCALE TRANSPORTATION SYSTEMS
E. M. Jones 1985 11 p Presented at the Conf. on Space Manufacturing, Princeton, N.J., 8 May 1985
(Contract W-7405-eng-36)
(DE85-009607; LA-UR-85-1128; CONF-8505136-1) Avail: NTIS HC A02/MF A01

The energy supply for large scale space transportation systems is described. Three-week voyages across 1 AU could be made in large sailing craft propelled by microwaves generated at power stations operating at 0.1 AU from the Sun. It is suggested that the power stations could be built of mercurian materials launched by mass driver to building sites in solar orbit. A Clarke Station 28 km in radius could generate 64 TW of microwaves and support the operation of a 1000-tonne, 1000-passenger vessel. The ability to build near-Sun power stations of mercurian materials will support high-speed transport and solar system development in general. DOE

23 CHEMISTRY AND MATERIALS (GENERAL)

Includes biochemistry and organic chemistry.

N85-32146*# National Aeronautics and Space Administration, Washington, D. C.
REMARKS ON PREPARATION OF INDANDIONE DETECTION REAGENTS
Jan Stepan and Vaclav Kral Aug. 1985 11 p refs Transl. into ENGLISH from Casopis Lekaru Ceskych (Prague), v. 92, no. 8, 1953 p 208-210 Transl. by Kanner (Leo) Associates, Redwood City, Calif.
(Contract NASw-4005)
(NASA-TM-77905; NAS 1.15:77905) Avail: NTIS HC A02/MF A01 CSCL 07C

A modified Claisen condensation with sliced sodium at a higher temperature was recommended for the production of ungranulated charcoal. A new ninhydrin production method by oxidation of benzaldiketohydrinden using available reagents was tried and was

unsuccessful. Triketohydrinden was obtained by boiling ninhydrin in acetic acid anhydrides. E.A.K.

24 COMPOSITE MATERIALS

Includes laminates.

N85-32147*# National Aeronautics and Space Administration. Marshall Space Flight Center, Huntsville, Ala.
DEVELOPMENT AND TEST OF ADVANCED COMPOSITE COMPONENTS. CENTER DIRECTORS DISCRETIONARY FUND PROGRAM
Gwyn Faile, Rose Hollis, Frank Ledbetter, Juan Maldonado, Jim Sledd, Jim Stuckey, Gerald Waggoner, and Erich Engler Jun. 1985 36 p
(NASA-TM-86512; NAS 1.15:86512) Avail: NTIS HC A03/MF A01 CSCL 11D

This report describes the design, analysis, fabrication, and test of a complex bathtub fitting. Graphite fibers in an epoxy matrix were utilized in manufacturing of 11 components representing four different design and layup concepts. Design allowables were developed for use in the final stress analysis. Strain gage measurements were taken throughout the static load test and correlation of test and analysis data were performed, yielding good understanding of the material behavior and instrumentation requirements for future applications. Author

N85-32148*# National Aeronautics and Space Administration. Lewis Research Center, Cleveland, Ohio.
GRAPHITE/PMR POLYIMIDE COMPOSITES WITH IMPROVED TOUGHNESS
Raymond D. Vannucci and Kenneth J. Bowles 1985 15 p refs Proposed for presentation at the 17th Natl. SAMPE Tech. Conf., Kiamesha Lake, N.Y., 22-24 Oct. 1985
(NASA-TM-87081; E-2661; NAS 1.15:87081) Avail: NTIS HC A02/MF A01 CSCL 11D

The toughness of composites made with modified PMR (polymerization of monomer reactants) polyimides and Celion 6000 graphite fibers was studied. Various types/levels of monomer reactants containing flexible links were incorporated into PMR resin compositions used to prepare composites. The composites were evaluated for toughness using instrumented drop weight and 10 deg off axis tensile tests at room temperature, and for strength using flexure and short beam shear tests at room temperature and at elevated temperature. The effect of resin composition on composite processability, thermo-oxidative stability, toughness and mechanical properties are discussed. Author

N85-32149*# National Aeronautics and Space Administration. Langley Research Center, Hampton, Va.
THERMAL EXPANSION OF SELECTED GRAPHITE REINFORCED POLYIMIDE-, EPOXY-, AND GLASS-MATRIX COMPOSITE
Stephen S. Tompkins Jul. 1985 20 p refs
(NASA-TM-87572; NAS 1.15:87572) Avail: NTIS HC A02/MF A01 CSCL 11D

The thermal expansion of three epoxy-matrix composites, a polyimide-matrix composite and a borosilicate glass-matrix composite, each reinforced with continuous carbon fibers, has been measured and compared. The expansion of a composite with a rubber toughened epoxy-matrix and P75S carbon fibers was very different from the expansion of two different single phase epoxy-matrix composites with P75S fibers although all three had the same stacking sequence. Reasonable agreement was obtained between measured thermal-expansion data and results from classical laminate theory. The thermal expansion of a material may change markedly as a result of thermal cycling. Microdamage, induced by 250 cycles between -156 C and 121 C in the graphite/polyimide laminate, caused a 53 percent decrease in the coefficient of thermal expansion. The thermal expansion of the graphite/glass laminate was not changed by 100 thermal cycles from -129 C to 38 C; however, a residual strain of about 10 x 10 to the minus 6 power was measured for the laminate tested. Author

N85-32150*# National Aeronautics and Space Administration. Langley Research Center, Hampton, Va.
INFLUENCE OF THE RESIN ON INTERLAMINAR MIXED-MODE FRACTURE
W. S. Johnson and P. D. Mangalgiri Jul. 1985 39 p refs
(NASA-TM-87571; NAS 1.15:87571) Avail: NTIS HC A03/MF A01 CSCL 11D

Both literature review data and new data on toughness behavior of seven matrix and adhesive systems in four types of tests were studied in order to assess the influence of the resin on interlaminar fracture. Mixed mode (i.e., various combinations of opening mode 1, G sub 1, and shearing mode 2; G sub 2) fracture toughness data showed that the mixed mode relationship for failure appears to be linear in terms of G sub 1 and G sub 2. The study further indicates that fracture of brittle resins is controlled by the G sub 1 component, and that fracture of many tough resins is controlled by total strain-energy release rate, G sub T. Regarding the relation of polymer structure and the mixed mode fracture: high mode 1 toughness requires resin dilatation; dilatation is low in unmodified epoxies at room temperature/dry conditions; dilatation is higher in plasticized epoxies, heated epoxies, and in modified epoxies; modification improves mode 2 toughness only slightly compared with mode 1 improvements. Analytical aspects of the cracked lap shear test specimen were explored. B.W.

N85-32151*# National Aeronautics and Space Administration. Langley Research Center, Hampton, Va.
COMPARISONS OF VARIOUS CONFIGURATIONS OF THE EDGE DELAMINATION TEST FOR INTERLAMINAR FRACTURE TOUGHNESS
T. Kevin OBrien, N. J. Johnston, I. S. Raju, D. H. Morris, and R. A. Simonds Jul. 1985 50 p refs Prepared in cooperation with Army Research and Technology Labs., Fort Eustis, Va.
(DA Proj. 1L1-61102-AH-45)
(NASA-TM-86433; NAS 1.15:86433; USAAVSCOM-TM-85-B-3) Avail: NTIS HC A03/MF A01 CSCL 11D

Various configurations of Edge Delamination Tension (EDT) test specimens, of both brittle (T300/5208) and toughened-matrix (T300/BP907) graphite reinforced composite laminates, were manufactured and tested. The mixed-mode interlaminar fracture toughness, G sub C, was measured using (30/30 sub 2/30/90 sub N)sub s, n=1 or 2, (35/-35/0/90) sub s and (35/0/-35/90) sub s layups designed to delaminate at low tensile strains. Laminates were made without inserts so that delaminations would form naturally between the central 90 deg plies and the adjacent angle plies. Laminates were also made with Teflon inserts implanted between the 90 deg plies and the adjacent angle (theta) plies at the straight edge to obtain a planar fracture surface. In addition, interlaminar tension fracture toughness, Glc, was measured from laminates with the same layup but with inserts in the midplane, between the central 90 deg plies, at the straight edge. All of the EDT configurations were useful for ranking the delamination resistance of composites with different matrix resins. Furthermore, the variety of layups and configurations available yield interlaminar fracture toughness measurements needed to generate delamination failure criteria. The influence of insert thickness and location, and coupon size on G sub c values were evaluated. B.W.

N85-32152# Dayton Univ., Ohio.
IMPROVED MATERIALS FOR COMPOSITES AND ADHESIVE JOINTS Final Report, 1 Sep. 1983 - 31 Aug. 1984
R. Servais, D. Anderson, H. Chai, W. Click, and J. Hartness Wright-Patterson AFB, Ohio AFWAL Dec. 1984 284 p
(Contract F33615-81-C-5056)
(AD-A154918; UDR-TR-84-134; AFWAL-TR-84-4189) Avail: NTIS HC A13/MF A01 CSCL 11/4

This report presents a summary of the work performed by the University of Dayton Research Institute during the period 1 Sept. 1983 through 31 Aug. 1984. Research was conducted in the

following areas: processing and evaluation of composites, adhesive-bonded joints, interface/interphase characterization, and mechanics of composites and adhesive-bonded joints.
Author (GRA)

N85-32153# Dayton Univ., Ohio.
IMPROVED MATERIALS FOR COMPOSITE AND ADHESIVE JOINTS Annual Report, 1 Sep. 1982 - 31 Aug. 1983
R. Kim, W. Click, J. Hartness, M. Koenig, and M. Rich Wright-Patterson AFB, Ohio AFWAL Jul. 1984 161 p
(Contract F33615-81-C-5056)
(AD-A155065; UDR-TR-83-117; AFWAL-TR-84-4074) Avail: NTIS HC A08/MF A01 CSCL 11/4

This report presents a summary of research conducted in the following areas: Processing and Evaluation of Composites, Adhesive Bonded Joints, Interface/Interphase Characterization, and Mechanics of Composites and Adhesive Bonded Joints.
Author (GRA)

N85-32154# Jortner Research and Engineering, Inc., Costa Mesa, Calif.
EFFECTS OF WEAK INTERFACES ON THERMOSTRUCTURAL BEHAVIOR OF CARBON-CARBON COMPOSITES Annual Report, 1 Dec. 1984 - 31 Mar. 1985
J. Jortner 31 Mar. 1985 59 p
(Contract N00014-82-C-0405)
(AD-A155330; JR/E-8526) Avail: NTIS HC A04/MF A01 CSCL 11/4

Continuing research into mechanical and thermal behavior of carbon-carbon composites is described. Results presented include a theory for tensile fracture of yarn-bundles in which the fiber-matrix interface is weak, a minimechanical shear-lag analysis of thermal expansion of 3D carbon-carbons showing that interconstituent slippage has large effects on thermal expansion test data, a discussion of the role of radial yarns during heat treatment of cylindrical 3D billets, and an initial analysis of the effects on constitutive behavior of strain-induced microscale rotations of fibers. GRA

N85-32155# Ohio State Univ., Columbus.
EXPERIMENTAL AND THEORETICAL ASSESSMENT OF A NEW TECHNIQUE FOR THE NON-DESTRUCTIVE EVALUATION OF LAMINATED PANELS Final Report, 18 Feb. 1982 - 30 Jun. 1984
V. H. Kenner 21 Feb. 1985 90 p
(Contract F33615-82-K-5009)
(AD-A155622; AFWAL-TR-84-4129) Avail: NTIS HC A05/MF A01 CSCL 11/4

The goal of the present research project was to evaluate a potential method of edge flaw detection in laminated structures. This method uses miniature dynamic force transducers to detect the changes in loading history arising from the (very low level) impact of steel spheres on the transducer, which is located on the surface of the examined object. A theoretical and experimental analysis of the low frequency vibration response of bonded joints showed that it is possible to distinguish between mechanically sound and debonded specimen using a low frequency analysis. This analysis has shown that it is possible to construct a field-usable instrument that would permit rapid inspection of bonded structures for degrading conditions that occur at the edges of bonded joints. This analysis is applicable to both composite and metal laminated structures. GRA

25 INORGANIC AND PHYSICAL CHEMISTRY

Includes chemical analysis, e.g., chromatography; combustion theory; electrochemistry; and photochemistry.

For related information see also *77 Thermodynamics and Statistical Physics.*

N85-32156*# National Aeronautics and Space Administration. Lewis Research Center, Cleveland, Ohio.
SHOCK TUBE MEASUREMENTS OF GROWTH CONSTANTS IN THE BRANCHED-CHAIN ETHANE-CARBON MONOXIDE-OXYGEN SYSTEM
Richard S. Brokaw, Theodore A. Brabbs, and Christopher A. Snyder Jul. 1985 15 p refs
(NASA-TM-87068; E-2574; NAS 1.15:87068) Avail: NTIS HC A02/MF A01 CSCL 07D

Exponential free radical growth constants have been measured for ethane carbon monoxide oxygen mixtures by monitoring the growth of oxygen atom concentration as manifested by CO flame band emission. Data were obtained over the temperature range of 1200 to 1700 K. The data were analyzed using an ethane oxidation mechanism involving seven elementary reaction steps. Calculated growth constants were close to experimental values at lower temperatures, up to about 1400 K, but at higher temperatures computed growth constants were considerably smaller than experiment. In attempts to explain these results additional branching reactions were added to the mechanism. However, these additional reactions did not appreciably change calculated growth constants.
Author

N85-32157# Carnegie-Mellon Univ., Pittsburgh, Pa. Dept. of Mechanical Engineering.
LARGE EDDY STRUCTURES IN TRANSITIONAL AND TURBULENT FLAMES Annual Report, 1 Jul. 1983 - 30 Jun. 1984
N. Chigier Jul. 1984 18 p
(Grant AF-AFOSR-0266-82)
(AD-A154520; AFOSR-85-0379TR) Avail: NTIS HC A02/MF A01 CSCL 21/2

A second generation experimental apparatus has been designed and constructed to provide a uniform co-flowing air stream with no physical enclosure around the flame. A new seeding system has been acquired that provides large quantities of small seeded particles in the secondary air to avoid bias in velocity measurements by LDV (Laser Doppler Velocimetry). More flame height measurements have been made which do no agree with the classical Hawthorne-Hotel data. The LDV electronics processing data acquisition and software systems have all been debugged, calibrated and made ready for measurements with sampling times of 150 KHz. Ionization and thermocouple probes have been designed and are under construction. Preliminary color schlieren photographs using rainbow schlieren have been made.
GRA

N85-32158# Air Force Inst. of Tech., Wright-Patterson AFB, Ohio.
CALCULATION OF MOLECULAR CONSTANTS POTENTIAL ENERGY CURVES AND FRANCK-CONDON FACTORS FOR LEAD OXIDE Summary Report
E. A. Dorko Apr. 1985 75 p
(AD-A154521; AU-AFIT-EN-TR-85-1) Avail: NTIS HC A04/MF A01 CSCL 07/4

This paper deals with the preparation of potential energy curves and Franck-Condon factors for diatomic molecules specifically lead oxide. The starting point for the calculations is the spectroscopic data which can include observations of transitions between rotational, vibrational, and electronic states. Once the data is gathered it can be used to calculate Dunham type coefficients or molecular constants, From these constants the potential energy curve can be calculated by an RKR analysis. From analysis (IPA)the wave functions can be calculated. Finally, Franck-Condon factors can be calculated. Calculations are presented for the diatomic molecule, lead oxide (PBO). GRA

N85-32159# Minnesota Univ., Minneapolis. Dept. of Mechanical Engineering.
HIGH TEMPERATURE SOLAR ELECTROTHERMAL PROCESSING 2. ZINC FROM ZINC OXIDE Interim Report
E. A. Fletcher, F. J. Macdonald, and D. Kunnerth 3 May 1985 42 p
(Contract N00014-82-K-0523)

(AD-A154747; TR-6) Avail: NTIS HC A03/MF A01 CSCL 07/4

The electrolytic decomposition potential of ZnO was studied in a solar furnace in the temperature range 600 to 1400K and in three electrolytes (NaOH, 0.33ZnF2-0.67NaF, and 0.13AlF3(-) 0.87NaF). From 600 to 1200K, the measured potentials were close to the thermodynamically predicted values for the reaction ZnO(s) yield Zn (stable phase) + 0.5O2(g), if provision is made for reasonable overvoltages. The overvoltages decreased with increasing temperature. In the range 1200 to 1400K, the direct chemical reaction of ZnO with the graphite cathode resulted in the formation of a gas film in a process analogous to a transition from nucleate to film boiling, which greatly decreased the current. Various materials were tested for use as electrodes and cell casings. Their behavior, experimental problems and methods for dealing with them, as well as the apparatus, are described and discussed. GRA

N85-32160# Air Force Office of Scientific Research, Bolling AFB, Washington, D.C.

STATUS OF BORON COMBUSTION RESEARCH

G. M. Faeth Oct. 1984 145 p

(AF Proj. 2308)

(AD-A154762; AFOSR-85-0466TR) Avail: NTIS HC A07/MF A01 CSCL 21/2

This report describes the proceedings of an AFOSR sponsored Specialists Meeting on Boron Combustion. The objectives of the meeting were to review current understanding and to recommend fundamental research needs concerning boron combustion. Combustion of both slurries and solid propellants containing boron was considered for airbreathing propulsion applications. Boron can provide more than twice the volumetric energy density of conventional hydrocarbon fuels for airbreathing propulsion systems - substantially improving the performance of volume-limited vehicles. Realizing this potential, however, has been difficult. Problems have been encountered in achieving adequate ignition, flame stability and combustion efficiency in practical sized combustors. There is also evidence of energy trapping by combustion product vapors during energy conversion to generate propulsive forces, which reduces system performance. Both of these problems become more acute at low combustion chamber pressures which are associated with high altitude operation. Several research problems were suggested in order to help resolve these difficulties. GRA

N85-32161# Minnesota Univ., Minneapolis. Dept. of Chemical Engineering and Materials Science.

INTERFACE CHEMISTRY OF Hg(1-x)Cd(x)Te Interim Report

P. Philip, A. Franciosi, and D. J. Peterman 8 May 1985 15 p

Prepared in cooperation with McDonnell Douglas Research Labs., St. Louis, MO

(Contract N00014-84-K-0545)

(AD-A154876; IR-2) Avail: NTIS HC A02/MF A01 CSCL 07/4

We present preliminary studies of temperature formation of the Hg1-xCdxTe(110)-Cr interface. For Cr coverages below 2A, Cr atoms replace Hg atoms in a 10-13 A thick semiconductor layer while elemental Te is released at the surface. The typical high coverage interface morphology consists of an elemental Te surface, a metallic Cr film, a Hg-depleted subsurface layer where Cr is bonded to Te, and finally the ternary semiconductor bulk. This complex interface chemistry is compared with recent results for Hg1-xCdxTe interfaces with simple and noble metals. GRA

N85-32162# Emory Univ., Atlanta, Ga. Dept. of Chemistry.

MULTIDIMENSIONAL LUMINESCENCE MEASUREMENTS Interim Report

I. M. Warner, G. Patonay, and M. Thomas 30 Apr. 1985 42 p

(Contract N00014-83-K-0026)

(AD-A154950; EMORY/DC/TR/4) Avail: NTIS HC A03/MF A01 CSCL 07/4

Luminescence spectroscopy has long been recognized as a tool for the quantititive and qualitative identification of a wide range of molecular systems. However, the resolving power of these techniques is often limited for similar compounds because absorption and emission peaks are typically broad banded and leads to overlapping spectra. To increase the resolving power of luminescence studies, recent studies have used multidimensional luminescence measurements (MLM) (use of two or more parameters of luminescence) to increase selectivity. Complex mixtures may be analyzed by rapidly acquiring fluorescence data as a function of multiple excitation and emission wavelengths. Advances in instrumentation and data reduction strategies allow the discrimination of mixtures in overlapping spectra by capitalizing on differences in fluorescence lifetime or fluorescence depolarization measurements. Fluorescence detected circular dichroism (FDCD) has been used to resolve optically active fluorescent compounds. Additionally, luminescence measurements may be combined with a range of measurements such as quenchometry and chromatography to yield very selective determinations. GRA

N85-32163# Chemical Research and Development Center, Aberdeen Proving Ground, Md.

PHASE BEHAVIOR AND QLS (QUASIELASTIC LIGHT SCATTERING) IN POTASSIUM LINOLEATE/N-ALKANOL MICROEMULSIONS Technical Report, Sep. 1983 - Jan. 1984

R. A. Mackay and R. P. Seiders Mar. 1985 20 p

(DA Proj. 1L1-61102-A-71-A)

(AD-A155028; CRDC-TR-84089) Avail: NTIS HC A02/MF A01 CSCL 07/4

We present here pseudo-ternary phase maps on three surfactant stabilized quaternary systems composed of water, hexadecane, and potassium linoleate (KL) as surfactant and the three saturated primary alcohols, 1-butanol, 1-pentanol, and 1-hexanol as cosurfactants. These systems exhibit phase behavior analogous to that of the potassium oleate/n-alkanol systems recently reported. Butanol gives a system with one large single-phase region extending from the water side to the oil side of the diagram. Pentanol yields two areas of single phase, a large upper water in oil (w/o) region and a smaller finger-like oil in water (o/w) region arcing up from the water apex to ca 20% emulsifier. The hexanol system reveals the largest expanse of the w/o region, but in the water-continuous corner only a metastable clear area was encountered. Quasielastic Light Scattering (QLS) measurements are also reported in all three systems, and an attempt is made to correlate these measurements to the phase behavior. The butanol system gave no QLS evidence of aggregation at three different compositions. The pentanol and hexanol system gave diffusion coefficients that suggest the existence of aggregates with corrrelation lengths in the 100- to 700-A range. In general, diffusion coefficients for the hexanol system were smaller than those at comparable compositions in the pentanol system. GRA

N85-32164# Army Natick Research and Development Command, Mass.

FEASIBILITY STUDY FOR SMALL GROUP WATER DESALINATION EQUIPMENT Final Report, Feb. - Aug. 1984

M. Holtzapple, A. Allen, and M. Rogers Aug. 1984 107 p

(DA Proj. 1L1-62724-AH-99)

(AD-A155106; NATICK/TR-85/042) Avail: NTIS HC A06/MF A01 CSCL 13/2

The ability for samll groups of soldiers to desalinate brackish or sea water will reduce their dependence on supply lines. Ten desalination options were reviewed for effectiveness in nine scenarios. Each option was rated according to a number of factors such as energy consumption, water recovery, logistics concerns, weight, and simplicity. The importance of each of these factors depended on the scenario being considered. These options included simple distillation, singlepass membrane distillation, multiplepass membrane distillation, multiple effect evaporation, heat pumps, vapor-compression, reverse osmosis without energy recovery, reverse osmosis with energy recovery, electrodialysis and ion exchange. The nine scenarios include: using waste heat from vehicles, using power take-off from vehicles, using a trailer mounted unit performing desalination on the move or in a fixed location, stowing a small desalination unit in vehicles to be used when needed, using waste heat at a fixed location, using a dedicated power source for a desalination unit at a fixed location, using waste heat from a microclimate cooling unit, and having a

soldier carry the desalination unit. From this analysis, it was determined that simple distillation, membrane distillation, reverse osmosis, and vapor-compression were viable options. GRA

N85-32165# Rocketdyne, Canoga Park, Calif.
BASIC RESEARCH IN NOVEL INORGANIC REAGENTS AND FLUOROCARBON CHEMISTRY Final Report, 4 Mar. 1981 - 30 Sep. 1984
C. J. Schack and K. O. Christe Feb. 1985 130 p
(Contract F49620-81-C-0020)
(AD-A155340; RI/RD85-121; AFOSR-85-0462TR) Avail: NTIS HC A07/MF A01 CSCL 07/3

A 44-month program was conducted on the preparation of dense, thermally stable fluorocarbon derivatives. The technical approach employed was the interaction of inorganic TeF5O- and SeF5O- reactants and selected fluorocarbons. Improved or innovative preparative methods were developed for the requisite inorganic reagents. Substitution-type reactions led to the formation of mono-substituted fluorocarbon derivatives, whereas bis-substituted products were obtained via addition of the inorganic groups to unsaturated fluoroolefins. Spectroscopic characterization of the synthesized compounds was employed to identify their molecular structures. The new compounds were shown to be thermally stable, and possessing densities only slightly less than the analogous iodo-substituted fluorocarbons. GRA

N85-32166# California Univ., Santa Barbara.
DESIGN OF MICELLES AS DEPHOSPHORYLATING AGENTS Final Report, 1 Sep. 1981 - 31 Aug. 1984
C. A. Bunton 6 May 1985 5 p
(Contract DAAG29-81-K-0122)
(AD-A155589; ARO-18290.12-CH) Avail: NTIS HC A02/MF A01 CSCL 07/3

The factors which control effects of selfassembling colloids upon desphosphorylation and the spontaneous hydrolysis of Mustard simulants have been examined. The colloids are aqueous micelles, alcohol-swollen micelles or microemulsions and aggregates of hydrophobic ammonium ions. The nucleophiles studied include hydroxide ion, alkoxide and aryloxide ions, peroxyanions, oximate and amidoximate ions, and hydroxamate and imidazolide ions. p-Nitrophenyl diphenyl phosphate was generally the substrate, although spontaneous hydrolysis of 2, 4-dinitrophenyl phosphate dianion was also examined. The nonfunctional surfactants were generally C16H33N+Me3X- where X = Br, Cl, MeSO3 or OH. The effects of functional groups, hydroxyethyl, oximate and hydroxamate were also examined. For all the bimolecular reactions studied rate enhancements by the colloidal species were due largely to increased reactant concentrations in the small colloidal particles. For spontaneous hydrolyses of 2, 4-dinitrophenyl phosphate and the Mustard simulant the medium effect of the colloidal particle was all important. GRA

N85-32167# Ballistic Research Labs., Aberdeen Proving Ground, Md.
IMBEDDED THERMOCOUPLES AS A SOLID PROPELLANT COMBUSTION PROBE Final Report
M. S. Miller, T. P. Coffee, and A. J. Kotlar Apr. 1985 41 p
(DA Proj. 1L1-61102-AH-43)
(AD-A155630; AD-F300620; BRL-MR-3440) Avail: NTIS HC A03/MF A01 CSCL 21/2

Recent work has shown the feasibility of using combustion zone temperature profiles to obtain overall reaction kinetics for heat release in that zone. Such a procedure gives new motivation to the old interest in measuring temperature profiles through the combustion wave of solid propellants. The only method presently capable of providing a continuous temperature profile from deep within the solid through the dark zone is the imbedded thermocouple technique. A comprehensive review of this technique was, therefore, undertaken in order to evaluate sources of error involved and to make an assessment of the potential for success in deriving overall kinetics from such a measurement. The results of this review along with original calculations of condensed phase response errors are reported herein. GRA

N85-32168# Yale Univ., New Haven, Conn. Dept. of Chemical Engineering.
AEROSOL ANALYSIS AND EMISSION SPECTROMETRY WITH FREE JETS Final Report
J. B. Fenn 31 Jan. 1985 56 p
(Contract DE-FG01-78ET-11384)
(DE85-010576; DOE/ET-11384/T1) Avail: NTIS HC A04/MF A01

The possibilities of using small supersonic free jets in vacuo for two applications in fossil fuel technology was explored. In one, the jet was used as a means of accelerating aerosol particles to impinge upon a transducer whose output signal would be proportional to the momentum and therefore the mass of the particle. The other was to take advantage of rotational cooling along with the absence of vibrational relaxation during the expansion and thus to analyze for trace constituents in flue gas by means of infrared spectrometry. Some progress was made, but more important results were embodied in a novel Electrospray Ion Source for mass spectrometric analysis of complex organic species, a new insight on the energy distribution in molecules undergoing elastic and inelastic scattering by surfaces. Advances were made in the development of computational methods for describing the interaction between evaporating and/or burning particles in the combustion of sprays and clouds. DOE

N85-32169# California Univ., Livermore. Lawrence Livermore Lab.
FACILITY FOR LARGE-SCALE HAZARDOUS GAS TESTING
R. P. Koopman Apr. 1985 30 p Presented at the Chlorine Inst. Chlorine Plant Operations Seminar, Houston, TX, 13 Feb. 1985
(Contract W-7405-eng-48)
(DE85-011852; UCRL-92602; CONF-850282-1) Avail: NTIS HC A03/MF A01

Design basis factors for both the facility and the spill tests are presented. Spill test results for two recent testing series are given for N2O4 and NH3. The data acquisition system includes measurements on atmospheric boundary layer, wind field, vapor cloud temperature and concentration, and surface heat flux measurements in addition to the spill area. DOE

N85-32170# GA Technologies, Inc., San Diego, Calif.
DECOMPOSITION OF SULFURIC ACID USING SOLAR THERMAL ENERGY
Feb. 1985 169 p
(Contract DE-AT03-82SF-11666)
(DE85-012288; GA-A-17573) Avail: NTIS HC A08/MF A01

A high temperature solar powered catalytic metallic reactor was built and tested as a first step in determining the potential applicability of metallic reactors to the Solar Fuels and Chemical Program. The temperature range of interest, 700 to 1000 C, provides a serious test of the capability thermal stresses. Without practical metallic reactors, we will have to await scientific and engineering breakthroughs in the fields of ceramics and structural design of brittle materials before ceramic heat exchangers become practical. The tests also provided the first opportunity to demonstrate a working catalytic chemical reactor on a solar power tower using engineering materials. The chemical reaction chosen for study was sulfuric acid decomposition, the key high temperature step to thermochemical production of hydrogen from water. This is a very clean reaction with no side reactions producing extraneous products; thus, the results may easily be extrapolated to the design of solar powered catalytic reactors for other fuels and chemical processes. The overall program was very successful in that all major test objectives were met. The sulfuric acid decomposition reaction went essentially to completion as predicted. The selected materials of construction, Incoloy 800H, Hastelloy C-276, and Inconel 825, performed satisfactorily. The temperature inside the cavity was very uniform and well within predicted values. No unacceptable corrosion was observed. The solar driven chemical reactor, located on top of the solar power tower, could be operated and controlled from the ground. The results of the test indicate that continued development of this concept is warranted. The next step in the development of high temperature metallic reactors is

the demonstration of such a system at higher pressures and solar flux levels. DOE

N85-32171# Mound Lab., Miamisburg, Ohio.
ELECTROCHEMISTRY OF HEXANITROAZOBENZENE (HNAB)
D. W. Firsich 1985 4 p refs Presented at the ADPA Meeting, Hilton Head, S. C., 11 Mar. 1985
(Contract DE-AC04-76DP-00053)
(DE85-010807; MLM-3238(CP); CONF-8503100-3) Avail: NTIS HC A02/MF A01

The electrochemical properties of hexanitroazobenzene (HNAB) are explored, including the characterization of its anion, dianion, protonated dianion and diprotonated dianion by cyclic voltammetry, controlled potential coulometry, and visible spectroscopy. The acid/base relationships of these species are defined. The chemistry demonstrated is shown to be useful in exploring the reactivity of HNAB with common metals, and is relevant to the synthesis of HNAB. DOE

N85-32952# Joint Publications Research Service, Arlington, Va.
CORRELATION OF INTENSITIES OF DIFFERENT SCATTERING CHANNELS Abstract Only
S. M. Burkitbayev, V. P. Kushnir, and E. A. Manykin *In its* USSR Rept.: Phys. and Math. (JPRS-UPM-85-004) 17 Jun. 1985 p 76 Transl. into ENGLISH from Dokl. Akad. Nauk SSSR, v. 279, no. 2, Nov. 1984 p 338-339 (For primary document see N85-32860 21-70)
Avail: NTIS HC A06/MF A01

26 METALLIC MATERIALS

Includes physical, chemical, and mechanical properties of metals, e.g., corrosion; and metallurgy.

N85-32172*# Cryo Support Services, Inc., New Castle, Del.
A SYSTEMATIC PLAN FOR THE CONTINUED STUDY OF DIMENSIONAL STABILITY OF METALLIC ALLOYS CONSIDERED FOR THE FABRICATION OF CRYOGENIC WIND TUNNEL MODELS
D. A. Wigley Jun. 1985 19 p refs Prepared for Kentron International, Inc.
(Contract NAS1-16000)
(NASA-CR-172449; NAS 1.26:172449) Avail: NTIS HC A02/MF A01 CSCL 11F

Interrelated research and development activities, phased development of stepped specimen program are documented and a sequence for a specific program of machining, validation and heat treatment cycles for one material are described. Proposed work for the next phase of dimensional stability research is presented and further technology development activities are proposed. E.A.K.

N85-32173*# Case Western Reserve Univ., Cleveland, Ohio. Dept. of Chemistry.
WHY CO BONDS SIDE-ON AT LOW COVERAGE AND BOTH SIDE-ON AND UPRIGHT AT HIGH COVERAGE ON THE Cr(110) SURFACE
S. P. Mehandru and Alfred B. Anderson [1985] 16 p refs
(Grant NAG3-341)
(NASA-CR-176071; NAS 1.26:176071) Avail: NTIS HC A02/MF A01 CSCL 11F

An atom superposition and electron delocalization molecular orbital study of CO adsorption on the Cr(110) surface shows a high coordinate lying down orientation is favored. This is a result of the large number of empty d-band energy levels in chromium, which allows the antibonding counterparts to sigma and pi donation bonds to the surface to be empty. When lying down, backbonding to CO pi sup * orbitals is enhanced. Repulsive interactions cause additional CO to stand upright at < 1/4 monolyer coverage. The results confirm the recent experimental study of Shinn and Madey. Author

N85-32174*# Case Western Reserve Univ., Cleveland, Ohio. Dept. of Chemistry.
MOLECULAR ORBITAL STUDIES IN OXIDATION: SULFATE FORMATION AND METAL-METAL OXIDE ADHESION Final Report, 30 Oct. 1982 - 31 Jul. 1985
Alfred B. Anderson 31 Jul. 1985 5 p refs
(Grant NAG3-341)
(NASA-CR-176070; NAS 1.26:176070) Avail: NTIS HC A02/MF A01 CSCL 11F

The chemical mechanisms for sulfate formation from sodium chloride and sulfur trioxide, which is a product of jet fuel combustion was determined. Molten sodium sulfate leads to hot corrosion of the protective oxide layers on turbine blades. How yttrium dopants in nidkel-aluminum alloys used in turbine blades reduce the spalling rate of protective alumina films and enhance their adhesion was also determined. Two other fulfate mechanisms were deduced and structure of carbon monoxide on a clean chronium and clean platinum-titanium alloys surfaces was determined. All studies were by use of the atom superposition and electron delocalization molecular orbital (ASED-MO) theory. Seven studies were completed. Their titles and abstracts are given. Author

N85-32175*# Case Western Reserve Univ., Cleveland, Ohio. Dept. of Chemistry.
ADSORPTION OF O2, SO2, AND SO3 ON NICKEL OXIDE. MECHANISM FOR SULFATE FORMATION
S. P. Mehandru (Delhi Univ., India) and Alfred B. Anderson [1985] 28 p refs
(Grant NAG3-341)
(NASA-CR-176072; NAS 1.26:176072) Avail: NTIS HC A03/MF A01 CSCL 11F

Calculations based on the atom superposition and electron delocalization molecular orbital (ASED-MO) technique suggest that O2 will adsorb perferentially end-on at an angle 45 deg from normal on a nickel cation site on the (100) surface of NiO. SO2 adsorption is also stronger on the nickel site; SO2 bonds through the sulfur atom is a plane perpendicular to the surface. Adsorption energies for SO3 on the nickel and oxygen sites are comparable in the perferred orientation in which the SO3 plane is parallel to the surface. On activation, SO3 adsorbed to an O2(-) site forms a trigonal pyramidal SO4 species which yields, with a low barrier, a tetrahedral sulfate anion. Subsequently the anion reorients on the surface. Possibilities for alternative mechanisms which require the formation of Ni3(+) or O2(-) are discussed. NiSO4 thus formed leads to the corrosion of Ni at high temperatures in the SO2+O2/SO3 The SO2+O2/SO3 atmosphere, as discussed in the experimental literature. Author

N85-32176*# Case Western Reserve Univ., Cleveland, Ohio. Dept. of Chemistry.
CO ADSORPTION ON (111) AND (100) SURFACES OF THE Pt SUB 3 Ti ALLOY. EVIDENCE FOR PARALLEL BINDING AND STRONG ACTIVATION OF CO
S. P. Mehandru, Alfred B. Anderson, and P. N. Ross (California Univ., Lawrence Berkeley Lab.) [1985] 25 p refs
(Grant NAG3-341; Contract DE-AC03-76SF-00098)
(NASA-CR-176077; NAS 1.26:176077) Avail: NTIS HC A02/MF A01 CSCL 11F

The CO adsorption on a 40 atom cluster model of the (111) surface and a 36 atom cluster model of the (100) surface of the Pt3Ti alloy was studied. Parallel binding to high coordinate sites associated with Ti and low CO bond scission barriers are predicted for both surfaces. The binding of CO to Pt sites occurs in an upright orientation. These orientations are a consequence of the nature of the CO pi donation interactions with the surface. On the Ti sites the orbitals donate to the nearly empty Ti 3d band and the antibonding counterpart orbitals are empty. On the Pt sites, however, they are in the filled Pt 5d region of the alloy band, which causes CO to bond in a vertical orientation by 5 delta donation from the carbon end. E.A.K.

N85-32177*# Kentron International, Inc., Hampton, Va.
MACHINING-INDUCED DEFORMATION IN STEPPED

SPECIMENS OF PH 13-8 Mo, 18 NICKEL MARAGING STEEL GRADE 200T1 AND GRAIN-REFINED HP 9-4-20
D. A. Wigley Jun. 1985 34 p refs Prepared in cooperation with Cryo Support Services, Inc., New Castle, Del.
(Contract NAS1-16000)
(NASA-CR-172450; NAS 1.26:172450) Avail: NTIS HC A03/MF A01 CSCL 11F

The results of a study to evaluate the dimensional changes created during machining and subsequent cycling to cryogenic temperatures for three different metallic alloys are presented. Experimental techniques are described and results presented for 18 Ni Grade 200 maraging steel, PH-13-8 Mo stainless steel, and Grain-refined HP 9-4-20. Author

N85-32178*# General Electric Co., Huntsville, Ala. Space Systems Div.
MPS SOLIDIFICATION MODEL. ANALYSIS AND CALCULATION OF MACROSEGREGATION IN A CASTING INGOT Final Report
David R. Poirier (Arizona Univ.) and Anna L. Maples May 1985 79 p refs
(Contract NAS8-36039)
(NASA-CR-171589; NAS 1.26:171589; Doc-85HV002) Avail: NTIS HC A05/MF A01 CSCL 11F

Work performed on several existing solidification models for which computer codes and documentation were developed is presented. The models describe the solidification of alloys in which there is a time varying zone of coexisting solid and liquid phases; i.e., the S/L zone. The primary purpose of the models is to calculate macrosegregation in a casting or ingot which results from flow of interdendritic liquid in this S/L zone during solidification. The flow, driven by solidification contractions and by gravity acting on density gradients in the interdendritic liquid, is modeled as flow through a porous medium. In Model 1, the steady state model, the heat flow characteristics are those of steady state solidification; i.e., the S/L zone is of constant width and it moves at a constant velocity relative to the mold. In Model 2, the unsteady state model, the width and rate of movement of the S/L zone are allowed to vary with time as it moves through the ingot. Each of these models exists in two versions. Models 1 and 2 are applicable to binary alloys; models 1M and 2M are applicable to multicomponent alloys. Author

N85-32179# Belgian Center for Corrosion Study, Brussels.
UNDERSTANDING AND LABORATORY PREDICTION OF THE ATMOSPHERIC CORROSION BEHAVIOR OF STEELS AND OF NON-FERROUS METALS AND ALLOYS Annual Report
M. Pourbaix 31 Jan. 1984 42 p
(Contract DAJA45-83-C-0011)
(AD-A154642) Avail: NTIS HC A03/MF A01 CSCL 11/6

The work during the second semi-annual period was essentially devoted to aluminum alloys. Accelerated tests were performed on Al-Mn, Al-Cu-Mg, Al-Zn-Cu-Mg and on 7075-T73 clad with Al-Zn, in a typical marine simulated atmosphere and in a typical industrial simulated atmosphere. The results were obtained as electrode potentials during wet periods versus time, weight loss and corrosion penetration versus time and corrosion morphology. The results were analyzed to see if there is a relationship between the values of the electrode potentials and the type and magnitude of corrosion during the accelerated test on hand, and for a comparison between the results of the accelerated tests and known behaviors of these materials in well defined natural exposure conditions, on another hand. It is hoped that, as a result of this, characteristic atmospheric condition can be simulated by accelerated laboratory tests and that these laboratory tests can provide indications on the type of corrosion and the corrosion magnitude in these natural conditions, and will allow a quick selection of materials for given exposure conditions. Limited series of electrode potentials measurements were made on samples exposed to natural conditions, in an attempt to improve our understanding of the correlation between accelerated and natural tests. GRA

N85-32180# Portland State Univ., Oreg.
ELECTRODEPOSITION OF CHROMIUM AND COPPER IN MAGNETIC FIELDS Final Report, 1 Jul. 1981 - 31 Dec. 1984
J. Dash Feb. 1985 7 p
(Contract DAAG29-81-C-0027)
(AD-A154648; ARO-15104.14-MS) Avail: NTIS HC A02/MF A01 CSCL 13/8

Our previous research had demonstrated several significant effects caused by the application of magnetic fields during electrolytic thinning and electrodeposition of metals. The purpose of the research supported by this contract was to continue studies of these effects. We sought to determine what applied magnetic field strength and other parameters of electrolysis would maximize the following effects: (1) improvement in the uniformity of both anode and cathode processes; (2) increase in the speed of electrodeposition; and (3) inhibition of hydrogen gas formation during electrodeposition. An additional goal of this research was to determine effects of magnetic fields on the properties of metallic deposits. GRA

N85-32181# Air Force Inst. of Tech., Wright-Patterson AFB, Ohio. School of Engineering.
THE EFFECT OF STRESS AND HOT CORROSION ON NICKEL-BASE SUPERALLOYS M.S. Thesis
S. J. Balsone Mar. 1985 118 p
(AF Proj. 2302)
(AD-A154722; AFIT/GAE/AA/85M-1) Avail: NTIS HC A06/MF A01 CSCL 11/6

This Thesis examines the effect of a molten salt environment on high temperature creep properties of Inconel 718. Sustained-load creep tests were conducted at 1472 F in laboratory air at stress levels in the range of 10 Ksi to 30 Ksi. Round bar tensile specimens were coated with a 90% Na2SO4/10% NaCl salt mixture by spraying a heated specimen with an aqueous salt solution. Creep data were collected over a 72 hour test period. Salt coated specimens were compared with uncoated specimens. Specimens were sectioned and mounted, and a metallographic analysis of the corrosion attack was conducted. Degradation of high temperature creep properties of Inconel 718 in the presence of molten salt is due primarily to oxide penetration into metal which has been depleted of alloying elements and to subsequent cracking along oxide-metal interfaces. Grain boundary sliding and void formation along the grain boundaries also occurred in the alloy-depleted zone of corrosion attack. In static hot corrosion tests on specimens of Rene 77 and Rene 80, cylindrical pins were salt coated and tested for 72 hours at 1652 F in laboratory air. Weight-change calculations and measurements of the depth of corrosion attack were made, and a metallographic analysis was done. GRA

N85-32182# Royal Aircraft Establishment, Farnborough (England).
THE EFFECT OF ABRASIVE BLASTING ON THE FATIGUE AND CORROSION OF AN ALUMINIUM-COPPER ALLOY
C. J. E. Smith and M. A. H. Hewins Aug. 1984 24 p
(AD-A154954; RAE-TR-84082; DRIC-BR-94938) Avail: NTIS HC A02/MF A01 CSCL 11/6

Rotating bending fatigue tests have established that glass bead and alumina grit blasting have only a slight effect on the fatigue properties of 2014-T6 aluminium alloy. Exposure to salt fog for 8 hours or alternate immersion in 3 1/2% salt solution for 3 days reduces the fatigue strength from 170 MPa to 107 MPa and 46 MPa respectively but substantial improvements in fatigue strength may be achieved by abrasive blast cleaning to remove the corrosion. Total immersion tests made in 3 1/2% salt solution to examine the effects of abrasive blasting on corrosion have demonstrated that the corrosion rate and type of pitting attack on 2014-T6 aluminium alloy sheet are dependent on the abrasive used and on the amount of corrosion which has occurred prior to blast cleaning. GRA

N85-32183# Naval Postgraduate School, Monterey, Calif.
THE EFFECT OF PRIOR PARENT PHASE COLD WORK ON MARTENSITE TRANSFORMATION IN Cu-Zn-Al SHAPE MEM-

ORY ALLOYS M.S. Thesis
G. E. Moore Dec. 1984 85 p
(AD-A155140; AD-F630645) Avail: NTIS HC A05/MF A01 CSCL 11/6

The effect of cold work upon the transformation kinetics of parent to martensite and martensite to parent was studied utilizing differential scanning calorimetry, X-ray diffraction, optical and transmission electron microscopy methods. Samples of a Cu-Zn-Al shape memory alloy were cold rolled above martensite start temperature to varying degrees of deformation. The cold worked samples displayed various deformation morphologies. The mechanisms by which these deformation morphologies were developed and the varying morphology crystallographic features were studied and characterized using X-ray diffraction and optical and transmission electron microscopy techniques. GRA

N85-32184# Naval Postgraduate School, Monterey, Calif.
THE EFFECT OF ALLOY ADDITIONS ON SUPERPLASTICITY IN THERMOMECHANICALLY PROCESSED HIGH MAGNESIUM ALUMINUM-MAGNESIUM ALLOYS M.S. Thesis
R. J. Self Dec. 1984 127 p
(AD-A155142; AD-F630645) Avail: NTIS HC A07/MF A01 CSCL 11/6

This research extends previous thesis work by Becker and Mills, and is concurrent with that of Stengel on the superplastic behavior of warm rolled high-Mg, Al-Mg alloys. In this work, the effect of various alloy additions were investigated. The following Al-Mg alloy compositions were studied: 8% Mg; 8% Mg-0.4% Cu; 8% Mg-0.4% Cu-0.5% Mn; 10% Mg; 10% Mg-0.4% Cu; 10% Mg-0.2% Mn. These materials were solution treated and hot worked at 440 C and then warm rolled at 300 C to 94% reduction. Tensile testing was then conducted for the as-rolled condition. The alloys were tested at temperatures ranging from room temperature to 300 C and at strain rates from .000056/sec to .14/sec. The copper addition has, on the same weight percentage basis, the same effect on superplasticity as does the addition of manganese to the alloy. The addition of small amounts (i.e., approximately 0.2 weight percent) of manganese appears to offer little advantage over the binary compositions in terms of super plasticity. GRA

N85-32185# Naval Postgraduate School, Monterey, Calif.
COMPARISON OF THE RESPONSE OF SHAPE MEMORY ALLOY ACTUATORS USING AIR-COOLING AND WATER-COOLING M.S. Thesis
R. E. Watson Dec. 1984 120 p
(AD-A155216) Avail: NTIS HC A06/MF A01 CSCL 11/6

Titanium-Nickel (Ti-Ni) alloy specimens with induced shape memory were subjected to various single step current inputs under water-cooled, natural convective air-cooling, and stagnant air-cooling conditions to determine cooling time constants and subsequent delay time for successive actuation. Power input, specimen recovery and reextension displacement with various loads applied to the coil shaped actuator, and temperature distributions along the coil were recorded as functions of time. Results suggested that liquid cooling was a viable method for increased actuator response time. A brief review of the phase transformations that give rise to the shape memory effect is included. GRA

N85-32186# Illinois Univ. at Urbana-Champaign, Savoy. Dept. of Metallurgy and Mining Engineering.
THE EFFECT OF DIFFUSIVE HYDROGEN SEGREGATION ON FRACTURE OF POLYCRYSTALLINE NICKEL
D. Lassila and H. K. Birnbaum May 1985 28 p
(Contract N00014-83-K-0468)
(AD-A155238) Avail: NTIS HC A03/MF A01 CSCL 11/6

Hydrogen embrittlement of polycrystalline nickel was studied under conditions which allowed the diffusion and segregation of hydrogen to grain boundaries to be controlled. It was shown that even at high solute concentrations of hydrogen, the fracture mode was ductile shear rupture, if transport of hydrogen to the grain boundaries was not allowed. As the amount of hydrogen segregation to the grain boundaries was increased the fracture mode became increasingly intergranular. Analysis of the temperature dependence of this transition from ductile rupture to transgranular fracture yields a hydrogen segregation enthalpy of 11.6 kJ/mole. The transition in the fracture mode was also observed at a constant temperature by increasing the solute hydrogen concentration. The kinetics of this fracture transition suggests that the high hydrogen segregation layer extends about 35 nm from the grain boundary. It is suggested that the fracture mechanism is a softening of the material in this segregation region due to the high hydrogen concentration. GRA

N85-32187# Battelle Columbus Labs., Ohio.
METALLURGICAL ORIGINS OF FRACTURE TOUGHNESS AND MICROSTRUCTURE AND FRACTURE TOUGHNESS OF AN HSLA (HIGH-STRENGTH/LOW-ALLOY) STEEL Final Report, 15 Aug. 1978 - 14 Aug. 81, 1 Jan. 1982 - 31 Dec. 1984
A. R. Rosenfield, J. P. Hirth, and J. G. Schroth 31 May 1985 11 p Prepared in cooperation with Ohio State Univ., Columbus
(Contracts DAAG29-78-C-0031; DAAG29-82-K-0033)
(AD-A155530; ARO-15689.9-MS; ARO-18399.7-MS) Avail: NTIS HC A02/MF A01 CSCL 11/6

The report discusses effects of composition and heat treatment on the fracture behavior of a group of steels based on ASTM A712A. Very low transition temperatures were observed in a number of cases. However, adverse effects of Cu on the K sub Ic value for cleavage and on the sharpness of the ductile/brittle transition are noted. At ambient temperatures, overaged Cu particles are beneficial for ductile fracture resistance. A new experimental method of evaluating the relative contributions of opening and shear to ductile crack growth was developed, along with a superdislocation model of the process. GRA

N85-32188# United Technologies Research Center, East Hartford, Conn.
A STUDY OF ADHERENT OXIDE SCALES
J. G. Smeggil and A. W. Funkenbusch May 1985 31 p
(Contract N00014-82-C-0618)
(AD-A155554; UTRC/R85-916564-1) Avail: NTIS HC A03/MF A01 CSCL 11/6

The effects whereby minor element additions (yttrium) improve oxide scale adherence were investigated. These studies have led to the proposal of a new and different mechanism for oxide adherence. This new mechanism involves the effects of interfacial segregation of indigenous alloy impurities such as sulfur. A new mechanism to account for the beneficial effects that small additions have on the adherence of oxide scales is proposed. Sulfur is known to be present at tramp levels (less than 100 ppm) within nickel and nickel-based alloys and it can segregate to metal surfaces. However, it has been disclosed here that such sulfur segregation can also markedly affect the adherence of the protective oxide scale. In the absence of elements like yttrium, such segregation effects weaken the bond between the protective scale and the substrate metal. The role of the yttrium is to interact with sulfur to form a refractory sulfide. This interaction lessens the amount of sulfur available to segregate to and concentrate at the critical scale-metal interface. The results of experiments involving Auger spectroscopy, optical, scanning electron microscopy, scanning electron microprobe and scanning transmission electron microscopy techniques in conjunction with isothermal and cyclic oxidation testing which have led us to propose this mechanism are presented. GRA

N85-32189# Pacific Northwest Lab., Richland, Wash.
MODIFICATION OF THE GRAIN SIZE OF SPUTTERED COPPER WITH ADDITIONS OF OXYGEN, KRYPTON, SILVER, OR YTTRIUM
R. W. Moss and M. D. Merz Apr. 1985 26 p Presented at the Intern. Conf. on Met. Coatings, Los Angeles, 15 Apr. 1985
(Contract DE-AC06-76RL-01830)
(DE85-010975; PNL-SA-12847; CONF-8504124-1) Avail: NTIS HC A03/MF A01

Several 800 to 1100 (MU)m thick films of oxygen free high conductivity (OFHC) copper and copper with additions of oxygen,

krypton, silver, or yttrium were deposited at rates of 0.5 to 1.2 (MU)m/min using an enhanced thermionically supported discharge (ETSD) sputtering apparatus. To obtain fine grained materials, several deposition parameters, such as partial pressure of oxygen in the sputtering gas, bias, and substrate temperature, were varied. Oxygen and krypton were incorporated by trapping the sputtering gas; silver and yttrium were added by means of the target design. The structures and microstructures were examined with standard X-ray diffraction (XRD), transmission electron microscopy (TEM), and optical microscopy techniques. The grain sizes varied from 20 (MU)m for the OFHC copper to 0.0075 (MU)m for the Cu-4 at.% Y deposits. XRD data indicated an amorphous structure on the Cu-9 at.% Y deposits. DOE

N85-32190# Joint Publications Research Service, Arlington, Va.
EAST EUROPE REPORT: SCIENCE AND TECHNOLOGY
21 Jun. 1985 31 p Transl. into ENGLISH from various East European articles
(JPRS-ESA-85-021) Avail: NTIS HC A03/MF A01

Scientific and technological materials from Eastern European foreign-language newspapers, periodicals and monographs, plus news agency releases and broadcasts are compiled. In particular, the handling of radioactive wastes, immunology, phase-shifting capacitors, computer technology, personal computers, and a new wear-resistant metal coating developed in East Germany are addressed. For individual title, see N85-32191.

N85-32191# Joint Publications Research Service, Arlington, Va.
NEW METAL COATING METHOD DEVELOPED
Tilo Scholze *In its* East Europe Rept.: Sci. and Technol. JPRS-ESA-85-021 21 Jun. 1985 p 6-7 Transl. into ENGLISH from Freiheit (Halle, East Germany), 29 Mar. 1985 p 8 (For primary document see N85-32190 21-26)
Avail: NTIS HC A03/MF A01

The East German Pumps and Compressors VEB Combine is employing a titanium nitride (TiN) coating applied via thin-film vapor deposition to increase the wear behavior characteristics of functioning structural components by 200 to 400%. In addition, machine tools and drill bits are also being coated with TiN to increase their service life. F.M.R.

N85-32919# Joint Publications Research Service, Arlington, Va.
NONEQUILIBRIUM KINETICS OF GROWTH OF OXIDE LAYER GRAINS DURING LASER HEATING OF METALS IN AIR Abstract Only
D. T. Alimov, V. A. Bobyrev, F. V. Bunkin, V. L. Zhuravskiy, V. S. Lukyanchuk, Ye. A. Morozova, S. A. Ubaydullayev, and P. K. Khabibullayev *In its* USSR Rept.: Phys. and Math. (JPRS-UPM-85-004) 17 Jun. 1985 p 52 Transl. into ENGLISH from Dokl. Akad. Nauk SSSR (Moscow), v. 297, no. 4, Dec. 1984 p 871-876 Original language document previously announced in IAA as A85-20090 (For primary document see N85-32860 21-70)
Avail: NTIS HC A06/MF A01

27 NONMETALLIC MATERIALS

Includes physical, chemical, and mechanical properties of plastics, elastomers, lubricants, polymers, textiles, adhesives, and ceramic materials.

N85-32192# Notre Dame Univ., Ind. Dept. of Chemical Engineering.
POLYMER SOLUTION-SUPERCRITICAL FLUID BEHAVIOR
A. K. McClellan, E. G. Bauman, and M. A. McHugh 10 Apr. 1985 23 p
(Contract N00014-83-K-0613)
(AD-A154514; TR-2) Avail: NTIS HC A02/MF A01 CSCL 07/4

Experimental pressure-temperature (P-T) data are presented for the polystyrene-toluene-carbon dioxide system and the polystyrene-toluene-ethane system. The P-T phase diagrams for these systems exhibit characteristics which are similar to the phase diagrams of simple binary solutions. The addition of supercritical carbon dioxide and supercritical ethane to the polystyrene-toluene solution shifts the lower critical solution temperature curve to lower temperatures. Polymer-organic solvent-supercritical fluid additive phase behavior is interpreted in terms of Patterns of Patterson's corresponding states model. Representative calculations using this model are shown for the poly(ethylene-co-propylene) hexane-supercritical ethane system. GRA

N85-32193# Princeton Univ., N. J. Dept. of Chemical Engineering.
BUBBLE DYNAMICS IN POLYMER SOLUTIONS UNDERGOING SHEAR Ph.D. Thesis. Interim Report
P. S. Kezios 1 Apr. 1985 177 p
(Contract N00014-79-C-0385)
(AD-A154575; Rept-160-6076-4) Avail: NTIS HC A09/MF A01 CSCL 20/4

Hydraulic cavitation and its effects have been reported to be substantially inhibited and subsequently suppressed by the addition of minute quantities of water-soluble polymer. Modelling the growth and collapse of a single cavitation bubble in water has been established as the fundamental theoretical approach to understanding this phenomenon. Laser-induced cavitation has been developed as a technique for the experimental investigation and confirmation of predicted spherical and nonspherical bubble dynamics in quiescent viscous fluids. The present experimental research has sought to form a link between previous theoretical and experimental efforts. Optical cavitation has been used to create model cavitation bubbles nonintrusively within a fluid undergoing a steady shear flow history. The flow-induced deformation of these single bubbles was recorded and analyzed. GRA

N85-32194# California Univ., Davis. Div. of Materials Science and Engineering.
FUNDAMENTAL INVESTIGATIONS OF FAILURE DURING SUPERPLASTIC FORMING PROCESS Annual Report, 1 Feb. 1984 - 31 Jan. 1985
B. Hidalgo-Prada and A. K. Mukherjee 12 Mar. 1985 18 p
(Grant AF-AFOSR-0081-82)
(AD-A154647; AFOSR-85-0392TR) Avail: NTIS HC A02/MF A01 CSCL 11/9

The effects of strain rate on the stress-strain behavior of Ni-modified Ti-6Al-4V (Ti-6Al-4V-2Ni) at superplastic forming temperature (815 C), were investigated. The microstructural evolution during superplastic deformation (SPD), produced strain hardening at low strain-rates and strain softening at high strain rates. Maximum attainable superplastic ductility, observed at intermediate strain softening. Metallographic evidence is presented to show that the observed strain hardening is due to deformation-enhanced grain growth in the alpha and beta phases, while the strain softening can be attributed, primarily, to grain size refinement, due to dynamic recrystallization. GRA

N85-32195# Illinois Univ. at Urbana-Champaign, Savoy. Dept. of Theoretical and Applied Mechanics.
THE SHEARING CONTRIBUTION IN TRANSFORMATION TOUGHENING OF BRITTLE MATERIALS
P. Sofronis and R. M. McMeeking Mar. 1985 50 p
(Contract N00014-81-K-0650)
(AD-A154656) Avail: NTIS HC A03/MF A01 CSCL 20/12

A simple constitutive law is proposed for the description of a ceramic composite which undergoes stress induced martensitic transformation. This law is used in finite element calculations to investigate the shear effect on the transformation zone near a crack tip. A formula describing the stress intensity factor change due to the shear contribution of the transformation is given. Significant loss of toughness is observed in the case of a stationary crack and is attributed entirely to the shear component of the transformation is given. Significant loss of toughness is observed in the case of a stationary crack and is attributed entirely to the shear component of the transformation. As the crack grows, the wake of the transformed material left behind the crack constitutes a source of toughening. This toughening is due to both dilatancy

and shear in the phase change and rises to a maximum level just after a propagation comparable with the zone height. Finally, it is shown that the shear component can be important when prediction of the fracture toughness of the transformation toughened ceramics are made. GRA

N85-32196# Utah Univ., Salt Lake City. Dept. of Chemistry.
INTERACTION OF SOLUTES WITH STRETCHED POLYMERS Final Report, 14 Dec. 1981 - 13 Dec. 1985
J. Michl and P. J. Phillips Feb. 1985 11 p
(Contract DAAG29-82-K-0024)
(AD-A154662; ARO-18621.11-CH) Avail: NTIS HC A02/MF A01 CSCL 07/4

Significant advances have been made in the understanding of polymer-solute interactions and in the understanding of solute properties. This report pertains to: Dielectric relaxation studies - solute molecules containing dipole moments have been used in order to obtain information on the location of molecules in polyethylene. FTIR and polarized UV spectroscopic studies have been enlightening for acridine in polyethylene. Electron microscopic studies; Solute orientation factors from spectral measurements- The orientation distribution functions of solutes in uniaxially stretched polyethylene can be characterized by their moments. GRA

N85-32197# Harvard Univ., Cambridge, Mass. Div. of Applied Sciences.
MATRIX FRACTURE IN FIBER-REINFORCED CERAMICS
B. Budiansky, J. W. Hutchinson, and A. G. Evans Mar. 1985 36 p
(Contract N00014-84-K-0510; Grants NSF DMR-83-16979; NSF MEA-82-13925)
(AD-A154704; MECH-64) Avail: NTIS HC A03/MF A01 CSCL 11/2

A fiber-reinforced ceramic subject to tensile stress in the fiber direction can undergo extensive matrix cracking normal to the fibers, while the fibers remain intact. In this paper, the critical conditions for the onset of widespread matrix cracking are studied analytically on the basis of fracture-mechanics theory. Two distinct situations concerning the fiber-matrix interface are contemplated: (1) unbonded fibers initially held in the matrix by thermal or other strain mismatches, but susceptible to frictional slip, and (2) fibers that initially are weakly bonded to the matrix, but may be debonded by the stresses near the tip of an advancing matrix crack. The results generalize those of the Aveston-Cooper-Kelley theory for case (1). Optimal thermal strain mismatches for maximum cracking strength are studied, and theoretical results are compared with experimental data for a SiC fiber, lithium-alumina-silicate glass matrix composite. GRA

N85-32198# Air Force Wright Aeronautical Labs., Wright-Patterson AFB, Ohio.
SYNTHESIS AND PROPERTIES OF ARYLETHERSULFONE THERMOSET SYSTEMS Final Technical Report, Apr. 1983 - Apr. 1984
P. M. Lindley, L. G. Picklesimer, B. Evans, J. J. Kane, and F. E. Arnold Mar. 1985 25 p
(AF Proj. 241-9; AF Proj. 230-3)
(AD-A154811; AFWAL-TR-84-4119) Avail: NTIS HC A02/MF A01 CSCL 11/9

A series of acetylene-terminated (AT) oligomeric arylether sulfones were synthesized which upon curing possess higher molecular weight between crosslinks than earlier AT sulfones. A correlation between varying chain length of the oligomer and initial/final glass transition temperature (Tg's) was established which provides the required processing parameters and use temperatures. In all cases the initial Tg was dependent on the flexibility of the oligomeric backbone. The more flexible backbone structures provided the lower Tg's for processing. The final Tg's (cured Tg) which establish end use-temperatures were dependent on the varying chain length of the oligomer, as well as, backbone flexibility. The longer more flexible backbones provided lower end use temperatures. Of the twelve systems synthesized and characterized, one was selected for scale-up (50 g.) and is currently being evaluated with respect to its neat resin mechanical properties. GRA

N85-32199# Royal Aircraft Establishment, Farnborough (England).
IMPORTANCE AND SIGNIFICANCE OF TRANSITION TEMPERATURES
W. A. Lee Nov. 1984 13 p
(AD-A154871; RAE-TM-MAT/STR-1050; DRIC-BR-94446) Avail: NTIS HC A02/MF A01 CSCL 07/4

The importance of the transition temperatures of polymers is described with particular emphasis on their practical significance. An outline of the RAE Transition Temperature Data Bank is provided and RAE publications in the transition temperature field are tabulated. GRA

N85-32200# Massachusetts Univ., Amherst. Materials Research Lab.
STRUCTURE-PROPERTY RELATIONSHIPS IN THERMOPLASTIC ELASTOMERS. PART 3: SEGMENTED POLYACETAL-POLYURETHANES
J. C. W. Chien 4 Apr. 1985 22 p
(Contract N00014-83-K-0083)
(AD-A154897; TR-10) Avail: NTIS HC A02/MF A01 CSCL 11/9

Dihydroxy terminated polyacetals had been synthesized from aldehydes and glycols and used as soft segments to obtain segmented polyurethane block copolymers. The glass transition temperature (T sub G) of PacPU with 1,350 M sub n polyacetals is raised to -38 C and none was observed for shorter polyacetal chains. The copolymers can be synthesized to have a broad range of mechanical properties such as modulus from 0.5 to 130 MPa, stress at break from 0.7 to 21 MPa and elongation at break from 66% to 1300% through the variation of the constituents and composition. The rheological properties are only slightly dependent on temperature for symmetrical diisocyanates but quite temperature sensitive with asymmetrical diisocyanate copolymers. The polyacetals are selected tω build in acid catalyzed thermal decomposition of the thermoplastic elastomers. The hard and soft segments have TGA decomposition peaks at 292 and 343 C, respectively. Most copolymers display 2 peaks at temperatures between these two limits. GRA

N85-32201# Massachusetts Inst. of Tech., Cambridge. Dept. of Chemistry.
RESISTANCE OF POLYANILINE FILMS AS A FUNCTION OF ELECTROCHEMICAL POTENTIAL AND THE FABRICATION OF POLYANILINE-BASED MICROELECTRONIC DEVICES Interim Report
E. W. Paul, A. J. Ricco, and M. S. Wrighton 16 May 1985 38 p
(Contract N00014-84-K-0553)
(AD-A154999; ONR-TR-4) Avail: NTIS HC A03/MF A01 CSCL 11/9

Anodic growth of polyaniline films on a Au microelectrode array has been carried out to add to the characterization of polyaniline and to fabricate polyaniline-based microelectronic devices, diodes and transistors, that function when the polyaniline-functionalized microelectrode array is immersed in an electrolyte solution. The microelectrode array is a set of eight Au electrodes, 0.1 micrometer thick, 4.4 micrometers wide and 50 micrometers long, each individually addressable and separated from each other by 1.7 micrometers. Polyaniline can be deposited in controlled amounts by electrochemical oxidation of aniline. When the polyaniline is deposited in sufficient amounts, two or more of the eight Au microelectrodes can be connected in the electrical sense. Current can pass between two connected microelectrodes when there is an applied potential between them. The magnitude of the current at a given applied potential depends on the electrochemical potential of the polyaniline. In 0.5 M NaHsSO4/H2O the current (at a fixed applied potential) is maximum at an electrochemical potential of approx +0.4 V vs SCE and declines by a factor of greater than 1,000,000 upon reduction to +0.1 or oxidation to +0.7 V vs SCE. Owing to the large change in

resistance upon change in electrochemical potential, the functionalized microelectrodes is crucial to device function, owing to the limited conductivity of the polyaniline. The switching time of a transistor-like device is faster than 0.1 s. GRA

N85-32202# National Bureau of Standards, Gaithersburg, Md. Inorganic Materials Div.
STRESS CORROSION OF CERAMIC MATERIALS Annual Report, 1 Oct. 1983 - 30 Sep. 1984
S. W. Freiman, G. S. White, A. C. Gonzalez, E. R. Fuller, Jr., and D. C. Greenspan May 1985 119 p
(Contract N00014-84-F-0019)
(AD-A155020) Avail: NTIS HC A06/MF A01 CSCL 11/2

Studies during the past year focussed on two distinct areas. They are: (1) the effect of modifying ions on environmentally enhanced crack growth in glasses, and (2) the relationship between crack growth and electrical failure in multilayer ceramic capacitors. Results of these investigations are summarized. B.W.

N85-32203# Naval Postgraduate School, Monterey, Calif.
THE EFFECT OF MOULD SIZE ON THE EXOTHERMIC REACTION AND COMPRESSIVE STRENGTH OF EPOXY RESIN CHOCKS M.S. Thesis
J. D. Stalnaker Dec. 1984 72 p
(AD-A155102) Avail: NTIS HC A04/MF A01 CSCL 13/9

A study was conducted on the effects of mould size on the exothermic reaction that occurs during the curing of epoxy resin chocks. Moulds of CHOCKFAST ORANGE were cast with lateral dimensions of 3 by 3 inches, 6 by 6 inches and 9 by 9 inches, with thicknesses of 1/2, 1 and 1-1/2 inches. Results showed that the degree of exotherm increased with increased chock thickness. The 1/2 inch thick samples showed very little temperature rise, with the temperature increasing linearly with time. The 1 inch thick samples, beginning with the 6 by 6 by 1 inch sample, and the 1-1/2 inch samples experienced a two stage exothermic reaction, with temperature increasing linearly, initially and then exponentially during the second stage. Stress versus strain pilots revealed a significant increase in ductility with the increased exotherms, resulting in substantially higher ultimate strengths. Chock specimens experiencing the second stage, exponential temperature rise has ultimate strengths consistently in excess of 20,000 psi, compared to 16,000 to 17,000 psi to those specimens that did not. GRA

N85-32204# Army Engineer Waterways Experiment Station, Vicksburg, Miss.
USER'S GUIDE FOR COMPUTER PROGRAM CGFAG, CONCRETE GENERAL FLEXURE ANALYSIS WITH GRAPHICS Final Report
W. A. Price, III, H. Miller, M. L. Waites, and E. T. Gates Sep. 1984 46 p
(AD-A155555; WES-INSTRUCTION-K-84-11) Avail: NTIS HC A03/MF A01 CSCL 09/2

This user's guide is designed to analyze cross sections of reinforced and nonreinforced concrete as they are subjected to any combination of axial loads and bending. This program is one of the oldest examples of computerized structural analysis. Its versatility in classifying irregular cross sections, bolted baseplates, and unreinforced sections has sustained a demand for it from its origin to the present. The program has been used for numerous applications through manipulation of the ratio r. The phase for differentiation of nonreinforced sections has been implemented to theorize footing pressure and to make stability analyses. The recent revisions can be credited with making output easier to interpret and providing the new capability, graphics output of the geometry and stress equation calculation. The format allows for the output to be separated into a summary page of detailed stress tables. This ratio governs development of the transformed area of reinforcement in compression. It is actually the ratio of the effective modulus of the reinforcement in compression to that of the reinforcement in tension. GRA

N85-32205# Celanese Research Corp., Summit, N.J.
ELECTRICAL AND MECHANICAL PROPERTIES OF INTERCALATED GRAPHITE FIBERS Final Report, Apr. 1981 - Apr. 1984
H. A. Goldberg Apr. 1985 89 p
(Contract DAAG29-81-C-0016)
(AD-A155560; ARO-17260.7-PH) Avail: NTIS HC A05/MF A01 CSCL 11/5

In order to understand the electrical and mechanical property changes which occur when graphite fibers are intercalated, it is essential that a better understanding of the properties of the fibers prior to intercalation be developed. Research aimed at elucidating the structure-property relationships in neat carbon and graphite fibers is presented. In particular, the changes with increasing heat treatment in both electronic and structural properties are discussed. The relative importance of crystallite size, three dimensional order, and the details of disordered regions between crystallites are demonstrated by analysis of: resistance versus temperature; piezoresistance; X-ray diffraction; and intercalation behavior. Crystallite size effects must be included in order to understand the electronic structure of the fibers studied here. Arguments which demonstrate the potential importance of the disordered regions between crystallites to the anamolous resistance-temperature behavior of low-modulus, high-strength fibers are presented. Three dimensional order is shown to increase continuously with heat treatment. The piezoresistance of carbon and graphite fibers is discussed in terms of a simple polycrystalline model, and useful qualitative information on the parameters needed for modelling the elastic properties of these material is obtained. GRA

N85-32206# Westinghouse Research and Development Center, Pittsburgh, Pa.
INTRODUCTION OF STRUCTURAL VARIATIONS INTO OXIDE POLYMERS AND THEIR EFFECT ON SINTERING AND CRYSTALLIZATION Final Report, 1 Jan. 1983 - 31 Dec. 1984
B. E. Yoldas 11 Feb. 1985 85 p
(Contract DAAG29-83-C-0006)
(AD-A155597; ARO-19804.1-MS) Avail: NTIS HC A05/MF A01 CSCL 11/2

Hydrolytic polycondensation of metal alkoxides produces polymeric units consisting of an oxide network framed by hydroxyl and organic groups. The morphology of the polymerization as well as the structure of these materials is determined by the kinetics of hydrolysis polymerization reactions. By controlling the kinetics of these reactions it is possible to produce modified ceramic materials with altered properties. In this work, by using three representative systems, i.e., silica, titania and zirconia, the effect of hydrolytic polycondensation parameters on the resultant materials was investigated. These parameters include: molecular separation of species, their ratios, the reaction medium, the concentration of catalyst, the reaction time, the temperature and the type of alkyl group in the alkoxide. In the silica system, the parameters that affect the hydrolytic polycondensation of titanium alkoxides Ti(OR)4 were investigated. In the zirconia system, it has been shown that the alkyl groups and molecular separation during the hydrolytic condensation have particular significance in the modification of the monoclinic tetragonal transformation of the resultant ZrO2. GRA

N85-32207# North Carolina Univ., Raleigh.
PERMEATION OF MIXED PENETRANTS THROUGH GLASSY POLYMER MEMBRANES Final Report, Feb. 1981 - Jan. 1985
R. T. Chern, H. B. Hopfenberg, and V. T. Stannett 15 Mar. 1985 248 p
(Contract DAAG29-81-K-0039)
(AD-A155605; ARO-17773.15-CH) Avail: NTIS HC A11/MF A01 CSCL 11/9

This report summarizes the results of research activities supported by the Army Research Office. Three important areas were investigated: (1) Selective permeation of mixed gaseous penetrants in glassy polymers; (2) Transport of a reactive penetrant in polymers; and (3) Effects of chemical modification resulted from exposure to reactive penetrants on the permeability of the polymer

to permanent gases. The results of the first study indicated that the penetrants in a gaseous mixture compete with each other for diffusion paths provided by the microvoid sorption sites existing typically in a glassy polymer when the polymer was vitrified. The permeability to a given penetrant in a mixture is depressed from its pure-component value simply due to the competition effect. In the second area, we found that polyimide, often quoted for its chemical stability, is susceptible to attack by a strong nucleophile, ammonia. Finally, through ESCA and permeability measurements, we demonstrated that high-temperature fluorination of polyethylene, which gives a relatively well defined surface fluorinated layer, is controlled by the diffusion rate of fluorine. On the other hand, room temperature fluorination tends to be reaction-controlled and results in a distribution of fluorine atoms throughout the thickness of the film. GRA

28 PROPELLANTS AND FUELS

Includes rocket propellants, igniters, and oxidizers; storage and handling; and aircraft fuels.

For related information see also *07 Aircraft Propulsion and Power, 20 Spacecraft Propulsion and Power,* and *44 Energy Production and Conversion.*

N85-32208# Defence Research Establishment, Ottawa. (Ontario).
OBSERVATIONS OF THE USE OF THE SETAPOINT DETECTOR
J. R. Coleman and L. D. Gallop Dec. 1984 16 p In ENGLISH and FRENCH
(AD-A154533; DREO-TN-84-33) Avail: NTIS HC A02/MF A01 CSCL 21/4

In a previous investigation, a variety of tests were used to study the low temperature flow behavior of aviation turbine fuels. These included both specification fuels, and others that had higher than usual freeze points, but whose use might become necessary in the future. One procedure employed the Setapoint detector, manufactured by Stanhope Seta Ltd. This device measures the resistance to passage of a fuel pumped back and forth across a screen during a programmed cooling regime. In an attempt to find the reason for certain abnormal test results obtained using the Setapoint detector, a review of experimental results was conducted. Visual observations made during the tests were considered in conjunction with the stop flow and flow points. A number of distinct modes of behaviour, some leading to aberrant results, were identified. The instrument appeared best suited to specification aviation fuels, and middle distillates that produce fine homogeneous wax deposits during the test. GRA

N85-32209# Weapons Systems Research Lab., Adelaide (Australia).
THE DETERMINATION OF DINITROTOLUENE IN SINGLE BASE PROPELLANTS
M. Mular Jun. 1984 32 p
(AD-A154672; AD-F630659; WSRL-0368-TM) Avail: NTIS HC A03/MF A01 CSCL 19/1

Six single base gun propellants of three different types (AR 2206, NH and FNH) were analysed for dinitrotoluene by three different methods, viz titanous chloride reduction, gas chromatography and high performance liquid chromatography (HPLC). In general, similar results were obtained by all three methods. Although any of the three methods can be used for the determination of dinitrotoluene, the HPLC method is recommended - the equipment is automated and microprocessor controlled, and analyses can be performed relatively quickly, with good precision and with the lowest relative standard deviation of the order of 0.3%. It is recommended that the HPLC method be adopted as a standard test method. GRA

N85-32210# Naval Surface Weapons Center, White Oak, Md.
SYNTHESIS OF ENERGETIC MATERIALS Annual Progress Report
H. G. Adolph, M. Chaykovsky, J. M. Goldwasser, W. M. Koppes, and T. C. Adams, Jr. 31 Mar. 1985 45 p
(AD-A154887) Avail: NTIS HC A03/MF A01 CSCL 07/3

The synthesis of polyformals from several nitro- and fluorodiols was investigated. Linear, difunctional polyformals were obtained from 3, 3, 5, 7, 7-pentanitro-5-azanonanediol, 3, 5, 5, 7-tetranitro-3, 7-diazanonanediol, 2, 2, 3, 3, 4, 4-hexa fluoropentanediol, and 2, 2, 3, 3, 4, 4, 5, 5-octafluorohexanediol. Procedures are given to prepare stable gumstocks from the first 3 of these, using FEFO as plasticizer. The fourth polymer was only partially miscible with FEFO. Efforts toward the synthesis of polyazabicyclooctanes and polyazaoxabicyclononanes were continued. An acyclic model compound for the latter system was synthesized and found to be marginally stable. Various approaches to the synthesis of azacyclooctadienes as precursers to bicyclononanes were investigated. A study of the chemistry of the 2, 6,-diazabicyclooctane ring system was iniatiated. Condensation reactions of 2, 3-disubstituted and 2, 3, 5, 6-tetrasubstituted 1, 4-dinitropiperazines with methylene diamine derivatives were investigated in efforts to prepare linear polycyclic nitramines. During this work, the first example of a 1,2-dinitramninoolefin was prepared. A new oxidizer of exceptionally high oxygen content, 2, 3, 5, 6-tetranitrato-1, 4-dinitropiperazine, was prepared but was found to decompose slowly at room temperature. GRA

N85-32211# Computer Sciences Corp., Bay St. Louis, Miss. Technical Services Lab.
TNT EQUIVALENCY OF EAK EXPLOSIVE Final Report, Oct. - Dec. 1984
L. Mars, R. Kukuvka, and J. Caltagirone Dover, N.J. Army Armament Research and Development Command Jun. 1985 42 p
(Contract MIPR-4311-1076)
(AD-A155737; AD-E401350; ARLCD-CR-85019) Avail: NTIS HC A03/MF A01 CSCL 19/1

Peak side-on blast overpressure and scaled positive impulse have been measured for EAK explosive. The equivalency testing addressed the cylindrical shipping container. High explosive equivalency values for each test series were obtained as a function of scaled distance by comparison to known pressure and impulse characteristics for TNT hemispherical surface bursts. GRA

N85-32212# Calspan Corp., Buffalo, N. Y.
CLOSED-BOMB COMBUSTION OF HIVELITE-BASED, VERY HIGH BURN RATE (VHBR) PROPELLANT
E. B. Fisher and C. C. Morphy Apr. 1985 118 p
(Contract DAAK11-80-C-0062)
(AD-A155740; AD-F300619; BRL-CR-542) Avail: NTIS HC A06/MF A01 CSCL 19/1

An experimental investigation of the combustion characteristics of a Hivelite-based, very-high-burn-rate (VHBR) propellant was conducted. The experiments were performed in a closed chamber, called the VHBR bomb, that was specially designed and constructed for these experiments. The device was designed with the same diameter as the propellant samples in order to maintain one dimensional combustion processes and transient wave phenomena to simplify subsequent interpretation and analysis. Propellant combustion was characterized by a low burn rate (about 1 m/s) until a pressure in the vicinity of 15-20 MPa is reached. After this pressure, which may represent the propellant crushing or break pressure, the combustion rate accelerated to levels from 10 to 180 m/s, depending on other test parameters. Tests conducted at different loading densities indicated that combustion rate was a strong function of pressure. Variation of sample weight at constant loading density demonstrated that increasing the amount of unburned propellant at the time the break pressure was reached also causes burn rate and thrust to increase. A coating that makes the outside surface of the sample slippery tended to reduce the apparent burn rate but use of a coating which retarded transmission of gas pressure along the periphery of the sample increased the apparent burn rate as well as thrust. Change of mounting interface properties caused significant

differences in the dynamic characteristics leading to increased thrust. GRA

N85-32213# Pacific Northwest Lab., Richland, Wash.
BIOMASS THERMOCHEMICAL CONVERSION PROGRAM Annual Report, 1984
G. F. Schiefelbein, D. J. Stevens, and M. A. Gerber Jan. 1985 68 p
(Contract DE-AC06-76RL-01830)
(DE85-011867; PNL-5442) Avail: NTIS HC A04/MF A01

The generation of scientific data and conversion process information that will lead to the establishment of cost effective process for converting biomass resources into clean fuels is studied. A data base is developed for biomass thermal conversion by investigating the fundamental aspects of conversion technologies and by exploring those parameters that are critical to the conversion processes. The research activities is divided into: (1) gasification technology; (2) liquid fuels technology; (3) direct combustion technology; and (4) program support activities. These activities are described in detail. Outstanding accomplishments include: (1) successful operation of 3-MW combustor/gas turbine system; (2) successful extended term operation of an indirectly heated, dual bed gasifier for producing medium-Btu gas; (3) determination that oxygen requirements for medium-Btu gasification of biomass in a pressurized, fluidized bed gasifier are low; (4) established interdependence of temperature and residence times on biomass pyrolysis oil yields; and (5) determination of preliminary technical feasibility of thermally gasifying high moisture biomass feedstocks. DOE

N85-32214# Sandia Labs., Albuquerque, N. Mex.
BURN FRONT VELOCITY AS A FUNCTION OF PELLET DENSITY IN IRON-POTASSIUM PERCHLORATE HEAT POWDERS
D. K. McCarthy, W. B. Leslie, and R. W. Dietzel May 1985 18 p refs
(Contract DE-AC04-76DP-00789)
(DE85-011448; SAND-83-1025) Avail: NTIS HC A02/MF A01

Using optical-electronic methods, burn front velocities have been measured for heat pellets of densities which varied between 2.77 Mg/m(3) and 4.92 Mg/m(3). Velocity was found to decline with increasing density above 3.5 Mg/m(3). At densities greater than 4.4 Mg/m(3), self quenching of the combustion was frequently observed. At densities above 5 Mg/m(3), pellets combustion was frequently observed. At densities above 5 Mg/m(3), pellets could not be ignited. DOE

31 ENGINEERING (GENERAL)

Includes vacuum technology; control engineering; display engineering; and cryogenics.

N85-32215*# Applied Cryogenics and Materials Consultants, New Castle, Del.
BASIC CRYOGENICS AND MATERIALS. PHASE 1 Supplemental Report
David A. Wigley Jun. 1985 20 p refs
(Contract NAS1-17571)
(NASA-CR-177932; NAS 1.26:177932) Avail: NTIS HC A02/MF A01 CSCL 20L

The effects of cryogenic temperatures on the mechanical and physical properties of materials are summarized. Heat capacity and thermal conductivity are considered in the context of conservation of liquid nitrogen, thermal stability of the gas stream, and the response time for changes in operating temperature. Particular attention is given to the effects of differential expansion and failure due to thermal fatigue. Factors affecting safety are discussed, including hazards created due to the inadvertent production of liquid oxygen and the physiological effects of exposure to liquid and gaseous nitrogen, such as cold burns and asphyxiation. The preference for using f.c.c. metals at low temperatures is explained in terms of their superior toughness. The limitations on the use of ferritic steels is also considered. Nonmetallic materials are discussed, mainly in the context of their LOX compatibility and their use in the form of foams and fibers as insultants, seals, and fiber reinforced composites. Author

N85-32216# California Univ., Los Angeles. Dept. of Materials Science and Engineering.
SINTERING STUDIES PROJECT Research Progress Report, 1 Apr. 1984 - 31 Mar. 1985
F. F. Lange and W. J. Knapp 13 May 1985 8 p
(Contract N00014-84-K-0286)
(AD-A154750) Avail: NTIS HC A02/MF A01 CSCL 13/8

A new concept explains the factors which influence the sinterability of ceramic (and metal) powders. This theory, based on the thermodynamics consideration of pore disappearance, is centered on the coordination number of distribution of pores within the initial powder compact and on the changes in the pore coordination number during sintering. Thermodynamic arguments show that only pores with a coordination number less than a critical value (R > R sub c) can disappear by diffusion. The coordination number of a pore is the number of touching particles that surround and the pore size. This concept suggested the following phenomena: (1) consolidation forces that increase bulk density will eliminate pores with high coordination numbers and thus increase the sinterability of the powder compact, (2) multiple-particle packing units containing pores with low coordination (R < R sub c) will first densify during sintering to increase the size and coordination number of pores between the densifying packing units, (3)grain growth, supported by dense packing units, will decrease the coordination number of pores enlarged by local densification. i.e., normal grain growth is advantageous to sinterability, and (4) compressive stress produced by either surface tension effects or hot pressing cause the dense regions to deform, thus closing pores between the dense regions and reducing their coordination number. GRA

N85-32217# Joint Publications Research Service, Arlington, Va.
EAST EUROPE REPORT: SCIENCE AND TECHNOLOGY
30 Jul. 1985 34 p Transl. into ENGLISH from various East European articles
(JPRS-ESA-85-023) Avail: NTIS HC A03/MF A01

Scientific and technological materials from Eastern European foreign language newspapers, periodicals and monographs, plus news agency releases and broadcasts are presented. In particular, a Bulgarian article on laser technology applications, a Romanian article on the importance of automation and robotization in the economy, and articles on immunopharmacology, immunology, drug manufacture, production of microelectronic equipment, genetic research, and biotechnology are addressed. For individual titles, see N85-32218 through N85-32219.

N85-32218# Joint Publications Research Service, Arlington, Va.
APPLICATIONS OF LASER TECHNOLOGY DESCRIBED c36
In its East Europe Rept.: Sci. and Technol. JPRS-ESA-85-023 30 Jul. 1985 p 1-6 Repr. from Bulgaria Today (Sofia), no. 448, 1985 p 14-15 (For primary document see N85-32217 21-31)
Avail: NTIS HC A03/MF A01

Laser technology applications in Bulgaria are reviewed. An optical laser light-reflecting system produced in Bulgaria has been operating successfully in the Intercosmos satellite program for three years. There are two producers of laser technology in the country: the Optics Scientific Research Institute in Sofia at the Metalchim State Economic Enterprise, and the Problem Scientific Research Laboratory in Sofia with its Kliment Ohridski Laser Technology Production Department. They produce 20 types of lasers which are used in electronics, mechanical engineering, medicine, environmental protection, and general scientific fields. They include the ELI-M interferometry laser (helium-neon single-phase), the LTA Granat-M, used in microelectronic engraving, the Solar system used to prepared seeds for sowing, laser microscopes, and small-size helium-neon lasers used in optical-control measurement. F.M.R.

N85-32219# Joint Publications Research Service, Arlington, Va.
IMPORTANCE OF AUTOMATION, ROBOTIZATION IN ECONOMY **c37**
Aristide Predoi *In its* East Europe Rept.: Sci. and Technol. JPRS-ESA-85-023 30 Jul. 1985 p 26-31 Transl. into ENGLISH from Era Socialista (Bucharest), no. 8, 25 Apr. 1985 p 9-11 (For primary document see N85-32217 21-31)
Avail: NTIS HC A03/MF A01

Two decades of Romanian progress in automation and robotization of industry are reviewed. Under the aegis of the Institute for Scientific Research and Technical Engineering for Automation and Telecommunications, the automation equipment field has grown from one enterprise in 1965 to six in 1985, with the percentage of domestic needs being supplied by native products growing from 48 to 98.5% in the same period. The proportion of production achieved using mechanized and automated systems averages 65% in 1985, will be 70% in 1987, and over 90% in 1990. Contribution to the drive for increased industrial automation is a transition to computer-aided research and design and to computerized production control based on an integrated computer system. F.M.R.

32 COMMUNICATIONS

Includes land and global communications; communications theory; and optical communications.

For related information see also *04 Aircraft Communications and Navigation* and *17 Spacecraft Communications, Command and Tracking.*

N85-32220# Naval Postgraduate School, Monterey, Calif.
RADAR TARGET IDENTIFICATION THROUGH ELECTROMAGNETIC SCATTERING STUDIES M.S. Thesis
M. Lolic Dec. 1984 117 p
(AD-A154596) Avail: NTIS HC A06/MF A01 CSCL 17/9

Radar target identification using electromagnetic scattering is discussed. Frequencies being used are those corresponding to wavelengths from half the target size to one-tenth the target dimensions. The frequency domain calibration of the free field radar range at the Naval Postgraduate School is performed and validated on several perfectly conducting metallic spheres. Measurements of the radar cross section and the phase of the return on several finite length, thin walled, right circular cylinders were done. GRA

N85-32221# Naval Postgraduate School, Monterey, Calif.
DESIGN OF A JAMMING SIMULATOR FOR A BINARY COMMUNICATION SYSTEM M.S. Thesis
T. J. Pantos Dec. 1984 78 p
(AD-A154617) Avail: NTIS HC A05/MF A01 CSCL 17/4

Two receivers for coherent Phase Shift Key (PSK) and Frequency Shift Key (FSK) transmission have been designed in order to validate theoretical studies involving jamming of digital communication receivers. Binary PSK and FSK signals were generated, transmitted, and processed by each receiver, and measurements of each receiver's performance were recorded as each system operated in the presence of White Gaussian Noise (WGN) as well as in the presence of a combination of White Gaussian Noise and a jammer waveform. The system's performance is expressed in terms of the probability of receiver error occuring during the transmission of digital information. The results are plotted as receiver Probability of error (Pe) versus signal-to-noise ratio (SNR) for fixed values of and jammer-to-signal ratio (JSR). Signal and receiver designs are presented and diagrams as well as schematics have been included for clarity. GRA

N85-32222# Stanford Univ., Calif. Dept. of Computer Science.
GLOBALLY-ASYNCHRONOUS LOCALLY-SYNCHRONOUS SYSTEMS Ph.D. Thesis
D. M. Chapiro Oct. 1984 132 p
(Contract MDA903-83-C-0335)
(AD-A154624; SU-STAN-CS-84-1026) Avail: NTIS HC A07/MF A01 CSCL 09/2

This thesis provides a new framework for the design of very high performance digital machines. The new theoretical results which are presented have practical implications, and lead to a better understanding of possibilities and limitations in the design of computers, communication hardware and other digital machinery. The discussion centers on different organizations for globally-asynchronous, locally-synchronous systems, and covers the following issues: organizations for complex digital systems, metastability as a limitation for high performance, structures for two classes of non-conventional architectures, optimization, performance, reliability, and design techniques. We present new algorithms to compile the specifications of such machines onto efficient circuits, and to verify the correctness of the resulting machines. The models we developed for the analysis of the tradeoffs between different variables that affect the safety of operation of these systems, show that the proposed organizations result in extremely fast and reliable digital machines. The proposed organizational schemes can be used within a wide range of architectures, and integrated circuits designed according to this methodology have been developed and tested. Author (GRA)

N85-32223# Naval Ocean Systems Center, San Diego, Calif.
USING SHIP WAKE PATTERNS TO EVALUATE SAR (SYNTHETIC APERTURE RADAR) OCEAN WAVE IMAGING MECHANISMS. JOINT US-CANADIAN OCEAN WAVE INVESTIGATION PROJECT Interim Technical Report, FY83 - FY84
R. R. Hammond, R. R. Buntzen, and E. E. Floren Feb. 1985 68 p
(NR Proj. ZR0-3103; NR Proj. ZR0-0001)
(AD-A154633; NOSC/TR-978) Avail: NTIS HC A04/MF A01 CSCL 17/9

The Joint Ocean Wave Investigation Project (JOWIP) was conducted to evaluate the detectability of ocean wave structures on imaging synthetic aperture radar (SAR). This project used Kelvin surface ship wake patterns generated under controlled and well documented surface environmental conditions to isolate SAR image parameters. Use of waves of known wavelength and direction provide the opportunity to evaluate the SAR contribution to ocean wave forecasting. SEASAT-like images made with L-band SAR are presented: (1) to suggest how ship-generated surface roughness combines with the velocity-bunching mechanism in calm ocean areas to produce the unusually narrow wakes observed for azimuth-traveling ships on SEASAT images; and (2) to estimate conditions under which SAR image modulation mechanisms can be expected to produce wake images. A method is described for using the Kelvin transverse ship wake wave component to quantitatively evaluate the contributions of various SAR ocean wave imaging mechanisms. It makes use of the narrow sector of surface roughness generated by a ship along its track to produce SAR images of the longest waves in its wake system on flat calm water. GRA

N85-32224# Scripps Institution of Oceanography, La Jolla, Calif. Marine Physical Lab.
VLF (VERY LOW FREQUENCY) WORKSHOP HELD AT SAN DIEGO CALIFORNIA, 24-25 JANUARY 1985
W. S. Hodgkiss 1985 265 p Workshop held at San Diego, Calif., 24-25 Jan. 1985
(Contracts N00014-80-C-0220; N00014-79-C-0472)
(AD-A154652; MPL-U-11/85; MPL-TM-376) Avail: NTIS HC A12/MF A01 CSCL 05/1

The focus of this classified workshop was on the frequency region 1 to 30 Hz. The program included presentations by the participants followed by a discussion covering areas of potential Navy interest and future research objectives. A summary of the presentations and discussion is contained in this report. GRA

N85-32225# Illinois Univ. at Urbana-Champaign, Savoy. Urbana Coordinated Science Lab.
ROUTING ALGORITHMS AND STOCHASTIC ANALYSIS FOR LARGE COMMUNICATIONS NETWORKS Research Summary

Report, 21 Aug. 1985 - 20 Aug. 1986
B. Hajek 20 Aug. 1985 8 p
(Contract N00014-82-K-0359)
(AD-A154654) Avail: NTIS HC A02/MF A01 CSCL 12/1

As part of our ONR sponsored research in the subtopic Linear-Time Stochastic Algorithms, we began investigating an optimization technique known as simulated annealing. We have succeeded in giving a necessary and sufficient condition for the annealing algorithms to converge. New algorithms have been developed for open-loop computation of optimal state-dependent routine strategies for a fluid-approximation communication network model with a single destination. One of the algorithms is an efficient combinatorial algorithm based on the solution of max-flow problems for networks the same size as the original network. A new theory of distributed resource allocation was proposed. The work addresses problems of route selection and scheduling in communication networks. In a large distributed communication network, the decisions that individual stations can make should sometimes be purposely limited a priori in order to facilitate the coordination of such decisions. Such limitations might be placed at one layer of protocol by mechanisms operating at a higher protocol level. GRA

N85-32226# Computer Sciences Corp., Falls Church, Va.
SECURE DIGITAL VOICE COMMUNICATIONS IN THE DEFENSE DATA NETWORK (DDN) Final Report, Mar. 1984 - Mar. 1985
M. Bernet, D. Gan, and C. Oesterreicher 15 Mar. 1985 147 p
(Contract DCA100-84-C-0030)
(AD-A154677) Avail: NTIS HC A07/MF A01 CSCL 17/2

This final report has investigated and validated one of the fourteen key features of the future, all-digital World-wide Digital Systems Architecture (WWDSA), namely the enhanced 2.4 Kbps secure voice survivability through the use of packetized voice and the use of packetized voice and the interconnection between the voice survivability through the use of packetized voice and the interconnection between the voice (DSN) phase implementation plan in the report, Secure Voice, as provided by the STU-IIs, can be implemented in the DDN in the late 1980s time-frame with no technical and minimum schedule risk. VIUs are proposed to interconnect, the family of secure voice terminals, called STU-IIs, to the DDN. VIUs contain modan, signalling and supervision (S/S), and processor modules and are supported by the implementation model of the protocol architecture that (with the TAC as processor module) was proposed in the report. An optimum system-level architecture employing the VIUs and the proposed in the implementation plan based on an extensive evaluation. GRA

N85-32227# Massachusetts Inst. of Tech., Cambridge. Lab. for Computer Science.
INTERACTIVE ON-LINE CONFERENCES Ph.D. Thesis
S. K. Sarin Dec. 1984 254 p
(Contract N00014-83-K-0125)
(AD-A154723; MIT/LCS/TR-330) Avail: NTIS HC A12/MF A01 CSCL 17/2

A real-time conference allows a group of users, each at his or her own workstation, to conduct a problem-solving meeting by collectively viewing and manipulating a shared space of on-line application information while using a voice communication channel for discussion and negotiation. A real-time conference thus supplements asynchronous communication services, such as electronic mail, by permitting simultaneous manipulation of shared information. Techniques are presented in this document for designing and implementing real-time conferences on distributed computer systems. Useful functions for real-time conferences are proposed: control over who may join a conference, and over concurrent participant commands within a conference, private spaces and transfer of information between shared and private spaces; display of status information describing who is present in a conference and who is entering commands; eliciting and collecting responses to be used in decision-making; planning a conference and making it known to potential participants; and maintaining and reviewing records of a conference. The tradeoffs involved in selecting a comprehensible set of commands for these functions are illustrated by the detailed design of a real-time conferencing system for joint editing of documents. GRA

N85-32228# Applied Science Associates, Inc., Apex, N.C.
SCATTERING FROM FOLIAGE COVERED TERRAIN Interim Report, Jan. 1984 - Jan. 1985
G. S. Brown Griffiss AFB, N.Y. RADC Mar. 1985 32 p
(Contract F19628-84-C-0012)
(AD-A154724; ASA-AF-85-1; RADC-TR-85-60) Avail: NTIS HC A03/MF A01 CSCL 20/3

A brief review of efforts directed toward modeling the effects of foliage covered rough terrain on electromagnetic scattering is presented. A two-way passage approach is proposed as an approximate method of solution. In this approach, an incident field is transmitted through a foliage layer in free space. The field transmitted through the foliage acts as an incident field upon the rough surface. The field scattered by the surface is taken to be a secondary incident field upon the foliage slab. The net scattered field is the sum of surface scattered field and the two fields scattered from the foliage. Although the Foldy-Twersky theory can be used to account for the propagation through the foliage, investigations of the method of smoothing are also being carried out. The method of smoothing is also proposed for use in the surface scattering part of the problem. Particular attention is directed toward the asymptotic evaluation of the first interaction terms in this formalism. GRA

N85-32229# University of Western Kentucky, Bowling Green.
CALIBRATION AND USE OF CLUTTER DATA FOR SIMULATION Final Technical Report
M. S. Longmire 1985 212 p
(Contract N00014-84-C-2034)
(AD-A154793) Avail: NTIS HC A10/MF A01 CSCL 17/5

Part 1 of this report describes calibration of the radiometer for the Background Measurements and Analysis Program (BMAP). Part 2 is an article with results bearing on two-dimensional signal processing. (It was published in Applied Optics 15 Feb., 1985). Part 3 consists of vugraphs and supplemental text for two BMAP reviews and an Optical Sciences Division colloquium. The purpose of BMAP is to collect natural infrared background data for use in simulating the performance of Infared Search and Tracks sets (IRSTs). Usually the objects sought by an IRST are effectively point sources; that is, their images are unresolved (no larger than a detector element). Thus, the point response of the BMAP sensor and electronics must be well characterized for the intended data use. The response to a bar source must also be determined in order to correct the data for certain instrumental artifacts. The BMAP instruments should also be radiometrically calibrated so that simulated signals added to the background data can be related, at least approximately, to radiances of targets. GRA

N85-32230# Coast Guard, Washington, D.C. Office of Research and Development.
APPLICATION OF ADAPTIVE NOISE CANCELLATION TO COAST GUARD VOICE COMMUNICATIONS Final Report
B. B. Peterson, K. U. Dykstra, and M. D. Sakahara Mar. 1985 104 p
(AD-A154798; USCG-D-5-85) Avail: NTIS HC A06/MF A01 CSCL 17/2

A variety of approaches to the digital filtering of voice signals corrupted by background engine noise are presented. These approaches include the standard Least Mean Square adaptive noise cancellation algorithm, an optimum fixed weight filter, a special type of notch filter and frequency domain adaptive noise cancellation. The filters have been implemented both off-line using FORTRAN programs on an LSI-11/2 microcomputer, and in real time using thee Texas Instruments TMS 320 microprocessor and in PDP-11 assembly language using an LSI-11/2. Frequency domain adaptive filtering was seen to be superior to the LMS time domain algorithm because its much greater computational efficiency allowed the analysis of much longer filters. A digital filter that exploits the engine noise by having a notch at each harmonic was seen to be more effective than any of the adaptive

filters. The digital filter equations are derived, starting with a particular periodic reference input. This adaptive filter is shown to be, in reality, an infinite impulse response, time invariant filter.
Author (GRA)

N85-32231# Naval Surface Weapons Center, Dahlgren, Va.
DOPPLER SATELLITE DATA CHARACTERISTICS Final Report
R. J. Anderle Oct. 1983 53 p
(AD-A154868; NSWC/TR-83-353) Avail: NTIS HC A04/MF A01 CSCL 20/14

Random, oscillator and ionospheric errors are reviewed for Doppler observations of satellites. For omnidirectional antennas, random errors of Doppler measurements over 30-second intervals exceeded 20 cm about 30 percent of the time yielding measurement precision in the satellite position of about 50 cm based on a pass of data. High gain antennas showed random errors of only a few centimeters, but gave a precision in position of only 4 m because of the short Doppler count normally made with the equipment considered. However, oscillator errors significantly degrade this precision unless stabilities of about 5X10 to the -13th power are achieved for averaging times of about 1000 seconds. If such oscillators are utilized, a higher precision in position determination can be realized for continuously counted Doppler data by exploiting the continuous character of the measurement in the processing of the data. Neglected higher order ionospheric effects produce measurement errors equivalent to a meter or more during periods of high solar activity. Author (GRA)

N85-32232# Mississippi Univ., University. Dept. of Electrical Engineering.
GUIDED-MODE LAUNCHING IN A SLAB WAVEGUIDE BY WAY OF DIFFRACTION AT THE EDGE OF A CONDUCTING SCREEN RESIDING ON ONE SURFACE OF THE SLAB Final Technical Report, 1 Jan. 1983 - 1 Jan. 1985
T. H. Farris and L. W. Pearson Mar. 1985 65 p
(Contract N00014-81-K-0256)
(AD-A154886) Avail: NTIS HC A04/MF A01 CSCL 09/1

The behavior of electromagnetic fields in the presence of a dielectric waveguide or in the presence of a perfectly electrically conducting (p.e.c.) half plane constitute two general classes of problems in the study of electromagnetics. In this report we consider the case of a p.e.c. half plane residing on one surface of a dielectric slab waveguide in a homogeneous, lossless medium. A transverse magnetic plane wave impinges on the waveguide from the side of the slab on which the half plane resides. The boundary conditions for the electric field tangential to the half plane are cast in a form amenable to a Wiener-Hopf solution, from which the scattered electric field in the interior of the slab waveguide is obtained in terms of a radiation integral. This integral is evaluated using the method of steepest descents, and the resulting electric field is separated into a geometrical optics contribution, a contribution from diffraction at the edge of the half plane, a contribution from refraction by the waveguide, and guided-mode contributions. GRA

N85-32233# Monroe (Richard L.) Associates, Washington, D.C.
A THEORY OF ELECTROMAGNETIC SHIELDING WITH APPLICATIONS TO MIL-STD-285, IEEE-299, AND EMP SIMULATION
R. L. Monroe Feb. 1985 209 p
(Contract DAAK21-83-C-0052; DA Proj. 1L1-62120-AH-25)
(AD-A154905; HDL-CR-85-052-1) Avail: NTIS HC A10/MF A01 CSCL 20/14

A shielding theory based on Impedance Boundary Conditions is developed and used to obtain formal expressions for the fields transmitted to the interior of a generalized metallic structure from an arbitrary, external, time harmonic, electromagnetic source. The structure is an assemblage of planar sheets that may be penetrated by a finite number of narrow rectangular slots. It includes both a single sheet (continuous or slotted) and a rectangular enclosure (continuous or slotted) as special cases. Explicit expressions are then derived for the transmitted electric and magnetic fields at points on the inside surfaces of plane sheets (continuous and slotted) and rectangular enclosures (continuous and slotted) when these structures are exposed to fields from elementary electric and magnetic dipoles and small rectangular loop antennas. These expressions are then used to obtain the shielding effectiveness of sheets and enclosures. GRA

N85-32234# Rome Air Development Center, Griffiss AFB, N.Y.
THE USE OF THE GLISTENING SURFACE CONCEPT IN ROUGH SURFACE SCATTERING Technical Report, Jun. 1983 - Jun. 1984
R. J. Papa, J. F. Lennon, and R. L. Taylor Jul. 1984 36 p
(AF Proj. 2305)
(AD-A154922; RADC-TR-84-159) Avail: NTIS HC A03/MF A01 CSCL 17/9

Calculations of diffuse power scattered from a rough surface have typically used the concept of a glistening surface over which a centerline-varying surface cross section is integrated. The usual form of that surface is derived for relatively smooth surfaces and contains several other constraints that are not always evident. In this report, we will address the limitations on this definition and several alternative forms that are less restrictive. We will compare them with a more realistic solution in which the azimuthal variation in the surface cross section is taken into account and the integration is across the entire signal footprint on the surface. The standard scattering surface dimensions are determined under constraints on both the antenna heights and the surface width. In the report, we analyze the effect of removing those constraints. In addition, we consider a second formulation in which one of the antenna terminals of the bistatic system is considered to be sufficiently distant so that it is treated as being at infinity. We examine the different boundary values for the glistening surface based on these different assumptions and compare the resultant scattered power levels with the azimuthally varying cross section results. One of the most important conclusions is that the use of the centerline normalized cross section models can lead to calculated diffuse power levels that are in disagreement with the results for the more exact solution in which both the azimuthal variation in sigma deg is accounted for and the integration is always across the entire radar footprint rather than a calculated glistening surface width. GRA

N85-32235# Rome Air Development Center, Griffiss AFB, N.Y.
AN ANALYSIS OF PHYSICAL OPTICS MODELS FOR ROUGH SURFACE SCATTERING Report, Jan. 1983 - Jun. 1984
R. J. Papa, J. F. Lennon, and R. L. Taylor Sep. 1984 35 p
(AD-A154960; RADC-TR-84-195) Avail: NTIS HC A03/MF A01 CSCL 17/2

Many techniques have been applied to analyze the effects of the environment (specifically rough surface scattering) on the performance of radar and communication systems. Physical Optics is one of the most frequently applied approaches. Several topics include the limitations and constraints that are inherent in the application of physical optics models, the ranges of its validity, different representations of normalized cross sections, alpha, and the parameter ranges in which those forms have to be used, and finally the effect of the different representations for alpha on the calculation of diffuse scattered power. It is shown that if the Rayleigh parameter dependence of alpha is taken into account and the surface shadowing is included, then the physical optics model for electromagnetic scattering can be applied to surfaces that represent an extensive range of roughness conditions. GRA

N85-32236# Royal Signals and Radar Establishment, Malvern (England).
ASPECTS OF SAR IMAGE SEGMENTATION
S. C. Giess Feb. 1985 26 p
(AD-A154965; RSRE-MEMO-3789; DRIC-BR-95551) Avail: NTIS HC A03/MF A01 CSCL 17/9

An expression for the speckle structure seen on Synthetic Aperture Radar (SAR) images is derived. This model is used to investigate the applicability of the simple segmentation operators usually used for image analysis to the problem of the segmentation

of SAR images. These simple operators are shown to be incapable of segmenting raw SAR images satisfactorily. However they can be applied to successfully to a area averaged SAR images provided certain constraints are met. Possible segmentation approaches are examined in the light of these constraints. GRA

N85-32237# Naval Postgraduate School, Monterey, Calif.
FIN LINE FILTERS TECHNOLOGY AND ELECTRONIC WARFARE M.S. Thesis
S. Vitalis Dec. 1984 100 p
(AD-A154975) Avail: NTIS HC A05/MF A01 CSCL 17/4

Waveguide E plane fin line filters with various numbers of inductive strips are analyzed using the MICRO-COMPACT (MPAC) computer program. The scattering parameters for the inductive strips are obtained from a spectral domain program (FINSTRIP). Filters were fabricated and tested in X-band (8-12 GHz). Good agreement between the predicted response from a MICRO-COMPACT (MPAC) program and the measured response from a network analyzer was obtained in the case of simple filters (two inductive strips). Some applications of fin line filter technology in electronic warfare are also shown. Author (GRA)

N85-32238# Naval Postgraduate School, Monterey, Calif.
AN ANALYSIS OF THE MATERIEL FIELDING PLAN FOR THE SINCGARS (SINGLE CHANNEL GROUND AND AIRBORNE RADIO SYSTEM) RADIO M.S. Thesis
C. M. Tegen Dec. 1984 87 p
(AD-A155101) Avail: NTIS HC A05/MF A01 CSCL 15/5

This thesis is an analysis of the materiel fielding plan (MFP) for the Army's Single Channel Ground and Airborne Radio System (SINCGARS). Objectives of the study are to identify major potential problem areas in the MFP, and to generate recommendations for resolving these problems. The study involves a specific analysis of the maintenance and supply support aspects of the MFP within the context of the Major System acquisition framework. Research included extensive field interviews with personnel in the functional management areas of the Communications and Electronics Command (CECOM), the Project Office, and the Department of Army Staff. Potential problems identified concern the redistribution of VRC-12 series and PRC-77 radios, the imbedded COMSEC modification, and the issue of warranties. Recommendations include purchasing a warranty for the original production contract, improving the planning for redistribution of old radios, and providing strict control over the design of the imbedded COMSEC modification. GRA

N85-32239# Naval Postgraduate School, Monterey, Calif.
EXPERIMENTAL EVALUATION OF A NEW FORM OF M-ary (M = 8) PHASE SHIFT KEYING INCLUDING DESIGN OF THE TRANSMITTER AND RECEIVER M.S. Thesis
G. E. Thompson Dec. 1984 48 p
(AD-A155103) Avail: NTIS HC A03/MF A01 CSCL 17/2

For transmitting digital information over bandpass channels, M-ary Phase Shift Keying 8(PSK) schemes are used to conserve bandwidth at the expense of signal power. A block of k bits is used to change the phase of the carrier. These k bits represent M possible phase shifts since M = 2. Common forms of M-ary PSK use equally spaced phase angles. For example, if M = 8 and k=3, 8-ary PSK,uses eight phase angles spaced 45 degrees apart. This thesis considers a hybrid form of PSK when M = 8 and k = 3. Each of eight blocks of data with three bits per block are represented by different phase shifts of the carrier. The phase angles are chosen to give an equal distance between states (symbols) when projected onto the sine axis and the cosine axis of a phasor diagram. Thus, when the three bits are recovered, using two coherent phase detectors, the separation of the decision regions (voltage levels) are equal. GRA

N85-32240# Rome Air Development Center, Griffiss AFB, N.Y.
COMPRESSION OF SPREAD SPECTRUM SIGNALS ON AN EXCESSIVELY DISPERSIVE CHANNEL
D. M. Haines Oct. 1984 18 p
(AF Proj. 4600)
(AD-A155184; RADC-TM-84-23) Avail: NTIS HC A02/MF A01 CSCL 09/4

There are several new techniques for correcting time dispersive distortion of wideband and/or spread spectrum signals using signal processing capabilities which can be embedded into modern communications systems. These include adaptive channel equalization and in the case of spread spectrum signals, synchronous correlation, matched filtering and Rake processing. This paper shows several distinct advantages in the combination of matched filtering and Rake processing for handling dispersion of spread spectrum signals. GRA

N85-32241# Rome Air Development Center, Hanscom AFB, Mass.
NULL SYNTHESIS WITH PHASE AND AMPLITUDE CONTROLS AT THE SUBARRAY OUTPUTS Report, 1 Mar. - 14 May 1984
R. L. Haupt Sep. 1984 26 p
(AF Proj. 2305)
(AD-A155187; RADC-TR-84-197) Avail: NTIS HC A03/MF A01 CSCL 09/5

This report investigates the generation of nulls in an antenna pattern by controlling the phase and amplitude of the subarray output signals. Although the nulls may be formed with any number of subarrays, the subarray configuration and desired null location have a major impact on the distortion problem resulting from subarray nulling is well known, but little theoretical analysis has been done to explain the cause of the distortion. This report offers a theoretical and graphical explanation of why the distortion occurs. GRA

N85-32242# Electromagnetic Compatibility Analysis Center, Annapolis, Md.
FIELD ANTENNA HANDBOOK
J. A. Kuch (IIT Research Inst., Chicago) Jun. 1984 107 p
(Contract F19628-80-C-0042)
(AD-A155204; ECAC-CR-83-200) Avail: NTIS HC A06/MF A01 CSCL 09/5

This handbook presents basic propagation theory, the fundamentals concerning antennas, and the design and use of tactical high frequency and very high frequency antennas. It is a field reference for basic antenna facts and a usage guide for antennas. GRA

N85-32243# Naval Research Lab., Washington, D. C.
HUFFMAN-CODED PULSE COMPRESSION WAVEFORMS Interim Report
F. F. Kretschmer, Jr. and F. C. Lin 23 May 1985 18 p
(AD-A155322; NRL-8894) Avail: NTIS HC A02/MF A01 CSCL 17/9

Radar pulse compression waveforms usually consist of constant amplitude signals whose phase or frequency is varied to obtain the desired bandwidth and sidelobe levels. However, with Huffman-coded waveforms, both the amplitude and phase vary from subpulse to subpulse. These codes are investigated in detail and compared in performance with other pulse compression waveforms. GRA

N85-32244# Naval Postgraduate School, Monterey, Calif.
SECURITY CONTROLS IN THE STOCKPOINT LOGISTICS INTEGRATED COMMUNICATIONS ENVIRONMENT (SPLICE) M.S. Thesis
D. S. Arseneault Mar. 1985 91 p
(AD-A155536) Avail: NTIS HC A05/MF A01 CSCL 09/2

This thesis examines security controls specified and implemented in the Stock Point Logistics Integrated Communications Environment (SPLICE) project. Controls provided by the Defense Data Network and the Tandem operating system are reviewed. Alternatives from current literature in areas of authentication, encryption, and dial-port protection are reviewed for the purpose of suggesting enhancements. Issues discussed apply to most interactive/decentralized systems in operation today and include administrative as well as technical recommendations. GRA

N85-32245# Texas Univ., Austin. Electrical Engineering Research Lab.
A MULTIPLYING SLOT ARRAY
N. Camilleri and T. Itoh 1 May 1985 145 p
(Contract DAAG29-84-K-0076)
(AD-A155570; TR-85-1; ARO-21438.13-EL) Avail: NTIS HC A07/MF A01 CSCL 09/5

In search of a high power millimeter wave source this paper describes a novel multiplying slot array with space combining capability. This device distributes the power of a fundamental oscillator to an array of slots that are resonant at the second harmonic. The second harmonic is produced at the diode on each of the slots and is then radiated and power combined in free-space. The feasibility of adequate single element conversion efficiency and the use of high density slot elements has been successfully demonstrated. Single slot conversion loss measured for X and Ka-band models produced encouraging results. An 8-element multiplying array exhibited better than -12 dB side lobe level at 70 GHz. The simplicity of construction of such a device makes it useful at millimeter wave frequencies. The possibility of monolithic design is very feasible due to the simplicity of the structure.
Author (GRA)

N85-32246# Naval Postgraduate School, Monterey, Calif.
HEAD-ON SCATTERING OF A TUBULAR CYLINDER OF FINITE LENGTH FOR RADAR TARGET IDENTIFICATION PURPOSES M.S. Thesis
D. Geller Mar. 1985 157 p
(AD-A155608) Avail: NTIS HC A08/MF A01 CSCL 17/9

This thesis studies the head-on backscattering of a finite tubular cylinder with a circular cross-section and a very thin conducting wall. At this aspect angle, the backscattered fields depend only on the first Fourier component of the circumferential variations of the Psi-current. Measurements of several scaled tubular cylinders were taken and the experimental results were compared to theoretical data available. This thesis is part of an ongoing project of target identification through the investigation of the cross section of a target over a broad frequency band. Author (GRA)

N85-32247# Computer Sciences Corp., Falls Church, Va. Systems Div.
FLEXIBLE SATELLITE COMMUNICATIONS SYSTEMS SIMULATOR, PHASE 3 Final Report, Mar. 1984 - Apr. 1985
D. F. Arnaud and J. H. Shattuck 16 May 1985 227 p
(Contract DCA100-77-C-0020)
(AD-A155647) Avail: NTIS HC A11/MF A01 CSCL 17/2

This FSCSS Phase 3 Final Report describes the work performed during Phase 3 of Contract DCA100-77-C-0020. The work reported here includes the implementation of additional features of the Flexible Satellite Communications Systems Simulator (FSCSS), the Phase 3 acceptance tests and the documentation of the FSCSS Version 3.0 software. The work performed during Phase 3 falls into the following five categories: (1) Enhancements to the input process; (2) Addition of a color graphics capability; (3) Enhancements to the output process; (4) Simulation capabilities enhancements; and (5) New devices. GRA

N85-32248# Naval Postgraduate School, Monterey, Calif.
BROADSIDE SCATTERING OF A TUBULAR CYLINDER FOR EVALUATION OF TARGET IDENTIFICATION M.S. Thesis
B. Haklay Mar. 1985 152 p
(AD-A155739; AD-F300619) Avail: NTIS HC A08/MF A01 CSCL 17/9

The concept of target identification through its backscattering cross section, in the resonance region was investigated. Measurements from the broadside aspect angle of several scaled tubular cylinders have been used for this purpose. The experimental results and theoretical approximation for some of the cylinders are presented. That data will serve as the baseline for further investigation in this project. Detection by radar is done by detecting the backscattered electromagnetic signal returned from a target. The backscattered signal originates from the surface currents excited on the object when it is irradiated by an incident electromagnetic wave. Different targets have different outer surface that cause different surface currents to flow on the target when identical incident waves are irradiating the targets. GRA

N85-32249# California Univ., Livermore. Lawrence Livermore Lab.
NUMERICAL MODELING OF SUBSURFACE COMMUNICATION
G. J. Burke, C. G. Dease, E. M. Didwall, and R. J. Lytle Feb. 1985 42 p refs
(Contract W-7405-eng-48)
(DE85-012818; UCID-20439) Avail: NTIS HC A03/MF A01 CSCL 17B

Techniques are described for numerical modeling of through-the-Earth communication. The basic problem considered is evaluation of the field at a surface or airborne station due to an antenna buried in the Earth. Equations are given for the field of a point source in a homogeneous or stratified earth. These expressions involve infinite integrals over wave number, sometimes known as Sommerfield integrals. Numerical techniques used for evaluating these integrals are outlined. The problem of determining the current on a real antenna in the Earth, including the effect of insulation, is considered. Results are included for the fields of a point source in homogeneous and stratified earths and the field of a finite insulated dipole. The results are for electromagnetic propagation in the ELF-VLF range, but the codes also can address propagation problems at higher frequencies. DOE

N85-32250# Sandia Labs., Albuquerque, N. Mex.
CALCULATION OF THE PROPAGATION CONSTANT IN A RECTANGULAR WAVEGUIDE CONTAINING AN INHOMOGENEOUS LONGITUDINALLY MAGNETIZED PLASMA
L. K. Warne Feb. 1985 36 p refs
(Contract DE-AC04-76DP-00789)
(DE85-012072; SAND-85-0219) Avail: NTIS HC A03/MF A01

An experiment is currently being conducted to monitor breakdown phenomena in nitrogen (G. Hays, 1100 Quarterly Report Solid State Sciences, July to September 1984, Sandia National Laboratories). The motivation is provided by current interest in atmospheric propagation of large amplitude short rise time electromagnetic fields. The gas sample in the experiment is contained within a quartz cell in a rectangular waveguide. The sample is also biased by a longitudinal magnetostatic field to help increase absorption. A small amplitude interferometer is then used to monitor the electron density in the cell. This report summarizes an analysis done in support of this experiment. Standard perturbation is used to calculate the propagation constant in the gas sample making it possible to relate the electron density in the sample to the phase shift measured by the interferometer. The effects of the quartz cell are also determined. DOE

N85-32511*# EISCAT Scientific Association, Kiruna (Sweden).
CRITERIA FOR SITE SELECTION AND FREQUENCY ALLOCATION (KEYNOTE PAPER), PART 5
J. Rottger *In* International Council of Scientific Unions Middle Atmosphere Program: Handbook for MAP. Vol. 14 Dec. 1985 p 234-244 refs (For primary document see N85-32466 21-46)
Avail: NTIS HC A17/MF A01; also avail. from SCOSTEP Secretariat, Illinois Univ., 1406 West Green St., Urbana, Ill. 61801 CSCL 17B

N85-32512*# Control Data Corp., Minneapolis, Minn.
FREQUENCY AND SITE SELECTION CRITERIA FOR MST RADARS, PART 5.1A
G. D. Nastrom *In* International Council of Scientific Unions Middle Atmosphere Program: Handbook for MAP. Vol. 14 Dec. 1984 p 245 refs (For primary document see N85-32466 21-46)
Avail: NTIS HC A17/MF A01; also avail from SCOSTEP Secretariat, Illinois Univ., 1406 West Green St., Urbana, Ill. 61801 CSCL 17B

N85-32513*# EISCAT Scientific Association, Kiruna (Sweden).
MOST DESIRABLE TERRAIN, E.G., FLAT VS VALLEY LOCATION, PART 5.1B

J. Rottger *In* International Council of Scientific Unions Middle Atmosphere Program: Handbook for MAP. Vol. 14 Dec. 1984 p 246-248 (For primary document see N85-32466 21-46)
Avail: NTIS HC A17/MF A01; also avail. from SCOSTEP Secretariat, Illinois Univ., 1406 West Green St., Urbana, Ill. 61801 CSCL 17B

N85-32514# National Oceanic and Atmospheric Administration, Boulder, Colo. Aeronomy Lab.
SUMMARY OF SESSION ON OPTIMUM TRANSMITTER AND ANTENNA CONFIGURATION FOR MST RADAR, PART 6
J. L. Green *In* International Council of Scientific Unions Middle Atmosphere Program: Handbook for MAP. Vol. 141 Dec. 1984 p 249-250 (For primary document see N85-32466 21-46)
Avail: NTIS HC A17/MF A01; also avail. from SCOSTEP Secretariat, Illinois Univ., 1406 West Green St., Urbana, Ill. 61801 CSCL 17B

N85-32517*# EISCAT Scientific Association, Kiruna (Sweden).
INCREASE OF ANTENNA AREA INSTEAD OF TRANSMITTER POWER, PART 6.3A
J. Rottger *In* International Council of Scientific Unions Middle Atmosphere Program: Handbook for MAP. Vol. 14 Dec. 1984 p 257-258 refs (For primary document see N85-32466 21-46)
Avail: NTIS HC A17/MF A01; also avail. from SCOSTEP Secretariat, Illinois Univ., 1406 West Green St., Urbana, Ill. 61801 CSCL 09C

N85-32518*# National Oceanic and Atmospheric Administration, Boulder, Colo. Aeronomy Lab.
TESTING AND OPTIMIZING MST COAXIAL COLLINEAR ARRAYS, PART 6.4A
J. M. Warnock and J. L. Green *In* International Council of Scientific Unions Middle Atmosphere Program: Handbook for MAP. Vol. 14 Dec. 1984 p 259-261 refs (For primary document see N85-32466 21-46)
Avail: NTIS HC A17/MF A01; also avail. from SCOSTEP Secretariat, Illinois Univ., 1406 West Green St., Urbana, Ill. 61801 CSCL 09C

N85-32519*# Cornell Univ., Ithaca, N.Y. School of Electrical Engineering.
OVERVIEW OF ON-LINE DATA PROCESSING FOR MST RADARS (KEYNOTE PAPER), PART 7
D. T. Farley *In* International Council of Scientific Unions Middle Atmosphere Program: Handbook for MAP. Vol. 14 Dec. 1984 p 262-267 (For primary document see N85-32466 21-46)
Avail: NTIS HC A17/MF A01; also avail. from SCOSTEP Secretariat, Illinois Univ., 1406 West Green St., Urbana, Ill. 61801 CSCL 17I

N85-32520*# Illinois Univ., Urbana. Dept. of Electrical Engineering.
CODING SCHEMES FOR IMPROVING MST RADAR PERFORMANCE, PART 7.1A
S. A. Bowhill *In* International Council of Scientific Unions Middle Atmosphere Program: Handbook for MAP. Vol. 14 Dec. 1984 p. 268-270 refs (For primary document see N85-32466 21-46) (Grant NGR14-005-181)
Avail: NTIS HC A17/MF A01; also avail. from SCOSTEP Secretariat, Illinois Univ., 1406 West Green St., Urbana, Ill. 61801 CSCL 17I

N85-32527*# Case Western Reserve Univ., Cleveland, Ohio. Dept. of Electrical Engineering and Applied Physics.
CRITERIA AND ALGORITHMS FOR SPECTRUM PARAMETERIZATION OF MST RADAR SIGNALS
P. K. Rastogi *In* International Council of Scientific Unions Middle Atmosphere Program: Handbook for MAP. Vol. 14 Dec. 1984 p 289-293 refs (For primary document see N85-32466 21-46)
Avail: NTIS HC A17/MF A01; also avail. from SCOSTEP secretariat, Illinois Univ., 1406 West Green St., Urbana, Ill. 61801 CSCL 17I

N85-32535*# Cornell Univ., Ithaca, N.Y. School of Electrical Engineering.
STATUS OF THE JICAMARCA RADAR
T. Farley *In* International Council of Scientific Unions Middle Atmosphere Program. Handbook for MAP. Vol. 14 Dec. 1984 p 319-320 (For primary document see N85-32466 21-46)
Avail: NTIS HC A17/MF A01; also available from SCOSTEP Secretariat, Illinois Univ., 1406 West Green Street, Urbana, Ill. 61801 CSCL 17I

N85-32536*# National Oceanic and Atmospheric Administration, Boulder, Colo. Aeronomy Lab.
RECENT RESULTS AT THE SUNSET RADAR
J. L. Green, J. M. Warnock, and W. L. Clark *In* International Council of Scientific Unions Middle Atmosphere Program. Handbook for MAP. Vol. 14 Dec. 1984 p 321-323 refs (For primary document see N85-32466 21-46)
Avail: NTIS HC A17/MF A01; also available from SCOSTEP Secretariat, Illinois Univ., 1406 West Green Street, Urbana, Ill. 61801 CSCL 04A

N85-32537*# Utah State Univ., Logan.
THE BOOT LAKE MF IMAGING RADAR
G. W. Adams and J. W. Brosnahan (Tycho Technology, Inc., Boulder, Colo.) *In* International Council of Scientific Unions Middle Atmosphere Program. Handbook for MAP. Vol. 14 Dec. 1984 p 324 ref (For primary document see N85-32466 21-46)
Avail: NTIS HC A17/MF A01; also available from SCOSTEP Secretariat, Illinois Univ., 1406 West Green Street, Urbana, Ill. 61801 CSCL 17I

N85-32538*# Georgia Inst. of Tech., Atlanta. School of Geophysical Sciences.
MENTOR: ADDING AN OUTLYING RECEIVER TO AN ST RADAR FOR METEOR-WIND MEASUREMENT
R. G. Roper *In* International Council of Scientific Unions Middle Atmosphere Program. Handbook for MAP. Vol. 14 Dec. 1984 p 325-329 (For primary document see N85-32466 21-46)
Avail: NTIS HC A17/MF A01; also available from SCOSTEP Secretariat, Illinois Univ., 1406 West Green Street, Urbana, Ill. 61801 CSCL 04A

N85-32539*# National Oceanic and Atmospheric Administration, Boulder, Colo. Aeronomy Lab.
SUMMARY OF PROGRESS AT THE POKER FLAT OBSERVATORY IN ALASKA
B. B. Balsley *In* International Council of Scientific Unions Middle Atmosphere Program. Handbook for MAP. Vol. 14 Dec. 1984 p 330 refs (For primary document see N85-32466 21-46)
Avail: NTIS HC A17/MF A01; also available from SCOSTEP Secretariat, Illinois Univ., 1406 West Green Street, Urbana, Ill. 61801 CSCL 04A

N85-32540*# Illinois Univ., Urbana. Dept. of Electrical and Computer Engineering.
URBANA RADAR SYSTEMS: POSSIBILITIES AND LIMITATIONS
O. Royrvik *In* International Council of Scientific Unions Middle Atmosphere Program. Handbook for MAP. Vol. 14 Dec. 1984 p 331-336 refs (For primary document see N85-32466 21-46)
Avail: NTIS HC A17/MF A01; also available from SCOSTEP Secretariat, Illinois Univ., 1406 West Green Street, Urbana, Ill. 61801 CSCL 17I

N85-32541*# Alaska Univ., Fairbanks. Geophysical Inst.
THE SONDRESTROM RADAR: PROGRESS AND PROPOSED UPGRADES FOR ST WORK
B. J. Watkins *In* International Council of Scientific Unions Middle Atmosphere Program. Handbook for MAP. Vol. 14 Dec. 1984 p 337-338 ref (For primary document see N85-32466 21-46)
Avail: NTIS HC A17/MF A01; also available from SCOSTEP Secretariat, Illinois Univ., 1406 West Green Street, Urbana, Ill. 61801 CSCL 17I

N85-32542*# National Oceanic and Atmospheric Administration, Boulder, Colo. Wave Propagation Lab.
PROGRESS AND PLANS FOR THE COLORADO WIND PROFILER NETWORK
R. G. Strauch *In* International Council of Scientific Unions Middle Atmosphere Program. Handbook for MAP. Vol. 14 Dec. 1984 p 339-340 refs (For primary document see N85-32466 21-46)
Avail: NTIS HC A17/MF A01; also available from SCOSTEP Secretariat, Illinois Univ., 1406 West Green Street, Urbana, Ill. 61801 CSCL 17I

N85-32543*# Kyoto Univ. (Japan). Radio Atmospheric Science Center.
THE MU RADAR NOW PARTLY IN OPERATION
S. Kato, T. Ogawa, T. Tsuda, T. Sato, I. Kimura, and S. Fukao *In* International Council of Scientific Unions Middle Atmosphere Program. Handbook for MAP. Vol. 14 Dec. 1984 p 341-349 refs (For primary document see N85-32466 21-46)
Avail: NTIS HC A17/MF A01; also available from SCOSTEP Secretariat, Illinois Univ., 1406 West Green Street, Urbana, Ill. 61801 CSCL 04B

N85-32544*# Pennsylvania State Univ., University Park. Dept. of Meteorology.
NETWORK ST RADAR AND RELATED MEASUREMENTS AT PENNSYLVANIA STATE UNIVERSITY Progress Report
D. W. Thomson, C. W. Fairall, and R. M. Peters *In* International Council of Scientific Unions Middle Atmosphere Program. Handbook for MAP. Vol. 14 Dec. 1984 p 350-355 (For primary document see N85-32466 21-46)
Avail: NTIS HC A17/MF A01; also available from SCOSTEP Secretariat, Illinois Univ., 1406 West Green Street, Urbana, Ill. 61801 CSCL 17I

N85-32545*# Science Research Council, Chilton (England). Rutherford Appleton Lab.
A NOTE ON THE PROPOSED UK VHF RADAR
A. J. Hall *In* International Council of Scientific Unions Middle Atmosphere Program. Handbook for MAP. Vol. 14 Dec. 1984 p 356 (For primary document see N85-32466 21-46)
Avail: NTIS HC A17/MF A01; also available from SCOSTEP Secretariat, Illinois Univ., 1406 West Green Street, Urbana, Ill. 61801 CSCL 17I

N85-32547*# Centre National d'Etudes des Telecommunications, Saint Maur des Fosses (France).
THE PROUST RADAR
M. Petitdidier *In* International Council of Scientific Unions Middle Atmosphere Program. Handbook for MAP. Vol. 14 Dec. 1984 p 360-361 (For primary document see N85-32466 21-46)
Avail: NTIS HC A17/MF A01; also available from SCOSTEP Secretariat, Illinois Univ., 1406 West Green Street, Urbana, Ill. 61801 CSCL 17I

N85-32548*# Northeast Radio Observatory Corp., Westford, Mass. Haystack Observatory. Haystack Observatory.
MILLSTONE HILL RADAR: CAPABILITIES FOR S/T OBSERVATIONS
G. B. Loriot *In* International Council of Scientific Unions Middle Atmosphere Program. Handbook for MAP. Vol. 14 Dec. 1984 p 362 (For primary document see N85-32466 21-46)
Avail: NTIS HC A17/MF A01; also available from SCOSTEP Secretariat, Illinois Univ., 1406 West Green Street, Urbana, Ill. 61801 CSCL 17I

N85-32549*# National Oceanic and Atmospheric Administration, Boulder, Colo. Aeronomy Lab.
THE PONAPE ST RADAR
D. A. Carter, W. L. Ecklund, and B. B. Balsley *In* International Council of Scientific Unions Middle Atmosphere Program. Handbook for MAP. Vol. 14 Dec. 1984 p 363 (For primary document see N85-32466 21-46)
Avail: NTIS HC A17/MF A01; also available from SCOSTEP Secretariat, Illinois Univ., 1406 West Green Street, Urbana, Ill. 61801 CSCL 17I

33 ELECTRONICS AND ELECTRICAL ENGINEERING

Includes test equipment and maintainability; components, e.g., tunnel diodes and transistors; microminiaturization; and integrated circuitry.

For related information see also *60 Computer Operations and Hardware* and *76 Solid-State Physics.*

N85-32251*# Electrotek Concepts, Inc., Knoxville, Tenn.
EXPERIMENTAL INVESTIGATION OF A VARIABLE SPEED CONSTANT FREQUENCY ELECTRIC GENERATING SYSTEM FROM A UTILITY PERSPECTIVE
J. I. Herrera, T. W. Reddoch, and J. S. Lawler May 1985 52 p refs
(Contracts NAS3-24105; DE-AI01-76ET-20320)
(NASA-CR-174950; NAS 1.26:174950; DOE/NASA/4105-1) Avail: NTIS HC A03/MF A01 CSCL 09C

As efforts are accelerated to improve the overall capability and performance of wind electric systems, increased attention to variable speed configurations has developed. A number of potentially viable configurations have emerged. Various attributes of variable speed systems need to be carefully tested to evaluate their performance from the utility points of view. With this purpose, the NASA experimental variable speed constant frequency (VSCF) system has been tested. In order to determine the usefulness of these systems in utility applications, tests are required to resolve issues fundamental to electric utility systems. Legitimate questions exist regarding how variable speed generators will influence the performance of electric utility systems; therefore, tests from a utility perspective, have been performed on the VSCF system and an induction generator at an operating power level of 30 kW on a system rated at 200 kVA and 0.8 power factor. Author

N85-32252*# Westinghouse Defense and Electronic Systems Center, Baltimore, Md. Advanced Tech. Labs.
STRIPE FILTERS ON MULTISPECTRAL LINEAR ARRAYS Final Report
J. H. Hall, F. C. Blaha, B. R. Frias, J. Halvis, and E. Hubbard 15 May 1982 118 p
(Contract NAS5-25622)
(NASA-CR-175305; NAS 1.26:175305) Avail: NTIS HC A06/MF A01 CSCL 09C

Dielectric interference filters deposited directly on top of existing 200 element charge coupled device linear imaging arrays were designed, fabricated and evaluated. The optical performance of the filters was verified with regard to crosstalk between adjacent detector elements. The filters showed an average in-band transmittance greater than 80% and a total out of band transmittance of less than 5%. Filter stability was adequate for operation in a space environment. The filter elements were definable in 12 to 25 micron element size compatible with existing silicon detectors. These type of measurement were made: (1) spectral transmission of the filter as deposited on witness plates; (2) spectral response of the silicon sensing device; (3) any optical interaction between filter and sensing device; (4) the response of the filter/sensor combination; and (5) repeatability and uniformity of filter characteristics. Detailed discussion of these evaluations are given. E.R.

N85-32253# Ceramphysics, Inc., Westerville, Ohio.
CAPACITIVE ENERGY STORAGE AT CRYOGENIC TEMPERATURES Final Report, 1 Sep. 1984 - 28 Feb. 1985
W. N. Lawless and C. F. Clark 15 Feb. 1985 43 p
(Contract F49620-84-C-0089)
(AD-A154508; AFOSR-85-0377TR) Avail: NTIS HC A03/MF A01 CSCL 10/2

A Phase 1 research program on capacitive energy storage at liquid-nitrogen temperatures is reported. A composition in the

cadmium-lead-niobate-tantalate family of ceramic ferroelectrics was chosen with a paraelectric to ferroelectric phase transition at 71 K (so-called CPN17 composition), and prototype multilayer capacitors (MLC's), 1 x 1 x 0.2 cc with 46 active layers, were fabricated for testing. Dielectric-constant, specific-heat, and electrocaloric data were measured on these MLC's in the range 77-100 K at electric fields up to 200 kV/cm. All the measured data can be explained and correlated very satisfactorily using a Ginzburg-Landau expansion of the free energy in combination with the TdS equation for dielectrics. Capacitive-energy-storage densities were computed from the measured electric-field dependence of the dielectric constant at 77 K using the Helmholtz integral. A state-switching phenomenon was observed. The zero-field specific heat of CPN17 is 0.15 J/g/K at 77 K and displays an excess specific heat centered around 82 K. GRA

N85-32254# Purdue Univ., Lafayette, Ind. Turner Lab. for Electroceramics.
MULTILAYER CAPACITOR DIELECTRICS PRODUCED FROM METALLO-ORGANIC PRECURSORS Annual Report, 1 Mar. 1984 - 28 Feb. 1985
R. W. Vest and G. M. Vest 29 Apr. 1985 72 p
(Contract N00014-83-K-0321)
(AD-A154592) Avail: NTIS HC A04/MF A01 CSCL 07/1

The metallo-organic decomposition (MOD) process for preparing films or powders has a number of advantages over conventional processes. The metallo-organic compounds used in the present study had oxygen as the hetero atom to bond a metal atom to an organic ligand. This report is divided into three parts. The first details studies of the kinetics of formation of BaTiO3 and PbTiO3 by the MOD process, and demonstrates that the temperatures required are more than 200 C lower than those needed if the finest available powders are used as precursors. The second part of the report describes a study of the defect structure and dielectric properties of Nd2O3 doped BaTiO3. The use of the MOD process to prepare the various compositions insured the formation of equilibrium phases. The third part of the report discusses preliminary studies of BaTiO3 film formation by the MOD process. GRA

N85-32255# Naval Postgraduate School, Monterey, Calif.
FIN-LINE HORN ANTENNAS M.S. Thesis
J. R. Musitano Dec. 1984 47 p
(AD-A154597) Avail: NTIS HC A03/MF A01 CSCL 09/1

A new, bilateral fin-line horn antenna is introduced and the results of testing discussed. Experimental return loss and absolute gain data are presented and used to make comparisons between the characteristics of conventional and fin-line horns. Classical analysis assuming Huygen source distribution and E-plane sectoral horn modeling is applied with limited success. GRA

N85-32256# National Materials Advisory Board, Washington, D.C.
MAGNETIC MATERIALS Final Report, 15 Mar. 1984 - 29 Mar. 1985
Mar. 1985 101 p
(Contract MDA903-82-C-0434)
(AD-A154679; NMAB-426) Avail: NTIS HC A06/MF A01 CSCL 20/3

The report describes the fundamental role that magnetic materials play in many of the electrical and electronic systems used by modern society. It reviews the status of magnetic materials in their current engineering applications and identifies technical issues whose resolution would lead to improved performance in such applications as well as for new applications of these materials. The report recommends more research in the areas of rare-earth permanent magnets, amorphous magnetic materials and recording media and lists a number of scientific challenges. GRA

N85-32257# General Electric Co., Cincinnati, Ohio. Aircraft Engine Business Group.
HIGH TEMPERATURE ELECTRONICS TECHNOLOGY: LIFE TEST REPORT Final Report, Oct. 1983 - Jun. 1984
D. J. LaCombe Sep. 1984 33 p
(Contract N00014-83-C-2393)
(AD-A154681; R84AEB592) Avail: NTIS HC A03/MF A01 CSCL 09/5

This report presents the results of a series of life tests of silicon Integrated Injection Logic (I2L) microcircuits designed to operate for long periods at temperatures as high as 300 C. The technology needed to design and fabricate these microcircuits was previously developed under Contract N00173-79-C-0010. Two life tests were conducted: an operating-life test at 300 C and a nonoperating-life test at 360 C. Ten chip packages, each containing four identical ring oscillator/counter test circuits, were tested at each temperature. A total of 80 microcircuits were fabricated using two different metallization processes. None of the 300 C test specimens failed; 24 circuits of the 40 completed 3206 hours, and 16 completed 2342 hours. Of the 40 circuits tested at 360 C, 4 experienced infant mortality failure at about 1000 hours, but the remaining 36 circuits ran without failure for 2618 hours. Posttest analysis indicates that metallization deterioration began with scattered formation of void and extruded gold crystals in the connecting runs. The overall test results were considered very encouraging, and operational life is estimated to more than 18,000 hours at 300 deg C. Continued development efforts are recommended. GRA

N85-32258# Massachusetts Inst. of Tech., Cambridge. Lab. of Computer Science.
PARALLEL SIMULATION OF DIGITAL LSI CIRCUITS M.S. Thesis
J. M. Arnold Feb. 1985 102 p
(Contract N00014-83-K-0125)
(AD-A154745; MIT/LCS/TR-333) Avail: NTIS HC A06/MF A01 CSCL 09/5

Integrated circuit technology has been advancing at phenomenal rate over the last several years, and promises to continue to do so. If circuit design is to keep pace with fabrication technology, radically new approaches to computer-aided design will be necessary. One appealing approach is general purpose parallel processing. This thesis explores the issues involved in developing a framework for circuit simulation which exploits the locality exhibited by circuit operation to achieve a high degree of parallelism. This framework maps the topology of the circuit onto the the multiprocessor, assigning the simulation of individual partitions to separate processors. A new form of snychronization is developed, based upon a history maintenance and roll back strategy. The circuit simulator PRSIM was designed and implemented to determine the efficacy of this approach. The results of several preliminary experiments are reported, along with an analysis of the behavior of PRSIM. GRA

N85-32259# Naval Research Lab., Washington, D. C.
THE PLASMA EROSION OPENING SWITCH
R. J. Commisso, G. Cooperstein, R. A. Meger, J. M. Neri, and P. F. Ottinger 14 May 1985 45 p
(AD-A154942; AD-F630641; NRL-MR-5560) Avail: NTIS HC A03/MF A01 CSCL 09/1

The Plasma Erosion Opening Switch (PEOS) can conduct high current (approx. MA), open quickly (<10ns), and withstand high voltage (approx. MV). This switching technique has been used in inductive energy storage experiments and can be used with existing generators for pulse compression, voltage multiplication and power multiplication. The PEOS is used routinely for other types of power conditioning including prepulse suppression, pulse sharpening and multimodule jitter reduction. This paper is a review of the PEOS work to date. It reviews basic physics principles of the PEOS and outlines the operational limits of a system that employs a PEOS. Examples of present applications of the PEOS are also discussed. GRA

N85-32260# Naval Postgraduate School, Monterey, Calif.
DESIGN OF A SIXTEEN-BIT PIPELINED ADDER USING CMOS BULK P-WELL TECHNOLOGY M.S. Thesis
W. R. Reid Dec. 1984 117 p

(AD-A155043) Avail: NTIS HC A06/MF A01 CSCL 09/1

The design of a sixteen-bit pipelined adder complementary metal oxide semiconductor circuit is presented. The adder is designed to maximize throughput and to provide for testability. Tutorial material on CMOS design is also presented. GRA

N85-32261# General Accounting Office, Washington, D. C. National Security and International Affairs Div.

GAO (GENERAL ACCOUNTING OFFICE) ASSESSMENT OF DOD'S VERY HIGH SPEED INTEGRATED CIRCUITS (VHSIC) TECHNOLOGY PROGRAM

8 May 1985 33 p

(AD-A155109; GAO/NSIAD-85-37) Avail: NTIS HC A03/MF A01 CSCL 05/1

GAO reviewed DOD's Very High Speed Integrated Circuits (VHSIC) program - an effort to develop and demonstrate advanced data and signal processing technology for defense systems. Although progress has been made, the development, demonstration, and independent verification of first generation VHSIC technology is behind schedule. Nevertheless, DOD believes that VHSIC technology must be used in defense systems and in 1982 expanded the program to promote near-term system applications. In light of the delays and other problems, GAO is concerned with DOD's decision to further expand subsidies to stimulate earlier application of VHSIC technology. To achieve the goals of the program, GAO believes that DOD should emphasize progress goals for already approved contractor subsidies and the demonstration and independent testing of first generation VHSIC technology. This report discusses the expansion of the program as well as the status of its original objectives, and recommends alternative ways for DOD to encourage system developers to promptly consider using VHSIC technology. GRA

N85-32262# Rockwell International Corp., Thousand Oaks, Calif. Microelectronics Research and Development Center.

LSI/VLSI ION IMPLANTED PLANAR GaAs IC PROCESSING Semiannual Report, 1 Feb. - 31 Jul. 1984

R. Vahrenkamp, D. Holmes, K. Elliot, and P. Griffith Mar. 1985 50 p

(Contract F49620-83-C-0042; ARPA Order 338419; AF Proj. 2305)

(AD-A155110; MRDC41129.9SA; AFOSR-85-0486TR) Avail: NTIS HC A03/MF A01 CSCL 20/12

The scope of this program is to complete and stabilize the development of a planar fabrication process for high speed digital integrated circuits on 3-in GaAs wafers. In the six-month period covered by this was made in the areas of materials characterization, uniformity evaluation, and gate array design. Annealing experiments were performed on as-grown GaAS wafers to evaluate methods of damage gettering to reduce the metal concentration in active layers and to improve the reproducibility of the implant process. The results were somewhat inconsistent because of unusually high manganese levels in the ingot. To help determine those factors which influence threshold voltage variation, a simple C-V technique was established. One feature illustrated by the C-V data is that most reported nonuniformities in the LEC material which has been reported is due to systematic rather than random variations in threshold voltages. The statistical variation in threshold are generally much smaller being on the order of 20 mV. Standard deviations due to the larger systematic variations have been typically 50 to 70 mV. The AR8 mask set is in the second phase of the ongoing gate array development program. The masking plates for fabricating the generic underlayers have been received in-house, and Mayo had completed the customization layers. The UCSB circuits have been placed on the mask. The customization layers are ready to be sent to the mask shop. GRA

N85-32263# Utah Univ., Salt Lake City. Dept. of Physics.

DEFECTS IN TETRAHEDRALLY COORDINATED AMORPHOUS SEMICONDUCTORS Interim Report

P. C. Taylor 1985 10 p

(Contract N00014-83-K-0535; Grant NSF DMR-83-04471)

(AD-A155150; Rept-5) Avail: NTIS HC A02/MF A01 CSCL 20/12

In the tetrahedrally coordinated amorphous semiconductors the dominant defects deep in the gap are attributed to dangling bonds on the group IV atoms. These defects are commonly thought to have effective electron-electron correlation energies Ueff which are positive, although some tight-binding estimates suggest negative Ueff. Defect states near the band gap edges are invoked to account for many experimental results including the usual appearance of an Urbach absorption edge. These shallow defect states are usually attributed to strained bonds but two-fold-coordinated group IV atoms have also been suggested. The application of light of near-band-gap energies alters the density of paramagnetic dangling bonds. For large spin densities (n(s) greater than or equal to 10 to the 17th power per cu cm) this increase is probably due to the creation of new defects, but it is possible that at lower densities (n(s) less than or equal to 10 to the 16th power per cu cm) the rearrangement of electronic charge in existing defects is important. Impurities also contribute to the defects observed in tetrahedral amorphous semiconductors. Particular species include trapped atomic and molecular hydrogen, trapped NO-2 molecules, singly-coordinated oxygen atoms and E' centers. GRA

N85-32264# Texas Univ. at Dallas, Richardson. Applied Research Lab.

A SAMPLING PHASEMETER DESIGN FOR PULSED CONTINUOUS WAVE SIGNALS

R. S. Bailey 11 Mar. 1985 26 p

(Contract N00014-80-C-0490)

(AD-A155237; ARL-TR-85-5) Avail: NTIS HC A03/MF A01 CSCL 14/2

A continuous wave phasemeter was designed with the capability to operate with short duration pulses of continuous wave signals (pulsed cw) in a background of noise. An exclusive-OR gate provides the phase detection between the input signal and a reference signal. Sample and hold devices are used to provide the capability of averaging phase fluctuations from one pulse to another. The unique concept of quadrature phase logic is implemented in achieving truly linear transfer curve even with the presence of noise in the input signal. GRA

N85-32265# Air Force Systems Command, Wright-Patterson AFB, Ohio. Foreign Technology Div.

A SMALL-SCALE SELF-EXCITED ROTOR ELECTROSTATIC GENERATOR

A. F. Kalganov 15 Apr. 1985 16 p Transl. into ENGLISH from Izv. Vyssh. Ucheb. Zaved., Elektromekh. (USSR), no. 4, Apr. 1960 p 2-26

(AD-A155264; AD-F300613; FTD-ID(RS)T-0162-85) Avail: NTIS HC A02/MF A01 CSCL 09/5

Electrostatic generators, as sources of high direct current voltage, are being used more and more extensively in science and technology. Rotor electrostatic generators with conductor-carriers occupy a significant place among these generators; rotor electrostatic generators develop a voltage in the hundreds of kV and have the advantage that they can be made self-exciting. This considerably simplifies servicing and operation of the generators and is especially important in a small-scale design. Theoretical and experimental works on electrostatic generators with conductor-carriers in the last 20 years have led to the development of various types to such generators. Soviet scientists have made a great contribution to these works. However, the procedure for engineering calculation of certain types of generators still has not been adequately developed. In particular, the Zan calculation does not take into account the effect of parasitic capacitances in generators of disc and cylinder types. GRA

N85-32266# Air Force Inst. of Tech., Wright-Patterson AFB, Ohio. School of Engineering.

ELECTRICAL PROPERTIES OF BULK GROWN NITROGEN DOPED SILICON M.S. Thesis

M. A. OLeary Mar. 1985 150 p

(AD-A155471; AFIT/GE/ENG/85M-3) Avail: NTIS

HC A07/MF A01 CSCL 20/12

The electrical parameters of a boule of nitrogen doped float zone silicon were studied by Hall effect analysis. Samples were annealed at temperatures ranging from 800 to 900 C. In addition, a section of this boule was neutron transmutated (NTD) to increase the n-type doping. Samples from the NTD section were annealed at 800 C. Resistivity and mobility varied considerably from sample to sample, but the variation is not a function of annealing temperature. The annealed Si:N samples were found to be inhomogeneous; however, the Si:N NTD samples were homogeneous. In addition, annealing activated deep energy levels. The shallow energy levels reported in studies on ion implanted nitrogen in silicon were not found. The only shallow energy level found was phosphorus. The conclusion is nitrogen does not go into substitutional sites in silicon to any great extent. Although what happens to nitrogen in silicon is unknown it is suggested that nitrogen may form silicon-nitride complexes and precipitates, This could be the mechanism for strengthening the lattice. GRA

N85-32267# Draper (Charles Stark) Lab., Inc., Cambridge, Mass.
HOT ISOSTATICALLY PRESSED Sm(2)(TM)17 MAGNETS Final Report, 14 Feb. 1983 - 13 Feb. 1985
K. Kumar and H. Newborn Apr. 1985 25 p
(Contract DAAG29-83-C-0009)
(AD-A155479; CSDL-R-1774; ARO-18688.2-MS) Avail: NTIS HC A02/MF A01 CSCL 09/1

High energy product TDK-type, 2-17,Sm (Cu, Fe, Zr, Co) z magnets were produced successfully using hot isostatic pressing (HIP). The best combination of properties was obtained in magnets containing about 26.5 wt% Samarium, 4 wt% Copper, 20 wt% Iron, 2 wt% Zirconium, and 0.4 wt% Oxygen, and balance cobalt. The maximum value of (BH) max measured was 24.8 MGOe for a magnet with B sub R = 10.7 kG and H sub ci = 15.5 kOe. With higher levels of Cu (up to 8 wt%) much higher H sub ci values (up to 28.5 kOe) were measured. A minimum amount of Zr was found to be essential to H sub ci development. HIPing was successfully performed at 1100 C. This resulted in near-complete densification with little grain growth. Post-HIP homogenization was found to lead to enhanced properties after solution treatment and aging, 825 C was determined as the optimum peak aging temperature. Magnets produced from coarse (15 min grind time) alloy powders (with low oxygen contamination) had the properties indicated above. These were substantially superior to magnets produced from conventionally made much finer (1 hour grind time) sinter grade powder, which contained a higher level of oxygen and showed lower H sub ci even after excess Sm was added to compensate for the higher oxygen. However, H sub ci values of up to 8 kOe were found to develop in magnets made from fine (1 hour grind time) powders which were processed for lower oxygen contamination in a glove box. GRA

N85-32268# California Univ., Los Angeles. Dept. of Physics.
DISCOVERY OF A NONPROPAGATING HYDRODYNAMIC SOLITON
J. R. Wu Jun. 1985 106 p
(AD-A155569; TR-43) Avail: NTIS HC A06/MF A01 CSCL 20/4

A new type water-surface-wave soliton, nonpropagating hydrodynamic soliton, has been discovered. This is a self-trapped, highly localized and stationary transverse water-surface-wave excitation which appears in a rectangular cross section resonator continuously excited parametrically by vertical oscillation. An experiment designed to create the soliton and the features of the soliton are described. The profiles of the soliton for various frequencies and amplitudes are measured. It is found that the profile of the soliton is accurately given by a hyperbolic secant function. The stability region that is the amplitude and frequency range of the drive in which individual soliton can be created without hysteresis is experimentally determined. The interaction between two solitons has been investigated. It is observed that an attractive force exists between two solitons with the same polarity and a repulsive force exists between two solitons with the opposite polarity. GRA

N85-32269# Oak Ridge National Lab., Tenn. Solid State Div.
Z-CONTRAST IMAGING AND ELECTRON CHANNELING ANALYSIS OF DOPANTS IN SEMICONDUCTORS
S. J. Pennycock, R. J. Culbertson, and E. Fogarassy Mar. 1985 7 p refs Presented at the 4th Oxford Conf. on Microscopy of Semiconducting Mater., Oxford, 25-27 Mar. 1985
(Contract DE-AC05-84OR-21400)
(DE85-011410; CONF-8503131-2) Avail: NTIS HC A02/MF A01

The determination of dopant distribution and lattice location are key elements in the microanalysis of semiconductor materials. Here two techniques for this purpose are described. The first allows the imaging and elemental mapping of heavy dopants in light semiconductors, and the second is a means for determining the substitutional fraction of dopants or impurities in any crystal structure. DOE

N85-32270# General Electric Co., Schenectady, N. Y.
THERMOELECTRIC PROPERTIES OF BETA-BORON AND SOME BORON COMPOUNDS Final Report, Aug. 1981 - Sep. 1984
G. A. Slack, J. H. Rosolowski, M. L. Miller, and I. C. Huseby Dec. 1984 144 p
(Contract DE-AC01-81NE-32084)
(DE85-011978; DOE/NE-32084/T1) Avail: NTIS HC A07/MF A01

The thermoelectric properties, that is the Seebeck coefficient, and electrical and thermal conductivity, of doped (BETA)-boron have been measured from 300 to 1600 K. Most of the useful doping elements are transition metals and occupy interstitial sites in the lattice. The highest figure of merit so far achieved at 1000 K is ZT = 0.11 for P-type, polycrystalline, hot-pressed (BETA)-boron doped with copper. Higher values may be achievable once a better P-type dopant is found. Some experiments on (B68Y, (ALPHA)-B12Al, B4C, and B6Si are described. Transition metals appear to be effective dopants for B68Y and B4C. DOE

N85-32515*# Illinois Univ., Urbana. Aeronomy Lab.
T/R SWITCH DESIGN FOR SHORT-RANGE MEASUREMENTS, PART 6.1A
B. Yu *In* International Council of Scientific Unions Middle Atmosphere Program: Handbook for MAP. Vol 14 Dec. 1984 p 251-252 refs (For primary document see N85-32466 21-46)
Avail: NTIS HC A17/MF A01; also avail. from SCOSTEP Secretariat, Illinois Univ., 1406 West Green St., Urbana, Ill. 61801 CSCL 09C

N85-32522*# National Oceanic and Atmospheric Administration, Boulder, Colo. Aeronomy Lab.
SIDELOBE REDUCTION OF BARKER CODES, PART 7.1C
J. L. Green *In* International Council of Scientific Unions Middle Atmosphere Program: Handbook for MAP. Vol. 14 Dec. 1984 p 273-275 refs (For primary document see N85-32466 21-46)
Avail: NTIS HC A17/MF A01; also avail. from SCOSTEP Secretariat, Illinois Univ., 1406 West Green St., Urbana, Ill. 61801 CSCL 09C

N85-32523*# Illinois Univ., Urbana. Coordinated Science Lab.
CONSTRUCTION OF COMPLEMENTARY CODE SEQUENCE SETS, PART 7.1D
D. V. Sarwate *In* International Council of Scientific Unions Middle Atmosphere Program: Handbook for MAP. Vol. 14 Dec. 1984 p 276-277 refs (For primary document see N85-32466 21-46)
Avail: NTIS HC A17/MF A01; also avail. from SCOSTEP Secretariat, Illinois Univ., 1406 West Green St., Urbana, Ill. 61801 CSCL 09C

N85-32524*# Centre National d'Etudes des Telecommunications, Saint Maur des Fosses (France).
PROUST RADAR: DECODING HARDWARE AND COHERENT INTEGRATION, PART 7.2A
M. Petitdidier *In* International Council of Scientific Unions Middle Atmosphere Program: Handbook for MAP. Vol. 14 Dec. 1984 p 278-279 (For primary document see N85-32466 21-46)
Avail: NTIS HC A17/MF A01; also avail. from SCOSTEP Secretar-

iat, Illinois Univ., 1406 West Green St., Urbana, Ill. 61801 CSCL 09C

N85-32525*# Tycho Technology, Inc., Boulder, Colo.
A HIGH-SPEED DIGITAL SIGNAL PROCESSOR FOR ATMOSPHERIC RADAR, PART 7.3A
J. W. Brosnahan and D. M. Woodard *In* International Council of Scientific Unions Middle Atmosphere Program: Handbook for MAP. Vol. 14 Dec. 1984 p 280-284 refs (For primary document see N85-32466 21-46)
Avail: NTIS HC A17/MF A01; also avail. from SCOSTEP Secretariat, Illinos Univ., 1406 West Green St., Urbana, Ill. 61801 CSCL 09C

N85-32787# Joint Publications Research Service, Arlington, Va.
DIGITAL INTEGRATED CIRCUITS
Pavel Polasek and Josef Halamik *In its* East Europe Rept.: Sci. and Technol. Selections on CSSR JPRS-ESA-84-017 31 May 1984 p 28-46 refs Transl. into ENGLISH from Sdelovaci Technika (Prague), no. 12, 1983 p 443-448 (For primary document see N85-32781 21-60)
Avail: NTIS HC A05/MF A01

34 FLUID MECHANICS AND HEAT TRANSFER

Includes boundary layers; hydrodynamics; fluidics; mass transfer; and ablation cooling.

For related information see also *02 Aerodynamics* and *77 Thermodynamics and Statistical Physics.*

N85-32271 Pennsylvania State Univ., University Park.
A MULTILEVEL-MULTIGRID METHOD FOR RECIRCULATING FLOWS Ph.D. Thesis
Robert Edwin Phillips 1984 144 p
Avail: Univ. Microfilms Order No. DA8506663

A solution algorithm is developed which can predict recirculating flow phenomena in an accurate and efficient manner. The algorithm is based on the multilevel solution scheme of Brandt. In addition, regions with large spatial gradients in the dependent variables are handled through the use of multigrid local refinement. The algorithm is first used to study a scalar diffusion equation and an advection diffusion equation. Comparisons with model problems which have exact analytical solutions point out the efficient and accurate manner in which the algorithm performs. Modifications are described which adapt the multilevel-multigrid algorithm for use in analyzing recirculating flow. The full algorithm for recirculating flow is then tested by comparison of predicted results with three test cases for which either numerical or experimental results are available. Dissert. Abstr.

N85-32272*# California Univ., Los Angeles. School of Engineering and Applied Science.
VAPOR-LIQUID PHASE SEPARATOR STUDIES Final Report, 1980-1983
S. W. K. Yuan, W. A. Hepler, and T. H. K. Frederking Aug. 1985 13 p refs
(Contract NCC2-64)
(NASA-CR-166545; T-6624; NAS 1.26:166545) Avail: NTIS HC A02/MF A01 CSCL 20D

A study of porous plug use for vapor-liquid phase seperation in spaceborne cryogenic systems was conducted. The three main topics addressed were: (1) the usefulness of porous media in designs that call for variable areas and flow rates; (2) the possibility of prediction of main parameters of porous plugs for a given material; and (3) prediction of all parameters of the plug, including secondary parameters. G.L.C.

N85-32273# Naval Postgraduate School, Monterey, Calif.
EVALUATION OF THE EFFECTS OF ROLL ANGLE ON THE NATURAL CONVECTION HEAT TRANSFER FROM AN ARRAY OF CYLINDRICAL SPINES M.S. Thesis
J. E. McClanahan Dec. 1984 51 p
(AD-A154594) Avail: NTIS HC A04/MF A01 CSCL 09/5

Electronically steered phased array antennae frequently exhibit degraded performance due to the lack of proper heat transfer between the interior crystalline materials and the environment. This causes higher than optimum temperature environments for the crystalline materials and a subsequent loss of reliability. One possible solution to such a problem considers a surface augmentation through the use of pin fins (or spines) to assist in the dissipation of the heat. Experimental data has been obtained that predicts the effect of roll angle upon the natural convection heat transfer from an array of cylindrical spines or pin fins. A correlation is presented that permits evaluation of the Nusselt Modulus as a function of the Rayleigh Modulus and the roll angle and it shows that maximum heat transfer is obtained at roll angles between 20 and 30 degrees. GRA

N85-32274# Purdue Univ., Lafayette, Ind. School of Mechanical Engineering.
INJECTION OF DRAG REDUCING ADDITIVES INTO TURBULENT WATER FLOWS: TWO-COMPONENT VELOCITY MEASUREMENTS AND MIXING LENGTH MODEL PREDICTIONS Annual Report, 1 Mar. 1984 - 28 Feb. 1985
T. S. Luchik, D. T. Walker, and W. G. Tiederman Apr. 1985 151 p
(Contract N00014-83-K-0183; NR Proj. RR0-2301)
(AD-A154604; PME-FM-85-1) Avail: NTIS HC A08/MF A01 CSCL 20/4

The basic goals are: To determine the mechanism(s) by which a drag-reducing additive modifies the turbulent momentum transport near a wall; and to develop optimal methods for injecting these additives into wall flows. The structural characteristics of channel flows well downstream of the additive injectors were deduced from two-component laser velocimeter measurements while a mixing length model was developed to predict the wall shear stress of water flows with additive injection. A three beam, two-color laser velocimeter was used to measure simultaneously the velocity components parallel and normal to the wall between the channel centerline and y+ approx. 11 for three channel flows. The baseline case was a fully developed water flow; the second a well mixed drag-reducing flow whose Reynolds number matched that of the water flow; a third was a well mixed drag-reducing flow whose wall shear stress matched that of the water flow. Profiles of the mean and root-mean-square velocities confirmed that the additives modify the buffer region of the flow. The major influence occurred through damping of the fluctuations of the normal velocity component. Eulerian burst detectors were developed by extensions of the quadrant two, VITA and u-level detection methods. When properly extended all three methods yielded an average time between bursts that agreed with previous flow visualization results. In these very dilute drag-reducing flows, the average time between burst increased the same amount as the streak spacing. GRA

N85-32275# Southwest Research Inst., San Antonio, Tex.
EXPERIMENTS ON THE INFLUENCE OF ACTIVE WALLS ON THE INITIAL AMPLITUDES AND GROWTHS OF INSTABILITY WAVES Final Report, 8 Feb. 1982 - 31 Jan. 1985
J. T. Park, H. S. Silvus, Jr., S. A. Cerwin, and H. L. Rogler Mar. 1985 127 p
(Contract N00014-82-C-0199)
(AD-A154630; SWRI-6984) Avail: NTIS HC A07/MF A01 CSCL 20/4

An active-wall device was developed to determine those characteristics of traveling surface waves which are important in drag reduction with compliant coatings. Feasibility of an active wall was demonstrated with a Kelvin-Helmholtz solution for flow over a semi-infinite surface with traveling surface waves. Analysis indicated that freestream disturbances and the secondary flow generated by the leading edge could be modified or eliminated. An all solid-state electromechanical device was built which produces short-wavelength traveling surface waves. The active wall nominally designed to cancel Tollmien-Schlichting waves in a

laminar boundary layer. Wave form, wave speed, frequency, and amplitude were independently selectable. The electronic subsystem was a hybrid analog/digital device, and wall motion was produced by piezoelectric ceramic elements. Surface displacement was measured with an electro-optical instrument developed for this research. Measurements of sinusoidal wall motion ranged in amplitude from 0.6 - 13 microns over a frequency span of 10-150 Hz. Maximum phase speed was 166 cm/s. A low turbulence water tunnel was designed and assembled for the active-wall experiments. Design velocity was 10 m/s in a test section. Longitudinal relative turbulence intensity in the test section was estimated to be less than 0.2%. GRA

N85-32276# Materials Research Labs., Ascot Vale (Australia).
WEAK SHOCK WAVES PROPAGATING IN FLUID-GAS MIXTURES
E. H. VanLeeuwen Feb. 1985 15 p
(AD-A154759; MRL-R-951) Avail: NTIS HC A02/MF A01 CSCL 20/4

The structure of a weak normal shock wave is investigated analytically for the one-dimensional flow of a fluid, containing gas bubbles. The relative motion of the gas bubbles follow a Stokes-drag law. It is shown that for large values of time the gas bubbles behave isothermally and the shock wave approaches a steady state. For small values of time the gas bubbles behave isentropically and move faster than the fluid. GRA

N85-32277# Wisconsin Univ., Madison. Mathematics Research Center.
A NUMERICAL STUDY OF TAYLOR-VORTEX FLOW Technical Summary Report
J. C. Strikwerda Apr. 1985 32 p
(Contract DAAG29-80-C-0041)
(AD-A154787; MRC-TSR-2808) Avail: NTIS HC A03/MF A01 CSCL 20/4

Results are presented of a numerical study of Taylor vortex flows. The computations were done with values of the Reynolds number and aspect ratio as used by T. B. Benjamin in his experiments. An extensive study was made of the two-cell and four-cell transitions and bifurcations. Good agreement was obtained with the experimental results. The flows were assumed to be axisymmetric so that the computation required only two spatial dimensions, although it required that all velocity components and the pressure be computed. A regularized central finite difference scheme was used to discretize the Navier-Stokes equations. The system of equations was solved by an iterative method similar to successive-over-relaxation. GRA

N85-32278# Wisconsin Univ., Madison. Mathematics Research Center.
LARGE-TIME BEHAVIOR OF VISCOUS SURFACE WAVES Technical Summary Report
J. T. Beale and T. Nishida Apr. 1985 21 p
(Contract DAAG29-80-C-0041; Grant NSF MCS-81-01639)
(AD-A154805; MRC-TSR-2809) Avail: NTIS HC A02/MF A01 CSCL 20/4

We consider the mathematical behavior of a viscous, incompressible fluid bounded above by an atmosphere of constant pressure and below by a horizontal bottom. After reviewing the existence and regularity theory for the equations governing the motion, we establish rates of decay for solutions near equilibrium. The function describing the height of the free surface decays like 1/square root of t; the velocity field decays like 1/t. These estimates are shown first for the linearization about equilibrium and then for the full nonlinear problem. Complete details will be given elsewhere. GRA

N85-32279# Wisconsin Univ., Madison. Mathematics Research Center.
INSTABILITY AND CHAOTIC BEHAVIOR IN A FREE-SURFACE FLOW Summary Report
W. G. Pritchard Mar. 1985 108 p
(Contract DAAG29-80-C-0041)
(AD-A154879; MRC-TSR-2807) Avail: NTIS HC A06/MF A01 CSCL 20/4

This paper describes some experimental observations of free-surface flows arising when fluid poured over the end of a flat plate into a reservoir well below the plate. This class of flows was found to be highly unstable with over seven hundred qualitatively different flows being observed in the experiment. At very small values of the flux the liquid fell from the plate into the reservoir in the form of droplets which developed periodically at a number of sites on the underside of the plate. As the flux was increased these sites were able to sustain continuous, unbroken streams and combinations of drip sites and continuous streams were possible. At still larger values of the flux there was a tendency for the liquid to fall in sheets and several combinations of sheet flows and continuous streams were observed, some of which flows exhibited a rather chaotic temporal behavior. At even larger flux values the flow resembled that of the classic waterfall, but here there were also some unexpected instabilities where the attachment line of the free surface of the liquid with the plate developed corrugations. GRA

N85-32280# Naval Postgraduate School, Monterey, Calif.
DESIGN OF A GENERATOR FOR NEAR-TANGENTIAL TRANSONIC SWIRLING OUTFLOW M.S. Thesis
P. E. Thrower-LeSesne Dec. 1984 118 p
(AD-A155163) Avail: NTIS HC A06/MF A01 CSCL 20/4

Two computer methods for the design of radial out-flow turning vanes are described. The key requirement was for vanes with simple shapes that could be machined easily and inexpensively in-house. Two design approaches, one using circular arcs for both suction and pressure sides and one for wedge-arc shaped sections were developed. Requirements for the general design procedure arose in two exploratory projects, a Rotary Detonative Wave Engine (RDWE) and a high speed Centrifugal Diffuser Test Device (CDTD). The RDWE was analyzed first and found to be potentially inefficient in its original configuration. Preliminary design for a high speed CDTD flow generator was completed, incorporating wedge-arc radial outflow vanes. An attempt to analyze the flow through the geometry using the Eidelman-Godnov Euler was initiated. GRA

N85-32281# Naval Ship Research and Development Center, Bethesda, Md.
A VARIABLE NODE FINITE ELEMENT METHOD APPLIED TO THE GAS DYNAMICS EQUATIONS Final Report
M. C. Mosher May 1985 50 p
(SR0-1403)
(AD-A155211; DTNSRDC-85/010) Avail: NTIS HC A03/MF A01 CSCL 20/4

The author's variable node finite element method has been extended to systems of partial differential equations in one space dimension and applied to the gas dynamics equations in conservation form with a numerical viscosity to smear out the discontinuities. The method for gas dynamics was implemented in the computer program VFEGD and tested successfully on a shock tube problem. Since the variable node method concentrates nodes in regions of large gradients, it makes possible automatic numerical detection of contact discontinuities and shocks. Once they have been detected, they can be sharpened and consequently their diffusion can be controlled. The program VFEGD, with modifications to detect and sharpen contacts and shocks, was also tested successfully on the shock tube problem. GRA

N85-32282# Army Military Personnel Center, Alexandria, Va.
AN INVESTIGATION INTO THE FLUIDIZATION AND HEAT TRANSFER OF LOW DENSITY PARTICLES IN A FLUIDIZED BED WITH APPLICATIONS Final Report
J. M. Modlin 10 May 1985 184 p
(AD-A155259; AD-F300613) Avail: NTIS HC A09/MF A01 CSCL 10/1

The lack of reliable data on the fluidization and heat transfer characteristics of low density particles in a fluidized bed has

prompted an experimental and analytical investigation into this subject. Seven groups of particles ranging in diameter from 0.25 mm to 2.0 mm and density from 2.5 to 32 pcf have been successfully fluidized and shown to be generally well predicted by classical fluidization and fluidized bed heat transfer theory. Two other groups of particles, also in this approximate range of particle diameter and density, are, however, unable to be fluidized due to significant inter-particle and static electric attractions. Using the experimental data and results as a basis of analysis, two application of low density particle fluidization in a building efficient energy management program are discussed. A fluidized bed can be incorporated into the wall cavity of a building for use as either a collector of solar energy or as a heat exchange medium in a building space heating/cooling program. As a solar collector, it is shown that the low density particle fluidized bed would thermally perform between comparable conventional liquid and air-cooled flat plate solar collectors. It would require less water pumping power and plumbing than the liquid collector and less air pumping power than the air collector. GRA

N85-32283# Ballistic Research Labs., Aberdeen Proving Ground, Md.

BLAF: A BLAST FIELD RECONSTRUCTION PROGRAM FROM PRESSURE HISTORIES

A. Celmins Mar. 1985 247 p

(AD-A155300; AD-F300613; BRL-TR-2645) Avail: NTIS HC A11/MF A01 CSCL 19/4

The BLAF programs (BLAFS, BLAFOP, and BLAFHI) are designed to reconstruct parts of a spherical blast field from selected pressure history observations. The reconstruction method is based on a model fitting to the observed flow field and a subsequent numerical integration of the flow governing equations. This manual gives a short outline of the theoretical background, a description of the program and specifications for the input data and their formats. The flow field reconstruction is done in three steps, each step being realized by an independent progrm, BLAFS for shock fitting, BLAFOP for blast field overpressure fitting and BLAFHI for blast field history calculations. The input for BLAFS consists of observed shock arrival times ts and overpressure ps at a number of distances r. the program determines a shock model function by adjusting all three components of each data point, ts, ps and r. It also accepts incomplete observations where either ts or ps is missing. The output of BLAFS consists of a set of shock model parameters with corresponding error estimates. The BLAFOP program uses as input the results from BLAFS and overpressure history observations at two or more positions. The output is a set of parameters (with error estimates) of an overpressure field function. The program BLAFHI uses the results of BLAFS and BLAFOP and computes histories of all components of the blast field (velocity, pressure, density, and dynamic pressure) at distances specified by the user. These computations are done by numerical integration of the flow governing equations. GRA

N85-32284# Naval Postgraduate School, Monterey, Calif.

THE INFLUENCE OF OIL CONTAMINATION ON THE NUCLEATE POOL-BOILING BEHAVIOR OF R-114 FROM A STRUCTURED SURFACE M.S. Thesis

J. T. Reilly Mar. 1985 124 p

(AD-A155609; NPS69-85-003) Avail: NTIS HC A06/MF A01 CSCL 13/1

The U.S. Navy currently uses refrigerant R-114 in centrifugal chilled-water air-conditioning plants aboard submarines and surface ships. The Navy hopes to reduce the size of these units and increase their performance by using enhanced evaporator and condenser surfaces. The external nucleate pool-boiling heat-transfer coefficient of a horizontal smooth copper tube in R-114-oil mixtures was measured for heat fluxes from 1 to 100 kW/sq m at two different saturation temperatures. A copper-nickel tube coated with the Union Carbide High Flux coating was similiarly tested. The High Flux coating was found to improve the heat-transfer coefficient by at least a factor of 7 in oil-free R-114. Oil resulted in about 20% reduction of the heat transfer coefficient of the High Flux surface at heat fluxes less than 30 kW/sq m and up to an 80 percent reduction at heat fluxes above 30 kW/sq m with greater than 6% oil. Under all conditions, the High Flux coated tube outperformed the smooth copper tube. GRA

N85-32285# Naval Postgraduate School, Monterey, Calif.

FILM CONDENSATION OF STEAM ON EXTERNALLY FINNED HORIZONTAL TUBES M.S. Thesis

F. A. Flook Mar. 1985 147 p

(AD-A155642) Avail: NTIS HC A07/MF A01 CSCL 13/1

Filmwise condensation measurements of steam were made on horizontal finned tubes under vacuum and near-atmospheric conditions. Data were obtained for copper tubes with fins of rectangular, triangular, trapezoidal, and parabolic cross sections, and for a commercially-available finned tube. A stainless steel finned tube was also tested to investigate the effect of thermal conductivity. Maximum enhancements of about 4.8 were obtained under vacuum conditions, and about 6.9 at atmospheric pressure, compared to a smooth tube having an outside diameter equal to the root diameter of the finned tubes. The optimum fin spacing was found to be about 2.0 mm for rectangularly shaped-fins with a fin-thickness of 1.0 mm, and fin height of 0.5 and 1.5 mm. Fins with a parabolic shape were shown to perform better than fins of rectangular shape, and fins were shown to degrade the performance of stainless steel tubes. The effects of vapor shear were also shown to have only a small influence on the steam-side heat transfer coefficient. A theoretical model proposed by Webb et al. was found to underpredict the experimental data. Several suggestions to modify this model are described. GRA

N85-32286# Pennsylvania Univ., Philadelphia. Dept. of Mechanical Engineering and Applied Mechanics.

NUMERICAL SOLUTIONS OF TURBULENT MODELS FOR FLOW OVER A FLAT PLATE WITH ANGLE OF ATTACK

N. T. Truncellito, H. Yeh, and N. Lior Mar. 1985 49 p refs Revised

(Contracts DE-AC04-78-CS-35365; EM-78-C-04-5365; EM-78-C-04-5319)

(DE85-010380; DOE/CS-35365/T1) Avail: NTIS HC A03/MF A01 CSCL 20D

Numerical solutions of the two-dimensional boundary layer equations were examined. An integral solution was constructed for laminar and turbulent flow, as well as finite difference solutions for zeroth- and first-order turbulence models. The models also account for buoyancy effects. A three part mixing length model was employed in the zeroth-order model, and an additional turbulent kinetic energy equation was utilized for the first-order model. The computational method utilized Patankar-Spalding coordinates and differs from other methods in that no matching procedure is required for the inner and outer flow regions. The Falkner-Skan velocity profile is applied as an edge boundary condition while variable wall temperature conditions can be imposed. The effects of freestream velocity and angle of attack on skin friction and heat transfer were established, and the velocity and temperature fields were determined. Results of the zeroth-order solution are in excellent agreement with the Colburn equation and several other data sources. These solutions provide correlations in terms of Nusselt number and skin friction coefficient versus local Reynolds number which can be used for estimating heat transfer and wind loadings on a flat plate. Results generated are especially useful in predicting the performance of solar system designs. DOE

N85-32287# Pennsylvania Univ., Philadelphia. Dept. of Mechanical Engineering and Applied Mechanics.

FORCED CONVECTION ON SOLAR COLLECTOR ARRAYS

R. N. Segall, N. Lior, and H. Yeh Mar. 1985 231 p

(Contract DE-AC04-78CS-35319)

(DE85-010381; ALO-5319-5) Avail: NTIS HC A11/MF A01

Experiments were performed in a wind tunnel to determine the local and average heat transfer coefficients for forced convection of air over an array of three inclined rectangular plates. In addition to the measurement of heat transfer coefficients, flow visualization by the use of tufts was done to survey the nature and direction of the flow at the surface of the plates. The local

Reynolds number ranged from 5500 to 750,000 and the Reynolds number based on the length of the plate ranged from 480,000 to 850,000. Three angles of attack (30, 45, and 60 deg) and two inter-plate distances between adjacent plates were investigated at zero yaw angle for each of the three plates positioned in the array. The aspect ratio of each plate was 1:1.19. The convection heat transfer coefficient was determined at 25 different locations on the surface of each plate by using an electrically-heated surface probe built for that purpose. The experimental precision in measuring h is within + or - 2%. The local convective heat transfer coefficients obtained were also integrated over the area of the plate to yield average values. DOE

N85-32288# Oak Ridge National Lab., Tenn.
TWO-PHASE FLOW VISUALIZATION IN A TRANSPARENT, ATMOSPHERIC PRESSURE, BOILING WATER LOOP
A. E. Levin, J. J. Carbajo, B. H. Montgomery, and J. L. Wantland 1985 26 p Presented at the ASME-ASCE Fluids Eng. Conf. and Joint Mech. Conf., Albuquerque, N. Mex., 24 Jun. 1985
(Contract DE-AC05-84CR-21400)
(DE84-016857; CONF-850614-1) Avail: NTIS HC A03/MF A01

The Simulant Boiling Flow Visualization (SBFV) loop, a transparent atmospheric pressure test apparatus employing boiling water as a simulant for boiling liquid sodium, has been designed and operated at Oak Ridge National Laboratory. The objective of testing in this loop has been to study two phase flow behavior that is phenomenologically similar to that observed in sodium boiling experiments, as part of the US Department of Energy Breeder Reactor Safety Program. A detailed description of the design of the SBFV loop is presented, as well as experimental results that show the similarity between low power boiling behavior in water and liquid sodium. Future tests are planned in a seven pin flow visualization bundle that will be installed in the SBFV loop. The design of this bundle is also discussed. DOE

N85-32289# California Univ., Berkeley. Lawrence Berkeley Lab.
IN-SITU MEASUREMENT OF WALL THERMAL PERFORMANCE: DATA INTERPRETATION AND APPARATUS DESIGN RECOMMENDATIONS
M. P. Modera, M. H. Sherman, and S. G. deVinuesa Sep. 1984 32 p Presented at Symp. on Thermal Insulation, Mater. and Systems, Dallas, Tex., 2 Dec. 1984
(Contract DE-AC03-76SF-00098)
(DE85-011979; LBL-17773; CONF-841202-3) Avail: NTIS HC A03/MF A01

Although the U-values of many building matrials have been determined by laboratory testing, the in-situ thermal performance of walls, under either static or dynamic conditions, is not so well documented. This report examines the use of field measurements of heat flow and surface temperatures to determine the dynamic as well as static thermal performance of walls. The measurement strategies examined include both active devices, which generate their own heat fluxes on the wall surfaces, and passive devices, which rely on the weather to induce the required fluxes and temperature differences. Data obtained with both devices are analyzed with the Simplified Thermal Parameter (STP) model, which was designed to characterize a wall from flux and temperature measurements rather than from assumed material characteristics. The active measurement data are also analyzed with a modified version of the STP model that takes into account lateral heat losses. Some possible sources of error for both active and passive measurement strategies are also examined, and recommendations for both measurement strategies are given. DOE

N85-32290# Los Alamos National Lab., N. Mex.
CHARACTERISTICS OF A NUMERICAL FLUID DYNAMICS SIMULATOR
K. H. A. Winkler, M. L. Norman, and J. L. Norton 28 Aug. 1985 16 p Presented at the Symp. on Algorithms, Architectures and the Future of Sci. Computation, Austin, Tex., 18 Mar. 1985
(Contract W-7405-eng-36)
(DE85-009602; LA-UR-85-1094; CONF-8503129-1) Avail: NTIS HC A02/MF A01

A concept of a real time Numerical Fluid Dynamics Simulator (NFDS) is described, and its characteristics are derived. The following characteristics are adopted as guiding principles: (1) that the performance characteristics (information output, throughput and storage) of the NFDS be defined by the maximum rate at which the research can absorb the results of his/her simulator, thus establishing an impedance match between man and machine; (2) that the NFDS off-load from the researcher's brain in every way possible the routine tasks of data analysis that can be done automatically; and (3) that the NFDS is operated as a dedicated experimental device and that the researcher has complete control over the apparatus and experiment. The NFDS is envisioned to be composed of simulation processors, data storage devices, and image processing devices of extremely high power and capacity, interconnected by very high throughput communication channels. Individual component performance requirements are presented for both real time and playback operating models of the NFDS, using problems of current interest in fluid dynamics as examples. DOE

N85-32291# Zumbrunnen (Allen D.), Salt Lake City, Utah.
HIGH-FREQUENCY FURNACE Final Technical Report
A. D. Zumbrunnen 30 Apr. 1985 31 p
(Contract DE-FG01-81CS-15077)
(DE85-011210; DOE/CS-15077/T13) Avail: NTIS HC A03/MF A01

An experimental furnace has been built for the purpose of evaluating a new technique for the high purity melting of certain metals and semiconductors. The melt is contained in a solidified skull of the same material being melted, thus avoiding crucible reactions that are a problem in conventional processing. A number of commercial applications of the invention are discussed, assuming that feasibility can be established. These include the melting and crystal growth of silicon, where the avoidance of crucible contamination would improve the energy conversion efficiency of solar cells; and the consolidation of titanium sponge and scrap, where energy savings and other process advantages would be realized. The production of ferrous and non-ferrous, specialty alloys is also discussed. Heating power is derived from the electrical, proximity effect which is used to concentrate a high-frequency (9.6 kHz) current in the melt zone. The power source is a conventional, 50 kW, solid-state inverter of the type used in induction heating practice. All heats were conducted on a cast iron workpiece in argon at atmospheric pressure. The melt temperature of the casting (2100 F) was not achieved in any test run; however, the ability of proximity effect to generate localized heating was clearly demonstrated. DOE

N85-32292# Argonne National Lab., Ill.
RESOLUTION OF THERMAL STRIPING ISSUE DOWNSTREAM OF A HORIZONTAL PIPE ELBOW IN STRATIFIED PIPE FLOW
T. M. Kuzay and K. E. Kasza 1985 10 p Presented at the Ann. Meeting of the Am. Nucl. Soc., Boston, 9 Jun. 1985
(Contract W-31-109-eng-38)
(DE85-006195; CONF-850610-4) Avail: NTIS HC A02/MF A01

A thermally stratified pipe flow produced by a thermal transient when passing through a horizontal elbow as a result of secondary flow gives rise to large thermal fluctuations on the inner curvature wall of the downstream piping. These fluctuations were measured in a specially instrumented horizontal pipe and elbow system on a test set-up using water in the Mixing Components Technology Facility (MCTF) at Argonne National Laboratory (ANL). This study is part of a larger program which is studying the influence of thermal buoyancy on general reactor component performance. This paper discusses the influence of pipe flow generated thermal oscillations on the thermal stresses induced in the pipe walls. The instrumentation was concentrated around the exit plane of the 90(0) sweep elbow, since prior tests had indicated that the largest thermal fluctuations would occur within about one hydraulic diameter downstream of the elbow exit. The thermocouples were located along the inner curvature of the piping and measured the near surface fluid temperature. The test matrix involved thermal downramps under turbulent flow conditions. DOE

N85-32293# Advisory Group for Aerospace Research and Development, Neuilly-Sur-Seine (France). Propulsion and Energetics Panel.

THREE-DIMENSIONAL TECHNIQUES APPLIED TO INTERNAL FLOWS IN PROPULSION SYSTEMS

Loughton, England May 1985 200 p refs Lectures held in Rome, 6-7 Jun., in Cologne, 10-11 Jun., and in Paris, 13-14 Jun. 1985

(AGARD-LS-140; ISBN-92-835-1503-X) Avail: NTIS HC A09/MF A01

Various topics related to 3-D computation techniques applied to internal flows in propulsion systems are discussed. The different mathematical models starting from the most complete one (time average Navier-Stokes equations with turbulent modeling) to the simplest one (small potential disturbance equation) are discussed. For viscous flows, different approximation levels are discussed: full averaged Navier-Stokes equations, thin shear layer approximation, parabolic approximation, boundary layer equations with coupling methods, and distributed losses model. The calculation of 3D rotational inviscid flow by a method based on the CLEBSCH representation is described. The equation for the potential is discretized with a classical finite element technique. Pressure correction calculation procedures for 3-D viscous steady flow are given. In this method the velocity field is calculated from momentum equation assuming that the pressure is given. The exact solution is obtained by adjusting the pressure distribution in order to satisfy the continuity equation. A discretization technique which leads to a reduction of numerical mixing is given. The pressure correction methods for partially parabolic and elliptic flow are used to evaluate the performance of different blade rows and cascades. A review is given of the different approaches for the numerical solutions of the complete Navier-Stokes equations. The problem of grid generation for 3-D applications is discussed as well as the treatment of boundary conditions for internal flows. A computer program for the solution of the 3-D Euler equations by means of a time marching method with a finite volume discretization is described. The treatment of boundary conditions by a technique based on the use of some selected compatibility relations associated to the time hyperbolic Euler system is discussed. For individual titles, see N85-32294 through N85-32301.

N85-32294# Cambridge Univ. (England). Dept. of Engineering.

THE CALCULATION OF FULLY THREE DIMENSIONAL FLOW THROUGH ANY TYPE OF TURBOMACHINE BLADE ROW

J. D. Denton *In* AGARD 3-D Computation Tech. Appl. to Internal Flows in Propulsion Systems May 1985 20 p refs (For primary document see N85-32293 21-34)

Avail: NTIS HC A09/MF A01

Various approximation levels, enabling the simplification of the full system of Reynolds averaged Navier-Stokes equations, are presented. The latter are considered as the highest level model of flow description and depend heavily on the turbulence models. Viscous approximations such as the thin shear layer and the parabolized Navier-Stokes models are discussed. The disturbed loss model, applied in turbomachinery applications, is intermediate between the viscous and inviscid approximations. The Euler equations, rotational flow models and the simplest potential flow are further discussed and their limitations are printed out. R.J.F.

N85-32295# Vrije Universiteit, Brussels (Belgium). Dept. of Fluid Mechanics.

AN ANALYSIS OF FLOW MODELS: FROM NAVIER-STOKES TO POTENTIAL FLOW EQUATIONS

Ch. Hirsch *In* AGARD 3-D Computation Tech. Appl. to Internal Flows in Propulsion Systems May 1985 28 p refs (For primary document see N85-32293 21-34)

Avail: NTIS HC A09/MF A01

A method to calculate the three dimensional, rotational flow of an inviscid, compressible fluid in turbomachines is presented. The approach is based on a finite element formulation and results are presented for the flow in a rectangular bend, a turbine stator and a centrifugal impeller. Author

N85-32296# Vrije Universiteit, Brussels (Belgium). Dept. of Fluid Mechanics.

COMPUTATION OF THREE-DIMENSIONAL, INVISCID, ROTATIONAL FLOWS

Ch. Hirsch and C. Lacor *In* AGARD 3-D Computation Tech. Appl. to Internal Flows in Propulsion Systems May 1985 28 p refs (For primary document see N85-32293 21-34)

Avail: NTIS HC A09/MF A01

Pressure correction calculation procedures for 3-D viscous flow are described. The conservation equations and the types of pressure correction methods are described. The advantages of the pressure correction approach are discussed. Calculations are compared with measurements for three turbulent 3-D flows, each requiring a more general calculation method than the last. Comparison of calculations with well documented, realistic, experimental test cases is essential and demonstrates the engineering usefulness of the methods. A fully elliptic calculation procedure is described in detail by using a simple example. This example is so simple (16 grid points) that a variety of calculation procedures can be explored with only the aid of a hand held calculator or small personal computer. Comparison with the SIMPLE algorithm is discussed and the advantages of parabolic and partially parabolic methods are discussed. R.J.F.

N85-32297# Virginia Polytechnic Inst. and State Univ., Blacksburg. Dept. of Mechanical Engineering.

AN ELLIPTIC CALCULATION PROCEDURE FOR 3-D VISCOUS FLOW

Joan G. Moore *In* AGARD 3-D Computation Tech. Appl. to Internal Flows in Propulsion Systems May 1985 16 p refs Sponsored in part by Rolls-Royce Ltd. (For primary document see N85-32293 21-34)

Avail: NTIS HC A09/MF A01

The computation of 3-D internal transonic flows by means of a 3-D Euler Code is discussed. A multidomain approach for time hyperbolic system is presented. This technique, based on the decomposition of the computational domain into several subdomains which may overlap one another, makes it possible to simplify some mesh generation problems and to fit discontinuities such as shocks and slip surfaces. A description of the 3-D Euler Code is given. The space discretization method and the treatment of boundary conditions are emphasized. Various applications of this code in turbomachinery are discussed. R.J.F.

N85-32298# Office National d'Etudes et de Recherches Aeronautiques, Paris (France).

A 3-D EULER METHOD FOR INTERNAL TRANSONIC FLOWS COMPUTATION WITH A MULTI-DOMAIN APPROACH

J. P. Veuillot and G. Meauze *In* AGARD 3-D Computation Tech. Appl. to Internal Flows in Propulsion Systems May 1985 21 p refs (For primary document see N85-32293 21-34)

Avail: NTIS HC A09/MF A01

The results of calculations of three dimensional viscous flow in two centrifugal compressor impellers and in two linear turbine cascades are considered and answers to thermodynamic questions are obtained. For the impellers, the calculations give the work and the losses, the total pressure ratio and the efficiency, and show where the inefficiency arises. The results for the turbines show the increase in loss within and downstream of the cascades and allow the buildup and decay of secondary kinetic energy to be followed. Author

N85-32299# Virginia Polytechnic Inst. and State Univ., Blacksburg. Dept. of Mechanical Engineering.

PERFORMANCE EVALUATION OF FLOW IN TURBOMACHINERY BLADE ROWS

John Moore *In* AGARD 3-D Computation Tech. Appl. to Internal Flows in Propulsion Systems May 1985 26 p refs Sponsored in part by Rolls-Royce Ltd. (For primary document see N85-32293 21-34)

Avail: NTIS HC A09/MF A01

The numerical solution of the complete Navier-Stokes equations for two dimensional nonsteady flow has only been accomplished

in the last decade. Most of the computations have been for external flows. However, in the past few years this capability has been extended to internal flows for relatively simple configurations. Both implicit and explicit approaches have been used in developing methods for computing internal flows. These methods are discussed briefly with emphasis on MacCormack's explicit finite difference algorithm. The capabilities and limitations of these approaches are discussed. In particular, attention is focused on grid generation, formulation of boundary conditions for internal flows, and constraints imposed by limited computer storage and speed. Results for axisymmetric and 3-D flows are presented. In addition, developments currently in progress are noted. Finally, future developments of this capability are addressed, along with their impact on the development of advanced propulsion systems. R.J.F.

N85-32300# Dayton Univ., Ohio. Dept. of Mechanical Engineering.
NUMERICAL SOLUTION OF THE NAVIER-STOKES EQUATIONS FOR 3-D INTERNAL FLOWS: AN EMERGING CAPABILITY
J. N. Scott *In* AGARD 3-D Computation Tech. Appl. to Internal Flows in Propulsion Systems May 1985 24 p refs (For primary document see N85-32293 21-34)
Avail: NTIS HC A09/MF A01

The accuracy of 3-D flow calculations is discussed. A good calculation procedure solves a set of finite difference equations reasonably quick. However, if the finite difference equations do not accurately reflect the governing differential equations, poor results will be obtained. For example, it is common practice in three dimensional flow calculations to use upwind differencing or more direct forms of numerical mixing to obtain well posed finite difference equations which are needed to maintain a stable calculation procedure. The erroneous numerical viscosity introduced can be of the same order as the natural laminar or laminar plus turbulent viscosities in the flows calculated. When numerical mixing is present a proper evaluation of viscosity or turbulence models cannot be made because the effects of numerical and physical mixing cannot be distinguished. A simple 2-D example is used to demonstrate a practical method of obtaining the finite difference form of the convection term in momentum or other conservation equations. The 2-D example introduces no numerical mixing, yet results in well posed, (i.e., strong center point coefficient) finite difference equations. The method consists of central differencing to eliminate numerical mixing and upwinded control volumes to obtain finite difference equations with strong point coefficients. An upwinding procedure for the control volumes which may be applied to three dimensional flow is given. Inviscid calculations of horseshoe vortex flow about a Rankine half body are presented. R.J.F.

N85-32301# Virginia Polytechnic Inst. and State Univ., Blacksburg. Dept. of Mechanical Engineering.
CALCULATION OF 3-D FLOW WITHOUT NUMERICAL MIXING
Joan G. Moore *In* AGARD 3-D Computation Tech. Appl. to Internal Flows in Propulsion Systems May 1985 15 p refs Sponsored in part by Rolls-Royce Ltd. (For primary document see N85-32293 21-34)
Avail: NTIS HC A09/MF A01

A suite of computer programs was developed to calculate the fully 3D inviscid flow through any type of turbomachine blade row. The method is based on a pseudo time dependent solution of the Euler equations with convergence accelerated by a multigrid approach. It is shock capturing and has no Mach number limitations. The basic version of the program can cope with any type of single blade row, compressor or turbine, with axial, mixed or radial flow. Special versions of the code were developed for blade rows with part pitch or part span splitter blades and also for two blade rows in relative rotation i.e., a complete stage. Viscous effects may be approximated by a transpiration type of boundary layer displacement model or by the inclusion of a body force term in the momentum equations. R.J.F.

N85-32880# Joint Publications Research Service, Arlington, Va.
THEORETICAL FOUNDATIONS OF TURBULENT FLOWS Abstract Only
V. V. Struminskiy *In its* USSR Rept.: Phys. and Math. (JPRS-UPM-85-004) 17 Jun. 1985 p 21 Transl. into ENGLISH from Dokl. Akad. Nauk SSSR (Moscow), v. 280, no. 3, Jan. 1985 p 570-574 (For primary document see N85-32860 21-70)
Avail: NTIS HC A06/MF A01

N85-32881# Joint Publications Research Service, Arlington, Va.
TOWARD THE PROPAGATION OF WAVES IN UNSTEADY MEDIA Abstract Only
V. I. Pavlov, M. Mamatkulov, and P. K. Khabibullayev *In its* USSR Rept.: Phys. and Math. (JPRS-UPM-85-004) 17 Jun. 1985 p 21 Transl. into ENGLISH from Izv. Akad. Nauk UZSSR: Ser. Fiz.-Mat. Nauk (Tashkent), no. 4, Jul. - Aug. 1984 p 44-47 (For primary document see N85-32860 21-70)
Avail: NTIS HC A06/MF A01

N85-32882# Joint Publications Research Service, Arlington, Va.
EXACT SOLUTIONS OF SINGULAR EQUATIONS FOR VISCOUS TRANSONIC FLOWS Abstract Only
Yu. V. Zasorin *In its* USSR Rept.: Phys. and Math. (JPRS-UPM-85-004) 17 Jun. 1985 p 22 Transl. into ENGLISH from Dokl. Akad. Nauk SSSR (Moscow), v. 278, no. 6, Oct. 1984 p 1347-1351 (For primary document see N85-32860 21-70)
Avail: NTIS HC A06/MF A01

N85-32883# Joint Publications Research Service, Arlington, Va.
EXPLOSION IN FLIGHT Abstract Only
L. V. Shurshalov *In its* USSR Rept.: Phys. and Math. (JPRS-UPM-85-004) 17 Jun. 1985 p 24 Transl. into ENGLISH from Izv. Akad. Nauk SSSR: Mekhan. Zhidkosti i Gaza (Moscow), no. 5, Sep. - Oct. 1984 p 126-129 Original language document announced in IAA as A85-16180 (For primary document see N85-32860 21-70)
Avail: NTIS HC A06/MF A01

35 INSTRUMENTATION AND PHOTOGRAPHY

Includes remote sensors; measuring instruments and gages; detectors; cameras and photographic supplies; and holography.

For aerial photography see *43 Earth Resources.* For related information see also *06 Aircraft Instrumentation,* and *19 Spacecraft Instrumentation.*

N85-32302*# National Aeronautics and Space Administration. Lewis Research Center, Cleveland, Ohio.
A COMPARISON OF ELECTRONIC HETERODYNE MOIRE DEFLECTOMETRY AND ELECTRONIC HETERODYNE HOLOGRAPHIC INTERFEROMETRY FOR FLOW MEASUREMENTS
Arthur J. Decker and Josef Stricker (Technion - Israel Inst. of Tech.) 1985 19 p refs Proposed for presentation at the Aerospace Technol. Conf. and Exposition, Long Beach, Calif., 14-17 Oct. 1985; sponsored by Society of Automotive Engineers (NASA-TM-87071; E-2643; NAS 1.15:87071) Avail: NTIS HC A02/MF A01 CSCL 14B

Electronic heterodyne moire deflectometry and electronic heterodyne holographic interferometry are compared as methods for the accurate measurement of refractive index and density change distributions of phase objects. Experimental results are presented to show that the two methods have comparable accuracy for measuring the first derivative of the interferometric fringe shift. The phase object for the measurements is a large crystal of KD*P, whose refractive index distribution can be changed accurately and repeatably for the comparison. Although the refractive index change causes only about one interferometric fringe shift over the entire crystal, the derivative shows considerable detail for the comparison.

As electronic phase measurement methods, both methods are very accurate and are intrinsically compatible with computer controlled readout and data processing. Heterodyne moire is relatively inexpensive and has high variable sensitivity. Heterodyne holographic interferometry is better developed, and can be used with poor quality optical access to the experiment. Author

N85-32303*# Texas Univ. at Dallas, Richardson. Center for Space Sciences.
A RETARDING ION MASS SPECTROMETER FOR THE DYNAMICS EXPLORER-1 Final Report
Willie Wright 10 Jul. 1985 128 p refs
(Contract NAS8-32831)
(NASA-CR-171588; NAS 1.26:171588) Avail: NTIS HC A07/MF A01 CSCL 14B

The Retarding Ion Mass Spectrometer (RIMS) for Dynamics Explorer-1 is an instrument designed to measure the details of the thermal plasma distribution. It combines the ion temperature determining capability of the retarding potential analyzer with the compositional capabilities of the mass spectrometer and adds multiple sensor heads to sample all directions relative to the spacecraft ram direction. This manual provides a functional description of the RIMS, the instrument calibration, and a description of the commands which can be stored in the instrument logic to control its operation. Author

N85-32304# Materials Research Labs., Ascot Vale (Australia).
PLASMA MASS AND EFFECTIVE INDUCTANCE IN A SMALL RAILGUN
A. J. Bedford Nov. 1984 15 p
(AD-A154644; MRL-R-947) Avail: NTIS HC A02/MF A01 CSCL 20/7

A series of firings of a small caliber plasma-driven electromagnetic railgun are described in which copper, aluminum and zinc foils are used to initiate the plasma. Three different masses of each type of foil are used. Projectile displacement-time profiles in the railgun bore are constructed from streak camera records and calculations based on experimental current vs time records are made to obtain effective inductance per unit length values (L'sub eff) for each firing. The effects of foil mass and species, plasma voltage and plasma leakage past the projectile are discussed in relation to the calculated L' sub eff values. Author (GRA)

N85-32305# Air Force Inst. of Tech., Wright-Patterson AFB, Ohio. School of Engineering.
VELOCITY AND TRANSIENT MEASUREMENTS IN A SHOCK TUBE USING A HOT-WIRE ANEMOMETER M.S. Thesis
S. M. McQueen Dec. 1984 116 p
(AD-A154694; AFIT/GAE/AA/84D-17) Avail: NTIS HC A06/MF A01 CSCL 14/2

This thesis investigated the suitability of the TSI IFA-100 intelligent flow analyzer system, with TSI 1210 and 1214-T1.5 hot-wire sensors, to measure the velocity behind the incident shock wave in a shock tube. Velocity fluctuations as a result of Karman vortex street formation behind a 3/16-inch cylinder were also measured. The range of Reynolds numbers was $23{,}000 < Re < 35{,}000$ in this configuration. Calibration of the hot-wire was accomplished from ambient temperature to 275 F with individual calibrations at discreet temperatures (i.e., 74 F, 175 F, 275 F) designed to cover the expected test conditions up to 200 F and 620 ft/s. Velocities measured ranged from 312 to 590 ft/s with 4% or better accuracy. Velocity fluctuations were measured and computed as turbulence intensities, and ranged from 1.75 to 9.52%. The results of the investigation showed favorable indication that velocity can be measured with reasonable accuracy in a shock tube with the IFA-100 system. GRA

N85-32306# Lincoln Lab., Mass. Inst. of Tech., Lexington.
NON-MODEL BASED ESTIMATION WITH APPLICATIONS TO SENSOR CALIBRATION USING MULTIPLE SENSORS
T. S. Lee 1 Apr. 1985 24 p
(Contract F19628-85-C-0002)
(AD-A154736; TR-714; ESD-TR-84-325) Avail: NTIS HC A02/MF A01 CSCL 12/1

A nonmodel based estimation procedure is introduced. The best estimate is defined to be the geometric center of the intersected error volume, and the error of the best estimate is defined as the distance of the intersected error volume measured from the center. Khachian's algorithm is extended to find the best estimate. When the algorithm is viewed as a system of nonlinear difference equations, conditions are established to test the existence of periodic solutions. A stopping rule is also introduced. A strategy for finding the error of the best estimate is described. Examples are given to illustrate the estimation procedure. GRA

N85-32307# Defence Research Establishment, Ottawa. (Ontario).
TEST EVALUATION OF THE HONEYWELL GG1111 SINGLE-DEGREE-OF-FREEDOM (SDF) STRAPDOWN GYROSCOPE
M. F. Vinnins and R. Apps Oct. 1984 31 p
(AD-A154768; DREO-TN-85-2) Avail: NTIS HC A03/MF A01 CSCL 17/7

Test results from the evaluation of a Honeywell GG1111 single-degree-of-freedom strapdown gyroscope are presented. Tests include both static and constant-rate tests in servo and in analog-torque-to-balance modes. Results of multiposition drift tests, drift stability, cool down sensitivity, temperature sensitivity, torque generator linearity, scale factor stability and torque generator sensitivity to IA rate changes are presented, described and discussed. GRA

N85-32308# Naval Air Test Center, Patuxent River, Md.
SSMIR (SOLID STATE MEMORY INSTRUMENTATION RECORDER): A NEW APPROACH TO ACQUIRING DATA DURING AN AIRCRAFT SEAT/SLED EJECTION SEQUENCE
D. M. Watters 15 Apr. 1985 19 p
(AD-A154780; NATC-TM-85-3-SY) Avail: NTIS HC A02/MF A01 CSCL 14/5

The current state of ejection seat/sled testing employs an Aydin/Vector Co., pulse code modulation/telemetry instrumentation package. While this system meets all channel/data rate requirements and has proven itself in field testing, some major deficiencies exist. Data turnaround is one drawback; up to several weeks are normally required to process and print out the results from any sled shot. A second major deficiency is the amount of data dropout that can occur. In an ejection seat test, orientation of the skull antenna or misalignment of sending and receiving antennas can result in loss of data. Current technology in data storage media and high speed controllers provides backup mode for data integrity and also permits faster data reduction. This paper summarizes an electrical/mechanical packaging design of a software controlled, nonvolatile data recording system which uses 8 megabits of bubble memory to provide 24 sec of data storage in parallel to the PCM/TM transmission. Preliminary laboratory bench testing of the Solid State Memory Instrumentation (SSMI) Recorder indicates that the bubble memory can withstand the high vibration g loads (20 Gs up to 2000 Hz) and environmental temperatures (85 C) encountered in ejection seat testing. Laboratory shock testing (ejection seat trainer) to 5 Gs has also been successful along with tower testing at the Naval Air Development Center to 25 Gs. GRA

N85-32309# Honeywell, Inc., Bloomington, Minn. Physical Sciences Center.
DEVELOPMENT OF WIDE BAND RECORDING MATERIALS Final Report, Jan. 1982 - Sep. 1984
T. J. Moravec Apr. 1985 35 p
(Contract F19628-82-C-0029)
(AD-A154961; RADC-TR-85-65) Avail: NTIS HC A03/MF A01 CSCL 14/5

This report is the final report of a program to develop hard carbon (diamond-like) coatings as environmentally protective coatings for laser disc optical recording media. Two methods for producing the hard carbon films on the metallic thin film media were studied: plasma CVD by a hydrocarbon gas (PCVD), and direct Carbon Ion Beam Deposition (CIBD). Both methods tended to remove the sensitive media layer before the hard carbon layer

could be formed. An additional oxide layer deposited on the metallic media solved this problem. This hard carbon/oxide/metallic media system was successful in resisting degradation due to moisture. GRA

N85-32310# Emory Univ., Atlanta, Ga. Dept. of Chemistry.
A MICROPROCESSOR-CONTROLLED, MULTICHANNEL FLUORIMETER FOR ANALYSIS OF SEA WATER
P. B. Oldham, G. Patonay, and I. M. Warner 30 Apr. 1985 29 p
(Contract N00014-83-K-0026)
(AD-A154986; EMORY/DC/TR/6) Avail: NTIS HC A03/MF A01 CSCL 08/10

The multichannel fluorimeter described provides good sensitivity and rapid data acquisition. The advantages of multichannel fluorescence detection are discussed with special reference to the continuous monitoring of in vivo chlorophyll fluorescence in sea waters. Experiments on chlorophyll a determinations indicate a detection limit of 5 times 10 to the minus 12th power M with a linear range over at least three orders of magnitudes of concentration. GRA

N85-32311# Department of the Army, Washington, D. C.
MICROWAVE SAW (SURFACE ACOUSTIC WAVE) MONOCHROMATOR Patent Application
A. Ballato, inventor (to Army) Filed 24 May 1985 134 p
(AD-D011718; US-Patent-Appl-SN-737627) Avail: NTIS HC A07/MF A01 CSCL 20/1

An acoustic surface wave device is configured as a bandpass filter. The device has similar groups of sinusoidal corrugations cut into portions of both the top and bottom surfaces of an otherwise flat piezoelectric substrate. A pair of input interdigital transducers is located upon one end of the top flat surface of the substrate. A similar pair of output interdigital transducers is located on the bottom flat surface of the substrate at the end opposite the input interdigital transducers. When an input RF spectral signal is applied to the input interdigital transducers, the transducers convert the electrical signal spectrum to a surface acoustic wave spectrum. When the surface acoustic wave spectrum strikes the corrugations cut into the top surface of the substrate, the corrugations selectively scatter certain spectral components into bulk vibration. The bulk vibration strikes the similar corrugations located upon the bottom of the substrate and the bulk vibratory energy is efficiently reconverted to surface acoustic vibration which propagates along the bottom surface of the substrate. GRA

N85-32312# Tri-Con Associates, Inc., Cambridge, Mass.
FABRICATION AND TEST OF MODIFIED QUADRUPOLE MASS SPECTROMETER Final Report, Apr. - Dec. 1984
C. G. Kuczun 10 Jan. 1985 23 p
(Contract F19628-84-C-0101)
(AD-A155186; AFGL-TR-85-0002) Avail: NTIS HC A02/MF A01 CSCL 14/2

The objective of this contract was to modify, fabricate, test, and deliver the electronics for a quadrupole ion/neutral mass spectrometer capable of making positive ion and neutral species measurements over a range of 1 to 70 atomic mass units (AMU) with a mass sampling rate of 100 per second. GRA

N85-32313# Santa Barbara Research Center, Goleta, Calif.
BACKGROUND EQUATORIAL ASTRONOMICAL MEASUREMENTS FOCAL PLANE ASSEMBLY (REFURBISHED HI STAR SOUTH) Final Technical Report, Feb. 1983 - Sep. 1984
R. O. Davis and C. B. Tacelli Sep. 1984 114 p
(Contract F19628-83-C-0062)
(AD-A155215; SBRC-41413; AFGL-TR-84-0224) Avail: NTIS HC A06/MF A01 CSCL 17/5

The objective of the contract was to revise the existing design and to disassemble, modify, reassemble, test, and deliver one customer-furnished HI STAR SOUTH Focal Plane Assembly (FPA) for use on the Background Equatorial Astronomical Measurements (BEAM) program. A second FPA was furnished by the customer for parts. The first part of this report discusses the changes made in the design and provides photographs and drawings showing the various stages of modification and assembly of the focal plane. The major portion of the report presents the final performance and environmental test data taken on the modified FPA. A brief description of the test setups used for each test is provided, with a summary of the method of measurement and the resultant data. The data taken on the spectral filters (transmission vs wavelength) are included in Appendix A. Appendix B gives the temperature sensor calibration curves. GRA

N85-32314# Aerospace Corp., El Segundo, Calif. Chemistry and Physics Lab.
THE ROLE OF LONG TERM LAMP FLUCTUATIONS IN THE RANDOM WALK OF FREQUENCY BEHAVIOR OF THE RUBIDIUM FREQUENCY STANDARD: A CASE STUDY
C. H. Volk and R. P. Frueholz 20 Mar. 1985 19 p
(Contract F04701-83-C-0084)
(AD-A155338; TR-0084A(5472-03)-2; SD-TR-85-01) Avail: NTIS HC A02/MF A01 CSCL 14/2

A long term frequency stability test performed on an EG&G prototype Rb atomic frequency standard revealed excellent performance for an Rb atomic clock. Also, some classic Rb clock behaviors were observed, namely, long term frequency drift, spontaneous frequency jumps and random walk of frequency noise for long averaging times. A careful analysis of the complete test record disclosed that the spontaneous frequency jumps and the random walk of frequency noise can be attributed to the behavior of the clock's discharge lamp. The long term frequency drift, however, was found not to be primarily lamp-related. Although results of only a single test on a single Rb clock are reported here, we believe that the results are applicable to Rb clock technology as a whole. GRA

N85-32315# Allied Bendix Corp., Kansas City, Mo.
IMPROVED COORDINATE MEASURING MACHINE CALIBRATION AND CONTROL
R. J. Russell May 1985 58 p refs
(Contract DE-AC04-76DP-00613)
(DE85-012053; BDX-613-3267) Avail: NTIS HC A04/MF A01 CSCL 14B

A method for calibrating and controlling the volumetric accuracy of a coordinate measuring machine (CMM) is discussed. The calibration standard required to implement this method has been designed and fabricated and its physical parameters evaluated. DOE

N85-32316# Geological Survey, Menlo Park, Calif.
COMPARISON OF SURVEY AND PHOTOGRAMMETRY METHODS TO POSITION GRAVITY DATA, YUCCA MOUNTAIN, NEVADA
D. A. Ponce, S. S. C. Wu, and J. B. Spielman 1985 14 p ref
(Contract DE-AI08-78ET-44802)
(DE85-011685; USGS-OFR-85-36) Avail: NTIS HC A02/MF A01

Locations of gravity stations at Yucca Mountain, Nevada, were determined by a survey using an electronic distance-measuring device and by a photogram-metric method. The data from both methods were compared to determine if horizontal and vertical coordinates developed from photogrammetry are sufficently accurate to position gravity data at the site. The results show that elevations from the photogrammetric data have a mean difference of 0.57 + or - 0.70 m when compared with those the surveyed data. Comparison of the horizontal control shows that the two methods agreed to within 0.01 minute. At a latitude of 45(0), an error of 0.01 minute (18m) corresponds to a gravity anomaly error of 0.015 mGal. Bouguer gravity anomalies are most sensitive to errors in elevation, thus elevation is the determining factor for use of photogrammetric or survey methods to position gravity data. Because gravity station positions are difficult to locate on aerial photographs, photogrammetric positions are not always exactly at the gravity station; therefore, large disagreements may appear when comparing electronic and photogrammetric measurements. DOE

N85-32317# Oak Ridge National Lab., Tenn.
FAILURE MECHANISMS IN METAL-SHEATHED THERMOCOU-

PLES
M. B. Herskovitz 22 May 1985 5 p Presented at the ASTM Comm. Meeting on Effects of Temp. on the Properties of Metals, Los Angeles, 22 May 1985
(Contract DE-AC05-84OR-21400)
(DE85-011929; CONF-8505102-1) Avail: NTIS HC A02/MF A01

This paper addresses industrial use of metal sheathed thermocouples and does not consider sophisticated, one of a kind research or test performance applications. Failures can result because of shortcomings in design, fabrication, installation, operation, and maintenance. These observations are based on personal laboratory and field experience and on information from several suppliers and users. Investigating the failure mechanisms of metal sheathed thermocouples is important because if we can reduce the failure rate, we can reduce product cost, and improve quality while becoming more efficient and cost effective. Failure mechanisms can be grouped according to the primary cause of failure; mechanical, chemical, electrical, and thermal. DOE

N85-32318# Allied Bendix Corp., Kansas City, Mo.
PLATING DENSITY STANDARDS Final Report
W. E. Holland May 1985 25 p
(Contract DE-AC04-76DP-00613)
(DE85-010014; BDX-613-3222) Avail: NTIS HC A02/MF A01

Methods of producing beta backscatter and eddy current standards from foils were developed. These methods reduce the uncertainty in thickness measurements of the standards by 50%. Additionally, these methods can produce standards that have an uncertainty of + or - 0.5% in mass per unit area and an uncertainty of + or - 1.5% in density. Six foils were weighed three times to evaluate the cleaning, handling, and weighing techniques. The foils were cleaned before each weighing. The largest standard deviation was + or - 0.007 mg, which was less than the basic uncertainty of the balance + or - 0.03 mg. An algorithm and software developed that are capable of measuring the areas of foil standards to an uncertainty of + or - 0.2%. The precision of actual measurements on 21 foils was + or - 0.05%. Four sets of standards were produced for the range 9 to 12 (MU)m. Poor foil thickness uniformity prevented full accuracy from being achieved; but in spite of this, activity curves (mass per unit area) for the sets lay in a + or - 2.5% band. This was excellent, considering that three times the standard deviation of the activity measurements (counts) was + or - 1.56% when the probe was not moved between readings. DOE

N85-32319# Los Alamos National Lab., N. Mex.
TAILORED VACUUM CHAMBERS FOR ac MAGNETS
A. Harvey 1985 4 p refs Presented at the Particle Accelerator Conf., Vancouver, British Columbia, 13-16 May 1985
(Contract W-7405-eng-36)
(DE85-010767; LA-UR-85-1167) Avail: NTIS HC A02/MF A01

The proposed LAMPF-II accelerator has a 60-Hz booster synchrotron and a 3-Hz main ring. To provide a vacuum enclosure inside the magnets with low eddy-current losses and minimal field distortion, yet capable of carrying RF image currents and providing beam stabilization, we propose an innovative combination pipe. Structurally, the enclosure is high-purity alumina ceramic, which is strong, radiation resistant, and has good vacuum properties. Applied to the chamber are thin, spaced, silver conductors using adapted thick-film technology. The conductor design can be tailored to the stabilization requirements, for example, longitudinal conductors for image currents, circumferential for transverse stabilization. The inside of the chamber has a thin, resistive coating to avoid charge build-up. The overall 60-Hz power loss is less than 100 W/m. DOE

N85-32379*# Geological Survey, Reston, Va.
LARGE FORMAT CAMERA PHOTOGRAPHS: A NEW TOOL FOR UNDERSTANDING ARID ENVIRONMENTS
Alta S. Walker *In* NASA. Goddard Space Flight Center Global Mega-Geomorphology Jul. 1985 p 89-90 (For primary document see N85-32357 21-42)
Avail: NTIS HC A07/MF A01 CSCL 14E

N85-32623# Tartu State Univ. (USSR).
MULTI-CHANNEL ELECTRIC AEROSOL SPECTROMETER
A. Mirme, M. Noppel, I. Peil, J. Salm, E. Tamm, and H. Tammet *In* Intern. Comm. for Cloud Phys. 11th Intern. Conf. on Atmosphere Aerosols, Condensation and Ice Nuclei, Vol. 2 1984 p 155-159 refs (For primary document see N85-32596 21-47)
Avail: NTIS HC A09/MF A01

N85-32625# Odessa State Univ. (USSR).
ANALYSIS OF PERFORMANCE OF DYNAMIC THERMAL DIFFUSION CHAMBER
G. N. Lipantov and G. L. Shingarev *In* Intern. Comm. for Cloud Phys. 11th Intern. Conf. on Atmosphere Aerosols, Condensation and Ice Nuclei, Vol. 2 1984 p 165-170 refs (For primary document see N85-32596 21-47)
Avail: NTIS HC A09/MF A01

N85-32627# Indian Inst. of Tropical Meteorology, Poona.
A THERMAL DIFFUSION CHAMBER FOR THE MEASUREMENT OF CLOUD CONDENSATION NUCLEI
S. Chaudhuri and K. G. Vernekar *In* Intern. Comm. for Cloud Phys. 11th Intern. Conf. on Atmosphere Aerosols, Condensation and Ice Nuclei, Vol. 2 1984 p 176-180 refs (For primary document see N85-32596 21-47)
Avail: NTIS HC A09/MF A01

N85-33048*# California Inst. of Tech., Pasadena.
HEXAGONAL UNIFORMLY REDUNDANT ARRAYS FOR CODED-APERTURE IMAGING
M. H. Finger and T. A. Prince *In its* Contrib. to the 19th Intern. Cosmic Ray Conf. 1985 4 p refs (For primary document see N85-33044 21-88)
(Grant NGR-05-002-160)
(Paper-OG-9.2-1) Avail: NTIS HC A03/MF A01 CSCL 03A

N85-33050*# California Inst. of Tech., Pasadena.
BALLOON-BORNE VIDEO CASSETTE RECORDERS FOR DIGITAL DATA STORAGE
W. E. Althouse and W. R. Cook *In its* Contrib. to the 19th Intern. Cosmic Ray Conf. 1985 3 p refs (For primary document see N85-33044 21-88)
(Grant NGR-05-002-160)
(Paper-OG-9.3-11) Avail: NTIS HC A03/MF A01 CSCL 14C

36 LASERS AND MASERS

Includes parametric amplifiers.

N85-32320# Battelle Columbus Labs., Ohio.
THREE-DIMENSIONAL PHOTOCHEMICAL MACHINING WITH LASERS Final Technical Report, 1 Jun. 1982 - 30 Sep. 1984
R. E. Schwerzel, W. A. Ivancic, D. R. Johnson, V. D. McGinniss, and V. E. Wood 28 Dec. 1984 254 p
(Contract F49620-82-C-0077)
(AD-A154711; AFOSR-85-0456TR) Avail: NTIS HC A12/MF A01 CSCL 13/8

The primary objective of this research has been to evaluate the technical feasibility of three-dimensional photochemical machining with lasers, or PCM. PCM is a concept for the rapid fabrication of high-precision three-dimensional solid objects by spatially selective photopolymerization (or, alternatively, depolymerization) at the intersection point of two intersecting laser beams. To obtain true spatially selective photochemistry, it is necessary to develop systems in which the first laser beam (Beam 1) will pump a photoinitiator or photosensitizer to an unreactive, and spontaneously reversible, metastable intermediate with an energy content less than that required to initiate the desired reaction. The second laser beam (Beam 2) then selectively pumps the intermediate species to an energy level above that required to fragment the photoinitiator and trigger the reaction. In this way, the photochemical reaction can be confined to the intersection point, with no reaction occurring in either beam above. GRA

N85-32321# Naval Research Lab., Washington, D. C.
THE 2-D SIMULATIONS OF THE NRL (NAVAL RESEARCH LABORATORY) LASER EXPERIMENT
J. G. Lyon 8 May 1985 37 p
(AD-A154915; NRL-MR-5491) Avail: NTIS HC A03/MF A01 CSCL 20/5

Two-dimensional gas-dynamic simulations of the NRL laser experiment have been performed to study the formation of aneurysms in the blast wave and to study the formation of structure internal to the blast front itself. In one set of simulations the debris shell was perturbed sinusoidally in mass and position and also perturbed to mimic the action of a slow jet of material leaving the target at slower speeds than the bulk of the debris. In all cases the blast wave remained stable to any aneurysm-like instability. Internal structure, however, was quite easily produced and grew as a function of time. In the other set of simulations the effect of a pre-heated channel upon the propagation of the blast wave was examined. Bulges in the blast wave shock front were produced in these simulations that could be the beginning of the aneurysm phenomenon, but the preheated channel by itself appears to be insufficient to produce the observed aneurysm.
GRA

N85-32322# Air Force Systems Command, Wright-Patterson AFB, Ohio. Foreign Technology Div.
A FAST DISCHARGE EXCIMER LASER WITH SYMMETRIC GEOMETRY
S. Y. Wen 19 Apr. 1985 10 p Transl. into ENGLISH from Dianzi Xuebao (China), v. 12, no. 1, Jan. 1984 p 104-106
(AD-A155294; AD-F300613; FTD-ID(RS)T-1626-84) Avail: NTIS HC A02/MF A01 CSCL 20/5

Up to date, the excimer lasers pumped by Blumlein circuit are mostly having an asymmetric geometry using single plate capacitors to store energy. The experiments of Schwab on N2 gas lasers showed that poor spatial symmetry of the laser beam is obtained from the single plate asymmetric laser. Beams with good spatial symmetry can be obtained from lasers of double plate structure. We have constructed a fast discharge excimer laser with symmetric geometry using glued and hot pressed double plate capacitor for energy storage. With this device, N2, XeF and KrF lasers with good spatial symmetry were obtained. Preliminary study on the parameters of the XeF excimer system was carried out with this experimental device. GRA

N85-32323# Physical Sciences, Inc., Andover, Mass.
THEORETICAL MODELING OF LASER INDUCED OPTICAL DEGRADATION Final Report, 19 Mar. 1982 - 18 Mar. 1983
R. G. Root, G. Weyl, M. G. Miller, and L. A. Popper May 1985 124 p
(Contract F29601-82-C-0050)
(AD-A155302; AD-F300614; BRL-CR-543) Avail: NTIS HC A06/MF A01 CSCL 20/6

Laser irradiation of optical elements can degrade the performance of an optical system. In this report methodology has been established for predicting the system performance of an irradiated optical system. Models required to implement the methodology have been developed & improved; the models predict: (1) the physical damage caused by laser irradiation, (2) the optical aberrations corresponding to the physical damage, and (3) the point spread function (or optical transfer function) for the optical system which includes the aberrations induced by laser irradiation. The optical aberrations caused by three types of physical damage have been modelled. The aberrations are represented as a local change in amplitude and phase of the light. Surface cracks effectively reduce the local transmission to zero. Exfoliation reduces the transmission slightly (approximately 0.08) but its main effect is to introduce a random phase difference between different flakes. Vaporization does not affect transmission, but it introduced potentially large phase differences over distances associated with variations in the vaporization dynamics. The point spread function has been calculated for a simple optical system which has optical aberrations produced by laser irradiation. The main features of the point spread function are: (1) a central spike whose proportional to the square of the area which is not damaged, and (2) a damage halo whose width is determined by the characteristic size of the individual damage elements and whose total height is proportional to the incoherent sum of the square of the area of each damaged element. GRA

N85-32324# Dartmouth Coll., Hanover, N.H.
CERENKOV MASER AND CERENKOV LASER DEVICES Final Report, 1 Jan. 1983 - 31 Dec. 1984
J. E. Walsh 3 Apr. 1985 49 p
(Contract DAAG29-83-K-0018)
(AD-A155443; ARO-19777.12-PH) Avail: NTIS HC A03/MF A01 CSCL 20/5

Cerenkov Masers were operated over a wavelength range extending from 1 cm to just below 1 mm, and power levels of 200-250 kW in the 1 cm range were obtained. In the 1 cm range, voltage-tuning over 1 octave was achieved, and at 3 mm, a single structure was tuned from 88 to 130 GHz. At the higher power levels, gas breakdown was used as a diagnostic tool. This work was described in a number of publications and a bibliography and abstracts are attached. A flat-grating cylindrical mirror-based device (the realivistic orotron) was also examined. Power levels comparable to or greater than the best that can be obtained from mm-wavelength, coupled-cavity, travelling-wave tubes were obtained. The voltage-tuning range of these devices was also substantial. Single resonators were tuned over a half octave range, about 30 GHz, and at higher frequencies (60-80 GHz) + or - 10 percent tuning was achieved. The peak power at shorter wavelengths was 10 kW, and in the 1 cm range, 30 kW levels were obtained. The development of the mm-wavelength Cerenkov source also led to consideration of far- to near-infrared Cerenkov lasers. These were compared to the undulator type of Free-Electron lasers, and their relative advantages and disadvantages explored. A proof-of-principle far-infrared experiment has been proposed.
GRA

N85-32325# OptiMetrics, Inc., Ann Arbor, Mich.
SHIP-TO-SHIP PROPAGATION: MARITIME DATA ANALYSES Final Report
J. L. Manning, J. A. Dowling, and J. R. Hummel Mar. 1985 127 p
(Contract N00228-82-C-8171)
(AD-A155484; OMI-116; NEPRF-CR-85-05) Avail: NTIS HC A07/MF A01 CSCL 20/6

An analysis of two sets of atmospheric optical and supporting meteorological data has been performed. The first data set was taken by an airborne differential absorption lidar (DIAL) system. From this data set, vertical water vapor density profiles were extracted and used to calculate transmittances for CW and pulsed DF lasers. Thermal blooming calculations also were made to compare the performance of a laser optimized using a standard atmosphere water profile with a laser optimized using DIAL-derived profiles. The difference was found to be small for the conditions used here. The second data set consisted of long-path atmospheric transmittance and radiosonde measurements made in support of a long focal length imaging demonstration (LFLID). Measured transmittances were compared with LOWTRAN 6 transmittance calculations. Good agreement was obtained in the 3 to 5 micrometer range. Comparisons for the 8 to 12 micrometer region showed calculated transmittances about a factor of 10 lower than measured values. GRA

N85-32326# National Bureau of Standards, Boulder, Colo. Quantum Physics Div.
DETECTION OF EXCITED STATES BY LASER-INDUCED FLUORESCENCE Final Report, Oct. 1982 - Sep. 1984
H. Tischer and A. V. Phelps Apr. 1985 36 p
(Contracts MIPR-FY1455-83-N0632; MIPR-FY1455-84-N0631)
(AD-A155558; AFWAL-TR-84-2113) Avail: NTIS HC A03/MF A01 CSCL 07/4

Laser absorption techniques have been developed for the measurement of densities of H2 (C 3 Pi sub u) metastable densities in H2 electrical discharges. Using this technique and a modulated

discharge we have found that the metastable density is proportional to discharge current density for current densities up to 10 A/sq cm. By using a pulsed laser to destroy the metastables we have obtained preliminary measurements of the metastable lifetime as a function of H2 density. GRA

N85-32327# United Technologies Research Center, East Hartford, Conn.
INVESTIGATION OF PLASMA PROCESSES IN ELECTRONIC TRANSITION LASERS Final Report, 1 Jun. 1976 - 30 May 1985
W. L. Nighan 30 May 1985 134 p
(Contract N00014-76-C-0847; Proj. RR0-1107)
(AD-A155598; UTRC/R85-922617-1) Avail: NTIS HC A07/MF A01 CSCL 20/5

This investigation consists of a report on investigations of the fundamental processes affecting the operation and performance of electrically excited lasers having potential utility in a variety of areas of importance to the Navy. Particular attention in this investigation has been focused on lasers of the rare gas-halide and mercury-halide classes which have very promising potential for development as efficient, scalable optical sources for the UV/visible regions of the spectrum. GRA

N85-32328# Sandia Labs., Albuquerque, N. Mex.
LASER BEAM INTERACTIONS WITH VAPOR PLUMES DURING Nd:YAG LASER WELDING ON ALUMINUM
H. C. Peebles, A. J. Russo, G. R. Hadley, and R. L. Akau 1985 2 p Presented at the IMOG Joining Subgroup Meeting, Los Alamos, N. Mex., 2 Apr. 1985
(Contract DE-AC04-76DP-00789)
(DE85-009793; SAND-84-2667C; CONF-8504128-2-Abst) Avail: NTIS HC A02/MF A01

Welds produced on pure aluminum targets using pulsed Nd:YAG lasers can be accurately described using a relatively simple conduction mode heat transfer model provided that the fraction of laser energy absorbed is known and the amount of metal vaporized is smalled however at laser fluences commonly used in many production welding schedules significant aluminum vaporization does occur. The possible mechanisms have been identified which could result in laser beam attenuation by the vapor plume. DOE

N85-32218# Joint Publications Research Service, Arlington, Va.
APPLICATIONS OF LASER TECHNOLOGY DESCRIBED
In its East Europe Rept.: Sci. and Technol. JPRS-ESA-85-023 30 Jul. 1985 p 1-6 Repr. from Bulgaria Today (Sofia), no. 448, 1985 p 14-15 (For primary document see N85-32217 21-31)
Avail: NTIS HC A03/MF A01

N85-32884# Joint Publications Research Service, Arlington, Va.
INVESTIGATION OF REPRODUCIBILITY OF EMISSION WAVELENGTH OF HELIUM-NEON LASER WITH EXTERNAL NEON ABSORPTION CELL (0.63 MICROMETERS) Abstract Only
V. Ye. Privalov and Ye. G. Chulyayeva *In its* USSR Rept.: Phys. and Math. (JPRS-UPM-85-004) 17 Jun. 1985 p 25 Transl. into ENGLISH from Optika i Spektroskopiya (Leningrad), v. 57, no. 5, Nov. 1984 p 909-912 (For primary document see N85-32860 21-70)
Avail: NTIS HC A06/MF A01

N85-32885# Joint Publications Research Service, Arlington, Va.
PROSPECTS FOR LASERS FOR FUSION ENERGY ASSESSED Abstract Only
N. Basov and V. Rozanov *In its* USSR Rept.: Phys. and Math. (JPRS-UPM-85-004) 17 Jun. 1985 p 26-27 Transl. into ENGLISH from Mosk. Komsomolets (Moscow), 20 Jan. 1985 p 4 (For primary document see N85-32860 21-70)
Avail: NTIS HC A06/MF A01

N85-32886# Joint Publications Research Service, Arlington, Va.
GENERATION OF SINGLE NANOSECOND HIGH-CONTRAST RADIATION PULES (LAMBDA=10.6 MICROMETERS) Abstract Only
V. V. Apollonov, G. G. Baytsur, V. V. Brytkov, S. I. Ziyenko, S. V. Muravev, V. R. Sorochenko, K. N. Firsov, Yu. A. Shakir, and V. A. Yamshchikov *In its* USSR Rept.: Phys. and Math. (JPRS-UPM-85-004) 17 Jun. 1985 p 28 Transl. into ENGLISH from Pis'ma v Zh. Tekhn. Fiz. (Leningrad), v. 10, no. 19, 12 Oct. 1984 p 1192-1196 (For primary document see N85-32860 21-70)
Avail: NTIS HC A06/MF A01

N85-32887# Joint Publications Research Service, Arlington, Va.
LASER ELEKTRONIKA-01 FOR AIR POLLUTION CONTROL LIDAR Abstract Only
In its USSR Rept.: Phys. and Math. (JPRS-UPM-85-004) 17 Jun. 1985 p 29 Transl. into ENGLISH from Sov. Rossiya (Moscow), 16 Dec. 1984 p 2 (For primary document see N85-32860 21-70)
Avail: NTIS HC A06/MF A01

N85-32888# Joint Publications Research Service, Arlington, Va.
INVESTIGATION OF INFLUENCE OF GAS EXIT MODES ON CHARACTERISTICS OF N2O - N2 - He DISCHARGE LASER Abstract Only
V. G. Testov, Yu. V. Konev, V. D. Menenkov, Yu. I. Grin, and G. I. Mishin *In its* USSR Rept.: Phys. and Math. (JPRS-UPM-85-004) 17 Jun. 1985 p 30 Transl. into ENGLISH from Zh. Tekhn. Fiz. (Leningrad), v. 54, no. 12, Dec. 1984 p 2305-2314 (For primary document see N85-32860 21-70)
Avail: NTIS HC A06/MF A01

N85-32889# Joint Publications Research Service, Arlington, Va.
INFLUENCE OF MIRROR ANISOTROPY AND BREWSTER WINDOW ORIENTATION ON RADIATION CHARACTERISTICS OF RING LASERS Abstract Only
V. S. Rubanov, V. N. Severikov, and A. I. Shevtsova *In its* USSR Rept.: Phys. and Math. (JPRS-UPM-85-004) 17 Jun. 1985 p 31 Transl. into ENGLISH from Dokl. Akad. Nauk BSSR (Minsk), v. 28, no. 12, Dec. 1984 p 1086-1089 (For primary document see N85-32860 21-70)
Avail: NTIS HC A06/MF A01

N85-32890# Joint Publications Research Service, Arlington, Va.
LASING ON LIF:F(-)2 - DYE CENTERS WITH TRANSVERSE PUMPING Abstract Only
F. V. Karpushko and V. P. Morozov *In its* USSR Rept.: Phys. and Math. (JPRS-UPM-85-004) 17 Jun. 1985 p 31 Transl. into ENGLISH from Zh. Prikl. Spektroskopii (Minsk), v. 41, no. 4, Oct. 1984 p 656-658 (For primary document see N85-32860 21-70)
Avail: NTIS HC A06/MF A01

N85-32891# Joint Publications Research Service, Arlington, Va.
PARTICIPATION OF SINGLET OXYGEN IN PHOTODESTRUCTION OF AIR-SATURATED SOLUTIONS OF COUMARIN DYES Abstract Only
O. V. Zinkovskaya, N. A. Kuznestova, and O. L. Kaliya *In its* USSR Rept.: Phys. and Math. (JPRS-UPM-85-004) 17 Jun. 1985 p 32 Transl. into ENGLISH from Zh. Prikl. Spektroskopii (Minsk), v. 41, no. 4, Oct. 1984 p 626-630 (For primary document see N85-32860 21-70)
Avail: NTIS HC A06/MF A01

N85-32892# Joint Publications Research Service, Arlington, Va.
THE POSSIBILITIES OF REMOTE ANALYSIS OF ATMOSPHERIC GASES BASED ON RAMAN SCATTERING SPECTROSCOPY Abstract Only
G. N. Glazov and S. A. Danichkin *In its* USSR Rept.: Phys. and Math. (JPRS-UPM-85-004) 17 Jun. 1985 p 32 Transl. into ENGLISH from Zh. Prikl. Spektroskopii (Minsk), v. 41, no. 4, Oct. 1984 p 609-614 Original language document announced in IAA as A85-20589 (For primary document see N85-32860 21-70)
Avail: NTIS HC A06/MF A01

N85-32893# Joint Publications Research Service, Arlington, Va.
CHOICE OF OPTIMUM SATURATING ABSORBER FOR YAG PASSIVE MODE-LOCKING LASER Abstract Only
M. I. Demchuk, V. P. Mikhaylov, and K. V. Yumashev *In its* USSR Rept.: Phys. and Math. (JPRS-UPM-85-004) 17 Jun. 1985 p 33 Transl. into ENGLISH from Zh. Prikl. Spektroskopii (Minsk), v. 41, no. 4, Oct. 1984 p 566-571 (For primary document see N85-32860 21-70)
Avail: NTIS HC A06/MF A01

N85-32895# Joint Publications Research Service, Arlington, Va.
OPERATION OF SOLID STATE LASERS EXPOSED TO ELECTRON BEAM Abstract Only
M. R. Bedilov, Kh. B. Beysembayeva, P. K. Khabibullayev, and R. P. Saidov *In its* USSR Rept.: Phys. and Math. (JPRS-UPM-85-004) 17 Jun. 1985 p 34 Transl. into ENGLISH from Kvantovaya Elektron. (Moscow), v. 11, no. 10, Oct. 1984 p 2121-2126 (For primary document see N85-32860 21-70)
Avail: NTIS HC A06/MF A01

N85-32896# Joint Publications Research Service, Arlington, Va.
ESTABLISHMENT OF STEADY-STATE POWER LEVEL IN PULSE-PERIODIC EXCIMER LASER Abstract Only
V. M. Borisov, F. I. Vysikaylo, A. Yu. Vinokhodov, and Yu. B. Kiryukhin *In its* USSR Rept.: Phys. and Math. (JPRS-UPM-85-004) 17 Jun. 1985 p 34 Transl. into ENGLISH from Kvantovaya Elektron. (Moscow), v. 11, no. 10, Oct. 1984 p 2069-2073 (For primary document see N85-32860 21-70)
Avail: NTIS HC A06/MF A01

N85-32897# Joint Publications Research Service, Arlington, Va.
THE PROBLEM OF BRIGHTNESS ENHANCEMENT DURING LASER FREQUENCY DOUBLING Abstract Only
V. S. Averbakh, A. I. Makarov, and A. K. Potemkin *In its* USSR Rept.: Phys. and Math. (JPRS-UPM-85-004) 17 Jun. 1985 p 35 Transl. into ENGLISH from Kvantovaya Elektron. (Moscow), v. 11, no. 10, Oct. 1984 p 2049-2058 (For primary document see N85-32860 21-70)
Avail: NTIS HC A06/MF A01

N85-32898# Joint Publications Research Service, Arlington, Va.
LASER RADIATION PROPAGATION IN INERTIALESS NONLINEAR MEDIUM Abstract Only
K. S. Gochelashvili, I. V. Chashey, and V. I. Shishov *In its* USSR Rept.: Phys. and Math. (JPRS-UPM-85-004) 17 Jun. 1985 p 35 Transl. into ENGLISH from Kvantovaya Elektron. (Moscow), v. 11, no. 10, Oct. 1984 p 2036-2040 (For primary document see N85-32860 21-70)
Avail: NTIS HC A06/MF A01

N85-32899# Joint Publications Research Service, Arlington, Va.
DYNAMICS OF EMISSION FROM DYE LASERS EMPLOYING SYNCHRONOUS PUMPING BY LIMITED PICOSECOND PULSE TRAIN Abstract Only
A. I. Kovrigin, V. A. Nekhayenko, S. M. Pershin, and A. A. Podshivalov *In its* USSR Rept.: Phys. and Math. (JPRS-UPM-85-004) 17 Jun. 1985 p 36 Transl. into ENGLISH from Kvantovaya Elektron. (Moscow), v. 11, no. 10, Oct. 1984 p 2007-2018 (For primary document see N85-32860 21-70)
Avail: NTIS HC A06/MF A01

N85-32900# Joint Publications Research Service, Arlington, Va.
HIGH-POWER TWO-FREQUENCY CW DYE LASER Abstract Only
V. I. Balykin and A. I. Sidorov *In its* USSR Rept.: Phys. and Math. (JPRS-UPM-85-004) 17 Jun. 1985 p 36-37 Transl. into ENGLISH from Kvantovaya Elektron. (Moscow), v. 11, no. 10, Oct. 1984 p 2001-2006 Original language document previously announced in IAA as A85-21024 (For primary document see N85-32860 21-70)
Avail: NTIS HC A06/MF A01

N85-32901# Joint Publications Research Service, Arlington, Va.
SATURATION EFFECT IN MULTILEVEL LASING MEDIA Abstract Only
V. I. Lvov, A. A. Stepanov, and V. A. Shcheglov *In its* USSR Rept.: Phys. and Math. (JPRS-UPM-85-004) 17 Jun. 1985 p 37 Transl. into ENGLISH from Kvantovaya Elektron. (Moscow), v. 11, no. 10, Oct. 1984 p 1975-1983 Original language document previously announced in IAA as A85-21021 (For primary document see N85-32860 21-70)
Avail: NTIS HC A06/MF A01

N85-32902# Joint Publications Research Service, Arlington, Va.
OPTICAL INHOMOGENEITIES IN A NANOSECOND-PULSE IODINE PHOTODISSOCIATION LASER WITH SLOW UV RADIATION PUMPING Abstract Only
I. Skala, M. Khvoyka, L. Pekarek, B. Kralikova, V. S. Zuyev, K. S. Korolkov, and Ye. P. Orlov *In its* USSR Rept.: Phys. and Math. (JPRS-UPM-85-004) 17 Jun. 1985 p 37-38 Transl. into ENGLISH from Kvantovaya Elektron. (Moscow), v. 11, no. 10, Oct. 1984 p 1940-1946 Original language document previously announced in IAA as A85-21018 (For primary document see N85-32860 21-70)
Avail: NTIS HC A06/MF A01

N85-32903# Joint Publications Research Service, Arlington, Va.
EXCIMER-LASER GENERATOR OF POWERFUL UV PICOSECOND PULSES SYNCHRONIZED WITH PICOSECOND PULSES IN VISIBLE AND IR BANDS Abstract Only
S. A. Akhmanov, A. M. Valshin, V. M. Gordiyenko, M. S. Dzhidzhoyev, S. V. Krayushkin, V. T. Platonenko, and V. K. Popov *In its* USSR Rept.: Phys. and Math. (JPRS-UPM-85-004) 17 Jun. 1985 p 38 Transl. into ENGLISH from Kvantovaya Elektron. (Moscow), v. 11, no. 10, Oct. 1984 p 1897-1898 (For primary document see N85-32860 21-70)
Avail: NTIS HC A06/MF A01

N85-32904# Joint Publications Research Service, Arlington, Va.
POSSIBILITY OF MEASUREMENT OF SMALL DISPLACEMENTS BY RING LASER Abstract Only
E. M. Belenov, M. V. Danileyko, and A. V. Uskov *In its* USSR Rept.: Phys. and Math. (JPRS-UPM-85-004) 17 Jun. 1985 p 38-39 Transl. into ENGLISH from Kvantovaya Elektron. (Moscow), v. 11, no. 10, Oct. 1984 p 1894-1896 Original language document previously announced in IAA as A85-21015 (For primary document see N85-32860 21-70)
Avail: NTIS HC A06/MF A01

N85-32905# Joint Publications Research Service, Arlington, Va.
INFRARED LASER HOLOGRAPHY USED IN FUSION PLASMA STUDIES Abstract Only
In its USSR Rept.: Phys. and Math. (JPRS-UPM-85-004) 17 Jun. 1985 p 40 Transl. into ENGLISH from Sov. Latviya (Riga), Mar. 1985 p 4 (For primary document see N85-32860 21-70)
Avail: NTIS HC A06/MF A01

N85-32906# Joint Publications Research Service, Arlington, Va.
TUNABLE LASERS WITH HIGH CONVERSION EFFICIENCY Abstract Only
In its USSR Rept.: Phys. and Math. (JPRS-UPM-85-004) 17 Jun. 1985 p 41 Transl. into ENGLISH from Mosk. Pravda (Moscow), no. 56 (19776), 7 Mar. 1985 p 1, columns 5-6 (For primary document see N85-32860 21-70)
Avail: NTIS HC A06/MF A01

N85-32907# Joint Publications Research Service, Arlington, Va.
SELF Q-MODULATION AND GENERATION OF SHORT PULSES IN DISTRIBUTED-FEEDBACK LASERS Abstract Only
R. A. Karamaliyev and Dao Suan Khay *In its* USSR Rept.: Phys. and Math. (JPRS-UPM-85-004) 17 Jun. 1985 p 42 Transl. into ENGLISH from Dokl. Akad. Nauk Azerbaydzhanskoy SSR (Baku), v. 40, no. 8, Aug. 1984 p 31-33 (For primary document see N85-32860 21-70)
Avail: NTIS HC A06/MF A01

N85-32908# Joint Publications Research Service, Arlington, Va.
LOW-THRESHOLD INJECTION InGaAsP/GaAs DOUBLE HETEROSTRUCTURE LASERS WITH SEPARATE LIMITING OBTAINED BY LIQUID-PHASE EPITAXY (LAMBDA = 0.78 DIVIDED BY 0.87 MICRONS, I SUB thr = 460 A/cm 2, T = 300 K) Abstract Only
Zh. I. Alfeerov, I. N. Arsentev, L. S. Vavilova, D. Z. Garbuzov, and V. V. sKrasovskiy *In its* USSR Rept.: Phys. and Math. (JPRS-UPM-85-004) 17 Jun. 1985 p 42-43 Transl. into ENGLISH from Prikl. Mat. i Mekhan. (Moscow), v. 48, no. 4, Jul. - Aug. 1984 p 1655-1659 (For primary document see N85-32860 21-70)
Avail: NTIS HC A06/MF A01

N85-32909# Joint Publications Research Service, Arlington, Va.
SPACE-TIME CHARACTERISTICS OF FIELD IN LONGITUDINAL PULSE-PERIOD DISCHARGE TYPICAL IN PUMPING OF SELF-TERMINATING LASERS Abstract Only
V. N. Kukharev *In its* USSR Rept.: Phys. and Math. (JPRS-UPM-85-004) 17 Jun. 1985 p 43 Transl. into ENGLISH from Zh. Tekhn. Fiz. (Leningrad), v. 54, no. 10, Oct. 1984 p 1910-1914 Previously announced in IAA as A85-36514 (For primary document see N85-32860 21-70)
Avail: NTIS HC A06/MF A01

N85-32910# Joint Publications Research Service, Arlington, Va.
INFLUENCE OF TECHNOLOGICAL FACTORS ON LUMINESCENCE CHARACTERISTICS OF InGaAsP/InP HETEROLASERS (LAMBDA = 1.55 MICRONS) Abstract Only
A. T. Gorelenok, V. G. Gruzdov, and I. S. Tarasov *In its* USSR Rept.: Phys. and Math. (JPRS-UPM-85-004) 17 Jun. 1985 p 43-44 Transl. into ENGLISH from Zh. Tekhn. Fiz. (Leningrad), v. 54, no. 10, Oct. 1984 p 2047-2050 (For primary document see N85-32860 21-70)
Avail: NTIS HC A06/MF A01

N85-32911# Joint Publications Research Service, Arlington, Va.
POWERFUL XeCl EXCIMER ELECTRIC DISCHARGE LASER WITH GOOD TEMPORAL STABILITY AND FAST RESPONSE TIME Abstract Only
M. S. Dzhidzhoyev, V. T. Platonenko, and V. K. Popov *In its* USSR Rept.: Phys. and Math. (JPRS-UPM-85-004) 17 Jun. 1985 p 44 Transl. into ENGLISH from Vestn. Mosk. Univ.: Fiz., Astron. (Moscow), v. 25, no. 5, Sep. - Oct. 1984 p 113-115 (For primary document see N85-32860 21-70)
Avail: NTIS HC A06/MF A01

N85-32912# Joint Publications Research Service, Arlington, Va.
SPECTRAL-LUMINESCENCE CHARACTERISTICS AND INDUCED EMISSION OF Nd-3(+) ION IN Gd(2-X)Nd(X)(WO4)3 CRYSTALS Abstract Only
V. A. Berenberg, A. O. Ivanov, L. I. Krutova, I. V. Mochalov, and V. S. Terpugov *In its* USSR Rept.: Phys. and Math. (JPRS-UPM-85-004) 17 Jun. 1985 p 44-45 Transl. into ENGLISH from Optika i Spektroskopiya (Leningrad), v. 57, no. 3, Sep. 1984 p 455-459 (For primary document see N85-32860 21-70)
Avail: NTIS HC A06/MF A01

N85-32913# Joint Publications Research Service, Arlington, Va.
ADJUSTMENT OF RADIATION WAVELENGTH OF MULTIMODE InP-GaInAsP INJECTION HETEROLASERS Abstract Only
Ya. E. Kirson, E. E. Klotynsh, and I. A. Churkste *In its* USSR Rept.: Phys. and Math. (JPRS-UPM-85-004) 17 Jun. 1985 p 48 Transl. into ENGLISH from Izv. Akad. Nauk Latviyskoy SSR: Ser. Fiz. i Tekhn. Nauk (Riga), no. 5, Oct. - Nov. 1984 p 15-18 (For primary document see N85-32860 21-70)
Avail: NTIS HC A06/MF A01

N85-32914# Joint Publications Research Service, Arlington, Va.
SELECTIVE POPULATION OF N = 3 OVIII LEVEL DURING EXPANSION OF LASER PLASMA IN HELIUM Abstract Only
S. P. Zhukov, V. V. Korukhov, B. I. Troshin, and A. A. Chernenko *In its* USSR Rept.: Phys. and Math. (JPRS-UPM-85-004) 17 Jun. 1985 p 48-49 Transl. into ENGLISH from Pisma Zh. Eksperim. i Teor. Fiz. (Moscow), v. 40, no. 8, Oct. 1984 p 340-342 (For primary document see N85-32860 21-70)
Avail: NTIS HC A06/MF A01

N85-32915# Joint Publications Research Service, Arlington, Va.
PASSIVE Q-MODULATION OF OPTICAL CAVITIES BY KCl CRYSTALS CONTAINING OH(-) -IONS Abstract Only
L. M. Sobolev, V. V. Bryukvin, I. A. Parfianovich, and E. E. Penzina *In its* USSR Rept.: Phys. and Math. (JPRS-UPM-85-004) 17 Jun. 1985 p 49 Transl. into ENGLISH from Optika i Spektroskopiya (Leningrad), v. 57, no. 5, Nov. 1984 p 954-956 (For primary document see N85-32860 21-70)
Avail: NTIS HC A06/MF A01

N85-32921# Joint Publications Research Service, Arlington, Va.
DOPPLER SPECTROMETER FOR MEASURING NARROW PHOTOCHEMICAL GAPS IN INHOMOGENEOUSLY BROADENED SPECTRA Abstract Only
K. K. Rebane and V. Palm *In its* USSR Rept.: Phys. and Math. (JPRS-UPM-85-004) 17 Jun. 1985 p 53-54 Transl. into ENGLISH from Izv. Akad. Nauk Estonskoy SSR: Fiz. Mat. (Tallinn), v. 33, no. 4 p 461-463 (For primary document see N85-32860 21-70)
Avail: NTIS HC A06/MF A01

N85-32953# Joint Publications Research Service, Arlington, Va.
ABSORPTION OF LASER RADIATION IN SUBSTANCE WITH ABSORPTION COEFFICIENT DEPENDING LINEARLY UPON TEMPERATURE Abstract Only
I. V. Yedvabnyy and S. A. Ubaydullayev *In its* USSR Rept.: Phys. and Math. (JPRS-85-004) 17 Jun. 1985 p 76 Transl. into ENGLISH from Izv. Akad. Nauk Uzb. SSR, Ser. Fiz.-Mat. Nauk (Tashkent), no. 5, Sep. - Oct. 1984 p 76-78 (For primary document see N85-32860 21-70)
Avail: NTIS HC A06/MF A01

N85-32971# Joint Publications Research Service, Arlington, Va.
ON ONE NONLINEAR PROBLEM OF LASER THERMOCHEMISTRY Abstract Only
F. V. Bunkin, V. A. Galaktionov, N. A. Kirichenko, S. P. Kurdyumov, and A. A. Samarskiy *In its* USSR Rept.: Phys. and Math. (JPRS-UPM-85-004) 17 Jun. 1985 p 89 Transl. into ENGLISH from Dokl. Akad. Nauk SSSR (Moscow), v. 279, no. 4, Dec. 1984 p 838-842 (For primary document see N85-32860 21-70)
Avail: NTIS HC A06/MF A01

37 MECHANICAL ENGINEERING

Includes auxiliary systems (non-power); machine elements and processes; and mechanical equipment.

N85-32329*# National Aeronautics and Space Administration. Lewis Research Center, Cleveland, Ohio.
SURFACE ROUGHNESS EFFECTS IN ELASTOHYDRODYNAMIC CONTACTS
John H. Tripp (Case Western Reserve Univ.) and Bernard J. Hamrock Jul. 1985 14 p refs Presented at the 11th Leeds-Lyon Symp. on Mixed Lubrication and Lubricated Wear, Leeds, Engl., 4-7 Sep. 1984
(NASA-TP-2488; E-2524; NAS 1.60:2488) Avail: NTIS HC A02/MF A01 CSCL 20K

Surface roughness effects in full-film EHL contacts were studied. A flow factor modification to the Reynolds equation was applied to piezoviscous-elastic line contacts. Results for ensemble-averaged film shape, pressure distribution, and other mechanical quantities were obtained. Asperities elongated in the flow direction by a factor exceeding two decreased both film shape and pressure extrema at constant load; isotropic or transverse asperities increased these extrema. The largest effects are displayed by traction, which increased by over 5% for isotropic or transverse asperities and by slightly less for longitudinal roughness. E.A.K.

N85-32330*# National Aeronautics and Space Administration. Lewis Research Center, Cleveland, Ohio.
MECHANICS OF A GASEOUS FILM BARRIER TO LUBRICANT WETTING OF ELASTOHYDRODYNAMICALLY LUBRICATED CONJUNCTIONS
Joseph M. Prahl (Case Western Reserve Univ.) and Bernard J. Hamrock Aug. 1985 17 p refs Presented at the 11th Leeds-Lyon Symp. on Mixed Lubrication and Lubricated Wear, Leeds, Engl.,

4-7 Sep. 1984
(Grant NCC3-30)
(NASA-TP-2500; E-2523; NAS 1.60:2500) Avail: NTIS HC A02/MF A01 CSCL 20K

Two analytical models, one based on simple hydrodynamic lubrication and the other on soft elastohydrodynamic lubrication, are presented and compared to delineate the dominant physical parameters that govern the mechanics of a gaseous film between a small droplet of lubricant and the outer race of a ball bearing. Both models are based on the balance of gravity forces, air drag forces, and air film lubrication forces and incorporate a drag coefficient C sub D and a lubrication coefficient C sub L to be determined from experiment. The soft elastohydrodynamic lubrication (EHL) model considers the effects of droplet deformation and solid-surface geometry; the simpler hydrodynamic lubrication (HL) model assumes that the droplet remains essentially spherical. The droplet's angular position depended primarily on the ratio of gas inertia to droplet gravity forces and on the gas Reynolds number and weakly on the ratio of droplet gravity forces to surface tension forces (Bond number) and geometric ratios for the soft EHL. An experimental configuration in which an oil droplet is supported by an air film on the rotating outer race of a ball bearing within a pressure-controlled chamber produced measurements of droplet angular position as a function of outer-race velocity droplet size and type, and chamber pressure. E.A.K.

N85-32331*# National Aeronautics and Space Administration. Lewis Research Center, Cleveland, Ohio.
HERTZIAN CONTACT IN TWO AND THREE DIMENSIONS
John H. Tripp (Case Western Reserve Univ.) Jul. 1985 27 p refs
(NASA-TP-2473; E-2256; NAS 1.60:2473) Avail: NTIS HC A03/MF A01 CSCL 20K

The basic solution to the problem of mechanical contact between elastically deforming solids was proposed by Hertz over a century ago and has been used by tribologists and others ever since in a steadily increasing number of applications. While the theoretical development is not conceptually difficult and treatments exist to suit all tastes, it is nonetheless interesting to trace the relationships among the solutions in different dimensions. Such an approach is used herein to shed light on the curious and sometimes perplexing behavior of line contacts. A number of the more frequently used contact expressions together as a convenient reference and for comparative purposes. Author

N85-32332*# Texas A&M Univ., College Station. Turbomachinery Lab.
A COMPARISON OF EXPERIMENTAL AND THEORETICAL RESULTS FOR ROTORDYNAMIC COEFFICIENTS OF FOUR ANNULAR GAS SEALS Progress Report
Dara W. Childs, Clayton Nelson, David Elrod, and Colby Nicks Jul. 1985 128 p refs
(Contract NAS8-33716)
(NASA-CR-176086; NAS 1.26:176086; TRC-Seals-5-85) Avail: NTIS HC A07/MF A01 CSCL 13K

The test facility and initial test program developed to experimentally measure the fluid forces induced by annular gas seals is described. A comparison of theoretically predicted and experimentally obtained data for smooth and honeycomb seals is provided. And a comparison of experimental data from the tests of three smooth-rotor/smooth-stator seals is provided. The leakage of the working fluid through the seal, the pressure gradient along the seal length, entrance pressure-loss data, and rotordynamic coefficients provide a basis for comparison. A short discussion on seal theory is included, and various rotordynamic coefficient identification schemes are described. Author

N85-32333*# National Aeronautics and Space Administration. Lewis Research Center, Cleveland, Ohio.
TAPE CASTING AS AN APPROACH TO AN ALL-CERAMIC TURBINE SHROUD SEAL
James D. Cawley Jul. 1985 11 p refs
(NASA-TM-87078; E-2607; NAS 1.15:87078) Avail: NTIS HC A02/MF A01 CSCL 11A

Gas path seals have a one-dimensional variation in material requirement. Tape casting is a method which allows the fabrication of thin ceramic sheets, which may be laminated to accommodate these requirements. Using tape casting, thin sheets of zirconia (0.25 mm) were fabricated. These castings were successfully laminated and fired without bloating or delamination, demonstrating the feasibility of this approach. Author

N85-32334*# Auburn Univ., Ala. Dept. of Mechanical Engineering.
MEASUREMENT OF DAMPING OF GRAPHITE EPOXY MATERIALS Monthly Report, 1-30 Jun. 1985
M. J. Crocker 1 Jul. 1985 12 p
(Contract NAS8-36146)
(NASA-CR-176073; NAS 1.26:176073) Avail: NTIS HC A02/MF A01 CSCL 13E

Work on a damping measurement test apparatus is discussed. The device is designed to excite tube specimens in a vacuum chamber. Also some experiments were conducted on a tube specimen to confirm previously reported results. A table of data showing the results of forced vibration tests using a half ring and a free-free boundary is given. The main purpose was to study the effect of the frequency resolution on the damping ratio measurements. R.J.F.

N85-32335# Mechanical Technology, Inc., Latham, N. Y.
FRICTION AND WEAR OF SOLID-LUBRICATED CONTACT IN GAS TURBINE ENGINE BEARINGS Final Report, Apr. 1983 - Sep. 1984
S. Gray and P. K. Gupta Nov. 1984 108 p
(Contract F33615-83-C-5037)
(AD-A155042; MTI-84TR72; AFWAL-TR-84-4143) Avail: NTIS HC A06/MF A01 CSCL 11/8

A study was performed for a high temperature solid lubricated ball bearing under conditions representative of a gas turbine engine. The performance predictions were compared to the experimental test behavior of complete ball bearings and showed good correlation. In the pin on disc type material sliding tests, the friction and wear performance of M-50, NC-132, and alpha silicon carbide pairs with HAC-1 type lubricant composite were determined. In the first test mode, to simulate the interactions between the cage material and other bearing elements, the pairing of HAC-1 with M-50 and NC-132 at conditions up to 30,000 rpm and 316 C showed that the HAC-1 and NC-132 pair gave the lowest friction and wear and more stable temperatures. In the second test mode, to simulate low speed skidding which occurs between the ball and race materials, rapid wear was found and friction was high. This test data was used to prepare traction coefficient models as input to the ADORE computer program for bearing performance simulation. The analysis predicted that due to the high traction coefficients, the interactive forces are quite large, erratic, and inducive to cage wear and breakage. The good agreement with full scale testing of bearings demonstrated the significance of this combined material evaluation computer modeling technique. GRA

N85-32336# Naval Postgraduate School, Monterey, Calif.
ULTRASONIC POSITION REFERENCE SYSTEMS FOR AN AUTONOMOUS SENTRY ROBOT AND A ROBOT MANIPULATOR ARM M.S. Thesis
W. M. Dunkin Mar. 1985 97 p
(AD-A155481) Avail: NTIS HC A05/MF A01 CSCL 09/2

This thesis proposes and develops two microprocessor controlled ultrasonic systems which provide absolute coordinate reference for an autonomous sentry robot and a robotic manipulator. These systems close the position control loop which has never been fully closed in robotics and provide a better testbed for testing path planning and manipulator arm trajectory control. Each system involves known points of reference and ranges to these points which are determined by timing the interval of propagation of the ultrasonic transmissions. With this data, a microprocessor calculates the positions in Cartesian coordinates. GRA

N85-32219# Joint Publications Research Service, Arlington, Va.
IMPORTANCE OF AUTOMATION, ROBOTIZATION IN ECONOMY
Aristide Predoi *In its* East Europe Rept.: Sci. and Technol. JPRS-ESA-85-023 30 Jul. 1985 p 26-31 Transl. into ENGLISH from Era Socialista (Bucharest), no. 8, 25 Apr. 1985 p 9-11 (For primary document see N85-32217 21-31)
Avail: NTIS HC A03/MF A01

N85-32786# Joint Publications Research Service, Arlington, Va.
ROBOTS, MANIPULATORS
J. Grecner *In its* East Europe Rept.: Sci. and Technol. Selections on CSSR JPRS-ESA-84-017 31 May 1984 p 25-28 Transl. into ENGLISH from Sdelovaci Technika (Prague), no. 12, 1983 p 441-442 (For primary document see N85-32781 21-60)
Avail: NTIS HC A05/MF A01

38 QUALITY ASSURANCE AND RELIABILITY

Includes product sampling procedures and techniques; and quality control.

N85-32337*# National Aeronautics and Space Administration. Lewis Research Center, Cleveland, Ohio.
RELIABILITY OF VOID DETECTION IN STRUCTURAL CERAMICS USING SCANNING LASER ACOUSTIC MICROSCOPY
Don J. Roth, Stanley J. Klima, James D. Kiser, and George Y. Baaklini (Cleveland State Univ.) 1985 54 p refs Presented at the Spring Meeting of the Am. Soc. for Nondestructive Testing, Washington, D.C., 11-14 Mar. 1985
(NASA-TM-87035; E-2591; NAS 1.15:87035) Avail: NTIS HC A04/MF A01 CSCL 14D

The reliability of scanning laser acoustic microscopy (SLAM) for detecting surface voids in structural ceramic test specimens was statistically evaluated. Specimens of sintered silicon nitride and sintered silicon carbide, seeded with surface voids, were examined by SLAM at an ultrasonic frequency of 100 MHz in the as fired condition and after surface polishing. It was observed that polishing substantially increased void detectability. Voids as small as 100 micrometers in diameter were detected in polished specimens with 0.90 probability at a 0.95 confidence level. In addition, inspection times were reduced up to a factor of 10 after polishing. The applicability of the SLAM technique for detection of naturally occurring flaws of similar dimensions to the seeded voids is discussed. A FORTRAN program listing is given for calculating and plotting flaw detection statistics. Author

N85-32338# Wisconsin Univ., Madison. Mathematics Research Center.
THE OPTIMALITY OF LOWER CONFIDENCE LIMITS FOR THE RELIABILITY OF SERIES SYSTEMS OBTAINED BY THE METHOD OF KEY TEST RESULTS OR OTHER RELATED TECHNIQUES Summary Report
B. Harris and A. P. Soms Mar. 1985 21 p
(Contract DAAG29-80-C-0041)
(AD-A154880; MRC-TSR-2803) Avail: NTIS HC A02/MF A01 CSCL 14/4

In order to obtain lower confidence limits for the reliability of series systems using binomial subsystem data, K. A. Weaver introduced the method of key test results. This work was extended by A. Winterbottom. In the present paper, conditions are obtained under which the method of key test results gives Buehler optimal lower confidence limits identical with those given by the ordering induced by the maximum likelihood estimator. GRA

39 STRUCTURAL MECHANICS

Includes structural element design and weight analysis; fatigue; and thermal stress.

For applications see *05 Aircraft Design, Testing and Performance* and *18 Spacecraft Design, Testing and Performance.*

N85-32339*# National Aeronautics and Space Administration. Langley Research Center, Hampton, Va.
A CRACKED ORTHOTROPIC SHEET STIFFENED BY A SEMI-INFINITE ORTHOTROPIC SHEET
C. A. Bigelow Washington Jul. 1985 26 p refs
(NASA-TP-2455; L-15972; NAS 1.60:2455) Avail: NTIS HC A02/MF A01 CSCL 20K

The stress intensity factor is determined for a cracked orthotropic sheet adhesively bonded to an orthotropic stringer. Since the stringer is modeled as a semiinfinite sheet, the solution is most appropriate for a crack tip located near a stringer edge. Both adherends are treated as homogeneous, orthotropic media. It is assumed they are in plane stress and the adhesive is in pure shear. From Green's functions and the complex variable theory of orthotropic elasticity developed by Lekhnitskiy, a set of integral equations is obtained. The integral equations are replaced by an equivalent set of algebraic equations which is solved to obtain the shear stress distribution in the adhesive layer. With these stresses, equations for the stress intensity factors at both crack tips are found. A parametric study is conducted to determine the sensitivity of the system to material properties and specimen configuration. Unless the crack tip is very close to or under the stringer the stress intensity factor is approximately that of an unstiffened sheet. However, as the crack propagates beneath the stringer, the stress intensity factor decreases significantly. Increasing the stiffness of the stringer or the adhesive also results in a decrease in the stress intensity factor. Author

N85-32340*# Akron Univ., Ohio. Dept. of Civil Engineering.
RESULTS OF AN INTERLABORATORY FATIGUE TEST PROGRAM CONDUCTED ON ALLOY 800H AT ROOM AND ELEVATED TEMPERATURES Final Report
J. R. Ellis Jul. 1985 38 p refs Sponsored in part by General Atomic Co.
(Grant NAG3-379)
(NASA-CR-174940; NAS 1.26:174940) Avail: NTIS HC A03/MF A01 CSCL 20K

The experimental approach adopted for low cycle fatigue tests of alloy 800H involved the use of electrohydraulic test systems, hour glass geometry specimens, diametral extensometers, and axial strain computers. Attempts to identify possible problem areas were complicated by the lack of reliable data for the heat of Alloy 800H under investigation. The method adopted was to generate definitive test data in an interlaboratory Fatigue Test Program. The laboratories participating in the program were Argonne National Laboratory, Battelle Columbus, Mar-Test, and NASA Lewis. Fatigue tests were conducted on both solid and turbular specimens at temperatures of 20, 593, and 760 C and strain ranges of 2.0, 1.0, and 0.5 percent. The subject test method can, under certain circumstances, produce fatigue data which are serious in error. This approach subsequently was abandoned at General Atomic Company in favor of parallel gage length specimens and axial extensiometers. F.M.R.

N85-32341*# Akron Univ., Ohio. Dept. of Civil Engineering.
A CONTINUOUS DAMAGE MODEL BASED ON STEPWISE-STRESS CREEP RUPTURE TESTS Final Report
D. N. Robinson Cleveland Jul. 1985 24 p refs
(Grant NAG3-379)
(NASA-CR-174941; NAS 1.26:174941) Avail: NTIS HC A02/MF A01 CSCL 20K

A creep damage accumulation model is presented that makes use of the Kachanov damage rate concept with a provision accounting for damage that results from a variable stress history. This is accomplished through the introduction of an additional term

in the Kachanov rate equation that is linear in the stress rate. Specification of the material functions and parameters in the model requires two types of constituting a data base: (1) standard constant-stress creep rupture tests, and (2) a sequence of two-step creep rupture tests. Author

N85-32342*# Southwest Research Inst., San Antonio, Tex.
MEASUREMENT AND ANALYSIS OF CRITICAL CRACK TIP PROCESSES DURING FATIGUE CRACK GROWTH Final Report
D. L. Davidson, S. J. Hudak, and R. J. Dexter Jun. 1985 108 p refs
(Contract NAS1-17641)
(NASA-CR-172597; NAS 1.26:172597) Avail: NTIS HC A06/MF A01 CSCL 20K

The mechanics of fatigue crack growth under constant-amplitudes and variable-amplitude loading were examined. Critical loading histories involving relatively simple overload and overload/underload cycles were studied to provide a basic understanding of the underlying physical processes controlling crack growth. The material used for this study was 7091-T7E69, a powder metallurgy aluminum alloy. Local crack-tip parameters were measured at various times before, during, and after the overloads, these include crack-tip opening loads and displacements, and crack-tip strain fields. The latter were useed, in combination with the materials cyclic and monotonic stress-strain properties, to compute crack-tip residual stresses. The experimental results are also compared with analytical predictions obtained using the FAST-2 computer code. The sensitivity of the analytical model to constant-amplitude fatigue crack growth rate properties and to through-thickness constrain are studied. E.A.K.

N85-32343# Northwestern Univ., Evanston, Ill. Dept. of Civil Engineering.
DYNAMIC FRACTURE OF CONCRETE AND OTHER HETEROGENEOUS MATERIALS Annual Report, 1 Nov. 1983 - 30 Oct. 1984
T. Belytschko, Z. Bazant, C. Chang, and H. Hyun Nov. 1984 33 p
(Grant AF-AFOSR-0009-83)
(AD-A154513; AFOSR-85-0447TR) Avail: NTIS HC A03/MF A01 CSCL 20/11

Closed form solutions have been developed for wave propagation problems in materials which have a constitutive equation with strain softening (SS). These solutions have been useful in assessing the performance of finite element programs and in examining the validity of SS models from physical grounds. The salient characteristics of these wave propagation solutions with SS is that the strain softening localizes into a domain of one-dimension smaller than the space of the problem: for example, in a one-dimensional wave propagation problem, the strain softening localizes to a single point where strain softening is first initiated. Furthermore, if the stress goes to zero as the strain increases in the SS discontinuity is introduced in the displacement. A more serious shortcoming is the absence of energy dissipation in the SS part of the continuum. This absence is due to the extreme localization of the SS phenomenon. Since strain-softening models are usually intended to model dissipative processes such as microcracking or crushing of material, the absence of dissipation is quite troublesome. To overcome this drawback of the SS continuum model, a nonlocal theory was examined. In a non-local theory, the stresses depend on an average of the strain in a volume about the point at which the stress is being computed. In this type of theory, the localization which is characteristic of strain softening solutions can be limited and a finite amount of energy dissipation which is relatively insensitive to element size, can be achieved. GRA

N85-32344# Wisconsin Univ., Madison. Mathematics Research Center.
MODELLING AND PARAMETER ESTIMATION FOR DISTRIBUTED VIBRATORY SYSTEMS Final Report, 1 Jul. 1983 - 30 Sep. 1984
D. L. Russell Mar. 1985 43 p
(Grants AF-AFOSR-0281-83; DAAG29-83-G-0056)
(AD-A154518; AFOSR-85-0444TR) Avail: NTIS HC A03/MF A01 CSCL 20/11

Citing data collected and analyzed with the University of Wisconsin MIPAC (Modelling, Information Processing and Control) Facility electronic measurement and analysis equipment, the investigators make some general comments concerning mathematical models which appear to be appropriate for modelling certain vibratory systems of distributed parameter type. Aspects discussed include: location of vibrational spectra, damping rates, and spectral displacement due to mass density and/or elasticity variations. Particular emphasis is placed on some properties of segmented beams. The article ends with a preliminary mathematical discussion of the feasibility of parameter identification, from vibrational spectrum data alone, in the wave and Euler-Bernoulli beam equations. Author (GRA)

N85-32345# SRI International Corp., Menlo Park, Calif.
DYNAMIC FRACTURE BEHAVIOR OF STRUCTURAL MATERIALS Annual Report, Feb. 1984 - Feb. 1985
J. H. Giovanola and D. A. Shockey 25 Mar. 1985 17 p
(Contract F49620-81-K-0007; SRI Proj. PYU-2777; AF Proj. 2306)
(AD-A154568; AFOSR-85-0460TR; AR-4) Avail: NTIS HC A02/MF A01 CSCL 20/11

To ensure safe design of Air Force structures, it is necessary to understand the mechanics of high-rate fracture and to have a knowledge of the dynamic fracture properties of component materials. In accord with this need, a research program is being conducted at SRI with the goals of developing a test procedure for obtaining reliable dynamic initiation toughness values and establishing the relationship between dynamic initiation and dynamic propagation toughness. This annual report summarizes the progress and results of the fourth research year. The capabilities of the one-point-bend impact test (1PBT) conceived by Kalthoff, et al., and further developed during previous years of this program were extended in two ways during this fourth research year. By adding ballast plates to the ends of a specimen plate we showed that the 1PBT could be applied to lower density materials and smaller specimens than heretofore possible. Second, we developed a model of the post-instability behavior of the impacted specimen that allows the test to be used to assess crack propagation as well as crack initiation behavior. To compare dynamic initiation and propagation toughness, we performed a series of one-point-bend experiments in which KId and KID were measured on the same specimen. The propagation toughness values were dependent on crack velocity and propagation distance, and were much larger than the initiation toughness. GRA

N85-32346# Illinois Univ. at Urbana-Champaign, Savoy. Dept. of Theoretical and Applied Mechanics.
MECHANICS OF NEAR TIP MICROCRACKING IN BRITTLE MATERIAL
P. Charalambides and R. M. McMeeking Mar. 1985 41 p
(Contract N00014-81-K-0650)
(AD-A154684) Avail: NTIS HC A03/MF A01 CSCL 20/12

A continuum mechanics description, of the phenomenon of stress induced microcracking has been used to study the near tip stress and strain fields and the size and shape of a small scale damaged zone for a stationary mode I crack in an elastic body. The microcrack density was found to characterize three regions of interest. In the outer region the microcrack density is zero and the stress and strain fields are purely those for linear elastic deformation. This elastic field constrains the microcracking deformation which in combination with material weakening due to microcracking causes stress relaxation in a region of intermediate microcracking. Very close to the crack tip the microcrack density is saturated and the stress field becomes again singular but with a lower stress intensity than would prevail in the absence of microcracking. In the case where very rapid microcracking occurs as the strain is increased, the intermediate microcracking zone is still present providing continuity of the strain field and a smooth transition of the stress field from the purely elastic region to the region with saturated microcrack density. GRA

N85-32347# Air Force Inst. of Tech., Wright-Patterson AFB, Ohio. School of Engineering.

STRAIN RATE SENSITIVITY ESTIMATION FROM HIGH VELOCITY IMPACT DATA M.S. Thesis

M. H. Bednarek Mar. 1985 73 p

(AD-A154703; AFIT/GAE/AA/85M-2) Avail: NTIS HC A04/MF A01 CSCL 20/11

This experimental study was designed to expand on the work accomplished by Sundararajan and Shewmon in estimating the strain rate sensitivity factors for various materials through the use of simple ballistic impact experiments. The study was divided into the following categories: development on an alternate method of estimating average strain rate, expand the existing data to include more relevant aerospace alloys, explore the effects of heat treatment or elevated temperatures on strain rate sensitivity, and to duplicate tests as a verification of assumptions. The experimental procedure involved impacting test specimens with hardened steel spheres of known velocities, the resulting crater depth and diameter could then be correlated to an average strain rate. The energy of impact and crater volume can be equated to an average dynamic flow pressure. The tests results compared favorably with those obtained by Sundararajan and Shewmon, however, their time of impact assumption resulted in errors exceeding 30% for high strain impacts while their crater relaxation profiles as a function of impact velocity was not justified for the materials tested. General observations showed that the materials tested showed a variation in dynamic hardness with increased temperature and increased severity of heat treatment resulted in material less tolerant to strain rate variation. Strain rate sensitivity factors were low for the precipitated hardened alloys, intermediate for the solid solution alloys, and intermediate for the powered metal alloys. GRA

N85-32348# Illinois Univ., Urbana. Dept. of Metallurgy and Mining Engineering.

THE MEASUREMENT OF STRAIN FIELDS BY X-RAY TOPOGRAPHIC CONTOUR MAPPING

S. R. Stock, H. Chen, and H. K. Birnbaum May 1985 37 p

(Contract N00014-83-K-0468)

(AD-A154870) Avail: NTIS HC A03/MF A01 CSCL 13/13

X-ray diffraction topography offers unique advantages for imaging dislocations and accumulated plastic deformation in single crystals. X-ray diffraction is much more sensitive to strains and samples larger volumes of material than does electron microscopy. Also, topography can be used non-destructively to examine a single specimen many times during the course of an experiment. With the advent of synchrotron radiation sources and of rapid imaging systems for laboratory sources, the emphasis in applying X-ray topography is shifting from characterization studies to dynamic, in situ observation of experiments. One such application is observation of plastic deformation during tensile or bending tests. An X-ray topographic method is described for measuring the magnitude of the components of the strain tensor as a function of position in single crystal specimens. Several variants of the technique are described for use with monochromatic or white X-radiation. Results are reported for some components of the deformation field surrounding a precipitate of beta-NbH. Possible applications of contour mapping are discussed. GRA

N85-32349# Naval Research Lab., Washington, D. C.

THE DYNAMICS OF SLACK MARINE CABLES Interim Report, Oct. 1983 - Jan. 1985

O. M. Griffin and F. Rosenthal 13 May 1985 63 p

(AD-A155022; NRL-MR-5559) Avail: NTIS HC A04/MF A01 CSCL 13/10

Cables are employed in a wide variety of marine and offshore operations. Common examples include moorings, power supply, salvage operations and umbilicals. Most of the computer models developed to date assume that the tension in the cable elements is above a threshold level such that the vibrational behavior of the cable is essentially that of a taut string. For many applications in which catenary effects are important, and umbilical applications where the cable tension may be required to be small, a significant amount of cable slack may be realized. Examples of slack cable applications include deep water moorings, horizontal cable segments between vertical legs of a cable array, the downstream vertical leg of a multiple-leg cable array, and guy lines of deep water guyed towers and semisubmersible platforms. Design analysis of cable structures such as these using conventional taut cable techniques could lead to incorrect conclusions and to inappropriate selection of the required cables. GRA

N85-32350# Army Construction Engineering Research Lab., Champaign, Ill.

FIELD TESTING OF A LIGHTWEIGHT RELOCATABLE STRUCTURE IN A TEMPERATE ENVIRONMENT Final Technical Report

A. M. Kao, J. S. Carr, and D. K. McBride Apr. 1985 30 p

(DA Proj. 4A1-62731-AT-41)

(AD-A155171; CERL-TR-M-85/10) Avail: NTIS HC A03/MF A01 CSCL 13/13

This report described field tests of a commercially available, off-the-shelf, lightweight relocatable structure (LRS) system selected for possible military use in a theater of operations. A panelized system manufactured by Kelly Klosure, Inc. was selected to determine the constructibility, durability, and habitability of the building system. The first stage tests were conducted in a desert environment (Fort Irwin, CA) and stage 2 tests were conducted in a temperate environment (Fort Leonard Wood, MO). The results of stage 1 tests are documented in U.S. Army Constructibility of the building varies, depending on size. The tests confirm that the 20-ft-wide X 8-ft-high buildings can be erected manually by unskilled troop labor using only hand tools. However, for 12-ft-high structures assembled using 4 X 8-ft panels, and for 12-ft-high structures on elevated foundation/baseplates, a crane is needed to help assemble components for the erection. Elevated foundation/baseplates greatly increase construction difficulty and construction times. GRA

N85-32351# Southwest Research Inst., San Antonio, Tex.

LITERATURE SURVEY OF UNDERGROUND CONSTRUCTION METHODS FOR APPLICATION TO HARDENED FACILITIES Final Report

A. Kao Apr. 1985 51 p

(Contract DACA88-84-M-0157; DA Proj. 4A1-62731-AT-41)

(AD-A155212; CERL-TR-M-85/11) Avail: NTIS HC A04/MF A01 CSCL 13/13

This report is a survey of current literature dealing with underground construction practices and will provide the Army with information for comparing the advantages and disadvantages for methods for constructing hardened facilities that can resist threat forces and are safe, cost effective and energy efficient. Current procedures and problems in underground construction were evaluated in the areas of cut and cover methods, deep shafts, tunneling, ground water control, security and survivability, costs, and energy savings. An example building was then taken for underground siting to compare the applicability of the alternative construction techniques described in the literature. The example related the choice of construction method to security/survivability potential and ground water control methods. The study showed that underground buildings can be more economical than conventional above-ground buildings over a 20- to 30-year life cycle because of energy savings. Since adequate technology is available to construct hardened underground facilities under virtually any ground conditions, the main constraint in construction projects remains economic viability rather than technical feasibility. In Europe, where security and survivability are important in facility design and construction, many NATO military facilities are built either underground or in the sides of mountains. Many of the installations are tunneled into rock in the mountainsides which is relatively fault-free and is not prone to flooding during construction. Often, the rock is so strong that the tunnel walls do not have to be lined. GRA

N85-32352# Rockwell International Corp., Thousand Oaks, Calif. Science Center.

INFLUENCE OF PARTICLE ARRANGEMENT ON SINTERING Annual Report, 1 Jul. - 30 Nov. 1984
F. F. Lange and B. J. Kellett Apr. 1985 22 p
(Contract N00014-84-C-0298)
(AD-A155337; SC5410.1AR) Avail: NTIS HC A02/MF A01 CSCL 13/8

The change in free energy of identical cylinders arranged in rings to enclose one pore shows that the pore can either shrink to an equilibrium size or disappear depending on the number of cylinders coordinating the pore and the grain boundary energy to surface energy ratio as expressed by the dihedral angle. The same result is obtained for symmetric, closed arrays of spheres (rings and polyhedral). The shrinkage and strain rates of these closed arrays depends on both the dihedral angle and pore's coordination number; viz, arrays with a lower coordination number. When arrays with different coordination numbers are packed together, the differential shrinkage strain and strain rate between the arrays. The movement of particles during initial mass transport, commonly termed rearrangement, is due in part to differential strains and strain rates between particle clusters. Longer range (transparticle) mass transport gives rise to grain growth within an array. Grain growth in a powder compact is driven by the difference in external surface curvature between particles within the different arrays. Grain growth will lower a pore's coordination number and thus will overcome the thermodynamic barrier to pore closure. GRA

N85-32353# Naval Ship Research and Development Center, Bethesda, Md.
DUCTILE FRACTURE OF DYNAMICALLY LOADED NAVAL STRUCTURES-COMPACT TENSION SPECIMEN TESTS AND ANALYSES Final Report
E. A. Rasmussen, W. E. Carr, and L. N. Gifford Feb. 1985 147 p
(ZR0-2303)
(AD-A155472; DTNSRDC/84/071) Avail: NTIS HC A07/MF A01 CSCL 20/11

A combined experimental/analytical research program aimed at extending the static J-integral to the case of dynamic inelastic fracture is described. This program was a first step toward the goal of quantifying the fracture response of naval structures containing flaws subjected to dynamic loading. One-inch thick HY-80 baseplate was used because of its known toughness and its widespread application in naval structures. For the experimental work, a drop weight test fixture was designed that permitted controllable, high rate loading of precracked compact tension specimens. A series of specimens was tested, and applied load, load point displacements, and back face strains were routinely measured with improving confidence and accuracy as the program progressed. For the analytical work, two-dimensional finite element analyses were performed in conjunction with the experiments in an effort both to further develop analytical techniques for dynamic fracture problems and to provide information on the specimen response in this test program. The analyses performed displayed variable correlation with the experimental results. GRA

N85-32354# SRI International Corp., Menlo Park, Calif.
DEVELOPMENT OF IMPROVED DYNAMIC FAILURE MODELS Final Technical Report, 10 Jan. 1981 - 30 Sep. 1984
D. A. Shockey, D. R. Curran, and L. Seaman 15 Feb. 1985 372 p
(Contract DAAG29-81-K-0123)
(AD-A155586; ARO-18159.3-MS) Avail: NTIS HC A16/MF A01 CSCL 20/11

Improved computational models were developed for dynamic failure by shear banding and ductile fracture. The research effort involved theory, experiments and numerical analyses. A high performance split Hopkinson torsion bar was constructed and used to measure flow stress, failure strain, and shear band instability strains in VAR 4340 steel at strain rates ranging between 800 and 6000 s-1. Taylor-type rod impact tests were performed to measure the dynamic flow curve as a function of temperature (to 947 C) and initial hardness. The fracture surface topography of tensile bars was quantitatively analyzed to ascertain details of the ductile fracture processs and seek their dependence on microstructure. Observations and data from the experiments guided the modifications to the failure models. Viability of the models was verified and their usefulness in ordnance design was demonstrated by incorporating the models into the C-HEMP finite difference code and simulating various armor penetration scenarios. GRA

N85-32355# Naval Postgraduate School, Monterey, Calif.
AN INVESTIGATION INTO THE COMPARISONS OF THE UNDERWATER SHOCK EFFECTS ON A STIFFENED FLAT PLATE TO THE PREDICTIVE NATURE OF A COMPUTER MODEL M.S. Thesis
J. R. Langan Mar. 1985 75 p
(AD-A155612) Avail: NTIS HC A04/MF A01 CSCL 18/3

An experiment was performed to study the effects of an underwater explosion on a submerged test panel. This is a part of an on-going research project sponsored by the Defense Nuclear Agency (DNA) to help predict the dynamic responses of naval structural members due to underwater shocks. An important element of this thesis was to validate a finite element/finite central difference computer code developed to forecast shell responses. Emphasis was placed upon attaining stiffener tripping and collecting invaluable dynamic flat plate tripping data. GRA

N85-32356# Army Armament Research and Development Command, Watervliet, N. Y. Large Caliber Weapon Systems Lab.
STRESS CONCENTRATION IN THE ELASTOPLASTIC STATE AND RESIDUAL STRESS AFTER UNLOADING Final Technical Report
Y. F. Cheng Mar. 1985 38 p Presented at the Army Symp. on Solid Mech., Newport, R.I., 1-3 Oct. 1984
(AD-A155628; AD-E440281; ARLCB-TR-85011) Avail: NTIS HC A03/MF A01 CSCL 20/11

Photoplasticity and photoelastic coating techniques have been successfully employed to study stress concentration in the elastoplastic state and residual stress after unloading. Principles are described herein, and examples of the application of both methods are given. The results show that stress concentration in the elastoplastic state is lower than that in the elastic state and decreases continuously as yielding progresses. A good agreement exists between results from both methods. GRA

42 GEOSCIENCES (GENERAL)

N85-32357*# National Aeronautics and Space Administration. Goddard Space Flight Center, Greenbelt, Md.
GLOBAL MEGA-GEOMORPHOLOGY
Robert S. Hayden, ed. (George Mason Univ., Fairfax, Va.) Jul. 1985 130 p refs Workshop held in Oracle, Ariz., 14-16 Jan. 1985; sponsored by NASA and the International Union of Geological Sciences
(NASA-CP-2312; Rept-85B0472; NAS 1.55:2312) Avail: NTIS HC A07/MF A01 CSCL 08G

The extension of space exploration to the Moon and to other planets has broadened the scope of geomorphology by providing information on landforms which have developed in environments that differ significantly in fundamental factors such as temperature, pressure and gravity from the environments in which Earth's landforms have been shaped. In some cases the landforming processes themselves appear to be significantly different than any found in the terrestrial environment. Some investigators have suggested that features observed on other planets, such as chaos terrian and labryinths on Mars, can help us understand Earth's early history better because they may have been formed by processes which were important in the early ages of Earth but have long ceased to be active here. Corresponding terrestrial landforms would have long since been altered or obliterated by

subsequent activity. For individual titles, see N85-32358 through N85-32385.

N85-32358*# Arizona Univ., Tucson. Dept. of Geosciences.
A NEW GLOBAL GEOMORPHOLOGY? Abstract Only c46
Victor R. Baker *In* NASA. Goddard Space Flight Center Global Mega-Geomorphology Jul. 1985 p 9 (For primary document see N85-32357 21-42)
Avail: NTIS HC A07/MF A01 CSCL 08G

Geomorphology is entering a new era of discovery and scientific excitement centered on expanding scales of concern in both time and space. The catalysts for this development include technological advances in global remote sensing systems, mathematical modeling, and the dating of geomorphic surfaces and processes. Even more important are new scientific questions centered on comparative planetary geomorphology, the interaction of tectonism with landscapes, the dynamics of late Cenozoic climatic changes, the influence of cataclysmic processes, the recognition of extremely ancient landforms, and the history of the world's hydrologic systems. These questions all involve feedback relationships with allied sciences that have recently yielded profound developments. G.L.C.

N85-32359*# Manchester Univ. (England). Faculty of Arts (Physical Geography).
GLOBAL GEOMORPHOLOGY c46
Ian Douglas *In* NASA. Goddard Space Flight Center Global Mega-Geomorphology Jul. 1985 p 10-17 refs (For primary document see N85-32357 21-42)
Avail: NTIS HC A07/MF A01 CSCL 08G

Any global view of landforms must include an evaluation of the link between plate tectonics and geomorphology. To explain the broad features of the continents and ocean floors, a basic distinction between the tectogene and cratogene part of the Earth's surface must be made. The tectogene areas are those that are dominated by crustal movements, earthquakes and volcanicity at the present time and are essentially those of the great mountain belts and mid ocean ridges. Cratogene areas comprise the plate interiors, especially the old lands of Gondwanaland and Laurasia. Fundamental as this division between plate margin areas and plate interiors is, it cannot be said to be a simple case of a distinction between tectonically active and stable areas. Indeed, in terms of megageomorphology, former plate margins and tectonic activity up to 600 million years ago have to be considered. G.L.C.

N85-32360*# California Inst. of Tech., Pasadena. Geological and Planetary Sciences Div.
MEGA-GEOMORPHOLOGY: MARS VIS A VIS EARTH c91
Robert P. Sharp *In* NASA. Goddard Space Flight Center Global Mega-Geomorphology Jul. 1985 p 18-20 (For primary document see N85-32357 21-42)
Avail: NTIS HC A07/MF A01 CSCL 03B

The areas of chaotic terrain, the giant chasma of the Valles Marineris region, the complex linear and circular depressions of Labyrinthus Noctis on Mars all suggest the possibility of large scale collapse of parts of the martian crust within equatorial and sub equatorial latitudes. It seems generally accepted that the above features are fossil, being perhaps, more than a billion years old. It is possible that parts of Earth's crust experienced similar episodes of large scale collapse sometime early in the evolution of the planet. G.L.C.

N85-32361*# George Mason Univ., Fairfax, Va. Dept. of Public Affairs (Geography).
GEOMORPHOLOGICAL SIMILARITY AND UNIQUENESS c46
Robert S. Hayden *In* NASA. Goddard Space Flight Center Global Mega-Geomorphology Jul. 1985 p 21-22 (For primary document see N85-32357 21-42)
Avail: NTIS HC A07/MF A01 CSCL 08G

Remote sensing technology, particularly the development of satellite imagery, has given geomorphology a valuable tool for the study of large area, regional landscapes. The small scale large area format of LANDSAT and other satellite imagery reduces the amount of detailed information provided for a given region. This can be an advantage for regional study as much of the local information that is filtered out tends to be detail which, while significant in small area studies, could mask regional patterns. G.L.C.

N85-32362*# University of Southern Illinois, Carbondale. Dept. of Geology.
REGIONAL LANDFORM THRESHOLDS c43
Dale F. Ritter *In* NASA. Goddard Space Flight Center Global Mega-Geomorphology Jul. 1985 p 23-26 (For primary document see N85-32357 21-42)
Avail: NTIS HC A07/MF A01 CSCL 08B

Remote sensing technology allows us to recognize manifestations of regional thresholds, especially in the spatial characteristics of process agents. For example, a change in river channel pattern over a short distance reflects a threshold alteration in the physical controls of discharge and/or sediment. It is, therefore, a valuable indication of conditions as they exist. However, we probably will have difficulty determining whether the systemic parameters are now close to threshold conditions at which a different change will occur. This, of course, is a temporal and magnitude problem which is difficult to solve from the spatial characteristics. G.L.C.

N85-32363*# Princeton Univ., N. J. Dept. of Geological and Geophysical Sciences.
SOME OBSERVATIONS ON PALEOGEOMORPHOLOGY c46
Sheldon Judson *In* NASA. Goddard Space Flight Center Global Mega-Geomorphology Jul. 1985 p 27-28 refs (For primary document see N85-32357 21-42)
Avail: NTIS HC A07/MF A01 CSCL 08G

Reconstruction of ancient landscapes and landscape processes have long been attempted, and continue to be, with varying degrees of success. The process is not trivial and demands a wide variety of data collected over broad areas by students in many disciplines and sub-disciplines. The last two or three decades have seen a tremendous growth in the volume and quality of these data. As a result some paleogeomorphic studies on regional or larger scales may be tried. G.L.C.

N85-32364*# Adelaide Univ. (Australia). Dept. of Geography.
ANCIENT LANDSCAPES: THEIR NATURE AND SIGNIFICANCE FOR THE QUESTION OF INHERITANCE c46
C. R. Twidale *In* NASA. Goddard Space Flight Center Global Mega-Geomorphology Jul. 1985 p 29-40 refs (For primary document see N85-32357 21-42)
Avail: NTIS HC A07/MF A01 CSCL 08G

It is widely believed that much of the world's scenery is youthful. Thornbury's assertion that little of the world's scenery is older than Tertiary and that most of it is no older than Pleistocene dies hard. Yet there is ample evidence, long recognized, that very ancient forms and surfaces (here the term surface is used in the sense of a planation surface, surface d'aplanissement or Einebnungsflache) are an integral part of the contemporary landscape, and that such features are not restricted to the low latitude regions, though they are well preserved there. Many of them were formed in environments very different from that in which they now occur and are thus inherited. Paleosurfaces of many age ranges have been recognized. They can conveniently be considered as of three types: exhumed, epigene and etch. G.L.C.

N85-32365*# Chevron Oil Field Research Co., La Habra, Calif.
GEOMORPHOLOGY, TECTONICS, AND EXPLORATION Abstract Only c46
Floyd F. Sabins *In* NASA. Goddard Space Flight Center Global Mega-Geomorphology Jul. 1985 p 41 (For primary document see N85-32357 21-42)
Avail: NTIS HC A07/MF A01 CSCL 08G

Explorationists interpret satellite images for tectonic features and patterns that may be clues to mineral and energy deposits. The tectonic features of interest range in scale from regional (sedimentary basins, fold belts) to local (faults, fractures) and are generally expressed as geomorphic features in remote sensing

images. Explorationists typically employ classic concepts of geomorphology and landform analysis for their interpretations, which leads to the question - Are there new and evolving concepts in geomorphology that may be applicable to tectonic analyses of images? G.L.C.

N85-32366*# New Mexico Inst. of Mining and Technology, Socorro.
MEGA-GEOMORPHOLOGY AND NEOTECTONICS c48
Laurence H. Lattman *In* NASA. Goddard Space Flight Center Global Mega-Geomorphology Jul. 1985 p 42-43 (For primary document see N85-32357 21-42)
Avail: NTIS HC A07/MF A01 CSCL 08G

For several decades, subtle neotectonic effects involving several square kilometers have been studied in detail using remote sensing, primarily various types of stereo-aerial photographs at scales of 1:10,000 to 1:80,000. These subtle effects, especially local uplifts associated with growing structures of differential compaction, have been detected by the effect on drainage patterns, changes in hydraulic geometry of individuals channels or groups of channels, tonal halos (soil) and fracture patterns. The studies were extended with the advent of thermal IR imagery particularly in tonal analysis, and SLAR primarily in fracture pattern studies. Lately, quantitative efforts have begun attempting to link measured uplift over known structures with measured changes in hydraulic geometry and alluvial deposition. Thus, efforts are now underway attempting to quantify the relationship between neo- (micro-) tectonic changes and geomorphic parameters of drainage systems. G.L.C.

N85-32367*# Cornell Univ., Ithaca, N.Y. Dept. of Geological Sciences.
ANDREAN EXAMPLES OF MEGA-GEOMORPHOLOGY THEMES c46
Arthur L. Bloom *In* NASA. Goddard Space Flight Center Global Mega-Geomorphology Jul. 1985 p 44-45 (For primary document see N85-32357 21-42)
Avail: NTIS HC A07/MF A01 CSCL 08G

Geomorphic (or physiographic) provinces have been a well known and useful method of regional landform classification for a century. Every earth scientist will recognize a phrase such as Appalachian Plateau or Southern Rocky Mountains as defining a discrete region of consistent geologic structure that has experienced a similar interval of erosion by a similar process or set of processes. The geomorphic provinces formalized in the United States by Fenneman in the 1920's continue to be highly satisfactory even though some boundaries were only vaguely drawn. Mosaics of LANDSAT images illustrate better than any earlier maps the validity and coherence of Fenneman's provinces. The concept of geomorphic provinces has been used subconsciously or intuitively, to describe the relief of the ocean floor and the topography of the Moon and other planets. G.L.C.

N85-32368*# Purdue Univ., Lafayette, Ind. Dept. of Geosciences.
SPACE IMAGERY AND SOME GEOMORPHOLOGICAL PROBLEMS OF THE GUIANA SHIELD, SOUTH AMERICA c43
Wilton N. Melhorn *In* NASA. Goddard Space Flight Center Global Mega-Geomorphology Jul. 1985 p 46-53 refs (For primary document see N85-32357 21-42)
Avail: NTIS HC A07/MF A01 CSCL 08B

Some ongoing involvement in regional geomorphologic research in South America is described. Because of association with LARS at Purdue University, there has been engagement, vicarious or adivsory, in projects which led to LANDSAT 1-2 mapping of the natural resources of Bolivia (1:8,000,000 scale), and preparation of a geographic information system which mapped the general hydrology, geology, soils, and vegetation of Ecuador (1:4,000,000 scale). Currently we are involved more specifically in geological-geomorphological mapping of the Venezuelan portion of the Guiana shield, and because of manuscript limitations only questions pertinent to this region are posed in the ensuing discussion. G.L.C.

N85-32369*# Woods Hole Oceanographic Institution, Mass. Dept. of Geology and Geophysics.
DEEP SEA MEGA-GEOMORPHOLOGY: PROGRESS AND PROBLEMS c48
Wilfred B. Bryan *In* NASA. Goddard Space Flight Center Global Mega-Geomorphology Jul. 1985 p 54-55 (For primary document see N85-32357 21-42)
Avail: NTIS HC A07/MF A01 CSCL 08C

Historically, marine geologists have always worked with mega-scale morphology. This is a consequence both of the scale of the ocean basins and of the low resolution of the observational remote sensing tools available until very recently. In fact, studies of deep sea morphology have suffered from a serious gap in observational scale. Traditional wide-beam echo sounding gave images on a scale of miles, while deep sea photography has been limited to scales of a few tens of meters. Recent development of modern narrow-beam echo sounding coupled with computer-controlled swath mapping systems, and development of high-resolution deep-towed side-scan sonar, are rapidly filling in the scale gap. These technologies also can resolve morphologic detail on a scale of a few meters or less. As has also been true in planetary imaging projects, the ability to observe phenomena over a range of scales has proved very effective in both defining processes and in placing them in proper context. G.L.C.

N85-32370*# Fort Lewis A&M Coll., Durango, Colo. Dept. of Geology.
ONE APPLICATION OF MEGA-GEOMORPHOLOGY IN EDUCATION c46
Robert W. Blair, Jr. *In* NASA. Goddard Space Flight Center Global Mega-Geomorphology Jul. 1985 p 56-58 refs (For primary document see N85-32357 21-42)
Avail: NTIS HC A07/MF A01 CSCL 08G

One advantage of a synoptic view displaying landform assemblages provided by imagery is that one can often identify geomorphic processes which have shaped the region and which may affect the habitability of the area over a human life time. Considering the continued growth of the world population and the resultant pressure and the exploitation of land, usually without any consideration given to geologic processes, it is imperative that we attempt to educate as large a segment of the population as we can about geologic processes and how they influence land use. Space platform imagery which exhibits regional landscapes can be used: (1) to show students the impact of geologic processes over relatively short periods of time (e.g., the Mount St. Helens lateral blast); (2) to display the effects of poor planning because of a lack of knowledge of the local geologic processes (e.g., the 1973 image of the Mississippi River flood around St. Louis, MO); and (3) to show the association of certain types of landforms with building materials and other resources (e.g., drumlins and gravel deposits). G.L.C.

N85-32371*# Geological Survey, Flagstaff, Ariz.
USE OF THE SYNOPTIC VIEW: EXAMPLES FROM EARTH AND OTHER PLANETS c43
Baerbel K. Lucchitta *In* NASA. Goddard Space Flight Center Global Mega-Geomorphology Jul. 1985 p 59-61 refs (For primary document see N85-32357 21-42)
Avail: NTIS HC A07/MF A01 CSCL 08B

Space technology has added the synoptic view to other techniques used in geomorphology. Synoptic views are provided by spacecraft images or by application of space technology to time-honored information systems. Examples of spacecraft images of Earth are LANDSAT, SEASAT, and the SIR (Shuttle Imaging Radar) series. Examples of applied space technologies include the digital conversion of topographic maps to shaded relief maps and digital correlation methods. From the study of other planets we have learned that synoptic views enable the deciphering of a planet's history: large features are identified and mapped before small ones; studies proceed from the general to the specific. On Earth, we generally recognize smaller features and study specific processes first, then extrapolate toward larger features and a general synthesis. With the advent of space images of Earth,

perhaps the time is ripe to employ the methods used for other planets to the study of terrestrial geology and geomorphology. The following examples illustrate the use of regional-scale studies on Earth: the application of synoptic-view images in Antarctica, the use of digital methods and correlations of multiple data sets in regional studies, and some benefits to our understanding of terrestrial geology that have been obtained from analyses of other planets. G.L.C.

N85-32372*# Geological Survey, Reston, Va.
GEOMORPHIC CLASSIFICATION OF ICELANDIC AND MARTIAN VOLCANOES: LIMITATIONS OF COMPARATIVE PLANETOLOGY RESEARCH FROM LANDSAT AND VIKING ORBITER IMAGES c46
Richard S. Williams, Jr. *In* NASA. Goddard Space Flight Center Global Mega-Geomorphology Jul. 1985 p 62-63 (For primary document see N85-32357 21-42)
Avail: NTIS HC A07/MF A01 CSCL 08K

Some limitations in using orbital images of planetary surfaces for comparative landform analyses are discussed. The principal orbital images used were LANDSAT MSS images of Earth and nominal Viking Orbiter images of Mars. Both are roughly comparable in having a pixel size which corresponds to about 100 m on the planetary surface. A volcanic landform on either planet must have a horizontal dimension of at least 200 m to be discernible on orbital images. A twofold bias is directly introduced into any comparative analysis of volcanic landforms on Mars versus those in Iceland because of this scale limitation. First, the 200-m cutoff of landforms may delete more types of volcanic landforms on Earth than on Mars or vice versa. Second, volcanic landforms in Iceland, too small to be resolved or orbital images, may be represented by larger counterparts on Mars or vice versa. R.J.F.

N85-32373*# Arizona State Univ., Tempe. Dept. of Geology.
AEOLIAN GEOMORPHOLOGY FROM THE GLOBAL PERSPECTIVE c91
Ronald Greeley *In* NASA. Goddard Space Flight Center Global Mega-Geomorphology Jul. 1985 p 64-67 ref (For primary document see N85-32357 21-42)
Avail: NTIS HC A07/MF A01 CSCL 03B

Any planet or satellite having a dynamic atmosphere and a solid surface has the potential for experiencing aeolian (wind) processes. A survey of the Solar System shows at least four planetary objects which potentially meet these criteria: Earth, Mars, Venus, and possibly Titan, the largest satellite of Saturn. While the basic process is the same among these four objects, the movement of particles by the atmosphere, the aeolian environment is drastically different. It ranges from the hot (730 K), dense atmosphere of Venus to the extremely cold desert (218 K) environment of Mars where the atmospheric surface pressure is only approximately 7.5 mb. In considering aeolian processes in the planetary perspective, all three terrestrial planets share some common areas of attention for research, especially in regard to wind erosion and dust storms. Relevant properties of planetary objects potentially subject to aeolian processes are given in tabular form. R.J.F.

N85-32374*# State Univ. of New York, Binghamton. Dept. of Geological Sciences.
GEOMORPHIC ANALYSES FROM SPACE IMAGERY c43
Marie Morisawa *In* NASA. Goddard Space Flight Center Global Mega-Geomorphology Jul. 1985 p 68-75 refs (For primary document see N85-32357 21-42)
Avail: NTIS HC A07/MF A01 CSCL 08B

One of the most obvious applications of space imagery to geomorphological analyses is in the study of drainage patterns and channel networks. LANDSAT, high altitude photography and other types of remote sensing imagery are excellent for depicting stream networks on a regional scale because of their broad coverage in a single image. They offer a valuable tool for comparing and analyzing drainage patterns and channel networks all over the world. Three aspects considered in this geomorphological study are: (1) the origin, evolution and rates of development of drainage systems; (2) the topological studies of network and channel arrangements; and (3) the adjustment of streams to tectonic events and geologic structure (i.e., the mode and rate of adjustment). R.J.F.

N85-32375*# California State Polytechnic Univ., Pomona. Dept. of Earth Sciences.
THE PROBLEM OF SCALE IN PLANETARY GEOMORPHOLOGY c91
Lisa A. Rossbacher *In* NASA. Goddard Space Flight Center Global Mega-Geomorphology Jul. 1985 p 76-78 (For primary document see N85-32357 21-42)
Avail: NTIS HC A07/MF A01 CSCL 03B

Recent planetary exploration has shown that specific landforms exhibit a significant range in size between planets. Similar features on Earth and Mars offer some of the best examples of this scale difference. The difference in heights of volcanic features between the two planets has been cited often; the Martian volcano Olympus Mons stands approximately 26 km high, but Mauna Loa rises only 11 km above the Pacific Ocean floor. Polygonally fractured ground in the northern plains of Mars has diameters up to 20 km across; the largest terrestrial polygons are only 500 m in diameter. Mars also has landslides, aeolian features, and apparent rift valleys larger than any known on Earth. No single factor can explain the variations in landform size between planets. Controls on variation on Earth, related to climate, lithology, or elevation, have seldom been considered in detail. The size differences between features on Earth and other planets seem to be caused by a complex group of interacting relationships. The major planetary parameters that may affect landform size are discussed. R.J.F.

N85-32376*# Miami Univ., Oxford, Ohio. Dept. of Geology.
QUANTITATIVE ANALYSIS IN MEGAGEOMORPHOLOGY c46
Larry Mayer *In* NASA. Goddard Space Flight Center Global Mega-Geomorphology Jul. 1985 p 79-80 (For primary document see N85-32357 21-42)
Avail: NTIS HC A07/MF A01 CSCL 08G

Megageomorphology is the study of regional topographic features and their relations to independent geomorphic variables that operate at the regional scale. These independent variables can be classified as either tectonic or climatic in nature. Quantitative megageomorphology stresses the causal relations between plate tectonic factors and landscape features or correlations between climatic factors and geomorphic processes. In addition, the cumulative effects of tectonics and climate on landscape evolution that simultaneously operate in a complex system of energy transfer is of interst. Regional topographic differentiation, say between continents and ocean floors, is largely the result of the different densities and density contrasts within the oceanic and continental lithosphere and their isostatic consequences. Regional tectonic processes that alter these lithospheric characteristics include rifting, collision, subduction, transpression and transtension. R.J.F.

N85-32377*# Jet Propulsion Lab., California Inst. of Tech., Pasadena.
USE OF SPACEBORNE IMAGING RADAR IN REGIONAL GEOMORPHIC STUDIES c43
John P. Ford *In* NASA. Goddard Space Flight Center Global Mega-Geomorphology Jul. 1985 p 81-83 refs (For primary document see N85-32357 21-42)
Avail: NTIS HC A07/MF A01 CSCL 17I

In the past two decades, the use of both photographic and non-photographic remote sensing from satellite platforms has provided a unique capability for the observation and study of Earth and planetary surfaces. A wide range of imaging sensors that operate in different portions of the electromagnetic spectrum have yielded images of large areas that formerly were unknown or that had not previously been observed at a simultaneous instant in time. In addition, remote sensors equipped with multispectral or multiband capabilities are capable of taking data at different wavelengths simultaneously. Notable examples include the LANDSAT series of multispectral scanners, thematic mappers, and return

beam vidicons. Synthetic aperture radar and LANDSAT imagery are discussed. R.J.F.

N85-32378*# London Univ. (England). Faculty of Science (Geography).
TECHNIQUES, PROBLEMS AND USES OF MEGA-GEOMORPHOLOGICAL MAPPING **c43**
Clifford Embleton *In* NASA. Goddard Space Flight Center Global Mega-Geomorphology Jul. 1985 p 84-88 refs (For primary document see N85-32357 21-42)
Avail: NTIS HC A07/MF A01 CSCL 08B

A plea for a program of global geomorphological mapping based on remote sensing data is presented. It is argued that the program is a necessary step in bringing together the rapidly evolving concepts of plate tectonics with the science of geomorphology. Geomorphologists are urged to bring temporal scales into their subject and to abandon their recent isolation from tectonics and geological history. It is suggested that a start be made with a new geomorphological map of Europe, utilizing the latest space technology. R.J.F.

N85-32379*# Geological Survey, Reston, Va.
LARGE FORMAT CAMERA PHOTOGRAPHS: A NEW TOOL FOR UNDERSTANDING ARID ENVIRONMENTS **c35**
Alta S. Walker *In* NASA. Goddard Space Flight Center Global Mega-Geomorphology Jul. 1985 p 89-90 (For primary document see N85-32357 21-42)
Avail: NTIS HC A07/MF A01 CSCL 14E

Large Format Camera (LFC) was developed by NASA to produce high resolution stereo photographs from space with maximum photogrammetric fidelity. The camera has a 30.5 cm focal length lens and an f/6.0 aperture. The optics are corrected to permit operation with black and white (b/w), natural color (col) and color infrared (cir) film. Interchangeable minus-haze and minus-blue filters are located near the aperture stop, and an antivignetting filter is provided on the front element of the lens. The field-of-view of the LFC along track is 73.7 degrees (ratio 1.5 x H) and across track is 41.1 degrees (ratio 0.75 x H). The frame format of the LFC is 23x46 cm with the long dimension in the direction of flight. The camera can be operated to produce 10, 60, 70, or 80 percent forward overlap for stereoscopic coverage. With 80 percent forward overlap, the stereo model base height ratio is 0.3 for successive frames and 1.2 if every fourth frame is used. The LFC magazine has a capacity of 2400 frames. Two horizon-looking stellar cameras, one directed 45 degrees forward and the other 45 degrees aft were used to photograph the star field in synchronism with exposures of the LFC. Post flight mensuration and calculation of the stellar photographs will provide altitude information for the LFC. R.J.F.

N85-32380*# Geological Survey, Reston, Va.
QUANTITATIVE ANALYSIS OF GEOMORPHIC PROCESSES USING SATELLITE IMAGE DATA AT DIFFERENT SCALES **c43**
Richard S. Williams, Jr. *In* NASA. Goddard Space Flight Center Global Mega-Geomorphology Jul. 1985 p 91-93 (For primary document see N85-32357 21-42)
Avail: NTIS HC A07/MF A01 CSCL 08B

When aerial and satellite photographs and images are used in the quantitative analysis of geomorphic processes, either through direct observation of active processes or by analysis of landforms resulting from inferred active or dormant processes, a number of limitations in the use of such data must be considered. Active geomorphic processes work at different scales and rates. Therefore, the capability of imaging an active or dormant process depends primarily on the scale of the process and the spatial-resolution characteristic of the imaging system. Scale is an important factor in recording continuous and discontinuous active geomorphic processes, because what is not recorded will not be considered or even suspected in the analysis of orbital images. If the geomorphic process of landform change caused by the process is less than 200 m in x to y dimension, then it will not be recorded. Although the scale factor is critical, in the recording of discontinuous active geomorphic processes, the repeat interval of orbital-image acquisition of a planetary surface also is a consideration in order to capture a recurring short-lived geomorphic process or to record changes caused by either a continuous or a discontinuous geomorphic process. R.J.F.

N85-32381*# Geological Survey, Reston, Va.
QUANTITATIVE GEOMORPHOLOGIC STUDIES FROM SPACE-BORNE PLATFORMS **c43**
Richard S. Williams, Jr. *In* NASA. Goddard Space Flight Center Global Mega-Geomorphology Jul. 1985 p 94-97 (For primary document see N85-32357 21-42)
Avail: NTIS HC A07/MF A01 CSCL 08B

Although LANDSAT images of our planet represent a quantum improvement in the availability of a global image-data set for independent or comparative regional geomorphic studies of landforms, such images have several limitations which restrict their suitability for quantitative geomorphic investigations. The three most serious deficiencies are: (1) photogrammetric inaccuracies, (2) two-dimensional nature of the data, and (3) spatial resolution. These deficiencies are discussed, as well as the use of stereoscopic images and laser altimeter data. R.J.F.

N85-32382*# National Aeronautics and Space Administration. Goddard Space Flight Center, Greenbelt, Md.
GLOBAL GEOMORPHOLOGY: REPORT OF WORKING GROUP NUMBER 1 **c46**
Ian Douglas (Manchester Univ., England) *In its* Global Mega-Geomorphology Jul. 1985 p 101-104 (For primary document see N85-32357 21-42)
Avail: NTIS HC A07/MF A01 CSCL 08G

Remote sensing was considered invaluable for seeing landforms in their regional context and in relationship to each other. Sequential images, such as those available from LANDSAT orbits provide a means of detecting landform change and the operation of large scale processes, such as major floods in semiarid regions. The use of remote sensing falls into two broad stages: (1) the characterization or accurate description of the features of the Earth's surface; and (2) the study of landform evolution. Recommendations for future research are made. R.J.F.

N85-32383*# National Aeronautics and Space Administration. Goddard Space Flight Center, Greenbelt, Md.
LANDSCAPE INHERITANCE: REPORT OF WORKING GROUP NUMBER 2 **c43**
C. R. Twidale (Adelaide Univ., Australia) *In its* Global Mega-Geomorphology Jul. 1985 p 105 (For primary document see N85-32357 21-42)
Avail: NTIS HC A07/MF A01 CSCL 08B

The conventional wisdom is, or until recently has been, that the earth's scenery is essentially youthful, much of it being of pleistocene age. The validity of this assertion was questioned, surfaces and forms of much greater antiquity being cited from several cratonic regions, and also from the older orogens. Exhumed forms, some of them of great age (one inselberg landscape of Archaean age was noted), are more common and extensive than has previously been supposed. Epigene forms of Mesozoic ate are increasingly being demonstrated from the world's cratons and orogens. Etch features also are more widely eveloped than has been realized. It was recommended that studies of denudation chronology be undertaken, possible in relation to contrasted cratonic regions. The nature and age range of surfaces that make up the shields ought to be analysed, the processes responsible for shaping the surfaces, and, in the case of the ancien epigene forms, the reasons for their survival. R.J.F.

N85-32384*# National Aeronautics and Space Administration. Goddard Space Flight Center, Greenbelt, Md.
PROCESS THRESHOLDS: REPORT OF WORKING GROUP NUMBER 3 **c43**
Richard S. Williams, Jr. (Geological Survey, Reston, Va.) *In its* Global Mega-Geomorphology Jul. 1985 p 106-108 (For primary document see N85-32357 21-42)

Avail: NTIS HC A07/MF A01 CSCL 08B

The Process Thresholds Working Group concerned itself with whether a geomorphic process to be monitored on satellite imagery must be global, regional, or local in its effect on the landscape. It was pointed out that major changes in types and magnitudes of processes operating in an area are needed to be detectable on a global scale. It was concluded from a review of geomorphic studies which used satellite images that they do record change in landscape over time (on a time-lapse basis) as a result of one or more processes. In fact, this may be one of the most important attributes of space imagery, in that one can document land form changes in the form of a permanent historical record. The group also discussed the important subject of the acquisition of basic data sets by different satellite imaging systems. Geomorphologists already have available one near-global basis data set resulting from the early LANDSAT program, especially images acquired by LANDSATs 1 and 2. Such historic basic data sets can serve as a benchmark for comparison with landscape changes that take place in the future. They can also serve as a benchmark for comparison with landscape changes that have occurred in the past (as recorded) by images, photography and maps. R.J.F.

N85-32385*# National Aeronautics and Space Administration. Goddard Space Flight Center, Greenbelt, Md.
PLANETARY PERSPECTIVE. REPORT OF WORKING GROUP NUMBER 4 c91
Lisa A. Rossbacher (California State Polytechnic Univ., Pomona) *In its* Global Mega-Geomorphology Jul. 1985 p 109-110 (For primary document see N85-32357 21-42)
Avail: NTIS HC A07/MF A01 CSCL 03B

The study of global megageomorphology from a planetary perspective requires that, philosophically, we view the Earth as a planet like any other; one among a number of bodies of varied size and composition which, together with the Sun, form the Solar System. A first step in the study of the Earth from the planetary perspective is the development of global distribution maps of surface factors as landforms, tectonics, and of key processes operating on Earth. Data of other types, such as gravity and magnetism, should also be included and, so far as possible, multiple data sets should be developed. The compilation of maps would serve as a catalyst for research and a basis for interpretation. They could be used scientifically to document changes such as glacial variations and their relationships to climate, volcanic eruptions and their effects, and coastal alterations. Slow and rapid changes should be studied together with the relationships between scale and the rapidity of change. A study of the relationship of geomorphology (i.e., surficial processes) to lithology and structure is needed. The planetary perspective can also help in the identification and investigation of exotic features such as suspect terrains. R.J.F.

N85-32386# Geological Survey, Washington, D.C.
WORLDWIDE DIRECTORY OF NATIONAL EARTH-SCIENCE AGENCIES AND RELATED INTERNATIONAL ORGANIZATIONS
E. J. Tinsley, comp. and Joyce P. Hollander, comp. 1984 107 p
(GS-Circ-934; LC-84-600161) Avail: NTIS HC A06/MF A01

The Directory provides addresses of government earth science agencies around the world that have functions similar to those of one or more of the operating divisions of the U.S. Geological Survey (USGS). It also lists addresses of major international organizations that are concerned with some phase of the earth sciences. The directory is arranged alphabetically by country name. The location of each country is shown on a small index map, which is keyed to one of 10 reference maps showing the major regions of the world. The principal functions of the agencies listed are keyed to those of the USGS and are indicated by code letters. Author

43 EARTH RESOURCES

Includes remote sensing of earth resources by aircraft and spacecraft; photogrammetry; and aerial photography.

For instrumentation see *35 Instrumentation and Photography.*

N85-32387# Air Force Geophysics Lab., Hanscom AFB, Mass.
GLOBAL GEOID AND GRAVITY ANOMALY PREDICTIONS USING THE COLLOCATION AND POINT MASS TECHNIQUES Scientific Interim Report, Jan. - Aug. 1984
R. P. Bessette and G. Hadgigeorge 6 Sep. 1984 25 p
(AD-A154517; AFGL-TR-84-0236; AFGL-AFSG-446) Avail: NTIS HC A02/MF A01 CSCL 08/5

We previously described (14,14) spherical-harmonic global adjustments of satellite altimetry using the AFGL short-arc technique supplemented with point masses to allow incorporation of short-wavelength geoidal detail. Recently, we have also investigated another technique to enhance short-wavelength detail: least squares collocation with noise. Both methods provide a means to determine a high resolution gravity field on a local, regional or global scale. Statistical comparisons of these two methods have been made in selected areas and the results tabulated. GRA

N85-32388# Army Engineer Waterways Experiment Station, Vicksburg, Miss. Environmental Lab.
HANDBOOK FOR OBTAINING AND USING AERIAL PHOTOGRAPHY TO MAP AQUATIC PLANT DISTRIBUTION Final Report
J. M. Leonard Nov. 1984 42 p
(AD-A154584; WES-IR-A-84-2) Avail: NTIS HC A03/MF A01 CSCL 06/3

Stepwise procedures are given for the tasks required in using low-altitude aerial photography to map aquatic plants. The tasks include problem identification, photomission design, acquisition of ground truth data, and photointerpretation and data presentation. The sources of existing aerial photographs and the general and technical requirements for aerial photography are given in Appendixes A and B, respectively. Author (GRA)

N85-32389# Army Military Personnel Center, Alexandria, Va.
MICROCOMPUTER PROCESSING OF LANDSAT THEMATIC MAPPER DATA FOR THE ACQUISITION OF MILITARY TACTICAL TERRAIN DATA Final Report
S. J. McGregor 12 Apr. 1985 129 p
(AD-A154781) Avail: NTIS HC A07/MF A01 CSCL 08/2

This thesis demonstrates the potential use of microcomputer digital image processing techniques for obtaining tactical terrain data from LANDSAT multispectral digital imagery. Militarily significant Level 1 and 2 land cover classes were mapped for three North Carolina study areas using a modified USGS land cover classification system, LANDSAT 4 Thematic Mapper data, and the Personal Image Processing System (APPLEPIPS). A site specific accuracy assessment technique, using a stratified, systematic, unaligned sampling design, was used to determine the classification accuracy of the three land cover maps. The classification accuracy was determined to meet the USGS minimum acceptable standard of 85 percent at the 0.05 confidence level. GRA

N85-32390# Army Engineer Topographic Labs., Fort Belvoir, Va.
BASIC FORMULAE FOR THE COMPUTATION OF THE DEFLECTION OF THE VERTICAL FROM ASTRONOMICAL STAR OBSERVATIONS
A. A. Baldini Mar. 1985 12 p
(AD-A154912; ETL-R-069) Avail: NTIS HC A02/MF A01 CSCL 08/5

In this report we deal with new concepts for determining the astrogeodetic deflection of the vertical, in the sense that we determine the xi and eta deflection components completely independently of the knowledge of the astronomic coordinates, latitude and longitude, hence reducing the time and cost of field work. The first part of this paper is devoted to finding a relationship

between the deflection components with respect to a star or stars positions. We have found that the xi and eta components are related to either the difference between the astronomic and geodetic star zenith distances; azimuths; parallactic angles, or are based on a star rate of change in azimuth and zenith distance with respect to time. Except for the last one, star pairs must be considered. In the second part of this paper, we consider a method that deals with the solution for the deflection components xi and eta from observation of star pairs, as function of the astronomic and geodetic zenith distances. The effect of errors in evaluating the deflection components xi and eta as well as the polar migration, are considered. GRA

N85-32391# Army Engineer Topographic Labs., Fort Belvoir, Va.
REALIZING THE FULL POTENTIAL OF THE VIDEO DISC FOR MAPPING APPLICATIONS
R. B. Lambert Mar. 1985 9 p Presented at the ASP-ACSM Convention, 10-15 Mar. 1985, Washington, DC
(AD-A154966; ETL-R-071) Avail: NTIS HC A02/MF A01 CSCL 08/2

Today, scientists at the US Army Engineer Topographic Laboratories (ETL) are investigating mapping applications of optical storage technology. Research efforts at ETL over the last several years have shown that a great potential exists for interactive optical video disc systems in storing and displaying maps, photographs and other graphic materials. ETL's resident demonstration video disc system has served well but cannot be easily adapted to new mapping applications. A new system being developed at ETL uses state-of-the-art Direct Read After Write (DRAW) video disc technology for in-house recording of video discs. ETL's hybrid approach to data storage brings analog and digital mapping data together for the first time on the same video disc. Planning and production operations for video discs are being streamlined and cartographic standards are being developed to improve the quality of video map displays. Author (GRA)

N85-32392# Army Engineer Topographic Labs., Fort Belvoir, Va.
OPTICAL STORAGE TECHNOLOGY FOR MAPPING
E. A. Wilkinson 1985 7 p Presented at the 1985 ASP-ACSM Convention, Washington, DC
(AD-A154989; ETL-R-073) Avail: NTIS HC A02/MF A01 CSCL 08/2

The paper map has long been a great service to man. But today, some map users find the paper map to be an inadequate tool for the job at hand. Problems with paper maps range from storage of large quantities of maps to deterioration and deformation with age. Optical disc technology can be used with the data already available on paper maps to provide a solution to some of these problems, as well as provide additional flexibility not found on the paper map. The limitations and expectations of each type of optical disc system pertaining to its use in the cartographic field need amplification. Much of this technology is changing as research teams are quickly discovering new capabilities and applications for optical disc systems. Applications in the mapping industry offer exciting changes to traditional forms of map use and provide the map user with an entire range of new ideas. GRA

N85-32393# Los Alamos National Lab., N. Mex.
NEW ESTIMATING PROCEDURES FOR SURFACE RUNOFF, SEDIMENT YIELD, AND CONTAMINANT TRANSPORT IN LOS ALAMOS COUNTY, NEW MEXICO
L. J. Lane, W. D. Purtymun, and N. M. Becker Apr. 1985 56 p refs
(Contract W-7405-eng-36)
(DE85-011890; LA-10335-MS) Avail: NTIS HC A04/MF A01

Procedures are developed to predict runoff, sediment yield, and contaminant transport from semiarid watersheds with alluvial stream channels. The procedures represent a synthesis of mathematical models to approximate the complex processes of runoff generation, streamflow routing and hydrograph development, sediment transport and yield, particle sorting and enrichment, and transport of sediment associated contaminants. The procedures are applied to a complex watershed channel system at Los Alamos, New Mexico, and used to compute plutonium transport and redistribution in alluvial stream channels. Mass balance calculations are used to compute the amount of plutonium discharge from the channel system and to compute the amount of plutonium discharge from the channel system and to compute the plutonium remaining in storage in the channel alluvium. DOE

N85-32362*# University of Southern Illinois, Carbondale. Dept. of Geology.
REGIONAL LANDFORM THRESHOLDS
Dale F. Ritter *In* NASA. Goddard Space Flight Center Global Mega-Geomorphology Jul. 1985 p 23-26 (For primary document see N85-32357 21-42)
Avail: NTIS HC A07/MF A01 CSCL 08B

N85-32368*# Purdue Univ., Lafayette, Ind. Dept. of Geosciences.
SPACE IMAGERY AND SOME GEOMORPHOLOGICAL PROBLEMS OF THE GUIANA SHIELD, SOUTH AMERICA
Wilton N. Melhorn *In* NASA. Goddard Space Flight Center Global Mega-Geomorphology Jul. 1985 p 46-53 refs (For primary document see N85-32357 21-42)
Avail: NTIS HC A07/MF A01 CSCL 08B

N85-32371*# Geological Survey, Flagstaff, Ariz.
USE OF THE SYNOPTIC VIEW: EXAMPLES FROM EARTH AND OTHER PLANETS
Baerbel K. Lucchitta *In* NASA. Goddard Space Flight Center Global Mega-Geomorphology Jul. 1985 p 59-61 refs (For primary document see N85-32357 21-42)
Avail: NTIS HC A07/MF A01 CSCL 08B

N85-32374*# State Univ. of New York, Binghamton. Dept. of Geological Sciences.
GEOMORPHIC ANALYSES FROM SPACE IMAGERY
Marie Morisawa *In* NASA. Goddard Space Flight Center Global Mega-Geomorphology Jul. 1985 p 68-75 refs (For primary document see N85-32357 21-42)
Avail: NTIS HC A07/MF A01 CSCL 08B

N85-32377*# Jet Propulsion Lab., California Inst. of Tech., Pasadena.
USE OF SPACEBORNE IMAGING RADAR IN REGIONAL GEOMORPHIC STUDIES
John P. Ford *In* NASA. Goddard Space Flight Center Global Mega-Geomorphology Jul. 1985 p 81-83 refs (For primary document see N85-32357 21-42)
Avail: NTIS HC A07/MF A01 CSCL 17I

N85-32378*# London Univ. (England). Faculty of Science (Geography).
TECHNIQUES, PROBLEMS AND USES OF MEGA-GEOMORPHOLOGICAL MAPPING
Clifford Embleton *In* NASA. Goddard Space Flight Center Global Mega-Geomorphology Jul. 1985 p 84-88 refs (For primary document see N85-32357 21-42)
Avail: NTIS HC A07/MF A01 CSCL 08B

N85-32380*# Geological Survey, Reston, Va.
QUANTITATIVE ANALYSIS OF GEOMORPHIC PROCESSES USING SATELLITE IMAGE DATA AT DIFFERENT SCALES
Richard S. Williams, Jr. *In* NASA. Goddard Space Flight Center Global Mega-Geomorphology Jul. 1985 p 91-93 (For primary document see N85-32357 21-42)
Avail: NTIS HC A07/MF A01 CSCL 08B

N85-32381*# Geological Survey, Reston, Va.
QUANTITATIVE GEOMORPHOLOGIC STUDIES FROM SPACEBORNE PLATFORMS
Richard S. Williams, Jr. *In* NASA. Goddard Space Flight Center Global Mega-Geomorphology Jul. 1985 p 94-97 (For primary document see N85-32357 21-42)
Avail: NTIS HC A07/MF A01 CSCL 08B

N85-32383*# National Aeronautics and Space Administration. Goddard Space Flight Center, Greenbelt, Md.
LANDSCAPE INHERITANCE: REPORT OF WORKING GROUP NUMBER 2
C. R. Twidale (Adelaide Univ., Australia) *In its* Global Mega-Geomorphology Jul. 1985 p 105 (For primary document see N85-32357 21-42)
Avail: NTIS HC A07/MF A01 CSCL 08B

N85-32384*# National Aeronautics and Space Administration. Goddard Space Flight Center, Greenbelt, Md.
PROCESS THRESHOLDS: REPORT OF WORKING GROUP NUMBER 3
Richard S. Williams, Jr. (Geological Survey, Reston, Va.) *In its* Global Mega-Geomorphology Jul. 1985 p 106-108 (For primary document see N85-32357 21-42)
Avail: NTIS HC A07/MF A01 CSCL 08B

44 ENERGY PRODUCTION AND CONVERSION

Includes specific energy conversion systems, e.g., fuel cells and batteries; global sources of energy; fossil fuels; geophysical conversion; hydroelectric power; and wind power.

For related information see also *07 Aircraft Propulsion and Power, 20 Spacecraft Propulsion and Power, 28 Propellants and Fuels,* and *85 Urban Technology and Transportation.*

N85-32394*# Jet Propulsion Lab., California Inst. of Tech., Pasadena.
PROCEEDINGS OF THE 24TH PROJECT INTEGRATION MEETING Progress Report, Mar. - Oct. 1984
D. Tustin Oct. 1984 646 p refs Meeting held in Pasadena, Calif., 2-3 Oct. 1984
(Contract NAS7-918; JPL Proj. 5101-259; Contract DE-AI01-76ET-20356)
(NASA-CR-176058; JPL-Pub-85-27; DOE/JPL-1012-104; NAS 1.26:176058; FSA-PR-24) Avail: NTIS HC A99/MF A01 CSCL 10A

Progress made by the Flat-Plate Solar Array Project is described. Reports on silicon sheet growth and characterization, silicon material, process development, high-efficiency cells, environmental isolation, engineering sciences, and reliability physics are presented along with copies of visual presentations made at the 24th Project Integration Meeting. For individual titles, see N85-32395 through N85-32453.

N85-32395*# Department of Energy, Washington, D. C.
HIGH-EFFICIENCY CRYSTALLINE SILICON TECHNOLOGY DEVELOPMENT
Morton B. Prince *In* JPL Proc. of the 24th Project Integration Meeting Oct. 1984 p 49-56 (For primary document see N85-32394 21-44)
Avail: NTIS HC A99/MF A01 CSCL 10A

The rationale for pursuing high efficiency crystalline silicon technology research is discussed. Photovoltaic energy systems are reviewed as to their cost effectiveness and their competitiveness with other energy systems. The parameters of energy system life are listed and briefly reviewed. E.R.

N85-32396*# Pennsylvania Univ., Philadelphia.
SUMMARY OF THE HIGH-EFFICIENCY CRYSTALLINE SOLAR CELL RESEARCH FORUM
M. Wolf *In* JPL Proc. of the 24th Project Integration Meeting Oct. 1984 p 57-74 (For primary document see N85-32394 21-44)
Avail: NTIS HC A99/MF A01 CSCL 10A

An outline is given listing the speeches given in each session and the pertinent points is some speeches. There were six session, besides the overview session they were: (1) high efficiency concepts; (2) surface/interface effects; (3) bulk effects; (4) modeling; and (5) high efficiency device processing. Besides the emphasis placed on increasing efficiency of energy conversion, a great amount of discussion was spent on ways to reduce recombination and reducing surface defects. E.R.

N85-32397*# Jet Propulsion Lab., California Inst. of Tech., Pasadena.
HIGH-EFFICIENCY MODULE AND ARRAY RESEARCH
R. G. Ross, Jr. *In its* Proc. of the 24th Project Integration Meeting Oct. 1984 p 75-76 (For primary document see N85-32394 21-44)
Avail: NTIS HC A99/MF A01 CSCL 10A

An outline is presented giving module high efficiency research activities and module technologies contributing to high efficiency. Some factors given on high efficiency are high cell packing factors, low optical losses, low electrical mismatch losses and low operating temperatures. Factors given which are associated with reliability of modules are high efficiency cells, narrow module borders, antisoiling coatings, and antireflection coatings on glass-air interfaces. E.R.

N85-32398*# Jet Propulsion Lab., California Inst. of Tech., Pasadena.
FLAT-PLATE MODULE EFFICIENCY VERSUS COST TRADEOFFS
R. W. Aster *In its* Proc. of the 24th Project Integration Meeting Oct. 1984 p 77-82 (For primary document see N85-32394 21-44)
Avail: NTIS HC A99/MF A01 CSCL 10A

The Five Year Research Plan energy cost methodology and in depth analyses based on the extensive data that are relevant to PV systems are used to facilitate the accomplishment of the $0.15/kWh energy cost goal. An equation is given for the five year energy cost methodology. The allocation guidelines are designed to be consistent with flat solar array (FSA) milestones for module cost, module efficiency, and the programmatic goal for energy cost. They are research targets that appear to be achievable, given prior accomplishments and planned activities in the areas of low cost silicon purification, low cost sheet material, high efficiency cell processing, low cost, long life encapsulants, and automated fabrication method. Extensive sensitivity analysis work has been performed that shows that these guidelines represent an efficient way to meet the intent of the DOE program. Author

N85-32399*# Department of Energy, Washington, D. C.
THE FUTURE OF CRYSTALLINE SILICON TECHNOLOGY IN THE US DEPARTMENT OF ENERGY PROGRAM
Anthony F. Scolaro *In* JPL Proc. of the 24th Project Integration Meeting Oct. 1984 p 83-86 (For primary document see N85-32394 21-44)
Avail: NTIS HC A99/MF A01 CSCL 10A

Two basic findings were presented in the outlined report. The first is that silicon has a very high potential efficiency, demonstrated improvement in reliability and a significant potential for cost reductions. The second is that the photovoltaic technology development process is highly uncertain, but crystalline silicon technology has a substantial knowledge base to draw from, improving its chances of success. Several issues to be addressed are outlined. E.R.

N85-32400*# Hughes Aircraft Co., Culver City, Calif.
GEORGETOWN UNIVERSITY PHOTOVOLTAIC HIGHER EDUCATION NATIONAL EXEMPLAR FACILITY (PHENEF)
Neil Marshall *In* JPL Proc. of the 24th Project Integration Meeting Oct. 1984 p 87-98 (For primary document see N85-32394 21-44)
Avail: NTIS HC A99/MF A01 CSCL 10A

Several photographs of this facility using photovoltaic (PV) cells are shown. An outline is given of the systems requirements, system design and wiring topology, a simplified block design, module electrical characteristics, PV module and PV module matching. E.R.

N85-32401*# Jet Propulsion Lab., California Inst. of Tech., Pasadena.
BLOCK V MODULE PROGRAM
M. I. Smokler *In its* Proc. of the 24th Project Integration Meeting Oct. 1984 p 99-105 (For primary document see N85-32394 21-44)
Avail: NTIS HC A99/MF A01 CSCL 10A

An outlined overview of this module program is given. Tables are given for the following characteristics: module power trend, packing factor trend, cell and circuit characteristics, module physical characteristics, electrical performance, cell efficiency trend, module efficiency trend and module cost trend. The principal improvements are larger modules and higher performance. E.R.

N85-32402*# Jet Propulsion Lab., California Inst. of Tech., Pasadena.
RELIABILITY PHYSICS
Edward F. Cuddihy and Ronald G. Ross, Jr. *In its* Proc. of the 24th Project Integration Meeting Oct. 1984 p 107-109 (For primary document see N85-32394 21-44)
Avail: NTIS HC A99/MF A01 CSCL 10A

Speakers whose topics relate to the reliability physics of solar arrays are listed and their topics briefly reviewed. Nine reports are reviewed ranging in subjects from studies of photothermal degradation in encapsulants and polymerizable ultraviolet stabilizers to interface bonding stability to electrochemical degradation of photovoltaic modules. E.R.

N85-32403*# Jet Propulsion Lab., California Inst. of Tech., Pasadena.
PHOTOTHERMAL DEGRADATION STUDIES OF ENCAPSULANTS
Ranty H. Liang *In its* Proc. of the 24th Project Integration Meeting Oct. 1984 p 111-119 (For primary document see N85-32394 21-44)
Avail: NTIS HC A99/MF A01 CSCL 10A

The reliability physics program at JPL is outlined. The overall objectives and approaches are given in the program. The objectives, approaches and conclusions are given for two specific parts of the programs. These two parts are mechanistic studies of photothermal degradation and performance characteristics of materials with respect to photothermal stresses. E.R.

N85-32404*# Jet Propulsion Lab., California Inst. of Tech., Pasadena.
PREDICTING PHOTOTHERMAL FIELD PERFORMANCE
C. C. Gonzalez and R. G. Ross, Jr. *In its* Proc. of the 24th Project Integration Meeting Oct. 1984 p 121-128 (For primary document see N85-32394 21-44)
Avail: NTIS HC A99/MF A01 CSCL 10A

Photothermal field performance in flat plate solar collectors was predicted. An analytical model which incorporates the measured dependency between transmittance loss and UV and temperature exposure levels was developed. The model uses SOLMET weather data extrapolated to 30 years for various sites and module mounting configurations. It is concluded that the temperature is the key to photothermally induced transmittance loss. The sensitivity of transmittance loss to UV level is nonlinear with minimum in curve near one sun. The ethylene vinyl acetate (EVA) results are consistent with 30 year life allocation. E.A.K.

N85-32405*# Toronto Univ. (Ontario).
MICROMOLECULAR MODELING
James Guillet *In* JPL Proc. of the 24th Project Integration Meeting Oct. 1984 p 129-135 (For primary document see N85-32394 21-44)
Avail: NTIS HC A99/MF A01 CSCL 10A

A reaction kinetics based model of the photodegradation process, which measures all important rate constants, and a computerized model capable of predicting the photodegradation rate and failure modes of a 30 year period, were developed. It is shown that the computerized photodegradation model for polyethylene correctly predicts failure of ELVAX 15 and cross linked ELVAX 150 on outdoor exposure. It is indicated that cross linking ethylene vinyl acetate (EVA) does not significantly change its degradation rate. It is shown that the effect of the stabilizer package is approximately equivalent on both polymers. The computerized model indicates that peroxide decomposers and UV absorbers are the most effective stabilizers. It is found that a combination of UV absorbers and a hindered amine light stabilizer (HALS) is the most effective stabilizer system. E.A.K.

N85-32406*# Polytechnic Inst. of New York, Farmingdale.
POLYMERIZABLE ULTRAVIOLET STABILIZERS
P. Gomez, S. K. Fu, and O. Vogl *In* JPL Proc. of the 24th Project Integration Meeting Oct. 1984 p 137-143 (For primary document see N85-32394 21-44)
Avail: NTIS HC A99/MF A01 CSCL 10A

Polymerizable ultraviolet stabilizers were examined. The objective was to synthesize polymerizable UV monomers, and to incorporate polymerizable UV stabilizers (benzotriazoles) into polymers. E.A.K.

N85-32407*# Springborn Labs., Inc., Enfield, Conn.
ENCAPSULATION MATERIALS RESEARCH
P. Willis *In* JPL Proc. of the 24th Project Integration Meeting Oct. 1984 p 145-164 (For primary document see N85-32394 21-44)
Avail: NTIS HC A99/MF A01 CSCL 10A

Encapsulation materials for solar cells were investigated. The different phases consisted of: (1) identification and development of low cost module encapsulation materials; (2) materials reliability examination; and (3) process sensitivity and process development. It is found that outdoor photothermal aging devices (OPT) are the best accelerated aging methods, simulate worst case field conditions, evaluate formulation and module performance and have a possibility for life assessment. Outdoor metallic copper exposure should be avoided, self priming formulations have good storage stability, stabilizers enhance performance, and soil resistance treatment is still effective. E.A.K.

N85-32408*# Case Western Reserve Univ., Cleveland, Ohio.
EVA-GLASS INTERFACE BOND STABILITY
Jack L. Koenig *In* JPL Proc. of the 24th Project Integration Meeting Oct. 1984 p 165-181 (For primary document see N85-32394 21-44)
Avail: NTIS HC A99/MF A01 CSCL 10A

The ethylene vinyl acetate/glass interface bond stability was investigated. Special methods to determine the structure of polymer/glass interface were developed. Structural changes related to hydrothermal degradation of polymer/glass interface are examined. Methods to inhibit the degradation reaction which occur at polymer/glass interface are developed. E.A.K.

N85-32409*# Cincinnati Univ., Ohio.
INTERFACIAL BONDING STABILITY
J. Boerio *In* JPL Proc. of the 24th Project Integration Meeting Oct. 1984 p 183-189 (For primary document see N85-32394 21-44)
Avail: NTIS HC A99/MF A01 CSCL 10A

Interfacial bonding stability by in situ ellipsometry was investigated. It is found that: (1) gamma MPS is an effective primer for bonding ethylene vinyl acetate (EVA) to aluminum; (2) ellipsometry is an effective in situ technique for monitoring the stability of polymer/metal interfaces; (3) the aluminized back surface of silicon wafers contain significant amounts of silicon and may have glass like properties. E.A.K.

N85-32410*# Jet Propulsion Lab., California Inst. of Tech., Pasadena.
TOPICS IN ELECTROCHEMICAL DEGRADATION OF PHOTOVOLTAIC MODULES
G. R. Mon *In its* Proc. of the 24th Project Integration Meeting Oct. 1984 p 191-205 (For primary document see N85-32394 21-44)
Avail: NTIS HC A99/MF A01 CSCL 10A

Electrochemical degradation of photovoltaic modules was

examined. It is found that the extent of electrochemical damage is dependent on the integrated leakage current. The PV electrochemical degradation mechanisms in the two polarities are different: (1) degradation rates in the two polarities are of the same order of magnitude; (2) center tapped grounded arrays are a preferred system configuration to minimize electrochemical degradation. The use of thicker pottant layers and polymer substrate films to reduce equilibrium leakage current values is suggested. A metallized substrate layer, if used, should be isolated from the pottant and the frame by polyester layers, and EVA modules appear to be consistent with 30 year life allocation levels for electrochemical damage. Temperature acceleration factors are well behaved and moderately well understood; humidity acceleration factors vary radically with module construction and materials and require additional research. E.A.K.

N85-32411*# Wilkes Coll., Wilkes-Barre, Pa.
POLYMER-WATER INTERACTION STUDIES
John Orehotsky *In its* Proc. of the 24th Project Integration Meeting Oct. 1984 p 207-237 (For primary document see N85-32394 21-44)
Avail: NTIS HC A99/MF A01 CSCL 10A

Polymer water interactions were investigated. The following interactions were studied: (1) water absorption and desorption kinetics in EVA and PVB; (2) humidity dependence of electrical properties of EVA and PVB; (3) plasticizer effects in PVB; and (4) radiation effects in PVB and EVA. E.A.K.

N85-32412*# Midwest Research Inst., Golden, Colo. Solar Energy Research Inst.
SILICON REFINEMENT BY CHEMICAL VAPOR TRANSPORT
J. Olson *In* JPL Proc. of the 24th Project Integration Meeting Oct. 1984 p 241-246 (For primary document see N85-32394 21-44)
Avail: NTIS HC A99/MF A01 CSCL 10A

Silicon refinement by chemical vapor transport is discussed. The operating characteristics of the purification process, including factors affecting the rate, purification efficiency and photovoltaic quality of the refined silicon were studied. The casting of large alloy plates was accomplished. A larger research scale reactor is characterized, and it is shown that a refined silicon product yields solar cells with near state of the art conversion efficiencies. E.A.K.

N85-32413*# Union Carbide Corp., Tonawanda, N.Y.
A FLUIDIZED-BED REACTOR FOR SILANE PYROLYSIS
S. Iya *In* JPL Proc. of the 24th Project Integration Meeting Oct. 1984 p 247-249 (For primary document see N85-32394 21-44)
Avail: NTIS HC A99/MF A01 CSCL 10A

The silane decomposition in a fluidized bed reactor was studied. The process feasibility and operating windows were determined. Long duration tests were conducted and silicon purity was demonstrated. A high purity linear was installed in the fluid bed reactor; the FBR product was melted and single crystallized. Product purity improvements are noted. E.A.K.

N85-32414*# Jet Propulsion Lab., California Inst. of Tech., Pasadena.
JPL IN-HOUSE FLUIDIZED-BED REACTOR RESEARCH
N. K. Rohatgi *In its* Proc. of the 24th Project Integration Meeting Oct. 1984 p 251-257 (For primary document see N85-32394 21-44)
Avail: NTIS HC A99/MF A01 CSCL 10A

Fluidized bed reactor research techniques for fabrication of quartz linears was reviewed. Silane pyrolysis was employed in this fabrication study. Metallic contaminant levels in the silicon particles were below levels detectable by emission spectroscopy. G.L.C.

N85-32415*# Washington Univ., Seattle.
MODELING OF THE SILANE FBR SYSTEM
M. P. Dudokovic, P. A. Ramachandran, and S. Lai *In* JPL Proc. of the 24th Project Integration Meeting Oct. 1984 p 259-273 (For primary document see N85-32394 21-44)
Avail: NTIS HC A99/MF A01 CSCL 10A

Development of a mathematical model for fluidized bed pyrolysis of silane that relates production rate and product properties (size, size distribution, presence or absence of fines) with bed size and operating conditions (temperature, feed concentration, flow rate, seed size, etc.) and development of user oriented algorithm for the model are considered. A parameter sensitivity study of the model was also developed. G.L.C.

N85-32416*# California Inst. of Tech., Pasadena.
SILICON PRODUCTION IN AN AEROSOL REACTOR
Jin Jwang Wu, M. K. Alam, B. Ellen Johnson, and Richard C. Flagan *In* JPL Proc. of the 24th Project Integration Meeting Oct. 1984 p 275-280 (For primary document see N85-32394 21-44)
Avail: NTIS HC A99/MF A01 CSCL 10A

An aerosol reactor for the growth of large silicon particles by silane pyrolysis was shown to demonstrate the following properties: (1) generate seed particles by pyrolysis of a small amount of silane; (2) mix seed aerosol with primary silane flow, limiting number concentration such that the amount of silane is sufficient to grow the desired size of particles from the seed; and (3) react the silane at a rate which is controlled such that the seed particles scavenge the condensible vapors rapidly enough to inhibit further nucleation. G.L.C.

N85-32417*# Jet Propulsion Lab., California Inst. of Tech., Pasadena.
HIGH-EFFICIENCY SILICON SOLAR CELL RESEARCH
Taher Daud *In its* Proc. of the 24th Project Integration Meeting Oct. 1984 p 281-282 (For primary document see N85-32394 21-44)
Avail: NTIS HC A99/MF A01 CSCL 10A

Progress reports on research in high-efficiency silicon solar cells were presented by eight contractors and JPL. The presentations covered the issues of Bulk and Surface Loss, Modeling, Measurements, and Proof of Concept. G.L.C.

N85-32418*# Florida Univ., Gainesville.
PHYSICS OF HEAVILY DOPED SILICON AND SOLAR-CELL PARAMETER MEASUREMENT
Fred A. Lindholm *In* JPL Proc. of the 24th Project Integration Meeting Oct. 1984 p 283-293 (For primary document see N85-32394 21-44)
Avail: NTIS HC A99/MF A01 CSCL 10A

A study of the physics of heavily doped silicon and solar cell parameter measurement was undertaken. The parameters investigated were energy gap, lifetime, recombination velocity, diffusivity, mobility and if N or P is high. G.L.C.

N85-32419*# Pennsylvania Univ., Philadelphia.
MEASURING BULK RECOMBINATION RATES AND BOUNDARY RECOMBINATION VELOCITIES
M. Wolf *In* JPL Proc. of the 24th Project Integration Meeting Oct. 1984 p 295-304 (For primary document see N85-32394 21-44)
Avail: NTIS HC A99/MF A01 CSCL 10A

A study was undertaken to measure bulk recombination rates and boundary recombination velocities in silicon solar cell materials. G.L.C.

N85-32420*# State Univ. of New York, Albany.
STUDIES OF OXYGEN- AND CARBON-RELATED DEFECTS IN HIGH-EFFICIENCY SILICON SOLAR CELLS
J. Corbett *In* JPL Proc. of the 24th Project Integration Meeting Oct. 1984 p 305-311 (For primary document see N85-32394 21-44)
Avail: NTIS HC A99/MF A01 CSCL 10A

Studies were conducted to investigate the vague nature of carbon and oxygen related defects in high efficiency silicon solar cells. High temperature tests were employed to perform these investigations. G.L.C.

N85-32421*# Research Triangle Inst., Research Triangle Park, N.C.
COMPREHENSIVE SILICON SOLAR-CELL COMPUTER MODELING
M. F. Lamorte *In* JPL Proc. of the 24th Project Integration Meeting Oct. 1984 p 313-323 (For primary document see N85-32394 21-44)
Avail: NTIS HC A99/MF A01 CSCL 10A

A comprehensive silicon solar cell computer modeling scheme was developed to perform the following tasks: (1) model and analysis of the net charge distribution in quasineutral regions; (2) experimentally determined temperature behavior of Spire Corp. n+pp+ solar cells where n+-emitter is formed by ion implantation of 75As or 31P; and (3) initial validation results of computer simulation program using Spire Corp. n+pp+ cells. G.L.C.

N85-32422*# Jet Propulsion Lab., California Inst. of Tech., Pasadena.
SENSITIVITY ANALYSIS OF HIGH-EFFICIENCY SILICON SOLAR-CELL DESIGN PARAMETERS
Anant R. Mokashi *In its* Proc. of the 24th Project Integration Meeting Oct. 1984 p 325-331 (For primary document see N85-32394 21-44)
Avail: NTIS HC A99/MF A01 CSCL 10A

Silicon solar cell design parameters were investigated to determine their bearing on cell efficiency. Among the parameters reviewed were: (1) bulk resistivity, (2) minority carrier lifetime cell thickness, (3) front junction depth, (4) front surface doping concentration, (5) front surface recombination velocity, and (6) back surface contact. The following were concluded: (1) there is good agreement between experimental and simulation results; (2) sheet material quality improvement is needed for high efficiency cells; (3) 20% cell of this design is feasible with 10 ms bulk lifetime material; and (4) for achieving efficiencies higher than 20% new cell designs including thin cells with light trapping and back surface field should be considered. G.L.C.

N85-32423*# Washington Univ., Seattle.
SILICON SURFACE PASSIVATION BY SILICON NITRIDE DEPOSITION
Larry C. Olsen *In* JPL Proc. of the 24th Project Integration Meeting Oct. 1984 p 333-345 (For primary document see N85-32394 21-44)
Avail: NTIS HC A99/MF A01 CSCL 10A

Silicon nitride deposition was studied as a method of passivation for silicon solar cell surfaces. The following three objectives were the thrust of the research: (1) the use of pecvd silicon nitride for passivation of silicon surfaces; (2) measurement techniques for surface recombination velocity; and (3) the importance of surface passivation to high efficiency solar cells. G.L.C.

N85-32424*# Sah (C. T.) Associates, Urbana, Ill.
IMPORTANT LOSS MECHANISMS IN HIGH-EFFICIENCY SOLAR CELLS
C. Tang Sah *In* JPL Proc. of the 24th Project Integration Meeting Oct. 1984 p 347-351 (For primary document see N85-32394 21-44)
Avail: NTIS HC A99/MF A01 CSCL 10A

A study was conducted to identify loss mechanisms in high efficiency silicon solar cells. The following were considered: (1) recombination loss mechanisms; (2) high efficiency cells; (3) very high efficiency cells; and (4) ultra high efficiency cells. G.L.C.

N85-32425*# Westinghouse Electric Corp., Pittsburgh, Pa.
DEVELOPMENT OF HIGH-EFFICIENCY SOLAR CELLS ON SILICON WEB
A. Rohatgi, D. L. Meier, R. B. Campbell, R. G. Seidensticker, and P. Rai-Choudhury *In* JPL Proc. of the 24th Project Integration Meeting Oct. 1984 p 353-363 (For primary document see N85-32394 21-44)
Avail: NTIS HC A99/MF A01 CSCL 10A

The development of high efficiency solar cells on a silicon web is discussed. Heat treatment effects on web quality; the influence of twin plane lamellae, trace impurities and stress on minority carrier lifetime; and the fabrication of cells are discussed. R.J.F.

N85-32426*# Westinghouse Electric Corp., Pittsburgh, Pa.
SIMULTANEOUS JUNCTION FORMATION
R. B. Campbell *In* JPL Proc. of the 24th Project Integration Meeting Oct. 1984 p 369-377 (For primary document see N85-32394 21-44)
Avail: NTIS HC A99/MF A01 CSCL 10A

High-risk, high-payoff improvements to a baseline process sequence of simultaneous junction formation of silicon solar cells are discussed. The feasibility of simultaneously forming front and back junctions of solar cells using liquid dopants on dendritic web silicon was studied. Simultaneous diffusion was compared to sequential diffusion. A belt furnace for the diffusion process was tested. R.J.F.

N85-32427*# California Inst. of Tech., Pasadena.
AMORPHOUS METALLIC FILMS IN SILICON METALLIZATION SYSTEMS
Marc-A. Nicolet, Hannu Kattelus, and Frank So *In* JPL Proc. of the 24th Project Integration Meeting Oct. 1984 p 379-387 (For primary document see N85-32394 21-44)
Avail: NTIS HC A99/MF A01 CSCL 10A

The general objective was to determine the potential of amorphous metallic thin films as a means of improving the stability of metallic contacts to a silicon substrate. The specific objective pursued was to determine the role of nitrogen in the formation and the resulting properties of amorphous thin-film diffusion barriers. Amorphous metallic films are attractive as diffusion barriers because of the low atomic diffusivity in these materials. Previous investigations revealed that in meeting this condition alone, good diffusion barriers are not necessarily obtained, because amorphous films can react with an adjacent medium (e.g., Si, Al) before they recrystallize. In the case of a silicon single-crystalline substrate, correlation exists between the temperature at which an amorphous metallic binary thin film reacts and the temperatures at which the films made of the same two metallic elements react individually. Amorphous binary films made of Zr and W were investigated. Both react with Si individually only at elevated temperatures. It was confirmed that such films react with Si only above 700 C when annealed in vacuum for 30 min. Amorphous W-N films were also investigated. They are more stable as barriers between Al and Si than polycrystalline W. Nitrogen effectively prevents the W-Al reaction that sets in at 500 C with polycrystalline W. R.J.F.

N85-32428*# Purdue Univ., Lafayette, Ind.
MOD SILVER METALLIZATION FOR PHOTOVOLTAICS
G. M. Vest and R. W. Vest *In* JPL Proc. of the 24th Project Integration Meeting Oct. 1984 p 389-403 Previously announced as N85-27381 (For primary document see N85-32394 21-44)
Avail: NTIS HC A99/MF A01 CSCL 10A

The development of flat plate solar arrays is reported. Photovoltaic cells require back side metallization and a collector grid system on the front surface. Metallo-organic decomposition (MOD) silver films can eliminate most of the present problems with silver conductors. The objectives are to: (1) identify and characterize suitable MO compounds; (2) develop generic synthesis procedures for the MO compounds; (3) develop generic fabrication procedures to screen printable MOD silver inks; (4) optimize processing conditions to produce grid patterns and photovoltaic cells; and (5) develop a model which describes the adhesion between the fired silver film and the silicon surface. E.A.K.

N85-32429*# Westinghouse Electric Corp., Pittsburgh, Pa.
LASER-ASSISTED SOLAR-CELL METALLIZATION PROCESSING
Subhadra Dutta *In* JPL Proc. of the 24th Project Integration Meeting Oct. 1984 p 405-420 (For primary document see N85-32394 21-44)
Avail: NTIS HC A99/MF A01 CSCL 10A

A photolytic metal deposition system using a focused continuous wave ultraviolet laser, a photolytic metal deposition system using a mask and ultraviolet flood illumination, and a pyrolytic metal deposition system using a focused continuous wave laser were studied. Fabrication of solar cells, as well as characterization to determine the effects of transient heat on solar cell junctions were investigated. R.J.F.

N85-32430*# Spectrolab, Inc., Sylmar, Calif.
A NON-NOBLE FRONT METALLIZATION PROCESS
Alexander Garcia, III *In* JPL Proc. of the 24th Project Integration Meeting Oct. 1984 p 421-431 (For primary document see N85-32394 21-44)
Avail: NTIS HC A99/MF A01 CSCL 10A

The optimization, evaluation, and demonstration of a solar cell metallization system is discussed. Screen printing, air firing, reducted atmospheres, and conductive air coating were studied. R.J.F.

N85-32431*# Superwave Technology, Inc., Santa Clara, Calif.
MICROWAVE-ENHANCED THIN-FILM DEPOSITION
S. Chitre *In* JPL Proc. of the 24th Project Integration Meeting Oct. 1984 p 433-435 (For primary document see N85-32394 21-44)
Avail: NTIS HC A99/MF A01 CSCL 10A

The deposition of semiconducting and insulating thin films at low temperatures using microwave technology was explored. The method of plasma formations, selection of a power source, the design of the microwave plasma cavity, the microwave circuitry, impedance matching, plasma diagnostics, the deposition chamber and the vacuum system were studied. R.J.F.

N85-32432*# ARCO Solar, Inc., Chatsworth, Calif.
PULSED EXCIMER LASER PROCESSING FOR COST-EFFECTIVE SOLAR CELLS
D. Wong *In* JPL Proc. of the 24th Project Integration Meeting Oct. 1984 p 437-446 (For primary document see N85-32394 21-44)
Avail: NTIS HC A99/MF A01 CSCL 10A

The goal was to demonstrate the cost effectiveness feasibility of fabricating 16% efficient solar cells on 125 mm diameter Cz wafers using pulsed excimer laser for junction formation, surface passivation, and front metallization. R.J.F.

N85-32433*# Spire Corp., Bedford, Mass.
EXCIMER LASER ANNEALING FOR FABRICATION OF LOW-COST SOLAR CELLS
A. C. Greenwald *In* JPL Proc. of the 24th Project Integration Meeting Oct. 1984 p 447-459 (For primary document see N85-32394 21-44)
Avail: NTIS HC A99/MF A01 CSCL 10A

The goal was to determine if a pulsed excimer laser annealing (PELA) is cost effective compared to a baseline process. An excimer laser pulsed annealing apparatus was built. Three hundred solar cells were fabricated. An economic analysis was performed. R.J.F.

N85-32434*# Springborn Labs., Inc., Enfield, Conn.
ENCAPSULATION PROCESSING AND MANUFACTURING YIELD ANALYSIS
P. Willis *In* JPL Proc. of the 24th Project Integration Meeting Oct. 1984 p 461-469 (For primary document see N85-32394 21-44)
Avail: NTIS HC A99/MF A01 CSCL 10A

The development of encapsulation processing and a manufacturing productivity analysis for photovoltaic cells are discussed. The goals were: (1) to understand the relationships between both formulation variables and process variables; (2) to define conditions required for optimum performance; (3) to predict manufacturing yield; and (4) to provide documentation to industry. R.J.F.

N85-32435*# Westinghouse Electric Corp., Pittsburgh, Pa.
SILICON DENDRITIC WEB GROWTH
S. Duncan *In* JPL Proc. of the 24th Project Integration Meeting Oct. 1984 p 473-481 (For primary document see N85-32394 21-44)
Avail: NTIS HC A99/MF A01 CSCL 10A

Technological goals for a silicon dendritic web growth program effort are presented. Principle objectives for this program include: (1) grow long web crystals front continuously replenished melt; (2) develop temperature distribution in web and melt; (3) improve reproductibility of growth; (4) develop configurations for increased growth rates (width and speed); (5) develop new growth system components as required for improved growth; and (6) evaluate quality of web growth. B.W.

N85-32436*# Westinghouse Electric Corp., Pittsburgh, Pa.
TEMPERATURE-STRESS MODELING
R. G. Seidensticker *In* JPL Proc. of the 24th Project Integration Meeting Oct. 1984 p 483-490 (For primary document see N85-32394 21-44)
Avail: NTIS HC A99/MF A01 CSCL 10A

Temperature-stress modeling for silicon dendritic web growth is described. Temperature/stress fields near growth front are examined. The effects of lateral temperature gradients are also explored. B.W.

N85-32437*# Jet Propulsion Lab., California Inst. of Tech., Pasadena.
SILICON RIBBON STRESS-STRAIN ACTIVITIES
B. K. Wada, C. F. Shih, C. P. Kuo, and W. M. Phillips *In its* Proc. of the 24th Project Integration Meeting Oct. 1984 p 491-515 (For primary document see N85-32394 21-44)
Avail: NTIS HC A99/MF A01 CSCL 10A

The finite element method is used to investigate stress/strain in silicon ribbon. Failure considerations such as residual stress, buckling material non-linearity and creep are discussed. Temperature profiles are presented. B.W.

N85-32438*# Kentucky Univ., Lexington.
ANALYSIS OF STRESS-STRAIN RELATIONSHIPS IN SILICON RIBBON
O. Dillon *In* JPL Proc. of the 24th Project Integration Meeting Oct. 1984 p 517-524 (For primary document see N85-32394 21-44)
Avail: NTIS HC A99/MF A01 CSCL 10A

An analysis of stress-strain relationships in silicon ribbon is presented. A model to present entire process, dynamical Transit Analysis is developed. It is found that knowledge of past-strain history is significant in modeling activities. B.W.

N85-32439*# Kentucky Univ., Lexington.
STRESS AND BUCKLING ANALYSIS
O. Dillon *In* JPL Proc. of the 24th Project Integration Meeting Oct. 1984 p 525-543 (For primary document see N85-32394 21-44)
Avail: NTIS HC A99/MF A01 CSCL 10A

An analysis is presented of elastic stress and buckling behavior due to thermal stresses in silicon ribbon. Thermal profiles for reducing stresses and improving flatness in wide ribbon are discussed. B.W.

N85-32440*# Mobil Tyco Solar Energy Corp., Waltham, Mass.
STRESS AND EFFICIENCY STUDIES IN EFG
J. P. Kalejs *In* JPL Proc. of the 24th Project Integration Meeting Oct. 1984 p 545-560 (For primary document see N85-32394 21-44)
Avail: NTIS HC A99/MF A01 CSCL 10A

Stress and efficiency studies in EFG were carried out for silicon sheet growth. Methods were developed to quantify influence of dislocation electrical activity on bulk lifetime. A new creep law formulation for silicon stress was developed. Bulk lifetime degradation due to increase in doping levels was also examined. B.W.

N85-32441*# Illinois Univ., Chicago.
SILICON SHEET SURFACE STUDIES
S. Danyluk *In* JPL Proc. of the 24th Project Integration Meeting Oct. 1984 p 561-570 (For primary document see N85-32394 21-44)

Avail: NTIS HC A99/MF A01 CSCL 10A

Several activities were performed in the area of silicon sheet surface studies. An interferometry technique was developed for measuring residual stresses in short, thin silicon sheets. Simulation of abrasion of silicon by diamond and by scrating and indentation tests was carried out. The wear rate in silicon was correlated with a wear model. B.W.

N85-32442*# Massachusetts Inst. of Tech., Cambridge.
ANALYSIS OF INCLINED GROWTH OF SILICON SHEET
Robert A. Brown *In* JPL Proc. of the 24th Project Integration Meeting Oct. 1984 p 571-573 (For primary document see N85-32394 21-44)
Avail: NTIS HC A99/MF A01 CSCL 10A

A general-purpose finite element program was developed for analysis of silicon sheet growth in inclined configurations. This program will be used to study parametric sensitivity of various growth geometries with respect to thermal control and growth rate, dopant segregation, thermal stress and interface morphology and instability. B.W.

N85-32443*# Mobil Tyco Solar Energy Corp., Waltham, Mass.
EDGE-DEFINED FILM-FED GROWTH OF THIN SILICON SHEETS
H. M. Ettouney and J. P. Kalejs *In* JPL Proc. of the 24th Project Integration Meeting Oct. 1984 p 575-586 (For primary document see N85-32394 21-44)
Avail: NTIS HC A99/MF A01 CSCL 10A

Finite element analysis was used on two length scales to understand crystal growth of thin silicon sheets. Thermal-capillary models of entire ribbon growth systems were developed. Microscopic modeling of morphological structure of melt/solid interfaces beyond the point of linear instability was carried out. The application to silicon system is discussed. B.W.

N85-32444*# Midwest Research Inst., Golden, Colo.
HIGH-PURITY SILICON CRYSTAL GROWTH
T. Ciszek *In* JPL Proc. of the 24th Project Integration Meeting Oct. 1984 p 587-605 (For primary document see N85-32394 21-44)
Avail: NTIS HC A99/MF A01 CSCL 10A

Crystal growth parameter effects on minority carrier lifetime and solar cell efficiencies were investigated using high purity techniques such as float zoning. Study objectives include the following: (1) optimize dopants and minority carrier lifetime in FZ material for high efficiency silicon solar cell applications; (2) improve the understanding of lifetime degradation mechanisms (point defects, impurities, thermal history, surface effects, etc.), and (3) crystallographic defect characterization of float zone and ribbon crystals via X-ray topography. B.W.

N85-32445*# Jet Propulsion Lab., California Inst. of Tech., Pasadena.
ADVANCED MODULE DEVELOPMENT OVERVIEW
M. I. Smokler *In* JPL Proc. of the 24th Project Integration Meeting Oct. 1984 p 609-611 (For primary document see N85-32394 21-44)
Avail: NTIS HC A99/MF A01 CSCL 10A

Crystalline silicon solar power modules are examined for reliability and cost effectiveness. A goal of 12% solar energy conversion efficiency is considered feasible at a cost of 12/kWh, and a decision is made to limit consideration to float zone silicon wafer and dendritic web silicone modules. A preliminary module packaging configuration of glass/ethylene vinyl acetate/plastic film is selected. Anticipated module efficiency levels are 12.6% at 25 C and 11.5% at NOCT (Nominal Operating Cell Temperature). F.M.R.

N85-32446*# Spire Corp., Bedford, Mass.
STATUS OF HIGH-EFFICIENCY MODULE DESIGN AND FABRICATION
M. B. Spitzer *In* JPL Proc. of the 24th Project Integration Meeting Oct. 1984 p 613-618 (For primary document see N85-32394 21-44)
Avail: NTIS HC A99/MF A01 CSCL 10A

The fabrication of high efficiency solar energy conversion modules (13% efficiency at NOCT - Nominal Operating Cell Temperature) is discussed, with emphasis placed on reducing NOCT, since reduced operating temperature improves both efficiency and module lifetime. F.M.R.

N85-32447*# Jet Propulsion Lab., California Inst. of Tech., Pasadena.
MODULE HIPOT AND GROUND CONTINUITY TEST RESULTS
John S. Griffith *In its* Proc. of the 24th Project Integration Meeting Oct. 1984 p 619-631 (For primary document see N85-32394 21-44)
Avail: NTIS HC A99/MF A01 CSCL 10A

Hipot (high voltage potential) and module frame continuity tests of solar energy conversion modules intended for deployment into large arrays are discussed. The purpose of the tests is to reveal potentially hazardous voltage conditions in installed modules, and leakage currents that may result in loss of power or cause ground fault system problems, i.e., current leakage potential and leakage voltage distribution. The tests show a combined failure rate of 36% (69% when environmental testing is included). These failure rates are believed easily corrected by greater care in fabrication. F.M.R.

N85-32448*# Jet Propulsion Lab., California Inst. of Tech., Pasadena.
PHOTOVOLTAIC MODULE SPREAD-OF-FLAME TESTING
R. S. Sugimura, D. H. Otth, and J. C. Arnett (ARCO Solar, Inc.) *In its* Proc. of the 24th Project Integration Meeting Oct. 1984 p 633-638 (For primary document see N85-32394 21-44)
Avail: NTIS HC A99/MF A01 CSCL 10A

Photovoltaic modules used in solar energy conversion are tested for flammability. Class B burning brand tests were conducted with the following results: module glass shattered and hydrocarbon encapsulants ignited. Penetration of back surface material was the prime cause of failure. Materials with greater flame and heat resistance are under consideration to increase back surface integrity up to Class A burning brand standard. The most promising is stainless steel foil. F.M.R.

N85-32449*# Jet Propulsion Lab., California Inst. of Tech., Pasadena.
IMPROVED NOMINAL OPERATING CELL TEMPERATURE (NOCT) TEST PROCEDURE
L. Wen and D. Berns *In its* Proc. of the 24th Project Integration Meeting Oct. 1984 p 639-642 (For primary document see N85-32394 21-44)
Avail: NTIS HC A99/MF A01 CSCL 10A

A procedure is developed to improve testing of Nominal Operating Cell Temperature (NOCT) as it applies to solar energy conversion modules. NOCT is a direct reflection of module thermal design and is closely related to the representative ambient temperature. It is also a key to array energy production and estimates of module lifetimes. Present NOCT test and evaluation procedures are inconsistent, producing significant scatter. Test refinements would specify a clear sky, the addition of 10% to the insolation level for ground reflection, the addition of a ground emission factor of 0.8 (at 30C ground temperature), an effective wind direction of 135 degrees from the North, and a module tilt of 30 degrees from the horizon. F.M.R.

N85-32450*# Jet Propulsion Lab., California Inst. of Tech., Pasadena.
THIN-FILM RELIABILITY AND ENGINEERING OVERVIEW
R. G. Ross, Jr. *In its* Proc. of the 24th Project Integration Meeting Oct. 1984 p 643-646 (For primary document see N85-32394 21-44)
Avail: NTIS HC A99/MF A01 CSCL 10A

The reliability and engineering technology base required for thin film solar energy conversions modules is discussed. The

emphasis is on the integration of amorphous silicon cells into power modules. The effort is being coordinated with SERI's thin film cell research activities as part of DOE's Amorphous Silicon Program. Program concentration is on temperature humidity reliability research, glass breaking strength research, point defect system analysis, hot spot heating assessment, and electrical measurements technology. F.M.R.

N85-32451*# Clemson Univ., S.C.
ACCELERATED STRESS FACTORS AND FAILURE/ DEGRADATION MECHANISMS IN TERRESTRIAL SOLAR CELLS
Jay W. Lathrop *In* JPL Proc. of the 24th Project Integration Meeting Oct. 1984 p 647-656 (For primary document see N85-32394 21-44)
Avail: NTIS HC A99/MF A01 CSCL 10A

Plans for the development of amorphous cell accelerated test measurement instrumentation are outlined. Diagrams for an 11-lamp ELH solar simulator and ac light source instrumentation are given. Examples of ac and dc analysis graphs are also provided. M.G.

N85-32452*# Jet Propulsion Lab., California Inst. of Tech., Pasadena.
FAILURE ANALYSIS OF THIN-FILM AMORPHOUS-SILICON SOLAR-CELL MODULES
Q. Kim *In* JPL Proc. of the 24th Project Integration Meeting Oct. 1984 p 657-662 (For primary document see N85-32394 21-44)
Avail: NTIS HC A99/MF A01 CSCL 10A

A failure analysis of thin film amorphous silicon solar cell modules was conducted. The purpose of this analysis is to provide information and data for appropriate corrective action that could result in improvements in product quality and reliability. Existing techniques were expanded in order to evaluate and characterize degradational performance of a-Si solar cells. Microscopic and macroscopic defects and flaws that significantly contribute to performance degradation were investigated. B.W.

N85-32453*# Jet Propulsion Lab., California Inst. of Tech., Pasadena.
REFERENCE-CELL CALIBRATION ACTIVITIES
R. Mueller *In* JPL Proc. of the 24th Project Integration Meeting Oct. 1984 p 663-668 (For primary document see N85-32394 21-44)
Avail: NTIS HC A99/MF A01 CSCL 10A

The use of secondary calibration in large area pulsed solar simulators (LAPSS) is discussed. It is argued that primary calibration in sunlight is time consuming, that only a limited sun calibration of a set of primary reference cells is required, that the LAPSS light source is filtered to closely match the am 1.5 direct spectrum, and that the temperal stability of the filtered LAPSS is excellent. There is the possibility of a lower error rate. Lower costs are anticipated. R.J.F.

N85-32454# ECO Energy Conversion, Newton, Mass.
A SAFE, HIGH-POWER-DENSITY LITHIUM BATTERY Final Report, Sep. 1984 - Feb. 1985
F. Walsh Mar. 1985 27 p
(Contract N00014-84-C-0724)
(AD-A155223) Avail: NTIS HC A03/MF A01 CSCL 10/3

The Li/SOCl2 battery has received attention because of its high theoretical energy/power density. However, practical Li/SOCl2 cells have not provided the desired power density and have suffered from concerns with cell safety on discharge. In previous work, ECO has shown that the use of a TAA-type catalyst significantly improves the safety of the Li/SOCl2 cell at high rate. The objective of this Phase 1 program was to determine whether a stacked disk electrode configuration with TAA-catalyzed cathodes would meet a high power-density design goal. Under the program, the effects of cathode thickness, preparation pressure, electrolyte gap and solute concentration on stacked-electrode cell performance and capacity were measured. The results of the Phase 1 program included the demonstration of stacked-electrode cell performance and capacity at levels suitable to meet a design goal of 400 W/kg with high energy density. Further work in a Phase 2 program will be required to demonstrate in laser-sealed fully-packaged cells that the results of Phase 1 can be practically applied to provide a safe high-rate, energy-dense power source for military applications. GRA

N85-32455# Los Alamos National Lab., N. Mex.
PERFORMANCE ANALYSIS OF MIXED PASSIVE SOLAR HEATING SYSTEMS
W. O. Wray and E. D. Best 1985 7 p Presented at Solar Buildings: Realities for Today, Trends for Tomorrow, Washington, D.C., 18 Mar. 1985
(Contract W-7405-eng-36)
(DE85-009624; LA-UR-85-1046; CONF-850388-2) Avail: NTIS HC A02/MF A01

The various situations in which interactions between south-facing systems serving a single thermal zone may affect the performance of the mixture are discussed. The nature of direct gain interactions with unvented Trombe walls was explored using a thermal network computer program. The results are compared with predictions from the simple design analysis procedures which neglect interactions. It is shown that system interactions can significantly improve the performance of a mixture under certain conditions. DOE

N85-32456# Los Alamos National Lab., N. Mex.
LOS ALAMOS OPTICAL MATERIALS RELIABILITY, MAINTAINABILITY, AND EXPOSURE TESTING PROGRAM Status Report
S. W. Moore Mar. 1985 20 p
(Contract W-7405-eng-36)
(DE85-011894; LA-10356-SR) Avail: NTIS HC A02/MF A01

Cost effectiveness of many solar materials is a major factor in bringing solar products into widespread use. This factor is affected by initial cost as well as by durability. The least costly material that will do a specific job is determined along with and its lifetime such that full life cycle costing can be ascertained by the manufacturer. To this end, material operating limitations, durabilities, and failure modes are being determined. DOE

45 ENVIRONMENT POLLUTION

Includes air, noise, thermal and water pollution; environment monitoring; and contamination control.

N85-32457# Committee on Government Operations (U. S. House).
REVIEW OF HAZARDOUS WASTE CLEANUP AND DISPOSAL EFFORTS AT TINKER AIR FORCE BASE
Washington GPO 1985 221 p refs Hearing before a Subcomm. of the Comm. on Govt. Operations, 98th Congr., 2nd Sess., 13 Dec. 1984
(GPO-43-294) Avail: Committee on Government Operations

The efforts to clean up and control hazardous wastes at Tinker Air Force Base are discussed. Ground water contamination, waste treatment, recycling, maintenance, and selection of disposal sites are discussed. R.J.F.

N85-32458 Committee on Energy and Commerce (U. S. House).
HAZARDOUS AIR POLLUTANTS
Washington GPO 1985 547 p refs Hearing before the Subcomm. on Health and the Environ. of the Comm. on Energy and Com., 98th Congr., 2nd Sess., 14 Dec. 1984
(GPO-43-064) Avail: Subcommittee on Health and the Environment

The accidental release of toxic substances with the air was discussed. The disaster in Bhopal, India was discussed in detail. Safety practices at Union Carbide, Federal regulations relative to toxic substances, and mortality statistics for West Virginia were covered. R.J.F.

N85-32459# Naval Ocean Systems Center, San Diego, Calif.
MARINE ENVIRONMENTAL QUALITY ASSESSMENT PROGRAM, FIVE-YEAR PLAN (FY 1984 - 1988)
A. Zirino and R. K. Johnston Oct. 1984 73 p
(NR Proj. F59-559; NR Proj. Y08-17)
(AD-A154715; NOSC/TD-761) Avail: NTIS HC A04/MF A01 CSCL 06/6

This document is the second five-year plan (FY84-FY88) of the Marine Environmental Quality Assessment (MEQA) Program. It updates the MEQA Exploratory Development (FY78-FY83) Program Plan and places emphasis on current environmental issues, such as the fate and effects of organotin leachates, real-time monitoring techniques, bio-chemical analysis and advanced bioassay procedures. GRA

N85-32460# Naval Postgraduate School, Monterey, Calif.
ASSESSMENT OF THE PERFORMANCE OF AN IN-FIELD GAUSSIAN PLUME/PUFF MODEL FOR OVERWATER USE Final Report, Oct. - Nov. 1984
C. E. Skupniewicz and G. E. Schacher Feb. 1985 53 p
(F59-551)
(AD-A155435; NPS61-85-002; NEPRF-CR-85-01) Avail: NTIS HC A04/MF A01 CSCL 20/4

A U.S. Navy chemical hazard forecast computer model is tested for consistency with Naval Postgraduate School field data which was used in its development. The model's attempt to forecast puff dispersion, overwater dispersion for burst release for which a parameterization has not been developed, are examined by comparison to relative dispersion data sets. The parameterizations developed from the NPS data set are compared to an independently derived set of parameterizations demonstrating the generic applicability of the model. It was found that the model predicts the total width over which a hazard might occur reasonably well, but underpredicts the downwind hazard distance. This is due to lack of separate consideration of meander effects. Author (GRA)

N85-32461# Radian Corp., Austin, Tex.
EMERGENCY MODELING OF HAZARDOUS AIR POLLUTANTS Final Report, Jun. 1983 - Sep. 1984
M. Hebets Tyndall AFB, Fla. Air Force Engineering and Services Center May 1985 246 p
(Contract F33615-83-D-4001)
(AD-A155441; AFESC/ESL-TR-84-55) Avail: NTIS HC A11/MF A01 CSCL 13/2

An updated atmospheric diffusion modeling capability has been developed for responding to accidents which emit toxic vapors into the atmosphere. The microcomputer-based Complex Hazardous Air Release Model (CHARM) has been adapted for use in Air Force propellant, fuel, and chemical handling operations. Air Force personnel can use the model to assess potential exposure to airborne toxic clouds which results from an emergency or accidental release of hazardous compounds. CHARM includes proven evaporation and atmospheric dispersion algorithms and includes a procedure for modeling the dispersion of denser-than-air gases. GRA

N85-32462# Walker (William W., Jr.), Concord, Mass.
EMPIRICAL METHODS FOR PREDICTING EUTROPHICATION IN IMPOUNDMENTS. REPORT 3. PHASE 2. MODEL REFINEMENTS
W. W. Walker, Jr. Mar. 1985 323 p
(Contract DACW39-78-C-0053-Rept-3)
(AD-A155483; WES-TR-E-81-9-3) Avail: NTIS HC A14/MF A01 CSCL 08/1

Empirical eutrophication models are useful tools for some aspects of reservoir water quality assessment and management. This report modifies existing model structures and parameter estimates to improve their generality and permit application under a wider spectrum of reservoir conditions. A network of models is assembled for predicting reservoir-average concentrations of total phosphorus, total nitrogen, chlorophyll-a, transparency, organic nitrogen, particulate phosphorus, and hypolimnetic oxygen depletion rate (near-dam) as functions of reservoir mean depth, hydraulic residence time, and inflow concentrations of total phosphorus, ortho-phosphorus, total nitrogen, and inorganic nitrogen. Models are tested against several independent lake and reservoir data sets compiled from the literature. An error analysis indicates that the prediction of chlorophyll-a, the most direct measure of eutrophication response, is limited more by variabilities in the biological responses to a given set of nutrient concentrations and other environmental conditions than by uncertainties in predicting pool nutrient levels from external loadings. Inflow available phosphorus concentration and mena depth are shown to explain most of the variance in reservoir tropic state indicators and hypolimnetic oxygen status. GRA

N85-32463# Pacific Northwest Lab., Richland, Wash.
VALMET: A VALLEY AIR POLLUTION MODEL Final Report
C. D. Whiteman and K. J. Allwine Apr. 1985 170 p refs Revised
(Contract DE-AC06-76RL-01830)
(DE85-010820; PNL-4728-Rev-1) Avail: NTIS HC A08/MF A01

An air quality model is described for predicting air pollution concentrations in deep mountain valleys arising from nocturnal down-valley transport and diffusion of an elevated pollutant plume, and the fumigation of the plume on the valley floor and sidewalls after sunrise. A technical description of the model, a discussion of the model's applications, the required model inputs, sample calculations and model outputs, and a full listing of the FORTRAN computer program are included. DOE

N85-32721*# Geological Survey, Denver, Colo. Federal Center.
SULFUR DIAGENESIS IN MARINE SEDIMENTS
Martin Goldhaber *In* NASA, Washington The Global Sulfur Cycle Jul. 1985 p 42-44 refs (For primary document see N85-32710 21-51)
Avail: NTIS HC A14/MF A01 CSCL 13B

N85-32726*# Michigan State Univ., Hickory Corners. Biology Station.
SULFUR CYCLING IN FRESHWATER SEDIMENTS Abstract Only
Michael J. Klug *In* NASA, Washington The Global Sulfur Cycle Jul. 1985 p 60-61 refs (For primary document see N85-32710 21-51)
Avail: NTIS HC A14/MF A01 CSCL 13B

N85-32727*# Reading Univ. (England).
SOME THOUGHTS ON GAIA AND THE SULFUR CYCLE
James E. Lovelock *In* NASA, Washington The Global Sulfur Cycle Jul. 1985 p 62-63 refs (For primary document see N85-32710 21-51)
Avail: NTIS HC A14/MF A01 CSCL 13B

N85-32729*# North Carolina Univ., Chapel Hill. Dept. of Marine Science.
SULFUR AND CARBON CYCLING IN ORGANIC-RICH MARINE SEDIMENTS Abstract Only
Christopher S. Martens *In* NASA, Washington The Global Sulfur Cycle Jul. 1985 p 66-67 refs (For primary document see N85-32710 21-51)
Avail: NTIS HC A14/MF A01 CSCL 13B

N85-32731*# Scripps Institution of Oceanography, San Diego, Calif.
POSSIBLE ROLES OF MANGANESE REDOX CHEMISTRY IN THE SULFUR CYCLE Abstract Only
Kenneth H. Nealson *In* NASA, Washington The Global Sulfur Cycle Jul. 1985 p 69 refs (For primary document see N85-32710 21-51)
Avail: NTIS HC A14/MF A01 CSCL 13B

N85-32733*# National Aeronautics and Space Administration. Ames Research Center, Moffett Field, Calif.
BIOGEOCHEMICAL CYCLING AND REMOTE SENSING
David L. Peterson *In* NASA, Washington The Global Sulfur Cycle

Jul. 1985 p 72-76 refs (For primary document see N85-32710 21-51)
Avail: NTIS HC A14/MF A01 CSCL 13B

N85-32742*# Michigan State Univ., Hickory Corners. Biology Station
SULFUR REDUCTION IN SEDIMENTS OF MARINE AND EVAPORITE ENVIRONMENTS
Michael J. Klug, Penelope Boston (National Center for Atmospheric Research, Boulder), Roger Francois (British Columbia Univ.), Ruth Ann Gyure (Purdue Univ.), Barbara Javor (Scripps Inst. of Oceanography, La Jolla, Calif.), Gordon Tribble (Hawaii Univ., Honolulu), and Appathurai Vairavamurthy (Florida State Univ.) *In* NASA, Washington The Global Sulfur Cycle Jul. 1985 p 128-157 refs (For primary document see N85-32710 21-51)
Avail: NTIS HC A14/MF A01 CSCL 13B

N85-32744*# North Carolina Univ., Chapel Hill. Dept. of Marine Sciences.
MICROANALYSIS OF DISSOLVED IRON AND PHOSPHATE IN PORE WATERS OF HYPERSALINE SEDIMENT
Robert Haddad and Timothy Shaw (Scripps Inst. of Oceanography, La Jolla, Calif.) *In* NASA, Washington The Global Sulfur Cycle Jul. 1985 p 183-193 (For primary document see N85-32710 21-51)
Avail: NTIS HC A14/MF A01 CSCL 13B

N85-32748*# National Aeronautics and Space Administration, Washington, D. C.
SULFUR CYCLE
R. Hariss and H. Niki *In its* The Global Sulfur Cycle Jul. 1985 p 234-238 refs (For primary document see N85-32710 21-51)
Avail: NTIS HC A14/MF A01 CSCL 13B

46 GEOPHYSICS

Includes aeronomy; upper and lower atmosphere studies; ionospheric and magnetospheric physics; and geomagnetism.

For space radiation see *93 Space Radiation.*

N85-32464*# Institute for Atmospheric Optics and Remote Sensing, Hampton, Va.
DATA ANALYSIS FOR LIDAR AND QUARTZ CRYSTAL MICROBALANCE SYSTEMS Final Report
Geoffrey S. Kent and Adarsh Deepak Jun. 1985 182 p refs (Contract NAS1-16253)
(NASA-CR-172601; NAS 1.26:172601) Avail: NTIS HC A09/MF A01 CSCL 04A

Results are presented of the analysis of data taken on the stratospheric aerosol, using lidar, Quartz Crystal Microbalance (QCM), and the SAGE and SAM II satellite systems. The main objective of the work reported has been to use the data, taken with the NASA-LaRC instruments to study the stratospheric effects of volcanic eruptions during the period between the launch of the SAGE and SAM II satellite systems and October 1980. Four significant volcanic eruptions, for which data are available, occurred during this period--Soufriere, Sierra Negra, Mt. St. Helens, and Ulawun. Data on these have been analyzed to determine the changes in stratospheric mass loading produced by the eruptions, and to study the dispersion of the newly injected material. Author

N85-32465*# National Aeronautics and Space Administration. Goddard Space Flight Center, Greenbelt, Md.
CRUSTAL DYNAMICS PROJECT DATA ANALYSIS FIXED STATION VLBI GEODETIC RESULTS
James W. Ryan and Chopo Ma 1985 134 p
(NASA-TM-86229; Rept-85B0522; NAS 1.15:86229) Avail: NTIS HC A07/MF A01 CSCL 08G

The Goddard VLBI group reports the results of analyzing the fixed observatory VLBI data available to the Crustal Dynamics Project through the end of 1984. All POLARIS/IRIS full-day data are included. The mobile site at Platteville, Colorado is also included since its occupation bears on the study of plate stability. Data from 1980 through 1984 were used to obtain the catalog of site and radio source positions labeled S284C. Using this catalog two types of one-day solutions were made: (1) to estimate site and baseline motions; and (2) to estimate Earth rotation parameters. A priori Earth rotation parameters were interpolated to the epoch of each observation from BIH Circular D. Author

N85-32466*# International Council of Scientific Unions, Urbana, Ill.
MIDDLE ATMOSPHERE PROGRAM. HANDBOOK FOR MAP. VOLUME 14: URSI/SCOSTEP WORKSHOP ON TECHNICAL ASPECTS OF MST RADAR
S. A. Bowhill, ed. (Illinois Univ., Urbana) and Belva Edwards, ed. Dec. 1984 381 p refs Workshop held in Urbana, Ill., 22-25 May 1984 Sponsored in part by UNESCO
(Contract NASw-3805)
(NASA-CR-176085; NAS 1.26:176085; MAP-HANDBOOK-14)
Avail: NTIS HC A17/MF A01; also available from SCOSTEP Secretariat, Illinois Univ., 1406 West Green Street, Urbana, Ill. 61801 CSCL 04B

Various topics relative to middle atmosphere research were discussed. meteorological and aeronomical requirements for mesosphere-stratosphere-troposphere (MST) radar networks, general circulation of the middle atmosphere, the interpretation of radar returns from clear air, spaced antenna and Doppler techniques for velocity measurement, and techniques for the study of gravity waves and turbulence are among the topics discussed. For individual titles, see N85-32467 through N85-32550.

N85-32467*# National Aeronautics and Space Administration. Goddard Space Flight Center, Greenbelt, Md.
METEOROLOGICAL AND AERONOMICAL REQUIREMENTS FOR MST RADAR NETWORKS (KEYNOTE PAPER), PART 1
c47
M. A. Geller *In* International Council of Scientific Unions Middle Atmosphere Program: Handbook for MAP. Vol. 14 Dec. 1984 p 1-4 (For primary document see N85-32466 21-45)
Avail: NTIS HC A17/MF A01; also avail. from SCOSTEP Secretariat, Illinois Univ., 1406 West Green St., Urbana, Ill. 61801 CSCL 04B

Mesosphere - stratosphere - troposphere (MST) radar are phase coherent radars that measure the amplitude and Doppler shift of radio waves that are scattered back to the receiving antennas. For a monostatic system, the line-of-sight projection of the wind vector is obtained if one assumes that the atmospheric scatterers are being swept along with the wind velocity. The three-dimensional wind is then derived either by using multiple beams or by beam swinging. The turbulence intensity is derived either by measuring the backscattered power or by deriving the width of the autocorrelation function for the wind. Furthermore, some information on sharp changes in the atmospheric static stability (e.g., at the tropopause) can be obtained by looking for specular reflections. The discussion addresses the question of how these MST measurement capabilities can contribute to various meteorological and aeronomical research areas. R.J.F.

N85-32468*# Cornell Univ., Ithaca, N.Y. School of Electrical Engineering.
TROPOSPHERIC-STRATOSPHERIC EXCHANGE, PART 1.1A
c47
C. R. Cornish *In* International Council of Scientific Unions Middle Atmosphere Program: Handbook for MAP. Vol. 14 Dec. 1984 p 4-5 refs (For primary document see N85-32466 21-46)
Avail: NTIS HC A17/MF A01; also avail. from SCOSTEP Secretariat, Illinois Univ., 1406 West Green St., Urbana, Ill. 61801 CSCL 04B

Much of the observational evidence of large scale tropospheric-stratospheric exchange has been obtained by radiosonde and satellite radiane data. So far mesosphere-stratosphere-troposphere (MST) radars have made mininal contributions, in part due to their recent use as a meteorological tool, intermittent operation at some facilities and sparse geographic distribution. However, as more

MST facilities come on-line in more locations, the good time and height resolution data throughtout the troposphere and much of the stratosphere obtainable by MST radars will enhance the detail of stratospheric and tropospheric circulations and interactions. On smaller scales MST radars have already been used to examine convective forcing from the troposphere into the stratosphere and subsequent launching of gravity waves (LARSEN et al., 1982). Observations of persistent turbulent layers in the stratosphere over Arecibo, attributable to inertial oscillations, appear to propagate away from a source region near the tropopause (SATO and WOODMAN, 1982). MST radars offer the availability of high resolution wind data in height and time needed to observe interactions between the troposphere and stratosphere. The lack of geographic coverage (e.g., equatorial regions) and insufficient data bases at many MST facilities presently inhibit studies of large-scale interactions. At present MST radars can be used to examine smaller scale interactions. R.J.F.

N85-32469*# Cornell Univ., Ithaca, N.Y.
OBSERVATIONS OF FRONTAL ZONE STRUCTURES WITH A VHF DOPPLER RADAR AND RADIOSONDES, PART 1.2A c47
M. F. Larsen and J. Rottger (EISCAT Scientific Association) *In* International Council of Scientific Unions Middle Atmosphere Program. Handbook for MAP. Vol. 14 Dec. 1984 p 7-13 refs (For primary document see N85-32466 21-46)
Avail: NTIS HC A17/MF A01; also avail. from SCOSTEP Secretariat, Illinois Univ., 1406 West Green St., Urbana, Ill. 61801 CSCL 04B

The SOUSY-VHF-Radar is a pulsed coherent radar operating at 53.5 MHz and located near Bad Lauterbert, West Germany. Since 1977, the facility, operated by the Max-Planck-Institut fur Aeronomie, has been used to make a series of frontal passage observations in the spring and fall. Experiments in winter have been difficult because part of the transmitting and receiving array is usually covered by snow during that part of the year. Wavelengths around 6 m are known to be sensitive to the vertical temperature structure of the atmosphere (GREEN and GAGE, 1980; RASTOGI and ROTTGER, 1982). Thus, it has been possible to use radars operating at frequencies near 500 MHz to locate the tropopause. Comparisons between radar data and radiosonde data have shown that there is a large gradient in the radar reflectivity at the height where the radiosonde tropopause occurs. An experiment carried out by ROTTGER (1979) on March 15 to 16, 1977, showed that the radar's sensitivity to the vertical temperature structure could also be used to locate the position of fronts. The SOUSY-VHF-Radar consists of a transmitting array, also used for receiving in some configurations, that can be scanned in the off-vertical direction but not at sufficiently low elevation angles to study the horizontal extent of structures. R.J.F.

N85-32470*# National Aeronautics and Space Administration. Goddard Space Flight Center, Greenbelt, Md.
EXCERPTS FROM THE PAPER: RESEARCH STATUS AND RECOMMENDATION FROM THE ALASKA WORKSHOP ON GRAVITY WAVES AND TURBULENCE IN THE MIDDLE ATMOSPHERE, PART 1.3A
D. C. Fritts (Alaska Univ., Fairbanks), M. A. Geller, B. B. Balsley (NOAA, Boulder), M. L. Chanin (Service d'Aeronomie du Centre Nationale de la Recherche Scientifique, Verrieres le Buisson, France), I. Hirota (Kyoto Univ.), J. R. Holton (Washington Univ., Seattle), S. Kato (Kyoto Univ.), R. S. Lindzen (MIT), M. R. Schoeberl, R. A. Vincent (Adelaide Univ.) et al *In* International Council of Scientific Unions Middle Atmosphere Program: Handbook for MAP. Vol. 14 Dec. 1984 p 14-22 refs Repr. from Bull. Am. Meteorol. Soc., no. 65 p 149-159 Workshop held in Fairbanks, Alaska, 18-22 Jul. 1983 (For primary document see N85-32466 21-46)
Avail: NTIS HC A17/MF A01; also avail. from SCOSTEP Secretariat, Illinois Univ., 1406 West Green St., Urbana, Ill. 61801 CSCL 04B

Internal gravity waves are disturbances whose intrinsic frequencies k(c - u) are smaller than the Brunt-Vaisala frequency (N). Their importance arises because: they are the major components of the total flow and temperature variability fields of the mesosphere (i.e., shears and lapse rates) and hence constitute the likely sources of turbulence; and they are associated with fluxes of momentum that communicate stresses over large distances. For example, gravity waves exert a drag on the flow in the upper mesosphere. However, in order for gravity waves to exert a net drag on the atmosphere, they must be attenuated. There are two general types of processes that seek to attenuate gravity waves: dissipation and saturation. Dissipation is any process that is effective independent of the wave amplitude, while saturation occurs when certain wave amplitude conditions are met. Radiative damping is an example of dissipation, while convective overturning is an example of saturation. The two processes are not mutually exclusive. R.J.F.

N85-32471*# National Aeronautics and Space Administration. Goddard Space Flight Center, Greenbelt, Md.
GRAVITY WAVES FROM THE STRATOSPHERE TO THE MESOSPHERE, PART 1.3B
M. R. Schoeberl *In* International Council of Scientific Unions Middle Atmosphere Program: Handbook for MAP. Vol. 14 Dec. 1984 p 23 ref (For primary document see N85-32466 21-46)
Avail: NTIS HC A17/MF A01; also avail. from SCOSTEP Secretariat, Illinois Univ., 1406 West Green St., Urbana, Ill. 61801 CSCL 04A

The propagation of gravity waves from the stratosphere to the mesosphere has important implications both for observers and those who are attempting to parameterize wave breaking in global models. As they propagate from the tropopause to their breaking level (here, assumed to be the mesosphere), gravity waves can encounter a refractive environment since the vertical group velocity is a function of the background wind. They may be focussed or scattered or dissipated before reaching the mesosphere. It is even conceivable that gravity waves may break stop breaking, and begin breaking again at high altitudes with a resultant loss of wave energy in the intervening region. From a modeling viewpoint, the important concern for large-scale flows is the total upward flux of gravity wave (pseudo) momentum entering the stratosphere and mesosphere. The refraction of gravity waves also presents a difficult problem for observers since waves passing through the tropopause may arrive a thousand kilometers upstream in the mesosphere. Since mesosphere - stratosphere - troposphere (MST) radars sense tropospheric and mesospheric conditions most accurately, they are ideally suited to assess the total gravity-wave flux through the tropopause and stratospause. Networks of radars making coordinated measurements may be required to accurately determine the upward flux of momentum as well as the flux convergence between layers. R.J.F.

N85-32472*# National Aeronautics and Space Administration. Goddard Space Flight Center, Greenbelt, Md.
THE SUPPRESSION OF CONVECTIVE WAVEBREAKING BY RADIATIVE TRANSFER PROCESSES, PART 1.3C
M. R. Schoeberl *In* International Council of Scientific Unions Middle Atmosphere Program: Handbook for MAP. Vol. 14 Dec. 1984 p 24-26 refs (For primary document see N85-32466 21-46)
Avail: NTIS HC A17/MF A01; Also avail. from SCOSTEP Secretariat, Illinois Univ., 1406 West Green St., Urbana, Ill. 61801 CSCL 04A

Schoeberl et al. (1983) suggested that convective wavebreaking of monochromatic gravity waves might be suppressed by radiative transfer processes if the vertical wavelength waves were sufficiently short. As the vertical wavelength or the gravity wave decreases, radiative transfer between adjacent vertical layers becomes increasingly important. This exchange can increase the radiative relaxation time scale so that the wave will no longer grow with altitude. Thus, very short vertical wavelength waves may dissipate radiatively rather than become convectively unstable. Apruzese and Strobel (1984) have revised the exchange coefficients used in Schoeberl et al. (1983). Also, Chao and Schoeberl (1984) pointed out that the computation made by LINDZEN (1981) of the convective diffusion rate may be a factor of two too low as the convective adjustment processes tends to minimize the thermal

transport by the wave. The purpose here is to revise the values given in Schoeberl et al. (1983). These results also suggest that the very thin turbulent layers observed by mesosphere-stratosphere-troposphere (MST) radars (e.g., WOODMAN, 1980) cannot be produced by the convective instability of monochromatic gravity waves with large horizontal scales. R.J.F.

N85-32473*# Illinois Univ., Urbana. Dept. of Atmospheric Sciences.
A NUMERICAL ANALYSIS OF TRANSIENT PLANETARY WAVES AND THE VERTICAL STRUCTURE IN A MESO-STRATO-TROPOSPHERE MODEL, PART 1.4A
Ke-Su Zhang and T. Sasamori *In* International Council of Scientific Unions Middle Atmosphere Program: Handbook for MAP. Vol. 14 Dec. 1984 p 27-35 refs (For primary document see N85-32466 21-46)
Avail: NTIS HC A17/MF A01; also avail. from SCOSTEP Secretariat, Illinos Univ., 1406 West Green St., Urbana, Ill. 61801 CSCL 04B

The structure of unstable planetary waves is computed by a quasi-geostrophic model extending from the surface up to 80 km by means of eigenvalue-eigenfunction techniques in spherical coordinates. Three kinds of unstable modes of distinct phase speeds and vertical structures are identified in the winter climate state: (1) the deep Green mode with its maximum amplitude in the stratosphere; (2) the deep Charney mode with its maximum amplitude in the troposphere: and (3) the shallow Charney mode which is largely confined to the troposphere. Both the Green mode and the deep Charney mode are characterized by very slow phase speeds. They are mainly supported by upward wave energy fluxes, but the local baroclinic energy conversion within the stratosphere also contributes in supporting these deep modes. The mesosphere and the troposphere are dynamically independent in the summer season decoupled by the deep stratospheric easterly. The summer mesosphere supports the easterly unstable waves 1-4. Waves 3 and 4 are identified with the observed mesospheric 2-day wave and 1.7-day wave, respectively. Author

N85-32474*# National Aeronautics and Space Administration. Goddard Space Flight Center, Greenbelt, Md.
GENERAL CIRCULATION OF THE MIDDLE ATMOSPHERE, PART 1.4B
M. R. Schoeberl *In* Intern. Council of Sci. Unions Middle Atmosphere Program: Handbook for Map. Vol. 14: URSI/SCOSTEP Workshop Dec. 1984 p 36-37 refs (For primary document see N85-32466 21-46)
Avail: NTIS HC A17/MF A01; also avail. from SCOSTEP Secretariat, Illinois Univ., 1406 West Green St., Urbana, Ill. 61801 CSCL 04A

In both the tropical and extratropical regions there are a large number of dynamical problems which can be addressed by mesosphere-stratosphere-troposphere (MST) radars. The distinct advantage the MST radar has over rocket observations is continuous data acquisition. Without a doubt, the time-space spectrum of the mesospheric flow field is rich in high frequency motions associated with gravity waves rather than turbulent (random) fluctuations, and these events are particularly amenable to analysis with continuous data sets. In addition to the high frequency motions these are longer period fluctuations in the upper stratosphere and mesosphere wind fields which, combined with temperature fields derived from satellite data or lidars, can greatly enhance our knowledge of the upper atmosphere. R.J.F.

N85-32475*# National Oceanic and Atmospheric Administration, Boulder, Colo.
PERFORMANCE OF THE COLORADO WIND-PROFILING NETWORK, PART 1.5A c47
R. G. Strauch, K. B. Earnshaw, D. A. Merritt, K. P. Moran, and D. W. vandeKamp *In* Intern. Council of Sci. Unions Middle Atmosphere Program: Handbook for Map. Vol. 14: URSI/SCOSTEP Workshop Dec. 1984 p 38-48 refs (For primary document see N85-32466 21-46)
Avail: NTIS HC A17/MF A01; also avail. from SCOSTEP Secretariat, Illinois Univ., 1406 West Green St., Urbana, Ill. 61801 CSCL 04B

The Wave Propagation Laboratory (WPL) has operated a network of radar wind Profilers in Colorado for about 1 year. The network consists of four VHF (50-MHz) radars and a UHF (915-MHz) radar. The Platteville VHF radar was developed by the Aeronomy Laboratory (AL) and has been operated jointly by WPL and AL for several years. The other radars were installed between February and May 1983. Experiences with these radars and some general aspects of tropospheric wind measurements with Doppler radar are discussed. R.J.F.

N85-32476*# EISCAT Scientific Association, Kiruna (Sweden).
VERTICAL TRANSPORT IN THE ATMOSPHERE: MEASUREMENT CAPABILITIES AND REQUIREMENTS OF VHF RADARS, PART 1.6A c47
J. Rottger *In* International Council of Scientific Union Middle Atmosphere Program: Handbook for MAP. Vol. 14 Dec. 1984 p 49-57 refs (For primary document see N85-32466 21-46)
Avail: NTIS HC A17/MF A01; also avail. from SCOSTEP Secretariat, Illinois Univ., 1406 West Green St., Urbana, Ill. 61801 CSCL 04B

Mass exchange, mixing on transport in the atmosphere involves reversible processes, i.e., any kind of organized motions such as wave and large scale flows, and nonreversible processes, i.e., molecular and turbulent diffusion. Without evaluating in detail the relative efficiency of these processes, an attempt is made to summarize those phenomena which can be qualitatively (and eventually also quantitatively) observed with VHF radars. Only mixing in the vertical direction is considered, since this appears to be the essential part of transport processes to which VHF radars can contribute better understanding. Mixing processes in the troposphere are discussed. Possible contributions of VHF radars to the study the mass exchange processes between the troposphere and stratosphere are studied. Transport in the middle atmosphere is briefly summarized, since it is in principle similar to transport in the lower atmosphere. R.J.F.

N85-32477*# National Oceanic and Atmospheric Administration, Boulder, Colo. Aeronomy Lab.
COMPARISON OF TROPOPAUSE ALTITUDE DETERMINATION BY THE PLATTEVILLE RADAR, SUNSET RADAR AND THE NWS RAWINSONDE c47
J. L. Green and K. S. Gage *In* International Council of Scientific Unions Middle Atmosphere Program: Handbook for MAP. Vol. 14 Dec. 1984 p 58-61 refs (For primary document see N85-32466 21-46)
Avail: NTIS HC A17/MF A01; also avail. from SCOSTEP Secretariat, Illinois Univ., 1406 West Green St., Urbana, Ill. 61801 CSCL 04B

During the month of March, 1981 the Sunset and Platteville Radar and Platteville Radar were operated primarily with vertical antenna beams. These radars are both VHF ST (Stratosphere-Troposphere) radars. The separation between them was 63 km, the Sunset site located in the foothills of the Rocky Mountains and the Platteville site was in the plains, just east of the mountains. Both radars were operated continuously for about three weeks with a time resolution of a few minutes. Both made measurements in the 4 to 20 km altitude interval with an altitude sampling of 1.2 km. The purpose is to compare the estimation of the altitude of the tropopause by these two radars with the altitude of the tropopause derived from standard NWS rawinsondes. R.J.F.

N85-32478*# Control Data Corp., Minneapolis, Minn.
SYNOPTIC-SCALE DYNAMICS WITH VERTICAL VELOCITY, PART 1.8A c47
G. D. Nastrom *In* International Council of Scientific Unions Middle Atmosphere Program: Handbook for MAP. Vol. 14 Dec. 1984 p 62-68 refs (For primary document see N85-32466 21-46)
Avail: NTIS HC A17/MF A01; also avail. from SCOSTEP Secretariat, Illinois Univ., 1406 West Green St., Urbana, Ill. 61801 CSCL 04B

Radar measurements of all three of the atmospheric velocity

components by the MST technique data from all the pioneering work of Woodman and Geillen (1974). The radar horizontal velocities have been compared with other standard measurements, such as radiosonde winds, in a number of studies and are now finding widespread acceptance within the meteorological community for research and operational forecasting purposes. Perhaps the single most interesting report recently is that the mesosphere-stratosphere-troposphere (MST) profiler winds are turning out to be one of the most useful pieces of data for predicting upslope snowfall in the cold season forecasting study of the PROFS Program (Reynolds, 1983). By contrast, the vertical velocities measured by MST radars have received relatively little attention, despite the facts that direct continuous measurement of vertical velocity is unique (i.e., it cannot be done with radiosondes) and that the vertical velocity is intimately linked with the dynamics of the atmosphere. Indeed, for many forecasting applications the vertical velocity is the single most important variable, yet it is usually inferred indirectly from other dynamical variables. The stratosphere-troposphere (ST) radars now available have the potential to change this situation. Some of the results from vertical velocity measurements which have direct application in synoptic scale dynamics. R.J.F.

N85-32479# Colorado Univ., Boulder.
PRACTICAL USE OF A TROPOPAUSE HEIGHT DETERMINATION ALGORITHM ON AN MST RADAR DATA SET, PART 1.8B **c47**
A. C. Riddle, K. S. Gage (NOAA, Boulder, Colo.), and B. B. Balsley (NOAA, Boulder, Colo.) *In* International Council of Scientific Unions Middle Atmosphere Program: Handbook for MAP. Vol. 14 Dec. 1984 p 69-73 refs (For primary document see N85-32466 21-46)
Avail: NTIS HC A17/MF A01; also avail. from SCOSTEP Secretariat, Illinois Univ., 1406 West Green St., Urbana, Ill. 61804 CSCL 04B

The possibility of detecting tropopause height from vertical incidence clear air radar returns was demonstrated by Gage and Green (1979). Following theoretical analysis by Gage et al. (1981) an objective method for tropopause height determination was presented by Gage and Green (1982). That method was adapted for use as a computer algorithm by Riddle et al. (1983). Further progress on an improved algorithm is reported. It is shown that this improved algorithm substantially reduces the number of misidentified tropopauses, while at the same time it increases the number of correctly identified tropopauses. Some of the problems of the algorithm are identified and suggestions are made for further improvement. R.J.F.

N85-32480*# Illinois Univ., Urbana. Dept. of Electrical and Computer Engineering.
SOME RECENT DEVELOPMENTS IN THE INTERPRETATION OF MST RADAR RETURNS FROM CLEAR AIR (KEYNOTE PAPER), PART 2
C. H. Liu *In* International Council of Scientific Unions Middle Atmosphere Program: Handbook for MAP. Vol. 14 Dec. 1984 p 74-79 refs (For primary document see N85-32466 21-46)
Avail: NTIS HC A17/MF A01; also avail. from SCOSTEP Secretariat, Illinois Univ., 1406 West Green St., Urbana, Ill. 61801 CSCL 04A

Mesosphere-stratosphere-troposphere (MST) radar returns from clear air come about through the interaction of electromagnetic waves with the inhomogeneous structures of refractive index in the atmosphere. In order to interpret the data correctly to obtain information concerning the dynamics of the atmosphere, one must first know how the various refractive index structures can affect the propagation and scattering of the radio waves. This can be achieved through theoretical and model studies. On the other hand, in order to carry out realistic theoretical studies, realistic models of the inhomogeneous structures of the atmospheric refractive index are needed. These are available only through observational data. Therefore the close interplays between theoretical and observational investigations are essential in making progress in this area. Some results on certain aspects of the problem are presented with emphasis on those aspects that may lead to new developments. R.J.F.

N85-32481*# Illinois Univ., Urbana. Dept. of Electrical and Computer Engineering.
MORPHOLOGY OF THE SCATTERING TARGETS: FRESNEL AND TURBULENT MECHANISMS, PART 2.1A
O. Royrvik *In* International Council of Scientific Unions Middle Atmosphere Program: Handbook for MAP. Vol. 14 Dec. 1984 p 80-83 (For primary document see N85-32466 21-46)
Avail: NTIS HC A17/MF A01; also avail. from SCOSTEP Secretariat, Illinois Univ., 1406 West Green St., Urbana, Ill. 61801 CSCL 04A

Refractive index fluctuations cause coherent scattering and reflection of VHF radio waves from the clear air in the altitude region between 0 and approximately 90 km. Similar echoes from the stratosphere/troposphere and the mesosphere are observed at UHF and MF/HF frequencies, respectively. The nature of the refractive index fluctuations has been studied for many years without producing a clear consensus on what mechanism causes them. It is believed that the irregularities can originate from two different mechanisms: turbulent mixing of the gradient of refractive index, and stable horizontally stratified laminae of sharp gradients in the refractive index. In order to explain observations of volume dependence and aspect sensitivity of the echo power in the MST region, a diversity of submechanisms has been proposed. They include isotropic and anisotropic turbulent scattering, Fresnel scattering and reflection, and diffuse reflection. Isotropic turbulent scattering is believed to cause a majority of the clear air echoes observed by MST radars. The mechanism requires active turbulence mixing of a preexisting gradient in the refractive index profile. R.J.F.

N85-32482*# EISCAT Scientific Association, Kiruna (Sweden).
SIGNAL STATISTICS OF THE RADAR ECHOES: ANGLE-OF-ARRIVAL STATISTICS, PART 2.2A
J. Rottger *In* International Council of Scientific Unions Middle Atmosphere Program: Handbook for MAP. Vol. 14 Dec. 1984 p 84-87 refs (For primary document see N85-32466 21-46)
Avail: NTIS HC A17/MF A01; also avail. from SCOSTEP Secretariat, Illinois Univ., 1406 West Green St., Urbana, Ill. 61801 CSCL 04A

The Doppler spectra, measured with a vertical antenna beam, are characterized by essentially two different kinds of distributions, one has a very narrow and the other a broad spectral width. The former is accepted as due to reflection whereas the latter is due to scattering. It can happen that both kinds of spectra are observed simultaneously. Superimposed on a fairly broad Gaussian signal spectrum, very narrow signal spikes are evident. Because some spikes occur at different Doppler frequencies, the subreflections have to be assumed to move with different radial velocities. To experimentally verify this reasonable assumption, it is proposed to measure the angle of arrival of the different signal returns. One can here make use of the essential advantage that the spikes can be filtered in frequency (called Doppler sortening or sharpening). By means of the cross spectrum analysis with the interferometer technique (measuring phase differences between spaced antennas), their angle of arrival can be measured. This will allow determination of the distribution of the angles of arrival. R.J.F.

N85-32483*# National Oceanic and Atmospheric Administration, Boulder, Colo. Aeronomy Lab.
A MODIFIED FRESNEL SCATTERING MODEL FOR THE PARAMETERIZATION OF FRESNEL RETURNS, PART 2.3A
K. S. Gage, W. L. Ecklund, and B. B. Balsley *In* International Council of Scientific Unions Middle Atmosphere Program: Handbook for MAP. Vol. 14 Dec. 1984 p 88-97 refs (For primary document see N85-32466 21-46)
Avail: NTIS HC A17/MF A01; also avail. from SCOSTEP Secretariat, Illinois Univ., 1406 West Green St., Urbana, Ill. 61801 CSCL 04A

A modified Fresnel scatter model is presented and the revised model is compared with observations from the Poker Flat, Alaska,

radar, the SOUSY radar and the Jimcamarca radar. The modifications to the original model have been made to better account for the pulse width dependence and height dependence of backscattered power observed at vertical incidence at lower VHF. Vertical profiles of backscattered power calculated using the revised model and routine radiosonde data show good agreement with observed backscattered power profiles. Relative comparisons of backscattered power using climatological data for the model agree fairly well with observed backscattered power profiles from Poker Flat, Jicamarca, and SOUSY. Author

N85-32484*# Illinois Univ., Urbana. Aeronomy Lab.
OBSERVATIONS OF MESOSPHERIC TURBULENCE BY ROCKET PROBE AND VHF RADAR, PART 2.4A
O. Royrvik and L. G. Smith *In* International Council of Scientific Unions Middle Atmosphere Program: Handbook for MAP. Vol. 14 Dec. 1984 p 98-105 refs (For primary document see N85-32466 21-46)
Avail: NTIS HC A17/MF A01; also avail. from SCOSTEP Secretariat, Illinois Univ., 1406 West Green St., Urbana, Ill. 61801 CSCL 04A

Data from the Jicamarca VHF radar and from a Languir probe fine-structure on a Nike Orion rocket launched from Punto Lobos, Peru, have been compared. A single mesospheric scattering layer was observed by the radar. The Langmuir probe detected irregularities in the electron-density profile in a narrow region between 85.2 and 86.6 km. It appears from a comparison between these two data sets that turbulence in the neutral atmosphere is the mechanism generating the refractive index irregularities.Author

N85-32485*# Illinois Univ., Urbana. Aeronomy Lab.
INTERPRETATION OF RADAR RETURNS FROM THE MESOSPHERE, PART 2.3A
O. Royrvik *In* International Council of Scientific Unions Middle Atmosphere Program: Handbook for MAP. Vol. 14 Dec. 1984 p 106-113 refs (For primary document see N85-32466 21-46)
Avail: NTIS HC A17/MF A01; also avail. from SCOSTEP Secretariat, Illinois Univ., 1406 West Green St., Urbana, Ill. 61801 CSCL 04A

The study of VHF radar signals from the mesosphere has shown that neutral atmosphere turbulence plays a central role in generating the refractive index irregularities that backscatter the radio waves. It follows that an increase in the turbulent energy dissipation rate will result in a decrease in signal correlation time and an increase in scattered signal power. Thus, in turbulence-generated radar echoes a negative correlation between echo power and signal correlation time (P/C) is expected. P/C also changes as a function of altitude, i.e., it is negative in the upper mesosphere but largely positive in the lower, with the latter thought to be a manifestation of partial reflection from stratified layers of refractive index gradient. Partial reflection would also explain the vertical aspect sensitivity of the scattered signal in the lower mesosphere. F.M.R.

N85-32486*# Illinois Univ., Urbana. Aeronomy Lab.
RADAR ECHOES AT 2.66 AND 40.92 MHz FROM THE MESOSPHERE, PART 2.6A
O. Royrvik *In* International Council of Scientific Unions Middle Atmosphere Program: Handbook for MAP. Vol. 14 Dec. 1984 p 114-120 refs (For primary document see N85-32466 21-46)
Avail: NTIS HC A17/MF A01; also avail. from SCOSTEP Secretariat, Illinois Univ., 1406 West Green St., Urbana, Ill. 61801 CSCL 04A

During recent decades, the ionospheric D region has been scanned extensively by radar in the frequency range from 1 to 60 MHz. Progress has been made in understanding the reflection/scattering of radio waves in that area. Rocket measurement of ion density irregularities were compared to radar echo observations at 2.75 MHz with the conclusion that the received radar signal was due to scattering from isotropic and homogeneous turbulence in the altitude region between 70 and 95 km. However, scattering cross sections at 2 and 6 mHz suggest that the radar echo from the region below 80 km is in part due to partial reflection from stratified layers. The VHF scattering cross section is aspect sensitive in the D region below about 75 km and tends to be isotropic at higher altitudes. Positive correlations between scattered signal power and signal correlation time (P/C) have been observed by VHF radars in the lower mesosphere, with the conclusion that it might be an additional indication of partial reflection from stratified layers. In the upper mesosphere where the P/C correlation is negative, it is generally believed that the scattering is caused by isotropic turbulence. Radar echoes at the 2.16 and 40.92 MHz ranges are compared, assuming that both result from turbulent scatter. Adjusting the radar Bragg wavelength, it was found that both sets are due to scattering from the same layer of turbulence-generated irregularities. F.M.R.

N85-32487*# Case Western Reserve Univ., Cleveland, Ohio. Dept. of Electrical Engineering and Applied Physics.
USEFULNESS OF MULTIFREQUENCY MST RADAR MEASUREMENTS, PART 2.6B
P. K. Rastogi and J. D. Mathews *In* International Council of Scientific Unions Middle Atmosphere Program: Handbook for MAP. Vol. 14 Dec. 1984 p 121-125 refs (For primary document see N85-32466 21-46)
Avail: NTIS HC A17/MF A01; also avail. from SCOSTEP Secretariat, Illinois Univ., 1406 West Green St., Urbana, Ill. 61801 CSCL 04A

Scattering of radio waves from atmospheric refractive-index irregularities induced by turbulence was invoked almost four decades ago to explain the characteristics of signals received on VHF/UHF ionospheric and tropospheric forward-scatter links. Due to the bistatic geometry of these links a slender, horizontally extended, common volume or cell is formed in space. The principal contribution to scattering arises from refractive-index fluctuations in this volume at the Bragg wave number K approx. sub B = K approx. sub i -k approx. sub s vectors. It has been surmised that the use of more than one frequency in probing the middle-atmosphere regions should help resolve several issues pertaining to the scattering mechanism. These issues are briefly re-examined in this note. The implications of the radar equation are discussed. The problems arising due to layered structure of turbulence and the choice of frequencies most suitable for multifrequency measurements are considered. B.W.

N85-32488*# Adelaide Univ. (Australia). Dept. of Physics.
RELATIONSHIP OF SPACED ANTENNA AND DOPPLER TECHNIQUES FOR VELOCITY MEASUREMENTS (KEYNOTE PAPER), PART 3
R. A. Vincent *In* International Council of Scientific Unions Middle Atmosphere Program: Handbook for MAP. Vol. 14 Dec. 1984 p 126-130 refs (For primary document see N85-32466 21-46)
Avail: NTIS HC A17/MF A01; also avail. from SCOSTEP Secretariat, Illinois Univ., 1406 West Green St., Urbana, Ill. 61804 CSCL 04A

The Doppler, spaced-antenna and interferometric methods of measuring wind velocities all use the same basic information, the Doppler shifts imposed on backscattered radio waves, but they process it in different ways. The Doppler technique is most commonly used at VHF since the narrow radar beams are readily available. However, the spaced antenna (SA) method has been successfully used with the SOUSY and Adelaide radars. At MF/HF the spaced antenna method is widely used since the large antenna arrays (diameter $>$ 1 km) required to generate narrow beams are expensive to construct. Where such arrays of this size are available then the Doppler method has been successfully used (e.g., Adelaide and Brisbane). In principle, the factors which influence the choice of beam pointing angle, the optimum antenna spacing will be the same whether operation is at MF or VHF. Many of the parameters which govern the efficient use of wind measuring systems have been discussed at previous MST workshops. Some of the points raised by these workshops are summarized. Author

N85-32489*# Saskatchewan Univ., Saskatoon. Inst. of Space and Atmospheric Studies.
A SIMPLE MODEL FOR TESTING THE EFFECTS OF GRAVITY-

WAVE-PRODUCED VERTICAL OSCILLATIONS OF SCATTERING IRREGULARITIES ON SPACED-ANTENNA, HORIZONTAL DRIFT MEASUREMENTS

C. E. Meek and I. M. Reid *In* International Council of Scientific Unions Middle Atmosphere Program: Handbook for MAP. Vol. 14 Dec. 1984 p 131-133 (For primary document see N85-32466 21-46)

Avail: NTIS HC A17/MF A01; also avail. from SCOSTEP Secretariat, Illinois Univ., 1406 West Green St., Urbana, Ill. 61801 CSCL 04A

It has been suggested that the velocities produced by the spaced antenna partial-reflection drift experiment may constitute a measure of the vertical oscillations due to short-period gravity waves rather than the mean horizontal flow. The contention is that the interference between say two scatterers, one of which is traveling upward, and the other down, will create a pattern which sweeps across the ground in the direction (or anti-parallel) of the wave propagation. Since the expected result, viz., spurious drift directions, is seldom, if ever, seen in spaced antenna drift velocities, this speculation is tested in an atmospheric model. B.W.

N85-32490*# EISCAT Scientific Association, Kiruna (Sweden).
POTENTIAL ADVANTAGES OF THE SPACED ANTENNA METHOD FOR OPERATIONAL WIND PROFILING, PART 3.1B

J. Rottger and M. F. Larsen (Cornell Univ.) *In* International Council of Scientific Unions Middle Atmosphere Program: Handbook for MAP. Vol. 14 Dec. 1984 p 134-138 refs (For primary document see N85-32466 21-46)

Avail: NTIS HC A17/MF A01; also avail. from SCOSTEP Secretariat, Illinois Univ., 1406 West Green St., Urbana, Ill. 61801 CSCL 04A

The problem of very short-range forecasting is twofold. It is necessary to understand the processes that are being forecasted, and data appropriate to the scale of interest has to be generated. Coherent VHF and UHF radars are being used for operational wind profiling and are providing part of the solution to the data-acquisition problem. The Profiler system operated by the Wave Propagation Laboratory at NOAA has already shown great promise. As a result, plans are being considred for expanding the network of radars to cover a larger area of the country. The Profiler uses what is commonly referred to as the Doppler method for measuring winds. Two beams are pointed off-vertical, and the Doppler shift of the echo determines the line-of-sight velocity. The velocity components along the beams are then translated to horizontal wind components. A number of possible advantages of the spaced antennas (SA) method for operational wind profiling are discussed. B.W.

N85-32491*# Saskatchewan Univ., Saskatoon. Inst. of Space and Atmospheric Studies.
CRITERIA FOR OPTIMUM SPACING OF SPACED ANTENNA, PART 3.2A

C. E. Meek *In* International Council of Scientific Unions Middle Atmosphere Program: Handbook for MAP. Vol. 14 Dec. 1984 p 139-143 (For primary document see N85-32466 21-46)

Avail: NTIS HC A17/MF A01; also avail. from SCOSTEP Secretariat, Illinois Univ., 1406 West Green St., Urbana, Ill. 61801 CSCL 04A

There are many factors affecting the spaced antenna drift results, only one of which is antenna spacing. Generally, good results are obtained at MF for receiver antenna spacings of 1-1.5 lambda, and at VHF (e.g., SOUSY) for spacings approx. 6 lambda. Since one of the factors, local atmospheric/ionospheric conditions, are difficult to predict, this paper will be restricted to a short discussion of relevant factors, and methods for comparing various antenna/analysis configurations. B.W.

N85-32492*# Stanford Univ., Calif. STARLAB.
ANISOTROPY OF THE PERMITTIVITY FIELD INFERRED FROM ASPECT-SENSITIVE RADAR ECHOES

A. T. Waterman *In* International Council of Scientific Unions Middle Atmosphere Program: Handbook for MAP. Vol. 14 Dec. 1984 p 144-147 refs (For primary document see N85-32466 21-46)

Avail: NTIS HC A17/MF A01; also avail. from SCOSTEP Secretariat, Illinois Univ., 1406 West Green St., Urbana, Ill. 61801 CSCL 04A

An attempt is made to draw some quantitative conclusions regarding the anisotropy of the clear-air back-scattering mechanism based on the measured variation of echo power with zenith angle. The measurements were made by the SOUSY group of the Max Planck Institute for Aeronomy at Lindau, FRG. They installed their 47-MHz transmitter and antenna feed in the 300-meter diameter reflector at Arecibo. The resulting 1.7-degree beam was stepped successively through seven 1.7-degree intervals from 1.7 to 11.7 degrees in zenith angle, obtaining about four minutes of data at each setting. This procedure was carried out in an eastward pointing azimuth and in a northward pointing azimuth, the entire set of measurements consuming an hour and twenty minutes. Range resolution was 150 meters. B.W.

N85-32493*# EISCAT Scientific Association, Kiruna (Sweden).
ACCURACY OF VELOCITY AND POWER DETERMINATION BY THE DOPPLER METHOD

J. Rottger *In* International Council of Scientific Unions Middle Atmosphere Program: Handbook for MAP. Vol. 14 Dec. 1984 p 148-149 refs (For primary document see N85-32466 21-46)

Avail: NTIS HC A17/MF A01; also avail. from SCOSTEP Secretariat, Illinois Univ., 1406 West Green St., Urbana, Ill. 61801

When designing a Mesosphere-Stratosphere-Troposphere (MST) radar antenna one has to trade between the choices to optimize the effective aperture or to optimize the sidelobe suppression. An optimization of the aperture increases the sensitivity. Suppression of side-lobes by tapering attenuates undesirable signals which spoil the estimates of reflectivity and velocity. Generally, any sidelobe effects are equivalent to a broadening of the antenna beam. The return signal is due to a product of the antenna pattern with the varying atmospheric reflectivity structures. Thus, knowing the antenna pattern, it is in principle possible to find the signal spectra, which, however, may be a tedious computational and ambiguous procedure. For vertically pointing main beams the sidelobe effects are efficiently suppressed because of the aspect sensitivity. It follows that sidelobes are a minor problem for spaced antenna methods. However, they can be crucial for Doppler methods, which need off-vertical beams. If a sidelobe is pointing towards the zenith a larger power may be received from the vertical than off-vertical directions, but quantitative estimates of this effect are not yet known. To get an error estimate of sidelobe effects with an off-vertical main beam a 1-dimensional example is considered. B.W.

N85-32494*# EISCAT Scientific Association, Kiruna (Sweden).
IMPROVEMENT OF VERTICAL VELOCITY MEASUREMENTS, PART 3.4B

J. Rottger *In* International Council of Scientific Unions Middle Atmosphere Program: Handbook for MAP. Vol. 14 Dec. 1984 p 150-155 refs (For primary document see N85-32466 21-46)

Avail: NTIS HC A17/MF A01; also avail. from SCOSTEP Secretariat, Illinois Univ., 1406 West Green St., Urbana, Ill. 61801 CSCL 04A

Vertical velocities are assumed to be measurable with vertically pointing antenna beams. An exact horizontal levelling and good phase calibration of the radar antenna system can yield real main-beam directions which do not significantly differ from calculated patterns. It is, thus, anticipated that antenna beams can be pointed exactly vertically. Because of area size and near-field limitations, VHF radar antennas have typically beam widths of more than several degrees. It is known that most of the reflectivity structures detected by vertically beaming VHF radars in the troposphere, stratosphere and lower mesosphere are aspect-sensitive. It cannot a priori be assumed that these structures are exactly horizontal. A few examples are investigated to support this statement. B.W.

N85-32495*# Alaska Univ., Fairbanks. Geophysical Inst.
ANTENNA INDUCED RANGE SMEARING IN MST RADARS

B. J. Watkins and P. E. Johnston *In* International Council of

Scientific Unions Middle Atmosphere Program: Handbook for MAP. Vol. 14 Dec. 1984 p 156-160 refs (For primary document see N85-32466 21-46)
Avail: NTIS HC A17/MF A01; also avail. from SCOSTEP Secretariat, Illinois Univ., 1406 West Green St., Urbana, Ill. 61801 CSCL 04A

There is considerable interest in developing stratosphere troposphere (ST) and mesosphere stratosphere troposphere (MST) radars for higher resolution to study small-scale turbulent structures and waves. At present most ST and MST radars have resolutions of 150 meters or larger, and are not able to distinguish the thin (40 - 100 m) turbulent layers that are known to occur in the troposphere and stratosphere, and possibly in the mesosphere. However the antenna beam width and sidelobe level become important considerations for radars with superior height resolution. The objective of this paper is to point out that for radars with range resolutions of about 150 meters or less, there may be significant range smearing of the signals from mesospheric altitudes due to the finite beam width of the radar antenna. At both stratospheric and mesospheric heights the antenna sidelobe level for lear equally spaced phased arrays may also produce range aliased signals. To illustrate this effect the range smearing functions for two vertically directed antennas have been calculated, (1) an array of 32 coaxial-collinear strings each with 48 elements that simulates the vertical beam of the Poker Flat, Glaska, MST radar; and (2) a similar, but smaller, array of 16 coaxial-collinear strings each with 24 elements. B.W.

N85-32496*# Illinois Univ., Urbana. Aeronomy Lab.
EFFECTS OF LINE-OF-SIGHT VELOCITY ON SPACED-ANTENNA MEASUREMENTS, PART 3.5A
O. Royrvik *In* International Council of Scientific Unions Middle Atmosphere Program: Handbook for MAP. Vol. 14 Dec. 1984 p 161-163 refs (For primary document see N85-32466 21-46)
Avail: NTIS HC A17/MF A01; also avail. from SCOSTEP Secretariat, Illinois Univ., 1406 West Green St., Urbana, Ill. 61801 CSCL 04A

Horizontal wind velocities in the upper atmosphere, particularly the mesosphere, have been measured using a multitude of different techniques. Most techniques are based on stated or unstated assumptions about the wind field that may or may not be true. Some problems with the spaced antenna drifts (SAD) technique that usually appear to be overlooked are investigated. These problems are not unique to the SAD technique; very similar considerations apply to measurement of horizontal wind using multiple-beam Doppler radars as well. Simply stated, the SAD technique relies on scattering from multiple scatterers within an antenna beam of fairly large beam width. The combination of signals with random phase gives rise to an interference pattern on the ground. This pattern will drift across the ground with a velocity twice that of the ionospheric irregularities from which the radar signals are scattered. By using spaced receivers and measuring time delays of the signal fading in different antennas, it is possible to estimate the horizontal drift velocities. B.W.

N85-32497*# EISCAT Scientific Association, Kiruna (Sweden).
INTERFEROMETER APPLICATIONS OF VHF RADARS, PART 3.6A
J. Rottger *In* International Council of Scientific Unions Middle Atmosphere Program: Handbook for MAP. Vol. 14 Dec. 1984 p 164-173 refs Presented at the Am. Meteorol. Soc. 22nd Conf. on Radar Meteorol., Zurich, 1984 Submitted for publication (For primary document see N85-32466 21-46)
Avail: NTIS HC A17/MF A01; also avail. from SCOSTEP Secretariat, Illinois Univ., 1406 West Green St., Urbana, Ill. 61801 CSCL 04B

Using a spaced antenna setup of a VHF radar, the spatial distribution of amplitudes and phases of the radar echoes from the troposphere, stratosphere and mesosphere can be measured. Combining in a suitable analysis procedure the complex digital samples from the different receiving antennas is consistent with the radar interferometer method. In addition to the well-known parameters measured with the commonly applied Doppler and drifts methods, i.e., reflectivity and mean fluctuation velocity, the interferometer technique allows to measure the regular spectrum of the returns. This technique, which was first applied with the spaced antenna system of the SOUSY-VHF-Radar in W. Germany, as well as some first examples of results are described here. These comprise the measurements of the horizontal and vertical velocities of the mean flow as well as of turbulence structures, the aspect sensitivity and the tilt of layers from which the baroclinicity can be estimated. Particularly, results of interferometer measurements of the vertical and horizontal phase velocities and wavelengths of gravity waves in the stratosphere are displayed. The latter results are also discussed in terms of the generation and propagation of these waves. B.W.

N85-32498*# Arecibo Ionospheric Observatory, Puerto Rico.
MESOSPHERIC MEASUREMENTS OF IRREGULARITY PATCHES USING A 3-ANTENNA INTERFEROMETER, PART 3.6B
H. M. Ierkic and J. Rottger (EISCAT Scientific Association) *In* International Council of Scientific Unions Middle Atmosphere Program: Handbook for MAP. Vol. 14 Dec. 1984 p 174-178 refs (For primary document see N85-32466 21-46)
Avail: NTIS HC A17/MF A01; also avail. from SCOSTEP Secretariat, Illinois Univ., 1406 West Green St., Urbana, Ill. 61801 CSCL 04A

Three events of mesospheric radar returns have been isolated to illustrate the potential of a three-antenna interferometer in the study of the neutral atmosphere. Contour plots of echo intensity and the presence of irregularities in isolated and well-defined regions are shown. These measurements were carried out using the SOUSY radar in the Harz mountains in Germany, on September 9, 1980. The system frequency is 53.5 MHz. Local time is 2 hours in advance of Universal time. The irregularities wavelength is 2.81 m and the three arms of the interferometer were sampled with 167 ms of time difference. To provide precise estimates of vertical velocities, the measured (radial) Doppler shift has to be corrected to subtract the contribution due to the horizontal motions. For near-vertical observations (zenith angle less than about 10 deg) it is readily shown that the rate of change of the measured phases are related to the velocities V sub eq, V sub ns (in the East-West and North-South directions). B.W.

N85-32499*# National Aeronautics and Space Administration. Goddard Space Flight Center, Greenbelt, Md.
TECHNIQUES FOR THE STUDY OF GRAVITY WAVES AND TURBULENCE (KEYNOTE PAPER), PART 4
M. R. Schoeberl *In* International Council of Scientific Unions Middle Atmosphere Program: Handbook for MAP. Vol. 14 Dec. 1984 p 179-182 refs (For primary document see N85-32466 21-46)
Avail: NTIS HC A17/MF A01; also avail. from SCOSTEP Secretariat, Illinois Univ., 1406 West Green St., Urbana, Ill. 61801 CSCL 04A

Probably one of the most important achievements mesosphere stratosphere troposphere (MST) radars can make toward increasing the understanding of the dynamics of the atmosphere is to determine the exact relationship between the generation of turbulence and the sources of high shear or convectively unstable flows. An important theoretical tool, the gravity-wave breaking through which one can begin to understand spontaneous generation of turbulence model is discussed. In this model, large amplitude gravity waves produce local regions where the Richardson number (N sup 2/[U sub Z] sup 2) is less than 1/4 thus giving rise to turbulent flows. Thus the appearance of turbulent layers can often be interpreted as a breaking-gravity-wave signature. Even though the techniques for studying gravity waves and turbulence may be quite different (and historically have resulted in somewhat separate bodies of literature), it is clear from the wave-breaking model that the phenomena are intimately linked. The techniques for measurements of gravity wave flow fields and turbulent regions by MST radar should show cognizance of some of the theoretical questions raised by the wave-breaking model. B.W.

N85-32500*# Case Western Reserve Univ., Cleveland, Ohio. Dept. of Electrical Engineering and Applied Physics.

DETERMINATION OF BILLOWS AND OTHER TURBULENT STRUCTURES, PART 4.1A **c47**

P. K. Rastogi *In* International Council of Scientific Unions Middle Atmosphere Program: Handbook for MAP. Vol. 14 Dec. 1984 p 183-185 refs (For primary document see N85-32466 21-46)

Avail: NTIS HC A17/MF A01; also avail. from SCOSTEP Secretariat, Illinois Univ., 1406 West Green St., Urbana, Ill. 61801 CSCL 04B

Billows are regular, wave-like arrays of cross-flow vortices that develop in stratified oceanic or atmospheric flows with large shear. Atmospheric billows can become manifest through condensation. Billows are frequently seen in their characteristic cloud forms in the lower atmosphere. Under suitable viewing conditions, billows can also be seen in noctilucent clouds that form near the polar mesosphere during the summer months. Other turbulent structures -- related to billows -- are the Kelvin-Helmholtz instability (KHI) and cat's eye structures that occur in fully developed turbulent shear flows. Shear flows may contain perturbations at many different horizontal wavelengths and vertical scales. Realistic theoretical models have been constructed to study the stability and growth of these perturbations. The extent to which billows and Kelvin-Helmholtz instability have been observed in the atmosphere with the use of radars is outlined. Most of these observations are confined to the troposphere. Suggestions are made for improved radar experiments that are required to detect these structures at higher altitudes. B.W.

N85-32501*# National Oceanic and Atmospheric Administration, Boulder, Colo. Aeronomy Lab.

SPECTRAL MEASUREMENTS OF TURBULENCE AND GRAVITY WAVES, PART 4.2A

K. S. Gage *In* International Council of Scientific Unions Middle Atmosphere Program: Handbook for MAP. Vol. 14 Dec. 1984 p 186-188 refs (For primary document see N85-32466 21-46)

Avail: NTIS HC A17/MF A01; also avail. from SCOSTEP Secretariat, Illinois Univ., 1406 West Green St., Urbana, Ill. 61801 CSCL 04A

Recently, it has become widely recognized that gravity waves play an important role in determining the large-scale circulation of the middle atmosphere. This realization has come about, in large measure, from the realization that Rayleigh friction plays an important role in the dynamics of the middle atmosphere. Since Rayleigh friction is intimately related to the saturation of vertically propagating gravity waves, an understanding of the saturation process has become a focal point for theoretical studies. With the advent of MST radar studies of the middle atmosphere, it has become possible to determine the spectrum of horizontal atmospheric velocity fluctuations over the range of scales which comprise the gravity-wave spectrum. It has been suggested that these spectra are comprised of buoyancy waves. The controversial interpretation of these spectra is discussed. B.W.

N85-32502*# Illinois Univ., Urbana. Dept. of Electrical and Computer Engineering.

GRAVITY-WAVE SPECTRA IN THE ATMOSPHERE OBSERVED BY MST RADAR, PART 4.2B

A. O. Scheffler and C. H. Liu *In* International Council of Scientific Unions Middle Atmosphere Program: Handbook for MAP. Vol. 14 Dec. 1984 p 189-191 refs (For primary document see N85-32466 21-46)

Avail: NTIS HC A17/MF A01; also avail. from SCOSTEP Secretariat, Illinois Univ., 1406 West Green St., Urbana, Ill. 61801 CSCL 04A

A universal spectrum of atmospheric buoyancy waves is proposed based on data from radiosonde, Doppler navigation, not-wire anemometer and Jimsphere balloon. The possible existence of such a universal spectrum clearly will have significant impact on several areas in the study of the middle atmosphere dynamics such as the parameterization of sub-grid scale gravity waves in global circulation models; the transport of trace constituents and heat in the middle atmosphere, etc. Therefore, it is important to examine more global wind data with temporal and spatial resolutions suitable for the investigation of the wave spectra. Mesosphere-stratosphere-troposphere (MST) radar observations offer an excellent opportunity for such studies. It is important to realize that radar measures the line-of-sight velocity which, in general, contains the combination of the vertical and horizontal components of the wave-associated particle velocity. Starting from a general oblique radar observation configuration, applying the dispersion relation for the gravity waves, the spectrum for the observed fluctuations in the line-of-sight gravity-wave spectrum is investigated through a filter function. The consequence of the filter function on data analysis is discussed. B.W.

N85-32503*# Air Force Geophysics Lab., Hanscom AFB, Mass.

HIGH RESOLUTION EVIDENCE FOR THE GARRETT-MUNK SPECTRUM OF STRATOSPHERIC GRAVITY WAVES

E. M. Dewan, N. Grossbard, A. F. Quesada, and R. E. Good *In* International Council of Scientific Unions Middle Atmosphere Program: Handbook for MAP. Vol. 14 Dec. 1984 p 192-196 refs (For primary document see N85-32466 21-46)

Avail: NTIS HC A17/MF A01; also avail. from SCOSTEP Secretariat, Illinois Univ., 1406 West Green St., Urbana, Ill. 61801 CSCL 04A

Vertical profiles of scalar horizontal winds have been measured at high resolution (10 m) in the 13 to 37 km region of the stratosphere. This resolution (at that range of altitude) represents the state-of-the-art, and is unique. The technique used smoke trails laid by rockets in the stratosphere, and were taken by AFGL at Wallops Island, VA, White Sands Missile Range, NM, and Ft. Churchill, Canada, in the 1977-78 time period. Two or three cameras were used to give the time-lapse photographs. The goal was to ascertain whether or not the internal waves of the stratosphere behave consistently with the Garrett-Munk model which was originally created for oceanic internal waves. Five profiles of horizontal wind are presented. It is concluded: (1) stratospheric internal waves obey the Garrett-Munk model for vertical wave numbers; (2) there is not statistically significant evidence for a break in the curve at high wave numbers when due allowance is made for aliasing effects; and (3) the power density level of the spectra are almost equal on a log-log scale in spite of the difference in time, season, and geographical location. B.W.

N85-32504*# National Oceanic and Atmospheric Administration, Boulder, Colo. Aeronomy Lab.

ON THE SPECTRUM OF ATMOSPHERIC VELOCITY FLUCTUATIONS SEEN BY MST/ST RADAR AND THEIR INTERPRETATION **c47**

K. S. Gage and G. D. Nastrom (Control Data Corp., Minneapolis) *In* International Council of Scientific Unions Middle Atmosphere Program: Handbook for MAP. Vol. 14 Dec. 1984 p 197-207 refs (For primary document see N85-32466 21-46)

Avail: NTIS HC A17/MF A01; also avail. from SCOSTEP Secretariat, Illinois Univ., 1406 West Green St., Urbana, Ill. 61801 CSCL 04B

The observations of the spectrum of atmospheric motions over the range of periods from a few minutes to many hours are considered that have been made with stratosphere-troposphere/mesosphere-stratosphere (ST/MST) radars in the past five years. This range of periods includes the periods associated with buoyancy waves and the scale of atmospheric motions often referred to by meteorologists as the mesoscale. The spectra of horizontal and vertical velocities are considered. Their interpretation is examined in terms of buoyancy wave theory and turbulence theory. To help in interpreting these spectra some recently determined aircraft wave number spectra are presented. B.W.

N85-32505*# Cornell Univ., Ithaca, N.Y. School of Electrical Engineering.

USE OF THE VAD TECHNIQUE AND MEASUREMENTS OF MOMENTUM FLUX IN THE STRATOSPHERE AT AERCIBO, PART 4.3A

C. R. Cornish and M. F. Larsen *In* International Council of Scientific Unions Middle Atmosphere Program: Handbook for MAP. Vol. 14

Dec. 1984 p 208-210 refs (For primary document see N85-32466 21-46)
Avail: NTIS HC A17/MF A01; also avail. from SCOSTEP Secretariat, Illinois Univ., 1406 West Green St., Urbana, Ill. 61801 CSCL 04A

The Arecibo 430-MHz radar was used in the velocity-azimuth display (VAD) mode to obtain radial velocity measurements at 16 azimuth directions from which the three-dimensional wind field and momentum flux can be calculated. The radar was operated on a nearly continuous basis for a seven-day period in May of 1982 and the elapsed time between start and finish of a VAD scan was approximately 35 minutes. Radial velocities were measured in the upper troposphere and lower stratosphere (6-24 km) with at height resolution of 150 meters at a zenith angle of 15 deg. Vertical and horizontal velocities are calculated from the sums and differences, respectively, of radial velocity pairs, i.e., at azimuth directions AZ and AZ + 180 degrees. Momentum flux at a particular azimuth is calculated by taking the difference between the square of radial velocities at AZ and AZ + 180 degrees. It should be noted that measurements of radial velocity pairs are not simultaneous but are time delayed by approximately 15-25 minutes. This period, the time required to rotate the antenna feed and take measurements at AZ and AZ + 180 deg, effectively limits sampling of velocities and momentum fluxes to longer period gravity waves and planetary waves. B.W.

N85-32506*# Georgia Inst. of Tech., Atlanta. School of Geophysical Sciences.
RELATIONSHIP OF ISOLATED TURBULENT REGIONS TO THE GENERAL TURBULENT BACKGROUND, PART 4.4A
R. G. Roper *In* International Council of Scientific Unions Middle Atmosphere Program: Handbook for Map. Vol. 14 Dec. 1984 p 211 (For primary document see N85-32466 21-46)
Avail: NTIS HC A17/MF A01; also avail. from SCOSTEP Secretariat, Illinois Univ., 1406 West Green St., Urbana, Ill. 61801 CSCL 04A

The atmosphere below 100 km is often referred to as the homosphere; the region above, the heterosphere. In the homosphere, constitutents are mixed, and average molecular weight is constant. In the heterosphere, diffusive separation occurs, and species tend to fractionate; average molecular weight decreases with height. Mixing in the homosphere has its source dynamical (wind) energy. Against this background turbulence, intermittent enhancements of turbulent intensity are observed. Some of these enhancements are long lived -- for example, a turbulent layer at approximately 86 km altitude seems to be almost a permanent feature of the (global) daytime D region, as oserved by partial reflection. This may well be a delineation of the mesopause level, since long-term radio meteor studies have shown approx. 85 km to be the breakpoint between thermospheric circulation above, and mesospheric circulation below. The use of stratosphere-troposphere (ST) radars in the lower atmosphere, and mesosphere-stratosphere-troposphere (MST) and partial-reflection radars in the mesosphere for height/time profiles of turbulent intensity is discussed. B.W.

N85-32507*# Alaska Univ., Fairbanks. Geophysical Inst.
ESTIMATION OF VERTICAL DIFFUSION FROM OBSERVATIONS OF ATMOSPHERIC TURBULENCE LAYERS, PART 4.4B
D. C. Fritts *In* International Council of Scientific Unions Middle Atmosphere Program: Handbook for MAP. Vol. 14 Dec. 1984 p 212-215 refs (For primary document see N85-32466 21-46)
Avail: NTIS HC A17/MF A01; also avail. from SCOSTEP Secretariat, Illinois Univ., 1406 West Green St., Urbana, Ill. 61801 CSCL 04A

There have been numerous studies addressing the turbulent diffusion in the stratosphere and mesosphere during the last two decades. The motivation for such studies was the need for an understanding of the thermal and constituent structure of the middle atmosphere. Observational estimates of the horizontal and/or vertical diffusion were obtained using chemical release, rocket vapor trail, aircraft, balloon, and radar techniques. During the same period, a number of theoretical studies were performed to infer the level of vertical diffusion needed to account for observed constituent profiles. There appears to be a discrepancy between the level of vertical diffusion required for the dissipation of gravity wave and tidal motions on the one hand and for the maintenance of observed temperature and constituent profiles on the other. A possible explanation of this discrepancy is outlined. Measurements that may help verify this explanation are suggested. B.W.

N85-32508*# Alaska Univ., Fairbanks. Geophysical Inst.
MOMENTUM FLUX MEASUREMENTS: TECHNIQUES AND NEEDS, PART 4.5A
D. C. Fritts *In* International Council of Scientific Unions Middle Atmosphere Program: Handbook for MAP. Vol. 14 Dec. 1984 p 216-218 refs (For primary document see N85-32466 21-46)
Avail: NTIS HC A17/MF A01; also avail. from SCOSTEP Secretariat, Illinois Univ., 1406 West Green St., Urbana, Ill. 61801 CSCL 04A

The vertical flux of horizontal momentum by internal gravity waves is now recognized to play a significant role in the large-scale circulation and thermal structure of the middle atmosphere. This is because a divergence of momentum flux due to wave dissipation results in an acceleration of the local mean flow towards the phase speed of the gravity wave. Such mean flow acceleration are required to offset the large zonal accelerations driven by Coriolis torques acting on the diabatic meridional circulation. Techniques and observations regarding the momentum flux distribution in the middle atmosphere are discussed. B.W.

N85-32509*# National Oceanic and Atmospheric Administration, Boulder, Colo.
TROPOSPHERIC GRAVITY WAVES OBSERVED BY THREE CLOSELY SPACED ST RADARS c47
D. A. Carter, B. B. Balsley, W. L. Ecklund, M. Crochet (L.S.E.E.T, Toulon, France), A. C. Riddle (Colorado Univ.), and R. Garello *In* International Council of Scientific Unions Middle Atmosphere Program: Handbook for MAP. Vol. 14 Dec. 1984 p 219-228 refs (For primary document see N85-32466 21-46)
Avail: NTIS HC A17/MF A01; also avail. from SCOSTEP Secretariat, Illinois Univ., 1406 West Green St., Urbana, Ill. 61801 CSCL 04B

Clear-air radar experiments were carried out on the southern coast of France during the (ALPEX) Alpine experiment program vertically directed stratosphere-troposphere-radars were set up with spacings of about 5 to 6 km. The temporal and spectral characteristics of the vertical velocity fluctuations were examined. The horizontal and vertical properties of gravity waves in the lower atmosphere were analyzed. The techniques used and the first results from this wave study are described. E.A.K.

N85-32510*# Saskatchewan Univ., Saskatoon. Inst. of Space and Atmospheric Studies.
DETERMINATION OF HORIZONTAL AND VERTICAL WAVELENGTHS OF GRAVITY WAVES IN THE MESOSPHERE BY SPACED WIND MEASUREMENTS
C. E. Meek *In* International Council of Scientific Unions Middle Atmosphere Program. Handbook for MAP. Vol. 14 Dec. 1984 p 229-233 refs (For primary document see N85-32466 21-46)
Avail: NTIS HC A17/MF A01; also avail. from SCOSTEP Secretariat, Illinois Univ., 1406 West Green St., Urbana, Ill. 61801 CSCL 04A

The reduction of spaced wind measurements taken over a range of heights is described. The equipment used is a medium frequency radar with one site consisting of a vertically pointing transmitter and space receiving antennas, and two remote receiving sites with spaced antennas. Assuming approximately horizontally stratified scatterers, horizontal winds are thus available at the corners of a triangle of side approx. 20 km in the GRAVNET system. E.A.K.

N85-32511*# EISCAT Scientific Association, Kiruna (Sweden).
CRITERIA FOR SITE SELECTION AND FREQUENCY ALLOCATION (KEYNOTE PAPER), PART 5 c32
J. Rottger *In* International Council of Scientific Unions Middle

Atmosphere Program: Handbook for MAP. Vol. 14 Dec. 1985 p 234-244 refs (For primary document see N85-32466 21-46)
Avail: NTIS HC A17/MF A01; also avail. from SCOSTEP Secretariat, Illinois Univ., 1406 West Green St., Urbana, Ill. 61801 CSCL 17B

Technical aspects of mesosphere-stratosphere-troposphere (MST) Radar on site and frequency selection were discussed. Recommendations on site selections are presented. Tests of interference will be conducted before selecting a site. A small directional antenna may be suitable to simulate sidelobe sensitivity of radars however, sophisticated data-processing methods make system sensitivity extremely good. The use of the complete data system to look for interference is recommended. There is the difficulty of allocation of frequencies -- almost continuous use by these radars will be made when the band 40 to 60 MHz is allocated to other services. E.A.K.

N85-32512*# Control Data Corp., Minneapolis, Minn.
FREQUENCY AND SITE SELECTION CRITERIA FOR MST RADARS, PART 5.1A c32
G. D. Nastrom *In* International Council of Scientific Unions Middle Atmosphere Program: Handbook for MAP. Vol. 14 Dec. 1984 p 245 refs (For primary document see N85-32466 21-46)
Avail: NTIS HC A17/MF A01; also avail from SCOSTEP Secretariat, Illinois Univ., 1406 West Green St., Urbana, Ill. 61801 CSCL 17B

The majority of mesosphere-stratosphere-troposphere (MST) and ST radars are located in or near mountainous terrain. When measuring horizontal velocities, the terrain is a small factor, but when measuring vertical velocities, the meteorological noise induced by rough terrain can severely limit the usefulness of the observations. When the variance of the vertical velocity is too large, it is not possible to suitably filter the data to detect the small synoptic-scale signal with reasonable statistical confidence. The variance of vertical velocity at all tropospheric levels is directly related to the low level wind speed during flow over rough terrain. It is suggested that the synoptic-scale vertical velocity can be measured by ST radars where the terrain is smooth. The large-scale vertical velocity cannot always be reliably determined from MST radar data when the underlying terrain is rough. The vertical velocity is potentially on of future radar site selections, taking into account the desired meteorological applications of the data and engineering design factors. If the synoptic-scale vertical velocity is a desired variable, the radar should not be located near mountains. E.A.K.

N85-32513*# EISCAT Scientific Association, Kiruna (Sweden).
MOST DESIRABLE TERRAIN, E.G., FLAT VS VALLEY LOCATION, PART 5.1B c32
J. Rottger *In* International Council of Scientific Unions Middle Atmosphere Program: Handbook for MAP. Vol. 14 Dec. 1984 p 246-248 (For primary document see N85-32466 21-46)
Avail: NTIS HC A17/MF A01; also avail. from SCOSTEP Secretariat, Illinois Univ., 1406 West Green St., Urbana, Ill. 61801 CSCL 17B

Ground reflections which are similar for all (Yagi) elements of a phased array and change the radiation pattern of the single elements are discussed. This consequently yields a change of the radiation pattern of the entire array. It is assumed that the radiation pattern of a Yagi antenna can be treated in a good approximation for the present purpose, similar to the pattern of a single dipole, if one confines to radiation angles which are roughly perpendicular to the main beam of the Yagi antenna. E.A.K.

N85-32514# National Oceanic and Atmospheric Administration, Boulder, Colo. Aeronomy Lab.
SUMMARY OF SESSION ON OPTIMUM TRANSMITTER AND ANTENNA CONFIGURATION FOR MST RADAR, PART 6 c32
J. L. Green *In* International Council of Scientific Unions Middle Atmosphere Program: Handbook for MAP. Vol. 141 Dec. 1984 p 249-250 (For primary document see N85-32466 21-46)
Avail: NTIS HC A17/MF A01; also avail. from SCOSTEP Secretariat, Illinois Univ., 1406 West Green St., Urbana, Ill. 61801 CSCL 17B

Interpret MST radar data and hardware incorporation into these systems are discussed. Two recent examples of this necessary interaction are cited: (1) in orbit to obtain the average vertical velocity related to meteorological systems, the radar antenna must be pointed with an accuracy of 0.1 degree; (2) antenna sidelobe reduction to reduce the number of spurious records is considered. Improvements in the MST or ST technique are examined and the following topics are discussed: T/R Switch Design for Short-Range Measurements. Practicality of Electron Beam Steering for MST/ST Radars. Increase of Antenna Area Instead of Transmitted Power. The use of Interferometer Techniques for Beam Steering. Testing and Optimizing MST Coaxial-Collinear Arrays. E.A.K.

N85-32515*# Illinois Univ., Urbana. Aeronomy Lab.
T/R SWITCH DESIGN FOR SHORT-RANGE MEASUREMENTS, PART 6.1A c33
B. Yu *In* International Council of Scientific Unions Middle Atmosphere Program: Handbook for MAP. Vol 14 Dec. 1984 p 251-252 refs (For primary document see N85-32466 21-46)
Avail: NTIS HC A17/MF A01; also avail. from SCOSTEP Secretariat, Illinois Univ., 1406 West Green St., Urbana, Ill. 61801 CSCL 09C

The positive intrinsic negative (PIN) diode switch which is designed to protect the receiver from burnout or damage on transmission and channel the echo signal to the receiver on reception is outlined. The receiver must be protected firmly. A schematic diagram of a transformer rectifier (TR-ATR) switch for the Urbana Radar is shown. The T/R switch consists of a half wavelength coaxial cavity with tuning condenser and PIN diodes. Two UM4300 PIN diodes were mounted between the inner and outer conductor. The dc biasing voltage required for the PIN diodes is supplied by a control circuit. On transmission, the PIN diodes are forward biased to about 0.5 amperes. On reception, about 10 volts reverse voltage is applied to the diodes, which produces an initial reverse current to speed the recovery time. The T/R switch characteristics are estimated and the result of testing at different peak transmitter powers from 410 kW to 1500 kW is shown. E.A.K.

N85-32516*# National Oceanic and Atmospheric Administration, Boulder, Colo. Aeronomy Lab.
PRACTICALITY OF ELECTRONIC BEAM STEERING FOR MST/ST RADARS, PART 6.2A c47
W. L. Clark and J. L. Green *In* International Council of Scientific Unions Middle Atmosphere Program: Handbook for MAP. Vol. 14 Dec. 1984 p 253-256 refs (For primary document see N85-32466 21-46)
Avail: NTIS HC A17/MF A01; also avail. from SCOSTEP Secretariat, Illinois Univ., 1406 West Green St., Urbana, Ill. 61801 CSCL 09C

Electronic beam steering is described as complex and expensive. The Sunset implementation of electronic steering is described, and it is demonstrated that such systems are cost effective, versatile, and no more complex than fixed beam alternatives, provided three or more beams are needed. The problem of determining accurate meteorological wind components in the presence of spatial variation is considered. A cost comparison of steerable and fixed systems allowing solution of this problem is given. The concepts and relations involved in phase steering are given, followed by the description of the Sunset ST radar steering system. The implications are discussed, references to the competing SAD method are provided, and a recommendation concerning the design of the future Doppler ST/MST systems is made. E.A.K.

N85-32517*# EISCAT Scientific Association, Kiruna (Sweden).
INCREASE OF ANTENNA AREA INSTEAD OF TRANSMITTER POWER, PART 6.3A c32
J. Rottger *In* International Council of Scientific Unions Middle Atmosphere Program: Handbook for MAP. Vol. 14 Dec. 1984 p 257-258 refs (For primary document see N85-32466 21-46)
Avail: NTIS HC A17/MF A01; also avail. from SCOSTEP Secretariat, Illinois Univ., 1406 West Green St., Urbana, Ill.

61801 CSCL 09C

An extension of the antenna area may be preferred to an increase of transmitter power, when it is considered that reflection often dominates the scatter contribution at near zenith angles. It is noticed that an increase of the antenna area A, linearly increases the contribution of reflection. This most likely occur at vertical incidence, since the mean generalized refractive index gradient (M) is largest in the vertical direction. The altitude ranges at which the echo power gets weak and we have to consider improvements of sensitivity are mostly larger than 5 to 8 km. It follows that the considerations are valid up to antenna diameters close to 200 m for wavelengths of 6 m. On the other hand the reflected component has to be larger than the scattered component which only holds for near zenith angles. E.A.K.

N85-32518*# National Oceanic and Atmospheric Administration, Boulder, Colo. Aeronomy Lab.

TESTING AND OPTIMIZING MST COAXIAL COLLINEAR ARRAYS, PART 6.4A c32

J. M. Warnock and J. L. Green *In* International Council of Scientific Unions Middle Atmosphere Program: Handbook for MAP. Vol. 14 Dec. 1984 p 259-261 refs (For primary document see N85-32466 21-46)

Avail: NTIS HC A17/MF A01; also avail. from SCOSTEP Secretariat, Illinois Univ., 1406 West Green St., Urbana, Ill. 61801 CSCL 09C

Many clear-air VHF wind profiles use coaxial collinear (COCO) arrays for their antenna. A COCO array is composed of long lines of half-wave dipoles spaced one-half wavelength apart. An inexpensive method of checking a COCO array is described and its performance is optimized by measuring and then correcting the relative rf phase among its lines at their feed point. This method also gives an estimate of the rf current amplitude among the lines. The strength and location of the sidelobes in the H-plane of the array can be estimated. E.A.K.

N85-32519*# Cornell Univ., Ithaca, N.Y. School of Electrical Engineering.

OVERVIEW OF ON-LINE DATA PROCESSING FOR MST RADARS (KEYNOTE PAPER), PART 7 c32

D. T. Farley *In* International Council of Scientific Unions Middle Atmosphere Program: Handbook for MAP. Vol. 14 Dec. 1984 p 262-267 (For primary document see N85-32466 21-46)

Avail: NTIS HC A17/MF A01; also avail. from SCOSTEP Secretariat, Illinois Univ., 1406 West Green St., Urbana, Ill. 61801 CSCL 17I

The most important aspects of the processing of MST radar data are discussed. The important points of on-line data processing for MST radar are reviewed. The goals of the on-line and now almost exclusively digital processing, procedures are to achieve good altitude resolution and coverage, good frequency (Doppler shift) resolution, and good time resolution, while avoiding, the problems of range and frequency ambiguity (aliasing), ground clutter, and interference. Achieving optimum results requires pulse compression and some coherent integration. The first allows full utilization of the average power capability of the transmitter and the second reduces the computing requirements. E.A.K.

N85-32520*# Illinois Univ., Urbana. Dept. of Electrical Engineering.

CODING SCHEMES FOR IMPROVING MST RADAR PERFORMANCE, PART 7.1A c32

S. A. Bowhill *In* International Council of Scientific Unions Middle Atmosphere Program: Handbook for MAP. Vol. 14 Dec. 1984 p. 268-270 refs (For primary document see N85-32466 21-46) (Grant NGR14-005-181)

Avail: NTIS HC A17/MF A01; also avail. from SCOSTEP Secretariat, Illinois Univ., 1406 West Green St., Urbana, Ill. 61801 CSCL 17I

The performance of a mesosphere-stratosphere-troposphere (MST) radar can be characterized by its system sensitivity and its range resolution. The former enables Doppler velocities to be determined even in the presence of very weak structures; the latter permits study of the fine structure within a turbulent region. Coding of transmitted signals has as its aim an increase in the effective radar sensitivity or range resolution without an increase in the peak transmitted power. This is accomplished by spreading the power in the frequency domain, giving better range resolution, without reducing the pulse width. Two basic techniques are used to accomplish this frequency dispersion: (1) using a type of pseudorandom code for the phase or amplitude within a single pulse, or within a finite sequence of pulses; (2) to code the frequency of the transmitted signal in some way. The various possibilities are discussed and are compared with the pulse-coding methods. E.A.K.

N85-32521*# National Oceanic and Atmospheric Administration, Boulder, Colo.

ELIMINATION OF RANGE-ALIASED ECHOES IN THE VHF RADARS

R. G. Strauch *In* International Council of Scientific Unions Middle Atmosphere Program: Handbook for MAP. Vol. 14 Dec. 1984 p 271-272 (For primary document see N85-32466 21-46)

Avail: NTIS HC A17/MF A01; also avail. from SCOSTEP Secretariat, Illinois Univ., 1406 West Green St., Urbana, Ill. 61801 CSCL 04A

Very high frequency radars designed to measure tropospheric wind profiles usually detect scattering to a maximum height of about 20 km. If the antenna elevation angle is 45 degrees or more above the horizon, the maximum range of interest is less than 30 km. A VHF pulsed Doppler radar wind Profiler can, therefore, be operated at high pulse repetition rates. The maximum bandwidth allowed is about 0.5 MHz so a radar with uncoded pulses can operate with a duty cycle of 1 to 10%, depending on the desired height resolution. It is possible to operate a tropospheric wind profiler that utilizes all the average power available from the transmitter without the complexity of coded pulses. However, the VHF radar can detect echoes from the mesosphere on occasion and, with high pulse repetition rates, these echoes occur at the same apparent range as the tropospheric echoes. These mesospheric echoes may be stronger than the tropospheric signals. The range-aliased mesospheric echoes can be greatly attenuated or effectively eliminated. E.A.K.

N85-32522*# National Oceanic and Atmospheric Administration, Boulder, Colo. Aeronomy Lab.

SIDELOBE REDUCTION OF BARKER CODES, PART 7.1C c33

J. L. Green *In* International Council of Scientific Unions Middle Atmosphere Program: Handbook for MAP. Vol. 14 Dec. 1984 p 273-275 refs (For primary document see N85-32466 21-46)

Avail: NTIS HC A17/MF A01; also avail. from SCOSTEP Secretariat, Illinois Univ., 1406 West Green St., Urbana, Ill. 61801 CSCL 09C

Barker codes can be realized as simple digital preprocessors, or with the use of a delay line, can be realized as an analogue device. Assuming the process observed has an autocorrelation time that is long compared to the code length, a gain in signal to noise, G = N where N is the number of elements in the code, may be realized. Typically Barker codes are implemented by shifting the phase of the transmitted signal by 0 or 180 degrees according to the code pattern. A typical detection scheme is shown where the output of the radar receiver is delayed by an analogue delay line or a shift register. The signal in each element of the delay line or shift register is continuously multiplied by the code and all elements are summed. A principal disadvantage was the sidelobe response. In the case of MST or ST radar echoes where there is a dynamic range as large as 60 dB, these unwanted sidelobes cause an increase in the apparent width of atmospheric layers, or some narrow layer to appear at several altitudes. The sidelobes of a Barker code may be reduced by tapering the response of the decoder. Optimum tapers, are shown. It is found that the sidelobe response is greatly reduced with very little loss in G. E.A.K.

N85-32523*# Illinois Univ., Urbana. Coordinated Science Lab.

CONSTRUCTION OF COMPLEMENTARY CODE SEQUENCE

SETS, PART 7.1D **c33**
D. V. Sarwate *In* International Council of Scientific Unions Middle Atmosphere Program: Handbook for MAP. Vol. 14 Dec. 1984 p 276-277 refs (For primary document see N85-32466 21-46)
Avail: NTIS HC A17/MF A01; also avail. from SCOSTEP Secretariat, Illinois Univ., 1406 West Green St., Urbana, Ill. 61801 CSCL 09C

A set of code sequences is a complementary code sequence set if the sum of the aperiodic autocorrelation functions for the sequences is zero everywhere except at the origin. A simple construction for sets of complementary code sequences is discussed. E.A.K.

N85-32524*# Centre National d'Etudes des Telecommunications, Saint Maur des Fosses (France).
PROUST RADAR: DECODING HARDWARE AND COHERENT INTEGRATION, PART 7.2A **c33**
M. Petitdidier *In* International Council of Scientific Unions Middle Atmosphere Program: Handbook for MAP. Vol. 14 Dec. 1984 p 278-279 (For primary document see N85-32466 21-46)
Avail: NTIS HC A17/MF A01; also avail. from SCOSTEP Secretariat, Illinois Univ., 1406 West Green St., Urbana, Ill. 61801 CSCL 09C

The Proust Radar decoding handware and coherent integration are specified. The specifications include characteristics, device description and enumeration of advantages and limitations. E.A.K.

N85-32525*# Tycho Technology, Inc., Boulder, Colo.
A HIGH-SPEED DIGITAL SIGNAL PROCESSOR FOR ATMOSPHERIC RADAR, PART 7.3A **c33**
J. W. Brosnahan and D. M. Woodard *In* International Council of Scientific Unions Middle Atmosphere Program: Handbook for MAP. Vol. 14 Dec. 1984 p 280-284 refs (For primary document see N85-32466 21-46)
Avail: NTIS HC A17/MF A01; also avail. from SCOSTEP Secretariat, Illinos Univ., 1406 West Green St., Urbana, Ill. 61801 CSCL 09C

The Model SP-320 device is a monolithic realization of a complex general purpose signal processor, incorporating such features as a 32-bit ALU, a 16-bit x 16-bit combinatorial multiplier, and a 16-bit barrel shifter. The SP-320 is designed to operate as a slave processor to a host general purpose computer in applications such as coherent integration of a radar return signal in multiple ranges, or dedicated FFT processing. Presently available is an I/O module conforming to the Intel Multichannel interface standard; other I/O modules will be designed to meet specific user requirements. The main processor board includes input and output FIFO (First In First Out) memories, both with depths of 4096 W, to permit asynchronous operation between the source of data and the host computer. This design permits burst data rates in excess of 5 MW/s. E.A.K.

N85-32526*# Illinois Univ., Urbana. Aeronomy Lab.
HARDWARE SCHEMES FOR FAST FOURIER TRANSFORM, PART 7.4A **c62**
G. R. Stitt and S. A. Bowhill *In* International Council of Scientific Unions Middle Atmosphere Program: Handbook for MAP. Vol. 14 Dec. 1984 p 285-288 refs (For primary document see N85-32466 21-46)
(Grants NsG-7506; NSF ATM-81-20371)
Avail: NTIS HC A17/MF A01; also avail. from SCOSTEP Secretariat, Illinois Univ., 1406 West Green St., Urbana, Ill. 61801 CSCL 09B

Real-time fast fourier transformer (FFT) processing of a MST radar data and cost-effective approaches to hardware FFT generation were studied. Previously devised hardware FFT configurations are described including the estimated number of chips used and the time required to perform a 1024-point FFT. The remaining entries in the table correspond to original designs, which presuppose the availability of a microcomputer and a modestly complicated hardware peripheral. These original designs, all of which implement a radix-4 FFT with twiddle factors, are assigned model numbers to make them easier to refer to. E.A.K.

N85-32527*# Case Western Reserve Univ., Cleveland, Ohio. Dept. of Electrical Engineering and Applied Physics.
CRITERIA AND ALGORITHMS FOR SPECTRUM PARAMETERIZATION OF MST RADAR SIGNALS **c32**
P. K. Rastogi *In* International Council of Scientific Unions Middle Atmosphere Program: Handbook for MAP. Vol. 14 Dec. 1984 p 289-293 refs (For primary document see N85-32466 21-46)
Avail: NTIS HC A17/MF A01; also avail. from SCOSTEP Secretariat, Illinois Univ., 1406 West Green St., Urbana, Ill. 61801 CSCL 17I

The power spectra [S(f)] of MST radar signals contain useful information about the variance of refractivity fluctuations, the mean radial velocity, and the radial velocity variance in the atmosphere. When noise and other contaminating signals are absent, these quantities can be obtained directly from the zeroth, first and second order moments of the spectra. A step-by-step procedure is outlined that can be used effectively to reduce large amounts of MST radar data-averaged periodograms measured in range and time to a parameterized form. The parameters to which a periodogram can be reduced are outlined and the steps in the procedure, that may be followed selectively, to arrive at the final set of reduced parameters are given. Examples of the performance of the procedure are given and its use with other radars are commented on. E.A.K.

N85-32528*# Colorado Univ., Boulder. CIRES.
INTERPOLATION PROBLEMS IN METEOR RADAR ANALYSIS, PART 7.6A
D. Tetenbaum and S. K. Avery *In* International Council of Scientific Unions Middle Atmosphere Program: Handbook for MAP. Vol. 14 Dec. 1984 p 294-296 refs (For primary document see N85-32466 21-46)
Avail: NTIS HC A17/MF A01; also avail. from SCOSTEP Secretariat, Illinois Univ., 1406 West Green St., Urbana, Ill. 61801 CSCL 04A

Meteor echoes come from random points in the observation volume, and are irregularly spaced in time. This precludes the use of fast fourier transformations (FFT) techniques on the raw data to give the spectrum of waves that are present. One way around this obstacle is to restrict our interest to a particular class of waves, and fit a corresponding model to the raw data. It is assumed that there is no horizontal variation across the observation volume for tides, but in the vertical this is certainly not the case. If, in addition, we are interested in other types of waves which may be present and whose periods are unknown, then examining the raw line-of-sight velocities does not tell us how to modify the model, since the line-of-sight direction is not fixed. This is the motivation for interpolation. Interpolation takes a temporal series of line-of-sight velocities, and transforms it to a temporal series of wind velocities for each orthogonal direction. The velocities along a given direction can then be examined readily for any waves in addition to tides. E.A.K.

N85-32529*# Saskatchewan Univ., Saskatoon. Inst. of Space and Atmospheric Studies.
PROBLEMS AND SOLUTIONS IN ANALYZING PARTIAL-REFLECTION DRIFT DATA BY CORRELATION TECHNIQUES **c65**
C. E. Meek *In* International Council of Scientific Unions Middle Atmosphere Programs: Handbook for MAP. Vol. 14 Dec. 1984 p 297-299 (For primary document see N85-32466 21-46)
Avail: NTIS HC A17/MF A01; also avail. from SCOSTEP Secretariat, Illinois Univ., 1406 West Green St., Urbana, Ill. 61801 CSCL 12A

Solutions in analyzing partial reflection drift data by correlation techniques are discussed. The problem of analyzing spaced antenna drift data breaks down into the general categories of raw data collection and storage, correlation calculation, interpretation of correlations, location of time lags for peak correlation, and velocity calculation. E.A.K.

N85-32530*# Colorado Univ., Boulder. CIRES.
DATA BASE MANAGEMENT: MSTRAC (KEYNOTE PAPER),

PART 8 **c81**

S. K. Avery and B. B. Balsley (NOAA, Boulder, Colo.) *In* International Council of Scientific Unions Middle Atmosphere Program: Handbook for MAP. Vol. 14 Dec. 1984 p 300-301 (For primary document see N85-32466 21-46)

Avail: NTIS HC A17/MF A01; also avail. from SCOSTEP Secretariat, Illinois Univ., 1406 West Green St., Urbana, Ill. 61801 CSCL 05A

Technical Aspects of MST radars were discussed. The name of the group is MST Radar Coordination (MSTRAC). The geophysical parameters to be included in the sample data tapes were determined. It was suggested that MSTRAC compile a catalog of existing data at each of the facilities. It is found that: (1) there is a community of interested users for MST data; (2) the initial responses from observatories indicates that interest in MSTRAC is not overwhelming, probably because of time involved; and (3) the program needs reassessment. E.A.K.

N85-32531*# Illinois Univ., Urbana.

SAMPLE INTERCHANGE OF MST RADAR DATA FROM THE URBANA RADAR

S. A. Bowhill and A. Rennier *In* International Council of Scientific Unions Middle Atmosphere Program. Handbook for MAP. Vol. 14 Dec. 1984 p 302-305 (For primary document see N85-32466 21-46)

(Grants NsG-7506; NSF ATM-81-20371)

Avail: NTIS HC A17/MF A01; also available from SCOSTEP Secretariat, Illinois Univ., 1406 West Green Street, Urbana, Ill. 61801 CSCL 04A

As a first step in interchange of data from the Urbana mesosphere-stratosphere-troposphere (MST) radar, a sample tape has been prepared in 9-track 1600-bpi IBM format. It includes all Urbana data for April 1978 (the first month of operation of the radar). The 300-ft tape contains 260 h of typical mesospheric power and line-of-sight velocity data. G.L.C.

N85-32532*# Control Data Corp., Minneapolis, Minn.

MST RADAR DATA MANAGEMENT **c81**

G. D. Nastrom *In* International Council of Scientific Unions Middle Atmosphere Program. Handbook for MAP. Vol. 14 Dec. 1984 p 306 refs (For primary document see N85-32466 21-46)

Avail: NTIS HC A17/MF A01; also available from SCOSTEP Secretariat, Illinois Univ., 1406 West Green Street, Urbana, Ill. 61801 CSCL 05A

One atmospheric variable which can be deduced from stratosphere-troposphere (ST) radar data other than wind speed and direction is C sub n sup 2, related to the eddy dissipation rate. The computation of C sub n sup 2 makes use of the transmitted power (average, or peak plus duty cycle), the range of the echoes, and the returned power. The returned power can be calibrated only if a noise source of known strength is imposed; e.g., in the absence of absolute calibration, one can compare the diurnal noise signal with the galactic sky temperature. Thus to compute C sub n sup 2 one needs the transmitter power, the returned signal as a function of height, and the returned noise at an altitude so high that it is not contaminated by any signal. Now C sub n sup 2 relates with the amount of energy within the inertial subrange, and for many research studies it may be desirable to relate this with background flow as well as shears or irregularities on the size of the sample volume. The latter are quantified by the spectral width. G.L.C.

N85-32533*# National Oceanic and Atmospheric Administration, Boulder, Colo.

DATA BASE FOR THE COLORADO PROFILING NETWORK **c81**

D. A. Merritt *In* International Council of Scientific Unions Middle Atmosphere Program. Handbook for MAP. Vol. 14 Dec. 1984 p 307-308 refs (For primary document see N85-32466 21-46)

Avail: NTIS HC A17/MF A01; also available from SCOSTEP Secretariat, Illinois Univ., 1406 West Green Street, Urbana, Ill. 61801 CSCL 05A

The Colorado profiling system developed by the Wave Propagation Laboratory (WPL) includes five (soon to be six) Doppler radar wind Profilers; four operate at 49 MHz (6 m) and are located at Platteville, Fleming, Lay Creek, and Cahone, and one operates at 915 MHz (33 cm) and is located at Denver. The sixth radar, now under construction, will operate at 405 MHz (UHF) and will be located at Boulder. Microwave radiometers and surface meteorological stations are at some of the radar sites. The data base for the wind Profilers is discussed. G.L.C.

N85-32534*# EISCAT Scientific Association, Kiruna (Sweden).

FURTHER DEVELOPMENTS OF EISCAT AS AN MST RADAR

J. Rottger (Max-Planck-Inst. fuer Aeronomie, Lindau, West Germany) *In* International Council of Scientific Unions Middle Atmosphere Program. Handbook for MAP. Vol. 14 Dec. 1984 p 309-318 refs (For primary document see N85-32466 21-46)

Avail: NTIS HC A17/MF A01; also available from SCOSTEP Secretariat, Illinois Univ., 1406 West Green Street, Urbana, Ill. 61801 CSCL 04A

The principal capabilities of EISCAT as an MST radar were described. Since the VHF transmitter of the EISCAT system is not yet delivered, only the UHF system could be used for radar experiments. Considerable developments in the year 1983 have now strongly improved the reliability of the operations. Most of the experiments were and will be done to investigate the high latitude ionosphere and thermosphere, but some time was also devoted to observations of the lower and middle atmosphere, particularly during the MAP/WINE compaign. G.L.C.

N85-32535*# Cornell Univ., Ithaca, N.Y. School of Electrical Engineering.

STATUS OF THE JICAMARCA RADAR **c32**

T. Farley *In* International Council of Scientific Unions Middle Atmosphere Program. Handbook for MAP. Vol. 14 Dec. 1984 p 319-320 (For primary document see N85-32466 21-46)

Avail: NTIS HC A17/MF A01; also available from SCOSTEP Secretariat, Illinois Univ., 1406 West Green Street, Urbana, Ill. 61801 CSCL 17I

The capabilities of the large 50-MHz radar at Jicamarca for mesosphere-stratosphere-troposphere MST observations were discussed in some detail. Hence this description will be quite brief and will concentrate on recent improvements in the facility. The radar is located about 20 km from Lima, Peru. It is well shielded by surrounding mountains, and most of the ground clutter is restricted to ranges of 15 km or less. The antenna consists of 18,432 half-wave dipoles (9216 crossed pairs) covering an area of 290 m by 290 m and divided up into 64 independent modules which can be individually phased and/or used as separate antennas in any way desired. The whole array can be steered about 3 degrees from the on-axis position (the limit is the beam width of the individual modules, which cannot be steered), and any polarization can be arranged. Even with this limited steerability it is straightforward to determine vector wind velocities by pointing segments of the antenna in different directions. The radar can also be used as in interferometer. G.L.C.

N85-32536*# National Oceanic and Atmospheric Administration, Boulder, Colo. Aeronomy Lab.

RECENT RESULTS AT THE SUNSET RADAR **c32**

J. L. Green, J. M. Warnock, and W. L. Clark *In* International Council of Scientific Unions Middle Atmosphere Program. Handbook for MAP. Vol. 14 Dec. 1984 p 321-323 refs (For primary document see N85-32466 21-46)

Avail: NTIS HC A17/MF A01; also available from SCOSTEP Secretariat, Illinois Univ., 1406 West Green Street, Urbana, Ill. 61801 CSCL 04A

The Sunset radar is a VHF, pulsed Doppler radar located in a narrow canyon near the Sunset townsite 15 km west of Boulder, CO. This facility is operated by the Aeronomy Laboratory, ERL, NOAA, exclusively for meteorological research and the development of the mesosphere-stratosphere-troposphere (MST) and stratosphere-troposphere (ST) radar technique. Recent results include a measurement of all three components of wind velocity for the Federal Administration. G.L.C.

N85-32537*# Utah State Univ., Logan.
THE BOOT LAKE MF IMAGING RADAR c32
G. W. Adams and J. W. Brosnahan (Tycho Technology, Inc., Boulder, Colo.) *In* International Council of Scientific Unions Middle Atmosphere Program. Handbook for MAP. Vol. 14 Dec. 1984 p 324 ref (For primary document see N85-32466 21-46)
Avail: NTIS HC A17/MF A01; also available from SCOSTEP Secretariat, Illinois Univ., 1406 West Green Street, Urbana, Ill. 61801 CSCL 17I

The Middle-Atmosphere Imaging Radar is located at the Boot Lake field site, 10 miles east of Brighton, Colorado. It operates at 2.66 MHz with a 50-kW peak pulse power in 30 microsecond pulses. Ten independent coaxial-collinear antennas are used; five are parallel and run east-west, the other five are parallel and run north-south. Each antenna consists of eight half-wave dipoles. All ten antennas or a crossed pair may be used for transmission; all ten are sampled by pairs in rapid sequence for reception. The system is now operating on a campaign basis as a Fourier interferometer by measuring the complex voltages on the ten antennas and Fourier transforming them independently. Multiple scatterers within a single range gate, now sorted by velocity, can be located individually by their phase angles. The transmitted signal cycles through four modes (N-S linear, right-hand circular, E-W linear, and left-hand circular). G.L.C.

N85-32538*# Georgia Inst. of Tech., Atlanta. School of Geophysical Sciences.
MENTOR: ADDING AN OUTLYING RECEIVER TO AN ST RADAR FOR METEOR-WIND MEASUREMENT c32
R. G. Roper *In* International Council of Scientific Unions Middle Atmosphere Program. Handbook for MAP. Vol. 14 Dec. 1984 p 325-329 (For primary document see N85-32466 21-46)
Avail: NTIS HC A17/MF A01; also available from SCOSTEP Secretariat, Illinois Univ., 1406 West Green Street, Urbana, Ill. 61801 CSCL 04A

Radar scattering from ionized meteor trails has been used for many years as a way to determine mesopause-level winds. Scattering occurs perpendicular to the trails, and since the ionizing efficiency of the incoming meteoroids depends on the cosine of the zenith angle of the radiant, echoes directly overhead are rare. Stratosphere-troposphere (ST) radars normally sample within 15 deg of the vertical, and thus receive few meteor echoes. Even the higher powdered mesosphere-stratosphere-troposphere (MST) radars are not good meteor radars, although they were used to successfully retrieved meteor winds from the Poker Flat, Alaska MST radar by averaging long data intervals. It has been suggested that a receiving station some distance from an ST radar could receive pulses being scattered from meteor trails, determine the particular ST beam in which the scattering occurred, measure the radial Doppler velocity, and thus determine the wind field. This concept has been named MENTOR (Meteor Echoes; No Transmitter, Only Receivers). G.L.C.

N85-32539*# National Oceanic and Atmospheric Administration, Boulder, Colo. Aeronomy Lab.
SUMMARY OF PROGRESS AT THE POKER FLAT OBSERVATORY IN ALASKA c32
B. B. Balsley *In* International Council of Scientific Unions Middle Atmosphere Program. Handbook for MAP. Vol. 14 Dec. 1984 p 330 refs (For primary document see N85-32466 21-46)
Avail: NTIS HC A17/MF A01; also available from SCOSTEP Secretariat, Illinois Univ., 1406 West Green Street, Urbana, Ill. 61801 CSCL 04A

A description of the status of the Poker Flat MST Radar as of early 1983 is included in the 1983 mesosphere-stratosphere-troposphere MST Workshop Proceedings. The Observatory continues to operate in a continuous data-taking mode, except for a three-week planned campaign experiment concurrent with the STATE rocket program during June 1983. Construction of the digital preprocessing system mentioned in the last status report is all but complete. This additional improvement should be operational by late summer. The possibility of steering the array also mentioned in the last status report is being investigated. A project is underway to electronically steer the one-quarter vertical section of the array. Steering will be in finite steps within about + or - 5 deg of vertical. Successful testing of this modification may lead to eventually steering the entire array in this manner. Data analysis of the data base (now more than four years in length) continues with well over one dozen extramural scientific groups participating. G.L.C.

N85-32540*# Illinois Univ., Urbana. Dept. of Electrical and Computer Engineering.
URBANA RADAR SYSTEMS: POSSIBILITIES AND LIMITATIONS c32
O. Royrvik *In* International Council of Scientific Unions Middle Atmosphere Program. Handbook for MAP. Vol. 14 Dec. 1984 p 331-336 refs (For primary document see N85-32466 21-46)
Avail: NTIS HC A17/MF A01; also available from SCOSTEP Secretariat, Illinois Univ., 1406 West Green Street, Urbana, Ill. 61801 CSCL 17I

The Aeronomy Laboratory Field Station of the University of Illinois at Urbana contains three different radar systems capable of probing various regions of the atmosphere below about 100 km. These are an mesosphere-stratosphere-troposphere (MST) radar, a VHF meteor radar and an MF partial-reflection radar. All three radars can measure winds and waves in the ionospheric D region. The MST radar is, in addition, capable of probing the lower stratosphere and upper troposphere. A sodium (Na) LIDAR is also located at the Field Station and provides an additional way of studing winds and waves in the mesosphere by observing temporal variations in the sodium density profile. G.L.C.

N85-32541*# Alaska Univ., Fairbanks. Geophysical Inst.
THE SONDRESTROM RADAR: PROGRESS AND PROPOSED UPGRADES FOR ST WORK c32
B. J. Watkins *In* International Council of Scientific Unions Middle Atmosphere Program. Handbook for MAP. Vol. 14 Dec. 1984 p 337-338 ref (For primary document see N85-32466 21-46)
Avail: NTIS HC A17/MF A01; also available from SCOSTEP Secretariat, Illinois Univ., 1406 West Green Street, Urbana, Ill. 61801 CSCL 17I

The capabilities and limitations of the Sondrestrom Radar for stratosphere-troposphere ST observations were previously presented. Recent progress and proposed upgrades are summarized. During the first year of operation (April 1983 to April 1984) there was only one ST experiment, mainly with the objective of evaluating the site and determining that the hardare and software were still operational after the radar's move from Alaska. The Sondrestrom site has about the same degree of ground clutter as the former Chatanika site and the data appear to be similar. The radar's operation continues to be incoherent-scatter observations of the ionosphere. The main radar parameters are summarized. G.L.C.

N85-32542*# National Oceanic and Atmospheric Administration, Boulder, Colo. Wave Propagation Lab.
PROGRESS AND PLANS FOR THE COLORADO WIND PROFILER NETWORK c32
R. G. Strauch *In* International Council of Scientific Unions Middle Atmosphere Program. Handbook for MAP. Vol. 14 Dec. 1984 p 339-340 refs (For primary document see N85-32466 21-46)
Avail: NTIS HC A17/MF A01; also available from SCOSTEP Secretariat, Illinois Univ., 1406 West Green Street, Urbana, Ill. 61801 CSCL 17I

Since January 1983, the Wave Propagation Laboratory (WPL) has placed four wind profiling radars in operation. These radars and the Platteville radar (originally developed by the Aeronomy Laboratory (AL0 and jointly operated by AL and WPL for several years) form the Colorado Wind Profiler Network. Plans and improvements for the Colorado Wind Profilers are summarized. G.L.C.

N85-32543*# Kyoto Univ. (Japan). Radio Atmospheric Science Center.
THE MU RADAR NOW PARTLY IN OPERATION c32
S. Kato, T. Ogawa, T. Tsuda, T. Sato, I. Kimura, and S. Fukao *In* International Council of Scientific Unions Middle Atmosphere

Program. Handbook for MAP. Vol. 14 Dec. 1984 p 341-349 refs (For primary document see N85-32466 21-46)
Avail: NTIS HC A17/MF A01; also available from SCOSTEP Secretariat, Illinois Univ., 1406 West Green Street, Urbana, Ill. 61801 CSCL 04B

The MU radar (middle- and upper-atmosphere radar) of RASC (Radio Atmospheric Science Center, Kyoto University) is now partly in operation, although the facility will be completed in 1985. The active array system of the radar makes it possible to steer the radar beam as fast as in each interpulse period. Various sophisticated experiments are expected to be performed by the system. A preliminary observation was successful to elucidate atmospheric motions during Typhoon No. 5 which approached the radar site in August, 1983. Author

N85-32544*# Pennsylvania State Univ., University Park. Dept. of Meteorology.
NETWORK ST RADAR AND RELATED MEASUREMENTS AT PENNSYLVANIA STATE UNIVERSITY Progress Report c32
D. W. Thomson, C. W. Fairall, and R. M. Peters *In* International Council of Scientific Unions Middle Atmosphere Program. Handbook for MAP. Vol. 14 Dec. 1984 p 350-355 (For primary document see N85-32466 21-46)
Avail: NTIS HC A17/MF A01; also available from SCOSTEP Secretariat, Illinois Univ., 1406 West Green Street, Urbana, Ill. 61801 CSCL 17I

Mesoscale meteorological measurements, analysis and prediction are some of the principal areas of research in the Department of Meteorology at Penn State. In anticipation of a staged turn-on of the three systems during the Summer and Fall of 1984, the nonconstruction-related efforts have focused on the software development necessary to allow essentially immediate use of network data. A 16-bit microcomputer has been programmed to serve as the network controller, communications interface and, at least for real-time purposes, the operational display system. Insofar as possible we have in this task built upon our substantial accumulated experience in working with the processing and display of Doppler sodar system signals. Once the radar-derived wind and turbulence profiles are communicated to the various interconnected Departmental computers they become just one component of a comprehensive data base which can be applied to a diverse set of ongoing basic and operational research programs. G.L.C.

N85-32545*# Science Research Council, Chilton (England). Rutherford Appleton Lab.
A NOTE ON THE PROPOSED UK VHF RADAR c32
A. J. Hall *In* International Council of Scientific Unions Middle Atmosphere Program. Handbook for MAP. Vol. 14 Dec. 1984 p 356 (For primary document see N85-32466 21-46)
Avail: NTIS HC A17/MF A01; also available from SCOSTEP Secretariat, Illinois Univ., 1406 West Green Street, Urbana, Ill. 61801 CSCL 17I

The proposal for the establishment of a VHF radar in the UK is still under active consideration, although for financial reasons no start has yet been made on an installation. Several changes have been made to the scheme as described and these are listed. (1) The initial installation will be suitable for stratosphere-troposphere (ST) operation only using 64 antennas and 2 power modules. (2) An existing site is being examined on the west coast of Wales, which because it is a former Loran ground station is provided with the buildings, power and communications facilities to enable a radar to be assembled much more quickly than a green field site would allow. Because the site is not within a mountain valley as originally intended, careful early attention will have to be given to the possible problems of local interference and sea-surface returns. (3) Preliminary discussions with the UK licensing authorities suggest that a frequency of 47 MHz is more likely than 50 MHz. (4) Minor changes are planned in the antenna array connection scheme of the 400-element mesosphere-stratosphere-troposphere (MST) array to allow more precise sidelobe suppression to be achieved in the receive mode. G.L.C.

N85-32546*# Adelaide Univ. (Australia). Dept. of Physics.
THE ADELAIDE VHF RADAR: CAPABILITIES AND FUTURE PLANS
B. H. Briggs, B. Candy, W. G. Elford, W. K. Hocking, P. T. May, and R. A. Vincent *In* International Council of Scientific Unions Middle Atmosphere Program. Handbook for MAP. Vol. 14 Dec. 1984 p 357-359 (For primary document see N85-32466 21-46)
Avail: NTIS HC A17/MF A01; also available from SCOSTEP Secretariat, Illinois Univ., 1406 West Green Street, Urbana, Ill. 61801 CSCL 04A

The VHF radar at Buckland Park, South Australia commenced operation in January, 1984. The radar is located adjacent to the 2-MHz ionospheric radar. The routine method for measuring horizontal wind velocity is the space antenna technique (SA) while the Doppler technique is used to measure vertical velocities. It is possible to swing the transmitting beam in the east-west plane, allowing Doppler measurements of the EW wind component. G.L.C.

N85-32547*# Centre National d'Etudes des Telecommunications, Saint Maur des Fosses (France).
THE PROUST RADAR c32
M. Petitdidier *In* International Council of Scientific Unions Middle Atmosphere Program. Handbook for MAP. Vol. 14 Dec. 1984 p 360-361 (For primary document see N85-32466 21-46)
Avail: NTIS HC A17/MF A01; also available from SCOSTEP Secretariat, Illinois Univ., 1406 West Green Street, Urbana, Ill. 61801 CSCL 17I

Specifications for the Proust incoherent scattering meteorological radar are presented. Both the transmitting and receiving facilities are detailed. G.L.C.

N85-32548*# Northeast Radio Observatory Corp., Westford, Mass. Haystack Observatory. Haystack Observatory.
MILLSTONE HILL RADAR: CAPABILITIES FOR S/T OBSERVATIONS c32
G. B. Loriot *In* International Council of Scientific Unions Middle Atmosphere Program. Handbook for MAP. Vol. 14 Dec. 1984 p 362 (For primary document see N85-32466 21-46)
Avail: NTIS HC A17/MF A01; also available from SCOSTEP Secretariat, Illinois Univ., 1406 West Green Street, Urbana, Ill. 61801 CSCL 17I

During the past several years, the 440-MHz radar at Millstone Hill has been modified to detect coherent echoes from clear-air turbulence in the stratosphere/troposphere (S/T) over the altitude range 4-25 km. Two distinct modes of data acquisition have been developed, and data reduction programs have been completed for one of these modes. This mode (I-mode) transmits a 10 microsec (1.5 km) pulse on the fully steerable antenna. Typically, the antenna is set at a low elevation angle (e.g., 15 deg.) to reduce the altitude resolution to approximately 1 km., and power spectra are collected at some 40 range gates. The antenna may be scanned in azimuth to obtain the total wind vector, held fixed to monitor wave motion, or scanned in elevation to monitor the horizontal extent of the turbulent activity. This steerability gives Millstone a flexible system to focus on localized events, such as lee waves or convective storms. An additional advantage at low elevations is the relatively large Doppler shift of the signal, since the LOS velocity contains a large component of the horizontal velocity. This shift separates the turbulence signal sufficiently far from the ground clutter to allow the spectral moments to be readily inferred. Some 500 hours of S/T I-mode data have been reduced to geophysical parameters, and reside on a data base at Millstone Hill. G.L.C.

N85-32549*# National Oceanic and Atmospheric Administration, Boulder, Colo. Aeronomy Lab.
THE PONAPE ST RADAR c32
D. A. Carter, W. L. Ecklund, and B. B. Balsley *In* International Council of Scientific Unions Middle Atmosphere Program. Handbook for MAP. Vol. 14 Dec. 1984 p 363 (For primary document see N85-32466 21-46)
Avail: NTIS HC A17/MF A01; also available from SCOSTEP

Secretariat, Illinois Univ., 1406 West Green Street, Urbana, Ill. 61801 CSCL 17I

In May, 1984, a 50-MHz ST radar was installed on the island of Ponape in the western equatorial Pacific (7 deg N, 158 deg E) by the Aeronomy Laboratory of NOAA. The radar consists of a 100 m x 100 m array with a single, vertically directed, beam and is initially transmitting micro sec. (2.25 km) pulses. The radar is operating continuously, with Doppler spectra being recorded at approximately 1 1/2 minute intervals and sent to Boulder for later analysis. One of the principal goals of the radar is to measure vertical motions in the troposphere and lower stratosphere at a location which is within the intertropical convergence zone during part of the year. First results, during generally fair weather conditions, show detectable echoes up to about 21 km with the tropopause at 17-18 km. Once daily balloon soundings are available locally from a NOAA Weather Service Office on the island, it is planned that this radar will be joined in the coming year by two others with oblique as well as vertical beams on two yet-to-be-selected equatorial islands as part of the TOGA (Tropical Oceans Global Atmosphere) program. G.L.C.

N85-32550*# National Oceanic and Atmospheric Administration, Boulder, Colo. Aeronomy lab.

MEASUREMENTS OF VERTICAL VELOCITY OVER FLAT TERRAIN BY ST RADAR AND OTHER RELATED USES OF THE RADAR DATA SET c47

J. L. Green and G. D. Nastrom (Control Data Corp., Minneapolis, Minn.) *In* International Council of Scientific Unions Middle Atmosphere Program. Handbook for MAP. Vol. 14 Dec. 1984 p 364-366 (For primary document see N85-32466 21-46)

Avail: NTIS HC A17/MF A01; also available from SCOSTEP Secretariat, Illinois Univ., 1406 West Green Street, Urbana, Ill. 61801 CSCL 04B

The need to study vertical velocity measurements from an ST radar located on the plains, far from the mountains is pointed out, as all presently available clear-air radars are located in or near mountains. The construction and operation of a VHF Doppler (ST) radar in the midwestern part of the United States to make meteorological measurements is also discussed. While primary interest is in measuring the synoptic-scale vertical velocities in the troposphere and lower stratosphere, it should be stressed, however, that the radar data set generated during the radar experiment would have many other valuable uses of interest to us and others some of whom are listed below. The required radar parameters, approximate costs, and recommended mode of operation are also detailed. G.L.C.

N85-32551# Geological Survey, Washington, D.C.

CHANGES IN THE ORGANIC MATERIAL IN LAKES IN THE BLAST ZONE OF MOUNT ST. HELENS, WASHINGTON: HYDROLOGIC EFFECTS OF THE ERUPTIONS

Diane M. McKnight, John M. Klein, and Robert C. Wissmar 1984 31 p refs

(GS-Circ-850-1) Avail: NTIS HC A03/MF A01

Large quantities of organic material were introduced into the nearby surface waters, either as soil and plants incorporated into pyroclastic, mudflow, or debris-avalanche deposits, or as blown-down timber swept into lakes by the lateral blast of hot volcanic gases. The resulting major increases in the concentration of dissolved organic material were one of the most significant changes in the water chemistry of surface waters of the blast zone. Increases in dissolved organic material were correlated with dense bacterial populations, and large increases in the concentrations of dissolved manganese, iron, and sulfur. The majority of the dissolved organic material was higher molecular weight, yellow organic acids. Many of the specific organic compounds identifiable by gas chromatography-mass spectrometry were derived from the pyrolysis of plant and soil organic material. These changes are discussed in detail. Author

N85-32552*# Lockheed Missiles and Space Co., Palo Alto, Calif.

ISEE-1 DATA REDUCTION AND ANALYSIS PLASMA COMPOSITION EXPERIMENT Final Report

W. Lennartsson and R. D. Sharp Mar. 1985 83 p refs

(Contract NAS5-25773)

(NASA-CR-175306; NAS 1.26:175306; LMSC-F018862) Avail: NTIS HC A05/MF A01 CSCL 03B

The plasma composition experiment covers energies from OeV to 17 keV/e and has a mass-per-charge range from less than 1 to about 150 amu. Measurements were made from the inner ring current region to the plasma sheet, magnetotail lobes, and the magnetopause boundary layers and beyond. Possibly the most significant results from the experiment are those related to energetic (0+) ions of terrestrial origin. These ions are found in every region of the magnetosphere reached by the spacecraft and can have energy and pitch-angle distributions that are similar to those traditionally associated with protons of solar wind origin. The (0+) ions are commonly the most numerous ions in the 0.1 - 17 keV/e energy range and are often a substantial part of the ion population at large distances as well, especially during geomagnetically disturbed conditions. An overview of results obtained for the (0+) and other ions with energies in the 0.1 - 17 keV/e range in the magnetosphere is given. Author

N85-32553# Air Force Inst. of Tech., Wright-Patterson AFB, Ohio. School of Engineering.

NUCLEAR THERMAL TRANSMITTANCE IN THE ATMOSPHERE USING LOWTRAN-6 COMPUTER CODE M.S. Thesis

J. M. Leonard Mar. 1985 66 p

(AD-A154669; AD-F630659; AFIT/GNE/ENP/85M-13) Avail: NTIS HC A04/MF A01 CSCL 04/1

The purpose of this thesis is to provide the nuclear weapons-effect analyst with accurate transmittance data for burst/target geometries and atmospheric conditions in which thermal radiation effects are of significance, yet without having to run a complex computer code for each specific case being investigated. Transmittance values for several realistic sets of atmospheric conditions were obtained using the 1962 U.S. Standard Atmospheric Model and the LOWTRAN Rural, Urban, Maritime, Tropospheric, and Stratospheric aerosol models. Boundary layer (0 - 2 km) transmittance calculations, using the Rural, Urban, and Maritime aerosols, were accomplished for sea-level visibilities of 5, 10, 15, and 23 km. A computer program was developed to weight the LOWTRAN-6 output transmittances according to a 6000 K Planckian distribution, simulating a nuclear weapon source. The geometry chosen is for the region where thermal radiation has a significant damage potential to Air Force systems; altitudes from sea-level to 20 kilometers, and ground ranges from 0 - 25 kilometers from weapon ground-zero. The results are displayed in a graphical format, providing the user with accurate nuclear thermal atmospheric transmittance data. GRA

N85-32554# KLD Associates, Inc., Huntington, N. Y.

ROBUST DETECTION AND CLASSIFICATION OF REGIONAL SEISMIC SIGNALS USING A TWO MODE/TWO STAGE CASCADED ADAPTIVE ARMA (CAARMA) MODEL Final Report, 15 Jul. 1983 - 14 Jul. 1984

B. Schnitta-Israel Mar. 1985 169 p

(Contract F49620-83-C-0137; ARPA Order 4787; AF Proj. 4787) (AD-A154710; KLD-TR-159; AFOSR-85-0395TR) Avail: NTIS HC A08/MF A01 CSCL 17/10

The objective of this contract was to tailor TRAPS (Transient Acoustic Processing System) to the seismic event monitoring application thus providing a powerful tool for the nuclear monitoring problem. The TRAPS is a three stage process. Stage one is a hybrid adaptive filter designed to perform noise elimination on each receiver component. This is beamformed and input into stage two which performs signal enhancement. Information resulting from stage one/two is used in stage three to calculate the location and classification of the detected event. While the original TRAPS succeeded in doubling the range of detection, study it did so with a standard beamformer. Task 1 was to ascertain if an adaptive beamformer (AB) incorporated into TRAPS would produce any gains. It is determined that TRAPS' Stage One followed by a standard beamformer was superior to an AB, yet an AB strategical-

ly placed between TRAPS' stage one and stage two provided some processing gain. GRA

N85-32555# Royal Norwegian Council for Scientific and Industrial Research, Kjeller.
THE NORWEGIAN SEISMIC ARRAY (NORSAR) Semiannual Technical Summary, 1 Apr. - 30 Sep. 1984 on Phase 3
L. B. Loughran Nov. 1984 74 p
(Contract F08606-84-C-0002; ARPA Order 1483)
(AD-A154751; NORSAR-CONTRIB-350) Avail: NTIS HC A04/MF A01 CSCL 17/10

The Norwegian Seismic Array (NORSAR) Detection Processing System operated during the period 1 April - 30 September 1984 with an average up time of 95.1%. A total of 2160 seismic events were reported in this period. A seismic waveform injection technique has been developed and applied to deep events in the Fiji Islands region. Preliminary results show no compelling evidence for significant deviations from the double couple mechanism; and the data are consistent with a stress drop in the range 10-100 bars. A new method for dynamic ray tracing is being developed, and has been tested against simple analytical models. An investigation of optimum data processing schemes for regional arrays has shown the need for operating over a relatively wide band of frequencies (2-8 Hz) in order to ensure adequate SNR for various signal paths (oceanic, mobile cratonic belt, shield). SNR gains of 2-4 dB (up to about 5 Hz) relative to conventional beamforming can be obtained using optimum weighting, whereas a simplified scheme of 0/1 weighting gives 1-2 dB less gain. GRA

N85-32556# Mission Research Corp., Santa Barbara, Calif.
EXPERIMENTAL AND ANALYTIC CHARACTERIZATION OF NONLINEAR SEISMIC ATTENUATION Final Report, 21 Mar. 1984 - 20 Mar. 1985
G. D. McCartor and W. R. Wortman 20 Mar. 1985 85 p
(Contract F49620-84-C-0049; ARPA Order 4397)
(AD-A154760; MRC-R-900) Avail: NTIS HC A05/MF A01 CSCL 08/11

In order to assess the existence and impact of mild nonlinear contributions to attenuation of seismic signals from underground explosions, data from the test SALMON have been studied. It's found that the moderate strain regime (epsilon approx. 10 to the third power) data are internally consistent with an attenuation function, Q, which is independent of amplitude over more than an order magnitude. However the attenuation is much greater than that found from small strain measurements in different experiments. Nonlinear constitutive relations are considered which allow an analytic solution for the expected transition to linear small strain behavior. GRA

N85-32557# Wisconsin Univ., Madison. Mathematics Research Center.
ON THE LIMITING CONFIGURATION OF INTERFACIAL GRAVITY WAVES Technical Summary Report
R. E. L. Turner and J.-M. VandenBroeck Mar. 1985 21 p
(Contract DAAG29-80-C-0041; Grants NSF MCS-82-00406; NSF MCS-80-01960)
(AD-A154821; MRC-TSR-2800) Avail: NTIS HC A02/MF A01 CSCL 08/5

Progressive gravity waves at the interface between two unbounded fluids are considered. The flow in each fluid is taken to be potential flow. The problem is converted into a set of integro-differential equations, reduced to a set of algebraic equations by discretization, and solved by Newton's method together with parameter variation. Meiron and Saffman's calculations showing the existence of overhanging waves are confirmed. However, the present calculations do not support Saffman and Yuen's conjecture that the waves are geometrically limited (i.e., that solutions exist until the interface intersects itself). It is proposed that along a solution branch starting with sinusoidal waves of small amplitude, one reaches solutions with vertical streamlines and then overhanging waves. Continuing on this branch one returns to nonoverhanging waves and thence back toward a wave with vertical streamlines. It is suggested that this succession of patterns and accompanying oscillation in wave characteristics is repeated indefinitely. Graphs of the results are included. GRA

N85-32558# Air Force Geophysics Lab., Hanscom AFB, Mass.
APPLICATION OF SATELLITE ACCELEROMETER DATA TO IMPROVE DENSITY MODELS Environmental Research Papers
F. A. Marcos 9 Aug. 1984 52 p
(AF Proj. 6690)
(AD-A154904; AFGL-TR-84-0211; AFGL-ERP-887) Avail: NTIS HC A04/MF A01 CSCL 04/1

Atmospheric density measurements obtained by the satellite accelerometer experiment provide data over a wide range of solar and geophysical conditions. These results are used in a preliminary evaluation of several atmospheric models. The model accuracies are compared by their mean values and standard deviations relative to the accelerometer data. Sources of model uncertainties and problems in reducing them are described. Long-term programs involving coordinated measurements, analyses of available data and theoretical studies are required along with development of more accurate indicators of solar and geomagnetic activity before models can show significant improvement. GRA

N85-32559# Emmanuel Coll., Boston, Mass.
EQUITORIAL SCINTILLATIONS: ADVANCES SINCE ISEA-6
S. Basu Hanscom AFB, Mass. AF Geophysics, Mass. Jan. 1985 49 p
(Contract F19628-84-K-0003)
(AD-A154962; AFGL-TR-85-0014; SR-1) Avail: NTIS HC A03/MF A01 CSCL 04/1

Since the last equatorial aeronomy meeting in 1980, our understanding of the morphology of equatorial scintillations has advanced greatly due to more intensive observations at the equatorial anomaly locations in the different longitude zones. The unmistakable effect of the sunspot cycle in controlling irregularity belt width and electron concentration responsible for strong scintillation in the GHz range has been demonstrated. The fact that night-time F-region dynamics is an important factor in controlling the magnitude of scintillations has been recognized by interpreting scintillation observations in the light of realistic models of total electron content at various longitudes. A hypothesis based on the alignment of the solar terminator with the geomagnetic flux tubes as an indicator of enhanced scintillation occurrence and another based on the influence of a transequatorial thermospheric neutral wind have been postulated to describe the observed longitudinal variation. GRA

N85-32560# Ohio State Univ., Columbus. Dept. of Geodetic Science and Surveying.
UPWARD CONTINUATION OF SURFACE GRAVITY ANOMALIES
J. Y. Cruz and P. Laskowski Hanscom AFB, Mass. AF Geophysics Lab. Dec. 1984 119 p
(Contract F19268-82-K-0022)
(AD-A154973; OSU-DGSS-360; AFGL-TR-84-0331; SR-8) Avail: NTIS HC A06/MF A01 CSCL 08/5

Investigations on the upward continuation of gravity anomalies given on the surface of the Earth's visible topography are reported. Results are compared for three upward continuation procedures: first, the direct Poisson integration of the original terrain-uncorrected surface anomalies; second, the direct Poisson integration of terrain-corrected (i.e., Faye) surface anomalies; and third, the so-called indirect method. In the indirect method the original anomaly field is basically split into three frequency ranges that are then modeled separately: the low frequencies are modeled by spherical harmonics; the medium frequencies are modeled by Poisson integration of residual surface anomalies with long-wavelength terrain correction applied; and the high frequencies are modeled by prism integration of the gravitational effects of certain shallow topographic masses of assumed constant density. GRA

N85-32561# Atmospheric and Environmental Research, Inc., Cambridge, Mass.
THE DIURNAL VARIATION OF THE NEUTRAL SODIUM SPECIES IN THE UPPER ATMOSPHERE: A MODEL STUDY
J. M. Rodriguez, M. K. W. Ko, and N. D. Sze 1 Aug. 1984 30 p
(Contract F19628-83-C-0123)
(AD-A154988; AFGL-TR-84-0204; SR-1) Avail: NTIS HC A03/MF A01 CSCL 04/1

A study is made to calculate the diurnal behavior of the neutral sodium species (Na, NaO, NaO2, and NaOH) in the mesosphere using a one-dimensional photochemical model. The calculated results for Na are compared with available observations. The model results show that NaO2 is an important reservior for the sodium species in the atmosphere, and that the diurnal variation of Na in the mesosphere is, to a large extent, determined by the diurnal behavior of atomic oxygen. The role of NaOH as a temporary reservior for sodium and its possible effect on stratospheric chlorine chemistry remains unclear, as there is insufficient information from observation of Na to determine the rate for the atmospheric production of NaOH. GRA

N85-32562# SRI International Corp., Menlo Park, Calif.
CHARACTERISTICS AND SOURCES OF E-REGION IONIZATION IN THE CONTINUOUS AURORA Final Report, 15 Dec. 1982 - 30 Sep. 1984
R. M. Robinson, J. D. Kelly, and R. R. Vondrak Hanscom AFB, Mass. AF Geophysics Lab. Oct. 1984 37 p
(Contract F19628-83-C-0001)
(AD-A155018; SRI-ESU-5401; AFGL-TR-84-0249) Avail: NTIS HC A03/MF A01 CSCL 04/1

The continuous aurora is defined as E-region ionization that is steady in time and uniformly distributed over a large portion of the auroral oval. We have studied the characteristics and sources of ionization in the continuous aurora using data from the Chatanika radar and the DMSP AND NOAA satellites. The predominant source of ionization in the continuous aurora is precipitating electrons. The energy distribution of these energetic electrons is approximately Maxwellian. Satellite measurements of electron fluxes can be used to infer the ionospheric electron density along the path of the satelllite in the altitude range 90 to 160 km. However, these calculations underestimate the actual electron density when other ionization sources are present. Precipitating protons, in particular, can occasionally produce ionization comparable to that produced by precipitating electrons. Measurements of proton fluxes measured by the NOAA 6 satellite were used to estimate the ionization produced by protons. These estimates were compared with the results of measurements made simultaneously by the Chatanika radar. Calculations based on linear transport theory were found to reproduce the observed profiles fairly well. In sunlit conditions photoioniaztion can also produce continuous auroral E region ionization. Chatanika radar data were used to examine the dependence of this source on solar zenith angle and solar flux. GRA

N85-32563# Naval Postgraduate School, Monterey, Calif.
DESIGN OF A FREESTANDING NOISE MEASUREMENT AND RECORDING SYSTEM TO PREDICT THE INTENSITY AND LOCATION OF ELECTROMAGNETIC RADIATION FROM EARTHQUAKES M.S. Thesis
M. V. Ross Dec. 1984 83 p
(AD-A155070) Avail: NTIS HC A05/MF A01 CSCL 08/11

The design, construction, and testing of a freestanding radio frequency (RF) noise measurement and recording system in the 30 MHz and 150 MHz range is presented. Placement of the system along the San Andreas fault to permit the establishment of a correlation between increased background RF noise to earthquake fault activity for potential as an earthquake prediction tool is described. GRA

N85-32564# Naval Research Lab., Washington, D. C.
NEWTON'S METHOD AS A DYNAMICAL SYSTEM: GLOBAL CONVERGENCE AND PREDICTABILITY Memorandum Report, 15 Sep. 1983 - 15 Sep. 1984
R. G. Holt and I. B. Schwartz 13 May 1985 16 p
(AD-A155170; NRL-MR-5536) Avail: NTIS HC A02/MF A01 CSCL 12/1

Newton's method as an iterative scheme to compute both unstable and stable fixed points of a discrete dynamical system is considered. It is shown for Newton iterations that the basins of attraction are intertwined in a complicated manner. This complex structure appears to be fractal, and its dimension is estimated. Consequences of predictability for the final state are given in terms of imprecision in the initial data. GRA

N85-32565# Massachusetts Inst. of Tech., Cambridge. Dept. of Earth Atmospheric and Planetary Sciences.
DEVELOPMENT OF ULTRASONIC MODELING TECHNIQUES FOR THE STUDY OF CRUSTAL INHOMOGENEITIES
J. T. Bullitt and M. N. Toksoz Aug. 1984 37 p
(Contract F19628-83-K-0027)
(AD-A155206; AFGL-TR-84-0227; SR-1) Avail: NTIS HC A03/MF A01 CSCL 08/11

The effects of topographic features on Rayleigh wave propagation and scattering are investigated in the laboratory using three-dimensional ultrasonic models. The effects of different topographic features on Rayleigh wave transmission and scattering are examined as a function of wavelength and of angle of incidence. In general, backscattered or reflected Rayleigh waves are small compared to transmitted waves. A significant fraction of the Rayleigh wave energy is scattered into body waves. Transmission and reflection coefficients transmitted or reflected energy scattered into body wave ranges from more than 90% at normal incidence to about zero at near-grazing incidence. At each angle, transmission coefficients vary strongly with frequency. Because of frequency-dependent phase shifts, the transmitted and reflected waves are distorted. The effect of the steps on wave propagation is demonstrated by convolving synthetic dispersed wave trains with the impulse response of the scale models. The ocean-continent margin of the western United States is modelled as a 60 deg ramp scaled to 60 km height. The Tibetan Plateau is modeled as a broad mesa scaled up to 40 km height. In both models the azimuthal dependence of transmitted Rayleigh waves is similar to that observed at WWSSN stations for Rayleigh waves crossing the modeled terrestrial structures. GRA

N85-32566# Ohio State Univ., Columbus. Dept. of Geodetic Science and Surveying.
SPLINES. THEIR EQUIVALENCE TO COLLOCATION
H. Sonkel Aug. 1984 60 p
(Contract F19628-82-K-0017)
(AD-A155250; OSU/DGSS-357; AFGL-TR-84-0215; SR-6) Avail: NTIS HC A04/MF A01 CSCL 12/1

The application of splines in geodesy was mainly restricted to the solution of one-dimensional problems like interpolation, differentiation, approximation, solution of differential equations, etc. Two-dimensional splines turned out to be an adequate tool for the representation of smooth surfaces based on grided data. The purpose of this paper is to present splines on the real line, on the circle, on the sphere, and on the two-dimensional plane in a common and simple framework: The Green's function and the frequency domain method. Splines of arbitrary degree, no matter what their domain of definition is, are shown to be recursively related to each other by convolutions of Green's functions. The close relation (and little difference, if any) between spline and collocation solutions is demonstrated. GRA

N85-32567# Boston Coll., Chestnut Hill, Mass. Space Data Analysis Lab.
IONOSPHERIC ELECTRON DENSITY PROFILE AND RELATED STUDIES Final Report, 1 Oct. 1980 - 15 Jul. 1984
B. Basu, D. T. Decker, J. M. Retterer, and P. M. Bakshi 15 Aug. 1984 74 p
(Contract F19628-81-K-0009)
(AD-A155257; AFGL-TR-84-0257) Avail: NTIS HC A04/MF A01 CSCL 04/1

We have studied photo-ionization of the neutral gas by

photons in the extreme ultraviolet (EUV) region of the solar spectrum along with the various particle-particle collisional processes that determine the energy dependence of the photoelectron flux. We have also studied the effects of plasma instabilities in determining the photoelectron energy spectrum in the 2-6 eV energy range. We describe a series of case studies, modeling the EDP(Electron Density Profile) using first-principle calculations and comparing the results to a variety of direct measurements. For cases in which simultaneous airflow emission measurements are available, we evaluate the emissions predicted by our model EDP and compare with the observed emissions. We have addressed the problem of specifying the flux incident on the atmosphere with a calculation of the magnetospheric loss-cone population resulting from pitch-angle diffusion. In an effort to describe the phenomena of ion conics, we have also studied both the means by which turbulence can be caused by precipitating electrons and the way in which the turbulence can accelerate ionospheric ions, using particle plasma simulation techniques. A simplified analysis shows no dependence upon beam current for the spherical geometry and a weak dependence for the cylindrical case. GRA

N85-32568# Aerospace Corp., El Segundo, Calif. Lab. Operations.
TRAPPING OF ION CONICS BY DOWNWARD PARALLEL ELECTRIC FIELDS
D. J. Gorney, Y. T. Chiu, and D. R. Croley 1 May 1985 29 p
(Contract F04701-83-C-0084)
(AD-A155306; TR-0084A(5940-05)-1; SD-TR-85-13) Avail: NTIS HC A03/MF A01 CSCL 04/1

Several examples of upflowing field-aligned electrons at altitudes between 1000 and 1500 km at high latitudes have been reported recently. The velocity-space distributions of these electrons suggest that they were accelerated out of the ionosphere by downward parallel electric fields, and parallel potential drops of a few tens to a few hundred volts over the altitude range 1000-6000 km are implied. The electron beams are associated with ion conics. Data from electrostatic analyzers onboard the S3-3 satellite show that ion conics can be trapped at low altitude by the downward electric field. Evidence for the parallel electric field is obtained not only from observations of upflowing electron beams but also from observations of retardation of downflowing electrons and local acceleration of downflowing ions. The inferred parallel electric fields have magnitudes large enough to locally balance the magnetic mirror force on perpendicular ion conics in the few hundred eV energy range. This electrostatic trapping has important consequences for wave heating of ion conics since it extends the residence time of ions in the heating region. It is demonstrated that this multi-pass heating mechanism leads to perpendicular ion heating far in excess of that predicted by present theories of ion conic heating. GRA

N85-32569# Centre National de la Recherche Scientifique, Verrieres-Le Buisson (France). Service d'Aeronomie.
[ACTIVITIES REPORT OF THE AERONOMY DEPARTMENT] Annual Report, 1983-1984 [RAPPORT D'ACTIVITE, 1983-1984]
1984 305 p refs In FRENCH
(G-774-1984) Avail: NTIS HC A14/MF A01

Irradiation climatology; stratospheric photochemistry; a Rayleigh lidar study of middle atmosphere structure; physics and dynamics of the atmosphere; upper atmosphere studies; experiments on Spacelab; solar system study from space; infrared astrophysics; and solar physics are discussed. Author (ESA)

N85-32358*# Arizona Univ., Tucson. Dept. of Geosciences.
A NEW GLOBAL GEOMORPHOLOGY? Abstract Only
Victor R. Baker *In* NASA. Goddard Space Flight Center Global Mega-Geomorphology Jul. 1985 p 9 (For primary document see N85-32357 21-42)
Avail: NTIS HC A07/MF A01 CSCL 08G

N85-32359*# Manchester Univ. (England). Faculty of Arts (Physical Geography).
GLOBAL GEOMORPHOLOGY
Ian Douglas *In* NASA. Goddard Space Flight Center Global Mega-Geomorphology Jul. 1985 p 10-17 refs (For primary document see N85-32357 21-42)
Avail: NTIS HC A07/MF A01 CSCL 08G

N85-32361*# George Mason Univ., Fairfax, Va. Dept. of Public Affairs (Geography).
GEOMORPHOLOGICAL SIMILARITY AND UNIQUENESS
Robert S. Hayden *In* NASA. Goddard Space Flight Center Global Mega-Geomorphology Jul. 1985 p 21-22 (For primary document see N85-32357 21-42)
Avail: NTIS HC A07/MF A01 CSCL 08G

N85-32363*# Princeton Univ., N. J. Dept. of Geological and Geophysical Sciences.
SOME OBSERVATIONS ON PALEOGEOMORPHOLOGY
Sheldon Judson *In* NASA. Goddard Space Flight Center Global Mega-Geomorphology Jul. 1985 p 27-28 refs (For primary document see N85-32357 21-42)
Avail: NTIS HC A07/MF A01 CSCL 08G

N85-32364*# Adelaide Univ. (Australia). Dept. of Geography.
ANCIENT LANDSCAPES: THEIR NATURE AND SIGNIFICANCE FOR THE QUESTION OF INHERITANCE
C. R. Twidale *In* NASA. Goddard Space Flight Center Global Mega-Geomorphology Jul. 1985 p 29-40 refs (For primary document see N85-32357 21-42)
Avail: NTIS HC A07/MF A01 CSCL 08G

N85-32365*# Chevron Oil Field Research Co., La Habra, Calif.
GEOMORPHOLOGY, TECTONICS, AND EXPLORATION Abstract Only
Floyd F. Sabins *In* NASA. Goddard Space Flight Center Global Mega-Geomorphology Jul. 1985 p 41 (For primary document see N85-32357 21-42)
Avail: NTIS HC A07/MF A01 CSCL 08G

N85-32366*# New Mexico Inst. of Mining and Technology, Socorro.
MEGAGEOMORPHOLOGY AND NEOTECTONICS
Laurence H. Lattman *In* NASA. Goddard Space Flight Center Global Mega-Geomorphology Jul. 1985 p 42-43 (For primary document see N85-32357 21-42)
Avail: NTIS HC A07/MF A01 CSCL 08G

N85-32367*# Cornell Univ., Ithaca, N.Y. Dept. of Geological Sciences.
ANDREAN EXAMPLES OF MEGA-GEOMORPHOLOGY THEMES
Arthur L. Bloom *In* NASA. Goddard Space Flight Center Global Mega-Geomorphology Jul. 1985 p 44-45 (For primary document see N85-32357 21-42)
Avail: NTIS HC A07/MF A01 CSCL 08G

N85-32370*# Fort Lewis A&M Coll., Durango, Colo. Dept. of Geology.
ONE APPLICATION OF MEGA-GEOMORPHOLOGY IN EDUCATION
Robert W. Blair, Jr. *In* NASA. Goddard Space Flight Center Global Mega-Geomorphology Jul. 1985 p 56-58 refs (For primary document see N85-32357 21-42)
Avail: NTIS HC A07/MF A01 CSCL 08G

N85-32372*# Geological Survey, Reston, Va.
GEOMORPHIC CLASSIFICATION OF ICELANDIC AND MARTIAN VOLCANOES: LIMITATIONS OF COMPARATIVE PLANETOLOGY RESEARCH FROM LANDSAT AND VIKING ORBITER IMAGES
Richard S. Williams, Jr. *In* NASA. Goddard Space Flight Center Global Mega-Geomorphology Jul. 1985 p 62-63 (For primary

document see N85-32357 21-42)
Avail: NTIS HC A07/MF A01 CSCL 08K

N85-32376*# Miami Univ., Oxford, Ohio. Dept. of Geology.
QUANTITATIVE ANALYSIS IN MEGAGEOMORPHOLOGY
Larry Mayer *In* NASA. Goddard Space Flight Center Global Mega-Geomorphology Jul. 1985 p 79-80 (For primary document see N85-32357 21-42)
Avail: NTIS HC A07/MF A01 CSCL 08G

N85-32382*# National Aeronautics and Space Administration. Goddard Space Flight Center, Greenbelt, Md.
GLOBAL GEOMORPHOLOGY: REPORT OF WORKING GROUP NUMBER 1
!an Douglas (Manchester Univ., England) *In its* Global Mega-Geomorphology Jul. 1985 p 101-104 (For primary document see N85-32357 21-42)
Avail: NTIS HC A07/MF A01 CSCL 08G

N85-32711*# California Univ., Santa Barbara. Dept. of Geology.
PRECAMBRIAN EVOLUTION AND THE ROCK RECORD
Stanley Awramik *In* NASA, Washington The Global Sulfur Cycle Jul. 1985 p 5-8 (For primary document see N85-32710 21-51)
Avail: NTIS HC A14/MF A01 CSCL 08G

N85-32716*# National Aeronautics and Space Administration. Ames Research Center, Moffett Field, Calif.
CARBON ISOTOPE GEOCHEMISTRY AND GEOBIOLOGY
David DesMarais *In* NASA, Washington The Global Sulfur Cycle Jul. 1985 p 19-25 refs (For primary document see N85-32710 21-51)
Avail: NTIS HC A14/MF A01 CSCL 13B

N85-32720*# University of South Florida, St. Petersburg. Dept. of Marine Science.
CARBON AND SULFUR CYCLING THROUGH GEOLOGIC TIME Abstract Only
Robert M. Garrels *In* NASA, Washington The Global Sulfur Cycle Jul. 1985 p 40-41 refs (For primary document see N85-32710 21-51)
Avail: NTIS HC A14/MF A01 CSCL 08G

N85-32723*# Oregon Univ., Eugene. Dept. of Geology.
GEOLOGY AND GEOCHEMISTRY OF SULFIDE AND SULFATE DEPOSITION Abstract Only
William T. Holser *In* NASA, Washington The Global Sulfur Cycle Jul. 1985 p 50-54 refs (For primary document see N85-32710 21-51)
Avail: NTIS HC A14/MF A01 CSCL 08G

N85-32958# Joint Publications Research Service, Arlington, Va.
BEAM DIFFUSION IN LINEAR IONOSPHERIC LAYER Abstract Only
V. D. Gusev and O. K. Vlasaova *In its* USSR Rept.: Phys. and Math. (JPRS-UPM-85-004) 17 Jun. 1985 p 79 Transl. into ENGLISH from Vestn. Mosk. Univ., Fiz., Astron., v. 25, no. 5, Sep. - Oct. 1984 p 74-81 (For primary document see N85-32860 21-70)
Avail: NTIS HC A06/MF A01

47 METEOROLOGY AND CLIMATOLOGY

Includes weather forecasting and modification.

N85-32570*# South Dakota School of Mines and Technology, Rapid City.
RAIN VOLUME ESTIMATION OVER AREAS USING SATELLITE AND RADAR DATA Semiannual Report, 1 Jan. - 30 Jun. 1985
Andre A. Doneaud and Thomas H. VonderHaar 30 Jun. 1985 22 p refs Prepared in cooperation with Colorado State Univ., Fort Collins
(Grant NAG5-386)
(NASA-CR-176050; NAS 1.26:176050) Avail: NTIS HC A02/MF A01 CSCL 04B

The feasibility of rain volume estimation over fixed and floating areas was investigated using rapid scan satellite data following a technique recently developed with radar data, called the Area Time Integral (ATI) technique. The radar and rapid scan GOES satellite data were collected during the Cooperative Convective Precipitation Experiment (CCOPE) and North Dakota Cloud Modification Project (NDCMP). Six multicell clusters and cells were analyzed to the present time. A two-cycle oscillation emphasizing the multicell character of the clusters is demonstrated. Three clusters were selected on each day, 12 June and 2 July. The 12 June clusters occurred during the daytime, while the 2 July clusters during the nighttime. A total of 86 time steps of radar and 79 time steps of satellite images were analyzed. There were approximately 12-min time intervals between radar scans on the average. B.W.

N85-32571*# Wisconsin Univ., Madison. Space Science and Engineering Center.
DIAGNOSTICS OF SEVERE CONVECTION AND SUBSYNOPTIC SCALE AGEOSTROPHIC CIRCULATIONS Final Report, 1 Jun. 1979 - 14 Sep. 1984
22 Jul. 1985 6 p refs
(Contract NAS8-33222)
(NASA-CR-171581; NAS 1.26:171581) Avail: NTIS HC A02/MF A01 CSCL 04B

Diagnostics of severe convection and subsynoptic scale ageostrophic circulations are reported. Mesoscale circulations through forcing of ageostrophic motion by adiabatic, diabatic and frictional processes were studied. The development and application of a hybrid isentropic sigma coordinate numerical model was examined. The numerical model simulates mesoscale ageostrophic circulations associated with propagating jet streaks and severe convection. A complete list of publications and these completed through support of the NASA severe storms research project is included. E.A.K.

N85-32572*# Atmospheric and Environmental Research, Inc., Cambridge, Mass.
GENERATION OF AVAILABLE POTENTIAL ENERGY AND THE ENERGY CYCLE DURING THE GLOBAL WEATHER EXPERIMENT Final Report, year 1
David A. Salstein and Richard D. Rosen Feb. 1985 32 p refs
(Contract NAS5-27745)
(NASA-CR-175301; NAS 1.26:175301) Avail: NTIS HC A03/MF A01 CSCL 04B

Two parallel sets of analyses, which in one case included and in the other omitted data observed by satellite based and other FGGE special observing systems are examined. The results of our previous work is extended in two separate, but not unrelated, ways. First, from these two parallel analyses, which are labeled FGGE (full FGGE system) and NOSAT (satellite omitted), it was discovered that the two sets of fields were quite close over much of the globe. Locally the influence of satellite based systems led to some differences, particularly over the Southern Hemisphere Oceans. The diabatic heating fields generated by the GLA FGGE analysis was also examined. From these fields, one can ascertain the role of total diabatic heating and of the various diabatic heating components in the atmospheric energy cycle, in particular in the generation of available potential energy. Author

N85-32573# National Severe Storms Lab., Norman, Okla.
THUNDERSTORM PHENOMENA AND WEATHER RADAR SCANNING STRATEGIES Final Report
Steve Vasiloff, Michael Istok, and R. J. Doviak Dec. 1984 19 p refs
(Contract DTFA01-80-Y-10524)
(DOT/FAA/PM-85/14) Avail: NTIS HC A02/MF A01

Examination of several thunderstorm cells' maximum reflectivity and updraft speed shows that growth rates of maximum reflectivity factor ranged from 4 to 7 dBZ/mn and those of maximum updraft speed ranged from 3 to 7 m/s/min Times of occurrence of

maximum values of reflectivity, storm height, and updraft speed are compared. The Air Force Geophysics Laboratory's storm analysis and tracking algorithms are used to evaluate interlaced and continguous (non-interlaced) scanning strategies. Eleven cell attributes are determined and compared for each strategy. The differences between attribute values obtained from successive contiguous scans are about the same as the differences between values obtained from interlaced and contiguous scans for the same time period. Thus, an interlaced scanning strategy may allow detection of some hazards (e.g., low altitude shear) in one-half the time expected using the proposed NEXRAD contiguous scanning strategy without significantly compromising the evaluation of storm attributes. Although these findings are incomplete because of the smalldata sample they suggest that the NEXRAD radar can provide more timely warnings of low altitude weather hazards in the terminal area if an interlaced scan strategy is used. Author

N85-32574# Fraunhofer-Inst. fuer Atmosphaerische Umweltforschung, Garmisch-Partenkirchen (West Germany).
VISIBILITY AND VERTICAL STRUCTURE MEASUREMENTS IN SOUTHERN GERMANY Final Technical Report, Dec. 1982 - Dec. 1984
R. Reiter, W. Carnuth, and W. Funk Dec. 1984 210 p
(Contract DAJA45-83-C-0023; DA Proj. 1T1-61102-BH-57)
(AD-A154714) Avail: NTIS HC A10/MF A01 CSCL 04/2

The objective was to obtain a body of data describing the vertical profile of the extinction coefficient of the lower atmosphere under a broad range of atmospheric conditions in Southern Germany. The lidar system used included both a ruby and neodymium-glass laser, both used with and without frequency doubling, allowing alternate measurements in wavelengths 347, 530, and 1060 nm. The received backscattered signals were recorded in such a way that almost-real time corrections for background luminosity, squared range, laser output, and input sensitivity could be made. Klett's inversion method was mainly used for the evaluation of the profiles. Conventional meteorological data were obtained in parallel, including aerosol characterization with Knollenberg counters. The report included graphic presentations of a number of data sets. Author (GRA)

N85-32575# Air Force Systems Command, Wright-Patterson AFB, Ohio. Foreign Technology Div.
METEOROLOGICAL WEAPONS
Z. Wei 13 Mar. 1985 8 p Transl. into ENGLISH from Kexue Shiyan (China), no. 4, 1984 p 35-36
(AD-A154735; FTD-ID(RS)T-1483-84) Avail: NTIS HC A02/MF A01 CSCL 04/2

Meteorological weapons are no more than military application of meteorological science and technology. In more detail, it is the military application of changing weather artifically. The reason why weather can be changed artificially is due to unstable factors (such as thermal factors and dynamical factors) in the atmosphere. What are such unstable factors? They can be illustrated through an example of firing a gun: Before shooting, the bullet is loaded, now consider it at the time when the bullet is being shot. Only after one click the bullet will be moving very rapidly, the instability of the atmosphere is just like that of a bullet ready to be shot. Only a small amount of energy can trigger a large amount of energy transfer. The result of such an energy transfer in the atmosphere will lead to changes of weather and climate in certain areas. If people have a certain purpose in their mind they can add a certain amount of energy to the atmosphere and change the weather in the direction that they expect. This is the basic principle behind changing weather artificially. GRA

N85-32576# University of Eastern Washington, Cheney.
PALEOENVIRONMENTAL INVESTIGATIONS AT SEED CAVE (WINDUST CAVE H-45FR46), FRANKLIN COUNTY, WASHINGTON Final Report
R. S. Thompson 1985 61 p
(Contract DACW68-83-M-5624)
(AD-A154777; Rept-100-41) Avail: NTIS HC A04/MF A01 CSCL 04/2

Investigations were conducted at Seed Cave to recover paleoenvironmental data being destroyed by relic collectors, Excavations exposed a profile over 5.5m in depth. Radiocarbon and stratigraphic evidence, combined with floral and faunal remains, indicates changes in local environment during the last 9000 years: 9000-6400 B.P. relatively cooler and moister; 6400-4100 B.P. considerably drier; 4100-3500 B.P. relatively moister conditions based on faunal and sediment data while the pollen spectra indicates conditions more arid than at present. Data for the last 3500 years indicate no substantial environmental changes around Seed Cave. GRA

N85-32577# Systems and Applied Sciences Corp., Vienna, Va.
AUTOMATED CELL DETECTION AS A MESOCYCLONE PRECURSOR TOOL Final Report, Oct. 1982 - Sep. 1984
F. I. Harris and P. J. Petrocchi Hanscom AFB, Mass. AF Geophysics Lab. 5 Oct. 1984 31 p
(Contract F19628-82-C-0023)
(AD-A154952; AFGL-TR-84-0266; AFGL-ERP-891) Avail: NTIS HC A03/MF A01 CSCL 04/2

Automated cell detection in radar observations of convective storm complexes has been explored as a severe storm indicator. Six-dB peaks were detected in the radar reflectivity fields and their characteristics were monitored as a function of time. It was found in a severe tornadic storm that the number of cells and the average intensity of the cells had trends that appear to be characteristic of super-cell storms with these trends being identifiable at least 45 min before the touchdown of the first tornado and 90 min before the touchdown of a maxi tornado. None of these trends could be detected in a storm system that produced only a funnel cloud. This second storm did produce a tornado vortex signature. It would appear that the peak detection algorithm has the potential of extending the warning period for severe weather associated with super-cell and for indicating the potential of extremely severe weather. Testing has been limited and therefore these results must be considered somewhat tentative.
Author (GRA)

N85-32578# Systems and Applied Sciences Corp., Vienna, Va.
REAL-TIME AUTOMATED DETECTION OF MESOCYCLONES AND TORNADO VORTEX SIGNATURES
J. G. Wieler Hanscom AFB, Mass. AF Geophys. Lab. 20 Oct. 1984 39 p
(Contract F19628-82-C-0023)
(AD-A154968; AFGL-TR-84-0282; SR-6) Avail: NTIS HC A03/MF A01 CSCL 04/2

An algorithm incorporating resolution-dependent shear and velocity thresholds for the detection of mesocyclones and tornado vortex signatures in real-time is presented. The algorithm identifies both cyclonic and anti-cyclonic shear areas, and characterizes them into six categories. Also, the three-dimensional average of each feature's rotational kinetic energy, momentum and horizontal and vertical extent are computed. Algorithm performance is discussed for four case studies. The results, verified by ground observations and output from the Tornado Vortex Signature algorithm, are very encouraging. GRA

N85-32579# Systems and Applied Sciences Corp., Monterey, Calif.
ACCURACY AND OPERATIONAL USE OF MEDIUM AND EXTENDED RANGE NUMERICAL ATMOSPHERIC FORECASTS: A REVIEW Final Report, Aug. 1983 - Feb. 1985
R. L. Elsberry, H. D. Hamilton, and P. A. Petit Feb. 1985 84 p
(Contract N00228-83-C-3101; AF Proj. 7W05)
(AD-A155027; NEPRF-CR-85-02) Avail: NTIS HC A05/MF A01 CSCL 04/2

The potential benefits of medium range (5-10 day) and extended range (10-15 day) atmospheric forecasts in support of the U.S. Navy are assessed. The present and likely near-future state of the art of medium range and extended range forecasting are surveyed, summarized, and related to specific operational requirements and applications of such forecasts. Conclusions regarding the required skill for longer-range forecasts are provided,

Several issues relating to forecast system at a central site, and to presentation, distribution and use of products, are presented.
Author (GRA)

N85-32580# Naval Postgraduate School, Monterey, Calif.
FORECASTING OF TROPICAL CYCLONE MOTION USING AN EOF (EMPIRICAL ORTHOGONAL FUNCTION) REPRESENTATION OF WIND FORCING M.S. Thesis
W. E. Wilson Dec. 1984 89 p
(AD-A155034) Avail: NTIS HC A05/MF A01 CSCL 04/2

Empirical Orthogonal Function (EOF) analysis is used to represent the environmental wind forcing of selected western North Pacific tropical cyclone tracks from 1979-1983. The EOF analysis is applied separately to the zonal and meridional wind components at 700, 400 and 250 mb on a 527-point grid with 288.7 km zonal and meridional spacing that is relocated with the storm center. The 527 EOF coefficients (for each level and component) are computed for a sample of 682 cases. The coefficient vectors are truncated to the first 35 coefficients based on a Monte Carlo selection criterion. These coefficients account for at least 82 percent of the variance in each field. The EOF coefficients, along with storm movement during the past 24 hours, position, date and intensity, are then used as potential predictors in a regression analysis forecast scheme for tropical cyclone motion. The EOF-based regression equations are tested on the dependent data cases. The mean 72-hour track forecast error is between 450 and 500 km. Therefore, it appears that this regression scheme has potential for operational applications. GRA

N85-32581# Naval Postgraduate School, Monterey, Calif.
AN EVALUATION OF DISCRETIZED CONDITIONAL PROBABILITY AND LINEAR REGRESSION THRESHOLD TECHNIQUES IN MODEL OUTPUT STATISTICS FORECASTING OF CLOUD AMOUNT AND CEILING OVER THE NORTH ATLANTIC OCEAN M.S. Thesis
M. H. Wooster Dec. 1984 188 p
(AD-A155100) Avail: NTIS HC A09/MF A01 CSCL 04/2

This thesis describes the application and evaluation of several statistical models in the forecasting of cloud amount and ceiling over coastal and open ocean areas of the North Atlantic Ocean. The focus of this study is to evaluate the applicability of previous Naval Postgraduate School model output statistics research in the area of horizontal marine visibility to the forecasting of cloud amount and ceiling over ocean areas. The models, including minimum probable error linear regression threshold techniques, maximum conditional probability and natural regression, utilize observed visibility data and model output parameters from the Navy Operational Global Atmospheric Prediction System (NOGAPS). Results show statistically similar results for the linear regression and maximum conditional probability models. Also included is the result of additional experimentation on the application of several measures of separability and cluster analysis to predictor selection. GRA

N85-32582# Naval Postgraduate School, Monterey, Calif.
PARAMETER ESTIMATION IN COMMUNICATION SYSTEM TRACKING SATELLITE OBSERVATIONS M.S. Thesis
V. A. Tsafaras Dec. 1984 83 p
(AD-A155137; AD-F630645) Avail: NTIS HC A05/MF A01 CSCL 17/2

The estimation of parameters from a satellite communication system is often through the use of Kalman filtering. In this work the location of the eye of a hurricane is estimated from satellite observation. A comparison with a posteriori meteorologist's analysis was attempted. An adaptive gating scheme was employed in the filter to accommodate manueuvers of the storm. The observations were at random intervals and also came from several different sources (aircraft and land based radar as well as satellite). GRA

N85-32583# Naval Postgraduate School, Monterey, Calif.
MEAN FLOW AND TURBULENCE IN COMPLEX TERRAIN M.S. Thesis
M. J. Buell Mar. 1985 271 p
(AD-A155138; AD-F630645) Avail: NTIS HC A12/MF A01 CSCL 04/2

Atmospheric models used to describe horizontal diffusion in the surface layer depend upon a detailed characterization of the mean flow and standard deviation of wind direction fluctuations (SD theta). Meteorological data were collected from 12 tower located across the coastal complex terrain of Vandenberg AFB, CA. from August 1983 to July 1984 in order to analyze these mean and turbulence parameters as a function of stability, time averaging, wind direction, wind speed, elevation and terrain. Three stability cases were chosen from Richardson Number criteria and found representative of specific flow regimes. SD theta was a function of stability with the largest values associated with the unstable (sea breeze) case and lower values with the stable (land breeze/drainage flow) and neutral (post-frontal) cases. All three stability cases showed varying degrees of SD theta dependence on time averaging, wind direction, wind speed, elevation, and terrain with greater time averaging dependence found in the unstable case, greater wind direction and terrain dependence noted in the stable case, and greater lower level height dependence found in both the stable and unstable cases. In contrast to most findings over homogeneous terrain, SD theta dependence on wind speed was found in all three stability cases with this dependence most important in the neutral case. GRA

N85-32584# Naval Postgraduate School, Monterey, Calif.
MESOSCALE FEATURES AND ATMOSPHERIC REFRACTION CONDITIONS OF THE ARCTIC MARGINAL ICE ZONE M.S. Thesis
J. A. McNitt Dec. 1984 129 p
(AD-A155139; AD-F630645) Avail: NTIS HC A07/MF A01 CSCL 04/1

This thesis summarizes the Marginal Ice Zone Experiment (MIZEX-83) conducted in the Arctic during the summer of 1983 and describes the mesoscale features and atmospheric refraction conditions. The three case studies examined are: warm air advection over dense pack ice causing strong elevated ducting and subrefraction; cold air advection over relatively open water causing shallow convection and normal refraction conditions; and large scale subsidence in the western quadrants of an anticyclone leading to super-refraction and weak ducting. Developing synoptic scale cyclones adjacent to the MIZEX-83 area often determined the airflow over the region. The observed large horizontal sea surface temperature gradients were the dominant forcing mechanisms on surface layer stability. Trapping layers associated with subsidence inversions can be located on satellite imagery by assuming that stratiform clouds form immediately below the inversion. Uniform cloud and refraction layers were not common during MIZEX-83 due to strong mesoscale variability. Factors affecting inversion height include subsidence and entrainment mixing. Bulk Richardson number value for locations over the open water and pack ice show significant variability in stability conditions across the MIZ. GRA

N85-32585# Schmitt (Rainer), Glashutten (West Germany).
INVESTIGATIONS OF MICRO-TURBULENCE IN THE BOTTOM OF THE BOUNDARY LAYER Interim Report
R. Schmitt Mar. 1985 23 p
(Contract DAJA45-83-C-0038)
(AD-A155148; AD-F630645; IR-3) Avail: NTIS HC A02/MF A01 CSCL 04/2

This third interim report deals with the second series of measurements in Western Germany. Data are presented for the period Jan. 1985 to March 1985: location STEINBACH (West Germany). GRA

N85-32586# Air Force Geophysics Lab., Hanscom AFB, Mass.
A SIMULATION OF WEATHER IN 3D SPACE Environmental Research Papers
I. I. Gringorten 16 Oct. 1984 35 p
(DA Proj. 667-0)
(AD-A155221; AFGL-TR-84-0267; AFGL-ERP-892) Avail: NTIS HC A03/MF A01 CSCL 04/2

A stochastic simulation process, known as the 3D-Boehm Sawtooth Wave model has been developed. It has greater versatility than previously applied models. For a real cloud cover, the input consists of the mean sky-cover and a scale parameter, depicted as a characteristic wavelength. The algorithm has been written and programmed to map the simulated clouds horizontally, or in vertical cross-section. Since the model requires climatology in the vertical, a procedure has been developed which takes the cumulative sky-cover as seen by a surface observer and produces estimates of mean cloudiness within any specified layer. GRA

N85-32587# Ophir Corp., Lakewood, Colo.
CIRCULATION ANALYSIS OF TWO SNOWSTORMS DURING THE SNOW-TWO PROGRAM Technical Report, 16 Jan. - 31 Aug. 1984
Y. L. Chen Sep. 1984 80 p
(Contract F19628-83-C-0130)
(AD-A155225; AFGL-TR-84-0255; SR-1) Avail: NTIS HC A05/MF A01 CSCL 04/2

In this study, the conditions during two snowstorm cases during SNOW TWO Project, 16-17 January and 23-24 January, 1984, were analyzed. In an effort to incorporate large-scale forcing, the kinematic method (so as to include the effects of latent heat release and convective transport was used to compute the large-scale vertical motion. This large-scale vertical motion computed, as well as other conditions studied for both cases, will provide useful information for the proper choice of initial conditions for future numerical simulations of cloud development. GRA

N85-32588# Dugway Proving Ground, Utah.
NOTES ON ATMOSPHERIC STABILITY, TURBULENCE, AND ITS MEASUREMENTS
C. A. Biltoft Mar. 1985 61 p
(AD-A155230; DPG-TR-85-204) Avail: NTIS HC A04/MF A01 CSCL 04/1

Modernization of Dugway's diffusion test capabilities include the procurement of state-of-the-art instrumentation and an upgrade in data collection methodology and modeling. Dispersion of a buoyant, passive plume is due to transport by mean atmospheric motions. Although K-theory and Gaussian diffusion equations are burdened by restrictive assumptions, these equations offer the most practical means of modeling the effects of turbulence on diffusing material. Turbulence occurs as vortex stretching in a sheared environment causes an energy cascade towards progressively smaller eddy sizes until viscous dissipation occurs. Direct turbulence measurements require an assortment of instrumentation due to the range of eddy sizes. Consequently, it is most economical to estimate turbulence from stability parameters and most models accept such turbulence estimators as input. The Obukhov Length, stability parameter obtained from principal turbulent *MSG DI4 drols processing-LAST input iGNORED ower profile data using flux-gradient relationships. LED scintillometers, acoustic sounders, radiometers, precision thermometers, and sonic anemometers are needed to upgrade Dugway's turbulence measurement capabilities. Data from these instruments will help define test go/no-go conditions, improve quality control, enhance posttest analysis capabilities, and provide improved input for diffusion modeling.
Author (GRA)

N85-32589# Systems and Applied Sciences Corp., Monterey, Calif.
MEDIUM RANGE ATMOSPHERIC FORECAST SYSTEM: EVALUATION REPORT Final Report, Aug. 1983 - Feb. 1985
P. A. Petit, H. D. Hamilton, and R. L. Elsberry Feb. 1985 82 p
(Contract N00228-83-C-3101; NR Proj. W05-13)
(AD-A155240; NEPRF-CR-85-04) Avail: NTIS HC A05/MF A01 CSCL 04/2

The Navy has little experience in evaluating the usefulness of numerical environmental predictions prepared for periods greater than 3 days. Recognizing this, the Naval Environmental Prediction Research Facility (NEPRF) embarked in 1983 in a project to develop a procedure which could establish the relevant accuracy and operational utility of a medium-range (5 to 10 day) atmospheric forecast system. The results of a comprehensive evaluation of the accuracy and utility--with respect to operational Navy applications--of medium range (5-7 day) atmospheric forecast system are presented. Several nonstandard, but operationally relevant, objective measures of forecast model skill are employed, along with more traditional measures. GRA

N85-32590# Scripps Institution of Oceanography, La Jolla, Calif. Visibility Lab.
A TRANSPORTABLE, MACHINE ORIENTED LIBRARY OF EUROPEAN SKY AND TERRAIN RADIANCE DISTRIBUTIONS WITH CONTEMPORARY RADIOMETRIC AND METEOROLOGICAL PROFILES Interim Report
R. W. Johnson and M. K. Oleinik Apr. 1984 32 p
(Contract F19628-82-C-0060)
(AD-A155254; SIO-REF-84-15; AFGL-TR-84-0096; SR-5) Avail: NTIS HC A03/MF A01 CSCL 04/2

A data set which contains nearly 500 arrays representing the measurements of visible spectrum sky and terrain radiance values first discussed in an earlier document has been organized into a readily transportable, machine readable library. A complementary data set including contemporary measurements of atmospheric volume scattering coefficients plus selected meteorological variables as a function of altitude has been included in a similar machine oriented format. The data base contents are described as are the storage tape formats and sample extraction procedures. Author (GRA)

N85-32591# Little (Arthur D.), Inc., Cambridge, Mass.
ABSORPTION AND SCATTERING PROPERTIES OF AEROSOLS OF AGGREGATED PARTICLES IN THE INFRARED SPECTRAL REGION Final Report, Apr. 1982 - Apr. 1985
J. R. Aronson, Simon, I., and E. M. Smith 30 Apr. 1985 34 p
(Contract DAAG29-82-C-0006)
(AD-A155475; ARO-17753.2-GS) Avail: NTIS HC A03/MF A01 CSCL 20/6

This report concerns the extension of a theory of particulate scattering to the difficult case of aggregated aerosols. Photoacoustic measurements of absorption and scattering in the infrared and visible spectral regions have been made for Silicon Dioxide and Carbon smokes to test the validity of the theory. The development of suitable screening materials for infrared radiation, particularly in the 3-5 and 8-13 micrometer regions is required by developments of modern infrared detection technology. Such smokescreen materials derive their value from either absorption or scattering phenomena or some combination of the two. Because scattering phenomena may be optimized with regard to wavelength of effective operation by suitable choice of particle size and refractive index, the corrollary is also true: viz. no one scattering material is likely to be equally valuable over all wavelengths. GRA

N85-32592# Naval Postgraduate School, Monterey, Calif.
THE EFFECTS OF SUBREFRACTIVE LAYERS AND ELEVATED DUCTS ON AIRBORNE RADAR AND ESM (ELECTRONIC SURVEILLANCE MEASURES) M.S. Thesis
D. D. Grau Mar. 1985 90 p
(AD-A155524) Avail: NTIS HC A05/MF A01 CSCL 17/9

This report is an investigation of the effects of anomalous propagation of radar waves, caused by subrefractive layers and elevated ducts, on aircraft radar performance and possible tactics. A test and evaluation of radar coverage for various environmental scenarios is conducted using the Integrated Refractive Effects Prediction System (IREPS) model. From the results of each scenario, a decision matrix is created and applied as an analysis tool for determining satisfactory flight profiles for a given mission. The findings are discussed for both a radiating and non-radiating aircraft perspective. Environmental data collected from the Mediterranean Sea and Northern Arabian Sea were analyzed and used to determine the test scenarios. GRA

N85-32593# Naval Postgraduate School, Monterey, Calif.
FORECASTING ATMOSPHERIC VISIBILITY OVER THE SUM-

MER NORTH ATLANTIC USING THE PRINCIPAL DISCRIMINANT METHOD M.S. Thesis
K. C. Elias Mar. 1985 113 p
(AD-A155537) Avail: NTIS HC A06/MF A01 CSCL 04/1

This thesis describes the application and evaluation of the Principal Discriminant Method (PDM) in the forecasting of horizontal visibility over selected physically homogeneous areas of the North Atlantic Ocean. The main focus is to propose a possible model output statistics (MOS) approach to operationally forecast visibility at the 00-hour model initialization time and the 24-hour and 48-hour model forecast projections, using as data the period 15 May to 7 July 1983. The technique involves the manipulation of observed visibility and the Fleet Numerical Oceanography Center's Navy Operational Global Atmospheric System (NOGAPS) model output parameters. Both two-and three-category visibility models were examined. The resulting zero-and one-class errors as well as the threat scores from the PDM model were compared with those obtained from maximum probability and natural regression studies. For the majority of the experiments performed, PDM was outperformed by the other techniques, although one trail run of an adjusted PDM technique gave results similar to those of the maximum probability techniques. GRA

N85-32594# Naval Postgraduate School, Monterey, Calif.
A NUMERICAL AND ANALYTICAL INVESTIGATION OF LEE CYCLOGENESIS Ph.D. Thesis
J. L. Hayes Mar. 1985 139 p
(AD-A155607) Avail: NTIS HC A07/MF A01 CSCL 04/1

The effect of topography on the evolution of a disturbance in a baroclinically unstable mean flow is studied using analytical and numerical simulations. In particular, dynamic mechanisms involved in cyclogenesis in the lee of long, meridional barriers similar to the Rocky Mountains are explored. The rapid growth observed in lee cyclogenesis is highly dependent on the superposition of a growing baroclinic wave with a steady, orographically forced wave of the same scale. As the baroclinic wave moves over the mountain, development is masked by the orographically-forced, high-pressure ridge. As it moves down the lee side of the mountain, the baroclinic wave appears to grow rapidly due to superposition with the forced, lee-side trough. Indications of enhanced, lee-side baroclinic instability are present in the numerical simulations, but the effect on wave development is minor compared to the effect of superposition. The rapid continuous-mode growth, which was demonstrated by Farrell (1982), is not observed in any of the simulations. GRA

N85-32595# Systems and Applied Sciences Corp., Monterey, Calif.
MEDIUM RANGE ATMOSPHERIC FORECAST SYSTEM: EVALUATION PLAN Final Report, Aug. 1983 - Feb. 1985
P. A. Petit, H. D. Hamilton, and R. L. Elsberry Feb. 1985 39 p
(Contract N00228-83-C-3101)
(AD-A155623; NEPRF-CR-85-03) Avail: NTIS HC A03/MF A01 CSCL 04/2

A plan for conducting a comprehensive evaluation of the accuracy and utility, with respect to operational Navy applications, of a medium range (5 to 10 day) atmospheric forecast system is presented. Detailed evaluation procedures for verification data collection and reduction for practical skill assessment are provided. GRA

N85-32596# International Commission for Cloud Physics, Laramie, Wyo. Committee on Nucleation.
ELEVENTH INTERNATIONAL CONFERENCE ON ATMOSPHERIC AEROSOLS, CONDENSATION AND ICE NUCLEI, VOLUME 2
Budapest Hungarian Meteorological Service 1984 192 p refs Conf. held in Budapest, 3-8 Sep. 1984 Submitted for publication 2 Vol.
(PB85-182418; ISBN-963-7701-842) Avail: NTIS HC A09/MF A01

Volume 2 contains papers presented at the Eleventh International Conference on Atmospheric Aerosols, Condensation and Ice Nuclei. Subjects covered are the physics and chemistry of tropospheric aerosols, observations and theory of condensation and ice nucleation. This particular session of the conference contains papers on the theory and laboratory investigation of ice nucleation. For individual titles, see N85-32597 through N85-32635.

N85-32597# Utah Univ., Salt Lake City. Dept. of Meteorology.
MECHANISM OF HETEROGENEOUS DEPOSITION ICE NUCLEATION NEAR WATER-SATURATION
N. Fukuta *In* Intern. Comm. for Cloud Phys. 11th Intern. Conf. on Atmosphere Aerosols, Condensation and Ice Nuclei, Vol. 2 1984 p 6-9 refs Sponsored in part by NOAA (For primary document see N85-32596 21-47)
(Grant NSF ATM-81-06792)
Avail: NTIS HC A09/MF A01

Experimental studies for deposition ice nucleation on aerosol particles show that, contrary to what the thermodynamic theory predicts, the supersaturation with respect to ice necessary to sustain a given nucleation level increases as the temperature becomes higher and the saturation ratio with with respect to water approaches unity. This mechanism was theoretically analyzed taking the similarity between the heterogeneous ice nucleations and two-dimensional nucleations involved in ice crystal plane growth into consideration: As the temperature increases under a constant ice-supersaturation, the saturation ratio with respect to water also increases resulting in a thicker adsorbed layer. As the layer thickens, the mechanism of ice nucleation must change from the simple deposition to the freezing via a transitional mechanism which has been shown to be more difficult than the others. The difficulty of transitional nucleation in adsorbed water layers, that occur in patches on hydrophobic nucleus surfaces drives the system to a higher ice-supersaturation in order to sustain the given nucleation level, with some compensation effect from the widened and thickened patches, causing the curlup effect in the nucleation isopleths. Author

N85-32598# Colorado State Univ., Fort Collins.
EXPERIMENTAL STUDIES OF THE KINETICS OF DEPOSITION NUCLEATION ON AN ICE NUCLEANT USED IN WEATHER MODIFICATION
P. J. Demott, W. G. Finnegan, R. D. Horn, and L. O. Grant *In* Intern. Comm. for Cloud Phys. 11th Intern. Conf. on Atmosphere Aerosols, Condensation and Ice Nuclei, Vol. 2 1984 p 10-14 refs (For primary document see N85-32596 21-47)
Avail: NTIS HC A09/MF A01

Large isothermal and controlled expansion cloud chambers are utilized to study the character and rate of ice nucleation from the vapor onto an ice nucleus. Methods for elucidating mechanisms for ice nucleation are reviewed. Preliminary results indicate that deposition nucleation becomes dominant at temperatures colder than -18 C, at below water saturation. Time constants for the process are approx. 20 minutes. Author

N85-32599# University of Northern Arizona, Flagstaff.
INACTIVATION OF SILVER IODIDE BY ATMOSPHERIC NUCLEATION INHIBITORS
R. G. Layton and G. Caple *In* Intern. Comm. for Cloud Phys. 11th Intern. Conf. on Atmosphere Aerosols, Condensation and Ice Nuclei, Vol. 2 1984 p 15-19 refs (For primary document see N85-32596 21-47)
Avail: NTIS HC A09/MF A01

The average ice nucleation temperature of drops of silver iodide aqueous suspension placed on blank polycarbonate Nuclepore filters was compared to that obtained using similar filters through which 2.4 cubic meters of air had been drawn. Although the aerosol trapped on the filter occasionally raised the nucleation temperature of the drops the usual case was for the temperature to be lowered. A weak correlation exists between the Aitken nuclei count and the amount of inhibition. Author

N85-32600# Central Aerological Observatory, Moscow (USSR).
ICE NUCLEATION BY SILVER IODINE PARTICLES WITH

NEARLY CRITICAL SIZES
M. Ya. Aksenov, H. V. Lisenkova, and N. O. Plaude *In* Intern. Comm. for Cloud Phys. 11th Intern. Conf. on Atmosphere Aerosols, Condensation and Ice Nuclei, Vol. 2 1984 p 20-24 refs (For primary document see N85-32596 21-47)
Avail: NTIS HC A09/MF A01

Silver iodide aerosols having mean cubic sizes in the range of 0.007 to 0.2 micro have been tested for their nucleating activity. Measurements of the number of particles activated as ice-forming nuclei at temperatures of -7, -10 and -20 C have shown that the nucleation activity increases monotonically with increasing particle sizes and does not exhibit any gap which was reported in the literature. The number of particles activated at T = 20 deg is found to exceed the total number of particles injected in the mixing cloud chamber, thus the process of ice multiplication may be suggested. Author

N85-32601# Ukrainian Scientific Hydrometeorological Inst. (USSR).
PHOTOINDUCED ACTIVE SITES ON ICE NUCLEATING AEROSOL OF SILVER IODIDE
R. A. Bakhanova and R. V. Oleynik *In* Intern. Comm. for Cloud Phys. 11th Intern. Conf. on Atmosphere Aerosols, Condensation and Ice Nuclei, Vol. 2 1984 p 25-29 refs (For primary document see N85-32596 21-47)
Avail: NTIS HC A09/MF A01

The effect of ultraviolet illumination on the ice nucleating ability of AgJ aerosol particles was investigated. In accordance with our suggestion the photochemical activation of AgJ particles is connected with the formation of atomic silver centres on AgJ surface. Author

N85-32602# Institute of Chemical Kinetics and Combustion, Novosibirsk (USSR).
EXPERIMENTAL INVESTIGATION OF PROPERTIES OF ICE-FORMING REAGENTS
N. A. Kakutkina, A. M. Baklanov, B. Z. Gorbunov, K. P. Koutzenogy, A. S. Safatov, A. I. Sidorov, N. A. Silin, and S. B. Khvan *In* Intern. Comm. for Cloud Phys. 11th Intern. Conf. on Atmosphere Aerosols, Condensation and Ice Nuclei, Vol. 2 1984 p 30-33 refs (For primary document see N85-32596 21-47)
Avail: NTIS HC A09/MF A01

A probability of forming an ice crystal on a particle or fraction of active particles is a function of a number of characteristics for medium temperature, supersaturation and particles themselves size, surface properties. The information on these dependences allows to optimize the usage of this ice-forming reagent. In addition, these dependences are the basis for verification of different theoretical concepts of ice formation. A great deal of experimental material on the study of ice-forming activity of various reagents at the Institute of Chemical Kinetics and Combustion has been accumulated. The results of investigating the ice-forming activity for aerosols of various substances depending on the characteristics of medium and aerosol system are presented. B.W.

N85-32603# University of Northern Arizona, Flagstaff. Dept. of Chemistry.
ICE ACTIVE BACTERIA AS CONDENSATION NUCLEI
J. R. Snider, G. Caple, D. Chapman, R. G. Layton, and D. C. Sands (Montana State Univ.) *In* Intern. Comm. for Cloud Phys. 11th Intern. Conf. on Atmosphere Aerosols, Condensation and Ice Nuclei, Vol. 2 1984 p 34-37 refs (For primary document see N85-32596 21-47)
Avail: NTIS HC A09/MF A01

Two strains of ice nucleating bacteria, Pscudomonas syringae and Erwinia herbicola, were filtered onto a .4 micro membrane filters, dried, and then stored in static humidity chambers. The number of visible drops was found to be correlated with the number of bacteria impregnated on the filter surface. A P. syringae mutant, which is not ice nucleating, produced no drops under comparable conditions. These preliminary findings appear to associate a condensation ability of the bacteria with their observed warm immersion freezing activity. Both properties of the bacteria may be mediated by a hydrophilic outer cell membrane, which is thought to be composed of polysaccharide. Activation energy for condensation is lowered by the presence of a wettable cell surface. These observations are significant in terms of the bacterias ability to remain hydrated and visible during airborne transport, and in relation to their potential mode of atmospheric ice nucleation. Author

N85-32604# High Mountain Geophysical Inst., Nalchik (USSR).
THE EFFECT OF SUPERSATURATION, TEMPERATURE AND PARTICLE SIZE ON ICE-NUCLEATING ABILITY OF ATMOSPHERIC AEROSOL
N. A. Berezinski, G. V. Stepanov, and V. G. Khorguani *In* Intern. Comm. for Cloud Phys. 11th Intern. Conf. on Atmosphere Aerosols, Condensation and Ice Nuclei, Vol. 2 1984 p 38-43 refs (For primary document see N85-32596 21-47)
Avail: NTIS HC A09/MF A01

Nowadays great attention is given to the water solid phase formation in clouds. However, small concentrations of natural ice-forming nuclei and difficulties in aerosol particle size differentiation make it difficult to study the different size particle activity. Besides the majority of experimental data on ice nucleation was obtained with the help of mixing and expansion chambers at low (-15 to -20 C) temperatures and uncontrolled supersaturations. That's why high-temperature region of ice nucleation (-6 to -15 C) and the effect of supersaturation remained practically unknown. In this work ice-nucleating ability of natural aerosol particles is studied by means of their capture on hydrophobic pads with subsequent investigation in thermo-diffusion chamber. Sampling was conducted by a universal cascade impactor mounted on board aircraft laboratory. At the first stage the giant 3 mm particles deposited, at the second-particles from 0.5 to 5 mm in diameter, at the third more than 0.02 mm. B.W.

N85-32605# Alaska Univ., Fairbanks. Geophysical Inst.
ICE CRYSTAL NUCLEATION ON HYGROSCOPIC AEROSOLS
Takeshi Ohtake *In* Intern. Comm. on Cloud Phys. 11th Intern. Conf. on Atmosphere Aerosols, Condensation and Ice Nuclei, Vol. 2 1984 p 44-48 refs Sponsored in part by Alaska State Funds (For primary document see N85-32596 21-47)
(Grant NSF DPP-83-8303964)
Avail: NTIS HC A09/MF A01

Aerosols were collected on hydrophobic membrane filters at remote polar areas for testing their ice nucleation ability at temperatures of -25 and -37 C with precisely controlled humidities. The observation showed that aerosol concentrations of 10-1000 particles per CW m in the atmosphere were nucleated to ice crystals with about 82% R.M. over water. The size range of the aerosols were determined to be between 0.01 and 0.6 micron in diameter. The concentration of the ice nucleated hygroscopic aerosols and the humidities forming ice crystals agree with those observed in the Antarctic atmosphere and cirrus clouds. Author

N85-32606# Main Geophysical Observatory, Leningrad (USSR).
ON THE EFFICIENCY OF THE MECHANISM OF ICE PARTICLES FORMATION IN THE VAPOR SUPERSATURATION FIELD AROUND A FREEZING DROPLET
V. V. Klingo, V. V. Sergeev, and B. Sh. Faizullin *In* Intern. Comm. for Cloud Phys. 11th Intern. Conf. on Atmosphere Aerosols, Condensation and Ice Nuclei, Vol. 2 1984 p 49-52 refs (For primary document see N85-32596 21-47)
Avail: NTIS HC A09/MF A01

The quantitative evaluation of the efficiency of the mechanism of ice nucleation in the water vapor transient supersaturation field surrounding a freezing cloud droplet was made. Author

N85-32607# Kentucky Univ., Lexington. Dept. of Chemical Engineering.
GENERATION OF LEAD, LEAD IODIDE AND IODIDE AEROSOLS AND THEIR ICE NUCLEATION
Yasuo Ueno *In* Intern. Comm. for Cloud Phys. 11th Intern. Conf. on Atmosphere Aerosols, Condensation and Ice Nuclei, Vol. 2 1984 p 53-55 refs (For primary document see N85-32596 21-47)
Avail: NTIS HC A09/MF A01

Test aerosols of lead, lead iodide and iodide were generated by a condensation method. The conditions under which monodisperse, fine or coarse aerosols might be formed were examined. The ice nucleation temperature of these typical aerosols could be individually marked using an ice nucleation chamber. An experiment of the reactivity of lead aerosol toward iodine vapor was carried out using lead aerosol and iodine vapor under different temperatures. The reactivity between lead aerosol and iodine vapor could be estimated from the number of ice crystal in the ice nucleation chamber. Author

N85-32608# Hebrew Univ., Jerusalem (Israel). Dept. of Atmospheric Sciences.
THE NUCLEATION OF ICE CRYSTALS DURING THE FREEZING OF LARGE SUPERCOOLED DROPS
A. Gagin and H. Nozyce *In* Intern. Comm. for Cloud Phys. 11th Intern. Conf. on Atmosphere Aerosols, Condensation and Ice Nuclei, Vol. 2 1984 p 56-65 refs (For primary document see N85-32596 21-47)
Avail: NTIS HC A09/MF A01

Laboratory experiments were conducted to study the possible mechanisms of secondary ice crystal production during the process of freezing of large supercooled drops. Secondary ice particle have been detected in the laboratory and their production seems to be attributable to nucleation at relatively high, transient, supersaturations occurring during the freezing of large drops and not to ice splinter ejection in the course of spike formation which frequently accompany the symmetric freezing of drops. These findings may provide a clue to the understanding of the rapid glaciation rates observed in maritime cumuli and in some summertime convective clouds. Author

N85-32609# Manchester Univ. (England). Dept. of Physics.
ICE NUCLEUS MEASUREMENTS
C. P. R. Saunders and R. Al-Naimi *In* Intern. Comm. for Cloud Phys. 11th Intern. Conf. on Atmosphere Aerosols, Condensation and Ice Nuclei, Vol. 2 1984 p 69-73 refs (For primary document see N85-32596 21-47)
Avail: NTIS HC A09/MF A01

The concentrations of natural ice nuclei have been studied using continuous flow chambers in order to determine deposition and condensation nucleus concentrations. Author

N85-32610# Main Geophysical Observatory, Leningrad (USSR).
ON THE PROBLEM OF POSSIBLE MECHANISM OF ICE NUCLEI FORMATION IN CONVECTIVE CLOUDS
V. Ya. Nikandrov, T. N. Gromova, D. D. Stalevich, and T. A. Pershina Intern. Comm. for Cloud Phys. 11th Intern. Conf. on Atmosphere Aerosols, Condensation and Ice Nuclei, Vol. 2 1984 p 74-78 refs (For primary document see N85-32596 21-47)
Avail: NTIS HC A09/MF A01

At the maturity stage of a powerful cumulus cloud over its top areas with high humidity deficit are set up at the expense of subsidence development. The evaporation process of drops caught in such conditions is very intensive. The low air pressure at high altitudes also promotes this process. The intensive vaporation results in a considerable cooling of drops, their freezing and subsequent destruction. The deformation and destruction of freezing drops is accompanied by their charging, as well as by the formation of a large number of ice nuclei. All these phenomena accelerate precipitation formation process and cloud electrization. The results of theoretical and laboratory studies are presented on drop behavior during intensive evaporation under the conditions of high humidity deficit and low pressure. B.W.

N85-32611# Colorado Univ., Boulder. Cooperative Inst. for Research in Environmental Science.
BACTERIAL ICE NUCLEI OF MARINE ORIGIN: SOME RECENT OBSERVATIONS
R. R. Fall and R. C. Schnell *In* Intern. Comm. for Cloud Phys. 11th Intern. Conf. on Atmosphere Aerosols, Condensation and Ice Nuclei, Vol. 2 1984 p 79-83 refs (For primary document see N85-32596 21-47)
Avail: NTIS HC A09/MF A01

The observations that terrestrial ice nuclei can have a biogenic origin, and that certain bacteria can initiate freezing at exceptionally warm temperature (-1.3 C) are now well documented. Less well understood are active ice nuclei (-2 C) found in sea water, marine fog and the marine atmosphere in general. Recently, the authors have observed that active ice nuclei can be produced by a salt tolerant bacterium isolated from marine algae cultures. The bacterium (strain FB 1032) exhibits properties similar to pseudomonas fluorescens biotype G, an ice nucleating bacterium found in terrestrial sources. A search for ice nuclei in sea water at La Jolla, California, revealed threshold nucleation at -2.8 C. From these samples several ice nucleation-active Erwinis species were isolated. Author

N85-32612# Central Aerological Observatory, Moscow (USSR).
AIRBORNE MEASUREMENTS OF ATMOSPHERIC ICE NUCLEI
M. V. Vychuzhanina, V. I. Miroshnichenko, I. P. Parshutkina, A. D. Solovjev, and B. N. Leskov (Ukrainian Scientific Hydrometeorological Inst.) *In* Intern. Comm. for Cloud Phys. 11th Intern. Conf. on Atmosphere Aerosols, Condensation and Ice Nuclei, Vol. 2 1984 p 84-88 (For primary document see N85-32596 21-47)
Avail: NTIS HC A09/MF A01

The results of aircraft measurements of ice nuclei over an experimental meteorological site in the Ukraine during the winter seasons of 1977 and 1979 to 1982 are given. Measurements were made with a mixing-type cloud chamber. Data on the vertical distribution of ice nuclei were obtained under different atmospheric conditions. Author

N85-32613# Indian Inst. of Tropical Meteorology, Poona.
AIRCRAFT OBSERVATIONS OF CONDENSATION AND ICE NUCLEI AT A TROPICAL STATION
S. K. Paul, S. K. Sharma, A. Mary Selvan, A. S. R. Murty, and Bh. V. Ramana Murty *In* Intern. Comm. for Cloud Phys. 11th Intern. Conf. on Atmosphere Aerosols, Condensation and Ice Nuclei, Vol. 2 1984 p 89-93 refs (For primary document see N85-32596 21-47)
Avail: NTIS HC A09/MF A01

Aircraft observations of large and giant CN, chloride particles, total aerosol and IN made in the summer monsoon season indicated the following. The chloride number increased with height while its mass decreased. The ice nuclei N, by and large, increased with height. On the days with higher rainfall, the size spectra of chloride particles were broader, bimodal and particles $< 15 <$ m were more. The total aerosol and IN were more on the days with higher rainfall. Author

N85-32614# Departamento de Fisica Fundamental, Valiadolid (Spain).
A STATISTICAL ANALYSIS OF ICE NUCLEI CONCENTRATIONS AT URBAN AND RURAL SITES IN VALLADOLID, SPAIN
P. J. Perez, J. A. Garcia, and J. Casanova *In* Intern. Comm. for Cloud Phys. 11th Intern. Conf. on Atmosphere Aerosols, Condensation and Ice Nuclei, Vol. 2 1984 p 94-98 refs (For primary document see N85-32596 21-47)
Avail: NTIS HC A09/MF A01

Daily concentrations of atmospheric ice nuclei were measured at ground level in Valiadolid, at urban and rural sites, during 1982. The data presented show that, in the region of the study, the concentrations of ice nuclei are negatively correlated with visibility and wind speed, and positively correlated with temperatures and atmospheric stability. The results suggest an influence of continental air masses over the ambient background concentration in IN. Author

N85-32615# Johann-Wolfgang-Goethe-Univ., Frankfurt am Main (West Germany). Inst. fuer Meteorologie und Geophysik.
SUPERSATURATION SPECT A OF ICE NUCLEI AT DIFFERENT LOCATIONS IN EUROPE AND OVER THE NORTH-ATLANTIC
D. Stein and H.-W. Georgii *In* Intern. Comm. for Clouds Phys. 11th Intern. Conf. on Atmosphere Aerosols, Condensation and Ice Nuclei, Vol. 2 1984 p 99-104 refs Sponsored in part by

Deutsch Forschungsgemeinschaft through Sonderforschungsbereich 73 Atmospheric Trace Constituents, the municipality of St. Moritz, Switzerland, and by the Republic of Malta (For primary document see N85-32596 21-47)
Avail: NTIS HC A09/MF A01

The concentration of ice nuclei was measured at different activation temperatures and supersaturations (ice) with a low-pressure diffusion chamber. The received supersaturation and temperature spectra at different locations in Europe and over the Atlantic were demonstrated between 9% and 20% supersaturation (ice) respectively -9 C and -18 C activation temperature. The results show great differences of the spectra combined with low concentrations absent of sources of ice nuclei while those sources impress the ice nuclei distribution at continental locations. Author

N85-32616# Wyoming Univ., Laramie. Dept. of Atmospheric Science.
CONCENTRATIONS OF ICE NUCLEI OF DIFFERENT MODES OF ACTIVITIES
G. Vali, T. Deshler, and D. C. Rogers (Research Council of Alberta) *In* Intern. Comm. for Cloud Phys. 11th Intern. Conf. on Atmosphere Aerosols, Condensation and Ice Nuclei, Vol. 2 1984 p 105-109 refs Sponsored in part by Bureau of Reclamation, and by NSF (For primary document see N85-32596 21-47)
Avail: NTIS HC A09/MF A01

Measurements of different ice nucleation modes are examined to construct a view of the characteristics of the total atmospheric ice nucleus population. Overall, it seems reasonable to maintain the working assumption that nucleation modes can in fact be instrumentally distinguished. The numerous physical tests used to evaluate instrument performance point to the same conclusion. The relative importance of various ice nucleation modes, of course, depend on the atmospheric conditions being considered. In terms of typical concentrations, contact-freezing and condensation-freezing nuclei seem to be more abundant; deposition and immersion-freezing nuclei are factors of 10 to 20 fewer. The variability of nucleus concentrations roughly amounts to factors of 20 to 60 to encompass 90% of the cases. Smaller ranges of variability at colder temperatures suggest a wider availability of nuclei of lesser activity--a result intuitively acceptable. R.J.F.

N85-32617# University Coll., Galway (Ireland).
THE NUCLEATION OF ICE AT VERY LOW TEMPERATURES AND PRESSURES
A. F. Roddy *In* Intern. Comm. for Cloud Phys. 11th Intern. Conf. on Atmosphere Aerosols, Condensation and Ice Nuclei, Vol. 2 1984 p 110-116 refs (For primary document see N85-32596 21-47)
Avail: NTIS HC A09/MF A01

The nucleation of ice is considered in the temperature range 120 to 160 K and at sub-millibar total pressures. These conditions are sometimes found in the real atmosphere in the mesopause region. At such times noctilucent clouds may occur. There is particular emphasis on the application of classical nucleation theory to the nucleation of cubic ice Ic by particles of meteoric origin. Author

N85-32618# Academia Sinica, Lanzhou (China).
OBSERVATIONS OF THE ATMOSPHERIC ICE NUCLEUS AT NORTHWEST CHINA
Zheng-Mo Ge *In* Intern. Comm. for Cloud Phys. 11th Intern. Conf. on Atmosphere Aerosols, Condensation and Ice Nuclei, Vol. 2 1984 p 117-121 refs (For primary document see N85-32596 21-47)
Avail: NTIS HC A09/MF A01

It is argued that the average concentration, the monthly variation and the daily variation of atmospheric ice nucleus in Lanzhou city are dependent upon the relation between atmospheric ice nucleus concentration and other essential meteorological factors. Wind direction, air pollution over cities and visibility are examined. R.J.F.

N85-32619# Indian Inst. of Tropical Meteorology, Poona.
ICE NUCLEATING CHARACTERISTICS OF CAPPARIS APHYLLA, AN INDIAN HERB
A. S. Ramchandra Murty, A. Mary Selvan, P. C. S. Devara, and Bh. V. Ramana Murty *In* Intern. Comm. for Clous Phys. 11th Intern. Conf. on Atmosphere Aerosols, Condensation and Ice Nuclei, Vol. 2 1984 p 122-126 refs (For primary document see N85-32596 21-47)
Avail: NTIS HC A09/MF A01

Capparis Aphylla, also known as greenwood of cair, is a herb grown in the forests located in different regions in India. It is in the form of a green bush without leaves and the stems contain iodine. This herb is known to have been used in India during ancient times in attempts for securing rain through the performance of the Kariristi, a sacrifice to God. The method involves, besides chanting of prayers, burning of the above herb with oils. In order to determine the ice nucleating property of the herb, drop freezing experiments were conducted. The dried herb was burnt and the ash so obtained was finely ground and this powder was mixed with double distilled water. The millimeter sized (diameter approximately 2 microns) water drops containing the powdered ash as suspension were used in the drop freezing experiments. The results showed that the herb can induce freezing of water drops at about -4 C. The ice nucleating ability of the herb has been attributed to the iodine contained in it. The results of the drop freezing experiments and the physical aspects of weather modification by Kariristi were discussed. Author

N85-32620# Desert Research Inst., Reno, Nev.
THE CAPTURE OF ICE NUCLEATING AND NON ICE-NUCLEATING AEROSOLS BY ICE PHASE PRECIPITATION
J. A. Warburton, L. G. Young, M. S. Owens, and R. H. Stone *In* Intern. Comm. for Cloud Phys. 11th Intern. Conf. on Atmosphere Aerosols, Condensation and Ice Nuclei, Vol. 2 1984 p 127-134 refs Sponsored in part by the State of Nevada (For primary document see N85-32596 21-47)
(Contract NA82RA-C-0098)
Avail: NTIS HC A09/MF A01

Chemical analyses of snow collected from five winter seasons in the Sierra Nevada, show that there is a positive correlation between the silver concentration and the snow water mass containing the silver which originates from AgI ice-nucleating aerosol sources in the region. When the same snow is analyzed for its indium content for those occasions when non ice-nucleating indium sesquioxide (In_2O_3) is released as aerosols, at the same rates and at the same locations as the AgI, the indium oxide is found to be removed at lesser rates than the silver iodide. In addition the indium concentration and the mass of snow containing it, do not appear to be positively correlated, but rather constant or slightly negatively correlated. It is considered that the differences in capture and removal of the two aerosol types are due to their different physical nucleating properties. The results of continuing experiments and theoretical modelling of the removal processes for the two types of aerosols will be presented. Author

N85-32621# Missouri Univ., Rolla. Graduate Center for Cloud Physics Research.
THE 100 YEARS OF AITKEN NUCLEI (AN) STUDY-REMINISCENCE, CURRENT AND FUTURE PROBLEMS
J. Podzimek and J. C. Carstens *In* Intern. Comm. for Cloud Phys. 11th Intern. Conf. on Atmosphere Aerosols, Condensation and Ice Nuclei, Vol. 2 1984 p 137-147 refs (For primary document see N85-32596 21-47)
Avail: NTIS HC A09/MF A01

Aitken nuclei (AN) measurements are reviewed and the principles of expansion techniques analyzed. Calculated values are compared to the recently published data obtained by different counters and for different test aerosol. The question whether one can make a universally valid calibration of AN counters is discussed in detail. Author

N85-32622# Colorado State Univ., Fort Collins. Dept. of Atmospheric Science.

PROPERTIES OF AEROSOL PARTICLES DETECTED BY SATELLITES IN COASTAL REGIONS

E. E. Hindman, P. A. Durkee, and W. Keunning *In* Intern. Comm. for Cloud Phys. 11th Intern. Conf. on Atmosphere Aerosols, Condensation and Ice Nuclei, Vol. 2 1984 p 148-154 refs (For primary document see N85-32596 21-47)

(Contract N00014-79-C-0793)

Avail: NTIS HC A09/MF A01

The particles detected in the marine boundary layer were primarily spherical, 1 to 6 microns in diameter and of oceanic origin. Optical depths 0.04 to 0.10 were resolved. The particles detected above the boundary layer were primarily submicron, partially hygroscopic and a mixture of rural, oceanic and possibly urban particles. These particles could mask radiation scattered by boundary layer particles. Near-simultaneous satellite radiometric measurements and airborne aerosol measurements have shown particles of oceanic origin are responsible for a majority of the scattered energy in cloud-free regions except when significant upper-level haze layers are present. R.J.F.

N85-32623# Tartu State Univ. (USSR).

MULTI-CHANNEL ELECTRIC AEROSOL SPECTROMETER c35

A. Mirme, M. Noppel, I. Peil, J. Salm, E. Tamm, and H. Tammet *In* Intern. Comm. for Cloud Phys. 11th Intern. Conf. on Atmosphere Aerosols, Condensation and Ice Nuclei, Vol. 2 1984 p 155-159 refs (For primary document see N85-32596 21-47)

Avail: NTIS HC A09/MF A01

Multi-channel electric mobility spectrometry is a most efficient technique for the rapid measurement of an unstable aerosol particle size spectrum. The measuring range of the spectrometer from 10 microns to 10 microns is achieved by applying diffusional and field charging mechanisms simultaneously. On-line data processing is carried out with a microcomputer. Experimental calibration ensures correctness of measurement. Author

N85-32624# Bhabha Atomic Research Centre, Bombay (India). Div. of Radiological Protection.

SUPERSATURATION OBTAINED IN A CONDENSATION NUCLEUS COUNTER

P. V. N. Mair, D. V. Paima, and K. G. Vohra *In* Intern. Comm. for Cloud Phys. 11th Intern. Conf. on Atmosphere Aerosols, Condensation and Ice Nuclei, Vol. 2 1984 p 160-164 refs (For primary document see N85-32596 21-47)

Avail: NTIS HC A09/MF A01

Supersaturation attained in two expansion type condensation nucleus counters was estimated by a new method. The method was used to investigate the behavior of a Gardner Counter and a laboratory counter of spherical geometry with aerosols of different concentrations and composition in air and argon. Results showed that cooling was less by 15 to 50% of isentropic value, supersaturations attained were lower and threshold size for detection considerably higher than what were predicted from isentropic behavior. Author

N85-32625# Odessa State Univ. (USSR).

ANALYSIS OF PERFORMANCE OF DYNAMIC THERMAL DIFFUSION CHAMBER c35

G. N. Lipantov and G. L. Shingarev *In* Intern. Comm. for Cloud Phys. 11th Intern. Conf. on Atmosphere Aerosols, Condensation and Ice Nuclei, Vol. 2 1984 p 165-170 refs (For primary document see N85-32596 21-47)

Avail: NTIS HC A09/MF A01

Using a thermal diffusion chamber, the influence of sampling and thermo-and diffusiophoretic effects on the results of atmospheric condensation nuclei activity measurements was studied. Under certain temperatures and air humidity there occurs supersaturation on the chamber inlet exceeding that of supersaturation estimated for linear distribution of temperature and vapor concentration. Thermo-and diffusiophoretic effects may result in 20% errors under the maximum supersaturation of 1%. R.J.F.

N85-32626# Ukrainian Scientific Hydrometeorological Inst. (USSR).

THE INVESTIGATION OF NATURAL AND ARTIFICIAL ICE NUCLEI BY THE IMPROVED MEMBRANE FILTER METHOD

A. V. Silaev, R. A. Bakhanova, I. V. Ivanshenko, and L. M. Tovstenko *In* Intern. Comm. for Cloud Phys. 11th Intern. Conf. on Atmosphere Aerosols, Condensation and Ice Nuclei, Vol. 2 1984 p 171-175 refs (For primary document see N85-32596 21-47)

Avail: NTIS HC A09/MF A01

The equipment and a procedure for a quick treatment of membrane filters were developed. The laboratory investigations of the influence of a mean diameter of filter pores, of total sample volume, of volume rate of sampling, and of hygroscopic admixtures to ice-forming aerosols upon the measured ice nuclei (IN) concentration were carried out. The aircraft measurements of IN concentration were fulfilled over some regions of the Ukraine and Moldavia. Author

N85-32627# Indian Inst. of Tropical Meteorology, Poona.

A THERMAL DIFFUSION CHAMBER FOR THE MEASUREMENT OF CLOUD CONDENSATION NUCLEI c35

S. Chaudhuri and K. G. Vernekar *In* Intern. Comm. for Cloud Phys. 11th Intern. Conf. on Atmosphere Aerosols, Condensation and Ice Nuclei, Vol. 2 1984 p 176-180 refs (For primary document see N85-32596 21-47)

Avail: NTIS HC A09/MF A01

A static thermal diffusion chamber for the measurement of cloud condensation nuclei (CCN) in the atmosphere was designed and fabricated at the institute. The chamber has a volume of 115 cc. An automatic electronic temperature controller was designed and used with the chamber for regulating the supersaturation in the chamber. The supersaturation in the chamber could be controlled with 2 percent accuracy. The theory relating to the steady state supersaturations in the chamber and the variations in the concentration of CCN under the steady state condition are studied. The details of the thermal diffusion chamber, accuracy of measurement and the result of the observations undertaken at Pune (India) are discussed. Author

N85-32628# Desert Research Inst., Reno, Nev.

STABLE GENERATION OF HIGHLY MONODISPERSE AEROSOLS

Jack Y. Des *In* Intern. Comm. for Cloud Phys. 11th Intern. Conf. on Atmosphere Aerosols, Condensation and Ice Nuclei, Vol. 2 1984 o 181-185 refs (For primary document see N85-32596 21-47)

Avail: NTIS HC A09/MF A01

A technique was developed to generate very stable outputs of highly monodisperse aerosols. The technique involves passing the output from a uniquely designed atomizer through the electrical mobility analyzers connected in series. The stability was monitored with a condensation nuclei (CN) counter while the dispersity was determined with a continuous flow diffusion (CFD) cloud condensation nuclei (CCN) counter. Author

N85-32629# Grenoble-1 Univ. (France).

BASIC ICE NUCLEATION MECHANISMS ON MONO AND MICROCRYSTALS AND ICE FORMING NUCLEI. THEORETICAL ANALYSIS AND EXPERIMENTAL RESULTS ACHIEVED IN THE LABORATORY OVER THE PAST TEN YEARS: REVIEW PAPER
Abstract Only

H. Andriambelona and R. Montmory *In* Intern. Comm. for Cloud Phys. 11th Intern. Conf. on Atmosphere Aerosols, Condensation and Ice Nuclei, Vol. 2 1984 p 186 (For primary document see N85-32596 21-47)

Avail: NTIS HC A09/MF A01

An analysis is given of measurements of PbI and AgI under different technical conditions. Adsorption measurements were completed by neutron diffraction spectroscopy. This brought to light many new aspects of the mechanisms of ice formation on ice forming materials, according to their surface state. In controlled conditions, PbI2 epitaxial thin films were produced which are perfectly flat and had a clean surface. Between 0 deg and -25 C, for a given water vapor pressure which lies between ice saturation and supercooled water saturation, no ice cluster will form on

PbI2 crystal faces. This negative result can be interpreted if we consider that these 0001 faces are hydrophobic and/or if we take ice substrate interface entropy into account. The forming of surface defects (ex. etch pits, macroscopic steps) causes the appearance of nucleation sites for ice. Most of these sites are capillary condensation sites on which the water molecules assemble after their diffusion on the hydrophobic faces and then form tridimensional condensation nuclei from which ice appears through freezing. Other ice nucleation sites can be produced by surface photolysis. For AgX, thin photolysis is obtained by irradiation.
R.J.F.

N85-32630# State Univ. of New York, Albany. Atmospheric Sciences Research Center.
ICE NUCLEATION OF SINGLE WATER DROPLET BY SILVER IODIDE: A LABORATORY OBSERVATION Abstract Only
Roger J. Cheng *In* Intern. Comm. for Cloud Phys. 11th Intern. Conf. on Atmosphere Aerosols, Condensation and Ice Nuclei, Vol. 2 1984 p 187 (For primary document see N85-32596 21-47)
Avail: NTIS HC A09/MF A01

Investigation of nucleation of single water droplet by silver iodide reveals two distinctive mechanisms of ice nucleation. A sophisticated system of high speed cinephotomicrographic apparatus and a miniature environmental controlled chamber built in under a high power microscope were utilized to provide detailed observations of the complete process of ice nucleation. Ice nucleation is observed instantly when silver iodide crystal, produced by smoke generator, is making contact with surface of a supercooled water droplet. Then a thin sheet of ice forms radially from the contact point, and eventually covers the whole body of the droplet. Numerous air bubbles are formed continuously at the ice water interface during freezing period. The duration of freezing process depends on the size of the droplet, its degree of supercooling and the environmental conditions. A two step nucleation process is suggested first, due to the different solubilities of silver iodide in water and in a solution of sodium iodide, the silver iodide nucleates and precipitates as droplets. Dissolved double salt grows by condensation in a high humidity condition. This is then followed by a second process in which the silver iodide crystal nucleates the formation of ice from the interior of the dilute.
R.J.F.

N85-32631# Ceskoslovenska Akademie Ved, Prague. Inst. of the Physics of the Atmosphere.
ICE-FORMING EFFICIENCY OF THE SOLUBLE AND INSOLUBLE PORTIONS OF DUST CONTAINED IN SNOW Abstract Only
Frantisek Anyz *In* Intern. Comm. for Cloud Phys. 11th Intern. Conf. on Atmosphere Aerosols, Condensation and Ice Nuclei, Vol. 2 1984 p 188 (For primary document see N85-32596 21-47)
Avail: NTIS HC A09/MF A01

During periods when snow covers the ground, practically no dust from the soil enters the atmosphere and that contained in the snow originates mainly from atmospheric immissions. Snow samples were collected both in industrial and relatively clean mountain areas of Czechoslovakia both from the snow surface and at various depths in the snow layer. After melting the snow samples, the average median freezing temperature of water drops about 3 mm in diameter, ranging from -3.2 C to -14.5 C, was found for each new sample. The freezing temperature was also measured after the removal of insoluble particles from the water by filtration or sedimentation and after reduction of the sample volume to 1/128 of the original by evaporation. The electrical conductivity of the melted snow samples was also measured. The results demonstrated that the insoluble particles were the most efficient ice nuclei. On the other hand, the freezing temperature after the removal of insoluble particles by filtration or sedimentation decreased only slightly in some samples. The electrical conductivity of snow water did not exhibit any explicit influence. The same freezing temperature was found in samples whose conductivity differed by a factor of 50.
Author

N85-32632# Colorado State Univ., Fort Collins. Dept. of Atmospheric Science.
CRITICAL SUPERSATURATIONS WITH RESPECT TO WATER FOR FAST CONDENSATION-FREEZING ICE NUCLEATION Abstract Only
R. R. Blumenstein, W. G. Finnegan, and L. O. Grant *In* Intern. Comm. for Cloud Phys. 11th Intern. Conf. on Atmosphere Aerosols, Condensation and Ice Nuclei, Vol. 2 1984 p 189 (For primary document see N85-32596 21-47)
Avail: NTIS HC A09/MF A01

Experiments using chemical kinetic methodology to study ice nucleation of hygroscopic ice nuclei resulted in the determination of two types of condensation freezing mechanisms. At water saturation, the rate of condensation freezing ice nucleation is relatively slow, requiring 10 to 60 minutes for nucleation of the entire nuclei population, depending on temperature. At critical levels of transitory supersaturation with respect to water, the rate of condensation freezing increases markedly and the yield of ice crystals produced increases as much as two orders of magnitude. In this case, all the ice crystals are produced within approximately two minutes. Results of studies of the fast mechanism are emphasized.
R.J.F.

N85-32633# Missouri Univ., Rolla. Dept. of Physics.
MONTE CARLO STUDIES OF H2O LAYERS ADSORBED ON A MODEL BASAL FACE OF AgI Abstract Only
Barbara N. Hale, Donald A. Reago, Jr., Richard C. Ward, and Walter E. Lundy *In* International Commission for Cloud Physics 11th Intern. Conf. on Atmosphere Aerosols, Condensation and Ice Nuclei, Vol. 2 1984 p 190 (For primary document see N85-32596 21-47)
(Grant NSF ATM-80-15790)
Avail: NTIS HC A09/MF A01

Effective pair potentials and Metropolis Monte Carlo methods are used to study the structure and state (liquid vs. solid) of a two layer (96 molecule periodic unit cell) and a four layer (192 molecule periodic unit cell) H2O system on a model rigid basal face of hexagonal AgI. Previous studies indicate that the model substrate is rapidly covered by an H O monolayer at 265 K. The present work uses the Monte Carlo method and the H2O-R2O central force potentials of Stillinger and Rahman to equilibrate the water layer systems and to calculate average binding energy per molecule, (two dimensional) ice Ih structure factors, average unit cell dipole moment and mean square O-O displacements at 200, 265 and 300 K. Results for two initial water layer states (unit cells taken from a melted sample at 300 K and from a model bulk ion Ih at 200 K) are discussed. The motivation is to investigate the probability and temperature dependence of ice Ih formation in adsorbed layers of different thickness. Preliminary results suggest: (1) that the monolayers adjacent to the AgX substrate take on a planar six membered ring structure at 200 and 265 K; and (2) that the four layer system displays a vertical layering more characteristic of ice Ih. Consideration is given to the possibility that a defect free AgX basal face will not provide a seeding environment necessary for ice Ih formation in the limited number of layers studied.
R.J.F.

N85-32634# Alaska Univ., Fairbanks. Geophysical Inst.
CONCENTRATION AND SOURCE AREAS OF ICE NUCLEI IN THE ALASKAN ATMOSPHERE Abstract Only
Andrew G. Fountain (Geological Survey, Tacoma, Wash.) and Takeshi Ohtake *In* International Commission for Cloud Physics 11th Intern. Conf. on Atmosphere Aerosols, Condensation and Ice Nuclei, Vol. 2 1984 p 191 (For primary document see N85-32596 21-47)
Avail: NTIS HC A09/MF A01

Atmospheric ice nucleus concentrations were measured daily for 10 months at three ground sites in Alaska to determine the influence of long range nucleus sources on the concentrations. The filter method, used to detect the nuclei at -20 C, employed several modifications in an attempt to increase the reliability of the results. The results indicate a seasonal variation in nucleus concentration with a winter minimum and a north to south trend in increasing average concentration. Eighteen episodes of high concentrations were observed of which 5/28 were correlated with

500 mb isobaric transport from Eurasia and 5/28 were coincident with 700 mb cyclogenesis over Alaska. This latter correlation has not been previously reported. These results suggest that local nucleus sources play a dominant role in the seasonal variation of their concentrations, while individual episodes are caused by external or regional influences. Observations of significant ice nucleus concentrations at temperatures below -30 C, suggests inefficiency in the vapor deposition mechanism of ice nucleation. Author

N85-32635# Utah Univ., Salt Lake City. Dept. of Meteorology.
CLOUD DROPLET NUCLEATION AND INITIAL GROWTH DERIVED FROM LIDAR DEPOLARIZATION STUDIES Abstract Only
K. Sassen, K. N. Liou, and G. Dodd *In* International Commission for Cloud Physics 11th Intern. Conf. on Atmosphere Aerosols, Condensation and Ice Nuclei, Vol. 2 1984 p 192 (For primary document see N85-32596 21-47)
Avail: NTIS HC A09/MF A01

Based on the operating geometry of a polarization ruby lidar system, a numerical model was developed which predicts the variations in single and multiple scattering parameters (at several wavelengths) as a function of height above cloud base for comparison to lidar data from maritime stratus clouds. In contrast to former attempts, utilizing homogeneous cloud models, laser backscattering, attenuation and multiple scattering induced depolarization quantities are computed from Hie scattering theory for a population of spherical drops whose number and size distribution are varied with height above cloud base according to the output from a cloud microphysical model. It is shown that the laser depolarization and backscattering received as a function of cloud depth are sensitive to the assumed cloud condensation nucleus spectrum and the updraft velocity at cloud base, indicating that polarization lidar and multi wavelength lidar techniques are uniquely suited for studies of the nucleation and initial growth of cloud droplet populations. R.J.F.

N85-32636# International Commission for Cloud Physics, Laramie, Wyo. Committee on Nucleation.
ELEVENTH INTERNATIONAL CONFERENCE ON ATMOSPHERIC AEROSOLS, CONDENSATION AND ICE NUCLEI, VOLUME 1
Budapest Hungarian Meteorological Service 1984 307 p refs Conf. held in Budapest, 3-8 Sep. 1984 Submitted for publication 2 Vol.
(PB85-182400) Avail: NTIS HC A14/MF A01

The text of papers presented at the Eleventh International Conference on Atmospheric Aerosols, Condensation and Ice Nuclei by a total of one hundred authors is given. Subjects covered are the physics and chemistry of tropospheric aerosols, observations and theory of condensation and ice nucleation. For individual titles, see N85-32637 through N85-32699.

N85-32637# University Coll., Galway (Ireland).
THE FIRST CONDENSATION NUCLEUS CONFERENCE
T. C. OConner *In* International Commission for Cloud Physics 11th Intern. Conf. on Atmospheric Aerosols, Condensation and Ice Nuclei, Vol. 1 1984 p 15-19 refs (For primary document see N85-32636 21-47)
Avail: NTIS HC A14/MF A01

A brief historical review is given of this series of international conferences on condensation nuclei, with particular reference to the first conference in Dublin in 1955. A selective bibliography of the principal papers by P. J. Nolan and co-workers and by L. W. Pollak and his co-workers on the determination of the size and concentration of condensation nuclei and on some applications of the Nolan-Pollak photoelectric nucleus counter is included. Author

N85-32638# National Center for Atmospheric Research, Boulder, Colo.
PRODUCTION OF STABLE EMBRYO PARTICLES IN DENSE ION TRACKS OF ALPHA PARTICLE EMISSIONS IN THE ATMOSPHERE
E. A. Martell *In* International Commission for Cloud Physics 11th Intern. Conf. on Atmospheric Aerosols, Condensation and Ice Nuclei, Vol. 1 1984 p 23-27 refs Sponsored by NSF (For primary document see N85-32636 21-47)
Avail: NTIS HC A14/MF A01

Alpha particle emissions from radon and its radioactive decay products in continental surface air provide a natural gas-to-particle conversion process. An initial separation of charge in the dense column of ions in each alpha track inhibits recombination. Track concentrations of radiolysis products, excited polyatomic molecules, and water vapor provide for growth of large positive ion clusters before recombination, resulting in the production of stable embryo particles. Author

N85-32639# Toulouse Univ. (France).
FORMATION OF PARTICLES IN THE AIR OF THE HUMID TROPICAL FORESTS
J. Servant and R. Delmas (Marien NGouabi Univ., Brazzaville, Congo Peoples' Republic) *In* International Commission for Cloud Physics 11th Intern. Conf. on Atmospheric Aerosols, Condensation and Ice Nuclei, Vol. 1 1984 p 28-34 refs (For primary document see N85-32636 21-47)
Avail: NTIS HC A14/MF A01

Particle size distributions of NH4+, SO4-, NO3-, NA+, and CA++ ions in the air of a tropical rain forest of the Ivory Coast are presented. From the measured size distributions the modes of formation of the NH4+, SO4- and NO3- ions ions are discussed. Author

N85-32640# Toulouse Univ. (France). Lab. Aerologie.
STUDY OF THE FORMATION OF PARTICLES FROM NATURAL HYDROCARBONS RELEASED BY VEGETATION
A. Lopez, S. Prieur, and J. Fontan *In* International Commission for Cloud Physics 11th Intern. Conf. on Atmospheric Aerosols, Condensation and Ice Nuclei, Vol. 1 1984 p 35-51 refs (For primary document see N85-32636 21-47)
Avail: NTIS HC A14/MF A01

The pine forest is a source of natural particles. The intensity of this source is calculated from measurements at ground level of concentration of Aitken nuclei and of radon, a naturally radioactive gas which was used as a tracer of the variations of the vertical stability of the lower layers of the atmosphere. The concentrations of the Aitken nuclei exhibit a diurnal cycle linked to the solar intensity. The formation of this particular matter results from the oxidation reactions of the gaseous emanations from the biomass with OH radicals and ozone. The rates of these different reactions vary with time over a period of 24 hr. Author

N85-32641# Bhabha Atomic Research Centre, Bombay (India). Air Monitoring Section.
EXPERIMENTAL STUDIES OF THE FORMATION OF AITKEN NUCLEI IN THE ATMOSPHERE
T. S. Muraleedharan, M. C. SubbaRamu, and K. G. Vohra *In* International Commission for Cloud Physics 11th Intern. Conf. on Atmospheric Aerosols, Condensation and Ice Nuclei, Vol. 1 1984 p 52-57 refs (For primary document see N85-32636 21-47)
Avail: NTIS HC A14/MF A01

Some of the atmospheric gas-phase reactions lead to the formation of Aitken nuclei. Monthly averages of the simultaneous measurements of Aitken nuclei in the atmosphere, Aitken nuclei formed in filtered air, sulphur dioxide, ethylene and alpha radioactivity in the atmosphere at Trombay, Bombay, were obtained from measurements. Correlation coefficients between Aitken nuclei formed and the other parameters were computed. The analysis of these results in the light of controlled experiments shows that most of the Aitken nuclei in the atmosphere are due to gas-to-particle conversion of sulphur dioxide and that ozone, ehtylene and atmospheric radioactivity have significant roles in the process of formation of Aitken nuclei in the atmosphere. Author

N85-32642# Kyoto Univ. (Japan). Inst. of Atomic Energy.
PHOTOCHEMICAL AEROSOL FORMATION IN POLLUTED ATMOSPHERE

M. Kasahara, K. Takahashi, Y. Moriguchi, and M. Kohno *In* International Commission for Cloud Physics 11th Intern. Conf. on Atmospheric Aerosols, Condensation and Ice Nuclei, Vol. 1 1984 p 58-62 refs (For primary document see N85-32636 21-47)
Avail: NTIS HC A14/MF A01

Laboratory tests were conducted to clarify the photochemical aerosol formation and growth mechanisms in various gaseous systems containing representative air pollutants such as SO2, NO2 and/or hydrocarbons. Photochemical aerosol formation and growth processes were examined by tracing the time change of total particle number concentration and particle size distribution. Photochemical aerosol forming potential in different gaseous systems was evaluated in terms of either gas-to-particle conversion rate or the number concentration of newly formed particles by UV irradiation. Author

N85-32643# Wien Univ. (Austria). Inst. fuer Experimentalphysik.
THE INFLUENCE OF BROWNIAN COAGULATION ON THE SIZE DISTRIBUTIONS OF ATMOSPHERIC AEROSOLS
A. Majerowicz and P. E. Wagner *In* International Commission for Cloud Physics 11th Intern. Conf. on Atmospheric Aerosols, Condensation and Ice Nuclei, Vol. 1 1984 p 63-67 refs Sponsored by Fonds zur Foerderung der Wissenschaftlichen Forschung in Oesterreich (For primary document see N85-32636 21-47)
Avail: NTIS HC A14/MF A01

A discussion is given of model calculations of Brownian coagulation combined with the formation of new particles in a bimodal aerosol, which was chosen as a model for nucleation and accumulation mode of the atmospheric aerosol. The formation and mutual interaction of the two modes are discussed. The stability of the bimodal aerosol in the presence of a constant spatially uniform aerosol source was checked. The obtained numerical results agree fairly well with the available experimental data. R.J.F.

N85-32644# Karpov (V. Y.) Physical Chemistry Inst., Moscow (USSR).
A STUDY OF TIME TRANSFORMATION OF NATURAL PHOTOCHEMICAL AEROSOLS
A. A. Lushnikov, Yu. V. Julanov, V. A. Zagainov, I. A. Hevskii, P. Yu. Makaveev, L. D. Stulov, and O. N. Nikitin *In* International Commission for Cloud Physics 11th Intern. Conf. on Atmospheric Aerosols, Condensation and Ice Nuclei, Vol. 1 1984 p 68-72 (For primary document see N85-32636 21-47)
Avail: NTIS HC A14/MF A01

Diurnal variations of the concentration levels of high dispersed and submicron fractions of atmospheric aerosols are measured in three different geographical regions of the USSR. A three step particle growth model is presented allowing correct reproducing the characteristic features of the time behavior of the concentration measured. The volume productivity of the smallest particle sources (2 to 10 particles/cubic centimeters sec) is evaluated. R.J.F.

N85-32645# Bhabha Atomic Research Centre, Bombay (India). Air Monitoring Section.
HUMAN ACTIVITY AND PRODUCTION RATE OF SECONDARY NUCLEI
P. V. Joshi and D. N. Kelkar *In* International Commission for Cloud Physics 11th Intern. Conf. on Atmospheric Aerosols, Condensation and Ice Nuclei, Vol. 1 1984 p 73-76 refs (For primary document see N85-32636 21-47)
Avail: NTIS HC A14/MF A01

Continuous measurements of Aitken nuclei concentration were carried out at a semiurban and a remote site. Production rates of secondary nuclei were calculated by subtracting a known fraction of the accumulation mode nuclei from the total nuclei concentrations. The peaks in the nuclei production rates were found to be associated with human activities like automobile transport or the cooking activities. Author

N85-32646# Indian Inst. of Trcpical Meteorology, Poona.
A NEW HYPOTHESIS FOR THE OBSERVED VERTICAL DISTRIBUTION OF ATMOSPHERIC AEROSOLS
A. Mary Selvam, A. S. RamachandraMurty, and Bh. V. RamanaMurty *In* International Commission for Cloud Physics 11th Intern. Conf. on Atmospheric Aerosols, Condensation and Ice Nuclei, Vol. 1 1984 p 77-81 refs (For primary document see N85-32636 21-47)
Avail: NTIS HC A14/MF A01

A simple model which can explain the observed vertical distribution and size spectrum of atmospheric aerosol is proposed. The model is based on a new physical hypothesis for the vertical mass exchange between the troposphere and the stratosphere. The vertical mass exchange takes place through a gravity wave feedback mechanism. There is close agreement between the model predicted aerosol distribution and size spectrum and the observed distributions. Author

N85-32647# Central Aerological Observatory, Moscow (USSR).
ON THE MECHANISMS RESPONSIBLE FOR THE FORMATION OF TYPICAL SIZE SPECTRA AND VERTICAL DISTRIBUTION OF TROPOSPHERIC AEROSOL PARTICLES
V. I. Smirnov *In* International Commission for Cloud Physics 11th Intern. Conf. on Atmospheric Aerosols, Condensation and Ice Nuclei, Vol. 1 1984 p 82-86 refs (For primary document see N85-32636 21-47)
Avail: NTIS HC A14/MF A01

A theoretical interpretation of the well known regularities in the structure of particle size spectra of the tropospheric aerosol and in the aerosol distribution in the vertical is given by taking into account aerosol generation from gases, primary condensation, coagulation, fragmentation of large particles, particle generation at the sea surface, sedimentation and scavenging. A new interpretation of the Junge spectrum is offered. Author

N85-32648# Academy of Sciences of the Georgian SSR, Tbilisi (USSR). Inst. of Geophysics.
ON THE TRANSFORMATION REGULARITIES OF TIME SERIES OF SOLID AEROSOL CONCENTRATIONS IN THE SURFACE ATMOSPHERIC LAYER
O. V. Lomaya, D. G. Tsintsadze, and G. N. Buka *In* International Commission for Cloud Physics 11th Intern. Conf. on Atmospheric Aerosols, Condensation and Ice Nuclei, Vol. 1 1984 p 87-91 refs (For primary document see N85-32636 21-47)
Avail: NTIS HC A14/MF A01

Time variations of solid aerosol weight concentrations in the surface atmospheric layer conducted in urban conditions are discussed. The combined analysis of time series of aerosol concentrations and various meteorological factors was carried out. The regularities of variations in time were studied. An explanation of reasons, causing them was found. Annual, daily and secular run of C depends on the corresponding variations of the number of aerosols coming into the layer under investigation as well as on the meteorological conditions. The temporal run of mean daily aerosol concentrations is well explained by the corresponding variability of the complex meteorological potential of air pollution, taking into account three meteorological factors; stratification of atmosphere in the lower 0.5 km layer, wind velocity in the near ground layer and the amount of precipitation falling during twenty-four hours. R.J.F.

N85-32649# Karpov (V. Y.) Physical Chemistry Inst., Moscow (USSR).
SIZE SPECTRA FOR THE SOURCE-ENHANCED COAGULATION WITH THE TURBULENT MASS TRANSFER
A. G. Sutugin *In* International Commission for Cloud Physics 11th Intern. Conf. on Atmospheric Aerosols, Condensation and Ice Nuclei, Vol. 1 1984 p 92-95 refs (For primary document see N85-32636 21-47)
Avail: NTIS HC A14/MF A01

An implicit method of integrating of the rigid systems of differential equations is applied for the solution of the coagulation equations. The method requires much less computation time than the routine Runge-Kutta procedure and, so, permits one to follow the spectrum evolution for considerably longer time interval. It is very useful for simulating of the retarded coagulation. The examples

of retarded systems are these with the dissociation of clusters and with the low collision efficiency. It is demonstrated that the time scale of the spectra evolution is much larger for such systems so settling of the self-preserving regime under the atmospheric conditions is impossible. The conditions for the neglection of the influence of the turbulent mass transfer on the coagulation are formulated. The mass transfer influence the size spectrum evolution near the source of fresh particles only. Author

N85-32650# Mainz Univ. (West Germany). Inst. for Meteorology.
OUR KNOWLEDGE ABOUT THE ATMOSPHERIC AEROSOL
R. Jaenicke *In* International Commission for Cloud Physics 11th Intern. Conf. on Atmospheric Aerosols, Condensation and Ice Nuclei, Vol. 1 1984 p 99-107 refs (For primary document see N85-32636 21-47)
Avail: NTIS HC A14/MF A01

A summary is given on what is known about atmospheric aerosols. The atmospheric aerosol has gained increasing interest in the past and our knowledge about it has grown. This mainly is caused through the availability of powerful tools for observations and measurements. However, these methods often promote the measurements of parameters which are more or less for understanding the aerosol. Author

N85-32651# Academia Sinica, Beijing (China). Inst. of Atmospheric Physics.
CHARACTERISTICS OF AEROSOL COMPOSITION IN A NON-URBAN AREA, NORTH CHINA
Wang Ming-xing, Ren Li-xin, and Lu Wei-xiu *In* International Commission for Cloud Physics 11th Intern. Conf. on Atmospheric Aerosols, Condensation and Ice Nuclei, Vol. 1 1984 p 108-112 refs (For primary document see N85-32636 21-47)
Avail: NTIS HC A14/MF A01

The basic results of a comprehensive measurement at Xinglong astronomical observing station are summarized. Fundamental characteristics of elemental concentrations and size distributions of aerosol are briefly discussed; it is found that the size distribution of Cl may show a bimodal under certain conditions, which may be a result of a mixture of marine air and polluted air. A comparison between the elemental concentrations sampled by different sampling devices shows that chemical reactions may preferably occur on filters and that the nonurban aerosol contains more acid pollutants than the polluted cities where black smoke is visibly observed. Author

N85-32652# Institute for Atmospheric Physics, Budapest (Hungary).
TRACE ELEMENT CONCENTRATIONS IN ATMOSPHERIC AEROSOL OVER HUNGARY
A. Meszaros, L. Haszpra, I. Kiss (Hungarian Academy of Sciences, Debrecen), E. Koltay (Hungarian Academy of Sciences, Debrecen), S. Laszlo (Hungarian Academy of Sciences, Debrecen), and Gy. Szabo (Hungarian Academy of Sciences, Debrecen) *In* International Commission for Cloud Physics 11th Intern. Conf. on Atmospheric Aerosols, Condensation and Ice Nuclei, Vol. 1 1984 p 113-117 refs (For primary document see N85-32636 21-47)
Avail: NTIS HC A14/MF A01

Seventy filter samples of atmospheric particles collected during one year at a rural site were analysed up to 20 elements by PIXE. The average concentrations and enrichment factors are presented and discussed. The most abundant element was sulfur that had no seasonal variation while other pollution elements like non crustal V and As had 2.5 higher average concentrations in winter than in summer. Soil derived elements had their maximum concentrations in summer. Interelement correlation matrix and factor analysis showed that four factors were sufficient to account to 77 and 75% of the total variance in winter and summer, respectively, but the very complex factor loading structure did not enable exact source opportionment. Author

N85-32653# Indian Inst. of Tropical Meteorology, Poona.
CHEMICAL COMPOSITION OF ATMOSPHERIC AEROSOL AT DELHI
L. T. Khemani, Medha S. Naik, G. A. Momin, R. Kumar, R. N. Chatterjee, G. Singh, and Bh. V. RamanaMurty *In* International Commission for Cloud Physics 11th Intern. Conf. on Atmospheric Aerosols, Condensation and Ice Nuclei, Vol. 1 1984 p 118-122 refs (For primary document see N85-32636 21-47)
Avail: NTIS HC A14/MF A01

The total atmospheric aerosol levels at Delhi (north India) were measured on 116 days between February to October 1980. The observations were stratified according to the season. The values of cross correlation of total suspended particles (TSP) and its components were evaluated. High TSP (209 microgram/cc.) levels were found during summer period associated with hot and dry weather in the region. Low TSP (109 microgram/cc.) were found during monsoon period. Most of the TSP mass was associated with the natural soil elements, such as Fe, Al, Mn, Ca and K. Only a fraction of the mass of the TSP was comprised of elements from anthropogenic sources, e.g., Pb, Ni, Cd, Sb, Cu and Zn. The aerosols at Delhi were potentially basic in nature unlike those in European countries which are acidic in nature and cause for acid rainfall. Author

N85-32654# Mainz Univ. (West Germany). Inst. for Meteorology.
MINERAL AEROSOLS AND SOURCE IDENTIFICATION
L. Schuetz and M. Sebert (Freiburg Univ., West Germany) *In* International Commission for Cloud Physics 11th Intern. Conf. on Atmospheric Aerosols, Condensation and Ice Nuclei, Vol. 1 1984 p 123-127 refs (For primary document see N85-32636 21-47)
Avail: NTIS HC A14/MF A01

Dry fractionated silt-clay size samples (particle radius < or = 5 micrometers) of a suite Saharan desert soils have been analyzed by X-ray diffraction for source characteristic mineral constituents. The same analysis applied to mineral aerosol samples collected at 3 desert sites during normal and sand-storm conditions yielded a comparison between soil mineral particles, which can be eroded and transported long distances, and soil-derived aerosol material. Within the soil dust samples the composition varies with different provinces. Material from the north shows certain enrichments of carbonates and in the south high abundance of kaolinite will be found. Palygorskite, exclusively found in the north, seems to be the only source-specific mineral which can be used for a larger source region. In contrast, airborne material was found to be extremely well mixed and does not reflect local or regional characteristics. Local components will be detected only temporarily under severe dust storm conditions. Author

N85-32655# Stockholm Univ. (Sweden). Dept. of Meteorology.
PHYSICAL AND CHEMICAL AEROSOL CHARACTERISTICS IN EXTREMELY CLEAN AIR MASSES AT CAPE GRIM, TASMANIA
J. Heintzenberg *In* International Commission for Cloud Physics 11th Intern. Conf. on Atmospheric Aerosols, Condensation and Ice Nuclei, Vol. 1 1984 p 128-132 refs (For primary document see N85-32636 21-47)
Avail: NTIS HC A14/MF A01

Fine particle aerosol samples were taken on a monthly basis at the Australian background station at Cape Grim, Tasmania. The aerosol deposits were analyzed for elemental carbon (PEC), Na+, SO4, Pb, Cd, and Mn. Continuous recordings of condensation nuclei and radon were used for the interpretation of the results. The first 17 months of data show metal concentrations comparable to data from other remote areas. PEC-concentrations were lower than Northern Hemisphere minima. Author

N85-32656# Mainz Univ. (West Germany). Inst. for Meteorology.
AITKEN PARTICLE SIZE DISTRIBUTION IN ANTARCTICA
R. Jaenicke and J. Stingl *In* International Commission for Cloud Physics 11th Intern. Conf. on Atmospheric Aerosols, Condensation and Ice Nuclei, Vol. 1 1984 p 133-137 refs (For primary document see N85-32636 21-47)
Avail: NTIS HC A14/MF A01

Since the summer expedition 1981/82, the German Antarctic Research Station Georgvon-Neumayer was available for aerosol studies. This is a unique opportunity to fill the gap still present in the global cover of the Aitken particle concentration. Aitken particles play a crucial role in air chemistry as a link between atmospheric trace gases and aerosols. The forming of Aitken particles occurs through gas-to-particle conversion thus acting as a sink for precursor gases, most probably sulfur and organic species. In addition, most human activities are connected with the production of high concentrations of Aitken particles. Thus, the presence of rather high concentrations of Aitken particles might serve as an indicator for anthropogenic activities. However, because of the limited residence time of Aitken particles, particles produced this way are not subject to intercontinental transport. The Aitken particle concentration in the Antarctic is known only vaguely and indicated to be around 5001cc. at the coast. G.L.C.

N85-32657# Washington Univ., Seattle. Cloud and Aerosol Research Group.

AIRBORNE MEASUREMENTS OF THE VERTICAL DISTRIBUTION OF ARCTIC HAZE

Lawrence F. Radke, Jamie H. Lyons, Ian H. Bailey (Western Australian Inst. of Tech.), and Peter V. Hobbs *In* International Commission for Cloud Physics 11th Intern. Conf. on Atmospheric Aerosols, Condensation and Ice Nuclei, Vol. 1 1984 p 138-142 refs (For primary document see N85-32636 21-47)

(Grant NSF DPP-82-09548)

Avail: NTIS HC A14/MF A01

The polar regions are sinks for most atmospheric trace constituents. Once introduced into the Arctic, the combination of differing source regions, great thermal stability, reduced photochemistry, low scavening rates, and slow meridional transport produce a vertically layered complex of very clean and quite polluted air of potentially long life. Early airborne observations made it clear that the particulate portion of this pollution contributed to a significant degradation of visibility, noting visibilities as low as 3 to 8 km. Recent work has clearly established that episodes of anthropogenic pollution (haze) are common at surface locations around the arctic rim during arctic winter. This haze contains secondary aerosol (mostly acid sulfate) and primary aerosol of industrial origins, together with various soil and volcanic material. Airborne measurements were designed to characterize the vertical structure and horizontal extent of arctic haze and to further define the arctic aerosol. G.L.C.

N85-32658# Colorado Univ., Boulder. Cooperative Inst. for Research in Environmental Sciences.

CONDENSATION NUCLEI AND AEROSOL SIZE DISTRIBUTION MEASUREMENTS IN ARCTIC HAZE

R. C. Schnell *In* International Commission for Cloud Physics 11th Intern. Conf. on Atmospheric Aerosols, Condensation and Ice Nuclei, Vol. 1 1984 p 143-147 refs (For primary document see N85-32636 21-47)

Avail: NTIS HC A14/MF A01

During March and April of 1983 an instrumented NOAA WP-3D aircraft flew 130 hours studying anthropogenic Arctic air pollution commonly known as Arctic Haze. All of the flights were conducted north of the Arctic Circle and covered the Arctic Ice Cap from Alaska across the pole to the Norwegian Arctic. The haze was observed to occur in distinct layers separated by cleaner air. Typical CN concentrations within haze layers were 800 to 1000 cc and 50 to 100 cc in the intervening clean air. Clouds within a haze layer reduced CN concentration to between 10 and 20 cm. The haze layers were further distinguished by generally containing a bi-modal particle distribution with the larger particle mode peaking in the 1 to 2 micrometer diameter range in concentrations of from 0.1 to 1 cc. Author

N85-32659# Academy of Sciences of the Georgian SSR, Tbilisi (USSR). Inst. of Geophysics.

AIRCRAFT INVESTIGATIONS OF THE DISTRIBUTION OF AEROSOLS IN THE LOWER TROPOSPHERE

A. G. Amiranashvili, T. G. Gzirishvili, A. I. Kartsivadze, and A. G. Nodia *In* International Commission for Cloud Physics 11th Intern. Conf. on Atmospheric Aerosols, Condensation and Ice Nuclei, Vol. 1 1984 p 148-153 refs (For primary document see N85-32636 21-47)

Avail: NTIS HC A14/MF A01

A long-term aircraft investigations of the vertical distribution of short-living radon decay products and large and gigantic aerosol particles in the lower 5 km atmospheric layer was conducted. It is revealed that the character of substiate affects much more the content of aerosols in the atmosphere than the content of products of radon decay. It is shown that the cumulus cloudiness exerts influence upon the content of aerosols of both types, increasing it in comparison with cloudless days. The quantitative evaluation of the turbulent mixing intensity in free atmosphere for cloudless days and for days with cumuli is carried out. Using the values of turbulence coefficient and aerosol particle concentrations at different levels the evaluation of sedimentation velocity of aerosols of different size was conducted. Author

N85-32660# Institute of Experimental Meteorology (USSR).

THE VARIABILITY OF AEROSOL MICROSTRUCTURE IN CONTINENTAL AND OCEANIC SURFACE LAYERS OF THE ATMOSPHERE IN ANTICYCLONES

N. V. Goncharov, O. A. Lipskaya, V. V. Smirnov, and A. D. Uvarov *In* International Commission for Cloud Physics 11th Intern. Conf. on Atmospheric Aerosols, Condensation and Ice Nuclei, Vol. 1 1984 p 154-158 refs (For primary document see N85-32636 21-47)

Avail: NTIS HC A14/MF A01

Data on the atmospheric D=0.01-20 micron aerosol dispersive composition and variability, generalized for summer and winter anticyclones typical of the center of the European territory of the USSR and the Southern Hemisphere oceans are presented. Author

N85-32661# Academy of Sciences (USSR), Moscow. Inst. of Atmospheric Physics.

VARIATION OF THE SUBMICRON AEROSOL STRUCTURE

G. I. Gorchakov, A. S. Emilenko, A. I. Kartsivadze (Academy of Sciences of the Georgian SSR, Tbilisi), D. M. Metreveli (Academy of Sciences of the Georgian SSR, Tbilisi), and V. N. Sidorov *In* International Commission for Cloud Physics 11th Intern. Conf. on Atmospheric Aerosols, Condensation and Ice Nuclei, Vol. 1 1984 p 159-163 refs (For primary document see N85-32636 21-47)

Avail: NTIS HC A14/MF A01

Microstructure parameters of the submicron aerosol and the particle refractive index are determined using data on the scattering matrix. Variation of the atmospheric aerosol particle size distributions in the submicron range and humidity influence on the aerosol microstructure have been studied. Efficiency of the main transformation processes of the background aerosol is evaluated. Author

N85-32662# Paris XII Univ., Creteil (France). Lab. de Physique des Aerosols et de Transfert des Contaminations.

SOME CONSIDERATIONS ABOUT THE NATURAL ATMOSPHERIC RADIOACTIVE AEROSOL

A. Renoux, G. Tymen (Univ. de Bretagne Occidentale), and G. Madelaine *In* International Commission for Cloud Physics 11th Intern. Conf. on Atmospheric Aerosols, Condensation and Ice Nuclei, Vol. 1 1984 p 164-169 refs (For primary document see N85-32636 21-47)

Avail: NTIS HC A14/MF A01

The natural atmospheric radioactivity especially arises from Radon 222, and in an inferior way, from Radon 220 (Thoron), both being radioactive gas emerging from the Earth. Their lived short daughters stick themselves upon the air particles, and make up the natural atmospheric aerosol. By studying this latter, we may drow up various atmospheric phenonenous, estimate the quantity of natural irradiation a given population may undertake, and, on a more theoric level, confirm the rightfulness of some Aerosol Physics and Atmospheric Electricity laws. G.L.C.

N85-32663# Wien Univ. (Austria). Inst. fuer Experimentalphysik.
VARIABILITY OF RURAL AEROSOLS UNDER STABLE WEATHER CONDITIONS
R. Hitzenberger, H. Horvath, M. Pimminger (Technische Univ., Vienna), and H. Puxbaum (Technische Univ., Vienna) *In* International Commission for Cloud Physics 11th Intern. Conf. on Atmospheric Aerosols, Condensation and Ice Nuclei, Vol. 1 1984 p 170-174 refs (For primary document see N85-32636 21-47)
Avail: NTIS HC A14/MF A01

Aerosol mass concentration, mass size distributions, extinction, scattering and absorption coefficients were measured in autumn before the heating period at two sites in Vienna and the Vienna woods, Austria, under very stable stagnant weather conditions. On some samples a chemical analysis was performed. No large difference was found between the aerosol at the two sites except a larger carbon content and absorption coefficient in Vienna both during and after the stagnant period. Variability of the aerosol properties (both chemical and physical) can be attributed to local sources only when the residence time of the air mass has been short (approx. two days). Author

N85-32664# Netherlands Energy Research Foundation, Petten.
MARINE AEROSOLS AT THE DUTCH NORTH SEA COAST: SIZE DISTRIBUTIONS AND FRACTIONATION OF TRACE ELEMENTS
J. F. vandeVate, R. K. A. M. Mallant, G. P. A. Kos, H. M. TenBrink, A. Plomp, and A. Vermetten *In* International Commission for Cloud Physics 11th Intern. Conf. on Atmospheric Aerosols, Condensation and Ice Nuclei, Vol. 1 1984 p 175-179 refs (For primary document see N85-32636 21-47)
Avail: NTIS HC A14/MF A01

Size distributions, concentrations and elemental composition of the North Sea marine aerosol and of micro-ocean aerosol were investigated. Surf had insignificant influence on size distributions; also identical size distributions were obtained at different heights 10 m to 850 m. Any continental influence appears almost exclusively in the particle diameter range around 0.1 micrometers. Fractionation factors relative to Na of 10 trace elements amounted to 10 .001 to .0001 104 at a coastal site; those from filtered sea water (micro-ocean) are roughly one order of magnitude smaller. Author

N85-32665# Johann-Wolfgang-Goethe-Univ., Frankfurt am Main (West Germany). Inst. fuer Meteorologie und Geophysik.
APPLICATION OF PARTICLE INDUCED X-RAY EMISSION ANALYSIS (PIXE) TO AEROSOL LONG RANGE TRANSPORT STUDIES
P. Metternich, H.-W. Georgii, and K. O. Groeneveld *In* International Commission for Cloud Physics 11th Intern. Conf. on Atmospheric Aerosols, Condensation and Ice Nuclei, Vol. 1 1984 p 180-184 refs (For primary document see N85-32636 21-47)
Avail: NTIS HC A14/MF A01

Using a combination of a size fractionating sampler and a multi-elemental technique such as PIXE, the levels and types of tropospheric aerosols were determined, both in the planetary boundary layer and the free atmosphere, under a variety of remote and pollution conditions. The elemental mass size functions obtained in these ground and aircraft measurements together with the corresponding air mass trajectories were used to assess the relationships between observed aerosol distributions and atmospheric transport mechanisms. Author

N85-32666# Mainz Univ. (West Germany). Inst. for Meteorology.
SAHARA DESERT DUST TRANSPORT TO THE SOUTH
G. A. DAlmeida and R. Jaenicke *In* International Commission for Cloud Physics 11th Intern. Conf. on Atmospheric Aerosols, Condensation and Ice Nuclei, Vol. 1 1984 p 185-190 refs (For primary document see N85-32636 21-47)
Avail: NTIS HC A14/MF A01

A network with 10 sunphotometers was established in the Sahara desert and close to its borders. The aim of this network was to monitor the flux of duct out of the Sahara. The transport to the South is the most important one as compared with the other wind directions. The results show roughly 400 millions of tons per year transported to the South. The respective figure for the transport to the West, North and East are 200, 100 millions of tons per year, and nothing. These results could be obtained simultaneously and do in part confirm earlier estimates. Author

N85-32667# Wisconsin Univ., Madison. Dept. of Meteorology.
SCAVENGING OF SUBMICRON AEROSOL PARTICLES BY SNOW CRYSTALS: THEORY AND EXPERIMENTS
P. K. Wang and D. Sauter *In* International Commission for Cloud Physics 11th Intern. Conf. on Atmospheric Aerosols, Condensation and Ice Nuclei, Vol. 1 1984 p 191-194 refs (For primary document see N85-32636 21-47)
(Grant EPA-R-809371-01-0)
Avail: NTIS HC A14/MF A01

A theoretical model is presented for the determination of collection efficiency of submicron aerosol particles by snow crystals. The model considers the removal of aerosol particles under the influence of combined effect of Browian diffusion, thermo- and diffusiophoretic forces, electric forces, and hydrodynamic effects. Experimental results are compared with theoretical predictions by the model. It is shown that reasonable agreement was obtained. Author

N85-32668# Academia Sinica, Beijing (China). Inst. of Atmospheric Physics.
MEASUREMENTS OF GIANT SALT NUCLEI FROM INLAND IN EAST CHINA
He Zhenzhen, Huang Meiyuan, Chen Yianjuan, Jing Anjian, Shen Znilai, Zhou Wenxian (Nanjing Meteorological Coll.), and Chen Jingrong *In* International Commission for Cloud Physics 11th Intern. Conf. on Atmospheric Aerosols, Condensation and Ice Nuclei, Vol. 1 1984 p 195-199 (For primary document see N85-32636 21-47)
Avail: NTIS HC A14/MF A01

The giant salt nuclei (d=2 microns) are important factors for physical processes of formating of warm clouds and precipitation. In order to investigate further the source region of the giant salt, the salt nuclei horizontal transport with air motion and the pattern of its distribution, three observation stations which are located on same latitude of about 30 N were established. Ningbo and Jiande were chosen as representatives of maritime (island), coastal and land stations respectively. The straight distance from Putuo to Ningbo and Jiande is 75 and 300 km respectively. Time measurements were made simultaneously at three stations at 2-hr interval from 0600 to 2000 (sometimes for all day) every day and with measuring at 1300 and after rainfall. The method of Liesegang's circle was used for distinguishing and count of salt nuclei, and the data obtained were corrected by magnification factor and collection efficiency of pump air speed and relative humidity. Author

N85-32669# Karpov (V. Y.) Physical Chemistry Inst., Moscow (USSR).
A PROBABILISTIC METHOD FOR PARTICLE SIZE ANALYSIS OF AEROSOLS
Yu. V. Julanov, A. A. Lushnikov, and I. A. Nevskii *In* International Commission for Cloud Physics 11th Intern. Conf. on Atmospheric Aerosols, Condensation and Ice Nuclei, Vol. 1 1984 p 200-203 refs (For primary document see N85-32636 21-47)
Avail: NTIS HC A14/MF A01

A mathematical model is presented and possibilties are discussed for the particle size analysis of aerosols by counters affording the multiple counting of particles. The total particle concentration can be determined by measuring the total dead time interval T sub 0 and dividing it into the total measurement time T:N = ln(T/T sub o). Author

N85-32670# Utrecht State Univ. (Netherlands). Inst. for Meteorology and Oceanography.
CLOUD CONDENSATION ON INSOLUBLE PARTICLES

J. C. H. VanDerHage *In* International Commission for Cloud Physics 11th Intern. Conf. on Atmospheric Aerosols, Condensation and Ice Nuclei, Vol. 1 1984 p 207-210 refs (For primary document see N85-32636 21-47)
Avail: NTIS HC A14/MF A01

Experimental evidence strongly suggest that condensation of water on insoluble particles is an adsorption process and not a nucleation process. Cloud condensation on insoluble particles is negligible due to the low concentration of insoluble CCN in a type atmospheric aerosol. The adsorption mechanisms and the consequences of its application to atmospheric processes are discussed here. Author

N85-32671# Atmospheric Environment Service, Downsview (Ontario).
OBSERVATIONS OF CLOUD DROPLETS, AEROSOL PARTICLES AND CLOUD CONDENSATION NUCLEI IN CONTINENTAL AIR MASSES
W. R. Leaitch, J. W. Strapp (Desert Research Inst.), R. S. Schemenauer, G. A. Isaac, and J. G. Hudson *In* International Commission for Cloud Physics 11th Intern. Conf. on Atmospheric Aerosols, Condensation and Ice Nuclei, Vol 1 1984 p 211-216 refs (For primary document see N85-32636 21-47)
Avail: NTIS HC A14/MF A01

Measurements are made of the concentrations of cloud droplets, aerosol particles larger than 0.18 micrometers and cloud condensation nuclei active at supersaturations $< 0.4\%$. Comparisons indicate that the maximum cloud supersaturation was usually $< 0.4\%$ and that the cloud droplet concentrations were strongly influenced by the updraft velocity. Author

N85-32672# Institute of Applied Geophysics, Moscow (USSR).
CONDENSATION PROPERTIES OF ATMOSPHERIC AEROSOL
A. G. Laktionov *In* International Commission for Cloud Physics 11th Intern. Conf. on Atmospheric Aerosols, Condensation and Ice Nuclei, Vol. 1 1984 p 217-221 refs (For primary document see N85-32636 21-47)
Avail: NTIS HC A14/MF A01

A new approach to calculating the condensation properties of atmospheric aerosols is proposed. The ionic composition of solution on aerosol particles and the values of ionic osmotic coefficient is taken into account. The relation between the masses of aerosol drops and their ionic composition at equilibrium humidity is computed. The condensation transformation of atmospheric aerosol distribution functions and its connection with the condensation nuclei distribution function is analyzed. Author

N85-32673# Ecole Normale Superieure, Abidjan (Ivory Coast).
A STATISTICAL STUDY OF CCN CONCENTRATION IN SUB-EQUATORIAL CLIMATE: THE PARTICULAR CASE OF THE TROPICAL WET FOREST
F. Desalmand, R. Serpolay (LAMP-IOPG du Puy de Dome, Clermont, France), and J. Baudet (Faculty des Sciences, Abdjan, Ivory Coast) *In* International Commission for Cloud Physics 11th Intern. Conf. on Atmospheric Aerosols, Condensation and Ice Nuclei, Vol 1 1984 p 222-226 refs (For primary document see N85-32636 21-47)
Avail: NTIS HC A14/MF A01

A statistical study of CCN concentration measurements carried out in the Ivory Coast with a static diffusion cloud chamber is presented. A number of measurements were taken at three supersaturations S during each of the two main seasons. Theoretical remarks about the dependence of the k-slope of the S-spectrum upon the size distribution and the activity of CCN are given with the equatorial forest as example of CCN source. The shape of the S-spectrum and the sense of variation of the size spectrum are quite correlated with meteorological conditions. Author

N85-32674# Institute of Applied Geophysics, Moscow (USSR).
INVESTIGATION OF THE FORMATION OF CLOUD PARTICLE SPECTRUM ON NATURAL CONDENSATION NUCLEI
N. A. Begalishvili, N. Sh. Bibilashvili, I. P. Metskhvarishvili, I. P. Prais, and E. G. Krachaturyan *In* International Commisiion for Cloud Physics 11th Intern. Conf. on Atmospheric Aerosols, Condensation and Ice Nuclei, Vol. 1 1984 p 227-231 refs (For primary document see N85-32636 21-47)
Avail: NTIS HC A14/MF A01

In analyzing the atmospheric aerosols the basic problem is the determination of disperse and chemical composition of particles. Dispersity of aerosols was determined by the method of optical and electron microscopy. As to chemical composition, the most promising is the application of the method of microchemical analysis, known as the method of Liezegang rings. The method was offered to investigate aerosol particles of some soluble salts, which form atmospheric condensation nuclei. Investigations showed the possibility of application of this method in determining the dispersity of chemical composition of particles of a wide variety of soluble and insoluable inorganic salts. Author

N85-32675# Max-Planck-Inst. fuer Meteorologie, Hamburg (West Germany).
A SIMPLE MODEL TO INVESTIGATE THE ACTIVATION PROCESS IN WATERCLOUDS
H. Grassl (Inst. fuer Meereskunde, Duesternbrooker, West Germany) and L. Levkov *In* International Commission for Cloud Physics 11th Intern. Conf. on Atmospheric Aerosols, Condensation and Ice Nuclei, Vol. 1 1984 p 232-238 Sponsored in part by Umweltbundesamt and the European Communities (For primary document see N85-32636 21-47)
Avail: NTIS HC A14/MF A01

The simple relations CCN = c(n) S sup k and N = n sup gamma between cloud condensation nuclei, CCN, supersaturation, S, number of aerosol particles, n, and cloud droplets, N, involve two empirical parameters, k and gamma, which are constants for a distinct aerosol type. Calculations of k and gamma, given n, S, size and composition of aerosol particles, show the same range of values as all measurements available in the open literature. This stimulates the search for a simple model allowing to calculate changes in cloud droplet number N for any given variation of an aerosol parameter and/or updraft. The model includes the reduction of maximum supersaturation S sub max with particle number n and calculations, via an iteration a value S sub max simultaneously fulfilling two relations for N. A main result is the change in most important parameters with cloud types. An increase in particle number is as important as an increase in updraft for the entire updraft range, while a change in the slope of the aerosol size distribution is extremely important for stratus clouds. Consequences for the optical depth of clouds are also discussed. Author

N85-32676# Naval Research Lab., Washington, D. C.
MEASUREMENTS OF THE CRITICAL SUPERSATURATION OF 0.029 TO 0.035 MICRON RADIUS PARTICLES AT WASHINGTON, DISTRICT OF COLUMBIA
J. W. Fitzgerald and G. M. Frick *In* International Commission for Cloud Physics 11th Intern. Conf. on Atmospheric Aerosols, Condensation and Ice Nuclei, Vol. 1 1984 p 239-243 refs (For primary document see N85-32636 21-47)
Avail: NTIS HC A14/MF A01

The critical supersaturation of 0.029 to 0.035 micrometers radius atmospheric aerosol particles was measured. From these measurements, estimates of the aerosol activation parameter B sup 0 and of the volume fraction epsilon sub V of water soluble material were obtained, the latter being calculated by assuming that the soluble material was ammonium sulfate. The value of epsilon sub V ranged from 0.2 to 0.58 and averaged 0.4 for all twenty measurements. Author

N85-32677# Desert Research Inst., Reno, Nev.
A RELATIONSHIP BETWEEN CLOUD DROPLET SIZE AND CCN CRITICAL SUPERSATURATION
J. C. Hudson and C. F. Rogers *In* International Commission for Cloud Physics 11th Intern. Conf. on Atmospheric Aerosols, Condensation and Ice Nuclei, Vol. 1 1984 p 244-248 refs (For primary document see N85-32636 21-47)
(Grant NSF ATM-82-10344)
Avail: NTIS HC A14/MF A01

In cloud measurements of CCN spectra demonstrate that cloud droplets grow almost exclusively on the nuclei with the lowest critical supersaturations, S sub c. Moreover larger droplets seem to be more likely to be grown on nuclei with lower S sub c. Experiments are described which have employed improved droplet size cuts which were also varied during the experiments. The results not only confirm the previous study but also establish a correlation between cloud droplet size and nucleus S sub c.
Author

N85-32678# Naval Research Lab., Washington, D. C.
FOG ACTIVATION AND SUPERSATURATION
H. Gerber, J. E. Jiusto (State Univ. of New York, Albany), and G. G. Lala (State Univ. of New York, Albany) *In* International Commission for Cloud Physics 11th Intern. Conf. on Atmospheric Aerosols, Condensation and Ice Nuclei, Vol. 1 1984 p 229-253 refs (For primary document see N85-32636 21-47)
Avail: NTIS HC A14/MF A01

Measurements made in radiation fog with a high resolution hygrometer and other instrumentation showed that the time constants of turbulent eddy dissipation and droplet growth were similar. Both must be considered in predicting fog microphysics. Thicker radiation fog was studies using the saturation hygrometer which measures 95% RH similar to or less than 105%, as well as other instrumentation including newly developed precision psychrometers, liquid water and visibility meters, droplet size spectrometers, and low wind speed indicators. The results described are limited to two cases of post sunrise radiation fog for which the relationships between supersaturation, turbulence, and droplet activation were studied.
Author

N85-32679# Academy of Sciences (USSR), Moscow. Inst. of Physical Chemistry.
ON THE QUESTION TO THE EFFECT OF SURFACTANTS ON THE SPECTRUM OF CLOUD DROPS IN THE PROCESS OF THEIR CONDENSATION GROWTH
S. P. Bakanov, B. V. Dejaguin, Yu. S. Kurghuin, and K. M. Merzhanov *In* International Commission for Cloud Physics 11th Intern. Conf. on Atmospheric Aerosols, Condensation and Ice Nuclei, Vol. 1 1984 p 254-259 refs (For primary document see N85-32636 21-47)
Avail: NTIS HC A14/MF A01

Introduction of a highly-disperse aerosol of higher fatty alcohols into the zone of an ascending current under cumuli results in that a greater part of droplets are passivated, and in the cumulus there are provided conditions for the preferable growth of large drops. An attempt was made to investigate theoretically the possibility of surfactants exerting their effect on the process of condensation growth of water containing nuclei, thus envisaging causing artificially rainfall from warm clouds. The following model was adopted as an investigation object: an air current ascending at a velocity mu, containing a fairy wide spectrum of water containing condensation nuclei saturated with surfactants vapors. The saturation degree amounts to about 100% and is retained constant during the whole process.
Author

N85-32680# Indian Inst. of Tropical Meteorology, Poona.
AIRCRAFT OBSERVATIONS OF CLOUD CONDENSATION NUCLEI IN MARITIME AND CONTINENTAL ENVIRONMENTS
A. S. Ramachandra, R. Vijayakumar, Poona Sikka, A. Mary Selvam, and Bh. V. Ramana Murty *In* International Commission for Cloud Physics 11th Intern. Conf. on Atmospheric Aerosols, Condensation and Ice Nuclei, Vol. 1 1984 p 260-264 refs (For primary document see N85-32636 21-47)
Avail: NTIS HC A14/MF A01

Aircraft observations of cloud condensation nuclei were made at different levels in the lower troposphere (up to 10000 ft ASL) over the Arabian Sea, about 100 km off the coast at Bombay (18 deg 51 min N, 72 deg 49 min E, 33 ft ASL) and over the Deccan Plateau region, about 200 km inland from the coast at Bombay. The concentration of CCN increased with height over the ocean and decreased over the land. Based on the dynamics of the atmospheric boundary layer, a theoretical model for the prediction of dispesion of aerosols in the atmosphere has been proposed.
Author

N85-32681# Academia Sinica, Beijing (China). Inst. of Atmospheric Physics.
THE DISTRIBUTION OF GIANT SALT NUCLEI INSIDE AND OUTSIDE CLOUD OVER THE BASIN OF XIN AND JIANG
Huang Mei-yuan and Shen Zhi-lai *In* International Commission for Cloud Physics 11th Intern. Conf. on Atmospheric Aerosols, Condensation and Ice Nuclei, Vol. 1 1984 p 265-269 refs (For primary document see N85-32636 21-47)
Avail: NTIS HC A14/MF A01

The giant salt nuclei are an important factor for formation of warm rain. The observations of various authors indicate that the distribution of giant salt nuclei on the ground is relative to weather background. Less attention is paid to the relation between the vertical distribution of salt nuclei and weather condition. Moreover, there is no information of giant salt nuclei in cloud. Twenty-five flights were flown for the observation of giant salt nuclei using method of Liesegang's circles and other parameters. 340 measurements were made at altitude from 1000m to 5500m inside and outside cloud. The distribution of giant salt nuclei in various weather situations are described. The distribution of giant salt nuclei in various clouds is given.
Author

N85-32682# Missouri Univ., Rolla. Dept. of Mechanical and Aerospace Engineering.
PROPERTIES OF FOREST DERIVED CLOUD CONDENSATION NUCLEI
J. Podzimek and F. Desalmand (University of Abidjan, Ivory Coast) *In* International Commission for Cloud Physics 11th Intern. Conf. on Atmospheric Aerosols, Condensation and Ice Nuclei, Vol. 1 1984 p 270-274 refs (For primary document see N85-32636 21-47)
Avail: NTIS HC A14/MF A01

Several typical examples of the cloud condensation nuclei (CCN) and Aitken nuclei (AN) measurements at a rural site in the savannah in the proximity of a river with tropical vegetation in Ivory Coast are mentioned. An explanation of the low AN counts and a very high CCN concentration based on a hypothetical inactive nucleus with several active spots is offered.
Author

N85-32683# Clermont-Ferrand Univ. (France).
INFLUENCE ON AN INDUSTRIAL SITE ON THE CHARACTERISTICS OF CCN SUPERSATURATION WITH AIR MASSES OF DIFFERENT ORIGIN
G. Gorbinet and R. Serpolay *In* International Commission for Cloud Physics 11th Intern. Conf. on Atmospheric Aerosols, Condensation and Ice Nuclei, Vol. 1 1984 p 275-279 refs (For primary document see N85-32636 21-47)
Avail: NTIS HC A14/MF A01

By treating with statistical methods a number of measurements on CCN concentrations performed on the industrial site of Lacq (South-West of France) and stratified according to three types of meteorological situations, it has been concluded that the CCN concentrations and their distributions are significantly different from a type to the other. It has been proved that the nuclei produced on the site modify the air masses of maritime and continental origin to such an extent that some of their microphysical features are inverted.
Author

N85-32684# Missouri Univ., Rolla. Dept. of Physics.
THEORETICAL STUDIES OF STRUCTURE AND STABILITY OF HYDRATES OF ATMOSPHERIC SULFUR SPECIES
Patricia L. Moore Plummer *In* International Commission for Cloud Physics 11th Intern. Conf. on Atmospheric Aerosols, Condensation and Ice Nuclei, Vol. 1 1984 p 280-284 refs Sponsored in part by NSF (For primary document see N85-32636 21-47)
Avail: NTIS HC A14/MF A01

Ab initio quantum mechanical calculations have been done for the monohydrates of many of the sulfur containing compounds of atmospheric importance. All of the species examined had at

least one stable monohydrate with stabilities ranging from 2 to 20 kcal/mole. Author

N85-32685# Desert Research Inst., Reno, Nev.
THE NUCLEI OF CLOUD FORMATION
W. C. Kocmond and J. G. Hudson *In* International Commission for Cloud Physics 11th Intern. Conf. on Atmospheric Aerosols, Condensation and Ice Nuclei, Vol. 1 1984 p 285-291 refs (For primary document see N85-32636 21-47)
Avail: NTIS HC A14/MF A01

The most important effects of nuclei occur when they are amplified by water condensation in atmospheric clouds. The extent of the influence of variations in CCN concentration and spectral shape on precipitation, cloud albedo and cloud chemistry is discussed. Refinements in the definition of cloud condensation nuclei (CCN) are traced. Author

N85-32686# North Carolina State Univ., Raleigh. Dept. of Marine, Earth and Atmospheric Sciences.
TRANSPORT AND FORMATION OF SUMMERTIME CLOUD CONDENSATION NUCLEI OVER THE ARCTIC OCEAN
V. K. Saxena and R. S. Rathore *In* International Commission for Cloud Physics 11th Intern. Conf. on Atmospheric Aerosols, Condensation and Ice Nuclei, Vol. 1 1984 p 292-298 refs (For primary document see N85-32636 21-47)
Avail: NTIS HC A14/MF A01

A field experiment was conducted to investigate the microphysics of Arctic stratus clouds using an instrumented four engine Electra aircraft which was based at Barrow, Alaska and operated by the National Center for Atmospheric Research. Real time, in situ measurements of cloud condensation nuclei (CCN) spectrum were made. A remarkable feature of the data set is that CCN concentrations increase sharply within clouds. Thus, it is suggested that the contribution of gas to particle conversion mechanism through cloud processes may prove significant during the Arctic summer. Our study of wind frequency and CCN wind rose revealed that the winds from Scandanavia and Eurasia were rich in CCN concentration. Furthermore, a trajectory analysis was performed which revealed central and eastern USSR may provide pollutant injections into the Arctic environment. Author

N85-32687# Bhabha Atomic Research Centre, Bombay (India).
A REVIEW ON THE FORMATION OF AEROSOL PARTICLES IN THE ATMOSPHERE Abstract Only
K. G. Vohra *In* International Commission for Cloud Physics 11th Intern. Conf. on Atmospheric Aerosols, Condensation and Ice Nuclei, Vol. 1 1984 p 299 (For primary document see N85-32636 21-47)
Avail: NTIS HC A14/MF A01

The basic processes of gas to particle conversion in the atmosphere play a vital role in the formation of Aitken nuclei, cloud condensation nuclei (CCN) and background aerosol. These processes are highly complex, involving very rapid chemical conversion of trace gases to particles, even at parts per billion level. A vital and ubiquitous source is ionizing radiation including cosmic rays and alpha, beta and gamma radiations from the decay of atmospheric radon. A number of studies have been reported in the literature on the formation of submicron aerosol with the above basic ingredients, under different conditions. These are reviewed in detail, with particular reference to the role of ionizing radiations and unsaturated hydrocarbons at trace levels in the formation and growth of aerosols in the natural atmosphere. Experiments conducted on spontaneous formation of particles in the filtered air, with simultaneous measurements of relevant trace gases are reviewed in detail. The basic mechanisms of formation of certain free radicals, and the role of these radicals in enhancing the oxidation of SO and formation of submicron aerosol particles are considered. B.W.

N85-32688# North Carolina State Univ., Raleigh. Dept. of Marine, Earth and Atmospheric Sciences.
AEROSOL FORMATION BY WAVE ACTION OVER ROSS SEA, ANTARTICA Abstract Only
V. K. Saxenta, T. B. Curtin, and F. P. Parungo (National Oceanic and Atmospheric Administration, Boulder, Colo.) *In* International Commission for Cloud Physics 11th Intern. Conf. on Atmospheric Aerosols, Condensation and Ice Nuclei, Vol. 1 1984 p 300 (For primary document see N85-32636 21-47)
Avail: NTIS HC A14/MF A01

Investigations were conducted to test a hypothesis regarding the origin of these organic particulates in the Antarctic coastal clouds. According to the current belief, these visible particulates are produced by the wave action over the surface of the Ross Sea off the annual ice edge. Processes leading to the transfer of organic material from the ocean to the atmosphere are already documented and experiments over the Atlantic coast have shown the abundance of organic material in sea surface films and bubble generated aerosols. The field experiment consisted of deploying a submicroscopic particulate sampling assembly (SPSA) at the air sea interface using a portable buoy and the Coast Guard, floatable helicopters. Simultaneous Nucleopore filter samples were thus obtained at the air sea interface and in the surface boundary layer. Aerosol particles ranging between 5 to 7 micro m in diameter were found in unanticipated concentrations in the surface boundary layer. The results indicate that aerosols formed over Ross sea influence the cloud forming processes over the Ross Ice Shelf. B.W.

N85-32689# Meteorologisches Observatorium, Radebeul (East Germany).
AN ELECTRON MICROSCOPIC STUDY OF URBAN AEROSOL Abstract Only
M. Zier and M. Gast *In* International Commisssion for Cloud Physics 11th Intern. Conf. on Atmospheric Aerosols, Condensation and Ice Nuclei, Vol. 1 1984 p 301 (For primary document see N85-32636 21-47)
Avail: NTIS HC A14/MF A01

The motor vehicle traffic is one of the main sources of aerosol particles in the surface layer of the atmosphere of a city. In order to quantify its influence aerosol particles were simultaneously sampled by membrane filters at three measuring points in a city under different meteorological conditions. The sampling height was 2 m above the ground. Two measuring points were situated in the center of the city in a distance of 4 m respectively 50 m from the kerb of a highway, the third one was in a suburban area. The particle size distributions of the sampled aerosol particles altogether and of the soot particles in particular were determined by electron microscopy. The differences between the particle size distributions are discussed taking into consideration meteorological parameters, the state of the surface of the highway wet or dry and the frequency of motor vehicles. Author

N85-32690# Nagoya Univ. (Japan). Water Research Inst.
SULFATES IN MARINE AEROSOLS OVER THE TROPICAL WESTERN PACIFIC OCEAN Abstract Only
Akira Ono *In* International Commission for Cloud Physics 11th Intern. Conf. on Atmospheric Aerosols, Condensation and Ice Nuclei, Vol. 1 1984 p 302 (For primary document see N85-32636 21-47)
Avail: NTIS HC A14/MF A01

To provide a better understanding on the nature and origin of sulfate in marine aerosols over the open ocean, field measurements of marine aerosols over the tropical Western Pacific Ocean were performed on board the R.V. Keifu-maru during the Summer MONEX of May 1979. The size fractionated aerosol samples were collected by an Andersen sampler for the coarse particle fraction and by an electrostatic sampler for the fine one. From the mass distribution of marine sulfate aerosols in relation to the size spectrum of aerosol particles, it is found that the aerosol particle below 1 micro m in diameter contain hardly any sea salt sulfate, while the contribution of sea salt sulfate increases in the size range larger than 1 micro m in diameter. The total concentration of excess sulfate found in aerosols over the tropical Western Pacific Ocean is 1.0 micro g/cu m, while the total concentration of sea salt sulfate is only 0.09 micro/cu m. This means that not only the predominant number of particles but also the majority of

the sulfate mass over the tropical Western Pacific Ocean is of excess sulfate origin. B.W.

N85-32691# Centre National de la Recherche Scientifique, Paris (France). Centre des Faibles Radioactivites.
GRANULOMETRIC STUDY OF THE ACIDITY AND SULFATE EXCESS IN MARINE AEROSOLS Abstract Only **c48**
Ba Cuong Nguyen, Bernard Bonsang, and Amdre Gaudry *In* International Commission for Cloud Physics 11th Intern. Conf. on Atmospheric Aerosols, Condensation and Ice Nuclei, Vol. 1 1984 p 303 (For primary document see N85-32636 21-47)
Avail: NTIS HC A14/MF A01

It is demonstrated from previous oceanographic cruises undertaken in various marine areas: littoral region, upwelling areas, and open ocean, that marine SO2 concentrations can be correlated with the primary productivity. One of the manifestation of the primary productivity leads to the production of organic sulfides in sea water which can be outgassed exhausted to the atmosphere. The SO2 produced after the oxidation in the air of the sulfides, may oxidize itself very quickly. A sulfate enrichment SO4/Na(+)>0.25 with respect to the sea salt composition in the marine aerosols was systematically observed. In order to study such a sulfate enrichment, aerosols have been sampled by means of a high volume cascade impactor during oceanographic cruises in several remote oceanic areas. After aqueous dissolution, sulfate, sodium and acidity has been determined in the aerosols collected on each stage of the impactor. The results show that the acidity in the aerosols and the SO4/Na(+) ratio simultaneously increases with the decreasing size of the particles. B.W.

N85-32692# Paris VII Univ. (France). Lab. de Chimie Minerals des Milieux Naturels.
VARIATIONS OF PARTICULATE SULFUR CONCENTRATIONS IN A COASTAL ATMOSPHERIC ENVIRONMENT IN CONNECTION WITH THE CHANGE OF AIR MASSES ORIGIN Abstract Only
Jaques Morelly, Thierry Marchal, Laurence Girard-Reydet, and Patrick Carlier *In* International Commission for Cloud Physics 11th Intern. Conf. on Atmospheric Aerosols, Condensation and Ice Nuclei, Vol. 1 1984 p 304 (For primary document see N85-32636 21-47)
Avail: NTIS HC A14/MF A01

A study of chemical composition of coastal aerosol was started recently at the extreme point of Brittany, which is a low industrialized area. Samples were collected with 6 stage cascade impactors during 4 periods subjected to various meteorological conditions December 1980, June 1981, February 1982, April 1982, April 1982. Analysis by X-ray fluorescence was performed for the detection of sulfur and other elements. Attention is focused here on the fluctuations of atmospheric concentrations in particulate sulfur. An attempt was made to distinguish the natural marine background and the anthropogenic contributions according to the origins of air masses arriving on the sampling zone and the evolution of their trajectories at 850 or 700 mbar. In situations of west winds unfavorable for the extension to Brittany of atmospheric pollution from Western Europe, variations in the size distribution of sulfur were observed. Man's impact appears when anticyclonic situations on Western Europe succeed to conditions of oceanic West winds. This evolution corresponds to a strong increase of initial concentrations of sulfur associated with the submicron aerosol. B.W.

N85-32693# Consiglio Nazionale delle Ricerche, Bologna (Italy).
CHARACTERIZATION OF INSOLUBLE PARTICLES ASSOCIATED WITH CLOUD DROPLETS Abstract Only
S. Fuzzi, D. Johnson (State Univ. of New York, Syracuse), J. Kadlecek (State Univ. Of New York, Albany), S. McLaren (State Univ. of New York, Albany), and N. Camarota *In* International Commission for Cloud Physics 11th Intern. Conf. on Atmospheric Aerosols, Condensation and Ice Nuclei, Vol. 1 1984 p 305 (For primary document see N85-32636 21-47)
Avail: NTIS HC A14/MF A01

A sampling program for cloud chemistry study has been carried on at Whiteface Mountain, New York for several years. During the winter 1983, both liquid and supercooled cloud droplet samples were collected. Part of the cloud water was filtered through .2 micron Nucleopore membrane and the insoluble residue on the filter was analyzed by computer assisted scanning electron microscopy, for individual particle imaging. A statistical representative sample was examined. The elemental composition of each individual particle was obtained by X-ray energy spectroscopy. The particles were divided in different classes, depending on their elemental composition and the results were examined in several different ways: (1) chemical variability between different cloud events; (2) chemical variability within a single long lasting event; (3) chemical variability as a function of particle size; and (4) particle number concentration per surface/volume unit. Computed air mass trajectories were also used in the analysis of the results. B.W.

N85-32694# Colorado State Univ., Fort Collins. Dept. of Atmospheric Science.
THE MEASURED RATE OF CONDENSATION NUCLEATION TO DROPLETS USING THE TECHNIQUES OF CHEMICAL KINETICS Abstract Only
R. R. Blumenstein, R. D. Horn, and L. O. Grant *In* International Commission for Cloud Physics 11th Intern. Conf. on Atmospheric Aerosols, Condensation and Ice Nuclei, Vol. 1 1984 p 306 (For primary document see N85-32636 21-47)
Avail: NTIS HC A14/MF A01

Results of laboratory experiments to determine the rate of condensation on a known aerosol population followed by growth to droplets are presented. Data was interpreted using the methodology of chemical kinetics where the rate of phase change is used to deduce and describe the mechanism. Rates of nucleation and growth were examined as a function of temperature and water vapor concentration. Separate experiments were conducted at water saturation and conditions of transitory supersaturation with respect to water. The experiments were conducted in a large cloud chamber at the Colorado State University Cloud Simulation and Aerosol Laboratory. Growth was monitored from dry aerosol to droplet and measured from 0.5 m diameter to equilibrium size with 0.1 sec resolution by a Particle Measuring System (PMS) forward scattering spectrometer probe (FSSP) adapted for use in the laboratory. The nucleant used was hydrosonic AgI-NaI nuclei. Temperatures were maintained above the threshold for ice nucleation. Results from this study can be applied to the study of condensation freezing processes. Author

N85-32695# Grenoble-1 Univ. (France).
THE INTERACTION OF POLYNUCLEAR AROMATIC HYDROCARBONS PAH'S WITH WATER VAPOR AND THEIR ROLE AS CONDENSATION NUCLEI IN THE FORMATION OF HAZE AND FOG Abstract Only
J. J. Batifol, M. B. Benoist, Y. Durand, and R. Montmory *In* International Commission for Cloud Physics 11th Intern. Conf. on Atmospheric Aerosols, Condensation and Ice Nuclei, Vol. 1 1984 p 307 refs (For primary document see N85-32636 21-47)
Avail: NTIS HC A14/MF A01

The interaction of approximately fifteen polynuclear aromatic hydrocarbons P.A.H.'s with water vapor was studied. Each P.A.H. has been examined separately. Certain P.A.H.'s are actual condensation nuclei as soon as the relative humidity has risen above approx. 98%, having no visible hysteresis. They have a higher role as CCN's at temperatures < O C. Other P.A.H.'s, amongst which fluoranthene can be found are very hydrophobic. Finally, anthracene is an ice forming nucleus at temperatures approx. -10 C. In the case of anthracene, the isotherms which found were similar when temperatures for which anthracene becomes ice forming have been reached, the isotherms are of type 3. The amount of hydrophilic sites decreases noticeably. In the case of fluoranthracene, the isotherms are of type 2. As for pyrene, the isotherms are of type 2, but the area taken up by hydrophilic sites is greater than for anthracene. B.W.

N85-32696# Desert Research Inst., Reno, Nev.
APPLICABILITY OF SURFACE CCN MEASUREMENTS Abstract Only

J. G. Hudson *In* International Commission for Cloud Physics 11th Intern. Conf. on Atmospheric Aerosols, Condensation and Ice Nuclei, Vol. 1 1984 p 308 (For primary document see N85-32636 21-47)
Avail: NTIS HC A14/MF A01

Simultaneous cloud condensation nuclei (CCN) measurements at two nearby surface locations < 20 km seem to show a high degree of homogeneity. These measurements were made in four separate field projects at various locations across the U.S. The measurements were continuous for several days at a time. A CCN spectrum was measured in two of the programs. Three of the projects involved significant elevation differences, e.g., 600 m. During periods when both locations were within the boundary layer below cloud or even within cloud the concentrations were often quite similar. These results indicate that surface CCN measurements may often be representative of cloud base concentrations. Since cloud base is where CCN play their most important role and the surface is the most convenient place to make the measurements this increases the value of CCN measurements.
Author

N85-32697# Roorkee Univ. (India). Dept. of Physics.
EFFECT OF IONS ON CLOUD FORMATION AND ITS ROLE IN SOLAR TERRESTRIAL RELATIONSHIP Abstract Only
Jagdish Rai and N. C. Varshneya *In* International Commission for Cloud Physics 11th Intern. Conf. on Atmospheric Aerosols, Condensation and Ice Nuclei, Vol. 1 1984 p 309-310 (For primary document see N85-32636 21-47)
Avail: NTIS HC A14/MF A01

In the past, various correlation between precipitation and atmospheric electrical parameters have been made. On the first sight these correlations seem to be conflicting but a careful examination reveals a systematic latitudinal dependence. These correlations can be explained through the part played by atmospheric ions in the formation and electrification of clouds. Condensation on hygroscopic particles is well known. In this paper the role of atmospheric ions in heterogeneous nucleation is discussed. The Helmholtz free energy for heterogeneous nucleation on neutral aerosol particles is explained. To see in turn the role of cloud condensation and ice nucleation processes on solar terrestrial relationship, the sun atmosphere system has been divided into different sections with solar constant and galactic and solar cosmic rays as inputs. Applying the method of system analysis to each section the energy outputs in the form of atmospheric electrical power, precipitation, wind, temperature etc., have been calculated.
B.W.

N85-32698# Karpov (V. Y.) Physical Chemistry Inst., Moscow (USSR).
ON THE TRANSPORT OF LARGE CONDENSATION NUCLEI IN THE ATMOSPHERE AT VARIOUS ALTITUDES OVER THE TERRITORY OF THE USSR Abstract Only
B. F. Sadovskij and I. V. Petrijanov *In* International Commission for Cloud Physics 11th Intern. Conf. on Atmospheric Aerosols, Condensation and Ice Nuclei, Vol. 1 1984 p 311 (For primary document see N85-32636 21-47)
Avail: NTIS HC A14/MF A01

Measurements of the concentration of large condensation nuclei of the diameter from 0.1 to 0.2 to 1 micro m have been carried out at various altitudes over the territory of the USSR. The vertical profiles of nucleus distributions have been obtained at different measurement levels up to 5 km altitude. A considerable increase in the concentration of particles over industrial complexes and a decrease in the number of particles with increasing distance from a pollution source have been noted. Concentrations of large nuclei were measured in an atmospheric haze and clouds. Some change in the number of nuclei in the immediate vicinity of clouds was observed. Data on the concentration of nuclei under conditions of temperature inversion have been obtained. An attempt to relate the change in the concentration of particles to meteorological factors is made.
Author

N85-32699# Drexel Univ., Philadelphia, Pa.
TEMPERATURE MEASUREMENTS ON SMALL DROPLETS Abstract Only
John Cooney *In* International Commission for Cloud Physics 11th Intern. Conf. on Atmospheric Aerosols, Condensation and Ice Nuclei, Vol. 1 1984 p 312 (For primary document see N85-32636 21-47)
Avail: NTIS HC A14/MF A01

Methods, designed to ascertain the temperature changes which take place in such droplets of 20 microns during a rapid growth phase are under continuing investigation. The principal means for achieving this is by monitoring light scattered from such droplets. The basic coherent antistokes Raman scatter (CARS) pattern from snall droplets arising from the 3rd order nonlinear polarization of the material C2H2 and H2O has been evaluated. With the details of the scattered field elucidated more realistic calculation of scatter signal intensities becomes possible. Unexpected findings arising from the theoretical work include significant enhancement in scatter intensity per unit mass of material, thus theory shows increases by factors of 30 to 40 in scattered field intensity over that from equivalent material in the bulk. In addition, in contrast with bulk CARS scatter patterns, Mie type scatter patterns appear thus giving rise to remarkably different scatter fields than observed from the bulk. Details of signal noise calculations and their impact on temperature measurement accuracies are given.
B.W.

N85-32467*# National Aeronautics and Space Administration. Goddard Space Flight Center, Greenbelt, Md.
METEOROLOGICAL AND AERONOMICAL REQUIREMENTS FOR MST RADAR NETWORKS (KEYNOTE PAPER), PART 1
M. A. Geller *In* International Council of Scientific Unions Middle Atmosphere Program: Handbook for MAP. Vol. 14 Dec. 1984 p 1-4 (For primary document see N85-32466 21-45)
Avail: NTIS HC A17/MF A01; also avail. from SCOSTEP Secretariat, Illinois Univ., 1406 West Green St., Urbana, Ill. 61801 CSCL 04B

N85-32468*# Cornell Univ., Ithaca, N.Y. School of Electrical Engineering.
TROPOSPHERIC-STRATOSPHERIC EXCHANGE, PART 1.1A
C. R. Cornish *In* International Council of Scientific Unions Middle Atmosphere Program: Handbook for MAP. Vol. 14 Dec. 1984 p 4-5 refs (For primary document see N85-32466 21-46)
Avail: NTIS HC A17/MF A01; also avail. from SCOSTEP Secretariat, Illinois Univ., 1406 West Green St., Urbana, Ill. 61801 CSCL 04B

N85-32469*# Cornell Univ., Ithaca, N.Y.
OBSERVATIONS OF FRONTAL ZONE STRUCTURES WITH A VHF DOPPLER RADAR AND RADIOSONDES, PART 1.2A
M. F. Larsen and J. Rottger (EISCAT Scientific Association) *In* International Council of Scientific Unions Middle Atmosphere Program. Handbook for MAP. Vol. 14 Dec. 1984 p 7-13 refs (For primary document see N85-32466 21-46)
Avail: NTIS HC A17/MF A01; also avail. from SCOSTEP Secretariat, Illinois Univ., 1406 West Green St., Urbana, Ill. 61801 CSCL 04B

N85-32475*# National Oceanic and Atmospheric Administration, Boulder, Colo.
PERFORMANCE OF THE COLORADO WIND-PROFILING NETWORK, PART 1.5A
R. G. Strauch, K. B. Earnshaw, D. A. Merritt, K. P. Moran, and D. W. vandeKamp *In* Intern. Council of Sci. Unions Middle Atmosphere Program: Handbook for Map. Vol. 14: URSI/SCOSTEP Workshop Dec. 1984 p 38-48 refs (For primary document see N85-32466 21-46)
Avail: NTIS HC A17/MF A01; also avail. from SCOSTEP Secretariat, Illinois Univ., 1406 West Green St., Urbana, Ill. 61801 CSCL 04B

N85-32476*# EISCAT Scientific Association, Kiruna (Sweden).
VERTICAL TRANSPORT IN THE ATMOSPHERE: MEASUREMENT CAPABILITIES AND REQUIREMENTS OF VHF RADARS, PART 1.6A
J. Rottger *In* International Council of Scientific Union Middle Atmosphere Program: Handbook for MAP. Vol. 14 Dec. 1984 p 49-57 refs (For primary document see N85-32466 21-46)
Avail: NTIS HC A17/MF A01; also avail. from SCOSTEP Secretariat, Illinois Univ., 1406 West Green St., Urbana, Ill. 61801 CSCL 04B

N85-32477*# National Oceanic and Atmospheric Administration, Boulder, Colo. Aeronomy Lab.
COMPARISON OF TROPOPAUSE ALTITUDE DETERMINATION BY THE PLATTSVILLE RADAR, SUNSET RADAR AND THE NWS RAWINSONDE
J. L. Green and K. S. Gage *In* International Council of Scientific Unions Middle Atmosphere Program: Handbook for MAP. Vol. 14 Dec. 1984 p 58-61 refs (For primary document see N85-32466 21-46)
Avail: NTIS HC A17/MF A01; also avail. from SCOSTEP Secretariat, Illinois Univ., 1406 West Green St., Urbana, Ill. 61801 CSCL 04B

N85-32478*# Control Data Corp., Minneapolis, Minn.
SYNOPTIC-SCALE DYNAMICS WITH VERTICAL VELOCITY, PART 1.8A
G. D. Nastrom *In* International Council of Scientific Unions Middle Atmosphere Program: Handbook for MAP. Vol. 14 Dec. 1984 p 62-68 refs (For primary document see N85-32466 21-46)
Avail: NTIS HC A17/MF A01; also avail. from SCOSTEP Secretariat, Illinois Univ., 1406 West Green St., Urbana, Ill. 61801 CSCL 04B

N85-32479# Colorado Univ., Boulder.
PRACTICAL USE OF A TROPOPAUSE HEIGHT DETERMINATION ALGORITHM ON AN MST RADAR DATA SET, PART 1.8B
A. C. Riddle, K. S. Gage (NOAA, Boulder, Colo.), and B. B. Balsley (NOAA, Boulder, Colo.) *In* International Council of Scientific Unions Middle Atmosphere Program: Handbook for MAP. Vol. 14 Dec. 1984 p 69-73 refs (For primary document see N85-32466 21-46)
Avail: NTIS HC A17/MF A01; also avail. from SCOSTEP Secretariat, Illinois Univ., 1406 West Green St., Urbana, Ill. 61804 CSCL 04B

N85-32500*# Case Western Reserve Univ., Cleveland, Ohio. Dept. of Electrical Engineering and Applied Physics.
DETERMINATION OF BILLOWS AND OTHER TURBULENT STRUCTURES, PART 4.1A
P. K. Rastogi *In* International Council of Scientific Unions Middle Atmosphere Program: Handbook for MAP. Vol. 14 Dec. 1984 p 183-185 refs (For primary document see N85-32466 21-46)
Avail: NTIS HC A17/MF A01; also avail. from SCOSTEP Secretariat, Illinois Univ., 1406 West Green St., Urbana, Ill. 61801 CSCL 04B

N85-32504*# National Oceanic and Atmospheric Administration, Boulder, Colo. Aeronomy Lab.
ON THE SPECTRUM OF ATMOSPHERIC VELOCITY FLUCTUATIONS SEEN BY MST/ST RADAR AND THEIR INTERPRETATION
K. S. Gage and G. D. Nastrom (Control Data Corp., Minneapolis) *In* International Council of Scientific Unions Middle Atmosphere Program: Handbook for MAP. Vol. 14 Dec. 1984 p 197-207 refs (For primary document see N85-32466 21-46)
Avail: NTIS HC A17/MF A01; also avail. from SCOSTEP Secretariat, Illinois Univ., 1406 West Green St., Urbana, Ill. 61801 CSCL 04B

N85-32509*# National Oceanic and Atmospheric Administration, Boulder, Colo.
TROPOSPHERIC GRAVITY WAVES OBSERVED BY THREE CLOSELY SPACED ST RADARS
D. A. Carter, B. B. Balsley, W. L. Ecklund, M. Crochet (L.S.E.E.T, Toulon, France), A. C. Riddle (Colorado Univ.), and R. Garello *In* International Council of Scientific Unions Middle Atmosphere Program: Handbook for MAP. Vol. 14 Dec. 1984 p 219-228 refs (For primary document see N85-32466 21-46)
Avail: NTIS HC A17/MF A01; also avail. from SCOSTEP Secretariat, Illinois Univ., 1406 West Green St., Urbana, Ill. 61801 CSCL 04B

N85-32516*# National Oceanic and Atmospheric Administration, Boulder, Colo. Aeronomy Lab.
PRACTICALITY OF ELECTRONIC BEAM STEERING FOR MST/ST RADARS, PART 6.2A
W. L. Clark and J. L. Green *In* International Council of Scientific Unions Middle Atmosphere Program: Handbook for MAP. Vol. 14 Dec. 1984 p 253-256 refs (For primary document see N85-32466 21-46)
Avail: NTIS HC A17/MF A01; also avail. from SCOSTEP Secretariat, Illinois Univ., 1406 West Green St., Urbana, Ill. 61801 CSCL 09C

N85-32550*# National Oceanic and Atmospheric Administration, Boulder, Colo. Aeronomy lab.
MEASUREMENTS OF VERTICAL VELOCITY OVER FLAT TERRAIN BY ST RADAR AND OTHER RELATED USES OF THE RADAR DATA SET
J. L. Green and G. D. Nastrom (Control Data Corp., Minneapolis, Minn.) *In* International Council of Scientific Unions Middle Atmosphere Program. Handbook for MAP. Vol. 14 Dec. 1984 p 364-366 (For primary document see N85-32466 21-46)
Avail: NTIS HC A17/MF A01; also available from SCOSTEP Secretariat, Illinois Univ., 1406 West Green Street, Urbana, Ill. 61801 CSCL 04B

N85-32725*# National Aeronautics and Space Administration. Ames Research Center, Moffett Field, Calif.
EVOLUTION OF THE ATMOSPHERE Abstract Only
James F. Kasting *In* NASA, Washington The Global Sulfur Cycle Jul. 1985 p 57-59 refs (For primary document see N85-32710 21-51)
Avail: NTIS HC A14/MF A01 CSCL 04B

48 OCEANOGRAPHY

Includes biological, dynamic and physical oceanography; and marine resources.

N85-32700# Army Cold Regions Research and Engineering Lab., Hanover, N. H.
NUMERICAL MODELING OF SEA ICE DYNAMICS AND ICE THICKNESS CHARACTERISTICS Final Report
W. D. Hibler, III Mar. 1985 59 p
(AD-A154600; CRREL-85-5) Avail: NTIS HC A04/MF A01 CSCL 08/12

A dynamic-thermodynamic sea ice model is extended to include a full thermodynamic code and a complete multilevel ice thickness distribution. The variable thickness formulation includes a more realistic parameterization of ice ridging than used in previous models. Seasonal simulations have been performed using this model and the results have been analyzed with particular emphasis on examination of the ridge buildup results off the Canadian Archipelago and off the North Slope. This report presents a complete description of this model and discusses progress made on examining and testing the variable thickness extensions. GRA

N85-32701# Office of Naval Research, Arlington, Va.
PHYSICAL OCEANOGRAPHY PROGRAM SCIENCE ABSTRACTS Annual Report, for Period Ending FY84
T. Spence 1 Apr. 1985 124 p
(AD-A154637) Avail: NTIS HC A06/MF A01 CSCL 08/10

The Office of Naval Research supports a broadly based oceanography effort. This volume documents the physical oceanographic aspects, which are presented as abstracts submitted by

the principal investigators. This report, which is published annually, is intended to communicate the diversity and scope of the physical oceanography effort. GRA

N85-32702# Woods Hole Oceanographic Institution, Mass.
HORIZONTAL AND VERTICAL STRUCTURE OF VELOCITY, POTENTIAL VORTICITY AND ENERGY IN THE GULF STREAM Ph.D. Thesis
M. M. Hall Feb. 1985 170 p
(Contract N00014-82-C-0019; Grant NSF OCE-82-08746)
(AD-A154753; WHOI-85-16) Avail: NTIS HC A08/MF A01 CSCL 08/3

A current meter mooring was deployed for one year at the mean position of the Gulf Stream at 68 deg W. Projecting the velocity onto along- and cross-stream components shows that the vertical structure of velocity at the site is described by a baroclinic along stream and decoupled, barotropic cross-stream component. The well defined relationship between thermocline temperature and cross stream component distance allows the use of the former as a horizontal coordinate and enables estimates of mass, momentum and kinetic energy fluxes of the Gulf Stream for four events when it passes over the morning site. Alternatively, an average vertical and horizontal velocity section of the Stream may be constructed, and using that, a potential vorticity section. There is a strong jump from low to high values of thermocline potential vorticity crossing the Stream from south to north. Time-series of vertical velocities were calculated and their rms sizes are large (0.05 cm/s). The Rossby number below the thermocline is estimated to be $>$ or $=$ 0.1, but in the thermocline it is about 0.3. Diagnostic calculations of the kinetic energy budgets in a quasi-geostrophic eddy resolving general circulation model suggest that downstream convergence of mean kinetic energy in the Gulf Stream is primarily balanced by mean geostrophic flow against a pressure gradient. Author (GRA)

N85-32703# Naval Postgraduate School, Monterey, Calif.
HYDROGRAPHIC DATA FROM THE OPTOMA (OCEAN PREDICTION THROUGH OBSERVATIONS, MODELING AND ANALYSIS) PROGRAM: OPTOMA15, 24 JANUARY TO 23 FEBRUARY 1985 Report, Oct. 1982 - Apr. 1985
P. A. Wittmann, E. A. Kelley, Jr., and C. N. K. Mooers Apr. 1985 114 p
(AD-A155012; NPS68-85-016) Avail: NTIS HC A06/MF A01 CSCL 08/10

The two cruises, Leg DI and DII, and one AXBT flight Leg P were undertaken in January and February 1985. This report presents the hydrographic data acquired by XBT, AXBT and CTD casts, from the cruises and the flight. GRA

N85-32704# Naval Postgraduate School, Monterey, Calif.
NUMERICAL SIMULATIONS OF THE RESPONSE OF INTENSE OCEAN CURRENTS TO ATMOSPHERIC FORCING Ph.D. Thesis
D. Adamec Mar. 1985 100 p
(AD-A155161) Avail: NTIS HC A05/MF A01 CSCL 08/3

This thesis studies the two and three-dimensional response of strong ocean currents to atmospheric forcing using numerical simulations. Surface cooling is explored as a possible mechanism for explaining an observed 100 km southward shift in the mean position of the Gulf Stream during winter. The magnitude and direction of the cross-stream circulation is highly dependent on whether or not a vertical mixing of momentum occurs when the water column convectively adjusts in response to surface cooling. A weak cross-stream flow toward the higher sea-surface temperatures occurs in the surface layer if momentum mixing does not occur, whereas a stronger flow toward lower sea-surface temperatures results if momentum mixing does take place. The response of three-dimensional simulations is very similar to the two-dimensional simulations in the immediate vicinity of the front. The response due to horizontal cooling gradients is not large enough to displace the Gulf Stream appreciably southward in any of the numerical simulations. By contrast, a moderate increase in the zonal wind stress is more effective in displacing the core of the current system than are strong gradients in the surface cooling. The position of the Gulf Stream has also been observed to change as it encounters changes in the bottom topography. The simulated adjustment of flow to a 200 m seamount is consistent with the conservation of potential vorticity. Inclusion of surface forcing does not affect the adjustment to the topography in any of the simulations, and does not steer the flow toward (away from) the topography so that the characteristics of the downstream flow are changed. GRA

N85-32705# Naval Postgraduate School, Monterey, Calif.
SIMULATION OF THE COUPLED ATMOSPHERIC AND OCEANIC BOUNDARY LAYER MODEL DURING MILDEX M.S. Thesis
J. W. Swaykos Dec. 1984 68 p
(AD-A155166) Avail: NTIS HC A04/MF A01 CSCL 04/1

A coupled, oceanic-atmospheric boundary layer model which provides single-station prediction capability is evaluated relative to boundary layer observations. The model is initialized and verified using data obtained during the 1983 Mixed Layer Dynamics Experiment (MILDEX). Model prediction of inversion height, lifting condensation level, air and sea temperatures, specific humidity and mixed layer depth are compared with observations. A significant model shortcoming is the over-prediction of cloud thickness. Consequently, shortwave radiation at the ocean surface is too low and the predicted ocean mixed layer depths are not realistic. Oceanic predictions resulting from independent specification of surface radiation more closely resembled observed oceanic variations. Atmospheric boundary layer model reformulation is required to alleviate the cloud thickness/shortwave radiation problem. GRA

N85-32706# Army Engineer Waterways Experiment Station, Vicksburg, Miss. Hydraulics Lab.
REVERIFICATION OF THE CHESAPEAKE BAY MODEL Final Report
M. A. Granat, L. F. Gulbrandsen, and V. R. Pankow Apr. 1985 301 p
(AD-A155486; WES/TR/HL-85-3) Avail: NTIS HC A14/MF A01 CSCL 08/8

The Chesapeake Bay hydraulic model, an 8.6 acre fixed-bed model, constructed to a horizontal scale ratio of 1:1000 and a vertical ratio of 1:100, reproduces the entire Chesapeake Bay estuarine system from the offshore Atlantic Ocean to the head of tide for all tributaries. The model is equipped with the necessary appurtenances to accurately reproduce and measure tidal heights, tidal currents, salinity distributions, and freshwater inflows. It is the largest and one of the most sophisticated estuarine models of its kind. Complete computer control and data acquisition capabilities ensure accurate and precise monitoring and control throughout the 14 acre shelter. During the summer of 1980, unusual concrete expansion on the model resulted in compression and unequal vertical concrete movement. Damaged areas were remolded and all existing and new expansion joints were widened and filled with a closed cell expansion material. Reverification of the model was required following this rehabilitation effort. This report provides all the necessary information to adequately assess model reverification and model operating capabilities. GRA

N85-32707# Naval Postgraduate School, Monterey, Calif.
COASTAL EROSION ALONG MONTEREY BAY M.S. Thesis
A. I. Sklavidis and W. R. LimaBlanco Mar. 1985 108 p
(AD-A155610) Avail: NTIS HC A06/MF A01 CSCL 08/3

Permanent beach erosion in Southern Monterey Bay, CA, is episodic, occurring infrequently when high tides coincide with stormy weather which allows wave action to erode the toe of the cliffs. This thesis uses precise aerial photogrammmetric techniques to measure cliff recession from 1946 through 1984. Maximum erosion occurs in the vicinity of Fort Ord (7.3 ft yr) and decreases to the south. A model is developed to predict cliff erosion based on the hypothesis that erosion occurs only when the water level due to combined tides, wave set-up and run-up exceeds the cliff elevation. The model combines predicted tidal elevations and wave heights. Shallow water wave heights at various locations are

calculated by transforming deep-water directional wave spectra provided by the Fleet Numerical Oceanography Center. Refraction of the wave energy is responsible for the variabillity of erosion rates along the shore. The bathymetry of Monterey Bay is such that the refracted wave energy is greater in the Fort Ord area than to the south. The erosion model was calibrated using the spectral wave climatology and aerial photographs covering an 18-year period. The model qualitatively replicates the temporal variability of the measured recession rates and gives a reasonable prediction of the spatial variation of the mean recession rates.
GRA

N85-32369*# Woods Hole Oceanographic Institution, Mass. Dept. of Geology and Geophysics.
DEEP SEA MEGA-GEOMORPHOLOGY: PROGRESS AND PROBLEMS
Wilfred B. Bryan *In* NASA. Goddard Space Flight Center Global Mega-Geomorphology Jul. 1985 p 54-55 (For primary document see N85-32357 21-42)
Avail: NTIS HC A07/MF A01 CSCL 08C

N85-32691# Centre National de la Recherche Scientifique, Paris (France). Centre des Faibles Radioactivites.
GRANULOMETRIC STUDY OF THE ACIDITY AND SULFATE EXCESS IN MARINE AEROSOLS Abstract Only
Ba Cuong Nguyen, Bernard Bonsang, and Amdre Gaudry *In* International Commission for Cloud Physics 11th Intern. Conf. on Atmospheric Aerosols, Condensation and Ice Nuclei, Vol. 1 1984 p 303 (For primary document see N85-32636 21-47)
Avail: NTIS HC A14/MF A01

51 LIFE SCIENCES (GENERAL)

Includes genetics.

N85-32708*# National Aeronautics and Space Administration. Ames Research Center, Moffett Field, Calif.
THE EVOLUTION OF COMPLEX AND HIGHER ORGANISMS
David Smilne, ed. (Evergreen State Coll.), David Raup, ed. (Chicago Univ.), John Billingham, ed., Karl Niklaus, ed. (Cornell Univ., Ithaca, N.Y.), and Kevin Padian, ed. (California Univ., Berkeley) 1985 113 p refs Original contains color illustrations
(NASA-SP-478; A-9363; NAS 1.21:478; LC-85-7159) Avail: NTIS HC A06/MF A01; SOD HC $8.50 as 033-000-00951-8 CSCL 06C

The evolution of Phanerozoic life has probably been influenced by extraterrestrial events and properties of the Earth-Moon system that have not, until now, been widely recognized. Tide range, gravitational strength, the Earth's axial tilt, and other planetary properties provide background conditions whose effects on evolution may be difficult to distinguish. Solar flares, asteroid impacts, supernovae, and passage of the solar system through galactic clouds can provide catastrophic changes on the Earth with consequent characteristic extinctions. Study of the fossil record and the evolution of complex Phanerozoic life can reveal evidence of past disturbances in space near the Earth. Conversely, better understanding of environmental influences caused by extraterrestrial factors and properties of the solar system can clarify aspects of evolution, and may aid in visualizing life on other planets with different properties. Author

N85-32709*# Management and Technical Services Co., Washington, D.C.
USSR SPACE LIFE SCIENCES DIGEST
Lydia Razran Hooke, Mike Radtke, and Joseph E. Rowe NASA Aug. 1985 85 p
(Contract NASw-3676)
(NASA-CR-3922; NAS 1.26:3922) Avail: NTIS HC A05/MF A01 CSCL 06B

The first issue of the bimonthly digest of USSR Space Life Sciences is presented. Abstracts are included for 49 Soviet periodical articles in 19 areas of aerospace medicine and space biology, published in Russian during the first quarter of 1985. Translated introductions and table of contents for nine Russian books on topics related to NASA's life science concerns are presented. Areas covered include: botany, cardiovascular and respiratory systems, cybernetics and biomedical data processing, endocrinology, gastrointestinal system, genetics, group dynamics, habitability and environmental effects, health and medicine, hematology, immunology, life support systems, man machine systems, metabolism, musculoskeletal system, neurophysiology, perception, personnel selection, psychology, radiobiology, reproductive system, and space biology. This issue concentrates on aerospace medicine and space biology. E.A.K.

N85-32710*# National Aeronautics and Space Administration, Washington, D. C.
THE GLOBAL SULFUR CYCLE
Dorian Sagan, ed. Jul. 1985 305 p refs Proc. of the Planetary Biol. Microbial Ecology's 1984 Summer Res. Prog., San Jose, Calif., 24 Jun. - 4 Aug. 1984
(NASA-TM-87570; NAS 1.15:87570) Avail: NTIS HC A14/MF A01 CSCL 13B

The results of the planetary biology microbial ecology's 1984 Summer Research Program, which examined various aspects of the global sulfur cycle are summarized. Ways in which sulfur flows through the many living and chemical species that inhabit the surface of the Earth were investigated. Major topics studied include: (1) sulfur cycling and metabolism of phototropic and filamentous sulfur bacteria; (2) sulfur reduction in sediments of marine and evaporite environments; (3) recent cyanobacterial mats; (4) microanalysis of community metabolism in proximity to the photic zone in potential stromatolites; and (5) formation and activity of microbial biofilms on metal sulfides and other mineral surfaces. Relationships between the global sulfur cycle and the understanding of the early evolution of the Earth and biosphere and current processes that affect global habitability are stressed. For individual titles, see N85-32711 through N85-32748.

N85-32711*# California Univ., Santa Barbara. Dept. of Geology.
PRECAMBRIAN EVOLUTION AND THE ROCK RECORD c46
Stanley Awramik *In* NASA, Washington The Global Sulfur Cycle Jul. 1985 p 5-8 (For primary document see N85-32710 21-51)
Avail: NTIS HC A14/MF A01 CSCL 08G

The Precambrian time which refers to geological time prior to the first appearance of animals with mineralized hard parts was investigated. Best estimates for this event are around 570 million years ago. Because the rock record begins some 3,800 million years ago the Precambrian encompasses about 84% of geologic time. The fossil record for this immense span of time is dominated by prokaryotes and the sedimentary structures produced by them. The first fossil remains that are considered eukaryotic are found in 1,000 million year old rocks. The first animals may be as old as 700 million years. The fossil records of the first 84% of the Earth's history are collected and described. E.A.K.

N85-32712*# Saskatchewan Univ., Saskatoon. Dept. of Applied Microbiology and Food Science.
AEROBIC SULFUR-OXIDIZING BACTERIA: ENVIRONMENTAL SELECTION AND DIVERSIFICATION Abstract Only
Douglas Caldwell *In* NASA, Washington The Global Sulfur Cycle Jul. 1985 p 9-10 refs (For primary document see N85-32710 21-51)
Avail: NTIS HC A14/MF A01 CSCL 06C

Sulfur-oxidizing bacteria oxidize reduced inorganic compounds to sulfuric acid. Lithotrophic sulfur oxidizer use the energy obtained from oxidation for microbial growth. Heterotrophic sulfur oxidizers obtain energy from the oxidation of organic compounds. In sulfur-oxidizing mixotrophs energy are derived either from the oxidation of inorganic or organic compounds. Sulfur-oxidizing bacteria are usually located within the sulfide/oxygen interfaces of springs, sediments, soil microenvironments, and the hypolimnion. Colonization of the interface is necessary since sulfide auto-oxidizes and because both oxygen and sulfide are needed for growth. The

environmental stresses associated with the colonization of these interfaces resulted in the evolution of morphologically diverse and unique aerobic sulfur oxidizers. E.A.K.

N85-32713*# National Aeronautics and Space Administration. Ames Research Center, Moffett Field, Calif.
ORIGIN OF LIFE
Sherwood Chang *In* NASA, Washington The Global Sulfur Cycle Jul. 1985 p 11-13 refs (For primary document see N85-32710 21-51)
Avail: NTIS HC A14/MF A01 CSCL 06C

The pathways of organic chemical synthesis, the chemical evolution on the early Earth leading to life was constrained by the development of the planet by accretion and core formation. The accretion and differentiation into the core-mantle-crust-atmosphere system strongly influenced the temperature and composition of the atmosphere, surface, and interior; but large gaps persist in our understanding of these processes. The time-span over which Earth acquired its volatiles, the composition of these volatiles, and the conditions under which outgassing of volatiles occurred to form the atmosphere, are unknown. Uncertainties in existing models for Earth accretion and early planetary development allows a wide range of possible prebiotic atmospheric compositions at the time and temperature when liquid water appeared and thermally-labile organic compounds could survive. These compositions range from strongly reducing atmospheres to mildly reducing ones. Author

N85-32714*# National Aeronautics and Space Administration. Ames Research Center, Moffett Field, Calif.
PROTOCYANOBACTERIA: OXYGENIC AND ANOXYGENIC PHOTOSYNTHESIS IN MAT-FORMING BACTERIA
Yehuda Cohen *In* NASA, Washington The Global Sulfur Cycle Jul. 1985 p 14-15 refs Prepared in cooperation with Hebrew Univ. (For primary document see N85-32710 21-51)
Avail: NTIS HC A14/MF A01 CSCL 06C

The oldest record of life is preserved in prePhanerozoic stromatolites dated 3500 million years old and is most likely of filamentous mat-forming cyanobacteria. The sedimentary records of cyanobacterial mats in stromatolites are the most abundant record of life throughout the prePhanerozoic. Stromatolites persisted into the Phanerozoic Eon, yet they become much less pronounced relative to earlier ones. The abundance and persistence of cyanobacterial mats throughout most of geological time point to the evolutionary success of these kinds of microbial communities and their possible role in the evolution of the Earth and atmosphere. E.A.K.

N85-32715*# National Aeronautics and Space Administration. Ames Research Center, Moffett Field, Calif.
SULFUR TRANSFORMATIONS AT THE HYDROGEN SULFIDE/OXYGEN INTERFACE IN STRATIFIED WATERS AND IN CYANOBACTERIAL MATS
Yehuda Cohen *In* NASA, Washington The Global Sulfur Cycle Jul. 1985 p 16-18 refs Prepared in cooperation with Hebrew Univ. (For primary document see N85-32710 21-51)
Avail: NTIS HC A14/MF A01 CSCL 06C

Stratified water bodies allow the development of several microbial plates along the water column. The microbial plates develop in relation to nutrient availability, light penetration, and the distribution of oxygen and sulfide. Sulfide is initially produced in the sediment by sulfate-reducing bacteria. It diffuses along the water column creating a zone of hydrogen sulfide/oxygen interface. In the chemocline of Solar Lake oxygen and sulfide coexist in a 0 to 10 cm layer that moves up and down during a diurnal cycle. The microbial plate at the chemocline is exposed to oxygen and hydrogen sulfide, alternating on a diurnal basis. The cyanobacteria occupying the interface switch from anoxygenic photosynthesis in the morning to oxygenic photosynthesis during the rest of the day which results in a temporal build up of elemental sulfur during the day and disappears at night due to both oxidation to thiosulfate and sulfate by thiobacilli, and reduction to hydrogen sulfide by Desulfuromonas sp. and anaerobically respiring cyanobacteria. Sulfate reduction was enhanced in the light at the surface of the cyanobacterial mats. Microsulfate reduction measurements showed enhanced activity of sulfate reduction even under high oxygen concentrations of 300 to 800 micrometer. Apparent aerobic SO sub 4 reduction activity is explained by the co-occurrence of H sub 2. The physiology of this apparent sulfate reduction activity is studied. E.A.K.

N85-32716*# National Aeronautics and Space Administration. Ames Research Center, Moffett Field, Calif.
CARBON ISOTOPE GEOCHEMISTRY AND GEOBIOLOGY c46
David DesMarais *In* NASA, Washington The Global Sulfur Cycle Jul. 1985 p 19-25 refs (For primary document see N85-32710 21-51)
Avail: NTIS HC A14/MF A01 CSCL 13B

Carbon isotope fractionation values were used to understand the history of the biosphere. For example, plankton analyses confirmed that marine extinctions at the end of the Cretaceous period were indeed severe (see Hsu's article in Sundquist and Broeker, 1984). Variations in the isotopic compositions of carbonates and evaporitic sulfates during the Paleozoic reflect the relative abundances of euxinic (anoxic) marine environments and organic deposits from terrestrial flora. The carbon isotopic composition of Precambrian sediments suggest that the enzyme ribulose bisphosphate carboxylase has existed for perhaps 3.5 billion years. E.A.K.

N85-32717*# California Univ., San Diego, La Jolla. Dept. of Chemistry.
DISTRIBUTION AND ABUNDANCE OF ORGANIC THIOLS Abstract Only
Robert Fahey *In* NASA, Washington The Global Sulfur Cycle Jul. 1985 p 26 refs (For primary document see N85-32710 21-51)
Avail: NTIS HC A14/MF A01 CSCL 06C

The role of glutathione (GSH) in protecting against the toxicity of oxygen and oxygen by products is well established for all eukaryotes studied except Entamoeba histolytica which lacks mitochrondria, chloroplasts, and microtubules. The GSH is not universal among prokaryotes. Entamoeba histolytica does not produce GSH or key enzymes of GSH metabolism. A general method of thiol analysis based upon fluorescent labeling with monobromobimane and HPLC separation of the resulting thiol derivatives was developed to determine the occurrence of GSH and other low molecular weight thiols in bacteria. Glutathione is the major thiol in cyanobacteria and in most bacteria closely related to the purple photosynthetic bacteria, but GSH was not found in archaebacteria, green bacteria, or GRAM positive bacteria. It suggested that glutathione metabolism was incorporated into eukaryotes at the time that mitochondria and chloroplasts were acquired by endosymbiosis. In Gram positive aerobes, coenzyme A occurs at millimolar levels and CoA disulfide reductases are identified. The CoA, rather than glutathione, may function in the oxygen detoxification processes of these organisms. E.A.K.

N85-32718*# Oldenburg Univ. (West Germany). Dept. of Geomicrobiology.
CYTOCHROMES AND IRON SULFUR PROTEINS IN SULFUR METABOLISM OF PHOTOTROPHIC BACTERIA
Ulrich Fischer *In* NASA, Washington The Global Sulfur Cycle Jul. 1985 p 27-29 refs (For primary document see N85-32710 21-51)
Avail: NTIS HC A14/MF A01 CSCL 06C

Dissimilatory sulfur metabolism in phototrophic sulfur bacteria provides the bacteria with electrons for photosynthetic electron transport chain and, with energy. Assimilatory sulfate reduction is necessary for the biosynthesis of sulfur-containing cell components. Sulfide, thiosulfate, and elemental sulfur are the sulfur compounds most commonly used by phototrophic bacteria as electron donors for anoxygenic photosynthesis. Cytochromes or other electron transfer proteins, like high-potential-iron-sulfur protein (HIPIP) function as electron acceptors or donors for most enzymatic steps during the oxidation pathways of sulfide or thiosulfate. Yet, hemeor

siroheme-containing proteins themselves undergo enzymatic activities in sulfur metabolism. Sirohemes comprise a porphyrin-like prosthetic group of sulfate reductase. eenzymatic reactions involve electron transfer. Electron donors or acceptors are necessary for each reaction. Cytochromes and iron sulfur problems, are able to transfer electrons. E.A.K.

N85-32719*# Houston Univ., Tex. Dept. of Biochemistry and Biophysical Science.
INSIGHTS INTO THE PHYLOGENETIC POSITIONS OF PHOTOSYNTHETIC BACTERIA OBTAINED FROM 5S rRNA AND 16S rRNA SEQUENCE DATA
George E. Fox *In* NASA, Washington The Global Sulfur Cycle Jul. 1985 p 30-39 refs (For primary document see N85-32710 21-51)
Avail: NTIS HC A14/MF A01 CSCL 06C

Comparisons of complete 16S ribosomal ribonucleic acid (rRNA) sequences established that the secondary structure of these molecules is highly conserved. Earlier work with 5S rRNA secondary structure revealed that when structural conservation exists the alignment of sequences is straightforward. The constancy of structure implies minimal functional change. Under these conditions a uniform evolutionary rate can be expected so that conditions are favorable for phylogenetic tree construction. E.A.K.

N85-32720*# University of South Florida, St. Petersburg. Dept. of Marine Science.
CARBON AND SULFUR CYCLING THROUGH GEOLOGIC TIME Abstract Only c46
Robert M. Garrels *In* NASA, Washington The Global Sulfur Cycle Jul. 1985 p 40-41 refs (For primary document see N85-32710 21-51)
Avail: NTIS HC A14/MF A01 CSCL 08G

Mathematical models of the coupled global systems of sedimentary reservoirs and fluxes are used to infer variations in reservoir sizes and rates of sedimentation over periods of hundreds of millions of years. Perhaps most interesting is the coupled sulfide/sulfate carbon/carbonate system that controls global oxygen and carbon dioxide production and consumption is discussed. B.W.

N85-32721*# Geological Survey, Denver, Colo. Federal Center.
SULFUR DIAGENESIS IN MARINE SEDIMENTS c45
Martin Goldhaber *In* NASA, Washington The Global Sulfur Cycle Jul. 1985 p 42-44 refs (For primary document see N85-32710 21-51)
Avail: NTIS HC A14/MF A01 CSCL 13B

Bacterial sulfate reduction occurs in all marine sediments that contain organic matter. Aqueous sulfide (HS-, H2S), one of the initial products of bacterial sulfide reduction, is extremely reactive with iron bearing minerals: sulfur is fixed into sediments as iron sulfide (first FeS and then Fe2S2). A working definition is given of sulfur diagenesis in marine sediments. Controls and consequences of sulfate reduction rates in marine sediments are examined. B.W.

N85-32722*# Barcelona Univ. (Spain). Dept. of Microbiology.
ECOPHYSIOLOGY OF PHOTOTROPHIC SULFUR BACTERIA IN LAKES: VERTICAL DISTRIBUTION OF PLANKTONIC POPULATIONS
Ricardo Guerrero *In* NASA, Washington The Global Sulfur Cycle Jul. 1985 p 45-49 refs (For primary document see N85-32710 21-51)
Avail: NTIS HC A14/MF A01 CSCL 16C

The study of purple and green sulfur bacterial populations in nature is of interest for the following reasons: (1) high quantities of biomass, with low species diversity can be collected; (2) study of planktonic life permits one to understand the mechanisms, structural as well as physiological, used to maintain their vertical position without sinking; and (3) they are capable of sulfur oxidations and reductions that act as important intermediates in the global sulfur cycle. Purple and green photosynthetic bacteria, moreover, may be responsible for certain geological deposits. Planktonic phototrophic sulfur bacteria were analyzed in relation to their vertical distribution in the water column. Factors, including competition for light, that determine their sedimentation rates and the numerical changes in species and populations were assessed. B.W.

N85-32723*# Oregon Univ., Eugene. Dept. of Geology.
GEOLOGY AND GEOCHEMISTRY OF SULFIDE AND SULFATE DEPOSITION Abstract Only c46
William T. Holser *In* NASA, Washington The Global Sulfur Cycle Jul. 1985 p 50-54 refs (For primary document see N85-32710 21-51)
Avail: NTIS HC A14/MF A01 CSCL 08G

Factors contributing to the geology and geochemistry of sulfide and sulfate deposition are discussed. The age curves of sulfur and oxygen isotopes in marine sulfate are assessed. B.W.

N85-32724*# California Univ., San Diego, La Jolla.
MICROBIOLOGY OF SOLAR SALT PONDS Abstract Only
Barbara Javor *In* NASA, Washington The Global Sulfur Cycle Jul. 1985 p 55-56 refs (For primary document see N85-32710 21-51)
Avail: NTIS HC A14/MF A01 CSCL 06C

Solar salt ponds are shallow ponds of brines that range in salinity from that of normal seawater (3.4 percent) through NaCl saturation. Some salterns evaporate brines to the potash stage of concentration (bitterns). All the brines (except the bitterns, which are devoid of life) harbor high concentrations of microorganisms. The high concentrations of microorganisms and their adaptation to life in the salt pond are discussed. B.W.

N85-32725*# National Aeronautics and Space Administration. Ames Research Center, Moffett Field, Calif.
EVOLUTION OF THE ATMOSPHERE Abstract Only c47
James F. Kasting *In* NASA, Washington The Global Sulfur Cycle Jul. 1985 p 57-59 refs (For primary document see N85-32710 21-51)
Avail: NTIS HC A14/MF A01 CSCL 04B

Theories on the origin of the Earth atmosphere and chemical composition are presented. The role of oxygenic photosynthesis on the determination of the Earth's origin is discussed. The research suggests that further analysis of the geologic record is needed to more accurately estimate the history of atmospheric oxygen. B.W.

N85-32726*# Michigan State Univ., Hickory Corners. Biology Station.
SULFUR CYCLING IN FRESHWATER SEDIMENTS Abstract Only c45
Michael J. Klug *In* NASA, Washington The Global Sulfur Cycle Jul. 1985 p 60-61 refs (For primary document see N85-32710 21-51)
Avail: NTIS HC A14/MF A01 CSCL 13B

Organic sulfur containing compounds represent greater than 80% of the total sulfur in sediments of eutrophic freshwater lakes. Although sedimentary sulfur is predominantly in the form of organic compounds, more sulfur is transformed by sulfate reduction than by any other process. Rates of sulfate reduction in these sediments average 7 mmol/sq m/day. This rate is 19 times greater than the net rate of production of inorganic sulfur from organic compounds on an annual basis. Author

N85-32727*# Reading Univ. (England).
SOME THOUGHTS ON GAIA AND THE SULFUR CYCLE c45
James E. Lovelock *In* NASA, Washington The Global Sulfur Cycle Jul. 1985 p 62-63 refs (For primary document see N85-32710 21-51)
Avail: NTIS HC A14/MF A01 CSCL 13B

The data hypothesis states that the composition, oxidation reduction state, and temperature of the troposphere are actively regulated by the biota for the biota. One of the early predictions of the Gaia hypothesis was that there should be a sulfur compound made by the biota in the oceans. It would need to be stable enough against oxidation in water to allow its transfer to the air.

Either the sulfur compound itself or its atmospheric oxidation product would have to return sulfur from the sea to the land surfaces. The most likely candidate for this role was dimethyl sulfide. Another sulfur compound of interest from a Gaian viewpoint CS2 (carbon disulfide) is discussed. Theories on the production of dimethyl sulfide and carbon disulfide related to the Gaian hypothesis are examined. B.W.

N85-32728*# Boston Univ., Mass. Dept. of Biology.
FROM MICROBIAL COMMUNITIES TO CELLS Abstract Only
Lynn Margulis *In* NASA, Washington The Global Sulfur Cycle Jul. 1985 p 64-65 refs (For primary document see N85-32710 21-51)
Avail: NTIS HC A14/MF A01 CSCL 06C

The eukraotic cell, the unit of structure of protoctists, plants, fungi, and animals, is not at all homologous to prokaryotic cells. Instead the eukaryotic cell is homologous to communities of microorganisms such as those of the sulfuretum. This research is based on the hypothesis that at least four different interacting community members entered the original associations that, when stabilized, led to the emergence of eukaryotic cells. These are: (1) host nucleocytoplasm (thermoplasma like archaebacteria); (2) mitochrondria (paracoccus or bdellovibryo like respiring bacteria; and (3) plastids (cyanobacteria) and undulipodia. Tubulin like protein was found in the free living spirochete Spirochaeta bajacaliforniensis and in several other spirochetes. The amino acid sequence was to see if the spirochete protein is homologous to the tubulin of undulipodial and mitotic spindle microtubules. B.W.

N85-32729*# North Carolina Univ., Chapel Hill. Dept. of Marine Science.
SULFUR AND CARBON CYCLING IN ORGANIC-RICH MARINE SEDIMENTS Abstract Only c45
Christopher S. Martens *In* NASA, Washington The Global Sulfur Cycle Jul. 1985 p 66-67 refs (For primary document see N85-32710 21-51)
Avail: NTIS HC A14/MF A01 CSCL 13B

Nearshore, continental shelf, and slope sediments are important sites of microbially mediated carbon and sulfur cycling. Marine geochemists investigated the rates and mechanisms of cycling processes in these environments by chemical distribution studies, in situ rate measurements, and steady state kinetic modeling. Pore water chemical distributions, sulfate reduction rates, and sediment water chemical fluxes were used to describe cycling on a ten year time scale in a small, rapidly depositing coastal basin, Cape Lookout Bight, and at general sites on the upper continental slope off North Carolina, U.S.A. In combination with 210 Pb sediment accumulation rates, these data were used to establish quantitative carbon and sulfur budgets as well as the relative importance of sulfate reduction and methanogeneis as the last steps in the degradation of organic matter. Author

N85-32730*# Stanford Univ., Palo Alto, Calif. Dept. of Microbiology.
CHEMOLITHOTROPHY AND PHYSIOLOGY OF BACTERIAL NUTRIENT LIMITATION Abstract Only
Abdul Matin *In* NASA, Washington The Global Sulfur Cycle Jul. 1985 p 68 refs (For primary document see N85-32710 21-51)
Avail: NTIS HC A14/MF A01 CSCL 06C

An overview of the physiology of chemolithotrophic bacteria, particularly the thiobacilli, was presented. In these bacteria unique physiological traits are expressed during nutrient limited growth. Different physiological types of chemolithotrophs, pathways of sulfur oxidation, and electron transport in the thiobacilli, problems encountered by chemolithotrophs in the generation of reducing power, and some explanations of the phenomenon of obligate chemolithotrophy were considered. Mixotrophy in the thiobacilli has been studied extensively both under nutrient excess and limitation. In nature, bacteria usually grow under nutrient limitation. Yet the bulk of our knowledge of microbial metabolic function is derived from bacteria grown in laboratory batch cultures containing a great abundance of nutrients. Microbial behavior in these two types of environments can be very different, indicating the need for basing an understanding of microbial ecology on studies that rely on cultivation of microorganisms under nutrient limitation. Nutrient limited bacteria differ in several ways from those growing in large quantities of nutrients. They have different surface structures and make a much fuller use of their metabolic potential, especially by the synthesis of unique pathways of catabolic enzymes. Author

N85-32731*# Scripps Institution of Oceanography, San Diego, Calif.
POSSIBLE ROLES OF MANGANESE REDOX CHEMISTRY IN THE SULFUR CYCLE Abstract Only c45
Kenneth H. Nealson *In* NASA, Washington The Global Sulfur Cycle Jul. 1985 p 69 refs (For primary document see N85-32710 21-51)
Avail: NTIS HC A14/MF A01 CSCL 13B

Sulfate reducing bacteria (SRB) are very potent MnO2 reducers by virtue of their sulfide production: H2S reacts rapidly with MnO2 to yield Mn(2), elemental sulfur, and water. In manganese rich zones, Mn cycles rapidly if sulfate is present to drive the reduction and the MnO2 precipitates and sinks into anaerobic zones. The production of sulfide (by organisms requiring organic carbon compounds) to reduce manganese oxides might act to couple the carbon and sulfur cycles in water bodies in which the two cycles are physically separated. Iron has been proposed for this provision of reducing power by (Jorgensen, 1983), but since MnS is soluble and FeS is very insoluble in water, it is equally likely that manganese rather than iron provides the electrons to the more oxidized surface layers. R.J.F.

N85-32732*# Georgia Univ., Athens. Dept. of Biochemistry.
SULFATE-REDUCING BACTERIA: MICROBIOLOGY AND PHYSIOLOGY Abstract Only
Harold D. Peck *In* NASA, Washington The Global Sulfur Cycle Jul. 1985 p 70-71 refs (For primary document see N85-32710 21-51)
Avail: NTIS HC A14/MF A01 CSCL 06C

The sulfate reducing bacteria, the first nonphotosynthetic anaerobic bacteria demonstrated to contain c type cytochromes, perform electron transfer coupled to phosphorylation. A new bioenergetic scheme for the formation of a proton gradient for growth of Desulfovibrio on organic substrates and sulfate involving vectors electron transfer and consistent with the cellular localization of enzymes and electron transfer components was proposed. Hydrogen is produced in the cytoplasm from organic substrates and, as a permease molecule diffuses rapidly across the cytoplasmic membrane, it is oxidized to protons and electrons by the periplasmic hydrogenase. The electrons only are transferred across the cytoplasmic membrane to the cytoplasm where they are used to reduce sulfate to sulfide. The protons are used for transport or to drive a reversible ATPOSE. The net effect is the transfer of protons across the cytoplasmic membrane with the intervention of a proton pump. This type of H2 cycling is relevant to the bioenergetics of other types of anaerobic microorganisms. R.J.F.

N85-32733*# National Aeronautics and Space Administration. Ames Research Center, Moffett Field, Calif.
BIOGEOCHEMICAL CYCLING AND REMOTE SENSING c45
David L. Peterson *In* NASA, Washington The Global Sulfur Cycle Jul. 1985 p 72-76 refs (For primary document see N85-32710 21-51)
Avail: NTIS HC A14/MF A01 CSCL 13B

Research is underway at the NASA Ames Research Center that is concerned with aspects of the nitrogen cycle in terrestrial ecosystems. An interdisciplinary research group is attempting to correlate nitrogen transformations, processes, and productivity with variables that can be remotely sensed. Recent NASA and other publications concerning biogeochemical cycling at global scales identify attributes of vegetation that could be related or explain the spatial variation in biologically functional variables. These functional variables include net primary productivity, annual nitrogen mineralization, and possibly the emission rate of nitrous oxide from soils. R.J.F.

N85-32734*# Ohio State Univ., Columbus. Dept. of Microbiology.
STRUCTURE AND PHYSIOLOGY OF BEGGIATOA AND THIOTHRIX
Thomas M. Schmidt *In* NASA, Washington The Global Sulfur Cycle Jul. 1985 p 77-78 refs (For primary document see N85-32710 21-51)
Avail: NTIS HC A14/MF A01 CSCL 06C

Beggiatoa and Thiothrix are genera of filamentous, colorless, sulfide oxidizing bacteria. These organisms are microaerophilic, oxidizing sulfide to sulfur in the presence of oxygen. The sulfur accumulates in intracellular sulfur globules - the outstanding morphological feature of these bacteria. Some strains are able to further oxidize the sulfur to sulfate aerobically or reduce the sulfur to sulfide anaerobically. This metabolic versatility makes these bacteria important links in aquatic sulfur cycles. Author

N85-32735*# Bonn Univ. (West Germany). Inst. of Microbiology.
PHOTOTROPHIC BACTERIA AND THEIR ROLE IN THE BIOGEOCHEMICAL SULFUR CYCLE
Hans G. Trueper *In* NASA, Washington The Global Sulfur Cycle Jul. 1985 p 79-82 refs (For primary document see N85-32710 21-51)
Avail: NTIS HC A14/MF A01 CSCL 06C

An essential step that cannot be bypassed in the biogeochemical cycle of sulfur today is dissimilatory sulfate reduction by anaerobic bacteria. The enormous amounts of sulfides produced by these are oxidized again either anaerobically by phototrophic bacteria or aerobically by thiobacilli and large chemotrophic bacteria (Beggiatoa, Thiovulum, etc.). Phototrophic bacteria use sulfide, sulfur, thiosulfate, and sulfite as electron donors for photosynthesis. The most obvious intermediate in their oxidative sulfur metabolism is a long chain polysulfide that appears as so called sulfur globules either inside (Chromatiaceae) or outside (Ectothiorhodospiraceae, Chlorobiaceae, and some of the Rhodospirillaceae) the cells. The assimilation of sulfur compounds in phototrophic bacteria is in principle identical with that of nonphototrophic bacteria. However, the Chlorobiaceae and some of the Chromatiaceae and Rhodospirillaceae, unable to reduce sulfate, rely upon reduced sulfur for biosynthetic purposes. R.J.F.

N85-32736*# University of Southern Illinois, Carbondale. Dept. of Botany.
THE ROLE OF SULFUR IN OSMOREGULATION AND SALINITY TOLERANCE IN CYANOBACTERIA, ALGAE, AND PLANTS Abstract Only
John H. Yopp *In* NASA, Washington The Global Sulfur Cycle Jul. 1985 p 83-86 refs (For primary document see N85-32710 21-51)
Avail: NTIS HC A14/MF A01 CSCL 06C

Organosulfur compounds are involved in osmoregulation and salinity tolerance in some cyanobacteria and photosynthetic eukaryotes. Glycinebetaine, the osmolyte of the halotolerant cyanobacterium, Aphanothece halcphytica, requires the sulfonium compound. S-adenosyl-methionine (SAM) for its synthesis. Glutamate is the nitrogen source, SAM is the methyl carbon and serine the carbon backbone source of this unique osmolyte. Inhibitor studies suggest that photorespiration interacts with sulfur metabolism to control betaine synthesis in cyanobacteria. The limiting factor for SAM synthesis is formate from photorespiration. SAM is, in turn, the methyl donor for betaine synthesis from serine. The nitrogen component of serine is from glutamate. Betaine synthesis is hypothesized to be regulated via potassium. The biosynthesis of dimethyl-B-propiothetin (DMPT, which is the same as beta-dimethyl sulfonioprpionate) and diacylsulfoquinovosylglycerol were elucidated as having their roles in osmoregulation and salinity tolerance. The relation between these sulfolipids and the sulfur cycle was discussed. R.J.F.

N85-32737*# Barcelona Univ. (Spain). Dept. of Microbiology.
SULFUR CYCLING AND METABOLISM OF PHOTOTROPHIC AND FILAMENTOUS SULFUR BACTERIA
Ricardo Guerrero, Daniel Brune (Bonn Univ.), Ricardo Poplawski (Hebrew Univ., Jerusalem), and Thomas M. Schmidt (Ohio State Univ., Columbus) *In* NASA, Washington The Global Sulfur Cycle Jul. 1985 p 87-89 refs (For primary document see N85-32710 21-51)
Avail: NTIS HC A14/MF A01 CSCL 06C

Phototrophic sulfur bacteria taken from different habitate (Alum Rock State Park, Palo Alto salt marsh, and Big Soda Lake) were grown on selective media, characterized by morphological and pigment analysis, and compared with bacteria maintained in pure culture. A study was made of the anaerobic reduction of intracellular sulfur globules by a phototrophic sulfur bacterium (Chromatium vinosum) and a filamentous aerobic sulfur bacterium (Beggiatoa alba). Buoyant densities of different bacteria were measured in Percoll gradients. This method was also used to separate different chlorobia in mixed cultures and to assess the relative homogeneity of cultures taken directly or enriched from natural samples (including the purple bacterial layer found at a depth of 20 meters at Big Soda Lake.) Interactions between sulfide oxidizing bacteria were studied. R.J.F.

N85-32738*# Bonn Univ. (West Germany). Inst. of Microbiology.
ENRICHMENTS FOR PHOTOTROPHIC BACTERIA AND CHARACTERIZATION BY MORPHOLOGY AND PIGMENT ANALYSIS
D. Brune *In* NASA, Washington The Global Sulfur Cycle Jul. 1985 p 90-107 refs (For primary document see N85-32710 21-51)
Avail: NTIS HC A14/MF A01 CSCL 06C

The purpose of this investigation was to examine several sulfide containing environments for the presence of phototrophic bacteria and to obtain enriched cultures of some of the bacteria present. The field sites were Alum Rock State Park, the Palo Alto salt marsh, the bay area salt ponds, and Big Soda Lake (near Fallon, Nevada). Bacteria from these sites were characterized by microscopic examination, measurement of in vitro absorption spectra, and analysis of carotenoid pigments. Field observations at one of the bay area salt ponds, in which the salt concentration was saturating (about 30 percent NaCl) and the sediments along the shore of the pond covered with a gypsum crust, revealed a layer of purple photosynthetic bacteria under a green layer in the gypsum crust. Samples of this gypsum crust were taken to the laboratory to measure light transmission through the crust and to try to identify the purple photosynthetic bacteria present in this extremely saline environment. R.J.F.

N85-32739*# Ohio State Univ., Columbus. Dept. of Microbiology.
ANAEROBIC REDUCTION OF ELEMENTAL SULFUR BY CHROMATIUM VINOSUM AND BEGGIATOA ALBA
Thomas M. Schmidt *In* NASA, Washington The Global Sulfur Cycle Jul. 1985 p 108-113 refs (For primary document see N85-32710 21-51)
Avail: NTIS HC A14/MF A01 CSCL 06C

The effect of sulfur globules on the buoyant density of Chromatium vinosum and Beggiatoa alba was examined. The potential use of sulfur as a terminal electron acceptor in the anaerobic metabolism of Beggiatoa alba is also examined. The effect of the reduction of intracellular sulfur was investigated during dark metabolism on the buoyant density of C. vinosum. It is hypothesized from the results that the sulfur reduction to sulfide is part of an anaerobic energy operating system. Carbon stored as PHB can be oxidized with the concomitant reduction of sulfur to sulfide. E.R.

N85-32740*# Barcelona Univ. (Spain). Dept. of Microbiology.
BUOYANT DENSITIES OF PHOTOTROPHIC SULFUR BACTERIA AND CYANOBACTERIA
Ricardo Guerrero *In* NASA, Washington The Global Sulfur Cycle Jul. 1985 p 114-116 (For primary document see N85-32710 21-51)
Avail: NTIS HC A14/MF A01 CSCL 06C

The buoyant densities of bacterial cells are greatly influenced by the accumulation of intracellular reserve material. The buoyant density of phototrophic bacteria that are planktonic is of particular

interest, since these organisms must remain in the photic zone of the water column for optimal growth. Separation of cells by their buoyant density may also be of use in separating and identifying organisms from a natural population. The bacteria used were obtained from pure cultures, enrichments, or samples taken directly from the environment. Author

N85-32741*# Hebrew Univ., Jerusalem (Israel). Dept. of Biochemistry.
INTERACTIONS AMONG SULFIDE-OXIDIZING BACTERIA
Ricardo Poplawski *In* NASA, Washington The Global Sulfur Cycle Jul. 1985 p 117-127 refs (For primary document see N85-32710 21-51)
Avail: NTIS HC A14/MF A01 CSCL 06C

The responses of different phototrophic bacteria in a competitive experimental system are studied, one in which primary factors such as H2S or light limited photometabolism. Two different types of bacteria shared one limited source of sulfide under specific conditions of light. The selection of a purple and a green sulfur bacteria and the cyanobacterium was based on their physiological similarity and also on the fact that they occur together in microbial mats. They all share anoxygenic photosynthesis, and are thus probably part of an evolutionary continuum of phototrophic organisms that runs from, strictly anaerobic physiology to the ability of some cyanobacteria to shift between anoxygenic bacterial style photosynthesis and the oxygenic kind typical of eukaryotes. Author

N85-32742*# Michigan State Univ., Hickory Corners. Biology Station.
SULFUR REDUCTION IN SEDIMENTS OF MARINE AND EVAPORITE ENVIRONMENTS c45
Michael J. Klug, Penelope Boston (National Center for Atmospheric Research, Boulder), Roger Francois (British Columbia Univ.), Ruth Ann Gyure (Purdue Univ.), Barbara Javor (Scripps Inst. of Oceanography, La Jolla, Calif.), Gordon Tribble (Hawaii Univ., Honolulu), and Appathurai Vairavamurthy (Florida State Univ.) *In* NASA, Washington The Global Sulfur Cycle Jul. 1985 p 128-157 refs (For primary document see N85-32710 21-51)
Avail: NTIS HC A14/MF A01 CSCL 13B

Transformations of sulfur in sediments of ponds ranging in salinities from that of normal seawater to those of brines saturated with sodium chloride were examined. The chemistry of the sediment and pore waters were focused on with emphasis on the fate of sulfate reduction. The effects of increasing salinity on both forms of sulfur and microbial activity were determined. A unique set of chemical profiles and sulfate-reducing activity was found for the sediments of each of the sites examined. The quantity of organic matter in the salt pond sediments was significantly greater than that occurring in the adjacent intertidal site. The total quantitative and qualitative distribution of volatile fatty acids was also greater in the salt ponds. Volatile fatty acids increased with salinity. E.R.

N85-32743*# National Aeronautics and Space Administration. Ames Research Center, Moffett Field, Calif.
CYANOBACTERIAL MATS: MICROANALYSIS OF COMMUNITY METABOLISM
Yehuda Cohen, David Bermudes (Boston Univ.), Ulrich Fischer (Oldenburg Univ.), Robert Haddad (North Carolina Univ., Chapel Hill), Lee Prufert (North Carolina Univ., Chapel Hill), Trudy Scheulderman-Suylen (Technische Hogeschool, Delft, Netherlands), and Timothy Shaw (Scripps Inst. of Oceanography, La Jolla, Calif.) *In* NASA, Washington The Global Sulfur Cycle Jul. 1985 p 158-182 (For primary document see N85-32710 21-51)
Avail: NTIS HC A14/MF A01 CSCL 06C

The microbial communities in two sites were studied using several approaches: (1) light microscopy; (2) the measurement of microprofiles of oxygen and sulfide at the surface of the microbial mat; (3) the study of diurnal variation of oxygen and sulfides; (4) in situ measurement of photosynthesis and sulfate reduction and study of the coupling of these two processes; (5) measurement of glutathione in the upper layers of the microbial mat as a possible oxygen quencher; (6) measurement of reduced iron as a possible intermediate electron donor along the established redoxcline in the mats; (7) measurement of dissolved phosphate as an indicator of processes of break down of organic matter in these systems; and (8) measurement of carbon dioxide in the interstitial water and its delta C-13 in an attempt to understand the flow of CO2 through the systems. Microbial processes of primary production and initial degradation at the most active zone of the microbial mat were analyzed. Author

N85-32744*# North Carolina Univ., Chapel Hill. Dept. of Marine Sciences.
MICROANALYSIS OF DISSOLVED IRON AND PHOSPHATE IN PORE WATERS OF HYPERSALINE SEDIMENT c45
Robert Haddad and Timothy Shaw (Scripps Inst. of Oceanography, La Jolla, Calif.) *In* NASA, Washington The Global Sulfur Cycle Jul. 1985 p 183-193 (For primary document see N85-32710 21-51)
Avail: NTIS HC A14/MF A01 CSCL 13B

Diurnal fluctuations of reduced iron concentrations, expected to occur in reduced sediments in the photic zone, were studied. Iron concentration was compared to O2-H2S, a microanalysis of sulfate reduction was performed, as well as an examination of diurnal concentration of dissolved phosphate and changes in interstitial CO2. The iron profiles suggest a strong correlation between iron remobilization and processes occurring in the light. Phosphate profiles suggest the removal of phosphate is strongly correlated with precipitation of oxidized iron in the upper 2 mm to 5 mm of the sediments. Pore water CO2 concentrations and carbon isotope ratios are presented. These data are from the analyses of minisediment cores collected from the 42 per mil salt pond and incubated in the laboratory under light and dark conditions. E.R.

N85-32745*# Boston Univ., Mass. Dept. of Biology.
GLUTATHIONE IN CYANOBACTERIA
David Bermudes *In* NASA, Washington The Global Sulfur Cycle Jul. 1985 p 194-199 (For primary document see N85-32710 21-51)
Avail: NTIS HC A14/MF A01 CSCL 06C

The effects of light and O2 on glutathione production were determined. Results of light and dark studies under normal and reduced oxygen tensions were compared to determine the effect of reduction in oxygen tension on glutathione levels. The growth rate of Anacystis nidulans and concurrent production of glutathione is presented. The generation of time of Anacystis nidulans was approximately 12 hours. Results of light and dark incubation of Aphanothece halophytica dominated planktonic microbial community from Pond 4 and Anacystis nidulans under high and low oxygen tension is also presented. It appears that light grown Anacystis nidulans cells have equal amounts of glutathione while dark grown cells produce more glutathione in the presence of increased O2. E.R.

N85-32746*# Oldenburg Univ. (West Germany). Dept. of Geomicrobiology.
MICROBIAL COMMUNITIES AND MICROPROFILES OF SULFIDE AND OXYGEN OF ALUM ROCK SULFUR SPRINGS
Ulrich Fischer *In* NASA, Washington The Global Sulfur Cycle Jul. 1985 p 200-217 refs (For primary document see N85-32710 21-51)
Avail: NTIS HC A14/MF A01 CSCL 06C

The microbial community of Alum Rock sulfur spring Site 3 was studied along one branch of the main stream and between the two branches, 150 cm distant from the source. The community at the source was dominated by green sulfur photosynthetic bacteria of the genus Chlorobium. At 15 cm to 35 cm from the source dominance in the community shifted to the genus Flexibacter at the surface of the mat and purple bacteria of the genus Chromatium underneath. At 50 cm to 80 cm colorless sulfur oxidizing bacteria of the genus Thiothrix began to appear. At 100 cm to 150 cm, the surface of the mat was still dominated by Flexibacter, but underneath dominance shifted to purple sulfur bacteria as above, as well as cyanobacteria of the genus Oscillatoria and Pseudonabaena. The measurements of temperature along the stream showed no significant gradient. Community variations appear to be controlled more by sulfide than temperature. Ten ml of the overlying water were taken and fixed immediately

to determine the sulfide concentration by the methylene blue method. A sulfide concentration of 106 micro-m was calculated for the overlying water. Author

N85-32747*# Saskatchewan Univ., Saskatoon. Dept. of Applied Microbiology and Food Science.
MICROBIAL COLONIZATION AND GROWTH ON METAL SULFIDES AND OTHER MINERAL SURFACES
Douglas Caldwell, Alfred R. Sundquist (California Univ., San Diego, La Jolla), John Lawrence, and Allen P. Doyle (Alaska Univ.) *In* NASA, Washington The Global Sulfur Cycle Jul. 1985 p 218-233 refs (For primary document see N85-32710 21-51)
Avail: NTIS HC A14/MF A01 CSCL 06C

To determine whether a bacterial film forms on sulfur minerals in situ, various sulfur containing and other minerals were incubated in Penitencia Creek. The rate of cell growth and attachment within the surface microenvironment of mineral surfaces was also determined. To determine whether surfaces enriched with soluble sulfur substrates (cysteine, glutathione, thioglycolate, sulfite, and thiosulfate) increased the rate of growth or attachment of natural communities, membrane enrichments were incubated. These rates were determined as described by Caldwell et al. (1981, 1983). The growth of Pseudomonas fluorescens, a heterotrophic sulfur oxidizer, was studied in batch cell suspensions and in continuous culture. In batch culture the cells were oxygen limited (growth rate 0.33 per hour under oxygen limitations and 0.52 per hour when vigorously aerated). Growth within the film was glucose limited. Several behavioral phenomena were observed for cells growing within the hydrodynamic boundary layer. Despite a flow of 10 cm per second in the environment, the bacteria were able to move freely in both directions within the hydrodynamic boundary layer. E.R.

N85-32748*# National Aeronautics and Space Administration, Washington, D. C.
SULFUR CYCLE **c45**
R. Hariss and H. Niki *In its* The Global Sulfur Cycle Jul. 1985 p 234-238 refs (For primary document see N85-32710 21-51)
Avail: NTIS HC A14/MF A01 CSCL 13B

Among the general categories of tropospheric sulfur sources, anthropogenic sources have been quantified the most accurately. Research on fluxes of sulfur compounds from volcanic sources is now in progress. Natural sources of reduced sulfur compounds are highly variable in both space and time. Variables, such as soil temperature, hydrology (tidal and water table), and organic flux into the soil, all interact to determine microbial production and subsequent emissions of reduced sulfur compounds from anaerobic soils and sediments. Available information on sources of COS, CS2, DMS, and H2S to the troposphere in the following paragraphs are summarized; these are the major biogenic sulfur species with a clearly identified role in tropospheric chemistry. The oxidation of SO2 to H2SO4 can often have a significant impact on the acidity of precipitation. A schematic representation of some important transformations and sinks for selected sulfur species is illustrated. E.R.

N85-32749# Baylor Coll. of Medicine, Houston, Tex. Dept. of Physiology.
PHYSICAL CHEMICAL STATE OF WATER IN LIVING CELLS Final Progress Report, period ending 1982
C. F. Hazlewood, D. C. Chang, and R. L. Vick May 1985 22 p (Contract N00014-76-C-0100)
(AD-A154566) Avail: NTIS HC A02/MF A01 CSCL 06/3

Overall Research Program (specific work tasks) outlined in the proposal include: physical properties of water in tissues, cells and subcellular organelles; physical properties of water in the brine shrimp artemia; effects of hemorrhagic shock on the physical properties of tissue water. Relaxation times and diffusion coefficients for water protons, hydrogen and isotopes of water were determined. The progress 1983 to 1984 pertains to: mechanisms of NMR relaxation; hypothesis of proteins dynamics and hemorrhagic shock. A biophysical study of cellular water and ions in excitable cells, functional role of ion-water-protein interactions in excitable cells, is summarized. Scientific findings include: (1) effects of the ionic enviornment on the gating properties of the excitable ionic channels; effect of internal Cs(+) ions on the early and late conductance in squid axon. The effect of internal sodium ions on the action potential and reversal potential in squid axons; (2) structure and function of the membrane proteins and the submembrane (cortical) protein network (a) structure of the squid axon membrane as seen after freeze-fracture, (b) possible role of cytoplasmic microtubule structure in the excitation properties of nerve axon; (3) Ionic mechanisms involved in the regulation of the resting potential; (a) Effects of ionic concentration on the resting potential in squid axons: evidence supporting a modification of the constant field equation, (b) differentiation between the excitable sodium channel and the major pathway for the resting sodium current; (4) Intracellular transport of Na(+) ions inside the nerve cell. GRA

N85-32750# Army Medical Research Inst. of Infectious Diseases, Fort Detrick, Md.
DIFFERENCES IN SUSCEPTIBILITY OF INBRED MICE TO BACILLUS ANTHRACIS
S. L. Welkos, T. J. Keener, and P. H. Gibbs 26 Apr. 1985 33 p (AD-A155646) Avail: NTIS HC A03/MF A01 CSCL 06/5

Animal species differ in their resistance both to infection by B. anthracis and to anthrax toxin. A mouse model was developed to study the basis of these host differences and the pathogenesis of infection. When infected with the virulent B. anthracis strain Volume 1B, all eight strains of inbred mice tested had low LD50 values (5 to 30 spores). However, analysis of time-to-death (TTD) data revealed significant differences between the strains, which could be divided into three groups: most susceptible (A/J, DBA/2J, and C3H/HeN); intermediate (C57BL/6J, C57L/J, and C58/J); and least susceptible (CBA/J and C57BR/cdJ). In contrast, the mice were distinctly susceptible or resistant to lethal infection by Sterne vaccine strain. The LD50 of the susceptible A/J and DBA/2J mice was approximately 1,000 Sterne spores; whereas the remaining six relatively resistant strains were killed only by 0.2 to 2 x 10,000,000 spores. Mice lethally infected with B. anthracis had an acute course, characterized by extensive gelatinous edema and large concentrations of bacilli in the blood and organs (e.g., 1,000,000,000 CFU/g spleen). To study susceptibility to anthrax toxin, the protective antigen (PA) and lethal factor (LF) components of the toxin were injected i.v. into A/J and CBA/J mice. As reported earlier for various animal species, susceptibilities of the mice to anthrax toxin appeared to be independent of that to infection. The toxin LD50 values for both strains were about 12 micrograms PA combined with 2.4 micrograms LF. GRA

N85-32751# Argonne National Lab., Ill.
INFLUENCE OF CHEMICAL FORM, FEEDING REGIMEN, AND ANIMAL SPECIES ON THE GASTROINTESTINAL ABSORPTION OF PLUTONIUM
M. H. Bhattacharyya, R. P. Larsen, N. Cohen, L. G. Ralston, R. D. Oldham, E. S. Moretti, and L. Ayres 1985 9 p refs Presented at the Seminar on the Speciation of Fission Products in the Environment, Oxford, 16 Apr. 1985 Prepared in cooperation with New York Univ., New York.
(Contract W-31-109-eng-38)
(DE85-010291; CONF-850473-1) Avail: NTIS HC A02/MF A01

The effect of chemical form and feeding regimen on the gastrointestinal (GI) absorption of plutonium in adult mice at plutonium concentrations relevant to the establishment of drinking water standards was evaluated. Mean fractional GI absorption values in fasted and fed adult mice are given. To assess the validity of extrapolating data from mice to humans, the GI absorption of Pu(VI) bicarbonate in adult baboons was also determined with a dual isotope method that does not require animal sacrifice. Fractional GI absorption values obtained by this method are also given. This method was validated in one baboon and are currently completing validation in two additional animals. At low plutonium concentrations, plutonium oxidation state [Pu(VI) vs Pu(IV)] and administration medium (bicarbonate vs nitrate vs citrate) had little effect on the GI absorption of plutonium in mice. Formation of

Pu(IV) polymers and animal feeding decreased the GI absorption of plutonium 5- to 10-fold. The GI absorption of Pu(VI) bicarbonate in both fed and fasted adult baboons appeared to be the same as in fed and fasted adult mice, respectively. DOE

N85-32752# Joint Publications Research Service, Arlington, Va.
USSR REPORT: LIFE SCIENCES. BIOMEDICAL AND BEHAVIORAL SCIENCES
25 Jul. 1985 117 p Transl. into ENGLISH from various Russian articles
(JPRS-UBB-85-020) Avail: NTIS HC A06/MF A01

Progress in the life sciences, biomedical, and behavioral sciences is reported. Topics discussed include: aerospace medicine, aerotechnology, biochemistry, bionics, biophysics, biotechnology, environmental issues, epidemiology, genetics, human factors engineering, immunology, laser effects, microbiology, military medicine, nonionizing electromagnetic radiation effects, pharmacology and toxicology, physiology, public health, and radiation biology. For individual titles, see N85-32753 through N85-32754.

N85-32753# Joint Publications Research Service, Arlington, Va.
REMOTE MEDICAL DIAGNOSIS **c52**
V. K. Yemelyanov *In its* USSR Rept.: Life Sci. Biomed. and JPRS-UBB-85-020 25 Jul. 1985 p 1-2 Transl. into ENGLISH from Sov. Litva (Vilnius, USSR), 12 Apr. 1985 p 4 (For primary document see N85-32752 21-51)
Avail: NTIS HC A06/MF A01

The use of aerospace medicine achievements to solve medical problems on Earth is discussed. Man's abilities, methods of controlling the organism's adaptation to changing and often harsh conditions of outer space are monitored. Special methods and the proper apparatus give recording and transmission of various physiological parameters that indicate the status of all of a cosmonaut's vitally important body systems. Remote diagnosis can be effectively applied to use on Earth. A well-developed network of satellites is available. The possibility to use this network to allow a hospital in remote region of the country to communicate and exchange information with leading centers of medicine is outlined. E.A.K.

N85-32754# Joint Publications Research Service, Arlington, Va.
HYDROPONICS DEVELOPMENTS FOR SPACESHIP GARDEN
Yu. Meshkov *In its* USSR Rept.: Life Sci. Biomed. and JPRS-UBB-85-020 25 Jul. 1985 p 3 Transl. into ENGLISH from Probl. i Resheniya, 5 Feb. 1985 p 6 (For primary document see N85-32752 21-51)
Avail: NTIS HC A06/MF A01

Developments in hydroponics aimed at developing kitchen gardens for spaceships are reported. Spacing of plants at various stages of development in hydroponic units to realize optimum use of area and to maximize the effectiveness of light from natural and artificial sources falling on plant was studied. It is found that if the efficiency of utilization of light energy is increased by 20 to 30 times, a comparable increase in the yield of biomass from square meter of area can be realized. A compact unit, the Samorod-Arktika for hydroponic cultivation of plants at outposts in Arctic regions was developed. The unit serves the same dual role for workers at polar outposts as in a spaceship garden: furnishes vitamins for the diet, and provides the psychological effect of greenery. Prospects for development of this technology to help solve worldwide problems of limited land, water and energy resources for agriculture are discussed. E.A.K.

52 AEROSPACE MEDICINE

Includes physiological factors; biological effects of radiation; and weightlessness.

N85-32755* National Aeronautics and Space Administration, Washington, D. C.
AEROSPACE MEDICINE AND BIOLOGY: A CONTINUING BIBLIOGRAPHY WITH INDEXES, SUPPLEMENT 273
Jul. 1985 87 p
(NASA-SP-7011(273); NAS 1.21:7011(273)) Avail: NTIS HC $7.00 CSCL 06E

This bibliography lists 265 reports, articles, and other documents introduced into the NASA scientific and technical information system in June 1985. Topics in aerospace medicine and biology, metabolism, human behavior, man machine systems, and injuries are included. R.J.F.

N85-32756# Air Force Systems Command, Wright-Patterson AFB, Ohio. Foreign Technology Div.
STUDIES OF CIRCULATORY AND METABOLIC CHANGES DURING KETAMINE NARCOSIS
I. Hensel, U. Braun, D. Kettler, D. Knoll, and J. Martel 13 Mar. 1985 16 p Transl. into ENGLISH from Der Anaesthesist, (West Germany), v. 21, no. 2, 1972 p 44-49
(AD-A154512; FTD-ID(RS)T-0079-85) Avail: NTIS HC A02/MF A01 CSCL 06/15

Among commonly used anesthetics, ketamine obviously occupies an unusual position. While most anesthetics exert a retarding effect on circulation and metabolism, ketamine clearly has the opposite effect. Figure 1 shows the synopsis of the most important circulatory characteristics after a representative individual test. The injection of ketamine in the animal test causes an increases in heart frequency (HF), HZV (lower curve), coronary blood supply (Vcor) and the myocardial O2 consumption, together with a reduction in coronary venous saturation (upper falling curve). The pressures and the rate of decrease are higher. Eight mongrel dogs weighing between 19 and 27 kg were pre-medicated with 1 mg of scopalamine and 30 minutes later received intravenously on average 20 mg/kg body weight of ketamine which produced in them a condition similar to narcosis. The behavior of PCO2, pH bases excess and the average arterial pressure, heart beat and the central venous pressure during ketamine is discussed. The change in heart beat and the plasma concentration of noradrenaline, adrenaline, glucose and free fatty acids during ketamine narcosis is reported. Oxygen consumption during ketamine narcosis after administration of a muscle relaxant and a morphine derivative is also reported. GRA

N85-32757# Dayton Univ., Ohio.
VISUAL PHENOMENA PRODUCED BY BINOCULARLY DISPARATE DYNAMIC VISUAL NOISE Final Technical Paper, Aug. 1981 - Sep. 1984
G. A. Geri and Y. Y. Zeevi May 1985 39 p Prepared in cooperation with Massachusetts Inst. of Tech.,
(Contract F33615-81-C-0005)
(AD-A154758; AFHRL-TP-85-4) Avail: NTIS HC A03/MF A01 CSCL 06/16

The use of helmet mounted displays in flight simulation requires that different visual stimuli be presented to the two eyes. Such disparate stimulation may result in perceptual problems which could adversely affect simulator training. A series of four experiments addressed several perceptual problems associated with the use of binocularly disparate stimuli. The stimulus used in all four experiments was the dynamic visual noise (DVN) stereophenomenon produced by viewing a detuned television receiver with the input to one eye attenuated by a light filter. The result is the percept of several counterdirectional dot-planes separated in depth. The purpose of the basic visual research reported here is to further elucidate the visual mechanisms underlying movement aftereffects (Experiment 1), binocular rivalry (Experiment 2), perceived visual acceleration (Experiment 3), and vergence and accommodation to perceived depth (Experiment 4). Each of these phenomena was induced by a form free texture stimulus perceived as moving in planes located at various distances from the observer. GRA

N85-32758# Hahnemann Medical Coll. and Hospital, Philadelphia, Pa. Dept. of Anatomy.
ANALYSIS OF LONG BONE AND VERTEBRAL FAILURE PATTERNS Final Scientific Report
J. A. C. Eurell 14 Feb. 1985 223 p

(Grant AF-AFOSR-0044-84)
(AD-A154796; AFOSR-85-0454TR) Avail: NTIS HC A10/MF A01 CSCL 06/5

This report documents five years of work on the normal anatomy of the rhesus monkey vertebral column, the vertebral column response to compressive loading, and the response of bone to hypokinesia. The surface of fractures of long bones were also examined. The rhesus monkey vertebral column was similar to the human spine anatomically, with the exception of the cartilaginous end plates which had unique islands of calcification. The primate vertebral column responded to compressive loading by bending or fracture of bone within individual vertebral bodies, burst injuries in spinal units, and stimulation of osteophyte formation in in vivo impacted spines. Bone formation appeared to be inhibited by hypokinesia in the femur, rib, and vertebral body of exposed rhesus monkeys. Torsional and straight fractures of long bones had varied surface texture due to different angles of fracture planes across the bone matrix. GRA

N85-32759# National Jewish Hospital and Research Center, Denver, Colo.
RESOURCE ALLOCATION IN CEREBRAL SPECIALIZATION OF FUNCTION: BEHAVIORAL AND ELECTROPHYSIOLOGICAL STUDIES Final Progress Report, 15 Mar. 1983 - 30 Sep. 1984
9 Apr. 1985 5 p
(Contract N00014-83-C-0318)
(AD-A155092) Avail: NTIS HC A02/MF A01 CSCL 05/10

The purpose of this project was to study, using both cognitive and electrophysiological methods the relationship between resource allocation theory and functional cerebral lateralization. A number of cognitive experiments have been completed during the period of this project. Two experiments were completed and analyzed that addressed the question of whether hemispheric differences in information processing may be characterized by differences in the way information is represented or the relative speed and accuracy with which the processes within a hemisphere can operate on a representational system. According to Anderson (1983) there are at least three types of representations of information which are qualitatively different: spatial images, temporal strings and abstract propositions. Theoretically, these representations differ in the way the information is encoded, the processes by which matches of incoming information are made against the current representation, and how new structures within a representational system are constructed. The unity of the concept of cerebral specialization with the allocation of resources model has proven useful in accounting for otherwise disparate research findings involving perception, cognition, and motor performance. Moreover, this approach suggests explanations for patterns of task interference that are not readily interpretable within the information processing framework. GRA

N85-32760# SRI International Corp., Menlo Park, Calif.
USAFSAM REVIEW AND ANALYSIS OF RADIOFREQUENCY RADIATION BIOEFFECTS LITERATURE Interim Report, 17 Mar. - 31 Dec. 1984
L. N. Heynick and P. Polson Mar. 1985 332 p
(Contract F33615-82-C-0610)
(AD-A155113; USAFSAM-TR-85-7; IR-5) Avail: NTIS HC A15/MF A01 CSCL 06/18

The objectives of this project are to acquire, review, and analyze on an ongoing bases, information on research pertaining to the biological effects of radiofrequency radiation (RFR) for the preparation of a computer data base of analyses at the USAF School of Aerospace Medicine (USAFSAM). The method in use is to: (1) select documents judged to be representative of prior and current research on various RFR-bioeffects topics, (2) analyze in detail the contents of each such document, and (3) assess the validity and significance of the results presented. In this fifth report, the major RFR-bioeffects topics are listed and the format used for analyzing each selected document is described. During the period covered by this report, 40 additional analyses were completed, for a total of 200 analyses. The texts of the additional analyses are presented in Appendix A. In addition to the text, each analysis includes information for computer retrieval by authors, key words, year of publication, and RFR parameters. Appendixes B and C are two cumulative indexes to reference citations for all of the analyses completed thus far. In Appendix B, each citation is listed under each pertinent major topic. Appendix C comprises a cumulative list of citations in alphabetical order by first author and without regard to topic. GRA

N85-32761# New York State Coll. of Agriculture and Life Sciences, Ithaca.
INTERACTION OF OPIATE AND PHENCYCLIDINE DERIVATIVES WITH THE ACETYLCHOLINE RECEPTOR Contractor Report, Jun. 1983 - Oct. 1984
R. E. Oswald Mar. 1985 32 p
(Contract DAAK11-83-C-0049)
(AD-A155119; CRDC-CR-85004) Avail: NTIS HC A03/MF A01 CSCL 06/15

The purpose of this work was to define the structural and biochemical environment of the AChR/I and the relationship of drug structure to the resultant pharmacological response. A number of drugs were tested using both biochemical and electrophysiological tests. For the most part, compounds consisted of benzomorphan and phencyclidine analogs, with the benzomorphans being the more thoroughly tested. Several important portions of the benzomorphan structure were identified, and the results of varying substitutents suggested that hydrophobicity parameters were the most important determinants of binding affinity. GRA

N85-32762# Aerospace Medical Div., Brooks AFB, Tex.
AIR FORCE TECHNICAL OBJECTIVE DOCUMENT, AEROSPACE MEDICAL DIVISION, FISCAL YEAR 1986 Annual Report
B. Phelps Jan. 1985 23 p
(AD-A155195; AMD-TR-85-4) Avail: NTIS HC A02/MF A01 CSCL 06/5

This TOD (Technical Objective Document) describes the planning method used within two of the Aerospace Medical Div.'s (AMD) laboratories to achieve our technical goals. Specifically, efforts are directed in the biotechnology program to man's adaptability, survivability, and performance capabilities within his operational environment. This research and development of AMD's functions is accomplished as interdisciplinary work by teams of biomedical scientists, engineers, and physical scientists within the Air Force laboratories and the industrial and academic communities. GRA

N85-32763# School of Aerospace Medicine, Brooks AFB, Tex.
PREDICTIVE MODEL OF ELECTRON BEAM INDUCED FLASH-BLINDNESS Final Report, Nov. 1983 - Oct. 1984
N. Miller and T. G. Wheeler Mar. 1985 22 p
(AF Proj. 7757)
(AD-A155260; AD-F300613; USAFSAM-TR-84-35) Avail: NTIS HC A02/MF A01 CSCL 06/16

The spectral characteristics of the Cerenkov radiation have been evaluated and converted to equivalent retinal irradiance from external sources. On the basis of the conversion, electron fluxes have been estimated for 2-sec recovery times from flashblindness. The electrons are assumed to have energies greater than 6 MeV and to be delivered in one or more bursts of 1 microsecond each over 1 sec. It is important to note that very little data exists on recovery times as short as 2 sec for either photopic and scotopic conditions. This situation is a direct result of the lack of definition of the critical tasks and their sensitivity to an interruption of background adaptation. The Cerenkov radiation produced within the eye by relativistic electrons can be compared to light from external sources by the relationships: 1 rad approx. = 4.6 scotopic td-sec and 1 rad approx. = 0.55 photopic td sec. Based on these conversion factors, the following estimates can be derived by extrapolation from existing data: (1) Absolute threshold is equivalent to the Cerenkov radiation from a 4.3-microrad electron beam and to a 0.5-mrad X-ray beam. (2) For low photopic levels of adaption (approximately 10 td), 100,000-rad electron beam would be required for a 2-sec recover time for foveal or parafoveal vision. (3) For the dark-adapted eye, a dose of 10 rads may cause a 2-sec

interruption in the detection of low-contrast, peripheral targets. GRA

N85-32764# Army Medical Research Inst. of Infectious Diseases, Fort Detrick, Md.
SPONTANEOUS TRANSITIONAL CELL CARCINOMA IN THE URINARY BLADDER OF A STRAIN 13 GUINEA PIG Case Report
C. J. Trahan and W. C. Mitchell May 1985 14 p
(AD-A155645) Avail: NTIS HC A02/MF A01 CSCL 06/5

Spontaneous tumors in guinea pigs are very rare. To date, only 318 cases have been reported. This report describes the clinical pathology, gross pathology, and light microscopy histopathology of a spontaneous transitional cell carcinoma in the urinary bladder of a male Strain 13 guinea pig. GRA

N85-32753# Joint Publications Research Service, Arlington, Va.
REMOTE MEDICAL DIAGNOSIS
V. K. Yemelyanov *In its* USSR Rept.: Life Sci. Biomed. and JPRS-UBB-85-020 25 Jul. 1985 p 1-2 Transl. into ENGLISH from Sov. Litva (Vilnius, USSR), 12 Apr. 1985 p 4 (For primary document see N85-32752 21-51)
Avail: NTIS HC A06/MF A01

53 BEHAVIORAL SCIENCES

Includes psychological factors; individual and group behavior; crew training and evaluation; and psychiatric research.

N85-32765*# Old Dominion Univ., Norfolk, Va.
AN ERROR-DEPENDENT MODEL OF INSTRUMENT-SCANNING BEHAVIOR IN COMMERCIAL AIRLINE PILOTS Ph.D. Thesis - May 1983
Dennis H. Jones Washington Jul. 1985 190 p refs
(Grant NGT-47-003-801)
(NASA-CR-3908; NAS 1.26:3908) Avail: NTIS HC A09/MF A01 CSCL 05I

A new flexible model of pilot instrument scanning behavior is presented which assumes that the pilot uses a set of deterministic scanning patterns on the pilot's perception of error in the state of the aircraft, and the pilot's knowledge of the interactive nature of the aircraft's systems. Statistical analyses revealed that a three stage Markov process composed of the pilot's three predicted lookpoints (LP), occurring 1/30, 2/30, and 3/30 of a second prior to each LP, accurately modelled the scanning behavior of 14 commercial airline pilots while flying steep turn maneuvers in a Boeing 737 flight simulator. The modelled scanning data for each pilot were not statistically different from the observed scanning data in comparisons of mean dwell time, entropy, and entropy rate. These findings represent the first direct evidence that pilots are using deterministic scanning patterns during instrument flight. The results are interpreted as direct support for the error dependent model and suggestions are made for further research that could allow for identification of the specific scanning patterns suggested by the model. Author

N85-32766# Naval Postgraduate School, Monterey, Calif.
REVIEW OF THE PSYCHOLOGICAL ISSUES RELATING TO THE EFFECTIVENESS OF STRUCTURED PROGRAMMING M.S. Thesis
C. A. C. McGrath Dec. 1984 61 p
(AD-A154593) Avail: NTIS HC A04/MF A01 CSCL 05/10

Claims have been made that the failure of empirical studies to establish the efficacy of structured programming is due to the lack of psychological models of the programming task. Many authors have pointed out that psychological research on the human information processing model might provide substance to the claim that structured programming facilitates a programmer's understanding of program logic. This thesis reviews the results of current psychological research and shows that at this time it is not possible to build a satisfactory psychological model of the programmer and his/her task. In order to define the programming task more clearly, the issues involving the psychological model are identified. GRA

N85-32767# Naval Submarine Medical Research Lab., Groton, Conn.
THE EFFECT OF SET SIZE ON TIME TO RECALL COLOR CODED INFORMATION Interim Report
A. R. Jacobsen 27 Mar. 1985 21 p
(AD-A155013; NSMRL-1044) Avail: NTIS HC A02/MF A01 CSCL 05/10

The ability of observers to accurately identify up to twenty different colors presented on a CRT screen was studied. The effect of set size on time to recall color-coded information was also investigated via a paired-associates paradigm in which each color was paired with a letter of the alphabet. On test trials the time between color presentation and the subject's verbal response with the appropriate letter were recorded. All twenty subjects were able to identify accurately all twenty colors. For sets of two through seven colors, increases in set size resulted in significant rises in time to recall. Subsequent increases in set sizes, up to twenty, resulted in little or no further increase in time to recall. The time to recall was also found to vary significantly to the different colors. Although no statistical differences were found among 16 of the 20 colors, the other 4 yielded significantly slower times to recall. GRA

N85-32768# American Coll. Testing Program, Iowa city, Iowa. Test Development Div.
MODELS FOR MULTIDIMENSIONAL TESTS AND HIERARCHICALLY STRUCTURED TRAINING MATERIALS Final Report, 1 Sep. 1981 - 28 Feb. 1985
M. D. Reckase May 1985 32 p
(Contract N00014-81-K-0817; RR0-4204)
(AD-A155231; RR-85-1-ONR) Avail: NTIS HC A03/MF A01 CSCL 14/2

Work on item response theory was extended to include two areas that had not been extensively researched previously. They include models for test items that require more than one ability for a correct response and models for the interaction between modules of instruction that have a hierarchical relationship. For both of these types of models, estimation procedures were developed for model parameters and extensive work was done to determine the appropriate interpretation of the parameter values. This report is a summary of work performed on these modules over a three year period. GRA

N85-32769# Texas A&M Univ., College Station. Dept. of Management.
SYMBOLIC AND INTERACTIONAL PERSPECTIVES ON LEADERSHIP: AN INTEGRATIVE FRAMEWORK
R. W. Griffin, K. D. Skivington, and G. Moorhead May 1985 52 p
(Contract N00014-83-C-0025)
(AD-A155247; TR-ONR-DG-15) Avail: NTIS HC A04/MF A01 CSCL 05/10

This paper presents the development of a Symbolic Interactional Leadership model. The model integrates three emergent streams of thought, symbolic action, reciprocal interactions, and interactional psychology, into a fresh approach which offers considerable advancement over simple, unidirectional, bivariate, static models. Implications for future theory and research are discussed. This model, while not yet a fully articulated theory, does represent a significant advancement over simple unidirectional, bivariate, static models. While likely to be subject to further refinement and development, the SIL model, then, may provide a useful framework for organizing existing theory and serving as a blueprint for future research. GRA

N85-32770# Colorado Univ., Boulder. Inst. of Cognitive Science.
CONCEPTUALIZING IN ASSEMBLY TASKS Interim Technical Report, 1983 - 1985

P. Baggett and A. Ehrenfeucht Apr. 1985 37 p
(Contracts N00014-85-K-0060; N00014-78-C-0433; N00014-84-C-0112)
(AD-A155564; ICS-TR-139) Avail: NTIS HC A03/MF A01 CSCL 05/10

This paper gives a method to determine a person's hypothetical conceptualization of an object, its breakdown into subassemblies, and so on, from the person's sequence of requests for pieces given a group of conceptualizations, there is a typical one. The hypothesis that assembly instructions presenting a typical conceptualization will yield better structural and functional performance than those presenting a minority one, is supported experimentally. Conceptualizations are derived from objects built from memory (and incorrectly) by people who first studied typical or minority instructions. A new distance measure determines how far these conceptualizations are from those presented in the instructions. People studying typical instructions yield typical conceptualizations, and importantly, people studying minority instructions also yield typical conceptualizations, although they are significantly less typical than those from typical instructions. From the theoretical construct of conceptualizations and the methods of measuring them a practical principle, and a way to implement it, are found. The principle: When a single set of procedural instructions is designed, it should present the conceptualization that the majority of people to be instructed by it bring to the situation naturally.
Author (GRA)

N85-32771# Walter Reed Army Inst. of Research, Washington, D.C. Div. of Neuropsychiatry.
HUMAN PERFORMANCE IN CONTINUOUS/SUSTAINED OPERATIONS AND THE DEMANDS OF EXTENDED WORK/REST SCHEDULES. AN ANNOTATED BIBLIOGRAPHY
G. P. Krueger, L. Cardenales-Ortiz, and C. A. Loveless May 1985 211 p
(AD-A155619; WRAIR-BB-85-1) Avail: NTIS HC A10/MF A01 CSCL 05/10

The performance of workers under conditions of sustained or continuous work is a particularly important topic to the military services. Available research data on the topic are scattered throughout diverse printed sources, many of which are difficult to locate. This annotated bibliography lists 399 references containing research data, conceptual position papers and different methodological approaches to studying human performance in continuous/sustained operations and extended work/rest schedules. The time frame covered in the references is from 1940 to 1985. GRA

54 MAN/SYSTEM TECHNOLOGY AND LIFE SUPPORT

Includes human engineering; biotechnology; and space suits and protective clothing.

N85-32772*# National Aeronautics and Space Administration. Ames Research Center, Moffett Field, Calif.
LIVING ALOFT: HUMAN REQUIREMENTS FOR EXTENDED SPACEFLIGHT
Mary M. Connors, Albert A. Harrison (California Univ., Davis), and Faren R. Akins (Santa Clara Univ., Calif.) Washington 1985 426 p refs Original contains color illustrations
(NASA-SP-483; NAS 1.21:483) Avail: NTIS HC A19/MF A01; SOD HC $14.00 as 033-000-00949-6 CSCL 06K

Human psychological and social adjustment to space is investigated. Studies and experiences bearing on human performance capability, psychological well being, and social organization, as they relate to space, were identified and assessed, and suggestions offered as to where further research could ease the Earth/space transition. Special emphasis was given to the variables of crew size, crew diversity, and mission duration, all of which can be expected to increase in future spaceflight. By providing a conceptual framework in which issues and related information can be integrated, the hope is to aid in discovering those conditions under which future space travelers can flourish. Author

N85-32773# Army Natick Research and Development Command, Mass.
THE EFFECTS OF PROLONGED FEEDING MEAL, READY-TO-EAT (MRE) OPERATIONAL RATIONS Final Technical Report, period ending 1983
E. Hirsch, H. L. Meiselman, R. D. Popper, G. Smits, and B. Jezior Oct. 1984 374 p
(DA Proj. 1L1-62724-AH-99)
(AD-A154763; NATICK/TR-85/035) Avail: NTIS HC A16/MF A01 CSCL 06/8

The US Army Natick Research and Development Center conducted a study to evaluate the effects of prolonged feeding Meal, Ready-to-Eat (MRE) operational rations on troop effectiveness. Two combat support companies, from the 25th Infantry Division, participated in this 34 day study while they were engaged in a field training exercise at the Pohakuloa Training Area on the Island of Hawaii. One company subsisted solely on MRE rations. The other company was fed an A ration breakfast, an MRE lunch, and an A ration dinner. The MRE food items were highly rated by the troops but these foods were not consumed in sufficient quantity. Average daily caloric intake was 2,189 calories per day for the MRE group and 2,950 calories per day for the control group. The major consequences of the low food intakes were body weight loss and some vitamin and mineral intakes that were below recommended levels. The MRE group lost 8.1 pounds and the control group lost 4.6 pounds. Both groups had intakes of niacin and magnesium that were below recommended levels. The MRE group also consumed less riboflavin, calcium, and iron than recommended. The other measures that were taken to evaluate the consequences of prolonged feeding the MRE did not reveal any major differences between the two companies. Questionairres on physical symptoms, mood morale and perceptions of leadership showed only minor differences between the two companies. The performance of the two companies did not differ on a test battery of cognitive and psychomotor tasks. GRA

N85-32774# Southwest Research Inst., San Antonio, Tex. Div. of Engineering and Materials Science.
A CREW EXPOSURE STUDY, PHASE 2. VOLUME 2. AT SEA, PART A Final Report, 15 May 1982 - 12 Apr. 1985
W. J. Astleford, J. C. Buckingham, H. L. Kaplan, R. J. Magott, and J. P. Riegel Apr. 1985 97 p
(Contract DTCG23-80-C-20015)
(AD-A155233; USCG-D-11-85-Vol-2-Pt-A) Avail: NTIS HC A05/MF A01 CSCL 06/10

The objective of this effort was to implement the Phase 1 test plan for characterizing occupational exposures of crew members on bulk liquid tankers to chemical substances, primarily cargo vapors. Additional chemical substances included nuisance dust, asbestos fibers, oil mist and silica dust. This report documents the measurement and monitoring data that were collected on six at-sea voyages that involved tankers carrying Subchapter O, Subchapter D and unregulated liquid products. The interpretation of these occupational exposures was based on a conservative method that makes use of the medical monitoring response level concept and current values of the ACGIH TLVs. This method was developed because the work routine that forms the basis for TLVs is not generally applicable to marine operations. Noise dosimetry was performed on two voyages in order to characterize the environment in an Engine Room and in the Deck Department of a state-of-the-art product tanker. This study concluded that the potential for unacceptable inhalation exposures is greatest during open tank gauging and entry into product tanks. Volume 2, Part A represents the body of the final report. The detailed voyage reports are contained in Part B. GRA

N85-32775# Naval Air Development Center, Warminster, Pa. Aircraft and Crew Systems Technology Directorate.
ANALYSIS OF THE TRANSIENT RESPONSE OF TEMPORAL ARTERY BLOOD FLOW DATA RELATIVE TO VARIOUS ANTI-G

SUIT PRESSURE SCHEDULES Final Report, 1983 - 1984
R. J. Crosbie 16 Oct. 1984 32 p
(AD-A155242; NADC-84143-60) Avail: NTIS HC A03/MF A01 CSCL 06/16

Recent incidences of G-induced loss of consciousness (LOC) by aircrew flying high performance aircraft have reestablished the operational need for increased G-protection for aircrewmen and have prompted a renewed interest in the development of new and improved G-protective equipment and techniques. Of current concern is the rapidity with which these high performance aircraft can achieve high G-levels. This high rate of G-onset creates a period during which the physiological response of the aircrewman and the protective action of his anti-G suit lab behind the G profile, and during which visual symptoms which normally precede LOC and serve to warn the pilot, do not occur. A method is presented for objectively measuring the relative effectiveness of various G protective equipment or techniques by comparing the quantitative response of a subject's mean Doppler flow velocity signal to a series of modest G profiles when using each protective system in turn. The method is applied to evaluate two configurations of the Navy's new servo controlled anti-G valve in comparison with the standard ALAR valve during exposure to G profiles having various rates of G onset. GRA

N85-32776# Air Force Human Resources Lab., Brooks AFB, Tex.
ADVANCED SIMULATOR FOR PILOT TRAINING AND HELMET-MOUNTED VISUAL DISPLAY CONFIGURATION COMPARISONS Interim Report, Jan. 1983 - Jan. 1984
R. R. Woodruff, D. C. Hubbard, and A. Shaw May 1985 24 p
(AF Proj. 1123)
(AD-A155326; AFHRL-TR-84-65) Avail: NTIS HC A02/MF A01 CSCL 05/9

This effort compared five flight simulator visual display configurations using a simulated aerial refueling task. The configurations were: (1) a helmet-mounted stereoscopic display with a 40 deg field of view (FOV), (2) a helmet-mounted biocular display with a 40 deg FOV, (3) the full Advanced Simulator for Pilot Training (ASPT) 300 FOV, (4) the ASPT visual display masked to present a 40 deg FOV, and (5) lead lanthanum zirconate titanate (PLZT) goggles (stereoscopic) using one ASPT window. Performance of pilots using the different display configurations was observed. The results indicated that horizontal position was maintained better with the wide-FOV ASPT display and that boom movement was minimized with the stereoscopic display. GRA

55 PLANETARY BIOLOGY

Includes exobiology; and extraterrestrial life.

N85-32777*# National Aeronautics and Space Administration. Ames Research Center, Moffett Field, Calif.
SEARCH FOR THE UNIVERSAL ANCESTORS
H. Hartman, ed. (MIT), J. G. Lawless, ed., and P. Morrison, ed. (MIT) Jul. 1985 145 p refs
(NASA-SP-477; A-8646; NAS 1.21:477) Avail: NTIS MF A01; SOD HC $3.75 as 033-000-009-3-4 CSCL 06C

By its nature, the study of the origins of life is multidisciplinary, requiring contributions from astronomers, biologists, chemists, geologists, physicists, and many others. Partial answers are provided to many questions about organic chemical evolution and the origin of life. It is observed that the gaps in our knowledge concerning the steps from the nonliving to the living are numerous. Among these gaps are: (1) a solar system formation with its accumulation of raw materials; (2) the synthesis of the life forming monomers, such as the amino acids, nucleotides, and lipids; (3) the condensation of these monomers into useful polymers, such as proteins and nucleic acids; (4) the sequestering of these materials into droplets of proteinoid or membrane-like structures; and (5) the development of a chemical memory (the genetic code) to pass on to the progeny the information acquired. Author

59 MATHEMATICAL AND COMPUTER SCIENCES (GENERAL)

N85-32977# Joint Publications Research Service, Arlington, Va.
NECESSARY AND SUFFICIENT CONDITIONS FOR SINGLE-EXTREMUM AND CONVEX PROBLEMS OF MATHEMATICAL PROGRAMMING Abstract Only
I. I. Gasanov and A. D. Rikun *In its* USSR Rept.: Phys. and Math. (JPRS-UPM-85-004) 17 Jun. 1985 p 96 Transl. into ENGLISH from Dokl. Akad. Nauk SSSR (Moscow), v. 278, no. 4, Oct. 1984 p 786-789 (For primary document see N85-32860 21-70)
Avail: NTIS HC A06/MF A01

N85-32978# Joint Publications Research Service, Arlington, Va.
ON THE PROBLEM OF LINEAR PROGRAMMING WITH APPROXIMATE DATA Abstract Only
G. M. Agayan, A. A. Ryutin, and A. N. Tikhonov *In its* USSR Rept.: Phys. and Math. (JPRS-UPM-85-005) Transl. into ENGLISH from Zh. Vychsl. Mat. i Mat. Fiz. (Moscow), v. 24, no. 9, Sep. 1984 p 1303-1311 (For primary document see N85-32860 21-70)
Avail: NTIS HC A06/MF A01

60 COMPUTER OPERATIONS AND HARDWARE

Includes computer graphics and data processing.
For components see *33 Electronics and Electrical Engineering.*

N85-32778# Massachusetts Inst. of Tech., Cambridge. Lab. for Computer Science.
TIGHT BOUNDS ON THE COMPLEXITY OF PARALLEL SORTING Interim Report
T. Leighton Mar. 1985 28 p
(Contract N00014-80-C-0622)
(AD-A154726; MIT/LCS/TM-272) Avail: NTIS HC A03/MF A01 CSCL 09/2

In this paper, we prove tight upper and lower bounds on the number of processors, information transfer, wire area and time needed to sort N-numbers in a bounded-degree fixed-connection network. GRA

N85-32779# Massachusetts Inst. of Tech., Cambridge. Lab. for Computer Science.
RESOURCE MANAGEMENT FOR THE TAGGED TOKEN DATAFLOW ARCHITECTURE
D. E. Culler Jan. 1985 116 p
(Contract N00014-75-C-0661)
(AD-A154773; MIT/LCS/TR-332) Avail: NTIS HC A06/MF A01 CSCL 09/2

The Taged Token Dataflow Architecture is multiprocessor based on the U-interpreter model of dataflow computation. It captures the essential execution mechanism of the U-interpreter precisely; operations are enabled for execution by the availability of operand data. However, computational resources in the model and the machine are viewed quite differently. This thesis addresses four major resource management issues essential to bridge the gap between the U-interpreter and the Tagged Token Dataflow Architecture: termination detection; token store overflow; Iteration identifier overflow; and program deadlock. This thesis offers a way to overcome the differences between the model and the machine through a concerted approach to resource management, involving the compiler and the run-time system. Program graphs based on the U-interpreter model is transformed into equivalent graphs which are more suitable for execution on the Tagged Token Dataflow Architecture, These graphs have predictable resource requirements and include special operations to engage the run-time

system. The run-time system has two responsibilities: dynamic allocation/deallocation of resources, and dynamic control of program execution. The work presented here is motivated by the need to however, it serves a more general goal as well. Resource management is a fundamental aspect of any dataflow machine, and the issues raised in this thesis should have a prominent role in the design and evaluation of dataflow architectures in general.
GRA

N85-32780# Naval Postgraduate School, Monterey, Calif.
REAL-TIME CONTOUR SURFACE DISPLAY GENERATION
M. J. Zyda Sep. 1984 43 p
(RR0-0001)
(AD-A155232; NPS52-84-013) Avail: NTIS HC A03/MF A01 CSCL 09/2

We present in this study the architectural specification and feasibility determination for a real-time contour display generator. We begin by examining a recently reported, highly decomposable algorithm for contour surface display generation. We establish a piece of the total algorithm as the algorithm component. The algorithm component is that part of the algorithm that can be executed in parallel, independently from the computations performed on any other algorithm subpart. We propose an architecture for the algorithm component, and model that architecture in order to determine the real-time capability of the algorithm. We then model the larger system of multiple algorithm component processors. This modeling effort is performed with respect to a particular application requiring real-time contour surface display generation. A VSLI feasibility computation is then performed on the proposed architecture. The study ends with a look at the impact of real-time contour surface display generation on the design of the graphics display system.
GRA

N85-32781# Joint Publications Research Service, Arlington, Va.
EAST EUROPE REPORT: SCIENCE AND TECHNOLOGY. SELECTIONS ON CSSR COMPUTER TECHNOLOGY
31 May 1984 80 p refs Transl. into ENGLISH from various East European articles
(JPRS-ESA-84-017) Avail: NTIS HC A05/MF A01

Various topics relative to Czechoslovakian electronics industries are discussed. Computers, CMOS, robots and manipulators, television receivers and electrical measurement are covered. For individual titles, see N85-32782 through N85-32788.

N85-32782# Joint Publications Research Service, Arlington, Va.
SELECTIONS ON CSSR COMPUTER TECHNOLOGY
Ladislav Suran and Rostislav Wasyluk *In its* East Europe Rept.: Sci. and Technol. Selections on CSSR JPRS-ESA-84-017 31 May 1984 p 1-4 Transl. into ENGLISH from Sdelovaci Technika (Prague), no. 1, 1983 p 18-19 (For primary document see N85-32781 21-60)
Avail: NTIS HC A05/MF01

In view of the advantages offered by CMOS technology, low power input and a wide range of operational voltages, demands for its introduction in Czechoslovakia appeared in the latter half of the 1970's. Key customers for CMOS circuits are telecommunication technology enterprises for automated electronic private branch exchanges and telephones, enterprises manufacturing communications technology for portable radio stations, and chromometrological enterprises for the production of electronic alarm clocks. Thus, by the end of 1970 the microelectronics sector of TESLA VUST (Research Institute of Communications Technology of the TESLA enterprise) started developing CMOS circuits with low and medium integration. Since 1980 this development has continued as part of state task AZ 09-119-102 in cooperation with the concern enterprise TESLA Piestany. Circuits of low and medium integration of the 4000 series were supplemented by circuits of high integration on the order of up to 10,000 elements per chip or chip area sizes in excess of 20 square millimeters. An outline of the circuits being developed and produced is given. Key properties of CMOS circuits of the 4000 series are listed.
R.J.F.

N85-32783# Joint Publications Research Service, Arlington, Va.
THE 8080 EMULATOR
Frantisek Michalek and Tomas Kolinek *In its* East Europe Rept.: Sci. and Technol. Selections on CSSR JPRS-ESA-84-017 31 May 1984 p 4-8 Transl. into ENGLISH from Sdelovaci Technika (Prague), no. 3, 1983 p 82 (For primary document see N85-32781 21-60)
Avail: NTIS HC A05/MF A01

Despite the various advantages offered by microprocessors, such as an efficient set of instructions, low consumption of energy and low price, there remain areas where microprocessors cannot find application for the time being. A microprocessor with extensive software is the MOS 8080 microprocessor. However, MOS microprocessors are slow and this led to development of the 8080 emulator which considerably speeds up the system's operation without calling for expensive readjustment of software. Microcomputers of the third generation already have a higher transmissivity than the mentioned emulator. The 8080 emulator fills in the gap between the usual fast bipolar processors and MOS microprocessors. Even though bipolar processors are adequately fast, they call for requisite development of an assembler and additional software. On the other hand, MOS microprocessors offer assemblers, higher programming languages and developmental systems, but are slow. The 8080 emulator is actually an 8080 microprocessor which operates at a higher speed. In addition to time loops, the 8080 software can be used directly with the 8080 emulator.
R.J.F.

N85-32784# Joint Publications Research Service, Arlington, Va.
R, L, C, G MEASUREMENT
Karel Kuegler *In its* East Europe Rept.: Sci. and Technol. Selection on CSSR JPRS-ESA-84-017 31 May 1984 p 8-16 Transl. into ENGLISH from Sdelovaci Technika (Prague), no. 5, 1983 p 161-163 (For primary document see N85-32781 21-60)
Avail: NTIS HC A05/MF A01

New methods for measuring voltages and currents throughout the range of used impedances are discussed. Dividing transformers, analog to digital convectors, voltmeters, and controllers are discussed.
R.J.F.

N85-32785# Joint Publications Research Service, Arlington, Va.
QUALITY ANALYSIS
Pavel Kyjovsky *In its* East Europe Rept.: Sci. and Technol. Selections on CSSR JPRS-ESA-84-017 31 May 1984 p 17-20 Transl. into ENGLISH from Sdelovaci Technika (Prague), no. 11, 1983 p 401-402 (For primary document see N85-32781 21-60)
Avail: NTIS HC A05/MF A01

Quality analysis and quality engineering are one of the means for intensifying the national economy that have an impact not only on the sphere of products, but also on the management and evaluation of entire production organisms in defining their economic and social utility. Quality analysis as such is a system oriented complex of methods, the ultimate objective of which is searching for and proposing improved or even basically new solutions relevant to the function of the analyzed object in order to improve its effectiveness. Examples of improvements in such products as switches, soldering apparatus, and transformers are discussed.
R.J.F.

N85-32786# Joint Publications Research Service, Arlington, Va. **c37**
ROBOTS, MANIPULATORS
J. Grecner *In its* East Europe Rept.: Sci. and Technol. Selections on CSSR JPRS-ESA-84-017 31 May 1984 p 25-28 Transl. into ENGLISH from Sdelovaci Technika (Prague), no. 12, 1983 p 441-442 (For primary document see N85-32781 21-60)
Avail: NTIS HC A05/MF A01

A plan for technological development, a new 16 bit microcomputer for an industrial robot and manipulator control system is discussed. Relatively high technical demands on the quality of the control system, mainly with regard to speed and reliability, were made. It was decided to adopt a modular concept design permitting a high degree of variability in the composition of the control system while meeting the basic prerequisite for develop-

ing effective international cooperation and specialization among relevant organizations in interested CEMA countries. The task solvers have recently started generating applicational software, which is being developed with adequate time lead. Another part of the task will be the development of a microprogram controlled connecting unit for connecting several sensor type subsystems and sensors typical of the new generation of adaptive industrial robots and manipulators. R.J.F.

N85-32787# Joint Publications Research Service, Arlington, Va.
DIGITAL INTEGRATED CIRCUITS **c33**
Pavel Polasek and Josef Halamik *In its* East Europe Rept.: Sci. and Technol. Selections on CSSR JPRS-ESA-84-017 31 May 1984 p 28-46 refs Transl. into ENGLISH from Sdelovaci Technika (Prague), no. 12, 1983 p 443-448 (For primary document see N85-32781 21-60)
Avail: NTIS HC A05/MF A01

The term semicustom designed integrated circuits denotes integrated circuits of an all purpose character in which the production of chips is completed by using one to three custom design stencil type exposure masks. This involves in most cases interconnecting masks that are used to devise the circuit function desired by the customer. Silicon plates with an all purpose gate matrix are produced up to the interconnection level and can be kept at this phase in storage, after which a customer's specific demands can be met very expediently. All purpose logic fields containing 200 logic gates on a chip and an all purpose chip to be expanded to 1,000 logic gates are discussed. The technology facilitates the devising of fast gates with a delay of approximately 5 ns and power dissipation of 1 mW. In assembly it will be possible to make use of the entire assortment of the currently used casings with 16, 18, 20, 24, 28 and 40 outlets. In addition to the development of the mentioned technology, a general methodology for design of the mentioned gate fields is currently under way. R.J.F.

N85-32788# Joint Publications Research Service, Arlington, Va.
GDR SEMICONDUCTOR PARTS **c76**
Jaroslav Tolasz *In its* East Europe Rept.: Sci. and Technol. Selections on CSS JPRS-ESA-84-017 31 May 1984 p 47-78 Transl. into ENGLISH from Sdelovaci Technika (Prague), no. 2, Feb. 1983 p 59 (For primary document see N85-32781 21-60)
Avail: NTIS HC A05/MF A01

In 1982 the Microelectronics Combine introduced on the market new parts in an unprecendented volume, mainly from the area of bipolar and unipolar integrated circuits, transistors, diodes, optoelectronic components, basic materials for the production of semiconductor components, X-ray tubes and technological systems. These new components are described. R.J.F.

61 COMPUTER PROGRAMMING AND SOFTWARE

Includes computer programs, routines, and algorithms.

N85-32789*# Intergraph Corp., Huntsville, Ala. Federal Systems Div.
ANALYSIS OF SPACECRAFT DATA Final Technical Report
1 Jun. 1984 8 p
(Contract NAS8-34005)
(NASA-CR-171587; NAS 1.26:171587; F85-227; IC/FSD-85-032)
Avail: NTIS HC A02/MF A01 CSCL 09B

A software program for the production and analysis of data from the Dynamics Explorer-A (DE-A) satellite was maintained and modified and new software initiated. A capability was developed to process DE-A plasma-wave instrument mission analysis files on the Tektronic 4027 color CRT, for which two programs were written. The algorithm for the calibration lookup table for the plasma-wave instrument data was modified and verified, and a production program to generate color FR-80 spectrograms was written. F.M.R.

N85-32790*# Intergraph Corp., Huntsville, Ala. Federal Systems Div.
ANALYSIS OF SPACECRAFT DATA Final Technical Report
6 Mar. 1985 17 p
(Contract NAS8-36038)
(NASA-CR-171597; NAS 1.26:171597; F85-229; IC/FSD-85-033)
Avail: NTIS HC A02/MF A01 CSCL 09B

Support was provided for the maintenance and modifications of software for the production and detailed analysis of data from the DE-A spacecraft and new software developed for this end. Software for the analysis of the data from the Spacelab Experimental Particle Accelerator (SEPAC) was also developed. Author

N85-32791*# Research Triangle Inst., Research Triangle Park, N.C. Center for Digital Systems Research.
CARE 3 USER FRIENDLY INTERFACE USER'S GUIDE
C. L. Conrad, W. F. Ingogly, S. E. McBride, and J. L. Pierce May 1985 73 p
(Contract NAS1-16489)
(NASA-CR-172608; NAS 1.26:172608) Avail: NTIS HC A04/MF A01 CSCL 09B

A user's guide to the use of the CARE 3 menu program is provided, which was designed to provide an interactive user friendly interface to the CARE III computer program. The CARE 3 menu program executes on the VAX 700 series computers under the VMS operating system. The result of a session with the CARE 3 menu program is the creation of an input file for execution by CARE 3. Author

N85-32792*# Vanderbilt Univ., Nashville, Tenn. Center for Intelligent Systems.
RESEARCH ON AN EXPERT SYSTEM FOR DATABASE OPERATION OF SIMULATION-EMULATION MATH MODELS. VOLUME 1, PHASE 1: RESULTS
K. Kawamura, G. O. Beale, J. D. Schaffer, B.-J. Hsieh, S. Padalkar, and J. J. Rodriguez-Moscoso 9 Aug. 1985 82 p refs
(Contract NAS8-36285)
(NASA-CR-176087; NAS 1.26:176087) Avail: NTIS HC A05/MF A01 CSCL 09B

The results of the first phase of Research on an Expert System for Database Operation of Simulation/Emulation Math Models, is described. Techniques from artificial intelligence (AI) were to bear on task domains of interest to NASA Marshall Space Flight Center. One such domain is simulation of spacecraft attitude control systems. Two related software systems were developed to and delivered to NASA. One was a generic simulation model for spacecraft attitude control, written in FORTRAN. The second was an expert system which understands the usage of a class of spacecraft attitude control simulation software and can assist the user in running the software. This NASA Expert Simulation System (NESS), written in LISP, contains general knowledge about digital simulation, specific knowledge about the simulation software, and self knowledge. Author

N85-32793*# Vanderbilt Univ., Nashville, Tenn. Center for Intelligent Systems.
RESEARCH ON AN EXPERT SYSTEM FOR DATABASE OPERATION OF SIMULATION-EMULATION MATH MODELS. VOLUME 2, PHASE 1: RESULTS
K. Kawamura, G. O. Beale, J. D. Schaffer, B.-J. Hsieh, S. Padalkar, and J. J. Rodriguez-Moscoso 9 Aug. 1985 178 p
(Contract NAS8-36285)
(NASA-CR-176088; NAS 1.26:176088) Avail: NTIS HC A08/MF A01 CSCL 09B

A reference manual is provided for NESS, a simulation expert system. This manual gives user information regarding starting and operating NASA expert simulation system (NESS). This expert system provides an intelligent interface to a generic simulation program for spacecraft attitude control problems. A menu of the functions the system can perform is provided. Control repeated returns to this menu after executing each user request. Author

N85-32794*# National Aeronautics and Space Administration. Dryden (Hugh L.) Flight Research Center, Edwards, Calif.
DESIGN OF AN EXPERT-SYSTEM FLIGHT STATUS MONITOR
Victoria A. Regenie and Eugene L. Duke Aug. 1985 11 p
Presented at the AIAA Guidance and Control Conf., Snowmass, Colo., 19-21 Aug. 1985
(NASA-TM-86739; H-1300; NAS 1.15:86739; AIAA-85-1980) Avail: NTIS HC A02/MF A01 CSCL 09B

The modern advanced avionics in new high-performance aircraft strains the capability of current technology to safely monitor these systems for flight test prior to their generalized use. New techniques are needed to improve the ability of systems engineers to understand and analyze complex systems in the limited time available during crucial periods of the flight test. The Dryden Flight Research Facility of NASA's Ames Research Center is involved in the design and implementation of an expert system to provide expertise and knowledge to aid the flight systems engineer. The need for new techniques in monitoring flight systems and the conceptual design of an expert-system flight status monitor is discussed. The status of the current project and its goals are described. Author

N85-32795*# National Aeronautics and Space Administration. Ames Research Center, Moffett Field, Calif.
THE NAS KERNEL BENCHMARK PROGRAM
David H. Bailey and John T. Barton Aug. 1985 17 p refs
(NASA-TM-86711; Rept-85195; NAS 1.15:86711) Avail: NTIS HC A02/MF A01 CSCL 09B

A collection of benchmark test kernels that measure supercomputer performance has been developed for the use of the NAS (Numerical Aerodynamic Simulation) program at the NASA Ames Research Center. This benchmark program is described in detail and the specific ground rules are given for running the program as a performance test. Author

N85-32796*# McDonnell-Douglas Technical Services Co., Inc., Huntsville, Ala.
SPACE STATION ECLS INTEGRATION ANALYSIS: SIMPLIFIED GENERAL CLUSTER SYSTEMS MODEL, ECLS SYSTEM ASSESSMENT PROGRAM ENHANCEMENTS
R. E. Ferguson Aug. 1985 92 p refs
(Contract NAS8-36407)
(NASA-CR-176089; NAS 1.26:176089; MDC-W5040) Avail: NTIS HC A05/MF A01 CSCL 09B

The data base verification of the ECLS Systems Assessment Program (ESAP) was documented and changes made to enhance the flexibility of the water recovery subsystem simulations are given. All changes which were made to the data base values are described and the software enhancements performed. The refined model documented herein constitutes the submittal of the General Cluster Systems Model. A source listing of the current version of ESAP is provided in Appendix A. Author

N85-32797# Naval Postgraduate School, Monterey, Calif.
DEVELOPMENT OF COMPUTER PROGRAMS USING THE METHOD OF IMAGES TO PREDICT THE SOUND FIELD IN A WEDGE OVERLAYING A FAST FLUID AND COMPARISON WITH LABORATORY EXPERIMENTS M.S. Thesis
P. K. LeSesne Dec. 1984 66 p
(AD-A154580) Avail: NTIS HC A04/MF A01 CSCL 09/2

Two computer programs using the method of images to determine the pressure amplitude and phase distribution in a wedge shaped medium overlaying a fast fluid bottom were studied. The WEDGE program used a source at infinity and was constrained to upslope, on axis predictions, while CROSS SLOPE, using a source at finite distance, made predictions anywhere within the medium. Comparison of the two programs suggest that an infinite source is not approached until the source exceeds 600 dump distances from the apex. The CROSS SLOPE prediction of pressure amplitude were in agreement with experimental data obtained in the upslope direction, and with sound field similar to that described by the theory of Buckingham, but of much richer variety. GRA

N85-32798# Softech, Inc., Waltham, Mass.
AdA (TRADEMARK) TRAINING CURRICULUM. ADVANCED AdA TOPICS L305 TEACHER'S GUIDE EXERCISES
Jul. 1984 82 p
(Contract DAAB07-83-C-K514)
(AD-A154621) Avail: NTIS HC A05/MF A01 CSCL 09/2

There are far more exercises in this booklet than can be solved during one presentation of L305. The instructors should select specific exercises for the class based on the class's mathematical background and programming ability, the pace of the course, and the degree of success solving previous exercises. The purpose of this Guide is to help instructors make this selection. Each exercise is designed for a certain point in the course. An accompanying diagram shows the point at which each exercise can be assigned. In most cases the exercise makes use of information presented as part of the indicated topic, and should be assigned after that topic has been presented. Because L305 emphasizes data abstraction and the construction of software out of components, solutions to most of the exercises are packages rather than subprograms. Thus, they are not executable by themselves. GRA

N85-32799# Massachusetts Inst. of Tech., Cambridge. Lab. for Computer Science.
CONSENSUS IN THE PRESENCE OF PARTIAL SYNCHRONY (PRELIMINARY VERSION) Interim Research Report
C. Dwork, N. Lynch, and L. Stockmeyer Oct. 1984 33 p
(Contract N00014-83-K-0125)
(AD-A154705; MIT/LCS/TM-270) Avail: NTIS HC A03/MF A01 CSCL 09/2

The problem of reaching agreement among separated processors is of fundamental importance to distributed computing, and has provided a rich set of interesting mathematical problems. Previous work has shown that if communication and processing are synchronous there exist consensus protocols resilient to large numbers of failures, the exact number depending on the particular type of faulty behavior to be tolerated. In contrast it has been shown that if either communication or processing are asynchronous, then there is no consensus protocol resilient to even one failure of the weakest type. This paper defines and studies the consensus problem in practically motivated situations which lie between the completely synchronous and the completely asynchronous cases. GRA

N85-32800# Advanced Information and Decision Systems, Mountain View, Calif.
THE DOCUMENTATION ASSISTANT: AN INTELLIGENT SYSTEM FOR DOCUMENTATION Final Report, 1 Jul. - 1 Dec. 1984
J. S. Dean, B. P. McCune, and S. G. Rosenbaum 22 Apr. 1985 68 p
(Contract N00014-83-C-0444)
(AD-A154709; AI/DS-TR-1047-020-1) Avail: NTIS HC A04/MF A01 CSCL 09/2

The purpose of this document is to describe a semi-automated system for the documentation of computer software; this system is called the documentation assistant (DA). To motivate this system, a general discussion of documentation issues and problems is interwoven with descriptions of how the DA would address many of these topics. A feasibility assessment and plan for this approach is presented. The documentation assistant project is a research effort at advanced information & decision systems. The purpose of this effort is to study advanced techniques which address one of the most pressing problems during the software life cycle: the process of documentation. Currently, the DA exists on paper only; one goal of the research effort is to develop a prototype version, which would be incorporated in the intelligent program editor (another research prototype being developed at AI&DS under ONR sponsorship). GRA

N85-32801# Massachusetts Inst. of Tech., Cambridge. Lab. for Computing Science.
SOFTWARE FOR INTERACTIVE ON-LINE CONFERENCES

Interim Report
S. K. Sarin and I. Greif Jul. 1984 35 p
(Contract N00014-83-K-0125)
(AD-A154742; MIT/LCS/TM-264) Avail: NTIS HC A03/MF A01 CSCL 09/2

A layered architecture for the implementation of real-time conferences is presented. In a real-time conference a group of users, each at his or her own workstation, share identical views of on-line application information. The users cooperate in a problem solving task by interactively modifying or editing the shared view or the underlying information, and can use a voice communication channel for discussion and negotiation. The lower layer in this architecture, named Ensemble, supports the sharing of arbitrary application-defined objects among the participants of a conference, these can be used in constructing real-time conferencing systems for many different applications. An example is presented of how the Ensemble functions can be used to implement a shared bitmap with independent participant cursors. The relation between this layered architecture and the ISO Open Systems Interconnection reference model is discussed. In particular, it is argued that Ensemble represents a plausible first step toward a Session-layer protocol development. Author (GRA)

N85-32802# Naval Postgraduate School, Monterey, Calif.
AN AUTOMATED QUALITY ASSURANCE SURVEILLANCE PLAN FOR ADP (AUTOMATED DATA PROCESSING) OPERATIONS UNDER THE NAVY'S COMMERCIAL ACTIVITIES PROGRAM M.S. Thesis
H. E. Morton Dec. 1984 177 p
(AD-A154767) Avail: NTIS HC A09/MF A01 CSCL 09/2

This thesis documents the process whereby a Navy Regional Data Automation Center implements an automated quality assurance program to ensure proper performance of a commercial service contract by a civilian contractor. The feasibility of implementing MIL-STD-105D on microcomputers is examined, along with the software tools necessary for that implementation. Finally, a system design and programs to effect such an implementation are proposed. GRA

N85-32803# Naval Postgraduate School, Monterey, Calif.
THE DESIGN AND IMPLEMENTATION OF AN OBJECT-ORIENTED, PRODUCTION-RULE INTERPRETER M.S. Thesis
H. M. McArthur Dec. 1984 212 p
(AD-A154769) Avail: NTIS HC A10/MF A01 CSCL 09/2

This thesis describes the design and implementation of two prototype interpreters for Omega, an object oriented, production rule programming language. The first implementation is a throw away prototype written in LISP; the second implementation is a more complete version written in C. The Omega language features two major components: a set of production rules executed through pattern-directed invocation, and a relational database of values and objects. We develop a simple system of rule selection and a list implementation of relations. The system's performance is evaluated in comparison with LISP and Prolog interpreters. The author concludes with a discussion of his experience in developing example applications, and recommend extensions to the language based on this experience. GRA

N85-32804# Colorado School of Mines, Golden. Center for Wave Phenomena.
QUALITATIVE ANALYSIS OF SIGN-BIT PROCESSING
I. Leroux 30 Apr. 1985 115 p
(Contract N00014-84-K-0049)
(AD-A154776; CWP-028) Avail: NTIS HC A06/MF A01 CSCL 09/2

This paper discusses the sign-bit processing in the Born inversion method. It shows on basic examples that in the absence of relative true amplitude, the Born inversion algorithm written by Bleistein-Cohen still provides an image of the subsurface. It implies that all the essential information provided by a wave train is contained in the phase only. Sign-bit digital recording means that only the sign of the true amplitude signal is recorded with one bit. In conventional seismic recording, 16 to 32 binary bits per sample point are recorded. The economic advantages of sign-bit acquisition are immediately obvious. Complete amplitude recovery comparable to full gain recording can be achieved by correct application of sign-bit techniques. Sign-bit data recording has interested the seismic exploration industry for many years because it provides an easy way to greatly decrease the number of channels in a data acquisition system. Sign-bit digital recording means that only the sign of the analog signal is recorded with one bit. In conventional seismic recording 16 to 32 binary bits are necessary for each sample point. So the economic advantages of sign-bit recording are obvious. It is necessary to check that the results obtained from usual seismic processings are valid and still provide good information. GRA

N85-32805# Softech, Inc., Fairborn, Ohio.
HLLM SOFTWARE SUPPORT Final Report, May 1980 - Nov. 1984
M. Moore Apr. 1985 330 p
(Contract F33615-79-C-1936)
(AD-A154828; AFWAL-TR-85-1009) Avail: NTIS HC A15/MF A01 CSCL 09/2

The purpose of this document is to provide a comprehensive assessment of the Instruction Set Architecture (ISA) designed to support the development of the advanced avionic computer referred to as a High Level Language Machine (HLLM). The assessment is with respect to the JOVIAL (J73) language as described by MIL-STD-1589B. The assessment is divided into four parts, each of which evaluates the ISA from a different perspective. Section 2 evaluates the ISA in terms of how the user programming language JOVIAL (J73) maps onto the ISA. Section 3 discusses just how well suited JOVIAL (J73) is for the ISA and the impact of the current ISA definition on a preprocessor developed to translate JOVIAL (J73) into the ISA features. Section 4 suggests what changes to the ISA would result in a more suitable architecture for JOVIAL (J73). GRA

N85-32806# Wisconsin Univ., Madison. Mathematics Research Center.
SIGMA - A STOCHASTIC-INTEGRATION GLOBAL MINIMIZATION ALGORITHM Summary Report
F. Aluffi-Pentini, V. Parisi, and F. Zirilli Mar. 1985 28 p
(Contracts DAJA37-81-C-0740; DAAG29-80-C-0041)
(AD-A154878; MRC-TSR-2806) Avail: NTIS HC A03/MF A01 CSCL 09/2

The paper gives a detailed description of a FORTRAN IV program based on a new method of finding a global (or absolute) minimizer of a function of N real variables, i.e., the point x in N-dimensional space (or possibly one of the points) such that not only the function increases if one moves away from x in any direction, (local or relative minimum), but also such that no other point exists where f has a lower value. The method, which was first proposed by the present authors in a paper which is to appear in the Journal of Optimization Theory and Applications, is based on ideas from statistical mechanics, and looks for a point of global minimum by following the solution trajectories of a stochastic differential equation representing the motion of particle (in N-space) under the action of a potential field and of a random perturbing force. The tests were performed by running the program on an extensive set of carefully selected tests were performed by running the program on an extensive set of carefully selected test problems of varying difficulty, and the performance was remarkably successful, even on very hard problems (e.g., problems with a single point of global minimum and up to about 10 to the 10th power points of non-global minimum). GRA

N85-32807# Mitre Corp., Bedford, Mass.
DESIGN GUIDELINES FOR USER-SYSTEM INTERFACE SOFTWARE Final Report
S. L. Smith and J. N. Mosier Sep. 1984 458 p
(Contract F19628-84-C-0001)
(AD-A154907; MTR-9420; ESD-TR-84-190) Avail: NTIS HC A20/MF A01 CSCL 09/2

In computer-based information systems, special attention

must be given to design of the user-system interface (USI) software. This report revises and expands previously published material, and proposes a more comprehensive set of guidelines for design of USI software in six functional areas: data entry; data display; sequence control; user guidance; data transmission; and data protection. GRA

N85-32808# Naval Postgraduate School, Monterey, Calif.
THE FORMAL SPECIFICATION OF AN ABSTRACT MACHINE: DESIGN AND IMPLEMENTATION M.S. Thesis
J. M. Yurchak Dec. 1984 152 p
(AD-A155167) Avail: NTIS HC A08/MF A01 CSCL 09/2

The high cost of porting software from one machine to another stems from the ad hoc way in which the programmer's problem solving abstraction interacts with the machine's physical resource abstraction. If this interaction could be formalized, the well known semantic gap would at least be better understood, if not narrowed significantly. This thesis applies techniques borrowed from contemporary research in abstract data type specification to design, specify and implement the physical resources of an abstract machine called AM. Author (GRA)

N85-32809# Performance Measurement Associates, Inc., Vienna, Va.
THE EFFECT OF COMMUNICATION-LANGUAGE DESIGNS ON SOFTWARE SPECIFICATIONS
E. M. Connelly and K. J. Garbelman Apr. 1985 116 p
(Contract N00014-82-C-0499; RR0-4209)
(AD-A155173; PMA-85-1) Avail: NTIS HC A06/MF A01 CSCL 09/2

The development of complete and accurate software-requirements specification is acknowledged to be a critical factor in the development of software that solves a customer's software problems. The development process usually involves the interaction of one or more customer representatives (users) with one or more software engineers. Among the difficulties frequently experienced in this interaction, one is that the users and the software engineers are each familiar with a different language - the argon common to their respective fields, but not common to both. The research described here was an original investigation of the effect of various language designs on the interaction of a non-programming user (experienced in inventory-control systems) with an experienced software engineer, as they endeavored to develop requirements specifications in a cooperative manner. The variations in language design that were studied included: the introduction of collective terms into an existing language, and the use of abbreviations. GRA

N85-32810# Naval Postgraduate School, Monterey, Calif.
A PASCAL INTERPRETER FOR THE FUNCTIONAL PROGRAMMING LANGUAGE ELC (EXTENDED LAMBDA CALCULUS) M.S. Thesis
R. P. Steen, Jr. Dec. 1984 256 p
(AD-A155218) Avail: NTIS HC A12/MF A01 CSCL 09/2

Functional programming is a methodology designed to eliminate many of the problems of past programming languages through actions such as the elimination of the assignment statement and the ability to program in an environment that is at a higher level of abstraction than any previous languages. In this thesis an interpreter, written in PASCAL, for the Extended Lambda Calculus is presented. Initially, the events leading to the development of functional programming is discussed followed by an in depth look at how the interpreter operates. Numerous example ELC programs are presented, including discussions of practical applications and statistical data about execution times and memory requirements. The Berkeley PASCAL source code for the interpreter is also included in Appendix C. GRA

N85-32811# Naval Postgraduate School, Monterey, Calif.
EXPERIENCE WITH OMEGA: IMPLEMENTATION OF A PROTOTYPE PROGRAMMING ENVIRONMENT: PART 1
B. J. MacLennan May 1985 63 p
(Proj. RR0-1408)
(AD-A155438; NPS52-85-006-Pt-1) Avail: NTIS HC A04/MF A01 CSCL 09/2

This is the first report of a series exploring the use of the alpha programming notation to prototype a programming environment. This environment includes an interpreter, unparser, syntax directed editor, command interpreter, debugger and code generator, and supports programming in a small applicative language. This report describes the interpreter, unparser, syntax directed editor, command interpreter and debugger for a subset of the language, namely arithmetic expressions. GRA

N85-32812# Air Force Inst. of Tech., Wright-Patterson AFB, Ohio. School of Engineering.
A COMPREHENSIVE STUDY OF THE AFIT (AIR FORCE INSTITUTE OF TECHNOLOGY) SOFTWARE DEVELOPMENT ENVIRONMENT M.S. Thesis
B. F. Balent Mar. 1985 278 p
(AD-A155450; AFIT/GCS/MA/85J-1) Avail: NTIS HC A13/MF A01 CSCL 09/2

This thesis studied the software development environment for the School of Engineering, Air Force Institute of Technology (AFIT). Its goal was to identify and solve the problems associated with software development performed by AFIT's students. This was accomplished by completing the engineering lifecycle stages of problem identification, problem requirements analysis, search, decision, specification, design, and implementation. The specification for this new software development system, dubbed Software Analysis and Design Engineering Environment (SANDEE), called for a phased development. The first phase called for a manual system of preprinted documentation forms with some computerization. The remaining three phases called for an expanding, interactive development environment using many state-of-the-art features. The specification also established standards for documentation and software development. GRA

N85-32813# Naval Postgraduate School, Monterey, Calif.
A MICROCOMPUTER TUTORIAL ON SPREADSHEETS AND DATABASES WITH A SIMULATED BUDGET PREPARATION M.S. Thesis
S. T. Cowen, III Mar. 1985 116 p
(AD-A155516) Avail: NTIS HC A06/MF A01 CSCL 05/1

The objective of this thesis is to illustrate to financial managers in the Fractical Comptrollership Course (PCC) some of the potential for microcomputers in budget preparation and execution. This will be accomplished through the use of a tutorial on electronic spreadsheets and databases, and a simulated budget generated using an electronic spreadsheet. The background of microcomputer implementation into the federal government and commercial industry and the problems encountered in this implementation are presented. The theory of tutorial development, along with a methodology which uses a layered procedure is discussed and used to develop the tutorial which resulted from this thesis. The tutorial manual is enclosed as Appendix A and the computer program is enclosed as Appendix B. It is recommended that this tutorial be included as a requirement for all PCC students. GRA

N85-32814# Naval Postgraduate School, Monterey, Calif.
SURVIVAL FUNCTION OF HYPO-EXPONENTIAL DISTRIBUTIONS M.S. Thesis
M. M. Lotfy and A. S. Abdelsamad Mar. 1985 85 p
(AD-A155518) Avail: NTIS HC A05/MF A01 CSCL 12/1

The reliability of a system is the probability that the system will survive or complete an intended mission of certain duration. Describing all possible ways that a system can survive a mission in reliability shorthand gives a simple approach to reliability computations. Reliability computation for a system defined by shorthand notation is greatly dependent upon the convolution problem. Assuming constant component failure rates, this paper presents an analytical approach and a computer program for computing the reliability of any convolution of independent and exponentially distributed random variables. GRA

N85-32815# Dalmo Victor Co., Belmont, Calif.
EVALUATION OF A SOFTWARE DESIGN APPROACH: DEVELOP A THREAT RESOLUTION MODULE IN AdA (TRADEMARK) Final Report, Apr. 1983 - Nov. 1984
S. J. Wersan, M. T. Minogue, and R. L. Simmen 5 Mar. 1985 120 p
(Contract DAAE07-83-C-R056)
(AD-A155599; R-3811-10968A; TACOM-TR-13073) Avail: NTIS HC A06/MF A01 CSCL 09/2

The vehicle integrated defense system (VIDS) incorporates several packages of application software written in Ada. This report describes the preliminary design and code generation of one of the critical packages, the threat resolution module (TRM). The necessary logic design, table, and file creation and other tasks to implement a preliminary TRM was accomplished. All programming was written in the DOD standard Higher Order Language of Ada. Work was done on the UNISTAR 200 workstation hosting an Ada Compiler developed by TeleSoft Corporation and targeting the MC68000 microcomputer. The operating system for the software development was UNIX. This report describes the feasibility of the VIDS-DMS software design approach by discussing the three principal topics of: (1) software algorithm design technology; (2) code generation, edit, and debug using Ada as the PDL; and (3) test of the preliminary TRM on a skeleton operating system (testbed). The annotated source code of the software as well as the object code for the TRM is delivered under separate cover with this report to TACOM. This data, in conjunction with the lessons learned during the experimental development project form the baseline for continued development of the VIDS-DMS feasibility demonstration model software. Author (GRA)

N85-32816# Air Force Inst. of Tech., Wright-Patterson AFB, Ohio. School of Engineering.
A COMPARISON AND ANALYSIS OF VINTR'S GLOBAL ROUTING ALGORITHM WITH THE LEE ROUTING ALGORITHM IN TWO-LAYER PRINTED CIRCUIT BOARDS M.S. Thesis
F. T. Chesley Mar. 1985 147 p
(AD-A155600; AFIT/GCS/ENG/85M-1) Avail: NTIS HC A07/MF A01 CSCL 12/1

Microcomputer software was designed and written to compare a standard routing technique (Lee) with an experimental, unpublished routing technique proposed by J. Vintr for two-layer printed circuit boards. Vintr's algorithm, as studied in this thesis, uses a four-iteration approach to minimize unroutable nets and minimize route distance. The unrouted nets and average route lengths were observed and analyzed for differing sizes of two-point nets. Analysis revealed a reduction of unroutable connections across iterations, but congestion played a heavy role in the overall success of finding paths. A recommendation is made that use of 8-bit microcomputers in design automation is impractical, and research in this area of technology can best be accomplished using larger computer systems. Author (GRA)

N85-32817# Naval Postgraduate School, Monterey, Calif.
A SIMPLE SOFTWARE ENVIRONMENT BASED ON OBJECTS AND RELATIONS
B. J. MacLennan Apr. 1985 32 p
(AD-A155704; NPS52-85-005) Avail: NTIS HC A03/MF A01 CSCL 09/2

This paper presents a simple programming system based on a clear separation of value-oriented programming and object-oriented programming. The value-oriented component is based on the model of objects and values connected by relations, and on production system-like rules to determine the alteration of these relations through time. It is shown that these few basic ideas permit simple prototyping of a software development environment. Author (GRA)

N85-32818# Stanford Univ., Calif. Systems Optimization Lab.
A PRACTICAL APPROACH TO KARMARKAR'S ALGORITHM
I. J. Lustig Jun. 1985 23 p
(Contracts N00014-85-K-0343; DE-AM03-76SF00326; DE-AT03-76ER-72018; Grants NSF DMS-84-20623; NSF DCR-84-13211; NSF ECS-83-12142)
(AD-A155714; SU-SOL-85-5) Avail: NTIS HC A02/MF A01 CSCL 12/1

A practical approach to implementing Karmarkar's algorithm is discussed. A variant of the algorithm is proposed which still has polynomial complexity and which eliminates the need for Karmarkar's canonical form. This method allows upper and lower bounds to be used and does not require knowledge of the objective value. Some heuristics are given which alleviate certain computational difficulties that arise when a practical implementation of the algorithm is attempted. A FORTRAN program is described that allows one to study its convergence properties. GRA

N85-32819# Oak Ridge Gaseous Diffusion Plant, Tenn.
LIQUID-PHASE COMPOSITIONS FROM VAPOR-PHASE ANALYSES 2: ADAPTATION OF THE PRAUSNITZ PROGRAM TO UF6 AND SOME OF ITS POTENTIAL IMPURITIES
H. D. Cochran and W. Davis, Jr. Mar. 1985 75 p refs
(Contract DE-AC05-84OT-21400)
(DE85-011521; K/OA-5762) Avail: NTIS HC A04/MF A01

The economic incentive to use vapor-phase samples of UF6 to determine the concentration of impurities in cylinders of UF6 rather than liquid-phase samples is discussed. A suitable model based on the Hayden-O'Connell equation of state to account for vapor-phase nonidealities was developed. Molecular parameters for UF6 and common impurities were obtained, and preliminary calculations were made for representative impurity concentrations. The results are compared with those of earlier calculations based on the Redlich-Kwong equation of state and Scatchard-Hildebrand regular solution theory. Recommendations are presented to sample and to analyze both vapor and liquid phases from UF6 cylinders so that the model may be validated. After the remaining parameters are obtained and after the model is validated, the Prausnitz model should provide a sound basis for determining liquid-phase composition from vapor-phase sample analyses of UF6 and its common impurities. DOE

N85-32820# California Univ., Livermore. Lawrence Livermore Lab.
PRAXIS RELEASE NOTES, VERSION 7.3
F. W. Holloway and A. DeGroot 3 May 1985 29 p
(Contract W-7405-eng-48)
(DE85-011862; UCID-20426) Avail: NTIS HC A03/MF A01

Release notes which are intended as a guide to those responsible for Nova software are presented. The notes assume extensive knowledge of the present Praxis language. Each improvement in Praxis is described. Many of the improvements have example programs which are contained within the chapter on example programs. Details on the specific areas within the compiler which are modified are included which will only be useful to those working on the compiler itself. The principal improvements made in this version of the compiler are: support under version 4.1 of the VMS operating system, ability to directly call the VMS Run Time Library, repair of two bugs introduced by version 7.2, and reintroduction and cleanup of the VMS System Service routines (OSI). DOE

62 COMPUTER SYSTEMS

Includes computer networks.

N85-32821*# Michigan Univ., Ann Arbor. Dept. of Electrical Engineering and Computer Science.
PERFORMANCE AND EVALUATION OF REAL-TIME MULTICOMPUTER CONTROL SYSTEMS Status Report, Sep. 1984 - Aug. 1985
Kang G. Shin Aug. 1985 11 p refs
(Grants NAG1-296; NAG1-492; NGT-23-005-801)
(NASA-CR-176098; NAS 1.26:176098) Avail: NTIS HC A02/MF A01 CSCL 09B

Three experiments on fault tolerant multiprocessors (FTMP)

were begun. They are: (1) measurement of fault latency in FTMP; (2) validation and analysis of FTMP synchronization protocols; and investigation of error propagation in FTMP. G.L.C.

N85-32822*# National Aeronautics and Space Administration. Langley Research Center, Hampton, Va.
CONCURRENT IMPLEMENTATION OF THE CRANK-NICOLSON METHOD FOR HEAT TRANSFER ANALYSIS
Jonathan B. Ransom and Robert E. Fulton (George Washington Univ., Hampton, Va.) Jun. 1985 27 p refs
(NASA-TM-86448; NAS 1.15:86448) Avail: NTIS HC A03/MF A01 CSCL 09B

To exploit the significant gains in computing speed provided by Multiple Instruction Multiple Data (MIMD) computers, concurrent methods for practical problems need to be investigated and test problems implemented on actual hardware. One such problem class is heat transfer analysis which is important in many aerospace applications. This paper compares the efficiency of two alternate implementations of heat transfer analysis on an experimental MIMD computer called the Finite Element Machine (FEM). The implicit Crank-Nicolson method is used to solve concurrently the heat transfer equations by both iterative and direct methods. Comparison of actual timing results achieved for the two methods and their significance relative to more complex problems are discussed. Author

N85-32823# Naval Postgraduate School, Monterey, Calif.
EVALUATION AND IMPLEMENTATION OF A FUNCTIONAL MICROPROGRAM GENERATOR M.S. Thesis
D. B. Stiltner Dec. 1984 223 p
(AD-A155164) Avail: NTIS HC A10/MF A01 CSCL 09/2

When a programmer writes a microprogram, as a part of a machine's instruction set or to implement an algorithm in microcode for faster execution, he must be concerned with the smallest details of the hardware in the machine. Microprogramming exists at the lowest (closest to the machine) level and is the most tedious computer language to program. In the field of computer design, where microprogramming is used most extensively, designers use microprogramming to perfect instruction sets and to optimize frequently used routines. A computer-aided design tool called a microcode generator is proposed in this thesis. It is an interactive, menu-driven functional programming tool. The user builds a microroutine by selecting functions from a series of menus as they are presented in a logical sequence. It is implemented in the language C on the Naval Postgraduate School Computer Science Department's VAX 780 computer using the Unix program development system components. The microcode generator is designed to produce microroutines targeted for a specific machine, the Am29203 Evaluation Board, an ALU implemented in bit-slice components. (Author). GRA

N85-32824# Air Force Inst. of Tech., Wright-Patterson AFB, Ohio. School of Engineering.
DEVELOPMENT OF A DEDICATED SPEECH WORK STATION M.S. Thesis
W. H. Lieber Dec. 1984 266 p
(AD-A155465; AFIT/GE/EE/84D-71) Avail: NTIS HC A12/MF A01 CSCL 09/2

This thesis project attempted to design and develop a dedicated speech work station which would accept one of sixteen possible analog signal inputs, digitize the input and store the resulting data in the expanded computer memory of a modified Cromeco S-100 bus microcomputer system. Once stored, the data could be relocated to magnetic floppy disk storage for graphically displayed on a CRT. As a result of the hardware and software developed under this thesis, bus microcomputer system can be configured as a dedicated stand alone speech work station. Hardware is now developed which provides an extended memory capability for storage of analog-to-digital sampled analog speech. Data storage is via a direct memory access capability. The hardware also supports providing an analog output from previously stored data samples via a digital-to-analog capability. Software is developed which controls the analog input to be sampled and the sampling rate to be used. The software also allows the sampled data to be graphically displayed 500 samples at a time on a video display screen or to be placed in or returned from more permanent storage on a magnetic disk. The detailed analysis, development, and fabrication of the hardware and software is also contained in the thesis. GRA

N85-32825# Naval Postgraduate School, Monterey, Calif.
THE ARCHITECTURAL REQUIREMENTS AND INTEGRATION ANALYSES OF A DATABASE SERVER FOR OFFICE AUTOMATION
S. A. Demurjian, D. K. Hsiao, and R. G. Marshall May 1985 21 p
(Proj. RR0-1408)
(AD-A155517; NPS52-85-008) Avail: NTIS HC A02/MF A01 CSCL 09/2

Office automation systems are growing both in use and in complexity. The development of a database management system for the office automation environment becomes a high priority, in order to provide an efficient and reliable way to manage the information needs of the office. Therefore, the specification of a database server for the office automation environment becomes a key area of concern. In addition to providing traditional database support, the database server must also provide new database support, so as to meet the unique and many needs of office automation environments. This paper focuses on the characterization and specification of a database server for the office automation environment. It also considers how such a database server can be effectively integrated into the office automation environment. The authors use both intuitive comparisons and queing-theory analyses to evaluate the various integration approaches. Further, they examine an experimental database system, known as the multibackend database system, as a candidate for the database server in the office automation environment. Author (GRA)

N85-32826# Naval Postgraduate School, Monterey, Calif.
MICROCOMPUTER NETWORK: INVESTIGATION AND IMPLEMENTATION M.S. Thesis
J. L. Egbert Mar. 1985 78 p
(AD-A155631) Avail: NTIS HC A05/MF A01 CSCL 09/2

This thesis presents an overview of microcomputer networks in general and the Lattice Net Microcomputer Network in particular. The Lattice Net is a network which has as its ultimate goal the use of power lines as a medium of transmission. The program presented herein is part of an on-going project to implement this system. This program works in conjunction with the code presented in another thesis Microlan File Transfer Program for Microprocessors by Roger D. Jaskot and Harold W. Henry. Author (GRA)

N85-32827# Massachusetts Inst. of Tech., Cambridge. Lab. for Information and Decision Systems.
BROADCASTING TOPOLOGY AND ROUTING INFORMATION IN COMPUTER NETWORKS M.S. Thesis
J. M. Spinelli May 1985 96 p
(Contract N00014-84-K-0357; DARPA Order 3045)
(AD-A155668; LIDS-TH-1470) Avail: NTIS HC A05/MF A01 CSCL 09/2

The topology problem in store and forward computer networks is that of keeping all nodes informed of the current operational status of each communication link in the network. The failure or repair of one or more communication links is called a topology change. Two efficient algorithms are presented for solving this problem. They require 0(l) communication and O(n) time for simple topology hanges in a network with l links and n nodes. The algorithms send messages only in resposne to topology changes, and each message usually contains information only about the links whose status has changed. The algorithms work properly in the presence of arbitrarily complex topology changes. The routing information problem is that of keeping each node informed of the packet transmission delay on each directed link in the network. Nodes need this information in order to make intelligent routing decisions. The two topology algorithms discussed above are used to also solve the routing information problem. The level of

difficulty in solving this problem is found to depend greatly on the particular properties of the topology algorithm used. Author (GRA)

N85-32828# Informatique Internatinale S.A., Rungis (France).
COMPARATIVE STUDY ON DATA SYSTEM ARCHITECTURES Final Report
P. Vielcanet, H. Horgen, T. Demoy (GIXI), and P. Howlett (Societe Francaise d'Equipmements pour la Navigation Aerienne) Paris ESA Nov. 1984 325 p refs
(Contract ESTEC-5524/83/NL-PP)
(ESA-CR(P)-2015) Avail: NTIS HC A14/MF A01

Space application of microprocessor based distributed processing systems set up for ground or airborne utilization was assessed for a manned space station and a large unmanned platform. The survey suggests that the transposition of ground based or airborne solutions to space applications is a technological challenge mainly with respect to space radiation hardening. However, promising trends towards compactness, performance, and reliability are noted. The selection of a qualification method for VLSI components is undecided. Commonality between space and ground computer systems seems achievable in the medium term for manned missions. Spacecraft performance, operational flexibility, and user convenience can be enhanced, at affordable cost, through increased spacecraft automation and autonomy. Many instances of autonomy, intelligence, and stringent requirements can be found in current ground process control applications. Critical reliability and availability requirements are met by specific airborne distributed computer systems implementations. Author (ESA)

N85-32526*# Illinois Univ., Urbana. Aeronomy Lab.
HARDWARE SCHEMES FOR FAST FOURIER TRANSFORM, PART 7.4A
G. R. Stitt and S. A. Bowhill *In* International Council of Scientific Unions Middle Atmosphere Program: Handbook for MAP. Vol. 14 Dec. 1984 p 285-288 refs (For primary document see N85-32466 21-46)
(Grants NsG-7506; NSF ATM-81-20371)
Avail: NTIS HC A17/MF A01; also avail. from SCOSTEP Secretariat, Illinois Univ., 1406 West Green St., Urbana, Ill. 61801 CSCL 09B

63 CYBERNETICS

Includes feedback and control theory.

For related information see also *54 Man/System Technology and Life Support.*

No abstracts in this category.

64 NUMERICAL ANALYSIS

Includes iteration, difference equations, and numerical approximation.

N85-32829*# National Aeronautics and Space Administration. Langley Research Center, Hampton, Va.
ON A VARIATIONAL APPROACH TO SOME PARAMETER ESTIMATION PROBLEMS
H. T. Banks (Brown Univ.) Jun. 1985 40 p refs Presented at the Intern. Conf. on Control Theory for Distributed Parameter Systems and Appl., Vorau, Austria, 9-14 Jul. 1984
(Contract NAS1-17070; Grant NSF DMS-82-05355; Contracts AF-AFOSR-0398-84; DAAG29-83-K-0029)
(NASA-CR-177935; ICASE-85-32; NAS 1.26:177935) Avail: NTIS HC A03/MF A01 CSCL 12A

Examples (1-D seismic, large flexible structures, bioturbation, nonlinear population dispersal) in which a variation setting can provide a convenient framework for convergence and stability arguments in parameter estimation problems are considered. Some of these examples are 1-D seismic, large flexible structures, bioturbation, and nonlinear population dispersal. Arguments for convergence and stability via a variational approach of least squares formulations of parameter estimation problems for partial differential equations is one aspect of the problem considered. Author

N85-32830*# National Aeronautics and Space Administration, Washington, D. C.
GENERALIZED FORMULATION OF A CLASS OF EXPLICIT AND IMPLICIT TVD SCHEMES
H. C. Yee Jul. 1985 25 p refs
(NASA-TM-86775; Rept-85343; NAS 1.15:86775) Avail: NTIS HC A02/MF A01 CSCL 12A

A one parameter family of second order explicit and implicit total variation diminishing (TVD) schemes is reformulated so that a simpler and wider group of limiters is included. The resulting scheme can be viewed as a symmetrical algorithm with a variety of numerical dissipation terms that are designed for weak solutions of hyperbolic problems. This is a generalization of Roe and Davis's recent works to a wider class of symmetric schemes other than Lax-Wendroff. The main properties of the present class of schemes are that they can be implicit, and when steady state calculations are sought, the numerical solution is independent of the time step. Author

N85-32831*# National Aeronautics and Space Administration. Ames Research Center, Moffett Field, Calif.
SIMULATION OF COMPLEX THREE-DIMENSIONAL FLOWS
George S. Diewert, Herbert J. Rothmund, and Kazuhiro Nakahashi Jul. 1985 15 p refs
(NASA-TM-86773; Rept-85228; NAS 1.15:86773) Avail: NTIS HC A02/MF A01 CSCL 12A

The concept of splitting is used extensively to simulate complex three dimensional flows on modern computer architectures. Used in all aspects, from initial grid generation to the determination of the final converged solution, splitting is used to enhance code vectorization, to permit solution driven grid adaption and grid enrichment, to permit the use of concurrent processing, and to enhance data flow through hierarchal memory systems. Three examples are used to illustrate these concepts to complex three dimensional flow fields: (1) interactive flow over a bump; (2) supersonic flow past a blunt based conical afterbody at incidence to a free stream and containing a centered propulsive jet; and (3) supersonic flow past a sharp leading edge delta wing at incidence to the free stream. Author

N85-32832# Yale Univ., New Haven, Conn. Dept. of Computer Science.
ON THE DEPENDENCE OF THE CONVERGENCE OF GUMMEL'S ALGORITHM ON THE REGULARITY OF THE SOLUTION
T. Kerkhoven Mar. 1985 22 p
(Contracts N00014-82-K-0184; DE-AC02-81-ER-10996)
(AD-A154628; YALEU/DCS/RR-366) Avail: NTIS HC A02/MF A01 CSCL 12/1

The convergence of a typical example from the class of highly successful decoupling algorithms for steady state semiconductor simulation, collectively known as Gummel's method, is considered for one, two, and three dimensional models. Because a nonlinear equation is solved for the potential u at every step, the considered version corresponds closely to the algorithms used for numerical computation in practice. As opposed to most earlier publications, the dependence of the regularity of the solution on the device geometry and the nature of the boundary conditions for the system of mixed boundary value problems is considered. From a detailed analysis of the boundary conditions for a typical two dimensional model we conclude that for a physically realistic device geometry the solution may be expected to be sufficiently regular for the algorithm to converge. GRA

N85-32833# Air Force Inst. of Tech., Wright-Patterson AFB, Ohio. School of Engineering.

OSCILLATORY SOLUTIONS OF THE PEACEMAN-RACHFORD ALTERNATING DIRECTION IMPLICIT METHOD AND A COMPARISON OF METHODS FOR THE SOLUTION OF THE TWO DIMENSIONAL HEAT DIFFUSION EQUATION M.S. Thesis

R. F. Kropf Jan. 1985 71 p
(AD-A154670; AD-F630659; AFIT/GNE/ENP/85M-11) Avail: NTIS HC A04/MF A01 CSCL 12/1

The two dimensional heat diffusion equation with Dirichlet boundary conditions was solved using the fully explicit, fully implicit, Crank-Nicolson implicit, and Peaceman-Rachford alternating direction implicit (ADI) methods. Comparisons of accuracy and time requirements were made. The possibility that the ADI method has stable oscillatory solutions with large time steps was investigated. Results of computations revealed that the ADI has stable oscillations for large time steps, in some cases producing large enough errors to render the solution unusable. Time steps greater than twice the square of the mesh spacing divided by the thermal diffusivity must be used with care. For small time steps, the Crank-Nicolson and ADI methods were the most accurate, and the ADI was the fastest method. The fully implicit method was the most accurate at large time steps, but the ADI, with a smaller time step to reduce the oscillatory error, was still the fastest method to reach a solution with the desired degree of accuracy. GRA

N85-32834# Boeing Computer Services Co., Tukwila, Wash.
NEW DEVELOPMENTS ON THE CORE FUNCTION FOR EFFICIENT IMPLEMENTATION OF THE DIFFICULT RESIDUE NUMBER SYSTEM OPERATIONS Final Report, Nov. 1983 - Feb. 1985

R. E. Altschul, D. D. Miller, J. N. Polky (Sigma Research, Inc.), J. R. King (Washington Univ.), and D. A. Technology Inc Uvelli (Seattle Silicon Technology, Inc.) Feb. 1985 93 p
(Contract N00014-84-C-0130)
(AD-A154678) Avail: NTIS HC A05/MF A01 CSCL 12/1

This paper develops new properties of the core function on a residue number system (RNS) which allows efficient implementation of the operations of comparison, overflow detection, sign determination, parity determination, scaling, and general division. Previously these operations have been considered difficult to implement in high speed hardware and have not taken advantage of the parallel structure of a residue class architecture. In 1977, Akushskii, Burcev and Pak introduced the core function and presented algorithms for these difficult operations. While these algorithms were superior to previous techniques, the evaluation of the core function required, in general, an iterative, complex procedure. Moreover, while these techniques were theoretically attractive, they were unable to construct a methodology for determining a suitable core function for a realistic moduli set. In the present work, a new method for evaluating the core function is introduced. This method utilizes a redundant modulus and its computational complexity is equivalent to that of the first iteration of the method of Akushskii, et al. While this new method requires additional hardware to carry on this redundant modulus calculation, it provides more information and allows more flexibility than the previous method. New and much more efficient algorithms for the difficult RNS operations are developed. In addtition, new structural properties of the core function are developed, and the optimality of the function is characterized. The selection of an optimal core function for any moduli set is cast as an integer programming problem. GRA

N85-32835# Air Force Inst. of Tech., Wright-Patterson AFB, Ohio. School of Engineering.
OPTIMAL LOW THRUST TRANSFER USING A FIRST-ORDER PERTURBATION MODEL M.S. Thesis

T. G. Black 6 Mar. 1985 43 p
(AD-A154761; AFIT/GA/AA/84D-1) Avail: NTIS HC A03/MF A01 CSCL 12/1

An analytic solution to the optimal low thrust problem is developed using a first-order perturbation approach for planar orbit transfers. This solution is verified by comparison with the solution obtained by integrating the equations of motion. For low vehicle accelerations the analytic solution yields results quite close to those obtained by the integrated solution. At higher acceleration levels, however, the analytic solution diverges from the integrated solution. For very low acceleration levels the analytic solution approaches the limiting case of the infinitesimally low thrust spiral solution. GRA

N85-32836# Massachusetts Inst. of Tech., Cambridge. Lab. for Computer Science.
A NEW FAULT-TOLERANT ALGORITHM FOR CLOCK SYNCHRONIZATION

J. Lundelius and N. Lynch Jul. 1984 33 p
(Contracts N00014-83-K-0125; DAAG29-84-K-0058; DAAG29-79-C-0155; Grant NSF DCR-83-02391)
(AD-A154771; MIT/LCS/TM-265) Avail: NTIS HC A03/MF A01 CSCL 09/2

We describe a new fault tolerant algorithm for solving a variant of Lamport's clock synchronization problem. The algorithm is designed for a system of distributed processes that communicate by sending messages. Each process has its own read only physical clock whose drift rate from real time is very small. By adding a value to its physical clock time, the process obtains its local time. The algorithm solves the problem of maintaining closely synchronized local times, assuming that processes' local times are closely synchronized initially. The algorithm is able to tolerate the failure of just under a third of the participating processes. It maintains synchronization to within a small constant, whose magnitude depends upon the rate of clock drift, the message delivery time, and the initial closeness of synchronization. We also give a characterization of how far the clocks drift from real time. Reintegration of a repaired process can be accomplished using a slight modification of the basic algorithm. A similar style algorithm can also be used to achieve synchronization initially. GRA

N85-32837# Aeronautical Research Associates of Princeton, Inc., N. J.
THEORY OF SOLITON WAVES Final Report

H. Segur 21 Nov. 1984 17 p
(Contract N00014-80-C-0048)
(AD-A154784; ARAP-536) Avail: NTIS HC A02/MF A01 CSCL 12/1

The long-range objective of the work performed under this contract has been to construct realistic models of water waves using solitons and other intrinsically nonlinear waves as the fundamental building blocks. In principle, both deterministic and statistical models could be constructed in this way, in deep water or in shallow water. The basic idea is that because water waves are known to be fundamentally nonlinear, one has a better chance of describing them with mathematical models that are also fundamentally nonlinear. This report describes the progress we have made in achieving that objective. GRA

N85-32838# Wisconsin Univ., Madison. Mathematics Research Center.
A NOTE ON A THEOREM OF R. DUFFIN Technical Summary Report

P. H. Rabinowitz Mar. 1985 21 p
(Contract DAAG29-80-C-0041; Grant NSF MCS-81-10556)
(AD-A154786; MRC-TSR-2802) Avail: NTIS HC A02/MF A01 CSCL 20/11

In an earlier paper, Duffin studied a model for the transverse vibrations of a string of n beads. This note looks at the same question in a more general setting. It establishes the existence of special solutions corresponding to high frequency oscillations which are positive in the coordinate system chosen as well as other nonpositive solutions. GRA

N85-32839# Wisconsin Univ., Madison.
SOBOLEV-POINCARE'S INEQUALITY AND THE NEUMANN PROBLEM FOR u SUB t = DIVERGENCE OF THE ABSOLUTE VALUE OF THE GRADIENT u TO THE p-2 POWER x THE GRADIENT u Technical Summary Report

I. Fukuda Apr. 1985 20 p
(Contract DAAG29-80-C-0041)

(AD-A154788; MRC-TSR-2811) Avail: NTIS HC A02/MF A01 CSCL 12/1

An equation is used as a model for a broad class of singular and degenerate parabolic equations. The degenerate type ($p > 2$) has been treated by many authors, but the behavior of solutions of the singular type ($1 < p < 2$) is less well understood. In this paper we establish the homogenization effect of the singular problem with Neumann boundary conditions. GRA

N85-32840# Wisconsin Univ., Madison. Mathematics Research Center.

ON THE TURNING LOZANGE OF CONSTANT SIDE WHOSE VERTICES ALTERNATE BETWEEN TWO FIXED CIRCLES OF A RING Technical Summary Report

I. J. Schoenberg Apr. 1985 10 p

(Contract DAAG29-80-C-0041)

(AD-A154803; MRC-TSR-2813) Avail: NTIS HC A02/MF A01 CSCL 12/1

This note is to call attention to the paper on a theorem about zig-zags between two circles. It explains the construction of a linkage composed of four equal bars P sub 1 P sub 2 = P sub 2 P sub 3 = P sub 3 P sub 4 = P 4 P 1 = d, joined at the points P sub k, with the following property: With P sub 1 and P sub 3 moving in the circular groove T, and P sub 3, P sub 4 moving in the circular groove T', it is shown that the lozange P sub 1 P sub 2 P sub 3 P sub 4 can be turned around. GRA

N85-32841# Wisconsin Univ., Madison. Mathematics Research Center.

THE DISTRIBUTION OF THE NUMBER OF EMPTY CELLS IN A GENERALIZED RANDOM ALLOCATION SCHEME Technical Summary Report

B. Harris, M. Marden, and C. J. Park Mar. 1985 26 p

(Contract DAAG29-80-C-0041)

(AD-A154806; MRC-TSR-2805) Avail: NTIS HC A03/MF A01 CSCL 12/1

The n balls are randomly distributed into N cells, so that no cell may contain more than one ball. This process is repeated m times. In addition, balls may disappear; such disappearances are independent and identically Bernoulli distributed. Conditions are given under which the number of empty cells has an asymptotically (N approaches infinity) standard normal distribution. GRA

N85-32842# Massachusetts Inst. of Tech., Cambridge. Lab. for Computer Science.

GENERALIZED PLANAR MATCHING Interim Research Report

F. Berman, T. Leighton, P. W. Shor, and L. Snyder Apr. 1985 39 p

(Contract N00014-80-C-0622; Grants NSF MCS-80-05387; AF-AFOSR-0326-82)

(AD-A154809; MIT/LCS/TM-273) Avail: NTIS HC A03/MF A01 CSCL 12/1

This paper proves that maximum planar H-matching (the problem of determining the maximum number of node-disjoint copies of the fixed graph H contained in a variable planar graph G) is NP-complete for any connected planar graph H with three or more nodes. It is also shown that perfect planar H-matching is NP-complete for any connected outerplanar graph H with three or more nodes, and is, somewhat surprisingly solvable in linear time for traingulated H with four or more nodes. The results generalize and unify several special-case results proved in the literature. The techniques can also be applied to solve a variety of problems, including the optimal tile salvage problem from wafer-scale integration. Although the authors prove that the optimal tile salvage problem and others like it are NP-complete, they also describe provably good approximation algorithms that are suitable for practical applications. Author (GRA)

N85-32843# Wisconsin Univ., Madison. Mathematics Research Center.

LOCAL EPI-CONTINUITY AND LOCAL OPTIMIZATION Technical Summary Report

S. M. Robinson Mar. 1985 24 p

(Contract DAAG29-80-C-0041; Grant NSF MCS-82-00632)

(AD-A154812; MRC-TSR-2798) Avail: NTIS HC A02/MF A01 CSCL 12/1

One of the fundamental questions in nonlinear optimization is how optimization problems behave when the functions defining them changed (e.g., by continuous deformation). Recently the study of epi-continuity has somewhat unified the results in this area. Here we show how to localize the concept of epi-continuity, and how to apply these localized ideas to ensure persistence and stability of local optimizing sets. We also show how these conditions follow from known properties of nonlinear programming problems. GRA

N85-32844# GRD, Inc., Warminster, Pa.

RECURSIVE NONLINEAR FILTERING THROUGH COMPLETE LINEARIZATION Technical Report, Mar. 1984 - Mar. 1985

T. F. Dyson Apr. 1985 79 p

(Contract N00014-84-C-0233)

(AD-A155029; TR-1) Avail: NTIS HC A05/MF A01 CSCL 12/1

Recursive filtering forms the foundation of all tracking and position estimation tasks when the target undergoes dynamic motion relative to the observer. Moreover, recursive filtering has an important role in stochastic signal detection. The typical application almost invariably involves dynamics equations which depend nonlinearly on the physical variables and sometimes even the sensor (observation) equation involves a nonlinear relation to the quantities to be estimated. In these common situations the practitioner nearly always resorts to a form of approximate linearization of the describing equations. Although highly successful in many useful application, it is commonly recognized that a variety of problems simply will not satisfactorily succumb to the usual Extended Kalman methods. For these situations present research in nonlinear filtering theory hold major portent. Indeed, the new understanding of nonlinear problems developed over the past 10 years leads to optimism for better, more refined approximate filtering techniques which may prove to be both accurate and more widely applicable. GRA

N85-32845# Stanford Univ., Calif. Dept. of Statistics.

DECOMPOSING THE JOINT DISTRIBUTION OF SEVERAL LINEAR COMBINATIONS OF UNIFORM SPACINGS

F. Huffer 25 Apr. 1985 28 p

(Contract N00014-76-C-0475)

(AD-A155056; SU-TR-356) Avail: NTIS HC A03/MF A01 CSCL 12/1

Using facts about divided differences, we prove an identity which can sometimes express the joint distribution of several linear combinations of uniform spacings as a sum of simpler distributions. This identity is useful in the exact computation of probabilities and expectations which arise in testing for uniformity. Examples are given. GRA

N85-32846# California Univ., Livermore. Lawrence Livermore Lab.

DYNA3D, INGRID, AND TAURUS: AN INTEGRATED, INTERACTIVE SOFTWARE SYSTEM FOR CRASHWORTHINESS ENGINEERING

D. J. Benson, J. O. Hallquist, and D. W. Stillman Apr. 1985 9 p Presented at the ASME Intern. Computers in Eng. Conf. and Exhibition, Boston, 4 Aug. 1985

(Contract W-7405-eng-48)

(DE85-010928; UCRL-92218; CONF-850862-2) Avail: NTIS HC A02/MF A01

An integrated, interactive set of finite element programs for crashworthiness analysis was developed. The DYNA3D has the following four capabilities that are critical for the efficient and accurate analysis of crashes: (1) fully nonlinear solid, shell, and beam elements for representing a structure; (2) a broad range of constitutive models for representing the materials; (3) sophisticated contact algorithms for the impact interactions; and (4) a rigid body capability to represent the bodies away from the impact zones at a greatly reduced cost without sacrificing any accuracy in the

momentum calculations. A general purpose mesh generator is used to generate the large and complex data files for DYNA3D, INGRID. The INGRID also doubles as a geometric modeller. The TAURUS, an interactive post processor, is used to display DYNA3D output. In addition to the standard monochrome hidden line display, time history plotting, and contouring, TAURUS generates interactive color displays on eight color video screens by plotting color bands superimposed on the mesh which indicate the value of the state variables. It is found that color is as important as hidden line removal in aiding the analyst in understanding results. The basic methodologies of the programs are presented along with several crashworthiness calculations. DOE

N85-32973# Joint Publications Research Service, Arlington, Va.
POISSON FORMULA FOR RADON TRANSFORMATION AND NUMERICAL IMAGE RECONSTRUCTION ALGORITHM Abstract Only
N. D. Vvedenskaya and S. G. Gindikin *In its* USSR Rept.: Phys. and Math. (JPRS-UPM-85-004) 17 Jun. 1985 p 90 Transl. into ENGLSH from Dokl. Akad. Nauk SSSR (Moscow), v. 279, no. 4, Dec. 1984 p 780-784 (For primary document see N85-32860 21-70)
Avail: NTIS HC A06/MF A01

N85-32974# Joint Publications Research Service, Arlington, Va.
ASYMPTOTICALLY STABLE SOLUTIONS OF SOME NON-LINEAR EQUATIONS Abstract Only
N. A. Kirichenko *In its* USSR Rept.: Phys. and Math. (JPRS-UPM-85-004) 17 Jun. 1985 p 91 Transl. into ENGLISH from Dokl. Akad. Nauk SSSR (Moscow), v. 280, no. 3, Jan. 1985 p 579-583 (For primary document see N85-32860 21-70)
Avail: NTIS HC A06/MF A01

65 STATISTICS AND PROBABILITY

Includes data sampling and smoothing; Monte Carlo method; and stochastic processes.

N85-32847*# National Aeronautics and Space Administration. Marshall Space Flight Center, Huntsville, Ala.
WEIBULL DISTRIBUTION BASED ON MAXIMUM LIKELIHOOD WITH INTERVAL INSPECTION DATA
Mario H. Rheinfurth 30 Jul. 1985 11 p
(NASA-TM-86515; NAS 1.15:86515) Avail: NTIS HC A02/MF A01 CSCL 12A

The two Weibull parameters based upon the method of maximum likelihood are determined. The test data used were failures observed at inspection intervals. The application was the reliability analysis of the SSME oxidizer turbine blades. Author

N85-32848# Wisconsin Univ., Madison. Mathematics Research Center.
ANALYSIS OF UNREPLICATED FACTORIALS ALLOWING FOR POSSIBLY FAULTY OBSERVATIONS Technical Summary Report
G. E. P. Box and R. D. Meyer Mar. 1985 16 p
(Contract DAAG29-80-C-0041; Grant NSF MCS-82-00632)
(AD-A154813; MRC-TSR-2799) Avail: NTIS HC A02/MF A01 CSCL 12/1

Normal probability plotting of the orthogonal contrasts (Daniel (1959)) is a useful diagnostic as well as inferential technique for analyzing unreplicated factorial experiments. In particular, the presence of one of more faulty observations is marked by a characteristic defect of the normal plot. In previous work, the authors introduced a more formal method of identifying active effects as a supplement to Daniel's graphical analysis. This work is extended here to allow for the possibility of faulty observations. GRA

N85-32849# Pennsylvania State Univ., University Park. Dept. of Statistics.
ANTISTARSHAPEDNESS, DISPERSIVENESS AND MIXTURES
J. Lynch 30 Apr. 1985 10 p
(Contract DAAG29-84-K-0007)
(AD-A155583; ARO-20063.3-MA) Avail: NTIS HC A02/MF A01 CSCL 12/1

Necessary and sufficient conditions are given for certain classes of distributions to be closed under mixtures. The relevant classes are defined in terms of antistarshapedness or dispersiveness. One of the main results characterizes distributions with log concave densities. A basic tool in the analysis of univariate survival data is the quantile plot. GRA

N85-32850# Florida State Univ., Tallahassee. Dept. of Statistics.
RECONCILING BAYESIAN AND FREQUENTIST EVIDENCE IN THE ONE-SIDED TESTING PROGRAM
G. Casella and R. L. Berger Apr. 1985 24 p
(Contract DAAG29-82-K-0168)
(AD-A155603; ARO-19367.26-MA) Avail: NTIS HC A02/MF A01 CSCL 12/1

For the one-sided hypothesis testing problem it is shown that it is possible to reconcile Bayesian evidence against H sub 0, expressed in terms of the posterior probability that H sub 0 is true, with frequentist evidence against h sub 0, expressed in terms of p-value. In fact, for many classes of prior distributions it is shown that the infimum of the Bayesian posteriors probability of H sub 0 is either equal to or bounded above by the p-value. The results are in direct contrast to recent work of Berger and Sellke (1985)in the two-sided (point null) case, where it was found that the p-value is much less than the Bayesian infimum. Some comments on the point null problem are given. Author (GRA)

N85-32529*# Saskatchewan Univ., Saskatoon. Inst. of Space and Atmospheric Studies.
PROBLEMS AND SOLUTIONS IN ANALYZING PARTIAL-REFLECTION DRIFT DATA BY CORRELATION TECHNIQUES
C. E. Meek *In* International Council of Scientific Unions Middle Atmosphere Programs: Handbook for MAP. Vol. 14 Dec. 1984 p 297-299 (For primary document see N85-32466 21-46)
Avail: NTIS HC A17/MF A01; also avail. from SCOSTEP Secretariat, Illinois Univ., 1406 West Green St., Urbana, Ill. 61801 CSCL 12A

N85-32975# Joint Publications Research Service, Arlington, Va.
OPTIMIZATION OF SAMPLING IN STATISTICAL PHYSICS EXPERIMENTS Abstract Only
M. Kh. Rafailov *In its* USSR Rept.: Phys. and Math. (JPRS-UPM-85-004) 17 Jun. 1985 p 92-93 Transl. into ENGLISH from Zh. Tekh. Fiz. (Leningrad), v. 54, no. 12, Dec. 1984 p 2349-2351 (For primary document see N85-32860 21-70)
Avail: NTIS HC A06/MF A01

66 SYSTEMS ANALYSIS

Includes mathematical modeling; network analysis; and operations research.

N85-32851*# National Aeronautics and Space Administration. Dryden (Hugh L.) Flight Research Center, Edwards, Calif.
IDENTIFICATION OF UNSTEADY AERODYNAMICS AND AEROELASTIC INTEGRO-DIFFERENTIAL SYSTEMS
Naren K. Gupta (Integrated Systems, Inc., Palo Alto, Calif.) and Kenneth W. Iliff Aug. 1985 32 p refs
(NASA-TM-86749; H-1313; NAS 1.15:86749) Avail: NTIS HC A03/MF A01 CSCL 12B

The problem of estimating integro-differential models based on test or simulation data is dealt with. The identification techniques proposed for estimating parameters in models described by differential equations need to be considerably extended to deal with the integral terms. Conditions under which the integral terms may be approximated by algebraic values are discussed. The integro-differential models discussed are related to indicial models proposed by aerodynamicists to describe unsteady flow. Author

N85-32852# Texas A&M Univ., College Station. Dept. of Management.
THE PRIMING EFFECT IN TASK DESIGN RESEARCH
T. C. Head, V. L. Yates, R. W. Griffin, and T. S. Bateman Apr. 1985 43 p
(Contract N00014-83-C-0025)
(AD-A154589; TR-ONR-DG-14) Avail: NTIS HC A03/MF A01 CSCL 12/2

This study, using a different operationalization from previous work, investigated the potential impact of the priming effect on task design research. The priming effect, as discussed by Salancik and Pfeffer (1977, 1978), is artificially increasing an attitude's saliency by including items describing that attitude on a questionnaire. Results of the study demonstrated a strong presence of priming effects. Further analyses of how the priming effect may manifest itself in common descriptive statistics (means, correlations, reliabilities) provided mixed findings. GRA

N85-32853# Naval Research Lab., Washington, D. C.
A VECTORIZED NEAREST-NEIGHBORS ALGORITHM OF ORDER N USING A MONOTONIC LOGICAL GRID
J. P. Boris 29 May 1985 49 p
(Proj. RR0-1109)
(AD-A155169; NRL-MR-5570) Avail: NTIS HC A03/MF A01 CSCL 12/1

When a large number of separate objects interact, N*(N-1)/2 interactions can occur. At any instant a given object may interact strongly with only a few of the N-1 others. Unfortunately, keeping lists of the other objects with which it interacts or recomputing these nearest neighbors each timestep is computationally expensive. This nearest neighbors problem has persisted in computational Physics and computational geometry for several decades. We need efficient algorithms which select important nearest-neighbor interactions without having to check and analyze N2 interactions. To date the best algorithms which scale as N, rather than N2, are scalar algorithms which address memory randomly. This report introduces an efficient 3D nearest-neighbors algorithm whose cost scales as N and which vectorizes easily using data from contiguous memory locations. A Monotonic Logical Grid (MLG) for storing the object data is defined dynamically so that objects which are adjacent in real space automatically have close address indices in the compact MLG data arrays. The data values for each object are stored at a location (i,j,k) in the MLG such that the X positions of all objects increase monotonically with index i, the Y positions increase monotonically with index j, and the Z positions increase monotonically with index k. SUch a well-structured mapping from the real positions to regular, compact data arrays can always be found. Further, when object motions result in a local violation of spatial monotonicity, another MLG always can be found nearby. This means that local changes in the object positions and hence spatial ordering do not trigger global changes in where these object data are stored in the MLG. GRA

N85-32854# Stanford Univ., Palo Alto, Calif. Dept. of Statistics.
A SIMULATION STUDY OF SYLVESTER'S PROBLEM IN THREE DIMENSIONS
K. A. Do and H. Solomon 2 May 1985 9 p
(Contract N00014-76-C-0475)
(AD-A155266; AD-F300613; SU-TR-357) Avail: NTIS HC A02/MF A01 CSCL 12/1

This note gives estimates of solutions to the Sylvester problem in three dimensions. These results suggest that the solutions in four and higher dimensions are very close to the solution for the n-dimensional sphere which is known. GRA

N85-32855# Air Force Inst. of Tech., Wright-Patterson AFB, Ohio. School of Engineering.
BAYESIAN VS MAP MULTIPLE MODEL ADAPTIVE ESTIMATION FOR FIELD OF VIEW EXPANSION IN TRACKING AIRBORNE TARGETS M.S. Thesis
P. A. Loving Mar. 1985 112 p
(AD-A155466; AFIT/GE/EE/85M-1) Avail: NTIS HC A06/MF A01 CSCL 12/1

Previous efforts have led to the development of a multiple model adaptive filter (MMAF) tracking algorithm which demonstrates significant improvements in performance against close-range, highly dynamic, airborne targets, over a direct correlation method currently in use. The basic elemental filter in the MMAF bank combines an enhanced correlator and a linear Kalman filter. Digital signal processing techniques are used to derive a target shape function from the forward looking infrared sensor data. This shape function is used as a template in the correlation algorithm which generates offset pseudo-measurements for the update portion of a linear Kalman filter. The multiple models are created by tuning the basic model for best performance against differing target maneuvering behavior and with physically different fields of view. The outputs of three independent elemental filters, each receiving data from a shared sensor are used to generate a single adaptive estimate of the state via a probabilistic weighted average (Bayesian form) or by selection of the one elemental filter associated with the highest probability (MAP form). The adaptive state estimate can produce target position predictions to be used in generating feedback control for maintaining the target in the center of the field of view. There are two main results from this effort. The addition of a third elemental filter to the baseline MMAF improves tracking performance over the two-element MMAF. Specifically, the peak error following a maneuver is significantly reduced. However, the MAP estimation approach does not differ significantly from the Bayesian approach. GRA

N85-32856# Purdue Univ., Lafayette, Ind. Dept. of Statistics.
A SHORT BIBLIOGRAPHY OF RECENT DEVELOPMENTS IN SELECTION AND RANKING PROCEDURES
S. S. Gupta May 1985 18 p
(Contract N00014-84-C-0167)
(AD-A155648; TR-85-11) Avail: NTIS HC A02/MF A01 CSCL 12/1

A short bibliography of recent developments (1965-1985) in selection and ranking - mainly the subset selection procedures is provided. The bibliography is divided into six parts: Theory; Applications; Books; Computer Packages; Proceedings of Conferences; and Two-stage selection procedures. GRA

67 THEORETICAL MATHEMATICS

Includes topology and number theory.

No abstracts in this category.

70 PHYSICS (GENERAL)

For geophysics see *46 Geophysics*. For astrophysics see *90 Astrophysics*. For solar physics see *92 Solar physics*.

N85-32857*# California Univ., Los Angeles.
PLANETARY DYNAMOS Final Technical Report
Friedrich H. Busse 19 Jul. 1985 12 p refs
(Grant NsG-7484)
(NASA-CR-176001; NAS 1.26:176001) Avail: NTIS HC A02/MF A01 CSCL 20C

The MAGSAT-program has added significantly to our knowledge of planetary magnetism. The accuracy of observations has been improved such that a reliable extrapolation of the magnetic field to the core surface is now much more feasible than it has been before, and the prospect of further MAGSAT missions raises the expectation that the time dependence of the geomagnetic field will be known with similar accuracy in the future. In the research support it has been attempted to develop dynamo theory with these applications in mind. G.L.C.

N85-32858# Texas Technological Univ., Lubbock. Dept. of Electrical Engineering.
COORDINATED RESEARCH PROGRAM IN PULSED POWER PHYSICS Annual Report, 1 Oct. 1983 - 31 Oct. 1984
M. Kristiansen, L. Hatfield, and G. Schaefer 20 Dec. 1984 213 p
(Grant AF-AFOSR-0032-84)
(AD-A154629; AFOSR-85-0457TR) Avail: NTIS HC A10/MF A01 CSCL 10/2

Work on three program elements, related to pulsed power research, is described. The program is a multi-investigator program whose main emphasis is on gaining a better understanding of repetitive opening and closing switch phenomena. The main effort is on diffuse discharge opening switches but considerable progress has also been made on understanding and describing fundamental, transient discharge phenomena. In addition several smaller studies have considered various novel ideas and concepts to determine their potential for further investigations. The three main projects are Opening Switches, Transient Processes in Triggered Electrical Breakdown of Gases, and Exploratory Concepts. The second one of these projects will not be carried on in its present form beyond this contract period since the Principal Investigator is moving to another university. GRA

N85-32859# Army Cold Regions Research and Engineering Lab., Hanover, N. H.
KINETIC FRICTION COEFFICIENT OF ICE
K. A. Forland and J. C. P. Tatinclaux Mar. 1985 47 p
(AD-A155035; CRREL-85-6) Avail: NTIS HC A03/MF A01 CSCL 08/12

This study investigates the relative influence of various parameters on the kinetic friction coefficient mu sub k between ice and different surfaces. Friction tests were performed with urea-doped, columnar ice, studying the parameters of normal pressure, velocity, type of material, material roughness, ice orientation, ice hardness and test configuration. Tests were conducted by pulling a sample of ice over a sheet of material and by pulling a sample of material over an ice sheet. An ambient temperature of -1.5 + or - 1 deg C was maintained throughout, and the ice surface hardness was measured using a specially designed apparatus. The results of the friction tests revealed that the behavior of mu sub k with varying velocity was significantly influenced by the test configuration and material roughness. The magnitude of the kinetic friction coefficient was also affected by varying normal pressure, surface roughness and ice hardness. Additional guidelines for standardized ice friction tests and future investigations were recommended. GRA

N85-32860# Joint Publications Research Service, Arlington, Va.
USSR REPORT: PHYSICS AND MATHEMATICS Abstracts Only
17 Jun. 1985 114 p Transl. into ENGLISH from various Russian articles
(JPRS-UPM-85-004) Avail: NTIS HC A06/MF A01

Work performed in the Soviet Union in the disciplines of physics and mathematics is reported. Categories presented include: acoustics, crystals and semiconductors, fluid mechanics, lasers and masers, mechanics of solids, molecule physics, nuclear physics, plasma physics, optics and spectroscopy, theoretical physics, and mathematics For individual titles, see N85-32861 through N85-32978.

N85-32861# Joint Publications Research Service, Arlington, Va.
THE KONSTANTINOV EFFECT AND ABSORPTION OF SOUND IN INHOMOGENEOUS MEDIA Abstract Only **c71**
F. F. Legusha *In its* USSR Rept.: Phys. and Math. (JPRS-UPM-85-004) 17 Jun. 1985 p 4 Transl. into ENGLISH from Usp. Fiz. Nauk (Moscow) v. 144, no. 3, Nov. 1984 p 509-522 (For primary document see N85-32860 21-70)
Avail: NTIS HC A06/MF A01

Experiments on the Konstantinov effect the absorption of sound at the boundary between two media are reviewed. The possibility of exploiting the phenomenon to intensify sound absorption in engineering acoustics is discussed. Visual observation methods for ultrasonic fields are employed to illustrate the design principles of various technical devices. Promising new media exhibiting the thermooptical effect include the vanadium-oxide-based (FTIROC) phase-transformation interference reversible optical reflector and spatial light-modulators based on the surface tension deformation of a liquid layer caused by radiation heating of the liquid. E.A.K.

N85-32862# Joint Publications Research Service, Arlington, Va.
TOWARD THE THEORY OF ACOUSTIC SCATTERING ON UNEVEN FREE SURFACE Abstract Only **c71**
A. G. Voronovich *In its* USSR Rept.: Phys. and Math. (JPRS-UPM-85-004) 17 Jun. 1985 p 4-5 Transl. into ENGLISH from Akust. Zh. (Moscow), v. 30 , no. 6, Nov. – Dec. 1984 p 747-753 (For primary document see N85-32860 21-70)
Avail: NTIS HC A06/MF A01

An approximate method is proposed for calculating the scattering of sound on uneven free surfaces based on a power-series expansion for increases in the logarithm of the scattering matrix. This corresponds to making allowances for the first terms of the series of perturbation theory, and that leads essentially to Kirchhoff's approximation for large-scale gradual irregularities. The cases of a horizontal plane and a periodic surface are analyzed as examples. An approximation is described that allows for processes which are significant for scattering on large and small-scale surface components responsible for scattering in mirror and nonmirror directions. E.A.K.

N85-32863# Joint Publications Research Service, Arlington, Va.
NEW APPROXIMATIONS AND FINDINGS OF THEORY OF NONLINEAR ACOUSTIC BEAMS Abstract Only **c71**
Yu. R. Lapidus and O. V. Rudenko *In its* USSR Rept.: Phys. and Math. (JPRS-UPM-85-004) 17 Jun. 1985 p 5 Transl. into ENGLISH from Akust. Zh. (Moscow), v. 30, no. 6, Nov. - Dec. 1984 p 797-802 (For primary document see N85-32860 21-70)
Avail: NTIS HC A06/MF A01

Approaches to the solution of problems arising in the theory of nonlinear propagation effects of high-intensity spatially localized acoustic waves are addressed. A modified theory is proposed that provides more complete information about nonlinear diffraction processes in acoustic beams. The domains of applicability of the first and second approximations are identified. The determination of peak values is explained. E.A.K.

N85-32864# Joint Publications Research Service, Arlington, Va.
REFLECTION OF ACOUSTIC BEAM FROM INHOMOGENEOUS BOUNDARY Abstract Only **c71**
A. D. Lapin *In its* USSR Rept.: Phys. and Math. (JPRS-UPM-85-004) 17 Jun. 1985 p 5 Transl. into ENGLISH from Akust. Zh. (Moscow), v. 30, no. 6, Nov. – Dec. 1984 p 836-838 (For primary document see N85-32860 21-70)
Avail: NTIS HC A06/MF A01

The effective coefficient of reflection of an acoustic beam incident normally on an inhomogeneous boundary characterized by elastic-type acoustic conductivity is calculated. The analysis is performed within the framework of the modified perturbation theory, with allowance for the terms of the second order with respect to the amplitude of inhomogeneities. It is found that practically all of the acoustic energy of the beam is converted to surface waves when the wave numbers of the bulk and surface waves are close to one another. E.A.K.

N85-32865# Joint Publications Research Service, Arlington, Va.
INFLUENCE ON BI-PHONON STATES ON RAMAN SCATTERING OF LIGHT IN MOLECULAR CRYSTALS Abstract Only **c76**
Yu. D. Zavorotnev, L. N. Ovander, and L. I. Stefanovich *In its* USSR Rept.: Phys. and Math. (JPRS-UPM-85-004) 17 Jun. 1985 p 6 Transl. into ENGLISH from Optika i Spektroskopiya (Leningrad), v. 57, no. 5, Nov. 1984 p 831-836 (For primary document see N85-32860 21-70)
Avail: NTIS HC A06/MF A01

The excitation of biphonons formed from intramolecular vibrations was investigated by the resonance Raman light scattering

method, in which the pumping frequency is close to the frequency of the two-particle state, the conditions of polariton Fermi resonance are satisfied. The connection between the energy flux of the scattered radiation and the nonlinear polarizability tensor is identified. Raman light scattering tensor selection rules which make it possible to investigate various bi-exciton states by choosing the scattering geometry are investigated. It is found through investigating those bi-phonon states formed from the phonons in the same zone that not all of the scattered radiation lines are resonant as the pumping frequency approaches a particular biphonon level. E.A.K.

N85-32866# Joint Publications Research Service, Arlington, Va.
X-RAY DIFFRACTOMETRIC MEASUREMENTS AND CALCULATIONS OF LIMITING VALUES OF DISCREPANCY BETWEEN LATTICES AND LAYER THICKNESSES, PREVENTING GENERATION OF DISLOCATIONS DURING GROWTH OF MULTILAYER HETEROSTRUCTURES Abstract Only **c76**
G. B. Bokiy and G. F. Kuznetsov *In its* USSR Rept.: Phys. and Math. (JPRS-UPM-85-004) 17 Jun. 1985 p 6-7 Transl. into ENGLISH from Dokl. Akad. Nauk SSSR (Moscow), v. 279, no. 4, Dec. 1984 p 876-880 (For primary document see N85-32860 21-70)
Avail: NTIS HC A06/MF A01

A theoretical functional relationship is proposed between the critical parameters for any heterolayer in a multilayer heterostructure and the experimentally measured discrepancies and thicknesses of all of the layers in the heterostructures; this relationship is verified experimentally by comparing data from X-ray diffractometry and X-ray topographic analyses. The generation of dislocations in each of the heterolayers of a dual heterostructure is confirmed by X-ray topography only when the actual thickness of the heterolayer exceeds its calculated critical thickness. Otherwise, no dislocations are generated during the growth processes when incongruities are registered in the dual heterostructures. The formulas derived can be used for X-ray diffractometry measurements and analysis of the characteristic parameters of any type of multilayer heterostructures. E.A.K.

N85-32867# Joint Publications Research Service, Arlington, Va.
INFLUENCE OF COHERENT LIGHT BEAMS ON FREE CARRIERS IN SEMICONDUCTORS Abstract Only **c76**
I. M. Dykman and P. M. Tomchuk *In its* USSR Rept.: Phys. and Math. (JPRS-UPM-85-004) 17 Jun. 1985 p 7 Transl. into ENGLISH from Fiz. Tverdogo Tela (Leningrad), v. 26, no. 9, Sep. 1984 p 2729-2733 (For primary document see N85-32860 21-70)
Avail: NTIS HC A06/MF A01

A semiconductor exposed to several coherent beams of light waves was examined. It is assumed that because psi is smaller than the width of the forbidden zone, the light is capable only of redistribution of the electron concentration, while the total number of electrons in the semiconductor remains constant. Wave interference modulates the probability of electron scattering and the power they absorb, exerting light pressure on the electron gas. A kinetic equation is derived for the problem which allows for these factors. The detection of effects caused by the formation of super lattices are discussed, and their parameters are defined. E.A.K.

N85-32868# Joint Publications Research Service, Arlington, Va.
LUMINESCENCE AND ABSORPTION OF INDIUM-ACTIVATED POTASSIUM-BORATE GLASSES SUBJECTED TO HIGH-POWER EXCITATION Abstract Only **c76**
S. Ye. Belyy, S. Ye. Zelenskiy, B. A. Okhrimenko, and S. M. Yablochkov *In its* USSR Rept.: Phys. and Math. (JPRS-UPM-85-004) 17 Jun. 1985 p 10 Transl. into ENGLISH from Zh. Prikl. Spektroskopii (Minsk), v. 41, no. 4, Oct. 1984 p 583-587 (For primary document see N85-32860 21-70)
Avail: NTIS HC A06/MF A01

The interaction between indium activated potassium borate glasses and the radiation from a pulsed neodymium laser is investigated. Specimens of K sub 2O . 7Bsub 2O sub 3 are irradiated by fourth harmonic focused radiation from a neodymium laser revealing a long, nonexponential component in the attenuation of the luminescence. This fact is interpreted within the framework of the model of recombination luminescence. The variations in the luminescence and absorption spectra of potassium borate glass are found to be stable and to be associated with the occurrence of new luminescence spectra caused by photoionization of In+ centers. E.A.K.

N85-32869# Joint Publications Research Service, Arlington, Va.
GENERATION AND AMPLIFICATION OF RADIATION DURING STIMULATED RAMAN SCATTERING IN CRYSTALS Abstract Only **c76**
S. N. Karpukhin and V. Ye. Yashin *In its* USSR Rept.: Phys. and Math. (JPRS-UPM-85-004) 17 Jun. 1985 p 10-11 Transl. into ENGLISH from Kvantovaya Elektron. (Moscow), v. 11, no. 10, Oct. 1984 p 1992-2000 Original language document announced in IAA as A85-21023 (For primary document see N85-32860 21-70)
Avail: NTIS HC A06/MF A01

The generation of Stokes radiation in focused beams under conditions of stimulated Raman scattering in calcite and barium nitrate crystals is investigated experimentally. High efficiency of pump energy to Stokes energy conversion (about 0.8) is obtained in the case of stimulated Raman counter scattering, which is thought to be a result of four photon parametric processes. The wave front reversal is determined for spatially homogeneous and inhomogeneous beams over a wide range of pump energy and divergence and lens focal length. V.L. (IAA)

N85-32870# Joint Publications Research Service, Arlington, Va.
ABSORPTION OF 10.6 MICROMETER LASER RADIATION IN ELECTRON-HOLE CONDENSATE IN GERMANIUM Abstract Only **c76**
V. P. Kalinushkin, A. A. Manenkov, G. N. Mikhaylova, and S. Yu. Sokolov *In its* USSR Rept.: Phys. and Math. (JPRS-UPM-85-004) 17 Jun. 1985 p 11 Transl. into ENGLISH from Dokl. Akad. Nauk SSSR (Moscow), v. 279, no. 1, Nov. 1984 p 88-90 (For primary document see N85-32860 21-70)
Avail: NTIS HC A06/MF A01

The absorption cross section of the electron hole fluid in uncompressed germanium and an irregularly deformed germanium crystal during the formation of small electron hole droplets were determined. The change in transmission of probe radiation from a CO2 laser by the specimen, caused by the generation of nonequilibrium carriers in the crystal, is measured at T = 300 and 1.6 K. The absorption cross section at T = 1.6 K was estimated by comparing the modulation percentages of probe radiation at 300 and 1.6 K. A modulation percentage of about 7 is obtained for deformed and undeformed germanium specimens at 1.6 K. The attenuation signal at T = 300 K in the deformed specimen was the same as that for the undeformed one. The experimental values obtained for the attenuation of radiation in an electron hole liquid are thus the same in irregularly deformed and uncompressed germanium. E.A.K.

N85-32871# Joint Publications Research Service, Arlington, Va.
CLASSICAL EMISSION OF RELATIVISTIC CHARGED PARTICLES DURING AXIAL CHANNELING Abstract Only **c76**
B. V. Kholomay *In its* USSR Rept.: Phys. and Math. (JPRS-UPM-85-004) 17 Jun. 1985 p 12 Transl. into ENGLISH from Vestn. Moskovskogo Univ.: Fiz., Astron. (Moscow), v. 25, no. 5, Sep. - Oct. 1984 p 125-128 (For primary document see N85-32860 21-70)
Avail: NTIS HC A06/MF A01

The relativistic equations of motion in arbitrary axisymmetrical electrical focusing fields are employed to study the high frequency emission of relativistic charged particles during axial channeling in crystals. A solution is sought to the relativistic steady state Hamilton-Jacobi equation in a cylindrical coordinate system. The basic principles of relativistic particle movement during axial channeling can be obtained for an arbitrary focusing electrical field on the assumption that the charge moves in a spiral and fluctuates little in the vicinity of the equilibrium radius. An expression

is derived for the spectral angular distribution of the time averaged total radiated power. E.A.K.

N85-32872# Joint Publications Research Service, Arlington, Va.
SYSTEM FOR ELECTRO-OPTICAL CERAMIC RECRYSTALLIZATION Abstract Only **c76**
M. G. Livinsh, T. Ya. Pinins, Ya. A. Seglinsh, and Yu. A. Zvirgzds *In its* USSR Rept.: Phys. and Math. (JPRS-UPM-85-004) 17 Jun. 1985 p 16 Transl. into ENGLISH from Izv. Akad. Nauk Latv. SSR: Ser. Fiz. i Tekhn. Nauk (Riga), no. 5, Oct. - Nov. 1984 p 42-45 (For primary document see N85-32860 21-70)
Avail: NTIS HC A06/MF A01

A hot pressing system to obtain electro-optical ceramic blanks up to 100 mm in diameter and up to 30 mm high is described which makes it possible to realize recrystallization in a vacuum and in an oxidizing atmosphere without cooling the specimen between cycles. The device consists of a press, heating chamber and support systems. Experimental operation of the first model of this system for 12 months proved the reliability and convenience of the design, but also disclosed a number of dificient elements, which were corrected in the present model. By using this system, the length of the technological recrystallization cycle can be shortened by up to 50% as compared with hot pressing in two separate systems; the number of rejects can be reduced during the recrystallization stage by reducing the number of heating cooling cycles; and optically homogeneous electro-optical ceramic can be produced which provides light transmission close to the theoretical limit. E.A.K.

N85-32873# Joint Publications Research Service, Arlington, Va.
DEFECT FORMATION IN AMORPHOUS HYDRATED SILICON SUBJECTED TO LASER RADIATION Abstract Only **c76**
G. M. Chukicheva, Yu. A. Zarifyants, S. N. Karyagin, P. K. Kashkarov, and A. V. Petrov *In its* USSR Rept.: Phys. and Math. (JPRS-UPM-85-004) 17 Jun. 1985 p 16-17 Transl. into ENGLISH from Fiz. i Tekhn. Poluprov. (Leningrad), v. 18, no. 10, Oct. 1984 p 1895-1896 (For primary document see N85-32860 21-70)
Avail: NTIS HC A06/MF A01

The reduction in capacitive photo emf in amorphous hydrated silicon exposed to pulses from an Nd laser is investigated by photoluminescence and electron paramagnetic resonance methods at 10 GHz. The photoluminescence spectral distribution of the a-Si:H film at 77 K shows a sharp increase in the intensity of the 0.85-eV band after irradiation of the specimen by laser pulses at approximately 0.1 MW/ sq cm, while the parameters of the primary band changed insignificantly. The increase in the intensity of the 0.85-eV band provides direct evidence of the formation of intrinsic defects in a-Si:H, similar to that observed elsewhere as the result of Ar+ ion implantation, electron bombardment and following long term irradiation with light at 5 W/sq cm. Spin centers are cited as one of the possible types of defects that are formed as the result of breaking the Si-H bonds. The shift in the g-factor of the electron paramagnetic resonance signal indicates a change in the coordination circumference of the Si centers. E.A.K.

N85-32874# Joint Publications Research Service, Arlington, Va.
QUASI-STEADY-STATE MELTING MODE DURING COMBINED LASER IRRADIATION OF SEMICONDUCTOR MATERIALS Abstract Only **c76**
V. N. Abakumov, V. N. Guman, and V. S. Yuferev *In its* USSR Rept.: Phys. and Math. (JPRS-UPM-85-004) 17 Jun. 1985 p 17 Transl. into ENGLISH from Fiz. i Tekhn. Poluprov. (Leningrad), v. 18, no. 10, Oct. 1984 p 1832-1835 (For primary document see N85-32860 21-70)
Avail: NTIS HC A06/MF A01

The concentration of heat sources created by the absorption of laser radiation striking a substance in the vicinity of a melting front, and their advancement along with the front, are investigated. A simple analytical solution to Stefan's problem for this laser irradiation mode is found. The temperature field distributions are obtained and expressions are derived for the rate of melting front movement during combined exposure to laser pulses with nanosecond, microsecond and millisecond durations. Although the analysis does not contradict experimental findings elsewhere, the theory cannot be compared quantitatively with those experiments inasmuch as the latter are qualitative in nature. E.A.K.

N85-32875# Joint Publications Research Service, Arlington, Va.
INTER-ZONE AUGER RECOMBINATION IN GaSb LASER STRUCTURES Abstract Only **c76**
B. L. Gelmont, Z. N. Sokolova, and V. B. Khalfin *In its* USSR Rept.: Phys. and Math. (JPRS-UPM-85-004) 17 Jun. 1985 p 17-18 Transl. into ENGLISH from Fiz. i Tekhn. Poluprov. (Leningrad), v. 18, no. 10, Oct. 1984 p 1803-1807 (For primary document see N85-32860 21-70)
Avail: NTIS HC A06/MF A01

The influence of interzone Auger recombination on the threshold current of heterolasers with an active region consisting of an undoped semiconductor in which the width of the forbidden zone is approximately the same as the spin-orbital splitting was investigated. The interzone Auger recombination weights are computed by Kane's model; the radiative recombination rates in GaSb laser heterostructures are computed. The threshold current density and internal luminescence quantum efficiency are found. It is demonstrated analytically that the fundamental Auger recombination mechanism essentially does not increase the threshold current density in GaSb lasers and lasers with similar solid solution composition. The threshold current densities are found to be significantly higher at room temperature, which is explained either on the basis of large optical losses in the structure, or recombination involving impurities. E.A.K.

N85-32876# Joint Publications Research Service, Arlington, Va.
PHOTO-ACOUSTIC EFFECT IN FINITE-DIMENSIONAL SEMICONDUCTORS Abstract Only **c76**
A. N. Vasilev and V. B. Sandomirskiy *In its* USSR Rept.: Phys. and Math. (JPRS-UPM-85-004) 17 Jun. 1985 p 18 Transl. into ENGLISH from Fiz. i Tekhn. Poluprov. (Leningrad), v. 18, no. 10, Oct. 1984 p 1751-1758 (For primary document see N85-32860 21-70)
Avail: NTIS HC A06/MF A01

The photoacoustic effect, defined as the generation of temperature waves in a specimen as a result of the absorption of unsteady radiation followed by the formation of acoustic oscillations in the specimen or the surrounding medium, is examined in a semiconductor of finite thickness with allowance for surface recombination and heat release from the rear boundary. The surface temperature is investigated numerically as a function of frequency. Approximate expressions are obtained for the heat sources in the specimen. Simple analytical expressions are obtained for the amplitude of the photoacoustic effect which agree quantitatively with the features of the graphs. The photoacoustic effect is shown to determine a number of the electronic, thermal, and geometric characteristics of the specimens. E.A.K.

N85-32877# Joint Publications Research Service, Arlington, Va.
EFFECT OF POWERFUL PULSED LOW-ENERGY ION STREAMS ON GaAs Abstract Only **c76**
Yu. A. Bityurin, S. V. Gaponov, Ye. B. Klyuyenkov, and M. D. Strikovskiy *In its* USSR Rept.: Phys. and Math. (JPRS-UPM-85-004) 17 Jun. 1985 p 18-19 Transl. into ENGLISH from Fiz. i Tekhn. Poluprov. (Leningrad), v. 18, no. 10, Oct. 1984 p 1729-1734 (For primary document see N85-32860 21-70)
Avail: NTIS HC A06/MF A01

The compensation effect of Gallium arsenide bombarded by intense streams of low energy arsenic ions is investigated in an experimental setup similar to that employed for laser spraying and epitaxy. It is found that compensation at irradiation temperatures of 350 to 500 C is associated with the migration of primary radiation defects in the GaAs, and the formation of intricate complexes in a nonlinear mode with respect to the radiation intensity. The radiation intensity has a strong influence on the depth of compensation, and the influence is not associated with change in the diffusion length of the vacancies. A phenomenological model of the process is proposed which assumes the accumulation of divacancy - donor atom complexes through an intermediate short

lived state. By combining high density of the bombarding stream and heating of the semiconductor, it is thus possible to obtain injected radiation stimulated self compensation under the radiation conditions. E.A.K.

N85-32878# Joint Publications Research Service, Arlington, Va.
INFLUENCE OF BACKGROUND ELECTRICALLY NEUTRAL ARGON ADMIXTURE ON MECHANICAL STRENGTH OF SILICON CRYSTALS Abstract Only **c76**
V. V. Kolomoyets, Yu. V. Simonenko, and A. V. Fedosov *In its* USSR Rept.: Phys. and Math. (JPRS-UPM-85-004) 17 Jun. 1985 p 19 Transl. into ENGLISH from Dokl. Akad. Nauk Ukr. SSR: Ser. A. Fiz.-Mat. i Tekhn. Nauki (Kiev), no. 10, Oct. 1984 p 61-63 (For primary document see N85-32860 21-70)
Avail: NTIS HC A06/MF A01

The influence of local elastic stresses on the mechanical characteristics of silicon crystals, which determines the reliability of silicon devices operating under severe mechanical conditions, is determined directly by comparing the effect of changing the resistance of uniaxially compressed crystals. Two batches of specimens were made from two Si ingots doped with electrically active phosphorous. One of the ingots was grown in argon, resulting in a residual background argon impurity; the other ingot was grown in a vacuum. It is found that specimens containing traces of argon broke down under mechanical stress of 15.8 plus or minum 1 tonne/cm sq 2, while specimens made from the ingot grown in a vacuum broke down at 21.8 + or - 1 tonne/cm sq. 2: the strength by approximately a factor of 1.4. E.A.K.

N85-32879# Joint Publications Research Service, Arlington, Va.
DEVELOPMENT OF ARTIFICIALLY PRODUCED PERTURBATIONS IN SUPERSONIC BOUNDARY LAYER Abstract Only **c76**
A. D. Kosinov and A. A. Maslov *In its* USSR Rept.: Phys. and Math. (JPRS-UPM-85-004) 17 Jun. 1985 p 20 Transl. into ENGLISH from Izv. Akad. Nauk SSSR: Mekhan. Zhidkosti i Gaza (Moscow), no. 5, Sep. - Oct. 1984 p 37-43 Original language document announced in IAA as A85-16177 (For primary document see N85-32860 21-70)
Avail: NTIS HC A06/MF A01

A method is proposed which uses an ac discharge to produce perturbations of regular amplitude in a supersonic boundary layer. This method is used to conduct an experimental study of the development of the boundary layer on a flat plate at a Mach number of 2.0. The Fourier components of the wave packet are determined. The data obtained are compared with calculations of the linear stability of a supersonic boundary layer carried out in the plane-parallel flow approximation. L.M. (IAA)

N85-32880# Joint Publications Research Service, Arlington, Va.
THEORETICAL FOUNDATIONS OF TURBULENT FLOWS Abstract Only **c34**
V. V. Struminskiy *In its* USSR Rept.: Phys. and Math. (JPRS-UPM-85-004) 17 Jun. 1985 p 21 Transl. into ENGLISH from Dokl. Akad. Nauk SSSR (Moscow), v. 280, no. 3, Jan. 1985 p 570-574 (For primary document see N85-32860 21-70)
Avail: NTIS HC A06/MF A01

Turbulent fluid motions can only be described by constructing more general solutions based on the Liouville equation and it was pointed out that since the Boltzmann equation can be derived from the principles of mechanics and statistics and that this equation can, in principal, describe only laminar motions of fluids. A general approach to obtaining such a solution is outlined based on the concept of groups of particles, some of which can be in an equilibrium state at the same time that others are in a nonequilibrium state. Each group is viewed as a particle-like dynamic entity and a system of coupled collision equations is constructed whose form is similar to the collision equation in the Boltzmann theory but which now describe the kinetics of the system of groups. This system of equations can be reduced to a closed system of equations for describing turbulent motions, in contrast to classical approaches to turbulence which lead to an infinite system which must be truncated. E.A.K.

N85-32881# Joint Publications Research Service, Arlington, Va.
TOWARD THE PROPAGATION OF WAVES IN UNSTEADY MEDIA Abstract Only **c34**
V. I. Pavlov, M. Mamatkulov, and P. K. Khabibullayev *In its* USSR Rept.: Phys. and Math. (JPRS-UPM-85-004) 17 Jun. 1985 p 21 Transl. into ENGLISH from Izv. Akad. Nauk UZSSR: Ser. Fiz.-Mat. Nauk (Tashkent), no. 4, Jul. - Aug. 1984 p 44-47 (For primary document see N85-32860 21-70)
Avail: NTIS HC A06/MF A01

Variation in the speed of sound in unsteady media caused by changes in physical and chemical properties are investigated analytically. A truncated equation is derived to describe wave propagation in unsteady media. Steady waves are found to exist in unsteady media when nonlinearity is taken into account. E.A.K.

N85-32882# Joint Publications Research Service, Arlington, Va.
EXACT SOLUTIONS OF SINGULAR EQUATIONS FOR VISCOUS TRANSONIC FLOWS Abstract Only **c34**
Yu. V. Zasorin *In its* USSR Rept.: Phys. and Math. (JPRS-UPM-85-004) 17 Jun. 1985 p 22 Transl. into ENGLISH from Dokl. Akad. Nauk SSSR (Moscow), v. 278, no. 6, Oct. 1984 p 1347-1351 (For primary document see N85-32860 21-70)
Avail: NTIS HC A06/MF A01

An exact solution is sought to the equation for viscous transonic flow. Explicit fundamental solutions are constructed for a system of hypoelliptical operators with singular coefficients. Asymptotic expansions of these solutions are found. The exact formula for the Green's function of certain boundary problems and the rate of decrease at infinity of the solutions of the homogeneous equation are investigated within the class of moderate growth distributions. E.A.K.

N85-32883# Joint Publications Research Service, Arlington, Va.
EXPLOSION IN FLIGHT Abstract Only **c34**
L. V. Shurshalov *In its* USSR Rept.: Phys. and Math. (JPRS-UPM-85-004) 17 Jun. 1985 p 24 Transl. into ENGLISH from Izv. Akad. Nauk SSSR: Mekhan. Zhidkosti i Gaza (Moscow), no. 5, Sep. - Oct. 1984 p 126-129 Original language document announced in IAA as A85-16180 (For primary document see N85-32860 21-70)
Avail: NTIS HC A06/MF A01

Godunov's finite-difference scheme using an axisymmetric flow model is used to investigate the explosion of a body (e.g., a meteoroid in the atmosphere) in flight. It is shown that, even for a relatively small contribution of kinetic energy (K sub 0 = 0.1 E sub 0), deviations from one-dimensional explosion flow are very significant, especially for a large initial density of the flying body. This is even more true when the kinetic energy K sub 0 is equal to or greater than the explosion energy E sub 0. L.M.

N85-32884# Joint Publications Research Service, Arlington, Va.
INVESTIGATION OF REPRODUCIBILITY OF EMISSION WAVELENGTH OF HELIUM-NEON LASER WITH EXTERNAL NEON ABSORPTION CELL (0.63 MICROMETERS) Abstract Only **c36**
V. Ye. Privalov and Ye. G. Chulyayeva *In its* USSR Rept.: Phys. and Math. (JPRS-UPM-85-004) 17 Jun. 1985 p 25 Transl. into ENGLISH from Optika i Spektroskopiya (Leningrad), v. 57, no. 5, Nov. 1984 p 909-912 (For primary document see N85-32860 21-70)
Avail: NTIS HC A06/MF A01

A stabilized LG-149-1 helium-neon laser with an external neon cell in a longitudinal magnetic field is investigated and found to provide wavelength reproducibility of 10 million, rather than the limiting values of 10 to the 8th power to 10 to the 9th power, due to shifts in the emission frequency. Frequency reproducibility is measured by a method utilizing a matrix of the frequency intervals formed by the published spread in the electrical parameters of the laser. The matrix provides a graphic representation of how changes in particular parameters influence shifts in frequency, and makes it possible to estimate the best-case situation. In the worse case, the frequency is combined, i.e., the reproducibility is determined by the sum of the diagonal elements of the matrix.

Recommendations are given for ways of providing instrument-instrument wavelength reproducibility of one to 10 the 8th power.
Author

N85-32885# Joint Publications Research Service, Arlington, Va.
PROSPECTS FOR LASERS FOR FUSION ENERGY ASSESSED Abstract Only **c36**
N. Basov and V. Rozanov *In its* USSR Rept.: Phys. and Math. (JPRS-UPM-85-004) 17 Jun. 1985 p 26-27 Transl. into ENGLISH from Mosk. Komsomolets (Moscow), 20 Jan. 1985 p 4 (For primary document see N85-32860 21-70)
Avail: NTIS HC A06/MF A01

The authors assess the status of laser thermonuclear fusion research in the USSR and abroad, reviewing some of its major advances as well as current objectives of scientists working in this field. The possible development of an experimental laser thermonuclear reactor is discussed. Such a laser must operate with a pulse repetition frequency of 1 to 10 pulses per second, and it must have a service life of about 100 million pulses. It will be made up of individual modules (10 to 20 modules) with an overall energy of 2 to 3 megajoules, and it will ensure stable focusing of radiation on a target about 1 centimeter in size from a distance of about 50 meters. Its efficiency will be adequate and its cost low enough. Lasers of several types (including carbon-dioxide lasers and chemical and excimer lasers based on a mixture of noble gases with halogen) can meet these requirements, but incorporating them in a single unit is quite difficult from the engineering standpoint. The development of modules of such lasers is also an important task. R.J.F.

N85-32886# Joint Publications Research Service, Arlington, Va.
GENERATION OF SINGLE NANOSECOND HIGH-CONTRAST RADIATION PULES (LAMBDA=10.6 MICROMETERS) Abstract Only **c36**
V. V. Apollonov, G. G. Baytsur, V. V. Brytkov, S. I. Ziyenko, S. V. Muravev, V. R. Sorochenko, K. N. Firsov, Yu. A. Shakir, and V. A. Yamshchikov *In its* USSR Rept.: Phys. and Math. (JPRS-UPM-85-004) 17 Jun. 1985 p 28 Transl. into ENGLISH from Pis'ma v Zh. Tekhn. Fiz. (Leningrad), v. 10, no. 19, 12 Oct. 1984 p 1192-1196 (For primary document see N85-32860 21-70)
Avail: NTIS HC A06/MF A01

The regenerative amplifier-based master oscillator of the Polinom laser system is described. The master oscillator is made up of three blocks: the first generates a high-contrast nanosecond pulse for injection into the regenerative amplifier; the second is the regenerative amplifer, which outputs a nanosecond pulse train; the third converts the pulse train to a single high-contrast pulse. A tunable LG-74 laser is the radiation source. The regenerative amplifier is made up of a pair of amplifier modules which produce a train of nanosecond pulses against the background of the intrinsic radiation. Measurements of the working parameters of each block are described. The Polinom laser system produces energy of 0.5 J, with half-height duration of 3 ns, contrast exceeding 1 million and divergence of approximately 0.0005. Author

N85-32887# Joint Publications Research Service, Arlington, Va.
LASER ELEKTRONIKA-01 FOR AIR POLLUTION CONTROL LIDAR Abstract Only **c36**
In its USSR Rept.: Phys. and Math. (JPRS-UPM-85-004) 17 Jun. 1985 p 29 Transl. into ENGLISH from Sov. Rossiya (Moscow), 16 Dec. 1984 p 2 (For primary document see N85-32860 21-70)
Avail: NTIS HC A06/MF A01

A station for high-altitude sounding of the atmosphere began monitoring the purity of the air over Tomsk yesterday. Data on the distribution of industrial emissions in the atmosphere are obtained with the aid of a multipurpose laser locator, or lidar, which is equipped with a large receiving mirror. Subsequent processing of the data makes it possible to determine sources of pollution. Specialists of the Institute of Atmospheric Optics of the USSR Academy of Sciences' Siberian Branch taught the laser its new occupation. The laser beam proved to be capable of obtaining information on the condition of every layer of air, including the stratosphere. A special computer-based unit of the station makes it possible to read this information in a matter of seconds. No measuring method had such accuracy and operational efficiency in the prelidar era. Within the framework of a Soviet-Bulgarian research program, industry of the People's Republic of Bulgaria has begun the series production of a laser complex, the Elektronika-01, which is based on the Tomsk lidar. Author

N85-32888# Joint Publications Research Service, Arlington, Va.
INVESTIGATION OF INFLUENCE OF GAS EXIT MODES ON CHARACTERISTICS OF N2O - N2 - He DISCHARGE LASER Abstract Only **c36**
V. G. Testov, Yu. V. Konev, V. D. Menenkov, Yu. I. Grin, and G. I. Mishin *In its* USSR Rept.: Phys. and Math. (JPRS-UPM-85-004) 17 Jun. 1985 p 30 Transl. into ENGLISH from Zh. Tekhn. Fiz. (Leningrad), v. 54, no. 12, Dec. 1984 p 2305-2314 (For primary document see N85-32860 21-70)
Avail: NTIS HC A06/MF A01

A N2O laser is investigated in order to determine the influence of the composition, initial conditions, droplet parameters and supersonic 1-dimensional flow modes. The variations in the gain in a rectangular channel of an N2O - N2 - He GDL are calculated. The amplifying properties are measured experimentally as a function of the braking parameters, the nozzle parameters, the distance from the exit section of the nozzle and from the axis in the transverse direction and the composition of the mixture in 3-dimensional and flat jets. The amplifying characteristics of N2O - N2 - He mixtures are analyzed. It is found that amplification drops off sharply as the braking parameters increase, due to thermal dissociation of the working N2O molecules. Inversion exceeding 1015 cm-3 is achieved, which is higher in CO2 systems; the braking parameters are significantly smaller. Comparison of the experimental findings for N2O - N2, N2O - He and N2O - N2 - He mixtures indicate significantly more inversion for 1-dimensional flow behind a tapered nozzle than for a nozzle with maximum expansion. Author

N85-32889# Joint Publications Research Service, Arlington, Va.
INFLUENCE OF MIRROR ANISOTROPY AND BREWSTER WINDOW ORIENTATION ON RADIATION CHARACTERISTICS OF RING LASERS Abstract Only **c36**
V. S. Rubanov, V. N. Severikov, and A. I. Shevtsova *In its* USSR Rept.: Phys. and Math. (JPRS-UPM-85-004) 17 Jun. 1985 p 31 Transl. into ENGLISH from Dokl. Akad. Nauk BSSR (Minsk), v. 28, no. 12, Dec. 1984 p 1086-1089 (For primary document see N85-32860 21-70)
Avail: NTIS HC A06/MF A01

The influence of the angle of rotation of the Brewster windows and the combined phase anisotropy of the cavity on the lasing polarization and energy characteristics of a ring laser is investigated. The polarization azimuths and elipticities are investigated in a triangular ring laser operating at lambda = 1.5 microns. The findings make it possible to assess the influence of magnetic fields on the frequency characteristics of ring lasers based on the actual phase anisotropy of the laser mirrors and the orientation accuracy of the Brewster exit windows of the active element.
Author

N85-32890# Joint Publications Research Service, Arlington, Va.
LASING ON LiF:F(-)2 - DYE CENTERS WITH TRANSVERSE PUMPING Abstract Only **c36**
F. V. Karpushko and V. P. Morozov *In its* USSR Rept.: Phys. and Math. (JPRS-UPM-85-004) 17 Jun. 1985 p 31 Transl. into ENGLISH from Zh. Prikl. Spektroskopii (Minsk), v. 41, no. 4, Oct. 1984 p 656-658 (For primary document see N85-32860 21-70)
Avail: NTIS HC A06/MF A01

Tunable lasing in an LiF:F-2 - color center crystal laser employing transverse pumping is described. Uniform transverse pumping of the active crystals is achieved by employing banks of 90 deg prisms, which satisfy the condition of total internal reflection for the pumping radiation. A tunable lasing line with 0.6 cm-1 and 80 mJ is achieved in the selective cavity of the device, employing a holographic selector with spatial frequency of 2100 mm-1 as the dispersing element. The pumping scheme can, in principle, be

used to obtain powerful tunable lasing in organic dye solutions without using amplifier stages. Author

N85-32891# Joint Publications Research Service, Arlington, Va.
PARTICIPATION OF SINGLET OXYGEN IN PHOTODESTRUCTION OF AIR-SATURATED SOLUTIONS OF COUMARIN DYES Abstract Only **c36**
O. V. Zinkovskaya, N. A. Kuznestova, and O. L. Kaliya *In its* USSR Rept.: Phys. and Math. (JPRS-UPM-85-004) 17 Jun. 1985 p 32 Transl. into ENGLISH from Zh. Prikl. Spektroskopii (Minsk), v. 41, no. 4, Oct. 1984 p 626-630 (For primary document see N85-32860 21-70)
Avail: NTIS HC A06/MF A01

The possibility of employing ground-based Raman-scattering lidars to investigate the molecular gas concentration profile of the atmosphere is studied. The random error of the method is analyzed; the efficiency of existing Raman scattering lidars is investigated, and the gas-analytic capabilities of lidars employing excimer lasers are studied using hypothetical systems with optimum sounding wavelengths as an example. It is found that UV band excimer lasers expand the capabilities of Raman scattering lidars significantly, and make them highly promising for numerous remote (up to 1 to 2 km altitude) atmospheric gas analysis tasks. Author

N85-32892# Joint Publications Research Service, Arlington, Va.
THE POSSIBILITIES OF REMOTE ANALYSIS OF ATMOSPHERIC GASES BASED ON RAMAN SCATTERING SPECTROSCOPY Abstract Only **c36**
G. N. Glazov and S. A. Danichkin *In its* USSR Rept.: Phys. and Math. (JPRS-UPM-85-004) 17 Jun. 1985 p 32 Transl. into ENGLISH from Zh. Prikl. Spektroskopii (Minsk), v. 41, no. 4, Oct. 1984 p 609-614 Original language document announced in IAA as A85-20589 (For primary document see N85-32860 21-70)
Avail: NTIS HC A06/MF A01

The use of ground lidars employing the Raman scattering effect for measuring the concentration profiles of atmospheric molecular gases is discussed. The random error in gas concentration measurements due to field fluctuations, shot noise, and fluctuations of the laser pulse energy is estimated. A complex index of probing efficiency is introduced which characterizes accuracy, sensitivity, spatial and temporal resolution, and range. The possibility of measuring background concentrations of CO2 at altitudes up to 10 km and CH4, NO, and SO2 at altitudes up to 1-2 km is demonstrated. V.L.

N85-32893# Joint Publications Research Service, Arlington, Va.
CHOICE OF OPTIMUM SATURATING ABSORBER FOR YAG PASSIVE MODE-LOCKING LASER Abstract Only **c36**
M. I. Demchuk, V. P. Mikhaylov, and K. V. Yumashev *In its* USSR Rept.: Phys. and Math. (JPRS-UPM-85-004) 17 Jun. 1985 p 33 Transl. into ENGLISH from Zh. Prikl. Spektroskopii (Minsk), v. 41, no. 4, Oct. 1984 p 566-571 (For primary document see N85-32860 21-70)
Avail: NTIS HC A06/MF A01

This study describes investigations conducted to develop optimization criteria for passive mode locking in YAG lasers. More than 90 passive shutters based on saturating absorbers with polymethine dyes in the liquid and solid phases, as well as alkali halide crystals with Z centers, are investigated. The findings make it possible to assess the limiting capabilities of passive mode locking YAG lasers for existing saturating absorber components, and to provide practical recommendations for the synthesis of new absorber components which provide the required set of laser parameters. A group of dyes is identified which provide the maximum energy and minimum ultrashort pulse length; these are dyes number 2681u in solution and film, number 7029, analogs of dye number 3955 containing ClO4 and F3DSO3 anions, as well as analog of dye number 1000 with a BF4 anion. The findings agree with the theory of passive mode locking of solid state lasers. Author

N85-32894# Joint Publications Research Service, Arlington, Va.
IN-CAVITY LASER IR SPECTRUM ANALYZER FOR INVESTIGATING NON-STEADY-STATE PROCESSES Abstract Only **c75**
V. A. Vratskiy and A. N. Kolerov *In its* USSR Rept.: Phys. and Math. (JPRS-UPM-85-004) 17 Jun. 1985 p 33 Transl. into ENGLISH from Zh. Prikl. Spektroskopii (Minsk), v. 41, no. 4, Oct. 1984 p 561-566 (For primary document see N85-32860 21-70)
Avail: NTIS HC A06/MF A01

An Li:F:F+2 in cavity IR spectrum analyzer is developed which provides sensitivity of approximately 5 x 10 to the minus 9th power 1/cm operating in the 870 to 1000 nm band. More than 200 new absorption lines are observed for atmospheric air, as well as a large number of highly excited transitions in the 925 to 960 nm band. The large number of absorption lines for atmospheric air results from weak transitions of water vapor, hydrocarbons and cyanogen compounds. The excited transition lines are caused by the occurrence of ionization products, as well as short-lived compounds formed through plasma chemical reactions. The characteristic variations in spectral intensity and form of the absorption line are determined. A method and instrumentation are developed for studying the dynamics of absorption (or emission) spectra that can be employed to investigate nonsteady state high speed phenomena in pulse plasma, explosion processes and the combustion of various flames, as well as to investigate the properties of intermediate products in plasma chemical reactions. Author

N85-32895# Joint Publications Research Service, Arlington, Va.
OPERATION OF SOLID STATE LASERS EXPOSED TO ELECTRON BEAM Abstract Only **c36**
M. R. Bedilov, Kh. B. Beysembayeva, P. K. Khabibullayev, and R. P. Saidov *In its* USSR Rept.: Phys. and Math. (JPRS-UPM-85-004) 17 Jun. 1985 p 34 Transl. into ENGLISH from Kvantovaya Elektron. (Moscow), v. 11, no. 10, Oct. 1984 p 2121-2126 (For primary document see N85-32860 21-70)
Avail: NTIS HC A06/MF A01

The basic findings from an investigation of the influence of the beam of electrons arising during the operation of a laser thermonuclear reactor on the characteristics of stimulated emission are presented. The experiments were conducted with ruby, YAG:Nd3+ garnet and various types of glass lasers. The temporal, energy and spectral characteristics are investigated for specimens of these materials irradiated by an electron beam with density of 10 to the 12th power to 10 to the 14th power e1/square centimeters. It is found experimentally that the degradation in the characteristics of the stimulated emission of a laser within the field of an electron beam is explained by defects formed in the active element, and by other factors as well. For example, defects are found in the substrates of the reflecting mirrors, which also degrade the performance. Contributing factors include the occurrence of color centers which absorb the exciting photon, reduced concentration of the active Cr 3+ ion, and the occurrence of defects absorbed in the lasing region. The findings are significant for the development of efficient laser thermonuclear reactors and radiation-resistant solid state lasers. 10 to the 12th power to 10 to the 14th power e1/square centimeters. Author

N85-32896# Joint Publications Research Service, Arlington, Va.
ESTABLISHMENT OF STEADY-STATE POWER LEVEL IN PULSE-PERIODIC EXCIMER LASER Abstract Only **c36**
V. M. Borisov, F. I. Vysikaylo, A. Yu. Vinokhodov, and Yu. B. Kiryukhin *In its* USSR Rept.: Phys. and Math. (JPRS-UPM-85-004) 17 Jun. 1985 p 34 Transl. into ENGLISH from Kvantovaya Elektron. (Moscow), v. 11, no. 10, Oct. 1984 p 2069-2073 (For primary document see N85-32860 21-70)
Avail: NTIS HC A06/MF A01

The characteristic time (or number of pulses) required for the lasing energy of a pulse-periodic excimer laser to drop from the monopulse energy level to the steady-state-value for a given pulse reposition frequency is studied. The experiments were performed on a pulseperiodic excimer laser with frequency variable from about 1 to 100 Hz. It was found that the pulse lasing energy drops to the defined value within 10 to 20 pulses, and is determined by a number of factors. An interpretation is provided for the dynamics of the change in the lasing energy from pulse to pulse. The behavior

observed is explained by the occurrence of acoustic waves in the loop, and the manner in which these waves interact with one another. Author

N85-32897# Joint Publications Research Service, Arlington, Va.
THE PROBLEM OF BRIGHTNESS ENHANCEMENT DURING LASER FREQUENCY DOUBLING Abstract Only c36
V. S. Averbakh, A. I. Makarov, and A. K. Potemkin *In its* USSR Rept.: Phys. and Math. (JPRS-UPM-85-004) 17 Jun. 1985 p 35 Transl. into ENGLISH from Kvantovaya Elektron. (Moscow), v. 11, no. 10, Oct. 1984 p 2049-2058 (For primary document see N85-32860 21-70)
Avail: NTIS HC A06/MF A01

The characteristics of the transformation of the spatial structure of powerful laser system beams when their frequencies are doubled in nonlinear crystals are investigated qualitatively. The aim is to derive a condition on the wavefront of the initial beam which must be satisfied in order to increase the brightness of second-harmonic radiation. The analysis is based on wave equations written in parabolic approximation for slowly fluctuating amplitudes of the interacting waves propagating in the direction of synchronism in the crystal. It is found that the change in brightness is determined by the ratio of the geometric component (characteristic angles) of the beam divergence to the diffraction component at the crystal input. An unchanged radiation brightness, and a 3.5-fold brightness enhancement are demonstrated experimentally as a function of the curvature of the wavefront for 88% power conversion in a KDP crystal with harmonic laser radiation of B = 5x10 to the 17th power w/square centimeters. Brightness enhancement is also observed in a KDP crystal cut for type-II synchronism (L = 2.5 cm). It is found that depolarization of no more than 0.3% is required in order to obtain near maximum brightness. B = 5x10 to the 17th power w/square centimeters. Author

N85-32898# Joint Publications Research Service, Arlington, Va.
LASER RADIATION PROPAGATION IN INERTIALESS NONLINEAR MEDIUM Abstract Only c36
K. S. Gochelashvili, I. V. Chashey, and V. I. Shishov *In its* USSR Rept.: Phys. and Math. (JPRS-UPM-85-004) 17 Jun. 1985 p 35 Transl. into ENGLISH from Kvantovaya Elektron. (Moscow), v. 11, no. 10, Oct. 1984 p 2036-2040 (For primary document see N85-32860 21-70)
Avail: NTIS HC A06/MF A01

The propagation of laser radiation in a nonlinear medium with smaller than average variations in the index of refraction is investigated. An equation is derived for the second-order coherence function for propagation over long distances, where a saturated fluctuation condition replaces exponential growth in perturbations in the wave. The equation is analyzed on the basis of a self-similar solution. Similar results are found to hold for a turbulent nonlinear medium as well. Author

N85-32899# Joint Publications Research Service, Arlington, Va.
DYNAMICS OF EMISSION FROM DYE LASERS EMPLOYING SYNCHRONOUS PUMPING BY LIMITED PICOSECOND PULSE TRAIN Abstract Only c36
A. I. Kovrigin, V. A. Nekhayenko, S. M. Pershin, and A. A. Podshivalov *In its* USSR Rept.: Phys. and Math. (JPRS-UPM-85-004) 17 Jun. 1985 p 36 Transl. into ENGLISH from Kvantovaya Elektron. (Moscow), v. 11, no. 10, Oct. 1984 p 2007-2018 (For primary document see N85-32860 21-70)
Avail: NTIS HC A06/MF A01

Synchronous pulsed emission of organic dye lasers pumped by a train of picosecond pulses from a mode-locked laser is examined theoretically and experimentally. A model is developed for the production of supershort light pulses. A four-level model of the active medium is employed, making it possible to investigate the mode-locking kinetics and to calculate the limiting emission parameters. Because the synchronous emission process is unsteady, it is found that the parameters in the pulse train change significantly, and that there is no complete time correlation between an emitted pulse and its corresponding pumping pulse. It is recommended that trains containing more than thirty pulses be employed in order to obtain synchronously tracking pulses with minimum duration, and that the length of the dye laser cavity be adjusted to obtain the maximum second-harmonic radiation energy in order to produce the shortest possible pulses. The experimental findings agree well with the theory; the minimum spectrally-limited pulse length achieved is 8 ps. Author

N85-32900# Joint Publications Research Service, Arlington, Va.
HIGH-POWER TWO-FREQUENCY CW DYE LASER Abstract Only c36
V. I. Balykin and A. I. Sidorov *In its* USSR Rept.: Phys. and Math. (JPRS-UPM-85-004) 17 Jun. 1985 p 36-37 Transl. into ENGLISH from Kvantovaya Elektron. (Moscow), v. 11, no. 10, Oct. 1984 p 2001-2006 Original language document previously announced in IAA as A85-21024 (For primary document see N85-32860 21-70)
Avail: NTIS HC A06/MF A01

The dual-frequency generation of a CW dye laser pumped by an argon laser was investigated experimentally. Stable dual-mode generation with an output power of 1.23 W and an efficiency of 14 percent, which is comparable to the efficiency of single-mode dye ring lasers, was achieved. The fluctuations of the frequency interval between the two modes and the width of each of the axial mode did not exceed 10 MHz. V.L.

N85-32901# Joint Publications Research Service, Arlington, Va.
SATURATION EFFECT IN MULTILEVEL LASING MEDIA Abstract Only c36
V. I. Lvov, A. A. Stepanov, and V. A. Shcheglov *In its* USSR Rept.: Phys. and Math. (JPRS-UPM-85-004) 17 Jun. 1985 p 37 Transl. into ENGLISH from Kvantovaya Elektron. (Moscow), v. 11, no. 10, Oct. 1984 p 1975-1983 Original language document previously announced in IAA as A85-21021 (For primary document see N85-32860 21-70)
Avail: NTIS HC A06/MF A01

An approach is proposed which makes it possible to adequately describe the saturation effect observed under conditions of resonance interaction between multifrequency emission and the active medium. The efficiency of the method proposed here is demonstrated for two typical cases, i.e., multilevel media with parallel and cascade transitions. V.L.

N85-32902# Joint Publications Research Service, Arlington, Va.
OPTICAL INHOMOGENEITIES IN A NANOSECOND-PULSE IODINE PHOTODISSOCIATION LASER WITH SLOW UV RADIATION PUMPING Abstract Only c36
I. Skala, M. Khvoyka, L. Pekarek, B. Kralikova, V. S. Zuyev, K. S. Korolkov, and Ye. P. Orlov *In its* USSR Rept.: Phys. and Math. (JPRS-UPM-85-004) 17 Jun. 1985 p 37-38 Transl. into ENGLISH from Kvantovaya Elektron. (Moscow), v. 11, no. 10, Oct. 1984 p 1940-1946 Original language document previously announced in IAA as A85-21018 (For primary document see N85-32860 21-70)
Avail: NTIS HC A06/MF A01

The evolution of the profile of the refractive index gradient of the active medium of an iodine nanosecond-pulse amplifier is investigated for the case where the pumping pulse duration is greater than the period of the radial acoustic oscillations of the gas in the laser cell. Two components, one of which increases monotonically with time and the other which oscillates rapidly, are identified in the refractive index gradient, and it is shown that high beam directivity can be achieved in this type of amplifier. The diameter of the amplifier and, consequently, its output energy are limited by the time of inversion and sound velocity. V.L.

N85-32903# Joint Publications Research Service, Arlington, Va.
EXCIMER-LASER GENERATOR OF POWERFUL UV PICOSECOND PULSES SYNCHRONIZED WITH PICOSECOND PULSES IN VISIBLE AND IR BANDS Abstract Only c36
S. A. Akhmanov, A. M. Valshin, V. M. Gordiyenko, M. S. Dzhidzhoyev, S. V. Krayushkin, V. T. Platonenko, and V. K. Popov *In its* USSR Rept.: Phys. and Math. (JPRS-UPM-85-004) 17 Jun. 1985 p 38 Transl. into ENGLISH from Kvantovaya Elektron. (Moscow), v. 11, no. 10, Oct. 1984 p 1897-1898 (For primary

document see N85-32860 21-70)
Avail: NTIS HC A06/MF A01

An XeCl excimer-laser based oscillator which produces powerful ultrashort UV pulses with durations of approximately 30 ns and energy of approximately 10 mJ at lambda = 0.308 micron is studied. The master oscillator is a YAlO3:Nd3+ yttrium aluminate passive mode-locked laser. A train of picosecond pulses from this device is used to drive a CDA-crystal-harmonic generator (lambda = 0.53 micron). Second-harmonic radiation from this stage drives a C160 dye laser (lambda = 616 nanometers), and the XeCl excimer oscillator then amplifies the second-harmonic of the C160 output. The system can be used for experiments on picosecond UV photolysis incorporating picosecond recordings of products by active spectroscopy, as well as for investigating laser annealing processes, etc. Author

N85-32904# Joint Publications Research Service, Arlington, Va.
POSSIBILITY OF MEASUREMENT OF SMALL DISPLACEMENTS BY RING LASER Abstract Only **c36**
E. M. Belenov, M. V. Danileyko, and A. V. Uskov *In its* USSR Rept.: Phys. and Math. (JPRS-UPM-85-004) 17 Jun. 1985 p 38-39 Transl. into ENGLISH from Kvantovaya Elektron. (Moscow), v. 11, no. 10, Oct. 1984 p 1894-1896 Original language document previously announced in IAA as A85-21015 (For primary document see N85-32860 21-70)
Avail: NTIS HC A06/MF A01

A system for measuring small displacements is presented which makes use of certain dynamic characteristics of ring lasers associated with energy redistribution between traveling waves propagating in the opposite directions. The minimum detectable amplitude, which is limited by emission intensity fluctuations, is estimated at 10 to the -18th - 10 to the -19th cm. A schematic diagram of the system is presented. V.L.

N85-32905# Joint Publications Research Service, Arlington, Va.
INFRARED LASER HOLOGRAPHY USED IN FUSION PLASMA STUDIES Abstract Only **c36**
In its USSR Rept.: Phys. and Math. (JPRS-UPM-85-004) 17 Jun. 1985 p 40 Transl. into ENGLISH from Sov. Latviya (Riga), Mar. 1985 p 4 (For primary document see N85-32860 21-70)
Avail: NTIS HC A06/MF A01

A method of producing holographic images using invisible infrared rays was proposed at the Georgian Academy of Sciences' Institute of Physics. It makes it possible not only to reproduce the object being depicted in three dimensions, but also literally to see through it. This makes it possible to detect in an object various internal impurities and flaws which are undetectable by other means. The transparent hologram is produced by means of an instantaneous flash of a powerful infrared laser, which is widely used in the welding and cutting of metals. The image is recorded on polymethyl methacrylate or transparent cellulose film. Infrared holography is also a good tool for the study of plasma as it is heated by laser radiation. Such plasma exists for only several millionths of a second. The accuracy of the measurements increases sharply in comparison with that of other methods. Such experiments are being conducted as part of the large-scale research program on controlled thermonuclear fusion. Infrared holography also holds promise for optics, and for inspecting the purity of materials in semiconductor technology. Author

N85-32906# Joint Publications Research Service, Arlington, Va.
TUNABLE LASERS WITH HIGH CONVERSION EFFICIENCY Abstract Only **c36**
In its USSR Rept.: Phys. and Math. (JPRS-UPM-85-004) 17 Jun. 1985 p 41 Transl. into ENGLISH from Mosk. Pravda (Moscow), no. 56 (19776), 7 Mar. 1985 p 1, columns 5-6 (For primary document see N85-32860 21-70)
Avail: NTIS HC A06/MF A01

Work by scientists of the Uzbek Academy of Sciences' Institute of Electronics is opening up new prospects for the utilization of laser technology. These scientists have succeeded in raising the smooth conversion efficiency of laser radiation to 75 percent. This is almost five times as high as the characteristics that were previously achieved. Quantum oscillators that are tunable over a wide range of the spectrum are finding use in spectroscopy, holography, chemistry, biology, and in the development of flexible laser systems. Author

N85-32907# Joint Publications Research Service, Arlington, Va.
SELF Q-MODULATION AND GENERATION OF SHORT PULSES IN DISTRIBUTED-FEEDBACK LASERS Abstract Only **c36**
R. A. Karamaliyev and Dao Suan Khay *In its* USSR Rept.: Phys. and Math. (JPRS-UPM-85-004) 17 Jun. 1985 p 42 Transl. into ENGLISH from Dokl. Akad. Nauk Azerbaydzhanskoy SSR (Baku), v. 40, no. 8, Aug. 1984 p 31-33 (For primary document see N85-32860 21-70)
Avail: NTIS HC A06/MF A01

The characteristics of the oscillatory mode of distributed-feedback dye lasers forming an optically-induced periodic gain structure are investigated. It is found analytically that short pulses in distributed-feedback lasers result from self-modulation of the Q-factor or the molecular loss coefficient. Distributed-feedback dye lasers are found to produce light pulses several tens of picoseconds long. Author

N85-32908# Joint Publications Research Service, Arlington, Va.
LOW-THRESHOLD INJECTION InGaAsP/GaAs DOUBLE HETEROSTRUCTURE LASERS WITH SEPARATE LIMITING OBTAINED BY LIQUID-PHASE EPITAXY (LAMBDA = 0.78 DIVIDED BY 0.87 MICRONS, I SUB thr = 460 A/cm 2, T = 300 K) Abstract Only **c36**
Zh. I. Alfeerov, I. N. Arsentev, L. S. Vavilova, D. Z. Garbuzov, and V. V. sKrasovskiy *In its* USSR Rept.: Phys. and Math. (JPRS-UPM-85-004) 17 Jun. 1985 p 42-43 Transl. into ENGLISH from Prikl. Mat. i Mekhan. (Moscow), v. 48, no. 4, Jul. - Aug. 1984 p 1655-1659 (For primary document see N85-32860 21-70)
Avail: NTIS HC A06/MF A01

Low-threshold infrared and red separate-limited double heterostructure lasers based on InGaAsP/GaAs structures with active region thickness d << d sub o = 0.1+0.03 micron, prepared by ordinary liquid-phase epitaxy, are described. The devices employ additional waveguide layers of InGaAsP between the narrow-zone active region and the wide-zone emitters. The active region is 2 to 10/6 micron thick, with the total thickness of the waveguide lasers comprising 0.4 micron. A minimum threshold of 460 A/sq cm (T = 300 K) is obtained for four-layer specimens. Continuous lasing is obtained at room temperature in lasers not employing strip designs. The drop in thresholds in double heterostructure lasers with separate limiting results from the fact that the absolute threshold current densities continue to drop as d becomes smaller in the region d < d sub o, in spite of the near-linear drop in r = f(d). E.A.K.

N85-32909# Joint Publications Research Service, Arlington, Va.
SPACE-TIME CHARACTERISTICS OF FIELD IN LONGITUDINAL PULSE-PERIOD DISCHARGE TYPICAL IN PUMPING OF SELF-TERMINATING LASERS Abstract Only **c36**
V. N. Kukharev *In its* USSR Rept.: Phys. and Math. (JPRS-UPM-85-004) 17 Jun. 1985 p 43 Transl. into ENGLISH from Zh. Tekhn. Fiz. (Leningrad), v. 54, no. 10, Oct. 1984 p 1910-1914 Previously announced in IAA as A85-36514 (For primary document see N85-32860 21-70)
Avail: NTIS HC A06/MF A01

Experimental findings on determining the field behavior in a pulse-periodic discharge with high repetition frequencies are presented. The spatial distribution of the potential in the plasma of a longitudinal pulse-periodic discharge, and the behavior of that distribution over the entire gas-discharge pulse, are investigated. It is found experimentally that the pulse discharge process at high repetition frequencies can be divided into three stages: during the first, the plasma column is polarized, which is followed by the transmission of recharging ionization waves, causing an alternate rise and fall in the voltage near the electrodes. The third stage is characterized by a practically linear potential distribution in the plasma column. The relationship between the features of the pulse-periodic discharge employed in pumping

self-terminating lasers and the operating characteristics of such lasers are discussed. The formation of the pulse structure in copper-vapor lasers is analyzed as an example. Author

N85-32910# Joint Publications Research Service, Arlington, Va.
INFLUENCE OF TECHNOLOGICAL FACTORS ON LUMINESCENCE CHARACTERISTICS OF InGaAsP/InP HETEROLASERS (LAMBDA = 1.55 MICRONS) Abstract Only c36
A. T. Gorelenok, V. G. Gruzdov, and I. S. Tarasov *In its* USSR Rept.: Phys. and Math. (JPRS-UPM-85-004) 17 Jun. 1985 p 43-44 Transl. into ENGLISH from Zh. Tekhn. Fiz. (Leningrad), v. 54, no. 10, Oct. 1984 p 2047-2050 (For primary document see N85-32860 21-70)
Avail: NTIS HC A06/MF A01

The influence of lattice parameter mismatch and the thicknesses of the intermediate layer and active region on the threshold current density, differential quantum efficiency and quantum radiation yield characteristics of InGaAsP/InP double heterostructure lasers are investigated. The lasers were created by liquid phase epitaxy on substrates of n-InP;Sn with (100) orientation in a step cooling process. The use of intermediate layers to prevent acceptors from entering the active region made it possible to reduce the threshold current density at 1.5 micro m to approximately 1 kA/sq cm, and to achieve threshold current densities of 4 - 4.5 kA/sq cm. Author

N85-32911# Joint Publications Research Service, Arlington, Va.
POWERFUL XeCl EXCIMER ELECTRIC DISCHARGE LASER WITH GOOD TEMPORAL STABILITY AND FAST RESPONSE TIME Abstract Only c36
M. S. Dzhidzhoyev, V. T. Platonenko, and V. K. Popov *In its* USSR Rept.: Phys. and Math. (JPRS-UPM-85-004) 17 Jun. 1985 p 44 Transl. into ENGLISH from Vestn. Mosk. Univ.: Fiz., Astron. (Moscow), v. 25, no. 5, Sep. - Oct. 1984 p 113-115 (For primary document see N85-32860 21-70)
Avail: NTIS HC A06/MF A01

An XeCl excimer laser producing approximately 300 mJ with a pulse length of approximately 15 ns, operating time of 100 ns and temporal stability exceeding + or - 3 ns is described. The pulse energy was measured by means of a calorimeter with galvanometer: at 3 atm, the maximum lasing energy for an HC1:Xa:Ha laser employing proportions of 3:30:2250 was 0.3 J with a pulse length of 15 ns. Because of its good temporal stability and fast response time, the system can be employed in conjunction with various laser devices, including passive mode locked YAG:Nd sup 3+ lasers. Author

N85-32912# Joint Publications Research Service, Arlington, Va.
SPECTRAL-LUMINESCENCE CHARACTERISTICS AND INDUCED EMISSION OF Nd-3(+) ION IN Gd(2-X)Nd(X)(WO4)3 CRYSTALS Abstract Only c36
V. A. Berenberg, A. O. Ivanov, L. I. Krutova, I. V. Mochalov, and V. S. Terpugov *In its* USSR Rept.: Phys. and Math. (JPRS-UPM-85-004) 17 Jun. 1985 p 44-45 Transl. into ENGLISH from Optika i Spektroskopiya (Leningrad), v. 57, no. 3, Sep. 1984 p 455-459 (For primary document see N85-32860 21-70)
Avail: NTIS HC A06/MF A01

Highly concentrated Gd(2-x)Nd(x)WO4)(3) crystals obtained by the Chokhral'skiy method on a Donets-3 commercial system are investigated. Spectroscopic measurements to determine the Stark levels and to identify transitions between levels were conducted by traditional absorption and luminescence analysis methods. The findings indicate that gadolinium neodymium tungstate crystals can be used effectively in solid state microlasers pumped by light pulses with durations of a few microseconds. Author

N85-32913# Joint Publications Research Service, Arlington, Va.
ADJUSTMENT OF RADIATION WAVELENGTH OF MULTIMODE InP-GaInAsP INJECTION HETEROLASERS Abstract Only c36
Ya. E. Kirson, E. E. Klotynsh, and I. A. Churkste *In its* USSR Rept.: Phys. and Math. (JPRS-UPM-85-004) 17 Jun. 1985 p 48 Transl. into ENGLISH from Izv. Akad. Nauk Latviyskoy SSR: Ser. Fiz. i Tekhn. Nauk (Riga), no. 5, Oct. - Nov. 1984 p 15-18 (For primary document see N85-32860 21-70)
Avail: NTIS HC A06/MF A01

The spectral tuning of injection lasers is investigated on the basis of a forbidden InP-GaInAsP mesastrip structure operating in the continuous mode at room temperature. In order to avoid heating of the active region when the pumping current changes, the laser was driven by 50 ns rectangular pulses at 2 MHz. Spectral recordings revealed that five mode jumps occur as the temperature increases from 0 to 45 C. The behavior of these modes is analyzed; it is found that the jumps are caused by heat induced changes in the parameters of the optical cavity. Increasing the pumping current beyond the threshold level also causes mode transfer, as the result of which the power averaged wavelength increases while the wavelength of the individual modes remains unchanged, at least for pumping current smaller than 2.5I sub thr. Author

N85-32914# Joint Publications Research Service, Arlington, Va.
SELECTIVE POPULATION OF N = 3 OVIII LEVEL DURING EXPANSION OF LASER PLASMA IN HELIUM Abstract Only c36
S. P. Zhukov, V. V. Korukhov, B. I. Troshin, and A. A. Chernenko *In its* USSR Rept.: Phys. and Math. (JPRS-UPM-85-004) 17 Jun. 1985 p 48-49 Transl. into ENGLISH from Pisma Zh. Eksperim. i Teor. Fiz. (Moscow), v. 40, no. 8, Oct. 1984 p 340-342 (For primary document see N85-32860 21-70)
Avail: NTIS HC A06/MF A01

The mechanism underlying the formation of inverse population of levels of multiply charged ions on the basis of recharging is realized experimentally for the first time. The experimental setup consisted of a neodymium glass laser, a vacuum chamber and a X-ray spectrograph. The experiments were conducted with spatial resolution along the plasma flame, using a pulse length of approximately 0.5 ns. It is found experimentally that when a laser plasma flame containing multiply charged oxygen ions expands, the OVIII oxygen levels become selectively populated due to recharging of the oxygen nuclei on helium ions. Author

N85-32915# Joint Publications Research Service, Arlington, Va.
PASSIVE Q-MODULATION OF OPTICAL CAVITIES BY KCl CRYSTALS CONTAINING OH(-) -IONS Abstract Only c36
L. M. Sobolev, V. V. Bryukvin, I. A. Parfianovich, and E. E. Penzina *In its* USSR Rept.: Phys. and Math. (JPRS-UPM-85-004) 17 Jun. 1985 p 49 Transl. into ENGLISH from Optika i Spektroskopiya (Leningrad), v. 57, no. 5, Nov. 1984 p 954-956 (For primary document see N85-32860 21-70)
Avail: NTIS HC A06/MF A01

The investigation of color centers in KCl-OH crystals additively colored in potassium vapors is described. It is found that irradiation of colored crystals by white light results in the formation of a series of F aggregate color centers which are stable at room temperature. The use of such crystals as passive laser shutters to Q modulate the cavity of a YAG-Nd(3+) laser (1.064 micro m) is described. It is found that working color centers that are thermally and optically stable at room temperature can be obtained by additive coloration of hydroxyl-doped KCl crystals in alkali metal vapors followed by exposure to light. Similar centers are unstable at room temperature if the KCl crystals contain no OH(-) ions, and cannot be used as passive shutters. An interpretation is given of the mechanism underlying the stabilization of working centers. Author

N85-32916# Joint Publications Research Service, Arlington, Va.
ACOUSTIC WAVE SCATTERING BY ROUND CYLINDRICAL SHELL REINFORCED WITH STRINGERS Abstract Only c71
A. P. Poddubnyak and A. R. Voloshin *In its* USSR Rept.: Phys. and Math. (JPRS-UPM-85-004) 17 Jun. 1985 p 50 Transl. into ENGLISH from Dokl. Nauk Ukr. SSR: Ser. A, Fiz.-Mat. i Tekhn. Nauki (Kiev), no. 10, Oct. 1984 p 45-47 (For primary document see N85-32860 21-70)
Avail: NTIS HC A06/MF A01

The influence of elastic ribs within a thin cylindrical shell submerged in liquid on the echo signal structure is investigated.

An elastic infinitely long round cylindrical shell stiffened internally by a regular system of stringers is struck by a plane pressure wave with its front parallel to the axis of the scatterer. Boundary conditions are assigned on the interface surface between the liquid and the elastic system (assuming the shell to contain a vacuum). The problem is solved in two stages: the scattering of sound by a shell within ribs is investigated, and then the wave field generated by oscillations of a ribbed shell is found. The scattered wave is found to consist of waves that are reflected and reradiated by the shell envelope itself with no influence from the reinforcing ribs, and three types of waves radiated by the shell under the influence of tangential and normal shifts, as well as rotation caused by interaction between the envelope and the ribs at the points of contact. If the shell thickness is set equal to zero, the problem becomes one of scattering of acoustic waves by a regular lattice of elastic ribs contained an acoustically soft round cylindrical shield. Author

N85-32917# Joint Publications Research Service, Arlington, Va.
IDENTIFICATION OF VIBRATIONAL-ROTATIONAL TRANSITIONS OF Os-192O4 WITHIN FREQUENCY TUNING LIMITS OF HIGH PRESSURE CO2 WAVEGUIDE LASER Abstract Only **c72**

Ye. N. Bazarov, G. A. Gerasimov, V. P. Gubin, V. L. Derbov, A. D. Novikov, S. Yu. Otrokhov, A. I. Sazonov, and V. U. Fomin *In its* USSR Rept.: Phys. and Math. (JPRS-UPM-85-004) 17 Jun. 1985 p 51 Transl. into ENGLISH from Optika i Spektroskopiya (Leningrad), v. 57, no. 3, Sep. 1984 p 434-438 (For primary document see N85-32860 21-70)
Avail: NTIS HC A06/MF A01

The transitions of the OsO4-192 molecule, the most common isotype modification of osmium tetroxide, are observed and identified; a set of molecular constants to describe these transitions within the framework of the Moret-Bially formalism is obtained. On the basis of preliminary calculation of the frequencies and intensities, the strongest lines are related to permitted transitions of the primary band nu sub 3. The tuning band of the laser employed covered 1.5 GHz. Transitions of the P- and R- branches of the nu sub 3 band of OsO4-192 at values of J exceeding 100 are observed in this range of lines. The spectra were observed and photographed from the screen of an oscilloscope swept in sync with the voltage applied to the piezoceramic of the laser. The absorption spectra of OsO4-192 on the CO2P14 and R16 lasing lines presented as an example. Author

N85-32918# Joint Publications Research Service, Arlington, Va.
TOWARD A THEORY OF EXCITATION OF ATOMS DURING NUCLEAR AND MAGNETIC NEUTRON SCATTERING Abstract Only **c72**

G. L. Yudin *In its* USSR Rept.: Phys. and Math. (JPRS-UPM-85-004) 17 Jun. 1985 p 51-52 Transl. into ENGLISH from Dokl. Akad. Nauk SSSR (Moscow), v. 297, no. 2, Nov. 1984 p 363-368 (For primary document see N85-32860 21-70)
Avail: NTIS HC A06/MF A01

A theory of atom excitation is proposed which combines the nuclear parts of the problem and makes it possible to find directly the atom excitation and ionization cross section in collisions with neutrons. The single-electron problem is examined in general form, and can be extended to the case of several electrons with allowance for suppression of magnetic scattering without difficulty. Magnetic neutron scattering on magnetoactive electrons is taken into account, as well as nuclear scattering caused by interaction between neutrons and nuclei. Author

N85-32919# Joint Publications Research Service, Arlington, Va.
NONEQUILIBRIUM KINETICS OF GROWTH OF OXIDE LAYER GRAINS DURING LASER HEATING OF METALS IN AIR Abstract Only **c26**

D. T. Alimov, V. A. Bobyrev, F. V. Bunkin, V. L. Zhuravskiy, V. S. Lukyanchuk, Ye. A. Morozova, S. A. Ubaydullayev, and P. K. Khabibullayev *In its* USSR Rept.: Phys. and Math. (JPRS-UPM-85-004) 17 Jun. 1985 p 52 Transl. into ENGLISH from Dokl. Akad. Nauk SSSR (Moscow), v. 297, no. 4, Dec. 1984 p 871-876 Original language document previously announced in IAA as A85-20090 (For primary document see N85-32860 21-70)
Avail: NTIS HC A06/MF A01

A study has been made of grain growth in the oxide layer during the heating of cobalt specimens by a 25W CO2 laser to 1200 C. The function of the grain size distribution following laser heating is shown to have two maxima corresponding to small and large grains. In contrast, isothermal oxidation of the same specimens in an electric oven leads to a gradual increase of grain size, i.e., the maximum of the size distribution function shifts in the direction of larger grain sizes. The results are explained in terms of nonequilibrium kinetics of grain growth during laser heating. V.L. (IAA)

N85-32920# Joint Publications Research Service, Arlington, Va.
RADIATIVE-COLLISION GENERATION OF SOUND IN GASES SUBJECTED TO SINGLE-PULSE OPTICAL EXCITATION Abstract Only **c72**

V. M. Shalayev and V. Z. Yakhnin *In its* USSR Rept.: Phys. and Math. (JPRS-UPM-85-004) 17 Jun. 1985 p 53 Transl. into ENGLISH from Zh. Eksperim. i Teor. Fiz. (Moscow), v. 87, no. 4, Oct. 1984 p 1211-1220 (For primary document see N85-32860 21-70)
Avail: NTIS HC A06/MF A01

The phenomenon of radiative-collision generation of sound caused by light-induced drift of gases subjected to single-pulse optical excitation is analyzed theortically. The spectral characteristics of the acoustic signal resulting from light-induced drift, and their relationship with the parameters of the medium and the radiation, are analyzed. Two mechanisms are found to underlie the generation of sound by light-induced drift: selective and diffusive. A necessary and sufficient condition for the development of a diffusive current of excited particles is that the intensity gradient of the inducing radiation be nonzero. The calculations provide the theoretical basis for a method for determining the transport scattering cross-sections of excited atoms and molecules from experimental data on the acoustic signal resulting from light-induced drift in the field of a single light pulse. The findings are applicable to laser acoustic sources as well. Author

N85-32921# Joint Publications Research Service, Arlington, Va.
DOPPLER SPECTROMETER FOR MEASURING NARROW PHOTOCHEMICAL GAPS IN INHOMOGENEOUSLY BROADENED SPECTRA Abstract Only **c36**

K. K. Rebane and V. Palm *In its* USSR Rept.: Phys. and Math. (JPRS-UPM-85-004) 17 Jun. 1985 p 53-54 Transl. into ENGLISH from Izv. Akad. Nauk Estonskoy SSR: Fiz. Mat. (Tallinn), v. 33, no. 4 p 461-463 (For primary document see N85-32860 21-70)
Avail: NTIS HC A06/MF A01

A method is proposed for measuring the contours of narrow photochemical gaps in spectra by using the Doppler frequency shift of the broadened lasing line. An experimental setup is described that incorporates a single-freqeuncy CR-699-21 CW Rh6G dye laser with a Doppler modulator that broadens the line by approximately 0.005 delta nu. A spectrally narrow gap is formed in the absorption spectrum of the object by exposing it to the beam from a monochromatic laser with frequency, line width of delta sub L (delta sub L < < delta 0.01 to 0.0001/cm) and intensity of approximately 10 mu W/sq mm until the transmission at frequency nu micron increases by a factor of 5 to 10. The photochemical gap width in the absorption spectrum of H-2 octaethylporphine in a polystyrene matrix at 1.5K was measured, yielding a half-width of (17 + or - 4)x0.001/cm. The Doppler-effect contour measurement method is promising for the measurement of super narrow gaps occurring, for example, in objects with high optical density. It can also be used with lasers having poor long-term stability, as well as multimode lasers. Author

N85-32922# Joint Publications Research Service, Arlington, Va.
RESONANT ENERGY TRANSFER DURING STRONG EXCITATION Abstract Only **c72**

A. S. Agabekyan *In its* USSR Rept.: Phys. and Math. (JPRS-UPM-85-004) 17 Jun. 1985 p 54 Transl. into ENGLISH from Zh.

Prikl. Spektroskopii (Minsk), v. 41, no. 4, Oct. 1984 p 677-680 (For primary document see N85-32860 21-70)
Avail: NTIS HC A06/MF A01

This study examines the kinetics of excitation attenuation and addresses the possible role of phase relationships in the energy transfer process in a donor-acceptor pair in which both ions are initially excited, and there are no processes involving up-conversion of the acceptor radiation frequency. Coherence of the energy transfer is found to be disturbed by competition between the energy transfer and ion decay processes. Regardless of the relationship between the system parameters, only noncoherent energy transfer can occur in a pair of excited ions which interact resonantly. Different limiting cases of energy transfer are investigated. Author

N85-32923# Joint Publications Research Service, Arlington, Va.
TRANSPARENCY OF WATER 9N 186 - 500 nm REGION Abstract Only c74
N. P. Romanov and V. S. Shuklin *In its* USSR Rept.: Phys. and Math. (JPRS-UPM-85-004) 17 Jun. 1985 p 54 Transl. into ENGLISH from Zh. Prikl. Spektroskopii (Minsk), v. 41, no. 4, Oct. 1984 p 647-652 Original language document previously announced in IAA as A85-20593 (For primary document see N85-32860 21-70)
Avail: NTIS HC A06/MF A01

A method involving partial steam condensation is described which makes it possible to obtain samples of clear water whose transparency is higher than that of samples obtained by any other techniques. The exponential extinction coefficients of the samples are determined spectrophotometrically in the wavelength range 186-500 nm at 23 + or - 0.5 C. Within the experimental uncertainty (+ or - 0.015 per m), the values obtained are equal to zero in the range 300-490 nm and coincide with the extinction coefficient due to molecular scattering at wavelengths of 230 nm and greater. An analysis of the results obtained shows that the absorption coefficient of water at wavelengths below 210 nm depends expontentially on the energy of the absorbed quanta. V.L. (IAA)

N85-32924# Joint Publications Research Service, Arlington, Va.
ACTIVATION ANALYSIS OF NATURAL WATER USING NEUTRONS OF VARIOUS ENERGIES Abstract Only c73
R. Kamidova and A. A. Abdullayev *In its* USSR Rept.: Phys. and Math. (JPRS-UPM-85-004) 17 Jun. 1985 p 55 Transl. into ENGLISH from Izv. Akad. Nauk USSR: Ser. Fiz.-Mat. Nauk (Tashkent), no. 4, Jul. - Aug. 1984 p 55-56 (For primary document see N85-32860 21-70)
Avail: NTIS HC A06/MF A01

This study investigates the use of activation methods with fast neutrons and protons for analyzing natural water of various origin. The induced activity of the radio nuclides formed by cyclotron irradiation of the specimens was measured by a Ge(Li) detector in conjunction with multichannel analyzer. The complete absorption gamma-lines and gamma lines resulting from the summation effect are identified. Analyses of natural water and investigation of the gamma-spectra of proton-irradiated specimens demonstrated the prospects of selective analysis methods. Thermal neutron activation is found to be best for analyzing natural water. Author

N85-32925# Joint Publications Research Service, Arlington, Va.
TRANSFORMATION OF CHARGED PARTICLE BEAMS BY CONCENTRATING ELECTRO-OPTICAL SYSTEMS Abstract Only c73
Ye. V. Shpak and S. Ya. Yavor *In its* USSR Rept.: Phys. and Math. (JPRS-UPM-85-004) 17 Jun. 1985 p 55 Transl. into ENGLISH from Zh. Tekhn. Fiz. (Leningrad), v. 54, no. 10, Oct. 1984 p 1992-1998 (For primary document see N85-32860 21-70)
Avail: NTIS HC A06/MF A01

Analytical expressions are derived which make it possible to use the characteristics of the initial phase contour of a given electro-optical system to fully characterize the crossover produced by the system. The formulas obtained are analogous to those in electron optics to relate the positions of the object and its image, as well as linear and angular magnification. The concentrating systems are investigated by finding the envelopes of the charged-particle beams and examining the movement of the representative points of the beam in phase space. The transformation of charged particle beams by a wide class electrooptical systems, including systems with a plane curvilinear axial trajectory, is investigated. Formulas are derived which determine the connection between the crossover position at the input and output of the concentrating system, as well as the angular and linear magnification during crossover-crossover conversion. Author

N85-32926# Joint Publications Research Service, Arlington, Va.
THERMAL CONTRACTION OF CURRENT FLOW THROUGH ELECTRODE TURBULENT BOUNDARY LAYER Abstract Only c75
A. V. Nedospasov, V. D. Khait, and A. E. Sheyndlin *In its* USSR Rept.: Phys. and Math. (JPRS-UPM-85-004) 17 Jun. 1985 p 56 Transl. into ENGLISH from Dokl. Akad. Nauk SSSR (Moscow), v. 280, no. 3, Jan. 1985 p 594-597 (For primary document see N85-32860 21-70)
Avail: NTIS HC A06/MF A01

The critical current at which contraction of the discharge in an MHD generator occurs in the presence of turbulent plasma flow along the electrode (anode) walls as a result of heat balance instability at the walls was calculated analytically as a function of the wall temperature. The peak in the current-voltage characteristic of the boundary layer on the electrode was taken as the point of instability. The resistivity and current were calculated by solving a nonlinear ordinary differential equation governing stationary heat flow in the boundary layer. Elsewhere the plasma was assumed to be in equilibrium. The conductivity was assumed to be an exponential function of the temperature only. Convective heat transfer along the electrode wall was ignored and it was assumed that the temperature of the electrode wall was determined by the balancing of heat flow to the wall from the plasma and the heat flow to the external surface of the wall, which was held constant. The theoretical results agreed well with measurements performed on K-1 and U-02 setups and on a burner with a laminar flow. The results how that the critical current increases rapidly above 2000 K. Author

N85-32927# Joint Publications Research Service, Arlington, Va.
MIRROR REFLECTION OF CHARGED PARTICLES FROM +AMORPHOUS AND POLYCRYSTALLINE SURFACES Abstract Only c72
M. A. Kumakhov *In its* USSR Rept.: Phys. and Math. (JPRS-UPM-85-004) 17 Jun. 1985 p 56 Transl. into ENGLISH from Dokl. Akad. Nauk SSSR (Moscow), v. 279, no. 4, Dec. 1984 p 862-863 (For primary document see N85-32860 21-70)
Avail: NTIS HC A06/MF A01

The interaction of a positively charged particle with the surface of a smooth amorphous or polycrystalline film (such as glass) is examined. The potential of the interaction between the particle and the surface of the substance is calculated for the case of glancing incidence, in contrast to the case of tunneling, by taking into consideration the repulsion from atoms throughout the entire depth of the substance. The angles of mirror reflection and, for comparison, the critical tunneling angles in silicon strips, are tabulated. The mirror reflection angles are smaller than the characteristic tunneling angles. Author

N85-32928# Joint Publications Research Service, Arlington, Va.
AN ATTEMPT TO DETECT INDUCED NEUTRON CAPTURE IN LASER RADIATION FIELD Abstract Only c73
S. M. Mironov and G. U. Muradyan *In its* USSR Rept.: Phys. and Math. (JPRS-UPM-85-004) 17 Jun. 1985 p 57 Transl. into ENGLISH from Yadernaya Fiz. (Moscow), v. 40, no. 12, Dec. 1984 p 1393-1395 (For primary document see N85-32860 21-70)
Avail: NTIS HC A06/MF A01

This study describes an experiment conducted to detect change in the neutron radiative capture cross-section of a La-139 nucleus induced by the electromagnetic field produced by laser radiation. The experiments employed a transit-time neutron spectrometer with a base of approximately 10.5 m. The neutron burst frequency

was 270 Hz; the cylinder pulse length was 100 nsec, and the accelerated electron current was approximately 1 A. Radiative capture events were recorded on a Romashka 11-section scintillation detector. A cross sectional change of 0.25 + or - 0 56 bn was observed for a neodymium laser with intensity of 100,000 W/sq cm, which disagrees by at least an order of magnitude with the predicted figure. It is suggested that the divergence is due to the properties of the medium containing the nucleus, rather than the individual properties of the ion, and that the electromagnetic field causes primarily redistribution of the s- and p-states of the decaying compound nucleus, leaving the probability of its formation practically unchanged. Author

N85-32929# Joint Publications Research Service, Arlington, Va.
TOWARD THE QUESTION OF MULTI-QUARK CONFIGURATIONS IN NUCLEI Abstract Only **c73**
V. R. Garsevanishvili and Z. R. Menteshashvili *In its* USSR Rept.: Phys. and Math. (JPRS-UPM-85-004) 17 Jun. 1985 p 58 Transl. into ENGLISH from Pisma v Zh. Eksperim. i Teor. Fiz. (Moscow), v. 40, no. 8, Oct. 1984 p 359-362 (For primary document see N85-32860 21-70)
Avail: NTIS HC A06/MF A01

Deep inelastic scattering of charged leptons on an A nucleus is investigated. The ratio of the structural functions of different nuclei are found to deviate from unity, which is explained by scattering on colorless multi-quark formations in the nuclei. A distinguishing feature of the model employed is the possibility of the existence in the nucleus of a superfast quark which carries the entire nuclear impulse in the extremal situation. Author

N85-32930# Joint Publications Research Service, Arlington, Va.
EXOTIC EVENTS OF p BAR p-COLLIDER: EXCITED QUARK OR EXCITED COLOR BOSON? Abstract Only **c73**
S. S. Gershteyn, G. V. Dzhikiya, and Yu. F. Pirogov *In its* USSR Rept.: Phys. and Math. (JPRS-UPM-85-004) 17 Jun. 1985 p 58-59 Transl. into ENGLISH from Yadernaya Fiz. (Moscow), v. 40, no. 12, Dec. 1984 p 1500-1514 (For primary document see N85-32860 21-70)
Avail: NTIS HC A06/MF A01

This study investigates exotic events with large missing transverse momenta (up to 90 GeV/c) observed on the CERN pp-collider, that require by their signature and effective cross section the existence of an object with a mass of about 180 GeV/sq c generated resonantly from hadron beam constituents and capable of decay into a Wjet and Zjet. Different hypotheses about the nature of the new heavy object are advanced; it is concluded that the object must be generated resonantly in q(q)g or qq collisions. Explanation of the exotic events requires either the existence of excited quarks or excited color bosons. The effective cross section of the occurrence of the exotic events is assessed on the basis of the hypothesis of an excited quark, and arguments are advanced in favor of that hypothesis. Correlations in energy spectra are calculated that provide experimental evidence on the spin of an excited quark and the structure of its interaction. Possible experiments for verifying the hypothesis of an excited quark, as well as alternative hypotheses, are discussed. Author

N85-32931# Joint Publications Research Service, Arlington, Va.
THE POSSIBILITY OF OBSERVING AND EXPLOITING THE GENERATION OF HIGH-ENERGY PHOTONS BY ELECTRONS IN THE FIELD OF AN INTENSE ELECTROMAGNETIC WAVE Abstract Only **c73**
I. F. Ginzburg, G. L. Kotkin, and S. I. Polityko *In its* USSR Rept.: Phys. and Math. (JPRS-UPM-85-004) 17 Jun. 1985 p 59 Transl. into ENGLISH from Yadernaya Fiz. (Moscow), v. 40, no. 12, Dec. 1984 p 1495-1499 (For primary document see N85-32860 21-70)
Avail: NTIS HC A06/MF A01

The generation of high-energy photons by electrons at the focal point of a laser beam is investigated. The electron generation of photons is described as a series of nonlinear Compton-effect-type processes in which the electrons absorb a large number of laser photons. The use of spectral measurements for the direct verification of quantum effects of nonlinear QED is described. Calculations for even a very high-power CO2 laser indicate that the high-energy part of the spectrum is severely suppressed in relation to the ordinary Compton-effect spectrum. The contriubution is insignificant when the ratio of photon energy to electron energy is greater than 0.5, indicating that this method is not feasible for obtaining high-energy photons. Author

N85-32932# Joint Publications Research Service, Arlington, Va.
SPATIAL PARITY VIOLATION IN ELASTIC NEUTRON-NUCLEI INTERACTION CHANNEL Abstract Only **c73**
V. P. Alfimenkov *In its* USSR Rept.: Phys. and Math. (JPRS-UPM-85-004) 17 Jun. 1985 p 61 Transl. into ENGLISH from Uspekhi Fiz. Nauk (Moscow), v. 14, no. 3, Nov. 1984 p 361-380 (For primary document see N85-32860 21-70)
Avail: NTIS HC A06/MF A01

Investigations of the spatial parity violation in weak interactions are traced historically, beginning with the Feinmann and Gell-Mann hypotheses on the universality of the weak interaction between fermions in 1957. The questionn of P-odd neutron-optical dichroism and birefringence in association with elastic neutron forward scattering amplitude as a function of neutron helicity is investigated. Experimental investigations which have been performed on the P-odd effect in elastic neutron-nuclei interaction channels are outlined for the case of cold or thermal neutrons, and resonance neutrons. Author

N85-32933# Joint Publications Research Service, Arlington, Va.
POSSIBILITY OF DEVELOPING CHARGED-PARTICLE ENERGY ANALYZER BASED ON HYPERBOLOIDAL AXISYMMETRICAL LENS Abstract Only **c73**
V. S. Gurov and E. P. Sheretov *In its* USSR Rept.: Phys. and Math. (JPRS-UPM-85-004) 17 Jun. 1985 p 61 Transl. into ENGLISH from Zh. Tekhn. Fiz. (Leningrad), v. 54, no. 12, Dec. 1984 p 2383-2386 (For primary document see N85-32860 21-70)
Avail: NTIS HC A06/MF A01

The parameters of energy analyzers based on axisymmetrical hyperboloid lenses are investigated as a function of a number of design factors: the geometric factor of the electrode system, the distance from the charged-particle point source, and the position and size of the selecting slits for different energies of the analyzed particles. Equations are derived to describe the movement of charged particles in the field of a hyperboloid axisymmetrical lens. The operating efficiency of energy analyzers with different geometries is compared. The optimum geometry for an energy analyzer based on a hyperboloid axisymmetrical lens is identified. Author

N85-32934# Joint Publications Research Service, Arlington, Va.
HIGH-ENERGY PHYSICS INSTITUTE BUILDING 3-TRILLION-EV ACCELERATOR Abstract Only **c73**
S. Kulinich *In its* USSR Rept.: Phys. and Math. (JPRS-UPM-85-004) 17 Jun. 1985 p 63 Transl. into ENGLISH from Mosk. Komsomolets (Moscow), 13 Feb. 1985 p 4 (For primary document see N85-32860 21-70)
Avail: NTIS HC A06/MF A01

The main thrust of research being done at the Institute of High-Energy Physics (IFVE) is reported. Capabilities and operating procedures of the Institute's proton synchrotron are described. To advance further into the field of high energy particle research, IFVE has begun building an accelerator accumulator complex (UNK) which will have a capacity of 3 trillion electron-volts. It is explained that the present proton synchrotron will be used as an injector for the first phase of this complex. High energy physics will be brought to the stage of probing the quark and developing a theory of the unified nature of interactions. Experiments will be conducted with both fixed targets and counter beams. Author

N85-32935# Joint Publications Research Service, Arlington, Va.
INVESTIGATION OF ION-ACOUSTIC PLASMA TURBULENCE IN FIELD OF POWERFUL ELECTROMAGNETIC WAVE BY CO2-LASER RADIATION SCATTERING Abstract Only **c75**
M. P. Brizhinev, V. V. Bulanin, B. G. Yeremin, A. V. Kostrov, A. V.

Petrov, and S. G. Revin *In its* USSR Rept.: Phys. and Math. (JPRS-UPM-85-004) 17 Jun. 1985 p 64 Transl. into ENGLISH from Pisma v Zh. Eksperim. Teor. Fiz. (Moscow), v. 40, no. 8, Oct. 1984 p 332-334 (For primary document see N85-32860 21-70)
Avail: NTIS HC A06/MF A01

Ion acoustic oscillations excited in a plasma by scattering of an electromagnetic wave (CO2 laser radiation) is investigated in order to obtain complete information regarding the ion acoustic amplitude and spectrum. The appearance of a beat signal from the photodetector and the signal produced by the accelerated electrons from the collector at the end of the chamber was found to be temporally correlated, indicating resonant interaction between the pumping wave and the plasma. The findings indicate that the action of a strong electromagnetic field on a plasma results in the excitation of long wave ion acoustic waves near the plasma resonance point with energy density significantly lower than the energy density of the Langmuir oscillations. The ion acoustic wave excitation found in the experiment can occur directly during the development of modulation stability, and as the result of secondary effects associated with electron acceleration by Langmuir waves. Author

N85-32936# Joint Publications Research Service, Arlington, Va.
SOLUTION OF PROBLEM OF EQUILIBRIUM CONFINEMENT OF PLASMA BY MAGNETIC FIELD IN AN INFINITE CIRCULAR CYLINDER Abstract Only **c75**
G. I. Sulkhanishvili *In its* USSR Rept.: Phys. and Math. (JPRS-UPM-85-004) 17 Jun. 1985 p 64-65 Transl. into ENGLISH from Soobsch. Akad. Nauk Gruzinskoy SSR (Tbilisi), v. 115, no. 1, Jul. 1984 p 25-28 (For primary document see N85-32860 21-70)
Avail: NTIS HC A06/MF A01

A modeling problem of the equilibrium confinement of plasma by a magnetic field in an infinite circular cylinder is solved. The solution of the problem is a function of the current for the projection of the magnetic field onto the plane of the cross section in the cylinder. The solution of the problem as stated is constructed with the help of a Bessel function of the first kind for the case in which the domain is a disc. The free boundary, i.e., the boundary between the plasma and the vacuum, is established. Author

N85-32937# Joint Publications Research Service, Arlington, Va.
INJECTION OF HYDROGEN MACROPARTICLES INTO T-10 TOKAMAK Abstract Only **c75**
A. P. Andreyev, B. V. Kuteyev, A. A. A. Lovtsyus, A. Ya. Lukin, S. V. Skoblikov, A. P. Umov, and L. D. Tsendin *In its* USSR Rept.: Phys. and Math. (JPRS-UPM-85-004) 17 Jun. 1985 p 65 Transl. into ENGLISH from Pisma v Zh. Tekhn. Fiz. (Leningrad), v. 10, no. 19, 12 Oct. 1984 p 1199-1203 (For primary document see N85-32860 21-70)
Avail: NTIS HC A06/MF A01

Initial experiments on the injection of hydrogen pellets with characteristic dimension d = h = 1.3 mm and velocity V sub p similar to or less than 0.7 km s sup-1 into the deuterium plasma of a T-10 tokamak are described. The interaction between the macroparticles and the tokamak plasma is investigated for a wide range of plasma parameters: B = 1.5 - 3 T, I sub p = 210 - 500 kA, T sub e(0) = 0.6 - 1 keV, N sub e = (1.5 - 6).10 to the 13th power cu. cm. The typical evaporation rate is found as a function of the small radius, and the variation in the average density along one of the center chords caused by macroparticle injection is analyzed. It is found that the injection of macroparticles increases the maximum concentration corresponding to stable discharge combustion by 20 to 50 percent. Injection initiated cutoff only for near critical plasma densities. No degradation in stability was observed as q was reduced from 4 to 2. Comparison with the analytical data shows that evaporation occurs more rapidly than the model predicts, possibly because the model employed an approximation of the monoenergetic electron stream. Author

N85-32938# Joint Publications Research Service, Arlington, Va.
CCD-BASED X-RAY SPECTROMETRY FOR ON-LINE DETERMINATION OF LASER PLASMA ELECTRON TEMPERATURE Abstract Only **c75**
V. V. Blazhenkov, O. P. Varnavskiy, A. M. Kirkin, A. M. Leontovich, V. V. Lidskiy, V. V. Lidskiy, R. G. Mirzoyan, and A. M. Mozharovskiy *In its* USSR Rept.: Phys. and Math. (JPRS-UPM-85-004) 17 Jun. 1985 p 65-66 Transl. into ENGLISH from Pisma Zh. Tekh. Fiz. (Leningrad), v. 10, no. 19, 12 Oct. 1984 p 1165-1169 (For primary document see N85-32860 21-70)
Avail: NTIS HC A06/MF A01

An A-1047 linear video signal generator incorporating two 1024-element photoregisters and a 24-mm charge coupled device (CCD) is employed to record plasma X radiation. The plasma was produced by an Nd:YAG mode-locked laser employing 08 x 80-mm active elements. The radiation spectrum of Mg XI and Mg X ions are analyzed. It is found that charge coupled devices can be used to record X-ray signals which produce blackening of approximately 0.1 photographically, without cooling the CCD to reduce noise or processing the signals to increase the dynamic range of the device. No degradation in performance was observed over three months of operation of the system. Author

N85-32939# Joint Publications Research Service, Arlington, Va.
RADIO-FREQUENCY RADIATION OF STORM CLOUDS Abstract Only
V. I. Arabadzhi, Ye. S. Prokhorov, and I. I. Epshteyn *In its* USSR Rept.: Phys. and Math. (JPRS-UPM-85-004) 17 Jun. 1985 p 66 Transl. into ENGLISH from Zh. Tekh. Fiz. (Leningrad), v. 54, no. 12, Dec. 1984 p 2427-2428 (For primary document see N85-32860 21-70)
Avail: NTIS HC A06/MF A01

It is proposed that the radio frequency radiation occurring during storms over water and during the disintegration of water droplets in storm clouds can be explained through the retardation of electrical discharges upon the destruction of water films. The electrical discharge, as in the balloelectric effect, takes the form of heavy and ultraheavy ions, escaping in all directions. The phenomenon is similar to the occurrence of X-ray bremsstrahlung. Author

N85-32940# Joint Publications Research Service, Arlington, Va.
LOWER BOUNDS OF PROPAGATION VELOCITY OF STEADY IONIZING WAVES IN FIELD OF STRONG ELECTROMAGNETIC WAVE Abstract Only **c72**
A. P. Budnik, A. S. Vakulovskiy, A. G. Popov, and P. N. Svirkunov *In its* USSR Rept.: Phys. and Math. (JPRS-UPM-85-004) 17 Jun. 1985 p 66 Transl. into ENGLISH from Zh. Tekh. Fiz. (Leningrad), v. 54, no. 12, Dec. 1984 p 2400-2402 (For primary document see N85-32860 21-70)
Avail: NTIS HC A06/MF A01

Lower bounds are obtained for the propagation velocity of steady plane ionizing waves in the field of an electromagnetic wave, taking into account photoionization by intrinsic ultraviolet emission and electron diffusion. It is shown that allowing for ionization of the excited states of atoms (molecules) can only increase the lower bounds of the wave velocity. An example of optical discharges in argon is presented for illustration. It is found that when the radiation intensity exceeds 150 MW/sq. cm, optical discharges propagate at a velocity exceeding the light detonation velocity. Author

N85-32941# Joint Publications Research Service, Arlington, Va.
AMPLIFICATION OF ELECTROMAGNETIC WAVE BY ELECTRON STREAM WITH NEGATIVE VELOCITY DIFFERENCES Abstract Only
Yu. I. Yevdokimenko, K. A. Lukin, and V. P. Shestopalov *In its* USSR Rept.: Phys. and Math. (JPRS-UPM-85-004) 17 Jun. 1985 p 67 Transl. into ENGLISH from Zh. Tekh. Fiz. (Leningrad), v. 54, no. 12, Dec. 1984 p 2359-2362 (For primary document see N85-32860 21-70)
Avail: NTIS HC A06/MF A01

It is demonstrated that an external electromagnetic or Langmuir wave can be amplified by a rectilinear stream of electrons when the phase of the wave changes abruptly in the path of the electrons. The interaction between a single velocity electron stream and the

longitudinal component of the field of a wave is modeled. It is shown that, in the nonlinear stage of amplification, the electrons separate into two groups: a group of trapped particles and a group of drifting particles. Most of energy transfer is via these drifting electrons. It is found that if n jumps occur in the phase of the wave in the path of the electrons, the wave may be amplified in initial electron velocity change interval n + 1, with the amplification intervals alternating with intervals in which the wave energy is absorbed. Author

N85-32942# Joint Publications Research Service, Arlington, Va.
ELECTROMAGNETIC WAVE AMPLIFICATION DURING CYCLOTRON RESONANCE IN A MEDIUM Abstract Only c75
G. K. Avetisyan and K. Z. Atsagortsyan *In its* USSR Rept.: Phys. and Math. (JPRS-85-004) 17 Jun. 1985 p 67 Transl. into ENGLISH from Zh. Tekh. Fiz. (Leningrad), v. 54, no. 12, Dec. 1984 p 2347-2349 (For primary document see N85-32860 21-70)
Avail: NTIS HC A06/MF A01

The possibility of electron beam amplification of an electromagnetic wave in a refracting medium in the presence of cyclotron resonance is investigated. The process of particle acceleration or multi-photon emission caused by nonlinear resonance is investigated from the viewpoint of wave amplification. The linear wave gain is found on the basis of self-consistent Maxwell-Vlasov equations for the case of kinetic instability of the electron beam. Formulas are derived for the behavior of the gain in different limiting cases. Author

N85-32943# Joint Publications Research Service, Arlington, Va.
PLASMODYNAMIC METHODS FOR GENERATING POWERFUL LIGHT PULSES Abstract Only c75
A. F. Aleksandrov and I. B. Timofeyev *In its* USSR Rept.: Phys. and Math. (JPRS-UPM-85-004) 17 Jun. 1985 p 68 Transl. into ENGLISH from Izv. Sib. Otd. Akad. Nauk SSSR, Ser. Tekh. Nauk (Novosibirsk, USSR), v. 16, no. 3, Oct. 1984 p 65-75 (For primary document see N85-32860 21-70)
Avail: NTIS HC A06/MF A01

The use of plasmodynamic methods to produce high power radiating plasmas are reviewed. The use of classical Z pinch geometry to produce microsecond pulses in inert gases is analyzed. The processes occurring in the initial stages of the discharge are found to be explained satisfactorily by the model of radiation magnetohydrodynamics. The generation of plasma focus discharges, mainly by erosion type magnetoplasma compressors, is discussed. A dense plasma jet exiting the nozzle of a powerful pulse plasmotron into the air is outlined. Plasmodynamic methods are found to be highly effective for producing high intensity radiation sources with brightness temperatures of 2 to 10 eV, making it possible to create better quality and more powerful sources in the ordinary and vacuum ultraviolet regions of the spectrum. Dynamic Z pinch geometry makes it possible to implement elongated linear or cavity type sources. The injection of a dense plasma into a gas makes it possible to produce strong open type sources with long pulse durations but relatively low brightness temperature. Author

N85-32944# Joint Publications Research Service, Arlington, Va.
CHARACTERISTICS OF OPTOGALVANIC EFFECT IN MEDIA WITH INVERSE POPULATIONS Abstract Only c75
V. S. Burakov, P. Ya. Misakov, P. A. Naumenkov, and S. N. Raykov *In its* USSR Rept.: Phys. and Math. (JPRS-UPM-85-004) 17 Jun. 1985 p 68-69 Transl. into ENGLISH from Dokl. Akad. Nauk BSSR (Minsk), v. 28, no. 12, Dec. 1984 p 1078-1081 (For primary document see N85-32860 21-70)
Avail: NTIS HC A06/MF A01

The basic characteristics of the optogalvanic effect during resonant interaction between laser radiation and glow discharge plasma in mixtures with inverse population of the investigated levels are investigated. Glow discharge in a helium-neon mixture consisting of the plasma produced by the active element in an LG-56 helium-neon laser is described. Glow discharge plasma in pure neon and the plasma of a neon filled hollow cathode are investigated for comparison. The experimental findings agree satisfactorily with qualitative estimates of the contribution of certain elementary processes to the formation of the optogalvanic response for positive-column plasma as well as hollow cathode plasma. Author

N85-32945# Joint Publications Research Service, Arlington, Va.
CYCLOTRON ABSORPTION OF FAST MAGNETOSONIC WAVE IN STELLARATOR Abstract Only c75
L. M. Kovrizhnykh and P. Ye. Moroz *In its* USSR Rept.: Phys. and Math. (JPRS-UPM-85-004) 17 Jun. 1985 p 69 Transl. into ENGLISH from Zh. Eksperim. i Teoreticheskoy (Moscow), v. 57, no. 5, Nov. 1984 p 1649-1651 (For primary document see N85-32860 21-70)
Avail: NTIS HC A06/MF A01

The helical nature of the confining magnetic field of a stellarator is investigated in which the absorption can be significantly greater than in a tokamak with similar present parameters. The possibility of strong absorption of the fast magnetosonic wave in a stellarator plasma is demonstrated theoretically for the case of cyclotron resonance conditions of the primary ions. Author

N85-32946# Joint Publications Research Service, Arlington, Va.
A SYSTEM OF MAGNETOHYDRODYNAMIC-TYPE EQUATIONS Abstract Only c75
Ye. V. Chizhonkov and M. V. Lomonosov *In its* USSR Rept.: Phys. and Math. (JPRS-UPM-85-004) 17 Jun. 1985 p 69 Transl. into ENGLISH from Prikl. Mat. i Mekh. (Moscow), v. 48, no. 4, Jul. - Aug. 1984 p 1074-1077 (For primary document see N85-32860 21-20)
Avail: NTIS HC A06/MF A01

Theorems for the existence and uniqueness of a generalized solution are proved for a system of steady state magnetohydrodynamic type equations. Second order approximation difference schemes are constructed for an extensive group of areas; an iterative method is proposed for solving the resulting system of nonlinear algebraic equations requiring on the order of O(h(-2)ln h(-1)ln epsilon(-1)) arithmetic operations to obtain a solution to within epsilon in the two dimensional case. A steady state system of magnetohydrodynamic equations for a viscous incompressible liquid with finite conductivity is studied as an example. Author

N85-32947# Joint Publications Research Service, Arlington, Va.
INVESTIGATION OF SPACE-TIME STRUCTURE OF GLOW OF LASER PLASMA COLLIDING WITH FLAT SCREEN Abstract Only c75
V. A. Boyko, B. A. Bryunetkin, F. V. Bunkin, B. Z. Gorbenko, V. I. derzhiyev, V. M. Dyakin, S. A. Mayorov, I. Yu. Skobelev, B. M. Stepanov, A. Ya. Fayenov et al *In its* USSR Rept.: Phys. and Math. (JPRS-UPM-85-004) 17 Jun. 1985 p 70 Transl. into ENGLISH from Zh. Tekh. Fiz. (Leningrad), v. 54, no. 10, Oct. 1984 p 1915-1922 (For primary document see N85-32860 21-70)
Avail: NTIS HC A06/MF A01

The space time behavior of the glow of a laser colliding with a flat screen is investigated with the help of a high speed Agat-SF photochronograph. The plasma was heated by an Nd laser producing pulse energy of 20 - 30 J, with the radiation focused into a 0.2 x 30 nm line. The Agat-SF photochronograph was employed to record the space time behavior of the plasma flow in the 400 -480 nm and 480 - 560 nm spectral bands. The behavior of the plasma glow during free expansion and during interaction with a flat screen are investigated. It is found that the presence of a screen intensifies the plasma glow at large distances from the target, and that the plasma glow in the 400 - 480 nm band is caused mainly by the line radiation spectrum of the Be II ion. It is found in general that the basic characteristics of recombinating laser plasma glow are closely associated with the structure of the shockwave front. Author

N85-32948# Joint Publications Research Service, Arlington, Va.
DIAMAGNETIC INSTABILITY OF CYCLOTRON WAVES IN PLASMA Abstract Only c75
L. V. Borodachev and A. K. Nekrasov *In its* USSR Rept.: Phys. and Math. (JPRS-UPM-85-004) 17 Jun. 1985 p 70 Transl. into ENGLISH from Vestn. Mosk. Univ., Fiz., Astron. (Moscow),

v. 25, no. 5, Sep. - Oct. 1984 p 91-98 (For primary document see N85-32860 21-70)
Avail: NTIS HC A06/MF A01

The existence of a diamagnetic effect is demonstrated for the first time by mathematical modeling of a magnetoactive plasma. The modulation instability of the pumping wave associated with the diamagnetic effect is investigated. Spontaneous focusing and compression increments are obtained. Numerical experiments are described in which the development of diamagnetic instability is investigated in detail. The theoretical estimates of the increments are compared with the numerical values, and the analytical relationships between the number and depth of magnetic holes and pumping intensity are verified. The analytical results agree well with the theory. Author

N85-32949# Joint Publications Research Service, Arlington, Va.
INFLUENCE OF ECR-HEATING ON MHD ACTIVITY OF PLASMA IN TOKAMAK-10 INSTALLATION Abstract Only c75
V. V. Alikayev and M. M. Stepanenko *In its* USSR Rept.: Phys. and Math. (JPRS-UPM-85-004) 17 Jun. 1985 p 71 Transl. into ENGLISH from Pisma v Zh. Esperim. i Teoreticheskoy Fiz. (Moscow), v. 40, no. 8, Oct. 1984 p 327-329 (For primary document see N85-32860 21-70)
Avail: NTIS HC A06/MF A01

A series of experiments was conducted on the T-10 tokamak to determine the influence of electron-cyclotron resonant (ECR) heating on the (2/1) mode intensity during heating near the resonance surface q = 2. An oscillogram of the envelope of the (2/1) mode signal shows that heating destabilizes the (2/1) mode (doubling the signal) in the presence of ECR heating near the surface q = 2; the mode is stabilized when heating occurs away from the surface (the signal is reduced by approximately an order of magnitude). The signal value is proportional to the product of the amplitude and frequency of the emf induced on the coil. The findings confirm in principle that the concept of stabilizing (2/1) MHD instability by increasing the electron temperature away from the rational surface q = 2 is fundamentally correct. Author

N85-32950# Joint Publications Research Service, Arlington, Va.
COMPARISON OF FINDINGS OF THEORIES DESCRIBING REFLECTION FROM REAL SURFACE WITH EXPERIMENTS IN REGION OF ULTRASOFT X-RADIATION Abstract Only c74
A. Ya. Grudskiy *In its* USSR Rept.: Phys. and Math. (JPRS-UPM-85-004) 17 Jun. 1985 p 72 Transl. into ENGLISH from Opt. Spektrosk. (Leningrad), v. 57, no. 5, Nov. 1984 p 880-883 (For primary document see N85-32860 21-70)
Avail: NTIS HC A06/MF A01

The reflection and scattering of ultrasoft X-radiation from real mirror surfaces is investigated and the experimental findings are compared with existing theoretical models describing the reflection of electromagnetic radiation from rough surfaces. It is found that P. Beckman's model describes the experimental findings well, and that the roughness of a real mirror can influence the calculation of the optical constants of materials based on the angular relationships of the coefficient of reflection. Thin layers can be applied in order to improve the quality of the substrate in preparing multilayer X-ray mirrors, indicating that it should be possible to develop multilayer coatings on complex surfaces such as spheres, paraboias and hyperbolas. Author

N85-32951# Joint Publications Research Service, Arlington, Va.
EFFECTIVE BRIGHTNESS OF ZERO-POINT FLUCTUATIONS OF THE ELECTROMAGNETIC VACUUM ACCOMPANYING PARAMETRIC SCATTERING OF LIGHT Abstract Only c74
O. N. Abroskina, G. Kh. Kitayeva, and A. N. Penin *In its* USSR Rept.: Phys. and Math. (JPRS-UPM-85-004) 17 Jun. 1985 p 75 Transl. into ENGLISH from Dokl. Akad. Nauk SSSR (Moscow), v. 280, no. 3, Jan. 1985 p 584-586 (For primary document see N85-32860 21-70)
Avail: NTIS HC A06/MF A01

The contribution of zero point fluctuations of the electromagnetic vacuum to three wave parametric interaction of electromagnetic radiation in a nonlinear medium was measured. The results agreed well with the theory, which predicts that the number of photons N sub 1 (channel 1) leaving the scattering medium as a result of parametric conversion of radiation in the presence of intense pumping radiation is related to the number of input photons N sub 2 (channel 2) by the relationship N sub 1 = F sub 12 (N sub 2 + 1), where F sub 12 is the parametric conversion factor, and the factor of unity added to N sub 2 is due to zero point fluctuation of the vacuum. The contribution of the zero-point fluctuations was determined by comparing the value of N sub 1 for N sub 2 = O and N sub 2 = O. The experiments were performed using 100 mW of pumping radiation at 488 nm. A lithium niobate crystal was used as the nonlinear medium. The radiation was recorded using a photomultiplier in the photon counting mode and with a digital synchronous detection circuit. It was verified that the brightness of the zero point fluctuations did not depend on the reflection and absorption of radiation in the medium.Author

N85-32952# Joint Publications Research Service, Arlington, Va.
CORRELATION OF INTENSITIES OF DIFFERENT SCATTERING CHANNELS Abstract Only c25
S. M. Burkitbayev, V. P. Kushnir, and E. A. Manykin *In its* USSR Rept.: Phys. and Math. (JPRS-UPM-85-004) 17 Jun. 1985 p 76 Transl. into ENGLISH from Dokl. Akad. Nauk SSSR, v. 279, no. 2, Nov. 1984 p 338-339 (For primary document see N85-32860 21-70)
Avail: NTIS HC A06/MF A01

The problem of determining the number of types of radiation sources and the spectrum of each source is investigated through the correlation spectroscopy of the observed combined spectrum by analyzing the correlations between channels differing in energy and/or types of radiation. The scattering of light by an ensemble of particles exhibiting Brownian movement is investigated as an example. It is assumed that the movement of individual particles is statistically independent of that of others. The different scattering channels are separated by introducing frequency filters with a passband that is much smaller than the characteristic widths of the sought spectrum on the one hand, and significantly greater than the characteristic frequencies of the intensity fluctuations on the other. An expression is derived for the non-Gaussian term of the cross correlation function for the fields passing through the filters. Author

N85-32953# Joint Publications Research Service, Arlington, Va.
ABSORPTION OF LASER RADIATION IN SUBSTANCE WITH ABSORPTION COEFFICIENT DEPENDING LINEARLY UPON TEMPERATURE Abstract Only c36
I. V. Yedvabnyy and S. A. Ubaydullayev *In its* USSR Rept.: Phys. and Math. (JPRS-85-004) 17 Jun. 1985 p 76 Transl. into ENGLISH from Izv. Akad. Nauk Uzb. SSR, Ser. Fiz.-Mat. Nauk (Tashkent), no. 5, Sep. - Oct. 1984 p 76-78 (For primary document see N85-32860 21-70)
Avail: NTIS HC A06/MF A01

Absorption wave propagation is investigated in a medium in which the absorbing component is unstable at temperatures below the decomposition temperature and the decomposition products are transparent to laser radiation. A formula is derived that relates the velocity of the absorption wave to the intensity of the laser radiation. Author

N85-32954# Joint Publications Research Service, Arlington, Va.
OPTICAL WAVEGUIDE ALONG FRONT OF EXOTHERMIC REACTION Abstract Only c74
P. B. Lerner and B. S. Lukyanchuk *In its* USSR Rept.: Phys. and Math. (JPRS-UPM-85-004) 17 Jun. 1985 p 77 Transl. into ENGLISH from Zh. Tekh. Fiz. (Leningrad), v. 54, no. 12, Dec. 1984 p 2397-2400 (For primary document see N85-32860 21-70)
Avail: NTIS HC A06/MF A01

The formation of an optical waveguide along an exothermic reaction front is investigated. The basic linear, and some nonlinear, optical characteristics of this waveguide are assessed. The front of a laminar flame along which laser radiation propagates is examined. The change in the profile of the index of refraction along the front is analyzed. The conditions are specified under

which a local maximum of the index of refraction can form near the front of an exothermic reaction, making waveguide light propagation possible. The characteristic parameters of the waveguide formed are estimated in parabolic approximation. The estimates indicate the possibility of observing such a waveguide experimentally. Author

N85-32955# Joint Publications Research Service, Arlington, Va.
ELECTROSTATIC ASTIGMATIC TUBULAR LENS Abstract Only **c74**
L. G. Grikman, Z. D. Iskakova, and I. A. Petrov *In its* USSR Rept.: Phys. and Math. (JPRS-UPM-85-004) 17 Jun. 1985 p 77 Transl. into ENGLISH from Zh. Tekh. Fiz. (Leningrad), v. 54, no. 12, Dec. 1984 p 2342-2346 (For primary document see N85-32860 21-70)
Avail: NTIS HC A06/MF A01

The electron optical properties are described for a new electrostatic astigmatic tubular lens with equal radius electrodes separated by an infinitely small clearance, whose facing edges each have two protrusions and notches that are bounded by lines parallel to the optical axis of the lens and planes perpendicular to that axis. The potential distribution is found, and the paraxial properties of the lens are examined. In addition to design simplicity, the lens has far greater optical strength than the astigmatic tubular lens with electrodes whose facing edges contain protrusions and notches bounded by the line of intersection of two cylinders with the same radius; the effect of the lens on a beam of charged particles is similar to that of a quadrupole lens with an axisymmetrical field component. Author

N85-32956# Joint Publications Research Service, Arlington, Va.
FLUCTUATIONS IN LIGHT INTENSITY DURING BACKSCATTERING IN TURBULENT MEDIUM Abstract Only **c74**
S. S. Kashkarov, T. N. Nesterova, and A. S. Smirnov *In its* USSR Rept.: Phys. and Math. (JPRS-UPM-85-004) 17 Jun. 1985 p 78 Transl. into ENGLISH from Izv. Vyssh. Ucheb. Zaved., Radiofiz. (Gorky, USSR), v. 28, no. 10, Oct. 1984 p 1272-1278 (For primary document see N85-32860 21-70)
Avail: NTIS HC A06/MF A01

Findings from measurements of the fluctuations in intensity of a spherical light wave reflected by a point scatter located behind a turbulent layer are presented. The relative dispersion of the intensity fluctuations of the scattered radiation is investigated as a function of the statistical moments of the intensity fluctuations in the radiation incident on the scatterer, and of the distance between the radiation source and the device which receives the scattered radiation. The relationships between the statisical moments of the fluctuations in the radiation incident on the scatterer and reflected therefrom agree with the predicted values. Increased numbers of scatterers cause changes in the flicker index of the backscattered radiation: the value of the flicker index of backscattered radiation is determined by the size of the fourth moment of the intensity fluctuations in the radiation incident on the scatterer. Author

N85-32957# Joint Publications Research Service, Arlington, Va.
RELAXATION LENS IN INHOMOGENEOUS BINARY MIXTURE Abstract Only **c74**
E. T. Bruk-Levinson, Z. Plokhotski, and I. V. Khodan *In its* USSR Rept.: Phys. and Math. (JPRS-UPM-85-004) 17 Jun. 1985 p 78-79 Transl. into ENGLISH from Dokl. Akad. Nauk BSSR (Minsk), v. 28, no. 12, Dec. 1984 p 1090-1093 (For primary document see N85-32860 21-70)
Avail: NTIS HC A06/MF A01

A quasioptical system, occurring in an inhomogeneous binary mixture, that can be interpreted as a thin relaxation lens with optical characteristics determined by the coefficient of diffusion of the mixture is demonstrated. A binary mixture of uniform concentration distribution is suddenly disturbed by adding a small amount of the same type of mixture, but with a higher concentration than one of the components. As a result of diffusion, the inhomogeneous distribution of the concentration in the mixture begins to relax, causing a corresponding relaxation in the distribution of the index of refraction. A light beam striking such a system is deflected, with angle of deflection being a function of time and coordinate. A linear formula is derived which relates the coefficient of diffusion with the time derivative of the logarithm of the angle of deflection of the incident light beam. The resulting formation is found to be focusing or defocusing, depending upon the ratio of the indices of refraction of the pure components. Author

N85-32958# Joint Publications Research Service, Arlington, Va.
BEAM DIFFUSION IN LINEAR IONOSPHERIC LAYER Abstract Only **c46**
V. D. Gusev and O. K. Vlasaova *In its* USSR Rept.: Phys. and Math. (JPRS-UPM-85-004) 17 Jun. 1985 p 79 Transl. into ENGLISH from Vestn. Mosk. Univ., Fiz., Astron., v. 25, no. 5, Sep. - Oct. 1984 p 74-81 (For primary document see N85-32860 21-70)
Avail: NTIS HC A06/MF A01

The use of the Einstein-Fokker equation to describe beam scattering in a medium with a regular gradient of the index of refraction is investigated for the case of oblique incidence of radio waves on an ionospheric layer. An equation describing the beam is derived in the parabolic cylindrical coordinate system, and an expression for beam dispersion is proposed. It is found that the arc length of the beam can be replaced with a coordinate along the unperturbed trajectory for the case of oblique propagation only when the permittivity layer is linear. The approach can be extended to other models of the medium by using machine processing. Author

N85-32959# Joint Publications Research Service, Arlington, Va.
COEFFICIENT OF OPTICAL ABSORPTION AND SCATTERED LIGHT CAPTURE EFFECT Abstract Only **c74**
L. I. Mitsay and V. A. Nemeenov *In its* USSR Rept.: Phys. and Math. (JPRS-UPM-85-004) 17 Jun. 1985 p 79-80 Transl. into ENGLISH from Kvantovaya Electron. (Moscow), v. 11, no. 10, Oct. 1984 p 2116-2120 (For primary document see N85-32860 21-70)
Avail: NTIS HC A06/MF A01

This study investigates the absorption of laser radiation scattered on optical inhomogeneities of a material. The laser radiation power scattered in the specimen and converted to heat is determined. Analytical expressions are obtained for KCl, CsI and ZnSe to estimate the contribution of scattering to the measured optical absorption coefficient. Analyses are made for large impurities, and for small ones uniformly distributed through the specimen. Computer modeling of the trajectories of random beams is employed to find the angular distribution of the light intensity scattered on large impurities. This distribution and the capture conditions, i.e., the form and index of refraction of the specimen, as well as the distribution of the laser radiation intensity in the cross section of the beam, are used to calculate the amount of scattered radiation that is converted to heat. Author

N85-32960# Joint Publications Research Service, Arlington, Va.
METHODS FOR MEASURING AND ANALYZING DISPERSION PROPERTIES OF MULTIMODE FIBER OPTIC LIGHTPIPES (A REVIEW) Abstract Only **c74**
T. V. Babkina, V. V. Grigoryants, and V. B. Smirnov *In its* USSR Rept.: Phys. and Math. (JPRS-UPM-85-004) 17 Jun. 1985 p 80 Transl. into ENGLISH from Kvantovaya Elektron. (Moscow), v. 11, no. 10, Oct. 1984 p 1899-1939 Original language document previously announced as A85-21017 (For primary document see N85-32860 21-70)
Avail: NTIS HC A06/MF A01

Data in the literature on the information characteristics of multimode fiber-optic waveguides are reviewed. In particular, attention is given to the principal mechanisms affecting pulse dispersion in waveguides, methods of dispersion calculation, and problems involved in experimental investigation and quantitative description of fiber-optic waveguides. Hardware implementations of various methods of dispersion pulse measurements are examined, as are problems related to the certification of waveguides. Finally, the effect of the manufacture-related defects of

the actual refraction index profile on the transmission band of a waveguide and ways to compensate for this effect are discussed.
V.L. (IAA)

N85-32961# Joint Publications Research Service, Arlington, Va.
STIMULATED MANDELSTAM-BRILLOUIN SCATTERING WITH DISTRIBUTED FEEDBACK Abstract Only **c74**
O. P. Zaskalko, A. N. Zozulya, Yu. I. Kyzylasov, N. N. Panaioti, V. P. Silin, V. T. Tikhonchuk, and I. L. Fabelinskiy *In its* USSR Rept.: Phys. and Math. (JPRS-UPM-85-004) 17 Jun. 1985 p 80-81 Transl. into ENGLISH from Zh. Eksperim. Teoreticheskoy Fiz. (Moscow), v. 57, no. 5, Nov. 1984 p 1582-1593 (For primary document see N85-32860 21-70)
Avail: NTIS HC A06/MF A01

Low-threshold stimulated Mandelstam-Brillouin scattering with distributed feedback is proposed and obtained experimentally for the case of nearly antiparallel pumping beams. The distributed feedback is achieved by Bragg diffraction of the Mandelstam-Brillouin radiation on a spatially-periodic lattice of the index of refraction induced in an optically-nonlinear medium (carbon bisulphide) by interference between two light beams. The use of distributed feedback makes it possible to obtain single-frequency Mandelstam-Brillouin radiation with good energy efficiency and little angular divergence. A theory is developed for the phenomenon which makes it possible to calculate the coefficient of conversion of the pumping energy to Mandelstam-Brillouin radiation and to determine the optimum direction of generation and the distribution of the amplitudes of the waves interacting in the nonlinear medium. Comparison of the experimental and theoretical findings indicates good agreement. The proposed Mandelstam-Brillouin converter system has a low lasing threshold, a high quantum yield, exhibits no higher Stokes components and has small angular divergence.
Author

N85-32962# Joint Publications Research Service, Arlington, Va.
INFLUENCE OF PHONON INTERACTION ON WIDTH AND FORM OF MANDELSTAM-BRILLOUIN OPTICAL SCATTERING LINE Abstract Only **c74**
S. V. Gantsevich, V. D. Kagan, R. Katilyus, and E. A. Rzayev *In its* USSR Rept.: Phys. and Math. (JPTS-UPM-85-004) 17 Jun. 1985 p 81 Transl. into ENGLISH from Zh. Eksperim. Teoreticheskoy Fiz. (Moscow), v. 57, no. 5, Nov. 1984 p 1734-1744 (For primary document see N85-32860 21-70)
Avail: NTIS HC A06/MF A01

The scattering of light on interacting long-wave low-frequency phonons is investigated theoretically for intensities significantly exceeding the equilibrium value. The analysis is performed for phonons interacting through dissipative electronic system. The adaptation of kinetic diagram techniques for studying light scattering is described. Nonlinear effects in the phonon system and their influence on the form of the Mandelstam-Brillouin scattering line are investigated. Non-Peierls interaction through the electron density wave is employed as a specific phonon-phonon interaction mechanism. An expression is derived for the intensity of the scattered light. Mandelstam-Brillouin scattering is analyzed for the case in which the phonon intensity increases along the specimen, which is typical for experimental conditions.
Author

N85-32963# Joint Publications Research Service, Arlington, Va.
SOLVABILITY OF SOME INVERSE PROBLEMS IN LASER RADIATION FOCUSING Abstract Only **c74**
A. V. Goncharskiy, I. N. Sisakyan, and V. V. Stepanov *In its* USSR Rept.: Phys. and Math. (JPRS-UPM-85-004) 17 Jun. 1985 p 82 Transl. into ENGLISH from Dokl. Akad. Nauk SSSR (Moscow), v. 279, no. 1, Nov. 1984 p 68-71 (For primary document see N85-32860 21-70)
Avail: NTIS HC A06/MF A01

The solvability of some inverse problems of coherent optics, and the following set of related problems are investigated: (1) selection of the model; (2) solvability of the synthesis problems; (3) uniqueness of solution of solvability problem; and (4) correctness of algorithms for solving inverse problem. The problem of focusing coherent radiation in an arbitrary focal curve with assigned intensity distribution is solved using the approximation of geometric optics. A theorem is presented that provides sufficient existence conditions for smooth solutions of the inverse synthesis problem. Programmable optical elements which focus laser radiation in an arbitrary focal curve have been developed on the basis of the present theory.
Author

N85-32964# Joint Publications Research Service, Arlington, Va.
INFLUENCE OF SPATIAL PUMPING SPECTRUM ON QUALITY OF PHASE CONJUGATE REFLECTION DURING 4-PHOTON INTERACTION Abstract Only **c74**
V. V. Ivaknik *In its* USSR Rept.: Phys. and Math. (JPRS-UPM-85-004) 17 Jun. 1985 p 82 Transl. into ENGLISH from Izv. Vyssh. Ucheb. Zaved., Fiz. (Tomsk, USSR), v. 27, no. 9, Sep. 1984 p 115-117 (For primary document see N85-32860 21-70)
Avail: NTIS HC A06/MF A01

The influence of the spatial spectrum of the pumping waves on the quality of phase conjugate reflection is investigated using the example of degenerate 4-photon interaction. A truncated equation is derived for 4-photon parametric interaction in a flat nonlinear layer. Relationships are found between the amplitudes of the spatial spectra of the object and signal waves at the output of the nonlinear medium; the kernel of the integral operator in the expression for the amplitude of the spatial spectra describes phase conjugate reflection quality by a 4-photon radiation converter. An expression is found for the amplitude of the field of the object wave at the output of the parametric radiation converter that indicates the possibility of describing said converter with the help of a phase conjugation diaphragm.
Author

N85-32965# Joint Publications Research Service, Arlington, Va.
NEW METHOD FOR CORRECTING CHROMATISM OF MIRROR-LENS OBJECTIVES Abstract Only **c74**
N. L. Sokolov *In its* USSR Rept: Phys. and Math. (JPRS-UPM-85-004) 17 Jun. 1985 p 83 Transl. into ENGLISH from Opt. Spektrosk. (Leningrad), v. 57, no. 2, Sep. 1984 p 543-545 (For primary document see N85-32860 21-70)
Avail: NTIS HC A06/MF A01

An analytical method developed for correcting spherochromatic aberrations is demonstrated by the example of developing a mirror-lens objective. Rather than trying to select only one type of optical glass for the mirror-lens objectives which is apochromatic over a wide portion of the spectrum, an apochromatic field aberration compensator is employed with enough optical strength to correct the curvature of the field of view. The method can be used to obtain an apochromatic system by combining a positive compensator in a parallel beam of rays with a Mangin mirror made of the same type of glass and to optimize that system as a part of the mirror-lens objective. The chromatism correction method has been used successfully to develop different versions of mirror-lens objectives.
Author

N85-32966# Joint Publications Research Service, Arlington, Va.
DIELECTRIC MIRROR WITH FERROMAGNETIC SUBSTRATE Abstract Only **c74**
M. S. Borisova and Ye. N. Chernykh *In its* USSR Rept.: Phys. and Math. (JPRS-UPM-85-004) 17 Jun. 1985 p 83 Transl. into ENGLISH from Opt. Spektrosk. (Leningrad), v. 57, no. 3, Sep. 1984 p 543-545 (For primary document see N85-32860 21-70)
Avail: NTIS HC A06/MF A01

The reflection matrix of a ferromagnetic mirror with a multilayer dielectric coating applied to increase the coefficient of reflection, to permit operation in the cavity of neon-helium laser operating in the 0.63 or 1.15 micron region, is investigated. The reflection matrix is defined for a mirror with a ferromagnetic substrate and isotropic dielectric layers. A 6-layer dielectric mirror consisting of alternating layers of cryolite and zinc sulphide on a ferromagnetic substrate is analyzed as an example. It is found that the 6-layer coating reduces the phase nonreciprocity from approximately 6 x 10 to the -3 to approximately 4 x 10 to the -4 while increasing the amplitude coefficient reflection for p-polarization from 0.77 to 0.98. The amplitude nonreciprocity drops by two orders of magnitude,

and the polarization characteristics of the mirror are improved.
Author

N85-32967# Joint Publications Research Service, Arlington, Va.
THE FARADAY EFFECT IN RUBY AND CORUNDUM IN STRONG MAGNETIC FIELDS Abstract Only **c74**
B. B. Bouko and A. K. Soyka *In its* USSR Rept.: Phys. and Math. (JPRS-UPM-85-004) 17 Jun. 1985 p 84 Transl. into ENGLISH from Dokl. Akad. Nauk SSSR (Minsk), v. 28, no. 11, Nov. 1984 p 984-987 (For primary document see N85-32860 21-70)
Avail: NTIS HC A06/MF A01

The Faraday rotation of the polarization plane of light in ruby and corundum is investigated experimentally at room temperature in strong pulsed magnetic fields of up to 810 KOe. The experiments employed geometrically identical specimens of corundum and ruby made from a single crystal (a laser ruby rod with corundum end pieces and cr sup 3+ ion concentration of approximately 1.6 x 10 to the 19/cc). The sounding radiation consisted of plane-polarized light from a helium-neon laser at 632.8 nm. The angle of rotation of the light polarization plane is found to vary linearly as the strength of the magnetic field. The Verde constants for ruby and corundum were found to be within 7% of 0.353 and 0.375 deg/(KOe. cm), respectively. The findings indicate that the Verde constant is determined, under the conditions present in the experiment, by the diamagnetic term caused by Zeeman splitting of degenerate energy states occurring in the Faraday effect, i.e., splitting of the lines at the same frequency (in the absence of the field), but with different polarization. The Verde constant is independent of the magnetic field and temperature in this case.
Author

N85-32968# Joint Publications Research Service, Arlington, Va.
OPTICAL IMAGE OF BOUNDED OBJECTS Abstract Only **c74**
Yu. V. Vorobev *In its* USSR Rept.: Phys. and Math. (JPRS-UPM-85-004) 17 Jun. 1985 p 84 Transl. into ENGLISH from Opt. Spektrosk. (Leningrad), v. 57, no. 5, Nov. 1984 p 921-926 (For primary document see N85-32860 21-70)
Avail: NTIS HC A06/MF A01

A study is made of the images of isolated bounded objects with characteristic dimensions assumed to be known a priori and comparable to the least resolved distance of the optical system. An eigenfunction expansion apparatus is developed for recovering images distorted by aberrations of the optical system and by diffraction for the case in which the response function is axisymmetrical. This approach makes it possible to compare different optical systems in representing bounded isolated objects. Reconstruction of the images of objects with dimensions smaller than the theoretical resolution limit is analyzed as an example. Author

N85-32969# Joint Publications Research Service, Arlington, Va.
TRANSMISSION OF LIGHT BY DISPERSE MEDIUM OF DENSELY PACKED OPTICALLY SOFT PARTICLES Abstract Only **c74**
V. P. Dik, A. P. Ivanov, and V. A. Loyko *In its* USSR Rept.: Phys. and Math. (JPRS-UPM-85-004) 17 Jun. 1985 p 85 Transl. into ENGLISH from Opt. Spektrosk. (Leningrad), vol. 57, no. 5, Nov. 1984 p 884-888 (For primary document see N85-32860 21-70)
Avail: NTIS HC A06/MF A01

The characteristics of light transmission by densely packed layers of soft particles, i.e., particles for which the relative index of refraction is near unity are investigated. The experiment was conducted by measuring the coefficient of transmission of a turbid medium in rarified and densely packed states with the same amount of disperse matter. It is found that the attenuation of radiation passing through a densely packed medium depends upon the scattering index: the more diffuse the medium, the smaller the scattering index. A thickness mode is found to occur in a rarefied disperse medium in the region in which the particles are suspended. This mode also occurs in a densely packed system, and begins with larger overlap coefficients than for a rarefied medium. The results indicate that clarification effects do not change the principles of light attenuation by thick weakly absorbing layers of a disperse medium.
Author

N85-32970# Joint Publications Research Service, Arlington, Va.
EQUATIONS OF MOTION FOR ELECTROMAGNETIC WAVES IN 4-DIMENSIONAL EUCLIDIAN SPACE Abstract Only
Yu. N. Vatolin *In its* USSR Rept.: Phys. and Math. (JPRS-UPM-85-004) 17 Jun. 1985 p 86 Transl. into ENGLISH from Dokl. Akad. Nauk SSSR (Moscow), v. 278, no. 6, Oct. 1984 p 1340-1343 (For primary document see N85-32860 21-70)
Avail: NTIS HC A06/MF A01

The possibility of extending Maxwell's equations to a space described by four Cartesian coordinates was investigated. New non-trivial relationships are found between the physical quantities characterizing the electromagnetic fields. The possibility of substantiating a purely electromagnetic nature of the mass of charged particles is analyzed. Formulas are derived that ensure the necessary existence conditions for physical realization of inertial frames of reference entirely electromagnetic in nature. The possibility of solving the problem of spontaneous particle self-action is investigated.
Author

N85-32971# Joint Publications Research Service, Arlington, Va.
ON ONE NONLINEAR PROBLEM OF LASER THERMOCHEMISTRY Abstract Only **c36**
F. V. Bunkin, V. A. Galaktionov, N. A. Kirichenko, S. P. Kurdyumov, and A. A. Samarskiy *In its* USSR Rept.: Phys. and Math. (JPRS-UPM-85-004) 17 Jun. 1985 p 89 Transl. into ENGLISH from Dokl. Akad. Nauk SSSR (Moscow), v. 279, no. 4, Dec. 1984 p 838-842 (For primary document see N85-32860 21-70)
Avail: NTIS HC A06/MF A01

The typical properties of the solutions of those equations describing the occurrence of several steady states, localization effects and complex changes in the temperature field caused by the thermal action of laser radiation on chemically active media are studied. Effective approximate methods are sought for finding the solutions. Surface heating of a metal specimen exposed to laser radiation is examined. The solution of a boundary problem to determine presence and number of steady-state solutions is investigated. The stability of the steady-state is analyzed by applying the theory of non-steady-state averaging to the boundary problem derived. The investigation is for the case of Gaussian distribution of the radiation intensity over the surface of the material; however, a number of important findings can also be obtained for an arbitrary distribution satisfying rather weak integrability conditions.
Author

N85-32972# Joint Publications Research Service, Arlington, Va.
EXISTENCE OF SMOOTH SOLUTIONS IN PROBLEMS OF ELECTROMAGNETIC RADIATION FOCUSING Abstract Only
A. V. Goncharskiy and V. V. Stepanov *In its* USSR Rept.: Phys. and Math. (JPRS-UPM-85-004) 17 Jun. 1985 p 89 Transl. into ENGLISH from Dokl. Akad. Nauk SSSR (Moscow), v. 279, no. 4, Dec. 1984 p 788-792 (For primary document see N85-32860 21-70)
Avail: NTIS HC A06/MF A01

The inverse problem of electromagnetic radiation focusing into a plane curve on which the intensity distribution of the focused radiation is assigned is solved. It is assumed that transformation of the phase of the incident radiation with the help of an optical element is sufficent to solve the focusing problem. Using the approximation of geometrical optics, the problem is reduced to calculating the eikonal of the wave reflected from the optical element. The theory serves as the basis of algorithms for synthesizing programmable optical elements employed for various laser radiation focusing tasks.
Author

N85-32973# Joint Publications Research Service, Arlington, Va.
POISSON FORMULA FOR RADON TRANSFORMATION AND NUMERICAL IMAGE RECONSTRUCTION ALGORITHM Abstract Only **c64**
N. D. Vvedenskaya and S. G. Gindikin *In its* USSR Rept.: Phys. and Math. (JPRS-UPM-85-004) 17 Jun. 1985 p 90 Transl. into

ENGLSH from Dokl. Akad. Nauk SSSR (Moscow), v. 279, no. 4, Dec. 1984 p 780-784 (For primary document see N85-32860 21-70)
Avail: NTIS HC A06/MF A01

An algorithm is presented for Radon transform inversion based on an analog of a Poisson formula, for image reconstruction in sectional radiography. The algorithm is employed to compute test functions consisting of the sum of the characteristic functions of circles multiplied by different constants. The numerical experiments indicated that no regularization is required when the initial functions are smooth, but it is necessary when reconstructing discontinuous functions. The study indicates that the transformation formula derived can be employed in computational image reconstruction algorithms. Author

N85-32974# Joint Publications Research Service, Arlington, Va.
ASYMPTOTICALLY STABLE SOLUTIONS OF SOME NON-LINEAR EQUATIONS Abstract Only **c64**
N. A. Kirichenko *In its* USSR Rept.: Phys. and Math. (JPRS-UPM-85-004) 17 Jun. 1985 p 91 Transl. into ENGLISH from Dokl. Akad. Nauk SSSR (Moscow), v. 280, no. 3, Jan. 1985 p 579-583 (For primary document see N85-32860 21-70)
Avail: NTIS HC A06/MF A01

A nonlinear equation of the form u'=(-1) to then (u'+f(u)) to the 2n where f(u)=K sub o squared u + epsilon u squared - u cubed, K sub o squared > o, epsilon is an arbitrary parameter, the dot denotes a time derivative, and (2n) denotes a spatial derivative or order 2n, was studied on the interval (O,R). Boundary conditions were u sup ((2f+1)/partial w.r.t. omega) = 0 for k=0,1,2... and n-1,2,... when x is an element of omega. This equation is of interest in models of laser heating of gaseous mixtures which include thermal conductivity, diffusion and thermal diffusion effects. The particular case n = 1 was analyzed in detail and compared with the case of n = 0; the results can be generalized to other values of n. The solutions were studied in the limits the of R goes to infinity and the limit of t goes to infinity. The solutions were described in terms of the phase plane diagram and curves of the quantity a (2 pi/t) = u sub max - u sub min were constructed. The solution trajectories were shown to be spatially periodic with the period T satisfying the condition mT = 2R, where m is an integer. The solution with the maximum spatial period, whose phase plane trajectory connects two consecutive saddle points (no cycles), was shown to be the asymptotically stable solution. This solution was also shown to be the asymptotically stable solution in the limit t goes to infinity for finite R. Author

N85-32975# Joint Publications Research Service, Arlington, Va.
OPTIMIZATION OF SAMPLING IN STATISTICAL PHYSICS EXPERIMENTS Abstract Only **c65**
M. Kh. Rafailov *In its* USSR Rept.: Phys. and Math. (JPRS-UPM-85-004) 17 Jun. 1985 p 92-93 Transl. into ENGLISH from Zh. Tekh. Fiz. (Leningrad), v. 54, no. 12, Dec. 1984 p 2349-2351 (For primary document see N85-32860 21-70)
Avail: NTIS HC A06/MF A01

Sample optimization was studied in order to ensure a steady experimental result in statistical physics, which is determined by the relationship between the size of the sampling set for the random quantity in question needed to ensure stationarity of the distribution function F(x) and the level of significance when the interaction function p(x,t) is known a priori. The findings can be applied to problems of experimental design - determining the optimum sample size necessary and sufficient for the statistical characteristics of the random quantity investigated to be stationary, as well as problems of separating quantities with different statistical properties and thus to identify anomalies in the phenomena in question. Author

N85-32976# Joint Publications Research Service, Arlington, Va.
A NEW PROBLEM IN MATHEMATICAL PHYSICS ASSOCIATED WITH THE PROBLEM OF COHERENT PHASE TRANSFORMATION Abstract Only
M. A. Grinfeld *In its* USSR Rept.: Phys. and Math. (JPRS-UPM-85-004) 17 Jun. 1985 p 95 Transl. into ENGLISH from Dokl. Akad. Nauk SSSR (Moscow), v. 279, no. 1, Nov. 1984 p 72-76 (For primary document see N85-32860 21-70)
Avail: NTIS HC A06/MF A01

The description of heterogeneous coherent phase equilibria in an elastic single component system is shown to lead, in the approximation of small intrinsic deformation, to a new problem in mathematical physics with an unknown bound. The low order terms of the resulting system of equilibrium equations coincide with the equations of the classical linear theory of elasticity (generally speaking, anisotropic); however, the problem remains strongly nonlinear overall, inasmuch as it contains an unknown bound and a boundary condition on it which is quadratic with respect to translation. The formulas obtained are used to find certain explicit solutions to the boundary problems. As an example, the problem of heterogeneous equilibria in an infinite rectangular isotropic beam with free faces and constant loading on the surfaces x squared = const can be examined. A modeling problem for the asymptote of small intrinsic deformation during coherent phase transformation is presented as a scalar analog of the vector problem considered initially. Author

N85-32977# Joint Publications Research Service, Arlington, Va.
NECESSARY AND SUFFICIENT CONDITIONS FOR SINGLE-EXTREMUM AND CONVEX PROBLEMS OF MATHEMATICAL PROGRAMMING Abstract Only **c59**
I. I. Gasanov and A. D. Rikun *In its* USSR Rept.: Phys. and Math. (JPRS-UPM-85-004) 17 Jun. 1985 p 96 Transl. into ENGLISH from Dokl. Akad. Nauk SSSR (Moscow), v. 278, no. 4, Oct. 1984 p 786-789 (For primary document see N85-32860 21-70)
Avail: NTIS HC A06/MF A01

Classes of mathematical programming problems are identified for which each point which satisfies the necessary conditions of the extremum is a global minimum of the problem. The latter property is important from the viewpoint of applications, inasmuch as many optimization algorithms fail to distinguish between extreme and the points which satisfy the necessary conditions of the extremum. A mathematical programming problem of the type min (fcx)/g sub i(x) <0, i = 1,2,...,m; h sub j(x) = 0, j = 1,2,...,1) is investigated. This problem is said to be essentially single extremum problem if the sets of local and global minima of the problem are the same. A function ph1 is introduced which is said to be locally pseudo convex (quasi convex) in x if there exists a vicinity x with respect to which ph1 is pseudo convex (quasi convex) in x. A restriction is presented for application to the planning of water protection measures. Author

N85-32978# Joint Publications Research Service, Arlington, Va.
ON THE PROBLEM OF LINEAR PROGRAMMING WITH APPROXIMATE DATA Abstract Only **c59**
G. M. Agayan, A. A. Ryutin, and A. N. Tikhonov *In its* USSR Rept.: Phys. and Math. (JPRS-UPM-85-005) Transl. into ENGLISH from Zh. Vychsl. Mat. i Mat. Fiz. (Moscow), v. 24, no. 9, Sep. 1984 p 1303-1311 (For primary document see N85-32860 21-70)
Avail: NTIS HC A06/MF A01

A regularization problem of linear programming is proposed for approximately assigned restrictions. Approximate information about the system of restriction is provided in the form of an individual approximate system and of a class of systems equivalent to the individual system in accuracy. The existence of a unique solution to the corresponding regularization problem was proved, and stable methods for solving it are proposed. In a numerical example, the results using are compared with the results of a solution by the simplex method. Author

71 ACOUSTICS

Includes sound generation, transmission and attenuation. For noise pollution see *45 Environment Pollution.*

N85-32979*# Tomberlin (Thomas J.), Consultant, Montreal (Quebec).

STATISTICAL METHODS FOR EFFICIENT DESIGN OF COMMUNITY SURVEYS OF RESPONSE TO NOISE: RANDOM COEFFICIENTS REGRESSION MODELS
Thomas J. Tomberlin Jul. 1985 26 p refs Prepared for Bionetics Corp.
(Contract NAS1-16978)
(NASA-CR-177933; NAS 1.26:177933) Avail: NTIS HC A03/MF A01 CSCL 20A

Research studies of residents' responses to noise consist of interviews with samples of individuals who are drawn from a number of different compact study areas. The statistical techniques developed provide a basis for those sample design decisions. These techniques are suitable for a wide range of sample survey applications. A sample may consist of a random sample of residents selected from a sample of compact study areas, or in a more complex design, of a sample of residents selected from a sample of larger areas (e.g., cities). The techniques may be applied to estimates of the effects on annoyance of noise level, numbers of noise events, the time-of-day of the events, ambient noise levels, or other factors. Methods are provided for determining, in advance, how accurately these effects can be estimated for different sample sizes and study designs. Using a simple cost function, they also provide for optimum allocation of the sample across the stages of the design for estimating these effects. These techniques are developed via a regression model in which the regression coefficients are assumed to be random, with components of variance associated with the various stages of a multi-stage sample design. Author

N85-32980# Texas Univ., Austin. Applied Research Lab.
THE MOVING THERMOACOUSTIC ARRAY: A THEORETICAL FEASIBILITY STUDY
N. P. Chotiros 17 Jan. 1985 70 p
(Contract N00014-82-K-0425)
(AD-A154510; ARL-TR-85-3) Avail: NTIS HC A04/MF A01 CSCL 17/1

A theoretical study of the feasibility of the moving thermoacoustic source as a sound projector in underwater acoustic applications is presented. Since the Doppler shift is direction dependent, it was found that the moving optoacoustic sources are potentially useful for direction finding by virtue of the extremely high Doppler shifts achievable. While the thermoacoustic array has certain advantages over conventional acoustic projectors, notably the noncontact property and the Doppler direction finding capability, its optoacoustic energy conversion efficiency is no better than that of the stationary thermoacoustic array. This conclusion was arrived at through mathematical analysis from basic principles, and supported by computer generated numerical examples. The conversion efficiency was found to be strongly dependent on the acoustic signal carrier frequency and on the optical signal waveform. It was found that the thermoacoustic conversion was most efficient when the optical energy was delivered as an impulse train. The efficiency is fundamentally limited by the physical properties of the medium, particularly the coefficient of thermal expansion and the specific heat. A different optoacoustic conversion process, which employs nonlinear physical reactions to generate sound, is being pursued. GRA

N85-32981# Texas Univ., Austin. Applied Research Lab.
THE SOUND FIELD OF A MOVING LASER-INDUCED ACOUSTIC ARRAY (THEORY)
Y. H. Berthelot and I. J. Busch-Vishniac 4 Dec. 1984 57 p
(Contract N00014-82-K-0425)
(AD-A154553; ARL-TR-84-21) Avail: NTIS HC A04/MF A01 CSCL 20/1

This report describes the theoretical investigation of the sound field radiated by a moving laser source. When an intensity modulated laser beam illuminates a column of water, it produces a highly directive thermoacoustic array (or optoacoustic antenna). This report discusses a time domain approach for predicting the pressure field radiated by a moving (subsonic, transonic, or supersonic) thermoacoustic array. The theory is based on a convolution type summation between the impulse response of the thermoacoustic array and the laser pulse intensity. The theoretical model is for both nearfield and farfield radiation and for any Mach number of the source. GRA

N85-32982# Cambridge Acoustical Associates, Inc., Mass.
ITERATION SOLUTION FOR A SUBMERGED FORCE-DRIVEN FINITE CYLINDER Final Report
R. Martinez Apr. 1985 105 p
(Contract N00014-83-C-0194)
(AD-A154587; U-1208-328) Avail: NTIS HC A06/MF A01 CSCL 20/1

A theoretical model has been developed to protect acoustic radiation from a submerged, finite-cylindrical shell internally stiffened by ring frames and with flat, movable end caps. Iterative techniques are developed to solve the associated fluid-structure coupled systems over a moderate range of frequencies which encompasses several fluid-loaded resonances. We demonstrate that such techniques generate essentially the exact solution in a reasonably small number of iterations. Comparison of computational costs to those for the exact result shows iteration to be economically advantageous for all frequencies considered. GRA

N85-32983# Federal Aviation Administration, Washington, D.C. Office of Environment and Energy.
FAA/GAMA (FEDERAL AVIATION ADMINISTRATION/ GENERAL AVIATION MANUFACTURER'S ASSOCIATION) PROPELLER AIRCRAFT NOISE TEST PROGRAM, SALINA MUNICIPAL AIRPORT, SALINA, KANSAS
Feb. 1985 44 p
(AD-A154818; FAA-EE-85-1) Avail: NTIS HC A03/MF A01 CSCL 20/1

In September, 1984, the FAA, with the cooperation and support of the General Aviation Manufacturers' Assoc. (GAMA), conducted a noise measurement program on small propeller-driven aircraft at Salina Municipal Airport, Salina, Kansas. The program objectives were: (1) to obtain takeoff noise data using prepared international and U.S. certification procedures for propeller-driven small airplanes; and (2) to measure the benefits of noise abatement takeoff procedures being developed by the manufacturers for inclusion in the Pilot's Operating Handbook. For the five twin and four single engine aircraft tested, the results show an average noise reduction of 4.4 decibels when using reduced power procedures after takeoff. GRA

N85-32984# Bolt, Beranek, and Newman, Inc., Canoga Park, Calif.
OVERGROUND EXCESS SOUND ATTENUATION (ESA). VOLUME 3: APPLICATION OF ESA DATA IN NOISEFILE Final Report, Aug. 1982 - Dec. 1984
D. W. Bishop Apr. 1985 56 p
(Contract F33615-82-C-0501)
(AD-A154820; BBN-5324-Vol-3; AFAMRL-TR-84-017-Vol-3) Avail: NTIS HC A04/MF A01 CSCL 20/4

This is the third report in the series concerning Overground Excess Attenuation, ESA. Different models and algorithms for computing ESA are compared in terms of differences in A-levels at varying distances for different aircraft noise spectra. ESA values from recent field measurement at Wright-Patterson AFB, Dayton OH, theoretical models, and from NOISEMAP and a SAE recommendation are compared. It is recommended that the current NOISEMAP ESA algorithms be replaced with ESA curves based on Dayton data acquired under moderate downwind propagation conditions. It is also recommended that additional ESA field data be acquired over irregular terrain where direct line-of-sight propagation does not exist. GRA

N85-32985# Mandex, Inc., Vienna, Va.
HELICOPTER NOISE SURVEY FOR SELECTED CITIES IN THE CONTIGUOUS US
R. Main, A. Joshi, D. Couts, and L. Hilten 20 Mar. 1985 320 p

(AD-A154893; FAA-EE-85-3) Avail: NTIS HC A14/MF A01 CSCL 20/1

The remainder of this report (after the introduction) is organized as follows. Chapter 2 describes the methodology used in the noise measurement surveys. Chapter 3 describes the noise monitoring equipment used. Chapters 4 through 8 present the noise measurement data obtained from the standard sets of helicopter maneuvers and from in-service (not test) helicopter operations at each of five cities surveyed. Each of these chapters is divided into sections with the following headings: Overview of Helicopter Operations, Land Use and Helicopter Noise Abatement Procedures; Standardized Maneuver Tests, and Actual In-Service Helicopter Operations. In addition, Chapter 7 (Chicago, IL) also contains a section which presents the noise data measured for actual in-service operations at a public use heliport. GRA

N85-32986# Bolt, Beranek, and Newman, Inc., Canoga Park, Calif.

LATERAL ATTENUATION OF AIRCRAFT FLIGHT NOISE Final Technical Report, Aug. 1982 - Dec. 1984

D. E. Bishop Mar. 1985 34 p

(Contract F33615-82-C-0501)

(AD-A154958; BBN-5668; AFAMRL-TR-85-018) Avail: NTIS HC A03/MF A01 CSCL 20/1

This report reviews models for calculating the lateral attenuation of aircraft flight noise, in particular, the change in attenuation for different elevation angles varying from aircraft directly overhead (90 deg. elevation angle) to a zero elevation angle. Sets of noise spectrum-dependent lateral attenuation values derived from theory and from experimental flight measurements were applied to sets of different aircraft noise spectra to determine A-level differences with elevation angle. The lateral attenuation based on the experimental data showed appreciably greater attenuation, but still less attenuation than the SAE model currently incorporated in the Integrated Noise Model (INM) aircraft noise computer program. Based on the experimental curves, a new generalized transition model was developed and is recommended as a replacement for current NOISEMAP lateral transition algorithm. GRA

N85-32987# Lockheed Missiles and Space Co., Palo Alto, Calif.

DISCRETE-ELEMENT ACOUSTIC ANALYSIS OF SUBMERGED STRUCTURES USING DOUBLY ASYMPTOTIC APPROXIMATIONS Final Report, 15 Apr. 1982 - 30 Sep. 1984

J. A. DeRuntz, Jr. 26 Apr. 1985 27 p

(Contract N00014-82-C-0353)

(AD-A154959; LMSC-F035672) Avail: NTIS HC A03/MF A01 CSCL 20/1

Doubly Asymptotic Approximations have been found to offer significant advantages for the treatment of steady-state fluid-structure interaction in vibration, acoustic-radiation, and acoustic-scattering problems for complex submerged structures. This paper describes the theoretical foundations, development, and verification of two boundary-element/finite-element processors that implement this approach. The first processor is SWEEPS, which determines the structural response of and surface pressure on a vibrating submerged body. The second is TARGET, which embodies a discretized form of the Helmholtz integral equation to obtain fluid pressures away from the body. To test these processors, two problems involving a spherical shell in an infinite fluid have been solved. The first problem is one of modal internal forcing; while the second is concerned with forcing by incident plane waves. The computational results exhibit excellent agreement with closed form plane waves. The computational results exhibit excellent agreement with closed form solutions. Author (GRA)

N85-32988# Science Applications International Corp., McLean, Va.

A RANDOM LAYER MODEL FOR REFLECTION FROM OCEAN BOTTOM SEDIMENTS

R. R. Greene and D. M. Rubenstein 8 Feb. 1985 41 p

(Contract N00014-83-C-0303)

(AD-A155019; SAIC-85/1036) Avail: NTIS HC A03/MF A01 CSCL 20/1

Sub-bottom sediment layering is identified as the cause of strong acoustic reflectivity from the sea floor in abyssal plains. A technique for estimating the reflectivity from layering statistics in deep sea sediment cases is developed. Preliminary calculations are carried out which exhibit the qualitative and quantitative behavior of observed bottom reflectivity. GRA

N85-32989# Naval Postgraduate School, Monterey, Calif.

PROPAGATION OF SOUND IN A LAYERED LABORATORY MODEL M.S. Thesis

M. Tarig and S. Rungsirotekomol Dec. 1984 76 p

(AD-A155141; AD-F630645) Avail: NTIS HC A05/MF A01 CSCL 20/1

The propagation of sound in a laboratory model consisting of a surface layer of water overlying a thick bottom layer of sand was experimentally investigated. The variations of pressure amplitude as a function of receiver depth, range, and transverse location were measured for the source at constant depth in the surface layer of water. Three frequencies for which only the lowest mode propagates were used in this investigation. The measurements of pressure amplitude as a function of depth and range were found in good agreement with normal mode theory, when absorption in the bottom was taken into consideration. GRA

N85-32990# Stanford Research Inst., Menlo Park, Calif.

SPEECH UNDERSTANDING RESEARCH Annual Technical Report, 1 Apr. 1974 - 31 Mar. 1975

D. E. Walker, W. H. Paxton, J. J. Robinson, G. G. Hendrix, and B. G. Deutsch Jun. 1975 385 p

(Contract DAHC04-75-C-0006; ARPA Order 2903)

(AD-A155462; ATR-3) Avail: NTIS HC A17/MF A01 CSCL 05/7

The following summary provides a perspective on the distinctive characteristics of the Stanford Research Institute contributions to the current system. The system control, embedded in the parser, focuses the operation of the entire system to minimize both storage requirements and the time spent on incorrect interpretations. A language definition system provides a means for integrating the various sources of knowledge in the system. The language definition itself, based on studies of protocols gathered from actual performances in task-oriented dialogs, includes information from acoustics, phonetics, phonology, prosodics, syntax, semantics, pragmatics, and discourse. A new semantic network representation, which partitions the net into spaces, has proved particularly well suited for working with the two task domains. Discourse procedures, building on the semantics, establish a discourse history so that information from previous utterances (and, ultimately, from the task environment) can be used in the analysis of the current utternce. Appendix A contains a listing of the language currently defined in the speech understanding system. Appendix B lists the reports and publications issued by the project staff. GRA

N85-32991# Weidlinger Associates, New York, N.Y.

ACOUSTIC RADIATION FROM CONCENTRIC SHELLS CONTAINING AN INNER FLUID

J. M. Klosner and R. Vasudevan Jan. 1985 71 p Prepared in cooperation with Polytechnic Inst. of New York

(Contract N00014-78-C-0820)

(AD-A155476; POLY-M/AE-85-1; TR-29) Avail: NTIS HC A04/MF A01 CSCL 20/1

The acoustic radiation characteristics of a fluid filled concentric shell structure are investigated by making use of the simple source surface integral method. The fluid field is described in terms of surface expansion functions, while the in vacuo structural modes, obtained by using the BOSOR4 structural program, are used as a basis for the shell motions. The structural code can be applied to branched shells of revolution, thereby obviating the need to introduce structural coupling of the two shells in a manner which is external to the main code. For illustrative purposes three types of internal harmonic excitations have been considered: (1) an axisymmetric unit pressure acting on the central region, (2) a unit line load acting on the central region, and (3) concentrated axial loads acting at the poles of the spherical closures. The far field

fluid pressures have been obtained for a wide range of frequencies for both the single shell and for the double shell with and without inner fluid. Because of numerical difficulties encountered when applying the integral methods to internal fluid problems, some simple approximations to the internal fluid problem were considered. The results obtained compare quite favorably with those of the exact solution over a wide range of frequencies. Author (GRA)

N85-32992# Science Applications International Corp., McLean, Va.
[UNDERSTANDING COHERENCE LOSSES INCURRED BY BOTTOM-RETAINED SIGNALS] Final Report, 13 Dec. 1982 - 10 Feb. 1985
C. W. Spofford Apr. 1985 73 p
(Contract N00014-83-C-0303)
(AD-A155559; SAIC-85/1683) Avail: NTIS HC A04/MF A01 CSCL 20/1

Tasks on this contract focused on understanding the coherence losses incurred by bottom-retained signals due to three mechanisms: sub-bottom roughness, random inhomogeneities in the sediment column, and partial reflections from near-surface layering in the sediment. Work in the first area is continuing and two as-yet-unpublished references are included here to document the status of that effort. The coupled-mode, master-equation model for spatial coherence developed by Dozier has been applied to analyze coherence data acquired in BEARING STAKE and in shallow water. The effects of near-surface layering in sediments produces a loss in frequency coherence i.e., a time spread of the signal) and anomalous bottom-loss behavior. GRA

N85-32861# Joint Publications Research Service, Arlington, Va.
THE KONSTANTINOV EFFECT AND ABSORPTION OF SOUND IN INHOMOGENEOUS MEDIA Abstract Only
F. F. Legusha *In its* USSR Rept.: Phys. and Math. (JPRS-UPM-85-004) 17 Jun. 1985 p 4 Transl. into ENGLISH from Usp. Fiz. Nauk (Moscow) v. 144, no. 3, Nov. 1984 p 509-522 (For primary document see N85-32860 21-70)
Avail: NTIS HC A06/MF A01

N85-32862# Joint Publications Research Service, Arlington, Va.
TOWARD THE THEORY OF ACOUSTIC SCATTERING ON UNEVEN FREE SURFACE Abstract Only
A. G. Voronovich *In its* USSR Rept.: Phys. and Math. (JPRS-UPM-85-004) 17 Jun. 1985 p 4-5 Transl. into ENGLISH from Akust. Zh. (Moscow), v. 30, no. 6, Nov. - Dec. 1984 p 747-753 (For primary document see N85-32860 21-70)
Avail: NTIS HC A06/MF A01

N85-32863# Joint Publications Research Service, Arlington, Va.
NEW APPROXIMATIONS AND FINDINGS OF THEORY OF NONLINEAR ACOUSTIC BEAMS Abstract Only
Yu. R. Lapidus and O. V. Rudenko *In its* USSR Rept.: Phys. and Math. (JPRS-UPM-85-004) 17 Jun. 1985 p 5 Transl. into ENGLISH from Akust. Zh. (Moscow), v. 30, no. 6, Nov. - Dec. 1984 p 797-802 (For primary document see N85-32860 21-70)
Avail: NTIS HC A06/MF A01

N85-32864# Joint Publications Research Service, Arlington, Va.
REFLECTION OF ACOUSTIC BEAM FROM INHOMOGENEOUS BOUNDARY Abstract Only
A. D. Lapin *In its* USSR Rept.: Phys. and Math. (JPRS-UPM-85-004) 17 Jun. 1985 p 5 Transl. into ENGLISH from Akust. Zh. (Moscow), v. 30, no. 6, Nov. - Dec. 1984 p 836-838 (For primary document see N85-32860 21-70)
Avail: NTIS HC A06/MF A01

N85-32916# Joint Publications Research Service, Arlington, Va.
ACOUSTIC WAVE SCATTERING BY ROUND CYLINDRICAL SHELL REINFORCED WITH STRINGERS Abstract Only
A. P. Poddubnyak and A. R. Voloshin *In its* USSR Rept.: Phys. and Math. (JPRS-UPM-85-004) 17 Jun. 1985 p 50 Transl. into ENGLISH from Dokl. Nauk Ukr. SSR: Ser. A, Fiz.-Mat. i Tekhn. Nauki (Kiev), no. 10, Oct. 1984 p 45-47 (For primary document see N85-32860 21-70)
Avail: NTIS HC A06/MF A01

72 ATOMIC AND MOLECULAR PHYSICS

Includes atomic structure and molecular spectra.

N85-32993# Naval Postgraduate School, Monterey, Calif.
FORM FACTOR EFFECTS ON MICROWAVE CERENKOV RADIATION M.S. Thesis
E. R. Turner Dec. 1984 51 p
(AD-A154577) Avail: NTIS HC A04/MF A01 CSCL 20/8

The effects of the electron bunch charge distribution on the production of microwave Cerenkov radiation in air are investigated. The representation of this distribution is presented in terms of a function called the form factor. Theory is developed which uses two dimensionless quantities to study the form factor effects. These are the emission length to wavelength ratio and the bunch length to wavelength ratio. A prediction is made for conditions which allows a concentration of radiation 90 deg. to the beam. Results are reported of experiments which were performed to measure the effects of the form factor using parameters available at the Naval Postgraduate School's linear accelerator. Findings from these experiments along with suggestions for further research are included. GRA

N85-32994# California Univ., Berkeley. Dept. of Chemistry.
NONRADIATIVE DAMPING OF MOLECULAR ELECTRONIC EXCITED STATES BY METAL SURFACES
D. H. Waldeck, A. P. Alivisatos, and C. B. Harris Mar. 1985 45 p
(Contract N00014-83-K-0632)
(AD-A154619; TR-2) Avail: NTIS HC A03/MF A01 CSCL 20/8

Eighteen years ago a series of extremely important experiments were reported which studied for the first time the effect of a metal on an electronically excited molecule located hundreds or thousands of angstroms away. In these experiments, the Langmoir-Blodgett monolayer assembly technique was used to create a variable thickness spacer layer on top of the metal, and a layer of the luminescent molecules was placed on top of the spacer. In the 1970's theoretical investigations showed that in the short distance regime the molecule nonradiatively transfers energy to the substrate. In this review we discuss the interaction of a molecular excited state with a smooth substrate. Both theoretical and experimental work is treated. This discussion will concentrate on the classical treatment of the interaction because of its astounding success in comparison with experiment. We do however discuss the shortcomings of the classical treatment and some recent approaches to correcting these limitations. The experimental work is considered in detail but we focus on the region close to the substrate, less than 500 away because the longer distance regime has been well reviewed. GRA

N85-32995# Thorn EMI, Hayes (England).
THE EFFECT OF METAL OVERLAYERS OF THERMIONIC DISPENSER CATHODES Final Technical Report, Dec. 1982 - 1984
H. B. Skinner and R. A. Tuck Mar. 1985 128 p
(Contract DAJA45-83-C-0009; DA Proj. 1T1-61102-BH-57)
(AD-A154795; EVT-905) Avail: NTIS HC A07/MF A01 CSCL 20/6

This study has been undertaken to further the understanding of the physics and chemistry of thermionic dispenser cathodes and to test a model for the mechanism of operation of these devices. The surface structure and work function of cathodes coated with a variety of metals has been investigated using surface analytical techniques, including Auger Electron Spectroscopy. The theoretical implications of the results are discussed. GRA

N85-32996# Chemical Dynamics Corp., Columbus, Ohio.
VIBRATIONALLY ENHANCED DISSOCIATION OF DIATOMIC MOLECULES Final Report, 20 Sep. 1982 - 19 Sep. 1984

B. C. Garrett, L. T. Redmon, and M. J. Redmon May 1985 186 p
(Contract F33615-82-C-2241)
(AD-A154827; CDTR-85-1; AFWAL-TR-85-2020) Avail: NTIS HC A09/MF A01 CSCL 07/4

The impact parameter method for electron impact excitation of diatomic molecules has been extended to treat dissociation and to include the effects of vibrational and rotational excitation. The method was found to agree well with previous theoretical calculations of excitation and dissociation cross sections for H2. The agreement with experimental cross sections is poorer but consistant with our understanding of the processes. The method has been applied to electron impact excitation and dissociation of O2, S2, HCl, and HgBr through optically allowed transitions. Vibrational excitation of the molecule can significantly affect the cross sections for these processes, either increasing or decreasing the cross sections by as much as 2 orders of magnitude, whereas, rotational excitation has a much smaller effect on the cross sections. GRA

N85-32997# Massachusetts Inst. of Tech., Cambridge. Dept. of Chemistry.
PROSPECTS FOR A NEW KIND OF SYNTHESIS: ASSEMBLY OF MOLECULAR COMPONENTS TO ACHIEVE FUNCTIONS Interim Report
M. S. Wrighton 16 May 1985 38 p
(Contract N00014-84-K-0553)
(AD-A155023; ONR-TR3) Avail: NTIS HC A03/MF A01 CSCL 07/4

Molecular sceintists now have an opportunity to add an important new dimension to synthesis. Preparation of chemical systems, comprising two or more components, to achieve a function is possible. While rational strategies exist for some simple systems, major advances in fundamental reaction chemistry at the molecular and macromolecular level, especially at interfaces are required to achieve practically significant synthetic objectives. Synthetic chemical systems inspired by nature and microelectronic devices illustrate some of the aspects of systems synthesis. These example systems include multi-component catalysts, the photosynthetic apparatus for solar energy conversion, diodes and transistors. GRA

N85-32998# Rochester Univ., N. Y. Dept. of Chemistry.
OVERLAP INTEGRALS FOR ATOM-METAL SURFACE INTERACTIONS Interim Report
W. C. Murphy and T. F. George May 1985 22 p
(Contract N00014-80-C-0472; Grants AF-AFOSR-0046-82; NSF CHE-83-20185)
(AD-A155038; TR-67) Avail: NTIS HC A02/MF A01 CSCL 07/4

Atom-metal surface overlap integrals are of utmost importance in surface energy calculations. Direct numerical evaluation of these triple integrals can be very time consuming. However, we have developed an exact algebraic expression, where formulas for the coefficients are given for both the general case and the special case where the parallel wavevector is zero. Some numerical examples of the overlap for H on A1 are given. Author (GRA)

N85-32999# Armed Forces Radiobiology Research Inst., Bethesda, Md.
PAIRED ION CHAMBER CONSTANTS FOR FISSION GAMMA-NEUTRON FIELDS
K. P. Ferlic Dec. 1984 34 p
(AD-A155069; AFRRI-TR84-8) Avail: NTIS HC A03/MF A01 CSCL 20/7

Paired ionization chamber constants are calculated for the 50 cc spherical ionization chambers used in dosimetry of the AFRRI TRIGA reactor. The calculations include the most recently available information on energy spectra for neutron and gamma radiation present in AFRRI reactor exposure rooms, as well as for kerma factors and W-values of neutrons. The constant kT, which expresses neutron sensitivity of the 50 cc tissue equivalent (TE) ion chamber filled with TE gas, ranged from 0.92 to 0.96 among the 18 different neutron spectra for which calculations were done. The constant kU, which expresses neutron sensitivity of the 50 cc graphite ion chamber filled with CO2, ranged from 0.07 to 0.11 among the same spectra. The constant hT, which expresses gamma sensitivity of the TE/TE ion chamber, was taken to be unity for all spectra. The constant hU, which expresses gamma sensitivity of the C/CO2 ion chamber, was 0.99 + or - 0.01(range) for all spectra. These calculations will serve as the basis for future dosimetry with the 50 cc ion chambers at the AFRRI TRIGA reactor. GRA

N85-33000# Oregon Univ., Eugene.
MULTIPHOTON PRODUCTION AND DETECTION OF ATOMS Final Report, 1 Aug. 1981 - 31 Jan. 1985
P. C. Engelking 1 Apr. 1985 15 p
(Contract DAAG29-81-K-0154)
(AD-A155561; ARO-18047.1-CH) Avail: NTIS HC A02/MF A01 CSCL 07/5

The production of atomic fragments from a compound using multiphoton dissociation was investigated for metal centered and hetero atom centered compounds. The atoms were detected by multiphoton ionization. Metal centered systems generated large amounts of the characteristic metal atoms, with a large kinetic energy release, indicating a direct dissociation Mechanism. P and S centered systems gave mainly diatomic fragments. Author (GRA)

N85-33001# Brookhaven National Lab., Upton, N. Y.
PHOTOELECTRON STUDIES OF AUTOIONIZING RYDBERG STATES IN HCl
M. G. White and J. R. Grover 1985 11 p refs Presented at the Workshop on Autoionization of Atoms and Small Mol., Argonne, Ill., 2 May 1985
(Contract DE-AC02-76CH-00016)
(DE85-011813; BNL-36421; CONF-850560-1) Avail: NTIS HC A02/MF A01

The results of a systematic investigation of electronically autoionizing Rydberg states in HCl are discussed. Vibrationally resolved photoelectron spectroscopy was used to map out the non-radiative decay of vibronic levels of 3psigma (YIELDS) in n(sub d sup 2)sigma Rydberg states converging to the A sup 2 (SIGMA) sup + (3psigma) sup-1 excited ionic state. The observed vibrational distributions of the resulting X sup 2 PI (1 PI) sup n-1 ionic state are compared with the results of model calculations of Terwilliger and Smith based on spectral analysis of the absorption spectrum. Overall, the X(sup 2) PI vibrational branching ratios are found to be in only rough qualitative agreement with the calculations and these results are discussed in relation to the approximations involved. DOE

N85-33002# Argonne National Lab., Ill.
[ACTIVITIES OF THE PHYSICS DIVISION] Annual Review, 1 Apr. 1983 - 31 Mar. 1984
Aug. 1984 268 p
(Contract W-31-109-eng-38)
(DE85-000784; ANL-84-24) Avail: NTIS HC A12/MF A01

Activities in medium-energy physics research include studies of pion reaction mechanisms, nuclear structure studies, two-nucleon physics with pions and electrons, weak interactions and particle searches. Research at the Superconducting Linac Accelerator includes studies on quasi-elastic processes and reaction strengths, heavy-ion fusion reactions, high angular momentum states in nuclei, accelerator mass spectrometry and equipment development at the Tandem-Linac Facility. Theoretical nuclear physics studies reveiwed are grouped in the areas: nuclear forces and subnucleon degrees of freedom, variational calculation of finite many-body systems, nuclear shell theory and nuclear structure, intermediate energy physics, heavy-ion reactions and other theoretical studies. The atomic and molecular physics research is detailed in the five ongoing programs: (1) photoionization-photoelectron research; (2) high-resolution laser-RF spectroscopy with atomic and molecular beams; (3) photon interactions involving

fast ions; (4) interactions of fast atomic and molecular ions with solid and gaseous targets; and (5) theoretical atomic physics.DOE

N85-32917# Joint Publications Research Service, Arlington, Va.
IDENTIFICATION OF VIBRATIONAL-ROTATIONAL TRANSITIONS OF Os-192O4 WITHIN FREQUENCY TUNING LIMITS OF HIGH PRESSURE CO2 WAVEGUIDE LASER Abstract Only
Ye. N. Bazarov, G. A. Gerasimov, V. P. Gubin, V. L. Derbov, A. D. Novikov, S. Yu. Otrokhov, A. I. Sazonov, and V. U. Fomin *In its* USSR Rept.: Phys. and Math. (JPRS-UPM-85-004) 17 Jun. 1985 p 51 Transl. into ENGLISH from Optika i Spektroskopiya (Leningrad), v. 57, no. 3, Sep. 1984 p 434-438 (For primary document see N85-32860 21-70)
Avail: NTIS HC A06/MF A01

N85-32918# Joint Publications Research Service, Arlington, Va.
TOWARD A THEORY OF EXCITATION OF ATOMS DURING NUCLEAR AND MAGNETIC NEUTRON SCATTERING Abstract Only
G. L. Yudin *In its* USSR Rept.: Phys. and Math. (JPRS-UPM-85-004) 17 Jun. 1985 p 51-52 Transl. into ENGLISH from Dokl. Akad. Nauk SSSR (Moscow), v. 297, no. 2, Nov. 1984 p 363-368 (For primary document see N85-32860 21-70)
Avail: NTIS HC A06/MF A01

N85-32920# Joint Publications Research Service, Arlington, Va.
RADIATIVE-COLLISION GENERATION OF SOUND IN GASES SUBJECTED TO SINGLE-PULSE OPTICAL EXCITATION Abstract Only
V. M. Shalayev and V. Z. Yakhnin *In its* USSR Rept.: Phys. and Math. (JPRS-UPM-85-004) 17 Jun. 1985 p 53 Transl. into ENGLISH from Zh. Eksperim. i Teor. Fiz. (Moscow), v. 87, no. 4, Oct. 1984 p 1211-1220 (For primary document see N85-32860 21-70)
Avail: NTIS HC A06/MF A01

N85-32922# Joint Publications Research Service, Arlington, Va.
RESONANT ENERGY TRANSFER DURING STRONG EXCITATION Abstract Only
A. S. Agabekyan *In its* USSR Rept.: Phys. and Math. (JPRS-UPM-85-004) 17 Jun. 1985 p 54 Transl. into ENGLISH from Zh. Prikl. Spektroskopii (Minsk), v. 41, no. 4, Oct. 1984 p 677-680 (For primary document see N85-32860 21-70)
Avail: NTIS HC A06/MF A01

N85-32927# Joint Publications Research Service, Arlington, Va.
MIRROR REFLECTION OF CHARGED PARTICLES FROM +AMORPHOUS AND POLYCRYSTALLINE SURFACES Abstract Only
M. A. Kumakhov *In its* USSR Rept.: Phys. and Math. (JPRS-UPM-85-004) 17 Jun. 1985 p 56 Transl. into ENGLISH from Dokl. Akad. Nauk SSSR (Moscow), v. 279, no. 4, Dec. 1984 p 862-863 (For primary document see N85-32860 21-70)
Avail: NTIS HC A06/MF A01

N85-32940# Joint Publications Research Service, Arlington, Va.
LOWER BOUNDS OF PROPAGATION VELOCITY OF STEADY IONIZING WAVES IN FIELD OF STRONG ELECTROMAGNETIC WAVE Abstract Only
A. P. Budnik, A. S. Vakulovskiy, A. G. Popov, and P. N. Svirkunov *In its* USSR Rept.: Phys. and Math. (JPRS-UPM-85-004) 17 Jun. 1985 p 66 Transl. into ENGLISH from Zh. Tekh. Fiz. (Leningrad), v. 54, no. 12, Dec. 1984 p 2400-2402 (For primary document see N85-32860 21-70)
Avail: NTIS HC A06/MF A01

73 NUCLEAR AND HIGH-ENERGY PHYSICS

Includes elementary and nuclear particles; and reactor theory.

For space radiation see *93 Space Radiation.*

N85-33003# National Bureau of Standards, Gaithersburg, Md. Nuclear Radiation Div.
A PRACTICAL GUIDE TO IONIZATION CHAMBER DOSIMETRY AT THE AFRRI REACTOR
L. J. Goodman Apr. 1985 44 p
(Grant DNA-IACRO-83-847; DA Proj. U99-QAXM)
(AD-A155185; AFRRI-CR-85-1) Avail: NTIS HC A03/MF A01 CSCL 06/18

This report provides the Armed Forces Radiobiology Research Institute (AFRRI) with practical guidance on the use of ionization chambers for performing mixed-field dosimetry at the TRIGA reactor. Experimental techniques, calculational formulas, physical constants, and correction factors are discussed, with emphasis on practice rather than theory in order to provide consistency and long-term continuity to the reactory dosimetry program at AFRRI. GRA

N85-33004# Armed Forces Radiobiology Research Inst., Bethesda, Md.
RHODIUM-103 AND INDIUM-115 INELASTIC SCATTERING REACTIONS FOR FISSION NEUTRON DOSIMETRY
G. H. Zeman Dec. 1984 21 p
(DA Proj. U99-QAXM)
Avail: NTIS HC A02/MF A01 CSCL 20/8

Neutron activation foil cross sections are calculated for shielded and unshielded configurations of the AFRRI TRIGA reactor. The neutron spectra used in the calculations ranged in average energy from 0.55 MeV to 3.4 MeV, and the total range of activation foil sensitivity factors (cross section per unit tissue-kerma) was + or - 8.5% for 103Rh (n,n') 13mRh, + or - 20% for 115In (n,n') 115mIn, and + or - 75% for 32S (n,p)32P. These results support the use of 103 Rh and 115 In activation foils as tissue-kerma dosimeters at the AFRRI TRIGA reactor. Author (GRA)

N85-33005# Los Alamos National Lab., N. Mex.
RADIATION TRANSPORT Progress Report, 1 Jan. - 31 Mar. 1984
R. D. ODell Feb. 1985 63 p
(Contract W-7405-eng-36)
(DE85-010333; LA-10271-PR) Avail: NTIS HC A04/MF A01

Research and development progress in radiation transport by the Los Alamos National Laboratory's Group X-6 for the second quarter of FY84 was reported. Included are unclassified tasks in the areas of fission reactor neutronics, deterministic transport methods, Monte Carlo radiation transport, and cross sections and physics. DOE

N85-33006# Argonne National Lab., Ill.
TRITIUM TECHNOLOGY REVIEW
P. A. Finn and D. K. Sze 1985 13 p Presented at the 6th Topical Meeting on the Technol. of Fusion Energy, San Francisco, 3 Mar. 1985
(Contract W-31-109-eng-38)
(DE85-010504; CONF-850310-82) Avail: NTIS HC A02/MF A01

The methods used in recovering, containing and controlling tritium in a fusion reactor system are discussed. Safety requirements, cost analysis, and breeding needs for tritium control are outlined. DOE

N85-33007# Stanford Linear Accelerator Center, Calif.
DETECTOR PROBLEMS AT THE SSC
S. G. Wojcicki Feb. 1985 16 p refs Presented at the Aspen Winter Phys. Conf., Aspen, Colo., 14 Jan. 1985
(Contracts DE-AC03-81ER-40050; DE-AC03-76SF-00515)
(DE85-010217; SU-SLAC-PUB-3582; CONF-850146-6) Avail:

NTIS HC A02/MF A01

Work was done to understand the nature of potential difficulties and the required R and D needs to exploit aluminosity of 10(33)cm (-2) sec (-1) at a hadron-hadron high energy collider. Desirable features of the detectors and the superconducting super collider environment in which they work are discussed. Lepton identification, tracking, calorimetry and computing and triggering are the specific detector aspects addressed. DOE

N85-33008# Oak Ridge National Lab., Tenn.
EMPIRICAL CORRELATION OF RESIDUAL GAMMA RADIATION RESULTING FROM OPERATION OF THE HEALTH PHYSICS RESEARCH REACTOR
T. L. Chou, G. E. Ragan, and C. S. Sims Apr. 1985 27 p refs (Contract DE-AC05-84OR-21400)
(DE85-012075; ORNL-6144) Avail: NTIS HC A03/MF A01

An empirical equation has been developed which gives gamma dose equivalent rate as a function of time, distance, and fission yield after a pulsed operation of Oak Ridge National Laboratory's (ORNL) unshielded Health Physics Research Reactor (HPRR). A related expression which is applicable to steady-state reactor operation has been mathematically derived from the aforementioned empirical equation. The two relations can be used to predict the gamma dose equivalent rate to within 25% for times between 1 minute and 90 minutes after reactor shutdown. Similar agreement is expected for up to several days. In most cases the relations are expected to overestimate the gamma dose equivalent rate. DOE

N85-33009# Argonne National Lab., Ill.
EVALUATED NUCLEAR-DATA FILE FOR NIOBIUM
A. B. Smith, D. L. Smith, and R. J. Howerton Mar. 1985 42 p refs Prepared in cooperation with California Univ., Livermore. Lawrence Livermore Lab.
(Contract W-31-109-eng-38)
(DE85-012095; ANL/NDM-88) Avail: NTIS HC A03/MF A01

A comprehensive evaluated nuclear-data file for elemental niobium is provided in the ENDF/B format. This file, extending over the energy range 10(-11) to 20 MeV, is suitable for comprehensive neutronic calculations, particularly those dealing with fusion-energy systems. It also provides dosimetry information. Attention is given to the internal consistancy of the file, energy balance, and the quantitative specification of uncertainties. Experimental data and previous evaluated files are compared. The results of integral tests are described and remaining outstanding problem areas are cited. DOE

N85-32924# Joint Publications Research Service, Arlington, Va.
ACTIVATION ANALYSIS OF NATURAL WATER USING NEUTRONS OF VARIOUS ENERGIES Abstract Only
R. Kamidova and A. A. Abdullayev *In its* USSR Rept.: Phys. and Math. (JPRS-UPM-85-004) 17 Jun. 1985 p 55 Transl. into ENGLISH from Izv. Akad. Nauk USSR: Ser. Fiz.-Mat. Nauk (Tashkent), no. 4, Jul. - Aug. 1984 p 55-56 (For primary document see N85-32860 21-70)
Avail: NTIS HC A06/MF A01

N85-32925# Joint Publications Research Service, Arlington, Va.
TRANSFORMATION OF CHARGED PARTICLE BEAMS BY CONCENTRATING ELECTRO-OPTICAL SYSTEMS Abstract Only
Ye. V. Shpak and S. Ya. Yavor *In its* USSR Rept.: Phys. and Math. (JPRS-UPM-85-004) 17 Jun. 1985 p 55 Transl. into ENGLISH from Zh. Tekhn. Fiz. (Leningrad), v. 54, no. 10, Oct. 1984 p 1992-1998 (For primary document see N85-32860 21-70)
Avail: NTIS HC A06/MF A01

N85-32928# Joint Publications Research Service, Arlington, Va.
AN ATTEMPT TO DETECT INDUCED NEUTRON CAPTURE IN LASER RADIATION FIELD Abstract Only
S. M. Mironov and G. U. Muradyan *In its* USSR Rept.: Phys. and Math. (JPRS-UPM-85-004) 17 Jun. 1985 p 57 Transl. into ENGLISH from Yadernaya Fiz. (Moscow), v. 40, no. 12, Dec. 1984 p 1393-1395 (For primary document see N85-32860 21-70)
Avail: NTIS HC A06/MF A01

N85-32929# Joint Publications Research Service, Arlington, Va.
TOWARD THE QUESTION OF MULTI-QUARK CONFIGURATIONS IN NUCLEI Abstract Only
V. R. Garsevanishvili and Z. R. Menteshashvili *In its* USSR Rept.: Phys. and Math. (JPRS-UPM-85-004) 17 Jun. 1985 p 58 Transl. into ENGLISH from Pisma v Zh. Eksperim. i Teor. Fiz. (Moscow), v. 40, no. 8, Oct. 1984 p 359-362 (For primary document see N85-32860 21-70)
Avail: NTIS HC A06/MF A01

N85-32930# Joint Publications Research Service, Arlington, Va.
EXOTIC EVENTS OF p BAR p-COLLIDER: EXCITED QUARK OR EXCITED COLOR BOSON? Abstract Only
S. S. Gershteyn, G. V. Dzhikiya, and Yu. F. Pirogov *In its* USSR Rept.: Phys. and Math. (JPRS-UPM-85-004) 17 Jun. 1985 p 58-59 Transl. into ENGLISH from Yadernaya Fiz. (Moscow), v. 40, no. 12, Dec. 1984 p 1500-1514 (For primary document see N85-32860 21-70)
Avail: NTIS HC A06/MF A01

N85-32931# Joint Publications Research Service, Arlington, Va.
THE POSSIBILITY OF OBSERVING AND EXPLOITING THE GENERATION OF HIGH-ENERGY PHOTONS BY ELECTRONS IN THE FIELD OF AN INTENSE ELECTROMAGNETIC WAVE Abstract Only
I. F. Ginzburg, G. L. Kotkin, and S. I. Polityko *In its* USSR Rept.: Phys. and Math. (JPRS-UPM-85-004) 17 Jun. 1985 p 59 Transl. into ENGLISH from Yadernaya Fiz. (Moscow), v. 40, no. 12, Dec. 1984 p 1495-1499 (For primary document see N85-32860 21-70)
Avail: NTIS HC A06/MF A01

N85-32932# Joint Publications Research Service, Arlington, Va.
SPATIAL PARITY VIOLATION IN ELASTIC NEUTRON-NUCLEI INTERACTION CHANNEL Abstract Only
V. P. Alfimenkov *In its* USSR Rept.: Phys. and Math. (JPRS-UPM-85-004) 17 Jun. 1985 p 61 Transl. into ENGLISH from Uspekhi Fiz. Nauk (Moscow), v. 14, no. 3, Nov. 1984 p 361-380 (For primary document see N85-32860 21-70)
Avail: NTIS HC A06/MF A01

N85-32933# Joint Publications Research Service, Arlington, Va.
POSSIBILITY OF DEVELOPING CHARGED-PARTICLE ENERGY ANALYZER BASED ON HYPERBOLOIDAL AXISYMMETRICAL LENS Abstract Only
V. S. Gurov and E. P. Sheretov *In its* USSR Rept.: Phys. and Math. (JPRS-UPM-85-004) 17 Jun. 1985 p 61 Transl. into ENGLISH from Zh. Tekhn. Fiz. (Leningrad), v. 54, no. 12, Dec. 1984 p 2383-2386 (For primary document see N85-32860 21-70)
Avail: NTIS HC A06/MF A01

N85-32934# Joint Publications Research Service, Arlington, Va.
HIGH-ENERGY PHYSICS INSTITUTE BUILDING 3-TRILLION-EV ACCELERATOR Abstract Only
S. Kulinich *In its* USSR Rept.: Phys. and Math. (JPRS-UPM-85-004) 17 Jun. 1985 p 63 Transl. into ENGLISH from Mosk. Komsomolets (Moscow), 13 Feb. 1985 p 4 (For primary document see N85-32860 21-70)
Avail: NTIS HC A06/MF A01

74 OPTICS

Includes light phenomena.

N85-33010# IBM Research Lab., San Jose, Calif.
NONLINEAR SPECTROSCOPY Final Report, 1 Jan. 1978 - 31 Dec. 1984
R. G. Brewer 20 Mar. 1985 592 p
(Contract N00014-78-C-0246)
(AD-A154708) Avail: NTIS HC A25/MF A01 CSCL 20/6

Work continued in the general area of Laser Spectroscopy, the emphasis being on coherent optical transients and precision spectroscopy. Both theoretical and experimental studies were conducted. The most notable experimental accomplishments include the development of new experimental techniques: (1) the laser frequency switching technique of observing coherent optical transients such as optical free induction decay and photon echoes for studying the dynamic properties of solids or gas phase collisions; (2) the extension of these ideas to the picosecond time scale using a novel traveling wave electro-optic phase modulator; (3) the frequency stabilization of dye lasers to a linewidth of approx., the 100 Hertz for precision spectroscopic measurements; and (4) the Raman heterodyne detection method for observing nuclear magnetic resonance with a sensitive optical probe. One of the interesting applications of ultrastable dye lasers has been in the area of solid state laser spectroscopy where the optical homogeneous linewidths are of the order of 1 kilohertz or less. Other theoretical studies include: (1) a generalized theory of two-photon processes; (2) oscillatory free induction decay which lead to a prediction of a new phenomenon that was later verified both in the optical and radio frequency regions; (3) an elegant theorem on coherent transients which sets a rigorous limit on the duration of any coherent transient emission signal; and (4) a theory of cumulative two-pulse photon echoes. GRA

N85-33011# Cornell Univ., Ithaca, N.Y. School of Electrical Engineering.
OBJECT IDENTIFICATION AND MANIPULATION USING SILHOUETTE MOMENTS Final Report, Jul. 1983 - Dec. 1984
A. P. Reeves and R. W. Taylor Apr. 1985 73 p
(Contract N00014-83-K-2027)
(AD-A154755) Avail: NTIS HC A04/MF A01 CSCL 17/5

The theory of silhouette moments are presented along with results for classifying clean and noisy images. Noise reduction by image averaging is examined comparatively in image and moment spaces. Results are presented for classifications using subsets of the complete moment set. An inverse moment transform procedure is developed and demonstrated. GRA

N85-33012# Massachusetts Univ., Amherst. Astronomy Research Facility.
SCRIBE DATA OF OCTOBER 23, 1983 FLIGHT
H. Sakai and G. Vanasse Aug. 1984 53 p
(Contract F19628-84-K-0009)
(AD-A154864; UMASS-ARF-84-004; AFGL-TR-84-0208; SR-1) Avail: NTIS HC A04/MF A01 CSCL 20/6

This document describes a cryogenic interferometer launched at 12:12 GMT from Holloman AFB, NM. The instrument package reached the ceiling altitude at approximately 14:00. The data measurement was terminated at approximately 16:00. The parameters pertinent to the data measurement are presented collectively in Figure 1. The on-board instrument functioned satisfactorily for most of this time period. The PCM telemetry data were found processable during this time except for a short period between 12:30 and 13:00. The interferometer sampling scheme worked satisfactorily. Only few interferogram data showed faulty sampling during the entire flight. Each interferogram scan took approximately 30 seconds covering the optical path difference range from 0 cm to its maximum value over 8.25 cm. The interferogram signals were recorded with adequate signal-to-noise ratio to warrant spectral resolution figure of 0.060265 1/cm. Author (GRA)

N85-33013# Emory Univ., Atlanta, Ga. Dept. of Chemistry.
OPTICAL OUTPUT STABILIZATION METHOD FOR DIRECT CURRENT ARC LAMPS Interim Report
P. B. Oldham, G. Patonay, and I. M. Warner 30 Apr. 1985 24 p
(Contract N00014-83-K-0026)
(AD-A154987; EMORY/DC/TR-5) Avail: NTIS HC A02/MF A01 CSCL 13/1

A simple, effective technique for stabilizing the optical output of direct current (dc) arc lamps is described. The large output fluctuation due to arc wander in a commercially available lamp and power supply is minimized by the introduction of an alternating current (ac) waveform superimposed on the dc source voltage in conjunction with detector averaging. Arc stability is monitored indirectly by the detection of arc excited fluorescence from a standard sample. The monitored lamp output is typically maintained to within 1% relative standard deviation (RSD) by this method. Data are presented supporting the theory that arc wander is significantly reduced by the addition of an ac component to the dc lamp power. Various methods of ac introduction are discussed along with the design of a controllable oscillator circuit. The effects of variations in ac voltage and frequency on optical output stability are examined. Author (GRA)

N85-33014# Naval Research Lab., Washington, D. C.
KALMAN FILTER TIME SERIES ANALYSIS OF GAMMA-RAY DATA FROM NaI(T1) DETECTORS FOR THE ND6620 COMPUTER Final Report
G. W. Phillips 8 May 1985 117 p
(AD-A154995; NRL-MR-5541) Avail: NTIS HC A06/MF A01 CSCL 20/6

The Kalman Filter technique is applied to time series gamma-ray data from NaI(T1) detectors. A set of standard spectra which contribute significantly to the data in the least-squares sense are first determined using regression analysis. The Kalman Filter computer program is then used to determine the time behavior for the intensities of the standards which contribute to the observed spectra. The program was written for the ND6620 computer in DEC RT-11 FORTRAN and is being transferred to the VAX 11/780. GRA

N85-33015# Army Cold Regions Research and Engineering Lab., Hanover, N. H.
ICE FOG AS AN ELECTRO-OPTICAL OBSCURANT
G. Koh Mar. 1985 19 p
(AD-A155059; CRREL-85-8) Avail: NTIS HC A02/MF A01 CSCL 20/6

The extinction of visible light and infrared radiation (at wavelengths of 3.5 and 10.6 microns) by ice fog is considered utilizing theoretical concepts and historical experimental data. The reliability of the spherical approximation of ice fog for Mie calculations is examined and judged adequate for forward scatter situations but limited for side and backscatter applications. The relative efficacy in penetrating ice fog as a function of size distribution is evaluated for the wavelengths considered. GRA

N85-32923# Joint Publications Research Service, Arlington, Va.
TRANSPARENCY OF WATER 9N 186 - 500 nm REGION Abstract Only
N. P. Romanov and V. S. Shuklin *In its* USSR Rept.: Phys. and Math. (JPRS-UPM-85-004) 17 Jun. 1985 p 54 Transl. into ENGLISH from Zh. Prikl. Spektroskopii (Minsk), v. 41, no. 4, Oct. 1984 p 647-652 Original language document previously announced in IAA as A85-20593 (For primary document see N85-32860 21-70)
Avail: NTIS HC A06/MF A01

N85-32950# Joint Publications Research Service, Arlington, Va.
COMPARISON OF FINDINGS OF THEORIES DESCRIBING REFLECTION FROM REAL SURFACE WITH EXPERIMENTS IN REGION OF ULTRASOFT X-RADIATION Abstract Only
A. Ya. Grudskiy *In its* USSR Rept.: Phys. and Math. (JPRS-UPM-85-004) 17 Jun. 1985 p 72 Transl. into ENGLISH from Opt. Spektrosk. (Leningrad), v. 57, no. 5, Nov. 1984 p 880-883 (For primary document see N85-32860 21-70)
Avail: NTIS HC A06/MF A01

N85-32951# Joint Publications Research Service, Arlington, Va.
EFFECTIVE BRIGHTNESS OF ZERO-POINT FLUCTUATIONS OF THE ELECTROMAGNETIC VACUUM ACCOMPANYING PARAMETRIC SCATTERING OF LIGHT Abstract Only
O. N. Abroskina, G. Kh. Kitayeva, and A. N. Penin *In its* USSR Rept.: Phys. and Math. (JPRS-UPM-85-004) 17 Jun. 1985 p 75 Transl. into ENGLISH from Dokl. Akad. Nauk SSSR (Moscow), v. 280, no. 3, Jan. 1985 p 584-586 (For primary document see

N85-32860 21-70)
Avail: NTIS HC A06/MF A01

N85-32954# Joint Publications Research Service, Arlington, Va.
OPTICAL WAVEGUIDE ALONG FRONT OF EXOTHERMIC REACTION Abstract Only
P. B. Lerner and B. S. Lukyanchuk *In its* USSR Rept.: Phys. and Math. (JPRS-UPM-85-004) 17 Jun. 1985 p 77 Transl. into ENGLISH from Zh. Tekh. Fiz. (Leningrad), v. 54, no. 12, Dec. 1984 p 2397-2400 (For primary document see N85-32860 21-70)
Avail: NTIS HC A06/MF A01

N85-32955# Joint Publications Research Service, Arlington, Va.
ELECTROSTATIC ASTIGMATIC TUBULAR LENS Abstract Only
L. G. Grikman, Z. D. Iskakova, and I. A. Petrov *In its* USSR Rept.: Phys. and Math. (JPRS-UPM-85-004) 17 Jun. 1985 p 77 Transl. into ENGLISH from Zh. Tekh. Fiz. (Leningrad), v. 54, no. 12, Dec. 1984 p 2342-2346 (For primary document see N85-32860 21-70)
Avail: NTIS HC A06/MF A01

N85-32956# Joint Publications Research Service, Arlington, Va.
FLUCTUATIONS IN LIGHT INTENSITY DURING BACKSCATTERING IN TURBULENT MEDIUM Abstract Only
S. S. Kashkarov, T. N. Nesterova, and A. S. Smirnov *In its* USSR Rept.: Phys. and Math. (JPRS-UPM-85-004) 17 Jun. 1985 p 78 Transl. into ENGLISH from Izv. Vyssh. Ucheb. Zaved., Radiofiz. (Gorky, USSR), v. 28, no. 10, Oct. 1984 p 1272-1278 (For primary document see N85-32860 21-70)
Avail: NTIS HC A06/MF A01

N85-32957# Joint Publications Research Service, Arlington, Va.
RELAXATION LENS IN INHOMOGENEOUS BINARY MIXTURE Abstract Only
E. T. Bruk-Levinson, Z. Plokhotski, and I. V. Khodan *In its* USSR Rept.: Phys. and Math. (JPRS-UPM-85-004) 17 Jun. 1985 p 78-79 Transl. into ENGLISH from Dokl. Akad. Nauk BSSR (Minsk), v. 28, no. 12, Dec. 1984 p 1090-1093 (For primary document see N85-32860 21-70)
Avail: NTIS HC A06/MF A01

N85-32959# Joint Publications Research Service, Arlington, Va.
COEFFICIENT OF OPTICAL ABSORPTION AND SCATTERED LIGHT CAPTURE EFFECT Abstract Only
L. I. Mitsay and V. A. Nemeenov *In its* USSR Rept.: Phys. and Math. (JPRS-UPM-85-004) 17 Jun. 1985 p 79-80 Transl. into ENGLISH from Kvantovaya Electron. (Moscow), v. 11, no. 10, Oct. 1984 p 2116-2120 (For primary document see N85-32860 21-70)
Avail: NTIS HC A06/MF A01

N85-32960# Joint Publications Research Service, Arlington, Va.
METHODS FOR MEASURING AND ANALYZING DISPERSION PROPERTIES OF MULTIMODE FIBER OPTIC LIGHTPIPES (A REVIEW) Abstract Only
T. V. Babkina, V. V. Grigoryants, and V. B. Smirnov *In its* USSR Rept.: Phys. and Math. (JPRS-UPM-85-004) 17 Jun. 1985 p 80 Transl. into ENGLISH from Kvantovaya Elektron. (Moscow), v. 11, no. 10, Oct. 1984 p 1899-1939 Original language document previously announced as A85-21017 (For primary document see N85-32860 21-70)
Avail: NTIS HC A06/MF A01

N85-32961# Joint Publications Research Service, Arlington, Va.
STIMULATED MANDELSTAM-BRILLOUIN SCATTERING WITH DISTRIBUTED FEEDBACK Abstract Only
O. P. Zaskalko, A. N. Zozulya, Yu. I. Kyzylasov, N. N. Panaioti, V. P. Silin, V. T. Tikhonchuk, and I. L. Fabelinskiy *In its* USSR Rept.: Phys. and Math. (JPRS-UPM-85-004) 17 Jun. 1985 p 80-81 Transl. into ENGLISH from Zh. Eksperim. Teoreticheskoy Fiz. (Moscow), v. 57, no. 5, Nov. 1984 p 1582-1593 (For primary document see N85-32860 21-70)
Avail: NTIS HC A06/MF A01

N85-32962# Joint Publications Research Service, Arlington, Va.
INFLUENCE OF PHONON INTERACTION ON WIDTH AND FORM OF MANDELSTAM-BRILLOUIN OPTICAL SCATTERING LINE Abstract Only
S. V. Gantsevich, V. D. Kagan, R. Katilyus, and E. A. Rzayev *In its* USSR Rept.: Phys. and Math. (JPTS-UPM-85-004) 17 Jun. 1985 p 81 Transl. into ENGLISH from Zh. Eksperim. Teoreticheskoy Fiz. (Moscow), v. 57, no. 5, Nov. 1984 p 1734-1744 (For primary document see N85-32860 21-70)
Avail: NTIS HC A06/MF A01

N85-32963# Joint Publications Research Service, Arlington, Va.
SOLVABILITY OF SOME INVERSE PROBLEMS IN LASER RADIATION FOCUSING Abstract Only
A. V. Goncharskiy, I. N. Sisakyan, and V. V. Stepanov *In its* USSR Rept.: Phys. and Math. (JPRS-UPM-85-004) 17 Jun. 1985 p 82 Transl. into ENGLISH from Dokl. Akad. Nauk SSSR (Moscow), v. 279, no. 1, Nov. 1984 p 68-71 (For primary document see N85-32860 21-70)
Avail: NTIS HC A06/MF A01

N85-32964# Joint Publications Research Service, Arlington, Va.
INFLUENCE OF SPATIAL PUMPING SPECTRUM ON QUALITY OF PHASE CONJUGATE REFLECTION DURING 4-PHOTON INTERACTION Abstract Only
V. V. Ivaknik *In its* USSR Rept.: Phys. and Math. (JPRS-UPM-85-004) 17 Jun. 1985 p 82 Transl. into ENGLISH from Izv. Vyssh. Ucheb. Zaved., Fiz. (Tomsk, USSR), v. 27, no. 9, Sep. 1984 p 115-117 (For primary document see N85-32860 21-70)
Avail: NTIS HC A06/MF A01

N85-32965# Joint Publications Research Service, Arlington, Va.
NEW METHOD FOR CORRECTING CHROMATISM OF MIRROR-LENS OBJECTIVES Abstract Only
N. L. Sokolov *In its* USSR Rept: Phys. and Math. (JPRS-UPM-85-004) 17 Jun. 1985 p 83 Transl. into ENGLISH from Opt. Spektrosk. (Leningrad), v. 57, no. 2, Sep. 1984 p 543-545 (For primary document see N85-32860 21-70)
Avail: NTIS HC A06/MF A01

N85-32966# Joint Publications Research Service, Arlington, Va.
DIELECTRIC MIRROR WITH FERROMAGNETIC SUBSTRATE Abstract Only
M. S. Borisova and Ye. N. Chernykh *In its* USSR Rept.: Phys. and Math. (JPRS-UPM-85-004) 17 Jun. 1985 p 83 Transl. into ENGLISH from Opt. Spektrosk. (Leningrad), v. 57, no. 3, Sep. 1984 p 543-545 (For primary document see N85-32860 21-70)
Avail: NTIS HC A06/MF A01

N85-32967# Joint Publications Research Service, Arlington, Va.
THE FARADAY EFFECT IN RUBY AND CORUNDUM IN STRONG MAGNETIC FIELDS Abstract Only
B. B. Bouko and A. K. Soyka *In its* USSR Rept.: Phys. and Math. (JPRS-UPM-85-004) 17 Jun. 1985 p 84 Transl. into ENGLISH from Dokl. Akad. Nauk SSSR (Minsk), v. 28, no. 11, Nov. 1984 p 984-987 (For primary document see N85-32860 21-70)
Avail: NTIS HC A06/MF A01

N85-32968# Joint Publications Research Service, Arlington, Va.
OPTICAL IMAGE OF BOUNDED OBJECTS Abstract Only
Yu. V. Vorobev *In its* USSR Rept.: Phys. and Math. (JPRS-UPM-85-004) 17 Jun. 1985 p 84 Transl. into ENGLISH from Opt. Spektrosk. (Leningrad), v. 57, no. 5, Nov. 1984 p 921-926 (For primary document see N85-32860 21-70)
Avail: NTIS HC A06/MF A01

N85-32969# Joint Publications Research Service, Arlington, Va.
TRANSMISSION OF LIGHT BY DISPERSE MEDIUM OF DENSELY PACKED OPTICALLY SOFT PARTICLES Abstract Only
V. P. Dik, A. P. Ivanov, and V. A. Loyko *In its* USSR Rept.: Phys. and Math. (JPRS-UPM-85-004) 17 Jun. 1985 p 85 Transl. into ENGLISH from Opt. Spektrosk. (Leningrad), vol. 57, no. 5,

Nov. 1984 p 884-888 (For primary document see N85-32860 21-70)
Avail: NTIS HC A06/MF A01

75 PLASMA PHYSICS

Includes magnetohydrodynamics and plasma fusion.
For ionospheric plasmas see *46 Geophysics*. For space plasmas see *90 Astrophysics*.

N85-33016# Naval Research Lab., Washington, D. C.
LOW FREQUENCY INSTABILITIES DRIVEN BY AN ION TEMPERATURE ANISOTROPY Memorandum Report, Oct. 1984 - Oct. 1985
Y. C. Lee and J. D. Huba 8 May 1985 42 p
(AD-A154902; NRL-MR-5552) Avail: NTIS HC A03/MF A01 CSCL 20/9

We present a detailed linear analysis of low frequency instabilities driven by an ion temperature anisotropy. In particular we investigate the electromagnetic ion cyclotron instability, the mirror instability, and the firehose instability. These instabilities require a high Beta plasma which is typical of an early time HANE plasma. The electromagnetic ion cyclotron and mirror instabilities also require ion temperature anisotrophy while the firehose instability requires ion temperature anisotrophy. In general, we expect the early time coupling shell to have ion temperature anisotrophy so that the firehose instability is not obviously relevant to HANE situations but is included for the sake of completeness. We have also included an analysis of the influence of an electron temperature for the sake of completeness. We have also included an analysis of the influence of an electron temperature anisotropy on the Magnetohydrodynamics instability. This is an extension and correction of the work of Basu and Coppi (1984). We discuss the application of this research to HANE phenomena. GRA

N85-33017# California Univ., Los Angeles. Center for Plasma Physics and Fusion Engineering.
CYCLOTRON RESONANCE IN A NONNEUTRAL PLASMA
S. A. Prasad, G. J. Morales, and B. D. Fried Apr. 1985 15 p
(Contract N00014-75-C-0476)
(AD-A155248; PPG-861) Avail: NTIS HC A02/MF A01 CSCL 20/9

Single component plasmas are found to exhibit a reversal in the roles of cyclotron and upper hybrid resonances familiar in neutral plasmas. There is a global resonance at the cyclotron frequency omega = Omega = qB/mc and a local field cancellation at layers where omega = Omega sub 1 = sq rt(Omega-squared-(omega sub p) squared), omega sub p being the local plasma frequency. Thermal effects limit the amplitude of the global resonance and produce energy absorption at the omega = Omega sub 1 layers. Author (GRA)

N85-33018# Louisiana State Univ., Baton Rouge. Dept. of Mechanical Engineering.
MODELING THE EXHAUST OF THE PULSED PLASMA THRUSTER Final Report, 1 Jun. - 15 Aug. 1980
D. W. Yannitell Feb. 1985 34 p
(Contract F49620-79-C-0038)
(AD-A155344; AFRPL-TR-85-005) Avail: NTIS HC A03/MF A01 CSCL 21/3

The work presented in this report is an investigation of the plasma flow on a Teflon Pulsed Plasma Thruster (PPT), and the resulting plume. The long range goal is a theoretical model of the flow, both between and beyond the thruster electrodes, that could aid in the improvement of performance, and also predict the contamination potential of the device. The overall model required consists of an internal portion interfaced with an external portion at the exit plane of the electrodes. Most of this report deals with the internal portion of the model. Specifically, the physics of the discharge and plasma acceleration between the electrodes are discussed, and a mathematical model is developed which appears to be consistant with the available experimental data. The investigation shows the necessity of certain additional information without which the model cannot be properly exercised. The validity of certain assumptions of magnetohydrodynamic theory is demonstrated for the nontypical plasma produced by the PPT, and logical consequences of the assumptions are considered vis a vis recently obtained electromagnetic data. A major difficulty in the modeling of the internal flow is the selection of the proper boundary conditions to be applied to the solution domain. These include conditions at the electrodes, the insulator, the ablating Teflon surfaces, and the interface with the vacuum ahead of, and behind, the plasma blobs. GRA

N85-33019# Naval Research Lab., Washington, D. C.
ELECTROSTATIC ION CYCLOTRON INSTABILITY DUE TO A NONUNIFORM ELECTRIC FIELD PERPENDICULAR TO THE EXTERNAL MAGNETIC FIELD
G. Ganguli, Y. C. Lee, and P. Palmadesso 28 May 1985 20 p (RR0-3302)
(AD-A155474; NRL-MR-5549) Avail: NTIS HC A02/MF A01 CSCL 20/3

We suggest a new mechanism that can destabilize the kinetic ion cyclotron waves in the presence of a nonuniform electric field perpendicular to the uniform ambient magnetic field. In the absence of the electric field the mode energy is positive while in the presence of a uniform electric field the mode energy and could be negative. However, when the electric field is nonuniform, it is possible for a finite region to be of negative wave energy surrounded by regions of positive wave energy. A nonlocal wave packet couples the two regions so that a flow of energy from the region of negative wave energy to the region of positive wave energy will cause the mode to grow. This gives rise to the instability. Author (GRA)

N85-33020# Naval Research Lab., Washington, D. C.
OPERATIONAL WINDOW FOR A PLASMA EROSION OPENING SWITCH USED FOR VOLTAGE MULTIPLICATION ON PULSED POWER GENERATORS
P. F. Ottinger 5 Jun. 1985 28 p
(AD-A155482; NRL-MR-5591) Avail: NTIS HC A03/MF A01 CSCL 09/5

The Plasma Erosion Opening Switch (PEOS) is a fast opening switch which has been shown to be capable of conducting megampere-level currents before opening in <10 ns. Such a switch can be used for inductive storage in order to compress the output from conventional pulsed power generator in order to achieve voltage and power multiplication. An operational window is described herein which illustrates the voltage regime made accessible for a given machine by the switch. Author (GRA)

N85-33021# Oak Ridge National Lab., Tenn.
MAGNETICS CALCULATIONS FOR AN ELMO BUMPY SQUARE
R. T. Santoro, N. A. Uckan, and R. J. Schmidt 1985 2 p Presented at the 6th Topical Meeting on the Technol. of Fusion Energy, San Francisco, 3 Mar. 1985 Prepared in cooperation with McDonnell Douglas Astronautics Co., St. Louis
(Contract DE-AC05-84OR-21400)
(DE85-011438; CONF-850310-90) Avail: NTIS HC A02/MF A01

Advanced ELMO Bumpy Torus (EBT) concepts were studied to determine the potential for new and different concepts as confinement experiments or as reactors. Several magnetic configurations based on the EBT confinement concept were developed including the ELMO Bumpy Square (EBS). The EBS was selected as a possible candidate for near-term study because of its potential for resolving critical EBT issues, for its desirability as a reactor, and for anticipated contributions to the physics and technology of fusion. Magnetics calculations in support of studies to assess the merits of an EBS are summarized. DOE

N85-33022# Los Alamos National Lab., N. Mex.
MAGNETIC FIELDS IN LASER HEATED PLASMAS
F. Amiranoff, J. Brackbill, D. Colombant, and N. Grandjouan 1984 15 p Presented at the CECAM Workshop Transport, Interactions,

and Instabilities in Laser-Plasmas, Orsay, France, 24 Sep. 1984 Prepared in cooperation with Ecole Polytechnique, Paris and Naval Research Lab., Washington, D.C.
(Contract W-7405-eng-36)
(DE85-010715; LA-UR-85-1251; CONF-8409229-2) Avail: NTIS HC A02/MF A01

With a fixed-ion code for the study of self-generated magnetic fields in laser heated plasmas, the inhibition of thermal transport and the effect of the Nernst term are modeled for a KrF laser. For various values of the flux limiter, the response of a foil to a focused laser is calculated without a magnetic field and compared with the response calculated with a magnetic field. The results are: the Nernst term convects the magnetic field to densities above critical, but the field does not strongly inhibit transport into the foil. The field is also transported to subcritical densities, where it inhibits thermal diffusion and enhance lateral transport by convection. DOE

N85-32894# Joint Publications Research Service, Arlington, Va.
IN-CAVITY LASER IR SPECTRUM ANALYZER FOR INVESTIGATING NON-STEADY-STATE PROCESSES Abstract Only
V. A. Vratskiy and A. N. Kolerov *In its* USSR Rept.: Phys. and Math. (JPRS-UPM-85-004) 17 Jun. 1985 p 33 Transl. into ENGLISH from Zh. Prikl. Spektroskopii (Minsk), v. 41, no. 4, Oct. 1984 p 561-566 (For primary document see N85-32860 21-70)
Avail: NTIS HC A06/MF A01

N85-32926# Joint Publications Research Service, Arlington, Va.
THERMAL CONTRACTION OF CURRENT FLOW THROUGH ELECTRODE TURBULENT BOUNDARY LAYER Abstract Only
A. V. Nedospasov, V. D. Khait, and A. E. Sheyndlin *In its* USSR Rept.: Phys. and Math. (JPRS-UPM-85-004) 17 Jun. 1985 p 56 Transl. into ENGLISH from Dokl. Akad. Nauk SSSR (Moscow), v. 280, no. 3, Jan. 1985 p 594-597 (For primary document see N85-32860 21-70)
Avail: NTIS HC A06/MF A01

N85-32935# Joint Publications Research Service, Arlington, Va.
INVESTIGATION OF ION-ACOUSTIC PLASMA TURBULENCE IN FIELD OF POWERFUL ELECTROMAGNETIC WAVE BY CO2-LASER RADIATION SCATTERING Abstract Only
M. P. Brizhinev, V. V. Bulanin, B. G. Yeremin, A. V. Kostrov, A. V. Petrov, and S. G. Revin *In its* USSR Rept.: Phys. and Math. (JPRS-UPM-85-004) 17 Jun. 1985 p 64 Transl. into ENGLISH from Pisma v Zh. Eksperim. Teor. Fiz. (Moscow), v. 40, no. 8, Oct. 1984 p 332-334 (For primary document see N85-32860 21-70)
Avail: NTIS HC A06/MF A01

N85-32936# Joint Publications Research Service, Arlington, Va.
SOLUTION OF PROBLEM OF EQUILIBRIUM CONFINEMENT OF PLASMA BY MAGNETIC FIELD IN AN INFINITE CIRCULAR CYLINDER Abstract Only
G. I. Sulkhanishvili *In its* USSR Rept.: Phys. and Math. (JPRS-UPM-85-004) 17 Jun. 1985 p 64-65 Transl. into ENGLISH from Soobsch. Akad. Nauk Gruzinskoy SSR (Tbilisi), v. 115, no. 1, Jul. 1984 p 25-28 (For primary document see N85-32860 21-70)
Avail: NTIS HC A06/MF A01

N85-32937# Joint Publications Research Service, Arlington, Va.
INJECTION OF HYDROGEN MACROPARTICLES INTO T-10 TOKAMAK Abstract Only
A. P. Andreyev, B. V. Kuteyev, A. A. A. Lovtsyus, A. Ya. Lukin, S. V. Skoblikov, A. P. Umov, and L. D. Tsendin *In its* USSR Rept.: Phys. and Math. (JPRS-UPM-85-004) 17 Jun. 1985 p 65 Transl. into ENGLISH from Pisma v Zh. Tekhn. Fiz. (Leningrad), v. 10, no. 19, 12 Oct. 1984 p 1199-1203 (For primary document see N85-32860 21-70)
Avail: NTIS HC A06/MF A01

N85-32938# Joint Publications Research Service, Arlington, Va.
CCD-BASED X-RAY SPECTROMETRY FOR ON-LINE DETERMINATION OF LASER PLASMA ELECTRON TEMPERATURE Abstract Only
V. V. Blazhenkov, O. P. Varnavskiy, A. M. Kirkin, A. M. Leontovich, V. V. Lidskiy, V. V. Lidskiy, R. G. Mirzoyan, and A. M. Mozharovskiy *In its* USSR Rept.: Phys. and Math. (JPRS-UPM-85-004) 17 Jun. 1985 p 65-66 Transl. into ENGLISH from Pisma Zh. Tekh. Fiz. (Leningrad), v. 10, no. 19, 12 Oct. 1984 p 1165-1169 (For primary document see N85-32860 21-70)
Avail: NTIS HC A06/MF A01

N85-32942# Joint Publications Research Service, Arlington, Va.
ELECTROMAGNETIC WAVE AMPLIFICATION DURING CYCLOTRON RESONANCE IN A MEDIUM Abstract Only
G. K. Avetisyan and K. Z. Atsagortsyan *In its* USSR Rept.: Phys. and Math. (JPRS-85-004) 17 Jun. 1985 p 67 Transl. into ENGLISH from Zh. Tekh. Fiz. (Leningrad), v. 54, no. 12, Dec. 1984 p 2347-2349 (For primary document see N85-32860 21-70)
Avail: NTIS HC A06/MF A01

N85-32943# Joint Publications Research Service, Arlington, Va.
PLASMODYNAMIC METHODS FOR GENERATING POWERFUL LIGHT PUSES Abstract Only
A. F. Aleksandrov and I. B. Timofeyev *In its* USSR Rept.: Phys. and Math. (JPRS-UPM-85-004) 17 Jun. 1985 p 68 Transl. into ENGLISH from Izv. Sib. Otd. Akad. Nauk SSSR, Ser. Tekh. Nauk (Novosibirsk, USSR), v. 16, no. 3, Oct. 1984 p 65-75 (For primary document see N85-32860 21-70)
Avail: NTIS HC A06/MF A01

N85-32944# Joint Publications Research Service, Arlington, Va.
CHARACTERISTICS OF OPTOGALVANIC EFFECT IN MEDIA WITH INVERSE POPULATIONS Abstract Only
V. S. Burakov, P. Ya. Misakov, P. A. Naumenkov, and S. N. Raykov *In its* USSR Rept.: Phys. and Math. (JPRS-UPM-85-004) 17 Jun. 1985 p 68-69 Transl. into ENGLISH from Dokl. Akad. Nauk BSSR (Minsk), v. 28, no. 12, Dec. 1984 p 1078-1081 (For primary document see N85-32860 21-70)
Avail: NTIS HC A06/MF A01

N85-32945# Joint Publications Research Service, Arlington, Va.
CYCLOTRON ABSORPTION OF FAST MAGNETOSONIC WAVE IN STELLARATOR Abstract Only
L. M. Kovrizhnykh and P. Ye. Moroz *In its* USSR Rept.: Phys. and Math. (JPRS-UPM-85-004) 17 Jun. 1985 p 69 Transl. into ENGLISH from Zh. Eksperim. i Teoreticheskoy (Moscow), v. 57, no. 5, Nov. 1984 p 1649-1651 (For primary document see N85-32860 21-70)
Avail: NTIS HC A06/MF A01

N85-32946# Joint Publications Research Service, Arlington, Va.
A SYSTEM OF MAGNETOHYDRODYNAMIC-TYPE EQUATIONS Abstract Only
Ye. V. Chizhonkov and M. V. Lomonosov *In its* USSR Rept.: Phys. and Math. (JPRS-UPM-85-004) 17 Jun. 1985 p 69 Transl. into ENGLISH from Prikl. Mat. i Mekh. (Moscow), v. 48, no. 4, Jul. - Aug. 1984 p 1074-1077 (For primary document see N85-32860 21-20)
Avail: NTIS HC A06/MF A01

N85-32947# Joint Publications Research Service, Arlington, Va.
INVESTIGATION OF SPACE-TIME STRUCTURE OF GLOW OF LASER PLASMA COLLIDING WITH FLAT SCREEN Abstract Only
V. A. Boyko, B. A. Bryunetkin, F. V. Bunkin, B. Z. Gorbenko, V. I. derzhiyev, V. M. Dyakin, S. A. Mayorov, I. Yu. Skobelev, B. M. Stepanov, A. Ya. Fayenov et al *In its* USSR Rept.: Phys. and Math. (JPRS-UPM-85-004) 17 Jun. 1985 p 70 Transl. into ENGLISH from Zh. Tekh. Fiz. (Leningrad), vol. 54, no. 10, Oct. 1984 p 1915-1922 (For primary document see N85-32860 21-70)
Avail: NTIS HC A06/MF A01

N85-32948# Joint Publications Research Service, Arlington, Va.
DIAMAGNETIC INSTABILITY OF CYCLOTRON WAVES IN PLASMA Abstract Only
L. V. Borodachev and A. K. Nekrasov *In its* USSR Rept.: Phys. and Math. (JPRS-UPM-85-004) 17 Jun. 1985 p 70 Transl. into

ENGLISH from Vestn. Mosk. Univ., Fiz., Astron. (Moscow), vol. 25, no. 5, Sep. - Oct. 1984 p 91-98 (For primary document see N85-32860 21-70)
Avail: NTIS HC A06/MF A01

N85-32949# Joint Publications Research Service, Arlington, Va.
INFLUENCE OF ECR-HEATING ON MHD ACTIVITY OF PLASMA IN TOKAMAK-10 INSTALLATION Abstract Only
V. V. Alikayev and M. M. Stepanenko *In its* USSR Rept.: Phys. and Math. (JPRS-UPM-85-004) 17 Jun. 1985 p 71 Transl. into ENGLISH from Pisma v Zh. Esperim. i Teoreticheskoy Fiz. (Moscow), v. 40, no. 8, Oct. 1984 p 327-329 (For primary document see N85-32860 21-70)
Avail: NTIS HC A06/MF A01

76 SOLID-STATE PHYSICS

Includes superconductivity.

For related information, see also *33 Electronics and Electrical Engineering* and *36 Lasers and Masers.*

N85-33023# Ohio State Univ., Columbus. Corrosion Center.
THE DEVELOPMENT AND EVALUATION OF POINT DEFECT MODELS FOR THE GROWTH OF PASSIVE FILMS ON SINGLE CRYSTAL, POLYCRYSTALLINE, AND AMORPHOUS METAL SURFACES Final Report, 1 Mar. 1982 - 30 Apr. 1985
D. D. MacDonald, M. Urquidi, and B. W. Wilde 30 Apr. 1985 105 p
(Contract N00014-82-K-0265)
(AD-A154685; FCC-4445-4) Avail: NTIS HC A06/MF A01 CSCL 20/2

The principal task of this program was to develop a better understanding of: (1) the mechanisms of the growth of passive films on metal surfaces; (2) the role of space charge in determining the properties of the film; and (3) passivity breakdown phenomena. Experimental data for the ac impedance and passivity breakdown properties of passive films on nickel are presented in Sections 2 and 3. Also a theoretical development of the point defect model is presented in Section 4. A comparison between the theoretical and experimental data for the growth of passive films on nickel and iron is included. In addition, the role of minor alloying elements (such as molybdenum) on pitting and passivity breakdown is considered theoretically, and the model is compared with experimental data for 18% Cr ferritic stainless steel. The results of this study indicate that the point defect model although at present in a crude state of development, is a reasonable first-approximation theory for explaining some of the basic phenomena related to the growth and breakdown of anodic passive films on metal surfaces. On the basis of data developed in this program it is recommended that further experiments be conducted to further refine the model. GRA

N85-33024# Cornell Univ., Ithaca, N.Y. School of Electrical Engineering.
MICROWAVE SEMICONDUCTOR RESEARCH: MATERIALS, DEVICES AND CIRCUITS AND GALLIUM ARSENIDE BALLISTIC ELECTRON TRANSISTORS Final Report, 1 May 1981 - 30 Apr. 1984
L. F. Eastman, D. W. Woodard, G. W. Wicks, J. Ballantyne, and C. L. Tang Apr. 1985 85 p
(Contract F49620-81-C-0082)
(AD-A154698) Avail: NTIS HC A05/MF A01 CSCL 20/12

This program covers the growth and assessment of Gallium Arsenide, and related compounds and alloys, for use in microwave, millimeter, and optical devices. It also covers the processing of the material into devices, and the testing of the devices. Both molecular beam epitaxy (MBE) and organo-metallic vapor phase epitaxy (OMVPE) are used for growth. Materials assessment is included. Short modulation doped heterojunction bipolar transistors, are covered. The following is a list of tasks pursued: growth and characterization of GaAs for high performance microwave devices, investigation of microwave field-effect transistor performance limits set by layer composition and contact geometry, use of MBE tailored profiles for GaAs power FET's for improved performance, MBE multiple GaAs-Al(x)Ga(1-x)As heterojunctions for confinement of electrons for improved FET performance, high speed receivers for optical communications, dynamic and spectral characteristics of semiconductor laser materials and structures, carrier dynamics in compound semiconductors studied with picosecond optical excitation, advanced design techniques for microwave GaAs FET amplifiers, wide band circuits and systems, and (ballistic task) Gallium arsenide ballistic electron transistors. GRA

N85-33025# Lincoln Lab., Mass. Inst. of Tech., Lexington.
SOLID STATE RESEARCH Quarterly Technical Report, 1 May - 31 Jul. 1984
A. L. McWhorter 15 Aug. 1984 114 p
(Contract F19628-85-C-0002)
(AD-A154783; Rept-1984-3; ESD-TR-84-042) Avail: NTIS HC A06/MF A01 CSCL 20/12

This report covers in detail the solid state research work of the Solid State Division at Lincoln Laboratory for the period 1 May through 31 July 1984. The topics covered are Solid State Device Research, Quantum Electronics, Materials Research, Microelectronics, and Analog Device Technology. Funding is primarily provided by the Air Force, with additional support provided by the Army, DARPA, Navy, NASA, and DOE. GRA

N85-33026# Minnesota Univ., St. Paul.
MICROSCOPIC CONTROL OF SEMICONDUCTOR SURFACE OXIDATION Interim Report
A. Franciosi, S. Chang, P. Philip, C. Caprile, and J. Joyce 15 Apr. 1985 21 p
(Contract N00014-84-K-0545; Grant NSF DMR-80-20164)
(AD-A154799; Rept-1) Avail: NTIS HC A02/MF A01 CSCL 07/4

The effect of ultrathin (0.1-10A) chromium overlayers on the reactivity with oxygen of Si(111) and GaAs(110) cleavage surfaces. Synchrotron radiation photoemission shows that for Cr coverages below a critical threshold coverage the overlayer does not affect substantially the oxygen absorption rate. For chromium coverage above threshold the overlayer sharply enhances the oxygen absorption kinetics so that most semiconductor atoms in the surface and near surface region appear oxidized at activated coverage corresponds to the onset of reactive interdiffusion at the Si(111)-Cr and GaAs(110)-Cr interfaces. Therefore we suggest that ultrathin Si-Cr and As-Cr reacted phases created at the surface act as activation layers for semiconductor oxidation. Author (GRA)

N85-33027# Wisconsin Univ., Madison. Mathematics Research Center.
A SECOND ORDER DIFFERENCE SCHEME FOR TRANSIENT SEMICONDUCTOR DEVICE SIMULATION Technical Summary Report
C. A. Ringhofer Mar. 1985 41 p
(Contract DAAG29-80-C-0041)
(AD-A154824; MRC-TSR-2801) Avail: NTIS HC A03/MF A01 CSCL 09/1

A second order scheme for the solution of the transient fundamental semiconductor device equations is presented which does not suffer from timestep restrictions due to the stiffness of the analytical problem. The second order accuracy as well as the stability properties are demonstrated on the simulation of a p-n-junction diode. GRA

N85-33028# California Univ., Livermore. Lawrence Livermore Lab.
A REVIEW OF THE PHYSICS AND RESPONSE MODELS FOR BURNOUT OF SEMICONDUCTOR DEVICES Final Report
W. J. Orvis, G. H. Khanaka, and J. H. Yee Dec. 1984 89 p
(Contract W-7405-ENG-48)
(AD-A155031; UCRL-53573; DE85-010936) Avail: NTIS HC A05/MF A01 CSCL 09/1

Physical mechanisms that cause semiconductor devices to

fail from electrical overstress--particularly, EMP-induced electrical stress--are described in light of the current literature and the authors' own research. A major concern is the cause and effects of second breakdown phenomena in p-n junction devices. Models of failure thresholds are evaluated for their inherent errors and for their ability to represent the relevant physics. Finally, the response models that relate electromagnetic stress parameters to appropriate failure-threshold parameters are discussed. Author (GRA)

N85-33029# Utah Univ., Salt Lake City. Dept. of Physics.
DOPING SUPERLATTICES IN ORGANOMETALLIC VPE InP Interim Report
J. S. Yuan, M. Gal, P. C. Taylor, and G. B. Stringfellow 1985 11 p
(Contract N00014-83-K-0535; Grant NSF DMR-83-04471)
(AD-A155151; Rept-6) Avail: NTIS HC A02/MF A01 CSCL 07/1

Doping superlattices (nipi structures) have been grown in InP using organometallic vapor phase epitaxy in an atmospheric pressure reactor using trimethylindium and phosphine in a hydrogen ambient. Then n- and p-type dopants were diethyltellurium and dimethylzinc, respectively. The 4 K photoluminescence spectra at various excitation intensities are presented for a structure consisting of six 200 A layers with doping levels of 1 x 10 to the 18th power and 3 x 10 to the 18th power/cc for n- and p-layers. The luminescence peak is found to occur at energies considerably less than the band gap of InP and to move to higher energies with increased excitation intensity, as expected for doping superlattices where the band gap, which is indirect in real space, increases with increasing excited carrier concentration. The total photoluminescence signal decays in several steps, each exponential, with time constants ranging from .00000006 to .0007 seconds at 4 K, typical of these spatially indirect band gap materials. GRA

N85-33030# Air Force Systems Command, Wright-Patterson AFB, Ohio. Foreign Technology Div.
DETERMINATION OF KINETIC PARAMETERS OF MOLECULAR BEAM EPITAXY
J. Zhong 17 Apr. 1985 16 p Transl. into ENGLISH from Guangxue Xuebao (China), v. 4, no. 3, Mar. 1984 p 257-263
(AD-A155222; FTD-ID(RS)T-1601-84) Avail: NTIS HC A02/MF A01 CSCL 20/12

A kinetic growth model for molecular beam epitaxy (MBE) was discussed. Furthermore, high energy electron diffraction (HEED) was used as a surface characterization method to provide evidence for this model. GaAs was used as an example to study the growth rate of molecular beam epitaxy. The relation between the growth rate and the flux of Ga was verified by quadrupole mass spectroscopy. The suitable Ga to Al partial pressure ratio for growing materials such as Ga(1-x)Al(x)As with specific values of x was investigated theoretically as well as experimentally. Furthermore, the relation between dopant concentration and the corresponding effusion cell temperature was given for Si, Sn and Be. Author (GRA)

N85-33031# Dayton Univ., Ohio.
A THEORY OF EXCITON PHOTOLUMINESCENCE FOR TWO TYPES OF NEUTRAL ACCEPTORS IN SILICON. A STUDY OF THE SYSTEMS Si:(B, In), Si:(Al), (Si), Si:(Ga, In), Si:(B, Al), Si:(B, Ga), AND Si:(Al, Ga) Interim Report, Jun. 1983 - Aug. 1984
D. S. Moroi, M. C. Ohmer, and D. H. Brown Feb. 1985 134 p Prepared in cooperation with Kent State Univ., OH
(Contract F33615-81-C-5095)
(AD-A155452; UDR-TR-85-10; AFWAL-TR-85-4031) Avail: NTIS HC A07/MF A01 CSCL 20/12

Rate equations for the densities of free excitons and excitons bound to two types of neutral acceptors in silicon are solved for steady state in the absence of saturation. These rate equations contain the terms for the tunneling of an exciton bound to one type of neutral impurity to another. The tunneling rates are calculated using a simple model of an exciton in a one-dimensional semi-infinite double potential well. The energy eigenvalue equation for an exciton in this potential well is derived for estimating the exciton tunneling time. The steady-state solutions of the rate equations yield an expression for the ratio of the bound exciton luminescence intensity as a function of the impurity concentrations. The relative photoluminescence intensities for the systems Si:(B,In), Si:(Al,In), Si:(Ga,In), Si(B,Al) Si:(B,Ga), and Si:(Al,Ga) are calculated for various values for the relative free exciton capture cross section ratios. This model predicts no exciton tunneling for any of the above systems for the low impurity concentration range. For the systems with large differences in the bound exciton energy levels such as Si:(B,In), Si:(Al,In), and Si:(Ga,In), it predicts quenching of shallow impurity bound exciton luminescence. For the systems with small differences in the bound exciton energy levels such as Si:(B,Al) and Si:(B,Ga), the theory predicts enhancement of shallow impurity bound exciton luminescence. For the system Si:(Al,Ga) in which the difference in the bound exciton energy levels is very small, gallium bound exciton luminescence dominates if the aluminum free exciton capture section is less than the gallium free exciton capture cross section. GRA

N85-33032# Michigan Univ., Ann Arbor.
RAMAN SCATTERING STUDIES IN SOLIDS Final Report, 18 Jan. 1982 - 17 Jan. 1985
R. D. Merlin 30 Apr. 1985 7 p
(Contract DAAG29-82-K-0057)
(AD-A155528; ARO-18406.12-PH) Avail: NTIS HC A02/MF A01 CSCL 07/4

This report deals with Raman scattering studies of semiconductor heterostructures and superlattices. The primary interest here is an investigation of donor and acceptor spectra in gallium arsenide-(aluminum, gallium) arsenide multiple quantum wells. Other studies refer to quasi two-dimensional electron systems in germanium/gallium arsenide and photoexcited GaAs space-charge layers. Laser-induced oxidation of metals is discussed. It has been found that irradiation leads to the growth of thick amorphous oxide layers. Author (GRA)

N85-33033# Puerto Rico Univ., Mayaguez. Dept. of Physics.
AN EPR (ELECTRON-PARAMAGNETIC-RESONANCE) AND ENDOR (ELECTRON-NUCLEAR-DOUBLE-RESONANCE) STUDY OF FERROELECTRIC AMMONIUM SULFATE Final Report, 22 Feb. 1982 - 21 Feb. 1985
C. E. Bailey 15 Apr. 1985 124 p
(Grant DAAG29-82-G-0004)
(AD-A155580; ARO-19268.4-PH-H) Avail: NTIS HC A06/MF A01 CSCL 07/4

EPR (electron-paramagnetic-resonance) and ENDOR (electron-nuclear-double-resonance) are extremely useful techniques because they measure the interaction between a paramagnetic center and those atoms surrounding the center. Thus they give information on translations and rotations in the crystal on a microscopic scale. Whenever a paramagnetic center is introduced (they are not usually present in the pure material) one must consider the possibility that the effects seen when the sample is taken through a phase transition may be more the properties of the introduced defect rather than those of the host crystal. It is for this reason that centers introduced by radiation damage and those produced by doping should be used and compared whenever possible. Several radiation damage centers in ammonium sulfate, deuterated ammonium sulfate, and lithium sulfate are investigated. These results give insights into the nature of the hydrogen bonding in these materials. Computer software that has been developed in these studies is discussed. GRA

N85-33034# Florida Univ., Gainesville. Dept. of Materials Science and Engineering.
ELECTROTRANSPORT IN THIN FILMS Final Report, 1981 - 1985
R. E. Hummel and R. T. DeHoff Apr. 1985 6 p
(Contract DAAG29-81-K-0149)
(AD-A155584; ARO-18112.3-MS) Avail: NTIS HC A02/MF A01 CSCL 07/4

Circuit failure in thin film metallization may be due to a combination of electrotransport, thermotransport and grain

boundary grooving. In cases where electrotransport and thermotransport are relatively slow, such as in gold, grain boundary grooving may eventually cause void formation and failure of a microelectronic device. Film combinations consisting of substrate/indium/gold significantly retard grain growth, thermal grooving and hole formation under conditions usually experienced in microelectronic circuits. It is believed that indium oxide near the grain boundaries and on the surface is responsible for the stabilization of the gold grain structure and the prevention of hole formation.
Author (GRA)

N85-33035# Sandia Labs., Albuquerque, N. Mex.
ELECTRONIC PHENOMENA NEAR SEMICONDUCTOR GRAIN BOUNDARIES
G. E. Pike 1985 4 p Presented at the 168th Meeting of the Electrochem. Soc., Las Vegas, Nev., 13 Oct. 1985
(Contract DE-AC04-76DP-00789)
(DE85-011543; SAND-85-10720; CONF-851048-1) Avail: NTIS HC A02/MF A01

Various electronic phenomena which are generally associated with grain boundaries in semiconductors are reviewed. At equilibrium majority carriers are trapped at the boundaries, and a corresponding space charge layer of ionized dopant forms on both sides of the boundary. This creates a potential barrier to free carriers. An applied dc voltage causes the barrier to lower and change shape in an asymmetric way. At high voltages hot majority carriers can produce impact ionized minority carriers which further reduce the barrier height. Small ac voltages cause anomalous apparent capacitances which are either positive or negative. DOE

N85-32788# Joint Publications Research Service, Arlington, Va.
GDR SEMICONDUCTOR PARTS
Jaroslav Tolasz *In its* East Europe Rept.: Sci. and Technol. Selections on CSS JPRS-ESA-84-017 31 May 1984 p 47-78 Transl. into ENGLISH from Sdelovaci Technika (Prague), no. 2, Feb. 1983 p 59 (For primary document see N85-32781 21-60)
Avail: NTIS HC A05/MF A01

N85-32865# Joint Publications Research Service, Arlington, Va.
INFLUENCE ON BI-PHONON STATES ON RAMAN SCATTERING OF LIGHT IN MOLECULAR CRYSTALS Abstract Only
Yu. D. Zavorotnev, L. N. Ovander, and L. I. Stefanovich *In its* USSR Rept.: Phys. and Math. (JPRS-UPM-85-004) 17 Jun. 1985 p 6 Transl. into ENGLISH from Optika i Spektroskopiya (Leningrad), v. 57, no. 5, Nov. 1984 p 831-836 (For primary document see N85-32860 21-70)
Avail: NTIS HC A06/MF A01

N85-32866# Joint Publications Research Service, Arlington, Va.
X-RAY DIFFRACTOMETRIC MEASUREMENTS AND CALCULATIONS OF LIMITING VALUES OF DISCREPANCY BETWEEN LATTICES AND LAYER THICKNESSES, PREVENTING GENERATION OF DISLOCATIONS DURING GROWTH OF MULTILAYER HETEROSTRUCTURES Abstract Only
G. B. Bokiy and G. F. Kuznetsov *In its* USSR Rept.: Phys. and Math. (JPRS-UPM-85-004) 17 Jun. 1985 p 6-7 Transl. into ENGLISH from Dokl. Akad. Nauk SSSR (Moscow), v. 279, no. 4, Dec. 1984 p 876-880 (For primary document see N85-32860 21-70)
Avail: NTIS HC A06/MF A01

N85-32867# Joint Publications Research Service, Arlington, Va.
INFLUENCE OF COHERENT LIGHT BEAMS ON FREE CARRIERS IN SEMICONDUCTORS Abstract Only
I. M. Dykman and P. M. Tomchuk *In its* USSR Rept.: Phys. and Math. (JPRS-UPM-85-004) 17 Jun. 1985 p 7 Transl. into ENGLISH from Fiz. Tverdogo Tela (Leningrad), v. 26, no. 9, Sep. 1984 p 2729-2733 (For primary document see N85-32860 21-70)
Avail: NTIS HC A06/MF A01

N85-32868# Joint Publications Research Service, Arlington, Va.
LUMINESCENCE AND ABSORPTION OF INDIUM-ACTIVATED POTASSIUM-BORATE GLASSES SUBJECTED TO HIGH-POWER EXCITATION Abstract Only
S. Ye. Belyy, S. Ye. Zelenskiy, B. A. Okhrimenko, and S. M. Yablochkov *In its* USSR Rept.: Phys. and Math. (JPRS-UPM-85-004) 17 Jun. 1985 p 10 Transl. into ENGLISH from Zh. Prikl. Specktroskopii (Minsk), v. 41, no. 4, Oct. 1984 p 583-587 (For primary document see N85-32860 21-70)
Avail: NTIS HC A06/MF A01

N85-32869# Joint Publications Research Service, Arlington, Va.
GENERATION AND AMPLIFICATION OF RADIATION DURING STIMULATED RAMAN SCATTERING IN CRYSTALS Abstract Only
S. N. Karpukhin and V. Ye. Yashin *In its* USSR Rept.: Phys. and Math. (JPRS-UPM-85-004) 17 Jun. 1985 p 10-11 Transl. into ENGLISH from Kvantovaya Elektron. (Moscow), v. 11, no. 10, Oct. 1984 p 1992-2000 Original language document announced in IAA as A85-21023 (For primary document see N85-32860 21-70)
Avail: NTIS HC A06/MF A01

N85-32870# Joint Publications Research Service, Arlington, Va.
ABSORPTION OF 10.6 MICROMETER LASER RADIATION IN ELECTRON-HQLE CONDENSATE IN GERMANIUM Abstract Only
V. P. Kalinushkin, A. A. Manenkov, G. N. Mikhaylova, and S. Yu. Sokolov *In its* USSR Rept.: Phys. and Math. (JPRS-UPM-85-004) 17 Jun. 1985 p 11 Transl. into ENGLISH from Dokl. Akad. Nauk SSSR (Moscow), v. 279, no. 1, Nov. 1984 p 88-90 (For primary document see N85-32860 21-70)
Avail: NTIS HC A06/MF A01

N85-32871# Joint Publications Research Service, Arlington, Va.
CLASSICAL EMISSION OF RELATIVISTIC CHARGED PARTICLES DURING AXIAL CHANNELING Abstract Only
B. V. Kholomay *In its* USSR Rept.: Phys. and Math. (JPRS-UPM-85-004) 17 Jun. 1985 p 12 Transl. into ENGLISH from Vestn. Moskovskogo Univ.: Fiz., Astron. (Moscow), v. 25, no. 5, Sep. - Oct. 1984 p 125-128 (For primary document see N85-32860 21-70)
Avail: NTIS HC A06/MF A01

N85-32872# Joint Publications Research Service, Arlington, Va.
SYSTEM FOR ELECTRO-OPTICAL CERAMIC RECRYSTALLIZATION Abstract Only
M. G. Livinsh, T. Ya. Pinins, Ya. A. Seglinsh, and Yu. A. Zvirgzds *In its* USSR Rept.: Phys. and Math. (JPRS-UPM-85-004) 17 Jun. 1985 p 16 Transl. into ENGLISH from Izv. Akad. Nauk Latv. SSR: Ser. Fiz. i Tekhn. Nauk (Riga), no. 5, Oct. - Nov. 1984 p 42-45 (For primary document see N85-32860 21-70)
Avail: NTIS HC A06/MF A01

N85-32873# Joint Publications Research Service, Arlington, Va.
DEFECT FORMATION IN AMORPHOUS HYDRATED SILICON SUBJECTED TO LASER RADIATION Abstract Only
G. M. Chukicheva, Yu. A. Zarifyants, S. N. Karyagin, P. K. Kashkarov, and A. V. Petrov *In its* USSR Rept.: Phys. and Math. (JPRS-UPM-85-004) 17 Jun. 1985 p 16-17 Transl. into ENGLISH from Fiz. i Tekhn. Poluprov. (Leningrad), v. 18, no. 10, Oct. 1984 p 1895-1896 (For primary document see N85-32860 21-70)
Avail: NTIS HC A06/MF A01

N85-32874# Joint Publications Research Service, Arlington, Va.
QUASI-STEADY-STATE MELTING MODE DURING COMBINED LASER IRRADIATION OF SEMICONDUCTOR MATERIALS Abstract Only
V. N. Abakumov, V. N. Guman, and V. S. Yuferev *In its* USSR Rept.: Phys. and Math. (JPRS-UPM-85-004) 17 Jun. 1985 p 17 Transl. into ENGLISH from Fiz. i Tekhn. Poluprov. (Leningrad), v. 18, no. 10, Oct. 1984 p 1832-1835 (For primary document see N85-32860 21-70)
Avail: NTIS HC A06/MF A01

N85-32875# Joint Publications Research Service, Arlington, Va.
INTER-ZONE AUGER RECOMBINATION IN GaSb LASER

STRUCTURES Abstract Only
B. L. Gelmont, Z. N. Sokolova, and V. B. Khalfin *In its* USSR Rept.: Phys. and Math. (JPRS-UPM-85-004) 17 Jun. 1985 p 17-18 Transl. into ENGLISH from Fiz. i Tekhn. Poluprov. (Leningrad), v. 18, no. 10, Oct. 1984 p 1803-1807 (For primary document see N85-32860 21-70)
Avail: NTIS HC A06/MF A01

N85-32876# Joint Publications Research Service, Arlington, Va.
PHOTO-ACOUSTIC EFFECT IN FINITE-DIMENSIONAL SEMICONDUCTORS Abstract Only
A. N. Vasilev and V. B. Sandomirskiy *In its* USSR Rept.: Phys. and Math. (JPRS-UPM-85-004) 17 Jun. 1985 p 18 Transl. into ENGLISH from Fiz. i Tekhn. Poluprov. (Leningrad), v. 18, no. 10, Oct. 1984 p 1751-1758 (For primary document see N85-32860 21-70)
Avail: NTIS HC A06/MF A01

N85-32877# Joint Publications Research Service, Arlington, Va.
EFFECT OF POWERFUL PULSED LOW-ENERGY ION STREAMS ON GaAs Abstract Only
Yu. A. Bityurin, S. V. Gaponov, Ye. B. Klyuyenkov, and M. D. Strikovskiy *In its* USSR Rept.: Phys. and Math. (JPRS-UPM-85-004) 17 Jun. 1985 p 18-19 Transl. into ENGLISH from Fiz. i Tekhn. Poluprov. (Leningrad), v. 18, no. 10, Oct. 1984 p 1729-1734 (For primary document see N85-32860 21-70)
Avail: NTIS HC A06/MF A01

N85-32878# Joint Publications Research Service, Arlington, Va.
INFLUENCE OF BACKGROUND ELECTRICALLY NEUTRAL ARGON ADMIXTURE ON MECHANICAL STRENGTH OF SILICON CRYSTALS Abstract Only
V. V. Kolomoyets, Yu. V. Simonenko, and A. V. Fedosov *In its* USSR Rept.: Phys. and Math. (JPRS-UPM-85-004) 17 Jun. 1985 p 19 Transl. into ENGLISH from Dokl. Akad. Nauk Ukr. SSR: Ser. A. Fiz.-Mat. i Tekhn. Nauki (Kiev), no. 10, Oct. 1984 p 61-63 (For primary document see N85-32860 21-70)
Avail: NTIS HC A06/MF A01

N85-32879# Joint Publications Research Service, Arlington, Va.
DEVELOPMENT OF ARTIFICIALLY PRODUCED PERTURBATIONS IN SUPERSONIC BOUNDARY LAYER Abstract Only
A. D. Kosinov and A. A. Maslov *In its* USSR Rept.: Phys. and Math. (JPRS-UPM-85-004) 17 Jun. 1985 p 20 Transl. into ENGLISH from Izv. Akad. Nauk SSSR: Mekhan. Zhidkosti i Gaza (Moscow), no. 5, Sep. - Oct. 1984 p 37-43 Original language document announced in IAA as A85-16177 (For primary document see N85-32860 21-70)
Avail: NTIS HC A06/MF A01

77 THERMODYNAMICS AND STATISTICAL PHYSICS

Includes quantum mechanics; and Bose and Fermi statistics.

For related information see also *25 Inorganic and Physical Chemistry* and *34 Fluid Mechanics and Heat Transfer.*

No abstracts in this category.

80 SOCIAL SCIENCES (GENERAL)

Includes educational matters.

No abstracts in this category.

81 ADMINISTRATION AND MANAGEMENT

Includes management planning and research.

N85-33036# Army Procurement Research Office, Fort Lee, Va.
FEASIBILITY OF APPLICATIONS OF COMPETITION DECISION ASSIST PACKAGE (CDAP) TO SPARE PARTS Final Report
V. G. Lankford and B. L. Stewart Jan. 1985 48 p
(AD-A154716; APRO-84-13) Avail: NTIS HC A03/MF A01 CSCL 14/1

Defense Acquisition Regulation Supplement No. 6, DOD Replenishment Parts Breakout Program, 1 June 1983, prescribes a screening of replenishment parts designed to reduce costs by breaking out parts for purchase from other than prime weapon system contractors. The US Army Audit Agency recommended that a cost model be constructed and implemented to: (1) estimate potential costs and price reductions attributable to breakout or increased competition, (2) compare the two figures, and (3) identify whether breakout or competition is cost effective. In September 1983, the Army Procurement Research Office (APRO) published the Competition Decision- Assist Package (CDAP), APRO Study Report 82-08, which described an automated model designed to calculate estimates of recurring costs associated with two producers involved in a competitive production effort. This model had been developed as a tool to assist in the economic evaluation of production competition for a major weapon system. The objective of this study was to determine if it is feasible and beneficial to modify the existing CDAP model so it can be applied to spare parts breakout or competition as an economic analysis model. While the CDAP model may be useful for some major assemblies/subassemblies where an extensive manpower effort for developing model input is warranted, it is impractical as a general purpose economic analysis model for spare parts breakout or competition. Other, more appropriate models exist. GRA

N85-33037# Massachusetts Inst. of Tech., Cambridge. Lab. for Computer Science.
DISTRIBUTED NAME MANAGEMENT Ph.D. Thesis
K. R. Sollins Feb. 1985 164 p
(Contracts N00014-75-C-0661; N00014-83-K-0125)
(AD-A154785; MIT/LCS/TR-331) Avail: NTIS HC A08/MF A01 CSCL 05/1

The problem being addressed in this research is the design of a naming facility achieving the following goals. First, two functions on names must be supported: accessing a named object, and acting as a place holder for the named object. Second, it must be possible to share those names. Third, communication of the names as well as communcation by use of the names must be possible. Finally, feasibility of implementation is a goal. In this research a name is defined to be an object that can be associated with another object and has an equality operation defined on it. Two functions are defined for a name; it can be used both to provide access to the named object and as a place holder for the named object. The assumed system model is a loosely coupled, distributed system. The research addresses this problem with: (1) a detailed analysis of the naming problem and the nature of names themselves; (2) a proposal for a set of mechanisms that addresses the problem above, including the proposal of two new types of objects and the mechanisms for their use; and (3) two examples of uses of the model. The model consists of private views of shared, local namespaces allowing shared use of names and supporting shared responsibility for management of the namespace. In addition the model provides for the the acceptance and deletion of names in stages. Author (GRA)

N85-33038# Office of Naval Research, London (England).
SPACE RESEARCH IN THE UNITED KINGDOM: AN ASSESSMENT
N. F. Ness 19 Apr. 1985 6 p
(AD-A155334; ONRL-R-1-85) Avail: NTIS HC A02/MF A01 CSCL 03/1

This report examines the history and funding of UK (United Kingdom) space research; discusses work in disciplines such as astronomy and astrophysics, solar system studies, and terrestrial studies; and considers prospects for the future. GRA

N85-32530*# Colorado Univ., Boulder. CIRES.
DATA BASE MANAGEMENT: MSTRAC (KEYNOTE PAPER), PART 8
S. K. Avery and B. B. Balsley (NOAA, Boulder, Colo.) *In* International Council of Scientific Unions Middle Atmosphere Program: Handbook for MAP. Vol. 14 Dec. 1984 p 300-301 (For primary document see N85-32466 21-46)
Avail: NTIS HC A17/MF A01; also avail. from SCOSTEP Secretariat, Illinois Univ., 1406 West Green St., Urbana, Ill. 61801 CSCL 05A

N85-32532*# Control Data Corp., Minneapolis, Minn.
MST RADAR DATA MANAGEMENT
G. D. Nastrom *In* International Council of Scientific Unions Middle Atmosphere Program. Handbook for MAP. Vol. 14 Dec. 1984 p 306 refs (For primary document see N85-32466 21-46)
Avail: NTIS HC A17/MF A01; also available from SCOSTEP Secretariat, Illinois Univ., 1406 West Green Street, Urbana, Ill. 61801 CSCL 05A

N85-32533*# National Oceanic and Atmospheric Administration, Boulder, Colo.
DATA BASE FOR THE COLORADO PROFILING NETWORK
D. A. Merritt *In* International Council of Scientific Unions Middle Atmosphere Program. Handbook for MAP. Vol. 14 Dec. 1984 p 307-308 refs (For primary document see N85-32466 21-46)
Avail: NTIS HC A17/MF A01; also available from SCOSTEP Secretariat, Illinois Univ., 1406 West Green Street, Urbana, Ill. 61801 CSCL 05A

82 DOCUMENTATION AND INFORMATION SCIENCE

Includes information storage and retrieval technology; micrography; and library science.

For computer documentation see *61 Computer Programming and Software.*

N85-33039# Naval Postgraduate School, Monterey, Calif.
THE HUMAN RESOURCE MANAGEMENT INFORMATION NETWORK (HRMIN): A COST COMPARISON IN ACCORDANCE WITH OFFICE OF MANAGEMENT AND BUDGET (OMB) CIRCULAR NO. A-76, 5 APRIL 1979 M.S. Thesis
G. M. Matyas Dec. 1984 88 p
(AD-A154583) Avail: NTIS HC A05/MF A01 CSCL 05/2

The Human Resource Management Information Network (HRMIN) was conceived and developed in-house by the Navy Military Personnel Command (NMPC) and the Navy Personnel Research and Development Center (NPRDC). This thesis is an attempt to ascertain the compliance of this in-house development with the Office of Management and Budget policy on the acquisition of commercial or industrial products and services needed by the government. A cost comparison of the in-house performance cost and the contract-out cost of providing the services required of HRMIN indicate that the present in-house performance is the most cost effective alternative. Therefore conversion to a contracted-out performance should not be undertaken. GRA

N85-33040# Air Force Inst. of Tech., Wright-Patterson AFB, Ohio. School of Engineering.
CONTINUED DEVELOPMENT OF A DATA BASE MANAGEMENT SYSTEM PERFORMANCE MONITOR: VOLUME 1 M.S. Thesis
T. D. Bruner Dec. 1984 76 p
(AD-A154635; AFIT/GCS/ENG/84D-6-Vol-1) Avail: NTIS HC A05/MF A01 CSCL 09/2

This thesis focuses on the problem of analyzing the performance data collected on a Data Base Management System (DBMS). The performance data parameters are categorized and presented to the user using a Data Support System (DSS). The generalized design for a DBMS performance monitor was used to design a user-friendly interface to DBMS performance data. The user interface to the DBMS performance monitor uses menus to allow the user to select DBMS performance parameter values can also be printed in the form of a performance report. The design was implemented on a VAX 11/780 computer system using the VMS operating system. The TOTAL DBMS was used to collect performance data. The performance values were collected using existing software monitors, job accounting, system error log, and a utility developed at AFIT to collect Data Manipulation Language (DML) response performance data. Author (GRA)

N85-33041# Air Force Office of Scientific Research, Bolling AFB, Washington, D.C.
AIR FORCE OFFICE OF SCIENTIFIC RESEARCH (AFOSR). TECHNICAL REPORT SUMMARIES: FIRST QUARTER (CY) Technical Report, Jan. - Mar. 1985
B. J. Wert Apr. 1985 206 p
(AD-A154757; AFOSR-85-0474TR) Avail: NTIS HC A10/MF A01 CSCL 05/2

The AFOSR Technical Report Summaries are published quarterly of each calendar year. They consist of a brief summary of each AFOSR technical report received in the Technical Information Division and submitted to the Defense Technical Information Center for that quarter. Personal author and subject indexes are included. GRA

N85-33042# RAND Corp., Santa Monica, Calif.
INVESTIGATION OF DBMS (DATA BASE MANAGEMENT SYSTEMS) FOR USE IN A RESEARCH ENVIRONMENT M.S. Thesis - California State Univ., 6 Jul. 1984
P. N. Rosenfeld Feb. 1985 105 p
(AD-A154862; RAND/P-7002) Avail: NTIS HC A06/MF A01 CSCL 09/2

This thesis is an investigative study on whether a data base management system has a place in a research environment. The study concentrated on the use of large social science data sets. The following topics were examined: (1) how social science data sets are used in a research environment; (2) the data usage and need of an existing research institution (The Rand Corporation); (3) the differences between research and business applications; (4) the possible DBMS configurations within a research environment; (5) the opinions of Rand computer users when rating importance of DBMS features; and (6) evaluation of commercial DBMS for use in a research environment. Conventional DBMS have been very successful with business/corporate data bases, but DBMS are not widely used with research data bases. There are significant differences between the business and research data management needs. These include different retrieval and update specifications, the need for statistical routines, and less financial data base support. Much of research analysis requires the use of statistical procedures. Hence, a DBMS configuration within a research environment must include some access to statistical procedures. Given these reguirements, there are a few commercial DBMS which could be considered for a research environment.
Author (GRA)

N85-33043# Defense Technical Information Center, Alexandria, Va.
THE FLOW OF SCIENTIFIC AND TECHNICAL INFORMATION IN THE US ARMY RESEARCH LABORATORIES Final Report
R. L. Bixby May 1985 52 p
(AD-A155050; DTIC/TR-85/4) Avail: NTIS HC A04/MF A01 CSCL 05/2

The Defense Technical Information Center (DTIC) provides information services to the Army, Navy, Air Force, other Department of Defense (DOD) agencies, other Government agencies, and Government contractors. In order to provide this information, DTIC needs to anticipate the information needs of its users. An understanding of the flow of scientific and technical information

(STINFO) within DTIC user organizations is necessary to provide the best services. This paper was undertaken to trace the flow of STINFO within the Department of the Army's research laboratories and to determine how the Army researcher gathers information. Recommendations are made as to how DTIC can better serve the information needs of the Army. Author (GRA)

83 ECONOMICS AND COST ANALYSIS

Includes cost effectiveness studies.

No abstracts in this category.

84 LAW AND POLITICAL SCIENCE

Includes space law; international law; international cooperation; and patent policy.

No abstracts in this category.

85 URBAN TECHNOLOGY AND TRANSPORTATION

Includes applications of space technology to urban problems; technology transfer; technology assessment; and surface and mass transportation.

For related information see *03 Air Transportation and Safety, 16 Space Transportation,* and *44 Energy Production and Conversion.*

No abstracts in this category.

88 SPACE SCIENCES (GENERAL)

N85-33044*# California Inst. of Tech., Pasadena. Space Radiation Lab.
CONTRIBUTIONS TO THE 19TH INTERNATIONAL COSMIC RAY CONFERENCE
1985 50 p refs Conf. held in La Jolla, Calif., 11-23 Aug. 1985
(Contract NAGw-685)
(NASA-CR-176060; NAS 1.26:176060; SRL-85-05-15) Avail: NTIS HC A03/MF A01 CSCL 03B

Various aspects of cosmic radiation, its measurements and their patterns are presented. Measurement techniques and variations in solar cosmic ray patterns and calculations of elemental abundances are reviewed. For individual titles, see N85-33045 through N85-33059.

N85-33045*# California Inst. of Tech., Pasadena.
COSMIC RAY He3 MEASUREMENTS **c93**
R. A. Mewaldt *In its* Contrib. to the 19th Intern. Cosmic Ray Conf. 1985 4 p refs (For primary document see N85-33044 21-88)
(Paper-OG-4.2-3) Avail: NTIS HC A03/MF A01 CSCL 03B

Cosmic ray 3He/4H3 observations, including a new measurement at approximately 65 MeV/nucleon from ISEE-3, are compared with interstellar propagation and solar modulation models in an effort to understand the origin of cosmic ray He nuclei. Author

N85-33046*# California Inst. of Tech., Pasadena.
INITIAL RESULTS FROM THE CALTECH/DSRI BALLOON-BORNE ISOTOPE EXPERIMENT **c93**
S. M. Schindler, A. Buffingtan (California Univ., San Diego), E. C. Christian, J. E. Grove, K. H. Lau, E. C. Stone, I. L. Rasmussen (Danish Space Research Inst.), and S. Laursen (Danish Space Research Inst.) *In its* Contrib. to the 19th Intern. Cosmic Ray Conf. 1985 4 p refs (For primary document see N85-33044 21-88)
(Grant NGR-05-006-160)
(Paper-OG-4.3-8) Avail: NTIS HC A03/MF A01 CSCL 03B

The Caltech/DSRI balloon-borne High Energy Isotope Spectrometer Telescope (HEIST) was flown successfully from Palestine, Texas on 14 May 1984. The experiment was designed to measure cosmic ray isotopic abundances from neon through iron, with incident particle energies from approximately 1.5 to 2.2 GeV/nucleon, depending on the element. During approximately 38 hours at float altitude, $>$ 10 to the 5th events were recorded with Z $>$ or $=$ 6 and incident energies $>$ 1.5 GeV/nucleon. We present results from the ongoing data analysis associated with both the pre-flight Bevalac calibration and the flight data. Author

N85-33047*# California Inst. of Tech., Pasadena.
MEASUREMENTS OF Fe AND Ar FRAGMENTATION CROSS SECTIONS **c93**
K. H. Lau, R. A. Mewaldt, and E. C. Stone *In its* Contrib. to the 19th Intern. Cosmic Ray Conf. 1985 4 p refs (For primary document see N85-33044 21-88)
(Contract NAS5-28449; Grant NGR-05-002-160)
(Paper-OG-7.2-20) Avail: NTIS HC A03/MF A01 CSCL 03B

Measurements are reported of the yields of individual isotopes of Cr to Co (Z $=$ 24 to 27) resulting from the fragmentation of 56Fe, and the isotopes of Mg to K (Z $=$ 12 to 19) resulting from the fragmentation of 40Ar. Author

N85-33048*# California Inst. of Tech., Pasadena.
HEXAGONAL UNIFORMLY REDUNDANT ARRAYS FOR CODED-APERTURE IMAGING **c35**
M. H. Finger and T. A. Prince *In its* Contrib. to the 19th Intern. Cosmic Ray Conf. 1985 4 p refs (For primary document see N85-33044 21-88)
(Grant NGR-05-002-160)
(Paper-OG-9.2-1) Avail: NTIS HC A03/MF A01 CSCL 03A

Uniformly redundant arrays are used in coded-aperture imaging, a technique for forming images without mirrors or lenses. This technique is especially important for the high energy X-ray and gamma-ray region above 20 kev. In this technique, a mask consisting of opaque (closed) and trasparent (open) areas is placed between the photon sources to be imaged and a position sensitive detector or a detector array. Each source casts a shadow pattern of the mask or aperture onto the detector. This shadow pattern may be viewed as an encoded signal for that source direction. If each possible source code is unique, the detected composite of overlapping shadow patterns may be decoded to produce an image of the source distribution. G.L.C.

N85-33049*# California Inst. of Tech., Pasadena.
A BALLOON-BORNE IMAGING GAMMA-RAY TELESCOPE **c89**
W. E. Althouse, W. R. Cook, A. C. Cummings, M. H. Finger, T. A. Prince, S. M. Schindler, C. H. Starr, and E. C. Stone *In its* Contrib. to the 19th Intern. Cosmic Ray Conf. 1985 4 p refs (For primary document see N85-33044 21-88)
(Grant NGR-05-002-160)
(Paper-OG-9.2-2) Avail: NTIS HC A03/MF A01 CSCL 03B

A balloon-borne coded-aperture gamma-ray telescope for galactic and extragalactic astronomy observations is described. The instrument, called GRIP (Gamma Ray Imaging Payload), is designed for measurements in the energy range from 30 keV to 5 MeV with an angular resolution of 0.6 deg over a 20 deg field of view. Distinguishing characteristics of the telescope are a rotating hexagonal coded-aperture mask and a thick NaI scintillation camera. Rotating hexagonal coded-apertures and the development of thick scintillation cameras are discussed. G.L.C.

N85-33050*# California Inst. of Tech., Pasadena.
BALLOON-BORNE VIDEO CASSETTE RECORDERS FOR DIGITAL DATA STORAGE c35
W. E. Althouse and W. R. Cook *In its* Contrib. to the 19th Intern. Cosmic Ray Conf. 1985 3 p refs (For primary document see N85-33044 21-88)
(Grant NGR-05-002-160)
(Paper-OG-9.3-11) Avail: NTIS HC A03/MF A01 CSCL 14C

A high-speed, high-capacity digital data storage system has been developed for a new balloon-borne gamma-ray telescope. The system incorporates sophisticated, yet easy to use and economical consumer products: the portable video cassette recorder (VCR) and a relatively newer item - the digital audio processor. The in-flight recording system employs eight VCRs and will provide a continuous data storage rate of 1.4 megabits/sec throughout a 40 hour balloon flight. Data storage capacity is 25 gigabytes and power consumption is only 10 watts. G.L.C.

N85-33051*# California Inst. of Tech., Pasadena.
THE ENERGY SPECTRUM OF JOVIAN ELECTRONS IN INTERPLANETARY SPACE Abstract Only c90
S. P. Christon, A. C. Cummings, E. C. Stone, and W. R. Webber (New Hampshire Univ., Durham) *In its* Contrib. to the 19th Intern. Cosmic Ray Conf. 1985 1 p refs (For primary document see N85-33044 21-88)
(Contract NAS7-918; Grant NGR-05-002-160)
(Paper-SH-1.5-18) Avail: NTIS HC A03/MF A01 CSCL 03B

The energy spectrum of electrons with energies approximately 10 to approximately 180 MeV measured with the electron telescope on the Voyager 1 and 2 spacecraft in interplanetary space from 1978 to 1983 is reported. The kinetic energy of electrons is determined by double dE/dx measurements from the first two detectors (D1,D2) of a stack of eight solid state detectors and by the range of particle penetration into the remaining six detectors (D3 to D8) which are interleaved with tungsten absorbers. G.L.C.

N85-33052*# California Inst. of Tech., Pasadena.
PRECISION MEASUREMENTS OF SOLAR ENERGETIC PARTICLE ELEMENTAL COMPOSITION c92
H. Breneman and E. C. Stone *In its* Contrib. to the 19th Intern. Cosmic Ray Conf. 1985 4 p refs (For primary document see N85-33044 21-88)
(Contract NAS7-918; Grant NGR-05-002-160)
(Paper-SH-2.1-4) Avail: NTIS HC A03/MF A01 CSCL 03B

Using data from the Cosmic Ray Subsystem (CRS) aboard the Voyager 1 and 2 spacecraft, solar energetic particle abundances or upper limits for all elements with $3 <= Z >= 30$ from a combined set of 10 solar flares during the 1977 to 1982 time period were determined. Statistically meaningful abundances have been determined for the first time for several rare elements including P, Cl, K, Ti and Mn, while the precision of the mean abundances for the more abundant elements has been improved by typically a factor of approximately 3 over previously reported values. G.L.C.

N85-33053*# California Inst. of Tech., Pasadena.
SOLAR CORONAL AND PHOTOSPHERIC ABUNDANCES FROM SOLAR ENERGETIC PARTICLE MEASUREMENTS c92
H. Breneman and E. C. Stone *In its* Contrib. to the 19th Intern. Cosmic Ray Conf. 1985 4 p refs (For primary document see N85-33044 21-88)
(Contract NAS7-918; Grant NGR-05-002-160)
(Paper-SH-2.1-5) Avail: NTIS HC A03/MF A01 CSCL 03B

Solar energetic particle (SEP) elemental abundance data from the Cosmic Ray Subsystem (CRS) aboard the Voyager 1 and 2 spacecraft are used to derive unfractionated coronal and photospheric abundances for elements with $3 = or < Z > or = 30$. The ionic charge-to-mass ratio (Q/M) is the principal organizing parameter for the fractionation of SEPs by acceleration and propagation processes and for flare-to-flare variability, making possible a single-parameter Q/M-dependent correction to the average SEP abundances to obtain unfractionated coronal abundances. A further correction based on first ionization potential allows the determination of unfractionated photospheric abundances. G.L.C.

N85-33054*# California Inst. of Tech., Pasadena.
LATITUDE VARIATION OF RECURRENT FLUXES IN THE OUTER SOLAR SYSTEM Abstract Only c90
S. P. Christon and E. C. Stone *In its* Contrib. to the 19th Intern. Cosmic Ray Conf. 1985 1 p ref Previously announced in IAA as A85-24782 (For primary document see N85-33044 21-88)
(Paper-SH-4.1-13) Avail: NTIS HC A03/MF A01 CSCL 03B

Recurrent low energy (not less than 0.5 MeV) proton flux enhancements, reliable indicators of corotating plasma inteaction regions in interplanetary space, have been observed on the Voyager 1 and 2 and Pioneer 11 spacecraft in the heliographic latitude range 2 deg S to 23 deg N and the heliocentric radial range 11 to 20 AU. After a period of rather high correlation between fluxes at different latitudes in early 1983, distinct differences develop. The evolution of the fluxes appears to be related to the temporal and latitudinal dynamics of solar coronal holes, suggesting that information about the latitudinal structure of solar wind stream sources propagates to these distances. Author (IAA)

N85-33055*# National Aeronautics and Space Administration. Goddard Space Flight Center, Greenbelt, Md.
DIFFERENTIAL MEASUREMENT OF COSMIC-RAY GRADIENT WITH RESPECT TO INTERPLANETARY CURRENT SHEET c93
S. P. Christon (California Inst. of Tech., Pasadena), A. C. Cummings (California Inst. of Tech., Pasadena), E. C. Stone (California Inst. of Tech., Pasadena), K. W. Behannon, and L. F. Burlaga *In* California Inst. of Tech. Contrib. to the 19th Intern. Cosmic Ray Conf. 1985 4 p refs Sponsored in cooperation with JPL (For primary document see N85-33044 21-88)
(Grant NGR-05-002-160)
(Paper-SH-4.2-9) Avail: NTIS HC A03/MF A01 CSCL 03B

Simultaneous magnetic field and charged particle measurements from the Voyager pacecraft at heliographic latitude separations from 10 deg to 21 deg are used to determine the latitude gradient of the galactic cosmic ray flux with respect to the interplanetary current sheet. By comparing the ratio of cosmic ray flux at Voyager 1 to that at Voyager 2 during periods when both spacecraft are first north and then south of the interplanetary current sheet, we find an estimate of the latitudinal gradient with respect to the current sheet of approximately -0.15 = or − 0.05%/deg under restricted interplanetary conditions. Author

N85-33056*# California Inst. of Tech., Pasadena.
CHANGES IN THE ENERGY SPECTRUM OF ANOMALOUS OXYGEN AND HELIUM DURING 1977 - 1985 c93
A. C. Cummings, E. C. Stone, and W. R. Webber (New Hampshire Univ., Durham) *In its* Contrib. to the 19th Intern. Cosmic Ray Conf. 1985 4 p refs (For primary document see N85-33044 21-88)
(Contract NAS7-918; Grant NGR-05-002-160)
(Paper-SH-4.6-1) Avail: NTIS HC A03/MF A01 CSCL 03B

Data from the cosmic-ray experiment on the Voyager spacecraft was used to assure the energy spectrum of anomalous O and He during the period 1977 to 1985. These spectra change dramatically after the middle of 1980, with the peak or plateau region of the differential spectrum shifting to a higher energy. This change appears to be related to the reversal of the solar magnetic field and could imply that particle drifts are important to the acceleration or propagation of these particles. Author

N85-33057*# California Inst. of Tech., Pasadena.
SOLAR CYCLE VARIATIONS OF THE ANOMALOUS COSMIC RAY COMPONENT Abstract Only c93
R. A. Mewaldt and E. C. Stone *In its* Contrib. to the 19th Intern. Cosmic Ray Conf. 1985 1 p (For primary document see N85-33044 21-88)
(Contracts NAS5-28441; NAS5-28449; Grant NGR-05-002-160)
(Paper-SH-4.6-2) Avail: NTIS HC A03/MF A01 CSCL 03B

The intensity of the anomalous cosmic ray component,

consisting of He, N, O, and Ne, has long been known to be especially sensitive to the effects of solar modulation. Following its discovery in 1972, this component dominated the quiet-time flux of cosmic ray nuclei below approximately 30 MeV/nucleon during the 1972 to 1978 solar minimum, but then became essentially unobservable at 1 AU with the approach of solar maximum conditions. One recent theoretical model predicts substantial differences in the intensity of the anomalous fluxes from one solar minimum period to the next because of the reversal of the solar magnetic field. Using data from the Caltech experiments on IMP-8 and ICE (ISEE-3), the intensity of anomalous O and He at 1 AU during the years 1972 to 1985 is reported. We hope to determine whether the anomalous fluxes will return to their 1972 to 1978 levels, as predicted by spherically symmetric modulation models, or whether they will fail to return to 1 AU, as suggested by modulation models in which gradient and curvature drifts dominate. Author

N85-33058*# New Hampshire Univ., Durham.
RADIAL AND LATITUDINAL GRADIENTS OF ANOMALOUS OXYGEN DURING 1977 - 1985 c93
W. R. Webber, A. C. Cummings (California Inst. of Tech., Pasadena), and E. C. Stone *In* California Inst. of Tech. Contrib. to the 19th Intern. Cosmic Ray Conf. 1985 4 p refs (For primary document see N85-33044 21-88)
(Contract NAS7-918; Grant NGR-05-002-160)
(Paper-SH-4.6-4) Avail: NTIS HC A03/MF A01 CSCL 03B

The radial gradient of anomalous O remained constant during 1977 to 85 at approximately 10 to 15%/AU although the intensity changes by more than a factor of 100. These results can be used to deduce that most of the modulation of the intensities of these particles is occurring beyond 27 AU. Evidence for a latitudinal gradient of approximately +3%/degree at low energies (7.1 to 10.6 MeV/nucl) was also found. Author

N85-33059*# California Inst. of Tech., Pasadena.
SOLAR MODULATION AND INTERPLANETARY GRADIENTS OF THE GALACTIC ELECTRON FLUX, 1977 - 1984 Abstract Only c93
S. P. Christon, A. C. Cummings, E. C. Stone, and W. R. Webber (New Hampshire Univ., Durham) *In its* Contrib. to the 19th Intern. Cosmic Ray Conf. 1985 1 p refs (For primary document see N85-33044 21-88)
(Contract NAS7-918; Grant NGR-05-002-160)
(Paper-SH-4.7-4) Avail: NTIS HC A03/MF A01 CSCL 03B

The flux of electrons with energy from approximately 10 to 180 MeV measured ith the electron telescope on the Voyager 1 and 2 spacecraft in the heliocentric radial range 1 to 22 AU between 1977 and 1984 is reported. Jovian electrons were clearly observable between 1978 and 1983 (radial range 2 to 12 AU) at energies below approximately 50 MeV. Above approximately 50 MeV the electron intensity exhibited temporal variations generally related to the 11 year modulation of protons > 75 MeV. The overall magnitude of the electron intensity changes between the maximum intensity observed in 1977 and the minimum intensity in 1981 was a factor approximately 2, also comparable to that observed for > 75 MeV protons. By early 1985 the electron intensity has apparently recovered to the level observed in 1977 whereas the proton intensity was still about 20% lower. A detailed interpretation of these electron variations in all energy channels depends on an accurate subtraction of background induced by energetic protons of a few 100 Mev. This subtraction is facilitated by calibration results at several energies. Further results on these temporal variations and limits on possible interplanetary gradients will be reported. Author

89 ASTRONOMY

Includes radio and gamma-ray astronomy; celestial mechanics; and astrometry.

N85-33060*# California Univ., Berkeley.
RESEARCH IN EXTREME ULTRAVIOLET AND FAR ULTRAVIOLET ASTRONOMY Semiannual Status Report, 1 Dec. 1984 - 31 May 1985
Simon E. Labov 11 Aug. 1985 34 p refs
(Grant NGR-05-003-450)
(NASA-CR-176068; NAS 1.26:176068) Avail: NTIS HC A03/MF A01 CSCL 03A

Instruments designed to explore different aspects of far and extreme ultraviolet cosmic radiation were studied. The far ultraviolet imager (FUVI) was flown on the Aries sounding rocket. Its unique large format 75mm detector mapped out the far ultraviolet background radiation with a resolution of only a few arc minutes. Analysis of this data indicates to what extent the FUVI background is extra galactic in origin. A power spectrum of the spatial fluctuations will have direct consequences for galactic evolution. J.W.G.

N85-33049*# California Inst. of Tech., Pasadena.
A BALLOON-BORNE IMAGING GAMMA-RAY TELESCOPE
W. E. Althouse, W. R. Cook, A. C. Cummings, M. H. Finger, T. A. Prince, S. M. Schindler, C. H. Starr, and E. C. Stone *In its* Contrib. to the 19th Intern. Cosmic Ray Conf. 1985 4 p refs (For primary document see N85-33044 21-88)
(Grant NGR-05-002-160)
(Paper-OG-9.2-2) Avail: NTIS HC A03/MF A01 CSCL 03B

90 ASTROPHYSICS

Includes cosmology; and interstellar and interplanetary gases and dust.

N85-33061# California Univ., Livermore. Lawrence Livermore Lab.
ENERGY AND TECHNOLOGY REVIEW
Apr. 1985 46 p
(Contract W-7405-eng-48)
(DE85-011767; UCRL-52000-85-4) Avail: NTIS HC A03/MF A01

Some topics covered are coal gasification, evolution of tandem mirror magnetic fusion, solar pond water heaters for industry, synthesis of elements in red giant stars, and Novette target physics experiments. This being the 10th Anniversary issue some topics covered in the 1st issue are reviewed. DOE

N85-33051*# California Inst. of Tech., Pasadena.
THE ENERGY SPECTRUM OF JOVIAN ELECTRONS IN INTERPLANETARY SPACE Abstract Only
S. P. Christon, A. C. Cummings, E. C. Stone, and W. R. Webber (New Hampshire Univ., Durham) *In its* Contrib. to the 19th Intern. Cosmic Ray Conf. 1985 1 p refs (For primary document see N85-33044 21-88)
(Contract NAS7-918; Grant NGR-05-002-160)
(Paper-SH-1.5-18) Avail: NTIS HC A03/MF A01 CSCL 03B

N85-33054*# California Inst. of Tech., Pasadena.
LATITUDE VARIATION OF RECURRENT FLUXES IN THE OUTER SOLAR SYSTEM Abstract Only
S. P. Christon and E. C. Stone *In its* Contrib. to the 19th Intern. Cosmic Ray Conf. 1985 1 p ref Previously announced in IAA as A85-24782 (For primary document see N85-33044 21-88)
(Paper-SH-4.1-13) Avail: NTIS HC A03/MF A01 CSCL 03B

91 LUNAR AND PLANETARY EXPLORATION

Includes planetology; and manned and unmanned flights. For spacecraft design see *18 Spacecraft Design Testing, and Performance.* For space stations see *15 Launch Vehicles and Space Vehicles.*

N85-33062*# Lunar and Planetary Inst., Houston, Tex.
WORKSHOP ON THE EARLY EARTH: THE INTERVAL FROM ACCRETION TO THE OLDER ARCHEAN
Kevin Burke, ed. and Lewis D. Ashwal, ed. 1985 104 p refs Workshop held in Houston, Tex., 23-24 Apr. 1984
(Contract NASw-3389)
(NASA-CR-176037; NAS 1.26:176037; LPI-TR-85-01) Avail: NTIS HC A06/MF A01 CSCL 03B

Presentation abstracts are compiled which address various issues in Earth developmental processes in the first one hundred million years. The session topics included: accretion of the Earth (processes accompanying immediately following the accretion, including core formation); impact records and other information from planets and the Moon relevant to early Earth history; isotopic patterns of the oldest rocks; and igneous, sedimentary, and metamorphic petrology of the oldest rocks. For individual titles, see N85-33063 through N85-33094.

N85-33063*# Oregon State Univ., Corvallis. Coll. of Oceanography.
THE RELATION BETWEEN THE AGE OF THE SUBCONDUCTING SLAB AND THE RECYCLING OF SEDIMENTS INTO THE MANTLE
Dallas Abbott and Sarah Hoffman *In* Lunar and Planetary Inst. Workshop on the Early Earth: The Interval from Accretion to the Older Archean 1985 p 1-3 refs (For primary document see N85-33062 21-91)
Avail: NTIS HC A06/MF A01 CSCL 03B

The recycling of sediments into the mantle has become an important issue because recent papers have suggested that the geochemical inverse models of the evolution of radiogenic isotope abundances over the history of the Earth have nonunique solutions. Both the recycling of continent-derived sediments into the mantle and mixing in the mantle could produce similar geochemical effects in the mean isotopic ratios of new igneous material emplaced in continents. Recent models of Archaean heat flow and of plate tectonics during early Earth history have demonstrated that higher internal heat production of the early Earth was mainly dissipated through a higher creation rate of oceanic lithosphere. If the seafloor creation rate was higher on the early Earth, then the residence time of any one piece of oceanic lithosphere on the surface would have been shorter. It is possible that a higher rate of recycling of oceanic lithosphere into the mantle could have resulted in some transport of sediment into the mantle. G.L.C.

N85-33064*# Scripps Institution of Oceanography, La Jolla, Calif.
CONSTRAINTS ON EARLY ATMOSPHERE FROM PLANETARY ACCRETION PROCESSES
G. Arrhenius *In* Lunar and Planetary Inst. Workshop on the Early Earth: The Interval from Accretion to the Older Archean 1985 p 4-7 refs (For primary document see N85-33062 21-91)
Avail: NTIS HC A06/MF A01 CSCL 03B

Evidence for composition and dynamics of release of the earliest volatiles was in lack of anything better being sought from the most ancient sediments known at the time, although they were recognized to be younger than three billion years. Origin of life on Earth was considered to require a lasting atmosphere with hydrogen and methane as major components. The new observations together with theoretical studies generated by the space program and by systematic exploration of the Earth's oceanic crust changed the climate of opinion in which the questions of the primordial atmosphere are discussed. Even though existing evidence does not permit conclusive choice of any specific scenario, the acceptance of specific model elements now forces the consideration of a series of consequences, some of which may be tested by observation. G.L.C.

N85-33065*# California Univ., San Diego, La Jolla.
THE COMPOSITION OF THE PRIMITIVE ATMOSPHERE AND THE SYNTHESIS OF ORGANIC COMPOUNDS ON THE EARLY EARTH
Jeffrey L. Bada and Stanley L. Miller *In* Lunar and Planetary Inst. Workshop on the Early Earth: The Interval from Accretion to the Older Archean 1985 p 8-10 refs (For primary document see N85-33062 21-91)
Avail: NTIS HC A06/MF A01 CSCL 03B

The generally accepted theory for the origin of life on the Earth requires that a large variety of organic compounds be present to form the first living organisms and to provide the energy sources for primitive life either directly or through various fermentation reactions. This can provide a strong constraint on discussions of the formation of the Earth and on the composition of the primitive atmosphere. In order for substantial amounts of organic compounds to have been present on the prebiological Earth, certain conditions must have existed. There is a large body of literature on the prebiotic synthesis of organic compounds in various postulated atmospheres. In this mixture of abiotically synthesized organic compounds, the amino acids are of special interest since they are utilized by modern organisms to synthesize structural materials and a large array of catalytic peptides. G.L.C.

N85-33066*# Harvard-Smithsonian Center for Astrophysics, Cambridge, Mass.
CONDITIONS DURING FORMATION OF THE EARTH
A. C. W. Cameron *In* Lunar and Planetary Inst. Workshop on the Early Earth: The Interval from Accretion to the Older Archean 1985 p 11-13 refs (For primary document see N85-33062 21-91)
Avail: NTIS HC A06/MF A01 CSCL 03B

The formation of the Earth starts with gravitational instabilities in the gas of primitive solar nebula, which form giant gaseous protoplanets. The envelopes of these are thermally evaporated, but solids can gravitationally settle to the center of the protoplanets, and most of the core and mantle of the Earth were formed at that time (age about 10,000 years). The protoearth then survived a period of high temperatures in the surrounding gas (age about 10 to the 5th years). While and after the gas was thermally stabilized and removed from the solar system, the Earth grew by bombardment of planetesimals and its early atmosphere was established. A late major collision led to formation of the Moon and loss of the primordial atmosphere (age about 10 to the 8th years). The present atmosphere resulted from still later accretion. The presence of this atmosphere spreads out the mantle cooling and solidification over hundreds of millions of years. G.L.C.

N85-33067*# New Mexico Inst. of Mining and Technology, Socorro. Dept. of Geoscience.
EARLY EVOLUTION OF THE CRUST-MANTLE SYSTEM
Kent C. Condie *In* Lunar and Planetary Inst. Workshop on the Early Earth: The Interval from Accretion to the Older Archean 1985 p 14-16 refs (For primary document see N85-33062 21-91)
Avail: NTIS HC A06/MF A01 CSCL 03B

Nd isotopic data indicate that most Archean igneous rocks including compositions ranging from komatiite to tonalite are derived from undepleted or depleted upper mantle sources. If sampling is representative, only a few require enriched sources. A major unresolved question is the fate of the material removed from the upper mantle leaving early depleted sources as residue. One possibility is that widespread depletion of the early mantle resulted from a period of early degassing and magmatism. Rare gas isotopic data, in particular 129Xe/130Xe ratios, seem to demand that the upper mantle was extensively degassed at or before 4.4 b.y. and this led to rapid growth of the atmosphere and oceans. The lower mantle, however, was not significantly degassed during this event. It is likely that such widespread degassing and magmatism of the upper mantle transferred significant quantities of incompatible elements into the uppermost mantle or crust. Once formed, such an enriched fraction should resist recycling into the

mantle and collect at or near the Earth's surface. One possibility is that it collects chiefly in a zone of partial melting, analogous to the present low-velocity zone at the base of the lithosphere.
G.L.C.

N85-33068*# California Univ., Los Angeles. Dept. of Earth and Space Sciences.
WAS CORE FORMATION VIOLENT ENOUGH TO HOMOGENIZE THE EARLY MANTLE?
Stephen A. Cooperman and William M. Kaula *In* Lunar and Planetary Inst. Workshop on the Early Earth: The Interval from Accretion to the Older Archean 1985 p 17-19 refs (For primary document see N85-33062 21-91)
Avail: NTIS HC A06/MF A01 CSCL 03B

The dynamics of iron, its thermal state and its phase in the accreting Earth probably played a major role in the Earth's early thermal evolution. Plausible impact thermal histories make it possible that pure iron was molten in the accreting Earth after it was about 10% grown. Hence, iron eutectic alloys (FeS, FeO) certainly were. Additionally, the initial temperature of the core is an important constraint on the secular cooling of the early Earth and on the strength of the early geodynamo. Whether iron is solid or molten would influence geochemical equilibria in the upper and lower mantle; the mode of core formation, by spherical or near-spherical blobs, stalk-like instabilities, or something more catastrophic would influence the partitioning of siderophiles between silicate and iron phases. Early descent of iron (during accretion) favors partitioning according to low-pressure phase equilibria, whereas late descent favors higher pressure. The later core formation occurs, the greater the heat pulse, due to the strong dependence of gravitational potential energy on planetary radius. The heat may homogenize the mantle if core formation is global; otherwise, heterogeneity of iron differentiation may leave some of the pre-archean mantle unaffected. The larger the chunks of proto-core (and hence smaller surface/volume ratios) the greater the heterogeneity. G.L.C.

N85-33069*# Florida State Univ., Tallahassee. Dept. of Geology.
THE PROBLEM OF THE EARTH'S CO2 CONTENT AND THE IRON CORE
G. W. DeVore *In* Lunar and Planetary Inst. Workshop on the Early Earth: The Interval from Accretion to the Older Archean 1985 p 20-22 refs (For primary document see N85-33062 21-91)
Avail: NTIS HC A06/MF A01 CSCL 03B

The near absence of metallic iron and the presence of magnetite and FeS in the C-1 chondrites imply that metallic iron was a minor phase present during the accretion process that formed the C-1 chondrites. If the C-1 chondrites provided the bulk of the initial planetary growth materials, the carbon reduction model is favored. The above estimates suggest that some 1240 to 227 times as much CO2 may have been produced during the formation of the core than can be accounted for in the crust and mantle. This discrepancy taken to the extreme suggests either that: (1) the Earth has lost more than 99 percent of its initial CO2 during early differentiation (this is highly unlikely) or: (2) the Earth has acquired some 90 percent of its present mass by the accretion of debris from previously reduced and differentiated but subsequently disrupted planetary bodies whereby the associated CO2 would not be captured, or: (3) the C-1 chondrites represent only a trivial fraction of the initial accretion materials present in the nebular cloud or: (4) condensed iron and anhydrous silicate phases were preferentially accreted during the initial formation of the planetary bodies. G.L.C.

N85-33070*# Brown Univ., Providence, R. I. Dept. of Geological Science.
CONSIDERATIONS OF LARGE SCALE IMPACT AND THE EARLY EARTH
R. A. F. Grieve and E. M. Parmentier *In* Lunar and Planetary Inst. Workshop on the Early Earth: The Interval from Accretion to the Older Archean 1985 p 23-24 refs (For primary document see N85-33062 21-91)
Avail: NTIS HC A06/MF A01 CSCL 03B

Bodies which have preserved portions of their earliest crust indicate that large scale impact cratering was an important process in early surface and upper crustal evolution. Large impact basins form the basic topographic, tectonic, and stratigraphic framework of the Moon and impact was responsible for the characteristics of the second order gravity field and upper crustal seismic properties. The Earth's crustal evolution during the first 800 my of its history is conjectural. The lack of a very early crust may indicate that thermal and mechanical instabilities resulting from intense mantle convection and/or bombardment inhibited crustal preservation. Whatever the case, the potential effects of large scale impact have to be considered in models of early Earth evolution. Preliminary models of the evolution of a large terrestrial impact basin was derived and discussed in detail. Author

N85-33071*# Oregon State Univ., Corvallis. Coll. of Oceanography.
HYDROTHERMAL ALTERATION IN THE 3.5 b.y. OLD ONVERWACHT GROUP OF SOUTH AFRICA
Roger Hart and Maarten J. deWit (Witwatersrand Univ., Johannesburg, South Africa) *In* Lunar and Planetary Inst. Workshop on the Early Earth: The Interval from Accretion to the Older Archean 1985 p 25-27 refs (For primary document see N85-33062 21-91)
Avail: NTIS HC A06/MF A01 CSCL 03B

K-Ar studies of authigenic and alteration phases from the 3.5 b.y. old Onverwacht group of South Africa delineate hydrothermal metamorphism that ended 3.3 b.y. years ago. A whole rock K-Ar errochron from analysis of barite, dolomite, chert, and serpentinite (komatiite) gives an age of 3.3 b.y. with an intercept of 1,678 + or - 103. The 3.3. b.y. age for the metamorphism in the Onverwacht was confirmed by the Argon isotopes stepwise heating experiments of komatiites and basaltic komatiites from the Onverwacht Group. In addition, the errochron suggests all the phase studied equilibrated with a reservoir of hydrothermal argon with relatively uniform isotopic composition. The concept of hydrothermal activity in the Onverwacht Group is discussed and illustrated with photographs. Author

N85-33072*# Oregon State Univ., Corvallis. Coll. of Oceanography.
THE DEGASSING HISTORY OF THE EARTH: NOBLE GAS STUDIES OF ARCHAEAN CHERTS AND ZERO AGE GLASSY SUBMARINE BASALTS
Roger Hart and Lewis Hogan *In* Lunar and Planetary Inst. Workshop on the Early Earth: The Interval from Accretion to the Older Archean 1985 p 28-30 refs (For primary document see N85-33062 21-91)
Avail: NTIS HC A06/MF A01 CSCL 03B

Recent noble gas studies suggests the Earth's atmosphere outgassed from the Earth's upper mantle synchronous with sea floor spreading, ocean ridge hydrothermal activity and the formation of continents by partial melting in subduction zones. The evidence for formation of the atmosphere by outgassing of the mantle is the presence of radionuclides H3.-4, Ar-040 and 136 Xe-136 in the atmosphere that were produced from K-40, U and Th in the mantle. How these radionuclides were formed is reviewed. Author

N85-33073*# Oregon State Univ., Corvallis. Coll. of Oceanography.
THE 3.5 b.y. OLD ONVERWACHT GROUP: A REMNANT OF ANCIENT OCEANIC CRUST
Sarah Hoffman *In* Lunar and Planetary Inst. Workshop on the Early Earth: The Interval from Accretion to the Older Archean 1985 p 31-33 refs (For primary document see N85-33062 21-91)
Avail: NTIS HC A06/MF A01 CSCL 03B

The interaction between seawater and submarine volcanic rock has had important consequences for the chemistry of the ocean during the Phanerozoic. Most extant terranes have been regionally metamorphosed to the amphibolite and granulite facies, so that their precursor lithologies and structures are not readily determinable. However, the 3.5 b.y. old supracrustal rocks of the Barberton Mountain Land, South Africa, have not been subjected to high

grade regional metamorphism, and therefore there was reason to hope that a laboratory investigation might reveal the extent to which these rocks had been exposed to subseafloor hydrothermal activity. Hart and de Wit describe bulk geochemical evidence from the entire suite as well as field evidence which support the concept of hydrothermal activity in the Barberton Mountain Land. Mineralogical and textural features which unequivocally mark it as a submarine sequence emplaced in a midocean ridge/fracture zone or back arc/fracture zone environment are briefly discussed.
Author

N85-33074*# Oregon State Univ., Corvallis. Coll. of Oceanography.
SUBMARINE HYDROTHERMAL ENVIRONMENTS AS SITES FOR THE ORIGIN AND EVOLUTION OF LIFE
Sarah Hoffman and John Baross *In* Lunar and Planetary Inst. Workshop on the Early Earth: The Interval from Accretion to the Older Archean 1985 p 34-36 refs (For primary document see N85-33062 21-91)
Avail: NTIS HC A06/MF A01 CSCL 03B

That life formed and evolved in hydrothermal environments is proposed. This hypothesis is plausible in terms of the tectonic, paleontological, and degassing history of the Earth. Submarine hydrothermal vents are the only contemporary geological environment which may truly be called primeval and which today continue to be a major source of gases and dissolved elements to the ocean. The microbial assemblages in present day hydrothermal systems therefore could be living analogues of the earliest microbial communities to develop on Earth. The evidence for the hypothesis is reviewed.
Author

N85-33075*# Minnesota Univ., Minneapolis. Dept. of Geology and Geophysics.
NOBLE GASES AND THE EARLY HISTORY OF THE EARTH: INAPPROPRIATE PARADIGMS AND ASSUMPTIONS INHIBIT RESEARCH AND COMMUNICATION
G. R. Huss and E. C. Alexander, Jr. *In* Lunar and Planetary Inst. Workshop on the Early Earth: The Interval from Accretion to the Older Archean 1985 p 37-38 refs (For primary document see N85-33062 21-91)
Avail: NTIS HC A06/MF A01 CSCL 03B

The development of models as tracers of nobel gases through the Earth's evolution is discussed. A new set of paradigms embodying present knowledge was developed. Several important areas for future research are: (1) measurement of the elemental and isotopic compositions of the five noble gases in a large number of terrestrial materials, thus better defining the composition and distribution of terrestrial noble gases; (2) determinations of relative diffusive behavior, chemical behavior, and the distribution between solid and melt of noble gases under mantle conditions are urgently needed; (3) disequilibrium behavior in the nebula needs investigation, and the behavior of plasmas and possible cryotrapping on cold nebular solids are considered.
E.A.K.

N85-33076*# Harvard Univ., Cambridge, Mass. Dept. of Geological Sciences.
CONSTRAINTS ON THE DEVELOPMENT OF THE EARLY CONTINENTAL CRUST FROM ISOTOPIC DATA
S. B. Jacobson *In* Lunar and Planetary Inst. Workshop on the Early Earth: The Interval from Accretion to the Older Archean 1985 p 39 (For primary document see N85-33062 21-91)
Avail: NTIS HC A06/MF A01 CSCL 03B

Aspects of the origin and development of the early (AE) continential crust are addressed by radiogenic isotope and trace element studies. The most important ones are: (1) at what time did the earliest continental crust form; (2) what was its composition; (3) by what processes did it grow and by what processes was it destroyed; (4) what were the rates of production and destruction as a function of time during this time period? Nd is isotopic data on the oldest terrestrial rocks indicate that the mantle at this time had already suffered substantial depletion in incompatible elements due to earlier continent forming events. Isotopic data on young volcanic rocks derived from the depleted mantle show no evidence of this early history. The observed isotopic patterns of Nd, Sr, Hf and Pb through time together with the presently observed age spectrum of crustal rocks are considered. These patterns can be modelled by a transport model in which the continental growth and destruction rates are allowed to vary as a function of time. It is suggest that the mass of the continents at 3.8 AE ago was about 25% of the current continental mass. However, due to the very high recycling rates obtained in the early Archean only a few percent of this crust has been preserved up to the present. E.A.K.

N85-33077*# Max-Planck-Inst. fuer Chemie, Mainz (West Germany).
ANORTHOSITIC OCEANIC CRUST IN THE ARCHEAN EARTH
E. Jagoutz, J. B. Dawson (Sheffield Univ.), S. Hoernes (Bonn Univ.), B. Spettel, and H. Waenke *In* Lunar and Planetary Inst. Workshop on the Early Earth: The Interval from Accretion to the Older Archean 1985 p 40-41 refs (For primary document see N85-33062 21-91)
Avail: NTIS HC A06/MF A01 CSCL 03B

Ultrapure minerals separated from eclogite inclusions in kimberlites were analyzed for Sm, Nd, Sr, and oxygen isotopes and for major and trace elements. Clinopyroxene (cpx) and garnet (gnt) are the only primary mineral phases in these rocks, and mineral phases and their alteration products. The WR sub calc. is the reconstructed bulk composition excluding all the contamination influences. Two groups of eclogites: are distinguished: (1) type A Noritic-anorthositic eclogites; and (2) type B Ti-ferrogabbroic eclogites. The oxygen isotopes are primary mantle-derived features of these rocks and are not caused by posteruption processes, as they were measured on unaltered, clean mineral separates and show a correlation with REE pattern and Sr and Nd isotopes. It is suggested that the variation of the oxygen isotopes are caused by crustal-level fluid-rock interaction at relatively low temperature. It is shown that oxygen isotopes variation in MORB basalts caused by the hydrothermal system are in the same range as the observed oxygen isotope variation in eclogites. A model to explain the new set of data is proposed. It is thought that some of these eclogites might be emplaced into the upper lithosphere or lower crust at the time corresponding to their internal isochron age. The calculated WR composition was used to estimate model ages for these rocks.
E.A.K.

N85-33078*# Arizona Univ., Tucson. Lunar and Planetary Lab.
A MODEL FOR CORE FORMATION IN THE EARLY EARTH
John H. Jones and Michael J. Drake *In* Lunar and Planetary Inst. Workshop on the Early Earth: The Interval from Accretion to the Older Archean 1985 p 42-44 refs (For primary document see N85-33062 21-91)
(Grant NsG-7576)
Avail: NTIS HC A06/MF A01 CSCL 03B

Two basic types exogenous models were proposed to account for siderophile and chalcophile element abundances in the Earth's upper mantle. The first model requires that the Earth be depleted in volatiles and that, after a core formation event which extracted the most siderophile elements into the core, additional noble siderophile elements (Pt, Ir, Au) were added as a late veneer and mixed into the mantle. The second model postulates a reduced Earth with approximately CI elemental abundances in which a primary core forming event depleted all siderophile elements in the mantle. The plausibility of models which require fine scale mixing of chondritic material into the upper mantle is analyzed. Mixing in liquids is more efficient, but large degrees of silicate partial melting will facilitate the separation of magma from residual solids. Any external events affecting the upper mantle of the Earth should also be evident in the Moon; but siderophile and chalcophile element abundance patterns inferred for the mantles of the Earth and Moon differ. There appear to be significant physical difficulties associated with chondritic veneer models.
E.A.K.

N85-33079*# California Univ., Los Angeles. Dept. of Earth and Space Sciences.
IMPLICATIONS FOR THE EARTH OF THE EARLY DYNAMICAL ENVIRONMENT

W. M. Kaula and S. A. Cooperman *In* Lunar and Planetary Inst. Workshop on the Early Earth: The Interval from Accretion to the Older Archean 1985 p 45-47 refs (For primary document see N85-33062 21-91)
Avail: NTIS HC A06/MF A01 CSCL 03B

The formation of the Earth, was mainly from sizeable bodies: perhaps moon sized. Models of interaction among small planetesimals which take into account only close encounters all lead to the formation of moon sized objects, thus leading to several 100 in the inner solar system. Longer term interactions, such as secular resonance sweepings, are needed to get these planetesimals together to form the observed terrestrial bodies. After the accumulation of the Earth, during which core formation certainly occurred, further impacts probably influenced the locations of rifting centers in the system of mantle convection and crustal differentiation. They may have affected craton stabilization by promoting lateral heterogeneity, but had little influence on the key problem of early recycling of sial. E.A.K.

N85-33080*# State Univ. of New York, Albany. Dept. of Geological Sciences.
A REVIEW OF TECTONIC ASPECTS OF THE LIMPOPO BELT AND OTHER ARCHEAN HIGH-GRADE GNEISSIC TERRANES
W. S. F. Kidd *In* Lunar and Planetary Inst. Workshop on the Early Earth: The Interval from Accretion to the Older Archean 1985 p 48-49 ref (For primary document see N85-33062 21-91)
Avail: NTIS HC A06/MF A01 CSCL 03B

Published information on the Archean high grade terrains varies a great deal in the detail available. Such information as exists indicates marked differences in the lithic types and proportions present in the central Limpopo belt compared with the better studies of the other Archean high grade terrains. These differences may be important because they are expressed by the presence in the Limpopo belt of subordinate, but significant quantities (about 5% each) of two rock suites likely to have formed on a shallow marine platform of significant size (Eriksson and Kidd, in prep.). These suites consist of thick sections dominantly consisting of either carbonate and calc-silicate, or of pure metaquartzites, often fuchsite bearing, whose lithic characters are unlike those expected for metacherts but are very like those expected for platform arenites. Isotopic ages suggest these sediments are probably older than 3.3 Ga and younger than 3.5 Ga. Studies lead to the conclusions that (1) continental fragments large enough to provide a substrate for significant platform arenite and carbonate sedimentation existed by 3.3 to 3.5 Ga ago; (2) Wilson cycle tectonics seems to adequately explain most major features of the Archean gneissic terranes; and (3) Tibetan-Himalayan style collisional tectonics 2.6 Ga and older accounts for the large scale relationships between the Limpopo belt and the adjacent Archean greenstone granitoid terrane cratons. By inference, other more fragmentary Archean gneissic terranes may have once been part of such collisional zones. R.J.F.

N85-33081*# Woods Hole Oceanographic Institution, Mass. Dept. of Chemistry.
A REVIEW OF NOBLE GAS GEOCHEMISTRY IN RELATION TO EARLY EARTH HISTORY
Mark D. Kurz *In* Lunar and Planetary Inst. Workshop on the Early Earth: The Interval from Accretion to the Older Archean 1985 p 50 refs (For primary document see N85-33062 21-91)
Avail: NTIS HC A06/MF A01 CSCL 03B

One of the most fundamental noble gas constraints on early Earth history is derived from isotopic differences in (129)Xe/(130)Xe between various terrestrial materials. The short half life (17 m.y.) of extinct (129I, parent of (129)Xe, means that these differences must have been produced within the first 100 m.y. after terrestrial accretion. The identification of large anomalies in (129)Xe/(130)Xe in mid ocean ridge basalts (MORB), with respect to atmospheric xenon, suggests that the atmosphere and upper mantle have remained separate since that time. This alone is a very strong argument for early catastrophic degassing, which would be consistent with an early fractionation resulting in core formation. However, noble gas isotopic systematics of oceanic basalts show that the mantle cannot necessarily be regarded as a homogeneous system, since there are significant variations in (3)He/(4)He, (40)Ar/(36)Ar, and (129)Xe/(130)Xe. Therefore, the early degassing cannot be considered to have acted on the whole mantle. The specific mechanisms of degassing, in particular the thickness and growth of the early crust, is an important variable in understanding present day noble gas inventories. Another constraint can be obtained from rocks that are thought to be derived from near the lithosphere asthenosphere boundary: ultramafic xenoliths. M.G.

N85-33082*# Louisiana State Univ., Baton Rouge. Dept. of Geology.
ARCHEAN SEDIMENTARY SYSTEMS AND CRUSTAL EVOLUTION
Donald R. Lowe *In* Lunar and Planetary Inst. Workshop on the Early Earth: The Interval from Accretion to the Older Archean 1985 p 51-53 refs (For primary document see N85-33062 21-91)
Avail: NTIS HC A06/MF A01 CSCL 03B

Current knowledge of preserved Archean sedimentary rocks suggests that they accumulated in at least three major depositional settings. These are represented generally by sedimentary units: (1) in early Archean, pre-3.0 Ga old greenstone belts, (2) on late Archean sialic cratons, and (3) in late Archean, post-3.0 Ga old greenstone belts. Research suggests that the Archean was characterized by at least two distinctive and largely diachronous styles of crustal evolution. Thick, stable early Archean simatic platforms, perhaps analogous to modern oceanic islands formed over hot spots, underwent a single cycle of cratonization to form stable continental blocks in the early Archean. Later formed Archean continents show a two stage evolution. The initial stage is reflected in the existence of older sialic material, perhaps representing incompletely cratonized areas or microcontinents of as yet unknown origin. During the second stage, late Archean greenstone belts, perhaps analogous to modern magmatic arcs or back arc basins, developed upon or adjacent to these older sialic blocks. The formation of this generation of Archean continents was largely complete by the end of the Archean. These results suggest that Archean greenstone belts may represent a considerable range of sedimentological and tectonic settings. R.J.F.

N85-33083*# National Aeronautics and Space Administration. Goddard Space Flight Center, Greenbelt, Md.
THE ORIGIN OF CONTINENTAL CRUST: OUTLINES OF A GENERAL THEORY
Paul D. Lowman, Jr. *In* Lunar and Planetary Inst. Workshop on the Early Earth: The Interval from Accretion to the Older Archean 1985 p 54-56 refs (For primary document see N85-33062 21-91)
Avail: NTIS HC A06/MF A01 CSCL 03B

The lower continental crust, formerly very poorly understood, has recently been investigated by various geological and geophysical techniques that are beginning to yield a generally agreed on though still vague model (Lowman, 1984). As typified by at least some exposed high grade terranes, such as the Scottish Scourian complex, the lower crust in areas not affected by Phanerozoic orogeny or crustal extension appears to consist of gently dipping granulite gneisses of intermediate bulk composition, formed from partly or largely supracrustal precursors. This model, to the degree that it is correct, has important implications for early crustal genesis and the origin of continental crust in general. Most important, it implies that except for areas of major overthrusting (which may of course be considerable) normal superposition relations prevail, and that since even the oldest exposed rocks are underlain by tens of kilometers of sial, true primordial crust may still survive in the lower crustal levels (of. Phinney, 1981). R.J.F.

N85-33084*# Scripps Institution of Oceanography, La Jolla, Calif.
THE ARAVALLI SEQUENCE OF RAJASTHAN, INDIA: A PRECAMBRIAN CONTINENTAL MARGIN?
J. D. Macdougall, R. Willis, G. W. Lugmair, A. B. Roy (Rajasthan Univ.), and K. Gopalan (Physical Research Lab., India) *In* Lunar and Planetary Inst. Workshop on the Early Earth: The Interval from Accretion to the Older Archean 1985 p 57-58 refs (For

primary document see N85-33062 21-91)
Avail: NTIS HC A06/MF A01 CSCL 03B

The extent to which plate tectonics in its present form operated during the Precambrian is unknown, but is a subject of considerable current interest. A remarkable succession of Precambrian rocks in Rajasthan, Northwestern India, which may help to shed more light on this question are discussed. Data indicates that the Aravalli sequence has a number of characteristics generally ascribed to active continental margins. Although much more work is required to bear this out, the evidence suggests that the processes operating in such an environment in the early Proterozoic or late Archean were not vastly different from today. R.J.F.

N85-33085*# Open Univ., Milton (England). Dept. of Earth Sciences.
CARBON AND NITROGEN IN THE DEEP EARTH
D. P. Mattey, L. P. Carr, R. H. Carr, I. P. Wright, and C. T. Pillinger *In* Lunar and Planetary Inst. Workshop on the Early Earth: The Interval from Accretion to the Older Archean 1985 p 59-61 refs (For primary document see N85-33062 21-91)
Avail: NTIS HC A06/MF A01 CSCL 03B

High sensitivity mass spectrometric techniques were utilized to study the C-N isotope systematics in basic igneous rocks and mantle materials in an attempt to ultimately constrain the primordial isotopic compositions of these elements and their subsequent fate during the early history of the Earth. Preliminary results obtained for a selection of submarine basaltic glasses and diamonds are summarized concentrating on: (1) the problem of whether isotopes are significantly fractionated during igneous processes; and on (2) the effects of crustal recycling. M.G.

N85-33086*# Lunar and Planetary Inst., Houston, Tex.
CRUSTAL RADIOGENIC HEAT PRODUCTION AND THE SELECTIVE SURVIVAL OF ANCIENT CONTINENTAL CRUST
Paul Morgan *In its* Workshop on the Early Earth: The Interval from Accretion to the Older Archean 1985 p 62-64 refs Previously announced in IAA as A85-30039 (For primary document see N85-33062 21-91)
(Contract NASw-3389)
Avail: NTIS HC A06/MF A01 CSCL 03B

It is pointed out that the oldest terrestrial rocks have so far revealed no evidence of the impact phase of Earth evolution. This observation suggests that processes other than impact were dominant at the time of stabilization of these units. However, a use of the oldest terrestrial rocks as a sample of the early terrestrial crust makes it necessary to consider the possibility that these rocks may represent a biased sample. In the present study, the global continental heat flow data set is used to provide further evidence that potassium, uranium, and thorium abundances are, on the average, low in surviving Archean crust relative to younger continental crust. An investigation is conducted of the implications of relatively low crustal radiogenic heat production to the stabilization of early continental crust, and possible Archean crustal stabilization models are discussed. G.R. (IAA)

N85-33087*# National Aeronautics and Space Administration. Ames Research Center, Moffett Field, Calif.
WATER LOSS FROM VENUS: IMPLICATIONS FOR THE EARTH'S EARLY ATMOSPHERE
Steven M. Richardson (Iowa State Univ. of Science and Technology, Ames), James B. Pollack, and Ray T. Reynolds *In* Lunar and Planetary Inst. Workshop on the Early Earth: The Interval from Accretion to the Older Archean 1985 p 65-67 refs (For primary document see N85-33062 21-91)
Avail: NTIS HC A06/MF A01 CSCL 03B

The atmosphere of Venus outgassed rapidly as a result of planetary heating during accretion, resulting in massive water loss. The processes affecting atmospheric chemistry following accretion have consisted largely of hydrogen escape and internal re-equilibrium. The initial bulk composition of Venus and Earth are assumed to have been roughly similar. Chemical speciation on Venus was controlled by the temperature and oxygen buffering capacity of the surface magma. It is also assumed that the surfaces of planetary bodies of the inner solar system were partly or wholly molten during accretion with a temperature estimated at 1273 to 1573 K. To investigate the range of reasonable initial atmospheric compositions on Venus, limits have to be set for the proportion of total hydrogen and the buffered fugacity of oxygen. Using the C/H ratio of 0.033 set for Earth, virtually all of the water generated during outgassing must later have been lost in order to bring the current CO2/H2O ratio for Venus up to its observed value of 10 sup 4 to 10 sup 5. The proportion of H2O decreases in model atmospheres with successfully higher C/H values, ultimately approaching the depleted values currently observed on Venus. Increasing C/H also results in a rapid increase in CO/H2O and provides an efficient mechanism for water loss by the reaction $CO + H2O = CO2 + H2$. This reaction, plus water loss mechanisms involving crustal iron, could have removed a very large volume of water from the Venusian atmosphere, even at a low C/H value. F.M.R.

N85-33088*# Geological Survey, Reston, Va.
CHEMICAL EVOLUTION OF THE EARTH: EQUILIBRIUM OR DISEQUILIBRIUM PROCESS?
Motoaki Sato *In* Lunar and Planetary Inst. Workshop on the Early Earth: The Interval from Accretion to the Older Archean 1985 p 68-70 refs (For primary document see N85-33062 21-91)
Avail: NTIS HC A06/MF A01 CSCL 03B

To explain the apparent chemical incompatibility of the Earth's core and mantle or the disequilibrium process, various core forming mechanisms have been proposed, i.e., rapid disequilibrium sinking of molten iron, an oxidized core or protocore materials, and meteorite contamination of the upper mantle after separation from the core. Adopting concepts used in steady state thermodynamics, a method is devised for evaluating how elements should distribute stable in the Earth's interior for the present gradients of temperature, pressure, and gravitational acceleration. Thermochemical modeling gives useful insights into the nature of chemical evolution of the Earth without overly speculative assumptions. Further work must be done to reconcile siderophile elements, rare gases, and possible light elements in the outer core. F.M.R.

N85-33089*# ORYX, Paris (France).
LARGE ARCUATE SCARS: A GEOLOGICAL LEGACY OF THE EARTH'S ACCRETIONARY PAST
John M. Saul *In* Lunar and Planetary Inst. Workshop on the Early Earth: The Interval from Accretion to the Older Archean 1985 p 71-73 refs (For primary document see N85-33062 21-91)
Avail: NTIS HC A06/MF A01 CSCL 03B

Immediately following accretion, the surface of the Earth was densely patterned with circular scars which were the surface expressions of 3-D craterform structures. In the course of geological time these structures would have become less and less visible due to the workings of the Earth's atmosphere, surface waters, and plate tectonics regime but there is no compelling reason to assume that they have been entirely eradicated. Furthermore, a very imperfect analogy with the other inner planets suggests that geological processes may not in fact be capable of totally erasing such deep features. Some illustrative examples of arcuate scars are discussed. M.G.

N85-33090*# Lunar and Planetary Inst., Houston, Tex.
LUNAR AND MARTIAN IMPACT BASINS: EXPOSED RECORDS OF TERRESTRIAL BOMBARDMENT?
Peter M. Schultz *In its* Workshop on the Early Earth: The Interval from Accretion to the Older Archean 1985 p 74-75 refs (For primary document see N85-33062 21-91)
Avail: NTIS HC A06/MF A01 CSCL 03B

The unrecycled surfaces of the Moon, Mercury, and Mars preserve the very early history of impact bombardment and its effect on crustal evolution. Previous studies indicated that the post accretion impact flux by large bodies on Mars may have been dificient, but systematic studies recently have revealed that this deficiency is largely the result of active erosional and depositional processes during the first 0.8 by. Ancient Martian impact basins larger than 300 km in diameter are revealed by

subtle but unequivocal topographic and structural control of drainage patterns. In addition, the largest basins have left a deep seated imprint of concentric and radial structural patterns that control the occurrence of most Martian volcanic and tectonic provinces. If 10(-6)/km(2) is considered to be a reasonable approximation for the density of impact basins (> 300 km) of the Moon and Mars, then the Earth should have recorded more than 500 impacts that resulted in basins larger than 300 km in diameter over its post accretion geologic history. If calibrated with the Moon, then most of these impacts occurred prior to 3.8 by.
M.G.

N85-33091*# California Inst. of Tech., Pasadena. Div. of Geological and Planetary Sciences.
THERMAL, DYNAMIC AND COMPOSITIONAL ASPECTS OF THE CORE-FORMING EARTH
D. J. Stevenson *In* Lunar and Planetary Inst. Workshop on the Early Earth: The Interval from Accretion to the Older Archean 1985 p 76-78 refs (For primary document see N85-33062 21-91)
Avail: NTIS HC A06/MF A01 CSCL 03B

Core formation is the most important and singular differentiation event in the history of a terrestrial planet. It almost certainly involved the downward migration of a partially or wholly molten iron alloy through a silicate and oxide mantle, and was contemporaneous with accretion. Several important, unresolved issues which have implications for mantle and core geochemistry, the thermal history of the Earth, and the origin of geomagnetism are addressed: whether the early Earth was molten; whether core formation involved low or high pressure geochemistry, or both; early Earth mantle homogenization; whether equilibration established between core forming material and the mantle through which it migrated; and how much iron is stranded and unable to reach the core.
Author

N85-33092*# California Univ., Los Angeles. Inst. of Geophysics and Planetary Physics.
EARTH'S PRIMORDIAL DIFFERENTIATION, AND ITS AFTER-EFFECTS
Paul H. Warren *In* Lunar and Planetary Inst. Workshop on the Early Earth: The Interval from Accretion to the Older Archean 1985 p 79-81 refs (For primary document see N85-33062 21-91)
Avail: NTIS HC A06/MF A01 CSCL 03B

The case for massive primordial melting on the Earth is circumstantial (i.e., based mainly on lunar evidence), but nonetheless compelling. The term magma ocean is probably a hyperbole. Among other things, ocean implies the system is virtually 100% liquid, with a mainly gas/liquid upper surface, and a water like viscosity of the order .01 poise. The preferred term for this phenomenon is magmasphere.
G.L.C.

N85-33093*# Leicester Univ. (England). Dept. of Geology.
CHEMICAL CONSTRAINTS ON THE EVOLUTION OF ARCHEAN CONTINENTAL CRUST
B. L. Weaver and J. Tarney *In* Lunar and Planetary Inst. Workshop on the Early Earth: The Interval from Accretion to the Older Archean 1985 p 82-83 refs (For primary document see N85-33062 21-91)
Avail: NTIS HC A06/MF A01 CSCL 03B

One of the challenges of Archean geochronology is to find isotopic systems that preserve an indication of a rock's primary age in spite of the effects of later metamorphism. Zircon dating has been used widely with considerable success but not without difficulty, especially in polymetamorphic terrains. Zircons in such cases commonly are found to have lost radiogenic Pb, and despite fractionizing the zircons or abrading them to remove disturbed portions; it often is not possible to define a pattern of Pb loss from which the original age can confidently be inferred. The refinement of techniques to enable extremely small samples, or even single crystals, to be analyzed has contributed greatly to solving the problem but even those techniques cannot resolve the micron scale isotopic heterogeneities within single zircons in which much of their history is recorded. That can only be done by ion microprobe. Progress reports on studies of four Archean rocks, each of which illustrates the power and potential of ion microprobe analysis in solving problems of Archean geochronology are discussed.
R.J.F.

N85-33094*# Australian National Univ., Canberra. Research School of Earth Sciences.
DATING ARCHEAN ZIRCON BY ION MICROPROBE: NEW LIGHT ON AN OLD PROBLEM
I. S. Williams, P. D. Kinny, L. P. Black (Bureau of Mineral Resources, Canberra, Australia), W. Compston, D. O. Froude, and T. R. Ireland *In* Lunar and Planetary Inst. Workshop on the Early Earth: The Interval from Accretion to the Older Archean 1985 p 84-86 refs (For primary document see N85-33062 21-91)
Avail: NTIS HC A06/MF A01 CSCL 03B

Ion microprobe analysis of zircons from three sites (Watersmeet Dome in northern Michigan, Mount Sones in eastern Antarctica, and Mount Narryer in western Australia) is discussed. Implications of the results to Archean geochronology and early Earth crust composition are addressed.
M.G.

N85-32360*# California Inst. of Tech., Pasadena. Geological and Planetary Sciences Div.
MEGAGEOMORPHOLOGY: MARS VIS A VIS EARTH
Robert P. Sharp *In* NASA. Goddard Space Flight Center Global Mega-Geomorphology Jul. 1985 p 18-20 (For primary document see N85-32357 21-42)
Avail: NTIS HC A07/MF A01 CSCL 03B

N85-32373*# Arizona State Univ., Tempe. Dept. of Geology.
AEOLIAN GEOMORPHOLOGY FROM THE GLOBAL PERSPECTIVE
Ronald Greeley *In* NASA. Goddard Space Flight Center Global Mega-Geomorphology Jul. 1985 p 64-67 ref (For primary document see N85-32357 21-42)
Avail: NTIS HC A07/MF A01 CSCL 03B

N85-32375*# California State Polytechnic Univ., Pomona. Dept. of Earth Sciences.
THE PROBLEM OF SCALE IN PLANETARY GEOMORPHOLOGY
Lisa A. Rossbacher *In* NASA. Goddard Space Flight Center Global Mega-Geomorphology Jul. 1985 p 76-78 (For primary document see N85-32357 21-42)
Avail: NTIS HC A07/MF A01 CSCL 03B

N85-32385*# National Aeronautics and Space Administration. Goddard Space Flight Center, Greenbelt, Md.
PLANETARY PERSPECTIVE. REPORT OF WORKING GROUP NUMBER 4
Lisa A. Rossbacher (California State Polytechnic Univ., Pomona) *In its* Global Mega-Geomorphology Jul. 1985 p 109-110 (For primary document see N85-32357 21-42)
Avail: NTIS HC A07/MF A01 CSCL 03B

92 SOLAR PHYSICS

Includes solar activity, solar flares, solar radiation and sunspots.

N85-33095 Institut d'Aeronomie Spatiale de Belgique, Brussels.
SOLAR RADIO FLUXES AS INDICES OF SOLAR ACTIVITY
Marcel Nicolet and Lucien Bossy 1984 206 p refs Submitted for publication
(Aeronomica-Acta-A-282-1984) Avail: Issuing Activity

Daily solar radio flux values at 9400, 3750, 2000, 1000, and 2800 MHz were used to study solar radio fluxes as indices of solar activity. Yearly mean values at each frequency, and mean ratios during periods of 18 or 6 months indicate a close connection between radio fluxes in the centimeter region; anomalies related to calibration problems can be detected. Regression analysis of the daily values of the fluxes over at least 25 yr and a test on the sensitivity may provide final information on the stability of the

data with respect to time and solar activity. The method is capable of detecting long-term trends corresponding to instrument drifts. Such information is essential to understanding of anomalies detected in the observations of UV and X-ray irradiances. However, such a method is based on a linear relationship. When a quadratic form, as observed in the decimeter region, is adopted, the effect of the various levels of activity in a solar cycle must be considered. Author (ESA)

N85-33096*# Lockheed Missiles and Space Co., Palo Alto, Calif.
SOFT X-RAY POLYCHROMATOR FOR THE SOLAR MAXIMUM MISSION Final Report
B. M. Haisch, M. Levay, R. A. Stern, K. T. Strong, C. J. Wolfson, and L. W. Acton Dec. 1984 86 p refs Original contains color illustrations
(Contract NAS5-23758)
(NASA-CR-175297; NAS 1.26:175297) Avail: NTIS HC A05/MF A01 CSCL 03B

The XRP was designed to measure the following temporal and spatial properties of the active and flaring Sun: electron temperature, departures from steady state, ion kinetic temperatures, and electron density. The Bent Crystal Spectrometer (BCS) is capable of measuring the broadening and blue shifts often observed in the impulsive phase of flares. The six simultaneous line fluxes indicative of six different temperatures of formation observable by the Flat Crystal Spectrometer (FCS) allows the derivation of the differential emission measure of the plasma at each raster point. During the operational periods of the XRP hundreds of flares of C-level (GOES classification) were observed and brighter in both the FCS and BCS, including 5 X-flares. Associated theoretical work in atomic physics, stimulated in part by the promise of XRP measurements, has benefitted from the experimental data on solar plasmas which the XRP has provided in abundance. Author

N85-33097# National Oceanic and Atmospheric Administration, Boulder, Colo.
SOLAR CYCLE VARIATION OF EPHEMERAL REGIONS Final Report, 1 Nov. 1983 - 1 Nov. 1984
K. L. Harvey Hanscom AFB, Mass. AF Geophysics Lab. 1 Dec. 1984 37 p
(Contract ESD-84-611; AF Proj. 2311)
(AD-A154967; AFGL-TR-84-0335) Avail: NTIS HC A03/MF A01 CSCL 03/2

Ephemeral active regions (ER) have been identified and counted for selected periods from 1970 to mid-1984 using the daily, full-disk photospheric magnetograms taken by the National Solar Observatory. The number of ephemeral regions varies nearly in phase with the solar cycle. At solar minimum, ER are distributed almost uniformly in latitude; by solar maximum, peaks in the latitude distribution are observed in the sunspot zones and in higher latitude bands. In the quiet sun, 37% of the He I lambda 10830 dark points, used as a proxy for X-ray bright points (XBP), are associated with ER; 63% overlie bipoles that appear to be the chance encounter of opposite polarity network. The percentages are somewhat different in coronal holes; 21% of the dark points in He I are associated with ephemeral regions and 79% with bipoles that apparently result from chance encounters of flux. The dark points observed in the quiet sun and in coronal holes, vary anti-correlated with the solar cycle. Little relations was found between the areal density of He I dark points and ephemeral regions within the boundaries of coronal holes and parameters of the high speed solar wind streams associated with coronal holes. This study suggests that (1) ephemeral regions are not small active regions and that they may be primarily a surface phenomena, possibly resulting from convection interacting with sub-photospheric fields, and (2) He I dark points, and therefore, XBP, are more often associated with the encounter of existing opposite polarity network flux, the occurrence of which is related to the amount of mixed polarity areas which varies inversely with the solar cycle. Author (GRA)

N85-33098# Colorado Univ., Boulder. Dept. of Astro-geophysics.
SOLAR CONVECTION Final Report, 1 Mar. 1977 - 30 Nov. 1983
J. Toomre and K. B. Gebbie 30 Apr. 1984 37 p
(Contract F19628-77-C-0104)
(AD-A155214; AFGL-TR-84-0130) Avail: NTIS HC A03/MF A01 CSCL 03/2

A thorough study of convective penetration into the solar atmosphere and convective motions in sub-atmospheric layers on the Sun was made. Non-linear anelastic and Boussinesq modal equations were developed and solved to describe solar and stellar convection. An explanation was developed for the lack of penetration of large-scale convective motions into the observable solar atmosphere through the discovery of buoyancy braking near the top of a supposedly unstable layer. Observations of motions in the solar atmosphere led to the discovery of a new scale of solar motion, the so-called mesogranulation. A technique was developed to use changes in the solar five-minute oscillations as a probe of internal solar structure. Using this technique, large-scale, sub-atmospheric convective eddies were discovered. GRA

N85-33099# American Science and Engineering, Inc., Cambridge, Mass. Space Systems Div.
A STUDY OF THE CYCLICAL VARIATIONS OF CORONAL HOLES AND THEIR RELATION TO OPEN MAGNETIC FIELDS Final Report, 8 Nov. 1983 - 30 Sep. 1984
J. M. Davis and D. F. Webb Dec. 1984 50 p
(Contract F19628-84-C-0037)
(AD-A155251; ASE-4928; AFGL-TR-85-0003) Avail: NTIS HC A03/MF A01 CSCL 03/2

This contract was a study of possible variations in the observed flux from coronal holes over a solar cycle and their relationship to solar magnetic fields. The variation of X-ray emission from coronal holes was measured and compared with data on photospheric magnetic field strength and models of open field structures from holes. The data set consisted of reduced X-ray images from AS&E rocket flights and digitized photospheric magnetic field strength data from Mt. Wilson and Kitt peak observatories over the period 1974 to 1981. The results are as follows. We found that soft X-ray emission from coronal holes could be detected in the rocket data, confirming earlier Skylab results. Also, this emission appeared to vary systematically over an 8-year period, from a minimum in mid-1974 to a maximum about one year after sunspot activity maximum. This conclusion is strengthened by three other observations: (1) HeI 10830 A coronal holes exhibited decreased contrast during this same period; (2) the particular holes that we measured were typical of those at each phase of the cycle in terms of their evolutionary and interplanetary characteristics; and (3) the X-ray hole emission followed a similar trend in Harvey et al.'s (1982) data whereby the photospheric field strength of near-equatorial holes increased systematically by a factor of three between 1975 and 1980. Further, our own measurements of field strengths within the X-ray hole boundaries were sparse but generally in agreement with the Harvey et al. trend. GRA

N85-33100# Alabama Univ., Huntsville.
HEATING OF THE DEEP CHROMOSPHERE DURING SOLAR FLARES Final Report, 1 Dec. 1983 - 30 Sep. 1984
A. G. Emslie 1 Oct. 1984 11 p
(Contract F19628-84-K-0002)
(AD-A155256; AFGL-TR-84-0291) Avail: NTIS HC A02/MF A01 CSCL 03/2

The role of the negative hydrogen ion, in the energy balance of the deep chromosphere is reassessed and quantitatively evaluated. We find that in quiet Sun conditions the negative hydrogen ion (H) is a heating agent, absorbing more photospheric radiation than it reradiates. We further propose that during flares a flux of UV radiation produces over ionization of the deep chromosphere (principally by ionizing neutral silicon) and that the increased electron density so produced causes an increase in the H + e yields H association rate and so an increased H abundance. The resulting increased absorption of photospheric radiation by the H ions produces heating compatible with observations. Author (GRA)

N85-33101# Adaptive Optics Associates, Inc., Cambridge, Mass.
SOLAR ADAPTIVE OPTICS Final Report, 17 Mar. 1982 - 30 Sep. 1984
A. Wirth and R. Ruquist Sep. 1984 110 p
(Contract F19628-82-C-0035)
(AD-A155434; AFGL-TR-84-0262) Avail: NTIS HC A06/MF A01 CSCL 03/1

The problem of imaging the solar surface is considered. A theoretical study is presented that indicates that traditional adaptive optic techniques are of limited usefulness for solar imaging. A new method for adaptive optic image sharpening for extended sources is described. The incoming wavefront has added to it controlled amounts of various aberrations. The image quality is sensed and an error signal derived that allows iterative corrections to the wavefront to be determined. The measure of the image quality that is used is an integrated power spectrum of the image plane distribution. It is shown that quantity is maximized for an unaberrated input wave. Results sharpen under conditions of moderately severe turbulence. GRA

N85-33102# Air Force Geophysics Lab., Hanscom AFB, Mass.
SEARCH FOR THE NORTH-SOUTH ASYMMETRY IN SOLAR ACTIVITY Interim Report
M. A. Shea and D. F. Smart 3 Jun. 1985 7 p
(AD-A155525; AFGL-TR-85-0119) Avail: NTIS HC A02/MF A01 CSCL 03/2

The use of the comprehensive flare index as a possible indicator of north-south asymmetry in solar activity is investigated. Using a data base extending from 1955 through 1980 we discuss several of the problems that were encountered in using this index as an indicator of possible north-south asymmetry in solar activity. Preliminary results indicate that even allowing for the large number of major flares for which the location on the Sun was decidedly more active than the Southern Hemisphere for the period 1959 through 1970. GRA

N85-33052*# California Inst. of Tech., Pasadena.
PRECISION MEASUREMENTS OF SOLAR ENERGETIC PARTICLE ELEMENTAL COMPOSITION
H. Breneman and E. C. Stone *In its* Contrib. to the 19th Intern. Cosmic Ray Conf. 1985 4 p refs (For primary document see N85-33044 21-88)
(Contract NAS7-918; Grant NGR-05-002-160)
(Paper-SH-2.1-4) Avail: NTIS HC A03/MF A01 CSCL 03B

N85-33053*# California Inst. of Tech., Pasadena.
SOLAR CORONAL AND PHOTOSPHERIC ABUNDANCES FROM SOLAR ENERGETIC PARTICLE MEASUREMENTS
H. Breneman and E. C. Stone *In its* Contrib. to the 19th Intern. Cosmic Ray Conf. 1985 4 p refs (For primary document see N85-33044 21-88)
(Contract NAS7-918; Grant NGR-05-002-160)
(Paper-SH-2.1-5) Avail: NTIS HC A03/MF A01 CSCL 03B

93 SPACE RADIATION

Includes cosmic radiation; and inner and outer Earth's radiation belts.

For biological effects of radiation see *52 Aerospace Medicine*. For theory see *73 Nuclear and High-Energy Physics*.

N85-33103*# California Inst. of Tech., Pasadena. Space Radiation Lab.
RESEARCH IN PARTICLES AND FIELDS Semiannual Status Report, 1 Apr. 1984 - 31 Mar. 1985
E. C. Stone, L. Davis, Jr., R. A. Mewaldt, and T. A. Prince 31 Mar. 1985 42 p refs
(Grant NGR-05-002-160)
(NASA-CR-176069; NAS 1.26:176069) Avail: NTIS HC A02/MF A01 CSCL 03B

Research activities in Cosmic Rays Gamma Rays, and Astrophysical Plasmas are covered The investigation of the astrophysical aspects of cosmic rays and gamma rays and of the radiation and electromagnetic field environment of the Earth and other planets are studied. These investigations are carried ut by means of energetic particle and photon detector systems flown on spacecraft and balloons. The emphasis is on precision measurements with high resolution in charge mass and energy. An extensive bibliography is given. Author

N85-33045*# California Inst. of Tech., Pasadena.
COSMIC RAY He3 MEASUREMENTS
R. A. Mewaldt *In its* Contrib. to the 19th Intern. Cosmic Ray Conf. 1985 4 p refs (For primary document see N85-33044 21-88)
(Paper-OG-4.2-3) Avail: NTIS HC A03/MF A01 CSCL 03B

N85-33046*# California Inst. of Tech., Pasadena.
INITIAL RESULTS FROM THE CALTECH/DSRI BALLOON-BORNE ISOTOPE EXPERIMENT
S. M. Schindler, A. Buffingtan (California Univ., San Diego), E. C. Christian, J. E. Grove, K. H. Lau, E. C. Stone, I. L. Rasmussen (Danish Space Research Inst.), and S. Laursen (Danish Space Research Inst.) *In its* Contrib. to the 19th Intern. Cosmic Ray Conf. 1985 4 p refs (For primary document see N85-33044 21-88)
(Grant NGR-05-006-160)
(Paper-OG-4.3-8) Avail: NTIS HC A03/MF A01 CSCL 03B

N85-33047*# California Inst. of Tech., Pasadena.
MEASUREMENTS OF Fe AND Ar FRAGMENTATION CROSS SECTIONS
K. H. Lau, R. A. Mewaldt, and E. C. Stone *In its* Contrib. to the 19th Intern. Cosmic Ray Conf. 1985 4 p refs (For primary document see N85-33044 21-88)
(Contract NAS5-28449; Grant NGR-05-002-160)
(Paper-OG-7.2-20) Avail: NTIS HC A03/MF A01 CSCL 03B

N85-33055*# National Aeronautics and Space Administration. Goddard Space Flight Center, Greenbelt, Md.
DIFFERENTIAL MEASUREMENT OF COSMIC-RAY GRADIENT WITH RESPECT TO INTERPLANETARY CURRENT SHEET
S. P. Christon (California Inst. of Tech., Pasadena), A. C. Cummings (California Inst. of Tech., Pasadena), E. C. Stone (California Inst. of Tech., Pasadena), K. W. Behannon, and L. F. Burlaga *In* California Inst. of Tech. Contrib. to the 19th Intern. Cosmic Ray Conf. 1985 4 p refs Sponsored in cooperation with JPL (For primary document see N85-33044 21-88)
(Grant NGR-05-002-160)
(Paper-SH-4.2-9) Avail: NTIS HC A03/MF A01 CSCL 03B

N85-33056*# California Inst. of Tech., Pasadena.
CHANGES IN THE ENERGY SPECTRUM OF ANOMALOUS OXYGEN AND HELIUM DURING 1977 - 1985
A. C. Cummings, E. C. Stone, and W. R. Webber (New Hampshire Univ., Durham) *In its* Contrib. to the 19th Intern. Cosmic Ray Conf. 1985 4 p refs (For primary document see N85-33044 21-88)
(Contract NAS7-918; Grant NGR-05-002-160)
(Paper-SH-4.6-1) Avail: NTIS HC A03/MF A01 CSCL 03B

N85-33057*# California Inst. of Tech., Pasadena.
SOLAR CYCLE VARIATIONS OF THE ANOMALOUS COSMIC RAY COMPONENT Abstract Only
R. A. Mewaldt and E. C. Stone *In its* Contrib. to the 19th Intern. Cosmic Ray Conf. 1985 1 p (For primary document see N85-33044 21-88)
(Contracts NAS5-28441; NAS5-28449; Grant NGR-05-002-160)
(Paper-SH-4.6-2) Avail: NTIS HC A03/MF A01 CSCL 03B

N85-33058*# New Hampshire Univ., Durham.
RADIAL AND LATITUDINAL GRADIENTS OF ANOMALOUS OXYGEN DURING 1977 - 1985
W. R. Webber, A. C. Cummings (California Inst. of Tech., Pasadena), and E. C. Stone *In* California Inst. of Tech. Contrib. to the 19th

Intern. Cosmic Ray Conf. 1985 4 p refs (For primary document see N85-33044 21-88)
(Contract NAS7-918; Grant NGR-05-002-160)
(Paper-SH-4.6-4) Avail: NTIS HC A03/MF A01 CSCL 03B

N85-33059*# California Inst. of Tech., Pasadena.
SOLAR MODULATION AND INTERPLANETARY GRADIENTS OF THE GALACTIC ELECTRON FLUX, 1977 - 1984 Abstract Only
S. P. Christon, A. C. Cummings, E. C. Stone, and W. R. Webber (New Hampshire Univ., Durham) *In its* Contrib. to the 19th Intern. Cosmic Ray Conf. 1985 1 p refs (For primary document see N85-33044 21-88)
(Contract NAS7-918; Grant NGR-05-002-160)
(Paper-SH-4.7-4) Avail: NTIS HC A03/MF A01 CSCL 03B

99 GENERAL

No abstracts in this category.

SUBJECT INDEX

Typical Subject Index Listing

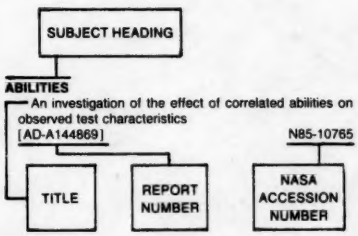

The subject heading is the key to the subject content of the document. Titles, report numbers, and accession numbers of pertinent documents are provided under each subject heading. When the title is insufficiently descriptive of the document content, a title extension has been added, separated from the title by three hyphens. The report number helps to indicate the type of document cited (e.g., NASA report, NASA translation, NASA contractor report). The NASA accession number is the number by which the document abstracts are arranged in this journal and by which the document is sold or requested. The titles, with title extensions if present, are arranged under each subject heading in ascending accession number order. The subject headings have been selected from the latest revision of the *NASA Thesaurus* (NASA SP-7051).

A

ABERRATION
Theoretical modeling of laser induced optical degradation
[AD-A155302] N85-32323
New method for correcting chromatism of mirror-lens objectives N85-32965
ABRASIVES
The effect of abrasive blasting on the fatigue and corrosion of an aluminium-copper alloy
[AD-A154954] N85-32182
ABSORBERS (MATERIALS)
Choice of optimum saturating absorber for YAG passive mode-locking laser N85-32893
ABSORPTION
Quasi-steady-state melting mode during combined laser irradiation of semiconductor materials N85-32874
ABSORPTION CROSS SECTIONS
Absorption of 10.6 micrometer laser radiation in electron-hole condensate in germanium N85-32870
An attempt to detect induced neutron capture in laser radiation field N85-32928
ABSORPTION SPECTRA
Doppler spectrometer for measuring narrow photochemical gaps in inhomogeneously broadened spectra N85-32921
ABSORPTIVITY
Variability of rural aerosols under stable weather conditions N85-32663
Absorption of laser radiation in substance with absorption coefficient depending linearly upon temperature N85-32953
Coefficient of optical absorption and scattered light capture effect N85-32959
ACCELERATED LIFE TESTS
Understanding and laboratory prediction of the atmospheric corrosion behavior of steels and of non-ferrous metals and alloys
[AD-A154642] N85-32179
High temperature electronics technology: Life test report
[AD-A154681] N85-32257
Accelerated stress factors and failure/degradation mechanisms in terrestrial solar cells N85-32451
ACCELERATION TOLERANCE
Analysis of the transient response of temporal artery blood flow data relative to various anti-G suit pressure schedules
[AD-A155242] N85-32775
ACCELEROMETERS
Application of satellite accelerometer data to improve density models
[AD-A154904] N85-32558
ACCIDENTS
Hazardous air pollutants
[GPO-43-064] N85-32458
ACCURACY
Accuracy and operational use of medium and extended range numerical atmospheric forecasts: A review
[AD-A155027] N85-32579
Medium range atmospheric forecast system: Evaluation report
[AD-A155240] N85-32589
Resource allocation in cerebral specialization of function: Behavioral and electrophysiological studies
[AD-A155092] N85-32759
ACIDITY
Granulometric study of the acidity and sulfate excess in marine aerosols N85-32691
ACOUSTIC ATTENUATION
Overground Excess Sound Attenuation (ESA). Volume 3: Application of ESA data in NOISEFILE
[AD-A154820] N85-32984
Lateral attenuation of aircraft flight noise
[AD-A154958] N85-32986
ACOUSTIC EXCITATION
Acoustic radiation from concentric shells containing an inner fluid
[AD-A155476] N85-32991
ACOUSTIC MEASUREMENT
Ultrasonic position reference systems for an autonomous sentry robot and a robot manipulator arm
[AD-A155481] N85-32336
FAA/GAMA (Federal Aviation Administration/General Aviation Manufacturer's Association) propeller aircraft noise test program, Salina Municipal Airport, Salina, Kansas
[AD-A154818] N85-32983
ACOUSTIC MICROSCOPES
Reliability of void detection in structural ceramics using scanning laser acoustic microscopy
[NASA-TM-87035] N85-32337
ACOUSTIC PROPAGATION
Microwave SAW (Surface Acoustic Wave) monochromator
[AD-D011718] N85-32311
ACOUSTIC SCATTERING
Toward the theory of acoustic scattering on uneven free surface N85-32862
Understanding coherence losses incurred by bottom-retained signals
[AD-A155559] N85-32992
ACOUSTIC VELOCITY
Trailing edge flow and aerodynamic sound. Part 1: Tonal pressure and velocity fluctuations. Part 2: Random pressure and velocity fluctuations
[AD-A154947] N85-32097
Toward the propagation of waves in unsteady media N85-32881
ACOUSTICS
USSR report: Physics and mathematics
[JPRS-UPM-85-004] N85-32860
Lateral attenuation of aircraft flight noise
[AD-A154958] N85-32986
ACOUSTO-OPTICS
The sound field of a moving laser-induced acoustic array (theory)
[AD-A154553] N85-32981
ACTIVATION
CO adsorption on (111) and (100) surfaces of the Pt sub 3 Ti alloy. Evidence for parallel binding and strong activation of CO
[NASA-CR-176077] N85-32176
A simple model to investigate the activation process in waterclouds N85-32675
Measurements of the critical supersaturation of 0.029 to 0.035 micron radius particles at Washington, District of Columbia N85-32676
Fog activation and supersaturation N85-32678
Luminescence and absorption of indium-activated potassium-borate glasses subjected to high-power excitation N85-32868
ACTIVATION ANALYSIS
Study of proton and neutron activation of metal samples in low Earth orbit
[NASA-CR-171596] N85-32130
ACTIVATION ENERGY
Thermoelectric properties of beta-boron and some boron compounds
[DE85-011978] N85-32270
Activation analysis of natural water using neutrons of various energies N85-32924
ACTIVITY (BIOLOGY)
Sulfur Cycle N85-32748
ACTUATORS
Comparison of the response of shape memory alloy actuators using air-cooling and water-cooling
[AD-A155216] N85-32185
ADAPTIVE FILTERS
Application of adaptive noise cancellation to Coast Guard voice communications
[AD-A154798] N85-32230
ADAPTIVE OPTICS
Solar adaptive optics
[AD-A155434] N85-33101
ADDITIVES
The effect of alloy additions on superplasticity in thermomechanically processed high magnesium aluminum-magnesium alloys
[AD-A155142] N85-32184
Z-contrast imaging and electron channeling analysis of dopants in semiconductors
[DE85-011410] N85-32269
Thermoelectric properties of beta-boron and some boron compounds
[DE85-011978] N85-32270
Injection of drag reducing additives into turbulent water flows: Two-component velocity measurements and mixing length model predictions
[AD-A154604] N85-32274
ADHESION TESTS
A study of adherent oxide scales
[AD-A155554] N85-32188
ADHESIVE BONDING
Improved materials for composites and adhesive joints
[AD-A154918] N85-32152
Improved materials for composite and adhesive joints
[AD-A155065] N85-32153
Experimental and theoretical assessment of a new technique for the non-destructive evaluation of laminated panels
[AD-A155622] N85-32155
Molecular orbital studies in oxidation: Sulfate formation and metal-metal oxide adhesion
[NASA-CR-176070] N85-32174
A cracked orthotropic sheet stiffened by a semi-infinite orthotropic sheet
[NASA-TP-2455] N85-32339
ADHESIVES
Influence of the resin on interlaminar mixed-mode fracture
[NASA-TM-87571] N85-32150
ADIABATIC CONDITIONS
Diagnostics of severe convection and subsynoptic scale ageostrophic circulations
[NASA-CR-171581] N85-32571
ADMIXTURES
Influence of background electrically neutral argon admixture on mechanical strength of silicon crystals N85-32878

ADSORPTION
Adsorption of O2, SO2, and SO3 on nickel oxide. Mechanism for sulfate formation
[NASA-CR-176072] N85-32175
CO adsorption on (111) and (100) surfaces of the Pt sub 3 Ti alloy. Evidence for parallel binding and strong activation of CO
[NASA-CR-176077] N85-32176
Cloud condensation on insoluble particles N85-32670

ADVECTION
A multilevel-multigrid method for recirculating flows N85-32271
Mesoscale features and atmospheric refraction conditions of the Arctic marginal ice zone
[AD-A155139] N85-32584

AERIAL EXPLOSIONS
Explosion in flight N85-32883

AERIAL PHOTOGRAPHY
Handbook for obtaining and using aerial photography to map aquatic plant distribution
[AD-A154584] N85-32388
Coastal erosion along Monterey Bay
[AD-A155610] N85-32707

AERIAL RECONNAISSANCE
Electronic reconnaissance aircraft of the Soviet Union Navy
[AD-A154706] N85-32091

AEROBES
Aerobic sulfur-oxidizing bacteria: Environmental selection and diversification N85-32712
Distribution and abundance of organic thiols N85-32717

AERODYNAMIC BALANCE
Recent developments in rotary-balance testing of fighter aircraft configurations at NASA Ames Research Center
[NASA-TM-86714] N85-32090

AERODYNAMIC CHARACTERISTICS
Quest for performance: The evolution of modern aircraft
[NASA-SP-468] N85-32089
Trailing edge flow and aerodynamic sound. Part 1: Tonal pressure and velocity fluctuations. Part 2: Random pressure and velocity fluctuations
[AD-A154947] N85-32097
Flight control system for a computer controlled aircraft with limited sensors
[AD-A155107] N85-32115

AERODYNAMIC CONFIGURATIONS
Recent developments in rotary-balance testing of fighter aircraft configurations at NASA Ames Research Center
[NASA-TM-86714] N85-32090
Wind tunnel drag evaluations of helicopter nose sections
[AD-A155489] N85-32100
Study of an efficient long-range Mach 2.7 supersonic transport configuration concept
[NASA-TM-86414] N85-32110

AERODYNAMIC DRAG
Wind tunnel drag evaluations of helicopter nose sections
[AD-A155489] N85-32100

AERODYNAMIC LOADS
Flight control system for a computer controlled aircraft with limited sensors
[AD-A155107] N85-32115

AERODYNAMIC NOISE
Trailing edge flow and aerodynamic sound. Part 1: Tonal pressure and velocity fluctuations. Part 2: Random pressure and velocity fluctuations
[AD-A154947] N85-32097

AERODYNAMIC STABILITY
Aerodynamic characteristics of the standard dynamics model in coning motion at Mach 0.6
[NASA-TM-86717] N85-32094

AERONAUTICAL ENGINEERING
The Naval Postgraduate School Flight Mechanics Laboratory: A feasibility study
[AD-A154578] N85-32127
DYNA3D, INGRID, and TAURUS: An integrated, interactive software system for crashworthiness engineering
[DE85-010928] N85-32846

AERONOMY
Equitorial scintillations: Advances since ISEA-6
[AD-A154962] N85-32559
Activities report of the Aeronomy Department
[G-774-1984] N85-32569

AEROSOLS
Aerosol analysis and emission spectrometry with free jets
[DE85-010576] N85-32168
Silicon production in an aerosol reactor N85-32416
Data analysis for lidar and quartz crystal microbalance systems
[NASA-CR-172601] N85-32464
Nuclear thermal transmittance in the atmosphere using LOWTRAN-6 computer code
[AD-A154669] N85-32553
Absorption and scattering properties of aerosols of aggregated particles in the infrared spectral region
[AD-A155475] N85-32591
Eleventh International Conference on Atmospheric Aerosols, Condensation and Ice Nuclei, volume 2
[PB85-182418] N85-32596
Mechanism of heterogeneous deposition ice nucleation near water-saturation N85-32597
Inactivation of silver iodide by atmospheric nucleation inhibitors N85-32599
Ice nucleation by silver iodine particles with nearly critical sizes N85-32600
Photoinduced active sites on ice nucleating aerosol of silver iodide N85-32601
Experimental investigation of properties of ice-forming reagents N85-32602
The effect of supersaturation, temperature and particle size on ice-nucleating ability of atmospheric aerosol N85-32604
Ice crystal nucleation on hygroscopic aerosols N85-32605
On the efficiency of the mechanism of ice particles formation in the vapor supersaturation field around a freezing droplet N85-32606
Generation of lead, lead iodide and iodide aerosols and their ice nucleation N85-32607
Aircraft observations of condensation and ice nuclei at a tropical station N85-32613
A statistical analysis of ice nuclei concentrations at urban and rural sites in Valladolid, Spain N85-32614
Supersaturation spect A of Ice Nuclei at different locations in Europe and over the North-Atlantic N85-32615
The capture of ice nucleating and non ice-nucleating aerosols by ice phase precipitation N85-32620
The 100 years of Aitken Nuclei (AN) study-reminiscence, current and future problems N85-32621
Properties of aerosol particles detected by satellites in coastal regions N85-32622
Multi-channel electric aerosol spectrometer N85-32623
Supersaturation obtained in a condensation nucleus counter N85-32624
The investigation of natural and artificial ice nuclei by the improved membrane filter method N85-32626
Stable generation of highly monodisperse aerosols N85-32628
Eleventh International Conference on Atmospheric Aerosols, Condensation and Ice Nuclei, volume 1
[PB85-182400] N85-32636
Photochemical aerosol formation in polluted atmosphere N85-32642
The influence of Brownian coagulation on the size distributions of atmospheric aerosols N85-32643
A study of time transformation of natural photochemical aerosols N85-32644
A new hypothesis for the observed vertical distribution of atmospheric aerosols N85-32646
On the mechanisms responsible for the formation of typical size spectra and vertical distribution of tropospheric aerosol particles N85-32647
On the transformation regularities of time series of solid aerosol concentrations in the surface atmospheric layer N85-32648
Our knowledge about the atmospheric aerosol N85-32650
Characteristics of aerosol composition in a nonurban area, north China N85-32651
Trace element concentrations in atmospheric aerosol over Hungary N85-32652
Chemical composition of atmospheric aerosol at Delhi N85-32653
Mineral aerosols and source identification N85-32654
Physical and chemical aerosol characteristics in extremely clean air masses at Cape Grim, Tasmania N85-32655
Aitken particle size distribution in Antarctica N85-32656
Airborne measurements of the vertical distribution of Arctic haze N85-32657
Condensation nuclei and aerosol size distribution measurements in Arctic haze N85-32658
Aircraft investigations of the distribution of aerosols in the lower troposphere N85-32659
The variability of aerosol microstructure in continental and oceanic surface layers of the atmosphere in anticyclones N85-32660
Variation of the submicron aerosol structure N85-32661
Some considerations about the natural atmospheric radioactive aerosol N85-32662
Variability of rural aerosols under stable weather conditions N85-32663
Marine aerosols at the Dutch North Sea coast: Size distributions and fractionation of trace elements N85-32664
Application of Particle Induced X-ray Emission analysis (PIXE) to aerosol long range transport studies N85-32665
Scavenging of submicron aerosol particles by snow crystals: Theory and experiments N85-32667
A probabilistic method for particle size analysis of aerosols N85-32669
Cloud condensation on insoluble particles N85-32670
Observations of cloud droplets, aerosol particles and cloud condensation nuclei in continental air masses N85-32671
Condensation properties of atmospheric aerosol N85-32672
Investigation of the formation of cloud particle spectrum on natural condensation nuclei N85-32674
A simple model to investigate the activation process in waterclouds N85-32675
Measurements of the critical supersaturation of 0.029 to 0.035 micron radius particles at Washington, District of Columbia N85-32676
On the question to the effect of surfactants on the spectrum of cloud drops in the process of their condensation growth N85-32679
Influence on an industrial site on the characteristics of CCN supersaturation with air masses of different origin N85-32683
Theoretical studies of structure and stability of hydrates of atmospheric sulfur species N85-32684
A review on the formation of aerosol particles in the atmosphere N85-32687
Aerosol formation by wave action over Ross Sea, Antartica N85-32688
An electron microscopic study of urban aerosol N85-32689
Sulfates in marine aerosols over the tropical Western Pacific Ocean N85-32690
Granulometric study of the acidity and sulfate excess in marine aerosols N85-32691
Variations of particulate sulfur concentrations in a coastal atmospheric environment in connection with the change of air masses origin N85-32692
Characterization of insoluble particles associated with cloud droplets N85-32693
The measured rate of condensation nucleation to droplets using the techniques of chemical kinetics N85-32694

AEROSPACE MEDICINE
USSR Space Life Sciences Digest
[NASA-CR-3922] N85-32709
USSR report: Life sciences. Biomedical and behavioral sciences
[JPRS-UBB-85-020] N85-32752
Remote medical diagnosis N85-32753
Aerospace medicine and biology: A continuing bibliography with indexes, supplement 273
[NASA-SP-7011(273)] N85-32755
Air force technical objective document, Aerospace Medical Division, Fiscal Year 1986
[AD-A155195] N85-32762

AEROSPACE SAFETY
Space Station crew safety alternatives study. Volume 2: Threat development
[NASA-CR-3855] N85-32133

AEROSPACE SYSTEMS
Robust control of multivariable and large space systems
[AD-A155117] N85-32140

AEROSPACE TECHNOLOGY TRANSFER
USSR report: Life sciences. Biomedical and behavioral sciences
[JPRS-UBB-85-020] N85-32752

AGING (MATERIALS)
Hot isostatically pressed Sm(2)(TM)17 magnets
[AD-A155479] N85-32267

AIR
Supersaturation obtained in a condensation nucleus counter N85-32624

AIR BREATHING ENGINES
Status of boron combustion research
[AD-A154762] N85-32160

AIR CONDITIONING EQUIPMENT
The influence of oil contamination on the nucleate pool-boiling behavior of R-114 from a structured surface
[AD-A155609] N85-32284

AIR COOLING
Comparison of the response of shape memory alloy actuators using air-cooling and water-cooling
[AD-A155216] N85-32185

AIR FILTERS
The investigation of natural and artificial ice nuclei by the improved membrane filter method N85-32626
AIR FLOW
Mesoscale features and atmospheric refraction conditions of the Arctic marginal ice zone [AD-A155139] N85-32584
AIR MASSES
A statistical analysis of ice nuclei concentrations at urban and rural sites in Valladolid, Spain N85-32614
Observations of cloud droplets, aerosol particles and cloud condensation nuclei in continental air masses N85-32671
Variations of particulate sulfur concentrations in a coastal atmospheric environment in connection with the change of air masses origin N85-32692
AIR POLLUTION
Hazardous air pollutants [GPO-43-064] N85-32458
VALMET: A valley air pollution model [DE85-010820] N85-32463
Eleventh International Conference on Atmospheric Aerosols, Condensation and Ice Nuclei, volume 2 [PB85-182418] N85-32596
Observations of the atmospheric ice nucleus at northwest China N85-32618
Photochemical aerosol formation in polluted atmosphere N85-32642
Human activity and production rate of secondary nuclei N85-32645
Characteristics of aerosol composition in a nonurban area, north China N85-32651
Trace element concentrations in atmospheric aerosol over Hungary N85-32652
Physical and chemical aerosol characteristics in extremely clean air masses at Cape Grim, Tasmania N85-32655
Condensation nuclei and aerosol size distribution measurements in Arctic haze N85-32658
Some considerations about the natural atmospheric radioactive aerosol N85-32662
Influence on an industrial site on the characteristics of CCN supersaturation with air masses of different origin N85-32683
Variations of particulate sulfur concentrations in a coastal atmospheric environment in connection with the change of air masses origin N85-32692
on the transport of large condensation nuclei in the atmosphere at various altitudes over the territory of the USSR N85-32698
Laser Elektronika-01 for air pollution control lidar N85-32887
AIR TRAFFIC CONTROL
Simulation studies of time-control procedures for the advanced air traffic control system [NASA-TP-2493] N85-32101
Status of the air traffic control system [GPO-40-343] N85-32107
AIR TRAFFIC CONTROLLERS (PERSONNEL)
Status of the air traffic control system [GPO-40-343] N85-32107
AIR TRANSPORTATION
Aviation system delays [S-HRG-98-1241] N85-32102
AIR WATER INTERACTIONS
Mesoscale features and atmospheric refraction conditions of the Arctic marginal ice zone [AD-A155139] N85-32584
Bacterial ice nuclei of marine origin: Some recent observations N85-32611
Properties of aerosol particles detected by satellites in coastal regions N85-32622
Numerical simulations of the response of intense ocean currents to atmospheric forcing [AD-A155161] N85-32704
Simulation of the coupled atmospheric and oceanic boundary layer model during MILDEX [AD-A155166] N85-32705
AIRBORNE/SPACEBORNE COMPUTERS
Comparative study on data system architectures --- spacecraft data processing [ESA-CR(P)-2015] N85-32628
AIRCRAFT ACCIDENTS
DYNA3D, INGRID, and TAURUS: An integrated, interactive software system for crashworthiness engineering [DE85-010928] N85-32846
AIRCRAFT COMPARTMENTS
The role of aircraft panel materials in cabin fires and their properties [FAA-CT-84-30] N85-32104
AIRCRAFT CONFIGURATIONS
Quest for performance: The evolution of modern aircraft [NASA-SP-468] N85-32089
AIRCRAFT CONTROL
Seat experiments for the full-scale transport aircraft controlled impact demonstration [AD-A155024] N85-32106
Flight control system for a computer controlled aircraft with limited sensors [AD-A155107] N85-32115
AIRCRAFT DESIGN
Preliminary sizing and performance of aircraft [NASA-TM-86357] N85-32111
Design of an expert-system flight status monitor [NASA-TM-86739] N85-32794
AIRCRAFT ENGINES
Component-specific modeling [NASA-CR-174925] N85-32119
AIRCRAFT EQUIPMENT
Simulation studies of time-control procedures for the advanced air traffic control system [NASA-TP-2493] N85-32101
AIRCRAFT FUELS
Observations of the use of the setapoint detector [AD-A154533] N85-32208
AIRCRAFT GUIDANCE
Simulation studies of time-control procedures for the advanced air traffic control system [NASA-TP-2493] N85-32101
AIRCRAFT MODELS
Development and validation of a general purpose linearization program for rigid aircraft models [NASA-TM-86737] N85-32122
AIRCRAFT NOISE
FAA/GAMA (Federal Aviation Administration/General Aviation Manufacturer's Association) propeller aircraft noise test program, Salina Municipal Airport, Salina, Kansas [AD-A154818] N85-32983
Overground Excess Sound Attenuation (ESA). Volume 3: Application of ESA data in NOISEFILE [AD-A154820] N85-32984
Helicopter noise survey for selected cities in the contiguous US [AD-A154893] N85-32985
Lateral attenuation of aircraft flight noise [AD-A154958] N85-32986
AIRCRAFT SAFETY
The role of aircraft panel materials in cabin fires and their properties [FAA-CT-84-30] N85-32104
AIRCRAFT STRUCTURES
Quest for performance: The evolution of modern aircraft [NASA-SP-468] N85-32089
Preliminary sizing and performance of aircraft [NASA-TM-86357] N85-32111
AIRFOILS
An evaluation of four methods of numerical analysis for two-dimensional airfoil flows [AD-A155202] N85-32098
AIRGLOW
SCRIBE data of October 23, 1983 flight [AD-A154864] N85-33012
AIRPORT PLANNING
Aviation system delays [S-HRG-98-1241] N85-32102
AITKEN NUCLEI
Eleventh International Conference on Atmospheric Aerosols, Condensation and Ice Nuclei, volume 2 [PB85-182418] N85-32596
Inactivation of silver iodide by atmospheric nucleation inhibitors N85-32599
Ice nucleus measurements N85-32609
The 100 years of Aitken Nuclei (AN) study-reminiscence, current and future problems N85-32621
Analysis of performance of dynamic thermal diffusion chamber N85-32625
Eleventh International Conference on Atmospheric Aerosols, Condensation and Ice Nuclei, volume 1 [PB85-182400] N85-32636
The first condensation nucleus conference N85-32637
Study of the formation of particles from natural hydrocarbons released by vegetation N85-32640
Experimental studies of the formation of Aitken nuclei in the atmosphere N85-32641
Human activity and production rate of secondary nuclei N85-32645
Aitken particle size distribution in Antarctica N85-32656
Properties of forest derived cloud condensation nuclei N85-32682
The nuclei of cloud formation N85-32685
Transport and formation of summertime cloud condensation nuclei over the Arctic Ocean N85-32686
A review on the formation of aerosol particles in the atmosphere N85-32687
The interaction of polynuclear aromatic hydrocarbons PAH's with water vapor and their role as condensation nuclei in the formation of haze and fog N85-32695
Applicability of surface CCN measurements N85-32696
on the transport of large condensation nuclei in the atmosphere at various altitudes over the territory of the USSR N85-32698
ALBEDO
Earth Albedo and the orbit of LAGEOS [NASA-TM-86210] N85-32131
ALCOHOLS
Phase behavior and QLS (Quasielastic Light Scattering) in potassium linoleate/n-alkanol microemulsions [AD-A155028] N85-32163
ALGAE
The role of sulfur in osmoregulation and salinity tolerance in cyanobacteria, algae, and plants N85-32736
ALGEBRA
A cracked orthotropic sheet stiffened by a semi-infinite orthotropic sheet [NASA-TP-2455] N85-32339
ALGORITHMS
Globally-asynchronous locally-synchronous systems [AD-A154624] N85-32222
Routing algorithms and stochastic analysis for large communications networks [AD-A154654] N85-32225
A multilevel-multigrid method for recirculating flows N85-32271
Non-model based estimation with applications to sensor calibration using multiple sensors [AD-A154736] N85-32306
Emergency modeling of hazardous air pollutants [AD-A155441] N85-32461
Practical use of a tropopause height determination algorithm on an MST radar data set, part 1.8B N85-32479
Criteria and algorithms for spectrum parameterization of MST radar signals N85-32527
Automated cell detection as a mesocyclone precursor tool [AD-A154952] N85-32577
Real-time automated detection of mesocyclones and tornado vortex signatures [AD-A154968] N85-32578
Consensus in the presence of partial synchrony (Preliminary version) [AD-A154705] N85-32799
SIGMA - A stochastic-integration global minimization algorithm [AD-A154878] N85-32806
A comparison and analysis of Vintr's global routing algorithm with the Lee routing algorithm in two-layer printed circuit boards [AD-A155600] N85-32816
A practical approach to Karmarkar's algorithm [AD-A155714] N85-32818
Evaluation and implementation of a functional microprogram generator [AD-A155164] N85-32823
Broadcasting topology and routing information in computer networks [AD-A155668] N85-32827
On the dependence of the convergence of Gummel's algorithm on the regularity of the solution [AD-A154628] N85-32832
A new fault-tolerant algorithm for clock synchronization [AD-A154771] N85-32836
A vectorized nearest-neighbors algorithm of order N using a monotonic logical grid [AD-A155169] N85-32853
Poisson formula for radon transformation and numerical image reconstruction algorithm N85-32973
ALKANES
Phase behavior and QLS (Quasielastic Light Scattering) in potassium linoleate/n-alkanol microemulsions [AD-A155028] N85-32163
ALLOYS
Results of an interlaboratory fatigue test program conducted on alloy 800H at room and elevated temperatures [NASA-CR-174940] N85-32340
ALPHA DECAY
Production of stable embryo particles in dense ion tracks of alpha particle emissions in the atmosphere N85-32638
ALPHA PARTICLES
Production of stable embryo particles in dense ion tracks of alpha particle emissions in the atmosphere N85-32638
ALTERNATING CURRENT
Tailored vacuum chambers for ac magnets [DE85-010767] N85-32319

ALTIMETERS
Global geoid and gravity anomaly predictions using the collocation and point mass techniques
[AD-A154517] N85-32387
ALTITUDE
Comparison of tropopause altitude determination by the Platteville Radar, Sunset Radar and the NWS Rawinsonde N85-32477
Observations of mesospheric turbulence by rocket probe and VHF radar, part 2.4A N85-32484
ALUMINUM
Thermoelectric properties of beta-boron and some boron compounds
[DE85-011978] N85-32270
Plasma mass and effective inductance in a small railgun
[AD-A154644] N85-32304
Laser beam interactions with vapor plumes during Nd:YAG laser welding on aluminum
[DE85-009793] N85-32328
ALUMINUM ALLOYS
Understanding and laboratory prediction of the atmospheric corrosion behavior of steels and of non-ferrous metals and alloys
[AD-A154642] N85-32179
The effect of abrasive blasting on the fatigue and corrosion of an aluminium-copper alloy
[AD-A154954] N85-32182
The effect of alloy additions on superplasticity in thermomechanically processed high magnesium aluminum-magnesium alloys
[AD-A155142] N85-32184
ALUMINUM OXIDES
Improved materials for composite and adhesive joints
[AD-A155065] N85-32153
The Faraday effect in ruby and corundum in strong magnetic fields N85-32967
AMBIENT TEMPERATURE
Results of an interlaboratory fatigue test program conducted on alloy 800H at room and elevated temperatures
[NASA-CR-174940] N85-32340
Improved Nominal Operating Cell Temperature (NOCT) test procedure N85-32449
AMINO ACIDS
Remarks on preparation of indandione detection reagents
[NASA-TM-77905] N85-32146
Cytochromes and iron sulfur proteins in sulfur metabolism of phototrophic bacteria N85-32718
AMMONIA
Facility for large-scale hazardous gas testing
[DE85-011852] N85-32169
AMORPHOUS MATERIALS
Amorphous metallic films in silicon metallization systems N85-32427
Mirror reflection of charged particles from + amorphous and polycrystalline surfaces N85-32927
The development and evaluation of point defect models for the growth of passive films on single crystal, polycrystalline, and amorphous metal surfaces
[AD-A154685] N85-33023
AMORPHOUS SEMICONDUCTORS
Defects in tetrahedrally coordinated amorphous semiconductors
[AD-A155150] N85-32263
Thin-film reliability and engineering overview N85-32450
Raman scattering studies in solids
[AD-A155528] N85-33032
AMPLIFICATION
Fin-line horn antennas
[AD-A154597] N85-32255
AMPLITUDE MODULATION
A sampling phasemeter design for pulsed continuous wave signals
[AD-A155237] N85-32264
AMPLITUDES
Huffman-coded pulse compression waveforms
[AD-A155322] N85-32243
ANAEROBES
Anaerobic reduction of elemental sulfur by Chromatium vinosum and Beggiatoa alba N85-32739
ANALOG DATA
Development of a dedicated speech work station
[AD-A155465] N85-32824
Solid state research
[AD-A154783] N85-33025
ANALOG TO DIGITAL CONVERTERS
R, L, C, G measurement N85-32784
Development of a dedicated speech work station
[AD-A155465] N85-32824
ANALYSIS (MATHEMATICS)
USSR report: Physics and mathematics
[JPRS-UPM-85-004] N85-32860
ANALYTICAL CHEMISTRY
The determination of dinitrotoluene in single base propellants
[AD-A154672] N85-32209
Marine environmental quality assessment program, five-year plan (FY 1984 - 1988)
[AD-A154715] N85-32459
ANALYZERS
Possiblity of developing charged-particle energy analyzer based on hyperboloidal axisymmetrical lens N85-32933
ANESTHETICS
Studies of circulatory and metabolic changes during ketamine narcosis
[AD-A154512] N85-32756
ANGLE OF ATTACK
Recent developments in rotary-balance testing of fighter aircraft configurations at NASA Ames Research Center
[NASA-TM-86714] N85-32090
Aerodynamic characteristics of the standard dynamics model in coning motion at Mach 0.6
[NASA-TM-86717] N85-32094
Numerical solutions of turbulent models for flow over a flat plate with angle of attack
[DE85-010380] N85-32286
ANGULAR DISTRIBUTION
Evaluated nuclear-data file for niobium
[DE85-012095] N85-33009
ANHYDRIDES
Remarks on preparation of indandione detection reagents
[NASA-TM-77905] N85-32146
ANILINE
Resistance of polyaniline films as a function of electrochemical potential and the fabrication of polyaniline-based microelectronic devices
[AD-A154999] N85-32201
ANISOTROPY
Anisotropy of the permittivity field inferred from aspect-sensitive radar echoes N85-32492
Influence of mirror anisotropy and Brewster window orientation on radiation characteristics of ring lasers N85-32889
Low frequency instabilities driven by an ion temperature anisotropy
[AD-A154902] N85-33016
ANNEALING
Electrical properties of bulk grown nitrogen doped silicon
[AD-A155471] N85-32266
ANNUAL VARIATIONS
Trace element concentrations in atmospheric aerosol over Hungary N85-32652
Chemical composition of atmospheric aerosol at Delhi N85-32653
The variability of aerosol microstructure in continental and oceanic surface layers of the atmosphere in anticyclones N85-32660
Numerical modeling of sea ice dynamics and ice thickness characteristics
[AD-A154600] N85-32700
ANODIC COATINGS
Resistance of polyaniline films as a function of electrochemical potential and the fabrication of polyaniline-based microelectronic devices
[AD-A154999] N85-32201
ANTARCTIC REGIONS
Use of the synoptic view: Examples from Earth and other planets N85-32371
Aerosol formation by wave action over Ross Sea, Antartica N85-32688
ANTENNA ARRAYS
Null synthesis with phase and amplitude controls at the subarray outputs
[AD-A155187] N85-32241
Evaluation of the effects of roll angle on the natural convection heat transfer from an array of cylindrical spines
[AD-A154594] N85-32273
A simple model for testing the effects of gravity-wave-produced vertical oscillations of scattering irregularities on spaced-antenna, horizontal drift measurements N85-32489
Criteria for optimum spacing of spaced antenna, part 3.2A N85-32491
Increase of antenna area instead of transmitter power, part 6.3A N85-32517
Summary of progress at the Poker Flat Observatory in Alaska N85-32539
ANTENNA DESIGN
Fin-line horn antennas
[AD-A154597] N85-32255
Most desirable terrain, e.g., flat vs valley location, part 5.1B N85-32513
Summary of session on optimum transmitter and antenna configuration for MST radar, part 6 N85-32514
ANTENNA RADIATION PATTERNS
Null synthesis with phase and amplitude controls at the subarray outputs
[AD-A155187] N85-32241
Anisotropy of the permittivity field inferred from aspect-sensitive radar echoes N85-32492
Effects of line-of-sight velocity on spaced-antenna measurements, part 3.5A N85-32496
Problems and solutions in analyzing partial-reflection drift data by correlation techniques N85-32529
ANTENNAS
The use of the glistening surface concept in rough surface scattering
[AD-A154922] N85-32234
Field antenna handbook
[AD-A155204] N85-32242
Numerical modeling of subsurface communication
[DE85-012818] N85-32249
Middle Atmosphere Program. Handbook for MAP. Volume 14: URSI/SCOSTEP Workshop on Technical Aspects of MST Radar
[NASA-CR-176085] N85-32466
ANTICYCLONES
Mesoscale features and atmospheric refraction conditions of the Arctic marginal ice zone
[AD-A155139] N85-32584
The variability of aerosol microstructure in continental and oceanic surface layers of the atmosphere in anticyclones N85-32660
ANTIGENS
Differences in susceptibility of inbred mice to bacillus anthracis
[AD-A155646] N85-32750
ANTIREFLECTION COATINGS
Los Alamos optical materials reliability, maintainability, and exposure testing program
[DE85-011894] N85-32456
APPROACH CONTROL
A preliminary investigation of handling qualities requirements for helicopter instrument flight during decelerating approach maneuvers and overshoot
[AD-A154650] N85-32125
APPROXIMATION
Improved Nominal Operating Cell Temperature (NOCT) test procedure N85-32449
Toward the propagation of waves in unsteady media N85-32881
On the problem of linear programming with approximate data N85-32978
Discrete-element acoustic analysis of submerged structures using doubly asymptotic approximations
[AD-A154959] N85-32987
AQUATIC PLANTS
Handbook for obtaining and using aerial photography to map aquatic plant distribution
[AD-A154584] N85-32388
ARC LAMPS
Optical output stabilization method for direct current arc lamps
[AD-A154987] N85-33013
ARCHAEOLOGY
Paleoenvironmental investigations at seed cave (Windust cave H-45FR46), Franklin County, Washington
[AD-A154777] N85-32576
ARCHITECTURE (COMPUTERS)
Globally-asynchronous locally-synchronous systems
[AD-A154624] N85-32222
Secure digital voice communications in the Defense Data Network (DDN)
[AD-A154677] N85-32226
Characteristics of a numerical fluid dynamics simulator
[DE85-009602] N85-32290
Resource management for the tagged token dataflow architecture
[AD-A154773] N85-32779
Real-time contour surface display generation
[AD-A155232] N85-32780
Software for interactive on-line conferences
[AD-A154742] N85-32801
HLLM software support
[AD-A154828] N85-32805
Comparative study on data system architectures — spacecraft data processing
[ESA-CR(P)-2015] N85-32828
Simulation of complex three-dimensional flows
[NASA-TM-86773] N85-32831
New developments on the core function for efficient implementation of the difficult residue number system operations
[AD-A154678] N85-32834
ARCTIC OCEAN
Transport and formation of summertime cloud condensation nuclei over the Arctic Ocean N85-32686

ARCTIC REGIONS
Mesoscale features and atmospheric refraction conditions of the Arctic marginal ice zone
[AD-A155139] N85-32584
Condensation nuclei and aerosol size distribution measurements in Arctic haze N85-32658
ARGON
New metal coating method developed N85-32191
Supersaturation obtained in a condensation nucleus counter N85-32624
Influence of background electrically neutral argon admixture on mechanical strength of silicon crystals N85-32878
Measurements of Fe and Ar fragmentation cross sections
[PAPER-OG-7.2-20] N85-33047
ARGON ISOTOPES
The degassing history of the Earth: Noble gas studies of Archaean cherts and zero age glassy submarine basalts N85-33072
ARMED FORCES (UNITED STATES)
Air force technical objective document, Aerospace Medical Division, Fiscal Year 1986
[AD-A155195] N85-32762
Feasibility of applications of Competition Decision Assist Package (CDAP) to spare parts
[AD-A154716] N85-33036
Air Force Office of Scientific Research (AFOSR). Technical report summaries: First quarter (CY)
[AD-A154757] N85-33041
ARRAYS
A multiplying slot array
[AD-A155570] N85-32245
The dynamics of slack marine cables
[AD-A155022] N85-32349
The Norwegian seismic array (NORSAR)
[AD-A154751] N85-32555
The moving thermoacoustic array: A theoretical feasibility study
[AD-A154510] N85-32980
ARTERIES
Analysis of the transient response of temporal artery blood flow data relative to various anti-G suit pressure schedules
[AD-A155242] N85-32775
ARTIFICIAL INTELLIGENCE
The documentation assistant: An intelligent system for documentation
[AD-A154709] N85-32800
ARTIFICIAL SATELLITES
Global geoid and gravity anomaly predictions using the collocation and point mass techniques
[AD-A154517] N85-32387
ASHES
Ice nucleating characteristics of Capparis Aphylla, an Indian herb N85-32619
ASPECT RATIO
A numerical study of Taylor-Vortex flow
[AD-A154787] N85-32277
Object identification and manipulation using silhouette moments
[AD-A154755] N85-33011
ASPHYXIA
Basic cryogenics and materials. Phase 1
[NASA-CR-177932] N85-32215
ASSEMBLING
Field testing of a lightweight relocatable structure in a temperate environment
[AD-A155171] N85-32350
ASTRONOMICAL COORDINATES
Basic formulae for the computation of the deflection of the vertical from astronomical star observations
[AD-A154912] N85-32390
ASTRONOMICAL SATELLITES
Mapping with QUASAT (quasar satellite) using short observation times
[AD-A155155] N85-32141
ASTRONOMY
Basic formulae for the computation of the deflection of the vertical from astronomical star observations
[AD-A154912] N85-32390
Space research in the United Kingdom: An assessment
[AD-A155334] N85-33038
ASTROPHYSICS
Space research in the United Kingdom: An assessment
[AD-A155334] N85-33038
Research in particles and fields
[NASA-CR-176069] N85-33103
ASYMMETRY
Search for the north-south asymmetry in solar activity
[AD-A155525] N85-33102
ASYMPTOTIC SERIES
Discrete-element acoustic analysis of submerged structures using doubly asymptotic approximations
[AD-A154959] N85-32987
ATLANTIC OCEAN
An evaluation of discretized conditional probability and linear regression threshold techniques in model output statistics forecasting of cloud amount and ceiling over the North Atlantic Ocean
[AD-A155100] N85-32581
ATMOSPHERIC ATTENUATION
Ship-to-ship propagation: Maritime data analyses
[AD-A155484] N85-32325
ATMOSPHERIC BOUNDARY LAYER
Facility for large-scale hazardous gas testing
[DE85-011852] N85-32169
Properties of aerosol particles detected by satellites in coastal regions N85-32622
Simulation of the coupled atmospheric and oceanic boundary layer model during MILDEX
[AD-A155166] N85-32705
ATMOSPHERIC CHEMISTRY
Activities report of the Aeronomy Department
[G-774-1984] N85-32569
Eleventh International Conference on Atmospheric Aerosols, Condensation and Ice Nuclei, volume 2
[PB85-182418] N85-32596
Ice nucleation by silver iodine particles with nearly critical sizes N85-32600
Airborne measurements of atmospheric ice nuclei N85-32612
A statistical analysis of ice nuclei concentrations at urban and rural sites in Valladolid, Spain N85-32614
Experimental studies of the formation of Aitken nuclei in the atmosphere N85-32641
Photochemical aerosol formation in polluted atmosphere N85-32642
The influence of Brownian coagulation on the size distributions of atmospheric aerosols N85-32643
The nuclei of cloud formation N85-32685
Characterization of insoluble particles associated with cloud droplets N85-32693
Sulfur Cycle N85-32748
ATMOSPHERIC CIRCULATION
Middle Atmosphere Program. Handbook for MAP. Volume 14: URSI/SCOSTEP Workshop on Technical Aspects of MST Radar
[NASA-CR-176085] N85-32466
Tropospheric-stratospheric exchange, part 1.1A N85-32468
Gravity waves from the stratosphere to the mesosphere, part 1.3B N85-32471
A numerical analysis of transient planetary waves and the vertical structure in a meso-strato-troposphere model, part 1.4A N85-32473
General circulation of the middle atmosphere, part 1.4B N85-32474
Performance of the Colorado wind-profiling network, part 1.5A N85-32475
Vertical transport in the atmosphere: Measurement capabilities and requirements of VHF radars, part 1.6A N85-32476
Synoptic-scale dynamics with vertical velocity, part 1.8A N85-32478
Determination of billows and other turbulent structures, part 4.1A N85-32500
Spectral measurements of turbulence and gravity waves, part 4.2A N85-32501
Gravity-wave spectra in the atmosphere observed by MST radar, part 4.2B N85-32502
Estimation of vertical diffusion from observations of Atmospheric turbulence layers, part 4.4B N85-32507
Momentum flux measurements: Techniques and needs, part 4.5A N85-32508
MST radar data management N85-32532
Data base for the Colorado profiling network N85-32533
Generation of available potential energy and the energy cycle during the global weather experiment
[NASA-CR-175301] N85-32572
Circulation analysis of two snowstorms during the SNOW-TWO program
[AD-A155225] N85-32587
Notes on atmospheric stability, turbulence, and its measurements
[AD-A155230] N85-32588
Sahara Desert dust transport to the south N85-32666
Measurements of giant salt nuclei from inland in east China N85-32668
Observations of cloud droplets, aerosol particles and cloud condensation nuclei in continental air masses N85-32671
Condensation properties of atmospheric aerosol N85-32672
Numerical simulations of the response of intense ocean currents to atmospheric forcing
[AD-A155161] N85-32704
ATMOSPHERIC COMPOSITION
Concentrations of ice nuclei of different modes of activities N85-32616
Observations of the atmospheric ice nucleus at northwest China N85-32618
The investigation of natural and artificial ice nuclei by the improved membrane filter method N85-32626
A thermal diffusion chamber for the measurement of cloud condensation nuclei N85-32627
Concentration and source areas of ice nuclei in the Alaskan atmosphere N85-32634
Eleventh International Conference on Atmospheric Aerosols, Condensation and Ice Nuclei, volume 1
[PB85-182400] N85-32636
Study of the formation of particles from natural hydrocarbons released by vegetation N85-32640
Experimental studies of the formation of Aitken nuclei in the atmosphere N85-32641
Photochemical aerosol formation in polluted atmosphere N85-32642
The influence of Brownian coagulation on the size distributions of atmospheric aerosols N85-32643
A study of time transformation of natural photochemical aerosols N85-32644
Human activity and production rate of secondary nuclei N85-32645
A new hypothesis for the observed vertical distribution of atmospheric aerosols N85-32646
On the transformation regularities of time series of solid aerosol concentrations in the surface atmospheric layer N85-32648
Our knowledge about the atmospheric aerosol N85-32650
Chemical composition of atmospheric aerosol at Delhi N85-32653
Aitken particle size distribution in Antarctica N85-32656
Condensation nuclei and aerosol size distribution measurements in Arctic haze N85-32658
Aircraft investigations of the distribution of aerosols in the lower troposphere N85-32659
The variability of aerosol microstructure in continental and oceanic surface layers of the atmosphere in anticyclones N85-32660
Theoretical studies of structure and stability of hydrates of atmospheric sulfur species N85-32684
A review on the formation of aerosol particles in the atmosphere N85-32687
The evolution of complex and higher organisms
[NASA-SP-478] N85-32708
Origin of life N85-32713
Evolution of the atmosphere N85-32725
Participation of singlet oxygen in photodestruction of air-saturated solutions of coumarin dyes N85-32891
The possibilities of remote analysis of atmospheric gases based on Raman scattering spectroscopy N85-32892
Constraints on early atmosphere from planetary accretion processes N85-33064
The composition of the primitive atmosphere and the synthesis of organic compounds on the early Earth N85-33065
The problem of the Earth's CO2 content and the iron core N85-33069
Water loss from Venus: Implications for the Earth's early atmosphere N85-33087
ATMOSPHERIC CONDUCTIVITY
Application of Particle Induced X-ray Emission analysis (PIXE) to aerosol long range transport studies N85-32665
ATMOSPHERIC DENSITY
Applied research and development for falling-sphere air density measuring systems
[AD-A155227] N85-32099
Application of satellite accelerometer data to improve density models
[AD-A154904] N85-32558
ATMOSPHERIC EFFECTS
Understanding and laboratory prediction of the atmospheric corrosion behavior of steels and of non-ferrous metals and alloys
[AD-A154642] N85-32179
ATMOSPHERIC ELECTRICITY
Some considerations about the natural atmospheric radioactive aerosol N85-32662
ATMOSPHERIC MODELS
VALMET: A valley air pollution model
[DE85-010820] N85-32463
A numerical analysis of transient planetary waves and the vertical structure in a meso-strato-troposphere model, part 1.4A N85-32473
Nuclear thermal transmittance in the atmosphere using LOWTRAN-6 computer code
[AD-A154669] N85-32553

Application of satellite accelerometer data to improve density models
[AD-A154904] N85-32558
Generation of available potential onergy and the energy cycle during the global weather experiment
[NASA-CR-175301] N85-32572
Accuracy and operational use of medium and extended range numerical atmospheric forecasts: A review
[AD-A155027] N85-32579
Mean flow and turbulence in complex terrain
[AD-A155138] N85-32583
Simulation of the coupled atmospheric and oceanic boundary layer model during MILDEX
[AD-A155166] N85-32705

ATMOSPHERIC MOISTURE
Water loss from Venus: Implications for the Earth's early atmosphere N85-33087

ATMOSPHERIC OPTICS
Airborne measurements of the vertical distribution of Arctic haze N85-32657

ATMOSPHERIC PHYSICS
Activities report of the Aeronomy Department
[G-774-1984] N85-32569
Photochemical aerosol formation in polluted atmosphere N85-32642

ATMOSPHERIC PRESSURE
Two-phase flow visualization in a transparent, atmospheric pressure, boiling water loop
[DE84-016857] N85-32288

ATMOSPHERIC RADIATION
Some considerations about the natural atmospheric radioactive aerosol N85-32662

ATMOSPHERIC REFRACTION
Gravity waves from the stratosphere to the mesosphere, part 1.3B N85-32471
Some recent developments in the interpretation of MST radar returns from clear air (keynote paper), part 2 N85-32480
Mesoscale features and atmospheric refraction conditions of the Arctic marginal ice zone
[AD-A155139] N85-32584

ATMOSPHERIC SCATTERING
Meteorological and aeronomical requirements for MST radar networks (keynote paper), part 1 N85-32467
Properties of aerosol particles detected by satellites in coastal regions N85-32622

ATMOSPHERIC SOUNDING
Laser Elektronika-01 for air pollution control lidar N85-32887

ATMOSPHERIC TURBULENCE
Middle Atmosphere Program. Handbook for MAP. Volume 14: URSI/SCOSTEP Workshop on Technical Aspects of MST Radar
[NASA-CR-176085] N85-32466
Excerpts from the paper: Research Status and Recommendation from the Alaska Workshop on Gravity Waves and Turbulence in the Middle Atmosphere, part 1.3A N85-32470
Morphology of the scattering targets: Fresnel and turbulent mechanisms, part 2.1A N85-32481
Interpretation of radar returns from the mesosphere, part 2.3A N85-32485
Radar echoes at 2.66 and 40.92 MHz from the mesosphere, part 2.6A N85-32486
Network ST radar and related measurements at Pennsylvania State University N85-32544
Notes on atmospheric stability, turbulence, and its measurements
[AD-A155230] N85-32588
A numerical and analytical investigation of lee cyclogenesis
[AD-A155607] N85-32594
Size spectra for the source-enhanced coagulation with the turbulent mass transfer N85-32649
Fog activation and supersaturation N85-32678

ATMOSPHERICS
A high-speed digital signal processor for atmospheric radar, part 7.3A N85-32525

ATOMIC EXCITATIONS
Study of proton and neutron activation of metal samples in low Earth orbit
[NASA-CR-171596] N85-32130

ATOMIC PHYSICS
Activities of the Physics Division
[DE85-000784] N85-33002

ATOMIC RECOMBINATION
Molecular orbital studies in oxidation: Sulfate formation and metal-metal oxide adhesion
[NASA-CR-176070] N85-32174

ATOMIZING
Stable generation of highly monodisperse aerosols N85-32628

ATOMS
Overlap integrals for atom-metal surface interactions
[AD-A155038] N85-32998

ATTENUATION
Experimental and analytic characterization of nonlinear seismic attenuation
[AD-A154760] N85-32556

AUDIO EQUIPMENT
Robust detection and classification of regional seismic signals using a two mode/two stage cascaded adaptive arma (CAARMA) model
[AD-A154710] N85-32554

AUGER EFFECT
Inter-zone auger recombination in GaSb laser structures N85-32875

AUGER SPECTROSCOPY
The effect of metal overlayers of thermionic dispenser cathodes
[AD-A154795] N85-32995

AURORAL IONIZATION
Characteristics and sources of E-region ionization in the continuous aurora
[AD-A155018] N85-32562

AUTOIONIZATION
Photoelectron studies of autoionizing Rydberg states in HCl
[DE85-011813] N85-33001

AUTOMATIC CONTROL
Importance of automation, robotization in economy N85-32219

AUTOMATION
NASA space station automation: AI-based technology review
[NASA-CR-176094] N85-32134
NASA space station automation: AI-based technology review. Executive summary
[NASA-CR-176096] N85-32135
East Europe report: Science and technology
[JPRS-ESA-85-023] N85-32217

AUTOREGRESSIVE PROCESSES
Robust detection and classification of regional seismic signals using a two mode/two stage cascaded adaptive arma (CAARMA) model
[AD-A154710] N85-32554

AVIONICS
Aviation system delays
[S-HRG-98-1241] N85-32102
HLLM software support
[AD-A154828] N85-32805

AXIAL FLOW
Classical emission of relativistic charged particles during axial channeling N85-32871

AXIAL STRAIN
Results of an interlaboratory fatigue test program conducted on alloy 800H at room and elevated temperatures
[NASA-CR-174940] N85-32340

AXISYMMETRIC FLOW
A panel method study of vortex sheets with special emphasis on sheets of axisymmetric geometry
[NASA-CR-177365] N85-32095
A numerical study of Taylor-Vortex flow
[AD-A154787] N85-32277

AZO COMPOUNDS
Electrochemistry of Hexanitroazobenzene (HNAB)
[DE85-010807] N85-32171
Synthesis of energetic materials
[AD-A154887] N85-32210

B

BACILLUS
Differences in susceptibility of inbred mice to bacillus anthracis
[AD-A155646] N85-32750

BACKGROUND NOISE
Application of adaptive noise cancellation to Coast Guard voice communications
[AD-A154798] N85-32230
Design of a freestanding noise measurement and recording system to predict the intensity and location of electromagnetic radiation from earthquakes
[AD-A155070] N85-32563

BACKGROUND RADIATION
Visibility and vertical structure measurements in southern Germany
[AD-A154714] N85-32574

BACKSCATTERING
Broadside scattering of a tubular cylinder for evaluation of target identification
[AD-A155739] N85-32248
Plating density standards
[DE85-010014] N85-32318
Meteorological and aeronomical requirements for MST radar networks (keynote paper), part 1 N85-32467
A modified Fresnel scattering model for the parameterization of Fresnel returns, part 2.3A N85-32483
Observations of mesospheric turbulence by rocket probe and VHF radar, part 2.4A N85-32484
Interpretation of radar returns from the mesosphere, part 2.3A N85-32485
Usefulness of multifrequency MST radar measurements, part 2.6B N85-32487
Relationship of spaced antenna and Doppler techniques for velocity measurements (keynote paper), part 3 N85-32488
Anisotropy of the permittivity field inferred from aspect-sensitive radar echoes N85-32492
Visibility and vertical structure measurements in southern Germany
[AD-A154714] N85-32574
Fluctuations in light intensity during backscattering in turbulent medium N85-32956

BACTERIA
Ice active bacteria as condensation nuclei N85-32603
Aerobic sulfur-oxidizing bacteria: Environmental selection and diversification N85-32712
Protocyanobacteria: Oxygenic and Anoxygenic photosynthesis in mat-forming bacteria N85-32714
Sulfur transformations at the hydrogen sulfide/oxygen interface in stratified waters and in cyanobacterial mats N85-32715
Distribution and abundance of organic thiols N85-32717
Cytochromes and iron sulfur proteins in sulfur metabolism of phototrophic bacteria N85-32718
Insights into the phylogenetic positions of photosynthetic bacteria obtained from 5S rRNA and 16S rRNA sequence data N85-32719
Ecophysiology of phototrophic sulfur bacteria in lakes: Vertical distribution of planktonic populations N85-32722
Chemolithotrophy and physiology of bacterial nutrient limitation N85-32730
Structure and physiology of Beggiatoa and Thiothrix N85-32734
Phototrophic bacteria and their role in the biogeochemical sulfur cycle N85-32735
Sulfur cycling and metabolism of phototrophic and filamentous sulfur bacteria N85-32737
Enrichments for phototrophic bacteria and characterization by morphology and pigment analysis N85-32738
Anaerobic reduction of elemental sulfur by Chromatium vinosum and Beggiatoa alba N85-32739
Buoyant densities of phototrophic sulfur bacteria and cyanobacteria N85-32740
Interactions among sulfide-oxidizing bacteria N85-32741
Cyanobacterial mats: Microanalysis of community metabolism N85-32743
Microanalysis of dissolved iron and phosphate in pore waters of hypersaline sediment N85-32744
Glutathione in cyanobacteria N85-32745
Microbial communities and microprofiles of sulfide and oxygen of alum rock sulfur springs N85-32746

BALL BEARINGS
Mechanics of a gaseous film barrier to lubricant wetting of elastohydrodynamically lubricated conjunctions
[NASA-TP-2500] N85-32330
Friction and wear of solid-lubricated contact in gas turbine engine bearings
[AD-A155042] N85-32335

BALLOON-BORNE INSTRUMENTS
A balloon-borne imaging gamma-ray telescope
[PAPER-OG-9.2-2] N85-33049
Balloon-borne video cassette recorders for digital data storage
[PAPER-OG-9.3-11] N85-33050

BANDPASS FILTERS
Microwave SAW (Surface Acoustic Wave) monochromator
[AD-D011718] N85-32311

BANDWIDTH
Experimental evaluation of a new form of M-ary (M = 8) phase shift keying including design of the transmitter and receiver
[AD-A155103] N85-32239

BASALT
The degassing history of the Earth: Noble gas studies of Archaean cherts and zero age glassy submarine basalts N85-33072

BAYES THEOREM
Reconciling Bayesian and frequentist evidence in the one-sided testing program
[AD-A155603] N85-32850
Bayesian vs MAP multiple model adaptive estimation for field of view expansion in tracking airborne targets
[AD-A155466] N85-32855

BEACHES
Coastal erosion along Monterey Bay
[AD-A155610] N85-32707

BEAM INJECTION
Injection of hydrogen macroparticles into T-10 tokamak N85-32937
BEAM INTERACTIONS
Laser beam interactions with vapor plumes during Nd:YAG laser welding on aluminum
[DE85-009793] N85-32328
BEAMS (RADIATION)
New approximations and findings of theory of nonlinear acoustic beams N85-32863
Reflection of acoustic beam from inhomogeneous boundary N85-32864
The problem of brightness enhancement during laser frequency doubling N85-32897
BEHAVIOR
Large-time behavior of viscous surface waves
[AD-A154805] N85-32278
Experimental and analytic characterization of nonlinear seismic attenuation
[AD-A154760] N85-32556
Sobolev-Poincare's inequality and the Neumann problem for u sub t = divergence of the absolute value of the gradient u to the p-2 power x the gradient u
[AD-A154788] N85-32839
BENDING
The effect of abrasive blasting on the fatigue and corrosion of an aluminium-copper alloy
[AD-A154954] N85-32182
User's guide for computer program CGFAG, Concrete General Flexure Analysis with Graphics
[AD-A155555] N85-32204
Thin-film reliability and engineering overview N85-32450
Analysis of long bone and vertebral failure patterns
[AD-A154796] N85-32758
BERNOULLI THEOREM
The distribution of the number of empty cells in a generalized random allocation scheme
[AD-A154806] N85-32841
BIBLIOGRAPHIES
Aerospace medicine and biology: A continuing bibliography with indexes, supplement 273
[NASA-SP-7011(273)] N85-32755
Human performance in continuous/sustained operations and the demands of extended work/rest schedules. An annotated bibliography
[AD-A155619] N85-32771
A short bibliography of recent developments in selection and ranking procedures
[AD-A155648] N85-32856
Air Force Office of Scientific Research (AFOSR). Technical report summaries: First quarter (CY)
[AD-A154757] N85-33041
BINARY ALLOYS
MPS solidification model. Analysis and calculation of macrosegregation in a casting ingot
[NASA-CR-171589] N85-32178
BINARY MIXTURES
Burn front velocity as a function of pellet density in iron-potassium perchlorate heat powders
[DE85-011448] N85-32214
Relaxation lens in inhomogeneous binary mixture N85-32957
BINDING
CO adsorption on (111) and (100) surfaces of the Pt sub 3 Ti alloy. Evidence for parallel binding and strong activation of CO
[NASA-CR-176077] N85-32176
BIOASSAY
Marine environmental quality assessment program, five-year plan (FY 1984 - 1988)
[AD-A154715] N85-32459
BIOASTRONAUTICS
Hydroponics developments for spaceship garden N85-32754
Aerospace medicine and biology: A continuing bibliography with indexes, supplement 273
[NASA-SP-7011(273)] N85-32755
BIOCHEMISTRY
Marine environmental quality assessment program, five-year plan (FY 1984 - 1988)
[AD-A154715] N85-32459
Interaction of opiate and phencyclidine derivatives with the acetylcholine receptor
[AD-A155119] N85-32761
The composition of the primitive atmosphere and the synthesis of organic compounds on the early Earth N85-33065
BIOCONVERSION
Biomass thermochemical conversion program
[DE85-011867] N85-32213
Aerobic sulfur-oxidizing bacteria: Environmental selection and diversification N85-32712
Distribution and abundance of organic thiols N85-32717
Cytochromes and iron sulfur proteins in sulfur metabolism of phototrophic bacteria N85-32718
BIOELECTRICITY
Physical chemical state of water in living cells
[AD-A154566] N85-32749
BIOGEOCHEMISTRY
Biogeochemical cycling and remote sensing N85-32733
Phototrophic bacteria and their role in the biogeochemical sulfur cycle N85-32735
BIOLOGICAL EVOLUTION
Origin of life N85-32713
Protocyanobacteria: Oxygenic and Anoxygenic photosynthesis in mat-forming bacteria N85-32714
Insights into the phylogenetic positions of photosynthetic bacteria obtained from 5S rRNA and 16S rRNA sequence data N85-32719
Search for the universal ancestors
[NASA-SP-477] N85-32777
Submarine hydrothermal environments as sites for the origin and evolution of life N85-33074
BIOLOGY
USSR Space Life Sciences Digest
[NASA-CR-3922] N85-32709
BIOMASS ENERGY PRODUCTION
Biomass thermochemical conversion program
[DE85-011867] N85-32213
BIONICS
USSR report: Life sciences. Biomedical and behavioral sciences
[JPRS-UBB-85-020] N85-32752
BIOSPHERE
Carbon isotope geochemistry and geobiology N85-32716
BIOSYNTHESIS
The role of sulfur in osmoregulation and salinity tolerance in cyanobacteria, algae, and plants N85-32736
BIOTECHNOLOGY
East Europe report: Science and technology
[JPRS-ESA-85-023] N85-32217
USSR report: Life sciences. Biomedical and behavioral sciences
[JPRS-UBB-85-020] N85-32752
Air force technical objective document, Aerospace Medical Division, Fiscal Year 1986
[AD-A155195] N85-32762
BITERNARY CODE
Construction of complementary code sequence sets, part 7.1D N85-32523
BLADDER
Spontaneous transitional cell carcinoma in the urinary bladder of a strain 13 guinea pig
[AD-A155645] N85-32764
BOILING
Two-phase flow visualization in a transparent, atmospheric pressure, boiling water loop
[DE84-016857] N85-32288
BOLTZMANN DISTRIBUTION
Theoretical foundations of turbulent flows N85-32680
BOMBER AIRCRAFT
Electronic reconnaissance aircraft of the Soviet Union Navy
[AD-A154706] N85-32091
BONDING
EVA-glass interface bond stability N85-32408
BORATES
Luminescence and absorption of indium-activated potassium-borate glasses subjected to high-power excitation N85-32868
BORON
Status of boron combustion research
[AD-A154762] N85-32160
BORON ALLOYS
Thermoelectric properties of beta-boron and some boron compounds
[DE85-011978] N85-32270
BORON COMPOUNDS
Thermoelectric properties of beta-boron and some boron compounds
[DE85-011978] N85-32270
BORON HYDRIDES
Closed-bomb combustion of Hivelite-based, Very High Burn Rate (VHBR) propellant
[AD-A155740] N85-32212
BOROSILICATE GLASS
Thermal expansion of selected graphite reinforced polyimide-, epoxy-, and glass-matrix composite
[NASA-TM-87572] N85-32149
BOSONS
Exotic events of p bar p-collider: Excited quark or excited color boson? N85-32930
BOUGUER LAW
Earth Albedo and the orbit of LAGEOS
[NASA-TM-86210] N85-32131
BOUNDARY LAYER CONTROL
Experiments on the influence of active walls on the initial amplitudes and growths of instability waves
[AD-A154630] N85-32275
BOUNDARY LAYER FLOW
An evaluation of four methods of numerical analysis for two-dimensional airfoil flows
[AD-A155202] N85-32098
BOUNDARY LAYER SEPARATION
An evaluation of four methods of numerical analysis for two-dimensional airfoil flows
[AD-A155202] N85-32098
BOUNDARY LAYER STABILITY
Mesoscale features and atmospheric refraction conditions of the Arctic marginal ice zone
[AD-A155139] N85-32584
Development of artificially produced perturbations in supersonic boundary layer N85-32879
BOUNDARY LAYERS
Applicability of surface CCN measurements N85-32696
BOUNDARY VALUE PROBLEMS
Scattering from foliage covered terrain
[AD-A154724] N85-32228
Oscillatory solutions of the Peaceman-Rachford alternating direction implicit method and a comparison of methods for the solution of the two dimensional heat diffusion equation
[AD-A154670] N85-32833
Sobolev-Poincare's inequality and the Neumann problem for u sub t = divergence of the absolute value of the gradient u to the p-2 power x the gradient u
[AD-A154788] N85-32839
Exact solutions of singular equations for viscous transsonic flows N85-32882
BRAIN
Resource allocation in cerebral specialization of function: Behavioral and electrophysiological studies
[AD-A155092] N85-32759
BRANCHING (MATHEMATICS)
A note on a theorem of R. Duffin
[AD-A154786] N85-32838
BREEDER REACTORS
Tritium technology review
[DE85-010504] N85-33006
BRIGHTNESS
The problem of brightness enhancement during laser frequency doubling N85-32897
BRIGHTNESS DISTRIBUTION
Effective brightness of zero-point fluctuations of the electromagnetic vacuum accompanying parametric scattering of light N85-32951
BRILLOUIN EFFECT
Stimulated Mandelstam-Brillouin scattering with distributed feedback N85-32961
BRINES
Microbiology of solar salt ponds N85-32724
BRITTLE MATERIALS
The shearing contribution in transformation toughening of brittle materials
[AD-A154656] N85-32195
Mechanics of near tip microcracking in brittle material
[AD-A154684] N85-32346
BRITTLENESS
Influence of the resin on interlaminar mixed-mode fracture
[NASA-TM-87571] N85-32150
Metallurgical origins of fracture toughness and microstructure and fracture toughness of an HSLA (High-Strength/Low-Alloy) steel
[AD-A155530] N85-32187
BROADBAND
Investigation of plasma processes in electronic transition lasers
[AD-A155598] N85-32327
BROWNIAN MOVEMENTS
The influence of Brownian coagulation on the size distributions of atmospheric aerosols N85-32643
Scavenging of submicron aerosol particles by snow crystals: Theory and experiments N85-32667
BUBBLE MEMORY DEVICES
SSMIR (Solid State Memory Instrumentation Recorder): A new approach to acquiring data during an aircraft seat/sled ejection sequence
[AD-A154780] N85-32308
BUBBLES
Magnetic materials
[AD-A154679] N85-32256
BUCKLING
Stress and buckling analysis N85-32439
BUDGETING
Pricing options for the space shuttle. Special study N85-32138
Space research in the United Kingdom: An assessment
[AD-A155334] N85-33038

BUMPY TORUSES
Magnetics calculations for an ELMO Bumpy Square [DE85-011438] N85-33021
BUOYANCY
Numerical solutions of turbulent models for flow over a flat plate with angle of attack [DE85-010380] N85-32286
Gravity-wave spectra in the atmosphere observed by MST radar, part 4.2B N85-32502
Buoyant densities of phototrophic sulfur bacteria and cyanobacteria N85-32740
BURNING RATE
The role of aircraft panel materials in cabin fires and their properties [FAA-CT-84-30] N85-32104
Closed-bomb combustion of Hivelite-based, Very High Burn Rate (VHBR) propellant [AD-A155740] N85-32212
BURNOUT
A review of the physics and response models for burnout of semiconductor devices [AD-A155031] N85-33028

C

CABLES
The dynamics of slack marine cables [AD-A155022] N85-32349
CADMIUM
Physical and chemical aerosol characteristics in extremely clean air masses at Cape Grim, Tasmania N85-32655
CALCULUS
A PASCAL interpreter for the functional programming language ELC (Extended lambda calculus) [AD-A155218] N85-32810
CALCULUS OF VARIATIONS
Generalized formulation of a class of explicit and implicit TVD schemes [NASA-TM-86775] N85-32830
CALIBRATING
Calibration and use of clutter data for simulation [AD-A154793] N85-32229
Background equatorial astronomical measurements focal plane assembly (refurbished HI STAR SOUTH) [AD-A155215] N85-32313
Improved coordinate measuring machine calibration and control [DE85-012053] N85-32315
Reference-cell calibration activities N85-32453
The 100 years of Aitken Nuclei (AN) study-reminiscence, current and future problems N85-32621
CAMERAS
Large format camera photographs: A new tool for understanding arid environments N85-32379
CANARD CONFIGURATIONS
Study of an efficient long-range Mach 2.7 supersonic transport configuration concept [NASA-TM-86414] N85-32110
CANCER
Spontaneous transitional cell carcinoma in the urinary bladder of a strain 13 guinea pig [AD-A155645] N85-32764
CANOPIES (VEGETATION)
Biogeochemical cycling and remote sensing N85-32733
CANTILEVER BEAMS
Influence of the resin on interlaminar mixed-mode fracture [NASA-TM-87571] N85-32150
CAPACITORS
East Europe report: Science and technology [JPRS-ESA-85-021] N85-32190
Stress corrosion of ceramic materials [AD-A155020] N85-32202
Capacitive energy storage at cryogenic temperatures [AD-A154508] N85-32253
A fast discharge excimer laser with symmetric geometry [AD-A155294] N85-32322
CARBON
Thermoelectric properties of beta-boron and some boron compounds [DE85-011978] N85-32270
Studies of oxygen- and carbon-related defects in high-efficiency silicon solar cells N85-32420
Physical and chemical aerosol characteristics in extremely clean air masses at Cape Grim, Tasmania N85-32655
Carbon and nitrogen in the deep Earth N85-33085
CARBON CYCLE
Carbon isotope geochemistry and geobiology N85-32716
Sulfur and carbon cycling in organic-rich marine sediments N85-32729
CARBON DIOXIDE
Polymer solution-supercritical fluid behavior [AD-A154514] N85-32192
Carbon isotope geochemistry and geobiology N85-32716
Carbon and sulfur cycling through geologic time N85-32720
Evolution of the atmosphere N85-32725
CARBON DIOXIDE LASERS
Identification of vibrational-rotational transitions of Os-192O4 within frequency tuning limits of high pressure CO2 waveguide laser N85-32917
The possibility of observing and exploiting the generation of high-energy photons by electrons in the field of an intense electromagnetic wave N85-32931
Investigation of ion-acoustic plasma turbulence in field of powerful electromagnetic wave by CO2-laser radiation scattering N85-32935
CARBON FIBERS
Thermal expansion of selected graphite reinforced polyimide-, epoxy-, and glass-matrix composite [NASA-TM-87572] N85-32149
Improved materials for composite and adhesive joints [AD-A155065] N85-32153
Electrical and mechanical properties of intercalated graphite fibers [AD-A155560] N85-32205
CARBON MONOXIDE
Shock tube measurements of growth constants in the branched-chain ethane-carbon monoxide-oxygen system [NASA-TM-87068] N85-32156
Why CO bonds side-on at low coverage and both side-on and upright at high coverage on the Cr(110) surface [NASA-CR-176071] N85-32173
CO adsorption on (111) and (100) surfaces of the Pt sub 3 Ti alloy. Evidence for parallel binding and strong activation of CO [NASA-CR-176077] N85-32176
The problem of the Earth's CO2 content and the iron core N85-33069
CARBON-CARBON COMPOSITES
Effects of weak interfaces on thermostructural behavior of carbon-carbon composites [AD-A155330] N85-32154
CARBONACEOUS MATERIALS
Development of wide band recording materials [AD-A154961] N85-32309
CARDIOVASCULAR SYSTEM
Studies of circulatory and metabolic changes during ketamine narcosis [AD-A154512] N85-32756
CAROTENE
Enrichments for phototrophic bacteria and characterization by morphology and pigment analysis N85-32738
CARTESIAN COORDINATES
Equations of motion for electromagnetic waves in 4-dimensional Euclidian space N85-32970
CASCADE FLOW
Notes on unsteady transonic cascade flows [AD-A154829] N85-32096
CASTING
MPS solidification model. Analysis and calculation of macrosegregation in a casting ingot [NASA-CR-171589] N85-32178
Tape casting as an approach to an all-ceramic turbine shroud seal [NASA-TM-87078] N85-32333
CATALOGS (PUBLICATIONS)
Data base management: MSTRAC (keynote paper), part 8 N85-32530
CATALYSTS
Decomposition of sulfuric acid using solar thermal energy [DE85-012288] N85-32170
A safe, high-power-density lithium battery [AD-A155223] N85-32454
CATENARIES
The dynamics of slack marine cables [AD-A155022] N85-32349
CATHODE RAY TUBES
The effect of set size on time to recall color coded information [AD-A155013] N85-32767
CATHODES
A safe, high-power-density lithium battery [AD-A155223] N85-32454
CAVITATION FLOW
Bubble dynamics in polymer solutions undergoing shear [AD-A154575] N85-32193
CEILINGS (METEOROLOGY)
An evaluation of discretized conditional probability and linear regression threshold techniques in model output statistics forecasting of cloud amount and ceiling over the North Atlantic Ocean [AD-A155100] N85-32581
CELESTIAL GEODESY
Basic formulae for the computation of the deflection of the vertical from astronomical star observations [AD-A154912] N85-32390
CELLS (BIOLOGY)
From microbial communities to cells N85-32728
Physical chemical state of water in living cells [AD-A154566] N85-32749
CENTRIFUGAL COMPRESSORS
A 3-D Euler method for internal transonic flows computation with a multi-domain approach N85-32298
CERAMICS
The shearing contribution in transformation toughening of brittle materials [AD-A154656] N85-32195
Matrix fracture in fiber-reinforced ceramics [AD-A154704] N85-32197
Stress corrosion of ceramic materials [AD-A155020] N85-32202
Sintering studies project [AD-A154750] N85-32216
Capacitive energy storage at cryogenic temperatures [AD-A154508] N85-32253
Tape casting as an approach to an all-ceramic turbine shroud seal [NASA-TM-87078] N85-32333
Friction and wear of solid-lubricated contact in gas turbine engine bearings [AD-A155042] N85-32335
Reliability of void detection in structural ceramics using scanning laser acoustic microscopy [NASA-TM-87035] N85-32337
System for electro-optical ceramic recrystallization N85-32872
CEREBRUM
Resource allocation in cerebral specialization of function: Behavioral and electrophysiological studies [AD-A155092] N85-32759
CERENKOV RADIATION
Cerenkov maser and Cerenkov laser devices [AD-A155443] N85-32324
Predictive model of electron beam induced flashblindness [AD-A155260] N85-32763
Form factor effects on microwave Cerenkov radiation [AD-A154577] N85-32993
CHANNEL MULTIPLIERS
Correlation of intensities of different scattering channels N85-32952
CHARCOAL
Remarks on preparation of indandione detection reagents [NASA-TM-77905] N85-32146
CHARGE CARRIERS
Influence of coherent light beams on free carriers in semiconductors N85-32867
CHARGE COUPLED DEVICES
CCD-based X-ray spectrometry for on-line determination of laser plasma electron temperature N85-32938
Solid state research [AD-A154783] N85-33025
CHARGE DISTRIBUTION
Form factor effects on microwave Cerenkov radiation [AD-A154577] N85-32993
CHARGE EXCHANGE
Evaluated nuclear-data file for niobium [DE85-012095] N85-33009
CHARGE TRANSFER
Polymer-water interaction studies N85-32411
CHARGED PARTICLES
Trapping of ion conics by downward parallel electric fields [AD-A155306] N85-32568
Classical emission of relativistic charged particles during axial channeling N85-32871
Transformation of charged particle beams by concentrating electro-optical systems N85-32925
Mirror reflection of charged particles from + amorphous and polycrystalline surfaces N85-32927
Possiblity of developing charged-particle energy analyzer based on hyperboloidal axisymmetrical lens N85-32933
CHEMICAL ANALYSIS
Remarks on preparation of indandione detection reagents [NASA-TM-77905] N85-32146
CHEMICAL BONDS
Why CO bonds side-on at low coverage and both side-on and upright at high coverage on the Cr(110) surface [NASA-CR-176071] N85-32173

Defects in tetrahedrally coordinated amorphous semiconductors
[AD-A155150] N85-32263
Interfacial bonding stability N85-32409

CHEMICAL COMPOSITION
The effect of diffusive hydrogen segregation on fracture of polycrystalline nickel
[AD-A155238] N85-32186
Chemical composition of atmospheric aerosol at Delhi N85-32653
Investigation of the formation of cloud particle spectrum on natural condensation nuclei N85-32674
Variations of particulate sulfur concentrations in a coastal atmospheric environment in connection with the change of air masses origin N85-32692
Liquid-phase compositions from vapor-phase analyses 2: Adaptation of the Prausnitz program to UF6 and some of its potential impurities
[DE85-011521] N85-32819

CHEMICAL ENGINEERING
Failure mechanisms in metal-sheathed thermocouples
[DE85-011929] N85-32317

CHEMICAL EVOLUTION
Origin of life N85-32713
Insights into the phylogenetic positions of photosynthetic bacteria obtained from 5S rRNA and 16S rRNA sequence data N85-32719
Search for the universal ancestors
[NASA-SP-477] N85-32777
Submarine hydrothermal environments as sites for the origin and evolution of life N85-33074

CHEMICAL PROPERTIES
Electrochemistry of Hexanitroazobenzene (HNAB)
[DE85-010807] N85-32171
Physical chemical state of water in living cells
[AD-A154566] N85-32749

CHEMICAL REACTIONS
Remarks on preparation of indandione detection reagents
[NASA-TM-77905] N85-32146
Interface chemistry of Hg(1-x)Cd(x)Te
[AD-A154876] N85-32161
Design of micelles as dephosphorylating agents
[AD-A155589] N85-32166
EVA-glass interface bond stability N85-32408
Experimental studies of the formation of Aitken nuclei in the atmosphere N85-32641
In-cavity laser IR spectrum analyzer for investigating non-steady-state processes N85-32894
Prospects for a new kind of synthesis: Assembly of molecular components to achieve functions
[AD-A155023] N85-32997

CHEMICAL REACTORS
Decomposition of sulfuric acid using solar thermal energy
[DE85-012288] N85-32170
Silicon production in an aerosol reactor N85-32416

CHEMICAL WARFARE
Design of micelles as dephosphorylating agents
[AD-A155589] N85-32166

CHEMILUMINESCENCE
Calculation of molecular constants potential energy curves and Franck-Condon factors for lead oxide
[AD-A154521] N85-32158

CHEMISORPTION
Why CO bonds side-on at low coverage and both side-on and upright at high coverage on the Cr(110) surface
[NASA-CR-176071] N85-32173

CHESAPEAKE BAY (US)
Reverification of the Chesapeake Bay model
[AD-A155486] N85-32706

CHINA
China has developed a new version of fighter aircraft
[AD-A155293] N85-32118

CHIPS (ELECTRONICS)
Digital integrated circuits N85-32787

CHLORINE
Facility for large-scale hazardous gas testing
[DE85-011852] N85-32169
Characteristics of aerosol composition in a nonurban area, north China N85-32651
Precision measurements of solar energetic particle elemental composition
[PAPER-SH-2.1-4] N85-33052

CHONDRITES
A model for core formation in the early Earth N85-33078

CHROMATOGRAPHY
Multidimensional luminescence measurements
[AD-A154950] N85-32162

CHROMIUM
Why CO bonds side-on at low coverage and both side-on and upright at high coverage on the Cr(110) surface
[NASA-CR-176071] N85-32173
Electrodeposition of chromium and copper in magnetic fields
[AD-A154648] N85-32180
Microscopic control of semiconductor surface oxidation
[AD-A154799] N85-33026
Measurements of Fe and Ar fragmentation cross sections
[PAPER-OG-7.2-20] N85-33047

CHROMIUM ALLOYS
A systematic plan for the continued study of dimensional stability of metallic alloys considered for the fabrication of cryogenic wind tunnel models
[NASA-CR-172449] N85-32172

CHROMOSPHERE
Heating of the deep chromosphere during solar flares
[AD-A155256] N85-33100

CHRONOLOGY
A new global geomorphology? N85-32358

CHUTES
Air carrier overwater emergency equipment and procedures
[PB85-917006] N85-32105

CIRCADIAN RHYTHMS
Human performance in continuous/sustained operations and the demands of extended work/rest schedules. An annotated bibliography
[AD-A155619] N85-32771

CIRCLES (GEOMETRY)
On the turning lozange of constant side whose vertices alternate between two fixed circles of a ring
[AD-A154803] N85-32840

CIRCUIT BOARDS
A comparison and analysis of Vintr's global routing algorithm with the Lee routing algorithm in two-layer printed circuit boards
[AD-A155600] N85-32816

CIRCUITS
Parallel simulation of digital LSI circuits
[AD-A154745] N85-32258

CIRCULAR CYLINDERS
Solution of problem of equilibrium confinement of plasma by magnetic field in an infinite circular cylinder N85-32936

CIRRUS CLOUDS
Ice crystal nucleation on hygroscopic aerosols N85-32605

CITIES
On the transformation regularities of time series of solid aerosol concentrations in the surface atmospheric layer N85-32648
An electron microscopic study of urban aerosol N85-32689
Helicopter noise survey for selected cities in the contiguous US
[AD-A154893] N85-32985

CIVIL AVIATION
An error-dependent model of instrument-scanning behavior in commercial airline pilots
[NASA-CR-3908] N85-32765

CLASSIFICATIONS
Geomorphic classification of Icelandic and Martian volcanoes: Limitations of comparative planetology research from LANDSAT and Viking orbiter images N85-32372

CLEANING
The effect of abrasive blasting on the fatigue and corrosion of an aluminium-copper alloy
[AD-A154954] N85-32182
Review of hazardous waste cleanup and disposal efforts at Tinker Air Force Base
[GPO-43-294] N85-32457

CLEAR AIR TURBULENCE
Millstone Hill radar: Capabilities for S/T observations N85-32548

CLIFFS
Coastal erosion along Monterey Bay
[AD-A155610] N85-32707

CLIMATE
Quantitative analysis in megageomorphology N85-32376
Meteorological weapons
[AD-A154735] N85-32575

CLIMATOLOGY
A modified Fresnel scattering model for the parameterization of Fresnel returns, part 2.3A N85-32483
Activities report of the Aeronomy Department
[G-774-1984] N85-32569
Paleoenvironmental investigations at seed cave (Windust cave H-45FR46), Franklin County, Washington
[AD-A154777] N85-32576
A simulation of weather in 3D space
[AD-A155221] N85-32586
Airborne measurements of the vertical distribution of Arctic haze N85-32657

CLOCKS
A new fault-tolerant algorithm for clock synchronization
[AD-A154771] N85-32836

CLOUD CHAMBERS
Construction of University of Missouri, Rolla's full scale cloud simulation chamber and applied research
[AD-A154682] N85-32128

CLOUD COVER
A simulation of weather in 3D space
[AD-A155221] N85-32586

CLOUD PHOTOGRAPHY
Radio-frequency radiation of storm clouds N85-32939

CLOUD PHYSICS
Eleventh International Conference on Atmospheric Aerosols, Condensation and Ice Nuclei, volume 2
[PB85-182418] N85-32596
Experimental studies of the kinetics of deposition nucleation on an ice nucleant used in weather modification N85-32598
Inactivation of silver iodide by atmospheric nucleation inhibitors N85-32599
Ice active bacteria as condensation nuclei N85-32603
The effect of supersaturation, temperature and particle size on ice-nucleating ability of atmospheric aerosol N85-32604
On the efficiency of the mechanism of ice particles formation in the vapor supersaturation field around a freezing droplet N85-32606
The nucleation of ice crystals during the freezing of large supercooled drops N85-32608
On the problem of possible mechanism of ice nuclei formation in convective clouds N85-32610
Bacterial ice nuclei of marine origin: Some recent observations N85-32611
Airborne measurements of atmospheric ice nuclei N85-32612
Aircraft observations of condensation and ice nuclei at a tropical station N85-32613
The nucleation of ice at very low temperatures and pressures N85-32617
The 100 years of Aitken Nuclei (AN) study-reminiscence, current and future problems N85-32621
A thermal diffusion chamber for the measurement of cloud condensation nuclei N85-32627
Stable generation of highly monodisperse aerosols N85-32628
Monte Carlo studies of H2O layers adsorbed on a model basal face of AgI N85-32633
Eleventh International Conference on Atmospheric Aerosols, Condensation and Ice Nuclei, volume 1
[PB85-182400] N85-32636
The first condensation nucleus conference N85-32637
Cloud condensation on insoluble particles N85-32670
Measurements of the critical supersaturation of 0.029 to 0.035 micron radius particles at Washington, District of Columbia N85-32676
A relationship between cloud droplet size and CCN critical supersaturation N85-32677
Fog activation and supersaturation N85-32678
On the question to the effect of surfactants on the spectrum of cloud drops in the process of their condensation growth N85-32679
Aircraft observations of cloud condensation nuclei in maritime and continental environments N85-32680
The distribution of giant salt nuclei inside and outside cloud over the basin of Xin and Jiang N85-32681
Characterization of insoluble particles associated with cloud droplets N85-32693
Applicability of surface CCN measurements N85-32696
Effect of ions on cloud formation and its role in solar terrestrial relationship N85-32697
on the transport of large condensation nuclei in the atmosphere at various altitudes over the territory of the USSR N85-32698

CLOUD SEEDING
Observations of cloud droplets, aerosol particles and cloud condensation nuclei in continental air masses N85-32671

CLOUDS
Stable generation of highly monodisperse aerosols N85-32628
Cloud droplet nucleation and initial growth derived from lidar depolarization studies N85-32635
A simple model to investigate the activation process in waterclouds N85-32675
A relationship between cloud droplet size and CCN critical supersaturation N85-32677
Properties of forest derived cloud condensation nuclei N85-32682

Influence on an industrial site on the characteristics of CCN supersaturation with air masses of different origin N85-32683

CLOUDS (METEOROLOGY)
An evaluation of discretized conditional probability and linear regression threshold techniques in model output statistics forecasting of cloud amount and ceiling over the North Atlantic Ocean [AD-A155100] N85-32581
A simulation of weather in 3D space [AD-A155221] N85-32586
Circulation analysis of two snowstorms during the SNOW-TWO program [AD-A155225] N85-32587
A thermal diffusion chamber for the measurement of cloud condensation nuclei N85-32627
Measurements of giant salt nuclei from inland in east China N85-32668
Investigation of the formation of cloud particle spectrum on natural condensation nuclei N85-32674
The nuclei of cloud formation N85-32685
The measured rate of condensation nucleation to droplets using the techniques of chemical kinetics N85-32694
Applicability of surface CCN measurements N85-32696

CLUSTER ANALYSIS
Decomposing the joint distribution of several linear combinations of uniform spacings [AD-A155056] N85-32845

CLUTTER
The use of the glistening surface concept in rough surface scattering [AD-A154922] N85-32234
Most desirable terrain, e.g., flat vs valley location, part 5.1B N85-32513

CMOS
Design of a sixteen-bit pipelined adder using CMOS bulk P-well technology [AD-A155043] N85-32260
East Europe report: Science and technology. Selections on CSSR computer technology [JPRS-ESA-84-017] N85-32781
Selections on CSSR computer technology N85-32782

COAGULATION
The influence of Brownian coagulation on the size distributions of atmospheric aerosols N85-32643
Size spectra for the source-enhanced coagulation with the turbulent mass transfer N85-32649

COAL GASIFICATION
Energy and Technology Review [DE85-011767] N85-33061

COASTAL WATER
Properties of aerosol particles detected by satellites in coastal regions N85-32622
Coastal erosion along Monterey Bay [AD-A155610] N85-32707

COASTS
Properties of aerosol particles detected by satellites in coastal regions N85-32622
Aircraft observations of cloud condensation nuclei in maritime and continental environments N85-32680

COATING
New metal coating method developed N85-32191

COATINGS
Stress concentration in the elastoplastic state and residual stress after unloading [AD-A155628] N85-32356
Dielectric mirror with ferromagnetic substrate N85-32966

COBALT
Measurements of Fe and Ar fragmentation cross sections [PAPER-OG-7.2-20] N85-33047

COBALT ALLOYS
Nonequilibrium kinetics of growth of oxide layer grains during laser heating of metals in air N85-32919

CODING
Construction of complementary code sequence sets, part 7.1D N85-32523

COEFFICIENT OF FRICTION
Friction and wear of solid-lubricated contact in gas turbine engine bearings [AD-A155042] N85-32335
Kinetic friction coefficient of ice [AD-A155035] N85-32859

COEFFICIENTS
Visibility and vertical structure measurements in southern Germany [AD-A154714] N85-32574

COGNITION
Resource allocation in cerebral specialization of function: Behavioral and electrophysiological studies [AD-A155092] N85-32759
Review of the psychological issues relating to the effectiveness of structured programming [AD-A154593] N85-32766

COGNITIVE PSYCHOLOGY
Conceptualizing in assembly tasks [AD-A155564] N85-32770

COHERENCE COEFFICIENT
Proust radar: Decoding hardware and coherent integration, part 7.2A N85-32524

COHERENT ELECTROMAGNETIC RADIATION
Solvability of some inverse problems in laser radiation focusing N85-32963

COHERENT LIGHT
Influence of coherent light beams on free carriers in semiconductors N85-32867

COHERENT RADAR
Observations of frontal zone structures with a VHF Doppler radar and radiosondes, part 1.2A N85-32469
Potential advantages of the spaced antenna method for operational wind profiling, part 3.1B N85-32490
Proust radar: Decoding hardware and coherent integration, part 7.2A N85-32524

COHERENT RADIATION
Laser radiation propagation in inertialess nonlinear medium N85-32898

COHERENT SCATTERING
Morphology of the scattering targets: Fresnel and turbulent mechanisms, part 2.1A N85-32481

COLD WORKING
The effect of prior parent phase cold work on martensite transformation in Cu-Zn-Al shape memory alloys [AD-A155140] N85-32183

COLLIMATORS
Soft X-ray polychromator for the Solar Maximum Mission [NASA-CR-175297] N85-33096

COLLISIONAL PLASMAS
Investigation of space-time structure of glow of laser plasma colliding with flat screen N85-32947

COLONIES
Cyanobacterial mats: Microanalysis of community metabolism N85-32743
Microbial communities and microprofiles of sulfide and oxygen of alum rock sulfur springs N85-32746
Microbial colonization and growth on metal sulfides and other mineral surfaces N85-32747

COLOR
Passive Q-modulation of optical cavities by KCl crystals containing OH(-) -ions N85-32915

COLOR CODING
The effect of set size on time to recall color coded information [AD-A155013] N85-32767

COMBINATORIAL ANALYSIS
Routing algorithms and stochastic analysis for large communications networks [AD-A154654] N85-32225

COMBUSTION
Aerosol analysis and emission spectrometry with free jets [DE85-010576] N85-32168
Biomass thermochemical conversion program [DE85-011867] N85-32213
In-cavity laser IR spectrum analyzer for investigating non-steady-state processes N85-32894

COMBUSTION EFFICIENCY
Closed-bomb combustion of Hivelite-based, Very High Burn Rate (VHBR) propellant [AD-A155740] N85-32212

COMBUSTION PRODUCTS
Ice nucleating characteristics of Capparis Aphylla, an Indian herb N85-32619

COMBUSTION STABILITY
Status of boron combustion research [AD-A154762] N85-32160
Closed-bomb combustion of Hivelite-based, Very High Burn Rate (VHBR) propellant [AD-A155740] N85-32212

COMMUNICATION
Numerical modeling of subsurface communication [DE85-012818] N85-32249

COMMUNICATION EQUIPMENT
Design of a jamming simulator for a binary communication system [AD-A154617] N85-32221
Globally-asynchronous locally-synchronous systems [AD-A154624] N85-32222

COMMUNICATION NETWORKS
Routing algorithms and stochastic analysis for large communications networks [AD-A154654] N85-32225
Broadcasting topology and routing information in computer networks [AD-A155668] N85-32827

COMPARTMENTS
The distribution of the number of empty cells in a generalized random allocation scheme [AD-A154806] N85-32841

COMPILERS
Resource management for the tagged token dataflow architecture [AD-A154773] N85-32779

COMPOSITE MATERIALS
A cracked orthotropic sheet stiffened by a semi-infinite orthotropic sheet [NASA-TP-2455] N85-32339

COMPRESSIBILITY
Analysis of long bone and vertebral failure patterns [AD-A154796] N85-32758

COMPRESSIBLE FLUIDS
An analysis of flow models: From Navier-Stokes to potential flow equations N85-32295

COMPRESSIVE STRENGTH
The effect of mould size on the exothermic reaction and compressive strength of epoxy resin chocks [AD-A155102] N85-32203

COMPTON EFFECT
The possibility of observing and exploiting the generation of high-energy photons by electrons in the field of an intense electromagnetic wave N85-32931

COMPUTATION
Survival function of hypo-exponential distributions [AD-A155518] N85-32814
On the dependence of the convergence of Gummel's algorithm on the regularity of the solution [AD-A154628] N85-32832
Ice fog as an electro-optical obscurant [AD-A155059] N85-33015
Magnetics calculations for an ELMO Bumpy Square [DE85-011438] N85-33021

COMPUTATIONAL FLUID DYNAMICS
Three-Dimensional Techniques Applied to Internal Flows in Propulsion Systems [AGARD-LS-140] N85-32293
The calculation of fully three dimensional flow through any type of turbomachine blade row N85-32294
An analysis of flow models: From Navier-Stokes to potential flow equations N85-32295
Computation of three-dimensional, inviscid, rotational flows N85-32296
An elliptic calculation procedure for 3-D viscous flow N85-32297
A 3-D Euler method for internal transonic flows computation with a multi-domain approach N85-32298
Performance evaluation of flow in turbomachinery blade rows N85-32299
Numerical solution of the Navier-Stokes equations for 3-D internal flows: An emerging capability N85-32300
Calculation of 3-D flow without numerical mixing N85-32301

COMPUTATIONAL GRIDS
Calculation of transonic steady and oscillatory pressures on a low aspect ratio model and comparison with experiment [NASA-TM-86449] N85-32092
Simulation of complex three-dimensional flows [NASA-TM-86773] N85-32831
A vectorized nearest-neighbors algorithm of order N using a monotonic logical grid [AD-A155169] N85-32853

COMPUTER AIDED DESIGN
NASA space station automation: AI-based technology review. Executive summary [NASA-CR-176096] N85-32135
Importance of automation, robotization in economy N85-32219
Design of a sixteen-bit pipelined adder using CMOS bulk P-well technology [AD-A155043] N85-32260
Design of a generator for near-tangential transonic swirling outflow [AD-A155163] N85-32280

COMPUTER AIDED MANUFACTURING
NASA space station automation: AI-based technology review [NASA-CR-176094] N85-32134
Importance of automation, robotization in economy N85-32219

COMPUTER ASSISTED INSTRUCTION
The Naval Postgraduate School Flight Mechanics Laboratory: A feasibility study [AD-A154578] N85-32127
A microcomputer tutorial on spreadsheets and databases with a simulated budget preparation [AD-A155516] N85-32813

COMPUTER DESIGN
East Europe report: Science and technology [JPRS-ESA-85-021] N85-32190
Globally-asynchronous locally-synchronous systems [AD-A154624] N85-32222

COMPUTER GRAPHICS
User's guide for computer program CGFAG, Concrete General Flexure Analysis with Graphics [AD-A155555] N85-32204
Flexible satellite communications systems simulator, phase 3 [AD-A155647] N85-32247
Realizing the full potential of the video disc for mapping applications [AD-A154966] N85-32391
Real-time contour surface display generation [AD-A155232] N85-32780
DYNA3D, INGRID, and TAURUS: An integrated, interactive software system for crashworthiness engineering [DE85-010928] N85-32846
COMPUTER INFORMATION SECURITY
Security controls in the Stockpoint Logistics Integrated Communications Environment (SPLICE) [AD-A155536] N85-32244
Design guidelines for user-system interface software [AD-A154907] N85-32807
COMPUTER NETWORKS
Interactive on-line conferences [AD-A154723] N85-32227
A high-speed digital signal processor for atmospheric radar, part 7.3A N85-32525
Microcomputer network: Investigation and implementation [AD-A155631] N85-32826
Broadcasting topology and routing information in computer networks [AD-A155668] N85-32827
COMPUTER PROGRAMMING
Review of the psychological issues relating to the effectiveness of structured programming [AD-A154593] N85-32766
Ada (trademark) training curriculum. Advanced Ada topics L305 teacher's guide exercises [AD-A154621] N85-32798
SIGMA - A stochastic-integration global minimization algorithm [AD-A154878] N85-32806
Design guidelines for user-system interface software [AD-A154907] N85-32807
Experience with omega: Implementation of a prototype programming environment: Part 1 [AD-A155438] N85-32811
Evaluation of a software design approach: Develop a threat resolution module in Ada (trademark) [AD-A155599] N85-32815
A simple software environment based on objects and relations [AD-A155704] N85-32817
Microcomputer network: Investigation and implementation [AD-A155631] N85-32826
New developments on the core function for efficient implementation of the difficult residue number system operations [AD-A154678] N85-32834
Continued development of a data base management system performance monitor: Volume 1 [AD-A154635] N85-33040
COMPUTER PROGRAMS
Calculation of transonic steady and oscillatory pressures on a low aspect ratio model and comparison with experiment [NASA-TM-86449] N85-32092
Tip vortex computer code SRATIP. User's guide [NASA-CR-172603] N85-32093
Preliminary sizing and performance of aircraft [NASA-TM-86357] N85-32111
Component-specific modeling [NASA-CR-174925] N85-32119
Microprocessor control design for a low-head crossflow turbine [AD-A155477] N85-32121
Development and validation of a general purpose linearization program for rigid aircraft models [NASA-TM-86737] N85-32122
Development of reduced order models for control system design using the OPTSYSX program [AD-A154552] N85-32124
Myoelectric control of a computer based expert system for flight control [AD-A154981] N85-32126
MPS solidification model. Analysis and calculation of macrosegregation in a casting ingot [NASA-CR-171589] N85-32178
User's guide for computer program CGFAG, Concrete General Flexure Analysis with Graphics [AD-A155555] N85-32204
Fin line filters technology and electronic warfare [AD-A154975] N85-32237
Calculation of 3-D flow without numerical mixing N85-32301
SSMIR (Solid State Memory Instrumentation Recorder): A new approach to acquiring data during an aircraft seat/sled ejection sequence [AD-A154780] N85-32308
Plating density standards [DE85-010014] N85-32318
An investigation into the comparisons of the underwater shock effects on a stiffened flat plate to the predictive nature of a computer model [AD-A155612] N85-32355
Analysis of inclined growth of silicon sheet N85-32442
Assessment of the performance of an in-field Gaussian plume/puff model for overwater use [AD-A155435] N85-32460
Nuclear thermal transmittance in the atmosphere using LOWTRAN-6 computer code [AD-A154669] N85-32553
An evaluation of discretized conditional probability and linear regression threshold techniques in model output statistics forecasting of cloud amount and ceiling over the North Atlantic Ocean [AD-A155100] N85-32581
Analysis of spacecraft data [NASA-CR-171587] N85-32789
Analysis of spacecraft data [NASA-CR-171597] N85-32790
CARE 3 user friendly interface user's guide [NASA-CR-172608] N85-32791
Design of an expert-system flight status monitor [NASA-TM-86739] N85-32794
The NAS kernel benchmark program [NASA-TM-86711] N85-32795
Development of computer programs using the method of images to predict the sound field in a wedge overlaying a fast fluid and comparison with laboratory experiments [AD-A154580] N85-32797
An automated quality assurance surveillance plan for ADP (Automated Data Processing) operations under the Navy's commercial activities program [AD-A154767] N85-32802
The design and implementation of an object-oriented, production-rule interpreter [AD-A154769] N85-32803
Qualitative analysis of sign-bit processing [AD-A154776] N85-32804
The formal specification of an abstract machine: Design and implementation [AD-A155167] N85-32808
A comprehensive study of the AFIT (Air Force Institute of Technology) software development environment [AD-A155450] N85-32812
Survival function of hypo-exponential distributions [AD-A155518] N85-32814
A practical approach to Karmarkar's algorithm [AD-A155714] N85-32818
Praxis release notes, version 7.3 [DE85-011862] N85-32820
Discrete-element acoustic analysis of submerged structures using doubly asymptotic approximations [AD-A154959] N85-32987
Speech understanding research [AD-A155462] N85-32990
An EPR (Electron-Paramagnetic-Resonance) and ENDOR (Electron-Nuclear-Double-Resonance) study of ferroelectric ammonium sulfate [AD-A155580] N85-33033
Continued development of a data base management system performance monitor: Volume 1 [AD-A154635] N85-33040
COMPUTER STORAGE DEVICES
SSMIR (Solid State Memory Instrumentation Recorder): A new approach to acquiring data during an aircraft seat/sled ejection sequence [AD-A154780] N85-32308
Development of a dedicated speech work station [AD-A155465] N85-32824
COMPUTER SYSTEMS DESIGN
A high-speed digital signal processor for atmospheric radar, part 7.3A N85-32525
Comparative study on data system architectures --- spacecraft data processing [ESA-CR(P)-2015] N85-32828
COMPUTER SYSTEMS PERFORMANCE
The 8080 emulator N85-32783
The NAS kernel benchmark program [NASA-TM-86711] N85-32795
COMPUTER SYSTEMS PROGRAMS
HLLM software support [AD-A154828] N85-32805
Design guidelines for user-system interface software [AD-A154907] N85-32807
The effect of communication-language designs on software specifications [AD-A155173] N85-32809
Evaluation of a software design approach: Develop a threat resolution module in Ada (trademark) [AD-A155599] N85-32815
A simple software environment based on objects and relations [AD-A155704] N85-32817
DYNA3D, INGRID, and TAURUS: An integrated, interactive software system for crashworthiness engineering [DE85-010928] N85-32846
COMPUTER SYSTEMS SIMULATION
Construction of University of Missouri, Rolla's full scale cloud simulation chamber and applied research [AD-A154682] N85-32128
COMPUTER TECHNIQUES
USAFSAM review and analysis of radiofrequency radiation bioeffects literature [AD-A155113] N85-32760
Design guidelines for user-system interface software [AD-A154907] N85-32807
New developments on the core function for efficient implementation of the difficult residue number system operations [AD-A154678] N85-32834
Distributed name management [AD-A154785] N85-33037
COMPUTERIZED SIMULATION
Simulation studies of time-control procedures for the advanced air traffic control system [NASA-TP-2493] N85-32101
Development and validation of a general purpose linearization program for rigid aircraft models [NASA-TM-86737] N85-32122
Numerical modeling of subsurface communication [DE85-012818] N85-32249
Parallel simulation of digital LSI circuits [AD-A154745] N85-32258
BLAF: A blast field reconstruction program from pressure histories [AD-A155300] N85-32263
Characteristics of a numerical fluid dynamics simulator [DE85-009602] N85-32290
An investigation into the comparisons of the underwater shock effects on a stiffened flat plate to the predictive nature of a computer model [AD-A155612] N85-32355
Micromolecular modeling N85-32405
Comprehensive silicon solar-cell computer modeling N85-32421
Emergency modeling of hazardous air pollutants [AD-A155441] N85-32461
Simulation of complex three-dimensional flows [NASA-TM-86773] N85-32831
COMPUTERS
Proust radar: Decoding hardware and coherent integration, part 7.2A N85-32524
East Europe report: Science and technology. Selections on CSSR computer technology [JPRS-ESA-84-017] N85-32781
CONCENTRATION (COMPOSITION)
Concentrations of ice nuclei of different modes of activities N85-32616
Observations of the atmospheric ice nucleus at northwest China N85-32618
Concentration and source areas of ice nuclei in the Alaskan atmosphere N85-32634
Human activity and production rate of secondary nuclei N85-32645
On the transformation regularities of time series of solid aerosol concentrations in the surface atmospheric layer N85-32648
Variability of rural aerosols under stable weather conditions N85-32663
Marine aerosols at the Dutch North Sea coast: Size distributions and fractionation of trace elements N85-32664
A statistical study of CCN concentration in subequatorial climate: The particular case of the tropical wet forest N85-32673
Sulfur Cycle N85-32748
CONCENTRIC CYLINDERS
Acoustic radiation from concentric shells containing an inner fluid [AD-A155476] N85-32991
CONCRETES
User's guide for computer program CGFAG, Concrete General Flexure Analysis with Graphics [AD-A155555] N85-32204
Dynamic fracture of concrete and other heterogeneous materials [AD-A154513] N85-32343

CONCURRENT PROCESSING
Concurrent implementation of the Crank-Nicolson method for heat transfer analysis
[NASA-TM-86448] N85-32822
Simulation of complex three-dimensional flows
[NASA-TM-86773] N85-32831
CONDENSATES
Aitken particle size distribution in Antarctica N85-32656
Properties of forest derived cloud condensation nuclei N85-32682
Influence on an industrial site on the characteristics of CCN supersaturation with air masses of different origin N85-32683
CONDENSATION
Remarks on preparation of indandione detection reagents
[NASA-TM-77905] N85-32146
Eleventh International Conference on Atmospheric Aerosols, Condensation and Ice Nuclei, volume 2
[PB85-182418] N85-32596
Ice active bacteria as condensation nuclei N85-32603
Generation of lead, lead iodide and iodide aerosols and their ice nucleation N85-32607
Ice nucleus measurements N85-32609
Airborne measurements of atmospheric ice nuclei N85-32612
Aircraft observations of condensation and ice nuclei at a tropical station N85-32613
Supersaturation spect A of Ice Nuclei at different locations in Europe and over the North-Atlantic N85-32615
The nuclei of cloud formation N85-32685
Transport and formation of summertime cloud condensation nuclei over the Arctic Ocean N85-32686
A review on the formation of aerosol particles in the atmosphere N85-32687
The measured rate of condensation nucleation to droplets using the techniques of chemical kinetics N85-32694
The interaction of polynuclear aromatic hydrocarbons PAH's with water vapor and their role as condensation nuclei in the formation of haze and fog N85-32695
Applicability of surface CCN measurements N85-32696
on the transport of large condensation nuclei in the atmosphere at various altitudes over the territory of the USSR N85-32698
CONDENSATION NUCLEI
Measurements of giant salt nuclei from inland in east China N85-32668
Cloud condensation on insoluble particles N85-32670
Observations of cloud droplets, aerosol particles and cloud condensation nuclei in continental air masses N85-32671
A statistical study of CCN concentration in subequatorial climate: The particular case of the tropical wet forest N85-32673
Investigation of the formation of cloud particle spectrum on natural condensation nuclei N85-32674
A simple model to investigate the activation process in waterclouds N85-32675
A relationship between cloud droplet size and CCN critical supersaturation N85-32677
On the question to the effect of surfactants on the spectrum of cloud drops in the process of their condensation growth N85-32679
Aircraft observations of cloud condensation nuclei in maritime and continental environments N85-32680
The distribution of giant salt nuclei inside and outside cloud over the basin of Xin and Jiang N85-32681
CONDENSING
Construction of University of Missouri, Rolla's full scale cloud simulation chamber and applied research
[AD-A154682] N85-32128
The 100 years of Aitken Nuclei (AN) study-reminiscence, current and future problems N85-32621
Supersaturation obtained in a condensation nucleus counter N85-32624
Analysis of performance of dynamic thermal diffusion chamber N85-32625
A thermal diffusion chamber for the measurement of cloud condensation nuclei N85-32627
Critical supersaturations with respect to water for fast condensation-freezing ice nucleation N85-32632
Eleventh International Conference on Atmospheric Aerosols, Condensation and Ice Nuclei, volume 1
[PB85-182400] N85-32636
The first condensation nucleus conference N85-32637
Cloud condensation on insoluble particles N85-32670
Condensation properties of atmospheric aerosol N85-32672
CONFERENCES
VLF (Very low frequency) workshop held at San Diego California, 24-25 January 1985
[AD-A154652] N85-32224
Middle Atmosphere Program. Handbook for MAP. Volume 14: URSI/SCOSTEP Workshop on Technical Aspects of MST Radar
[NASA-CR-176085] N85-32466
Data base management: MSTRAC (keynote paper), part 8 N85-32530
Eleventh International Conference on Atmospheric Aerosols, Condensation and Ice Nuclei, volume 2
[PB85-182418] N85-32596
Eleventh International Conference on Atmospheric Aerosols, Condensation and Ice Nuclei, volume 1
[PB85-182400] N85-32636
Software for interactive on-line conferences
[AD-A154742] N85-32801
Workshop on the Early Earth: The Interval from Accretion to the Older Archean
[NASA-CR-176037] N85-33062
CONFIDENCE LIMITS
The optimality of lower confidence limits for the reliability of series systems obtained by the method of key test results or other related techniques
[AD-A154880] N85-32338
CONFINEMENT
Magnetics calculations for an ELMO Bumpy Square
[DE85-011438] N85-33021
CONGRESSIONAL REPORTS
Aviation system delays
[S-HRG-98-1241] N85-32102
Status of the air traffic control system
[GPO-40-343] N85-32107
Review of hazardous waste cleanup and disposal efforts at Tinker Air Force Base
[GPO-43-294] N85-32457
Hazardous air pollutants
[GPO-43-064] N85-32458
CONICAL BODIES
Aerodynamic characteristics of the standard dynamics model in coning motion at Mach 0.6
[NASA-TM-86717] N85-32094
CONICS
Trapping of ion conics by downward parallel electric fields
[AD-A155306] N85-32568
CONIFERS
Study of the formation of particles from natural hydrocarbons released by vegetation N85-32640
CONSERVATION
Basic cryogenics and materials. Phase 1
[NASA-CR-177932] N85-32215
CONSTANTS
Large-time behavior of viscous surface waves
[AD-A154805] N85-32278
On the turning lozange of constant side whose vertices alternate between two fixed circles of a ring
[AD-A154803] N85-32840
CONSTRAINTS
On the limiting configuration of interfacial gravity waves
[AD-A154821] N85-32557
Detector problems at the SSC
[DE85-010217] N85-33007
CONSTRUCTION
Construction of University of Missouri, Rolla's full scale cloud simulation chamber and applied research
[AD-A154682] N85-32128
Field testing of a lightweight relocatable structure in a temperate environment
[AD-A155171] N85-32350
Literature survey of underground construction methods for application to hardened facilities
[AD-A155212] N85-32351
CONSTRUCTION MATERIALS
Field testing of a lightweight relocatable structure in a temperate environment
[AD-A155171] N85-32350
CONTACTS (GEOLOGY)
The 3.5 b.y. old Onverwacht Group: A remnant of ancient oceanic crust N85-33073
CONTAMINANTS
New estimating procedures for surface runoff, sediment yield, and contaminant transport in Los Alamos County, New Mexico
[DE85-011890] N85-32393
CONTAMINATION
The influence of oil contamination on the nucleate pool-boiling behavior of R-114 from a structured surface
[AD-A155609] N85-32284
JPL in-house fluidized-bed reactor research N85-32414
CONTINENTS
The origin of continental crust: Outlines of a general theory N85-33083
Crustal radiogenic heat production and the selective survival of ancient continental crust N85-33086
CONTINUOUS RADIATION
A sampling phasemeter design for pulsed continuous wave signals
[AD-A155237] N85-32264
CONTINUOUS WAVE LASERS
High-power two-frequency CW dye laser N85-32900
CONTINUUM MECHANICS
Mechanics of near tip microcracking in brittle material
[AD-A154684] N85-32346
CONTOURS
Real-time contour surface display generation
[AD-A155232] N85-32780
CONTRACTORS
The flow of scientific and technical information in the US Army Research Laboratories
[AD-A155050] N85-33043
CONTRAST
Reconciling Bayesian and frequentist evidence in the one-sided testing program
[AD-A155603] N85-32850
CONTROL EQUIPMENT
Improved coordinate measuring machine calibration and control
[DE85-012053] N85-32315
Robots, Manipulators N85-32786
CONTROL SYSTEMS DESIGN
Performance improvements of a highly integrated digital electronic control system for an F-15 airplane
[NASA-TM-86748] N85-32120
A preliminary investigation of handling qualities requirements for helicopter instrument flight during decelerating approach maneuvers and overshoot
[AD-A154650] N85-32125
Research on an expert system for database operation of simulation-emulation math models. Volume 1, Phase 1: Results
[NASA-CR-176087] N85-32792
CONTROL THEORY
Robust control of multivariable and large space systems
[AD-A155117] N85-32140
CONTROLLED ATMOSPHERES
Hydroponics developments for spaceship garden N85-32754
CONTROLLERS
Microprocessor control design for a low-head crossflow turbine
[AD-A155477] N85-32121
Secure digital voice communications in the Defense Data Network (DDN)
[AD-A154677] N85-32226
CONVECTION
Automated cell detection as a mesocyclone precursor tool
[AD-A154952] N85-32577
On the problem of possible mechanism of ice nuclei formation in convective clouds N85-32610
Magnetic fields in laser heated plasmas
[DE85-010715] N85-33022
Solar convection
[AD-A155214] N85-33098
CONVECTION CLOUDS
Mesoscale features and atmospheric refraction conditions of the Arctic marginal ice zone
[AD-A155139] N85-32584
CONVECTION CURRENTS
Diagnostics of severe convection and subsynoptic scale ageostrophic circulations
[NASA-CR-171581] N85-32571
CONVECTIVE HEAT TRANSFER
Evaluation of the effects of roll angle on the natural convection heat transfer from an array of cylindrical spines
[AD-A154594] N85-32273
CONVERGENCE
On the dependence of the convergence of Gummel's algorithm on the regularity of the solution
[AD-A154628] N85-32632
COOLANTS
Resolution of thermal striping issue downstream of a horizontal pipe elbow in stratified pipe flow
[DE85-006195] N85-32292
COOLING
Observations of the use of the setapoint detector
[AD-A154533] N85-32208
COORDINATES
A note on a theorem of R. Duffin
[AD-A154786] N85-32838
COORDINATION
Improved coordinate measuring machine calibration and control
[DE85-012053] N85-32315

COPOLYMERS
Structure-property relationships in thermoplastic elastomers. Part 3: Segmented polyacetal-polyurethanes
[AD-A154897] N85-32200
COPPER
Electrodeposition of chromium and copper in magnetic fields
[AD-A154648] N85-32180
The effect of abrasive blasting on the fatigue and corrosion of an aluminium-copper alloy
[AD-A154954] N85-32182
Modification of the grain size of sputtered copper with additions of oxygen, krypton, silver, or yttrium
[DE85-010975] N85-32189
Plasma mass and effective inductance in a small railgun
[AD-A154644] N85-32304
CORONAL HOLES
Solar cycle variation of ephemeral regions
[AD-A154967] N85-33097
A study of the cyclical variations of coronal holes and their relation to open magnetic fields
[AD-A155251] N85-33099
CORRECTION
Computation of three-dimensional, inviscid, rotational flows N85-32296
CORRELATION
Effect of ions on cloud formation and its role in solar terrestrial relationship N85-32697
CORROSION
Decomposition of sulfuric acid using solar thermal energy
[DE85-012288] N85-32170
Understanding and laboratory prediction of the atmospheric corrosion behavior of steels and of non-ferrous metals and alloys
[AD-A154642] N85-32179
The effect of abrasive blasting on the fatigue and corrosion of an aluminium-copper alloy
[AD-A154954] N85-32182
Polymer-water interaction studies N85-32411
CORRUGATING
Microwave SAW (Surface Acoustic Wave) monochromator
[AD-D011718] N85-32311
COSMIC RAYS
Contributions to the 19th International Cosmic Ray Conference
[NASA-CR-176060] N85-33044
Cosmic ray He3 measurements
[PAPER-OG-4.2-3] N85-33045
Initial results from the Caltech/DSRI balloon-borne isotope experiment
[PAPER-OG-4.3-8] N85-33046
Measurements of Fe and Ar fragmentation cross sections
[PAPER-OG-7.2-20] N85-33047
Precision measurements of solar energetic particle elemental composition
[PAPER-SH-2.1-4] N85-33052
Research in extreme ultraviolet and far ultraviolet astronomy
[NASA-CR-176068] N85-33060
Research in particles and fields
[NASA-CR-176069] N85-33103
COST ANALYSIS
Pricing options for the space shuttle. Special study N85-32138
High-efficiency crystalline silicon technology development N85-32395
Flat-plate module efficiency versus cost tradeoffs N85-32398
Los Alamos optical materials reliability, maintainability, and exposure testing program
[DE85-011894] N85-32456
Tritium technology review
[DE85-010504] N85-33006
Feasibility of applications of Competition Decision Assist Package (CDAP) to spare parts
[AD-A154716] N85-33036
The Human Resource Management Information Network (HRMIN): A cost comparison in accordance with Office of Management and Budget (OMB) Circular no. A-76, 5 April 1979
[AD-A154583] N85-33039
COST EFFECTIVENESS
The future of crystalline silicon technology in the US Department of Energy program N85-32399
Advanced module development overview N85-32445
The effect of communication-language designs on software specifications
[AD-A155173] N85-32809
Feasibility of applications of Competition Decision Assist Package (CDAP) to spare parts
[AD-A154716] N85-33036
The Human Resource Management Information Network (HRMIN): A cost comparison in accordance with Office of Management and Budget (OMB) Circular no. A-76, 5 April 1979
[AD-A154583] N85-33039
COST ESTIMATES
Pricing options for the space shuttle. Special study N85-32138
Clarke Stations and mercurian mass-drivers: Energy for large-scale transportation systems
[DE85-009607] N85-32145
COULOMETRY
Electrochemistry of Hexanitroazobenzene (HNAB)
[DE85-010807] N85-32171
COUNTERS
The 100 years of Aitken Nuclei (AN) study-reminiscence, current and future problems N85-32621
Supersaturation obtained in a condensation nucleus counter N85-32624
CRACK INITIATION
A cracked orthotropic sheet stiffened by a semi-infinite orthotropic sheet
[NASA-TP-2455] N85-32339
CRACK PROPAGATION
Metallurgical origins of fracture toughness and microstructure and fracture toughness of an HSLA (High-Strength/Low-Alloy) steel
[AD-A155530] N85-32187
Stress corrosion of ceramic materials
[AD-A155020] N85-32202
A cracked orthotropic sheet stiffened by a semi-infinite orthotropic sheet
[NASA-TP-2455] N85-32339
Measurement and analysis of critical crack tip processes during fatigue crack growth
[NASA-CR-172597] N85-32342
CRACK TIPS
A cracked orthotropic sheet stiffened by a semi-infinite orthotropic sheet
[NASA-TP-2455] N85-32339
CRASH LANDING
Air carrier overwater emergency equipment and procedures
[PB85-917006] N85-32105
CRASHWORTHINESS
The role of aircraft panel materials in cabin fires and their properties
[FAA-CT-84-30] N85-32104
Seat experiments for the full-scale transport aircraft controlled impact demonstration
[AD-A155024] N85-32106
DYNA3D, INGRID, and TAURUS: An integrated, interactive software system for crashworthiness engineering
[DE85-010928] N85-32846
CREEP PROPERTIES
The effect of stress and hot corrosion on nickel-base superalloys
[AD-A154722] N85-32181
CREEP STRENGTH
The effect of stress and hot corrosion on nickel-base superalloys
[AD-A154722] N85-32181
CREEP TESTS
The effect of stress and hot corrosion on nickel-base superalloys
[AD-A154722] N85-32181
A continuous damage model based on stepwise-stress creep rupture tests
[NASA-CR-174941] N85-32341
CREWS
A crew exposure study. Phase II. Volume 2. At sea. Part A
[AD-A155233] N85-32774
CRITICAL PRESSURE
Liquid-phase compositions from vapor-phase analyses 2: Adaptation of the Prausnitz program to UF6 and some of its potential impurities
[DE85-011521] N85-32819
CROSS FLOW
Microprocessor control design for a low-head crossflow turbine
[AD-A155477] N85-32121
CRUDE OIL
A crew exposure study. Phase II. Volume 2. At sea. Part A
[AD-A155233] N85-32774
CRUSTAL FRACTURES
Megageomorphology and neotectonics N85-32366
CRYOGENIC EQUIPMENT
Vapor-liquid phase separator studies
[NASA-CR-166545] N85-32272
CRYOGENIC FLUID STORAGE
Vapor-liquid phase separator studies
[NASA-CR-166545] N85-32272
CRYOGENIC FLUIDS
Basic cryogenics and materials. Phase 1
[NASA-CR-177932] N85-32215
CRYOGENIC WIND TUNNELS
A systematic plan for the continued study of dimensional stability of metallic alloys considered for the fabrication of cryogenic wind tunnel models
[NASA-CR-172449] N85-32172
CRYOGENICS
Capacitive energy storage at cryogenic temperatures
[AD-A154508] N85-32253
SCRIBE data of October 23, 1983 flight
[AD-A154864] N85-33012
CRYPTOGRAPHY
Security controls in the Stockpoint Logistics Integrated Communications Environment (SPLICE)
[AD-A155536] N85-32244
CRYSTAL DEFECTS
Studies of oxygen- and carbon-related defects in high-efficiency silicon solar cells N85-32420
High-purity silicon crystal growth N85-32444
Defect formation in amorphous hydrated silicon subjected to laser radiation N85-32873
An EPR (Electron-Paramagnetic-Resonance) and ENDOR (Electron-Nuclear-Double-Resonance) study of ferroelectric ammonium sulfate
[AD-A155580] N85-33033
CRYSTAL GROWTH
High-frequency furnace
[DE85-011210] N85-32291
Silicon production in an aerosol reactor N85-32416
Silicon dendritic web growth N85-32435
Temperature-stress modeling N85-32436
Silicon ribbon stress-strain activities N85-32437
Analysis of stress-strain relationships in silicon ribbon N85-32438
Stress and buckling analysis N85-32439
Stress and efficiency studies in EFG N85-32440
Silicon sheet surface studies N85-32441
Analysis of inclined growth of silicon sheet N85-32442
Edge-defined film-fed growth of thin silicon sheets N85-32443
High-purity silicon crystal growth N85-32444
Failure analysis of thin-film amorphous-silicon solar-cell modules N85-32452
Ice crystal nucleation on hygroscopic aerosols N85-32605
The nucleation of ice crystals during the freezing of large supercooled drops N85-32606
X-ray diffractometric measurements and calculations of limiting values of discrepancy between lattices and layer thicknesses, preventing generation of dislocations during growth of multilayer heterostructures N85-32866
Nonequilibrium kinetics of growth of oxide layer grains during laser heating of metals in air N85-32919
The development and evaluation of point defect models for the growth of passive films on single crystal, polycrystalline, and amorphous metal surfaces
[AD-A154685] N85-33023
Chemical constraints on the evolution of Archean continental crust N85-33093
CRYSTAL LATTICES
Interfacial bonding stability N85-32409
Raman scattering studies in solids
[AD-A155528] N85-33032
CRYSTAL OPTICS
Generation and amplification of radiation during stimulated Raman scattering in crystals N85-32869
CRYSTAL STRUCTURE
Z-contrast imaging and electron channeling analysis of dopants in semiconductors
[DE85-011410] N85-32269
Silicon dendritic web growth N85-32435
Temperature-stress modeling N85-32436
Silicon ribbon stress-strain activities N85-32437
Analysis of stress-strain relationships in silicon ribbon N85-32438
Stress and buckling analysis N85-32439
Stress and efficiency studies in EFG N85-32440
Silicon sheet surface studies N85-32441
Analysis of inclined growth of silicon sheet N85-32442
Edge-defined film-fed growth of thin silicon sheets N85-32443
High-purity silicon crystal growth N85-32444
Influence on bi-phonon states on Raman scattering of light in molecular crystals N85-32865
X-ray diffractometric measurements and calculations of limiting values of discrepancy between lattices and layer thicknesses, preventing generation of dislocations during growth of multilayer heterostructures N85-32866
Classical emission of relativistic charged particles during axial channeling N85-32871

Influence of background electrically neutral argon admixture on mechanical strength of silicon crystals N85-32878

Low-threshold injection InGaAsP/GaAs double heterostructure lasers with separate limiting obtained by liquid-phase epitaxy (lambda = 0.78 divided by 0.87 microns, I sub thr = 460 A/cm 2, T = 300 K) N85-32908

An EPR (Electron-Paramagnetic-Resonance) and ENDOR (Electron-Nuclear-Double-Resonance) study of ferroelectric ammonium sulfate [AD-A155580] N85-33033

CRYSTAL SURFACES

The development and evaluation of point defect models for the growth of passive films on single crystal, polycrystalline, and amorphous metal surfaces [AD-A154685] N85-33023

CRYSTALLIZATION

Interaction of solutes with stretched polymers [AD-A154662] N85-32196

Introduction of structural variations into oxide polymers and their effect on sintering and crystallization [AD-A155597] N85-32206

A fluidized-bed reactor for silane pyrolysis N85-32413

CRYSTALLOGRAPHY

X-ray diffractometric measurements and calculations of limiting values of discrepancy between lattices and layer thicknesses, preventing generation of dislocations during growth of multilayer heterostructures N85-32866

CRYSTALS

High temperature electronics technology: Life test report [AD-A154681] N85-32257

Monte Carlo studies of H2O layers adsorbed on a model basal face of AgI N85-32633

USSR report: Physics and mathematics [JPRS-UPM-85-004] N85-32860

Lasing on LiF:F(-)2 - dye centers with transverse pumping N85-32890

The problem of brightness enhancement during laser frequency doubling N85-32897

CULTURE TECHNIQUES

Chemolithotrophy and physiology of bacterial nutrient limitation N85-32730

Microbial colonization and growth on metal sulfides and other mineral surfaces N85-32747

CUMULUS CLOUDS

Aircraft investigations of the distribution of aerosols in the lower troposphere N85-32659

CURRENT DENSITY

Detection of excited states by laser-induced fluorescence [AD-A155558] N85-32326

Influence of technological factors on luminescence characteristics of InGaAsP/InP heterolasers (lambda = 1.55 microns) N85-32910

CURRENT SHEETS

Contributions to the 19th International Cosmic Ray Conference [NASA-CR-176060] N85-33044

Differential measurement of cosmic-ray gradient with respect to interplanetary current sheet [PAPER-SH-4.2-9] N85-33055

CYANO COMPOUNDS

Protocyanobacteria: Oxygenic and Anoxygenic photosynthesis in mat-forming bacteria N85-32714

Sulfur transformations at the hydrogen sulfide/oxygen interface in stratified waters and in cyanobacterial mats N85-32715

CYANOGEN

Cyanobacterial mats: Microanalysis of community metabolism N85-32743

Microanalysis of dissolved iron and phosphate in pore waters of hypersaline sediment N85-32744

Glutathione in cyanobacteria N85-32745

CYCLES

Possible roles of manganese redox chemistry in the sulfur cycle N85-32731

Biogeochemical cycling and remote sensing N85-32733

Phototrophic bacteria and their role in the biogeochemical sulfur cycle N85-32735

Sulfur cycling and metabolism of phototrophic and filamentous sulfur bacteria N85-32737

CYCLIC COMPOUNDS

Synthesis of energetic materials [AD-A154887] N85-32210

Influence of particle arrangement on sintering [AD-A155337] N85-32352

CYCLIC HYDROCARBONS

Synthesis of energetic materials [AD-A154887] N85-32210

CYCLIC LOADS

Results of an interlaboratory fatigue test program conducted on alloy 800H at room and elevated temperatures [NASA-CR-174940] N85-32340

CYCLOGENESIS

A numerical and analytical investigation of lee cyclogenesis [AD-A155607] N85-32594

CYCLONES

Real-time automated detection of mesocyclones and tornado vortex signatures [AD-A154968] N85-32578

Forecasting of tropical cyclone motion using an EOF (Empirical Orthogonal Function) representation of wind forcing [AD-A155034] N85-32580

CYCLOTRON RADIATION

Activation analysis of natural water using neutrons of various energies N85-32924

Diamagnetic instability of cyclotron waves in plasma N85-32948

Electrostatic ion cyclotron instability due to a nonuniform electric field perpendicular to the external magnetic field [AD-A155474] N85-33019

CYCLOTRON RESONANCE

Electromagnetic wave amplification during cyclotron resonance in a medium N85-32942

Influence of ECR-heating on MHD activity of plasma in tokamak-10 installation N85-32949

Cyclotron resonance in a nonneutral plasma [AD-A155248] N85-33017

CYCLOTRONS

Cyclotron absorption of fast magnetosonic wave in stellarator N85-32945

Low frequency instabilities driven by an ion temperature anisotropy [AD-A154902] N85-33016

CYLINDRICAL BODIES

The effect of stress and hot corrosion on nickel-base superalloys [AD-A154722] N85-32181

TNT equivalency of EAK explosive [AD-A155737] N85-32211

Evaluation of the effects of roll angle on the natural convection heat transfer from an array of cylindrical spines [AD-A154594] N85-32273

CYLINDRICAL SHELLS

Acoustic wave scattering by round cylindrical shell reinforced with stringers N85-32916

Iteration solution for a submerged force-driven finite cylinder [AD-A154587] N85-32982

Acoustic radiation from concentric shells containing an inner fluid [AD-A155476] N85-32991

CYTOCHROMES

Cytochromes and iron sulfur proteins in sulfur metabolism of phototrophic bacteria N85-32718

CYTOPLASM

Physical chemical state of water in living cells [AD-A154566] N85-32749

D

DAMAGE

A continuous damage model based on stepwise-stress creep rupture tests [NASA-CR-174941] N85-32341

DAMAGE ASSESSMENT

Theoretical modeling of laser induced optical degradation [AD-A155302] N85-32323

DAMPING

Measurement of damping of graphite epoxy materials [NASA-CR-176073] N85-32334

Nonradiative damping of molecular electronic excited states by metal surfaces [AD-A154619] N85-32994

DAMPING TESTS

Measurement of damping of graphite epoxy materials [NASA-CR-176073] N85-32334

DARK ADAPTATION

Glutathione in cyanobacteria N85-32745

DATA ACQUISITION

SSMIR (Solid State Memory Instrumentation Recorder): A new approach to acquiring data during an aircraft seat/sled ejection sequence [AD-A154780] N85-32308

Microcomputer processing of LANDSAT Thematic Mapper data for the acquisition of military tactical terrain data [AD-A154781] N85-32389

Problems and solutions in analyzing partial-reflection drift data by correlation techniques N85-32529

Continued development of a data base management system performance monitor: Volume 1 [AD-A154635] N85-33040

DATA BASE MANAGEMENT SYSTEMS

Data base management: MSTRAC (keynote paper), part 8 N85-32530

Analysis of spacecraft data [NASA-CR-171587] N85-32789

The architectural requirements and integration analysis of a database server for office automation [AD-A155517] N85-32825

Continued development of a data base management system performance monitor: Volume 1 [AD-A154635] N85-33040

Investigation of DBMS (Data Base Management Systems) for use in a research environment [AD-A154862] N85-33042

DATA BASES

Realizing the full potential of the video disc for mapping applications [AD-A154966] N85-32391

A transportable, machine oriented library of european sky and terrain radiance distributions with contemporary radiometric and meteorological profiles [AD-A155254] N85-32590

USAFSAM review and analysis of radiofrequency radiation bioeffects literature [AD-A155113] N85-32760

Research on an expert system for database operation of simulation-emulation math models. Volume 1, Phase 1: Results [NASA-CR-176087] N85-32792

The architectural requirements and integration analysis of a database server for office automation [AD-A155517] N85-32825

Investigation of DBMS (Data Base Management Systems) for use in a research environment [AD-A154862] N85-33042

DATA LINKS

Broadcasting topology and routing information in computer networks [AD-A155668] N85-32827

DATA MANAGEMENT

Distributed name management [AD-A154785] N85-33037

DATA PROCESSING

Overview of on-line data processing for MST radars (keynote paper), part 7 N85-32519

The Norwegian seismic array (NORSAR) [AD-A154751] N85-32555

Analysis of spacecraft data [NASA-CR-171597] N85-32790

An automated quality assurance surveillance plan for ADP (Automated Data Processing) operations under the Navy's commercial activities program [AD-A154767] N85-32802

Design guidelines for user-system interface software [AD-A154907] N85-32807

DATA PROCESSING TERMINALS

Secure digital voice communications in the Defense Data Network (DDN) [AD-A154677] N85-32226

DATA REDUCTION

Use of MMLE3 to determine lower order equivalent systems in the time domain [AD-A154700] N85-32112

In-situ measurement of wall thermal performance: Data interpretation and apparatus design recommendations [DE85-011979] N85-32289

SSMIR (Solid State Memory Instrumentation Recorder): A new approach to acquiring data during an aircraft seat/sled ejection sequence [AD-A154780] N85-32308

A modified Fresnel scattering model for the parameterization of Fresnel returns, part 2.3A N85-32483

Overview of on-line data processing for MST radars (keynote paper), part 7 N85-32519

Analysis of spacecraft data [NASA-CR-171597] N85-32790

DATA RETRIEVAL

Sample interchange of MST radar data from the Urbana radar N85-32531

DATA SIMULATION

Calibration and use of clutter data for simulation [AD-A154793] N85-32229

DATA STORAGE

Characteristics of a numerical fluid dynamics simulator [DE85-009602] N85-32290

Problems and solutions in analyzing partial-reflection drift data by correlation techniques N85-32529

Sample interchange of MST radar data from the Urbana radar N85-32531

Development of a dedicated speech work station
[AD-A155465] N85-32824

DATA TRANSMISSION
Proust radar: Decoding hardware and coherent integration, part 7.2A N85-32524
Design guidelines for user-system interface software
[AD-A154907] N85-32807

DECAY
Aircraft investigations of the distribution of aerosols in the lower troposphere N85-32659

DECISION MAKING
Interactive on-line conferences
[AD-A154723] N85-32227

DECODING
Proust radar: Decoding hardware and coherent integration, part 7.2A N85-32524

DECOMPOSITION
Decomposition of sulfuric acid using solar thermal energy
[DE85-012288] N85-32170
Decomposing the joint distribution of several linear combinations of uniform spacings
[AD-A155056] N85-32845

DECOUPLING
On the dependence of the convergence of Gummel's algorithm on the regularity of the solution
[AD-A154628] N85-32832

DEFECTS
Experimental and theoretical assessment of a new technique for the non-destructive evaluation of laminated panels
[AD-A155622] N85-32155
Defects in tetrahedrally coordinated amorphous semiconductors
[AD-A155150] N85-32263
Reliability of void detection in structural ceramics using scanning laser acoustic microscopy
[NASA-TM-87035] N85-32337

DEFENSE PROGRAM
Evaluation of a software design approach: Develop a threat resolution module in Ada (trademark)
[AD-A155599] N85-32815
The flow of scientific and technical information in the US Army Research Laboratories
[AD-A155050] N85-33043

DEFLECTION
A comparison of electronic heterodyne moire deflectometry and electronic heterodyne holographic interferometry for flow measurements
[NASA-TM-87071] N85-32302
Basic formulae for the computation of the deflection of the vertical from astronomical star observations
[AD-A154912] N85-32390

DEFORMATION
Machining-induced deformation in stepped specimens of PH 13-8 Mo, 18 nickel maraging steel grade 200T1 and grain-refined HP 9-4-20
[NASA-CR-172450] N85-32177
Bubble dynamics in polymer solutions undergoing shear
[AD-A154575] N85-32193
The effect of mould size on the exothermic reaction and compressive strength of epoxy resin chocks
[AD-A155102] N85-32203
A comparison of electronic heterodyne moire deflectometry and electronic heterodyne holographic interferometry for flow measurements
[NASA-TM-87071] N85-32302
Development of improved dynamic failure models
[AD-A155586] N85-32354
Local epi-continuity and local optimization
[AD-A154812] N85-32843

DEGASSING
The degassing history of the Earth: Noble gas studies of Archaean cherts and zero age glassy submarine basalts N85-33072

DEGRADATION
Theoretical modeling of laser induced optical degradation
[AD-A155302] N85-32323
Topics in electrochemical degradation of photovoltaic modules N85-32410
Accelerated stress factors and failure/degradation mechanisms in terrestrial solar cells N85-32451

DELAY
Aviation system delays
[S-HRG-98-1241] N85-32102

DELTA WINGS
China has developed a new version of fighter aircraft
[AD-A155293] N85-32118

DENDRITIC CRYSTALS
Silicon dendritic web growth N85-32435
Temperature-stress modeling N85-32436
Silicon ribbon stress-strain activities N85-32437
Analysis of stress-strain relationships in silicon ribbon N85-32438
Advanced module development overview N85-32445

DENSITOMETERS
Applied research and development for falling-sphere air density measuring systems
[AD-A155227] N85-32099

DENSITY (MASS/VOLUME)
An investigation into the fluidization and heat transfer of low density particles in a fluidized bed with applications
[AD-A155259] N85-32282
A safe, high-power-density lithium battery
[AD-A155223] N85-32454
Buoyant densities of phototrophic sulfur bacteria and cyanobacteria N85-32740

DENSITY MEASUREMENT
Applied research and development for falling-sphere air density measuring systems
[AD-A155227] N85-32099
Application of satellite accelerometer data to improve density models
[AD-A154904] N85-32558

DEOXYGENATION
Noble gases and the early history of the Earth: Inappropriate paradigms and assumptions inhibit research and communication N85-33075

DEPENDENCE
A modified Fresnel scattering model for the parameterization of Fresnel returns, part 2.3A N85-32483
Observations of mesospheric turbulence by rocket probe and VHF radar, part 2.4A N85-32484
On the dependence of the convergence of Gummel's algorithm on the regularity of the solution
[AD-A154628] N85-32832

DEPOSITION
Modification of the grain size of sputtered copper with additions of oxygen, krypton, silver, or yttrium
[DE85-010975] N85-32189
Laser-assisted solar-cell metallization processing N85-32429
Microwave-enhanced thin-film deposition N85-32431
Experimental studies of the kinetics of deposition nucleation on an ice nucleant used in weather modification N85-32598
Ice nucleus measurements N85-32609
Geology and geochemistry of sulfide and sulfate deposition N85-32723
Archean sedimentary systems and crustal evolution N85-33082

DESALINIZATION
Feasibility study for small group water desalination equipment
[AD-A155106] N85-32164

DESIGN ANALYSIS
A small-scale self-excited rotor electrostatic generator
[AD-A155264] N85-32265
Sensitivity analysis of high-efficiency silicon solar-cell design parameters N85-32422

DESTRUCTIVE TESTS
Seat experiments for the full-scale transport aircraft controlled impact demonstration
[AD-A155024] N85-32106

DETECTION
Experimental and theoretical assessment of a new technique for the non-destructive evaluation of laminated panels
[AD-A155622] N85-32155
A microprocessor-controlled, multichannel fluorimeter for analysis of sea water
[AD-A154986] N85-32310
Detection of excited states by laser-induced fluorescence
[AD-A155558] N85-32326
Automated cell detection as a mesocyclone precursor tool
[AD-A154952] N85-32577
Real-time automated detection of mesocyclones and tornado vortex signatures
[AD-A154968] N85-32578
Resource management for the tagged token dataflow architecture
[AD-A154773] N85-32779
Analysis of unreplicated factorials allowing for possibly faulty observations
[AD-A154813] N85-32848
An attempt to detect induced neutron capture in laser radiation field N85-32928

DETECTORS
Kalman filter time series analysis of gamma-ray data from NaI(T1) detectors for the ND6620 computer
[AD-A154995] N85-33014

DETONATION WAVES
The 2-D simulations of the NRL (Naval Research Laboratory) laser experiment
[AD-A154915] N85-32321

DF LASERS
Ship-to-ship propagation: Maritime data analyses
[AD-A155484] N85-32325

DIAGNOSIS
Remote medical diagnosis N85-32753

DIAMAGNETISM
Diamagnetic instability of cyclotron waves in plasma N85-32948

DIAMINES
Remarks on preparation of indandione detection reagents
[NASA-TM-77905] N85-32146

DIATOMIC MOLECULES
Vibrationally enhanced dissociation of diatomic molecules
[AD-A154827] N85-32996

DICHROISM
Multidimensional luminescence measurements
[AD-A154950] N85-32162

DIELECTRIC POLARIZATION
Interaction of solutes with stretched polymers
[AD-A154662] N85-32196

DIELECTRICS
Guided-mode launching in a slab waveguide by way of diffraction at the edge of a conducting screen residing on one surface of the slab
[AD-A154886] N85-32232

DIFFERENCE EQUATIONS
Non-model based estimation with applications to sensor calibration using multiple sensors
[AD-A154736] N85-32306

DIFFERENTIAL EQUATIONS
Development of reduced order models for control system design using the OPTSYSX program
[AD-A154552] N85-32124
Size spectra for the source-enhanced coagulation with the turbulent mass transfer N85-32649
SIGMA - A stochastic-integration global minimization algorithm
[AD-A154878] N85-32806
Identification of unsteady aerodynamics and aeroelastic integro-differential systems
[NASA-TM-86749] N85-32851
Exact solutions of singular equations for viscous transsonic flows N85-32882

DIFFRACTION
Guided-mode launching in a slab waveguide by way of diffraction at the edge of a conducting screen residing on one surface of the slab
[AD-A154886] N85-32232
Optical image of bounded objects N85-32968

DIFFUSION
Permeation of mixed penetrants through glassy polymer membranes
[AD-A155605] N85-32207
A multilevel-multigrid method for recirculating flows N85-32271
Simultaneous junction formation N85-32426
Notes on atmospheric stability, turbulence, and its measurements
[AD-A155230] N85-32585
Scavenging of submicron aerosol particles by snow crystals: Theory and experiments N85-32667

DIFFUSION COEFFICIENT
Relaxation lens in inhomogeneous binary mixture N85-32957

DIFFUSION THEORY
Oscillatory solutions of the Peaceman-Rachford alternating direction implicit method and a comparison of methods for the solution of the two dimensional heat diffusion equation
[AD-A154670] N85-32833

DIGITAL DATA
A high-speed digital signal processor for atmospheric radar, part 7.3A N85-32525

DIGITAL FILTERS
Application of adaptive noise cancellation to Coast Guard voice communications
[AD-A154798] N85-32230

DIGITAL SIMULATION
Flexible satellite communications systems simulator, phase 3
[AD-A155647] N85-32247
Research on an expert system for database operation of simulation-emulation math models. Volume 1, Phase 1: Results
[NASA-CR-176087] N85-32792
Research on an expert system for database operation of simulation-emulation math models. Volume 2, Phase 1: Results
[NASA-CR-176088] N85-32793

DIGITAL SYSTEMS
Performance improvements of a highly integrated digital electronic control system for an F-15 airplane
[NASA-TM-86748] N85-32120

Myoelectric control of a computer based expert system for flight control
[AD-A154981] N85-32126
Design of a jamming simulator for a binary communication system
[AD-A154617] N85-32221
Globally-asynchronous locally-synchronous systems
[AD-A154624] N85-32222
Secure digital voice communications in the Defense Data Network (DDN)
[AD-A154677] N85-32226
Experimental evaluation of a new form of M-ary (M = 8) phase shift keying including design of the transmitter and receiver
[AD-A155103] N85-32239
Microcomputer processing of LANDSAT Thematic Mapper data for the acquisition of military tactical terrain data
[AD-A154781] N85-32389
Realizing the full potential of the video disc for mapping applications
[AD-A154966] N85-32391
Bayesian vs MAP multiple model adaptive estimation for field of view expansion in tracking airborne targets
[AD-A155466] N85-32855

DIMENSIONAL STABILITY
A systematic plan for the continued study of dimensional stability of metallic alloys considered for the fabrication of cryogenic wind tunnel models
[NASA-CR-172449] N85-32172

DIMENSIONS
A simulation study of Sylvester's problem in three dimensions
[AD-A155266] N85-32854
Photo-acoustic effect in finite-dimensional semiconductors N85-32876

DIODES
Resistance of polyaniline films as a function of electrochemical potential and the fabrication of polyaniline-based microelectronic devices
[AD-A154999] N85-32201
A microprocessor-controlled, multichannel fluorimeter for analysis of sea water
[AD-A154986] N85-32310
T/R switch design for short-range measurements, part 6.1A N85-32515

DIPOLE ANTENNAS
Artificial and natural icing tests YEH-60A quick fix helicopter
[AD-A155147] N85-32116

DIPOLES
Testing and optimizing MST coaxial collinear arrays, part 6.4A N85-32518

DIRECT CURRENT
A small-scale self-excited rotor electrostatic generator
[AD-A155264] N85-32265
Optical output stabilization method for direct current arc lamps
[AD-A154987] N85-33013

DIRECTION FINDING
The moving thermoacoustic array: A theoretical feasibility study
[AD-A154510] N85-32980

DIRECTIONAL SOLIDIFICATION (CRYSTALS)
MPS solidification model. Analysis and calculation of macrosegregation in a casting ingot
[NASA-CR-171589] N85-32178

DIRECTORIES
Worldwide directory of national Earth-science agencies and related international organizations
[GS-CIRC-934] N85-32386

DISASTERS
Hazardous air pollutants
[GPO-43-064] N85-32458

DISCRIMINANT ANALYSIS (STATISTICS)
Forecasting atmospheric visibility over the summer north Atlantic using the principal discriminant method
[AD-A155537] N85-32593

DISPENSERS
The effect of metal overlayers of thermionic dispenser cathodes
[AD-A154795] N85-32995

DISPERSING
Assessment of the performance of an in-field Gaussian plume/puff model for overwater use
[AD-A155435] N85-32460
Investigation of the formation of cloud particle spectrum on natural condensation nuclei N85-32674

DISPERSIONS
Transmission of light by disperse medium of densely packed optically soft particles N85-32969

DISPLACEMENT MEASUREMENT
Improved coordinate measuring machine calibration and control
[DE85-012053] N85-32315
Possibility of measurement of small displacements by ring laser N85-32904

DISPLAY DEVICES
Advanced simulator for pilot training and helmet-mounted visual display configuration comparisons
[AD-A155326] N85-32776
Design guidelines for user-system interface software
[AD-A154907] N85-32807

DISSIPATION
Evaluation of the effects of roll angle on the natural convection heat transfer from an array of cylindrical spines
[AD-A154594] N85-32273

DISSOCIATION
Vibrationally enhanced dissociation of diatomic molecules
[AD-A154827] N85-32996

DISTANCE MEASURING EQUIPMENT
Comparison of survey and photogrammetry methods to position gravity data, Yucca Mountain, Nevada
[DE85-011685] N85-32316

DISTRIBUTED PROCESSING
Consensus in the presence of partial synchrony (Preliminary version)
[AD-A154705] N85-32799
Comparative study on data system architectures --- spacecraft data processing
[ESA-CR(P)-2015] N85-32828
A new fault-tolerant algorithm for clock synchronization
[AD-A154771] N85-32836

DISTRIBUTION FUNCTIONS
Antistarshapedness, dispersiveness and mixtures
[AD-A155583] N85-32849

DITCHING (LANDING)
Air carrier overwater emergency equipment and procedures
[PB85-917006] N85-32105

DIURNAL VARIATIONS
The diurnal variation of the neutral sodium species in the upper atmosphere: A model study
[AD-A154988] N85-32561
A study of time transformation of natural photochemical aerosols N85-32644

DMSP SATELLITES
Fluxgate magnetometer (SSM) for the defense meteorological satellite program (DMSP) block 5D-2, flight 7
[AD-A155229] N85-32143

DOCUMENTATION
The documentation assistant: An intelligent system for documentation
[AD-A154709] N85-32800

DOMAINS
Use of MMLE3 to determine lower order equivalent systems in the time domain
[AD-A154700] N85-32112

DOPED CRYSTALS
Z-contrast imaging and electron channeling analysis of dopants in semiconductors
[DE85-011410] N85-32269
Physics of heavily doped silicon and solar-cell parameter measurement N85-32418
Influence of background electrically neutral argon admixture on mechanical strength of silicon crystals N85-32878
Doping superlattices in organometallic VPE InP
[AD-A155151] N85-33029

DOPES
Molecular orbital studies in oxidation: Sulfate formation and metal-metal oxide adhesion
[NASA-CR-176070] N85-32174

DOPPLER EFFECT
A derivation of relativistic effects in satellite tracking
[AD-A154620] N85-32132
Accuracy of velocity and power determination by the Doppler method N85-32493
Coding schemes for improving MST radar performance, part 7.1A N85-32520
The moving thermoacoustic array: A theoretical feasibility study
[AD-A154510] N85-32980

DOPPLER RADAR
Middle Atmosphere Program. Handbook for MAP. Volume 14: URSI/SCOSTEP Workshop on Technical Aspects of MST Radar
[NASA-CR-176085] N85-32466
Observations of frontal zone structures with a VHF Doppler radar and radiosondes, part 1.2A N85-32469
Performance of the Colorado wind-profiling network, part 1.5A N85-32475
Relationship of spaced antenna and Doppler techniques for velocity measurements (keynote paper), part 3 N85-32488
On the spectrum of atmospheric velocity fluctuations seen by MST/ST radar and their interpretation N85-32504
Coding schemes for improving MST radar performance, part 7.1A N85-32520
Real-time automated detection of mesocyclones and tornado vortex signatures
[AD-A154968] N85-32578

DOSIMETERS
Results from radiation monitoring equipment experiments on STS-41C, 41D, 41G and 51A
[AD-A154676] N85-32142
A crew exposure study. Phase II. Volume 2. At sea. Part A
[AD-A155233] N85-32774
Paired ion chamber constants for fission gamma-neutron fields
[AD-A155069] N85-32999
A practical guide to ionization chamber dosimetry at the AFRRI reactor
[AD-A155185] N85-33003

DRAG REDUCTION
Injection of drag reducing additives into turbulent water flows: Two-component velocity measurements and mixing length model predictions
[AD-A154604] N85-32274
Experiments on the influence of active walls on the initial amplitudes and growths of instability waves
[AD-A154630] N85-32275

DRAINAGE
Geomorphic analyses from space imagery N85-32374
New estimating procedures for surface runoff, sediment yield, and contaminant transport in Los Alamos County, New Mexico
[DE85-011890] N85-32393

DRIFT (INSTRUMENTATION)
Criteria for optimum spacing of spaced antenna, part 3.2A N85-32491
Problems and solutions in analyzing partial-reflection drift data by correlation techniques N85-32529

DRIFT RATE
Test evaluation of the Honeywell GG1111 Single-Degree-of-Freedom (SDF) strapdown gyroscope
[AD-A154768] N85-32307

DROP SIZE
A relationship between cloud droplet size and CCN critical supersaturation N85-32677
Fog activation and supersaturation N85-32678
On the question to the effect of surfactants on the spectrum of cloud drops in the process of their condensation growth N85-32679
The distribution of giant salt nuclei inside and outside cloud over the basin of Xin and Jiang N85-32681

DROP TESTS
Graphite/PMR polyimide composites with improved toughness
[NASA-TM-87081] N85-32148

DROPS (LIQUIDS)
Instability and chaotic behavior in a free-surface flow
[AD-A154879] N85-32279
Ice nucleation of single water droplet by silver iodide: A laboratory observation N85-32630
Cloud droplet nucleation and initial growth derived from lidar depolarization studies N85-32635
Characterization of insoluble particles associated with cloud droplets N85-32693
The measured rate of condensation nucleation to droplets using the techniques of chemical kinetics N85-32694

DRUGS
Interaction of opiate and phencyclidine derivatives with the acetylcholine receptor
[AD-A155119] N85-32761

DUCTILITY
Metallurgical origins of fracture toughness and microstructure and fracture toughness of an HSLA (High-Strength/Low-Alloy) steel
[AD-A155530] N85-32187
Development of improved dynamic failure models
[AD-A155586] N85-32354

DURABILITY
Thin-film reliability and engineering overview N85-32450

DUST
Ice-forming efficiency of the soluble and insoluble portions of dust contained in snow N85-32631
Sahara Desert dust transport to the south N85-32666

DYE LASERS
Lasing on LiF:F(-)2 - dye centers with transverse pumping N85-32890
Dynamics of emission from dye lasers employing synchronous pumping by limited picosecond pulse train N85-32899
High-power two-frequency CW dye laser N85-32900

Self Q-modulation and generation of short pulses in distributed-feedback lasers N85-32907
Doppler spectrometer for measuring narrow photochemical gaps in inhomogeneously broadened spectra N85-32921
DYES
Lasing on LiF:F(-)2 - dye centers with transverse pumping N85-32890
Choice of optimum saturating absorber for YAG passive mode-locking laser N85-32893
DYNAMIC CHARACTERISTICS
Dynamic fracture behavior of structural materials [AD-A154568] N85-32345
The dynamics of slack marine cables [AD-A155022] N85-32349
Ductile fracture of dynamically loaded naval structures-compact tension specimen tests and analyses [AD-A155472] N85-32353
Hydrographic data from the OPTOMA (Ocean Prediction Through Observations, Modeling and Analysis) program: OPTOMA15, 24 January to 23 February 1985 [AD-A155012] N85-32703
DYNAMIC CONTROL
Bayesian vs MAP multiple model adaptive estimation for field of view expansion in tracking airborne targets [AD-A155466] N85-32855
DYNAMIC LOADS
In-situ measurement of wall thermal performance: Data interpretation and apparatus design recommendations [DE85-011979] N85-32289
The dynamics of slack marine cables [AD-A155022] N85-32349
DYNAMIC MODELS
Mechanics of a gaseous film barrier to lubricant wetting of elastohydrodynamically lubricated conjunctions [NASA-TP-2500] N85-32330
Development of improved dynamic failure models [AD-A155586] N85-32354
Numerical modeling of sea ice dynamics and ice thickness characteristics [AD-A154600] N85-32700
DYNAMIC PRESSURE
Strain rate sensitivity estimation from high velocity impact data [AD-A154703] N85-32347
DYNAMIC STABILITY
Newton's method as a dynamical system: Global convergence and predictability [AD-A155170] N85-32564
DYNAMIC STRUCTURAL ANALYSIS
User's guide for computer program CGFAG, Concrete General Flexure Analysis with Graphics [AD-A155555] N85-32204
Dynamic fracture behavior of structural materials [AD-A154568] N85-32345
DYNAMIC TESTS
Seat experiments for the full-scale transport aircraft controlled impact demonstration [AD-A155024] N85-32106
DYNAMICS EXPLORER 1 SATELLITE
A retarding ion mass spectrometer for the Dynamics Explorer-1 [NASA-CR-171588] N85-32303
DYNAMO THEORY
Planetary Dynamos [NASA-CR-176001] N85-32857

E

E REGION
Characteristics and sources of E-region ionization in the continuous aurora [AD-A155018] N85-32562
EARTH (PLANET)
Earth Albedo and the orbit of LAGEOS [NASA-TM-86210] N85-32131
Megageomorphology: Mars vis a vis Earth N85-32360
Workshop on the Early Earth: The Interval from Accretion to the Older Archean [NASA-CR-176037] N85-33062
EARTH ATMOSPHERE
Medium range atmospheric forecast system: Evaluation plan [AD-A155623] N85-32595
Production of stable embryo particles in dense ion tracks of alpha particle emissions in the atmosphere N85-32638
Photochemical aerosol formation in polluted atmosphere N85-32642
Evolution of the atmosphere N85-32725
Constraints on early atmosphere from planetary accretion processes N85-33064
The composition of the primitive atmosphere and the synthesis of organic compounds on the early Earth N85-33065
The degassing history of the Earth: Noble gas studies of Archaean cherts and zero age glassy submarine basalts N85-33072
Water loss from Venus: Implications for the Earth's early atmosphere N85-33087
EARTH CORE
Origin of life N85-32713
Was core formation violent enough to homogenize the early mantle? N85-33068
The problem of the Earth's CO2 content and the iron core N85-33069
A model for core formation in the early Earth N85-33078
Implications for the Earth of the early dynamical environment N85-33079
Chemical evolution of the Earth: Equilibrium or disequilibrium process? N85-33088
Thermal, dynamic and compositional aspects of the core-forming Earth N85-33091
EARTH CRUST
Megageomorphology: Mars vis a vis Earth N85-32360
Crustal dynamics project data analysis fixed station VLBI geodetic results [NASA-TM-86229] N85-32465
Development of ultrasonic modeling techniques for the study of crustal inhomogeneities [AD-A155206] N85-32565
Origin of life N85-32713
Workshop on the Early Earth: The Interval from Accretion to the Older Archean [NASA-CR-176037] N85-33062
Early evolution of the crust-mantle system N85-33067
Considerations of large scale impact and the early Earth N85-33070
The 3.5 b.y. old Onverwacht Group: A remnant of ancient oceanic crust N85-33073
Constraints on the development of the early continental crust from isotopic data N85-33076
Anorthositic oceanic crust in the Archean Earth N85-33077
Archean sedimentary systems and crustal evolution N85-33082
The origin of continental crust: Outlines of a general theory N85-33083
Crustal radiogenic heat production and the selective survival of ancient continental crust N85-33086
Large arcuate scars: A geological legacy of the Earth's accretionary past N85-33089
EARTH MANTLE
Origin of life N85-32713
Workshop on the Early Earth: The Interval from Accretion to the Older Archean [NASA-CR-176037] N85-33062
The relation between the age of the subconducting slab and the recycling of sediments into the mantle N85-33063
Constraints on early atmosphere from planetary accretion processes N85-33064
Early evolution of the crust-mantle system N85-33067
Was core formation violent enough to homogenize the early mantle? N85-33068
Constraints on the development of the early continental crust from isotopic data N85-33076
A model for core formation in the early Earth N85-33078
Carbon and nitrogen in the deep Earth N85-33085
Chemical evolution of the Earth: Equilibrium or disequilibrium process? N85-33088
Thermal, dynamic and compositional aspects of the core-forming Earth N85-33091
EARTH OBSERVATIONS (FROM SPACE)
Large format camera photographs: A new tool for understanding arid environments N85-32379
Quantitative geomorphologic studies from spaceborne platforms N85-32381
Process thresholds: Report of Working Group Number 3 N85-32384
Planetary perspective. Report of Working Group Number 4 N85-32385
Properties of aerosol particles detected by satellites in coastal regions N85-32622
EARTH PLANETARY STRUCTURE
Development of ultrasonic modeling techniques for the study of crustal inhomogeneities [AD-A155206] N85-32565
Conditions during formation of the Earth N85-33066
Constraints on the development of the early continental crust from isotopic data N85-33076
Anorthositic oceanic crust in the Archean Earth N85-33077
A model for core formation in the early Earth N85-33078
Implications for the Earth of the early dynamical environment N85-33079
Chemical evolution of the Earth: Equilibrium or disequilibrium process? N85-33088
Earth's primordial differentiation, and its after-effects N85-33092
EARTH RESOURCES
Handbook for obtaining and using aerial photography to map aquatic plant distribution [AD-A154584] N85-32388
EARTH ROTATION
Crustal dynamics project data analysis fixed station VLBI geodetic results [NASA-TM-86229] N85-32465
EARTH SURFACE
Geomorphological similarity and uniqueness N85-32361
Quantitative analysis of geomorphic processes using satellite image data at different scales N85-32380
Quantitative geomorphologic studies from spaceborne platforms N85-32381
Global geomorphology: Report of Working Group Number 1 N85-32382
Landscape inheritance: Report of Working Group Number 2 N85-32383
Planetary perspective. Report of Working Group Number 4 N85-32385
Upward continuation of surface gravity anomalies [AD-A154973] N85-32560
Large arcuate scars: A geological legacy of the Earth's accretionary past N85-33089
EARTH TIDES
Interpolation problems in meteor radar analysis, part 7.6A N85-32528
EARTH-MOON SYSTEM
The evolution of complex and higher organisms [NASA-SP-478] N85-32708
EARTHQUAKES
Design of a freestanding noise measurement and recording system to predict the intensity and location of electromagnetic radiation from earthquakes [AD-A155070] N85-32563
EATING
The effects of prolonged feeding meal, ready-to-eat (MRE) operational rations [AD-A154763] N85-32773
ECLOGITE
Anorthositic oceanic crust in the Archean Earth N85-33077
ECOLOGY
The global sulfur cycle [NASA-TM-87570] N85-32710
Sulfur cycling and metabolism of phototrophic and filamentous sulfur bacteria N85-32737
ECONOMIC ANALYSIS
Quality analysis N85-32785
ECONOMY
Quality analysis N85-32785
ECOSYSTEMS
Global geomorphology N85-32359
Biogeochemical cycling and remote sensing N85-32733
EDDY CURRENTS
Plating density standards [DE85-010014] N85-32318
EDDY VISCOSITY
MST radar data management N85-32532
EDGES
Experimental and theoretical assessment of a new technique for the non-destructive evaluation of laminated panels [AD-A155622] N85-32155
EDITING ROUTINES (COMPUTERS)
Experience with omega: Implementation of a prototype programming environment: Part 1 [AD-A155438] N85-32811
EDUCATION
The Naval Postgraduate School Flight Mechanics Laboratory: A feasibility study [AD-A154578] N85-32127
One application of mega-geomorphology in education N85-32370
Ada (trademark) training curriculum. Advanced Ada topics L305 teacher's guide exercises [AD-A154621] N85-32798
EFFICIENCY
Application of adaptive noise cancellation to Coast Guard voice communications [AD-A154798] N85-32230
Physics of heavily doped silicon and solar-cell parameter measurement N85-32418
Sensitivity analysis of high-efficiency silicon solar-cell design parameters N85-32422

Silicon surface passivation by silicon nitride deposition N85-32423
Important loss mechanisms in high-efficiency solar cells N85-32424
Stress and efficiency studies in EFG N85-32440

EFFLUENTS
Influence on an industrial site on the characteristics of CCN supersaturation with air masses of different origin N85-32683

EFFUSIVES
Changes in the organic material in lakes in the blast zone of Mount St. Helens, Washington: Hydrologic effects of the eruptions
[GS-CIRC-850-1] N85-32551

EJECTION SEATS
SSMIR (Solid State Memory Instrumentation Recorder): A new approach to acquiring data during an aircraft seat/sled ejection sequence
[AD-A154780] N85-32308

EJECTORS
Applied research and development for falling-sphere air density measuring systems
[AD-A155227] N85-32099

ELASTIC DEFORMATION
Hertzian contact in two and three dimensions
[NASA-TP-2473] N85-32331

ELASTIC SCATTERING
Spatial parity violation in elastic neutron-nuclei interaction channel N85-32932
Evaluated nuclear-data file for niobium
[DE85-012095] N85-33009

ELASTOHYDRODYNAMICS
Surface roughness effects in elastohydrodynamic contacts
[NASA-TP-2488] N85-32329
Mechanics of a gaseous film barrier to lubricant wetting of elastohydrodynamically lubricated conjunctions
[NASA-TP-2500] N85-32330

ELASTOMERS
Structure-property relationships in thermoplastic elastomers. Part 3: Segmented polyacetal-polyurethanes
[AD-A154897] N85-32200

ELASTOSTATICS
Ductile fracture of dynamically loaded naval structures-compact tension specimen tests and analyses
[AD-A155472] N85-32353

ELECTRIC BATTERIES
A safe, high-power-density lithium battery
[AD-A155223] N85-32454

ELECTRIC BRIDGES
R, L, C, G measurement N85-32784

ELECTRIC CONDUCTORS
Tailored vacuum chambers for ac magnets
[DE85-010767] N85-32319

ELECTRIC DIPOLES
Numerical modeling of subsurface communication
[DE85-012818] N85-32249

ELECTRIC DISCHARGES
Coordinated research program in pulsed power physics
[AD-A154629] N85-32858
Powerful XeCl excimer electric discharge laser with good temporal stability and fast response time N85-32911

ELECTRIC EQUIPMENT TESTS
Module Hipot and ground continuity test results N85-32447

ELECTRIC FIELDS
A theory of electromagnetic shielding with applications to MIL-STD-285, IEEE-299, and EMP simulation
[AD-A154905] N85-32233
Trapping of ion conics by downward parallel electric fields
[AD-A155306] N85-32568
Electrostatic ion cyclotron instability due to a nonuniform electric field perpendicular to the external magnetic field
[AD-A155474] N85-33019

ELECTRIC FILTERS
Stripe filters on multispectral linear arrays
[NASA-CR-175305] N85-32252

ELECTRIC GENERATORS
Experimental investigation of a variable speed constant frequency electric generating system from a utility perspective
[NASA-CR-174950] N85-32251
Operational window for a plasma erosion opening switch used for voltage multiplication on pulsed power generators
[AD-A155482] N85-33020

ELECTRIC NETWORKS
Microcomputer network: Investigation and implementation
[AD-A155631] N85-32826

ELECTRIC POTENTIAL
Module Hipot and ground continuity test results N85-32447
R, L, C, G measurement N85-32784

ELECTRIC POWER SUPPLIES
Experimental investigation of a variable speed constant frequency electric generating system from a utility perspective
[NASA-CR-174950] N85-32251

ELECTRICAL ENGINEERING
Failure mechanisms in metal-sheathed thermocouples
[DE85-011929] N85-32317

ELECTRICAL IMPEDANCE
R, L, C, G measurement N85-32784

ELECTRICAL INSULATION
Failure mechanisms in metal-sheathed thermocouples
[DE85-011929] N85-32317

ELECTRICAL MEASUREMENT
Modelling and parameter estimation for distributed vibratory systems
[AD-A154518] N85-32344
East Europe report: Science and technology. Selections on CSSR computer technology
[JPRS-ESA-84-017] N85-32781
R, L, C, G measurement N85-32784

ELECTRICAL PROPERTIES
Electrochemistry of Hexanitroazobenzene (HNAB)
[DE85-010807] N85-32171
Electrical properties of bulk grown nitrogen doped silicon
[AD-A155471] N85-32266
Failure analysis of thin-film amorphous-silicon solar-cell modules N85-32452
Electronic phenomena near semiconductor grain boundaries
[DE85-011543] N85-33035

ELECTRICAL RESISTANCE
Resistance of polyaniline films as a function of electrochemical potential and the fabrication of polyaniline-based microelectronic devices
[AD-A154999] N85-32201

ELECTRICAL RESISTIVITY
Electrical and mechanical properties of intercalated graphite fibers
[AD-A155560] N85-32205

ELECTRO-OPTICAL PHOTOGRAPHY
Magnetic materials
[AD-A154679] N85-32256

ELECTRO-OPTICS
Advanced simulator for pilot training and helmet-mounted visual display configuration comparisons
[AD-A155325] N85-32776
System for electro-optical ceramic recrystallization N85-32872
Transformation of charged particle beams by concentrating electro-optical systems N85-32925

ELECTROACOUSTIC TRANSDUCERS
The moving thermoacoustic array: A theoretical feasibility study
[AD-A154510] N85-32980

ELECTROCHEMICAL OXIDATION
Resistance of polyaniline films as a function of electrochemical potential and the fabrication of polyaniline-based microelectronic devices
[AD-A154999] N85-32201

ELECTROCHEMISTRY
Electrochemistry of Hexanitroazobenzene (HNAB)
[DE85-010807] N85-32171
Topics in electrochemical degradation of photovoltaic modules N85-32410
Characteristics of optogalvanic effect in media with inverse populations N85-32944

ELECTRODEPOSITION
Electrodeposition of chromium and copper in magnetic fields
[AD-A154648] N85-32180

ELECTRODES
Thermal contraction of current flow through electrode turbulent boundary layer N85-32926

ELECTROENCEPHALOGRAPHY
Resource allocation in cerebral specialization of function: Behavioral and electrophysiological studies
[AD-A155092] N85-32759

ELECTROHYDRAULIC FORMING
Results of an interlaboratory fatigue test program conducted on alloy 800H at room and elevated temperatures
[NASA-CR-174940] N85-32340

ELECTROLYSIS
High temperature solar electrothermal processing 2. Zinc from zinc oxide
[AD-A154747] N85-32159

ELECTROLYTES
Electrodeposition of chromium and copper in magnetic fields
[AD-A154648] N85-32180

ELECTROMAGNETIC ABSORPTION
Cyclotron absorption of fast magnetosonic wave in stellarator N85-32945

ELECTROMAGNETIC FIELDS
Guided-mode launching in a slab waveguide by way of diffraction at the edge of a conducting screen residing on one surface of the slab
[AD-A154886] N85-32232
Calculation of the propagation constant in a rectangular waveguide containing an inhomogeneous longitudinally magnetized plasma
[DE85-012072] N85-32250
Lower bounds of propagation velocity of steady ionizing waves in field of strong electromagnetic wave N85-32940
Equations of motion for electromagnetic waves in 4-dimensional Euclidian space N85-32970
Research in particles and fields
[NASA-CR-176069] N85-33103

ELECTROMAGNETIC INTERFERENCE
Stripe filters on multispectral linear arrays
[NASA-CR-175305] N85-32252

ELECTROMAGNETIC NOISE
The role of long term lamp fluctuations in the random walk of frequency behavior of the rubidium frequency standard: A case study
[AD-A155338] N85-32314
Design of a freestanding noise measurement and recording system to predict the intensity and location of electromagnetic radiation from earthquakes
[AD-A155070] N85-32563

ELECTROMAGNETIC PROPERTIES
A review of the physics and response models for burnout of semiconductor devices
[AD-A155031] N85-33028

ELECTROMAGNETIC PROPULSION
Plasma mass and effective inductance in a small railgun
[AD-A154644] N85-32304

ELECTROMAGNETIC PULSES
A theory of electromagnetic shielding with applications to MIL-STD-285, IEEE-299, and EMP simulation
[AD-A154905] N85-32233
Plasmodynamic methods for generating powerful light puses N85-32943
Methods for measuring and analyzing dispersion properties of multimode fiber optic lightpipes (a review) N85-32960

ELECTROMAGNETIC RADIATION
Numerical modeling of subsurface communication
[DE85-012818] N85-32249
Some recent developments in the interpretation of MST radar returns from clear air (keynote paper), part 2 N85-32480
Design of a freestanding noise measurement and recording system to predict the intensity and location of electromagnetic radiation from earthquakes
[AD-A155070] N85-32563
USAFSAM review and analysis of radiofrequency radiation bioeffects literature
[AD-A155113] N85-32760
Investigation of ion-acoustic plasma turbulence in field of powerful electromagnetic wave by CO2-laser radiation scattering N85-32935
Lower bounds of propagation velocity of steady ionizing waves in field of strong electromagnetic wave N85-32940
Amplification of electromagnetic wave by electron stream with negative velocity differences N85-32941
Electromagnetic wave amplification during cyclotron resonance in a medium N85-32942
Effective brightness of zero-point fluctuations of the electromagnetic vacuum accompanying parametric scattering of light N85-32951
Existence of smooth solutions in problems of electromagnetic radiation focusing N85-32972
Ice fog as an electro-optical obscurant
[AD-A155059] N85-33015

ELECTROMAGNETIC SCATTERING
Radar target identification through electromagnetic scattering studies
[AD-A154596] N85-32220
Scattering from foliage covered terrain
[AD-A154724] N85-32228
Head-on scattering of a tubular cylinder of finite length for radar target identification purposes
[AD-A155608] N85-32246
Broadside scattering of a tubular cylinder for evaluation of target identification
[AD-A155739] N85-32248

ELECTROMAGNETIC SHIELDING
A theory of electromagnetic shielding with applications to MIL-STD-285, IEEE-299, and EMP simulation
[AD-A154905] N85-32233

ELECTROMECHANICAL DEVICES
Experiments on the influence of active walls on the initial amplitudes and growths of instability waves
[AD-A154630] N85-32275
ELECTRON BEAMS
Practicality of electronic beam steering for MST/ST radars, part 6.2A N85-32516
Trapping of ion conics by downward parallel electric fields
[AD-A155306] N85-32568
Operation of solid state lasers exposed to electron beam N85-32895
Amplification of electromagnetic wave by electron stream with negative velocity differences N85-32941
ELECTRON BUNCHING
Form factor effects on microwave Cerenkov radiation
[AD-A154577] N85-32993
ELECTRON CYCLOTRON HEATING
Influence of ECR-heating on MHD activity of plasma in tokamak-10 installation N85-32949
ELECTRON DENSITY (CONCENTRATION)
Characteristics and sources of E-region ionization in the continuous aurora
[AD-A155018] N85-32562
Soft X-ray polychromator for the Solar Maximum Mission
[NASA-CR-175297] N85-33096
ELECTRON DIFFRACTION
Determination of kinetic parameters of molecular beam epitaxy
[AD-A155222] N85-33030
ELECTRON ENERGY
CCD-based X-ray spectrometry for on-line determination of laser plasma electron temperature N85-32938
Contributions to the 19th International Cosmic Ray Conference
[NASA-CR-176060] N85-33044
The energy spectrum of Jovian electrons in interplanetary space
[PAPER-SH-1.5-18] N85-33051
Solar modulation and interplanetary gradients of the galactic electron flux, 1977 - 1984
[PAPER-SH-4.7-4] N85-33059
ELECTRON IMPACT
Vibrationally enhanced dissociation of diatomic molecules
[AD-A154827] N85-32996
ELECTRON MICROSCOPY
Modification of the grain size of sputtered copper with additions of oxygen, krypton, silver, or yttrium
[DE85-010975] N85-32189
Z-contrast imaging and electron channeling analysis of dopants in semiconductors
[DE85-011410] N85-32269
Aerosol formation by wave action over Ross Sea, Antartica N85-32688
An electron microscopic study of urban aerosol N85-32689
ELECTRON OPTICS
Practicality of electronic beam steering for MST/ST radars, part 6.2A N85-32516
Electrostatic astigmatic tubular lens N85-32955
ELECTRON PARAMAGNETIC RESONANCE
Defect formation in amorphous hydrated silicon subjected to laser radiation N85-32873
An EPR (Electron-Paramagnetic-Resonance) and ENDOR (Electron-Nuclear-Double-Resonance) study of ferroelectric ammonium sulfate
[AD-A155580] N85-33033
ELECTRON PLASMA
Influence of ECR-heating on MHD activity of plasma in tokamak-10 installation N85-32949
ELECTRON RADIATION
Radio-frequency radiation of storm clouds N85-32939
ELECTRON SPECTROSCOPY
Activities of the Physics Division
[DE85-000784] N85-33002
ELECTRON STATES
Calculation of molecular constants potential energy curves and Franck-Condon factors for lead oxide
[AD-A154521] N85-32158
Nonradiative damping of molecular electronic excited states by metal surfaces
[AD-A154619] N85-32994
ELECTRON TRANSFER
Sulfate-reducing bacteria: Microbiology and physiology N85-32732
ELECTRON TUNNELING
A theory of exciton photoluminescence for two types of neutral acceptors in silicon. A study of the systems Si:(B, IN), Si:(Al), (Si), Si:(Ga, In), Si:(B, Al), Si:(B, Ga), and Si:(Al, GA)
[AD-A155452] N85-33031
ELECTRONIC AIRCRAFT
Electronic reconnaissance aircraft of the Soviet Union Navy
[AD-A154706] N85-32091
ELECTRONIC CONTROL
Performance improvements of a highly integrated digital electronic control system for an F-15 airplane
[NASA-TM-86748] N85-32120
A microprocessor-controlled, multichannel fluorimeter for analysis of sea water
[AD-A154986] N85-32310
ELECTRONIC EQUIPMENT
Resistance of polyaniline films as a function of electrochemical potential and the fabrication of polyaniline-based microelectronic devices
[AD-A154999] N85-32201
Prospects for a new kind of synthesis: Assembly of molecular components to achieve functions
[AD-A155023] N85-32997
ELECTRONIC EQUIPMENT TESTS
East Europe report: Science and technology
[JPRS-ESA-85-021] N85-32190
ELECTRONIC WARFARE
Fin line filters technology and electronic warfare
[AD-A154975] N85-32237
ELECTRONS
Detection of excited states by laser-induced fluorescence
[AD-A155558] N85-32326
Solar modulation and interplanetary gradients of the galactic electron flux, 1977 - 1984
[PAPER-SH-4.7-4] N85-33059
ELECTROPHYSIOLOGY
Interaction of opiate and phencyclidine derivatives with the acetylcholine receptor
[AD-A155119] N85-32761
ELECTROSTATIC GENERATORS
A small-scale self-excited rotor electrostatic generator
[AD-A155264] N85-32265
ELECTROSTATIC PROBES
Observations of mesospheric turbulence by rocket probe and VHF radar, part 2.4A N85-32484
ELECTROSTATICS
Electrostatic astigmatic tubular lens N85-32955
ELEVATION
Comparison of survey and photogrammetry methods to position gravity data, Yucca Mountain, Nevada
[DE85-011685] N85-32316
ELLIPSOMETERS
Interfacial bonding stability N85-32409
EMBEDDED COMPUTER SYSTEMS
HLLM software support
[AD-A154828] N85-32805
EMERGENCIES
Emergency modeling of hazardous air pollutants
[AD-A155441] N85-32461
EMISSION
Improved Nominal Operating Cell Temperature (NOCT) test procedure N85-32449
Dynamics of emission from dye lasers employing synchronous pumping by limited picosecond pulse train N85-32899
Spectral-luminescence characteristics and induced emission of Nd-3(+) ion in Gd(2-x)Nd(x)(WO4)3 crystals N85-32912
SCRIBE data of October 23, 1983 flight
[AD-A154864] N85-33012
EMISSION SPECTRA
Aerosol analysis and emission spectrometry with free jets
[DE85-010576] N85-32168
Ionospheric electron density profile and related studies
[AD-A155257] N85-32567
Investigation of reproducibility of emission wavelength of helium-neon laser with external neon absorption cell (0.63 micrometers) N85-32884
ENCAPSULATING
Photothermal degradation studies of encapsulants N85-32403
Encapsulation processing and manufacturing yield analysis N85-32434
ENERGETIC PARTICLES
Characteristics and sources of E-region ionization in the continuous aurora
[AD-A155018] N85-32562
Contributions to the 19th International Cosmic Ray Conference
[NASA-CR-176060] N85-33044
Solar coronal and photospheric abundances from solar energetic particle measurements
[PAPER-SH-2.1-5] N85-33053
ENERGY ABSORPTION
Cyclotron resonance in a nonneutral plasma
[AD-A155248] N85-33017
ENERGY BANDS
Doping superlattices in organometallic VPE InP
[AD-A155151] N85-33029
ENERGY CONVERSION EFFICIENCY
Status of boron combustion research
[AD-A154762] N85-32160
High-efficiency crystalline silicon technology development N85-32395
Summary of the high-efficiency crystalline solar cell research forum N85-32396
High-efficiency module and array research N85-32397
Flat-plate module efficiency versus cost tradeoffs N85-32398
The future of crystalline silicon technology in the US Department of Energy program N85-32399
Georgetown University Photovoltaic Higher Education National Exemplar Facility (PHENEF) N85-32400
Block V module program N85-32401
Photothermal degradation studies of encapsulants N85-32403
Advanced module development overview N85-32445
ENERGY DISSIPATION
Interpretation of radar returns from the mesosphere, part 2.3A N85-32485
ENERGY LEVELS
Establishment of steady-state power level in pulse-periodic excimer laser N85-32896
ENERGY SPECTRA
Paired ion chamber constants for fission gamma-neutron fields
[AD-A155069] N85-32999
Changes in the energy spectrum of anomalous oxygen and helium during 1977 - 1985
[PAPER-SH-4.6-1] N85-33056
ENERGY STORAGE
Capacitive energy storage at cryogenic temperatures
[AD-A154508] N85-32253
A fast discharge excimer laser with symmetric geometry
[AD-A155294] N85-32322
ENERGY TECHNOLOGY
Proceedings of the 24th Project Integration Meeting
[NASA-CR-176058] N85-32394
High-efficiency crystalline silicon technology development N85-32395
Energy and Technology Review
[DE85-011767] N85-33061
ENERGY TRANSFER
Meteorological weapons
[AD-A154735] N85-32575
Resonant energy transfer during strong excitation N85-32922
ENGINE CONTROL
Performance improvements of a highly integrated digital electronic control system for an F-15 airplane
[NASA-TM-86748] N85-32120
ENGINE FAILURE
Weibull distribution based on maximum likelihood with interval inspection data
[NASA-TM-86515] N85-32847
ENGINE PARTS
Component-specific modeling
[NASA-CR-174925] N85-32119
ENGINEERING MANAGEMENT
Thin-film reliability and engineering overview N85-32450
ENGINES
FAA/GAMA (Federal Aviation Administration/General Aviation Manufacturer's Association) propeller aircraft noise test program, Salina Municipal Airport, Salina, Kansas
[AD-A154818] N85-32983
ENTHALPY
Liquid-phase compositions from vapor-phase analyses 2: Adaptation of the Prausnitz program to UF6 and some of its potential impurities
[DE85-011521] N85-32819
ENVIRONMENT EFFECTS
Thin-film reliability and engineering overview N85-32450
ENVIRONMENT MANAGEMENT
Marine environmental quality assessment program, five-year plan (FY 1984 - 1988)
[AD-A154715] N85-32459
ENVIRONMENT MODELS
Empirical methods for predicting eutrophication in impoundments. Report 3. Phase 2. Model refinements
[AD-A155483] N85-32462
ENVIRONMENTAL CONTROL
Space station ECLSS integration analysis: Simplified General Cluster Systems Model, ECLS System Assessment Program enhancements
[NASA-CR-176089] N85-32796

ENVIRONMENTAL QUALITY
Marine environmental quality assessment program, five-year plan (FY 1984 - 1988)
[AD-A154715] N85-32459
Air force technical objective document, Aerospace Medical Division, Fiscal Year 1986
[AD-A155195] N85-32762

ENVIRONMENTAL SURVEYS
Marine environmental quality assessment program, five-year plan (FY 1984 - 1988)
[AD-A154715] N85-32459

ENVIRONMENTAL TESTS
Module Hipot and ground continuity test results N85-32447

EPINEPHRINE
Studies of circulatory and metabolic changes during ketamine narcosis
[AD-A154512] N85-32756

EPITAXY
Microwave semiconductor research: Materials, devices and circuits and gallium arsenide ballistic electron transistors
[AD-A154698] N85-33024

EPOXY MATRIX COMPOSITES
Improved materials for composites and adhesive joints
[AD-A154918] N85-32152
Improved materials for composite and adhesive joints
[AD-A155065] N85-32153

EPOXY RESINS
Improved materials for composite and adhesive joints
[AD-A155065] N85-32153
The effect of mould size on the exothermic reaction and compressive strength of epoxy resin chocks
[AD-A155102] N85-32203

EQUATIONS
On the dependence of the convergence of Gummel's algorithm on the regularity of the solution
[AD-A154628] N85-32832

EQUATIONS OF MOTION
Optimal low thrust transfer using a first-order perturbation model
[AD-A154761] N85-32835
Classical emission of relativistic charged particles during axial channeling N85-32871
Theoretical foundations of turbulent flows N85-32880
Equations of motion for electromagnetic waves in 4-dimensional Euclidian space N85-32970

EQUATIONS OF STATE
BLAF: A blast field reconstruction program from pressure histories
[AD-A155300] N85-32283
Liquid-phase compositions from vapor-phase analyses 2: Adaptation of the Prausnitz program to UF6 and some of its potential impurities
[DE85-011521] N85-32819
A system of magnetohydrodynamic-type equations N85-32946
A new problem in mathematical physics associated with the problem of coherent phase transformation N85-32976

EQUATORIAL REGIONS
Equitorial scintillations: Advances since ISEA-6
[AD-A154962] N85-32559

EQUILIBRIUM EQUATIONS
A new problem in mathematical physics associated with the problem of coherent phase transformation N85-32976

EROSION
Coastal erosion along Monterey Bay
[AD-A155610] N85-32707
Operational window for a plasma erosion opening switch used for voltage multiplication on pulsed power generators
[AD-A155482] N85-33020

ERROR ANALYSIS
Performance and evaluation of real-time multicomputer control systems
[NASA-CR-176098] N85-32821

ERRORS
In-situ measurement of wall thermal performance: Data interpretation and apparatus design recommendations
[DE85-011979] N85-32289
Comparison of survey and photogrammetry methods to position gravity data, Yucca Mountain, Nevada
[DE85-011685] N85-32316

ESTIMATES
The optimality of lower confidence limits for the reliability of series systems obtained by the method of key test results or other related techniques
[AD-A154880] N85-32338
Parameter estimation in communication system tracking satellite observations
[AD-A155137] N85-32582
Identification of unsteady aerodynamics and aeroelastic integro-differential systems
[NASA-TM-86749] N85-32851
A simulation study of Sylvester's problem in three dimensions
[AD-A155266] N85-32854

ETHANE
Shock tube measurements of growth constants in the branched-chain ethane-carbon monoxide-oxygen system
[NASA-TM-87068] N85-32156

ETHERS
Synthesis and properties of arylethersulfone thermoset systems
[AD-A154811] N85-32198

EULER EQUATIONS OF MOTION
An elliptic calculation procedure for 3-D viscous flow N85-32297
Calculation of 3-D flow without numerical mixing N85-32301

EUROPE
A transportable, machine oriented library of european sky and terrain radiance distributions with contemporary radiometric and meteorological profiles
[AD-A155254] N85-32590
Supersaturation spect A of Ice Nuclei at different locations in Europe and over the North-Atlantic N85-32615

EUTROPHICATION
Empirical methods for predicting eutrophication in impoundments. Report 3. Phase 2. Model refinements
[AD-A155483] N85-32462
Sulfur cycling in freshwater sediments N85-32726

EVALUATION
Improved materials for composite and adhesive joints
[AD-A155065] N85-32153
Fabrication and test of modified quadrupole mass spectrometer
[AD-A155186] N85-32312

EVAPORATION
Emergency modeling of hazardous air pollutants
[AD-A155441] N85-32461

EVOLUTION (DEVELOPMENT)
The evolution of complex and higher organisms
[NASA-SP-478] N85-32708

EXCHANGING
Tropospheric-stratospheric exchange, part 1.1A N85-32468

EXCIMER LASERS
A fast discharge excimer laser with symmetric geometry
[AD-A155294] N85-32322
Investigation of plasma processes in electronic transition lasers
[AD-A155598] N85-32327
Pulsed excimer laser processing for cost-effective solar cells N85-32432
Excimer laser annealing for fabrication of low-cost solar cells N85-32433
Establishment of steady-state power level in pulse-periodic excimer laser N85-32896
Saturation effect in multilevel lasing media N85-32901
Excimer-laser generator of powerful UV picosecond pulses synchronized with picosecond pulses in visible and IR bands N85-32903
Powerful XeCl excimer electric discharge laser with good temporal stability and fast response time N85-32911

EXCIMERS
A fast discharge excimer laser with symmetric geometry
[AD-A155294] N85-32322

EXCITATION
Detection of excited states by laser-induced fluorescence
[AD-A155558] N85-32326
Toward a theory of excitation of atoms during nuclear and magnetic neutron scattering N85-32918
Radiative-collision generation of sound in gases subjected to single-pulse optical excitation N85-32920
Resonant energy transfer during strong excitation N85-32922
Exotic events of p bar p-collider: Excited quark or excited color boson? N85-32930
Vibrationally enhanced dissociation of diatomic molecules
[AD-A154827] N85-32996

EXCITONS
A theory of exciton photoluminescence for two types of neutral acceptors in silicon. A study of the systems Si:(B, IN), Si:(Al), (Si), Si:(Ga, In), Si:(B, Al), Si:(B, Ga), and Si:(Al, GA)
[AD-A155452] N85-33031

EXHAUST GASES
Influence on an industrial site on the characteristics of CCN supersaturation with air masses of different origin N85-32683

EXOBIOLOGY
The global sulfur cycle
[NASA-TM-87570] N85-32710
Aerospace medicine and biology: A continuing bibliography with indexes, supplement 273
[NASA-SP-7011(273)] N85-32755
Search for the universal ancestors
[NASA-SP-477] N85-32777

EXOTHERMIC REACTIONS
The effect of mould size on the exothermic reaction and compressive strength of epoxy resin chocks
[AD-A155102] N85-32203
Optical waveguide along front of exothermic reaction N85-32954

EXPANSION
Acoustic radiation from concentric shells containing an inner fluid
[AD-A155476] N85-32991

EXPERT SYSTEMS
Myoelectric control of a computer based expert system for flight control
[AD-A154981] N85-32126
NASA space station automation: AI-based technology review
[NASA-CR-176094] N85-32134
NASA space station automation: AI-based technology review. Executive summary
[NASA-CR-176096] N85-32135
Research on an expert system for database operation of simulation-emulation math models. Volume 1, Phase 1: Results
[NASA-CR-176087] N85-32792
Research on an expert system for database operation of simulation-emulation math models. Volume 2, Phase 1: Results
[NASA-CR-176088] N85-32793
Design of an expert-system flight status monitor
[NASA-TM-86739] N85-32794

EXPLOSIVES
Electrochemistry of Hexanitroazobenzene (HNAB)
[DE85-010807] N85-32171
The determination of dinitrotoluene in single base propellants
[AD-A154672] N85-32209
TNT equivalency of EAK explosive
[AD-A155737] N85-32211

EXPONENTIAL FUNCTIONS
Survival function of hypo-exponential distributions
[AD-A155518] N85-32814

EXPOSURE
Los Alamos optical materials reliability, maintainability, and exposure testing program
[DE85-011894] N85-32456
A crew exposure study. Phase II. Volume 2. At sea. Part A
[AD-A155233] N85-32774

EXTENSOMETERS
Results of an interlaboratory fatigue test program conducted on alloy 800H at room and elevated temperatures
[NASA-CR-174940] N85-32340

EXTINCTION
Visibility and vertical structure measurements in southern Germany
[AD-A154714] N85-32574
Ice fog as an electro-optical obscurant
[AD-A155059] N85-33015

EXTRATERRESTRIAL RADIATION
Results from radiation monitoring equipment experiments on STS-41C, 41D, 41G and 51A
[AD-A154676] N85-32142

EXTREMELY LOW FREQUENCIES
Numerical modeling of subsurface communication
[DE85-012818] N85-32249

EYE (ANATOMY)
Predictive model of electron beam induced flashblindness
[AD-A155260] N85-32763

EYE MOVEMENTS
An error-dependent model of instrument-scanning behavior in commercial airline pilots
[NASA-CR-3908] N85-32765

F

F REGION
Equitorial scintillations: Advances since ISEA-6
[AD-A154962] N85-32559

F-15 AIRCRAFT
Recent developments in rotary-balance testing of fighter aircraft configurations at NASA Ames Research Center
[NASA-TM-86714] N85-32090
Performance improvements of a highly integrated digital electronic control system for an F-15 airplane
[NASA-TM-86745] N85-32120

FABRICATION
Resistance of polyaniline films as a function of electrochemical potential and the fabrication of polyaniline-based microelectronic devices
[AD-A154999] N85-32201
Parallel simulation of digital LSI circuits
[AD-A154745] N85-32258
Fabrication and test of modified quadrupole mass spectrometer
[AD-A155186] N85-32312
Three-dimensional photochemical machining with lasers
[AD-A154711] N85-32320
Tape casting as an approach to an all-ceramic turbine shroud seal
[NASA-TM-87078] N85-32333
Status of high-efficiency module design and fabrication N85-32446
FACTORIALS
Analysis of unreplicated factorials allowing for possibly faulty observations
[AD-A154813] N85-32848
FAILURE
Fundamental investigations of failure during superplastic forming process
[AD-A154647] N85-32194
Accelerated stress factors and failure/degradation mechanisms in terrestrial solar cells N85-32451
Analysis of long bone and vertebral failure patterns
[AD-A154796] N85-32758
FAILURE ANALYSIS
Failure mechanisms in metal-sheathed thermocouples
[DE85-011929] N85-32317
Dynamic fracture of concrete and other heterogeneous materials
[AD-A154513] N85-32343
Development of improved dynamic failure models
[AD-A155586] N85-32354
Failure analysis of thin-film amorphous-silicon solar-cell modules N85-32452
FAILURE MODES
A continuous damage model based on stepwise-stress creep rupture tests
[NASA-CR-174941] N85-32341
Thin-film reliability and engineering overview N85-32450
FALKNER-SKAN EQUATION
Numerical solutions of turbulent models for flow over a flat plate with angle of attack
[DE85-010380] N85-32286
FALLING SPHERES
Applied research and development for falling-sphere air density measuring systems
[AD-A155227] N85-32099
FAR FIELDS
Notes on unsteady transonic cascade flows
[AD-A154829] N85-32096
FARADAY EFFECT
The Faraday effect in ruby and corundum in strong magnetic fields N85-32967
FAST FOURIER TRANSFORMATIONS
Hardware schemes for fast Fourier transform, part 7.4A N85-32526
Interpolation problems in meteor radar analysis, part 7.6A N85-32528
FATIGUE (BIOLOGY)
Human performance in continuous/sustained operations and the demands of extended work/rest schedules. An annotated bibliography
[AD-A155619] N85-32771
FATIGUE (MATERIALS)
The effect of abrasive blasting on the fatigue and corrosion of an aluminium-copper alloy
[AD-A154954] N85-32182
Measurement and analysis of critical crack tip processes during fatigue crack growth
[NASA-CR-172597] N85-32342
FATIGUE TESTS
The effect of abrasive blasting on the fatigue and corrosion of an aluminium-copper alloy
[AD-A154954] N85-32182
Results of an interlaboratory fatigue test program conducted on alloy 800H at room and elevated temperatures
[NASA-CR-174940] N85-32340
FAULT TOLERANCE
Performance and evaluation of real-time multicomputer control systems
[NASA-CR-176098] N85-32621
A new fault-tolerant algorithm for clock synchronization
[AD-A154771] N85-32836
FEASIBILITY ANALYSIS
Rain volume estimation over areas using satellite and radar data
[NASA-CR-176050] N85-32570
Feasibility of applications of Competition Decision Assist Package (CDAP) to spare parts
[AD-A154716] N85-33036
FEEDBACK
Self Q-modulation and generation of short pulses in distributed-feedback lasers N85-32907
FEEDBACK CONTROL
Ultrasonic position reference systems for an autonomous sentry robot and a robot manipulator arm
[AD-A155481] N85-32336
FERROELECTRICITY
Capacitive energy storage at cryogenic temperatures
[AD-A154508] N85-32253
FERROMAGNETIC FILMS
Dielectric mirror with ferromagnetic substrate N85-32966
FIBER COMPOSITES
Basic cryogenics and materials. Phase 1
[NASA-CR-177932] N85-32215
Measurement of damping of graphite epoxy materials
[NASA-CR-176073] N85-32334
FIBER OPTICS
Methods for measuring and analyzing dispersion properties of multimode fiber optic lightpipes (a review) N85-32960
FILE MAINTENANCE (COMPUTERS)
Analysis of spacecraft data
[NASA-CR-171597] N85-32790
CARE 3 user friendly interface user's guide
[NASA-CR-172608] N85-32791
FILM CONDENSATION
Film condensation of steam on externally finned horizontal tubes
[AD-A155642] N85-32285
FILMS
Modification of the grain size of sputtered copper with additions of oxygen, krypton, silver, or yttrium
[DE85-010975] N85-32189
FILTRATION
The investigation of natural and artificial ice nuclei by the improved membrane filter method N85-32626
FINANCE
A microcomputer tutorial on spreadsheets and databases with a simulated budget preparation
[AD-A155516] N85-32813
FINANCIAL MANAGEMENT
A microcomputer tutorial on spreadsheets and databases with a simulated budget preparation
[AD-A155516] N85-32813
FINITE DIFFERENCE THEORY
Calculation of transonic steady and oscillatory pressures on a low aspect ratio model and comparison with experiment
[NASA-TM-86449] N85-32092
A numerical study of Taylor-Vortex flow
[AD-A154787] N85-32277
Performance evaluation of flow in turbomachinery blade rows N85-32299
Numerical solution of the Navier-Stokes equations for 3-D internal flows: An emerging capability N85-32300
An investigation into the comparisons of the underwater shock effects on a stiffened flat plate to the predictive nature of a computer model
[AD-A155612] N85-32355
Generalized formulation of a class of explicit and implicit TVD schemes
[NASA-TM-86775] N85-32830
Oscillatory solutions of the Peaceman-Rachford alternating direction implicit method and a comparison of methods for the solution of the two dimensional heat diffusion equation
[AD-A154670] N85-32833
FINITE ELEMENT METHOD
A variable node finite element method applied to the gas dynamics equations
[AD-A155211] N85-32281
Ductile fracture of dynamically loaded naval structures-compact tension specimen tests and analyses
[AD-A155472] N85-32353
An investigation into the comparisons of the underwater shock effects on a stiffened flat plate to the predictive nature of a computer model
[AD-A155612] N85-32355
Analysis of inclined growth of silicon sheet N85-32442
Edge-defined film-fed growth of thin silicon sheets N85-32443
Concurrent implementation of the Crank-Nicolson method for heat transfer analysis
[NASA-TM-86448] N85-32822
DYNA3D, INGRID, and TAURUS: An integrated, interactive software system for crashworthiness engineering
[DE85-010928] N85-32846
Photo-acoustic effect in finite-dimensional semiconductors N85-32876
FINS
Fin line filters technology and electronic warfare
[AD-A154975] N85-32237
Film condensation of steam on externally finned horizontal tubes
[AD-A155642] N85-32285
FIRE DAMAGE
The role of aircraft panel materials in cabin fires and their properties
[FAA-CT-84-30] N85-32104
Photovoltaic module spread-of-flame testing N85-32448
FISSION
Paired ion chamber constants for fission gamma-neutron fields
[AD-A155089] N85-32999
FISSION PRODUCTS
Paired ion chamber constants for fission gamma-neutron fields
[AD-A155089] N85-32999
FITTINGS
Development and test of advanced composite components. Center Directors discretionary fund program
[NASA-TM-86512] N85-32147
FLAME IONIZATION
Large eddy structures in transitional and turbulent flames
[AD-A154520] N85-32157
FLAME PROPAGATION
Wall flames and implications for upward flame spread
[FAA-CT-85-2] N85-32103
Optical waveguide along front of exothermic reaction N85-32954
FLAME RETARDANTS
Photovoltaic module spread-of-flame testing N85-32448
FLAME SPECTROSCOPY
Shock tube measurements of growth constants in the branched-chain ethane-carbon monoxide-oxygen system
[NASA-TM-87068] N85-32156
FLAME STABILITY
Wall flames and implications for upward flame spread
[FAA-CT-85-2] N85-32103
FLAMES
Large eddy structures in transitional and turbulent flames
[AD-A154520] N85-32157
Status of boron combustion research
[AD-A154762] N85-32160
In-cavity laser IR spectrum analyzer for investigating non-steady-state processes N85-32894
FLAMMABILITY
The role of aircraft panel materials in cabin fires and their properties
[FAA-CT-84-30] N85-32104
Photovoltaic module spread-of-flame testing N85-32448
FLASH BLINDNESS
Predictive model of electron beam induced flashblindness
[AD-A155260] N85-32763
FLAT PLATES
Instability and chaotic behavior in a free-surface flow
[AD-A154879] N85-32279
Numerical solutions of turbulent models for flow over a flat plate with angle of attack
[DE85-010380] N85-32286
An investigation into the comparisons of the underwater shock effects on a stiffened flat plate to the predictive nature of a computer model
[AD-A155612] N85-32355
Proceedings of the 24th Project Integration Meeting
[NASA-CR-176058] N85-32394
Flat-plate module efficiency versus cost tradeoffs N85-32398
Block V module program N85-32401
Reliability physics N85-32402
MOD silver metallization for photovoltaics N85-32428
Development of artificially produced perturbations in supersonic boundary layer N85-32879
FLEXIBILITY
User's guide for computer program CGFAG, Concrete General Flexure Analysis with Graphics
[AD-A155555] N85-32204
Thin-film reliability and engineering overview N85-32450
FLEXING
Graphite/PMR polyimide composites with improved toughness
[NASA-TM-87061] N85-32148
FLIGHT CHARACTERISTICS
In-flight evaluation of pure time delays in pitch and roll
[NASA-TM-86744] N85-32123

FLIGHT CONTROL
Flight control system for a computer controlled aircraft with limited sensors
[AD-A155107] N85-32115
Myoelectric control of a computer based expert system for flight control
[AD-A154981] N85-32126
FLIGHT HAZARDS
Space Station crew safety alternatives study. Volume 2: Threat development
[NASA-CR-3855] N85-32133
FLIGHT MECHANICS
The Naval Postgraduate School Flight Mechanics Laboratory: A feasibility study
[AD-A154578] N85-32127
FLIGHT SIMULATION
A preliminary investigation of handling qualities requirements for helicopter instrument flight during decelerating approach maneuvers and overshoot
[AD-A154650] N85-32125
FLIGHT SIMULATORS
Advanced simulator for pilot training and helmet-mounted visual display configuration comparisons
[AD-A155326] N85-32776
FLIGHT TESTS
Artificial and natural icing tests YEH-60A quick fix helicopter
[AD-A155147] N85-32116
Design of an expert-system flight status monitor
[NASA-TM-86739] N85-32794
FLOAT ZONES
Advanced module development overview N85-32445
FLOATS
Air carrier overwater emergency equipment and procedures
[PB85-917006] N85-32105
FLOW CHARACTERISTICS
Investigation of influence of gas exit modes on characteristics of N2O - N2 - He discharge laser N85-32888
FLOW CHARTS
Resource management for the tagged token dataflow architecture
[AD-A154773] N85-32779
FLOW DISTORTION
Development of artificially produced perturbations in supersonic boundary layer N85-32879
FLOW DISTRIBUTION
BLAF: A blast field reconstruction program from pressure histories
[AD-A155300] N85-32283
Techniques for the study of gravity waves and turbulence (keynote paper), part 4 N85-32499
FLOW EQUATIONS
The calculation of fully three dimensional flow through any type of turbomachine blade row N85-32294
FLOW MEASUREMENT
Injection of drag reducing additives into turbulent water flows: Two-component velocity measurements and mixing length model predictions
[AD-A154604] N85-32274
FLOW STABILITY
Experiments on the influence of active walls on the initial amplitudes and growths of instability waves
[AD-A154630] N85-32275
Instability and chaotic behavior in a free-surface flow
[AD-A154879] N85-32279
FLOW THEORY
Explosion in flight N85-32883
FLOW VELOCITY
A panel method study of vortex sheets with special emphasis on sheets of axisymmetric geometry
[NASA-CR-177365] N85-32095
FLOW VISUALIZATION
Two-phase flow visualization in a transparent, atmospheric pressure, boiling water loop
[DE84-016857] N85-32288
FLUID BOUNDARIES
The Konstantinov effect and absorption of sound in inhomogeneous media N85-32861
FLUID DYNAMICS
Notes on unsteady transonic cascade flows
[AD-A154829] N85-32096
Experiments on the influence of active walls on the initial amplitudes and growths of instability waves
[AD-A154630] N85-32275
Characteristics of a numerical fluid dynamics simulator
[DE85-009602] N85-32290
FLUID FILLED SHELLS
Acoustic radiation from concentric shells containing an inner fluid
[AD-A155476] N85-32991
FLUID FLOW
Observations of the use of the setapoint detector
[AD-A154533] N85-32208
Weak shock waves propagating in fluid-gas mixtures
[AD-A154759] N85-32276
FLUID MECHANICS
Bubble dynamics in polymer solutions undergoing shear
[AD-A154575] N85-32193
Experiments on the influence of active walls on the initial amplitudes and growths of instability waves
[AD-A154630] N85-32275
USSR report: Physics and mathematics
[JPRS-UPM-85-004] N85-32860
FLUID PRESSURE
Polymer solution-supercritical fluid behavior
[AD-A154514] N85-32192
FLUIDIZED BED PROCESSORS
An investigation into the fluidization and heat transfer of low density particles in a fluidized bed with applications
[AD-A155259] N85-32282
A fluidized-bed reactor for silane pyrolysis N85-32413
JPL in-house fluidized-bed reactor research N85-32414
Modeling of the silane FBR system N85-32415
FLUORESCENCE
Multidimensional luminescence measurements
[AD-A154950] N85-32162
A microprocessor-controlled, multichannel fluorimeter for analysis of sea water
[AD-A154986] N85-32310
Detection of excited states by laser-induced fluorescence
[AD-A155558] N85-32326
FLUORINE
Synthesis of energetic materials
[AD-A154887] N85-32210
FLUOROCARBONS
Basic research in novel inorganic reagents and fluorocarbon chemistry
[AD-A155340] N85-32165
FLUX (RATE)
Use of the VAD technique and measurements of momentum flux in the stratosphere at Aercibo, part 4.3A N85-32505
Momentum flux measurements: Techniques and needs, part 4.5A N85-32508
Characteristics and sources of E-region ionization in the continuous aurora
[AD-A155018] N85-32562
Horizontal and vertical structure of velocity, potential vorticity and energy in the gulf stream
[AD-A154753] N85-32702
Sulfur Cycle N85-32748
Solar cycle variation of ephemeral regions
[AD-A154967] N85-33097
FOCUSING
Background equatorial astronomical measurements focal plane assembly (refurbished HI STAR SOUTH)
[AD-A155215] N85-32313
Existence of smooth solutions in problems of electromagnetic radiation focusing N85-32972
FOG
Fog activation and supersaturation N85-32678
The interaction of polynuclear aromatic hydrocarbons PAH's with water vapor and their role as condensation nuclei in the formation of haze and fog N85-32695
Ice fog as an electro-optical obscurant
[AD-A155059] N85-33015
FOILS (MATERIALS)
Plasma mass and effective inductance in a small railgun
[AD-A154644] N85-32304
Plating density standards
[DE85-010014] N85-32318
Rhodium-103 and Indium-115 inelastic scattering reactions for fission neutron dosimetry N85-33004
FOLIAGE
Scattering from foliage covered terrain
[AD-A154724] N85-32228
FOOD CHAIN
From microbial communities to cells N85-32728
FORCED CONVECTION
Forced convection on solar collector arrays
[DE85-010381] N85-32287
FORECASTING
New estimating procedures for surface runoff, sediment yield, and contaminant transport in Los Alamos County, New Mexico
[DE85-011890] N85-32393
Forecasting atmospheric visibility over the summer north Atlantic using the principal discriminant method
[AD-A155537] N85-32593
FORESTS
Study of the formation of particles from natural hydrocarbons released by vegetation N85-32640
FORMATIONS
Implications for the Earth of the early dynamical environment N85-33079
FORMULAS (MATHEMATICS)
Aspects of SAR image segmentation
[AD-A154965] N85-32236
FORTRAN
Reliability of void detection in structural ceramics using scanning laser acoustic microscopy
[NASA-TM-87035] N85-32337
SIGMA - A stochastic-integration global minimization algorithm
[AD-A154878] N85-32806
FOSSILS
Cyanobacterial mats: Microanalysis of community metabolism N85-32743
FOURIER ANALYSIS
Head-on scattering of a tubular cylinder of finite length for radar target identification purposes
[AD-A155608] N85-32246
Analysis of spacecraft data
[NASA-CR-171587] N85-32789
SCRIBE data of October 23, 1983 flight
[AD-A154864] N85-33012
FOURIER TRANSFORMATION
In-situ measurement of wall thermal performance: Data interpretation and apparatus design recommendations
[DE85-011979] N85-32289
Qualitative analysis of sign-bit processing
[AD-A154776] N85-32804
FRACTURE MECHANICS
Influence of the resin on interlaminar mixed-mode fracture
[NASA-TM-87571] N85-32150
Comparisons of various configurations of the edge delamination test for interlaminar fracture toughness
[NASA-TM-86433] N85-32151
Effects of weak interfaces on thermostructural behavior of carbon-carbon composites
[AD-A155330] N85-32154
The shearing contribution in transformation toughening of brittle materials
[AD-A154656] N85-32195
Stress corrosion of ceramic materials
[AD-A155020] N85-32202
Dynamic fracture behavior of structural materials
[AD-A154568] N85-32345
Ductile fracture of dynamically loaded naval structures-compact tension specimen tests and analyses
[AD-A155472] N85-32353
Development of improved dynamic failure models
[AD-A155586] N85-32354
FRACTURE STRENGTH
Influence of the resin on interlaminar mixed-mode fracture
[NASA-TM-87571] N85-32150
Comparisons of various configurations of the edge delamination test for interlaminar fracture toughness
[NASA-TM-86433] N85-32151
Metallurgical origins of fracture toughness and microstructure and fracture toughness of an HSLA (High-Strength/Low-Alloy) steel
[AD-A155530] N85-32187
Thin-film reliability and engineering overview N85-32450
FRACTURES (MATERIALS)
Dynamic fracture behavior of structural materials
[AD-A154568] N85-32345
FREE ELECTRON LASERS
Cerenkov maser and Cerenkov laser devices
[AD-A155443] N85-32324
FREE ENERGY
Influence of particle arrangement on sintering
[AD-A155337] N85-32352
FREE FLOW
Experiments on the influence of active walls on the initial amplitudes and growths of instability waves
[AD-A154630] N85-32275
Numerical solutions of turbulent models for flow over a flat plate with angle of attack
[DE85-010380] N85-32286
FREE JETS
Aerosol analysis and emission spectrometry with free jets
[DE85-010576] N85-32168
FREE RADICALS
Shock tube measurements of growth constants in the branched-chain ethane-carbon monoxide-oxygen system
[NASA-TM-87068] N85-32156
FREEZING
On the problem of possible mechanism of ice nuclei formation in convective clouds N85-32610
Supersaturation spect A of Ice Nuclei at different locations in Europe and over the North-Atlantic N85-32615

Concentrations of ice nuclei of different modes of activities N85-32616
Ice nucleating characteristics of Capparis Aphylla, an Indian herb N85-32619
Ice-forming efficiency of the soluble and insoluble portions of dust contained in snow N85-32631
Critical supersaturations with respect to water for fast condensation-freezing ice nucleation N85-32632

FREQUENCIES
The problem of brightness enhancement during laser frequency doubling N85-32897

FREQUENCY ASSIGNMENT
Criteria for site selection and frequency allocation (keynote paper), part 5 N85-32511
Frequency and site selection criteria for MST radars, part 5.1A N85-32512

FREQUENCY DISTRIBUTION
Coding schemes for improving MST radar performance, part 7.1A N85-32520

FREQUENCY MULTIPLIERS
A phase-locked frequency multiplier for the signal averaging of the vibration of the Wessex helicopter input spiral bevel pinion
[AD-A154914] N85-32113

FREQUENCY RANGES
VLF (Very low frequency) workshop held at San Diego California, 24-25 January 1985
[AD-A154652] N85-32224

FREQUENCY SHIFT
Design of a jamming simulator for a binary communication system
[AD-A154617] N85-32221
Mesospheric measurements of irregularity patches using a 3-antenna interferometer, part 3.6B N85-32498
Doppler spectrometer for measuring narrow photochemical gaps in inhomogeneously broadened spectra N85-32921

FREQUENCY STANDARDS
The role of long term lamp fluctuations in the random walk of frequency behavior of the rubidium frequency standard: A case study
[AD-A155338] N85-32314

FRESH WATER
Sulfur cycling in freshwater sediments N85-32726

FRESNEL DIFFRACTION
Morphology of the scattering targets: Fresnel and turbulent mechanisms, part 2.1A N85-32481

FRESNEL REGION
A modified Fresnel scattering model for the parameterization of Fresnel returns, part 2.3A N85-32483

FRICTION
Numerical solutions of turbulent models for flow over a flat plate with angle of attack
[DE85-010380] N85-32286
Surface roughness effects in elastohydrodynamic contacts
[NASA-TP-2488] N85-32329

FRONTS (METEOROLOGY)
Observations of frontal zone structures with a VHF Doppler radar and radiosondes, part 1.2A N85-32469
Thunderstorm phenomena and weather radar scanning strategies
[DOT/FAA/PM-85/14] N85-32573

FUEL TESTS
Observations of the use of the setapoint detector
[AD-A154533] N85-32208

FUNCTIONAL ANALYSIS
Conceptualizing in assembly tasks
[AD-A155564] N85-32770

FUNCTIONS (MATHEMATICS)
On the dependence of the convergence of Gummel's algorithm on the regularity of the solution
[AD-A154628] N85-32832
New developments on the core function for efficient implementation of the difficult residue number system operations
[AD-A154678] N85-32834
USSR report: Physics and mathematics
[JPRS-UPM-85-004] N85-32860

FURNACES
High-frequency furnace
[DE85-011210] N85-32291

FUSELAGES
Wind tunnel drag evaluations of helicopter nose sections
[AD-A155489] N85-32100

G

GADOLINIUM
Spectral-luminescence characteristics and induced emission of Nd-3(+) ion in Gd(2-x)Nd(x)(WO4)3 crystals N85-32912

GALACTIC RADIATION
Differential measurement of cosmic-ray gradient with respect to interplanetary current sheet
[PAPER-SH-4.2-9] N85-33055

GALLIUM ANTIMONIDES
Inter-zone auger recombination in GaSb laser structures N85-32875

GALLIUM ARSENIDE LASERS
Low-threshold injection InGaAsP/GaAs double heterostructure lasers with separate limiting obtained by liquid-phase epitaxy (lambda = 0.78 divided by 0.87 microns, I sub thr = 460 A/cm 2, T = 300 K) N85-32908
Influence of technological factors on luminescence characteristics of InGaAsP/InP heterolasers (lambda = 1.55 microns) N85-32910

GALLIUM ARSENIDES
NASA space station automation: AI-based technology review
[NASA-CR-176094] N85-32134
LSI/VLSI ion implanted planar GaAs IC processing
[AD-A155110] N85-32262
Effect of powerful pulsed low-energy ion streams on GaAs N85-32877
Microwave semiconductor research: Materials, devices and circuits and gallium arsenide ballistic electron transistors
[AD-A154698] N85-33024
Microscopic control of semiconductor surface oxidation
[AD-A154799] N85-33026
Determination of kinetic parameters of molecular beam epitaxy
[AD-A155222] N85-33030
Raman scattering studies in solids
[AD-A155528] N85-33032

GAMMA RAY SPECTRA
Paired ion chamber constants for fission gamma-neutron fields
[AD-A155069] N85-32999
Kalman filter time series analysis of gamma-ray data from NaI(T1) detectors for the ND6620 computer
[AD-A154995] N85-33014

GAMMA RAYS
Study of proton and neutron activation of metal samples in low Earth orbit
[NASA-CR-171596] N85-32130
Results from radiation monitoring equipment experiments on STS-41C, 41D, 41G and 51A
[AD-A154676] N85-32142
A practical guide to ionization chamber dosimetry at the AFRRI reactor
[AD-A155185] N85-33003
Empirical correlation of residual gamma radiation resulting from operation of the Health Physics Research Reactor
[DE85-012075] N85-33008
Kalman filter time series analysis of gamma-ray data from NaI(T1) detectors for the ND6620 computer
[AD-A154995] N85-33014
A balloon-borne imaging gamma-ray telescope
[PAPER-OG-9.2-2] N85-33049
Balloon-borne video cassette recorders for digital data storage
[PAPER-OG-9.3-11] N85-33050
Research in particles and fields
[NASA-CR-176069] N85-33103

GARNETS
Anorthositic oceanic crust in the Archean Earth N85-33077

GAS ANALYSIS
Participation of singlet oxygen in photodestruction of air-saturated solutions of coumarin dyes N85-32891
The possibilities of remote analysis of atmospheric gases based on Raman scattering spectroscopy N85-32892

GAS CHROMATOGRAPHY
The determination of dinitrotoluene in single base propellants
[AD-A154672] N85-32209

GAS DENSITY
Emergency modeling of hazardous air pollutants
[AD-A155441] N85-32461

GAS DISCHARGE TUBES
Space-time characteristics of field in longitudinal pulse-period discharge typical in pumping of self-terminating lasers N85-32909

GAS DYNAMICS
A variable node finite element method applied to the gas dynamics equations
[AD-A155211] N85-32281
The 2-D simulations of the NRL (Naval Research Laboratory) laser experiment
[AD-A154915] N85-32321
Mechanics of a gaseous film barrier to lubricant wetting of elastohydrodynamically lubricated conjunctions
[NASA-TP-2500] N85-32330
A comparison of experimental and theoretical results for rotordynamic coefficients of four annular gas seals
[NASA-CR-176086] N85-32332

GAS EXPLOSIONS
Explosion in flight N85-32883

GAS FLOW
BLAF: A blast field reconstruction program from pressure histories
[AD-A155300] N85-32283
Investigation of influence of gas exit modes on characteristics of N2O - N2 - He discharge laser N85-32888

GAS MIXTURES
Weak shock waves propagating in fluid-gas mixtures
[AD-A154759] N85-32276
Asymptotically stable solutions of some nonlinear equations N85-32974

GAS TURBINE ENGINES
Tape casting as an approach to an all-ceramic turbine shroud seal
[NASA-TM-87078] N85-32333

GAS TURBINES
The effect of stress and hot corrosion on nickel-base superalloys
[AD-A154722] N85-32181

GAS-LIQUID INTERACTIONS
Mechanics of a gaseous film barrier to lubricant wetting of elastohydrodynamically lubricated conjunctions
[NASA-TP-2500] N85-32330

GASES
Emergency modeling of hazardous air pollutants
[AD-A155441] N85-32461

GASIFICATION
Biomass thermochemical conversion program
[DE85-011867] N85-32213

GASTROINTESTINAL SYSTEM
Influence of chemical form, feeding regimen, and animal species on the gastrointestinal absorption of plutonium
[DE85-010291] N85-32751

GATES (CIRCUITS)
Digital integrated circuits N85-32767

GEARS
A phase-locked frequency multiplier for the signal averaging of the vibration of the Wessex helicopter input spiral bevel pinion
[AD-A154914] N85-32113
Proposal for modifications to the Wessex helicopter main rotor gearbox vibration monitoring program
[AD-A155196] N85-32117

GENERAL AVIATION AIRCRAFT
Quest for performance: The evolution of modern aircraft
[NASA-SP-468] N85-32089

GENERATORS
Design of a generator for near-tangential transonic swirling outflow
[AD-A155163] N85-32280

GENETIC ENGINEERING
East Europe report: Science and technology
[JPRS-ESA-85-023] N85-32217

GENETICS
Search for the universal ancestors
[NASA-SP-477] N85-32777

GEOBOTANY
Carbon isotope geochemistry and geobiology N85-32716

GEOCHEMISTRY
Global Mega-Geomorphology
[NASA-CP-2312] N85-32357
Carbon isotope geochemistry and geobiology N85-32716
Geology and geochemistry of sulfide and sulfate deposition N85-32723
Microbiology of solar salt ponds N85-32724
Workshop on the Early Earth: The Interval from Accretion to the Older Archean
[NASA-CR-176037] N85-33062
The relation between the age of the subconducting slab and the recycling of sediments into the mantle N85-33063
The 3.5 b.y. old Onverwacht Group: A remnant of ancient oceanic crust N85-33073
A review of noble gas geochemistry in relation to early Earth history N85-33081
The Aravalli sequence of Rajasthan, India: A Precambrian continental margin? N85-33084
Carbon and nitrogen in the deep Earth N85-33085
Chemical evolution of the Earth: Equilibrium or disequilibrium process? N85-33086
Thermal, dynamic and compositional aspects of the core-forming Earth N85-33091

GEOCHRONOLOGY
Global Mega-Geomorphology
[NASA-CP-2312] N85-32357
Some observations on paleogeomorphology N85-32363

Landscape inheritance: Report of Working Group Number 2 N85-32383
Precambrian evolution and the rock record N85-32711
Origin of life N85-32713
The 3.5 b.y. old Onverwacht Group: A remnant of ancient oceanic crust N85-33073
Archean sedimentary systems and crustal evolution N85-33082
The Aravalli sequence of Rajasthan, India: A Precambrian continental margin? N85-33084
Chemical constraints on the evolution of Archean continental crust N85-33093
Dating Archean zircon by ion microprobe: New light on an old problem N85-33094

GEODESY
Crustal dynamics project data analysis fixed station VLBI geodetic results [NASA-TM-86229] N85-32465
SPLINES. Their equivalence to collocation [AD-A155250] N85-32566

GEODETIC COORDINATES
Basic formulae for the computation of the deflection of the vertical from astronomical star observations [AD-A154912] N85-32390

GEODYNAMICS
Precambrian evolution and the rock record N85-32711
Thermal, dynamic and compositional aspects of the core-forming Earth N85-33091

GEOLOGICAL FAULTS
Design of a freestanding noise measurement and recording system to predict the intensity and location of electromagnetic radiation from earthquakes [AD-A155070] N85-32563

GEOLOGICAL SURVEYS
Worldwide directory of national Earth-science agencies and related international organizations [GS-CIRC-934] N85-32386

GEOLOGY
Global Mega-Geomorphology [NASA-CP-2312] N85-32357
Space imagery and some geomorphological problems of the Guiana Shield, South America N85-32368
One application of mega-geomorphology in education N85-32370
Worldwide directory of national Earth-science agencies and related international organizations [GS-CIRC-934] N85-32386
Carbon and sulfur cycling through geologic time N85-32720
Geology and geochemistry of sulfide and sulfate deposition N85-32723

GEOMAGNETISM
Fluxgate magnetometer (SSM) for the defense meteorological satellite program (DMSP) block 5D-2, flight 7 [AD-A155229] N85-32143
Planetary Dynamos [NASA-CR-176001] N85-32857

GEOMETRICAL OPTICS
Solvability of some inverse problems in laser radiation focusing N85-32963
Existence of smooth solutions in problems of electromagnetic radiation focusing N85-32972

GEOMETRICAL THEORY OF DIFFRACTION
Guided-mode launching in a slab waveguide by way of diffraction at the edge of a conducting screen residing on one surface of the slab [AD-A154886] N85-32232

GEOMETRY
A fast discharge excimer laser with symmetric geometry [AD-A155294] N85-32322
Photo-acoustic effect in finite-dimensional semiconductors N85-32876

GEOMORPHOLOGY
Global Mega-Geomorphology [NASA-CP-2312] N85-32357
A new global geomorphology? N85-32358
Global geomorphology N85-32359
Megageomorphology: Mars vis a vis Earth N85-32360
Geomorphological similarity and uniqueness N85-32361
Regional landform thresholds N85-32362
Some observations on paleogeomorphology N85-32363
Ancient landscapes: Their nature and significance for the question of inheritance N85-32364
Geomorphology, tectonics, and exploration N85-32365
Megageomorphology and neotectonics N85-32366
Andrean examples of mega-geomorphology themes N85-32367
Space imagery and some geomorphological problems of the Guiana Shield, South America N85-32368
Deep sea mega-geomorphology: Progress and problems N85-32369
One application of mega-geomorphology in education N85-32370
Use of the synoptic view: Examples from Earth and other planets N85-32371
Geomorphic classification of Icelandic and Martian volcanoes: Limitations of comparative planetology research from LANDSAT and Viking orbiter images N85-32372
Aeolian geomorphology from the global perspective N85-32373
Geomorphic analyses from space imagery N85-32374
The problem of scale in planetary geomorphology N85-32375
Quantitative analysis in megageomorphology N85-32376
Use of spaceborne imaging radar in regional geomorphic studies N85-32377
Techniques, problems and uses of mega-geomorphological mapping N85-32378
Quantitative analysis of geomorphic processes using satellite image data at different scales N85-32380
Quantitative geomorphologic studies from spaceborne platforms N85-32381
Global geomorphology: Report of Working Group Number 1 N85-32382
Process thresholds: Report of Working Group Number 3 N85-32384
Planetary perspective. Report of Working Group Number 4 N85-32385
Precambrian evolution and the rock record N85-32711
Considerations of large scale impact and the early Earth N85-33070

GEOPHYSICAL SATELLITES
Application of satellite accelerometer data to improve density models [AD-A154904] N85-32558

GEOPHYSICS
Global Mega-Geomorphology [NASA-CP-2312] N85-32357
Deep sea mega-geomorphology: Progress and problems N85-32369
The origin of continental crust: Outlines of a general theory N85-33083

GEOTEMPERATURE
Crustal radiogenic heat production and the selective survival of ancient continental crust N85-33086

GERMANIUM
Thermoelectric properties of beta-boron and some boron compounds [DE85-011978] N85-32270
Absorption of 10.6 micrometer laser radiation in electron-hole condensate in germanium N85-32870
Raman scattering studies in solids [AD-A155528] N85-33032

GLASS
EVA-glass interface bond stability N85-32408
Thin-film reliability and engineering overview N85-32450
Luminescence and absorption of indium-activated potassium-borate glasses subjected to high-power excitation N85-32868

GLASS LASERS
Operation of solid state lasers exposed to electron beam N85-32895

GLOBAL AIR POLLUTION
The global sulfur cycle [NASA-TM-87570] N85-32710

GLOBAL ATMOSPHERIC RESEARCH PROGRAM
Generation of available potential energy and the energy cycle during the global weather experiment [NASA-CR-175301] N85-32572

GLOBAL POSITIONING SYSTEM
The potential of the NAVSTAR global positioning system for the Corps of Engineers, civil works [AD-A154913] N85-32109
A derivation of relativistic effects in satellite tracking [AD-A154620] N85-32132

GLOW DISCHARGES
Characteristics of optogalvanic effect in media with inverse populations N85-32944
Investigation of space-time structure of glow of laser plasma colliding with flat screen N85-32947

GLUTATHIONE
Distribution and abundance of organic thiols N85-32717
Glutathione in cyanobacteria N85-32745

GNEISS
Dating Archean zircon by ion microprobe: New light on an old problem N85-33094

GOES SATELLITES
Rain volume estimation over areas using satellite and radar data [NASA-CR-176050] N85-32570

GOLD
Resistance of polyaniline films as a function of electrochemical potential and the fabrication of polyaniline-based microelectronic devices [AD-A154999] N85-32201

GOVERNMENT PROCUREMENT
Feasibility of applications of Competition Decision Assist Package (CDAP) to spare parts [AD-A154716] N85-33036

GRAIN BOUNDARIES
The effect of stress and hot corrosion on nickel-base superalloys [AD-A154722] N85-32181
The effect of diffusive hydrogen segregation on fracture of polycrystalline nickel [AD-A155238] N85-32186
Influence of particle arrangement on sintering [AD-A155337] N85-32352
Electrotransport in thin films [AD-A155584] N85-33034
Electronic phenomena near semiconductor grain boundaries [DE85-011543] N85-33035

GRAIN SIZE
Modification of the grain size of sputtered copper with additions of oxygen, krypton, silver, or yttrium [DE85-010975] N85-32189
Nonequilibrium kinetics of growth of oxide layer grains during laser heating of metals in air N85-32919

GRAPHITE
Electrical and mechanical properties of intercalated graphite fibers [AD-A155560] N85-32205
Paired ion chamber constants for fission gamma-neutron fields [AD-A155069] N85-32999

GRAPHITE-EPOXY COMPOSITES
Development and test of advanced composite components. Center Directors discretionary fund program [NASA-TM-86512] N85-32147
Comparisons of various configurations of the edge delamination test for interlaminar fracture toughness [NASA-TM-86433] N85-32151
Measurement of damping of graphite epoxy materials [NASA-CR-176073] N85-32334

GRAPHITE-POLYIMIDE COMPOSITES
Graphite/PMR polyimide composites with improved toughness [NASA-TM-87081] N85-32148
Thermal expansion of selected graphite reinforced polyimide-, epoxy-, and glass-matrix composite [NASA-TM-87572] N85-32149

GRAVITATIONAL FIELDS
Global geoid and gravity anomaly predictions using the collocation and point mass techniques [AD-A154517] N85-32387
The evolution of complex and higher organisms [NASA-SP-478] N85-32708

GRAVITY ANOMALIES
Comparison of survey and photogrammetry methods to position gravity data, Yucca Mountain, Nevada [DE85-011685] N85-32316
Global geoid and gravity anomaly predictions using the collocation and point mass techniques [AD-A154517] N85-32387
Upward continuation of surface gravity anomalies [AD-A154973] N85-32560

GRAVITY WAVES
Middle Atmosphere Program. Handbook for MAP. Volume 14: URSI/SCOSTEP Workshop on Technical Aspects of MST Radar [NASA-CR-176085] N85-32466
Excerpts from the paper: Research Status and Recommendation from the Alaska Workshop on Gravity Waves and Turbulence in the Middle Atmosphere, part 1.3A N85-32470
Gravity waves from the stratosphere to the mesosphere, part 1.3B N85-32471
The suppression of convective wavebreaking by radiative transfer processes, part 1.3C N85-32472
A simple model for testing the effects of gravity-wave-produced vertical oscillations of scattering irregularities on spaced-antenna, horizontal drift measurements N85-32489
Interferometer applications of VHF radars, part 3.6A N85-32497
Techniques for the study of gravity waves and turbulence (keynote paper), part 4 N85-32499
Spectral measurements of turbulence and gravity waves, part 4.2A N85-32501

Gravity-wave spectra in the atmosphere observed by MST radar, part 4.2B N85-32502
High resolution evidence for the Garrett-Munk spectrum of stratospheric gravity waves N85-32503
On the spectrum of atmospheric velocity fluctuations seen by MST/ST radar and their interpretation N85-32504
Use of the VAD technique and measurements of momentum flux in the stratosphere at Aercibo, part 4.3A N85-32505
Momentum flux measurements: Techniques and needs, part 4.5A N85-32508
Tropospheric gravity waves observed by three closely spaced ST radars N85-32509
Determination of horizontal and vertical wavelengths of gravity waves in the mesosphere by spaced wind measurements N85-32510
On the limiting configuration of interfacial gravity waves
[AD-A154821] N85-32557
A new hypothesis for the observed vertical distribution of atmospheric aerosols N85-32646

GREEN'S FUNCTIONS
A cracked orthotropic sheet stiffened by a semi-infinite orthotropic sheet
[NASA-TP-2455] N85-32339
Exact solutions of singular equations for viscous transsonic flows N85-32882

GROUND BASED CONTROL
Simulation studies of time-control procedures for the advanced air traffic control system
[NASA-TP-2493] N85-32101

GROUND EFFECT (COMMUNICATIONS)
Most desirable terrain, e.g., flat vs valley location, part 5.1B N85-32513

GROUND TRUTH
Handbook for obtaining and using aerial photography to map aquatic plant distribution
[AD-A154584] N85-32388

GROUP DYNAMICS
Symbolic and interactional perspectives on leadership: An integrative framework
[AD-A155247] N85-32769

GROWTH
Cloud droplet nucleation and initial growth derived from lidar depolarization studies N85-32635
Chemolithotrophy and physiology of bacterial nutrient limitation N85-32730
Sulfate-reducing bacteria: Microbiology and physiology N85-32732
Microbial colonization and growth on metal sulfides and other mineral surfaces N85-32747

GUINEA PIGS
Spontaneous transitional cell carcinoma in the urinary bladder of a strain 13 guinea pig
[AD-A155645] N85-32764

GULF STREAM
Horizontal and vertical structure of velocity, potential vorticity and energy in the gulf stream
[AD-A154753] N85-32702
Numerical simulations of the response of intense ocean currents to atmospheric forcing
[AD-A155161] N85-32704

GUN PROPELLANTS
The determination of dinitrotoluene in single base propellants
[AD-A154672] N85-32209

GYROSCOPES
Test evaluation of the Honeywell GG1111 Single-Degree-of-Freedom (SDF) strapdown gyroscope
[AD-A154768] N85-32307

GYROSCOPIC STABILITY
Test evaluation of the Honeywell GG1111 Single-Degree-of-Freedom (SDF) strapdown gyroscope
[AD-A154768] N85-32307

H

HADRONS
Detector problems at the SSC
[DE85-010217] N85-33007

HALF LIFE
Study of proton and neutron activation of metal samples in low Earth orbit
[NASA-CR-171596] N85-32130

HALL EFFECT
Electrical properties of bulk grown nitrogen doped silicon
[AD-A155471] N85-32266

HARBORS
LORAN-C harbor and harbor entrance survey: Charleston, South Carolina
[AD-A154875] N85-32108

HARMONIC ANALYSIS
Acoustic radiation from concentric shells containing an inner fluid
[AD-A155476] N85-32991

HARMONIC OSCILLATORS
A multiplying slot array
[AD-A155570] N85-32245

HARMONIC RADIATION
The problem of brightness enhancement during laser frequency doubling N85-32897

HARMONICS
Upward continuation of surface gravity anomalies
[AD-A154973] N85-32560

HAZARDS
Facility for large-scale hazardous gas testing
[DE85-011852] N85-32169

HAZE
The measurement of aircraft windscreen haze and its effect on visual performance
[AD-A154949] N85-32114
Airborne measurements of the vertical distribution of Arctic haze N85-32657
Condensation nuclei and aerosol size distribution measurements in Arctic haze N85-32658
The interaction of polynuclear aromatic hydrocarbons PAH's with water vapor and their role as condensation nuclei in the formation of haze and fog N85-32695

HEALTH PHYSICS RESEARCH REACTOR
Empirical correlation of residual gamma radiation resulting from operation of the Health Physics Research Reactor
[DE85-012075] N85-33008

HEART RATE
Studies of circulatory and metabolic changes during ketamine narcosis
[AD-A154512] N85-32756

HEAT EXCHANGERS
An investigation into the fluidization and heat transfer of low density particles in a fluidized bed with applications
[AD-A155259] N85-32282

HEAT FLUX
Wall flames and implications for upward flame spread
[FAA-CT-85-2] N85-32103
Facility for large-scale hazardous gas testing
[DE85-011852] N85-32169

HEAT MEASUREMENT
The effect of prior parent phase cold work on martensite transformation in Cu-Zn-Al shape memory alloys
[AD-A155140] N85-32183

HEAT RESISTANT ALLOYS
The effect of stress and hot corrosion on nickel-base superalloys
[AD-A154722] N85-32181
Strain rate sensitivity estimation from high velocity impact data
[AD-A154703] N85-32347

HEAT SOURCES
Burn front velocity as a function of pellet density in iron-potassium perchlorate heat powders
[DE85-011448] N85-32214
Crustal radiogenic heat production and the selective survival of ancient continental crust N85-33086

HEAT TRANSFER
Wall flames and implications for upward flame spread
[FAA-CT-85-2] N85-32103
Imbedded thermocouples as a solid propellant combustion probe
[AD-A155630] N85-32167
An investigation into the fluidization and heat transfer of low density particles in a fluidized bed with applications
[AD-A155259] N85-32282
Numerical solutions of turbulent models for flow over a flat plate with angle of attack
[DE85-010380] N85-32286
Forced convection on solar collector arrays
[DE85-010381] N85-32287
Resolution of thermal striping issue downstream of a horizontal pipe elbow in stratified pipe flow
[DE85-006195] N85-32292
Concurrent implementation of the Crank-Nicolson method for heat transfer analysis
[NASA-TM-86448] N85-32822
Oscillatory solutions of the Peaceman-Rachford alternating direction implicit method and a comparison of methods for the solution of the two dimensional heat diffusion equation
[AD-A154670] N85-32833

HEAT TRANSFER COEFFICIENTS
The influence of oil contamination on the nucleate pool-boiling behavior of R-114 from a structured surface
[AD-A155609] N85-32284

HEAT TRANSMISSION
MPS solidification model. Analysis and calculation of macrosegregation in a casting ingot
[NASA-CR-171589] N85-32178
In-situ measurement of wall thermal performance: Data interpretation and apparatus design recommendations
[DE85-011979] N85-32289

HEAT TREATMENT
Metallurgical origins of fracture toughness and microstructure and fracture toughness of an HSLA (High-Strength/Low-Alloy) steel
[AD-A155530] N85-32187
Electrical and mechanical properties of intercalated graphite fibers
[AD-A155560] N85-32205
Strain rate sensitivity estimation from high velocity impact data
[AD-A154703] N85-32347

HEIGHT
Practical use of a tropopause height determination algorithm on an MST radar data set, part 1.8B N85-32479

HELICOPTERS
Wind tunnel drag evaluations of helicopter nose sections
[AD-A155489] N85-32100
A phase-locked frequency multiplier for the signal averaging of the vibration of the Wessex helicopter input spiral bevel pinion
[AD-A154914] N85-32113
Artificial and natural icing tests YEH-60A quick fix helicopter
[AD-A155147] N85-32116
Proposal for modifications to the Wessex helicopter main rotor gearbox vibration monitoring program
[AD-A155196] N85-32117
Helicopter noise survey for selected cities in the contiguous US
[AD-A154893] N85-32985

HELIUM
Investigation of influence of gas exit modes on characteristics of N2O - N2 - He discharge laser N85-32888
Selective population of N = 3 OVIII level during expansion of laser plasma in helium N85-32914
Changes in the energy spectrum of anomalous oxygen and helium during 1977 - 1985
[PAPER-SH-4.6-1] N85-33056
Solar cycle variations of the anomalous cosmic ray component
[PAPER-SH-4.6-2] N85-33057

HELIUM ISOTOPES
Cosmic ray He3 measurements
[PAPER-OG-4.2-3] N85-33045
Constraints on early atmosphere from planetary accretion processes N85-33064
The degassing history of the Earth: Noble gas studies of Archaean cherts and zero age glassy submarine basalts N85-33072

HELIUM-NEON LASERS
Applications of laser technology described N85-32218
Investigation of reproducibility of emission wavelength of helium-neon laser with external neon absorption cell (0.63 micrometers) N85-32884
Dielectric mirror with ferromagnetic substrate N85-32966

HELMET MOUNTED DISPLAYS
Advanced simulator for pilot training and helmet-mounted visual display configuration comparisons
[AD-A155326] N85-32776

HEMODYNAMIC RESPONSES
Analysis of the transient response of temporal artery blood flow data relative to various anti-G suit pressure schedules
[AD-A155242] N85-32775

HETERODYNING
A comparison of electronic heterodyne moire deflectometry and electronic heterodyne holographic interferometry for flow measurements
[NASA-TM-87071] N85-32302

HETEROGENEITY
Mechanism of heterogeneous deposition ice nucleation near water-saturation N85-32597

HEURISTIC METHODS
A practical approach to Karmarkar's algorithm
[AD-A155714] N85-32818

HIERARCHIES
Models for multidimensional tests and hierarchically structured training materials
[AD-A155231] N85-32768

HIGH ALTITUDE
Applied research and development for falling-sphere air density measuring systems
[AD-A155227] N85-32099

HIGH ENERGY INTERACTIONS
High-energy Physics Institute building 3-trillion-ev accelerator N85-32934
HIGH FREQUENCIES
Field antenna handbook
[AD-A155204] N85-32242
High-frequency furnace
[DE85-011210] N85-32291
HIGH LEVEL LANGUAGES
HLLM software support
[AD-A154828] N85-32805
The formal specification of an abstract machine: Design and implementation
[AD-A155167] N85-32808
Evaluation of a software design approach: Develop a threat resolution module in Ada (trademark)
[AD-A155599] N85-32815
HIGH POWER LASERS
High-power two-frequency CW dye laser N85-32900
HIGH PRESSURE
Identification of vibrational-rotational transitions of Os-192O4 within frequency tuning limits of high pressure CO2 waveguide laser N85-32917
HIGH RESOLUTION
The determination of dinitrotoluene in single base propellants
[AD-A154672] N85-32209
Antenna induced range smearing in MST radars N85-32495
High resolution evidence for the Garrett-Munk spectrum of stratospheric gravity waves N85-32503
HIGH STRENGTH STEELS
Metallurgical origins of fracture toughness and microstructure and fracture toughness of an HSLA (High-Strength/Low-Alloy) steel
[AD-A155530] N85-32187
HIGH TEMPERATURE
Recession of graphitic nozzles in rocket motors N85-32144
Shock tube measurements of growth constants in the branched-chain ethane-carbon monoxide-oxygen system
[NASA-TM-87068] N85-32156
The effect of stress and hot corrosion on nickel-base superalloys
[AD-A154722] N85-32181
High temperature electronics technology: Life test report
[AD-A154681] N85-32257
Results of an interlaboratory fatigue test program conducted on alloy 800H at room and elevated temperatures
[NASA-CR-174940] N85-32340
HIGH TEMPERATURE TESTS
Friction and wear of solid-lubricated contact in gas turbine engine bearings
[AD-A155042] N85-32335
HIGH VOLTAGES
Module Hipot and ground continuity test results N85-32447
HISTOLOGY
Spontaneous transitional cell carcinoma in the urinary bladder of a strain 13 guinea pig
[AD-A155645] N85-32764
HISTORIES
Quest for performance: The evolution of modern aircraft
[NASA-SP-468] N85-32089
Ancient landscapes: Their nature and significance for the question of inheritance N85-32364
One application of mega-geomorphology in education N85-32370
Space research in the United Kingdom: An assessment
[AD-A155334] N85-33038
Noble gases and the early history of the Earth: Inappropriate paradigms and assumptions inhibit research and communication N85-33075
HOLE DISTRIBUTION (ELECTRONICS)
Absorption of 10.6 micrometer laser radiation in electron-hole condensate in germanium N85-32870
HOLOGRAPHIC INTERFEROMETRY
A comparison of electronic heterodyne moire deflectometry and electronic heterodyne holographic interferometry for flow measurements
[NASA-TM-87071] N85-32302
HOLOGRAPHY
Infrared laser holography used in fusion plasma studies N85-32905
HOMOGENEITY
Numerical modeling of subsurface communication
[DE85-012818] N85-32249
A cracked orthotropic sheet stiffened by a semi-infinite orthotropic sheet
[NASA-TP-2455] N85-32339
HORIZONTAL ORIENTATION
Resolution of thermal striping issue downstream of a horizontal pipe elbow in stratified pipe flow
[DE85-006195] N85-32292
On the spectrum of atmospheric velocity fluctuations seen by MST/ST radar and their interpretation N85-32504
Tropospheric gravity waves observed by three closely spaced ST radars N85-32509
Determination of horizontal and vertical wavelengths of gravity waves in the mesosphere by spaced wind measurements N85-32510
Horizontal and vertical structure of velocity, potential vorticity and energy in the gulf stream
[AD-A154753] N85-32702
HORN ANTENNAS
Fin-line horn antennas
[AD-A154597] N85-32255
HOT CORROSION
The effect of stress and hot corrosion on nickel-base superalloys
[AD-A154722] N85-32181
Thin-film reliability and engineering overview N85-32450
HOT PRESSING
Hot isostatically pressed Sm(2)(TM)17 magnets
[AD-A155479] N85-32267
System for electro-optical ceramic recrystallization N85-32872
HOT-WIRE ANEMOMETERS
Velocity and transient measurements in a shock tube using a hot-wire anemometer
[AD-A154694] N85-32305
HUMAN BEHAVIOR
Resource allocation in cerebral specialization of function: Behavioral and electrophysiological studies
[AD-A155092] N85-32759
HUMAN BEINGS
Review of the psychological issues relating to the effectiveness of structured programming
[AD-A154593] N85-32766
HUMAN FACTORS ENGINEERING
Space Station crew safety alternatives study. Volume 2: Threat development
[NASA-CR-3855] N85-32133
USSR report: Life sciences. Biomedical and behavioral sciences
[JPRS-UBB-85-020] N85-32752
Living aloft: Human requirements for extended spaceflight
[NASA-SP-483] N85-32772
Design guidelines for user-system interface software
[AD-A154907] N85-32807
HUMAN PERFORMANCE
Resource allocation in cerebral specialization of function: Behavioral and electrophysiological studies
[AD-A155092] N85-32759
Conceptualizing in assembly tasks
[AD-A155564] N85-32770
HUMAN RESOURCES
The Human Resource Management Information Network (HRMIN): A cost comparison in accordance with Office of Management and Budget (OMB) Circular no. A-76, 5 April 1979
[AD-A154583] N85-33039
HUMIDITY
Ice active bacteria as condensation nuclei N85-32603
Ice crystal nucleation on hygroscopic aerosols N85-32605
Variation of the submicron aerosol structure N85-32661
Condensation properties of atmospheric aerosol N85-32672
Measurements of the critical supersaturation of 0.029 to 0.035 micron radius particles at Washington, District of Columbia N85-32676
HURRICANES
Parameter estimation in communication system tracking satellite observations
[AD-A155137] N85-32582
HYBRID COMPUTERS
Experiments on the influence of active walls on the initial amplitudes and growths of instability waves
[AD-A154630] N85-32275
HYDRATES
Theoretical studies of structure and stability of hydrates of atmospheric sulfur species N85-32684
Defect formation in amorphous hydrated silicon subjected to laser radiation N85-32873
HYDRATION
Hydrothermal alteration in the 3.5 b.y. old Onverwacht Group of South Africa N85-33071
HYDROCARBONS
Study of the formation of particles from natural hydrocarbons released by vegetation N85-32640
The interaction of polynuclear aromatic hydrocarbons PAH's with water vapor and their role as condensation nuclei in the formation of haze and fog N85-32695
HYDROCHLORIC ACID
Photoelectron studies of autoionizing Rydberg states in HCl
[DE85-011813] N85-33001
HYDRODYNAMICS
Discovery of a nonpropagating hydrodynamic soliton
[AD-A155569] N85-32268
Mechanics of a gaseous film barrier to lubricant wetting of elastohydrodynamically lubricated conjunctions
[NASA-TP-2500] N85-32330
HYDROGEN
Detection of excited states by laser-induced fluorescence
[AD-A155558] N85-32326
Sulfate-reducing bacteria: Microbiology and physiology N85-32732
HYDROGEN EMBRITTLEMENT
The effect of diffusive hydrogen segregation on fracture of polycrystalline nickel
[AD-A155238] N85-32186
HYDROGEN IONS
Heating of the deep chromosphere during solar flares
[AD-A155256] N85-33100
HYDROGEN ISOTOPES
Cosmic ray He3 measurements
[PAPER-OG-4.2-3] N85-33045
HYDROGEN PLASMA
Injection of hydrogen macroparticles into T-10 tokamak N85-32937
HYDROGEN SULFIDE
Sulfur transformations at the hydrogen sulfide/oxygen interface in stratified waters and in cyanobacterial mats N85-32715
HYDROGEOLOGY
Deep sea mega-geomorphology: Progress and problems N85-32369
Understanding coherence losses incurred by bottom-retained signals
[AD-A155559] N85-32992
HYDROGRAPHY
Hydrographic data from the OPTOMA (Ocean Prediction Through Observations, Modeling and Analysis) program: OPTOMA15, 24 January to 23 February 1985
[AD-A155012] N85-32703
HYDROLOGY
Megageomorphology and neotectonics N85-32366
Space imagery and some geomorphological problems of the Guiana Shield, South America N85-32368
Changes in the organic material in lakes in the blast zone of Mount St. Helens, Washington: Hydrologic effects of the eruptions
[GS-CIRC-850-1] N85-32551
HYDROMECHANICS
Experiments on the influence of active walls on the initial amplitudes and growths of instability waves
[AD-A154630] N85-32275
HYDROPONICS
Hydroponics developments for spaceship garden N85-32754
HYDROTHERMAL STRESS ANALYSIS
EVA-glass interface bond stability N85-32408
Hydrothermal alteration in the 3.5 b.y. old Onverwacht Group of South Africa N85-33071
HYDROTHERMAL SYSTEMS
Submarine hydrothermal environments as sites for the origin and evolution of life N85-33074
HYDROXYL RADICALS
Passive Q-modulation of optical cavities by KCl crystals containing OH(-) -ions N85-32915
HYGROMETERS
Fog activation and supersaturation N85-32678
HYPERBOLIC FUNCTIONS
Generalized formulation of a class of explicit and implicit TVD schemes
[NASA-TM-86775] N85-32830
HYPEROXIA
Distribution and abundance of organic thiols N85-32717
HYPOKINESIA
Analysis of long bone and vertebral failure patterns
[AD-A154796] N85-32758

I

ICE
Mesoscale features and atmospheric refraction conditions of the Arctic marginal ice zone
[AD-A155139] N85-32584
The nucleation of ice at very low temperatures and pressures N85-32617
The capture of ice nucleating and non ice-nucleating aerosols by ice phase precipitation N85-32620

ICE FORMATION
Artificial and natural icing tests YEH-60A quick fix helicopter
[AD-A155147] N85-32116
Ice nucleation of single water droplet by silver iodide: A laboratory observation N85-32630
Ice-forming efficiency of the soluble and insoluble portions of dust contained in snow N85-32631
Monte Carlo studies of H2O layers adsorbed on a model basal face of AgI N85-32633
ICE NUCLEI
Eleventh International Conference on Atmospheric Aerosols, Condensation and Ice Nuclei, volume 2
[PB85-182418] N85-32596
Mechanism of heterogeneous deposition ice nucleation near water-saturation N85-32597
Experimental studies of the kinetics of deposition nucleation on an ice nucleant used in weather modification N85-32598
Inactivation of silver iodide by atmospheric nucleation inhibitors N85-32599
Ice nucleation by silver iodine particles with nearly critical sizes N85-32600
Photoinduced active sites on ice nucleating aerosol of silver iodide N85-32601
Experimental investigation of properties of ice-forming reagents N85-32602
Ice active bacteria as condensation nuclei N85-32603
The effect of supersaturation, temperature and particle size on ice-nucleating ability of atmospheric aerosol N85-32604
Ice crystal nucleation on hygroscopic aerosols N85-32605
On the efficiency of the mechanism of ice particles formation in the vapor supersaturation field around a freezing droplet N85-32606
Generation of lead, lead iodide and iodide aerosols and their ice nucleation N85-32607
The nucleation of ice crystals during the freezing of large supercooled drops N85-32608
Ice nucleus measurements N85-32609
On the problem of possible mechanism of ice nuclei formation in convective clouds N85-32610
Bacterial ice nuclei of marine origin: Some recent observations N85-32611
Airborne measurements of atmospheric ice nuclei N85-32612
Aircraft observations of condensation and ice nuclei at a tropical station N85-32613
A statistical analysis of ice nuclei concentrations at urban and rural sites in Valladolid, Spain N85-32614
Supersaturation spect A of Ice Nuclei at different locations in Europe and over the North-Atlantic N85-32615
Concentrations of ice nuclei of different modes of activities N85-32616
Observations of the atmospheric ice nucleus at northwest China N85-32618
Ice nucleating characteristics of Capparis Aphylla, an Indian herb N85-32619
The capture of ice nucleating and non ice-nucleating aerosols by ice phase precipitation N85-32620
The investigation of natural and artificial ice nuclei by the improved membrane filter method N85-32626
Basic ice nucleation mechanisms on mono and microcrystals and ice forming nuclei. Theoretical analysis and experimental results achieved in the laboratory over the past ten years: Review paper N85-32629
Ice-forming efficiency of the soluble and insoluble portions of dust contained in snow N85-32631
Critical supersaturations with respect to water for fast condensation-freezing ice nucleation N85-32632
Concentration and source areas of ice nuclei in the Alaskan atmosphere N85-32634
Eleventh International Conference on Atmospheric Aerosols, Condensation and Ice Nuclei, volume 1
[PB85-182400] N85-32636
Effect of ions on cloud formation and its role in solar terrestrial relationship N85-32697
ICELAND
Geomorphic classification of Icelandic and Martian volcanoes: Limitations of comparative planetology research from LANDSAT and Viking orbiter images N85-32372
IDENTIFYING
Distributed name management
[AD-A154785] N85-33037
IGNITION
Burn front velocity as a function of pellet density in iron-potassium perchlorate heat powders
[DE85-011448] N85-32214
IMAGE ANALYSIS
Resource allocation in cerebral specialization of function: Behavioral and electrophysiological studies
[AD-A155092] N85-32759
IMAGE FILTERS
Hexagonal uniformly redundant arrays for coded-aperture imaging
[PAPER-OG-9.2-1] N85-33048
IMAGE PROCESSING
Aspects of SAR image segmentation
[AD-A154965] N85-32236
Microcomputer processing of LANDSAT Thematic Mapper data for the acquisition of military tactical terrain data
[AD-A154781] N85-32389
Object identification and manipulation using silhouette moments
[AD-A154755] N85-33011
IMAGERY
Geomorphic classification of Icelandic and Martian volcanoes: Limitations of comparative planetology research from LANDSAT and Viking orbiter images N85-32372
Geomorphic analyses from space imagery N85-32374
Process thresholds: Report of Working Group Number 3 N85-32384
IMAGES
Infrared laser holography used in fusion plasma studies N85-32905
Optical image of bounded objects N85-32968
IMAGING RADAR
The Boot Lake MF imaging radar N85-32537
IMAGING TECHNIQUES
Z-contrast imaging and electron channeling analysis of dopants in semiconductors
[DE85-011410] N85-32269
One application of mega-geomorphology in education N85-32370
Hexagonal uniformly redundant arrays for coded-aperture imaging
[PAPER-OG-9.2-1] N85-33048
IMMUNOLOGY
East Europe report: Science and technology
[JPRS-ESA-85-021] N85-32190
East Europe report: Science and technology
[JPRS-ESA-85-023] N85-32217
IMPACT DAMAGE
Considerations of large scale impact and the early Earth N85-33070
IMPACT RESISTANCE
Strain rate sensitivity estimation from high velocity impact data
[AD-A154703] N85-32347
IMPELLERS
A 3-D Euler method for internal transonic flows computation with a multi-domain approach N85-32298
IMPROVEMENT
Improved coordinate measuring machine calibration and control
[DE85-012053] N85-32315
IMPURITIES
Z-contrast imaging and electron channeling analysis of dopants in semiconductors
[DE85-011410] N85-32269
Raman scattering studies in solids
[AD-A155528] N85-33032
INCOHERENT SCATTER RADAR
The Proust radar N85-32547
INCOHERENT SCATTERING
The Sondrestrom radar: Progress and proposed upgrades for ST work N85-32541
INCOMPRESSIBLE FLOW
Experiments on the influence of active walls on the initial amplitudes and growths of instability waves
[AD-A154630] N85-32275
INCONEL (TRADEMARK)
Decomposition of sulfuric acid using solar thermal energy
[DE85-012288] N85-32170
The effect of stress and hot corrosion on nickel-base superalloys
[AD-A154722] N85-32181
INDEXES (DOCUMENTATION)
Air Force Office of Scientific Research (AFOSR). Technical report summaries: First quarter (CY)
[AD-A154757] N85-33041
INDIUM
Luminescence and absorption of indium-activated potassium-borate glasses subjected to high-power excitation N85-32868
INDIUM ARSENIDES
Low-threshold injection InGaAsP/GaAs double heterostructure lasers with separate limiting obtained by liquid-phase epitaxy (lambda = 0.78 divided by 0.87 microns, I sub thr = 460 A/cm 2, T = 300 K) N85-32908
Adjustment of radiation wavelength of multimode InP-GaInAsP injection heterolasers N85-32913
INDIUM PHOSPHIDES
Influence of technological factors on luminescence characteristics of InGaAsP/InP heterolasers (lambda = 1.55 microns) N85-32910
Adjustment of radiation wavelength of multimode InP-GaInAsP injection heterolasers N85-32913
INDUCTANCE
Plasma mass and effective inductance in a small railgun
[AD-A154644] N85-32304
INDUSTRIAL AREAS
Influence on an industrial site on the characteristics of CCN supersaturation with air masses of different origin N85-32683
INDUSTRIAL MANAGEMENT
Quality analysis N85-32785
INDUSTRIAL SAFETY
A crew exposure study. Phase II. Volume 2. At sea. Part A
[AD-A155233] N85-32774
INDUSTRIES
Quality analysis N85-32785
INELASTIC SCATTERING
Toward the question of multi-quark configurations in nuclei N85-32929
Evaluated nuclear-data file for niobium
[DE85-012095] N85-33009
INEQUALITIES
On the dependence of the convergence of Gummel's algorithm on the regularity of the solution
[AD-A154628] N85-32832
Sobolev-Poincare's inequality and the Neumann problem for u sub t = divergence of the absolute value of the gradient u to the p-2 power x the gradient u
[AD-A154788] N85-32839
INFECTIOUS DISEASES
Differences in susceptibility of inbred mice to bacillus anthracis
[AD-A155646] N85-32750
INFORMATION DISSEMINATION
Data base management: MSTRAC (keynote paper), part 8 N85-32530
USSR Space Life Sciences Digest
[NASA-CR-3922] N85-32709
Remote medical diagnosis N85-32753
The Human Resource Management Information Network (HRMIN): A cost comparison in accordance with Office of Management and Budget (OMB) Circular no. A-76, 5 April 1979
[AD-A154583] N85-33039
The flow of scientific and technical information in the US Army Research Laboratories
[AD-A155050] N85-33043
INFORMATION FLOW
The flow of scientific and technical information in the US Army Research Laboratories
[AD-A155050] N85-33043
INFORMATION SYSTEMS
Design guidelines for user-system interface software
[AD-A154907] N85-32807
The flow of scientific and technical information in the US Army Research Laboratories
[AD-A155050] N85-33043
INFORMATION TRANSFER
Myoelectric control of a computer based expert system for flight control
[AD-A154981] N85-32126
Tight bounds on the complexity of parallel sorting
[AD-A154726] N85-32778
The flow of scientific and technical information in the US Army Research Laboratories
[AD-A155050] N85-33043
INFRARED ASTRONOMY
Activities report of the Aeronomy Department
[G-774-1984] N85-32569
INFRARED DETECTORS
Background equatorial astronomical measurements focal plane assembly (refurbished HI STAR SOUTH)
[AD-A155215] N85-32313
Absorption and scattering properties of aerosols of aggregated particles in the infrared spectral region
[AD-A155475] N85-32591
Bayesian vs MAP multiple model adaptive estimation for field of view expansion in tracking airborne targets
[AD-A155466] N85-32855
INFRARED IMAGERY
Object identification and manipulation using silhouette moments
[AD-A154755] N85-33011
INFRARED INTERFEROMETERS
SCRIBE data of October 23, 1983 flight
[AD-A154864] N85-33012
INFRARED LASERS
Cerenkov maser and Cerenkov laser devices
[AD-A155443] N85-32324

Infrared laser holography used in fusion plasma studies N85-32905
INFRARED RADIATION
Calibration and use of clutter data for simulation [AD-A154793] N85-32229
Absorption and scattering properties of aerosols of aggregated particles in the infrared spectral region [AD-A155475] N85-32591
Ice fog as an electro-optical obscurant [AD-A155059] N85-33015
INFRARED SPECTRA
Stress corrosion of ceramic materials [AD-A155020] N85-32202
Absorption and scattering properties of aerosols of aggregated particles in the infrared spectral region [AD-A155475] N85-32591
In-cavity laser IR spectrum analyzer for investigating non-steady-state processes N85-32894
INGOTS
MPS solidification model. Analysis and calculation of macrosegregation in a casting ingot [NASA-CR-171589] N85-32178
INHOMOGENEITY
Reflection of acoustic beam from inhomogeneous boundary N85-32864
Relaxation lens in inhomogeneous binary mixture N85-32957
INJECTION LASERS
Low-threshold injection InGaAsP/GaAs double heterostructure lasers with separate limiting obtained by liquid-phase epitaxy (lambda = 0.78 divided by 0.87 microns, I sub thr = 460 A/cm 2, T = 300 K) N85-32908
Adjustment of radiation wavelength of multimode InP-GaInAsP injection heterolasers N85-32913
INORGANIC CHEMISTRY
Basic research in novel inorganic reagents and fluorocarbon chemistry [AD-A155340] N85-32165
INORGANIC COMPOUNDS
Aerobic sulfur-oxidizing bacteria: Environmental selection and diversification N85-32712
INPUT
Microwave SAW (Surface Acoustic Wave) monochromator [AD-D011718] N85-32311
Visibility and vertical structure measurements in southern Germany [AD-A154714] N85-32574
INPUT/OUTPUT ROUTINES
Flight control system for a computer controlled aircraft with limited sensors [AD-A155107] N85-32115
Flexible satellite communications systems simulator, phase 3 [AD-A155647] N85-32247
INSOLATION
Improved Nominal Operating Cell Temperature (NOCT) test procedure N85-32449
INSPECTION
Infrared laser holography used in fusion plasma studies N85-32905
INSTRUCTORS
Ada (trademark) training curriculum. Advanced Ada topics L305 teacher's guide exercises [AD-A154621] N85-32798
INSTRUMENT LANDING SYSTEMS
A preliminary investigation of handling qualities requirements for helicopter instrument flight during decelerating approach maneuvers and overshoot [AD-A154650] N85-32125
INSULATION
Basic cryogenics and materials. Phase 1 [NASA-CR-177932] N85-32215
INTEGRAL EQUATIONS
A cracked orthotropic sheet stiffened by a semi-infinite orthotropic sheet [NASA-TP-2455] N85-32339
INTEGRATED CIRCUITS
Globally-asynchronous locally-synchronous systems [AD-A154624] N85-32222
Parallel simulation of digital LSI circuits [AD-A154745] N85-32258
GAO (General Accounting Office) assessment of DOD's Very High Speed Integrated Circuits (VHSIC) technology program [AD-A155109] N85-32261
LSI/VLSI ion implanted planar GaAs IC processing [AD-A155110] N85-32262
Tight bounds on the complexity of parallel sorting [AD-A154726] N85-32778
Digital integrated circuits N85-32787
Development of a dedicated speech work station [AD-A155465] N85-32824
INTEGRATED OPTICS
Solar adaptive optics [AD-A155494] N85-33101
INTERDIGITAL TRANSDUCERS
Microwave SAW (Surface Acoustic Wave) monochromator [AD-D011718] N85-32311
INTERFACES
Improved materials for composite and adhesive joints [AD-A155065] N85-32153
Interface chemistry of Hg(1-x)Cd(x)Te [AD-A154876] N85-32161
EVA-glass interface bond stability N85-32408
Interfacial bonding stability N85-32409
On the limiting configuration of interfacial gravity waves [AD-A154821] N85-32557
INTERFACIAL TENSION
Effects of weak interfaces on thermostructural behavior of carbon-carbon composites [AD-A155330] N85-32154
Hertzian contact in two and three dimensions [NASA-TP-2473] N85-32331
The Konstantinov effect and absorption of sound in inhomogeneous media N85-32861
INTERFEROMETERS
Mesospheric measurements of irregularity patches using a 3-antenna interferometer, part 3.6B N85-32498
INTERFEROMETRY
Status of the Jicamarca radar N85-32535
SCRIBE data of October 23, 1983 flight [AD-A154864] N85-33012
INTERLAYERS
X-ray diffractometric measurements and calculations of limiting values of discrepancy between lattices and layer thicknesses, preventing generation of dislocations during growth of multilayer heterostructures N85-32866
INTERNAL COMBUSTION ENGINES
Friction and wear of solid-lubricated contact in gas turbine engine bearings [AD-A155042] N85-32335
INTERNAL WAVES
Excerpts from the paper: Research Status and Recommendation from the Alaska Workshop on Gravity Waves and Turbulence in the Middle Atmosphere, part 1.3A N85-32470
On the limiting configuration of interfacial gravity waves [AD-A154821] N85-32557
Theory of soliton waves [AD-A154784] N85-32837
INTERNATIONAL SUN EARTH EXPLORER 1
ISEE-1 data reduction and analysis plasma composition experiment [NASA-CR-175306] N85-32552
INTERPLANETARY SPACE
The energy spectrum of Jovian electrons in interplanetary space [PAPER-SH-1.5-18] N85-33051
INTERPOLATION
Interpolation problems in meteor radar analysis, part 7.6A N85-32528
INTERPROCESSOR COMMUNICATION
Broadcasting topology and routing information in computer networks [AD-A155668] N85-32827
INTERSTELLAR RADIATION
Contributions to the 19th International Cosmic Ray Conference [NASA-CR-176060] N85-33044
INTERVALS
Weibull distribution based on maximum likelihood with interval inspection data [NASA-TM-86515] N85-32847
INVARIANCE
Application of adaptive noise cancellation to Coast Guard voice communications [AD-A154798] N85-32230
INVENTIONS
East Europe report: Science and technology [JPRS-ESA-85-021] N85-32190
INVERSE SCATTERING
Solvability of some inverse problems in laser radiation focusing N85-32963
INVISCID FLOW
An evaluation of four methods of numerical analysis for two-dimensional airfoil flows [AD-A155202] N85-32098
An analysis of flow models: From Navier-Stokes to potential flow equations N85-32295
Numerical solution of the Navier-Stokes equations for 3-D internal flows: An emerging capability N85-32300
Calculation of 3-D flow without numerical mixing N85-32301
IODIDES
Generation of lead, lead iodide and iodide aerosols and their ice nucleation N85-32607
IODINE
Ice nucleating characteristics of Capparis Aphylla, an Indian herb N85-32619
Ice nucleation of single water droplet by silver iodide: A laboratory observation N85-32630
Monte Carlo studies of H2O layers adsorbed on a model basal face of AgI N85-32633
IODINE LASERS
Optical inhomogeneities in a nanosecond-pulse iodine photodissociation laser with slow UV radiation pumping N85-32902
ION ACOUSTIC WAVES
Investigation of ion-acoustic plasma turbulence in field of powerful electromagnetic wave by CO2-laser radiation scattering N85-32935
ION EXCHANGING
Feasibility study for small group water desalination equipment [AD-A155106] N85-32164
ION INJECTION
ISEE-1 data reduction and analysis plasma composition experiment [NASA-CR-175306] N85-32552
Effect of powerful pulsed low-energy ion streams on GaAs N85-32877
ION MICROSCOPES
Chemical constraints on the evolution of Archean continental crust N85-33093
ION PLATING
New metal coating method developed N85-32191
ION SOURCES
Aerosol analysis and emission spectrometry with free jets [DE85-010576] N85-32168
ION TEMPERATURE
Low frequency instabilities driven by an ion temperature anisotropy [AD-A154902] N85-33016
Soft X-ray polychromator for the Solar Maximum Mission [NASA-CR-175297] N85-33096
IONIC REACTIONS
Polymer-water interaction studies N85-32411
Resonant energy transfer during strong excitation N85-32922
IONIZATION CHAMBERS
Paired ion chamber constants for fission gamma-neutron fields [AD-A155069] N85-32999
A practical guide to ionization chamber dosimetry at the AFRRI reactor [AD-A155185] N85-33003
IONIZATION CROSS SECTIONS
Toward a theory of excitation of atoms during nuclear and magnetic neutron scattering N85-32918
Contributions to the 19th International Cosmic Ray Conference [NASA-CR-176060] N85-33044
IONIZATION POTENTIALS
Contributions to the 19th International Cosmic Ray Conference [NASA-CR-176060] N85-33044
IONIZING RADIATION
USAFSAM review and analysis of radiofrequency radiation bioeffects literature [AD-A155113] N85-32760
Lower bounds of propagation velocity of steady ionizing waves in field of strong electromagnetic wave N85-32940
IONOSPHERE
Fluxgate magnetometer (SSM) for the defense meteorological satellite program (DMSP) block 5D-2, flight 7 [AD-A155229] N85-32143
Doppler satellite data characteristics [AD-A154868] N85-32231
Further developments of EISCAT as an MST radar N85-32534
Urbana radar systems: Possibilities and limitations N85-32540
The Sondrestrom radar: Progress and proposed upgrades for ST work N85-32541
The Adelaide VHF radar: Capabilities and future plans N85-32546
Ionospheric electron density profile and related studies [AD-A155257] N85-32567
Beam diffusion in linear ionospheric layer N85-32958
IONOSPHERIC DISTURBANCES
Equitorial scintillations: Advances since ISEA-6 [AD-A154962] N85-32559

IONOSPHERIC DRIFT
A simple model for testing the effects of gravity-wave-produced vertical oscillations of scattering irregularities on spaced-antenna, horizontal drift measurements N85-32489
Effects of line-of-sight velocity on spaced-antenna measurements, part 3.5A N85-32496
IONOSPHERIC ELECTRON DENSITY
Ionospheric electron density profile and related studies
[AD-A155257] N85-32567
IONOSPHERIC ION DENSITY
Radar echoes at 2.66 and 40.92 MHz from the mesosphere, part 2.6A N85-32486
IONS
Production of stable embryo particles in dense ion tracks of alpha particle emissions in the atmosphere N85-32638
Formation of particles in the air of the humid tropical forests N85-32639
Effect of ions on cloud formation and its role in solar terrestrial relationship N85-32697
Electrostatic ion cyclotron instability due to a nonuniform electric field perpendicular to the external magnetic field
[AD-A155474] N85-33019
IRON
Burn front velocity as a function of pellet density in iron-potassium perchlorate heat powders
[DE85-011448] N85-32214
Microanalysis of dissolved iron and phosphate in pore waters of hypersaline sediment N85-32744
Multiphoton production and detection of atoms
[AD-A155561] N85-33000
Initial results from the Caltech/DSRI balloon-borne isotope experiment
[PAPER-OG-4.3-8] N85-33046
Measurements of Fe and Ar fragmentation cross sections
[PAPER-OG-7.2-20] N85-33047
Was core formation violent enough to homogenize the early mantle? N85-33068
The problem of the Earth's CO2 content and the iron core N85-33069
IRRADIATION
Theoretical modeling of laser induced optical degradation
[AD-A155302] N85-32323
Effect of powerful pulsed low-energy ion streams on GaAs N85-32877
IRREGULARITIES
Mesospheric measurements of irregularity patches using a 3-antenna interferometer, part 3.6B N85-32498
ISOSTATIC PRESSURE
Hot isostatically pressed Sm(2)(TM)17 magnets
[AD-A155479] N85-32267
ISOTOPE EFFECT
Constraints on the development of the early continental crust from isotopic data N85-33076
ISOTOPES
Contributions to the 19th International Cosmic Ray Conference
[NASA-CR-176060] N85-33044
Initial results from the Caltech/DSRI balloon-borne isotope experiment
[PAPER-OG-4.3-8] N85-33046
Measurements of Fe and Ar fragmentation cross sections
[PAPER-OG-7.2-20] N85-33047
ISOTOPIC LABELING
Constraints on the development of the early continental crust from isotopic data N85-33076
ITERATION
Newton's method as a dynamical system: Global convergence and predictability
[AD-A155170] N85-32564
A practical approach to Karmarkar's algorithm
[AD-A155714] N85-32818
New developments on the core function for efficient implementation of the difficult residue number system operations
[AD-A154678] N85-32834

J

JAMMING
Design of a jamming simulator for a binary communication system
[AD-A154617] N85-32221
JET LAG
Human performance in continuous/sustained operations and the demands of extended work/rest schedules. An annotated bibliography
[AD-A155619] N85-32771
JET MIXING FLOW
Large eddy structures in transitional and turbulent flames
[AD-A154520] N85-32157
JOINTS (JUNCTIONS)
Improved materials for composites and adhesive joints
[AD-A154918] N85-32152
Improved materials for composite and adhesive joints
[AD-A155065] N85-32153
Experimental and theoretical assessment of a new technique for the non-destructive evaluation of laminated panels
[AD-A155622] N85-32155
Resolution of thermal striping issue downstream of a horizontal pipe elbow in stratified pipe flow
[DE85-006195] N85-32292
Simultaneous junction formation N85-32426
Pulsed excimer laser processing for cost-effective solar cells N85-32432
JUPITER SATELLITES
The energy spectrum of Jovian electrons in interplanetary space
[PAPER-SH-1.5-18] N85-33051

K

KALMAN FILTERS
Parameter estimation in communication system tracking satellite observations
[AD-A155137] N85-32582
Bayesian vs MAP multiple model adaptive estimation for field of view expansion in tracking airborne targets
[AD-A155466] N85-32855
Kalman filter time series analysis of gamma-ray data from NaI(T1) detectors for the ND6620 computer
[AD-A154995] N85-33014
KARMAN VORTEX STREET
Velocity and transient measurements in a shock tube using a hot-wire anemometer
[AD-A154694] N85-32305
KELVIN-HELMHOLTZ INSTABILITY
A panel method study of vortex sheets with special emphasis on sheets of axisymmetric geometry
[NASA-CR-177365] N85-32095
KERNEL FUNCTIONS
The NAS kernel benchmark program
[NASA-TM-86711] N85-32795
KINETIC ENERGY
Numerical solutions of turbulent models for flow over a flat plate with angle of attack
[DE85-010380] N85-32286
KINETIC FRICTION
Kinetic friction coefficient of ice
[AD-A155035] N85-32859
KINETICS
Calculation of molecular constants potential energy curves and Franck-Condon factors for lead oxide
[AD-A154521] N85-32158
The effect of prior parent phase cold work on martensite transformation in Cu-Zn-Al shape memory alloys
[AD-A155140] N85-32183
Microscopic control of semiconductor surface oxidation
[AD-A154799] N85-33026
Determination of kinetic parameters of molecular beam epitaxy
[AD-A155222] N85-33030
KIRCHHOFF LAW OF RADIATION
Toward the theory of acoustic scattering on uneven free surface N85-32862
KNOWLEDGE
A simple software environment based on objects and relations
[AD-A155704] N85-32817
KRYPTON
Modification of the grain size of sputtered copper with additions of oxygen, krypton, silver, or yttrium
[DE85-010975] N85-32189
KRYPTON FLUORIDE LASERS
Magnetic fields in laser heated plasmas
[DE85-010715] N85-33022

L

LABORATORIES
The flow of scientific and technical information in the US Army Research Laboratories
[AD-A155050] N85-33043
LAGEOS (SATELLITE)
Earth Albedo and the orbit of LAGEOS
[NASA-TM-86210] N85-32131
LAKES
Empirical methods for predicting eutrophication in impoundments. Report 3. Phase 2. Model refinements
[AD-A155483] N85-32462
Changes in the organic material in lakes in the blast zone of Mount St. Helens, Washington: Hydrologic effects of the eruptions
[GS-CIRC-850-1] N85-32551
Sulfur cycling in freshwater sediments N85-32726
LAMINAR BOUNDARY LAYER
Experiments on the influence of active walls on the initial amplitudes and growths of instability waves
[AD-A154630] N85-32275
LAMINAR FLOW
Numerical solutions of turbulent models for flow over a flat plate with angle of attack
[DE85-010380] N85-32286
Theoretical foundations of turbulent flows N85-32880
LAMINAR WAKES
A panel method study of vortex sheets with special emphasis on sheets of axisymmetric geometry
[NASA-CR-177365] N85-32095
LAMINATES
Comparisons of various configurations of the edge delamination test for interlaminar fracture toughness
[NASA-TM-86433] N85-32151
Experimental and theoretical assessment of a new technique for the non-destructive evaluation of laminated panels
[AD-A155622] N85-32155
LAND USE
Microcomputer processing of LANDSAT Thematic Mapper data for the acquisition of military tactical terrain data
[AD-A154781] N85-32389
LANDFORMS
Global Mega-Geomorphology
[NASA-CP-2312] N85-32357
The problem of scale in planetary geomorphology N85-32375
Global geomorphology: Report of Working Group Number 1 N85-32382
Planetary perspective. Report of Working Group Number 4 N85-32385
LANDSAT SATELLITES
Geomorphic classification of Icelandic and Martian volcanoes: Limitations of comparative planetology research from LANDSAT and Viking orbiter images N85-32372
Use of spaceborne imaging radar in regional geomorphic studies N85-32377
Quantitative geomorphologic studies from spaceborne platforms N85-32381
Microcomputer processing of LANDSAT Thematic Mapper data for the acquisition of military tactical terrain data
[AD-A154781] N85-32389
LANGUAGE PROGRAMMING
The effect of communication-language designs on software specifications
[AD-A155173] N85-32809
LARGE SCALE INTEGRATION
Parallel simulation of digital LSI circuits
[AD-A154745] N85-32258
LARGE SPACE STRUCTURES
NASA space station automation: AI-based technology review
[NASA-CR-176094] N85-32134
NASA space station automation: AI-based technology review. Executive summary
[NASA-CR-176096] N85-32135
LASER ANNEALING
Excimer laser annealing for fabrication of low-cost solar cells N85-32433
LASER APPLICATIONS
East Europe report: Science and technology
[JPRS-ESA-85-023] N85-32217
Three-dimensional photochemical machining with lasers
[AD-A154711] N85-32320
Laser-assisted solar-cell metallization processing N85-32429
Tunable lasers with high conversion efficiency N85-32906
The sound field of a moving laser-induced acoustic array (theory)
[AD-A154553] N85-32981
Raman scattering studies in solids
[AD-A155528] N85-33032
LASER CAVITIES
Generation of single nanosecond high-contrast radiation pules (lambda=10.6 micrometers) N85-32886
Influence of mirror anisotropy and Brewster window orientation on radiation characteristics of ring lasers N85-32889

LASER CUTTING
Applications of laser technology described N85-32218
LASER DAMAGE
Theoretical modeling of laser induced optical degradation
[AD-A155302] N85-32323
LASER FUSION
Prospects for lasers for fusion energy assessed N85-32885
Energy and Technology Review
[DE85-011767] N85-33061
LASER HEATING
Quasi-steady-state melting mode during combined laser irradiation of semiconductor materials N85-32874
Nonequilibrium kinetics of growth of oxide layer grains during laser heating of metals in air N85-32919
Coefficient of optical absorption and scattered light capture effect N85-32959
On one nonlinear problem of laser thermochemistry N85-32971
Asymptotically stable solutions of some nonlinear equations N85-32974
Magnetic fields in laser heated plasmas
[DE85-010715] N85-33022
LASER INTERFEROMETRY
Applications of laser technology described N85-32218
Possibility of measurement of small displacements by ring laser N85-32904
LASER MATERIALS
Saturation effect in multilevel lasing media N85-32901
LASER MICROSCOPY
Applications of laser technology described N85-32218
LASER MODE LOCKING
Choice of optimum saturating absorber for YAG passive mode-locking laser N85-32893
Dynamics of emission from dye lasers employing synchronous pumping by limited picosecond pulse train N85-32899
LASER MODES
Self Q-modulation and generation of short pulses in distributed-feedback lasers N85-32907
LASER OUTPUTS
Z-contrast imaging and electron channeling analysis of dopants in semiconductors
[DE85-011410] N85-32269
The 2-D simulations of the NRL (Naval Research Laboratory) laser experiment
[AD-A154915] N85-32321
Visibility and vertical structure measurements in southern Germany
[AD-A154714] N85-32574
Luminescence and absorption of indium-activated potassium-borate glasses subjected to high-power excitation N85-32868
Generation and amplification of radiation during stimulated Raman scattering in crystals N85-32869
Absorption of 10.6 micrometer laser radiation in electron-hole condensate in germanium N85-32870
Defect formation in amorphous hydrated silicon subjected to laser radiation N85-32873
Establishment of steady-state power level in pulse-periodic excimer laser N85-32896
The problem of brightness enhancement during laser frequency doubling N85-32897
Excimer-laser generator of powerful UV picosecond pulses synchronized with picosecond pulses in visible and IR bands N85-32903
Investigation of ion-acoustic plasma turbulence in field of powerful electromagnetic wave by CO2-laser radiation scattering N85-32935
Characteristics of optogalvanic effect in media with inverse populations N85-32944
Absorption of laser radiation in substance with absorption coefficient depending linearly upon temperature N85-32953
Optical waveguide along front of exothermic reaction N85-32954
Coefficient of optical absorption and scattered light capture effect N85-32959
The sound field of a moving laser-induced acoustic array (theory)
[AD-A154553] N85-32981
Multiphoton production and detection of atoms
[AD-A155561] N85-33000
LASER PLASMAS
Investigation of plasma processes in electronic transition lasers
[AD-A155598] N85-32327
Selective population of N = 3 OVIII level during expansion of laser plasma in helium N85-32914
CCD-based X-ray spectrometry for on-line determination of laser plasma electron temperature N85-32938
Investigation of space-time structure of glow of laser plasma colliding with flat screen N85-32947
Magnetic fields in laser heated plasmas
[DE85-010715] N85-33022
LASER PUMPING
Three-dimensional photochemical machining with lasers
[AD-A154711] N85-32320
A fast discharge excimer laser with symmetric geometry
[AD-A155294] N85-32322
Lasing on LiF:F(-)2 - dye centers with transverse pumping N85-32890
Dynamics of emission from dye lasers employing synchronous pumping by limited picosecond pulse train N85-32899
Stimulated Mandelstam-Brillouin scattering with distributed feedback N85-32961
Influence of spatial pumping spectrum on quality of phase conjugate reflection during 4-photon interaction N85-32964
LASER RANGE FINDERS
Applications of laser technology described N85-32218
LASER SPECTROSCOPY
Applications of laser technology described N85-32218
Activities of the Physics Division
[DE85-000784] N85-33002
Nonlinear spectroscopy
[AD-A154708] N85-33010
LASER WELDING
Laser beam interactions with vapor plumes during Nd:YAG laser welding on aluminum
[DE85-009793] N85-32328
LASER WINDOWS
Influence of mirror anisotropy and Brewster window orientation on radiation characteristics of ring lasers N85-32889
LASERS
USSR report: Physics and mathematics
[JPRS-UPM-85-004] N85-32860
Inter-zone auger recombination in GaSb laser structures N85-32875
The problem of brightness enhancement during laser frequency doubling N85-32897
Low-threshold injection InGaAsP/GaAs double heterostructure lasers with separate limiting obtained by liquid-phase epitaxy (lambda = 0.78 divided by 0.87 microns, I sub thr = 460 A/cm 2, T = 300 K) N85-32908
An attempt to detect induced neutron capture in laser radiation field N85-32928
The sound field of a moving laser-induced acoustic array (theory)
[AD-A154553] N85-32981
LATERAL CONTROL
Resource allocation in cerebral specialization of function: Behavioral and electrophysiological studies
[AD-A155092] N85-32759
LATTICE PARAMETERS
Z-contrast imaging and electron channeling analysis of dopants in semiconductors
[DE85-011410] N85-32269
LATTICE VIBRATIONS
X-ray diffractometric measurements and calculations of limiting values of discrepancy between lattices and layer thicknesses, preventing generation of dislocations during growth of multilayer heterostructures N85-32866
Doping superlattices in organometallic VPE InP
[AD-A155151] N85-33029
LAUNCHING
Guided-mode launching in a slab waveguide by way of diffraction at the edge of a conducting screen residing on one surface of the slab
[AD-A154886] N85-32232
LAYERS
Tailored vacuum chambers for ac magnets
[DE85-010767] N85-32319
LEACHING
Marine environmental quality assessment program, five-year plan (FY 1984 - 1988)
[AD-A154715] N85-32459
LEAD OXIDES
Calculation of molecular constants potential energy curves and Franck-Condon factors for lead oxide
[AD-A154521] N85-32158
LEADERSHIP
Symbolic and interactional perspectives on leadership: An integrative framework
[AD-A155247] N85-32769
LEARNING THEORY
Models for multidimensional tests and hierarchically structured training materials
[AD-A155231] N85-32768
LEAST SQUARES METHOD
A practical approach to Karmarkar's algorithm
[AD-A155714] N85-32818
On a variational approach to some parameter estimation problems
[NASA-CR-177935] N85-32829
Kalman filter time series analysis of gamma-ray data from NaI(T1) detectors for the ND6620 computer
[AD-A154995] N85-33014
LEGENDRE FUNCTIONS
Object identification and manipulation using silhouette moments
[AD-A154755] N85-33011
LENS DESIGN
Possiblity of developing charged-particle energy analyzer based on hyperboloidal axisymmetrical lens N85-32933
Electrostatic astigmatic tubular lens N85-32955
Relaxation lens in inhomogeneous binary mixture N85-32957
New method for correcting chromatism of mirror-lens objectives N85-32965
LEPTONS
Toward the question of multi-quark configurations in nuclei N85-32929
LIBRARIES
A transportable, machine oriented library of european sky and terrain radiance distributions with contemporary radiometric and meteorological profiles
[AD-A155254] N85-32590
LIFE (DURABILITY)
Improved Nominal Operating Cell Temperature (NOCT) test procedure N85-32449
LIFE CYCLE COSTS
An analysis of the materiel fielding plan for the SINCGARS (Single Channel Ground and Airborne Radio System) radio
[AD-A155101] N85-32238
LIFE RAFTS
Air carrier overwater emergency equipment and procedures
[PB85-917006] N85-32105
LIFE SCIENCES
Life sciences flight experiments program mission science requirements document. The first life sciences dedicated Spacelab mission, part 1
[NASA-TM-87494] N85-32137
USSR Space Life Sciences Digest
[NASA-CR-3922] N85-32709
Search for the universal ancestors
[NASA-SP-477] N85-32777
LIFE SUPPORT SYSTEMS
Space station ECLSS integration analysis: Simplified General Cluster Systems Model, ECLS System Assessment Program enhancements
[NASA-CR-176089] N85-32796
LIFEBOATS
Air carrier overwater emergency equipment and procedures
[PB85-917006] N85-32105
LIFT DEVICES
Trailing edge flow and aerodynamic sound. Part 1: Tonal pressure and velocity fluctuations. Part 2: Random pressure and velocity fluctuations
[AD-A154947] N85-32097
LIFT DRAG RATIO
Study of an efficient long-range Mach 2.7 supersonic transport configuration concept
[NASA-TM-86414] N85-32110
LIGHT (VISIBLE RADIATION)
Visual phenomena produced by binocularly disparate dynamic visual noise
[AD-A154758] N85-32757
Ice fog as an electro-optical obscurant
[AD-A155059] N85-33015
LIGHT AMPLIFIERS
Optical inhomogeneities in a nanosecond-pulse iodine photodissociation laser with slow UV radiation pumping N85-32902
LIGHT BEAMS
Influence of coherent light beams on free carriers in semiconductors N85-32867
Fluctuations in light intensity during backscattering in turbulent medium N85-32956
Coefficient of optical absorption and scattered light capture effect N85-32959
LIGHT SCATTERING
Phase behavior and QLS (Quasielastic Light Scattering) in potassium linoleate/n-alkanol microemulsions
[AD-A155028] N85-32163
Temperature measurements on small droplets N85-32699
Influence on bi-phonon states on Raman scattering of light in molecular crystals N85-32865
Generation and amplification of radiation during stimulated Raman scattering in crystals N85-32869

Effective brightness of zero-point fluctuations of the electromagnetic vacuum accompanying parametric scattering of light N85-32951
Correlation of intensities of different scattering channels N85-32952
Coefficient of optical absorption and scattered light capture effect N85-32959
Stimulated Mandelstam-Brillouin scattering with distributed feedback N85-32961
Influence of phonon interaction on width and form of Mandelstam-Brillouin optical scattering line N85-32962
Transmission of light by disperse medium of densely packed optically soft particles N85-32969
Ice fog as an electro-optical obscurant
[AD-A155059] N85-33015

LIGHT TRANSMISSION
Ship-to-ship propagation: Maritime data analyses
[AD-A155484] N85-32325
Transmission of light by disperse medium of densely packed optically soft particles N85-32969

LINEAR EQUATIONS
A new problem in mathematical physics associated with the problem of coherent phase transformation N85-32976

LINEAR PROGRAMMING
Study of an efficient long-range Mach 2.7 supersonic transport configuration concept
[NASA-TM-86414] N85-32110
A practical approach to Karmarkar's algorithm
[AD-A155714] N85-32818
On the problem of linear programming with approximate data N85-32978

LINEAR SYSTEMS
Routing algorithms and stochastic analysis for large communications networks
[AD-A154654] N85-32225
Decomposing the joint distribution of several linear combinations of uniform spacings
[AD-A155056] N85-32845

LINEARITY
Large-time behavior of viscous surface waves
[AD-A154805] N85-32278
Test evaluation of the Honeywell GG1111 Single-Degree-of-Freedom (SDF) strapdown gyroscope
[AD-A154768] N85-32307

LINEARIZATION
Development and validation of a general purpose linearization program for rigid aircraft models
[NASA-TM-86737] N85-32122

LINKAGES
On the turning lozange of constant side whose vertices alternate between two fixed circles of a ring
[AD-A154803] N85-32840

LIPIDS
The role of sulfur in osmoregulation and salinity tolerance in cyanobacteria, algae, and plants N85-32736

LIQUEFIED NATURAL GAS
Facility for large-scale hazardous gas testing
[DE85-011852] N85-32169

LIQUID COOLING
Comparison of the response of shape memory alloy actuators using air-cooling and water-cooling
[AD-A155216] N85-32185

LIQUID FLOW
Instability and chaotic behavior in a free-surface flow
[AD-A154879] N85-32279

LIQUID FUELS
Biomass thermochemical conversion program
[DE85-011867] N85-32213

LIQUID METAL FAST BREEDER REACTORS
Resolution of thermal striping issue downstream of a horizontal pipe elbow in stratified pipe flow
[DE85-006195] N85-32292

LIQUID NITROGEN
Basic cryogenics and materials. Phase 1
[NASA-CR-177932] N85-32215

LIQUID OXYGEN
Basic cryogenics and materials. Phase 1
[NASA-CR-177932] N85-32215

LIQUID PHASE EPITAXY
Low-threshold injection InGaAsP/GaAs double heterostructure lasers with separate limiting obtained by liquid-phase epitaxy (lambda = 0.78 divided by 0.87 microns, I sub thr = 460 A/cm 2, T = 300 K)
N85-32908

LIQUID PHASES
Phase behavior and QLS (Quasielastic Light Scattering) in potassium linoleate/n-alkanol microemulsions
[AD-A155028] N85-32163
Liquid-phase compositions from vapor-phase analyses 2: Adaptation of the Prausnitz program to UF6 and some of its potential impurities
[DE85-011521] N85-32819

LIQUID SURFACES
Instability and chaotic behavior in a free-surface flow
[AD-A154879] N85-32279

LIQUID WASTES
Review of hazardous waste cleanup and disposal efforts at Tinker Air Force Base
[GPO-43-294] N85-32457

LIQUID-SOLID INTERFACES
MPS solidification model. Analysis and calculation of macrosegregation in a casting ingot
[NASA-CR-171589] N85-32178
Polymer-water interaction studies N85-32411

LIQUIDS
Weak shock waves propagating in fluid-gas mixtures
[AD-A154759] N85-32276

LITHIUM CHLORIDES
A safe, high-power-density lithium battery
[AD-A155223] N85-32454

LITHIUM FLUORIDES
Lasing on LiF:F(-)2 - dye centers with transverse pumping N85-32890
In-cavity laser IR spectrum analyzer for investigating non-steady-state processes N85-32894

LITHOSPHERE
Conditions during formation of the Earth N85-33066
Anorthositic oceanic crust in the Archean Earth N85-33077

LOADS (FORCES)
The effect of stress and hot corrosion on nickel-base superalloys
[AD-A154722] N85-32181
A comparison of experimental and theoretical results for rotordynamic coefficients of four annular gas seals
[NASA-CR-176086] N85-32332
Measurement and analysis of critical crack tip processes during fatigue crack growth
[NASA-CR-172597] N85-32342
Analysis of long bone and vertebral failure patterns
[AD-A154796] N85-32758

LOGIC CIRCUITS
Design of a sixteen-bit pipelined adder using CMOS bulk P-well technology
[AD-A155043] N85-32260
Digital integrated circuits N85-32787

LOGISTICS MANAGEMENT
An analysis of the materiel fielding plan for the SINCGARS (Single Channel Ground and Airborne Radio System) radio
[AD-A155101] N85-32238
Security controls in the Stockpoint Logistics Integrated Communications Environment (SPLICE)
[AD-A155536] N85-32244

LONG DURATION SPACE FLIGHT
Living aloft: Human requirements for extended spaceflight
[NASA-SP-483] N85-32772

LONG RANGE WEATHER FORECASTING
Accuracy and operational use of medium and extended range numerical atmospheric forecasts: A review
[AD-A155027] N85-32579

LONG TERM EFFECTS
Predicting photothermal field performance N85-32404
Topics in electrochemical degradation of photovoltaic modules N85-32410

LONG WAVE RADIATION
Influence of phonon interaction on width and form of Mandelstam-Brillouin optical scattering line N85-32962

LORAN C
LORAN-C harbor and harbor entrance survey: Charleston, South Carolina
[AD-A154875] N85-32108

LOSSES
Important loss mechanisms in high-efficiency solar cells N85-32424

LOW ASPECT RATIO
Calculation of transonic steady and oscillatory pressures on a low aspect ratio model and comparison with experiment
[NASA-TM-86449] N85-32092

LOW FREQUENCIES
Upward continuation of surface gravity anomalies
[AD-A154973] N85-32560
Influence of phonon interaction on width and form of Mandelstam-Brillouin optical scattering line N85-32962

LOW LEVEL TURBULENCE
Mean flow and turbulence in complex terrain
[AD-A155138] N85-32583

LOW PRESSURE
The nucleation of ice at very low temperatures and pressures N85-32617

LOW TEMPERATURE
Polymer solution-supercritical fluid behavior
[AD-A154514] N85-32192
Synthesis and properties of arylethersulfone thermoset systems
[AD-A154811] N85-32198
The nucleation of ice at very low temperatures and pressures N85-32617

LUBRICATION
Surface roughness effects in elastohydrodynamic contacts
[NASA-TP-2488] N85-32329
Mechanics of a gaseous film barrier to lubricant wetting of elastohydrodynamically lubricated conjunctions
[NASA-TP-2500] N85-32330

LUMINAIRES
The role of long term lamp fluctuations in the random walk of frequency behavior of the rubidium frequency standard: A case study
[AD-A155338] N85-32314

LUMINESCENCE
The space shuttle glow
[AD-A154937] N85-32139
Multidimensional luminescence measurements
[AD-A154950] N85-32162
Luminescence and absorption of indium-activated potassium-borate glasses subjected to high-power excitation N85-32868
Influence of technological factors on luminescence characteristics of InGaAsP/InP heterolasers (lambda = 1.55 microns) N85-32910
Spectral-luminescence characteristics and induced emission of Nd-3(+) ion in Gd(2-x)Nd(x)(WO4)3 crystals N85-32912
Plasmodynamic methods for generating powerful light puses N85-32943

LUMINOSITY
Visibility and vertical structure measurements in southern Germany
[AD-A154714] N85-32574

LUMINOUS INTENSITY
Fluctuations in light intensity during backscattering in turbulent medium N85-32956

LUNAR CRATERS
Lunar and Martian impact basins: Exposed records of terrestrial bombardment? N85-33090

LUNAR SURFACE
Lunar and Martian impact basins: Exposed records of terrestrial bombardment? N85-33090

M

MACHINING
Machining-induced deformation in stepped specimens of PH 13-8 Mo, 18 nickel maraging steel grade 200T1 and grain-refined HP 9-4-20
[NASA-CR-172450] N85-32177

MAGMA
Anorthositic oceanic crust in the Archean Earth N85-33077
Earth's primordial differentiation, and its after-effects N85-33092

MAGNESIUM
Measurements of Fe and Ar fragmentation cross sections
[PAPER-OG-7.2-20] N85-33047

MAGNESIUM ALLOYS
The effect of alloy additions on superplasticity in thermomechanically processed high magnesium aluminum-magnesium alloys
[AD-A155142] N85-32184

MAGNET COILS
Magnetics calculations for an ELMO Bumpy Square
[DE85-011438] N85-33021

MAGNETIC COMPRESSION
Magnetics calculations for an ELMO Bumpy Square
[DE85-011438] N85-33021

MAGNETIC DIPOLES
Numerical modeling of subsurface communication
[DE85-012818] N85-32249

MAGNETIC FIELD CONFIGURATIONS
Magnetics calculations for an ELMO Bumpy Square
[DE85-011438] N85-33021

MAGNETIC FIELDS
Electrodeposition of chromium and copper in magnetic fields
[AD-A154648] N85-32180
Magnetic materials
[AD-A154679] N85-32256
Analysis of spacecraft data
[NASA-CR-171587] N85-32789
Investigation of reproducibility of emission wavelength of helium-neon laser with external neon absorption cell (0.63 micrometers) N85-32884
Solution of problem of equilibrium confinement of plasma by magnetic field in an infinite circular cylinder N85-32936
The Faraday effect in ruby and corundum in strong magnetic fields N85-32967
Magnetic fields in laser heated plasmas
[DE85-010715] N85-33022

MAGNETIC FILMS
Development of wide band recording materials
[AD-A154961] N85-32309
MAGNETIC MATERIALS
Magnetic materials
[AD-A154679] N85-32256
MAGNETIC MIRRORS
Energy and Technology Review
[DE85-011767] N85-33061
MAGNETIC RECORDING
Balloon-borne video cassette recorders for digital data storage
[PAPER-OG-9.3-11] N85-33050
MAGNETIC SIGNALS
Fluxgate magnetometer (SSM) for the defense meteorological satellite program (DMSP) block 5D-2, flight 7
[AD-A155229] N85-32143
MAGNETIC SIGNATURES
Solar cycle variation of ephemeral regions
[AD-A154967] N85-33097
MAGNETIC TAPES
A transportable, machine oriented library of european sky and terrain radiance distributions with contemporary radiometric and meteorological profiles
[AD-A155254] N85-32590
MAGNETIC VARIATIONS
A study of the cyclical variations of coronal holes and their relation to open magnetic fields
[AD-A155251] N85-33099
MAGNETO-OPTICS
Magnetic materials
[AD-A154679] N85-32256
Development of wide band recording materials
[AD-A154961] N85-32309
MAGNETOACTIVITY
Diamagnetic instability of cyclotron waves in plasma N85-32948
MAGNETOELASTIC WAVES
Cyclotron absorption of fast magnetosonic wave in stellarator N85-32945
MAGNETOHYDRODYNAMIC FLOW
Thermal contraction of current flow through electrode turbulent boundary layer N85-32926
Modeling the exhaust of the pulsed plasma thruster
[AD-A155344] N85-33018
MAGNETOHYDRODYNAMIC GENERATORS
Thermal contraction of current flow through electrode turbulent boundary layer N85-32926
MAGNETOHYDRODYNAMIC STABILITY
Diamagnetic instability of cyclotron waves in plasma N85-32948
Low frequency instabilities driven by an ion temperature anisotropy
[AD-A154902] N85-33016
MAGNETOHYDRODYNAMICS
Planetary Dynamos
[NASA-CR-176001] N85-32857
Plasmodynamic methods for generating powerful light puses N85-32943
A system of magnetohydrodynamic-type equations N85-32946
MAGNETOMETERS
Fluxgate magnetometer (SSM) for the defense meteorological satellite program (DMSP) block 5D-2, flight 7
[AD-A155229] N85-32143
MAGNETOSONIC RESONANCE
Cyclotron absorption of fast magnetosonic wave in stellarator N85-32945
MAGNETOSPHERE
ISEE-1 data reduction and analysis plasma composition experiment
[NASA-CR-175306] N85-32552
MAGNETOSPHERIC ELECTRON DENSITY
Ionospheric electron density profile and related studies
[AD-A155257] N85-32567
MAGNETOSPHERIC INSTABILITY
Ionospheric electron density profile and related studies
[AD-A155257] N85-32567
MAGNETS
Hot isostatically pressed Sm(2)(TM)17 magnets
[AD-A155479] N85-32267
Tailored vacuum chambers for ac magnets
[DE85-010767] N85-32319
MAINTAINABILITY
Los Alamos optical materials reliability, maintainability, and exposure testing program
[DE85-011894] N85-32456
MAN MACHINE SYSTEMS
Myoelectric control of a computer based expert system for flight control
[AD-A154981] N85-32126
Importance of automation, robotization in economy N85-32219
Design guidelines for user-system interface software
[AD-A154907] N85-32807
A PASCAL interpreter for the functional programming language ELC (Extended lambda calculus)
[AD-A155218] N85-32810
MANAGEMENT INFORMATION SYSTEMS
The Human Resource Management Information Network (HRMIN): A cost comparison in accordance with Office of Management and Budget (OMB) Circular no. A-76, 5 April 1979
[AD-A154583] N85-33039
MANAGEMENT PLANNING
Quality analysis N85-32785
MANAGEMENT SYSTEMS
Symbolic and interactional perspectives on leadership: An integrative framework
[AD-A155247] N85-32769
MANDELSTAM REPRESENTATION
Stimulated Mandelstam-Brillouin scattering with distributed feedback N85-32961
MANGANESE
Physical and chemical aerosol characteristics in extremely clean air masses at Cape Grim, Tasmania N85-32655
Possible roles of manganese redox chemistry in the sulfur cycle N85-32731
Precision measurements of solar energetic particle elemental composition
[PAPER-SH-2.1-4] N85-33052
MANIPULATORS
Ultrasonic position reference systems for an autonomous sentry robot and a robot manipulator arm
[AD-A155481] N85-32336
East Europe report: Science and technology. Selections on CSSR computer technology
[JPRS-ESA-84-017] N85-32781
Robots, Manipulators N85-32786
MANNED SPACE FLIGHT
Living aloft: Human requirements for extended spaceflight
[NASA-SP-483] N85-32772
MANUALS
A retarding ion mass spectrometer for the Dynamics Explorer-1
[NASA-CR-171588] N85-32303
Ada (trademark) training curriculum. Advanced Ada topics L305 teacher's guide exercises
[AD-A154621] N85-32798
MANUFACTURING
Encapsulation processing and manufacturing yield analysis N85-32434
GDR semiconductor parts N85-32788
MAPPING
Mapping with QUASAT (quasar satellite) using short observation times
[AD-A155155] N85-32141
The measurement of strain fields by X-ray topographic contour mapping
[AD-A154870] N85-32348
Use of the synoptic view: Examples from Earth and other planets N85-32371
Techniques, problems and uses of mega-geomorphological mapping N85-32378
Planetary perspective. Report of Working Group Number 4 N85-32385
Realizing the full potential of the video disc for mapping applications
[AD-A154966] N85-32391
Optical storage technology for mapping
[AD-A154989] N85-32392
MAPS
Planetary perspective. Report of Working Group Number 4 N85-32385
MARAGING STEELS
Machining-induced deformation in stepped specimens of PH 13-8 Mo, 18 nickel maraging steel grade 200T1 and grain-refined HP 9-4-20
[NASA-CR-172450] N85-32177
MARINE BIOLOGY
Marine environmental quality assessment program, five-year plan (FY 1984 - 1988)
[AD-A154715] N85-32459
MARINE ENVIRONMENTS
Understanding and laboratory prediction of the atmospheric corrosion behavior of steels and of non-ferrous metals and alloys
[AD-A154642] N85-32179
Using ship wake patterns to evaluate SAR (Synthetic Aperture Radar) ocean wave imaging mechanisms. Joint US-Canadian Ocean Wave Investigation Project
[AD-A154633] N85-32223
Marine environmental quality assessment program, five-year plan (FY 1984 - 1988)
[AD-A154715] N85-32459
Forecasting atmospheric visibility over the summer north Atlantic using the principal discriminant method
[AD-A155537] N85-32593
Bacterial ice nuclei of marine origin: Some recent observations N85-32611
Marine aerosols at the Dutch North Sea coast: Size distributions and fractionation of trace elements N85-32664
Sulfates in marine aerosols over the tropical Western Pacific Ocean N85-32690
Granulometric study of the acidity and sulfate excess in marine aerosols N85-32691
Sulfur diagenesis in marine sediments N85-32721
Sulfur reduction in sediments of marine and evaporite environments N85-32742
Submarine hydrothermal environments as sites for the origin and evolution of life N85-33074
MARINE TECHNOLOGY
The dynamics of slack marine cables
[AD-A155022] N85-32349
Physical oceanography program science abstracts
[AD-A154637] N85-32701
MARKING
Resource management for the tagged token dataflow architecture
[AD-A154773] N85-32779
MARS (PLANET)
Megageomorphology: Mars vis a vis Earth N85-32360
MARS CRATERS
Lunar and Martian impact basins: Exposed records of terrestrial bombardment? N85-33090
MARS SURFACE
Lunar and Martian impact basins: Exposed records of terrestrial bombardment? N85-33090
MARS VOLCANOES
Geomorphic classification of Icelandic and Martian volcanoes: Limitations of comparative planetology research from LANDSAT and Viking orbiter images N85-32372
MARTENSITIC TRANSFORMATION
The effect of prior parent phase cold work on martensite transformation in Cu-Zn-Al shape memory alloys
[AD-A155140] N85-32183
MASERS
Cerenkov maser and Cerenkov laser devices
[AD-A155443] N85-32324
USSR report: Physics and mathematics
[JPRS-UPM-85-004] N85-32860
MASS
Plasma mass and effective inductance in a small railgun
[AD-A154644] N85-32304
MASS SPECTROMETERS
A retarding ion mass spectrometer for the Dynamics Explorer-1
[NASA-CR-171588] N85-32303
Fabrication and test of modified quadrupole mass spectrometer
[AD-A155186] N85-32312
Analysis of spacecraft data
[NASA-CR-171587] N85-32789
MASS SPECTROSCOPY
Aerosol analysis and emission spectrometry with free jets
[DE85-010576] N85-32168
MASS TRANSFER
New estimating procedures for surface runoff, sediment yield, and contaminant transport in Los Alamos County, New Mexico
[DE85-011890] N85-32393
Vertical transport in the atmosphere: Measurement capabilities and requirements of VHF radars, part 1.6A N85-32476
A new hypothesis for the observed vertical distribution of atmospheric aerosols N85-32646
Size spectra for the source-enhanced coagulation with the turbulent mass transfer N85-32649
MATCHED FILTERS
Compression of spread spectrum signals on an excessively dispersive channel
[AD-A155184] N85-32240
MATCHING
Generalized planar matching
[AD-A154809] N85-32842
MATERIAL ABSORPTION
Influence of chemical form, feeding regimen, and animal species on the gastrointestinal absorption of plutonium
[DE85-010291] N85-32751
MATERIALS HANDLING
A systematic plan for the continued study of dimensional stability of metallic alloys considered for the fabrication of cryogenic wind tunnel models
[NASA-CR-172449] N85-32172
TNT equivalency of EAK explosive
[AD-A155737] N85-32211

Basic cryogenics and materials. Phase 1
[NASA-CR-177932] N85-32215

MATHEMATICAL MODELS
Aerodynamic characteristics of the standard dynamics model in coning motion at Mach 0.6
[NASA-TM-86717] N85-32094
Development of reduced order models for control system design using the OPTSYSX program
[AD-A154552] N85-32124
Injection of drag reducing additives into turbulent water flows: Two-component velocity measurements and mixing length model predictions
[AD-A154604] N85-32274
Theoretical modeling of laser induced optical degradation
[AD-A155302] N85-32323
A continuous damage model based on stepwise-stress creep rupture tests
[NASA-CR-174941] N85-32341
Modelling and parameter estimation for distributed vibratory systems
[AD-A154518] N85-32344
Development of improved dynamic failure models
[AD-A155586] N85-32354
A new global geomorphology? N85-32358
Modeling of the silane FBR system N85-32415
Comprehensive silicon solar-cell computer modeling N85-32421
Emergency modeling of hazardous air pollutants
[AD-A155441] N85-32461
The Norwegian seismic array (NORSAR)
[AD-A154751] N85-32555
The diurnal variation of the neutral sodium species in the upper atmosphere: A model study
[AD-A154988] N85-32561
Development of ultrasonic modeling techniques for the study of crustal inhomogeneities
[AD-A155206] N85-32565
Diagnostics of severe convection and subsynoptic scale ageostrophic circulations
[NASA-CR-171581] N85-32571
Scavenging of submicron aerosol particles by snow crystals: Theory and experiments N85-32667
A probabilistic method for particle size analysis of aerosols N85-32669
A simple model to investigate the activation process in watercloudsN85-32675
Numerical modeling of sea ice dynamics and ice thickness characteristics
[AD-A154600] N85-32700
Carbon and sulfur cycling through geologic time N85-32720
An error-dependent model of instrument-scanning behavior in commercial airline pilots
[NASA-CR-3908] N85-32765
Optimal low thrust transfer using a first-order perturbation model
[AD-A154761] N85-32835
Theory of soliton waves
[AD-A154784] N85-32837
Identification of unsteady aerodynamics and aeroelastic integro-differential systems
[NASA-TM-86749] N85-32851
Diamagnetic instability of cyclotron waves in plasma N85-32948
Asymptotically stable solutions of some nonlinear equations N85-32974
Iteration solution for a submerged force-driven finite cylinder
[AD-A154587] N85-32982
Overground Excess Sound Attenuation (ESA). Volume 3: Application of ESA data in NOISEFILE
[AD-A154820] N85-32984
Lateral attenuation of aircraft flight noise
[AD-A154958] N85-32986
Modeling the exhaust of the pulsed plasma thruster
[AD-A155344] N85-33018
Feasibility of applications of Competition Decision Assist Package (CDAP) to spare parts
[AD-A154716] N85-33036

MATHEMATICAL PROGRAMMING
New developments on the core function for efficient implementation of the difficult residue number system operations
[AD-A154678] N85-32834
Necessary and sufficient conditions for single-extremum and convex problems of mathematical programming N85-32977

MATHEMATICS
Ada (trademark) training curriculum. Advanced Ada topics L305 teacher's guide exercises
[AD-A154621] N85-32798

MATRIX MATERIALS
Matrix fracture in fiber-reinforced ceramics
[AD-A154704] N85-32197

MAXIMUM LIKELIHOOD ESTIMATES
Robust detection and classification of regional seismic signals using a two mode/two stage cascaded adaptive arma (CAARMA) model
[AD-A154710] N85-32554
On a variational approach to some parameter estimation problems
[NASA-CR-177935] N85-32829
Weibull distribution based on maximum likelihood with interval inspection data
[NASA-TM-86515] N85-32847

MAXWELL EQUATION
Equations of motion for electromagnetic waves in 4-dimensional Euclidian space N85-32970

MEASUREMENT
Use of the VAD technique and measurements of momentum flux in the stratosphere at Aercibo, part 4.3A N85-32505

MEASURING INSTRUMENTS
Improved coordinate measuring machine calibration and control
[DE85-012053] N85-32315

MECHANICAL PROPERTIES
Improved materials for composite and adhesive joints
[AD-A155065] N85-32153
Basic cryogenics and materials. Phase 1
[NASA-CR-177932] N85-32215

MECHANIZATION
Importance of automation, robotization in economy N85-32219

MEDIA
Toward the propagation of waves in unsteady media N85-32881

MEDICAL SCIENCE
USSR Space Life Sciences Digest
[NASA-CR-3922] N85-32709

MELTING
Quasi-steady-state melting mode during combined laser irradiation of semiconductor materials N85-32874

MELTING POINTS
Ice-forming efficiency of the soluble and insoluble portions of dust contained in snow N85-32631

MELTS (CRYSTAL GROWTH)
Silicon dendritic web growth N85-32435
Temperature-stress modeling N85-32436
Silicon ribbon stress-strain activities N85-32437

MEMBRANES
Silicon dendritic web growth N85-32435
Temperature-stress modeling N85-32436
Silicon ribbon stress-strain activities N85-32437
Analysis of stress-strain relationships in silicon ribbon N85-32438
Stress and buckling analysis N85-32439
Stress and efficiency studies in EFG N85-32440
Silicon sheet surface studies N85-32441
Edge-defined film-fed growth of thin silicon sheets N85-32443
The investigation of natural and artificial ice nuclei by the improved membrane filter method N85-32626

MEMORY
The effect of set size on time to recall color coded information
[AD-A155013] N85-32767

MERCURY CADMIUM TELLURIDES
Interface chemistry of Hg(1-x)Cd(x)Te
[AD-A154876] N85-32161

MESOPAUSE
The nucleation of ice at very low temperatures and pressures N85-32617

MESOSCALE PHENOMENA
Diagnostics of severe convection and subsynoptic scale ageostrophic circulations
[NASA-CR-171581] N85-32571

MESOSPHERE
Gravity waves from the stratosphere to the mesosphere, part 1.3B N85-32471
A numerical analysis of transient planetary waves and the vertical structure in a meso-strato-troposphere model, part 1.4A N85-32473
Morphology of the scattering targets: Fresnel and turbulent mechanisms, part 2.1A N85-32481
Observations of mesospheric turbulence by rocket probe and VHF radar, part 2.4A N85-32484
Interpretation of radar returns from the mesosphere, part 2.3A N85-32485
Radar echoes at 2.66 and 40.92 MHz from the mesosphere, part 2.6A N85-32486
Antenna induced range smearing in MST radars N85-32495
Effects of line-of-sight velocity on spaced-antenna measurements, part 3.5A N85-32496
Mesospheric measurements of irregularity patches using a 3-antenna interferometer, part 3.6B N85-32498
Spectral measurements of turbulence and gravity waves, part 4.2A N85-32501
Relationship of isolated turbulent regions to the general turbulent background, part 4.4A N85-32506
Estimation of vertical diffusion from observations of Atmospheric turbulence layers, part 4.4B N85-32507
Momentum flux measurements: Techniques and needs, part 4.5A N85-32508
Sample interchange of MST radar data from the Urbana radar N85-32531
Urbana radar systems: Possibilities and limitations N85-32540
Progress and plans for the Colorado Wind Profiler Network N85-32542

METABOLISM
The role of sulfur in osmoregulation and salinity tolerance in cyanobacteria, algae, and plants N85-32736
Sulfur cycling and metabolism of phototrophic and filamentous sulfur bacteria N85-32737
Anaerobic reduction of elemental sulfur by Chromatium vinosum and Beggiatoa alba N85-32739
Interactions among sulfide-oxidizing bacteria N85-32741
Studies of circulatory and metabolic changes during ketamine narcosis
[AD-A154512] N85-32756

METAL COATINGS
East Europe report: Science and technology
[JPRS-ESA-85-021] N85-32190

METAL FILMS
Amorphous metallic films in silicon metallization systems N85-32427

METAL OXIDES
Molecular orbital studies in oxidation: Sulfate formation and metal-metal oxide adhesion
[NASA-CR-176070] N85-32174
A study of adherent oxide scales
[AD-A155554] N85-32188

METAL POWDER
Sintering studies project
[AD-A154750] N85-32216

METAL SHEETS
A theory of electromagnetic shielding with applications to MIL-STD-285, IEEE-299, and EMP simulation
[AD-A154905] N85-32233

METAL SURFACES
Why CO bonds side-on at low coverage and both side-on and upright at high coverage on the Cr(110) surface
[NASA-CR-176071] N85-32173
Nonradiative damping of molecular electronic excited states by metal surfaces
[AD-A154619] N85-32994
The effect of metal overlayers of thermionic dispenser cathodes
[AD-A154795] N85-32995

METAL VAPORS
Passive Q-modulation of optical cavities by KCl crystals containing OH(-) -ions N85-32915

METAL-METAL BONDING
Molecular orbital studies in oxidation: Sulfate formation and metal-metal oxide adhesion
[NASA-CR-176070] N85-32174

METALLIZING
High temperature electronics technology: Life test report
[AD-A154681] N85-32257
Amorphous metallic films in silicon metallization systems N85-32427
Laser-assisted solar-cell metallization processing N85-32429
A non-noble front metallization process N85-32430
Pulsed excimer laser processing for cost-effective solar cells N85-32432

METALLOGRAPHY
The effect of stress and hot corrosion on nickel-base superalloys
[AD-A154722] N85-32181

METALS
Study of proton and neutron activation of metal samples in low Earth orbit
[NASA-CR-171596] N85-32130
High-frequency furnace
[DE85-011210] N85-32291
On one nonlinear problem of laser thermochemistry N85-32971
The effect of metal overlayers of thermionic dispenser cathodes
[AD-A154795] N85-32995

METAMORPHISM (GEOLOGY)
Hydrothermal alteration in the 3.5 b.y. old Onverwacht Group of South Africa N85-33071
The 3.5 b.y. old Onverwacht Group: A remnant of ancient oceanic crust N85-33073

METASTABLE STATE
Globally-asynchronous locally-synchronous systems
[AD-A154624] N85-32222

Detection of excited states by laser-induced fluorescence
[AD-A155558] N85-32326

METEOR TRAILS
Interpolation problems in meteor radar analysis, part 7.6A N85-32528
MENTOR: Adding an outlying receiver to an ST radar for meteor-wind measurement N85-32538

METEORITE CRATERS
Large arcuate scars: A geological legacy of the Earth's accretionary past N85-33089

METEORITES
MENTOR: Adding an outlying receiver to an ST radar for meteor-wind measurement N85-32538
Explosion in flight N85-32883

METEOROLOGICAL INSTRUMENTS
Notes on atmospheric stability, turbulence, and its measurements
[AD-A155230] N85-32586

METEOROLOGICAL PARAMETERS
Experimental investigation of properties of ice-forming reagents N85-32602

METEOROLOGICAL RADAR
Middle Atmosphere Program. Handbook for MAP. Volume 14: URSI/SCOSTEP Workshop on Technical Aspects of MST Radar
[NASA-CR-176085] N85-32466
Meteorological and aeronomical requirements for MST radar networks (keynote paper), part 1 N85-32467
Tropospheric-stratospheric exchange, part 1.1A N85-32468
Gravity waves from the stratosphere to the mesosphere, part 1.3B N85-32471
The suppression of convective wavebreaking by radiative transfer processes, part 1.3C N85-32472
General circulation of the middle atmosphere, part 1.4B N85-32474
Performance of the Colorado wind-profiling network, part 1.5A N85-32475
Vertical transport in the atmosphere: Measurement capabilities and requirements of VHF radars, part 1.6A N85-32476
Comparison of tropopause altitude determination by the Plattsville Radar, Sunset Radar and the NWS Rawinsonde N85-32477
Synoptic-scale dynamics with vertical velocity, part 1.8A N85-32478
Practical use of a tropopause height determination algorithm on an MST radar data set, part 1.8B N85-32479
Morphology of the scattering targets: Fresnel and turbulent mechanisms, part 2.1A N85-32481
Usefulness of multifrequency MST radar measurements, part 2.6B N85-32487
Anisotropy of the permittivity field inferred from aspect-sensitive radar echoes N85-32492
Accuracy of velocity and power determination by the Doppler method N85-32493
Determination of billows and other turbulent structures, part 4.1A N85-32500
Spectral measurements of turbulence and gravity waves, part 4.2A N85-32501
Gravity-wave spectra in the atmosphere observed by MST radar, part 4.2B N85-32502
Momentum flux measurements: Techniques and needs, part 4.5A N85-32508
Tropospheric gravity waves observed by three closely spaced ST radars N85-32509
Determination of horizontal and vertical wavelengths of gravity waves in the mesosphere by spaced wind measurements N85-32510
Criteria for site selection and frequency allocation (keynote paper), part 5 N85-32511
Frequency and site selection criteria for MST radars, part 5.1A N85-32512
Summary of session on optimum transmitter and antenna configuration for MST radar, part 6 N85-32514
Practicality of electronic beam steering for MST/ST radars, part 6.2A N85-32516
Testing and optimizing MST coaxial collinear arrays, part 6.4A N85-32518
Overview of on-line data processing for MST radars (keynote paper), part 7 N85-32519
Coding schemes for improving MST radar performance, part 7.1A N85-32520
Elimination of range-aliased echoes in the VHF radars N85-32521
Sidelobe reduction of Barker codes, part 7.1C N85-32522
A high-speed digital signal processor for atmospheric radar, part 7.3A N85-32525
Hardware schemes for fast Fourier transform, part 7.4A N85-32526
Criteria and algorithms for spectrum parameterization of MST radar signals N85-32527
Interpolation problems in meteor radar analysis, part 7.6A N85-32528
Data base management: MSTRAC (keynote paper), part 8 N85-32530
Sample interchange of MST radar data from the Urbana radar N85-32531
MST radar data management N85-32532
Data base for the Colorado profiling network N85-32533
Further developments of EISCAT as an MST radar N85-32534
Status of the Jicamarca radar N85-32535
Recent results at the Sunset radar N85-32536
The Boot Lake MF imaging radar N85-32537
MENTOR: Adding an outlying receiver to an ST radar for meteor-wind measurement N85-32538
Summary of progress at the Poker Flat Observatory in Alaska N85-32539
Urbana radar systems: Possibilities and limitations N85-32540
The Sondrestrom radar: Progress and proposed upgrades for ST work N85-32541
Progress and plans for the Colorado Wind Profiler Network N85-32542
The MU radar now partly in operation N85-32543
Network ST radar and related measurements at Pennsylvania State University N85-32544
A note on the proposed UK VHF radar N85-32545
The Adelaide VHF radar: Capabilities and future plans N85-32546
The Proust radar N85-32547
Millstone Hill radar: Capabilities for S/T observations N85-32548
The Ponape ST radar N85-32549
Measurements of vertical velocity over flat terrain by ST radar and other related uses of the radar data set N85-32550
Automated cell detection as a mesocyclone precursor tool
[AD-A154952] N85-32577

METEOROLOGY
Middle Atmosphere Program. Handbook for MAP. Volume 14: URSI/SCOSTEP Workshop on Technical Aspects of MST Radar
[NASA-CR-176085] N85-32466
Generation of available potential energy and the energy cycle during the global weather experiment
[NASA-CR-175301] N85-32572
Meteorological weapons
[AD-A154735] N85-32575
A transportable, machine oriented library of european sky and terrain radiance distributions with contemporary radiometric and meteorological profiles
[AD-A155254] N85-32590
Medium range atmospheric forecast system: Evaluation plan
[AD-A155623] N85-32595

MICE
Differences in susceptibility of inbred mice to bacillus anthracis
[AD-A155646] N85-32750

MICROANALYSIS
Z-contrast imaging and electron channeling analysis of dopants in semiconductors
[DE85-011410] N85-32269
Cyanobacterial mats: Microanalysis of community metabolism N85-32743
Microanalysis of dissolved iron and phosphate in pore waters of hypersaline sediment N85-32744

MICROBALANCES
Data analysis for lidar and quartz crystal microbalance systems
[NASA-CR-172601] N85-32464

MICROBIOLOGY
The global sulfur cycle
[NASA-TM-87570] N85-32710

MICROCOMPUTERS
Microcomputer processing of LANDSAT Thematic Mapper data for the acquisition of military tactical terrain data
[AD-A154781] N85-32389
Robots, Manipulators N85-32786
An automated quality assurance surveillance plan for ADP (Automated Data Processing) operations under the Navy's commercial activities program
[AD-A154767] N85-32802
A comparison and analysis of Vintr's global routing algorithm with the Lee routing algorithm in two-layer printed circuit boards
[AD-A155600] N85-32816
Development of a dedicated speech work station
[AD-A155465] N85-32824
Microcomputer network: Investigation end implementation
[AD-A155631] N85-32826

MICROCRACKS
Mechanics of near tip microcracking in brittle material
[AD-A154684] N85-32346

MICROCRYSTALS
Basic ice nucleation mechanisms on mono and microcrystals and ice forming nuclei. Theoretical analysis and experimental results achieved in the laboratory over the past ten years: Review paper N85-32629

MICROELECTRONICS
Resistance of polyaniline films as a function of electrochemical potential and the fabrication of polyaniline-based microelectronic devices
[AD-A154999] N85-32201
East Europe report: Science and technology
[JPRS-ESA-85-023] N85-32217
High temperature electronics technology: Life test report
[AD-A154681] N85-32257
Selections on CSSR computer technology N85-32782
GDR semiconductor parts N85-32788
Prospects for a new kind of synthesis: Assembly of molecular components to achieve functions
[AD-A155023] N85-32997
Solid state research
[AD-A154783] N85-33025
Electrotransport in thin films
[AD-A155584] N85-33034

MICROMETEOROLOGY
Investigations of micro-turbulence in the bottom of the boundary layer
[AD-A155148] N85-32585

MICROORGANISMS
Protocyanobacteria: Oxygenic and Anoxygenic photosynthesis in mat-forming bacteria N85-32714
Sulfur transformations at the hydrogen sulfide/oxygen interface in stratified waters and in cyanobacterial mats N85-32715
Microbiology of solar salt ponds N85-32724
Some thoughts on GAIA and the sulfur cycle N85-32727
From microbial communities to cells N85-32728
Microbial colonization and growth on metal sulfides and other mineral surfaces N85-32747
Sulfur Cycle N85-32748

MICROPROCESSORS
Microprocessor control design for a low-head crossflow turbine
[AD-A155477] N85-32121
A microprocessor-controlled, multichannel fluorimeter for analysis of sea water
[AD-A154986] N85-32310
Ultrasonic position reference systems for an autonomous sentry robot and a robot manipulator arm
[AD-A155481] N85-32336
The 8080 emulator N85-32783

MICROPROGRAMMING
Evaluation and implementation of a functional microprogram generator
[AD-A155164] N85-32823

MICROSCOPY
Modification of the grain size of sputtered copper with additions of oxygen, krypton, silver, or yttrium
[DE85-010975] N85-32189

MICROSTRUCTURE
Metallurgical origins of fracture toughness and microstructure and fracture toughness of an HSLA (High-Strength/Low-Alloy) steel
[AD-A155530] N85-32187
Fundamental investigations of failure during superplastic forming process
[AD-A154647] N85-32194
The variability of aerosol microstructure in continental and oceanic surface layers of the atmosphere in anticyclones N85-32660
Variation of the submicron aerosol structure N85-32661

MICROWAVE AMPLIFIERS
Clarke Stations and mercurian mass-drivers: Energy for large-scale transportation systems
[DE85-009607] N85-32145

MICROWAVE CIRCUITS
Microwave semiconductor research: Materials, devices and circuits and gallium arsenide ballistic electron transistors
[AD-A154698] N85-33024

MICROWAVE EQUIPMENT
Microwave semiconductor research: Materials, devices and circuits and gallium arsenide ballistic electron transistors
[AD-A154698] N85-33024

MICROWAVE RADIOMETERS
Network ST radar and related measurements at Pennsylvania State University N85-32544

MICROWAVES
Microwave SAW (Surface Acoustic Wave) monochromator [AD-D011718] N85-32311
Microwave-enhanced thin-film deposition N85-32431
Form factor effects on microwave Cerenkov radiation [AD-A154577] N85-32993
MIDDLE ATMOSPHERE
Middle Atmosphere Program. Handbook for MAP. Volume 14: URSI/SCOSTEP Workshop on Technical Aspects of MST Radar [NASA-CR-176085] N85-32466
Excerpts from the paper: Research Status and Recommendation from the Alaska Workshop on Gravity Waves and Turbulence in the Middle Atmosphere, part 1.3A N85-32470
General circulation of the middle atmosphere, part 1.4B N85-32474
Sample interchange of MST radar data from the Urbana radar N85-32531
The MU radar now partly in operation N85-32543
MIE SCATTERING
Ice fog as an electro-optical obscurant [AD-A155059] N85-33015
MIG AIRCRAFT
China has developed a new version of fighter aircraft [AD-A155293] N85-32118
MILITARY AIR FACILITIES
Review of hazardous waste cleanup and disposal efforts at Tinker Air Force Base [GPO-43-294] N85-32457
MILITARY TECHNOLOGY
Meteorological weapons [AD-A154735] N85-32575
Air Force Office of Scientific Research (AFOSR). Technical report summaries: First quarter (CY) [AD-A154757] N85-33041
MILLIMETER WAVES
A multiplying slot array [AD-A155570] N85-32245
MINERAL DEPOSITS
Geomorphology, tectonics, and exploration N85-32365
Sulfur reduction in sediments of marine and evaporite environments N85-32742
MINERAL EXPLORATION
Geomorphology, tectonics, and exploration N85-32365
MINERALS
Mineral aerosols and source identification N85-32654
Microbial colonization and growth on metal sulfides and other mineral surfaces N85-32747
The effects of prolonged feeding meal, ready-to-eat (MRE) operational rations [AD-A154763] N85-32773
MINORITY CARRIERS
High-purity silicon crystal growth N85-32444
MIRROR FUSION
Energy and Technology Review [DE85-011767] N85-33061
MIRRORS
Influence of mirror anisotropy and Brewster window orientation on radiation characteristics of ring lasers N85-32889
Mirror reflection of charged particles from + amorphous and polycrystalline surfaces N85-32927
Comparison of findings of theories describing reflection from real surface with experiments in region of ultrasoft X-radiation N85-32950
Dielectric mirror with ferromagnetic substrate N85-32966
MISSION PLANNING
Life sciences flight experiments program mission science requirements document. The first life sciences dedicated Spacelab mission, part 1 [NASA-TM-87494] N85-32137
MIXING
Large eddy structures in transitional and turbulent flames [AD-A154520] N85-32157
Numerical solution of the Navier-Stokes equations for 3-D internal flows: An emerging capability N85-32300
MIXTURES
Antistarshapedness, dispersiveness and mixtures [AD-A155583] N85-32849
MODELS
MPS solidification model. Analysis and calculation of macrosegregation in a casting ingot [NASA-CR-171589] N85-32178
Numerical modeling of subsurface communication [DE85-012818] N85-32249
Numerical solutions of turbulent models for flow over a flat plate with angle of attack [DE85-010380] N85-32286
A modified Fresnel scattering model for the parameterization of Fresnel returns, part 2.3A N85-32483
Review of the psychological issues relating to the effectiveness of structured programming [AD-A154593] N85-32766
On the dependence of the convergence of Gummel's algorithm on the regularity of the solution [AD-A154628] N85-32832
Cosmic ray He3 measurements [PAPER-OG-4.2-3] N85-33045
MOIRE EFFECTS
A comparison of electronic heterodyne moire deflectometry and electronic heterodyne holographic interferometry for flow measurements [NASA-TM-87071] N85-32302
MOLECULAR BEAM EPITAXY
Determination of kinetic parameters of molecular beam epitaxy [AD-A155222] N85-33030
MOLECULAR EXCITATION
Nonradiative damping of molecular electronic excited states by metal surfaces [AD-A154619] N85-32994
MOLECULAR GASES
Participation of singlet oxygen in photodestruction of air-saturated solutions of coumarin dyes N85-32891
The possibilities of remote analysis of atmospheric gases based on Raman scattering spectroscopy N85-32892
MOLECULAR INTERACTIONS
USSR report: Physics and mathematics [JPRS-UPM-85-004] N85-32860
MOLECULAR ORBITALS
Why CO bonds side-on at low coverage and both side-on and upright at high coverage on the Cr(110) surface [NASA-CR-176071] N85-32173
Molecular orbital studies in oxidation: Sulfate formation and metal-metal oxide adhesion [NASA-CR-176070] N85-32174
MOLECULAR OSCILLATIONS
Vibrationally enhanced dissociation of diatomic molecules [AD-A154827] N85-32996
MOLECULAR STRUCTURE
Interaction of solutes with stretched polymers [AD-A154662] N85-32196
Polymerizable ultraviolet stabilizers N85-32406
Insights into the phylogenetic positions of photosynthetic bacteria obtained from 5S rRNA and 16S rRNA sequence data N85-32719
X-ray diffractometric measurements and calculations of limiting values of discrepancy between lattices and layer thicknesses, preventing generation of dislocations during growth of multilayer heterostructures N85-32866
MOLECULAR WEIGHT
Relationship of isolated turbulent regions to the general turbulent background, part 4.4A N85-32506
MOLTEN SALTS
The effect of stress and hot corrosion on nickel-base superalloys [AD-A154722] N85-32181
MOMENTS
Object identification and manipulation using silhouette moments [AD-A154755] N85-33011
MOMENTUM
Techniques for the study of gravity waves and turbulence (keynote paper), part 4 N85-32499
Momentum flux measurements: Techniques and needs, part 4.5A N85-32508
MONITORS
Results from radiation monitoring equipment experiments on STS-41C, 41D, 41G and 51A [AD-A154676] N85-32142
MONKEYS
Analysis of long bone and vertebral failure patterns [AD-A154796] N85-32758
MONOCHROMATORS
Microwave SAW (Surface Acoustic Wave) monochromator [AD-D011718] N85-32311
MONOMERS
Graphite/PMR polyimide composites with improved toughness [NASA-TM-87081] N85-32148
MONTE CARLO METHOD
Forecasting of tropical cyclone motion using an EOF (Empirical Orthogonal Function) representation of wind forcing [AD-A155034] N85-32580
Monte Carlo studies of H2O layers adsorbed on a model basal face of AgI N85-32633
Radiation transport [DE85-010333] N85-33005
MONTEREY BAY (CA)
Coastal erosion along Monterey Bay [AD-A155610] N85-32707
MORPHOLOGY
Understanding and laboratory prediction of the atmospheric corrosion behavior of steels and of non-ferrous metals and alloys [AD-A154642] N85-32179
Enrichments for phototrophic bacteria and characterization by morphology and pigment analysis N85-32738
MOTION SICKNESS
Mission operations requirements document for D-1 Experiment 102, Vestibular Experiments in Spacelab [NASA-TM-87495] N85-32129
MOTOR VEHICLES
An electron microscopic study of urban aerosol N85-32689
MULTIPROCESSING (COMPUTERS)
Performance and evaluation of real-time multicomputer control systems [NASA-CR-176098] N85-32821
Concurrent implementation of the Crank-Nicolson method for heat transfer analysis [NASA-TM-86448] N85-32822
MULTISPECTRAL BAND SCANNERS
Stripe filters on multispectral linear arrays [NASA-CR-175305] N85-32252
Use of spaceborne imaging radar in regional geomorphic studies N85-32377
Quantitative geomorphologic studies from spaceborne platforms N85-32381
MULTISPECTRAL LINEAR ARRAYS
Stripe filters on multispectral linear arrays [NASA-CR-175305] N85-32252
MULTIVARIATE STATISTICAL ANALYSIS
Robust control of multivariable and large space systems [AD-A155117] N85-32140

N

N-TYPE SEMICONDUCTORS
Electrical properties of bulk grown nitrogen doped silicon [AD-A155471] N85-32266
NAMING
Distributed name management [AD-A154785] N85-33037
NASA PROGRAMS
Life sciences flight experiments program mission science requirements document. The first life sciences dedicated Spacelab mission, part 1 [NASA-TM-87494] N85-32137
NATURAL LANGUAGE (COMPUTERS)
Experience with omega: Implementation of a prototype programming environment: Part 1 [AD-A155438] N85-32811
NAVIER-STOKES EQUATION
The calculation of fully three dimensional flow through any type of turbomachine blade row N85-32294
Performance evaluation of flow in turbomachinery blade rows N85-32299
NAVIGATION
LORAN-C harbor and harbor entrance survey: Charleston, South Carolina [AD-A154875] N85-32108
The potential of the NAVSTAR global positioning system for the Corps of Engineers, civil works [AD-A154913] N85-32109
NAVIGATION AIDS
LORAN-C harbor and harbor entrance survey: Charleston, South Carolina [AD-A154875] N85-32108
NEODYMIUM
Spectral-luminescence characteristics and induced emission of Nd-3(+) ion in Gd(2-x)Nd(x)(WO4)3 crystals N85-32912
NEODYMIUM ISOTOPES
Constraints on the development of the early continental crust from isotopic data N85-33076
NEODYMIUM LASERS
Laser beam interactions with vapor plumes during Nd:YAG laser welding on aluminum [DE85-009793] N85-32328
Luminescence and absorption of indium-activated potassium-borate glasses subjected to high-power excitation N85-32868
Defect formation in amorphous hydrated silicon subjected to laser radiation N85-32873
Selective population of N = 3 OVIII level during expansion of laser plasma in helium N85-32914
Passive Q-modulation of optical cavities by KCl crystals containing OH(-) -ions N85-32915

NEON
Initial results from the Caltech/DSRI balloon-borne isotope experiment
[PAPER-OG-4.3-8] N85-33046
Solar cycle variations of the anomalous cosmic ray component
[PAPER-SH-4.6-2] N85-33057
NERNST-ETTINGSHAUSEN EFFECT
Magnetic fields in laser heated plasmas
[DE85-010715] N85-33022
NEUMANN PROBLEM
Sobolev-Poincare's inequality and the Neumann problem for u sub t = divergence of the absolute value of the gradient u to the p-2 power x the gradient u
[AD-A154788] N85-32839
NEUROMUSCULAR TRANSMISSION
Physical chemical state of water in living cells
[AD-A154566] N85-32749
NEUTRAL ATMOSPHERES
The diurnal variation of the neutral sodium species in the upper atmosphere: A model study
[AD-A154988] N85-32561
NEUTRON ACTIVATION ANALYSIS
Activation analysis of natural water using neutrons of various energies N85-32924
Rhodium-103 and Indium-115 inelastic scattering reactions for fission neutron dosimetry N85-33004
NEUTRON CROSS SECTIONS
An attempt to detect induced neutron capture in laser radiation field N85-32928
Rhodium-103 and Indium-115 inelastic scattering reactions for fission neutron dosimetry N85-33004
Radiation transport
[DE85-010333] N85-33005
NEUTRON FLUX DENSITY
Study of proton and neutron activation of metal samples in low Earth orbit
[NASA-CR-171596] N85-32130
NEUTRON IRRADIATION
Study of proton and neutron activation of metal samples in low Earth orbit
[NASA-CR-171596] N85-32130
NEUTRON SCATTERING
Toward a theory of excitation of atoms during nuclear and magnetic neutron scattering N85-32918
NEUTRON SOURCES
Radiation transport
[DE85-010333] N85-33005
NEUTRON SPECTRA
Paired ion chamber constants for fission gamma-neutron fields
[AD-A155069] N85-32999
NEVADA
Comparison of survey and photogrammetry methods to position gravity data, Yucca Mountain, Nevada
[DE85-011685] N85-32316
NICKEL
The effect of diffusive hydrogen segregation on fracture of polycrystalline nickel
[AD-A155238] N85-32186
NICKEL OXIDES
Adsorption of O2, SO2, and SO3 on nickel oxide. Mechanism for sulfate formation
[NASA-CR-176072] N85-32175
NIOBIUM
Evaluated nuclear-data file for niobium
[DE85-012095] N85-33009
NITRO COMPOUNDS
Electrochemistry of Hexanitroazobenzene (HNAB)
[DE85-010807] N85-32171
NITROBENZENES
Electrochemistry of Hexanitroazobenzene (HNAB)
[DE85-010807] N85-32171
NITROGEN
Calculation of the propagation constant in a rectangular waveguide containing an inhomogeneous longitudinally magnetized plasma
[DE85-012072] N85-32250
Biogeochemical cycling and remote sensing N85-32733
Solar cycle variations of the anomalous cosmic ray component
[PAPER-SH-4.6-2] N85-33057
Carbon and nitrogen in the deep Earth N85-33085
NITROGEN COMPOUNDS
Synthesis of energetic materials
[AD-A154887] N85-32210
NITROGEN DIOXIDE
Facility for large-scale hazardous gas testing
[DE85-011852] N85-32169
NITROGEN IONS
Electrical properties of bulk grown nitrogen doped silicon
[AD-A155471] N85-32266
NITROGEN LASERS
Investigation of influence of gas exit modes on characteristics of N2O - N2 - He discharge laser N85-32888
NITROGEN OXIDES
Emergency modeling of hazardous air pollutants
[AD-A155441] N85-32461
NOCTURNAL VARIATIONS
VALMET: A valley air pollution model
[DE85-010820] N85-32463
NOISE
Visual phenomena produced by binocularly disparate dynamic visual noise
[AD-A154758] N85-32757
NOISE MEASUREMENT
Design of a freestanding noise measurement and recording system to predict the intensity and location of electromagnetic radiation from earthquakes
[AD-A155070] N85-32563
FAA/GAMA (Federal Aviation Administration/General Aviation Manufacturer's Association) propeller aircraft noise test program, Salina Municipal Airport, Salina, Kansas
[AD-A154818] N85-32983
Overground Excess Sound Attenuation (ESA). Volume 3: Application of ESA data in NOISEFILE
[AD-A154820] N85-32984
Helicopter noise survey for selected cities in the contiguous US
[AD-A154893] N85-32985
NOISE POLLUTION
Statistical methods for efficient design of community surveys of response to noise: Random coefficients regression models
[NASA-CR-177933] N85-32979
NOISE PROPAGATION
Overground Excess Sound Attenuation (ESA). Volume 3: Application of ESA data in NOISEFILE
[AD-A154820] N85-32984
NOISE REDUCTION
FAA/GAMA (Federal Aviation Administration/General Aviation Manufacturer's Association) propeller aircraft noise test program, Salina Municipal Airport, Salina, Kansas
[AD-A154818] N85-32983
NOISE SPECTRA
Overground Excess Sound Attenuation (ESA). Volume 3: Application of ESA data in NOISEFILE
[AD-A154820] N85-32984
Lateral attenuation of aircraft flight noise
[AD-A154958] N85-32986
NONDESTRUCTIVE TESTS
Experimental and theoretical assessment of a new technique for the non-destructive evaluation of laminated panels
[AD-A155622] N85-32155
Reliability of void detection in structural ceramics using scanning laser acoustic microscopy
[NASA-TM-87035] N85-32337
NONLINEAR EQUATIONS
Non-model based estimation with applications to sensor calibration using multiple sensors
[AD-A154736] N85-32306
NONLINEAR FILTERS
Recursive nonlinear filtering through complete linearization
[AD-A155029] N85-32844
NONLINEAR PROGRAMMING
Local epi-continuity and local optimization
[AD-A154812] N85-32843
NONLINEAR SYSTEMS
Aerodynamic characteristics of the standard dynamics model in coning motion at Mach 0.6
[NASA-TM-86717] N85-32094
On the dependence of the convergence of Gummel's algorithm on the regularity of the solution
[AD-A154628] N85-32832
Theory of soliton waves
[AD-A154784] N85-32837
NONLINEARITY
New approximations and findings of theory of nonlinear acoustic beams N85-32863
Toward the propagation of waves in unsteady media N85-32881
Nonlinear spectroscopy
[AD-A154708] N85-33010
NONUNIFORM MAGNETIC FIELDS
Electrostatic ion cyclotron instability due to a nonuniform electric field perpendicular to the external magnetic field
[AD-A155474] N85-33019
NORMAL DENSITY FUNCTIONS
The distribution of the number of empty cells in a generalized random allocation scheme
[AD-A154806] N85-32841
NOSE CONES
Applied research and development for falling-sphere air density measuring systems
[AD-A155227] N85-32099
NOSES (FOREBODIES)
Wind tunnel drag evaluations of helicopter nose sections
[AD-A155489] N85-32100
NOZZLE GEOMETRY
Investigation of influence of gas exit modes on characteristics of N2O - N2 - He discharge laser N85-32888
NUCLEAR CAPTURE
An attempt to detect induced neutron capture in laser radiation field N85-32928
Evaluated nuclear-data file for niobium
[DE85-012095] N85-33009
NUCLEAR ELECTRIC POWER GENERATION
East Europe report: Science and technology
[JPRS-ESA-85-023] N85-32217
NUCLEAR FUELS
East Europe report: Science and technology
[JPRS-ESA-85-021] N85-32190
NUCLEAR FUSION
Prospects for lasers for fusion energy assessed N85-32885
Infrared laser holography used in fusion plasma studies N85-32905
Tritium technology review
[DE85-010504] N85-33006
NUCLEAR INTERACTIONS
Study of proton and neutron activation of metal samples in low Earth orbit
[NASA-CR-171596] N85-32130
Contributions to the 19th International Cosmic Ray Conference
[NASA-CR-176060] N85-33044
NUCLEAR MAGNETIC RESONANCE
An EPR (Electron-Paramagnetic-Resonance) and ENDOR (Electron-Nuclear-Double-Resonance) study of ferroelectric ammonium sulfate
[AD-A155580] N85-33033
NUCLEAR PHYSICS
USSR report: Physics and mathematics
[JPRS-UPM-85-004] N85-32860
High-energy Physics Institute building 3-trillion-ev accelerator N85-32934
Activities of the Physics Division
[DE85-000784] N85-33002
NUCLEAR REACTOR CONTROL
Tritium technology review
[DE85-010504] N85-33006
NUCLEAR REACTORS
Operation of solid state lasers exposed to electron beam N85-32895
NUCLEAR SCATTERING
Toward the question of multi-quark configurations in nuclei N85-32929
NUCLEAR WEAPONS
Nuclear thermal transmittance in the atmosphere using LOWTRAN-6 computer code
[AD-A154669] N85-32553
NUCLEATION
Ice nucleation by silver iodine particles with nearly critical sizes N85-32600
The nucleation of ice crystals during the freezing of large supercooled drops N85-32608
Concentrations of ice nuclei of different modes of activities N85-32616
The nucleation of ice at very low temperatures and pressures N85-32617
Ice nucleating characteristics of Capparis Aphylla, an Indian herb N85-32619
The capture of ice nucleating and non ice-nucleating aerosols by ice phase precipitation N85-32620
Supersaturation obtained in a condensation nucleus counter N85-32624
Basic ice nucleation mechanisms on mono and microcrystals and ice forming nuclei. Theoretical analysis and experimental results achieved in the laboratory over the past ten years: Review paper N85-32629
Ice nucleation of single water droplet by silver iodide: A laboratory observation N85-32630
Ice-forming efficiency of the soluble and insoluble portions of dust contained in snow N85-32631
Critical supersaturations with respect to water for fast condensation-freezing ice nucleation N85-32632
Concentration and source areas of ice nuclei in the Alaskan atmosphere N85-32634
Cloud droplet nucleation and initial growth derived from lidar depolarization studies N85-32635
Eleventh International Conference on Atmospheric Aerosols, Condensation and Ice Nuclei, volume 1
[PB85-182400] N85-32636
The first condensation nucleus conference N85-32637

The influence of Brownian coagulation on the size distributions of atmospheric aerosols N85-32643
Measurements of giant salt nuclei from inland in east China N85-32668
Cloud condensation on insoluble particles N85-32670
The measured rate of condensation nucleation to droplets using the techniques of chemical kinetics N85-32694
Effect of ions on cloud formation and its role in solar terrestrial relationship N85-32697

NUCLEI
A thermal diffusion chamber for the measurement of cloud condensation nuclei N85-32627

NUCLEI (NUCLEAR PHYSICS)
Solar cycle variations of the anomalous cosmic ray component
[PAPER-SH-4.6-2] N85-33057
Radial and latitudinal gradients of anomalous oxygen during 1977 - 1985
[PAPER-SH-4.6-4] N85-33058

NUCLEONS
Cosmic ray He3 measurements
[PAPER-OG-4.2-3] N85-33045
Initial results from the Caltech/DSRI balloon-borne isotope experiment
[PAPER-OG-4.3-8] N85-33046

NULL ZONES
Null synthesis with phase and amplitude controls at the subarray outputs
[AD-A155187] N85-32241
Reconciling Bayesian and frequentist evidence in the one-sided testing program
[AD-A155603] N85-32850

NUMERICAL ANALYSIS
Numerical modeling of subsurface communication
[DE85-012818] N85-32249
Numerical solutions of turbulent models for flow over a flat plate with angle of attack
[DE85-010380] N85-32286
A numerical analysis of transient planetary waves and the vertical structure in a meso-strato-troposphere model, part 1.4A N85-32473
Circulation analysis of two snowstorms during the SNOW-TWO program
[AD-A155225] N85-32587
Numerical simulations of the response of intense ocean currents to atmospheric forcing
[AD-A155161] N85-32704
Overlap integrals for atom-metal surface interactions
[AD-A155038] N85-32998

NUMERICAL CONTROL
Flight control system for a computer controlled aircraft with limited sensors
[AD-A155107] N85-32115
Speech understanding research
[AD-A155462] N85-32990

NUMERICAL STABILITY
A numerical and analytical investigation of lee cyclogenesis
[AD-A155607] N85-32594

NUMERICAL WEATHER FORECASTING
Accuracy and operational use of medium and extended range numerical atmospheric forecasts: A review
[AD-A155027] N85-32579
Medium range atmospheric forecast system: Evaluation plan
[AD-A155623] N85-32595

NUSSELT NUMBER
Numerical solutions of turbulent models for flow over a flat plate with angle of attack
[DE85-010380] N85-32286

NUTRITION
Chemolithotrophy and physiology of bacterial nutrient limitation N85-32730
Influence of chemical form, feeding regimen, and animal species on the gastrointestinal absorption of plutonium
[DE85-010291] N85-32751

O

OBSERVATION
Observations of mesospheric turbulence by rocket probe and VHF radar, part 2.4A N85-32484
Analysis of unreplicated factorials allowing for possibly faulty observations
[AD-A154813] N85-32848

OCCULTATION
Ice fog as an electro-optical obscurant
[AD-A155059] N85-33015

OCEAN BOTTOM
Global geomorphology N85-32359
Deep sea mega-geomorphology: Progress and problems N85-32369
Sulfur and carbon cycling in organic-rich marine sediments N85-32729
A random layer model for reflection from ocean bottom sediments
[AD-A155019] N85-32988
Understanding coherence losses incurred by bottom-retained signals
[AD-A155559] N85-32992
The 3.5 b.y. old Onverwacht Group: A remnant of ancient oceanic crust N85-33073
Anorthositic oceanic crust in the Archean Earth N85-33077

OCEAN CURRENTS
Horizontal and vertical structure of velocity, potential vorticity and energy in the gulf stream
[AD-A154753] N85-32702
Hydrographic data from the OPTOMA (Ocean Prediction Through Observations, Modeling and Analysis) program: OPTOMA15, 24 January to 23 February 1985
[AD-A155012] N85-32703
Numerical simulations of the response of intense ocean currents to atmospheric forcing
[AD-A155161] N85-32704

OCEAN DYNAMICS
Physical oceanography program science abstracts
[AD-A154637] N85-32701

OCEAN MODELS
Anorthositic oceanic crust in the Archean Earth N85-33077

OCEAN SURFACE
Using ship wake patterns to evaluate SAR (Synthetic Aperture Radar) ocean wave imaging mechanisms. Joint US-Canadian Ocean Wave Investigation Project
[AD-A154633] N85-32223
Numerical simulations of the response of intense ocean currents to atmospheric forcing
[AD-A155161] N85-32704
Simulation of the coupled atmospheric and oceanic boundary layer model during MILDEX
[AD-A155166] N85-32705

OCEANOGRAPHIC PARAMETERS
Hydrographic data from the OPTOMA (Ocean Prediction Through Observations, Modeling and Analysis) program: OPTOMA15, 24 January to 23 February 1985
[AD-A155012] N85-32703

OCEANOGRAPHY
Physical oceanography program science abstracts
[AD-A154637] N85-32701

OCEANS
Global Mega-Geomorphology
[NASA-CP-2312] N85-32357
The variability of aerosol microstructure in continental and oceanic surface layers of the atmosphere in anticyclones N85-32660
Some thoughts on GAIA and the sulfur cycle N85-32727

OILS
The influence of oil contamination on the nucleate pool-boiling behavior of R-114 from a structured surface
[AD-A155609] N85-32284

ON-LINE SYSTEMS
Interactive on-line conferences
[AD-A154723] N85-32227
Overview of on-line data processing for MST radars (keynote paper), part 7 N85-32519

ONBOARD EQUIPMENT
Flight control system for a computer controlled aircraft with limited sensors
[AD-A155107] N85-32115
SCRIBE data of October 23, 1983 flight
[AD-A154864] N85-33012

ONE DIMENSIONAL FLOW
Explosion in flight N85-32883

OPERATING TEMPERATURE
Status of high-efficiency module design and fabrication N85-32446

OPERATIONS RESEARCH
The priming effect in task design research
[AD-A154589] N85-32852
Necessary and sufficient conditions for single-extremum and convex problems of mathematical programming N85-32977

OPERATORS (MATHEMATICS)
Aspects of SAR image segmentation
[AD-A154965] N85-32236

OPTICAL CORRECTION PROCEDURE
New method for correcting chromatism of mirror-lens objectives N85-32965

OPTICAL EQUIPMENT
Optical storage technology for mapping
[AD-A154989] N85-32392
Microwave semiconductor research: Materials, devices and circuits and gallium arsenide ballistic electron transistors
[AD-A154698] N85-33024

OPTICAL MEASUREMENT
SCRIBE data of October 23, 1983 flight
[AD-A154864] N85-33012

OPTICAL MEMORY (DATA STORAGE)
Realizing the full potential of the video disc for mapping applications
[AD-A154966] N85-32391
Optical storage technology for mapping
[AD-A154989] N85-32392

OPTICAL PROPERTIES
Failure analysis of thin-film amorphous-silicon solar-cell modules N85-32452
Properties of aerosol particles detected by satellites in coastal regions N85-32622
Radiative-collision generation of sound in gases subjected to single-pulse optical excitation N85-32920
Nonlinear spectroscopy
[AD-A154708] N85-33010
Optical output stabilization method for direct current arc lamps
[AD-A154987] N85-33013

OPTICAL RADAR
Data analysis for lidar and quartz crystal microbalance systems
[NASA-CR-172601] N85-32464
Visibility and vertical structure measurements in southern Germany
[AD-A154714] N85-32574
Cloud droplet nucleation and initial growth derived from lidar depolarization studies N85-32635
Laser Elektronika-01 for air pollution control lidar N85-32887
Participation of singlet oxygen in photodestruction of air-saturated solutions of coumarin dyes N85-32891

OPTICAL REFLECTION
Influence of spatial pumping spectrum on quality of phase conjugate reflection during 4-photon interaction N85-32964

OPTICAL RESONANCE
Saturation effect in multilevel lasing media N85-32901

OPTICAL WAVEGUIDES
Optical waveguide along front of exothermic reaction N85-32954
Methods for measuring and analyzing dispersion properties of multimode fiber optic lightpipes (a review) N85-32960

OPTIMIZATION
Globally-asynchronous locally-synchronous systems
[AD-A154624] N85-32222
Application of adaptive noise cancellation to Coast Guard voice communications
[AD-A154798] N85-32230
Testing and optimizing MST coaxial collinear arrays, part 6.4A N85-32518
The Norwegian seismic array (NORSAR)
[AD-A154751] N85-32555
New developments on the core function for efficient implementation of the difficult residue number system operations
[AD-A154678] N85-32834
Optimal low thrust transfer using a first-order perturbation model
[AD-A154761] N85-32835
Generalized planar matching
[AD-A154809] N85-32842
Local epi-continuity and local optimization
[AD-A154812] N85-32843
Optimization of sampling in statistical physics experiments N85-32975
Necessary and sufficient conditions for single-extremum and convex problems of mathematical programming N85-32977

ORBITAL ASSEMBLY
NASA space station automation: AI-based technology review
[NASA-CR-176094] N85-32134
NASA space station automation: AI-based technology review. Executive summary
[NASA-CR-176096] N85-32135

ORBITAL MANEUVERING VEHICLES
NASA space station automation: AI-based technology review
[NASA-CR-176094] N85-32134
NASA space station automation: AI-based technology review. Executive summary
[NASA-CR-176096] N85-32135

ORBITAL SPACE STATIONS
Comparative study on data system architectures — spacecraft data processing
[ESA-CR(P)-2015] N85-32828

ORDNANCE
Development of improved dynamic failure models
[AD-A155586] N85-32354

ORGANIC COMPOUNDS
Aerosol analysis and emission spectrometry with free jets
[DE85-010576] N85-32168
Distribution and abundance of organic thiols N85-32717
ORGANIC MATERIALS
Changes in the organic material in lakes in the blast zone of Mount St. Helens, Washington: Hydrologic effects of the eruptions
[GS-CIRC-850-1] N85-32551
ORGANIZATIONS
Worldwide directory of national Earth-science agencies and related international organizations
[GS-CIRC-934] N85-32386
The flow of scientific and technical information in the US Army Research Laboratories
[AD-A155050] N85-33043
ORGANOMETALLIC COMPOUNDS
Multilayer capacitor dielectrics produced from metallo-organic precursors
[AD-A154592] N85-32254
Marine environmental quality assessment program, five-year plan (FY 1984 - 1988)
[AD-A154715] N85-32459
Doping superlattices in organometallic VPE InP
[AD-A155151] N85-33029
ORTHOTROPIC PLATES
A cracked orthotropic sheet stiffened by a semi-infinite orthotropic sheet
[NASA-TP-2455] N85-32339
OSCILLATING FLOW
Development of artificially produced perturbations in supersonic boundary layer N85-32879
OSCILLATIONS
A simple model for testing the effects of gravity-wave-produced vertical oscillations of scattering irregularities on spaced-antenna, horizontal drift measurements N85-32489
OSCILLATORS
A multiplying slot array
[AD-A155570] N85-32245
Generation of single nanosecond high-contrast radiation pules (lambda=10.6 micrometers) N85-32886
OSMIUM ISOTOPES
Identification of vibrational-rotational transitions of Os-192O4 within frequency tuning limits of high pressure CO2 waveguide laser N85-32917
OSMOSIS
Condensation properties of atmospheric aerosol N85-32672
The role of sulfur in osmoregulation and salinity tolerance in cyanobacteria, algae, and plants N85-32736
OUTLETS
Investigation of influence of gas exit modes on characteristics of N2O - N2 - He discharge laser N85-32888
OUTPUT
Microwave SAW (Surface Acoustic Wave) monochromator
[AD-D011718] N85-32311
Optical output stabilization method for direct current arc lamps
[AD-A154987] N85-33013
OVERPRESSURE
TNT equivalency of EAK explosive
[AD-A155737] N85-32211
BLAF: A blast field reconstruction program from pressure histories
[AD-A155300] N85-32283
OXIDATION
Shock tube measurements of growth constants in the branched-chain ethane-carbon monoxide-oxygen system
[NASA-TM-87068] N85-32156
Basic research in novel inorganic reagents and fluorocarbon chemistry
[AD-A155340] N85-32165
Molecular orbital studies in oxidation: Sulfate formation and metal-metal oxide adhesion
[NASA-CR-176070] N85-32174
A study of adherent oxide scales
[AD-A155554] N85-32188
Aerobic sulfur-oxidizing bacteria: Environmental selection and diversification N85-32712
Some thoughts on GAIA and the sulfur cycle N85-32727
Possible roles of manganese redox chemistry in the sulfur cycle N85-32731
Sulfate-reducing bacteria: Microbiology and physiology N85-32732
Structure and physiology of Beggiatoa and Thiothrix N85-32734
Interactions among sulfide-oxidizing bacteria N85-32741
Nonequilibrium kinetics of growth of oxide layer grains during laser heating of metals in air N85-32919
Raman scattering studies in solids
[AD-A155528] N85-33032
OXIDATION-REDUCTION REACTIONS
Anaerobic reduction of elemental sulfur by Chromatium vinosum and Beggiatoa alba N85-32739
Microscopic control of semiconductor surface oxidation
[AD-A154799] N85-33026
OXIDES
The effect of stress and hot corrosion on nickel-base superalloys
[AD-A154722] N85-32181
The diurnal variation of the neutral sodium species in the upper atmosphere: A model study
[AD-A154988] N85-32561
OXYGEN
Shock tube measurements of growth constants in the branched-chain ethane-carbon monoxide-oxygen system
[NASA-TM-87068] N85-32156
Modification of the grain size of sputtered copper with additions of oxygen, krypton, silver, or yttrium
[DE85-010975] N85-32189
Studies of oxygen- and carbon-related defects in high-efficiency silicon solar cells N85-32420
Sulfur transformations at the hydrogen sulfide/oxygen interface in stratified waters and in cyanobacterial mats N85-32715
Distribution and abundance of organic thiols N85-32717
Evolution of the atmosphere N85-32725
Microbial communities and microprofiles of sulfide and oxygen of alum rock sulfur springs N85-32746
Changes in the energy spectrum of anomalous oxygen and helium during 1977 - 1985
[PAPER-SH-4.6-1] N85-33056
Solar cycle variations of the anomalous cosmic ray component
[PAPER-SH-4.6-2] N85-33057
Radial and latitudinal gradients of anomalous oxygen during 1977 - 1985
[PAPER-SH-4.6-4] N85-33058
OXYGEN ATOMS
Adsorption of O2, SO2, and SO3 on nickel oxide. Mechanism for sulfate formation
[NASA-CR-176072] N85-32175
OXYGEN IONS
ISEE-1 data reduction and analysis plasma composition experiment
[NASA-CR-175306] N85-32552

P

P-N JUNCTIONS
A second order difference scheme for transient semiconductor device simulation
[AD-A154824] N85-33027
A review of the physics and response models for burnout of semiconductor devices
[AD-A155031] N85-33028
PACIFIC OCEAN
Sulfates in marine aerosols over the tropical Western Pacific Ocean N85-32690
PACKAGING
Sintering studies project
[AD-A154750] N85-32216
PAIR PRODUCTION
Paired ion chamber constants for fission gamma-neutron fields
[AD-A155069] N85-32999
PALEOBIOLOGY
Precambrian evolution and the rock record N85-32711
PALEONTOLOGY
Global Mega-Geomorphology
[NASA-CP-2312] N85-32357
Some observations on paleogeomorphology N85-32363
Paleoenvironmental investigations at seed cave (Windust cave H-45FR46), Franklin County, Washington
[AD-A154777] N85-32576
Precambrian evolution and the rock record N85-32711
PANEL METHOD (FLUID DYNAMICS)
A panel method study of vortex sheets with special emphasis on sheets of axisymmetric geometry
[NASA-CR-177365] N85-32095
PANELS
Experimental and theoretical assessment of a new technique for the non-destructive evaluation of laminated panels
[AD-A155622] N85-32155
An investigation into the comparisons of the underwater shock effects on a stiffened flat plate to the predictive nature of a computer model
[AD-A155612] N85-32355
PARABOLIC DIFFERENTIAL EQUATIONS
Sobolev-Poincare's inequality and the Neumann problem for u sub t = divergence of the absolute value of the gradient u to the p-2 power x the gradient u
[AD-A154788] N85-32839
PARALLEL PROCESSING (COMPUTERS)
Parallel simulation of digital LSI circuits
[AD-A154745] N85-32258
Tight bounds on the complexity of parallel sorting
[AD-A154726] N85-32778
PARAMAGNETISM
An EPR (Electron-Paramagnetic-Resonance) and ENDOR (Electron-Nuclear-Double-Resonance) study of ferroelectric ammonium sulfate
[AD-A155580] N85-33033
PARAMETER IDENTIFICATION
Modelling and parameter estimation for distributed vibratory systems
[AD-A154518] N85-32344
Physics of heavily doped silicon and solar-cell parameter measurement N85-32418
Measuring bulk recombination rates and boundary recombination velocities N85-32419
PARAMETERIZATION
Assessment of the performance of an in-field Gaussian plume/puff model for overwater use
[AD-A155435] N85-32460
A modified Fresnel scattering model for the parameterization of Fresnel returns, part 2.3A N85-32483
Criteria and algorithms for spectrum parameterization of MST radar signals N85-32527
On a variational approach to some parameter estimation problems
[NASA-CR-177935] N85-32829
PARITY
Spatial parity violation in elastic neutron-nuclei interaction channel N85-32932
PARSING ALGORITHMS
Speech understanding research
[AD-A155462] N85-32990
PARTIAL DIFFERENTIAL EQUATIONS
A derivation of relativistic effects in satellite tracking
[AD-A154620] N85-32132
A variable node finite element method applied to the gas dynamics equations
[AD-A155211] N85-32281
On a variational approach to some parameter estimation problems
[NASA-CR-177935] N85-32829
PARTIAL PRESSURE
Determination of kinetic parameters of molecular beam epitaxy
[AD-A155222] N85-33030
PARTICLE BEAMS
Injection of hydrogen macroparticles into T-10 tokamak N85-32937
PARTICLE EMISSION
Production of stable embryo particles in dense ion tracks of alpha particle emissions in the atmosphere N85-32638
Application of Particle Induced X-ray Emission analysis (PIXE) to aerosol long range transport studies N85-32665
PARTICLE MASS
Aerosol analysis and emission spectrometry with free jets
[DE85-010576] N85-32168
PARTICLE PRECIPITATION
Characteristics and sources of E-region ionization in the continuous aurora
[AD-A155018] N85-32562
PARTICLE PRODUCTION
Formation of particles in the air of the humid tropical forests N85-32639
PARTICLE SIZE DISTRIBUTION
Large eddy structures in transitional and turbulent flames
[AD-A154520] N85-32157
Photoinduced active sites on ice nucleating aerosol of silver iodide N85-32601
Experimental investigation of properties of ice-forming reagents N85-32602
The effect of supersaturation, temperature and particle size on ice-nucleating ability of atmospheric aerosol N85-32604
Multi-channel electric aerosol spectrometer N85-32623
Formation of particles in the air of the humid tropical forests N85-32639
The influence of Brownian coagulation on the size distributions of atmospheric aerosols N85-32643
A new hypothesis for the observed vertical distribution of atmospheric aerosols N85-32646

On the mechanisms responsible for the formation of typical size spectra and vertical distribution of tropospheric aerosol particles N85-32647
Our knowledge about the atmospheric aerosol N85-32650
Characteristics of aerosol composition in a nonurban area, north China N85-32651
Variation of the submicron aerosol structure N85-32661
Variability of rural aerosols under stable weather conditions N85-32663
Marine aerosols at the Dutch North Sea coast: Size distributions and fractionation of trace elements N85-32664
A probabilistic method for particle size analysis of aerosols N85-32669
An electron microscopic study of urban aerosol N85-32689

PARTICLE TELESCOPES
The energy spectrum of Jovian electrons in interplanetary space
[PAPER-SH-1.5-18] N85-33051

PARTICLES
Absorption and scattering properties of aerosols of aggregated particles in the infrared spectral region
[AD-A155475] N85-32591
Ice-forming efficiency of the soluble and insoluble portions of dust contained in snow N85-32631
Study of the formation of particles from natural hydrocarbons released by vegetation N85-32640
A study of time transformation of natural photochemical aerosols N85-32644
Measurements of the critical supersaturation of 0.029 to 0.035 micron radius particles at Washington, District of Columbia N85-32676

PARTICULATE SAMPLING
Physical and chemical aerosol characteristics in extremely clean air masses at Cape Grim, Tasmania N85-32655

PASCAL (PROGRAMMING LANGUAGE)
A PASCAL interpreter for the functional programming language ELC (Extended lambda calculus)
[AD-A155218] N85-32810

PASSIVITY
Silicon surface passivation by silicon nitride deposition N85-32423
The development and evaluation of point defect models for the growth of passive films on single crystal, polycrystalline, and amorphous metal surfaces
[AD-A154685] N85-33023

PATTERN RECOGNITION
Automated cell detection as a mesocyclone precursor tool
[AD-A154952] N85-32577
Object identification and manipulation using silhouette moments
[AD-A154755] N85-33011

PELLETS
Burn front velocity as a function of pellet density in iron-potassium perchlorate heat powders
[DE85-011448] N85-32214

PENETRATION
The effect of stress and hot corrosion on nickel-base superalloys
[AD-A154722] N85-32181
Ice fog as an electro-optical obscurant
[AD-A155059] N85-33015

PERCEPTION
Resource allocation in cerebral specialization of function: Behavioral and electrophysiological studies
[AD-A155092] N85-32759
The effects of prolonged feeding meal, ready-to-eat (MRE) operational rations
[AD-A154763] N85-32773

PERFORMANCE TESTS
Fin-line horn antennas
[AD-A154597] N85-32255
Fabrication and test of modified quadrupole mass spectrometer
[AD-A155186] N85-32312
Module Hipot and ground continuity test results N85-32447

PERMEABILITY
Permeation of mixed penetrants through glassy polymer membranes
[AD-A155605] N85-32207

PERTURBATION THEORY
Calculation of the propagation constant in a rectangular waveguide containing an inhomogeneous longitudinally magnetized plasma
[DE85-012072] N85-32250
Reflection of acoustic beam from inhomogeneous boundary N85-32864

PETROLOGY
Dating Archean zircon by ion microprobe: New light on an old problem N85-33094

PHARMACOLOGY
East Europe report: Science and technology
[JPRS-ESA-85-023] N85-32217
Interaction of opiate and phencyclidine derivatives with the acetylcholine receptor
[AD-A155119] N85-32761

PHASE CONJUGATION
Influence of spatial pumping spectrum on quality of phase conjugate reflection during 4-photon interaction N85-32964

PHASE DIAGRAMS
Phase behavior and QLS (Quasielastic Light Scattering) in potassium linoleate/n-alkanol microemulsions
[AD-A155028] N85-32163

PHASE LOCKED SYSTEMS
A phase-locked frequency multiplier for the signal averaging of the vibration of the Wessex helicopter input spiral bevel pinion
[AD-A154914] N85-32113
Practicality of electronic beam steering for MST/ST radars, part 6.2A N85-32516

PHASE MATCHING
Huffman-coded pulse compression waveforms
[AD-A155322] N85-32243

PHASE MODULATION
Experimental evaluation of a new form of M-ary (M = 8) phase shift keying including design of the transmitter and receiver
[AD-A155103] N85-32239

PHASE SHIFT
Design of a jamming simulator for a binary communication system
[AD-A154617] N85-32221

PHASE SHIFT CIRCUITS
East Europe report: Science and technology
[JPRS-ESA-85-021] N85-32190

PHASE SHIFT KEYING
Experimental evaluation of a new form of M-ary (M = 8) phase shift keying including design of the transmitter and receiver
[AD-A155103] N85-32239

PHASE TRANSFORMATIONS
Comparison of the response of shape memory alloy actuators using air-cooling and water-cooling
[AD-A155216] N85-32185
The shearing contribution in transformation toughening of brittle materials
[AD-A154656] N85-32195
Aerobic sulfur-oxidizing bacteria: Environmental selection and diversification N85-32712
Sulfur transformations at the hydrogen sulfide/oxygen interface in stratified waters and in cyanobacterial mats N85-32715
The Konstantinov effect and absorption of sound in inhomogeneous media N85-32861
An EPR (Electron-Paramagnetic-Resonance) and ENDOR (Electron-Nuclear-Double-Resonance) study of ferroelectric ammonium sulfate
[AD-A155580] N85-33033

PHASED ARRAYS
Null synthesis with phase and amplitude controls at the subarray outputs
[AD-A155187] N85-32241
Evaluation of the effects of roll angle on the natural convection heat transfer from an array of cylindrical spines
[AD-A154594] N85-32273
Most desirable terrain, e.g., flat vs valley location, part 5.1B N85-32513

PHONONS
Influence on bi-phonon states on Raman scattering of light in molecular crystals N85-32865
Influence of phonon interaction on width and form of Mandelstam-Brillouin optical scattering line N85-32962

PHOSPHATES
Design of micelles as dephosphorylating agents
[AD-A155589] N85-32166
Microanalysis of dissolved iron and phosphate in pore waters of hypersaline sediment N85-32744

PHOSPHORUS
Multiphoton production and detection of atoms
[AD-A155561] N85-33000
Precision measurements of solar energetic particle elemental composition
[PAPER-SH-2.1-4] N85-33052

PHOSPHORYLATION
Design of micelles as dephosphorylating agents
[AD-A155589] N85-32166

PHOTOACOUSTIC SPECTROSCOPY
Photo-acoustic effect in finite-dimensional semiconductors N85-32876

PHOTOCHEMICAL REACTIONS
The diurnal variation of the neutral sodium species in the upper atmosphere: A model study
[AD-A154988] N85-32561
Photochemical aerosol formation in polluted atmosphere N85-32642
A study of time transformation of natural photochemical aerosols N85-32644

PHOTODISSOCIATION
Optical inhomogeneities in a nanosecond-pulse iodine photodissociation laser with slow UV radiation pumping N85-32902
Multiphoton production and detection of atoms
[AD-A155561] N85-33000

PHOTOELASTICITY
Stress concentration in the elastoplastic state and residual stress after unloading
[AD-A155628] N85-32356

PHOTOELECTRON SPECTROSCOPY
Photoelectron studies of autoionizing Rydberg states in HCl
[DE85-011813] N85-33001

PHOTOELECTRONS
Ionospheric electron density profile and related studies
[AD-A155257] N85-32567

PHOTOGEOLOGY
Quantitative geomorphologic studies from spaceborne platforms N85-32381

PHOTOGRAMMETRY
Comparison of survey and photogrammetry methods to position gravity data, Yucca Mountain, Nevada
[DE85-011685] N85-32316
Coastal erosion along Monterey Bay
[AD-A155610] N85-32707

PHOTOINTERPRETATION
Handbook for obtaining and using aerial photography to map aquatic plant distribution
[AD-A154584] N85-32388

PHOTOIONIZATION
Ionospheric electron density profile and related studies
[AD-A155257] N85-32567
Activities of the Physics Division
[DE85-000784] N85-33002

PHOTOLUMINESCENCE
A theory of exciton photoluminescence for two types of neutral acceptors in silicon. A study of the systems Si:(B, IN), Si:(Al), (Si), Si:(Ga, In), Si:(B, Al), Si:(B, Ga), and Si:(Al, GA)
[AD-A155452] N85-33031

PHOTOMETERS
Sahara Desert dust transport to the south N85-32666

PHOTONICS
Influence of spatial pumping spectrum on quality of phase conjugate reflection during 4-photon interaction N85-32964

PHOTONS
The possibility of observing and exploiting the generation of high-energy photons by electrons in the field of an intense electromagnetic wave N85-32931
Influence of spatial pumping spectrum on quality of phase conjugate reflection during 4-photon interaction N85-32964

PHOTOSENSITIVITY
Three-dimensional photochemical machining with lasers
[AD-A154711] N85-32320

PHOTOSPHERE
Contributions to the 19th International Cosmic Ray Conference
[NASA-CR-176080] N85-33044
Solar coronal and photospheric abundances from solar energetic particle measurements
[PAPER-SH-2.1-5] N85-33053
Heating of the deep chromosphere during solar flares
[AD-A155256] N85-33100

PHOTOSYNTHESIS
Protocyanobacteria: Oxygenic and Anoxygenic photosynthesis in mat-forming bacteria N85-32714
Cytochromes and iron sulfur proteins in sulfur metabolism of phototrophic bacteria N85-32718
Insights into the phylogenetic positions of photosynthetic bacteria obtained from 5S rRNA and 16S rRNA sequence data N85-32719
Ecophysiology of phototrophic sulfur bacteria in lakes: Vertical distribution of planktonic populations N85-32722
Anaerobic reduction of elemental sulfur by Chromatium vinosum and Beggiatoa alba N85-32739
Interactions among sulfide-oxidizing bacteria N85-32741
Cyanobacterial mats: Microanalysis of community metabolism N85-32743
Microanalysis of dissolved iron and phosphate in pore waters of hypersaline sediment N85-32744
Glutathione in cyanobacteria N85-32745
Microbial communities and microprofiles of sulfide and oxygen of alum rock sulfur springs N85-32746

PHOTOTROPISM
The global sulfur cycle [NASA-TM-87570] N85-32710
Phototrophic bacteria and their role in the biogeochemical sulfur cycle N85-32735
Sulfur cycling and metabolism of phototrophic and filamentous sulfur bacteria N85-32737
Enrichments for phototrophic bacteria and characterization by morphology and pigment analysis N85-32738
Buoyant densities of phototrophic sulfur bacteria and cyanobacteria N85-32740
Interactions among sulfide-oxidizing bacteria N85-32741
Cyanobacterial mats: Microanalysis of community metabolism N85-32743
Glutathione in cyanobacteria N85-32745

PHOTOVOLTAIC CELLS
High-efficiency crystalline silicon technology development N85-32395
Flat-plate module efficiency versus cost tradeoffs N85-32398
Georgetown University Photovoltaic Higher Education National Exemplar Facility (PHENEF) N85-32400
Photothermal degradation studies of encapsulants N85-32403
Topics in electrochemical degradation of photovoltaic modules N85-32410
Polymer-water interaction studies N85-32411
Encapsulation processing and manufacturing yield analysis N85-32434
Photovoltaic module spread-of-flame testing N85-32448

PHOTOVOLTAIC EFFECT
Predicting photothermal field performance N85-32404
Micromolecular modeling N85-32405
Silicon refinement by chemical vapor transport N85-32412
MOD silver metallization for photovoltaics N85-32428

PHYSICAL OPTICS
An analysis of physical optics models for rough surface scattering [AD-A154960] N85-32235

PHYSIOCHEMISTRY
Ecophysiology of phototrophic sulfur bacteria in lakes: Vertical distribution of planktonic populations N85-32722

PHYSIOLOGICAL RESPONSES
Empirical methods for predicting eutrophication in impoundments. Report 3. Phase 2. Model refinements [AD-A155483] N85-32462
USAFSAM review and analysis of radiofrequency radiation bioeffects literature [AD-A155113] N85-32760

PHYSIOLOGY
Chemolithotrophy and physiology of bacterial nutrient limitation N85-32730
Structure and physiology of Beggiatoa and Thiothrix N85-32734
Sulfur cycling and metabolism of phototrophic and filamentous sulfur bacteria N85-32737

PICOSECOND PULSES
Dynamics of emission from dye lasers employing synchronous pumping by limited picosecond pulse train N85-32899

PIEZOELECTRIC CERAMICS
Experiments on the influence of active walls on the initial amplitudes and growths of instability waves [AD-A154630] N85-32275

PIEZOELECTRIC TRANSDUCERS
Microwave SAW (Surface Acoustic Wave) monochromator [AD-D011718] N85-32311

PILOT PERFORMANCE
An error-dependent model of instrument-scanning behavior in commercial airline pilots [NASA-CR-3908] N85-32765
Human performance in continuous/sustained operations and the demands of extended work/rest schedules. An annotated bibliography [AD-A155619] N85-32771

PILOT TRAINING
Advanced simulator for pilot training and helmet-mounted visual display configuration comparisons [AD-A155326] N85-32776

PIPE FLOW
Resolution of thermal striping issue downstream of a horizontal pipe elbow in stratified pipe flow [DE85-006195] N85-32292

PIPES (TUBES)
Film condensation of steam on externally finned horizontal tubes [AD-A155642] N85-32285
Resolution of thermal striping issue downstream of a horizontal pipe elbow in stratified pipe flow [DE85-006195] N85-32292

PITCH (INCLINATION)
In-flight evaluation of pure time delays in pitch and roll [NASA-TM-86744] N85-32123

PLANAR STRUCTURES
LSI/VLSI ion implanted planar GaAs IC processing [AD-A155110] N85-32262
Generalized planar matching [AD-A154809] N85-32842

PLANE STRAIN
A cracked orthotropic sheet stiffened by a semi-infinite orthotropic sheet [NASA-TP-2455] N85-32339

PLANE WAVES
Guided-mode launching in a slab waveguide by way of diffraction at the edge of a conducting screen residing on one surface of the slab [AD-A154886] N85-32232

PLANETARY ATMOSPHERES
Aeolian geomorphology from the global perspective N85-32373

PLANETARY COMPOSITION
Workshop on the Early Earth: The Interval from Accretion to the Older Archean [NASA-CR-176037] N85-33062
Conditions during formation of the Earth N85-33066
Early evolution of the crust-mantle system N85-33067
Was core formation violent enough to homogenize the early mantle? N85-33068
The problem of the Earth's CO2 content and the iron core N85-33069
A review of noble gas geochemistry in relation to early Earth history N85-33081
Carbon and nitrogen in the deep Earth N85-33085
Chemical evolution of the Earth: Equilibrium or disequilibrium process? N85-33088
Thermal, dynamic and compositional aspects of the core-forming Earth N85-33091
Earth's primordial differentiation, and its after-effects N85-33092

PLANETARY CRATERS
Considerations of large scale impact and the early Earth N85-33070

PLANETARY ENVIRONMENTS
The global sulfur cycle [NASA-TM-87570] N85-32710

PLANETARY EVOLUTION
Global geomorphology: Report of Working Group Number 1 N85-32382
Landscape inheritance: Report of Working Group Number 2 N85-32383
Protocyanobacteria: Oxygenic and Anoxygenic photosynthesis in mat-forming bacteria N85-32714
Workshop on the Early Earth: The Interval from Accretion to the Older Archean [NASA-CR-176037] N85-33062
Conditions during formation of the Earth N85-33066
Early evolution of the crust-mantle system N85-33067
Was core formation violent enough to homogenize the early mantle? N85-33068
Considerations of large scale impact and the early Earth N85-33070
Noble gases and the early history of the Earth: Inappropriate paradigms and assumptions inhibit research and communication N85-33075
A review of noble gas geochemistry in relation to early Earth history N85-33081
Archean sedimentary systems and crustal evolution N85-33082
Crustal radiogenic heat production and the selective survival of ancient continental crust N85-33086
Large arcuate scars: A geological legacy of the Earth's accretionary past N85-33089
Thermal, dynamic and compositional aspects of the core-forming Earth N85-33091

PLANETARY GEOLOGY
The problem of scale in planetary geomorphology N85-32375
Landscape inheritance: Report of Working Group Number 2 N85-32383

PLANETARY MAGNETIC FIELDS
Planetary Dynamos [NASA-CR-176001] N85-32657

PLANETARY SURFACES
Considerations of large scale impact and the early Earth N85-33070

PLANETARY WAVES
A numerical analysis of transient planetary waves and the vertical structure in a meso-strato-troposphere model, part 1.4A N85-32473

PLANETOLOGY
Geomorphic classification of Icelandic and Martian volcanoes: Limitations of comparative planetology research from LANDSAT and Viking orbiter images N85-32372

PLANKTON
Properties of forest derived cloud condensation nuclei N85-32682
Ecophysiology of phototrophic sulfur bacteria in lakes: Vertical distribution of planktonic populations N85-32722

PLANTS (BOTANY)
Ice nucleating characteristics of Capparis Aphylla, an Indian herb N85-32619
The role of sulfur in osmoregulation and salinity tolerance in cyanobacteria, algae, and plants N85-32736
Hydroponics developments for spaceship garden N85-32754

PLASMA COMPOSITION
ISEE-1 data reduction and analysis plasma composition experiment [NASA-CR-175306] N85-32552

PLASMA DYNAMICS
Plasmodynamic methods for generating powerful light puses N85-32943

PLASMA ELECTRODES
Space-time characteristics of field in longitudinal pulse-period discharge typical in pumping of self-terminating lasers N85-32909

PLASMA ENGINES
Modeling the exhaust of the pulsed plasma thruster [AD-A155344] N85-33018

PLASMA EQUILIBRIUM
Solution of problem of equilibrium confinement of plasma by magnetic field in an infinite circular cylinder N85-32936

PLASMA FOCUS
Plasmodynamic methods for generating powerful light puses N85-32943

PLASMA OSCILLATIONS
Low frequency instabilities driven by an ion temperature anisotropy [AD-A154902] N85-33016

PLASMA PHYSICS
USSR report: Physics and mathematics [JPRS-UPM-85-004] N85-32860
Modeling the exhaust of the pulsed plasma thruster [AD-A155344] N85-33018

PLASMA POTENTIALS
Space-time characteristics of field in longitudinal pulse-period discharge typical in pumping of self-terminating lasers N85-32909

PLASMA PUMPING
Space-time characteristics of field in longitudinal pulse-period discharge typical in pumping of self-terminating lasers N85-32909

PLASMA RADIATION
Plasmodynamic methods for generating powerful light puses N85-32943
Characteristics of optogalvanic effect in media with inverse populations N85-32944
Investigation of space-time structure of glow of laser plasma colliding with flat screen N85-32947

PLASMA RESONANCE
Influence of ECR-heating on MHD activity of plasma in tokamak-10 installation N85-32949
Cyclotron resonance in a nonneutral plasma [AD-A155248] N85-33017

PLASMA TURBULENCE
Investigation of ion-acoustic plasma turbulence in field of powerful electromagnetic wave by CO2-laser radiation scattering N85-32935

PLASMA WAVES
Analysis of spacecraft data [NASA-CR-171587] N85-32789

PLASMAS (PHYSICS)
The space shuttle glow [AD-A154937] N85-32139
The plasma erosion opening switch [AD-A154942] N85-32259
Plasma mass and effective inductance in a small railgun [AD-A154644] N85-32304
Microwave-enhanced thin-film deposition N85-32431
In-cavity laser IR spectrum analyzer for investigating non-steady-state processes N85-32894
Infrared laser holography used in fusion plasma studies N85-32905
Operational window for a plasma erosion opening switch used for voltage multiplication on pulsed power generators [AD-A155482] N85-33020
Research in particles and fields [NASA-CR-176069] N85-33103

PLASTIC DEFORMATION
Fundamental investigations of failure during superplastic forming process
[AD-A154647] N85-32194
Dynamic fracture of concrete and other heterogeneous materials
[AD-A154513] N85-32343
The measurement of strain fields by X-ray topographic contour mapping
[AD-A154870] N85-32348
PLASTICIZERS
Synthesis of energetic materials
[AD-A154887] N85-32210
Polymer-water interaction studies N85-32411
PLATES (TECTONICS)
Global geomorphology N85-32359
Techniques, problems and uses of mega-geomorphological mapping N85-32378
Planetary perspective. Report of Working Group Number 4 N85-32385
The Aravalli sequence of Rajasthan, India: A Precambrian continental margin? N85-33084
PLATING
Plating density standards
[DE85-010014] N85-32318
PLATINUM ALLOYS
CO adsorption on (111) and (100) surfaces of the Pt sub 3 Ti alloy. Evidence for parallel binding and strong activation of CO
[NASA-CR-176077] N85-32176
PLUGS
Vapor-liquid phase separator studies
[NASA-CR-166545] N85-32272
PLUMES
Laser beam interactions with vapor plumes during Nd:YAG laser welding on aluminum
[DE85-009793] N85-32328
Assessment of the performance of an in-field Gaussian plume/puff model for overwater use
[AD-A155435] N85-32460
VALMET: A valley air pollution model
[DE85-010820] N85-32463
Modeling the exhaust of the pulsed plasma thruster
[AD-A155344] N85-33018
PLUTONIUM
Influence of chemical form, feeding regimen, and animal species on the gastrointestinal absorption of plutonium
[DE85-010291] N85-32751
POINT DEFECTS
Thin-film reliability and engineering overview N85-32450
The development and evaluation of point defect models for the growth of passive films on single crystal, polycrystalline, and amorphous metal surfaces
[AD-A154685] N85-33023
POISONS
Emergency modeling of hazardous air pollutants
[AD-A155441] N85-32461
POISSON DENSITY FUNCTIONS
Upward continuation of surface gravity anomalies
[AD-A154973] N85-32560
POISSON EQUATION
Poisson formula for radon transformation and numerical image reconstruction algorithm N85-32973
POLAR REGIONS
Airborne measurements of the vertical distribution of Arctic haze N85-32657
POLARIZATION (WAVES)
The Faraday effect in ruby and corundum in strong magnetic fields N85-32967
POLARIZATION CHARACTERISTICS
Influence of mirror anisotropy and Brewster window orientation on radiation characteristics of ring lasers N85-32889
POLLUTION MONITORING
VALMET: A valley air pollution model
[DE85-010820] N85-32463
Laser Elektronika-01 for air pollution control lidar N85-32887
POLLUTION TRANSPORT
VALMET: A valley air pollution model
[DE85-010820] N85-32463
Application of Particle Induced X-ray Emission analysis (PIXE) to aerosol long range transport studies N85-32665
Sahara Desert dust transport to the south N85-32666
Measurements of giant salt nuclei from inland in east China N85-32668
on the transport of large condensation nuclei in the atmosphere at various altitudes over the territory of the USSR N85-32698
POLYCRYSTALS
The effect of diffusive hydrogen segregation on fracture of polycrystalline nickel
[AD-A155238] N85-32186
Electrical and mechanical properties of intercalated graphite fibers
[AD-A155560] N85-32205
Thermoelectric properties of beta-boron and some boron compounds
[DE85-011978] N85-32270
Basic ice nucleation mechanisms on mono and microcrystals and ice forming nuclei. Theoretical analysis and experimental results achieved in the laboratory over the past ten years: Review paper N85-32629
Mirror reflection of charged particles from + amorphous and polycrystalline surfaces N85-32927
The development and evaluation of point defect models for the growth of passive films on single crystal, polycrystalline, and amorphous metal surfaces
[AD-A154685] N85-33023
POLYESTERS
Polymerizable ultraviolet stabilizers N85-32406
POLYETHYLENES
Interaction of solutes with stretched polymers
[AD-A154662] N85-32196
POLYIMIDE RESINS
Graphite/PMR polyimide composites with improved toughness
[NASA-TM-87081] N85-32148
Permeation of mixed penetrants through glassy polymer membranes
[AD-A155605] N85-32207
POLYIMIDES
Graphite/PMR polyimide composites with improved toughness
[NASA-TM-87081] N85-32148
POLYMER CHEMISTRY
Bubble dynamics in polymer solutions undergoing shear
[AD-A154575] N85-32193
Importance and significance of transition temperatures
[AD-A154871] N85-32199
POLYMER PHYSICS
Importance and significance of transition temperatures
[AD-A154871] N85-32199
POLYMERIZATION
Graphite/PMR polyimide composites with improved toughness
[NASA-TM-87081] N85-32148
Introduction of structural variations into oxide polymers and their effect on sintering and crystallization
[AD-A155597] N85-32206
Three-dimensional photochemical machining with lasers
[AD-A154711] N85-32320
Polymerizable ultraviolet stabilizers N85-32406
POLYMERS
EVA-glass interface bond stability N85-32408
POLYNUCLEAR ORGANIC COMPOUNDS
The interaction of polynuclear aromatic hydrocarbons PAH's with water vapor and their role as condensation nuclei in the formation of haze and fog N85-32695
POLYSTYRENE
Polymer solution-supercritical fluid behavior
[AD-A154514] N85-32192
POLYURETHANE RESINS
Structure-property relationships in thermoplastic elastomers. Part 3: Segmented polyacetal-polyurethanes
[AD-A154897] N85-32200
POROSITY
MPS solidification model. Analysis and calculation of macrosegregation in a casting ingot
[NASA-CR-171589] N85-32178
POROUS MATERIALS
Vapor-liquid phase separator studies
[NASA-CR-166545] N85-32272
PORTABLE EQUIPMENT
Field testing of a lightweight relocatable structure in a temperate environment
[AD-A155171] N85-32350
POSITION (LOCATION)
The potential of the NAVSTAR global positioning system for the Corps of Engineers, civil works
[AD-A154913] N85-32109
Parameter estimation in communication system tracking satellite observations
[AD-A155137] N85-32582
POTASSIUM
Passive Q-modulation of optical cavities by KCl crystals containing OH(-) -ions N85-32915
Measurements of Fe and Ar fragmentation cross sections
[PAPER-OG-7.2-20] N85-33047
Precision measurements of solar energetic particle elemental composition
[PAPER-SH-2.1-4] N85-33052
POTASSIUM CHLORIDES
Passive Q-modulation of optical cavities by KCl crystals containing OH(-) -ions N85-32915
POTASSIUM COMPOUNDS
Phase behavior and QLS (Quasielastic Light Scattering) in potassium linoleate/n-alkanol microemulsions
[AD-A155028] N85-32163
Luminescence and absorption of indium-activated potassium-borate glasses subjected to high-power excitation N85-32868
POTASSIUM PERCHLORATES
Burn front velocity as a function of pellet density in iron-potassium perchlorate heat powders
[DE85-011448] N85-32214
POTENTIAL ENERGY
Generation of available potential energy and the energy cycle during the global weather experiment
[NASA-CR-175301] N85-32572
Horizontal and vertical structure of velocity, potential vorticity and energy in the gulf stream
[AD-A154753] N85-32702
POTENTIAL FLOW
The calculation of fully three dimensional flow through any type of turbomachine blade row N85-32294
On the limiting configuration of interfacial gravity waves
[AD-A154821] N85-32557
POWDER (PARTICLES)
Multilayer capacitor dielectrics produced from metallo-organic precursors
[AD-A154592] N85-32254
POWDER METALLURGY
Hot isostatically pressed Sm(2)(TM)17 magnets
[AD-A155479] N85-32267
POWER CONDITIONING
The plasma erosion opening switch
[AD-A154942] N85-32259
PRECAMBRIAN PERIOD
Precambrian evolution and the rock record N85-32711
PRECIPITATION (METEOROLOGY)
Measurements of giant salt nuclei from inland in east China N85-32668
PREDICTION ANALYSIS TECHNIQUES
Wall flames and implications for upward flame spread
[FAA-CT-85-2] N85-32103
Injection of drag reducing additives into turbulent water flows: Two-component velocity measurements and mixing length model predictions
[AD-A154804] N85-32274
Assessment of the performance of an in-field Gaussian plume/puff model for overwater use
[AD-A155435] N85-32460
Accuracy and operational use of medium and extended range numerical atmospheric forecasts: A review
[AD-A155027] N85-32579
Forecasting of tropical cyclone motion using an EOF (Empirical Orthogonal Function) representation of wind forcing
[AD-A155034] N85-32580
An evaluation of discretized conditional probability and linear regression threshold techniques in model output statistics forecasting of cloud amount and ceiling over the North Atlantic Ocean
[AD-A155100] N85-32581
Medium range atmospheric forecast system: Evaluation report
[AD-A155240] N85-32589
Forecasting atmospheric visibility over the summer north Atlantic using the principal discriminant method
[AD-A155537] N85-32593
A numerical and analytical investigation of lee cyclogenesis
[AD-A155607] N85-32594
Simulation of the coupled atmospheric and oceanic boundary layer model during MILDEX
[AD-A155166] N85-32705
On the problem of linear programming with approximate data N85-32978
PREDICTIONS
Understanding and laboratory prediction of the atmospheric corrosion behavior of steels and of non-ferrous metals and alloys
[AD-A154642] N85-32179
Resource management for the tagged token dataflow architecture
[AD-A154773] N85-32779
PRESSURE
Computation of three-dimensional, inviscid, rotational flows N85-32296
PRESSURE DISTRIBUTION
Trailing edge flow and aerodynamic sound. Part 1: Tonal pressure and velocity fluctuations. Part 2: Random pressure and velocity fluctuations
[AD-A154947] N85-32097
PRESSURE ICE
Kinetic friction coefficient of ice
[AD-A155035] N85-32859

PRIMITIVE EARTH ATMOSPHERE
The composition of the primitive atmosphere and the synthesis of organic compounds on the early Earth N85-33065
The problem of the Earth's CO2 content and the iron core N85-33069
PRINTED CIRCUITS
Digital integrated circuits N85-32787
A comparison and analysis of Vintr's global routing algorithm with the Lee routing algorithm in two-layer printed circuit boards
[AD-A155600] N85-32816
PRINTERS
Flexible satellite communications systems simulator, phase 3
[AD-A155647] N85-32247
PROBABILITY THEORY
Reliability of void detection in structural ceramics using scanning laser acoustic microscopy
[NASA-TM-87035] N85-32337
Decomposing the joint distribution of several linear combinations of uniform spacings
[AD-A155056] N85-32845
Analysis of unreplicated factorials allowing for possibly faulty observations
[AD-A154813] N85-32848
Antistarshapedness, dispersiveness and mixtures
[AD-A155583] N85-32849
PROBLEM SOLVING
The formal specification of an abstract machine: Design and implementation
[AD-A155167] N85-32808
A comprehensive study of the AFIT (Air Force Institute of Technology) software development environment
[AD-A155450] N85-32812
A new fault-tolerant algorithm for clock synchronization
[AD-A154771] N85-32836
A simulation study of Sylvester's problem in three dimensions
[AD-A155266] N85-32854
Solution of problem of equilibrium confinement of plasma by magnetic field in an infinite circular cylinder N85-32936
Solvability of some inverse problems in laser radiation focusing N85-32963
On the problem of linear programming with approximate data N85-32978
PRODUCTION PLANNING
Robots, Manipulators N85-32786
PRODUCTIVITY
Encapsulation processing and manufacturing yield analysis N85-32434
Human activity and production rate of secondary nuclei N85-32645
PROGRAM VERIFICATION (COMPUTERS)
Discrete-element acoustic analysis of submerged structures using doubly asymptotic approximations
[AD-A154959] N85-32987
PROGRAMMING LANGUAGES
The design and implementation of an object-oriented, production-rule interpreter
[AD-A154769] N85-32803
Praxis release notes, version 7.3
[DE85-011862] N85-32820
Evaluation and implementation of a functional microprogram generator
[AD-A155164] N85-32823
PROGRESS
High-efficiency silicon solar cell research N85-32417
PROPAGATION MODES
Adjustment of radiation wavelength of multimode InP-GaInAsP injection heterolasers N85-32913
PROPAGATION VELOCITY
Lower bounds of propagation velocity of steady ionizing waves in field of strong electromagnetic wave N85-32940
Amplification of electromagnetic wave by electron stream with negative velocity differences N85-32941
PROPELLANTS
Closed-bomb combustion of Hivelite-based, Very High Burn Rate (VHBR) propellant
[AD-A155740] N85-32212
PROPULSION
Clarke Stations and mercurian mass-drivers: Energy for large-scale transportation systems
[DE85-009607] N85-32145
Three-Dimensional Techniques Applied to Internal Flows in Propulsion Systems
[AGARD-LS-140] N85-32293
PROPULSION SYSTEM PERFORMANCE
Performance improvements of a highly integrated digital electronic control system for an F-15 airplane
[NASA-TM-86748] N85-32120
PROTECTIVE COATINGS
A study of adherent oxide scales
[AD-A155554] N85-32188
Development of wide band recording materials
[AD-A154961] N85-32309
Encapsulation materials research N85-32407
PROTON ENERGY
Solar modulation and interplanetary gradients of the galactic electron flux, 1977 - 1984
[PAPER-SH-4.7-4] N85-33059
PROTON FLUX DENSITY
Study of proton and neutron activation of metal samples in low Earth orbit
[NASA-CR-171596] N85-32130
Latitude variation of recurrent fluxes in the outer solar system
[PAPER-SH-4.1-13] N85-33054
PROTON IRRADIATION
Study of proton and neutron activation of metal samples in low Earth orbit
[NASA-CR-171596] N85-32130
PROTON-PROTON REACTIONS
Exotic events of p bar p-collider: Excited quark or excited color boson? N85-32930
PROTONS
Sulfate-reducing bacteria: Microbiology and physiology N85-32732
Solar modulation and interplanetary gradients of the galactic electron flux, 1977 - 1984
[PAPER-SH-4.7-4] N85-33059
PROTOPLANETS
Implications for the Earth of the early dynamical environment N85-33079
PROTOTYPES
The design and implementation of an object-oriented, production-rule interpreter
[AD-A154769] N85-32803
PSYCHOLOGICAL FACTORS
Living aloft: Human requirements for extended spaceflight
[NASA-SP-483] N85-32772
PSYCHOLOGY
Review of the psychological issues relating to the effectiveness of structured programming
[AD-A154593] N85-32766
The priming effect in task design research
[AD-A154589] N85-32852
PSYCHOMETRICS
Conceptualizing in assembly tasks
[AD-A155564] N85-32770
PSYCHOMOTOR PERFORMANCE
The effects of prolonged feeding meal, ready-to-eat (MRE) operational rations
[AD-A154763] N85-32773
PULSE AMPLITUDE
A modified Fresnel scattering model for the parameterization of Fresnel returns, part 2.3A N85-32483
PULSE COMMUNICATION
Design of a jamming simulator for a binary communication system
[AD-A154617] N85-32221
PULSE COMPRESSION
Huffman-coded pulse compression waveforms
[AD-A155322] N85-32243
PULSE DURATION
A sampling phasemeter design for pulsed continuous wave signals
[AD-A155237] N85-32264
A modified Fresnel scattering model for the parameterization of Fresnel returns, part 2.3A N85-32483
Establishment of steady-state power level in pulse-periodic excimer laser N85-32896
PULSE GENERATORS
Coordinated research program in pulsed power physics
[AD-A154629] N85-32858
Operational window for a plasma erosion opening switch used for voltage multiplication on pulsed power generators
[AD-A155482] N85-33020
PULSE MODULATION
Effect of powerful pulsed low-energy ion streams on GaAs N85-32877
Self Q-modulation and generation of short pulses in distributed-feedback lasers N85-32907
PULSE RADAR
Huffman-coded pulse compression waveforms
[AD-A155322] N85-32243
Observations of frontal zone structures with a VHF Doppler radar and radiosondes, part 1.2A N85-32469
PULSED LASERS
Detection of excited states by laser-induced fluorescence
[AD-A155558] N85-32326
Pulsed excimer laser processing for cost-effective solar cells N85-32432
Excimer-laser generator of powerful UV picosecond pulses synchronized with picosecond pulses in visible and IR bands N85-32903
Powerful XeCl excimer electric discharge laser with good temporal stability and fast response time N85-32911
The moving thermoacoustic array: A theoretical feasibility study
[AD-A154510] N85-32980
PULSED RADIATION
Generation of single nanosecond high-contrast radiation pules (lambda=10.6 micrometers) N85-32886
Laser radiation propagation in inertialess nonlinear medium N85-32898
PURITY
JPL in-house fluidized-bed reactor research N85-32414
High-purity silicon crystal growth N85-32444
PYROLYSIS
A fluidized-bed reactor for silane pyrolysis N85-32413
Modeling of the silane FBR system N85-32415
Silicon production in an aerosol reactor N85-32416

Q

Q VALUES
Study of proton and neutron activation of metal samples in low Earth orbit
[NASA-CR-171596] N85-32130
QUADRATIC EQUATIONS
A new problem in mathematical physics associated with the problem of coherent phase transformation N85-32976
QUADRUPOLES
Fabrication and test of modified quadrupole mass spectrometer
[AD-A155186] N85-32312
QUALITATIVE ANALYSIS
Qualitative analysis of sign-bit processing
[AD-A154776] N85-32804
QUALITY CONTROL
Quality analysis N85-32785
An automated quality assurance surveillance plan for ADP (Automated Data Processing) operations under the Navy's commercial activities program
[AD-A154767] N85-32802
QUANTITATIVE ANALYSIS
Quantitative analysis in megageomorphology N85-32376
Quantitative analysis of geomorphic processes using satellite image data at different scales N85-32380
Quantitative geomorphologic studies from spaceborne platforms N85-32381
QUANTUM CHROMODYNAMICS
Toward the question of multi-quark configurations in nuclei N85-32929
Spatial parity violation in elastic neutron-nuclei interaction channel N85-32932
QUANTUM ELECTRONICS
Solid state research
[AD-A154783] N85-33025
QUANTUM MECHANICS
Earth Albedo and the orbit of LAGEOS
[NASA-TM-86210] N85-32131
Theoretical studies of structure and stability of hydrates of atmospheric sulfur species N85-32684
QUARKS
Toward the question of multi-quark configurations in nuclei N85-32929
Exotic events of p bar p-collider: Excited quark or excited color boson? N85-32930
QUARTZ
Dating Archean zircon by ion microprobe: New light on an old problem N85-33094
QUARTZ CRYSTALS
JPL in-house fluidized-bed reactor research N85-32414
Data analysis for lidar and quartz crystal microbalance systems
[NASA-CR-172601] N85-32464
QUEUEING THEORY
The architectural requirements and integration analysis of a database server for office automation
[AD-A155517] N85-32825

R

RADAR
The use of the glistening surface concept in rough surface scattering
[AD-A154922] N85-32234

RADAR ANTENNAS
Accuracy of velocity and power determination by the Doppler method N85-32493
Improvement of vertical velocity measurements, part 3.4B N85-32494
Mesospheric measurements of irregularity patches using a 3-antenna interferometer, part 3.6B N85-32498
Summary of progress at the Poker Flat Observatory in Alaska N85-32539
A note on the proposed UK VHF radar N85-32545

RADAR CROSS SECTIONS
Radar target identification through electromagnetic scattering studies
[AD-A154596] N85-32220
The use of the glistening surface concept in rough surface scattering
[AD-A154922] N85-32234
Head-on scattering of a tubular cylinder of finite length for radar target identification purposes
[AD-A155608] N85-32246

RADAR DATA
Hardware schemes for fast Fourier transform, part 7.4A N85-32526
Criteria and algorithms for spectrum parameterization of MST radar signals N85-32527

RADAR ECHOES
Morphology of the scattering targets: Fresnel and turbulent mechanisms, part 2.1A N85-32481
Signal statistics of the radar echoes: Angle-of-arrival statistics, part 2.2A N85-32482
A modified Fresnel scattering model for the parameterization of Fresnel returns, part 2.3A N85-32483
Observations of mesospheric turbulence by rocket probe and VHF radar, part 2.4A N85-32484
Interpretation of radar returns from the mesosphere, part 2.3A N85-32485
Radar echoes at 2.66 and 40.92 MHz from the mesosphere, part 2.6A N85-32486
Anisotropy of the permittivity field inferred from aspect-sensitive radar echoes N85-32492
Interferometer applications of VHF radars, part 3.6A N85-32497
Most desirable terrain, e.g., flat vs valley location, part 5.1B N85-32513
Interpolation problems in meteor radar analysis, part 7.6A N85-32528
The effects of subrefractive layers and elevated ducts on airborne radar and ESM (Electronic Surveillance Measures)
[AD-A155524] N85-32592

RADAR IMAGERY
Using ship wake patterns to evaluate SAR (Synthetic Aperture Radar) ocean wave imaging mechanisms. Joint US-Canadian Ocean Wave Investigation Project
[AD-A154633] N85-32223
Use of spaceborne imaging radar in regional geomorphic studies N85-32377
The Boot Lake MF imaging radar N85-32537

RADAR MEASUREMENT
Middle Atmosphere Program. Handbook for MAP. Volume 14: URSI/SCOSTEP Workshop on Technical Aspects of MST Radar
[NASA-CR-176085] N85-32466
Gravity waves from the stratosphere to the mesosphere, part 1.3B N85-32471
General circulation of the middle atmosphere, part 1.4B N85-32474
Performance of the Colorado wind-profiling network, part 1.5A N85-32475
Vertical transport in the atmosphere: Measurement capabilities and requirements of VHF radars, part 1.6A N85-32476
Comparison of tropopause altitude determination by the Plattsville Radar, Sunset Radar and the NWS Rawinsonde N85-32477
Synoptic-scale dynamics with vertical velocity, part 1.8A N85-32478
Practical use of a tropopause height determination algorithm on an MST radar data set, part 1.8B N85-32479
Usefulness of multifrequency MST radar measurements, part 2.6B N85-32487
Use of the VAD technique and measurements of momentum flux in the stratosphere at Aercibo, part 4.3A N85-32505

RADAR NETWORKS
Middle Atmosphere Program. Handbook for MAP. Volume 14: URSI/SCOSTEP Workshop on Technical Aspects of MST Radar
[NASA-CR-176085] N85-32466
Meteorological and aeronomical requirements for MST radar networks (keynote paper), part 1 N85-32467
Performance of the Colorado wind-profiling network, part 1.5A N85-32475
Comparison of tropopause altitude determination by the Plattsville Radar, Sunset Radar and the NWS Rawinsonde N85-32477

RADAR RECEPTION
Criteria for site selection and frequency allocation (keynote paper), part 5 N85-32511
Sidelobe reduction of Barker codes, part 7.1C N85-32522

RADAR SCATTERING
An analysis of physical optics models for rough surface scattering
[AD-A154960] N85-32235
A modified Fresnel scattering model for the parameterization of Fresnel returns, part 2.3A N85-32483
Observations of mesospheric turbulence by rocket probe and VHF radar, part 2.4A N85-32484
Interpretation of radar returns from the mesosphere, part 2.3A N85-32485
Radar echoes at 2.66 and 40.92 MHz from the mesosphere, part 2.6A N85-32486

RADAR SIGNATURES
The use of the glistening surface concept in rough surface scattering
[AD-A154922] N85-32234
Automated cell detection as a mesocyclone precursor tool
[AD-A154952] N85-32577

RADAR TARGETS
Radar target identification through electromagnetic scattering studies
[AD-A154596] N85-32220
Head-on scattering of a tubular cylinder of finite length for radar target identification purposes
[AD-A155608] N85-32246
Broadside scattering of a tubular cylinder for evaluation of target identification
[AD-A155739] N85-32248
Morphology of the scattering targets: Fresnel and turbulent mechanisms, part 2.1A N85-32481

RADAR TRANSMISSION
Criteria and algorithms for spectrum parameterization of MST radar signals N85-32527

RADAR TRANSMITTERS
Summary of session on optimum transmitter and antenna configuration for MST radar, part 6 N85-32514
Increase of antenna area instead of transmitter power, part 6.3A N85-32517

RADIAL DISTRIBUTION
Testing and optimizing MST coaxial collinear arrays, part 6.4A N85-32518

RADIAL VELOCITY
Use of the VAD technique and measurements of momentum flux in the stratosphere at Aercibo, part 4.3A N85-32505
Coding schemes for improving MST radar performance, part 7.1A N85-32520

RADIANCE
A transportable, machine oriented library of european sky and terrain radiance distributions with contemporary radiometric and meteorological profiles
[AD-A155254] N85-32590

RADIANT FLUX DENSITY
Existence of smooth solutions in problems of electromagnetic radiation focusing N85-32972

RADIANT HEATING
The Konstantinov effect and absorption of sound in inhomogeneous media N85-32861

RADIATION
Most desirable terrain, e.g., flat vs valley location, part 5.1B N85-32513

RADIATION ABSORPTION
Detection of excited states by laser-induced fluorescence
[AD-A155558] N85-32326
Absorption and scattering properties of aerosols of aggregated particles in the infrared spectral region
[AD-A155475] N85-32591
Luminescence and absorption of indium-activated potassium-borate glasses subjected to high-power excitation N85-32868
Absorption of laser radiation in substance with absorption coefficient depending linearly upon temperature N85-32953
A practical guide to ionization chamber dosimetry at the AFRRI reactor
[AD-A155185] N85-33003

RADIATION DETECTORS
Detector problems at the SSC
[DE85-010217] N85-33007
Research in extreme ultraviolet and far ultraviolet astronomy
[NASA-CR-176068] N85-33060

RADIATION DISTRIBUTION
Research in particles and fields
[NASA-CR-176069] N85-33103

RADIATION DOSAGE
A practical guide to ionization chamber dosimetry at the AFRRI reactor
[AD-A155185] N85-33003
Empirical correlation of residual gamma radiation resulting from operation of the Health Physics Research Reactor
[DE85-012075] N85-33008

RADIATION EFFECTS
Polymer-water interaction studies N85-32411
Nuclear thermal transmittance in the atmosphere using LOWTRAN-6 computer code
[AD-A154669] N85-32553
USSR report: Life sciences. Biomedical and behavioral sciences
[JPRS-UBB-85-020] N85-32752
USAFSAM review and analysis of radiofrequency radiation bioeffects literature
[AD-A155113] N85-32760
Empirical correlation of residual gamma radiation resulting from operation of the Health Physics Research Reactor
[DE85-012075] N85-33008

RADIATION MEASURING INSTRUMENTS
Results from radiation monitoring equipment experiments on STS-41C, 41D, 41G and 51A
[AD-A154676] N85-32142

RADIATION PROTECTION
East Europe report: Science and technology
[JPRS-ESA-85-023] N85-32217

RADIATION SOURCES
Radiative-collision generation of sound in gases subjected to single-pulse optical excitation N85-32920
Correlation of intensities of different scattering channels N85-32952

RADIATION SPECTRA
Correlation of intensities of different scattering channels N85-32952

RADIATION TRANSPORT
Radiation transport
[DE85-010333] N85-33005

RADIATIVE HEAT TRANSFER
Performance analysis of mixed passive solar heating systems
[DE85-009624] N85-32455

RADIATIVE TRANSFER
The suppression of convective wavebreaking by radiative transfer processes, part 1.3C N85-32472

RADIO EQUIPMENT
An analysis of the materiel fielding plan for the SINCGARS (Single Channel Ground and Airborne Radio System) radio
[AD-A155101] N85-32238

RADIO FREQUENCIES
VLF (Very low frequency) workshop held at San Diego California, 24-25 January 1985
[AD-A154652] N85-32224
Microwave SAW (Surface Acoustic Wave) monochromator
[AD-D011718] N85-32311
Radio-frequency radiation of storm clouds N85-32939

RADIO FREQUENCY INTERFERENCE
Most desirable terrain, e.g., flat vs valley location, part 5.1B N85-32513
Design of a freestanding noise measurement and recording system to predict the intensity and location of electromagnetic radiation from earthquakes
[AD-A155070] N85-32563
Radio-frequency radiation of storm clouds N85-32939

RADIO INTERFEROMETERS
Interferometer applications of VHF radars, part 3.6A N85-32497

RADIO METEOROLOGY
Meteorological and aeronomical requirements for MST radar networks (keynote paper), part 1 N85-32467
Tropospheric-stratospheric exchange, part 1.1A N85-32468
Observations of frontal zone structures with a VHF Doppler radar and radiosondes, part 1.2A N85-32469
Gravity waves from the stratosphere to the mesosphere, part 1.3B N85-32471
General circulation of the middle atmosphere, part 1.4B N85-32474
Performance of the Colorado wind-profiling network, part 1.5A N85-32475
Vertical transport in the atmosphere: Measurement capabilities and requirements of VHF radars, part 1.6A N85-32476
Comparison of tropopause altitude determination by the Plattsville Radar, Sunset Radar and the NWS Rawinsonde N85-32477
Synoptic-scale dynamics with vertical velocity, part 1.8A N85-32478

Sample interchange of MST radar data from the Urbana radar N85-32531
MST radar data management N85-32532
Data base for the Colorado profiling network N85-32533
Further developments of EISCAT as an MST radar N85-32534
Status of the Jicamarca radar N85-32535
Recent results at the Sunset radar N85-32536
The Boot Lake MF imaging radar N85-32537
MENTOR: Adding an outlying receiver to an ST radar for meteor-wind measurement N85-32538
Summary of progress at the Poker Flat Observatory in Alaska N85-32539
Urbana radar systems: Possibilities and limitations N85-32540
The Sondrestrom radar: Progress and proposed upgrades for ST work N85-32541
Progress and plans for the Colorado Wind Profiler Network N85-32542
The MU radar now partly in operation N85-32543
Network ST radar and related measurements at Pennsylvania State University N85-32544
A note on the proposed UK VHF radar N85-32545
The Adelaide VHF radar: Capabilities and future plans N85-32546
The Proust radar N85-32547
Millstone Hill radar: Capabilities for S/T observations N85-32548
The Ponape ST radar N85-32549
Measurements of vertical velocity over flat terrain by ST radar and other related uses of the radar data set N85-32550

RADIO SPECTRA
Microwave SAW (Surface Acoustic Wave) monochromator [AD-D011718] N85-32311

RADIO WAVE REFRACTION
Beam diffusion in linear ionospheric layer N85-32958

RADIO WAVES
Meteorological and aeronomical requirements for MST radar networks (keynote paper), part 1 N85-32467
Morphology of the scattering targets: Fresnel and turbulent mechanisms, part 2.1A N85-32481
Relationship of spaced antenna and Doppler techniques for velocity measurements (keynote paper), part 3 N85-32488

RADIOACTIVE AGE DETERMINATION
Paleoenvironmental investigations at seed cave (Windust cave H-45FR46), Franklin County, Washington [AD-A154777] N85-32576
Dating Archean zircon by ion microprobe: New light on an old problem N85-33094

RADIOACTIVE WASTES
East Europe report: Science and technology [JPRS-ESA-85-021] N85-32190

RADIOBIOLOGY
A practical guide to ionization chamber dosimetry at the AFRRI reactor [AD-A155185] N85-33003

RADIOGENIC MATERIALS
The relation between the age of the subconducting slab and the recycling of sediments into the mantle N85-33063

RADIOGRAPHY
Poisson formula for radon transformation and numerical image reconstruction algorithm N85-32973

RADIOLYSIS
Production of stable embryo particles in dense ion tracks of alpha particle emissions in the atmosphere N85-32638

RADIOMETERS
Calibration and use of clutter data for simulation [AD-A154793] N85-32229

RADIOSONDES
Ship-to-ship propagation: Maritime data analyses [AD-A155484] N85-32325
Observations of frontal zone structures with a VHF Doppler radar and radiosondes, part 1.2A N85-32469
A modified Fresnel scattering model for the parameterization of Fresnel returns, part 2.3A N85-32483
Gravity-wave spectra in the atmosphere observed by MST radar, part 4.2B N85-32502

RADON
Production of stable embryo particles in dense ion tracks of alpha particle emissions in the atmosphere N85-32638
Study of the formation of particles from natural hydrocarbons released by vegetation N85-32640
Aircraft investigations of the distribution of aerosols in the lower troposphere N85-32659
Poisson formula for radon transformation and numerical image reconstruction algorithm N85-32973

RADON ISOTOPES
Some considerations about the natural atmospheric radioactive aerosol N85-32662

RAILGUN ACCELERATORS
Plasma mass and effective inductance in a small railgun [AD-A154644] N85-32304

RAIN
Rain volume estimation over areas using satellite and radar data [NASA-CR-176050] N85-32570
The distribution of giant salt nuclei inside and outside cloud over the basin of Xin and Jiang N85-32681

RAIN FORESTS
Formation of particles in the air of the humid tropical forests N85-32639

RAMAN SPECTRA
Temperature measurements on small droplets N85-32699
Influence on bi-phonon states on Raman scattering of light in molecular crystals N85-32865
Generation and amplification of radiation during stimulated Raman scattering in crystals N85-32869
Participation of singlet oxygen in photodestruction of air-saturated solutions of coumarin dyes N85-32891
Raman scattering studies in solids [AD-A155528] N85-33032

RAMAN SPECTROSCOPY
Participation of singlet oxygen in photodestruction of air-saturated solutions of coumarin dyes N85-32891
The possibilities of remote analysis of atmospheric gases based on Raman scattering spectroscopy N85-32892

RANDOM PROCESSES
Statistical methods for efficient design of community surveys of response to noise: Random coefficients regression models [NASA-CR-177933] N85-32979

RANDOM VARIABLES
A random layer model for reflection from ocean bottom sediments [AD-A155019] N85-32988

RANDOM WALK
The role of long term lamp fluctuations in the random walk of frequency behavior of the rubidium frequency standard: A case study [AD-A155338] N85-32314

RANKING
A short bibliography of recent developments in selection and ranking procedures [AD-A155648] N85-32856

RARE GAS-HALIDE LASERS
Investigation of plasma processes in electronic transition lasers [AD-A155598] N85-32327

RARE GASES
Noble gases and the early history of the Earth: Inappropriate paradigms and assumptions inhibit research and communication N85-33075
A review of noble gas geochemistry in relation to early Earth history N85-33081

RATIONS
The effects of prolonged feeding meal, ready-to-eat (MRE) operational rations [AD-A154763] N85-32773

RAWINSONDES
Comparison of tropopause altitude determination by the Plattsville Radar, Sunset Radar and the NWS Rawinsonde N85-32477
A modified Fresnel scattering model for the parameterization of Fresnel returns, part 2.3A N85-32483

RAYLEIGH WAVES
Development of ultrasonic modeling techniques for the study of crustal inhomogeneities [AD-A155206] N85-32565

REACTION KINETICS
Design of micelles as dephosphorylating agents [AD-A155589] N85-32166
Imbedded thermocouples as a solid propellant combustion probe [AD-A155630] N85-32167
Introduction of structural variations into oxide polymers and their effect on sintering and crystallization [AD-A155597] N85-32206
Multilayer capacitor dielectrics produced from metallo-organic precursors [AD-A154592] N85-32254
Experimental studies of the kinetics of deposition nucleation on an ice nucleant used in weather modification N85-32598
The measured rate of condensation nucleation to droplets using the techniques of chemical kinetics N85-32694
Resonant energy transfer during strong excitation N85-32922

REACTION TIME
The effect of set size on time to recall color coded information [AD-A155013] N85-32767

REACTIVITY
Microscopic control of semiconductor surface oxidation [AD-A154799] N85-33026

REACTOR PHYSICS
Radiation transport [DE85-010333] N85-33005

REACTOR SAFETY
Two-phase flow visualization in a transparent, atmospheric pressure, boiling water loop [DE84-016857] N85-32288
Tritium technology review [DE85-010504] N85-33006

REAGENTS
Basic research in novel inorganic reagents and fluorocarbon chemistry [AD-A155340] N85-32165

REAL TIME OPERATION
Interactive on-line conferences [AD-A154723] N85-32227
Hardware schemes for fast Fourier transform, part 7.4A N85-32526
Real-time contour surface display generation [AD-A155232] N85-32780
Software for interactive on-line conferences [AD-A154742] N85-32801

REAL VARIABLES
SIGMA - A stochastic-integration global minimization algorithm [AD-A154878] N85-32806

RECIRCULATIVE FLUID FLOW
A multilevel-multigrid method for recirculating flows N85-32271

RECOMBINATION REACTIONS
Measuring bulk recombination rates and boundary recombination velocities N85-32419
Silicon surface passivation by silicon nitride deposition N85-32423
Inter-zone auger recombination in GaSb laser structures N85-32875

RECONNAISSANCE AIRCRAFT
Electronic reconnaissance aircraft of the Soviet Union Navy [AD-A154706] N85-32091

RECORDING
Development of wide band recording materials [AD-A154961] N85-32309
Design of a freestanding noise measurement and recording system to predict the intensity and location of electromagnetic radiation from earthquakes [AD-A155070] N85-32563

RECRYSTALLIZATION
System for electro-optical ceramic recrystallization N85-32872

RECTANGULAR WAVEGUIDES
Calculation of the propagation constant in a rectangular waveguide containing an inhomogeneous longitudinally magnetized plasma [DE85-012072] N85-32250

RECTIFIERS
T/R switch design for short-range measurements, part 6.1A N85-32515

RECURSIVE FUNCTIONS
Recursive nonlinear filtering through complete linearization [AD-A155029] N85-32844

RED GIANT STARS
Energy and Technology Review [DE85-011767] N85-33061

REDUCTION (CHEMISTRY)
Possible roles of manganese redox chemistry in the sulfur cycle N85-32731
Phototrophic bacteria and their role in the biogeochemical sulfur cycle N85-32735
Sulfur reduction in sediments of marine and evaporite environments N85-32742
Cyanobacterial mats: Microanalysis of community metabolism N85-32743
Microanalysis of dissolved iron and phosphate in pore waters of hypersaline sediment N85-32744

REDUNDANCY
Hexagonal uniformly redundant arrays for coded-aperture imaging [PAPER-OG-9.2-1] N85-33048

REFLECTANCE
Usefulness of multifrequency MST radar measurements, part 2.6B N85-32487
Thunderstorm phenomena and weather radar scanning strategies [DOT/FAA/PM-85/14] N85-32573

A random layer model for reflection from ocean bottom sediments
[AD-A155019] N85-32988

REFLECTION
Improved Nominal Operating Cell Temperature (NOCT) test procedure N85-32449
Mirror reflection of charged particles from + amorphous and polycrystalline surfaces N85-32927
Dielectric mirror with ferromagnetic substrate N85-32966

REFRACTION
The effects of subrefractive layers and elevated ducts on airborne radar and ESM (Electronic Surveillance Measures)
[AD-A155524] N85-32592

REFRACTIVITY
A comparison of electronic heterodyne moire deflectometry and electronic heterodyne holographic interferometry for flow measurements
[NASA-TM-87071] N85-32302
Some recent developments in the interpretation of MST radar returns from clear air (keynote paper), part 2 N85-32480
Morphology of the scattering targets: Fresnel and turbulent mechanisms, part 2.1A N85-32481
A modified Fresnel scattering model for the parameterization of Fresnel returns, part 2.3A N85-32483
Observations of mesospheric turbulence by rocket probe and VHF radar, part 2.4A N85-32484
Interpretation of radar returns from the mesosphere, part 2.3A N85-32485
Usefulness of multifrequency MST radar measurements, part 2.6B N85-32487
Variation of the submicron aerosol structure N85-32661
Beam diffusion in linear ionospheric layer N85-32958
Transmission of light by disperse medium of densely packed optically soft particles N85-32969

REFRACTORY PERIOD
Relaxation lens in inhomogeneous binary mixture N85-32957

REFUELING
NASA space station automation: AI-based technology review. Executive summary
[NASA-CR-176096] N85-32135

REGOLITH
Earth's primordial differentiation, and its after-effects N85-33092

REGRESSION ANALYSIS
Statistical methods for efficient design of community surveys of response to noise: Random coefficients regression models
[NASA-CR-177933] N85-32979
Kalman filter time series analysis of gamma-ray data from NaI(T1) detectors for the ND6620 computer
[AD-A154995] N85-33014

REGRESSION COEFFICIENTS
Statistical methods for efficient design of community surveys of response to noise: Random coefficients regression models
[NASA-CR-177933] N85-32979

REINFORCING FIBERS
Matrix fracture in fiber-reinforced ceramics
[AD-A154704] N85-32197

RELATIVISTIC EFFECTS
A derivation of relativistic effects in satellite tracking
[AD-A154620] N85-32132

RELATIVISTIC PARTICLES
Classical emission of relativistic charged particles during axial channeling N85-32871

RELIABILITY
Globally-asynchronous locally-synchronous systems
[AD-A154624] N85-32222
The optimality of lower confidence limits for the reliability of series systems obtained by the method of key test results or other related techniques
[AD-A154880] N85-32338
Reliability physics N85-32402
Advanced module development overview N85-32445
Thin-film reliability and engineering overview N85-32450
Los Alamos optical materials reliability, maintainability, and exposure testing program
[DE85-011894] N85-32456
Further developments of EISCAT as an MST radar N85-32534
Survival function of hypo-exponential distributions
[AD-A155518] N85-32814
Ice fog as an electro-optical obscurant
[AD-A155059] N85-33015

RELIABILITY ANALYSIS
Weibull distribution based on maximum likelihood with interval inspection data
[NASA-TM-86515] N85-32847

REMOTE CONTROL
Remote medical diagnosis N85-32753

REMOTE HANDLING
NASA space station automation: AI-based technology review. Executive summary
[NASA-CR-176096] N85-32135

REMOTE SENSING
A new global geomorphology? N85-32358
Geomorphological similarity and uniqueness N85-32361
Regional landform thresholds N85-32362
Megageomorphology and neotectonics N85-32366
Andrean examples of mega-geomorphology themes N85-32367
Space imagery and some geomorphological problems of the Guiana Shield, South America N85-32368
Deep sea mega-geomorphology: Progress and problems N85-32369
Use of the synoptic view: Examples from Earth and other planets N85-32371
Geomorphic analyses from space imagery N85-32374
Use of spaceborne imaging radar in regional geomorphic studies N85-32377
Techniques, problems and uses of mega-geomorphological mapping N85-32378
Global geomorphology: Report of Working Group Number 1 N85-32382
Process thresholds: Report of Working Group Number 3 N85-32384
Biogeochemical cycling and remote sensing N85-32733
Remote medical diagnosis N85-32753
Participation of singlet oxygen in photodestruction of air-saturated solutions of coumarin dyes N85-32891
The possibilities of remote analysis of atmospheric gases based on Raman scattering spectroscopy N85-32892

REMOTE SENSORS
Characteristics and sources of E-region ionization in the continuous aurora
[AD-A155018] N85-32562

REPLENISHMENT
Feasibility of applications of Competition Decision Assist Package (CDAP) to spare parts
[AD-A154716] N85-33036

REPORTS
High-efficiency silicon solar cell research N85-32417

RESEARCH
High-efficiency silicon solar cell research N85-32417
Activities report of the Aeronomy Department
[G-774-1984] N85-32589
Air force technical objective document, Aerospace Medical Division, Fiscal Year 1986
[AD-A155195] N85-32762
Air Force Office of Scientific Research (AFOSR). Technical report summaries: First quarter (CY)
[AD-A154757] N85-33041
Investigation of DBMS (Data Base Management Systems) for use in a research environment
[AD-A154862] N85-33042
The flow of scientific and technical information in the US Army Research Laboratories
[AD-A155050] N85-33043

RESEARCH AND DEVELOPMENT
A comprehensive study of the AFIT (Air Force Institute of Technology) software development environment
[AD-A155450] N85-32812

RESEARCH FACILITIES
The flow of scientific and technical information in the US Army Research Laboratories
[AD-A155050] N85-33043

RESEARCH MANAGEMENT
The Human Resource Management Information Network (HRMIN): A cost comparison in accordance with Office of Management and Budget (OMB) Circular no. A-76, 5 April 1979
[AD-A154583] N85-33039
Investigation of DBMS (Data Base Management Systems) for use in a research environment
[AD-A154862] N85-33042

RESERVOIRS
Empirical methods for predicting eutrophication in impoundments. Report 3. Phase 2. Model refinements
[AD-A155483] N85-32462
Carbon and sulfur cycling through geologic time N85-32720

RESIDUAL STRESS
Measurement and analysis of critical crack tip processes during fatigue crack growth
[NASA-CR-172597] N85-32342
Stress concentration in the elastoplastic state and residual stress after unloading
[AD-A155628] N85-32356

RESOLUTION
Optical image of bounded objects N85-32968

RESONANCE SCATTERING
Influence on bi-phonon states on Raman scattering of light in molecular crystals N85-32865

RESOURCE ALLOCATION
Routing algorithms and stochastic analysis for large communications networks
[AD-A154654] N85-32225
Resource allocation in cerebral specialization of function: Behavioral and electrophysiological studies
[AD-A155092] N85-32759

RESOURCES MANAGEMENT
Resource management for the tagged token dataflow architecture
[AD-A154773] N85-32779

RESPONSES
Interaction of opiate and phencyclidine derivatives with the acetylcholine receptor
[AD-A155119] N85-32761
The effect of set size on time to recall color coded information
[AD-A155013] N85-32767
Models for multidimensional tests and hierarchically structured training materials
[AD-A155231] N85-32768
Powerful XeCl excimer electric discharge laser with good temporal stability and fast response time N85-32911

RETINAL ADAPTATION
Predictive model of electron beam induced flashblindness
[AD-A155260] N85-32763

REVERBERATION
Toward the theory of acoustic scattering on uneven free surface N85-32862

REVERSE OSMOSIS
Feasibility study for small group water desalination equipment
[AD-A155106] N85-32164

REVISIONS
Modification of the grain size of sputtered copper with additions of oxygen, krypton, silver, or yttrium
[DE85-010975] N85-32189
Progress and plans for the Colorado Wind Profiler Network N85-32542

REYNOLDS NUMBER
A numerical study of Taylor-Vortex flow
[AD-A154787] N85-32277
Numerical solutions of turbulent models for flow over a flat plate with angle of attack
[DE85-010380] N85-32286

RIBONUCLEIC ACIDS
Insights into the phylogenetic positions of photosynthetic bacteria obtained from 5S rRNA and 16S rRNA sequence data N85-32719

RIBOSE
Insights into the phylogenetic positions of photosynthetic bacteria obtained from 5S rRNA and 16S rRNA sequence data N85-32719

RING LASERS
Influence of mirror anisotropy and Brewster window orientation on radiation characteristics of ring lasers N85-32889
Possibility of measurement of small displacements by ring laser N85-32904

RINGS (MATHEMATICS)
On the turning lozange of constant side whose vertices alternate between two fixed circles of a ring
[AD-A154803] N85-32840

ROBOTICS
NASA space station automation: AI-based technology review
[NASA-CR-176094] N85-32134
NASA space station automation: AI-based technology review. Executive summary
[NASA-CR-176096] N85-32135
East Europe report: Science and technology
[JPRS-ESA-85-021] N85-32190
East Europe report: Science and technology
[JPRS-ESA-85-023] N85-32217
Importance of automation, robotization in economy N85-32219
Ultrasonic position reference systems for an autonomous sentry robot and a robot manipulator arm
[AD-A155481] N85-32336

ROBOTS
Ultrasonic position reference systems for an autonomous sentry robot and a robot manipulator arm
[AD-A155481] N85-32336
East Europe report: Science and technology. Selections on CSSR computer technology
[JPRS-ESA-84-017] N85-32781
Robots, Manipulators N85-32786

ROCK MECHANICS
Precambrian evolution and the rock record N85-32711

ROCKET ENGINES
Modeling the exhaust of the pulsed plasma thruster [AD-A155344] N85-33018
ROCKET NOZZLES
Recession of graphitic nozzles in rocket motors N85-32144
ROCKS
Hydrothermal alteration in the 3.5 b.y. old Onverwacht Group of South Africa N85-33071
The 3.5 b.y. old Onverwacht Group: A remnant of ancient oceanic crust N85-33073
The Aravalli sequence of Rajasthan, India: A Precambrian continental margin? N85-33084
ROLL
In-flight evaluation of pure time delays in pitch and roll [NASA-TM-86744] N85-32123
ROSS ICE SHELF
Aerosol formation by wave action over Ross Sea, Antartica N85-32688
ROTARY STABILITY
Recent developments in rotary-balance testing of fighter aircraft configurations at NASA Ames Research Center [NASA-TM-86714] N85-32090
ROTARY WINGS
Tip vortex computer code SRATIP. User's guide [NASA-CR-172603] N85-32093
ROTATING GENERATORS
A small-scale self-excited rotor electrostatic generator [AD-A155264] N85-32265
ROTATION
Aerodynamic characteristics of the standard dynamics model in coning motion at Mach 0.6 [NASA-TM-86717] N85-32094
ROTOR SPEED
A comparison of experimental and theoretical results for rotordynamic coefficients of four annular gas seals [NASA-CR-176086] N85-32332
ROTORS
A panel method study of vortex sheets with special emphasis on sheets of axisymmetric geometry [NASA-CR-177365] N85-32095
A phase-locked frequency multiplier for the signal averaging of the vibration of the Wessex helicopter input spiral bevel pinion [AD-A154914] N85-32113
Proposal for modifications to the Wessex helicopter main rotor gearbox vibration monitoring program [AD-A155196] N85-32117
ROUTES
Routing algorithms and stochastic analysis for large communications networks [AD-A154654] N85-32225
RUBIDIUM
The role of long term lamp fluctuations in the random walk of frequency behavior of the rubidium frequency standard: A case study [AD-A155338] N85-32314
RUBY
The Faraday effect in ruby and corundum in strong magnetic fields N85-32967
RUBY LASERS
Visibility and vertical structure measurements in southern Germany [AD-A154714] N85-32574
Operation of solid state lasers exposed to electron beam N85-32895
RUPTURING
A continuous damage model based on stepwise-stress creep rupture tests [NASA-CR-174941] N85-32341
RURAL AREAS
Trace element concentrations in atmospheric aerosol over Hungary N85-32652
RYDBERG SERIES
Photoelectron studies of autoionizing Rydberg states in HCl [DE85-011813] N85-33001

S

S WAVES
Radar echoes at 2.66 and 40.92 MHz from the mesosphere, part 2.6A N85-32486
SAFETY
Basic cryogenics and materials. Phase 1 [NASA-CR-177932] N85-32215
SAFETY FACTORS
Space Station crew safety alternatives study. Volume 2: Threat development [NASA-CR-3855] N85-32133
SAHARA DESERT (AFRICA)
Sahara Desert dust transport to the south N85-32666
SAILS
Clarke Stations and mercurian mass-drivers: Energy for large-scale transportation systems [DE85-009607] N85-32145
SALINITY
Microbiology of solar salt ponds N85-32724
The role of sulfur in osmoregulation and salinity tolerance in cyanobacteria, algae, and plants N85-32736
Sulfur reduction in sediments of marine and evaporite environments N85-32742
Microanalysis of dissolved iron and phosphate in pore waters of hypersaline sediment N85-32744
SALT BEDS
Microbiology of solar salt ponds N85-32724
SALTS
Measurements of giant salt nuclei from inland in east China N85-32668
The distribution of giant salt nuclei inside and outside cloud over the basin of Xin and Jiang N85-32681
SAMPLES
Optimization of sampling in statistical physics experiments N85-32975
SAMPLING
Optimization of sampling in statistical physics experiments N85-32975
SANDS
Propagation of sound in a layered laboratory model [AD-A155141] N85-32989
SATELLITE ATTITUDE CONTROL
Research on an expert system for database operation of simulation-emulation math models. Volume 1, Phase 1: Results [NASA-CR-176087] N85-32792
Research on an expert system for database operation of simulation-emulation math models. Volume 2, Phase 1: Results [NASA-CR-176088] N85-32793
SATELLITE IMAGERY
Regional landform thresholds N85-32362
Geomorphology, tectonics, and exploration N85-32365
Quantitative analysis of geomorphic processes using satellite image data at different scales N85-32380
SATELLITE NETWORKS
Remote medical diagnosis N85-32753
SATELLITE OBSERVATION
Doppler satellite data characteristics [AD-A154868] N85-32231
Use of the synoptic view: Examples from Earth and other planets N85-32371
Rain volume estimation over areas using satellite and radar data [NASA-CR-176050] N85-32570
Parameter estimation in communication system tracking satellite observations [AD-A155137] N85-32582
SATELLITE ORIENTATION
Doppler satellite data characteristics [AD-A154868] N85-32231
SATELLITE TRACKING
A derivation of relativistic effects in satellite tracking [AD-A154620] N85-32132
SATURATION
Saturation effect in multilevel lasing media N85-32901
SATURATION (CHEMISTRY)
Mechanism of heterogeneous deposition ice nucleation near water-saturation N85-32597
SAWTOOTH WAVEFORMS
A simulation of weather in 3D space [AD-A155221] N85-32586
SCALE (CORROSION)
A study of adherent oxide scales [AD-A155554] N85-32188
SCALE (RATIO)
The problem of scale in planetary geomorphology N85-32375
Quantitative analysis of geomorphic processes using satellite image data at different scales N85-32380
SCALE MODELS
Reverification of the Chesapeake Bay model [AD-A155486] N85-32706
SCALING LAWS
TNT equivalency of EAK explosive [AD-A155737] N85-32211
SCANNING
An error-dependent model of instrument-scanning behavior in commercial airline pilots [NASA-CR-3908] N85-32765
SCATTERING
Guided-mode launching in a slab waveguide by way of diffraction at the edge of a conducting screen residing on one surface of the slab [AD-A154886] N85-32232
SCATTERING AMPLITUDE
Measurement and analysis of critical crack tip processes during fatigue crack growth [NASA-CR-172597] N85-32342
SCATTERING COEFFICIENTS
Variability of rural aerosols under stable weather conditions N85-32663
SCATTERING CROSS SECTIONS
Study of proton and neutron activation of metal samples in low Earth orbit [NASA-CR-171596] N85-32130
The use of the glistening surface concept in rough surface scattering [AD-A154922] N85-32234
An analysis of physical optics models for rough surface scattering [AD-A154960] N85-32235
Head-on scattering of a tubular cylinder of finite length for radar target identification purposes [AD-A155608] N85-32246
Radar echoes at 2.66 and 40.92 MHz from the mesosphere, part 2.6A N85-32486
SCHEDULING
Simulation studies of time-control procedures for the advanced air traffic control system [NASA-TP-2493] N85-32101
Aviation system delays [S-HRG-98-1241] N85-32102
SCHWARZSCHILD METRIC
A derivation of relativistic effects in satellite tracking [AD-A154620] N85-32132
SCINTILLATION
Equitorial scintillations: Advances since ISEA-6 [AD-A154962] N85-32559
SEA ICE
Numerical modeling of sea ice dynamics and ice thickness characteristics [AD-A154600] N85-32700
SEA WATER
A microprocessor-controlled, multichannel fluorimeter for analysis of sea water [AD-A154986] N85-32310
Granulometric study of the acidity and sulfate excess in marine aerosols N85-32691
SEALS (STOPPERS)
A comparison of experimental and theoretical results for rotordynamic coefficients of four annular gas seals [NASA-CR-176086] N85-32332
Tape casting as an approach to an all-ceramic turbine shroud seal [NASA-TM-87078] N85-32333
SEAS
Aerosol formation by wave action over Ross Sea, Antartica N85-32688
SEATS
Seat experiments for the full-scale transport aircraft controlled impact demonstration [AD-A155024] N85-32106
SECONDARY FLOW
Experiments on the influence of active walls on the initial amplitudes and growths of instability waves [AD-A154630] N85-32275
SECURITY
Literature survey of underground construction methods for application to hardened facilities [AD-A155212] N85-32351
SEDIMENT TRANSPORT
New estimating procedures for surface runoff, sediment yield, and contaminant transport in Los Alamos County, New Mexico [DE85-011890] N85-32393
SEDIMENTARY ROCKS
Carbon isotope geochemistry and geobiology N85-32716
Archean sedimentary systems and crustal evolution N85-33082
SEDIMENTS
Sulfur diagenesis in marine sediments N85-32721
Sulfur cycling in freshwater sediments N85-32726
Sulfur and carbon cycling in organic-rich marine sediments N85-32729
Sulfur reduction in sediments of marine and evaporite environments N85-32742
Microanalysis of dissolved iron and phosphate in pore waters of hypersaline sediment N85-32744
A random layer model for reflection from ocean bottom sediments [AD-A155019] N85-32988
Archean sedimentary systems and crustal evolution N85-33082
SEISMIC ENERGY
Development of ultrasonic modeling techniques for the study of crustal inhomogeneities [AD-A155206] N85-32565

SEISMIC WAVES
Robust detection and classification of regional seismic signals using a two mode/two stage cascaded adaptive arma (CAARMA) model
[AD-A154710] N85-32554
The Norwegian seismic array (NORSAR)
[AD-A154751] N85-32555
Experimental and analytic characterization of nonlinear seismic attenuation
[AD-A154760] N85-32556
Design of a freestanding noise measurement and recording system to predict the intensity and location of electromagnetic radiation from earthquakes
[AD-A155070] N85-32563
Qualitative analysis of sign-bit processing
[AD-A154776] N85-32804

SEISMOLOGY
The Norwegian seismic array (NORSAR)
[AD-A154751] N85-32555

SELECTION
A short bibliography of recent developments in selection and ranking procedures
[AD-A155648] N85-32856

SEMANTICS
The formal specification of an abstract machine: Design and implementation
[AD-A155167] N85-32808

SEMICONDUCTING FILMS
Microwave-enhanced thin-film deposition N85-32431

SEMICONDUCTOR DEVICES
Microwave semiconductor research: Materials, devices and circuits and gallium arsenide ballistic electron transistors
[AD-A154698] N85-33024
A second order difference scheme for transient semiconductor device simulation
[AD-A154824] N85-33027
A review of the physics and response models for burnout of semiconductor devices
[AD-A155031] N85-33028

SEMICONDUCTOR JUNCTIONS
A second order difference scheme for transient semiconductor device simulation
[AD-A154824] N85-33027

SEMICONDUCTORS (MATERIALS)
Interface chemistry of Hg(1-x)Cd(x)Te
[AD-A154876] N85-32161
Z-contrast imaging and electron channeling analysis of dopants in semiconductors
[DE85-011410] N85-32269
On the dependence of the convergence of Gummel's algorithm on the regularity of the solution
[AD-A154628] N85-32832
Influence on bi-phonon states on Raman scattering of light in molecular crystals N85-32865
Influence of coherent light beams on free carriers in semiconductors N85-32867
Quasi-steady-state melting mode during combined laser irradiation of semiconductor materials N85-32874
Photo-acoustic effect in finite-dimensional semiconductors N85-32876
Effect of powerful pulsed low-energy ion streams on GaAs N85-32877
A second order difference scheme for transient semiconductor device simulation
[AD-A154824] N85-33027
Raman scattering studies in solids
[AD-A155528] N85-33032
Electronic phenomena near semiconductor grain boundaries
[DE85-011543] N85-33035

SENSITIVITY
Test evaluation of the Honeywell GG1111 Single-Degree-of-Freedom (SDF) strapdown gyroscope
[AD-A154768] N85-32307
Visibility and vertical structure measurements in southern Germany
[AD-A154714] N85-32574
Rhodium-103 and Indium-115 inelastic scattering reactions for fission neutron dosimetry N85-33004

SEPARATORS
Vapor-liquid phase separator studies
[NASA-CR-166545] N85-32272

SEQUENCING
Construction of complementary code sequence sets, part 7.1D N85-32523

SEQUENTIAL COMPUTERS
Construction of complementary code sequence sets, part 7.1D N85-32523

SERIES (MATHEMATICS)
The optimality of lower confidence limits for the reliability of series systems obtained by the method of key test results or other related techniques
[AD-A154880] N85-32338

SERVICE LIFE
High temperature electronics technology: Life test report
[AD-A154681] N85-32257
Los Alamos optical materials reliability, maintainability, and exposure testing program
[DE85-011894] N85-32456

SET THEORY
Construction of complementary code sequence sets, part 7.1D N85-32523

SHAKERS
Measurement of damping of graphite epoxy materials
[NASA-CR-176073] N85-32334

SHALLOW WATER
Propagation of sound in a layered laboratory model
[AD-A155141] N85-32989

SHAPE MEMORY ALLOYS
The effect of prior parent phase cold work on martensite transformation in Cu-Zn-Al shape memory alloys
[AD-A155140] N85-32183
Comparison of the response of shape memory alloy actuators using air-cooling and water-cooling
[AD-A155216] N85-32185

SHEAR FLOW
Techniques for the study of gravity waves and turbulence (keynote paper), part 4 N85-32499

SHEAR STRENGTH
Graphite/PMR polyimide composites with improved toughness
[NASA-TM-87081] N85-32148

SHEAR STRESS
A cracked orthotropic sheet stiffened by a semi-infinite orthotropic sheet
[NASA-TP-2455] N85-32339

SHEARING
The shearing contribution in transformation toughening of brittle materials
[AD-A154656] N85-32195

SHELLS (STRUCTURAL FORMS)
An investigation into the comparisons of the underwater shock effects on a stiffened flat plate to the predictive nature of a computer model
[AD-A155612] N85-32355

SHELTERS
Field testing of a lightweight relocatable structure in a temperate environment
[AD-A155171] N85-32350

SHIELDING
Rhodium-103 and Indium-115 inelastic scattering reactions for fission neutron dosimetry N85-33004

SHIPS
LORAN-C harbor and harbor entrance survey: Charleston, South Carolina
[AD-A154875] N85-32108

SHOCK FRONTS
The 2-D simulations of the NRL (Naval Research Laboratory) laser experiment
[AD-A154915] N85-32321

SHOCK TUBES
Shock tube measurements of growth constants in the branched-chain ethane-carbon monoxide-oxygen system
[NASA-TM-87068] N85-32156
A variable node finite element method applied to the gas dynamics equations
[AD-A155211] N85-32281
Velocity and transient measurements in a shock tube using a hot-wire anemometer
[AD-A154694] N85-32305

SHOCK WAVE PROPAGATION
Weak shock waves propagating in fluid-gas mixtures
[AD-A154759] N85-32276

SHORT CIRCUITS
Thin-film reliability and engineering overview N85-32450

SHORT WAVE RADIATION
Global geoid and gravity anomaly predictions using the collocation and point mass techniques
[AD-A154517] N85-32387

SIDELOBE REDUCTION
Criteria for site selection and frequency allocation (keynote paper), part 5 N85-32511
Sidelobe reduction of Barker codes, part 7.1C N85-32522

SIDELOBES
Accuracy of velocity and power determination by the Doppler method N85-32493

SIDESLIP
Aerodynamic characteristics of the standard dynamics model in coning motion at Mach 0.6
[NASA-TM-86717] N85-32094

SIGNAL DETECTION
Robust detection and classification of regional seismic signals using a two mode/two stage cascaded adaptive arma (CAARMA) model
[AD-A154710] N85-32554

SIGNAL DETECTORS
Calibration and use of clutter data for simulation
[AD-A154793] N85-32229

SIGNAL DISTORTION
Compression of spread spectrum signals on an excessively dispersive channel
[AD-A155184] N85-32240

SIGNAL ENCODING
Coding schemes for improving MST radar performance, part 7.1A N85-32520

SIGNAL MEASUREMENT
A sampling phasemeter design for pulsed continuous wave signals
[AD-A155237] N85-32264
Visibility and vertical structure measurements in southern Germany
[AD-A154714] N85-32574

SIGNAL PROCESSING
A phase-locked frequency multiplier for the signal averaging of the vibration of the Wessex helicopter input spiral bevel pinion
[AD-A154914] N85-32113
Calibration and use of clutter data for simulation
[AD-A154793] N85-32229
Compression of spread spectrum signals on an excessively dispersive channel
[AD-A155184] N85-32240
A high-speed digital signal processor for atmospheric radar, part 7.3A N85-32525
Qualitative analysis of sign-bit processing
[AD-A154776] N85-32804
Bayesian vs MAP multiple model adaptive estimation for field of view expansion in tracking airborne targets
[AD-A155486] N85-32855
Solid state research
[AD-A154783] N85-33025

SIGNAL REFLECTION
A random layer model for reflection from ocean bottom sediments
[AD-A155019] N85-32988

SIGNAL TO NOISE RATIOS
Sidelobe reduction of Barker codes, part 7.1C N85-32522
Qualitative analysis of sign-bit processing
[AD-A154776] N85-32804

SIGNAL TRANSMISSION
Testing and optimizing MST coaxial collinear arrays, part 6.4A N85-32518
Criteria and algorithms for spectrum parameterization of MST radar signals N85-32527

SIGNATURES
Real-time automated detection of mesocyclones and tornado vortex signatures
[AD-A154968] N85-32578

SIGNS AND SYMPTOMS
The effects of prolonged feeding meal, ready-to-eat (MRE) operational rations
[AD-A154763] N85-32773

SILANES
A fluidized-bed reactor for silane pyrolysis N85-32413
Modeling of the silane FBR system N85-32415
Silicon production in an aerosol reactor N85-32416

SILICATES
Chemical constraints on the evolution of Archean continental crust N85-33093
Dating Archean zircon by ion microprobe: New light on an old problem N85-33094

SILICON
High temperature electronics technology: Life test report
[AD-A154681] N85-32257
Electrical properties of bulk grown nitrogen doped silicon
[AD-A155471] N85-32266
Thermoelectric properties of beta-boron and some boron compounds
[DE85-011978] N85-32270
High-frequency furnace
[DE85-011210] N85-32291
Predicting photothermal field performance N85-32404
Interfacial bonding stability N85-32409
Silicon refinement by chemical vapor transport N85-32412
JPL in-house fluidized-bed reactor research N85-32414
Silicon production in an aerosol reactor N85-32416
Physics of heavily doped silicon and solar-cell parameter measurement N85-32418
Measuring bulk recombination rates and boundary recombination velocities N85-32419
Studies of oxygen- and carbon-related defects in high-efficiency silicon solar cells N85-32420
Comprehensive silicon solar-cell computer modeling N85-32421

Sensitivity analysis of high-efficiency silicon solar-cell design parameters N85-32422
Silicon surface passivation by silicon nitride deposition N85-32423
Important loss mechanisms in high-efficiency solar cells N85-32424
Development of high-efficiency solar cells on silicon web N85-32425
Simultaneous junction formation N85-32426
Amorphous metallic films in silicon metallization systems N85-32427
Silicon dendritic web growth N85-32435
Temperature-stress modeling N85-32436
Silicon ribbon stress-strain activities N85-32437
Analysis of stress-strain relationships in silicon ribbon N85-32438
Stress and buckling analysis N85-32439
Stress and efficiency studies in EFG N85-32440
Silicon sheet surface studies N85-32441
Analysis of inclined growth of silicon sheet N85-32442
Edge-defined film-fed growth of thin silicon sheets N85-32443
High-purity silicon crystal growth N85-32444
Thin-film reliability and engineering overview N85-32450
Defect formation in amorphous hydrated silicon subjected to laser radiation N85-32873
Influence of background electrically neutral argon admixture on mechanical strength of silicon crystals N85-32878
Microscopic control of semiconductor surface oxidation [AD-A154799] N85-33026
A theory of exciton photoluminescence for two types of neutral acceptors in silicon. A study of the systems Si:(B, IN), Si:(Al), (Si), Si:(Ga, In), Si:(B, Al), Si:(B, Ga), and Si:(Al, GA) [AD-A155452] N85-33031

SILICON CARBIDES
Reliability of void detection in structural ceramics using scanning laser acoustic microscopy [NASA-TM-87035] N85-32337

SILICON COMPOUNDS
A fluidized-bed reactor for silane pyrolysis N85-32413
Advanced module development overview N85-32445

SILICON FILMS
The development and evaluation of point defect models for the growth of passive films on single crystal, polycrystalline, and amorphous metal surfaces [AD-A154685] N85-33023

SILICON JUNCTIONS
The future of crystalline silicon technology in the US Department of Energy program N85-32399
Advanced module development overview N85-32445

SILICON NITRIDES
Reliability of void detection in structural ceramics using scanning laser acoustic microscopy [NASA-TM-87035] N85-32337
Silicon surface passivation by silicon nitride deposition N85-32423

SILICON POLYMERS
EVA-glass interface bond stability N85-32408
Interfacial bonding stability N85-32409
Topics in electrochemical degradation of photovoltaic modules N85-32410
Polymer-water interaction studies N85-32411

SILVER
Modification of the grain size of sputtered copper with additions of oxygen, krypton, silver, or yttrium [DE85-010975] N85-32189
MOD silver metallization for photovoltaics N85-32428
Ice nucleation of single water droplet by silver iodide: A laboratory observation N85-32630
Monte Carlo studies of H2O layers adsorbed on a model basal face of AgI N85-32633

SILVER IODIDES
Inactivation of silver iodide by atmospheric nucleation inhibitors N85-32599
Ice nucleation by silver iodine particles with nearly critical sizes N85-32600
Photoinduced active sites on ice nucleating aerosol of silver iodide N85-32601

SIMPLEX METHOD
A practical approach to Karmarkar's algorithm [AD-A155714] N85-32818

SIMULATION
Two-phase flow visualization in a transparent, atmospheric pressure, boiling water loop [DE84-016857] N85-32288
The 2-D simulations of the NRL (Naval Research Laboratory) laser experiment [AD-A154915] N85-32321
A simulation of weather in 3D space [AD-A155221] N85-32586
Numerical modeling of sea ice dynamics and ice thickness characteristics [AD-A154600] N85-32700
On the dependence of the convergence of Gummel's algorithm on the regularity of the solution [AD-A154628] N85-32832
The priming effect in task design research [AD-A154589] N85-32852
A simulation study of Sylvester's problem in three dimensions [AD-A155266] N85-32854

SIMULATORS
Construction of University of Missouri, Rolla's full scale cloud simulation chamber and applied research [AD-A154682] N85-32128
Design of a jamming simulator for a binary communication system [AD-A154617] N85-32221
Flexible satellite communications systems simulator, phase 3 [AD-A155647] N85-32247
Reference-cell calibration activities N85-32453

SINE WAVES
Microwave SAW (Surface Acoustic Wave) monochromator [AD-D011718] N85-32311

SINGLE CRYSTALS
The measurement of strain fields by X-ray topographic contour mapping [AD-A154870] N85-32348
A fluidized-bed reactor for silane pyrolysis N85-32413
Basic ice nucleation mechanisms on mono and microcrystals and ice forming nuclei. Theoretical analysis and experimental results achieved in the laboratory over the past ten years: Review paper N85-32629
Spectral-luminescence characteristics and induced emission of Nd-3(+) ion in Gd(2-x)Nd(x)(WO4)3 crystals N85-32912
The development and evaluation of point defect models for the growth of passive films on single crystal, polycrystalline, and amorphous metal surfaces [AD-A154685] N85-33023

SINTERING
Introduction of structural variations into oxide polymers and their effect on sintering and crystallization [AD-A155597] N85-32206
Sintering studies project [AD-A154750] N85-32216
Hot isostatically pressed Sm(2)(TM)17 magnets [AD-A155479] N85-32267
Reliability of void detection in structural ceramics using scanning laser acoustic microscopy [NASA-TM-87035] N85-32337
Influence of particle arrangement on sintering [AD-A155337] N85-32352

SITE SELECTION
Criteria for site selection and frequency allocation (keynote paper), part 5 N85-32511
Frequency and site selection criteria for MST radars, part 5.1A N85-32512

SITES
Literature survey of underground construction methods for application to hardened facilities [AD-A155212] N85-32351

SIZE (DIMENSIONS)
The effect of set size on time to recall color coded information [AD-A155013] N85-32767

SIZE DISTRIBUTION
Ice fog as an electro-optical obscurant [AD-A155059] N85-33015

SIZING (SHAPING)
Preliminary sizing and performance of aircraft [NASA-TM-86357] N85-32111

SKIN FRICTION
Numerical solutions of turbulent models for flow over a flat plate with angle of attack [DE85-010380] N85-32286

SKULL
SSMIR (Solid State Memory Instrumentation Recorder): A new approach to acquiring data during an aircraft seat/sled ejection sequence [AD-A154760] N85-32308

SKY
A transportable, machine oriented library of european sky and terrain radiance distributions with contemporary radiometric and meteorological profiles [AD-A155254] N85-32590

SKY RADIATION
Improved Nominal Operating Cell Temperature (NOCT) test procedure N85-32449

SLABS
Guided-mode launching in a slab waveguide by way of diffraction at the edge of a conducting screen residing on one surface of the slab [AD-A154886] N85-32232

SLEEP DEPRIVATION
Human performance in continuous/sustained operations and the demands of extended work/rest schedules. An annotated bibliography [AD-A155619] N85-32771

SLIDING
The effect of stress and hot corrosion on nickel-base superalloys [AD-A154722] N85-32181

SLIDING FRICTION
Kinetic friction coefficient of ice [AD-A155035] N85-32859

SLOTS
A multiplying slot array [AD-A155570] N85-32245

SLURRY PROPELLANTS
Status of boron combustion research [AD-A154762] N85-32160

SNOW
The capture of ice nucleating and non ice-nucleating aerosols by ice phase precipitation N85-32620
Ice-forming efficiency of the soluble and insoluble portions of dust contained in snow N85-32631
Scavenging of submicron aerosol particles by snow crystals: Theory and experiments N85-32667

SNOWSTORMS
Circulation analysis of two snowstorms during the SNOW-TWO program [AD-A155225] N85-32587

SOCIAL FACTORS
Symbolic and interactional perspectives on leadership: An integrative framework [AD-A155247] N85-32769

SODIUM
The diurnal variation of the neutral sodium species in the upper atmosphere: A model study [AD-A154988] N85-32561
Physical and chemical aerosol characteristics in extremely clean air masses at Cape Grim, Tasmania N85-32655

SOFTWARE ENGINEERING
The effect of communication-language designs on software specifications [AD-A155173] N85-32809
A comprehensive study of the AFIT (Air Force Institute of Technology) software development environment [AD-A155450] N85-32812

SOIL EROSION
Mineral aerosols and source identification N85-32654

SOIL MAPPING
Space imagery and some geomorphological problems of the Guiana Shield, South America N85-32368

SOIL SCIENCE
Mineral aerosols and source identification N85-32654

SOILS
Numerical modeling of subsurface communication [DE85-012818] N85-32249
Mineral aerosols and source identification N85-32654
Biogeochemical cycling and remote sensing N85-32733

SOLAR ACTIVITY
Doppler satellite data characteristics [AD-A154868] N85-32231

SOLAR ACTIVITY EFFECTS
Solar radio fluxes as indices of solar activity [AERONOMICA-ACTA-A-282-1984] N85-33095

SOLAR ARRAYS
Forced convection on solar collector arrays [DE85-010381] N85-32287
Proceedings of the 24th Project Integration Meeting [NASA-CR-176058] N85-32394
High-efficiency module and array research N85-32397
Flat-plate module efficiency versus cost tradeoffs N85-32398
Block V module program N85-32401
Reliability physics N85-32402
MOD silver metallization for photovoltaics N85-32428

SOLAR ATMOSPHERE
Solar convection [AD-A155214] N85-33098

SOLAR CELLS
High-efficiency crystalline silicon technology development N85-32395
Summary of the high-efficiency crystalline solar cell research forum N85-32396

High-efficiency module and array research N85-32397
The future of crystalline silicon technology in the US Department of Energy program N85-32399
Predicting photothermal field performance N85-32404
Polymerizable ultraviolet stabilizers N85-32406
Encapsulation materials research N85-32407
Topics in electrochemical degradation of photovoltaic modules N85-32410
Polymer-water interaction studies N85-32411
Silicon refinement by chemical vapor transport N85-32412
High-efficiency silicon solar cell research N85-32417
Physics of heavily doped silicon and solar-cell parameter measurement N85-32418
Measuring bulk recombination rates and boundary recombination velocities N85-32419
Studies of oxygen- and carbon-related defects in high-efficiency silicon solar cells N85-32420
Comprehensive silicon solar-cell computer modeling N85-32421
Sensitivity analysis of high-efficiency silicon solar-cell design parameters N85-32422
Silicon surface passivation by silicon nitride deposition N85-32423
Important loss mechanisms in high-efficiency solar cells N85-32424
Development of high-efficiency solar cells on silicon web N85-32425
Simultaneous junction formation N85-32426
Laser-assisted solar-cell metallization processing N85-32429
A non-noble front metallization process N85-32430
Pulsed excimer laser processing for cost-effective solar cells N85-32432
Excimer laser annealing for fabrication of low-cost solar cells N85-32433
High-purity silicon crystal growth N85-32444
Advanced module development overview N85-32445
Status of high-efficiency module design and fabrication N85-32446
Photovoltaic module spread-of-flame testing N85-32448
Improved Nominal Operating Cell Temperature (NOCT) test procedure N85-32449
Thin-film reliability and engineering overview N85-32450
Accelerated stress factors and failure/degradation mechanisms in terrestrial solar cells N85-32451
Failure analysis of thin-film amorphous-silicon solar-cell modules N85-32452
Reference-cell calibration activities N85-32453

SOLAR COLLECTORS
An investigation into the fluidization and heat transfer of low density particles in a fluidized bed with applications [AD-A155259] N85-32282
Forced convection on solar collector arrays [DE85-010381] N85-32287
Advanced module development overview N85-32445
Status of high-efficiency module design and fabrication N85-32446
Module Hipot and ground continuity test results N85-32447
Photovoltaic module spread-of-flame testing N85-32448
Improved Nominal Operating Cell Temperature (NOCT) test procedure N85-32449
Thin-film reliability and engineering overview N85-32450

SOLAR CORONA
Contributions to the 19th International Cosmic Ray Conference [NASA-CR-176060] N85-33044
Solar coronal and photospheric abundances from solar energetic particle measurements [PAPER-SH-2.1-5] N85-33053
Latitude variation of recurrent fluxes in the outer solar system [PAPER-SH-4.1-13] N85-33054
A study of the cyclical variations of coronal holes and their relation to open magnetic fields [AD-A155251] N85-33099

SOLAR COSMIC RAYS
Solar coronal and photospheric abundances from solar energetic particle measurements [PAPER-SH-2.1-5] N85-33053
Differential measurement of cosmic-ray gradient with respect to interplanetary current sheet [PAPER-SH-4.2-9] N85-33055
Changes in the energy spectrum of anomalous oxygen and helium during 1977 - 1985 [PAPER-SH-4.6-1] N85-33056
Solar cycle variations of the anomalous cosmic ray component [PAPER-SH-4.6-2] N85-33057
Radial and latitudinal gradients of anomalous oxygen during 1977 - 1985 [PAPER-SH-4.6-4] N85-33058
Solar modulation and interplanetary gradients of the galactic electron flux, 1977 - 1984 [PAPER-SH-4.7-4] N85-33059

SOLAR CYCLES
Contributions to the 19th International Cosmic Ray Conference [NASA-CR-176060] N85-33044
Solar cycle variations of the anomalous cosmic ray component [PAPER-SH-4.6-2] N85-33057
Radial and latitudinal gradients of anomalous oxygen during 1977 - 1985 [PAPER-SH-4.6-4] N85-33058
Solar modulation and interplanetary gradients of the galactic electron flux, 1977 - 1984 [PAPER-SH-4.7-4] N85-33059
Solar cycle variation of ephemeral regions [AD-A154967] N85-33097
A study of the cyclical variations of coronal holes and their relation to open magnetic fields [AD-A155251] N85-33099

SOLAR ENERGY
Proceedings of the 24th Project Integration Meeting [NASA-CR-176058] N85-32394
Reliability physics N85-32402

SOLAR ENERGY CONVERSION
Proceedings of the 24th Project Integration Meeting [NASA-CR-176058] N85-32394
Summary of the high-efficiency crystalline solar cell research forum N85-32396
Silicon refinement by chemical vapor transport N85-32412
Performance analysis of mixed passive solar heating systems [DE85-009624] N85-32455
Prospects for a new kind of synthesis: Assembly of molecular components to achieve functions [AD-A155023] N85-32997

SOLAR FLARES
Contributions to the 19th International Cosmic Ray Conference [NASA-CR-176060] N85-33044
Precision measurements of solar energetic particle elemental composition [PAPER-SH-2.1-4] N85-33052
Solar coronal and photospheric abundances from solar energetic particle measurements [PAPER-SH-2.1-5] N85-33053
Soft X-ray polychromator for the Solar Maximum Mission [NASA-CR-175297] N85-33096
Heating of the deep chromosphere during solar flares [AD-A155256] N85-33100
Search for the north-south asymmetry in solar activity [AD-A155525] N85-33102

SOLAR FLUX
Solar modulation and interplanetary gradients of the galactic electron flux, 1977 - 1984 [PAPER-SH-4.7-4] N85-33059

SOLAR FURNACES
High temperature solar electrothermal processing 2. Zinc from zinc oxide [AD-A154747] N85-32159
Decomposition of sulfuric acid using solar thermal energy [DE85-012288] N85-32170

SOLAR GENERATORS
Advanced module development overview N85-32445
Module Hipot and ground continuity test results N85-32447
Thin-film reliability and engineering overview N85-32450

SOLAR HEATING
Performance analysis of mixed passive solar heating systems [DE85-009624] N85-32455

SOLAR MAGNETIC FIELD
Differential measurement of cosmic-ray gradient with respect to interplanetary current sheet [PAPER-SH-4.2-9] N85-33055
A study of the cyclical variations of coronal holes and their relation to open magnetic fields [AD-A155251] N85-33099

SOLAR MAXIMUM MISSION
Soft X-ray polychromator for the Solar Maximum Mission [NASA-CR-175297] N85-33096

SOLAR OBSERVATORIES
Solar cycle variation of ephemeral regions [AD-A154967] N85-33097
Solar adaptive optics [AD-A155434] N85-33101

SOLAR PHYSICS
Activities report of the Aeronomy Department [G-774-1984] N85-32569

SOLAR PROTONS
Latitude variation of recurrent fluxes in the outer solar system [PAPER-SH-4.1-13] N85-33054

SOLAR RADIATION
Clarke Stations and mercurian mass-drivers: Energy for large-scale transportation systems [DE85-009607] N85-32145

SOLAR RADIO EMISSION
Solar radio fluxes as indices of solar activity [AERONOMICA-ACTA-A-282-1984] N85-33095

SOLAR REFLECTORS
MOD silver metallization for photovoltaics N85-32428

SOLAR SYSTEM
Space research in the United Kingdom: An assessment [AD-A155334] N85-33038

SOLAR TERRESTRIAL INTERACTIONS
Effect of ions on cloud formation and its role in solar terrestrial relationship N85-32697

SOLAR WIND
Soft X-ray polychromator for the Solar Maximum Mission [NASA-CR-175297] N85-33096

SOLAR X-RAYS
A study of the cyclical variations of coronal holes and their relation to open magnetic fields [AD-A155251] N85-33099

SOLID LUBRICANTS
Friction and wear of solid-lubricated contact in gas turbine engine bearings [AD-A155042] N85-32335

SOLID MECHANICS
USSR report: Physics and mathematics [JPRS-UPM-85-004] N85-32860

SOLID PROPELLANT COMBUSTION
Imbedded thermocouples as a solid propellant combustion probe [AD-A155630] N85-32167
Closed-bomb combustion of Hivelite-based, Very High Burn Rate (VHBR) propellant [AD-A155740] N85-32212

SOLID PROPELLANT IGNITION
Status of boron combustion research [AD-A154762] N85-32160

SOLID PROPELLANT ROCKET ENGINES
Recession of graphitic nozzles in rocket motors N85-32144

SOLID PROPELLANTS
Closed-bomb combustion of Hivelite-based, Very High Burn Rate (VHBR) propellant [AD-A155740] N85-32212

SOLID STATE
SSMIR (Solid State Memory Instrumentation Recorder): A new approach to acquiring data during an aircraft seat/sled ejection sequence [AD-A154780] N85-32308

SOLID STATE DEVICES
Experiments on the influence of active walls on the initial amplitudes and growths of instability waves [AD-A154630] N85-32275
Solid state research [AD-A154783] N85-33025

SOLIDIFICATION
MPS solidification model. Analysis and calculation of macrosegregation in a casting ingot [NASA-CR-171589] N85-32178

SOLITARY WAVES
Theory of soliton waves [AD-A154784] N85-32837

SOLUBILITY
Bubble dynamics in polymer solutions undergoing shear [AD-A154575] N85-32193
Measurements of the critical supersaturation of 0.029 to 0.035 micron radius particles at Washington, District of Columbia N85-32676

SOLUTES
Interaction of solutes with stretched polymers [AD-A154662] N85-32196

SOLUTIONS
Discovery of a nonpropagating hydrodynamic soliton [AD-A155569] N85-32268
SPLINES. Their equivalence to collocation [AD-A155250] N85-32566

SONAR
The moving thermoacoustic array: A theoretical feasibility study [AD-A154510] N85-32980

SORPTION
Permeation of mixed penetrants through glassy polymer membranes
[AD-A155605] N85-32207
SOUND FIELDS
Development of computer programs using the method of images to predict the sound field in a wedge overlaying a fast fluid and comparison with laboratory experiments
[AD-A154580] N85-32797
The Konstantinov effect and absorption of sound in inhomogeneous media N85-32861
The sound field of a moving laser-induced acoustic array (theory)
[AD-A154553] N85-32981
SOUND GENERATORS
Radiative-collision generation of sound in gases subjected to single-pulse optical excitation N85-32920
SOUND TRANSMISSION
Development of computer programs using the method of images to predict the sound field in a wedge overlaying a fast fluid and comparison with laboratory experiments
[AD-A154580] N85-32797
The Konstantinov effect and absorption of sound in inhomogeneous media N85-32861
Propagation of sound in a layered laboratory model
[AD-A155141] N85-32989
SOUND WAVES
Qualitative analysis of sign-bit processing
[AD-A154776] N85-32804
New approximations and findings of theory of nonlinear acoustic beams N85-32863
Reflection of acoustic beam from inhomogeneous boundary N85-32864
Acoustic wave scattering by round cylindrical shell reinforced with stringers N85-32916
Radiative-collision generation of sound in gases subjected to single-pulse optical excitation N85-32920
Iteration solution for a submerged force-driven finite cylinder
[AD-A154587] N85-32982
Acoustic radiation from concentric shells containing an inner fluid
[AD-A155476] N85-32991
SOUNDING ROCKETS
Radar echoes at 2.66 and 40.92 MHz from the mesosphere, part 2.6A N85-32486
Research in extreme ultraviolet and far ultraviolet astronomy
[NASA-CR-176068] N85-33060
SPACE COMMUNICATION
Interpolation problems in meteor radar analysis, part 7.6A N85-32528
SPACE FLIGHT STRESS
Mission operations requirements document for D-1 Experiment 102, Vestibular Experiments in Spacelab
[NASA-TM-87495] N85-32129
SPACE LABORATORIES
Life sciences flight experiments program mission science requirements document. The first life sciences dedicated Spacelab mission, part 1
[NASA-TM-87494] N85-32137
SPACE MISSIONS
Life sciences flight experiments program mission science requirements document. The first life sciences dedicated Spacelab mission, part 1
[NASA-TM-87494] N85-32137
SPACE PLATFORMS
Comparative study on data system architectures --- spacecraft data processing
[ESA-CR(P)-2015] N85-32828
SPACE SHUTTLES
Pricing options for the space shuttle. Special study N85-32138
The space shuttle glow
[AD-A154937] N85-32139
SPACE STATIONS
Space Station crew safety alternatives study. Volume 2: Threat development
[NASA-CR-3855] N85-32133
NASA space station automation: AI-based technology review
[NASA-CR-176094] N85-32134
Automation study for space station subsystems and mission ground support
[NASA-CR-176097] N85-32136
Space station ECLSS integration analysis: Simplified General Cluster Systems Model, ECLS System Assessment Program enhancements
[NASA-CR-176089] N85-32796
SPACE TRANSPORTATION SYSTEM FLIGHTS
Clarke Stations and mercurian mass-drivers: Energy for large-scale transportation systems
[DE85-009607] N85-32145
SPACEBORNE ASTRONOMY
Mapping with QUASAT (quasar satellite) using short observation times
[AD-A155155] N85-32141
SPACEBORNE EXPERIMENTS
Study of proton and neutron activation of metal samples in low Earth orbit
[NASA-CR-171596] N85-32130
USSR Space Life Sciences Digest
[NASA-CR-3922] N85-32709
SPACEBORNE PHOTOGRAPHY
Large format camera photographs: A new tool for understanding arid environments N85-32379
SPACECRAFT
Clarke Stations and mercurian mass-drivers: Energy for large-scale transportation systems
[DE85-009607] N85-32145
SPACECRAFT COMMUNICATION
Automation study for space station subsystems and mission ground support
[NASA-CR-176097] N85-32136
SPACECRAFT COMPONENTS
Results from radiation monitoring equipment experiments on STS-41C, 41D, 41G and 51A
[AD-A154676] N85-32142
Background equatorial astronomical measurements focal plane assembly (refurbished HI STAR SOUTH)
[AD-A155215] N85-32313
SPACECRAFT ENVIRONMENTS
Automation study for space station subsystems and mission ground support
[NASA-CR-176097] N85-32136
Hydroponics developments for spaceship garden N85-32754
SPACECRAFT LAUNCHING
Pricing options for the space shuttle. Special study N85-32138
SPACECRAFT POWER SUPPLIES
Automation study for space station subsystems and mission ground support
[NASA-CR-176097] N85-32136
SPACECRAFT RADIATORS
Automation study for space station subsystems and mission ground support
[NASA-CR-176097] N85-32136
SPACECREWS
Living aloft: Human requirements for extended spaceflight
[NASA-SP-483] N85-32772
SPACELAB
Mission operations requirements document for D-1 Experiment 102, Vestibular Experiments in Spacelab
[NASA-TM-87495] N85-32129
SPACELAB PAYLOADS
Activities report of the Aeronomy Department
[G-774-1984] N85-32569
SPACETENNAS
Relationship of spaced antenna and Doppler techniques for velocity measurements (keynote paper), part 3 N85-32488
A simple model for testing the effects of gravity-wave-produced vertical oscillations of scattering irregularities on spaced-antenna, horizontal drift measurements N85-32489
Potential advantages of the spaced antenna method for operational wind profiling, part 3.1B N85-32490
Criteria for optimum spacing of spaced antenna, part 3.2A N85-32491
Accuracy of velocity and power determination by the Doppler method N85-32493
Interferometer applications of VHF radars, part 3.6A N85-32497
SPACING
Decomposing the joint distribution of several linear combinations of uniform spacings
[AD-A155056] N85-32845
SPAIN
A statistical analysis of ice nuclei concentrations at urban and rural sites in Valladolid, Spain N85-32614
SPARE PARTS
Feasibility of applications of Competition Decision Assist Package (CDAP) to spare parts
[AD-A154716] N85-33036
SPATIAL DISTRIBUTION
Influence of particle arrangement on sintering
[AD-A155337] N85-32352
Interferometer applications of VHF radars, part 3.6A N85-32497
Aircraft investigations of the distribution of aerosols in the lower troposphere N85-32659
The distribution of giant salt nuclei inside and outside cloud over the basin of Xin and Jiang N85-32681
Resource allocation in cerebral specialization of function: Behavioral and electrophysiological studies
[AD-A155092] N85-32759
SPATIAL RESOLUTION
Three-dimensional photochemical machining with lasers
[AD-A154711] N85-32320
Selective population of N = 3 OVIII level during expansion of laser plasma in helium N85-32914
Hexagonal uniformly redundant arrays for coded-aperture imaging
[PAPER-OG-9.2-1] N85-33048
Research in extreme ultraviolet and far ultraviolet astronomy
[NASA-CR-176068] N85-33060
SPECIFIC HEAT
Basic cryogenics and materials. Phase 1
[NASA-CR-177932] N85-32215
SPECIFICATIONS
The Proust radar N85-32547
An automated quality assurance surveillance plan for ADP (Automated Data Processing) operations under the Navy's commercial activities program
[AD-A154767] N85-32802
SPECIMEN GEOMETRY
A cracked orthotropic sheet stiffened by a semi-infinite orthotropic sheet
[NASA-TP-2455] N85-32339
Results of an interlaboratory fatigue test program conducted on alloy 800H at room and elevated temperatures
[NASA-CR-174940] N85-32340
SPECTRA
Criteria and algorithms for spectrum parameterization of MST radar signals N85-32527
Paleoenvironmental investigations at seed cave (Windust cave H-45FR46), Franklin County, Washington
[AD-A154777] N85-32576
SPECTRAL SENSITIVITY
Paired ion chamber constants for fission gamma-neutron fields
[AD-A155069] N85-32999
SPECTROGRAMS
Analysis of spacecraft data
[NASA-CR-171587] N85-32789
SPECTROMETERS
A microprocessor-controlled, multichannel fluorimeter for analysis of sea water
[AD-A154986] N85-32310
Research in extreme ultraviolet and far ultraviolet astronomy
[NASA-CR-176068] N85-33060
SPECTROPHOTOMETRY
Transparency of water 9n 186 - 500 nm region N85-32923
SPECTROSCOPIC ANALYSIS
Initial results from the Caltech/DSRI balloon-borne isotope experiment
[PAPER-OG-4.3-8] N85-33046
Dating Archean zircon by ion microprobe: New light on an old problem N85-33094
SPECTROSCOPIC TELESCOPES
A balloon-borne imaging gamma-ray telescope
[PAPER-OG-9.2-2] N85-33049
Balloon-borne video cassette recorders for digital data storage
[PAPER-OG-9.3-11] N85-33050
SPECTROSCOPY
Calculation of molecular constants potential energy curves and Franck-Condon factors for lead oxide
[AD-A154521] N85-32158
Multidimensional luminescence measurements
[AD-A154950] N85-32162
Basic research in novel inorganic reagents and fluorocarbon chemistry
[AD-A155340] N85-32165
Aerosol analysis and emission spectrometry with free jets
[DE85-010576] N85-32168
Electrochemistry of Hexanitroazobenzene (HNAB)
[DE85-010807] N85-32171
Multi-channel electric aerosol spectrometer N85-32623
USSR report: Physics and mathematics
[JPRS-UPM-85-004] N85-32860
SPECTRUM ANALYSIS
High resolution evidence for the Garrett-Munk spectrum of stratospheric gravity waves N85-32503
A relationship between cloud droplet size and CCN critical supersaturation N85-32677
In-cavity laser IR spectrum analyzer for investigating non-steady-state processes N85-32894
Spectral-luminescence characteristics and induced emission of Nd-3(+) ion in Gd(2-x)Nd(x)(WO4)3 crystals N85-32912
Doppler spectrometer for measuring narrow photochemical gaps in inhomogeneously broadened spectra N85-32921

A balloon-borne imaging gamma-ray telescope
[PAPER-OG-9.2-2] N85-33049

SPECULAR REFLECTION
Aspects of SAR image segmentation
[AD-A154965] N85-32236

SPEECH
Speech understanding research
[AD-A155462] N85-32990

SPEED CONTROL
Experimental investigation of a variable speed constant frequency electric generating system from a utility perspective
[NASA-CR-174950] N85-32251

SPHERES
SPLINES. Their equivalence to collocation
[AD-A155250] N85-32566

SPILLING
Facility for large-scale hazardous gas testing
[DE85-011852] N85-32169

SPIN-ORBIT INTERACTIONS
Inter-zone auger recombination in GaSb laser structures N85-32875

SPLINE FUNCTIONS
SPLINES. Their equivalence to collocation
[AD-A155250] N85-32566

SPLINES
SPLINES. Their equivalence to collocation
[AD-A155250] N85-32566

SPREAD SPECTRUM TRANSMISSION
Compression of spread spectrum signals on an excessively dispersive channel
[AD-A155184] N85-32240

SPUTTERING
Modification of the grain size of sputtered copper with additions of oxygen, krypton, silver, or yttrium
[DE85-010975] N85-32189

STABILITY
Notes on atmospheric stability, turbulence, and its measurements
[AD-A155230] N85-32588

STABILITY TESTS
Recent developments in rotary-balance testing of fighter aircraft configurations at NASA Ames Research Center
[NASA-TM-86714] N85-32090

STABILIZATION
Optical output stabilization method for direct current arc lamps
[AD-A154987] N85-33013

STABILIZERS (AGENTS)
Micromolecular modeling N85-32405
Polymerizable ultraviolet stabilizers N85-32406

STABLE OSCILLATIONS
Oscillatory solutions of the Peaceman-Rachford alternating direction implicit method and a comparison of methods for the solution of the two dimensional heat diffusion equation
[AD-A154670] N85-32833

STAINLESS STEELS
Machining-induced deformation in stepped specimens of PH 13-8 Mo, 18 nickel maraging steel grade 200T1 and grain-refined HP 9-4-20
[NASA-CR-172450] N85-32177
Film condensation of steam on externally finned horizontal tubes
[AD-A155642] N85-32285

STANDARDS
Improved coordinate measuring machine calibration and control
[DE85-012053] N85-32315

STARS
Basic formulae for the computation of the deflection of the vertical from astronomical star observations
[AD-A154912] N85-32390

STATISTICAL ANALYSIS
Reliability of void detection in structural ceramics using scanning laser acoustic microscopy
[NASA-TM-87035] N85-32337
Signal statistics of the radar echoes: Angle-of-arrival statistics, part 2.2A N85-32482
A statistical analysis of ice nuclei concentrations at urban and rural sites in Valladolid, Spain N85-32614
A statistical study of CCN concentration in subequatorial climate: The particular case of the tropical wet forest N85-32673
An error-dependent model of instrument-scanning behavior in commercial airline pilots
[NASA-CR-3908] N85-32765
Theory of soliton waves
[AD-A154784] N85-32837
Optimization of sampling in statistical physics experiments N85-32975

STATISTICAL CORRELATION
Solar radio fluxes as indices of solar activity
[AERONOMICA-ACTA-A-282-1984] N85-33095

STATISTICAL DISTRIBUTIONS
The distribution of the number of empty cells in a generalized random allocation scheme
[AD-A154806] N85-32841
Decomposing the joint distribution of several linear combinations of uniform spacings
[AD-A155056] N85-32845
Antistarshapedness, dispersiveness and mixtures
[AD-A155583] N85-32849

STATISTICAL WEATHER FORECASTING
An evaluation of discretized conditional probability and linear regression threshold techniques in model output statistics forecasting of cloud amount and ceiling over the North Atlantic Ocean
[AD-A155100] N85-32581

STEADY STATE
MPS solidification model. Analysis and calculation of macrosegregation in a casting ingot
[NASA-CR-171589] N85-32178
Weak shock waves propagating in fluid-gas mixtures
[AD-A154759] N85-32276
Radar echoes at 2.66 and 40.92 MHz from the mesosphere, part 2.6A N85-32486
Generalized formulation of a class of explicit and implicit TVD schemes
[NASA-TM-86775] N85-32830
On the dependence of the convergence of Gummel's algorithm on the regularity of the solution
[AD-A154628] N85-32832
Quasi-steady-state melting mode during combined laser irradiation of semiconductor materials N85-32874
Establishment of steady-state power level in pulse-periodic excimer laser N85-32896
A system of magnetohydrodynamic-type equations N85-32946
On one nonlinear problem of laser thermochemistry N85-32971
Chemical evolution of the Earth: Equilibrium or disequilibrium process? N85-33088
Soft X-ray polychromator for the Solar Maximum Mission
[NASA-CR-175297] N85-33096

STEAM
Film condensation of steam on externally finned horizontal tubes
[AD-A155642] N85-32285

STEEL STRUCTURES
Experimental and theoretical assessment of a new technique for the non-destructive evaluation of laminated panels
[AD-A155622] N85-32155

STEELS
Decomposition of sulfuric acid using solar thermal energy
[DE85-012288] N85-32170
Understanding and laboratory prediction of the atmospheric corrosion behavior of steels and of non-ferrous metals and alloys
[AD-A154642] N85-32179
Development of improved dynamic failure models
[AD-A155586] N85-32354

STEERING
Practicality of electronic beam steering for MST/ST radars, part 6.2A N85-32516

STELLAR EVOLUTION
Search for the universal ancestors
[NASA-SP-477] N85-32777
Noble gases and the early history of the Earth: Inappropriate paradigms and assumptions inhibit research and communication N85-33075

STELLAR MOTIONS
Solar convection
[AD-A155214] N85-33098

STELLARATORS
Cyclotron absorption of fast magnetosonic wave in stellarator N85-32945

STEREOPHOTOGRAPHY
Large format camera photographs: A new tool for understanding arid environments N85-32379

STIGMATISM
Electrostatic astigmatic tubular lens N85-32955

STOCHASTIC PROCESSES
Routing algorithms and stochastic analysis for large communications networks
[AD-A154654] N85-32225
A simulation of weather in 3D space
[AD-A155221] N85-32586
SIGMA - A stochastic-integration global minimization algorithm
[AD-A154878] N85-32806

STORMS
Radio-frequency radiation of storm clouds N85-32939

STRAIN RATE
Fundamental investigations of failure during superplastic forming process
[AD-A154647] N85-32194
Strain rate sensitivity estimation from high velocity impact data
[AD-A154703] N85-32347
Influence of particle arrangement on sintering
[AD-A155337] N85-32352

STRAPDOWN INERTIAL GUIDANCE
Test evaluation of the Honeywell GG1111 Single-Degree-of-Freedom (SDF) strapdown gyroscope
[AD-A154768] N85-32307

STRATA
Radar echoes at 2.66 and 40.92 MHz from the mesosphere, part 2.6A N85-32486

STRATIFICATION
Numerical modeling of subsurface communication
[DE85-012818] N85-32249

STRATIFIED FLOW
Resolution of thermal striping issue downstream of a horizontal pipe elbow in stratified pipe flow
[DE85-006195] N85-32292

STRATIGRAPHY
Paleoenvironmental investigations at seed cave (Windust cave H-45FR46), Franklin County, Washington
[AD-A154777] N85-32576
Sulfur transformations at the hydrogen sulfide/oxygen interface in stratified waters and in cyanobacterial mats N85-32715
The Aravalli sequence of Rajasthan, India: A Precambrian continental margin? N85-33084

STRATOSPHERE
Tropospheric-stratospheric exchange, part 1.1A N85-32468
Gravity waves from the stratosphere to the mesosphere, part 1.3B N85-32471
A numerical analysis of transient planetary waves and the vertical structure in a meso-strato-troposphere model, part 1.4A N85-32473
Vertical transport in the atmosphere: Measurement capabilities and requirements of VHF radars, part 1.6A N85-32476
Morphology of the scattering targets: Fresnel and turbulent mechanisms, part 2.1A N85-32481
Antenna induced range smearing in MST radars N85-32495
High resolution evidence for the Garrett-Munk spectrum of stratospheric gravity waves N85-32503
Relationship of isolated turbulent regions to the general turbulent background, part 4.4A N85-32506
Estimation of vertical diffusion from observations of Atmospheric turbulence layers, part 4.4B N85-32507
Further developments of EISCAT as an MST radar N85-32534
Urbana radar systems: Possibilities and limitations N85-32540
Millstone Hill radar: Capabilities for S/T observations N85-32548
The Ponape ST radar N85-32549
Measurements of vertical velocity over flat terrain by ST radar and other related uses of the radar data set N85-32550
Activities report of the Aeronomy Department
[G-774-1984] N85-32569
A new hypothesis for the observed vertical distribution of atmospheric aerosols N85-32646
Theoretical studies of structure and stability of hydrates of atmospheric sulfur species N85-32684

STRATUS CLOUDS
Transport and formation of summertime cloud condensation nuclei over the Arctic Ocean N85-32686

STREAK CAMERAS
Coordinated research program in pulsed power physics
[AD-A154629] N85-32858

STREAMS
Geomorphic analyses from space imagery N85-32374

STRESS (PHYSIOLOGY)
Status of the air traffic control system
[GPO-40-343] N85-32107

STRESS (PSYCHOLOGY)
Status of the air traffic control system
[GPO-40-343] N85-32107

STRESS ANALYSIS
Development and test of advanced composite components. Center Directors discretionary fund program
[NASA-TM-86512] N85-32147
The shearing contribution in transformation toughening of brittle materials
[AD-A154656] N85-32195
Matrix fracture in fiber-reinforced ceramics
[AD-A154704] N85-32197

User's guide for computer program CGFAG, Concrete General Flexure Analysis with Graphics [AD-A155555] N85-32204
Dynamic fracture of concrete and other heterogeneous materials [AD-A154513] N85-32343
Stress and buckling analysis N85-32439

STRESS CONCENTRATION
Mechanics of near tip microcracking in brittle material [AD-A154684] N85-32346
Stress concentration in the elastoplastic state and residual stress after unloading [AD-A155628] N85-32356

STRESS CORROSION
The effect of stress and hot corrosion on nickel-base superalloys [AD-A154722] N85-32181

STRESS CORROSION CRACKING
Stress corrosion of ceramic materials [AD-A155020] N85-32202

STRESS INTENSITY FACTORS
A cracked orthotropic sheet stiffened by a semi-infinite orthotropic sheet [NASA-TP-2455] N85-32339

STRESS RELAXATION
Mechanics of near tip microcracking in brittle material [AD-A154684] N85-32346

STRESS-STRAIN RELATIONSHIPS
Component-specific modeling [NASA-CR-174925] N85-32119
Effects of weak interfaces on thermostructural behavior of carbon-carbon composites [AD-A155330] N85-32154
Fundamental investigations of failure during superplastic forming process [AD-A154647] N85-32194
Hertzian contact in two and three dimensions [NASA-TP-2473] N85-32331
Analysis of stress-strain relationships in silicon ribbon N85-32438

STRESSES
Machining-induced deformation in stepped specimens of PH 13-8 Mo, 18 nickel maraging steel grade 200T1 and grain-refined HP 9-4-20 [NASA-CR-172450] N85-32177
Sintering studies project [AD-A154750] N85-32216
Thin-film reliability and engineering overview N85-32450

STRINGERS
A cracked orthotropic sheet stiffened by a semi-infinite orthotropic sheet [NASA-TP-2455] N85-32339
Acoustic wave scattering by round cylindrical shell reinforced with stringers N85-32916

STRONGLY COUPLED PLASMAS
Low frequency instabilities driven by an ion temperature anisotropy [AD-A154902] N85-33016

STRUCTURAL ANALYSIS
Iteration solution for a submerged force-driven finite cylinder [AD-A154587] N85-32982

STRUCTURAL BASINS
Lunar and Martian impact basins: Exposed records of terrestrial bombardment? N85-33090

STRUCTURAL ENGINEERING
Field testing of a lightweight relocatable structure in a temperate environment [AD-A155171] N85-32350
Proceedings of the 24th Project Integration Meeting [NASA-CR-176058] N85-32394

STRUCTURAL PROPERTIES (GEOLOGY)
Global Mega-Geomorphology [NASA-CP-2312] N85-32357
Andrean examples of mega-geomorphology themes N85-32367
Lunar and Martian impact basins: Exposed records of terrestrial bombardment? N85-33090
Earth's primordial differentiation, and its after-effects N85-33092

STRUCTURAL STABILITY
A systematic plan for the continued study of dimensional stability of metallic alloys considered for the fabrication of cryogenic wind tunnel models [NASA-CR-172449] N85-32172

STRUCTURAL VIBRATION
Experimental and theoretical assessment of a new technique for the non-destructive evaluation of laminated panels [AD-A155622] N85-32155

SUBROUTINES
Evaluation and implementation of a functional microprogram generator [AD-A155164] N85-32823

SUBSTRATES
Microwave SAW (Surface Acoustic Wave) monochromator [AD-D011718] N85-32311
Thin-film reliability and engineering overview N85-32450

SULFATES
Sulfates in marine aerosols over the tropical Western Pacific Ocean N85-32690
Granulometric study of the acidity and sulfate excess in marine aerosols N85-32691
Geology and geochemistry of sulfide and sulfate deposition N85-32723
Phototrophic bacteria and their role in the biogeochemical sulfur cycle N85-32735
Sulfur reduction in sediments of marine and evaporite environments N85-32742

SULFATION
Molecular orbital studies in oxidation: Sulfate formation and metal-metal oxide adhesion [NASA-CR-176070] N85-32174
Adsorption of O2, SO2, and SO3 on nickel oxide. Mechanism for sulfate formation [NASA-CR-176072] N85-32175

SULFIDES
The global sulfur cycle [NASA-TM-87570] N85-32710
Sulfur diagenesis in marine sediments N85-32721
Geology and geochemistry of sulfide and sulfate deposition N85-32723
Sulfate-reducing bacteria: Microbiology and physiology N85-32732
Structure and physiology of Beggiatoa and Thiothrix N85-32734
Enrichments for phototrophic bacteria and characterization by morphology and pigment analysis N85-32738
Interactions among sulfide-oxidizing bacteria N85-32741
Sulfur reduction in sediments of marine and evaporite environments N85-32742
Microbial communities and microprofiles of sulfide and oxygen of alum rock sulfur springs N85-32746
Microbial colonization and growth on metal sulfides and other mineral surfaces N85-32747

SULFONES
Synthesis and properties of arylethersulfone thermoset systems [AD-A154811] N85-32198

SULFUR
Theoretical studies of structure and stability of hydrates of atmospheric sulfur species N85-32684
Variations of particulate sulfur concentrations in a coastal atmospheric environment in connection with the change of air masses origin N85-32692
The global sulfur cycle [NASA-TM-87570] N85-32710
Sulfur transformations at the hydrogen sulfide/oxygen interface in stratified waters and in cyanobacterial mats N85-32715
Cytochromes and iron sulfur proteins in sulfur metabolism of phototrophic bacteria N85-32718
Carbon and sulfur cycling through geologic time N85-32720
Ecophysiology of phototrophic sulfur bacteria in lakes: Vertical distribution of planktonic populations N85-32722
Sulfur cycling in freshwater sediments N85-32726
Some thoughts on GAIA and the sulfur cycle N85-32727
Sulfur and carbon cycling in organic-rich marine sediments N85-32729
Possible roles of manganese redox chemistry in the sulfur cycle N85-32731
Phototrophic bacteria and their role in the biogeochemical sulfur cycle N85-32735
The role of sulfur in osmoregulation and salinity tolerance in cyanobacteria, algae, and plants N85-32736
Sulfur cycling and metabolism of phototrophic and filamentous sulfur bacteria N85-32737
Anaerobic reduction of elemental sulfur by Chromatium vinosum and Beggiatoa alba N85-32739
Sulfur Cycle N85-32748
Multiphoton production and detection of atoms [AD-A155561] N85-33000

SULFUR DIOXIDES
Experimental studies of the formation of Aitken nuclei in the atmosphere N85-32641

SULFUR OXIDES
Adsorption of O2, SO2, and SO3 on nickel oxide. Mechanism for sulfate formation [NASA-CR-176072] N85-32175

SULFURIC ACID
Decomposition of sulfuric acid using solar thermal energy [DE85-012288] N85-32170
Aerobic sulfur-oxidizing bacteria: Environmental selection and diversification N85-32712

SUMMER
Aircraft observations of condensation and ice nuclei at a tropical station N85-32613
Transport and formation of summertime cloud condensation nuclei over the Arctic Ocean N85-32686

SUN
Solar convection [AD-A155214] N85-33098
Heating of the deep chromosphere during solar flares [AD-A155256] N85-33100
Search for the north-south asymmetry in solar activity [AD-A155525] N85-33102

SUNSPOT CYCLE
Equitorial scintillations: Advances since ISEA-6 [AD-A154962] N85-32559

SUNSPOTS
Solar cycle variation of ephemeral regions [AD-A154967] N85-33097

SUPERCOMPUTERS
The NAS kernel benchmark program [NASA-TM-86711] N85-32795

SUPERCONDUCTORS
Detector problems at the SSC [DE85-010217] N85-33007

SUPERCOOLING
The nucleation of ice crystals during the freezing of large supercooled drops N85-32608

SUPERCRITICAL PRESSURES
Polymer solution-supercritical fluid behavior [AD-A154514] N85-32192

SUPERHIGH FREQUENCIES
Paired ion chamber constants for fission gamma-neutron fields [AD-A155069] N85-32999

SUPERLATTICES
Doping superlattices in organometallic VPE InP [AD-A155151] N85-33029

SUPERPLASTICITY
The effect of alloy additions on superplasticity in thermomechanically processed high magnesium aluminum-magnesium alloys [AD-A155142] N85-32184

SUPERSATURATION
Experimental investigation of properties of ice-forming reagents N85-32602
The effect of supersaturation, temperature and particle size on ice-nucleating ability of atmospheric aerosol N85-32604
On the efficiency of the mechanism of ice particles formation in the vapor supersaturation field around a freezing droplet N85-32606
Supersaturation spect A of Ice Nuclei at different locations in Europe and over the North-Atlantic N85-32615
Supersaturation obtained in a condensation nucleus counter N85-32624
Analysis of performance of dynamic thermal diffusion chamber N85-32625
Critical supersaturations with respect to water for fast condensation-freezing ice nucleation N85-32632
A simple model to investigate the activation process in waterclouds N85-32675
Measurements of the critical supersaturation of 0.029 to 0.035 micron radius particles at Washington, District of Columbia N85-32676
A relationship between cloud droplet size and CCN critical supersaturation N85-32677
Fog activation and supersaturation N85-32678

SUPERSONIC AIRCRAFT
Study of an efficient long-range Mach 2.7 supersonic transport configuration concept [NASA-TM-86414] N85-32110

SUPERSONIC BOUNDARY LAYERS
Development of artificially produced perturbations in supersonic boundary layer N85-32879

SUPERSONIC FLIGHT
China has developed a new version of fighter aircraft [AD-A155293] N85-32118

SUPERSONIC TRANSPORTS
Study of an efficient long-range Mach 2.7 supersonic transport configuration concept [NASA-TM-86414] N85-32110

SURFACE ACOUSTIC WAVE DEVICES
Microwave SAW (Surface Acoustic Wave) monochromator [AD-D011718] N85-32311

SURFACE DIFFUSION
The use of the glistening surface concept in rough surface scattering [AD-A154922] N85-32234
An analysis of physical optics models for rough surface scattering [AD-A154960] N85-32235

Mean flow and turbulence in complex terrain
[AD-A155138] N85-32583
SURFACE FINISHING
New metal coating method developed N85-32191
Reliability of void detection in structural ceramics using scanning laser acoustic microscopy
[NASA-TM-87035] N85-32337
MOD silver metallization for photovoltaics N85-32428
SURFACE PROPERTIES
Using ship wake patterns to evaluate SAR (Synthetic Aperture Radar) ocean wave imaging mechanisms. Joint US-Canadian Ocean Wave Investigation Project
[AD-A154633] N85-32223
Toward the theory of acoustic scattering on uneven free surface N85-32862
Acoustic radiation from concentric shells containing an inner fluid
[AD-A155476] N85-32991
Considerations of large scale impact and the early Earth N85-33070
Solar cycle variation of ephemeral regions
[AD-A154967] N85-33097
SURFACE REACTIONS
Overlap integrals for atom-metal surface interactions
[AD-A155038] N85-32998
SURFACE ROUGHNESS
Using ship wake patterns to evaluate SAR (Synthetic Aperture Radar) ocean wave imaging mechanisms. Joint US-Canadian Ocean Wave Investigation Project
[AD-A154633] N85-32223
The use of the glistening surface concept in rough surface scattering
[AD-A154922] N85-32234
An analysis of physical optics models for rough surface scattering
[AD-A154960] N85-32235
Surface roughness effects in elastohydrodynamic contacts
[NASA-TP-2488] N85-32329
Toward the theory of acoustic scattering on uneven free surface N85-32862
SURFACE ROUGHNESS EFFECTS
Comparison of findings of theories describing reflection from real surface with experiments in region of ultrasoft X-radiation N85-32950
SURFACE STABILITY
Experiments on the influence of active walls on the initial amplitudes and growths of instability waves
[AD-A154630] N85-32275
Instability and chaotic behavior in a free-surface flow
[AD-A154879] N85-32279
Interfacial bonding stability N85-32409
SURFACE TEMPERATURE
Facility for large-scale hazardous gas testing
[DE85-011852] N85-32169
SURFACE WAVES
Discovery of a nonpropagating hydrodynamic soliton
[AD-A155569] N85-32268
Large-time behavior of viscous surface waves
[AD-A154805] N85-32278
Upward continuation of surface gravity anomalies
[AD-A154973] N85-32560
Solid state research
[AD-A154783] N85-33025
SURFACTANTS
On the question to the effect of surfactants on the spectrum of cloud drops in the process of their condensation growth N85-32679
SURGES
Resolution of thermal striping issue downstream of a horizontal pipe elbow in stratified pipe flow
[DE85-006195] N85-32292
Nonlinear spectroscopy
[AD-A154708] N85-33010
SURVEILLANCE
An automated quality assurance surveillance plan for ADP (Automated Data Processing) operations under the Navy's commercial activities program
[AD-A154767] N85-32802
SURVEILLANCE RADAR
The effects of subrefractive layers and elevated ducts on airborne radar and ESM (Electronic Surveillance Measures)
[AD-A155524] N85-32592
SWITCHES
The plasma erosion opening switch
[AD-A154942] N85-32259
Coordinated research program in pulsed power physics
[AD-A154629] N85-32858
Operational window for a plasma erosion opening switch used for voltage multiplication on pulsed power generators
[AD-A155482] N85-33020
SWITCHING
The plasma erosion opening switch
[AD-A154942] N85-32259
SWITCHING CIRCUITS
T/R switch design for short-range measurements, part 6.1A N85-32515
Coordinated research program in pulsed power physics
[AD-A154629] N85-32858
SYMBIOSIS
From microbial communities to cells N85-32728
SYMMETRY
Possiblity of developing charged-particle energy analyzer based on hyperboloidal axisymmetrical lens N85-32933
SYNCHRONISM
Globally-asynchronous locally-synchronous systems
[AD-A154624] N85-32222
Consensus in the presence of partial synchrony (Preliminary version)
[AD-A154705] N85-32799
A new fault-tolerant algorithm for clock synchronization
[AD-A154771] N85-32836
SYNCHROTRON RADIATION
Microscopic control of semiconductor surface oxidation
[AD-A154799] N85-33026
SYNCHROTRONS
Tailored vacuum chambers for ac magnets
[DE85-010767] N85-32319
High-energy Physics Institute building 3-trillion-ev accelerator N85-32934
SYNOPTIC MEASUREMENT
Diagnostics of severe convection and subsynoptic scale ageostrophic circulations
[NASA-CR-171581] N85-32571
SYNOPTIC METEOROLOGY
Frequency and site selection criteria for MST radars, part 5.1A N85-32512
SYNTAX
Speech understanding research
[AD-A155462] N85-32990
SYNTHESIS
Electrochemistry of Hexanitroazobenzene (HNAB)
[DE85-010807] N85-32171
SYNTHESIS (CHEMISTRY)
Synthesis and properties of arylethersulfone thermoset systems
[AD-A154811] N85-32198
Synthesis of energetic materials
[AD-A154887] N85-32210
Origin of life N85-32713
The composition of the primitive atmosphere and the synthesis of organic compounds on the early Earth N85-33065
SYNTHETIC APERTURE RADAR
Using ship wake patterns to evaluate SAR (Synthetic Aperture Radar) ocean wave imaging mechanisms. Joint US-Canadian Ocean Wave Investigation Project
[AD-A154633] N85-32223
Aspects of SAR image segmentation
[AD-A154965] N85-32236
SYNTHETIC FUELS
Biomass thermochemical conversion program
[DE85-011867] N85-32213
SYSTEM FAILURES
Problems and solutions in analyzing partial-reflection drift data by correlation techniques N85-32529
SYSTEMS ANALYSIS
A numerical study of Taylor-Vortex flow
[AD-A154787] N85-32277
The optimality of lower confidence limits for the reliability of series systems obtained by the method of key test results or other related techniques
[AD-A154880] N85-32338
Space station ECLSS integration analysis: Simplified General Cluster Systems Model, ECLS System Assessment Program enhancements
[NASA-CR-176089] N85-32796
A comprehensive study of the AFIT (Air Force Institute of Technology) software development environment
[AD-A155450] N85-32812
Survival function of hypo-exponential distributions
[AD-A155518] N85-32814
SYSTEMS ENGINEERING
Development of reduced order models for control system design using the OPTSYSX program
[AD-A154552] N85-32124
The documentation assistant: An intelligent system for documentation
[AD-A154709] N85-32800
A comprehensive study of the AFIT (Air Force Institute of Technology) software development environment
[AD-A155450] N85-32812
Evaluation of a software design approach: Develop a threat resolution module in Ada (trademark)
[AD-A155599] N85-32815
Distributed name management
[AD-A154785] N85-33037
SYSTEMS INTEGRATION
Performance improvements of a highly integrated digital electronic control system for an F-15 airplane
[NASA-TM-86748] N85-32120
High temperature electronics technology: Life test report
[AD-A154681] N85-32257
Characteristics of a numerical fluid dynamics simulator
[DE85-009602] N85-32290
SYSTEMS MANAGEMENT
NASA space station automation: AI-based technology review
[NASA-CR-176094] N85-32134
Analysis of spacecraft data
[NASA-CR-171597] N85-32790

T

TANKER SHIPS
A crew exposure study. Phase II. Volume 2. At sea. Part A
[AD-A155233] N85-32774
TARGET RECOGNITION
Radar target identification through electromagnetic scattering studies
[AD-A154596] N85-32220
Broadside scattering of a tubular cylinder for evaluation of target identification
[AD-A155739] N85-32248
Bayesian vs MAP multiple model adaptive estimation for field of view expansion in tracking airborne targets
[AD-A155466] N85-32855
TASKS
Resource allocation in cerebral specialization of function: Behavioral and electrophysiological studies
[AD-A155092] N85-32759
Conceptualizing in assembly tasks
[AD-A155564] N85-32770
TECHNOLOGY ASSESSMENT
GAO (General Accounting Office) assessment of DOD's Very High Speed Integrated Circuits (VHSIC) technology program
[AD-A155109] N85-32261
Space station ECLSS integration analysis: Simplified General Cluster Systems Model, ECLS System Assessment Program enhancements
[NASA-CR-176089] N85-32796
Detector problems at the SSC
[DE85-010217] N85-33007
TECHNOLOGY UTILIZATION
A systematic plan for the continued study of dimensional stability of metallic alloys considered for the fabrication of cryogenic wind tunnel models
[NASA-CR-172449] N85-32172
Deep sea mega-geomorphology: Progress and problems N85-32369
Use of the synoptic view: Examples from Earth and other planets N85-32371
TECTONICS
Global Mega-Geomorphology
[NASA-CP-2312] N85-32357
Global geomorphology N85-32359
Quantitative analysis in megageomorphology N85-32376
Techniques, problems and uses of mega-geomorphological mapping N85-32378
Planetary perspective. Report of Working Group Number 4 N85-32365
A review of tectonic aspects of the Limpopo belt and other Archean high-grade gneissic terranes N85-33080
TELECOMMUNICATION
An analysis of physical optics models for rough surface scattering
[AD-A154960] N85-32235
Security controls in the Stockpoint Logistics Integrated Communications Environment (SPLICE)
[AD-A155536] N85-32244
Parameter estimation in communication system tracking satellite observations
[AD-A155137] N85-32582
TELECONFERENCING
Software for interactive on-line conferences
[AD-A154742] N85-32801
TELEOPERATORS
NASA space station automation: AI-based technology review
[NASA-CR-176094] N85-32134
NASA space station automation: AI-based technology review. Executive summary
[NASA-CR-176096] N85-32135

TELEVISION RECEIVERS
East Europe report: Science and technology. Selections on CSSR computer technology
[JPRS-ESA-84-017] N85-32781
TEMPERATURE DEPENDENCE
Remarks on preparation of indandione detection reagents
[NASA-TM-77905] N85-32146
Absorption of laser radiation in substance with absorption coefficient depending linearly upon temperature N85-32953
TEMPERATURE DISTRIBUTION
Quasi-steady-state melting mode during combined laser irradiation of semiconductor materials N85-32874
On one nonlinear problem of laser thermochemistry N85-32971
TEMPERATURE EFFECTS
Friction and wear of solid-lubricated contact in gas turbine engine bearings
[AD-A155042] N85-32335
Interfacial bonding stability N85-32409
TEMPERATURE GRADIENTS
Temperature measurements on small droplets N85-32699
TEMPERATURE MEASUREMENT
In-situ measurement of wall thermal performance: Data interpretation and apparatus design recommendations
[DE85-011979] N85-32289
Temperature measurements on small droplets N85-32699
TEMPERATURE PROFILES
Imbedded thermocouples as a solid propellant combustion probe
[AD-A155630] N85-32167
TEMPORAL DISTRIBUTION
Resource allocation in cerebral specialization of function: Behavioral and electrophysiological studies
[AD-A155092] N85-32759
TENSILE PROPERTIES
Effects of weak interfaces on thermostructural behavior of carbon-carbon composites
[AD-A155330] N85-32154
TENSILE STRESS
Matrix fracture in fiber-reinforced ceramics
[AD-A154704] N85-32197
A continuous damage model based on stepwise-stress creep rupture tests
[NASA-CR-174941] N85-32341
TENSILE TESTS
Graphite/PMR polyimide composites with improved toughness
[NASA-TM-87081] N85-32148
TERRAIN
The use of the glistening surface concept in rough surface scattering
[AD-A154922] N85-32234
Geomorphological similarity and uniqueness N85-32361
Ancient landscapes: Their nature and significance for the question of inheritance N85-32364
Landscape inheritance: Report of Working Group Number 2 N85-32383
Process thresholds: Report of Working Group Number 3 N85-32384
Microcomputer processing of LANDSAT Thematic Mapper data for the acquisition of military tactical terrain data
[AD-A154781] N85-32389
Mean flow and turbulence in complex terrain
[AD-A155138] N85-32583
A transportable, machine oriented library of european sky and terrain radiance distributions with contemporary radiometric and meteorological profiles
[AD-A155254] N85-32590
A review of tectonic aspects of the Limpopo belt and other Archean high-grade gneissic terranes N85-33080
TERRAIN ANALYSIS
Scattering from foliage covered terrain
[AD-A154724] N85-32228
TEST CHAMBERS
Analysis of performance of dynamic thermal diffusion chamber N85-32625
A thermal diffusion chamber for the measurement of cloud condensation nuclei N85-32627
Stable generation of highly monodisperse aerosols N85-32628
TEST FACILITIES
Decomposition of sulfuric acid using solar thermal energy
[DE85-012288] N85-32170
Georgetown University Photovoltaic Higher Education National Exemplar Facility (PHENEF) N85-32400
TESTS
Experiments on the influence of active walls on the initial amplitudes and growths of instability waves
[AD-A154630] N85-32275
THEMATIC MAPPING
Microcomputer processing of LANDSAT Thematic Mapper data for the acquisition of military tactical terrain data
[AD-A154781] N85-32389
THEOREMS
A note on a theorem of R. Duffin
[AD-A154786] N85-32838
A system of magnetohydrodynamic-type equations N85-32946
THEORETICAL PHYSICS
USSR report: Physics and mathematics
[JPRS-UPM-85-004] N85-32860
THERMAL ANALYSIS
Improved Nominal Operating Cell Temperature (NOCT) test procedure N85-32449
THERMAL BATTERIES
Burn front velocity as a function of pellet density in iron-potassium perchlorate heat powders
[DE85-011448] N85-32214
THERMAL BLOOMING
Ship-to-ship propagation: Maritime data analyses
[AD-A155484] N85-32325
THERMAL CONDUCTIVITY
Basic cryogenics and materials. Phase 1
[NASA-CR-177932] N85-32215
In-situ measurement of wall thermal performance: Data interpretation and apparatus design recommendations
[DE85-011979] N85-32289
THERMAL DEGRADATION
Photothermal degradation studies of encapsulants N85-32403
Micromolecular modeling N85-32405
THERMAL DIFFUSION
Analysis of performance of dynamic thermal diffusion chamber N85-32625
A thermal diffusion chamber for the measurement of cloud condensation nuclei N85-32627
THERMAL ENERGY
Decomposition of sulfuric acid using solar thermal energy
[DE85-012288] N85-32170
THERMAL ENVIRONMENTS
Improved Nominal Operating Cell Temperature (NOCT) test procedure N85-32449
THERMAL EXPANSION
Thermal expansion of selected graphite reinforced polyimide-, epoxy-, and glass-matrix composite
[NASA-TM-87572] N85-32149
THERMAL FATIGUE
Basic cryogenics and materials. Phase 1
[NASA-CR-177932] N85-32215
THERMAL INSULATION
Performance analysis of mixed passive solar heating systems
[DE85-009624] N85-32455
THERMAL PLASMAS
A retarding ion mass spectrometer for the Dynamics Explorer-1
[NASA-CR-171588] N85-32303
THERMAL PROTECTION
Artificial and natural icing tests YEH-60A quick fix helicopter
[AD-A155147] N85-32116
THERMAL RADIATION
Nuclear thermal transmittance in the atmosphere using LOWTRAN-6 computer code
[AD-A154669] N85-32553
THERMAL SIMULATION
Simulation of the coupled atmospheric and oceanic boundary layer model during MILDEX
[AD-A155166] N85-32705
THERMAL STABILITY
Graphite/PMR polyimide composites with improved toughness
[NASA-TM-87081] N85-32148
Basic research in novel inorganic reagents and fluorocarbon chemistry
[AD-A155340] N85-32165
Basic cryogenics and materials. Phase 1
[NASA-CR-177932] N85-32215
THERMAL STRESSES
Accelerated stress factors and failure/degradation mechanisms in terrestrial solar cells N85-32451
THERMIONIC CATHODES
The effect of metal overlayers of thermionic dispenser cathodes
[AD-A154795] N85-32995
THERMOCHEMISTRY
High temperature solar electrothermal processing 2. Zinc from zinc oxide
[AD-A154747] N85-32159
Biomass thermochemical conversion program
[DE85-011867] N85-32213
THERMOCOUPLES
Imbedded thermocouples as a solid propellant combustion probe
[AD-A155630] N85-32167
Resolution of thermal striping issue downstream of a horizontal pipe elbow in stratified pipe flow
[DE85-006195] N85-32292
Failure mechanisms in metal-sheathed thermocouples
[DE85-011929] N85-32317
THERMODYNAMIC EQUILIBRIUM
Condensation properties of atmospheric aerosol N85-32672
THERMODYNAMIC PROPERTIES
Meteorological weapons
[AD-A154735] N85-32575
Numerical modeling of sea ice dynamics and ice thickness characteristics
[AD-A154600] N85-32700
THERMODYNAMICS
Effects of weak interfaces on thermostructural behavior of carbon-carbon composites
[AD-A155330] N85-32154
Polymer solution-supercritical fluid behavior
[AD-A154514] N85-32192
Sintering studies project
[AD-A154750] N85-32216
The sound field of a moving laser-induced acoustic array (theory)
[AD-A154553] N85-32981
Chemical evolution of the Earth: Equilibrium or disequilibrium process? N85-33088
THERMOPLASTIC RESINS
Structure-property relationships in thermoplastic elastomers. Part 3: Segmented polyacetal-polyurethanes
[AD-A154897] N85-32200
THERMOSETTING RESINS
Synthesis and properties of arylethersulfone thermoset systems
[AD-A154811] N85-32198
THERMOSPHERE
Further developments of EISCAT as an MST radar N85-32534
THICK FILMS
MOD silver metallization for photovoltaics N85-32428
THICKNESS
X-ray diffractometric measurements and calculations of limiting values of discrepancy between lattices and layer thicknesses, preventing generation of dislocations during growth of multilayer heterostructures N85-32866
THIN FILMS
New metal coating method developed N85-32191
Multilayer capacitor dielectrics produced from metallo-organic precursors
[AD-A154592] N85-32254
Development of wide band recording materials
[AD-A154961] N85-32309
Microwave-enhanced thin-film deposition N85-32431
Failure analysis of thin-film amorphous-silicon solar-cell modules N85-32452
Electrotransport in thin films
[AD-A155584] N85-33034
THIN WALLS
Head-on scattering of a tubular cylinder of finite length for radar target identification purposes
[AD-A155608] N85-32246
THIOLS
Distribution and abundance of organic thiols N85-32717
THREAT EVALUATION
Space Station crew safety alternatives study. Volume 2: Threat development
[NASA-CR-3855] N85-32133
Evaluation of a software design approach: Develop a threat resolution module in Ada (trademark)
[AD-A155599] N85-32815
THREE DIMENSIONAL BODIES
Three-dimensional photochemical machining with lasers
[AD-A154711] N85-32320
On the dependence of the convergence of Gummel's algorithm on the regularity of the solution
[AD-A154628] N85-32832
THREE DIMENSIONAL FLOW
Three-Dimensional Techniques Applied to Internal Flows in Propulsion Systems
[AGARD-LS-140] N85-32293
An analysis of flow models: From Navier-Stokes to potential flow equations N85-32295
Computation of three-dimensional, inviscid, rotational flows N85-32296
An elliptic calculation procedure for 3-D viscous flow N85-32297
A 3-D Euler method for internal transonic flows computation with a multi-domain approach N85-32298

Performance evaluation of flow in turbomachinery blade rows N85-32299
Numerical solution of the Navier-Stokes equations for 3-D internal flows: An emerging capability N85-32300
Simulation of complex three-dimensional flows [NASA-TM-86773] N85-32831

THRESHOLD CURRENTS
Inter-zone auger recombination in GaSb laser structures N85-32875

THRUSTORS
Modeling the exhaust of the pulsed plasma thruster [AD-A155344] N85-33018

THUNDERSTORMS
Thunderstorm phenomena and weather radar scanning strategies [DOT/FAA/PM-85/14] N85-32573

TIDES
Reverification of the Chesapeake Bay model [AD-A155486] N85-32706
Coastal erosion along Monterey Bay [AD-A155610] N85-32707

TIME
The sound field of a moving laser-induced acoustic array (theory) [AD-A154553] N85-32981

TIME DEPENDENCE
Use of MMLE3 to determine lower order equivalent systems in the time domain [AD-A154700] N85-32112
MPS solidification model. Analysis and calculation of macrosegregation in a casting ingot [NASA-CR-171589] N85-32178
In-situ measurement of wall thermal performance: Data interpretation and apparatus design recommendations [DE85-011979] N85-32289
Mean flow and turbulence in complex terrain [AD-A155138] N85-32583

TIME FUNCTIONS
Use of MMLE3 to determine lower order equivalent systems in the time domain [AD-A154700] N85-32112

TIME LAG
Use of MMLE3 to determine lower order equivalent systems in the time domain [AD-A154700] N85-32112
In-flight evaluation of pure time delays in pitch and roll [NASA-TM-86744] N85-32123
Robust detection and classification of regional seismic signals using a two mode/two stage cascaded adaptive arma (CAARMA) model [AD-A154710] N85-32554

TIME MEASUREMENT
Investigation of space-time structure of glow of laser plasma colliding with flat screen N85-32947
The sound field of a moving laser-induced acoustic array (theory) [AD-A154553] N85-32981

TIME SERIES ANALYSIS
On the spectrum of atmospheric velocity fluctuations seen by MST/ST radar and their interpretation N85-32504
On the transformation regularities of time series of solid aerosol concentrations in the surface atmospheric layer N85-32848
Kalman filter time series analysis of gamma-ray data from NaI(T1) detectors for the ND6620 computer [AD-A154995] N85-33014

TIN COMPOUNDS
Marine environmental quality assessment program, five-year plan (FY 1984 - 1988) [AD-A154715] N85-32459

TISSUES (BIOLOGY)
Physical chemical state of water in living cells [AD-A154566] N85-32749

TITANIUM
Precision measurements of solar energetic particle elemental composition [PAPER-SH-2.1-4] N85-33052

TITANIUM ALLOYS
CO adsorption on (111) and (100) surfaces of the Pt sub 3 Ti alloy. Evidence for parallel binding and strong activation of CO [NASA-CR-176077] N85-32176
Fundamental investigations of failure during superplastic forming process [AD-A154647] N85-32194

TITANIUM CHLORIDES
The determination of dinitrotoluene in single base propellants [AD-A154072] N85-32209

TITANIUM NITRIDES
New metal coating method developed N85-32191

TOKAMAK DEVICES
Injection of hydrogen macroparticles into T-10 tokamak N85-32937
Influence of ECR-heating on MHD activity of plasma in tokamak-10 installation N85-32949

TOLERANCES (PHYSIOLOGY)
The role of sulfur in osmoregulation and salinity tolerance in cyanobacteria, algae, and plants N85-32736
A crew exposure study. Phase II. Volume 2. At sea. Part A [AD-A155233] N85-32774

TOLUENE
Polymer solution-supercritical fluid behavior [AD-A154514] N85-32192

TOPOGRAPHY
The measurement of strain fields by X-ray topographic contour mapping [AD-A154870] N85-32348
Geomorphological similarity and uniqueness N85-32351
Regional landform thresholds N85-32362
Some observations on paleogeomorphology N85-32363
Ancient landscapes: Their nature and significance for the question of inheritance N85-32364
Quantitative analysis in megageomorphology N85-32376
Landscape inheritance: Report of Working Group Number 2 N85-32383
Process thresholds: Report of Working Group Number 3 N85-32384
Frequency and site selection criteria for MST radars, part 5.1A N85-32512
Upward continuation of surface gravity anomalies [AD-A154973] N85-32560

TOPOLOGY
Global Mega-Geomorphology [NASA-CP-2312] N85-32357
Broadcasting topology and routing information in computer networks [AD-A155668] N85-32827

TORNADOES
Automated cell detection as a mesocyclone precursor tool [AD-A154952] N85-32577
Real-time automated detection of mesocyclones and tornado vortex signatures [AD-A154968] N85-32578

TORQUE
Test evaluation of the Honeywell GG1111 Single-Degree-of-Freedom (SDF) strapdown gyroscope [AD-A154768] N85-32307

TOUGHNESS
Graphite/PMR polyimide composites with improved toughness [NASA-TM-87081] N85-32148

TOXIC HAZARDS
Space Station crew safety alternatives study. Volume 2: Threat development [NASA-CR-3855] N85-32133
Review of hazardous waste cleanup and disposal efforts at Tinker Air Force Base [GPO-43-294] N85-32457
Hazardous air pollutants [GPO-43-064] N85-32458
Emergency modeling of hazardous air pollutants [AD-A155441] N85-32461
Air force technical objective document, Aerospace Medical Division, Fiscal Year 1986 [AD-A155195] N85-32762
A crew exposure study. Phase II. Volume 2. At sea. Part A [AD-A155233] N85-32774

TOXICITY
Distribution and abundance of organic thiols N85-32717

TOXINS AND ANTITOXINS
Differences in susceptibility of inbred mice to bacillus anthracis [AD-A155646] N85-32750

TRACE ELEMENTS
Marine aerosols at the Dutch North Sea coast: Size distributions and fractionation of trace elements N85-32664
Anorthositic oceanic crust in the Archean Earth N85-33077

TRAFFIC
An electron microscopic study of urban aerosol N85-32689

TRAILING EDGES
Trailing edge flow and aerodynamic sound. Part 1: Tonal pressure and velocity fluctuations. Part 2: Random pressure and velocity fluctuations [AD-A154947] N85-32097

TRAINING DEVICES
Models for multidimensional tests and hierarchically structured training materials [AD-A155231] N85-32768

TRAJECTORY OPTIMIZATION
SIGMA - A stochastic-integration global minimization algorithm [AD-A154878] N85-32806

TRANSDUCERS
Experimental and theoretical assessment of a new technique for the non-destructive evaluation of laminated panels [AD-A155622] N85-32155

TRANSFER ORBITS
Optimal low thrust transfer using a first-order perturbation model [AD-A154761] N85-32635

TRANSFORMATIONS
Transformation of charged particle beams by concentrating electro-optical systems N85-32925

TRANSFORMERS
T/R switch design for short-range measurements, part 6.1A N85-32515

TRANSIENT RESPONSE
Analysis of the transient response of temporal artery blood flow data relative to various anti-G suit pressure schedules [AD-A155242] N85-32775

TRANSITION TEMPERATURE
Synthesis and properties of arylethersulfone thermoset systems [AD-A154811] N85-32198
Importance and significance of transition temperatures [AD-A154871] N85-32199

TRANSMISSION LINES
Fin line filters technology and electronic warfare [AD-A154975] N85-32237
Microcomputer network: Investigation and implementation [AD-A155631] N85-32826

TRANSMITTANCE
Ship-to-ship propagation: Maritime data analyses [AD-A155484] N85-32325
Nuclear thermal transmittance in the atmosphere using LOWTRAN-6 computer code [AD-A154869] N85-32553

TRANSONIC FLOW
Calculation of transonic steady and oscillatory pressures on a low aspect ratio model and comparison with experiment [NASA-TM-86449] N85-32092
Notes on unsteady transonic cascade flows [AD-A154829] N85-32096
Design of a generator for near-tangential transonic swirling outflow [AD-A155163] N85-32280
An elliptic calculation procedure for 3-D viscous flow N85-32297
Exact solutions of singular equations for viscous transonic flows N85-32882

TRANSPARENCE
The measurement of aircraft windscreen haze and its effect on visual performance [AD-A154949] N85-32114
Transparency of water 9n 186 - 500 nm region N85-32923

TRANSPORT AIRCRAFT
Seat experiments for the full-scale transport aircraft controlled impact demonstration [AD-A155024] N85-32106

TRANSPORT PROPERTIES
Silicon refinement by chemical vapor transport N85-32412
Influence of chemical form, feeding regimen, and animal species on the gastrointestinal absorption of plutonium [DE85-010291] N85-32751
Electrotransport in thin films [AD-A155584] N85-33034
The relation between the age of the subconducting slab and the recycling of sediments into the mantle N85-33063

TRANSVERSE WAVES
Guided-mode launching in a slab waveguide by way of diffraction at the edge of a conducting screen residing on one surface of the slab [AD-A154886] N85-32232

TRAPPING
Trapping of ion conics by downward parallel electric fields [AD-A155306] N85-32568

TRAVELING WAVES
Experiments on the influence of active walls on the initial amplitudes and growths of instability waves [AD-A154630] N85-32275

TREES (PLANTS)
Insights into the phylogenetic positions of photosynthetic bacteria obtained from 5S rRNA and 16S rRNA sequence data N85-32719

TRIBOLOGY
Hertzian contact in two and three dimensions [NASA-TP-2473] N85-32331
TRIGGER CIRCUITS
Coordinated research program in pulsed power physics [AD-A154629] N85-32858
TRITIUM
Tritium technology review [DE85-010504] N85-33006
TROMBE WALLS
Performance analysis of mixed passive solar heating systems [DE85-009624] N85-32455
TROPICAL REGIONS
Aircraft observations of condensation and ice nuclei at a tropical station N85-32613
Formation of particles in the air of the humid tropical forests N85-32639
A statistical study of CCN concentration in subequatorial climate: The particular case of the tropical wet forest N85-32673
Properties of forest derived cloud condensation nuclei N85-32682
Sulfates in marine aerosols over the tropical Western Pacific Ocean N85-32690
TROPICAL STORMS
Forecasting of tropical cyclone motion using an EOF (Empirical Orthogonal Function) representation of wind forcing [AD-A155034] N85-32580
TROPOPAUSE
Comparison of tropopause altitude determination by the Platteville Radar, Sunset Radar and the NWS Rawinsonde N85-32477
Practical use of a tropopause height determination algorithm on an MST radar data set, part 1.8B N85-32479
The Ponape ST radar N85-32549
TROPOSPHERE
Meteorological and aeronomical requirements for MST radar networks (keynote paper), part 1 N85-32467
Tropospheric-stratospheric exchange, part 1.1A N85-32468
A numerical analysis of transient planetary waves and the vertical structure in a meso-strato-troposphere model, part 1.4A N85-32473
Performance of the Colorado wind-profiling network, part 1.5A N85-32475
Vertical transport in the atmosphere: Measurement capabilities and requirements of VHF radars, part 1.6A N85-32476
Morphology of the scattering targets: Fresnel and turbulent mechanisms, part 2.1A N85-32481
Antenna induced range smearing in MST radars N85-32495
Frequency and site selection criteria for MST radars, part 5.1A N85-32512
Urbana radar systems: Possibilities and limitations N85-32540
Progress and plans for the Colorado Wind Profiler Network N85-32542
Millstone Hill radar: Capabilities for S/T observations N85-32548
The Ponape ST radar N85-32549
Measurements of vertical velocity over flat terrain by ST radar and other related uses of the radar data set N85-32550
Eleventh International Conference on Atmospheric Aerosols, Condensation and Ice Nuclei, volume 1 [PB85-182400] N85-32636
A new hypothesis for the observed vertical distribution of atmospheric aerosols N85-32646
On the mechanisms responsible for the formation of typical size spectra and vertical distribution of tropospheric aerosol particles N85-32647
Application of Particle Induced X-ray Emission analysis (PIXE) to aerosol long range transport studies N85-32665
Aircraft observations of cloud condensation nuclei in maritime and continental environments N85-32680
Sulfur Cycle N85-32748
TROPOSPHERIC WAVES
Tropospheric gravity waves observed by three closely spaced ST radars N85-32509
Elimination of range-aliased echoes in the VHF radars N85-32521
TUBE CATHODES
The effect of metal overlayers of thermionic dispenser cathodes [AD-A154795] N85-32995
TUBES
Electrostatic astigmatic tubular lens N85-32955
TUNABLE LASERS
Generation of single nanosecond high-contrast radiation pules (lambda=10.6 micrometers) N85-32886
Lasing on LiF:F(-)2 - dye centers with transverse pumping N85-32890
Tunable lasers with high conversion efficiency N85-32906
Identification of vibrational-rotational transitions of Os-192O4 within frequency tuning limits of high pressure CO2 waveguide laser N85-32917
TUNGSTATES
Spectral-luminescence characteristics and induced emission of Nd-3(+) ion in Gd(2-x)Nd(x)(WO4)3 crystals N85-32912
TURBINE BLADES
Component-specific modeling [NASA-CR-174925] N85-32119
Three-Dimensional Techniques Applied to Internal Flows in Propulsion Systems [AGARD-LS-140] N85-32293
A 3-D Euler method for internal transonic flows computation with a multi-domain approach N85-32298
Calculation of 3-D flow without numerical mixing N85-32301
TURBINE ENGINES
Component-specific modeling [NASA-CR-174925] N85-32119
TURBINE WHEELS
A comparison of experimental and theoretical results for rotordynamic coefficients of four annular gas seals [NASA-CR-176086] N85-32332
TURBINES
Microprocessor control design for a low-head crossflow turbine [AD-A155477] N85-32121
Observations of the use of the setapoint detector [AD-A154533] N85-32208
TURBOJET ENGINES
China has developed a new version of fighter aircraft [AD-A155293] N85-32118
TURBOMACHINERY
Three-Dimensional Techniques Applied to Internal Flows in Propulsion Systems [AGARD-LS-140] N85-32293
An analysis of flow models: From Navier-Stokes to potential flow equations N85-32295
Calculation of 3-D flow without numerical mixing N85-32301
A comparison of experimental and theoretical results for rotordynamic coefficients of four annular gas seals [NASA-CR-176086] N85-32332
TURBULENCE
Large eddy structures in transitional and turbulent flames [AD-A154520] N85-32157
Experiments on the influence of active walls on the initial amplitudes and growths of instability waves [AD-A154630] N85-32275
Velocity and transient measurements in a shock tube using a hot-wire anemometer [AD-A154694] N85-32305
Observations of mesospheric turbulence by rocket probe and VHF radar, part 2.4A N85-32484
Mesospheric measurements of irregularity patches using a 3-antenna interferometer, part 3.6B N85-32496
Techniques for the study of gravity waves and turbulence (keynote paper), part 4 N85-32499
Spectral measurements of turbulence and gravity waves, part 4.2A N85-32501
Relationship of isolated turbulent regions to the general turbulent background, part 4.4A N85-32506
TURBULENCE EFFECTS
Fluctuations in light intensity during backscattering in turbulent medium N85-32956
TURBULENT BOUNDARY LAYER
Trailing edge flow and aerodynamic sound. Part 1: Tonal pressure and velocity fluctuations. Part 2: Random pressure and velocity fluctuations [AD-A154947] N85-32097
An evaluation of four methods of numerical analysis for two-dimensional airfoil flows [AD-A155202] N85-32098
Recession of graphitic nozzles in rocket motors N85-32144
Investigations of micro-turbulence in the bottom of the boundary layer [AD-A155148] N85-32585
Thermal contraction of current flow through electrode turbulent boundary layer N85-32926
TURBULENT DIFFUSION
Estimation of vertical diffusion from observations of Atmospheric turbulence layers, part 4.4B N85-32507
MST radar data management N85-32532
TURBULENT FLOW
Injection of drag reducing additives into turbulent water flows: Two-component velocity measurements and mixing length model predictions [AD-A154604] N85-32274
Numerical solutions of turbulent models for flow over a flat plate with angle of attack [DE85-010380] N85-32286
Determination of billows and other turbulent structures, part 4.1A N85-32500
Recent results at the Sunset radar N85-32536
Theoretical foundations of turbulent flows N85-32880
TURBULENT MIXING
Vertical transport in the atmosphere: Measurement capabilities and requirements of VHF radars, part 1.6A N85-32476
Morphology of the scattering targets: Fresnel and turbulent mechanisms, part 2.1A N85-32481
TURBULENT WAKES
Trailing edge flow and aerodynamic sound. Part 1: Tonal pressure and velocity fluctuations. Part 2: Random pressure and velocity fluctuations [AD-A154947] N85-32097
TWO DIMENSIONAL BODIES
On the dependence of the convergence of Gummel's algorithm on the regularity of the solution [AD-A154628] N85-32832
TWO DIMENSIONAL FLOW
An evaluation of four methods of numerical analysis for two-dimensional airfoil flows [AD-A155202] N85-32098
TWO-WAVELENGTH LASERS
High-power two-frequency CW dye laser N85-32900

U

U.S.S.R.
on the transport of large condensation nuclei in the atmosphere at various altitudes over the territory of the USSR N85-32698
USSR Space Life Sciences Digest [NASA-CR-3922] N85-32709
ULTRAHIGH FREQUENCIES
Potential advantages of the spaced antenna method for operational wind profiling, part 3.1B N85-32490
ULTRASHORT PULSED LASERS
Optical inhomogeneities in a nanosecond-pulse iodine photodissociation laser with slow UV radiation pumping N85-32902
ULTRASONIC RADIATION
Development of ultrasonic modeling techniques for the study of crustal inhomogeneities [AD-A155206] N85-32565
ULTRASONICS
Reliability of void detection in structural ceramics using scanning laser acoustic microscopy [NASA-TM-87035] N85-32337
ULTRAVIOLET ABSORPTION
Micromolecular modeling N85-32405
Heating of the deep chromosphere during solar flares [AD-A155256] N85-33100
ULTRAVIOLET ASTRONOMY
Research in extreme ultraviolet and far ultraviolet astronomy [NASA-CR-176068] N85-33060
ULTRAVIOLET MICROSCOPY
Interaction of solutes with stretched polymers [AD-A154662] N85-32196
ULTRAVIOLET PHOTOMETRY
Research in extreme ultraviolet and far ultraviolet astronomy [NASA-CR-176068] N85-33060
ULTRAVIOLET RADIATION
Polymerizable ultraviolet stabilizers N85-32406
Photoinduced active sites on ice nucleating aerosol of silver iodide N85-32601
Excimer-laser generator of powerful UV picosecond pulses synchronized with picosecond pulses in visible and IR bands N85-32903
ULTRAVIOLET SPECTROSCOPY
Transparency of water 9n 186 - 500 nm region N85-32923
UNDERGROUND EXPLOSIONS
Experimental and analytic characterization of nonlinear seismic attenuation [AD-A154760] N85-32556
UNDERGROUND STRUCTURES
Literature survey of underground construction methods for application to hardened facilities [AD-A155212] N85-32351
UNDERWATER ACOUSTICS
Development of computer programs using the method of images to predict the sound field in a wedge overlaying a fast fluid and comparison with laboratory experiments [AD-A154580] N85-32797
The moving thermoacoustic array: A theoretical feasibility study [AD-A154510] N85-32980

Discrete-element acoustic analysis of submerged structures using doubly asymptotic approximations [AD-A154959] N85-32987
A random layer model for reflection from ocean bottom sediments [AD-A155019] N85-32988
Propagation of sound in a layered laboratory model [AD-A155141] N85-32989
Understanding coherence losses incurred by bottom-retained signals [AD-A155559] N85-32992

UNDERWATER ENGINEERING
The dynamics of slack marine cables [AD-A155022] N85-32349

UNDERWATER EXPLOSIONS
An investigation into the comparisons of the underwater shock effects on a stiffened flat plate to the predictive nature of a computer model [AD-A155612] N85-32355

UNDERWATER STRUCTURES
Discrete-element acoustic analysis of submerged structures using doubly asymptotic approximations [AD-A154959] N85-32987

UNITED STATES
Helicopter noise survey for selected cities in the contiguous US [AD-A154893] N85-32985

UNIVERSITIES
The Naval Postgraduate School Flight Mechanics Laboratory: A feasibility study [AD-A154578] N85-32127

UNSTEADY FLOW
Identification of unsteady aerodynamics and aeroelastic integro-differential systems [NASA-TM-86749] N85-32851
Toward the propagation of waves in unsteady media N85-32881

UNSTEADY STATE
MPS solidification model. Analysis and calculation of macrosegregation in a casting ingot [NASA-CR-171589] N85-32178
Toward the propagation of waves in unsteady media N85-32881

UPPER ATMOSPHERE
Observations of mesospheric turbulence by rocket probe and VHF radar, part 2.4A N85-32484
The MU radar now partly in operation N85-32543

URANIUM FLUORIDES
Liquid-phase compositions from vapor-phase analyses 2: Adaptation of the Prausnitz program to UF6 and some of its potential impurities [DE85-011521] N85-32819

USER MANUALS (COMPUTER PROGRAMS)
Tip vortex computer code SRATIP. User's guide [NASA-CR-172603] N85-32093
User's guide for computer program CGFAG, Concrete General Flexure Analysis with Graphics [AD-A155555] N85-32204
BLAF: A blast field reconstruction program from pressure histories [AD-A155300] N85-32283
CARE 3 user friendly interface user's guide [NASA-CR-172608] N85-32791
Research on an expert system for database operation of simulation-emulation math models. Volume 2, Phase 1: Results [NASA-CR-176088] N85-32793
Praxis release notes, version 7.3 [DE85-011862] N85-32820

USER REQUIREMENTS
Design guidelines for user-system interface software [AD-A154907] N85-32807
The effect of communication-language designs on software specifications [AD-A155173] N85-32809
Praxis release notes, version 7.3 [DE85-011862] N85-32820
The flow of scientific and technical information in the US Army Research Laboratories [AD-A155050] N85-33043

UTILITIES
Experimental investigation of a variable speed constant frequency electric generating system from a utility perspective [NASA-CR-174950] N85-32251

V

VACUUM APPARATUS
Effective brightness of zero-point fluctuations of the electromagnetic vacuum accompanying parametric scattering of light N85-32951

VACUUM CHAMBERS
Tailored vacuum chambers for ac magnets [DE85-010767] N85-32319

VACUUM DEPOSITION
New metal coating method developed N85-32191

VACUUM TESTS
Measurement of damping of graphite epoxy materials [NASA-CR-176073] N85-32334

VALLEYS
VALMET: A valley air pollution model [DE85-010820] N85-32463

VALVES
Sobolev-Poincare's inequality and the Neumann problem for u sub t = divergence of the absolute value of the gradient u to the p-2 power x the gradient u [AD-A154788] N85-32839

VANADIUM OXIDES
The Konstantinov effect and absorption of sound in inhomogeneous media N85-32861

VANES
Design of a generator for near-tangential transonic swirling outflow [AD-A155163] N85-32280

VAPOR DEPOSITION
New metal coating method developed N85-32191

VAPOR PHASE EPITAXY
Doping superlattices in organometallic VPE InP [AD-A155151] N85-33029

VAPOR PHASES
Liquid-phase compositions from vapor-phase analyses 2: Adaptation of the Prausnitz program to UF6 and some of its potential impurities [DE85-011521] N85-32819
Microwave semiconductor research: Materials, devices and circuits and gallium arsenide ballistic electron transistors [AD-A154698] N85-33024

VAPORS
Status of boron combustion research [AD-A154762] N85-32160
Silicon refinement by chemical vapor transport N85-32412
A crew exposure study. Phase II. Volume 2. At sea. Part A [AD-A155233] N85-32774

VARIATIONS
On the transformation regularities of time series of solid aerosol concentrations in the surface atmospheric layer N85-32648
Object identification and manipulation using silhouette moments [AD-A154755] N85-33011
Optical output stabilization method for direct current arc lamps [AD-A154987] N85-33013

VECTOR SPACES
Simulation of complex three-dimensional flows [NASA-TM-86773] N85-32831

VEGETATION
Space imagery and some geomorphological problems of the Guiana Shield, South America N85-32368

VEGETATION GROWTH
Hydroponics developments for spaceship garden N85-32754

VELOCITY
BLAF: A blast field reconstruction program from pressure histories [AD-A155300] N85-32283
Numerical solutions of turbulent models for flow over a flat plate with angle of attack [DE85-010380] N85-32286
Horizontal and vertical structure of velocity, potential vorticity and energy in the gulf stream [AD-A154753] N85-32702

VELOCITY MEASUREMENT
Improvement of vertical velocity measurements, part 3.4B N85-32494
Problems and solutions in analyzing partial-reflection drift data by correlation techniques N85-32529

VENUS ATMOSPHERE
Water loss from Venus: Implications for the Earth's early atmosphere N85-33087

VERTEBRAE
Analysis of long bone and vertebral failure patterns [AD-A154796] N85-32758

VERTEBRAL COLUMN
Analysis of long bone and vertebral failure patterns [AD-A154796] N85-32758

VERTICAL AIR CURRENTS
Tropospheric gravity waves observed by three closely spaced ST radars N85-32509
Thunderstorm phenomena and weather radar scanning strategies [DOT/FAA/PM-85/14] N85-32573

VERTICAL DISTRIBUTION
Observations of mesospheric turbulence by rocket probe and VHF radar, part 2.4A N85-32484
Visibility and vertical structure measurements in southern Germany [AD-A154714] N85-32574
A new hypothesis for the observed vertical distribution of atmospheric aerosols N85-32646
On the mechanisms responsible for the formation of typical size spectra and vertical distribution of tropospheric aerosol particles N85-32647

VERTICAL MOTION
A simple model for testing the effects of gravity-wave-produced vertical oscillations of scattering irregularities on spaced-antenna, horizontal drift measurements N85-32489
Estimation of vertical diffusion from observations of Atmospheric turbulence layers, part 4.4B N85-32507

VERTICAL ORIENTATION
Improvement of vertical velocity measurements, part 3.4B N85-32494
Determination of horizontal and vertical wavelengths of gravity waves in the mesosphere by spaced wind measurements N85-32510
Trapping of ion conics by downward parallel electric fields [AD-A155306] N85-32568
Visibility and vertical structure measurements in southern Germany [AD-A154714] N85-32574
Horizontal and vertical structure of velocity, potential vorticity and energy in the gulf stream [AD-A154753] N85-32702

VERY HIGH FREQUENCIES
Field antenna handbook [AD-A155204] N85-32242
A modified Fresnel scattering model for the parameterization of Fresnel returns, part 2.3A N85-32483
Observations of mesospheric turbulence by rocket probe and VHF radar, part 2.4A N85-32484
Usefulness of multifrequency MST radar measurements, part 2.6B N85-32487
Potential advantages of the spaced antenna method for operational wind profiling, part 3.1B N85-32490
Improvement of vertical velocity measurements, part 3.4B N85-32494
Interferometer applications of VHF radars, part 3.6A N85-32497
Testing and optimizing MST coaxial collinear arrays, part 6.4A N85-32518
Elimination of range-aliased echoes in the VHF radars N85-32521
A note on the proposed UK VHF radar N85-32545

VERY LONG BASE INTERFEROMETRY
Mapping with QUASAT (quasar satellite) using short observation times [AD-A155155] N85-32141
Crustal dynamics project data analysis fixed station VLBI geodetic results [NASA-TM-86229] N85-32465

VERY LOW FREQUENCIES
VLF (Very low frequency) workshop held at San Diego California, 24-25 January 1985 [AD-A154652] N85-32224
Numerical modeling of subsurface communication [DE85-012818] N85-32249

VESTIBULAR TESTS
Mission operations requirements document for D-1 Experiment 102, Vestibular Experiments in Spacelab [NASA-TM-87495] N85-32129

VESTIBULES
Mission operations requirements document for D-1 Experiment 102, Vestibular Experiments in Spacelab [NASA-TM-87495] N85-32129

VHSIC (CIRCUITS)
GAO (General Accounting Office) assessment of DOD's Very High Speed Integrated Circuits (VHSIC) technology program [AD-A155109] N85-32261

VIBRATION
A phase-locked frequency multiplier for the signal averaging of the vibration of the Wessex helicopter input spiral bevel pinion [AD-A154914] N85-32113
Proposal for modifications to the Wessex helicopter main rotor gearbox vibration monitoring program [AD-A155196] N85-32117
Calculation of molecular constants potential energy curves and Franck-Condon factors for lead oxide [AD-A154521] N85-32158

VIBRATION DAMPING
A comparison of experimental and theoretical results for rotordynamic coefficients of four annular gas seals [NASA-CR-176086] N85-32332
Modelling and parameter estimation for distributed vibratory systems [AD-A154518] N85-32344

VIBRATION MEASUREMENT
Measurement of damping of graphite epoxy materials [NASA-CR-176073] N85-32334
VIBRATIONAL SPECTRA
Modelling and parameter estimation for distributed vibratory systems [AD-A154518] N85-32344
VIDEO DATA
Balloon-borne video cassette recorders for digital data storage [PAPER-OG-9.3-11] N85-33050
VIDEO DISKS
Realizing the full potential of the video disc for mapping applications [AD-A154966] N85-32391
VIKING ORBITER SPACECRAFT
Geomorphic classification of Icelandic and Martian volcanoes: Limitations of comparative planetology research from LANDSAT and Viking orbiter images N85-32372
VISCOSITY
Large-time behavior of viscous surface waves [AD-A154805] N85-32278
VISCOUS FLOW
Tip vortex computer code SRATIP. User's guide [NASA-CR-172603] N85-32093
Large-time behavior of viscous surface waves [AD-A154805] N85-32278
Computation of three-dimensional, inviscid, rotational flows N85-32296
A 3-D Euler method for internal transonic flows computation with a multi-domain approach N85-32298
Exact solutions of singular equations for viscous transsonic flows N85-32882
VISIBILITY
The measurement of aircraft windscreen haze and its effect on visual performance [AD-A154949] N85-32114
Forecasting atmospheric visibility over the summer north Atlantic using the principal discriminant method [AD-A155537] N85-32593
Ice fog as an electro-optical obscurant [AD-A155059] N85-33015
VISIBLE SPECTRUM
Absorption and scattering properties of aerosols of aggregated particles in the infrared spectral region [AD-A155475] N85-32591
Transparency of water 9n 186 - 500 nm region N85-32923
VISION
Visual phenomena produced by binocularly disparate dynamic visual noise [AD-A154758] N85-32757
VISUAL DISCRIMINATION
An error-dependent model of instrument-scanning behavior in commercial airline pilots [NASA-CR-3908] N85-32765
VISUAL PERCEPTION
The measurement of aircraft windscreen haze and its effect on visual performance [AD-A154949] N85-32114
Visual phenomena produced by binocularly disparate dynamic visual noise [AD-A154758] N85-32757
VISUAL STIMULI
Visual phenomena produced by binocularly disparate dynamic visual noise [AD-A154758] N85-32757
VITAMINS
The effects of prolonged feeding meal, ready-to-eat (MRE) operational rations [AD-A154763] N85-32773
VOICE COMMUNICATION
Secure digital voice communications in the Defense Data Network (DDN) [AD-A154677] N85-32226
Interactive on-line conferences [AD-A154723] N85-32227
Application of adaptive noise cancellation to Coast Guard voice communications [AD-A154798] N85-32230
Software for interactive on-line conferences [AD-A154742] N85-32601
VOIDS
Reliability of void detection in structural ceramics using scanning laser acoustic microscopy [NASA-TM-87035] N85-32337
VOLCANOES
Data analysis for lidar and quartz crystal microbalance systems [NASA-CR-172601] N85-32464
Changes in the organic material in lakes in the blast zone of Mount St. Helens, Washington: Hydrologic effects of the eruptions [GS-CIRC-850-1] N85-32551
VOLCANOLOGY
Andrean examples of mega-geomorphology themes N85-32367
VOLT-AMPERE CHARACTERISTICS
Electrochemistry of Hexanitroazobenzene (HNAB) [DE85-010807] N85-32171
VOLTMETERS
R, L, C, G measurement N85-32784
VORTEX SHEDDING
Trailing edge flow and aerodynamic sound. Part 1: Tonal pressure and velocity fluctuations. Part 2: Random pressure and velocity fluctuations [AD-A154947] N85-32097
VORTEX SHEETS
A panel method study of vortex sheets with special emphasis on sheets of axisymmetric geometry [NASA-CR-177365] N85-32095
VORTICES
Large eddy structures in transitional and turbulent flames [AD-A154520] N85-32157
Determination of billows and other turbulent structures, part 4.1A N85-32500
VORTICITY
Horizontal and vertical structure of velocity, potential vorticity and energy in the gulf stream [AD-A154753] N85-32702
VORTICITY EQUATIONS
A numerical study of Taylor-Vortex flow [AD-A154787] N85-32277
VULNERABILITY
Literature survey of underground construction methods for application to hardened facilities [AD-A155212] N85-32351

W

WAFERS
Interfacial bonding stability N85-32409
WAKES
Using ship wake patterns to evaluate SAR (Synthetic Aperture Radar) ocean wave imaging mechanisms. Joint US-Canadian Ocean Wave Investigation Project [AD-A154633] N85-32223
WALL FLOW
Injection of drag reducing additives into turbulent water flows: Two-component velocity measurements and mixing length model predictions [AD-A154604] N85-32274
Experiments on the influence of active walls on the initial amplitudes and growths of instability waves [AD-A154630] N85-32275
WALL TEMPERATURE
Numerical solutions of turbulent models for flow over a flat plate with angle of attack [DE85-010380] N85-32286
WALLS
Wall flames and implications for upward flame spread [FAA-CT-85-2] N85-32103
Construction of University of Missouri, Rolla's full scale cloud simulation chamber and applied research [AD-A154682] N85-32128
In-situ measurement of wall thermal performance: Data interpretation and apparatus design recommendations [DE85-011979] N85-32289
WARNING SYSTEMS
Automated cell detection as a mesocyclone precursor tool [AD-A154952] N85-32577
WASHINGTON
Changes in the organic material in lakes in the blast zone of Mount St. Helens, Washington: Hydrologic effects of the eruptions [GS-CIRC-850-1] N85-32551
WASTE DISPOSAL
Review of hazardous waste cleanup and disposal efforts at Tinker Air Force Base [GPO-43-294] N85-32457
WASTE ENERGY UTILIZATION
Feasibility study for small group water desalination equipment [AD-A155106] N85-32164
WATER
Two-phase flow visualization in a transparent, atmospheric pressure, boiling water loop [DE84-016857] N85-32288
Polymer-water interaction studies N85-32411
Mechanism of heterogeneous deposition ice nucleation near water-saturation N85-32597
Ice nucleation of single water droplet by silver iodide: A laboratory observation N85-32630
Critical supersaturations with respect to water for fast condensation-freezing ice nucleation N85-32632
Monte Carlo studies of H2O layers adsorbed on a model basal face of AgI N85-32633
Cloud condensation on insoluble particles N85-32670
Interactions among sulfide-oxidizing bacteria N85-32741
Physical chemical state of water in living cells [AD-A154566] N85-32749
Transparency of water 9n 186 - 500 nm region N85-32923
Activation analysis of natural water using neutrons of various energies N85-32924
WATER FLOW
Injection of drag reducing additives into turbulent water flows: Two-component velocity measurements and mixing length model predictions [AD-A154604] N85-32274
Reverification of the Chesapeake Bay model [AD-A155486] N85-32706
WATER HEATING
Energy and Technology Review [DE85-011767] N85-33061
WATER LANDING
Air carrier overwater emergency equipment and procedures [PB85-917006] N85-32105
WATER MANAGEMENT
Empirical methods for predicting eutrophication in impoundments. Report 3. Phase 2. Model refinements [AD-A155483] N85-32462
WATER QUALITY
Empirical methods for predicting eutrophication in impoundments. Report 3. Phase 2. Model refinements [AD-A155483] N85-32462
WATER RECLAMATION
Space station ECLSS integration analysis: Simplified General Cluster Systems Model, ECLS System Assessment Program enhancements [NASA-CR-176089] N85-32796
WATER RESOURCES
Feasibility study for small group water desalination equipment [AD-A155106] N85-32164
WATER VAPOR
Ship-to-ship propagation: Maritime data analyses [AD-A155484] N85-32325
On the efficiency of the mechanism of ice particles formation in the vapor supersaturation field around a freezing droplet N85-32606
Basic ice nucleation mechanisms on mono and microcrystals and ice forming nuclei. Theoretical analysis and experimental results achieved in the laboratory over the past ten years: Review paper N85-32629
A simple model to investigate the activation process in waterclouds N85-32675
The interaction of polynuclear aromatic hydrocarbons PAH's with water vapor and their role as condensation nuclei in the formation of haze and fog N85-32695
WATER WAVES
Discovery of a nonpropagating hydrodynamic soliton [AD-A155569] N85-32268
Coastal erosion along Monterey Bay [AD-A155610] N85-32707
Theory of soliton waves [AD-A154784] N85-32837
WAVE AMPLIFICATION
Amplification of electromagnetic wave by electron stream with negative velocity differences N85-32941
Electromagnetic wave amplification during cyclotron resonance in a medium N85-32942
WAVE DISPERSION
Beam diffusion in linear ionospheric layer N85-32958
Methods for measuring and analyzing dispersion properties of multimode fiber optic lightpipes (a review) N85-32960
Optical image of bounded objects N85-32968
WAVE EQUATIONS
Qualitative analysis of sign-bit processing [AD-A154776] N85-32804
WAVE FUNCTIONS
Overlap integrals for atom-metal surface interactions [AD-A155038] N85-32998
WAVE INTERACTION
Some recent developments in the interpretation of MST radar returns from clear air (keynote paper), part 2 N85-32480
WAVE PACKETS
Electrostatic ion cyclotron instability due to a nonuniform electric field perpendicular to the external magnetic field [AD-A155474] N85-33019
WAVE PROPAGATION
Field antenna handbook [AD-A155204] N85-32242
Numerical modeling of subsurface communication [DE85-012818] N85-32249
Dynamic fracture of concrete and other heterogeneous materials [AD-A154513] N85-32343

Gravity waves from the stratosphere to the mesosphere, part 1.3B N85-32471
Gravity-wave spectra in the atmosphere observed by MST radar, part 4.2B N85-32502
Experimental and analytic characterization of nonlinear seismic attenuation
[AD-A154760] N85-32556
Development of ultrasonic modeling techniques for the study of crustal inhomogeneities
[AD-A155206] N85-32565
The effects of subrefractive layers and elevated ducts on airborne radar and ESM (Electronic Surveillance Measures)
[AD-A155524] N85-32592
New approximations and findings of theory of nonlinear acoustic beams N85-32863
Reflection of acoustic beam from inhomogeneous boundary N85-32864
Toward the propagation of waves in unsteady media N85-32881
Laser radiation propagation in inertialess nonlinear medium N85-32898

WAVE REFLECTION
Most desirable terrain, e.g., flat vs valley location, part 5.1B N85-32513
A random layer model for reflection from ocean bottom sediments
[AD-A155019] N85-32988

WAVE SCATTERING
Development of ultrasonic modeling techniques for the study of crustal inhomogeneities
[AD-A155206] N85-32565
Acoustic wave scattering by round cylindrical shell reinforced with stringers N85-32916
Investigation of ion-acoustic plasma turbulence in field of powerful electromagnetic wave by CO2-laser radiation scattering N85-32935

WAVEFORMS
Huffman-coded pulse compression waveforms
[AD-A155322] N85-32243

WAVEGUIDE FILTERS
Fin line filters technology and electronic warfare
[AD-A154975] N85-32237

WAVEGUIDES
Guided-mode launching in a slab waveguide by way of diffraction at the edge of a conducting screen residing on one surface of the slab
[AD-A154886] N85-32232

WAVELENGTHS
Increase of antenna area instead of transmitter power, part 6.3A N85-32517
Investigation of reproducibility of emission wavelength of helium-neon laser with external neon absorption cell (0.63 micrometers) N85-32684

WEAK INTERACTIONS (FIELD THEORY)
Spatial parity violation in elastic neutron-nuclei interaction channel N85-32932

WEAPON SYSTEMS
Meteorological weapons
[AD-A154735] N85-32575

WEATHER
Middle Atmosphere Program. Handbook for MAP. Volume 14: URSI/SCOSTEP Workshop on Technical Aspects of MST Radar
[NASA-CR-176085] N85-32466
Investigations of micro-turbulence in the bottom of the boundary layer
[AD-A155148] N85-32585
A simulation of weather in 3D space
[AD-A155221] N85-32586

WEATHER FORECASTING
Automated cell detection as a mesocyclone precursor tool
[AD-A154952] N85-32577
Forecasting of tropical cyclone motion using an EOF (Empirical Orthogonal Function) representation of wind forcing
[AD-A155034] N85-32580

WEATHER MODIFICATION
Meteorological weapons
[AD-A154735] N85-32575
Experimental studies of the kinetics of deposition nucleation on an ice nucleant used in weather modification N85-32598
Ice nucleating characteristics of Capparis Aphylla, an Indian herb N85-32619

WEIBULL DENSITY FUNCTIONS
Weibull distribution based on maximum likelihood with interval inspection data
[NASA-TM-86515] N85-32847

WEIGHT (MASS)
Preliminary sizing and performance of aircraft
[NASA-TM-86357] N85-32111

WEIGHTLESSNESS
Mission operations requirements document for D-1 Experiment 102, Vestibular Experiments in Spacelab
[NASA-TM-87495] N85-32129
Analysis of the transient response of temporal artery blood flow data relative to various anti-G suit pressure schedules
[AD-A155242] N85-32775

WETTING
Mechanics of a gaseous film barrier to lubricant wetting of elastohydrodynamically lubricated conjunctions
[NASA-TP-2500] N85-32330

WIND (METEOROLOGY)
Aeolian geomorphology from the global perspective N85-32373
Diagnostics of severe convection and subsynoptic scale ageostrophic circulations
[NASA-CR-171581] N85-32571
Notes on atmospheric stability, turbulence, and its measurements
[AD-A155230] N85-32588

WIND DIRECTION
Practicality of electronic beam steering for MST/ST radars, part 6.2A N85-32516
Mean flow and turbulence in complex terrain
[AD-A155138] N85-32583

WIND MEASUREMENT
Facility for large-scale hazardous gas testing
[DE85-011852] N85-32169
Performance of the Colorado wind-profiling network, part 1.5A N85-32475
Potential advantages of the spaced antenna method for operational wind profiling, part 3.1B N85-32490
Determination of horizontal and vertical wavelengths of gravity waves in the mesosphere by spaced wind measurements N85-32510
Elimination of range-aliased echoes in the VHF radars N85-32521
Data base for the Colorado profiling network N85-32533

WIND PROFILES
Performance of the Colorado wind-profiling network, part 1.5A N85-32475
Potential advantages of the spaced antenna method for operational wind profiling, part 3.1B N85-32490
High resolution evidence for the Garrett-Munk spectrum of stratospheric gravity waves N85-32503
On the spectrum of atmospheric velocity fluctuations seen by MST/ST radar and their interpretation N85-32504
Relationship of isolated turbulent regions to the general turbulent background, part 4.4A N85-32506
Testing and optimizing MST coaxial collinear arrays, part 6.4A N85-32518
Elimination of range-aliased echoes in the VHF radars N85-32521
Data base for the Colorado profiling network N85-32533
Recent results at the Sunset radar N85-32536
Progress and plans for the Colorado Wind Profiler Network N85-32542

WIND TUNNEL MODELS
A systematic plan for the continued study of dimensional stability of metallic alloys considered for the fabrication of cryogenic wind tunnel models
[NASA-CR-172449] N85-32172
Machining-induced deformation in stepped specimens of PH 13-8 Mo, 18 nickel maraging steel grade 200T1 and grain-refined HP 9-4-20
[NASA-CR-172450] N85-32177

WIND TUNNEL TESTS
Aerodynamic characteristics of the standard dynamics model in coning motion at Mach 0.6
[NASA-TM-86717] N85-32094
Wind tunnel drag evaluations of helicopter nose sections
[AD-A155489] N85-32100

WIND TURBINES
Experimental investigation of a variable speed constant frequency electric generating system from a utility perspective
[NASA-CR-174950] N85-32251

WIND VELOCITY
Improved Nominal Operating Cell Temperature (NOCT) test procedure N85-32449
Synoptic-scale dynamics with vertical velocity, part 1.8A N85-32478
Relationship of spaced antenna and Doppler techniques for velocity measurements (keynote paper), part 3 N85-32488
Effects of line-of-sight velocity on spaced-antenna measurements, part 3.5A N85-32496
Use of the VAD technique and measurements of momentum flux in the stratosphere at Aercibo, part 4.3A N85-32505
Tropospheric gravity waves observed by three closely spaced ST radars N85-32509
Data base for the Colorado profiling network N85-32533
Status of the Jicamarca radar N85-32535
Recent results at the Sunset radar N85-32536
Mean flow and turbulence in complex terrain
[AD-A155138] N85-32583

WIND VELOCITY MEASUREMENT
Relationship of spaced antenna and Doppler techniques for velocity measurements (keynote paper), part 3 N85-32488
The Adelaide VHF radar: Capabilities and future plans N85-32546
Millstone Hill radar: Capabilities for S/T observations N85-32548

WINDSHIELDS
The measurement of aircraft windscreen haze and its effect on visual performance
[AD-A154949] N85-32114

WING TIP VORTICES
Tip vortex computer code SRATIP. User's guide
[NASA-CR-172603] N85-32093

WINTER
Airborne measurements of atmospheric ice nuclei N85-32612

WORK-REST CYCLE
Human performance in continuous/sustained operations and the demands of extended work/rest schedules. An annotated bibliography
[AD-A155619] N85-32771

WORKSTATIONS
NASA space station automation: AI-based technology review. Executive summary
[NASA-CR-176096] N85-32135

X

X RAY ANALYSIS
Application of Particle Induced X-ray Emission analysis (PIXE) to aerosol long range transport studies N85-32665

X RAY DIFFRACTION
Modification of the grain size of sputtered copper with additions of oxygen, krypton, silver, or yttrium
[DE85-010975] N85-32189
The measurement of strain fields by X-ray topographic contour mapping
[AD-A154870] N85-32348

X RAY FLUORESCENCE
Variations of particulate sulfur concentrations in a coastal atmospheric environment in connection with the change of air masses origin N85-32692

X RAY SCATTERING
Comparison of findings of theories describing reflection from real surface with experiments in region of ultrasoft X-radiation N85-32950

X RAY SPECTROSCOPY
CCD-based X-ray spectrometry for on-line determination of laser plasma electron temperature N85-32938
Soft X-ray polychromator for the Solar Maximum Mission
[NASA-CR-175297] N85-33096

X RAYS
Comparison of findings of theories describing reflection from real surface with experiments in region of ultrasoft X-radiation N85-32950
Contributions to the 19th International Cosmic Ray Conference
[NASA-CR-176060] N85-33044

XENON
Powerful XeCl excimer electric discharge laser with good temporal stability and fast response time N85-32911

XENON ISOTOPES
The degassing history of the Earth: Noble gas studies of Archaean cherts and zero age glassy submarine basalts N85-33072

Y

YAG LASERS
Choice of optimum saturating absorber for YAG passive mode-locking laser N85-32893
Operation of solid state lasers exposed to electron beam N85-32895
Passive Q-modulation of optical cavities by KCl crystals containing OH(-) -ions N85-32915

YTTRIUM
A study of adherent oxide scales
[AD-A155554] N85-32188
Modification of the grain size of sputtered copper with additions of oxygen, krypton, silver, or yttrium
[DE85-010975] N85-32189

Z

ZERO POINT ENERGY
Effective brightness of zero-point fluctuations of the electromagnetic vacuum accompanying parametric scattering of light N85-32951
ZINC
Plasma mass and effective inductance in a small railgun
[AD-A154644] N85-32304
ZINC OXIDES
High temperature solar electrothermal processing 2. Zinc from zinc oxide
[AD-A154747] N85-32159
ZIRCONIUM
Chemical constraints on the evolution of Archean continental crust N85-33093
ZIRCONIUM COMPOUNDS
Dating Archean zircon by ion microprobe: New light on an old problem N85-33094

PERSONAL AUTHOR INDEX

Typical Personal Author Index Listing

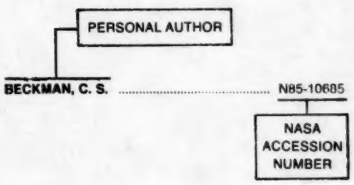

Listings in this index are arranged alphabetically by personal author. The NASA accession number denotes the number by which the citation is identified.

A

ABAKUMOV, V. N. N85-32874
ABBOTT, D. N85-33063
ABDELSAMAD, A. S. N85-32814
ABDULLAYEV, A. A. N85-32924
ABROSKINA, O. N. N85-32951
ACTON, L. W. N85-33096
ADAMEC, D. N85-32704
ADAMS, G. W. N85-32537
ADAMS, T. C., JR. N85-32210
ADOLPH, H. G. N85-32210
AGABEKYAN, A. S. N85-32922
AGAYAN, G. M. N85-32978
AKAU, R. L. N85-32328
AKHMANOV, S. A. N85-32903
AKINS, F. R. N85-32772
AKSENOV, M. Y. N85-32600
AL-NAIMI, R. N85-32609
ALAM, M. K. N85-32416
ALCABIN, M. N85-32101
ALEKSANDROV, A. F. N85-32943
ALEXANDER, E. C., JR. N85-33075
ALFEEROV, Z. I. N85-32908
ALFIMENKOV, V. P. N85-32932
ALIKAYEV, V. V. N85-32949
ALIMOV, D. T. N85-32919
ALIVISATOS, A. P. N85-32994
ALLEN, A. N85-32164
ALLWINE, K. J. N85-32463
ALTHOUSE, W. E. N85-33049
N85-33050
ALTSCHUL, R. E. N85-32834
ALUFFI-PENTINI, F. N85-32806
AMIRANASHVILI, A. G. N85-32659
AMIRANOFF, F. N85-33022
ANDERLE, R. J. N85-32231
ANDERSON, A. B. N85-32173
N85-32174
N85-32175
N85-32176
ANDERSON, D. N85-32152
ANDREYEV, A. P. N85-32937
ANDRIAMBELONA, H. N85-32629
ANDRIES, M. G. N85-32120
ANJIAN, J. N85-32668
ANTONIEWICZ, R. F. N85-32122
ANYZ, F. N85-32631
APOLLONOV, V. V. N85-32886
APPS, R. N85-32307
ARABADZHI, V. I. N85-32939
ARNAUD, D. F. N85-32247
ARNETT, J. C. N85-32448
ARNOLD, F. E. N85-32198
ARNOLD, J. M. N85-32258
ARONSON, J. R. N85-32591
ARRHENIUS, G. N85-33064
ARSENEAULT, D. S. N85-32244
ARSENTEV, I. N. N85-32908
ASHWAL, L. D. N85-33062
ASTER, R. W. N85-32398
ASTLEFORD, W. J. N85-32774
ATSAGORTSYAN, K. Z. N85-32942
AVERBAKH, V. S. N85-32897
AVERY, S. K. N85-32528
N85-32530
AVETISYAN, G. K. N85-32942
AWRAMIK, S. N85-32711
AYRES, L. N85-32751

B

BAAKLINI, G. Y. N85-32337
BABKINA, T. V. N85-32960
BABRAUSKAS, V. N85-32104
BADA, J. L. N85-33065
BAGGETT, P. N85-32770
BAILEY, C. E. N85-33033
BAILEY, D. H. N85-32795
BAILEY, I. H. N85-32657
BAILEY, R. S. N85-32264
BAKANOV, S. P. N85-32679
BAKER, V. R. N85-32358
BAKHANOVA, R. A. N85-32601
N85-32626
BAKLANOV, A. M. N85-32602
BAKSHI, P. M. N85-32567
BALDINI, A. A. N85-32390
BALENT, B. F. N85-32812
BALLANTYNE, J. N85-33024
BALLATO, A. N85-32311
BALSLEY, B. B. N85-32470
N85-32479
N85-32483
N85-32509
N85-32530
N85-32539
N85-32549
BALSONE, S. J. N85-32181
BALYKIN, V. I. N85-32900
BANKS, H. T. N85-32829
BAROSS, J. N85-33074
BARTON, J. T. N85-32795
BASOV, N. N85-32885
BASU, B. N85-32567
BASU, S. N85-32559
BATEMAN, T. S. N85-32852
BATIFOL, J. J. N85-32695
BAUDET, J. N85-32673
BAUMAN, E. G. N85-32192
BAYTSUR, G. G. N85-32886
BAZANT, Z. N85-32343
BAZAROV, Y. N. N85-32917
BEALE, G. O. N85-32792
N85-32793
BEALE, J. T. N85-32278
BECKER, N. M. N85-32393
BEDFORD, A. J. N85-32304
BEDILOV, M. R. N85-32895
BEDNAREK, M. H. N85-32347
BEGALISHVILI, N. A. N85-32674
BEHANNON, K. W. N85-33055
BELENOV, E. M. N85-32904
BELYTSCHKO, T. N85-32343
BELYY, S. Y. N85-32868
BENNETT, R. M. N85-32092
BENOIST, M. B. N85-32695
BENSON, D. J. N85-32846
BERENBERG, V. A. N85-32912
BEREZINSKI, N. A. N85-32604
BERGER, R. L. N85-32850
BERMAN, F. N85-32842
BERMUDES, D. N85-32743
N85-32745
BERNET, M. N85-32226
BERNS, D. N85-32449
BERRY, D. T. N85-32123
BERTHELOT, Y. H. N85-32981
BESSETTE, R. P. N85-32387
BEST, E. D. N85-32455
BEYSEMBAYEVA, K. B. N85-32895
BHATTACHARYYA, M. H. N85-32751
BIBILASHVILI, N. S. N85-32674
BIGELOW, C. A. N85-32339
BILLINGHAM, J. N85-32708
BILTOFT, C. A. N85-32568
BIRNBAUM, H. K. N85-32186
N85-32348
BISHOP, D. E. N85-32986
BISHOP, D. W. N85-32984
BITYURIN, Y. A. N85-32877
BIXBY, R. L. N85-33043
BLACK, L. P. N85-33094
BLACK, T. G. N85-32835
BLAHA, F. C. N85-32252
BLAIR, R. W., JR. N85-32370
BLAKE, W. K. N85-32097
BLAZHENKOV, V. V. N85-32938
BLOOM, A. L. N85-32367
BLUMENSTEIN, R. R. N85-32632
N85-32694
BOBYREV, V. A. N85-32919
BOERIO, J. N85-32409
BOKIY, G. B. N85-32866
BONSANG, B. N85-32891
BORIS, J. P. N85-32853
BORISOV, V. M. N85-32896
BORISOVA, M. S. N85-32966
BORODACHEV, L. V. N85-32948
BOSSY, L. N85-33095
BOSTON, P. N85-32742
BOUKO, B. B. N85-32967
BOWHILL, S. A. N85-32466
N85-32520
N85-32526
N85-32531
BOWLES, K. J. N85-32148
BOX, G. E. P. N85-32848
BOYKO, V. A. N85-32947
BRABBS, T. A. N85-32156
BRACKBILL, J. N85-33022
BRAUN, U. N85-32756
BRENEMAN, H. N85-33052
N85-33053
BREWER, R. G. N85-33010
BRIGGS, B. H. N85-32548
BRIZHINEV, M. P. N85-32935
BROKAW, R. S. N85-32156
BROSNAHAN, J. W. N85-32525
N85-32537
BROWN, D. H. N85-33031
BROWN, G. S. N85-32228
BROWN, R. A. N85-32442
BRUK-LEVINSON, E. T. N85-32957
BRUNE, D. N85-32737
N85-32738
BRUNER, T. D. N85-33040
BRYAN, W. B. N85-32369
BRYTKOV, V. V. N85-32886
BRYUKVIN, V. V. N85-32915
BRYUNETKIN, B. A. N85-32947
BUCKINGHAM, J. C. N85-32774
BUDIANSKY, B. N85-32197
BUDNIK, A. P. N85-32940
BUELL, M. J. N85-32583
BUFFINGTAN, A. N85-33046
BUKA, G. N. N85-32648
BULANIN, V. V. N85-32935
BULLITT, J. T. N85-32565
BUNKIN, F. V. N85-32919
N85-32947
N85-32971
BUNTON, C. A. N85-32166
BUNTZEN, R. R. N85-32223
BURAKOV, V. S. N85-32944
BURCHAM, F. W., JR. N85-32120
BURKE, G. J. N85-32249
BURKE, K. N85-33062
BURKE, R. N85-32098
BURKITBAYEV, S. M. N85-32952
BURLAGA, L. F. N85-33055
BUSCH-VISHNIAC, I. J. N85-32981
BUSSE, F. H. N85-32957

C

CALDWELL, D. N85-32712
N85-32747
CALTAGIRONE, J. N85-32211
CAMAROTA, N. N85-32693
CAMERON, A. C. W. N85-33066
CAMILLERI, N. N85-32245
CAMPBELL, R. B. N85-32425
N85-32426
CANDY, B. N85-32546
CANNON, M. R. N85-32106
CAPLE, G. N85-32599
N85-32603
CAPRILE, C. N85-33026
CARBAJO, J. J. N85-32288
CARDENALES-ORTIZ, L. N85-32771
CARLIER, P. N85-32692
CARNUTH, W. N85-32574
CARR, J. S. N85-32350
CARR, L. P. N85-33085
CARR, R. H. N85-33085
CARR, W. E. N85-32353
CARSTENS, J. C. N85-32621
CARTER, D. A. N85-32509
N85-32549
CASANOVA, J. N85-32614
CASELLA, G. N85-32850
CASH, S. E. N85-32142
CAWLEY, J. D. N85-32333
CELMINS, A. N85-32283
CERWIN, S. A. N85-32275
CHAI, H. N85-32152
CHANG, C. N85-32343
CHANG, D. C. N85-32749
CHANG, S. N85-32713
N85-33026
CHANIN, M. L. N85-32470
CHAPIRO, D. M. N85-32222
CHAPMAN, D. N85-32603
CHARALAMBIDES, P. N85-32346
CHASHEY, I. V. N85-32898
CHATTERJEE, R. N. N85-32653
CHAUDHURI, S. N85-32627
CHAYKOVSKY, M. N85-32210
CHEESEMAN, P. C. N85-32135
CHEN, H. N85-32348
CHEN, Y. L. N85-32587
CHENG, R. J. N85-32630
CHENG, Y. F. N85-32356
CHERN, R. T. N85-32207
CHERNENKO, A. A. N85-32914
CHERNYKH, Y. N. N85-32966
CHESLEY, F. T. N85-32816
CHIEN, J. C. W. N85-32200
CHIGIER, N. N85-32157
CHILDS, D. W. N85-32332
CHITRE, S. N85-32431
CHIU, Y. T. N85-32568
CHIZHONKOV, Y. V. N85-32946
CHOTIROS, N. P. N85-32980
CHOU, T. L. N85-33008
CHRISTE, K. O. N85-32165
CHRISTIAN, E. C. N85-33046
CHRISTON, S. P. N85-33051
N85-33054
N85-33055
N85-33059
CHUKICHEVA, G. M. N85-32873
CHULYAYEVA, Y. G. N85-32884
CHURKSTE, I. A. N85-32913
CISZEK, T. N85-32444
CLARK, C. F. N85-32253
CLARK, W. L. N85-32516
N85-32536
CLICK, W. N85-32152
N85-32153
COCHRAN, H. D. N85-32819
COFFEE, T. P. N85-32167
COHEN, N. N85-32751
COHEN, Y. N85-32714
N85-32715
N85-32743
COLEMAN, J. R. N85-32208
COLOMBANT, D. N85-33022
COMMISSO, R. J. N85-32259
COMPSTON, W. N85-33094
CONDIE, K. C. N85-33067
CONNELLY, E. M. N85-32809
CONNORS, M. M. N85-32772
CONRAD, C. L. N85-32791
COOK, W. R. N85-33049
N85-33050
COONEY, J. N85-32699
COOPER, L. N85-32104
COOPERMAN, S. A. N85-33068
N85-33079
COOPERSTEIN, G. N85-32259
CORBETT, J. N85-32420
CORNISH, C. R. N85-32468
N85-32505
COUTS, D. N85-32985
COWEN, S. T., III N85-32813
CROCHET, M. N85-32509
CROCKER, M. J. N85-32334
CROLEY, D. R. N85-32568
CROSBIE, R. J. N85-32775
CRUZ, J. Y. N85-32560
CUDDIHY, E. F. N85-32402
CULBERTSON, R. J. N85-32269
CULLER, D. E. N85-32779
CUMMINGS, A. C. N85-33049
N85-33051
N85-33055
N85-33056
N85-33058
N85-33059
CUNNINGHAM, T. B. N85-32140
CURRAN, D. R. N85-32354
CURTIN, T. B. N85-32688

D

DALGARNO, A. N85-32139
DALMEIDA, G. A. N85-32666
DANICHKIN, S. A. N85-32892
DANILEYKO, M. V. N85-32904
DANYLUK, S. N85-32441
DASH, J. N85-32180
DAUD, T. N85-32417
DAVIDSON, D. L. N85-32342
DAVIS, J. M. N85-33099
DAVIS, L., JR. N85-33103
DAVIS, R. O. N85-32313
DAVIS, W., JR. N85-32819
DAWSON, J. B. N85-33077
DEAN, J. S. N85-32800
DEASE, C. G. N85-32249
DECKER, A. J. N85-32302
DECKER, D. T. N85-32567
DEEPAK, A. N85-32464
DEGROOT, A. N85-32820
DEHOFF, R. T. N85-33034
DEJAGUIN, B. V. N85-32679
DELMAS, R. N85-32639
DEMCHUK, M. I. N85-32893
DEMOTT, P. J. N85-32598
DEMOY, T. N85-32828
DEMURJIAN, S. A. N85-32825
DENTON, J. D. N85-32294
DERBOV, V. L. N85-32917
DERUNTZ, J. A., JR. N85-32987
DERZHIYEV, V. I. N85-32947
DES, J. Y. N85-32628
DESALMAND, F. N85-32673
N85-32682
DESHLER, T. N85-32616
DESMARAIS, D. N85-32716
DEUTSCH, B. G. N85-32990
DEVARA, P. C. S. N85-32619
DEVINUESA, S. G. N85-32289
DEVORE, G. W. N85-33069
DEWAN, E. M. N85-32503
DEWIT, M. J. N85-33071
DEXTER, R. J. N85-32342
DIDWALL, E. M. N85-32249
DIETZEL, R. W. N85-32214
DIEWERT, G. S. N85-32831
DIK, V. P. N85-32969
DILLON, O. N85-32438
N85-32439
DO, K. A. N85-32854
DODD, G. N85-32635
DONEAUD, A. A. N85-32570
DORKO, E. A. N85-32158
DOUGLAS, I. N85-32359
N85-32382
DOVIAK, R. J. N85-32573
DOWLING, J. A. N85-32325
DOYLE, A. P. N85-32747
DOYLE, J. D. N85-32140
DRAKE, M. J. N85-33078
DUDOKOVIC, M. P. N85-32415
DUKE, E. L. N85-32122
N85-32794
DUNCAN, S. N85-32435
DUNKIN, W. M. N85-32336
DURAND, Y. N85-32695
DURKEE, P. A. N85-32622
DUTTA, S. N85-32429
DWORK, C. N85-32799
DYAKIN, V. M. N85-32947
DYKMAN, I. M. N85-32867
DYKSTRA, K. U. N85-32230
DYSON, T. F. N85-32844
DZHIDZHOYEV, M. S. N85-32903
N85-32911
DZHIKIYA, G. V. N85-32930

E

EARNSHAW, K. B. N85-32475
EASTMAN, L. F. N85-33024
ECKLUND, W. L. N85-32483
N85-32509
N85-32549
EDWARDS, B. N85-32466
EGBERT, J. L. N85-32826
EHRENFEUCHT, A. N85-32770
ELFORD, W. G. N85-32546
ELIAS, K. C. N85-32593
ELLIOT, K. N85-32262
ELLIS, J. R. N85-32340
ELROD, D. N85-32332
ELSBERRY, R. L. N85-32579
N85-32589
N85-32595
EMBLETON, C. N85-32378
EMILENKO, A. S. N85-32661
EMSLIE, A. G. N85-33100
ENGELKING, P. C. N85-33000
ENGLER, E. N85-32147
EPSHTEYN, I. I. N85-32939
ERZBERGER, H. N85-32101
ETTOUNEY, H. M. N85-32443
EURELL, J. A. C. N85-32758
EVANS, A. G. N85-32197
EVANS, B. N85-32198

F

FABELINSKIY, I. L. N85-32961
FAETH, G. M. N85-32160
FAHEY, R. N85-32717
FAILE, G. N85-32147
FAIRALL, C. W. N85-32544
FAIZULLIN, B. S. N85-32606
FALL, R. R. N85-32611
FARLEY, D. T. N85-32519
FARLEY, T. N85-32535
FARRIS, T. H. N85-32232
FAYENOV, A. Y. N85-32947
FEDOSOV, A. V. N85-32878
FENN, J. B. N85-32168
FERGUSON, R. E. N85-32796
FERLIC, K. P. N85-32999
FETTERMAN, D. E., JR. N85-32111
FIELDS, M. E. N85-32142
FINGER, M. H. N85-33048
N85-33049
FINN, P. A. N85-33006
FINNEGAN, W. G. N85-32598
N85-32632
FIRSCHEIN, O. N85-32134
N85-32135
FIRSICH, D. W. N85-32171
FIRSOV, K. N. N85-32886
FISCHER, U. N85-32718
N85-32743
N85-32746
FISHER, E. B. N85-32212
FITZGERALD, J. W. N85-32676
FLAGAN, R. C. N85-32416
FLETCHER, E. A. N85-32159
FLOOK, F. A. N85-32265
FLOREN, E. E. N85-32223
FOGARASSY, E. N85-32269
FOMIN, V. U. N85-32917
FONTAN, J. N85-32640
FORD, J. P. N85-32377
FORLAND, K. A. N85-32859
FOUNTAIN, A. G. N85-32634
FOX, G. E. N85-32719
FRANCIOSI, A. N85-32161
N85-33026
FRANCOIS, R. N85-32742
FREDERKING, T. H. K. N85-32272
FREIMAN, S. W. N85-32202
FRIAS, B. R. N85-32252
FRICK, G. M. N85-32676
FRIED, B. D. N85-33017
FRITTS, D. C. N85-32470
N85-32507
N85-32508

FROUDE, D. O. N85-33094
FRUEHOLZ, R. P. N85-32314
FRYKLUND, D. H. N85-32099
FU, S. K. N85-32406
FUKAO, S. N85-32543
FUKUDA, I. N85-32839
FUKUTA, N. N85-32597
FULLER, E. R., JR. N85-32202
FULTON, R. E. N85-32822
FUNK, W. N85-32574
FUNKENBUSCH, A. W. N85-32188
FUZZI, S. N85-32693

G

GAGE, K. S. N85-32477
N85-32479
N85-32483
N85-32501
N85-32504
GAGIN, A. N85-32608
GAL, M. N85-33029
GALAKTIONOV, V. A. N85-32971
GALL, P. D. N85-32110
GALLOP, L. D. N85-32208
GAN, D. N85-32226
GANGULI, G. N85-33019
GANTSEVICH, S. V. N85-32962
GAPONOV, S. V. N85-32877
GARBELMAN, K. J. N85-32809
GARBUZOV, D. Z. N85-32908
GARCIA, A., III N85-32430
GARCIA, J. A. N85-32614
GARELLO, R. N85-32509
GARRELS, R. M. N85-32720
GARRETT, B. C. N85-32996
GARSEVANISHVILI, V. R. N85-32929
GASANOV, I. I. N85-32977
GAST, M. N85-32689
GATES, E. T. N85-32204
GAUDRY, A. N85-32691
GAZLAY, R. L. N85-32108
GE, Z. M. N85-32618
GEBBIE, K. B. N85-33098
GELLER, D. N85-32246
GELLER, M. A. N85-32467
N85-32470
GELMONT, B. L. N85-32875
GENCO, L. V. N85-32114
GEORGE, T. F. N85-32998
GEORGEFF, M. P. N85-32134
N85-32135
GEORGII, H. W. N85-32615
N85-32665
GERASIMOV, G. A. N85-32917
GERBER, H. N85-32678
GERBER, M. A. N85-32213
GERI, G. A. N85-32757
GERSHTEYN, S. S. N85-32930
GIBBS, P. H. N85-32750
GIBSON, L. R. N85-32132
GIESS, S. C. N85-32236
GIFFORD, L. N. N85-32353
GINDIKIN, S. G. N85-32973
GINZBURG, I. F. N85-32931
GIOVANOLA, J. H. N85-32345
GIRARD-REYDET, L. N85-32692
GLAESER, P. B. N85-32126
GLAZOV, G. N. N85-32892
GOCHELASHVILI, K. S. N85-32898
GOLDBERG, H. A. N85-32205
GOLDBERG, J. N85-32135
GOLDHABER, M. N85-32721
GOLDWASSER, J. M. N85-32210
GOMEZ, P. N85-32406
GONCHAROV, N. V. N85-32660
GONCHARSKIY, A. V. N85-32963
N85-32972
GONZALEZ, A. C. N85-32202
GONZALEZ, C. C. N85-32404
GOOD, R. E. N85-32503
GOODMAN, L. J. N85-33003
GOPALAN, K. N85-33084
GORBENKO, B. Z. N85-32947
GORBINET, G. N85-32683
GORBUNOV, B. Z. N85-32602
GORCHAKOV, G. I. N85-32661
GORDIYENKO, V. M. N85-32903
GORELENOK, A. T. N85-32910
GORNEY, D. J. N85-32568
GRANAT, M. A. N85-32706
GRANDJOUAN, N. N85-33022
GRANT, L. O. N85-32598
N85-32632
N85-32694
GRASSL, H. N85-32675
GRAU, D. D. N85-32592
GRAY, S. N85-32335
GRECNER, J. N85-32786
GREELEY, R. N85-32373
GREEN, J. L. N85-32477
N85-32514
N85-32516
N85-32518
N85-32522
N85-32536
N85-32550
GREENE, R. R. N85-32988
GREENSPAN, D. C. N85-32202
GREENWALD, A. C. N85-32433
GREIF, I. N85-32801
GRIEVE, R. A. F. N85-33070
GRIFFIN, O. M. N85-32349
GRIFFIN, R. W. N85-32769
N85-32852
GRIFFITH, J. S. N85-32447
GRIFFITH, P. N85-32262
GRIGORYANTS, V. V. N85-32960
GRIKMAN, L. G. N85-32955
GRIN, Y. I. N85-32888
GRINFELD, M. A. N85-32976
GRINGORTEN, I. I. N85-32586
GROENEVELD, K. O. N85-32665
GROMOVA, T. N. N85-32610
GROSSBARD, N. N85-32503
GROVE, J. E. N85-33046
GROVER, J. R. N85-33001
GRUDSKIY, A. Y. N85-32950
GRUZDOV, V. G. N85-32910
GUBIN, V. P. N85-32917
GUERRERO, R. N85-32722
N85-32737
N85-32740
GUILLET, J. N85-32405
GULBRANDSEN, L. F. N85-32706
GUMAN, V. N. N85-32874
GUPTA, N. K. N85-32851
GUPTA, P. K. N85-32335
GUPTA, S. S. N85-32856
GUROV, V. S. N85-32933
GUSEV, V. D. N85-32958
GYURE, R. A. N85-32742
GZIRISHVILI, T. G. N85-32659

H

HADDAD, R. N85-32743
N85-32744
HADGIGEORGE, G. N85-32387
HADLEY, G. R. N85-32328
HAINES, D. M. N85-32240
HAISCH, B. M. N85-33096
HAJEK, B. N85-32225
HAKLAY, B. N85-32248
HALAMIK, J. N85-32787
HALE, B. N. N85-32633
HALL, A. J. N85-32545
HALL, J. H. N85-32252
HALL, M. M. N85-32702
HALLQUIST, J. O. N85-32846
HALVIS, J. N85-32252
HAMILTON, H. D. N85-32579
N85-32589
N85-32595
HAMMOND, R. R. N85-32223
HAMROCK, B. J. N85-32329
N85-32330
HANKS, M. L. N85-32116
HARISS, R. N85-32748
HARKLEROAD, M. N85-32103
N85-32104
HARRIS, B. N85-32338
N85-32841
HARRIS, C. B. N85-32994
HARRIS, F. I. N85-32577
HARRISON, A. A. N85-32772
HART, R. N85-33071
N85-33072
HARTMAN, H. N85-32777
HARTNESS, J. N85-32152
N85-32153
HARVEY, A. N85-32319
HARVEY, K. L. N85-33097
HASEMI, Y. N85-32103
HASZPRA, L. N85-32652
HATFIELD, L. N85-32658
HAUPT, R. L. N85-32241
HAYDEN, R. S. N85-32357
N85-32361
HAYES, J. L. N85-32594
HAZLEWOOD, C. F. N85-32749
HEAD, T. C. N85-32852
HEBETS, M. N85-32461
HEINTZENBERG, J. N85-32655
HENDRIX, G. G. N85-32990
HENSEL, I. N85-32756
HEPLER, W. A. N85-32272
HERRERA, J. I. N65-32251
HERSKOVITZ, M. B. N85-32317
HEVSKII, I. A. N85-32644
HEWINS, M. A. H. N85-32182
HEYNICK, L. N. N85-32760
HIBLER, W. D., III N85-32700
HIDALGO-PRADA, B. N85-32194
HILTEN, L. N85-32985
HINDMAN, E. E. N85-32622
HIROTA, I. N85-32470
HIRSCH, C. N85-32295
N85-32296
HIRSCH, E. N85-32773
HIRTH, J. P. N85-32187
HITZENBERGER, R. N85-32663
HOBBS, P. V. N85-32657
HOCKING, W. K. N85-32548
HODGKISS, W. S. N85-32224
HOERNES, S. N85-33077
HOFFMAN, S. N85-33063
N85-33073
N85-33074
HOGAN, L. N85-33072
HOLLAND, W. E. N85-32318
HOLLANDER, J. P. N85-32386
HOLLIS, R. N85-32147
HOLLOWAY, F. W. N85-32820
HOLMES, D. N85-32262
HOLSER, W. T. N85-32723
HOLT, R. G. N85-32564
HOLTON, J. R. N85-32470
HOLTZAPPLE, M. N85-32164
HOOKE, L. R. N85-32709
HOPFENBERG, H. B. N85-32207
HORGEN, H. N85-32828
HORN, R. D. N85-32598
N85-32694
HORVATH, H. N85-32663
HOWERTON, R. J. N85-33009
HOWLETT, P. N85-32828
HSIAO, D. K. N85-32825
HSIEH, B. J. N85-32792
N85-32793
HUBA, J. D. N85-33016
HUBBARD, D. C. N85-32776
HUBBARD, E. N85-32252
HUDAK, S. J. N85-32342
HUDSON, J. C. N85-32677
HUDSON, J. G. N85-32671
N85-32685
N85-32696
HUFFER, F. N85-32845
HUMMEL, J. R. N85-32325
HUMMEL, R. E. N85-33034
HUSEBY, I. C. N85-32270
HUSS, G. R. N85-33075
HUTCHINSON, J. W. N85-32197
HYUN, H. N85-32343

I

IERKIC, H. M. N85-32498
ILIFF, K. W. N85-32851
INGOGLY, W. F. N85-32791
IRELAND, T. R. N85-33094
ISAAC, G. A. N85-32671
ISKAKOVA, Z. D. N85-32955
ISTOK, M. N85-32573
ITOH, T. N85-32245
IVAKNIK, V. V. N85-32964
IVANCIC, W. A. N85-32320
IVANOV, A. O. N85-32912
IVANOV, A. P. N85-32969
IVANSHENKO, I. V. N85-32626
IYA, S. N85-32413

J

JACOBSEN, A. R. N85-32767
JACOBSON, S. B. N85-33076
JAENICKE, R. N85-32650
N85-32656
N85-32666
JAGOUTZ, E. N85-33077
JAVOR, B. N85-32724
N85-32742
JERMEY, C. N85-32094

JEZIOR, B. N85-32773
JINGRONG, C. N85-32668
JIUSTO, J. E. N85-32678
JOHNSON, B. E. N85-32416
JOHNSON, D. N85-32693
JOHNSON, D. R. N85-32320
JOHNSON, R. W. N85-32590
JOHNSON, W. S. N85-32150
JOHNSTON, K. J. N85-32141
JOHNSTON, N. J. N85-32151
JOHNSTON, P. E. N85-32495
JOHNSTON, R. K. N85-32459
JONES, D. H. N85-32765
JONES, E. M. N85-32145
JONES, J. H. N85-33078
JORTNER, J. N85-32154
JOSHI, A. N85-32985
JOSHI, P. V. N85-32645
JOYCE, J. N85-33026
JUDSON, S. N85-32363
JULANOV, Y. V. N85-32644
N85-32669

K

KADLECEK, J. N85-32693
KAGAN, V. D. N85-32962
KAKUTKINA, N. A. N85-32602
KALEJS, J. P. N85-32440
N85-32443
KALGANOV, A. F. N85-32265
KALINUSHKIN, V. P. N85-32870
KALIYA, O. L. N85-32891
KAMIDOVA, R. N85-32924
KANE, J. J. N85-32198
KAO, A. N85-32351
KAO, A. M. N85-32350
KAPLAN, H. L. N85-32774
KARAMALIYEV, R. A. N85-32907
KARPUKHIN, S. N. N85-32869
KARPUSHKO, F. V. N85-32890
KARTSIVADZE, A. I. N85-32659
N85-32661
KARYAGIN, S. N. N85-32873
KASAHARA, M. N85-32642
KASHKAROV, P. K. N85-32873
KASHKAROV, S. S. N85-32956
KASTING, J. F. N85-32725
KASZA, K. E. N85-32292
KATILYUS, R. N85-32962
KATO, S. N85-32470
N85-32543
KATTELUS, H. N85-32427
KAULA, W. M. N85-33068
N85-33079
KAUTZ, W. H. N85-32134
N85-32135
KAWAMURA, K. N85-32792
N85-32793
KEENER, T. J. N85-32750
KELKAR, D. N. N85-32645
KELLETT, B. J. N85-32352
KELLEY, E. A., JR. N85-32703
KELLY, J. B. N85-32120
KELLY, J. D. N85-32562
KENNER, V. H. N85-32155
KENT, G. S. N85-32464
KERELIUK, S. N85-32125
KERKHOVEN, T. N85-32832
KESWANI, S. T. N85-32144
KETTLER, D. N85-32756
KEUNNING, W. N85-32622
KEZIOS, P. S. N85-32193
KHABIBULLAYEV, P. K. N85-32881
N85-32895
N85-32919
KHAIT, V. D. N85-32926
KHALFIN, V. B. N85-32875
KHANAKA, G. H. N85-33028
KHAY, D. S. N85-32907
KHEMANI, L. T. N85-32653
KHODAN, I. V. N85-32957
KHOLOMAY, B. V. N85-32871
KHORGUANI, V. G. N85-32604
KHVAN, S. B. N85-32602
KHVOYKA, M. N85-32902
KIDD, W. S. F. N85-33080
KIM, Q. N85-32452
KIM, R. N85-32153
KIMURA, I. N85-32543
KING, J. R. N85-32834
KINNY, P. D. N85-33094
KIRICHENKO, N. A. N85-32971
N85-32974
KIRKIN, A. M. N85-32938
KIRSON, Y. E. N85-32913
KIRYUKHIN, Y. B. N85-32896
KISER, J. D. N85-32337
KISS, I. N85-32652
KITAYEVA, G. K. N85-32951
KLEIN, J. M. N85-32551
KLIMA, S. J. N85-32337
KLINGO, V. V. N85-32606
KLOSNER, J. M. N85-32991
KLOTYNSH, E. E. N85-32913
KLUG, M. J. N85-32726
N85-32742
KLYUYENKOV, Y. B. N85-32877
KNAPP, W. J. N85-32216
KNOLL, D. N85-32756
KO, M. K. W. N85-32561
KOCMOND, W. C. N85-32685
KOENIG, J. L. N85-32408
KOENIG, M. N85-32153
KOH, G. N85-33015
KOHNO, M. N85-32642
KOLEROV, A. N. N85-32894
KOLINEK, T. N85-32783
KOLOMOYETS, V. V. N85-32678
KOLTAY, E. N85-32652
KONEV, Y. V. N85-32888
KOOPMAN, R. P. N85-32169
KOPPES, W. M. N85-32210
KOROLKOV, K. S. N85-32902
KORUKHOV, V. V. N85-32914
KOS, G. P. A. N85-32664
KOSINOV, A. D. N85-32879
KOSTROV, A. V. N85-32935
KOTKIN, G. L. N85-32931
KOTLAR, A. J. N85-32167
KOUTZENOGY, K. P. N85-32602
KOVRIGIN, A. I. N85-32899
KOVRIZHNYKH, L. M. N85-32945
KRACHATURYAN, E. G. N85-32674
KRAL, V. N85-32146
KRALIKOVA, B. N85-32902
KRAYUSHKIN, S. V. N85-32903
KRETSCHMER, F. F., JR. N85-32243
KRISTIANSEN, M. N85-32858
KROPF, R. F. N85-32833
KRUEGER, G. P. N85-32771
KRUTOVA, L. I. N85-32912
KUCH, J. A. N85-32242
KUCZUN, C. G. N85-32312
KUEGLER, K. N85-32784
KUKHAREV, V. N. N85-32909
KUKUVKA, R. N85-32211
KULINICH, S. N85-32934
KUMAKHOV, M. A. N85-32927
KUMAR, K. N85-32267
KUMAR, R. N85-32653
KUNNERTH, D. N85-32159
KUO, C. P. N85-32437
KURDYUMOV, S. P. N85-32971
KURGHUIN, Y. S. N85-32679
KURZ, M. D. N85-33081
KUSHNIR, V. P. N85-32952
KUTEYEV, B. V. N85-32937
KUZAY, T. M. N85-32292
KUZNESTOVA, N. A. N85-32891
KUZNETSOV, G. F. N85-32866
KYJOVSKY, P. N85-32785
KYZYLASOV, Y. I. N85-32961

L

LABOV, S. E. N85-33060
LACOMBE, D. J. N85-32257
LACOR, C. N85-32296
LAI, S. N85-32415
LAIRD, C. E. N85-32130
LAKTIONOV, A. G. N85-32672
LALA, G. G. N85-32678
LAMBERT, R. B. N85-32391
LAMORTE, M. F. N85-32421
LANE, L. J. N85-32393
LANGAN, J. R. N85-32355
LANGE, F. F. N85-32216
N85-32352
LANKFORD, V. G. N85-33036
LAPIDUS, Y. R. N85-32863
LAPIN, A. D. N85-32864
LARSEN, M. F. N85-32469
N85-32490
N85-32505
LARSEN, R. P. N85-32751
LASKOWSKI, P. N85-32560
LASSILA, D. N85-32186
LASZLO, S. N85-32652
LATHROP, J. W. N85-32451
LATTMAN, L. H. N85-32366
LAU, K. H. N85-33046
N85-33047
LAURSEN, S. N85-33046
LAWLER, J. S. N85-32251
LAWLESS, J. G. N85-32777
LAWLESS, W. N. N85-32253
LAWRENCE, J. N85-32747
LAYTON, R. G. N85-32599
N85-32603
LEAITCH, W. R. N85-32671
LEDBETTER, F. N85-32147
LEE, T. S. N85-32306
LEE, W. A. N85-32199
LEE, Y. C. N85-33016
N85-33019
LEGUSHA, F. F. N85-32861
LEIGHTON, T. N85-32778
N85-32842
LENNARTSSON, W. N85-32552
LENNON, J. F. N85-32234
N85-32235
LEONARD, J. M. N85-32388
N85-32553
LEONTOVICH, A. M. N85-32938
LERNER, P. B. N85-32954
LEROUX, I. N85-32804
LESESNE, P. K. N85-32797
LESKOV, B. N. N85-32612
LESLIE, W. B. N85-32214
LEVAY, M. N85-33096
LEVIN, A. E. N85-32288
LEVITT, K. N. N85-32134
N85-32135
LEVKOV, L. N85-32675
LEVY, R. N85-32093
LI-XIN, R. N85-32651
LIANG, R. H. N85-32403
LIDSKIY, V. V. N85-32938
N85-32938
LIEBER, W. H. N85-32824
LIMABLANCO, W. R. N85-32707
LIN, F. C. N85-32243
LIN, S. J. N85-32093
LINDHOLM, F. A. N85-32418
LINDLEY, P. M. N85-32198
LINDZEN, R. S. N85-32470
LIOR, N. N85-32286
N85-32287
LIOU, K. N. N85-32635
LIPANTOV, G. N. N85-32625
LIPSKAYA, O. A. N85-32660
LISENKOVA, H. V. N85-32600
LIU, C. H. N85-32480
N85-32502
LIVINSH, M. G. N85-32872
LOFTIN, L. K., JR. N85-32089
LOLIC, M. N85-32220
LOMAYA, O. V. N85-32648
LOMONOSOV, M. V. N85-32946
LONGMIRE, M. S. N85-32229
LOPEZ, A. N85-32640
LORIOT, G. B. N85-32548
LOTFY, M. M. N85-32814
LOUGHRAN, L. B. N85-32555
LOVELESS, C. A. N85-32771
LOVELOCK, J. E. N85-32727
LOVING, P. A. N85-32855
LOVTSYUS, A. A. A. N85-32937
LOWE, D. R. N85-33082
LOWMAN, P. D., JR. N85-33083
LOYKO, V. A. N85-32969
LUCCHITTA, B. K. N85-32371
LUCHIK, T. S. N85-32274
LUGMAIR, G. W. N85-33084
LUKIN, A. Y. N85-32937
LUKIN, K. A. N85-32941
LUKYANCHUK, B. S. N85-32954
LUKYANCHUK, V. S. N85-32919
LUNDELIUS, J. N85-32836
LUNDY, W. E. N85-32633
LUSHNIKOV, A. A. N85-32644
N85-32669
LUSTIG, I. J. N85-32818
LVOV, V. I. N85-32901
LYNCH, J. N85-32849
LYNCH, N. N85-32799
N85-32836
LYON, J. G. N85-32321
LYONS, J. H. N85-32657
LYTLE, R. J. N85-32249

M

MA, C. N85-32465

MABEY, D. G. N85-32092
MACDONALD, D. D. N85-33023
MACDONALD, F. J. N85-32159
MACDOUGALL, J. D. N85-33084
MACKAY, R. A. N85-32163
MACLENNAN, B. J. N85-32811
N85-32817
MADELAINE, G. N85-32662
MADONNA, R. G. N85-32142
MAGOTT, R. J. N85-32774
MAIN, R. N85-32985
MAIR, P. V. N. N85-32624
MAIR, R. S. N85-32100
MAJEROWICZ, A. N85-32643
MAKAROV, A. I. N85-32897
MAKAVEEV, P. Y. N85-32644
MALCOLM, G. N. N85-32090
MALDONADO, J. N85-32147
MALLANT, R. K. A. M. N85-32664
MAMATKULOV, M. N85-32881
MANENKOV, A. A. N85-32870
MANGALGIRI, P. D. N85-32150
MANNING, J. L. N85-32325
MANYKIN, E. A. N85-32952
MAPLES, A. L. N85-32178
MARCHAL, T. N85-32692
MARCOS, F. A. N85-32558
MARDEN, M. N85-32841
MARGULIS, L. N85-32728
MARS, L. N85-32211
MARSHALL, N. N85-32400
MARSHALL, R. G. N85-32825
MARTEL, J. N85-32756
MARTELL, E. A. N85-32638
MARTENS, C. S. N85-32729
MARTINEZ, R. N85-32982
MASLOV, A. A. N85-32879
MATHEWS, J. D. N85-32487
MATIN, A. N85-32730
MATTEY, D. P. N85-33085
MATYAS, G. M. N85-33039
MAY, P. T. N85-32546
MAYER, L. N85-32376
MAYOROV, S. A. N85-32947
MCARTHUR, H. M. N85-32803
MCBRIDE, D. K. N85-32350
MCBRIDE, S. E. N85-32791
MCCARTHY, D. K. N85-32214
MCCARTOR, G. D. N85-32556
MCCLANAHAN, J. E. N85-32273
MCCLELLAN, A. K. N85-32192
MCCLELLAN, M. R. N85-32142
MCCUNE, B. P. N85-32800
MCFADDEN, P. D. N85-32113
N85-32117
MCGINNISS, V. D. N85-32320
MCGRATH, C. A. C. N85-32766
MCGREGOR, S. J. N85-32389
MCHUGH, M. A. N85-32192
MCKNIGHT, D. M. N85-32551
MCKNIGHT, R. L. N85-32119
MCLAREN, S. N85-32693
MCMEEKING, R. M. N85-32195
N85-32346
MCNITT, J. A. N85-32584
MCQUEEN, S. M. N85-32305
MCWHORTER, A. L. N85-33025
MEAUZE, G. N85-32298
MEEK, C. E. N85-32489
N85-32491
N85-32510
N85-32529
MEGER, R. A. N85-32259
MEHANDRU, S. P. N85-32173
N85-32175
N85-32176
MEI-YUAN, H. N85-32681
MEIER, D. L. N85-32425
MEISELMAN, H. L. N85-32773
MEIYUAN, H. N85-32668
MELHORN, W. N. N85-32368
MENENKOV, V. D. N85-32888
MENTESHASHVILI, Z. R. N85-32929
MERLIN, R. D. N85-33032
MERRITT, D. A. N85-32475
N85-32533
MERZ, M. D. N85-32189
MERZHANOV, K. M. N85-32679
MESHKOV, Y. N85-32754
MESZAROS, A. N85-32652
METREVELI, D. M. N85-32651
METSKHVARISHVILI, I. P. N85-32674
METTERNICH, P. N85-32665
MEWALDT, R. A. N85-33045
N85-33047
N85-33057
N85-33103
MEYER, R. D. N85-32848
MICHALEK, F. N85-32783
MICHL, J. N85-32196
MIKHAYLOV, V. P. N85-32893
MIKHAYLOVA, G. N. N85-32870
MILLER, D. D. N85-32834
MILLER, H. N85-32204
MILLER, M. G. N85-32323
MILLER, M. L. N85-32270
MILLER, M. S. N85-32167
MILLER, N. N85-32763
MILLER, S. L. N85-33065
MING-XING, W. N85-32651
MINOGUE, M. T. N85-32815
MIRME, A. N85-32623
MIRONOV, S. M. N85-32928
MIROSHNICHENKO, V. I. N85-32612
MIRZOYAN, R. G. N85-32938
MISAKOV, P. Y. N85-32944
MISHIN, G. I. N85-32888
MITCHELL, W. C. N85-32764
MITSAY, L. I. N85-32959
MOCHALOV, I. V. N85-32912
MODERA, M. P. N85-32289
MODLIN, J. M. N85-32282
MOKASHI, A. R. N85-32422
MOMIN, G. A. N85-32653
MON, G. R. N85-32410
MONROE, R. L. N85-32233
MONTGOMERY, B. H. N85-32288
MONTMORY, R. N85-32629
N85-32695
MOOERS, C. N. K. N85-32703
MOORE, G. E. N85-32183
MOORE, J. N85-32299
MOORE, J. G. N85-32297
N85-32301
MOORE, M. N85-32805
MOORE, S. W. N85-32456
MOORHEAD, G. N85-32769
MORALES, G. J. N85-33017
MORAN, K. P. N85-32475
MORAVEC, T. J. N85-32309
MORELLY, J. N85-32692
MORETTI, E. S. N85-32751
MORGAN, M. N85-32125
MORGAN, P. N85-33086
MORIGUCHI, Y. N85-32642
MORISAWA, M. N85-32374
MOROI, D. S. N85-33031
MOROZ, P. Y. N85-32945
MOROZOV, V. P. N85-32890
MOROZOVA, Y. A. N85-32919
MORPHY, C. C. N85-32212
MORRIS, D. H. N85-32151
MORRISON, P. N85-32777
MORTON, H. E. N85-32802
MOSHER, M. C. N85-32281
MOSIER, J. N. N85-32807
MOSS, R. W. N85-32189
MOZHAROVSKIY, A. M. N85-32938
MUELLER, R. N85-32453
MUKHERJEE, A. K. N85-32194
MULAR, M. N85-32209
MURADYAN, G. U. N85-32928
MURALEEDHARAN, T. S. N85-32641
MURAVEV, S. V. N85-32886
MURPHY, W. C. N85-32998
MURTY, A. S. R. N85-32613
N85-32619
MURTY, B. V. R. N85-32613
N85-32619
N85-32680
MUSITANO, J. R. N85-32255

N

NAIK, M. S. N85-32653
NAKAHASHI, K. N85-32831
NASTROM, G. D. N85-32478
N85-32504
N85-32512
N85-32532
N85-32550
NAUMENKOV, P. A. N85-32944
NEALSON, K. H. N85-32731
NEDOSPASOV, A. V. N85-32926
NEKHAYENKO, V. A. N85-32899
NEKRASOV, A. K. N85-32948
NELSON, C. N85-32332
NELSON, S. W. N85-32124
NEMEENOV, V. A. N85-32959
NERI, J. M. N85-32259
NESS, N. F. N85-33038
NESTEROVA, T. N. N85-32956
NEUMANN, P. N85-32134
N85-32135
NEVSKII, I. A. N85-32669
NEWBORN, H. N85-32267
NGUYEN, B. C. N85-32691
NICKS, C. N85-32332
NICOLET, M. N85-33095
NICOLET, M. A. N85-32427
NIGHAN, W. L. N85-32327
NIKANDROV, V. Y. N85-32610
NIKI, H. N85-32748
NIKITIN, O. N. N85-32644
NIKLAUS, K. N85-32708
NISHIDA, T. N85-32278
NIXON, D. N85-32096
NODIA, A. G. N85-32659
NOPPEL, M. N85-32623
NORMAN, M. L. N85-32290
NORTON, J. L. N85-32290
NOVIKOV, A. D. N85-32917
NOZYCE, H. N85-32608

O

OBRIEN, P. J. N85-32101
OBRIEN, T. K. N85-32151
OCONNER, T. C. N85-32637
ODELL, R. D. N85-33005
OESTERREICHER, C. N85-32226
OGAWA, T. N85-32543
OHMER, M. C. N85-33031
OHTAKE, T. N85-32605
N85-32634
OKHRIMENKO, B. A. N85-32868
OLDHAM, P. B. N85-32310
N85-33013
OLDHAM, R. D. N85-32751
OLEARY, M. A. N85-32266
OLEINIK, M. K. N85-32590
OLEYNIK, R. V. N85-32601
OLSEN, L. C. N85-32423
OLSON, J. N85-32412
ONO, A. N85-32690
OREHOTSKY, J. N85-32411
ORLOV, Y. P. N85-32902
ORVIS, W. J. N85-33028
OSWALD, R. E. N85-32761
OTROKHOV, S. Y. N85-32917
OTTH, D. H. N85-32448
OTTINGER, P. F. N85-32259
N85-33020
OVANDER, L. N. N85-32865
OWENS, M. S. N85-32620

P

PADALKAR, S. N85-32792
N85-32793
PADIAN, K. N85-32708
PAIMA, D. V. N85-32624
PALM, V. N85-32921
PALMADESSO, P. N85-33019
PANAIOTI, N. N. N85-32961
PANKOW, V. R. N85-32706
PANTOS, T. J. N85-32221
PAPA, R. J. N85-32234
N85-32235
PARFIANOVICH, I. A. N85-32915
PARISI, V. N85-32806
PARK, C. J. N85-32841
PARK, J. T. N85-32275
PARK, W. N85-32134
N85-32135
PARMENTIER, E. M. N85-33070
PARSHUTKINA, I. P. N85-32612
PARUNGO, F. P. N85-32688
PATONAY, G. N85-32162
N85-32310
N85-33013
PAUL, E. W. N85-32201
PAUL, S. K. N85-32613
PAVLOV, V. I. N85-32881
PAXTON, W. H. N85-32990
PEARSON, L. W. N85-32232
PECK, H. D. N85-32732
PEEBLES, H. C. N85-32328
PEERCY, R. L., JR. N85-32133
PEIL, I. N85-32623
PEKAREK, L. N85-32902
PENIN, A. N. N85-32951
PENNYCOCK, S. J. N85-32269
PENZINA, E. E. N85-32915
PEREZ, P. J. N85-32614
PERSHIN, S. M. N85-32899

PERSHINA, T. A. N85-32610
PETERMAN, D. J. N85-32161
PETERS, R. M. N85-32544
PETERSON, B. B. N85-32230
PETERSON, D. L. N85-32733
PETIT, P. A. N85-32579
N85-32589
N85-32595
PETITDIDIER, M. N85-32524
N85-32547
PETRIJANOV, I. V. N85-32698
PETROCCHI, P. J. N85-32577
PETROV, A. V. N85-32873
N85-32935
PETROV, I. A. N85-32955
PHELPS, A. V. N85-32326
PHELPS, B. N85-32762
PHILIP, P. N85-32161
N85-33026
PHILLIPS, G. W. N85-33014
PHILLIPS, P. J. N85-32196
PHILLIPS, R. E. N85-32271
PHILLIPS, W. M. N85-32437
PICKLESIMER, L. G. N85-32198
PIERCE, J. L. N85-32791
PIKE, G. E. N85-33035
PILLINGER, C. T. N85-33085
PIMMINGER, M. N85-32663
PININS, T. Y. N85-32872
PIROGOV, Y. F. N85-32930
PLATONENKO, V. T. N85-32903
N85-32911
PLAUDE, N. O. N85-32600
PLOKHOTSKI, Z. N85-32957
PLOMP, A. N85-32664
PLUMMER, P. L. M. N85-32684
PODDUBNYAK, A. P. N85-32916
PODSHIVALOV, A. A. N85-32899
PODZIMEK, J. N85-32621
N85-32682
POGGIO, A. A. N85-32134
N85-32135
POIRIER, D. R. N85-32178
POLASEK, P. N85-32787
POLITYKO, S. I. N85-32931
POLKY, J. N. N85-32834
POLLACK, J. B. N85-33087
POLSON, P. N85-32760
PONCE, D. A. N85-32316
POPLAWSKI, R. N85-32737
N85-32741
POPOV, A. G. N85-32940
POPOV, V. K. N85-32903
N85-32911
POPPER, L. A. N85-32323
POPPER, R. D. N85-32773
POTEMKIN, A. K. N85-32897
POURBAIX, M. N85-32179
PRAHL, J. M. N85-32330
PRAIS, I. P. N85-32674
PRASAD, S. A. N85-33017
PREDOI, A. N85-32219
PRICE, W. A., III N85-32204
PRIEUR, S. N85-32640
PRINCE, M. B. N85-32395
PRINCE, T. A. N85-33048
N85-33049
N85-33103
PRITCHARD, W. G. N85-32279
PRIVALOV, V. Y. N85-32884
PROKHOROV, Y. S. N85-32939
PRUFERT, L. N85-32743
PURTYMUN, W. D. N85-32393
PUTNAM, T. W. N85-32120
PUXBAUM, H. N85-32663

Q

QUESADA, A. F. N85-32503
QUINTIERE, J. G. N85-32103
N85-32104

R

RAASCH, R. F. N85-32133
RABINOWITZ, P. H. N85-32838
RADKE, L. F. N85-32657
RADTKE, M. N85-32709
RAFAILOV, M. K. N85-32975
RAGAN, G. E. N85-33008
RAI-CHOUDHURY, P. N85-32425
RAI, J. N85-32697
RAJU, I. S. N85-32151
RALSTON, L. G. N85-32751
RAMACHANDRA, A. S. N85-32680
RAMACHANDRAMURTY, A. S. N85-32646
RAMACHANDRAN, P. A. N85-32415
RAMANAMURTY, B. V. N85-32646
N85-32653
RAMSEY, D. C. N85-32121
RANSOM, J. B. N85-32822
RASMUSSEN, E. A. N85-32353
RASMUSSEN, I. L. N85-33046
RASTOGI, P. K. N85-32487
N85-32500
N85-32527
RATHORE, R. S. N85-32686
RAUP, D. N85-32708
RAYKOV, S. N. N85-32944
REAGO, D. A., JR. N85-32633
REBANE, K. K. N85-32921
RECKASE, M. D. N85-32768
REDDOCH, T. W. N85-32251
REDMON, L. T. N85-32996
REDMON, M. J. N85-32996
REEVES, A. P. N85-33011
REGENIE, V. A. N85-32794
REID, I. M. N85-32489
REID, W. R. N85-32260
REIGHTLER, K. S., JR. N85-32127
REILLY, J. T. N85-32284
REITER, R. N85-32574
RENNIER, A. N85-32531
RENOUX, A. N85-32662
RETTERER, J. M. N85-32567
REVIN, S. G. N85-32935
REYNOLDS, R. T. N85-33087
RHEINFURTH, M. H. N85-32847
RICCO, A. J. N85-32201
RICH, F. J. N85-32143
RICH, M. N85-32153
RICHARDSON, S. M. N85-33087
RIDDLE, A. C. N85-32479
N85-32509
RIEGEL, J. P. N85-32774
RIKUN, A. D. N85-32977
RINGHOFER, C. A. N85-33027
RITTER, D. F. N85-32362
ROBERTSON, K. D. N85-32109
ROBINSON, D. N. N85-32341
ROBINSON, J. J. N85-32990
ROBINSON, R. M. N85-32562
ROBINSON, S. M. N85-32843
ROCKOFF, L. A. N85-32133
RODDY, A. F. N85-32617
RODRIGUEZ-MOSCOSO, J. J. N85-32792
N85-32793
RODRIGUEZ, J. M. N85-32561
ROGERS, C. F. N85-32677
ROGERS, D. B. N85-32126
ROGERS, D. C. N85-32616
ROGERS, M. N85-32164
ROGLER, H. L. N85-32275
ROHATGI, A. N85-32425
ROHATGI, N. K. N85-32414
ROM, R. J. N85-32134
N85-32135
ROMANOV, N. P. N85-32923
ROOT, R. G. N85-32323
ROPER, R. G. N85-32506
N85-32538
ROSEN, R. D. N85-32572
ROSENBAUM, S. G. N85-32800
ROSENFELD, P. N. N85-33042
ROSENFIELD, A. R. N85-32187
ROSENTHAL, F. N85-32349
ROSOLOWSKI, J. H. N85-32270
ROSS, M. V. N85-32563
ROSS, P. N. N85-32176
ROSS, R. G., JR. N85-32397
N85-32402
N85-32404
N85-32450
ROSSBACHER, L. A. N85-32375
N85-32385
ROTH, D. J. N85-32337
ROTHMUND, H. J. N85-32831
ROTTGER, J. N85-32469
N85-32476
N85-32482
N85-32490
N85-32493
N85-32494
N85-32497
N85-32498
N85-32511
N85-32513
N85-32517
N85-32534
ROWE, J. E. N85-32709
ROY, A. B. N85-33084
ROYRVIK, O. N85-32481
N85-32484
N85-32485
N85-32486
N85-32496
N85-32540
ROZANOV, V. N85-32885
RUBANOV, V. S. N85-32889
RUBENSTEIN, D. M. N85-32988
RUBINCAM, D. P. N85-32131
RUDENKO, O. V. N85-32863
RUMMEL, J. A. N85-32137
RUNGSIROTEKOMOL, S. N85-32989
RUQUIST, R. N85-33101
RUSSELL, D. L. N85-32344
RUSSELL, R. J. N85-32315
RUSSO, A. J. N85-32328
RYAN, J. W. N85-32465
RYUTIN, A. A. N85-32978
RZAYEV, E. A. N85-32962

S

SABINS, F. F. N85-32365
SADOVSKIJ, B. F. N85-32698
SAFATOV, A. S. N85-32602
SAGAN, D. N85-32710
SAH, C. T. N85-32424
SAIDOV, R. P. N85-32895
SAKAHARA, M. D. N85-32230
SAKAI, H. N85-33012
SALM, J. N85-32623
SALSTEIN, D. A. N85-32572
SAMARSKIY, A. A. N85-32971
SANDOMIRSKIY, V. B. N85-32876
SANDS, D. C. N85-32603
SANTORO, R. T. N85-33021
SARIN, S. K. N85-32227
N85-32801
SARWATE, D. V. N85-32523
SASAMORI, T. N85-32473
SASSEN, K. N85-32635
SATO, M. N85-33088
SATO, T. N85-32543
SAUL, J. M. N85-33089
SAUNDERS, C. P. R. N85-32609
SAUTER, D. N85-32667
SAXENA, V. K. N85-32686
N85-32688
SAZONOV, A. I. N85-32917
SCHACHER, G. E. N85-32460
SCHACK, C. J. N85-32165
SCHAEFER, G. N85-32858
SCHAFFER, J. D. N85-32792
N85-32793
SCHEFFLER, A. O. N85-32502
SCHEMENAUER, R. S. N85-32671
SCHEULDERMAN-SUYLEN, T. N85-32743
SCHIEFELBEIN, G. F. N85-32213
SCHIFF, L. B. N85-32090
N85-32094
SCHINDLER, S. M. N85-33046
N85-33049
SCHMIDT, R. J. N85-33021
SCHMIDT, T. M. N85-32734
N85-32737
N85-32739
SCHMITT, R. N85-32585
SCHNELL, R. C. N85-32611
N85-32658
SCHNITTA-ISRAEL, B. N85-32554
SCHOEBERL, M. R. N85-32470
N85-32471
N85-32472
N85-32474
N85-32499
SCHOENBERG, I. J. N85-32640
SCHOLZE, T. N85-32191
SCHROEDER, R. A. N85-32112
SCHROTH, J. G. N85-32187
SCHUETZ, L. N85-32654
SCHULTZ, P. M. N85-33090
SCHWARTZ, I. B. N85-32564
SCHWERZEL, R. E. N85-32320
SCOLARO, A. F. N85-32399
SCOTT, J. N. N85-32300
SEAMAN, L. N85-32354
SEBERT, M. N85-32654
SEGALL, R. N. N85-32287
SEGLINSH, Y. A. N85-32872
SEGUR, H. N85-32837
SEIDENSTICKER, R. G. N85-32425
N85-32436
SEIDERS, R. P. N85-32163

SELF, R. J. N85-32184
SELVAM, A. M. N85-32646
N85-32680
SELVAN, A. M. N85-32613
N85-32619
SERGEEV, V. V. N85-32606
SERPOLAY, R. N85-32673
N85-32683
SERVAIS, R. N85-32152
SERVANT, J. N85-32639
SEVERIKOV, V. N. N85-32889
SHAKIR, Y. A. N85-32886
SHALAYEV, V. M. N85-32920
SHARMA, S. K. N85-32613
SHARP, R. D. N85-32552
SHARP, R. P. N85-32360
SHATTUCK, J. H. N85-32247
SHAW, A. N85-32776
SHAW, T. N85-32743
N85-32744
SHCHEGLOV, V. A. N85-32901
SHEA, M. A. N85-33102
SHERETOV, E. P. N85-32933
SHERMAN, M. H. N85-32269
SHESTOPALOV, V. P. N85-32941
SHEVTSOVA, A. I. N85-32889
SHEYNDLIN, A. E. N85-32926
SHIH, C. F. N85-32437
SHIN, K. G. N85-32821
SHINGAREV, G. L. N85-32625
SHISHOV, V. I. N85-32898
SHOCKEY, D. A. N85-32345
N85-32354
SHOR, P. W. N85-32842
SHPAK, Y. V. N85-32925
SHUKLIN, V. S. N85-32923
SHURSHALOV, L. V. N85-32883
SIDOROV, A. I. N85-32602
N85-32900
SIDOROV, V. N. N85-32661
SIKKA, P. N85-32680
SILAEV, A. V. N85-32626
SILIN, N. A. N85-32602
SILIN, V. P. N85-32961
SILVUS, H. S., JR. N85-32275
SIMMEN, R. L. N85-32815
SIMON, , I. N85-32591
SIMON, R. S. N85-32141
SIMONDS, R. A. N85-32151
SIMONENKO, Y. V. N85-32878
SIMS, C. S. N85-33008
SINGH, G. N85-32653
SISAKYAN, I. N. N85-32963
SKALA, I. N85-32902
SKINNER, H. B. N85-32995
SKIVINGTON, K. D. N85-32769
SKLAVIDIS, A. I. N85-32707
SKOBELEV, I. Y. N85-32947
SKOBLIKOV, S. V. N85-32937
SKRASOVSKIY, V. V. N85-32908
SKUPNIEWICZ, C. E. N85-32460
SLACK, G. A. N85-32270
SLEDD, J. N85-32147
SMART, D. F. N85-33102
SMEGGIL, J. G. N85-32188
SMILNE, D. N85-32708
SMIRNOV, A. S. N85-32956
SMIRNOV, V. B. N85-32960
SMIRNOV, V. I. N85-32647
SMIRNOV, V. V. N85-32660
SMITH, A. B. N85-33009
SMITH, C. J. E. N85-32182
SMITH, D. L. N85-33009
SMITH, E. M. N85-32591
SMITH, L. G. N85-32484
SMITH, S. L. N85-32807
SMITS, G. N85-32773
SMOKLER, M. I. N85-32401
N85-32445
SNIDER, J. R. N85-32603
SNYDER, C. A. N85-32156
SNYDER, L. N85-32842
SO, F. N85-32427
SOBOLEV, L. M. N85-32915
SOFRONIS, P. N85-32195
SOKOLOV, N. L. N85-32965
SOKOLOV, S. Y. N85-32870
SOKOLOVA, Z. N. N85-32875
SOLLINS, K. R. N85-33037
SOLOMON, H. N85-32854
SOLOVJEV, A. D. N85-32612
SOMS, A. P. N85-32338
SONKEL, H. N85-32566
SOROCHENKO, V. R. N85-32886
SOYKA, A. K. N85-32967
SPENCE, T. N85-32701
SPENCER, J. H. N85-32141
SPETTEL, B. N85-33077
SPIELMAN, J. B. N85-32316
SPINELLI, J. M. N85-32827
SPITZER, M. B. N85-32446
SPOFFORD, C. W. N85-32992
STALEVICH, D. D. N85-32610
STALNAKER, J. D. N85-32203
STANNETT, V. T. N85-32207
STARR, C. H. N85-33049
STECKLER, K. N85-32104
STEEN, R. P., JR. N85-32810
STEFANOVICH, L. I. N85-32865
STEIN, D. N85-32615
STEPAN, J. N85-32146
STEPANENKO, M. M. N85-32949
STEPANOV, A. A. N85-32901
STEPANOV, B. M. N85-32947
STEPANOV, G. V. N85-32604
STEPANOV, V. V. N85-32963
N85-32972
STERN, R. A. N85-33096
STEVENS, D. J. N85-32213
STEVENSON, D. J. N85-33091
STEWART, B. L. N85-33036
STILLMAN, D. W. N85-32846
STILTNER, D. B. N85-32823
STINGL, J. N85-32656
STITT, G. R. N85-32526
STOCK, S. R. N85-32348
STOCKMEYER, L. N85-32799
STONE, E. C. N85-33046
N85-33047
N85-33049
N85-33051
N85-33052
N85-33053
N85-33054
N85-33055
N85-33056
N85-33057
N85-33058
N85-33059
N85-33103
STONE, R. H. N85-32620
STRAPP, J. W. N85-32671
STRAUCH, R. G. N85-32475
N85-32521
N85-32542
STRICKER, J. N85-32302
STRIKOVSKIY, M. D. N85-32877
STRIKWERDA, J. C. N85-32277
STRINGFELLOW, G. B. N85-33029
STRONG, K. T. N85-33096
STRUMINSKIY, V. V. N85-32880
STUCKEY, J. N85-32147
STULOV, L. D. N85-32644
SUBBARAMU, M. C. N85-32641
SUGIMURA, R. S. N85-32448
SUGIOKA, I. N85-32095
SULKHANISHVILI, G. I. N85-32936
SULLIVAN, P. J. N85-32116
SUNDQUIST, A. R. N85-32747
SURAN, L. N85-32782
SUTUGIN, A. G. N85-32649
SVIRKUNOV, P. N. N85-32940
SWAYKOS, J. W. N85-32705
SZABO, G. N85-32652
SZE, D. K. N85-33006
SZE, N. D. N85-32561

T

TACELLI, C. B. N85-32313
TAKAHASHI, K. N85-32642
TAMM, E. N85-32623
TAMMET, H. N85-32623
TANG, C. L. N85-33024
TARASOV, I. S. N85-32910
TARIG, M. N85-32989
TARNEY, J. N85-33093
TASK, H. L. N85-32114
TATINCLAUX, J. C. P. N85-32859
TAVARES, E. J. N85-32116
TAYLOR, P. C. N85-32263
N85-33029
TAYLOR, R. L. N85-32234
N85-32235
TAYLOR, R. W. N85-33011
TEGEN, C. M. N85-32238
TENBRINK, H. M. N85-32664
TERPUGOV, V. S. N85-32912
TESTOV, V. G. N85-32888
TETENBAUM, D. N85-32528
TEWARSON, A. N85-32104
THOMAS, M. N85-32162
THOMPSON, G. E. N85-32239
THOMPSON, R. S. N85-32576
THOMSON, D. W. N85-32544
THROWER-LESESNE, P. E. N85-32280
TIEDERMAN, W. G. N85-32274
TIKHONCHUK, V. T. N85-32961
TIKHONOV, A. N. N85-32978
TIMOFEYEV, I. B. N85-32943
TINSLEY, E. J. N85-32386
TISCHER, H. N85-32326
TOBIAS, L. N85-32101
TOKSOZ, M. N. N85-32565
TOLASZ, J. N85-32786
TOMBERLIN, T. J. N85-32979
TOMCHUK, P. M. N85-32867
TOMPKINS, S. S. N85-32149
TOOMRE, J. N85-33098
TOVSTENKO, L. M. N85-32626
TRAHAN, C. J. N85-32764
TRIBBLE, G. N85-32742
TRIPP, J. H. N85-32329
N85-32331
TROSHIN, B. I. N85-32914
TRUEPER, H. G. N85-32735
TRUNCELLITO, N. T. N85-32286
TSAFARAS, V. A. N85-32582
TSENDIN, L. D. N85-32937
TSINTSADZE, D. G. N85-32648
TSUDA, T. N85-32543
TUCK, R. A. N85-32995
TURNER, E. R. N85-32993
TURNER, R. E. L. N85-32557
TUSTIN, D. N85-32394
TWIDALE, C. R. N85-32364
N85-32383
TYMEN, G. N85-32662
TZUOO, K. N85-32096

U

UBAYDULLAYEV, S. A. N85-32919
N85-32953
UCKAN, N. A. N85-33021
UENO, Y. N85-32607
UMOV, A. P. N85-32937
URQUIDI, M. N85-33023
USKOV, A. V. N85-32904
UVAROV, A. D. N85-32660
UVELLI, D. A. T. N85-32834

V

VAHRENKAMP, R. N85-32262
VAIRAVAMURTHY, A. N85-32742
VAKULOVSKIY, A. S. N85-32940
VALL, G. N85-32616
VALSHIN, A. M. N85-32903
VANASSE, G. N85-33012
VANDEKAMP, D. W. N85-32475
VANDENBROECK, J. M. N85-32557
VANDERHAGE, J. C. H. N85-32670
VANDEVATE, J. F. N85-32664
VANLEEUWEN, E. H. N85-32276
VANNUCCI, R. D. N85-32148
VARNAVSKIY, O. P. N85-32938
VARSHNEYA, N. C. N85-32697
VASILEV, A. N. N85-32876
VASILOFF, S. N85-32573
VASUDEVAN, R. N85-32991
VATOLIN, Y. N. N85-32970
VAVILOVA, L. S. N85-32908
VERMETTEN, A. N85-32664
VERNEKAR, K. G. N85-32627
VEST, G. M. N85-32254
N85-32426
VEST, R. W. N85-32254
N85-32428
VEUILLOT, J. P. N85-32298
VICK, R. L. N85-32749
VIELCANET, P. N85-32828
VIJAYAKUMAR, R. N85-32680
VINCENT, R. A. N85-32470
N85-32488
N85-32546
VINNINS, M. F. N85-32307
VINOKHODOV, A. Y. N85-32896
VITALIS, S. N85-32237
VLASAOVA, O. K. N85-32958
VOGL, O. N85-32406
VOHRA, K. G. N85-32624
N85-32641
N85-32687
VOLK, C. H. N85-32314

VOLOSHIN, A. R. N85-32916
VONDERHAAR, T. H. N85-32570
VONDRAK, R. R. N85-32562
VOROBEV, Y. V. N85-32968
VORONOVICH, A. G. N85-32862
VRATSKIY, V. A. N85-32894
VVEDENSKAYA, N. D. N85-32973
VYCHUZHANINA, M. V. N85-32612
VYSIKAYLO, F. I. N85-32896

W

WADA, B. K. N85-32437
WAENKE, H. N85-33077
WAGGONER, G. N85-32147
WAGNER, P. E. N85-32643
WAITES, M. L. N85-32204
WALDECK, D. H. N85-32994
WALKER, A. S. N85-32379
WALKER, D. E. N85-32990
WALKER, D. T. N85-32274
WALKER, W. W., JR. N85-32462
WALSH, F. N85-32454
WALSH, J. E. N85-32324
WANG, P. K. N85-32667
WANTLAND, J. L. N85-32288
WARBURTON, J. A. N85-32620
WARD, R. C. N85-32633
WARNE, L. K. N85-32250
WARNER, I. M. N85-32162
N85-32310
N85-33013
WARNOCK, J. M. N85-32518
N85-32536
WARREN, P. H. N85-33092
WASYLUK, R. N85-32782
WATERMAN, A. T. N85-32492
WATKINS, B. J. N85-32495
N85-32541
WATSON, R. E. N85-32185
WATTERS, D. M. N85-32308
WEAVER, B. L. N85-33093
WEBB, D. F. N85-33099
WEBB, T. P. N85-32115
WEBBER, W. R. N85-33051
N85-33056
N85-33058
N85-33059
WEI-XIU, L. N85-32651
WEI, Z. N85-32575
WEISS, N. R. N85-32131
WELKOS, S. L. N85-32750
WEN, L. N85-32449
WEN, S. Y. N85-32322
WENXIAN, Z. N85-32668
WERSAN, S. J. N85-32815
WERT, B. J. N85-33041
WEYL, G. N85-32323
WHEELER, T. G. N85-32763
WHITE, D. R. N85-32128
WHITE, G. S. N85-32202
WHITE, M. G. N85-33001
WHITEMAN, C. D. N85-32463
WICKS, G. W. N85-33024
WIDNALL, S. E. N85-32095
WIELER, J. G. N85-32578
WIGLEY, D. A. N85-32172
N85-32177
N85-32215
WILDE, B. W. N85-33023
WILKINSON, E. A. N85-32392
WILLIAMS, I. S. N85-33094
WILLIAMS, R. S., JR. N85-32372
N85-32380
N85-32381
N85-32384
WILLIS, P. N85-32407
N85-32434
WILLIS, R. N85-33084
WILSON, W. E. N85-32580
WINKLER, K. H. A. N85-32290
WIRTH, A. N85-33101
WISSMAR, R. C. N85-32551
WITTMANN, P. A. N85-32703
WOJCICKI, S. G. N85-33007
WOLF, M. N85-32396
N85-32419
WOLFSON, C. J. N85-33096
WONG, D. N85-32432
WOOD, V. E. N85-32320
WOODARD, D. M. N85-32525
WOODARD, D. W. N85-33024
WOODRUFF, R. R. N85-32776
WOOSTER, M. H. N85-32581
WORATSCHEK, R. N85-32116
WORTMAN, W. R. N85-32556
WRAY, W. O. N85-32455
WRIGHT, I. P. N85-33085
WRIGHT, W. N85-32303
WRIGHTON, M. S. N85-32201
N85-32997
WU, J. J. N85-32416
WU, J. R. N85-32268
WU, S. S. C. N85-32316
WYNNE, E. C. N85-32092

Y

YABLOCHKOV, S. M. N85-32868
YAKHNIN, V. Z. N85-32920
YAMSHCHIKOV, V. A. N85-32886
YANNITELL, D. W. N85-33018
YASHIN, V. Y. N85-32869
YATES, V. L. N85-32852
YAVOR, S. Y. N85-32925
YEDVABNYY, I. V. N85-32953
YEE, H. C. N85-32830
YEE, J. H. N85-33028
YEH, H. N85-32286
N85-32287
YEMELYANOV, V. K. N85-32753
YEREMIN, B. G. N85-32935
YEVDOKIMENKO, Y. I. N85-32941
YIANJUAN, C. N85-32668
YOLDAS, B. E. N85-32206
YOPP, J. H. N85-32736
YOUNG, L. G. N85-32620
YU, B. N85-32515
YUAN, J. S. N85-33029
YUAN, S. W. K. N85-32272
YUDIN, G. L. N85-32918
YUFEREV, V. S. N85-32874
YUMASHEV, K. V. N85-32893
YURCHAK, J. M. N85-32808

Z

ZAGAINOV, V. A. N85-32644
ZARIFYANTS, Y. A. N85-32873
ZASKALKO, O. P. N85-32961
ZASORIN, Y. V. N85-32882
ZAVOROTNEV, Y. D. N85-32865
ZEEVI, Y. Y. N85-32757
ZELENSKIY, S. Y. N85-32868
ZEMAN, G. H. N85-33004
ZHANG, K. S. N85-32473
ZHENZHEN, H. N85-32668
ZHI-LAI, S. N85-32681
ZHONG, J. N85-33030
ZHUKOV, S. P. N85-32914
ZHURAVSKIY, V. L. N85-32919
ZIER, M. N85-32689
ZIMMERMANN, R. E. N85-32106
ZINKOVSKAYA, O. V. N85-32891
ZIRILLI, F. N85-32806
ZIRINO, A. N85-32459
ZIYENKO, S. I. N85-32886
ZNILAI, S. N85-32668
ZOZULYA, A. N. N85-32961
ZUMBRUNNEN, A. D. N85-32291
ZUYEV, V. S. N85-32902
ZVIRGZDS, Y. A. N85-32872
ZYDA, M. J. N85-32780

CORPORATE SOURCE INDEX

Typical Corporate Source Index Listing

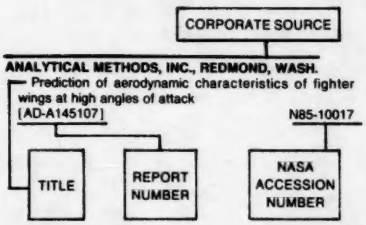

Listings in this index are arranged alphabetically by corporate source. The title of the document provides the user with a brief description of the subject matter. The report number helps to indicate the type of document cited (e.g., NASA report, translation, NASA contractor report). The NASA accession number denotes the number by which the citation is identified. The titles are arranged under each corporate source in ascending accession number order.

A

ACADEMIA SINICA, BEIJING (CHINA).
Characteristics of aerosol composition in a nonurban area, north China N85-32651
Measurements of giant salt nuclei from inland in east China N85-32668
The distribution of giant salt nuclei inside and outside cloud over the basin of Xin and Jiang N85-32681

ACADEMIA SINICA, LANZHOU (CHINA).
Observations of the atmospheric ice nucleus at northwest China N85-32618

ACADEMY OF SCIENCES OF THE GEORGIAN SSR, TBILISI (USSR).
On the transformation regularities of time series of solid aerosol concentrations in the surface atmospheric layer N85-32648
Aircraft investigations of the distribution of aerosols in the lower troposphere N85-32659

ACADEMY OF SCIENCES (USSR), MOSCOW.
Variation of the submicron aerosol structure N85-32661
On the question to the effect of surfactants on the spectrum of cloud drops in the process of their condensation growth N85-32679

ACCUMETRICS CORP., ROCKPORT, MISS.
Applied research and development for falling-sphere air density measuring systems
[AD-A155227] N85-32099

ADAPTIVE OPTICS ASSOCIATES, INC., CAMBRIDGE, MASS.
Solar adaptive optics
[AD-A155434] N85-33101

ADELAIDE UNIV. (AUSTRALIA).
Ancient landscapes: Their nature and significance for the question of inheritance N85-32364
Relationship of spaced antenna and Doppler techniques for velocity measurements (keynote paper), part 3 N85-32488
The Adelaide VHF radar: Capabilities and future plans N85-32546

ADVANCED INFORMATION AND DECISION SYSTEMS, MOUNTAIN VIEW, CALIF.
The documentation assistant: An intelligent system for documentation
[AD-A154709] N85-32800

ADVISORY GROUP FOR AEROSPACE RESEARCH AND DEVELOPMENT, NEUILLY-SUR-SEINE (FRANCE).
Three-Dimensional Techniques Applied to Internal Flows in Propulsion Systems
[AGARD-LS-140] N85-32293

AERONAUTICAL RESEARCH ASSOCIATES OF PRINCETON, INC., N. J.
Theory of soliton waves
[AD-A154784] N85-32837

AERONAUTICAL RESEARCH LABS., MELBOURNE (AUSTRALIA).
A phase-locked frequency multiplier for the signal averaging of the vibration of the Wessex helicopter input spiral bevel pinion
[AD-A154914] N85-32113
Proposal for modifications to the Wessex helicopter main rotor gearbox vibration monitoring program
[AD-A155196] N85-32117

AEROSPACE CORP., EL SEGUNDO, CALIF.
The role of long term lamp fluctuations in the random walk of frequency behavior of the rubidium frequency standard: A case study
[AD-A155336] N85-32314
Trapping of ion conics by downward parallel electric fields
[AD-A155306] N85-32568

AEROSPACE MEDICAL DIV., BROOKS AFB, TEX.
Air force technical objective document, Aerospace Medical Division, Fiscal Year 1986
[AD-A155195] N85-32762

AEROSPACE MEDICAL RESEARCH LABS., WRIGHT-PATTERSON AFB, OHIO.
The measurement of aircraft windscreen haze and its effect on visual performance
[AD-A154949] N85-32114
Myoelectric control of a computer based expert system for flight control
[AD-A154981] N85-32126

AIR FORCE ACADEMY, COLO.
Flight control system for a computer controlled aircraft with limited sensors
[AD-A155107] N85-32115

AIR FORCE GEOPHYSICS LAB., HANSCOM AFB, MASS.
Fluxgate magnetometer (SSM) for the defense meteorological satellite program (DMSP) block 5D-2, flight 7
[AD-A155229] N85-32143
Global geoid and gravity anomaly predictions using the collocation and point mass techniques
[AD-A154517] N85-32387
High resolution evidence for the Garrett-Munk spectrum of stratospheric gravity waves N85-32503
Application of satellite accelerometer data to improve density models
[AD-A154904] N85-32558
A simulation of weather in 3D space
[AD-A155221] N85-32586
Search for the north-south asymmetry in solar activity
[AD-A155525] N85-33102

AIR FORCE HUMAN RESOURCES LAB., BROOKS AFB, TEX.
Advanced simulator for pilot training and helmet-mounted visual display configuration comparisons
[AD-A155326] N85-32776

AIR FORCE INST. OF TECH., WRIGHT-PATTERSON AFB, OHIO.
Use of MMLE3 to determine lower order equivalent systems in the time domain
[AD-A154700] N85-32112
Microprocessor control design for a low-head crossflow turbine
[AD-A155477] N85-32121
Calculation of molecular constants potential energy curves and Franck-Condon factors for lead oxide
[AD-A154521] N85-32158
The effect of stress and hot corrosion on nickel-base superalloys
[AD-A154722] N85-32181
Electrical properties of bulk grown nitrogen doped silicon
[AD-A155471] N85-32266
Velocity and transient measurements in a shock tube using a hot-wire anemometer
[AD-A154694] N85-32305
Strain rate sensitivity estimation from high velocity impact data
[AD-A154703] N85-32347
Nuclear thermal transmittance in the atmosphere using LOWTRAN-6 computer code
[AD-A154669] N85-32553
A comprehensive study of the AFIT (Air Force Institute of Technology) software development environment
[AD-A155450] N85-32812
A comparison and analysis of Vintr's global routing algorithm with the Lee routing algorithm in two-layer printed circuit boards
[AD-A155600] N85-32816
Development of a dedicated speech work station
[AD-A155465] N85-32824
Oscillatory solutions of the Peaceman-Rachford alternating direction implicit method and a comparison of methods for the solution of the two dimensional heat diffusion equation
[AD-A154670] N85-32833
Optimal low thrust transfer using a first-order perturbation model
[AD-A154761] N85-32835
Bayesian vs MAP multiple model adaptive estimation for field of view expansion in tracking airborne targets
[AD-A155486] N85-32855
Continued development of a data base management system performance monitor: Volume 1
[AD-A154635] N85-33040

AIR FORCE OFFICE OF SCIENTIFIC RESEARCH, BOLLING AFB, WASHINGTON, D.C.
Status of boron combustion research
[AD-A154762] N85-32160
Air Force Office of Scientific Research (AFOSR). Technical report summaries: First quarter (CY)
[AD-A154757] N85-33041

AIR FORCE SYSTEMS COMMAND, WRIGHT-PATTERSON AFB, OHIO.
Electronic reconnaissance aircraft of the Soviet Union Navy
[AD-A154706] N85-32091
China has developed a new version of fighter aircraft
[AD-A155293] N85-32118
A small-scale self-excited rotor electrostatic generator
[AD-A155264] N85-32265
A fast discharge excimer laser with symmetric geometry
[AD-A155294] N85-32322
Meteorological weapons
[AD-A154735] N85-32575
Studies of circulatory and metabolic changes during ketamine narcosis
[AD-A154512] N85-32756
Determination of kinetic parameters of molecular beam epitaxy
[AD-A155222] N85-33030

AIR FORCE TECHNICAL APPLICATIONS CENTER, PATRICK AFB, FLA.
Results from radiation monitoring equipment experiments on STS-41C, 41D, 41G and 51A
[AD-A154676] N85-32142

AIR FORCE WRIGHT AERONAUTICAL LABS., WRIGHT-PATTERSON AFB, OHIO.
Synthesis and properties of arylethersulfone thermoset systems
[AD-A154811] N85-32198

AKRON UNIV., OHIO.
Results of an interlaboratory fatigue test program conducted on alloy 800H at room and elevated temperatures
[NASA-CR-174940] N85-32340
A continuous damage model based on stepwise-stress creep rupture tests
[NASA-CR-174941] N85-32341

ALABAMA UNIV., HUNTSVILLE.
Heating of the deep chromosphere during solar flares
[AD-A155256] N85-33100

ALASKA UNIV., FAIRBANKS.
Antenna induced range smearing in MST radars N85-32495
Estimation of vertical diffusion from observations of Atmospheric turbulence layers, part 4.4B N85-32507
Momentum flux measurements: Techniques and needs, part 4.5A N85-32508

The Sondrestrom radar: Progress and proposed upgrades for ST work N85-32541
Ice crystal nucleation on hygroscopic aerosols N85-32605
Concentration and source areas of ice nuclei in the Alaskan atmosphere N85-32634

ALLIED BENDIX CORP., KANSAS CITY, MO.
Improved coordinate measuring machine calibration and control
[DE85-012053] N85-32315
Plating density standards
[DE85-010014] N85-32318

AMERICAN COLL. TESTING PROGRAM, IOWA CITY, IOWA.
Models for multidimensional tests and hierarchically structured training materials
[AD-A155231] N85-32768

AMERICAN SCIENCE AND ENGINEERING, INC., CAMBRIDGE, MASS.
A study of the cyclical variations of coronal holes and their relation to open magnetic fields
[AD-A155251] N85-33099

APPLIED CRYOGENICS AND MATERIALS CONSULTANTS, NEW CASTLE, DEL.
Basic cryogenics and materials. Phase 1
[NASA-CR-177932] N85-32215

APPLIED SCIENCE ASSOCIATES, INC., APEX, N.C.
Scattering from foliage covered terrain
[AD-A154724] N85-32228

ARCO SOLAR, INC., CHATSWORTH, CALIF.
Pulsed excimer laser processing for cost-effective solar cells N85-32432

ARECIBO IONOSPHERIC OBSERVATORY, PUERTO RICO.
Mesospheric measurements of irregularity patches using a 3-antenna interferometer, part 3.6B N85-32498

ARGONNE NATIONAL LAB., ILL.
Resolution of thermal striping issue downstream of a horizontal pipe elbow in stratified pipe flow
[DE85-006195] N85-32292
Influence of chemical form, feeding regimen, and animal species on the gastrointestinal absorption of plutonium
[DE85-010291] N85-32751
Activities of the Physics Division
[DE85-000784] N85-33002
Tritium technology review
[DE85-010504] N85-33006
Evaluated nuclear-data file for niobium
[DE85-012095] N85-33009

ARIZONA STATE UNIV., TEMPE.
Aeolian geomorphology from the global perspective N85-32373

ARIZONA UNIV., TUCSON.
A new global geomorphology? N85-32358
A model for core formation in the early Earth N85-33078

ARMED FORCES RADIOBIOLOGY RESEARCH INST., BETHESDA, MD.
Paired ion chamber constants for fission gamma-neutron fields
[AD-A155069] N85-32999
Rhodium-103 and Indium-115 inelastic scattering reactions for fission neutron dosimetry N85-33004

ARMY ARMAMENT RESEARCH AND DEVELOPMENT COMMAND, WATERVLIET, N. Y.
Stress concentration in the elastoplastic state and residual stress after unloading
[AD-A155628] N85-32356

ARMY AVIATION ENGINEERING FLIGHT ACTIVITY, EDWARDS AFB, CALIF.
Artificial and natural icing tests YEH-60A quick fix helicopter
[AD-A155147] N85-32116

ARMY COLD REGIONS RESEARCH AND ENGINEERING LAB., HANOVER, N. H.
Numerical modeling of sea ice dynamics and ice thickness characteristics
[AD-A154600] N85-32700
Kinetic friction coefficient of ice
[AD-A155035] N85-32859
Ice fog as an electro-optical obscurant
[AD-A155059] N85-33015

ARMY CONSTRUCTION ENGINEERING RESEARCH LAB., CHAMPAIGN, ILL.
Field testing of a lightweight relocatable structure in a temperate environment
[AD-A155171] N85-32350

ARMY ENGINEER TOPOGRAPHIC LABS., FORT BELVOIR, VA.
The potential of the NAVSTAR global positioning system for the Corps of Engineers, civil works
[AD-A154913] N85-32109
Basic formulae for the computation of the deflection of the vertical from astronomical star observations
[AD-A154912] N85-32390
Realizing the full potential of the video disc for mapping applications
[AD-A154966] N85-32391
Optical storage technology for mapping
[AD-A154989] N85-32392

ARMY ENGINEER WATERWAYS EXPERIMENT STATION, VICKSBURG, MISS.
User's guide for computer program CGFAG, Concrete General Flexure Analysis with Graphics
[AD-A155555] N85-32204
Handbook for obtaining and using aerial photography to map aquatic plant distribution
[AD-A154584] N85-32388
Reverification of the Chesapeake Bay model
[AD-A155486] N85-32706

ARMY MEDICAL RESEARCH INST. OF INFECTIOUS DISEASES, FORT DETRICK, MD.
Differences in susceptibility of inbred mice to bacillus anthracis
[AD-A155646] N85-32750
Spontaneous transitional cell carcinoma in the urinary bladder of a strain 13 guinea pig
[AD-A155645] N85-32764

ARMY MILITARY PERSONNEL CENTER, ALEXANDRIA, VA.
An investigation into the fluidization and heat transfer of low density particles in a fluidized bed with applications
[AD-A155259] N85-32282
Microcomputer processing of LANDSAT Thematic Mapper data for the acquisition of military tactical terrain data
[AD-A154781] N85-32389

ARMY NATICK RESEARCH AND DEVELOPMENT COMMAND, MASS.
Feasibility study for small group water desalination equipment
[AD-A155106] N85-32164
The effects of prolonged feeding meal, ready-to-eat (MRE) operational rations
[AD-A154763] N85-32773

ARMY PROCUREMENT RESEARCH OFFICE, FORT LEE, VA.
Feasibility of applications of Competition Decision Assist Package (CDAP) to spare parts
[AD-A154716] N85-33036

ARMY RESEARCH AND TECHNOLOGY LABS., FORT EUSTIS, VA.
Comparisons of various configurations of the edge delamination test for interlaminar fracture toughness
[NASA-TM-86433] N85-32151

ATMOSPHERIC AND ENVIRONMENTAL RESEARCH, INC., CAMBRIDGE, MASS.
The diurnal variation of the neutral sodium species in the upper atmosphere: A model study
[AD-A154988] N85-32561
Generation of available potential energy and the energy cycle during the global weather experiment
[NASA-CR-175301] N85-32572

ATMOSPHERIC ENVIRONMENT SERVICE, DOWNSVIEW (ONTARIO).
Observations of cloud droplets, aerosol particles and cloud condensation nuclei in continental air masses N85-32671

AUBURN UNIV., ALA.
Measurement of damping of graphite epoxy materials
[NASA-CR-176073] N85-32334

AUSTRALIAN NATIONAL UNIV., CANBERRA.
Dating Archean zircon by ion microprobe: New light on an old problem N85-33094

B

BALLISTIC RESEARCH LABS., ABERDEEN PROVING GROUND, MD.
Imbedded thermocouples as a solid propellant combustion probe
[AD-A155630] N85-32167
BLAF: A blast field reconstruction program from pressure histories
[AD-A155300] N85-32283

BARCELONA UNIV. (SPAIN).
Ecophysiology of phototrophic sulfur bacteria in lakes: Vertical distribution of planktonic populations N85-32722
Sulfur cycling and metabolism of phototrophic and filamentous sulfur bacteria N85-32737
Buoyant densities of phototrophic sulfur bacteria and cyanobacteria N85-32740

BATTELLE COLUMBUS LABS., OHIO.
Metallurgical origins of fracture toughness and microstructure and fracture toughness of an HSLA (High-Strength/Low-Alloy) steel
[AD-A155530] N85-32187
Three-dimensional photochemical machining with lasers
[AD-A154711] N85-32320

BAYLOR COLL. OF MEDICINE, HOUSTON, TEX.
Physical chemical state of water in living cells
[AD-A154566] N85-32749

BELGIAN CENTER FOR CORROSION STUDY, BRUSSELS.
Understanding and laboratory prediction of the atmospheric corrosion behavior of steels and of non-ferrous metals and alloys
[AD-A154642] N85-32179

BHABHA ATOMIC RESEARCH CENTRE, BOMBAY (INDIA).
Supersaturation obtained in a condensation nucleus counter N85-32624
Experimental studies of the formation of Aitken nuclei in the atmosphere N85-32641
Human activity and production rate of secondary nuclei N85-32645
A review on the formation of aerosol particles in the atmosphere N85-32687

BIONETICS CORP., HAMPTON, VA.
Statistical methods for efficient design of community surveys of response to noise: Random coefficients regression models
[NASA-CR-177933] N85-32979

BOEING COMPUTER SERVICES CO., TUKWILA, WASH.
New developments on the core function for efficient implementation of the difficult residue number system operations
[AD-A154678] N85-32834

BOLT, BERANEK, AND NEWMAN, INC., CANOGA PARK, CALIF.
Overground Excess Sound Attenuation (ESA). Volume 3: Application of ESA data in NOISEFILE
[AD-A154820] N85-32984
Lateral attenuation of aircraft flight noise
[AD-A154958] N85-32986

BONN UNIV. (WEST GERMANY).
Phototrophic bacteria and their role in the biogeochemical sulfur cycle N85-32735
Enrichments for phototrophic bacteria and characterization by morphology and pigment analysis N85-32738

BOSTON COLL., CHESTNUT HILL, MASS.
Ionospheric electron density profile and related studies
[AD-A155257] N85-32567

BOSTON UNIV., MASS.
From microbial communities to cells N85-32728
Glutathione in cyanobacteria N85-32745

BROOKHAVEN NATIONAL LAB., UPTON, N. Y.
Photoelectron studies of autoionizing Rydberg states in HCl
[DE85-011813] N85-33001

BROWN UNIV., PROVIDENCE, R. I.
Considerations of large scale impact and the early Earth N85-33070

C

CALIFORNIA INST. OF TECH., PASADENA.
Megageomorphology: Mars vis a vis Earth N85-32360
Silicon production in an aerosol reactor N85-32416
Amorphous metallic films in silicon metallization systems N85-32427
Contributions to the 19th International Cosmic Ray Conference
[NASA-CR-176060] N85-33044
Cosmic ray He3 measurements
[PAPER-OG-4.2-3] N85-33045
Initial results from the Caltech/DSRI balloon-borne isotope experiment
[PAPER-OG-4.3-8] N85-33046
Measurements of Fe and Ar fragmentation cross sections
[PAPER-OG-7.2-20] N85-33047
Hexagonal uniformly redundant arrays for coded-aperture imaging
[PAPER-OG-9.2-1] N85-33048
A balloon-borne imaging gamma-ray telescope
[PAPER-OG-9.2-2] N85-33049
Balloon-borne video cassette recorders for digital data storage
[PAPER-OG-9.3-11] N85-33050
The energy spectrum of Jovian electrons in interplanetary space
[PAPER-SH-1.5-18] N85-33051
Precision measurements of solar energetic particle elemental composition
[PAPER-SH-2.1-4] N85-33052

Solar coronal and photospheric abundances from solar energetic particle measurements
[PAPER-SH-2.1-5] N85-33053
Latitude variation of recurrent fluxes in the outer solar system
[PAPER-SH-4.1-13] N85-33054
Changes in the energy spectrum of anomalous oxygen and helium during 1977 - 1985
[PAPER-SH-4.6-1] N85-33056
Solar cycle variations of the anomalous cosmic ray component
[PAPER-SH-4.6-2] N85-33057
Solar modulation and interplanetary gradients of the galactic electron flux, 1977 - 1984
[PAPER-SH-4.7-4] N85-33059
Thermal, dynamic and compositional aspects of the core-forming Earth N85-33091
Research in particles and fields
[NASA-CR-176069] N85-33103

CALIFORNIA STATE POLYTECHNIC UNIV., POMONA.
The problem of scale in planetary geomorphology N85-32375

CALIFORNIA UNIV., BERKELEY.
Nonradiative damping of molecular electronic excited states by metal surfaces
[AD-A154619] N85-32994
Research in extreme ultraviolet and far ultraviolet astronomy
[NASA-CR-176068] N85-33060

CALIFORNIA UNIV., BERKELEY. LAWRENCE BERKELEY LAB.
In-situ measurement of wall thermal performance: Data interpretation and apparatus design recommendations
[DE85-011979] N85-32289

CALIFORNIA UNIV., DAVIS.
Fundamental investigations of failure during superplastic forming process
[AD-A154647] N85-32194

CALIFORNIA UNIV., LIVERMORE. LAWRENCE LIVERMORE LAB.
Facility for large-scale hazardous gas testing
[DE85-011852] N85-32169
Numerical modeling of subsurface communication
[DE85-012818] N85-32249
Praxis release notes, version 7.3
[DE85-011862] N85-32820
DYNA3D, INGRID, and TAURUS: An integrated, interactive software system for crashworthiness engineering
[DE85-010928] N85-32846
Evaluated nuclear-data file for niobium
[DE85-012095] N85-33009
A review of the physics and response models for burnout of semiconductor devices
[AD-A155031] N85-33028
Energy and Technology Review
[DE85-011767] N85-33061

CALIFORNIA UNIV., LOS ANGELES.
Sintering studies project
[AD-A154750] N85-32216
Discovery of a nonpropagating hydrodynamic soliton
[AD-A155569] N85-32268
Vapor-liquid phase separator studies
[NASA-CR-166545] N85-32272
Planetary Dynamos
[NASA-CR-176001] N85-32857
Cyclotron resonance in a nonneutral plasma
[AD-A155248] N85-33017
Was core formation violent enough to homogenize the early mantle? N85-33068
Implications for the Earth of the early dynamical environment N85-33079
Earth's primordial differentiation, and its after-effects N85-33092

CALIFORNIA UNIV., SAN DIEGO, LA JOLLA.
Distribution and abundance of organic thiols N85-32717
Microbiology of solar salt ponds N85-32724
The composition of the primitive atmosphere and the synthesis of organic compounds on the early Earth N85-33065

CALIFORNIA UNIV., SANTA BARBARA.
Design of micelles as dephosphorylating agents
[AD-A155589] N85-32166
Precambrian evolution and the rock record N85-32711

CALSPAN CORP., BUFFALO, N. Y.
Closed-bomb combustion of Hivelite-based, Very High Burn Rate (VHBR) propellant
[AD-A155740] N85-32212

CAMBRIDGE ACOUSTICAL ASSOCIATES, INC., MASS.
Iteration solution for a submerged force-driven finite cylinder
[AD-A154587] N85-32982

CAMBRIDGE UNIV. (ENGLAND).
The calculation of fully three dimensional flow through any type of turbomachine blade row N85-32294

CARNEGIE-MELLON UNIV., PITTSBURGH, PA.
Large eddy structures in transitional and turbulent flames
[AD-A154520] N85-32157

CASE WESTERN RESERVE UNIV., CLEVELAND, OHIO.
Why CO bonds side-on at low coverage and both side-on and upright at high coverage on the Cr(110) surface
[NASA-CR-176071] N85-32173
Molecular orbital studies in oxidation: Sulfate formation and metal-metal oxide adhesion
[NASA-CR-176070] N85-32174
Adsorption of O2, SO2, and SO3 on nickel oxide. Mechanism for sulfate formation
[NASA-CR-176072] N85-32175
CO adsorption on (111) and (100) surfaces of the Pt sub 3 Ti alloy. Evidence for parallel binding and strong activation of CO
[NASA-CR-176077] N85-32176
EVA-glass interface bond stability N85-32408
Usefulness of multifrequency MST radar measurements, part 2.6B N85-32487
Determination of billows and other turbulent structures, part 4.1A N85-32500
Criteria and algorithms for spectrum parameterization of MST radar signals N85-32527

CELANESE RESEARCH CORP., SUMMIT, N.J.
Electrical and mechanical properties of intercalated graphite fibers
[AD-A155560] N85-32205

CENTRAL AEROLOGICAL OBSERVATORY, MOSCOW (USSR).
Ice nucleation by silver iodine particles with nearly critical sizes N85-32600
Airborne measurements of atmospheric ice nuclei N85-32612
On the mechanisms responsible for the formation of typical size spectra and vertical distribution of tropospheric aerosol particles N85-32647

CENTRE NATIONAL D'ETUDES DES TELECOMMUNICATIONS, SAINT MAUR DES FOSSES (FRANCE).
Proust radar: Decoding hardware and coherent integration, part 7.2A N85-32524
The Proust radar N85-32547

CENTRE NATIONAL DE LA RECHERCHE SCIENTIFIQUE, PARIS (FRANCE).
Granulometric study of the acidity and sulfate excess in marine aerosols N85-32691

CENTRE NATIONAL DE LA RECHERCHE SCIENTIFIQUE, VERRIERES-LE BUISSON (FRANCE).
Activities report of the Aeronomy Department
[G-774-1984] N85-32569

CERAMPHYSICS, INC., WESTERVILLE, OHIO.
Capacitive energy storage at cryogenic temperatures
[AD-A154508] N85-32253

CESKOSLOVENSKA AKADEMIE VED, PRAGUE.
Ice-forming efficiency of the soluble and insoluble portions of dust contained in snow N85-32631

CHEMICAL DYNAMICS CORP., COLUMBUS, OHIO.
Vibrationally enhanced dissociation of diatomic molecules
[AD-A154827] N85-32996

CHEMICAL RESEARCH AND DEVELOPMENT CENTER, ABERDEEN PROVING GROUND, MD.
Phase behavior and QLS (Quasielastic Light Scattering) in potassium linoleate/n-alkanol microemulsions
[AD-A155028] N85-32163

CHEVRON OIL FIELD RESEARCH CO., LA HABRA, CALIF.
Geomorphology, tectonics, and exploration N85-32365

CINCINNATI UNIV., OHIO.
Interfacial bonding stability N85-32409

CLEMSON UNIV., S.C.
Accelerated stress factors and failure/degradation mechanisms in terrestrial solar cells N85-32451

CLERMONT-FERRAND UNIV. (FRANCE).
Influence on an industrial site on the characteristics of CCN supersaturation with air masses of different origin N85-32683

COAST GUARD, WASHINGTON, D.C.
LORAN-C harbor and harbor entrance survey: Charleston, South Carolina
[AD-A154875] N85-32108
Application of adaptive noise cancellation to Coast Guard voice communications
[AD-A154798] N85-32230

COLORADO SCHOOL OF MINES, GOLDEN.
Qualitative analysis of sign-bit processing
[AD-A154776] N85-32804

COLORADO STATE UNIV., FORT COLLINS.
Rain volume estimation over areas using satellite and radar data
[NASA-CR-176050] N85-32570
Experimental studies of the kinetics of deposition nucleation on an ice nucleant used in weather modification N85-32596
Properties of aerosol particles detected by satellites in coastal regions N85-32622
Critical supersaturations with respect to water for fast condensation-freezing ice nucleation N85-32632
The measured rate of condensation nucleation to droplets using the techniques of chemical kinetics N85-32694

COLORADO UNIV., BOULDER.
Practical use of a tropopause height determination algorithm on an MST radar data set, part 1.8B N85-32479
Interpolation problems in meteor radar analysis, part 7.6A N85-32528
Data base management: MSTRAC (keynote paper), part 8 N85-32530
Bacterial ice nuclei of marine origin: Some recent observations N85-32611
Condensation nuclei and aerosol size distribution measurements in Arctic haze N85-32658
Conceptualizing in assembly tasks
[AD-A155564] N85-32770
Solar convection
[AD-A155214] N85-33098

COMMITTEE ON APPROPRIATIONS (U. S. SENATE).
Aviation system delays
[S-HRG-98-1241] N85-32102

COMMITTEE ON ENERGY AND COMMERCE (U. S. HOUSE).
Hazardous air pollutants
[GPO-43-064] N85-32458

COMMITTEE ON GOVERNMENT OPERATIONS (U. S. HOUSE).
Review of hazardous waste cleanup and disposal efforts at Tinker Air Force Base
[GPO-43-294] N85-32457

COMMITTEE ON PUBLIC WORKS AND TRANSPORTATION (U. S. HOUSE).
Status of the air traffic control system
[GPO-40-343] N85-32107

COMPUTER SCIENCES CORP., BAY ST. LOUIS, MISS.
TNT equivalency of EAK explosive
[AD-A155737] N85-32211

COMPUTER SCIENCES CORP., FALLS CHURCH, VA.
Secure digital voice communications in the Defense Data Network (DDN)
[AD-A154677] N85-32226
Flexible satellite communications systems simulator, phase 3
[AD-A155647] N85-32247

CONGRESSIONAL BUDGET OFFICE, WASHINGTON, D. C.
Pricing options for the space shuttle. Special study N85-32138

CONSIGLIO NAZIONALE DELLE RICERCHE, BOLOGNA (ITALY).
Characterization of insoluble particles associated with cloud droplets N85-32693

CONTROL DATA CORP., MINNEAPOLIS, MINN.
Synoptic-scale dynamics with vertical velocity, part 1.8A N85-32478
Frequency and site selection criteria for MST radars, part 5.1A N85-32512
MST radar data management N85-32532

CORNELL UNIV., ITHACA, N.Y.
Andrean examples of mega-geomorphology themes N85-32367
Tropospheric-stratospheric exchange, part 1.1A N85-32468
Observations of frontal zone structures with a VHF Doppler radar and radiosondes, part 1.2A N85-32469
Use of the VAD technique and measurements of momentum flux in the stratosphere at Aercibo, part 4.3A N85-32505
Overview of on-line data processing for MST radars (keynote paper), part 7 N85-32519
Status of the Jicamarca radar N85-32535
Object identification and manipulation using silhouette moments
[AD-A154755] N85-33011
Microwave semiconductor research: Materials, devices and circuits and gallium arsenide ballistic electron transistors
[AD-A154698] N85-33024

CRYO SUPPORT SERVICES, INC., NEW CASTLE, DEL.
A systematic plan for the continued study of dimensional stability of metallic alloys considered for the fabrication of cryogenic wind tunnel models
[NASA-CR-172449] N85-32172

Machining-induced deformation in stepped specimens of PH 13-8 Mo, 18 nickel maraging steel grade 200T1 and grain-refined HP 9-4-20
[NASA-CR-172450] N85-32177

D

DALMO VICTOR CO., BELMONT, CALIF.
Evaluation of a software design approach: Develop a threat resolution module in Ada (trademark)
[AD-A155599] N85-32815
DARTMOUTH COLL., HANOVER, N.H.
Cerenkov maser and Cerenkov laser devices
[AD-A155443] N85-32324
DAYTON UNIV., OHIO.
Improved materials for composites and adhesive joints
[AD-A154918] N85-32152
Improved materials for composite and adhesive joints
[AD-A155065] N85-32153
Numerical solution of the Navier-Stokes equations for 3-D internal flows: An emerging capability N85-32300
Visual phenomena produced by binocularly disparate dynamic visual noise
[AD-A154758] N85-32757
A theory of exciton photoluminescence for two types of neutral acceptors in silicon. A study of the systems Si:(B, IN), Si:(Al), (Si), Si:(Ga, In), Si:(B, Al), Si:(B, Ga), and Si:(Al, GA)
[AD-A155452] N85-33031
DEFENCE RESEARCH ESTABLISHMENT, OTTAWA. (ONTARIO).
Observations of the use of the setapoint detector
[AD-A154533] N85-32208
Test evaluation of the Honeywell GG1111 Single-Degree-of-Freedom (SDF) strapdown gyroscope
[AD-A154768] N85-32307
DEFENSE TECHNICAL INFORMATION CENTER, ALEXANDRIA, VA.
The flow of scientific and technical information in the US Army Research Laboratories
[AD-A155050] N85-33043
DEPARTAMENTO DE FISICA FUNDAMENTAL, VALIADOLID (SPAIN).
A statistical analysis of ice nuclei concentrations at urban and rural sites in Valladolid, Spain N85-32614
DEPARTMENT OF ENERGY, WASHINGTON, D. C.
High-efficiency crystalline silicon technology development N85-32395
The future of crystalline silicon technology in the US Department of Energy program N85-32399
DEPARTMENT OF THE ARMY, WASHINGTON, D. C.
Microwave SAW (Surface Acoustic Wave) monochromator
[AD-D011718] N85-32311
DESERT RESEARCH INST., RENO, NEV.
The capture of ice nucleating and non ice-nucleating aerosols by ice phase precipitation N85-32620
Stable generation of highly monodisperse aerosols N85-32628
A relationship between cloud droplet size and CCN critical supersaturation N85-32677
The nuclei of cloud formation N85-32685
Applicability of surface CCN measurements N85-32696
DRAPER (CHARLES STARK) LAB., INC., CAMBRIDGE, MASS.
Hot isostatically pressed Sm(2)(TM)17 magnets
[AD-A155479] N85-32267
DREXEL UNIV., PHILADELPHIA, PA.
Temperature measurements on small droplets N85-32699
DUGWAY PROVING GROUND, UTAH.
Notes on atmospheric stability, turbulence, and its measurements
[AD-A155230] N85-32588

E

ECO ENERGY CONVERSION, NEWTON, MASS.
A safe, high-power-density lithium battery
[AD-A155223] N85-32454
ECOLE NORMALE SUPERIEURE, ABIDJAN (IVORY COAST).
A statistical study of CCN concentration in subequatorial climate: The particular case of the tropical wet forest N85-32673
ECOLE POLYTECHNIQUE, PARIS (FRANCE).
Magnetic fields in laser heated plasmas
[DE85-010715] N85-33022
EISCAT SCIENTIFIC ASSOCIATION, KIRUNA (SWEDEN).
Vertical transport in the atmosphere: Measurement capabilities and requirements of VHF radars, part 1.6A N85-32476
Signal statistics of the radar echoes: Angle-of-arrival statistics, part 2.2A N85-32482
Potential advantages of the spaced antenna method for operational wind profiling, part 3.1B N85-32490
Accuracy of velocity and power determination by the Doppler method N85-32493
Improvement of vertical velocity measurements, part 3.4B N85-32494
Interferometer applications of VHF radars, part 3.6A N85-32497
Criteria for site selection and frequency allocation (keynote paper), part 5 N85-32511
Most desirable terrain, e.g., flat vs valley location, part 5.1B N85-32513
Increase of antenna area instead of transmitter power, part 6.3A N85-32517
Further developments of EISCAT as an MST radar N85-32534
ELECTROMAGNETIC COMPATIBILITY ANALYSIS CENTER, ANNAPOLIS, MD.
Field antenna handbook
[AD-A155204] N85-32242
ELECTROTEK CONCEPTS, INC., KNOXVILLE, TENN.
Experimental investigation of a variable speed constant frequency electric generating system from a utility perspective
[NASA-CR-174950] N85-32251
EMMANUEL COLL., BOSTON, MASS.
Equitorial scintillations: Advances since ISEA-6
[AD-A154962] N85-32559
EMORY UNIV., ATLANTA, GA.
Multidimensional luminescence measurements
[AD-A154950] N85-32162
A microprocessor-controlled, multichannel fluorimeter for analysis of sea water
[AD-A154986] N85-32310
Optical output stabilization method for direct current arc lamps
[AD-A154987] N85-33013

F

FEDERAL AVIATION ADMINISTRATION, WASHINGTON, D.C.
FAA/GAMA (Federal Aviation Administration/General Aviation Manufacturer's Association) propeller aircraft noise test program, Salina Municipal Airport, Salina, Kansas
[AD-A154818] N85-32983
FLORIDA STATE UNIV., TALLAHASSEE.
Reconciling Bayesian and frequentist evidence in the one-sided testing program
[AD-A155603] N85-32850
The problem of the Earth's CO2 content and the iron core N85-33069
FLORIDA UNIV., GAINESVILLE.
Physics of heavily doped silicon and solar-cell parameter measurement N85-32418
Electrotransport in thin films
[AD-A155584] N85-33034
FORT LEWIS A&M COLL., DURANGO, COLO.
One application of mega-geomorphology in education N85-32370
FRAUNHOFER-INST. FUER ATMOSPHAERISCHE UMWELTFORSCHUNG, GARMISCH-PARTENKIRCHEN (WEST GERMANY).
Visibility and vertical structure measurements in southern Germany
[AD-A154714] N85-32574

G

GA TECHNOLOGIES, INC., SAN DIEGO, CALIF.
Decomposition of sulfuric acid using solar thermal energy
[DE85-012288] N85-32170
GENERAL ACCOUNTING OFFICE, WASHINGTON, D. C.
GAO (General Accounting Office) assessment of DOD's Very High Speed Integrated Circuits (VHSIC) technology program
[AD-A155109] N85-32261
GENERAL ELECTRIC CO., CINCINNATI, OHIO.
Component-specific modeling
[NASA-CR-174925] N85-32119
High temperature electronics technology: Life test report
[AD-A154681] N85-32257
GENERAL ELECTRIC CO., HUNTSVILLE, ALA.
MPS solidification model. Analysis and calculation of macrosegregation in a casting ingot
[NASA-CR-171589] N85-32178
GENERAL ELECTRIC CO., SCHENECTADY, N. Y.
Thermoelectric properties of beta-boron and some boron compounds
[DE85-011978] N85-32270
GEOLOGICAL SURVEY, DENVER, COLO.
Sulfur diagenesis in marine sediments N85-32721
GEOLOGICAL SURVEY, FLAGSTAFF, ARIZ.
Use of the synoptic view: Examples from Earth and other planets N85-32371
GEOLOGICAL SURVEY, MENLO PARK, CALIF.
Comparison of survey and photogrammetry methods to position gravity data, Yucca Mountain, Nevada
[DE85-011685] N85-32316
GEOLOGICAL SURVEY, RESTON, VA.
Geomorphic classification of Icelandic and Martian volcanoes: Limitations of comparative planetology research from LANDSAT and Viking orbiter images N85-32372
Large format camera photographs: A new tool for understanding arid environments N85-32379
Quantitative analysis of geomorphic processes using satellite image data at different scales N85-32380
Quantitative geomorphologic studies from spaceborne platforms N85-32381
Chemical evolution of the Earth: Equilibrium or disequilibrium process? N85-33088
GEOLOGICAL SURVEY, WASHINGTON, D.C.
Worldwide directory of national Earth-science agencies and related international organizations
[GS-CIRC-934] N85-32386
Changes in the organic material in lakes in the blast zone of Mount St. Helens, Washington: Hydrologic effects of the eruptions
[GS-CIRC-850-1] N85-32551
GEORGE MASON UNIV., FAIRFAX, VA.
Geomorphological similarity and uniqueness N85-32361
GEORGIA INST. OF TECH., ATLANTA.
Relationship of isolated turbulent regions to the general turbulent background, part 4.4A N85-32506
MENTOR: Adding an outlying receiver to an ST radar for meteor-wind measurement N85-32538
GEORGIA UNIV., ATHENS.
Sulfate-reducing bacteria: Microbiology and physiology N85-32732
GRD, INC., WARMINSTER, PA.
Recursive nonlinear filtering through complete linearization
[AD-A155029] N85-32844
GRENOBLE-1 UNIV. (FRANCE).
Basic ice nucleation mechanisms on mono and microcrystals and ice forming nuclei. Theoretical analysis and experimental results achieved in the laboratory over the past ten years: Review paper N85-32629
The interaction of polynuclear aromatic hydrocarbons PAH's with water vapor and their role as condensation nuclei in the formation of haze and fog N85-32695

H

HAHNEMANN MEDICAL COLL. AND HOSPITAL, PHILADELPHIA, PA.
Analysis of long bone and vertebral failure patterns
[AD-A154796] N85-32758
HARVARD COLL. OBSERVATORY, CAMBRIDGE, MASS.
The space shuttle glow
[AD-A154937] N85-32139
HARVARD-SMITHSONIAN CENTER FOR ASTROPHYSICS, CAMBRIDGE, MASS.
Conditions during formation of the Earth N85-33086
HARVARD UNIV., CAMBRIDGE, MASS.
Matrix fracture in fiber-reinforced ceramics
[AD-A154704] N85-32197
Constraints on the development of the early continental crust from isotopic data N85-33076
HEBREW UNIV., JERUSALEM (ISRAEL).
The nucleation of ice crystals during the freezing of large supercooled drops N85-32608
Protocyanobacteria: Oxygenic and Anoxygenic photosynthesis in mat-forming bacteria N85-32714
Sulfur transformations at the hydrogen sulfide/oxygen interface in stratified waters and in cyanobacterial mats N85-32715
Interactions among sulfide-oxidizing bacteria N85-32741
HIGH MOUNTAIN GEOPHYSICAL INST., NALCHIK (USSR).
The effect of supersaturation, temperature and particle size on ice-nucleating ability of atmospheric aerosol N85-32604
HONEYWELL, INC., BLOOMINGTON, MINN.
Development of wide band recording materials
[AD-A154961] N85-32309

HONEYWELL SYSTEMS AND RESEARCH CENTER, MINNEAPOLIS, MINN.
Robust control of multivariable and large space systems
[AD-A155117] N85-32140
HOUSTON UNIV., TEX.
Insights into the phylogenetic positions of photosynthetic bacteria obtained from 5S rRNA and 16S rRNA sequence data N85-32719
HUGHES AIRCRAFT CO., CULVER CITY, CALIF.
Automation study for space station subsystems and mission ground support
[NASA-CR-176097] N85-32136
Georgetown University Photovoltaic Higher Education National Exemplar Facility (PHENEF) N85-32400

I

IBM RESEARCH LAB., SAN JOSE, CALIF.
Nonlinear spectroscopy
[AD-A154708] N85-33010
ILLINOIS UNIV. AT URBANA-CHAMPAIGN, SAVOY.
The effect of diffusive hydrogen segregation on fracture of polycrystalline nickel
[AD-A155238] N85-32186
The shearing contribution in transformation toughening of brittle materials
[AD-A154656] N85-32195
Routing algorithms and stochastic analysis for large communications networks
[AD-A154654] N85-32225
Mechanics of near tip microcracking in brittle material
[AD-A154684] N85-32346
ILLINOIS UNIV., CHICAGO.
Silicon sheet surface studies N85-32441
ILLINOIS UNIV., URBANA.
The measurement of strain fields by X-ray topographic contour mapping
[AD-A154870] N85-32348
A numerical analysis of transient planetary waves and the vertical structure in a meso-strato-troposphere model, part 1.4A N85-32473
Some recent developments in the interpretation of MST radar returns from clear air (keynote paper), part 2 N85-32480
Morphology of the scattering targets: Fresnel and turbulent mechanisms, part 2.1A N85-32481
Observations of mesospheric turbulence by rocket probe and VHF radar, part 2.4A N85-32484
Interpretation of radar returns from the mesosphere, part 2.3A N85-32485
Radar echoes at 2.66 and 40.92 MHz from the mesosphere, part 2.6A N85-32486
Effects of line-of-sight velocity on spaced-antenna measurements, part 3.5A N85-32496
Gravity-wave spectra in the atmosphere observed by MST radar, part 4.2B N85-32502
T/R switch design for short-range measurements, part 6.1A N85-32515
Coding schemes for improving MST radar performance, part 7.1A N85-32520
Construction of complementary code sequence sets, part 7.1D N85-32523
Hardware schemes for fast Fourier transform, part 7.4A N85-32526
Sample interchange of MST radar data from the Urbana radar N85-32531
Urbana radar systems: Possibilities and limitations N85-32540
INDIAN INST. OF TROPICAL METEOROLOGY, POONA.
Aircraft observations of condensation and ice nuclei at a tropical station N85-32613
Ice nucleating characteristics of Capparis Aphylla, an Indian herb N85-32619
A thermal diffusion chamber for the measurement of cloud condensation nuclei N85-32627
A new hypothesis for the observed vertical distribution of atmospheric aerosols N85-32646
Chemical composition of atmospheric aerosol at Delhi N85-32653
Aircraft observations of cloud condensation nuclei in maritime and continental environments N85-32680
INFORMATIQUE INTERNATINALE S.A., RUNGIS (FRANCE).
Comparative study on data system architectures
[ESA-CR(P)-2015] N85-32828
INSTITUT D'AERONOMIE SPATIALE DE BELGIQUE, BRUSSELS.
Solar radio fluxes as indices of solar activity
[AERONOMICA-ACTA-A-282-1984] N85-33095
INSTITUTE FOR ATMOSPHERIC OPTICS AND REMOTE SENSING, HAMPTON, VA.
Data analysis for lidar and quartz crystal microbalance systems
[NASA-CR-172601] N85-32464
INSTITUTE FOR ATMOSPHERIC PHYSICS, BUDAPEST (HUNGARY).
Trace element concentrations in atmospheric aerosol over Hungary N85-32652
INSTITUTE OF APPLIED GEOPHYSICS, MOSCOW (USSR).
Condensation properties of atmospheric aerosol N85-32672
Investigation of the formation of cloud particle spectrum on natural condensation nuclei N85-32674
INSTITUTE OF CHEMICAL KINETICS AND COMBUSTION, NOVOSIBIRSK (USSR).
Experimental investigation of properties of ice-forming reagents N85-32602
INSTITUTE OF EXPERIMENTAL METEOROLOGY (USSR).
The variability of aerosol microstructure in continental and oceanic surface layers of the atmosphere in anticyclones N85-32660
INTERGRAPH CORP., HUNTSVILLE, ALA.
Analysis of spacecraft data
[NASA-CR-171587] N85-32789
Analysis of spacecraft data
[NASA-CR-171597] N85-32790
INTERNATIONAL COMMISSION FOR CLOUD PHYSICS, LARAMIE, WYO.
Eleventh International Conference on Atmospheric Aerosols, Condensation and Ice Nuclei, volume 2
[PB85-182418] N85-32596
Eleventh International Conference on Atmospheric Aerosols, Condensation and Ice Nuclei, volume 1
[PB85-182400] N85-32636
INTERNATIONAL COUNCIL OF SCIENTIFIC UNIONS, URBANA, ILL.
Middle Atmosphere Program. Handbook for MAP. Volume 14: URSI/SCOSTEP Workshop on Technical Aspects of MST Radar
[NASA-CR-176085] N85-32466

J

JET PROPULSION LAB., CALIFORNIA INST. OF TECH., PASADENA.
Use of spaceborne imaging radar in regional geomorphic studies N85-32377
Proceedings of the 24th Project Integration Meeting
[NASA-CR-176058] N85-32394
High-efficiency module and array research N85-32397
Flat-plate module efficiency versus cost tradeoffs N85-32398
Block V module program N85-32401
Reliability physics N85-32402
Photothermal degradation studies of encapsulants N85-32403
Predicting photothermal field performance N85-32404
Topics in electrochemical degradation of photovoltaic modules N85-32410
JPL in-house fluidized-bed reactor research N85-32414
High-efficiency silicon solar cell research N85-32417
Sensitivity analysis of high-efficiency silicon solar-cell design parameters N85-32422
Silicon ribbon stress-strain activities N85-32437
Advanced module development overview N85-32445
Module Hipot and ground continuity test results N85-32447
Photovoltaic module spread-of-flame testing N85-32448
Improved Nominal Operating Cell Temperature (NOCT) test procedure N85-32449
Thin-film reliability and engineering overview N85-32450
Failure analysis of thin-film amorphous-silicon solar-cell modules N85-32452
Reference-cell calibration activities N85-32453
JOHANN-WOLFGANG-GOETHE-UNIV., FRANKFURT AM MAIN (WEST GERMANY).
Supersaturation spect A of Ice Nuclei at different locations in Europe and over the North-Atlantic N85-32615
Application of Particle Induced X-ray Emission analysis (PIXE) to aerosol long range transport studies N85-32665
JOINT PUBLICATIONS RESEARCH SERVICE, ARLINGTON, VA.
East Europe report: Science and technology
[JPRS-ESA-85-021] N85-32190
New metal coating method developed N85-32191
East Europe report: Science and technology
[JPRS-ESA-85-023] N85-32217
Applications of laser technology described N85-32218
Importance of automation, robotization in economy N85-32219
USSR report: Life sciences. Biomedical and behavioral sciences
[JPRS-UBB-85-020] N85-32752
Remote medical diagnosis N85-32753
Hydroponics developments for spaceship garden N85-32754
East Europe report: Science and technology. Selections on CSSR computer technology
[JPRS-ESA-84-017] N85-32781
Selections on CSSR computer technology N85-32782
The 8080 emulator N85-32783
R, L, C, G measurement N85-32784
Quality analysis N85-32785
Robots, Manipulators N85-32786
Digital integrated circuits N85-32787
GDR semiconductor parts N85-32788
USSR report: Physics and mathematics
[JPRS-UPM-85-004] N85-32860
The Konstantinov effect and absorption of sound in inhomogeneous media N85-32861
Toward the theory of acoustic scattering on uneven free surface N85-32862
New approximations and findings of theory of nonlinear acoustic beams N85-32863
Reflection of acoustic beam from inhomogeneous boundary N85-32864
Influence on bi-phonon states on Raman scattering of light in molecular crystals N85-32865
X-ray diffractometric measurements and calculations of limiting values of discrepancy between lattices and layer thicknesses, preventing generation of dislocations during growth of multilayer heterostructures N85-32866
Influence of coherent light beams on free carriers in semiconductors N85-32867
Luminescence and absorption of indium-activated potassium-borate glasses subjected to high-power excitation N85-32868
Generation and amplification of radiation during stimulated Raman scattering in crystals N85-32869
Absorption of 10.6 micrometer laser radiation in electron-hole condensate in germanium N85-32870
Classical emission of relativistic charged particles during axial channeling N85-32871
System for electro-optical ceramic recrystallization N85-32872
Defect formation in amorphous hydrated silicon subjected to laser radiation N85-32873
Quasi-steady-state melting mode during combined laser irradiation of semiconductor materials N85-32874
Inter-zone auger recombination in GaSb laser structures N85-32875
Photo-acoustic effect in finite-dimensional semiconductors N85-32876
Effect of powerful pulsed low-energy ion streams on GaAs N85-32877
Influence of background electrically neutral argon admixture on mechanical strength of silicon crystals N85-32878
Development of artificially produced perturbations in supersonic boundary layer N85-32879
Theoretical foundations of turbulent flows N85-32880
Toward the propagation of waves in unsteady media N85-32881
Exact solutions of singular equations for viscous transsonic flows N85-32882
Explosion in flight N85-32883
Investigation of reproducibility of emission wavelength of helium-neon laser with external neon absorption cell (0.63 micrometers) N85-32884
Prospects for lasers for fusion energy assessed N85-32885
Generation of single nanosecond high-contrast radiation pules (lambda=10.6 micrometers) N85-32886
Laser Elektronika-01 for air pollution control lidar N85-32887
Investigation of influence of gas exit modes on characteristics of N2O - N2 - He discharge laser N85-32888
Influence of mirror anisotropy and Brewster window orientation on radiation characteristics of ring lasers N85-32889
Lasing on LiF:F(-)2 - dye centers with transverse pumping N85-32890
Participation of singlet oxygen in photodestruction of air-saturated solutions of coumarin dyes N85-32891
The possibilities of remote analysis of atmospheric gases based on Raman scattering spectroscopy N85-32892
Choice of optimum saturating absorber for YAG passive mode-locking laser N85-32893
In-cavity laser IR spectrum analyzer for investigating non-steady-state processes N85-32894
Operation of solid state lasers exposed to electron beam N85-32895

Establishment of steady-state power level in pulse-periodic excimer laser N85-32896
The problem of brightness enhancement during laser frequency doubling N85-32897
Laser radiation propagation in inertialess nonlinear medium N85-32898
Dynamics of emission from dye lasers employing synchronous pumping by limited picosecond pulse train N85-32899
High-power two-frequency CW dye laser N85-32900
Saturation effect in multilevel lasing media N85-32901
Optical inhomogeneities in a nanosecond-pulse iodine photodissociation laser with slow UV radiation pumping N85-32902
Excimer-laser generator of powerful UV picosecond pulses synchronized with picosecond pulses in visible and IR bands N85-32903
Possibility of measurement of small displacements by ring laser N85-32904
Infrared laser holography used in fusion plasma studies N85-32905
Tunable lasers with high conversion efficiency N85-32906
Self Q-modulation and generation of short pulses in distributed-feedback lasers N85-32907
Low-threshold injection InGaAsP/GaAs double heterostructure lasers with separate limiting obtained by liquid-phase epitaxy (lambda = 0.78 divided by 0.87 microns, I sub thr = 460 A/cm 2, T = 300 K) N85-32908
Space-time characteristics of field in longitudinal pulse-period discharge typical in pumping of self-terminating lasers N85-32909
Influence of technological factors on luminescence characteristics of InGaAsP/InP heterolasers (lambda = 1.55 microns) N85-32910
Powerful XeCl excimer electric discharge laser with good temporal stability and fast response time N85-32911
Spectral-luminescence characteristics and induced emission of Nd-3(+) ion in Gd(2-x)Nd(x)(WO4)3 crystals N85-32912
Adjustment of radiation wavelength of multimode InP-GaInAsP injection heterolasers N85-32913
Selective population of N = 3 OVIII level during expansion of laser plasma in helium N85-32914
Passive Q-modulation of optical cavities by KCl crystals containing OH(-) -ions N85-32915
Acoustic wave scattering by round cylindrical shell reinforced with stringers N85-32916
Identification of vibrational-rotational transitions of Os-192O4 within frequency tuning limits of high pressure CO2 waveguide laser N85-32917
Toward a theory of excitation of atoms during nuclear and magnetic neutron scattering N85-32918
Nonequilibrium kinetics of growth of oxide layer grains during laser heating of metals in air N85-32919
Radiative-collision generation of sound in gases subjected to single-pulse optical excitation N85-32920
Doppler spectrometer for measuring narrow photochemical gaps in inhomogeneously broadened spectra N85-32921
Resonant energy transfer during strong excitation N85-32922
Transparency of water 9n 186 - 500 nm region N85-32923
Activation analysis of natural water using neutrons of various energies N85-32924
Transformation of charged particle beams by concentrating electro-optical systems N85-32925
Thermal contraction of current flow through electrode turbulent boundary layer N85-32926
Mirror reflection of charged particles from + amorphous and polycrystalline surfaces N85-32927
An attempt to detect induced neutron capture in laser radiation field N85-32928
Toward the question of multi-quark configurations in nuclei N85-32929
Exotic events of p bar p-collider: Excited quark or excited color boson? N85-32930
The possibility of observing and exploiting the generation of high-energy photons by electrons in the field of an intense electromagnetic wave N85-32931
Spatial parity violation in elastic neutron-nuclei interaction channel N85-32932
Possiblity of developing charged-particle energy analyzer based on hyperboloidal axisymmetrical lens N85-32933
High-energy Physics Institute building 3-trillion-ev accelerator N85-32934
Investigation of ion-acoustic plasma turbulence in field of powerful electromagnetic wave by CO2-laser radiation scattering N85-32935
Solution of problem of equilibrium confinement of plasma by magnetic field in an infinite circular cylinder N85-32936
Injection of hydrogen macroparticles into T-10 tokamak N85-32937
CCD-based X-ray spectrometry for on-line determination of laser plasma electron temperature N85-32938
Radio-frequency radiation of storm clouds N85-32939
Lower bounds of propagation velocity of steady ionizing waves in field of strong electromagnetic wave N85-32940
Amplification of electromagnetic wave by electron stream with negative velocity differences N85-32941
Electromagnetic wave amplification during cyclotron resonance in a medium N85-32942
Plasmodynamic methods for generating powerful light puses N85-32943
Characteristics of optogalvanic effect in media with inverse populations N85-32944
Cyclotron absorption of fast magnetosonic wave in stellarator N85-32945
A system of magnetohydrodynamic-type equations N85-32946
Investigation of space-time structure of glow of laser plasma colliding with flat screen N85-32947
Diamagnetic instability of cyclotron waves in plasma N85-32948
Influence of ECR-heating on MHD activity of plasma in tokamak-10 installation N85-32949
Comparison of findings of theories describing reflection from real surface with experiments in region of ultrasoft X-radiation N85-32950
Effective brightness of zero-point fluctuations of the electromagnetic vacuum accompanying parametric scattering of light N85-32951
Correlation of intensities of different scattering channels N85-32952
Absorption of laser radiation in substance with absorption coefficient depending linearly upon temperature N85-32953
Optical waveguide along front of exothermic reaction N85-32954
Electrostatic astigmatic tubular lens N85-32955
Fluctuations in light intensity during backscattering in turbulent medium N85-32956
Relaxation lens in inhomogeneous binary mixture N85-32957
Beam diffusion in linear ionospheric layer N85-32958
Coefficient of optical absorption and scattered light capture effect N85-32959
Methods for measuring and analyzing dispersion properties of multimode fiber optic lightpipes (a review) N85-32960
Stimulated Mandelstam-Brillouin scattering with distributed feedback N85-32961
Influence of phonon interaction on width and form of Mandelstam-Brillouin optical scattering line N85-32962
Solvability of some inverse problems in laser radiation focusing N85-32963
Influence of spatial pumping spectrum on quality of phase conjugate reflection during 4-photon interaction N85-32964
New method for correcting chromatism of mirror-lens objectives N85-32965
Dielectric mirror with ferromagnetic substrate N85-32966
The Faraday effect in ruby and corundum in strong magnetic fields N85-32967
Optical image of bounded objects N85-32968
Transmission of light by disperse medium of densely packed optically soft particles N85-32969
Equations of motion for electromagnetic waves in 4-dimensional Euclidian space N85-32970
On one nonlinear problem of laser thermochemistry N85-32971
Existence of smooth solutions in problems of electromagnetic radiation focusing N85-32972
Poisson formula for radon transformation and numerical image reconstruction algorithm N85-32973
Asymptotically stable solutions of some nonlinear equations N85-32974
Optimization of sampling in statistical physics experiments N85-32975
A new problem in mathematical physics associated with the problem of coherent phase transformation N85-32976
Necessary and sufficient conditions for single-extremum and convex problems of mathematical programming N85-32977
On the problem of linear programming with approximate data N85-32978

JORTNER RESEARCH AND ENGINEERING, INC., COSTA MESA, CALIF.
Effects of weak interfaces on thermostructural behavior of carbon-carbon composites
[AD-A155330] N85-32154

K

KARPOV (V. Y.) PHYSICAL CHEMISTRY INST., MOSCOW (USSR).
A study of time transformation of natural photochemical aerosols N85-32644
Size spectra for the source-enhanced coagulation with the turbulent mass transfer N85-32649
A probabilistic method for particle size analysis of aerosols N85-32669
on the transport of large condensation nuclei in the atmosphere at various altitudes over the territory of the USSR N85-32698

KENT STATE UNIV., OHIO.
A theory of exciton photoluminescence for two types of neutral acceptors in silicon. A study of the systems Si:(B, IN), Si:(Al), (Si), Si:(Ga, In), Si:(B, Al), Si:(B, Ga), and Si:(Al, GA)
[AD-A155452] N85-33031

KENTRON INTERNATIONAL, INC., HAMPTON, VA.
A systematic plan for the continued study of dimensional stability of metallic alloys considered for the fabrication of cryogenic wind tunnel models
[NASA-CR-172449] N85-32172
Machining-induced deformation in stepped specimens of PH 13-8 Mo, 18 nickel maraging steel grade 200T1 and grain-refined HP 9-4-20
[NASA-CR-172450] N85-32177

KENTUCKY UNIV., LEXINGTON.
Analysis of stress-strain relationships in silicon ribbon N85-32438
Stress and buckling analysis N85-32439
Generation of lead, lead iodide and iodide aerosols and their ice nucleation N85-32607

KLD ASSOCIATES, INC., HUNTINGTON, N. Y.
Robust detection and classification of regional seismic signals using a two mode/two stage cascaded adaptive arma (CAARMA) model
[AD-A154710] N85-32554

KYOTO UNIV. (JAPAN).
The MU radar now partly in operation N85-32543
Photochemical aerosol formation in polluted atmosphere N85-32642

L

LEICESTER UNIV. (ENGLAND).
Chemical constraints on the evolution of Archean continental crust N85-33093

LINCOLN LAB., MASS. INST. OF TECH., LEXINGTON.
Non-model based estimation with applications to sensor calibration using multiple sensors
[AD-A154736] N85-32306
Solid state research
[AD-A154783] N85-33025

LITTLE (ARTHUR D.), INC., CAMBRIDGE, MASS.
Absorption and scattering properties of aerosols of aggregated particles in the infrared spectral region
[AD-A155475] N85-32591

LOCKHEED MISSILES AND SPACE CO., PALO ALTO, CALIF.
ISEE-1 data reduction and analysis plasma composition experiment
[NASA-CR-175306] N85-32552
Discrete-element acoustic analysis of submerged structures using doubly asymptotic approximations
[AD-A154959] N85-32987
Soft X-ray polychromator for the Solar Maximum Mission
[NASA-CR-175297] N85-33096

LOFTIN (LAURENCE K., JR.), NEWPORT NEWS, VA.
Quest for performance: The evolution of modern aircraft
[NASA-SP-468] N85-32089

LONDON UNIV. (ENGLAND).
Techniques, problems and uses of mega-geomorphological mapping N85-32378

LOS ALAMOS NATIONAL LAB., N. MEX.
Clarke Stations and mercurian mass-drivers: Energy for large-scale transportation systems
[DE85-009607] N85-32145
Characteristics of a numerical fluid dynamics simulator
[DE85-009602] N85-32290
Tailored vacuum chambers for ac magnets
[DE85-010767] N85-32319
New estimating procedures for surface runoff, sediment yield, and contaminant transport in Los Alamos County, New Mexico
[DE85-011890] N85-32393
Performance analysis of mixed passive solar heating systems
[DE85-009624] N85-32455

Los Alamos optical materials reliability, maintainability, and exposure testing program
[DE85-011894] N85-32456
Radiation transport
[DE85-010333] N85-33005
Magnetic fields in laser heated plasmas
[DE85-010715] N85-33022

LOUISIANA STATE UNIV., BATON ROUGE.
Modeling the exhaust of the pulsed plasma thruster
[AD-A155344] N85-33018
Archean sedimentary systems and crustal evolution N85-33082

LUNAR AND PLANETARY INST., HOUSTON, TEX.
Workshop on the Early Earth: The Interval from Accretion to the Older Archean
[NASA-CR-176037] N85-33062
Crustal radiogenic heat production and the selective survival of ancient continental crust N85-33086
Lunar and Martian impact basins: Exposed records of terrestrial bombardment? N85-33090

M

MAIN GEOPHYSICAL OBSERVATORY, LENINGRAD (USSR).
On the efficiency of the mechanism of ice particles formation in the vapor supersaturation field around a freezing droplet N85-32606
On the problem of possible mechanism of ice nuclei formation in convective clouds N85-32610

MAINZ UNIV. (WEST GERMANY).
Our knowledge about the atmospheric aerosol N85-32650
Mineral aerosols and source identification N85-32654
Aitken particle size distribution in Antarctica N85-32656
Sahara Desert dust transport to the south N85-32666

MANAGEMENT AND TECHNICAL SERVICES CO., WASHINGTON, D.C.
USSR Space Life Sciences Digest
[NASA-CR-3922] N85-32709

MANCHESTER UNIV. (ENGLAND).
Global geomorphology N85-32359
Ice nucleus measurements N85-32609

MANDEX, INC., VIENNA, VA.
Helicopter noise survey for selected cities in the contiguous US
[AD-A154893] N85-32985

MASSACHUSETTS INST. OF TECH., CAMBRIDGE.
A panel method study of vortex sheets with special emphasis on sheets of axisymmetric geometry
[NASA-CR-177365] N85-32095
Resistance of polyaniline films as a function of electrochemical potential and the fabrication of polyaniline-based microelectronic devices
[AD-A154999] N85-32201
Interactive on-line conferences
[AD-A154723] N85-32227
Parallel simulation of digital LSI circuits
[AD-A154745] N85-32258
Analysis of inclined growth of silicon sheet N85-32442
Development of ultrasonic modeling techniques for the study of crustal inhomogeneities
[AD-A155206] N85-32565
Visual phenomena produced by binocularly disparate dynamic visual noise
[AD-A154758] N85-32757
Tight bounds on the complexity of parallel sorting
[AD-A154726] N85-32778
Resource management for the tagged token dataflow architecture
[AD-A154773] N85-32779
Consensus in the presence of partial synchrony (Preliminary version)
[AD-A154705] N85-32799
Software for interactive on-line conferences
[AD-A154742] N85-32801
Broadcasting topology and routing information in computer networks
[AD-A155668] N85-32827
A new fault-tolerant algorithm for clock synchronization
[AD-A154771] N85-32836
Generalized planar matching
[AD-A154809] N85-32842
Prospects for a new kind of synthesis: Assembly of molecular components to achieve functions
[AD-A155023] N85-32997
Distributed name management
[AD-A154785] N85-33037

MASSACHUSETTS UNIV., AMHERST.
Structure-property relationships in thermoplastic elastomers. Part 3: Segmented polyacetal-polyurethanes
[AD-A154897] N85-32200
SCRIBE data of October 23, 1983 flight
[AD-A154864] N85-33012

MATERIALS RESEARCH LABS., ASCOT VALE (AUSTRALIA).
Weak shock waves propagating in fluid-gas mixtures
[AD-A154759] N85-32276
Plasma mass and effective inductance in a small railgun
[AD-A154644] N85-32304

MAX-PLANCK-INST. FUER CHEMIE, MAINZ (WEST GERMANY).
Anorthositic oceanic crust in the Archean Earth N85-33077

MAX-PLANCK-INST. FUER METEOROLOGIE, HAMBURG (WEST GERMANY).
A simple model to investigate the activation process in waterclouds N85-32675

MCDONNELL-DOUGLAS ASTRONAUTICS CO., ST. LOUIS, MO.
Magnetics calculations for an ELMO Bumpy Square
[DE85-011438] N85-33021

MCDONNELL-DOUGLAS RESEARCH LABS., ST. LOUIS, MO.
Interface chemistry of Hg(1-x)Cd(x)Te
[AD-A154876] N85-32161

MCDONNELL-DOUGLAS TECHNICAL SERVICES CO., INC., HUNTSVILLE, ALA.
Space station ECLSS integration analysis: Simplified General Cluster Systems Model, ECLS System Assessment Program enhancements
[NASA-CR-176089] N85-32796

MECHANICAL TECHNOLOGY, INC., LATHAM, N. Y.
Friction and wear of solid-lubricated contact in gas turbine engine bearings
[AD-A155042] N85-32335

METEOROLOGISCHES OBSERVATORIUM, RADEBEUL (EAST GERMANY).
An electron microscopic study of urban aerosol N85-32689

MIAMI UNIV., OXFORD, OHIO.
Quantitative analysis in megageomorphology N85-32376

MICHIGAN STATE UNIV., HICKORY CORNERS.
Sulfur cycling in freshwater sediments N85-32726
Sulfur reduction in sediments of marine and evaporite environments N85-32742

MICHIGAN UNIV., ANN ARBOR.
Performance and evaluation of real-time multicomputer control systems
[NASA-CR-176098] N85-32821
Raman scattering studies in solids
[AD-A155528] N85-33032

MIDWEST RESEARCH INST., GOLDEN, COLO.
Silicon refinement by chemical vapor transport N85-32412
High-purity silicon crystal growth N85-32444

MINNESOTA UNIV., MINNEAPOLIS.
High temperature solar electrothermal processing 2. Zinc from zinc oxide
[AD-A154747] N85-32159
Interface chemistry of Hg(1-x)Cd(x)Te
[AD-A154876] N85-32161
Noble gases and the early history of the Earth: Inappropriate paradigms and assumptions inhibit research and communication N85-33075

MINNESOTA UNIV., ST. PAUL.
Microscopic control of semiconductor surface oxidation
[AD-A154799] N85-33026

MISSION RESEARCH CORP., SANTA BARBARA, CALIF.
Experimental and analytic characterization of nonlinear seismic attenuation
[AD-A154760] N85-32556

MISSISSIPPI UNIV., UNIVERSITY.
Guided-mode launching in a slab waveguide by way of diffraction at the edge of a conducting screen residing on one surface of the slab
[AD-A154886] N85-32232

MISSOURI UNIV., ROLLA.
Construction of University of Missouri, Rolla's full scale cloud simulation chamber and applied research
[AD-A154682] N85-32128
The 100 years of Aitken Nuclei (AN) study-reminiscence, current and future problems N85-32621
Monte Carlo studies of H2O layers adsorbed on a model basal face of AgI N85-32633
Properties of forest derived cloud condensation nuclei N85-32682
Theoretical studies of structure and stability of hydrates of atmospheric sulfur species N85-32684

MITRE CORP., BEDFORD, MASS.
Design guidelines for user-system interface software
[AD-A154907] N85-32807

MOBIL TYCO SOLAR ENERGY CORP., WALTHAM, MASS.
Stress and efficiency studies in EFG N85-32440
Edge-defined film-fed growth of thin silicon sheets N85-32443

MONROE (RICHARD L.) ASSOCIATES, WASHINGTON, D.C.
A theory of electromagnetic shielding with applications to MIL-STD-285, IEEE-299, and EMP simulation
[AD-A154905] N85-32233

MOUND LAB., MIAMISBURG, OHIO.
Electrochemistry of Hexanitroazobenzene (HNAB)
[DE85-010807] N85-32171

N

NAGOYA UNIV. (JAPAN).
Sulfates in marine aerosols over the tropical Western Pacific Ocean N85-32690

NATIONAL AERONAUTICAL ESTABLISHMENT, OTTAWA (ONTARIO).
A preliminary investigation of handling qualities requirements for helicopter instrument flight during decelerating approach maneuvers and overshoot
[AD-A154650] N85-32125

NATIONAL AERONAUTICS AND SPACE ADMINISTRATION, WASHINGTON, D. C.
Remarks on preparation of indandione detection reagents
[NASA-TM-77905] N85-32146
The global sulfur cycle
[NASA-TM-87570] N85-32710
Sulfur Cycle N85-32748
Aerospace medicine and biology: A continuing bibliography with indexes, supplement 273
[NASA-SP-7011(273)] N85-32755
Generalized formulation of a class of explicit and implicit TVD schemes
[NASA-TM-86775] N85-32830

NATIONAL AERONAUTICS AND SPACE ADMINISTRATION. AMES RESEARCH CENTER, MOFFETT FIELD, CALIF.
Recent developments in rotary-balance testing of fighter aircraft configurations at NASA Ames Research Center
[NASA-TM-86714] N85-32090
Aerodynamic characteristics of the standard dynamics model in coning motion at Mach 0.6
[NASA-TM-86717] N85-32094
Simulation studies of time-control procedures for the advanced air traffic control system
[NASA-TP-2493] N85-32101
In-flight evaluation of pure time delays in pitch and roll
[NASA-TM-86744] N85-32123
The evolution of complex and higher organisms
[NASA-SP-478] N85-32708
Origin of life N85-32713
Protocyanobacteria: Oxygenic and Anoxygenic photosynthesis in mat-forming bacteria N85-32714
Sulfur transformations at the hydrogen sulfide/oxygen interface in stratified waters and in cyanobacterial mats N85-32715
Carbon isotope geochemistry and geobiology N85-32716
Evolution of the atmosphere N85-32725
Biogeochemical cycling and remote sensing N85-32733
Cyanobacterial mats: Microanalysis of community metabolism N85-32743
Living aloft: Human requirements for extended spaceflight
[NASA-SP-483] N85-32772
Search for the universal ancestors
[NASA-SP-477] N85-32777
The NAS kernel benchmark program
[NASA-TM-86711] N85-32795
Simulation of complex three-dimensional flows
[NASA-TM-86773] N85-32831
Water loss from Venus: Implications for the Earth's early atmosphere N85-33087

NATIONAL AERONAUTICS AND SPACE ADMINISTRATION. DRYDEN (HUGH L.) FLIGHT RESEARCH CENTER, EDWARDS, CALIF.
Performance improvements of a highly integrated digital electronic control system for an F-15 airplane
[NASA-TM-86748] N85-32120
Development and validation of a general purpose linearization program for rigid aircraft models
[NASA-TM-86737] N85-32122
Design of an expert-system flight status monitor
[NASA-TM-86739] N85-32794

Identification of unsteady aerodynamics and aeroelastic integro-differential systems
[NASA-TM-86749] N85-32851

NATIONAL AERONAUTICS AND SPACE ADMINISTRATION. GODDARD SPACE FLIGHT CENTER, GREENBELT, MD.

Earth Albedo and the orbit of LAGEOS
[NASA-TM-86210] N85-32131
Global Mega-Geomorphology
[NASA-CP-2312] N85-32357
Global geomorphology: Report of Working Group Number 1 N85-32382
Landscape inheritance: Report of Working Group Number 2 N85-32383
Process thresholds: Report of Working Group Number 3 N85-32384
Planetary perspective. Report of Working Group Number 4 N85-32385
Crustal dynamics project data analysis fixed station: VLBI geodetic results
[NASA-TM-86229] N85-32465
Meteorological and aeronomical requirements for MST radar networks (keynote paper), part 1 N85-32467
Excerpts from the paper: Research Status and Recommendation from the Alaska Workshop on Gravity Waves and Turbulence in the Middle Atmosphere, part 1.3A N85-32470
Gravity waves from the stratosphere to the mesosphere, part 1.3B N85-32471
The suppression of convective wavebreaking by radiative transfer processes, part 1.3C N85-32472
General circulation of the middle atmosphere, part 1.4B N85-32474
Techniques for the study of gravity waves and turbulence (keynote paper), part 4 N85-32499
Differential measurement of cosmic-ray gradient with respect to interplanetary current sheet
[PAPER-SH-4.2-9] N85-33055
The origin of continental crust: Outlines of a general theory N85-33083

NATIONAL AERONAUTICS AND SPACE ADMINISTRATION. JOHNSON (LYNDON B.) SPACE CENTER,

Mission operations requirements document for D-1 Experiment 102, Vestibular Experiments in Spacelab
[NASA-TM-87495] N85-32129
Life sciences flight experiments program mission science requirements document. The first life sciences dedicated Spacelab mission, part 1
[NASA-TM-87494] N85-32137

NATIONAL AERONAUTICS AND SPACE ADMINISTRATION. LANGLEY RESEARCH CENTER, HAMPTON, VA.

Calculation of transonic steady and oscillatory pressures on a low aspect ratio model and comparison with experiment
[NASA-TM-86449] N85-32092
Study of an efficient long-range Mach 2.7 supersonic transport configuration concept
[NASA-TM-86414] N85-32110
Preliminary sizing and performance of aircraft
[NASA-TM-86357] N85-32111
Thermal expansion of selected graphite reinforced polyimide-, epoxy-, and glass-matrix composite
[NASA-TM-87572] N85-32149
Influence of the resin on interlaminar mixed-mode fracture
[NASA-TM-87571] N85-32150
Comparisons of various configurations of the edge delamination test for interlaminar fracture toughness
[NASA-TM-86433] N85-32151
A cracked orthotropic sheet stiffened by a semi-infinite orthotropic sheet
[NASA-TP-2455] N85-32339
Concurrent implementation of the Crank-Nicolson method for heat transfer analysis
[NASA-TM-86448] N85-32822
On a variational approach to some parameter estimation problems
[NASA-CR-177935] N85-32829

NATIONAL AERONAUTICS AND SPACE ADMINISTRATION. LEWIS RESEARCH CENTER, CLEVELAND, OHIO.

Graphite/PMR polyimide composites with improved toughness
[NASA-TM-87081] N85-32148
Shock tube measurements of growth constants in the branched-chain ethane-carbon monoxide-oxygen system
[NASA-TM-87068] N85-32156
A comparison of electronic heterodyne moire deflectometry and electronic heterodyne holographic interferometry for flow measurements
[NASA-TM-87071] N85-32302
Surface roughness effects in elastohydrodynamic contacts
[NASA-TP-2488] N85-32329
Mechanics of a gaseous film barrier to lubricant wetting of elastohydrodynamically lubricated conjunctions
[NASA-TP-2500] N85-32330
Hertzian contact in two and three dimensions
[NASA-TP-2473] N85-32331
Tape casting as an approach to an all-ceramic turbine shroud seal
[NASA-TM-87078] N85-32333
Reliability of void detection in structural ceramics using scanning laser acoustic microscopy
[NASA-TM-87035] N85-32337

NATIONAL AERONAUTICS AND SPACE ADMINISTRATION. MARSHALL SPACE FLIGHT CENTER, HUNTSVILLE, ALA.

Development and test of advanced composite components. Center Directors discretionary fund program
[NASA-TM-86512] N85-32147
Weibull distribution based on maximum likelihood with interval inspection data
[NASA-TM-86515] N85-32847

NATIONAL BUREAU OF STANDARDS, BOULDER, COLO.

Detection of excited states by laser-induced fluorescence
[AD-A155558] N85-32326

NATIONAL BUREAU OF STANDARDS, GAITHERSBURG, MD.

Wall flames and implications for upward flame spread
[FAA-CT-85-2] N85-32103
The role of aircraft panel materials in cabin fires and their properties
[FAA-CT-84-30] N85-32104
Stress corrosion of ceramic materials
[AD-A155020] N85-32202
A practical guide to ionization chamber dosimetry at the AFRRI reactor
[AD-A155185] N85-33003

NATIONAL CENTER FOR ATMOSPHERIC RESEARCH, BOULDER, COLO.

Production of stable embryo particles in dense ion tracks of alpha particle emissions in the atmosphere N85-32638

NATIONAL JEWISH HOSPITAL AND RESEARCH CENTER, DENVER, COLO.

Resource allocation in cerebral specialization of function: Behavioral and electrophysiological studies
[AD-A155092] N85-32759

NATIONAL MATERIALS ADVISORY BOARD, WASHINGTON, D. C.

Magnetic materials
[AD-A154679] N85-32256

NATIONAL OCEANIC AND ATMOSPHERIC ADMINISTRATION, BOULDER, COLO.

Performance of the Colorado wind-profiling network, part 1.5A N85-32475
Comparison of tropopause altitude determination by the Plattsville Radar, Sunset Radar and the NWS Rawinsonde N85-32477
A modified Fresnel scattering model for the parameterization of Fresnel returns, part 2.3A N85-32483
Spectral measurements of turbulence and gravity waves, part 4.2A N85-32501
On the spectrum of atmospheric velocity fluctuations seen by MST/ST radar and their interpretation N85-32504
Tropospheric gravity waves observed by three closely spaced ST radars N85-32509
Summary of session on optimum transmitter and antenna configuration for MST radar, part 6 N85-32514
Practicality of electronic beam steering for MST/ST radars, part 6.2A N85-32516
Testing and optimizing MST coaxial collinear arrays, part 6.4A N85-32518
Elimination of range-aliased echoes in the VHF radars N85-32521
Sidelobe reduction of Barker codes, part 7.1C N85-32522
Data base for the Colorado profiling network N85-32533
Recent results at the Sunset radar N85-32536
Summary of progress at the Poker Flat Observatory in Alaska N85-32539
Progress and plans for the Colorado Wind Profiler Network N85-32542
The Ponape ST radar N85-32549
Measurements of vertical velocity over flat terrain by ST radar and other related uses of the radar data set N85-32550
Solar cycle variation of ephemeral regions
[AD-A154967] N85-33097

NATIONAL SEVERE STORMS LAB., NORMAN, OKLA.

Thunderstorm phenomena and weather radar scanning strategies
[DOT/FAA/PM-85/14] N85-32573

NATIONAL TRANSPORTATION SAFETY BOARD, WASHINGTON, D. C.

Air carrier overwater emergency equipment and procedures
[PB85-917006] N85-32105

NAVAL AIR DEVELOPMENT CENTER, WARMINSTER, PA.

Analysis of the transient response of temporal artery blood flow data relative to various anti-G suit pressure schedules
[AD-A155242] N85-32775

NAVAL AIR TEST CENTER, PATUXENT RIVER, MD.

SSMIR (Solid State Memory Instrumentation Recorder): A new approach to acquiring data during an aircraft seat/sled ejection sequence
[AD-A154780] N85-32308

NAVAL OCEAN SYSTEMS CENTER, SAN DIEGO, CALIF.

Using ship wake patterns to evaluate SAR (Synthetic Aperture Radar) ocean wave imaging mechanisms. Joint US-Canadian Ocean Wave Investigation Project
[AD-A154633] N85-32223
Marine environmental quality assessment program, five-year plan (FY 1984 - 1988)
[AD-A154715] N85-32459

NAVAL POSTGRADUATE SCHOOL, MONTEREY, CALIF.

Wind tunnel drag evaluations of helicopter nose sections
[AD-A155489] N85-32100
Development of reduced order models for control system design using the OPTSYSX program
[AD-A154552] N85-32124
The Naval Postgraduate School Flight Mechanics Laboratory: A feasibility study
[AD-A154578] N85-32127
The effect of prior parent phase cold work on martensite transformation in Cu-Zn-Al shape memory alloys
[AD-A155140] N85-32183
The effect of alloy additions on superplasticity in thermomechanically processed high magnesium aluminum-magnesium alloys
[AD-A155142] N85-32184
Comparison of the response of shape memory alloy actuators using air-cooling and water-cooling
[AD-A155216] N85-32185
The effect of mould size on the exothermic reaction and compressive strength of epoxy resin chocks
[AD-A155102] N85-32203
Radar target identification through electromagnetic scattering studies
[AD-A154596] N85-32220
Design of a jamming simulator for a binary communication system
[AD-A154617] N85-32221
Fin line filters technology and electronic warfare
[AD-A154975] N85-32237
An analysis of the materiel fielding plan for the SINCGARS (Single Channel Ground and Airborne Radio System) radio
[AD-A155101] N85-32238
Experimental evaluation of a new form of M-ary (M = 8) phase shift keying including design of the transmitter and receiver
[AD-A155103] N85-32239
Security controls in the Stockpoint Logistics Integrated Communications Environment (SPLICE)
[AD-A155536] N85-32244
Head-on scattering of a tubular cylinder of finite length for radar target identification purposes
[AD-A155608] N85-32246
Broadside scattering of a tubular cylinder for evaluation of target identification
[AD-A155739] N85-32248
Fin-line horn antennas
[AD-A154597] N85-32255
Design of a sixteen-bit pipelined adder using CMOS bulk P-well technology
[AD-A155043] N85-32260
Evaluation of the effects of roll angle on the natural convection heat transfer from an array of cylindrical spines
[AD-A154594] N85-32273
Design of a generator for near-tangential transonic swirling outflow
[AD-A155163] N85-32280
The influence of oil contamination on the nucleate pool-boiling behavior of R-114 from a structured surface
[AD-A155609] N85-32284
Film condensation of steam on externally finned horizontal tubes
[AD-A155642] N85-32285
Ultrasonic position reference systems for an autonomous sentry robot and a robot manipulator arm
[AD-A155481] N85-32336

An investigation into the comparisons of the underwater shock effects on a stiffened flat plate to the predictive nature of a computer model
[AD-A155612] N85-32355
Assessment of the performance of an in-field Gaussian plume/puff model for overwater use
[AD-A155435] N85-32460
Design of a freestanding noise measurement and recording system to predict the intensity and location of electromagnetic radiation from earthquakes
[AD-A155070] N85-32563
Forecasting of tropical cyclone motion using an EOF (Empirical Orthogonal Function) representation of wind forcing
[AD-A155034] N85-32580
An evaluation of discretized conditional probability and linear regression threshold techniques in model output statistics forecasting of cloud amount and ceiling over the North Atlantic Ocean
[AD-A155100] N85-32581
Parameter estimation in communication system tracking satellite observations
[AD-A155137] N85-32582
Mean flow and turbulence in complex terrain
[AD-A155138] N85-32583
Mesoscale features and atmospheric refraction conditions of the Arctic marginal ice zone
[AD-A155139] N85-32584
The effects of subrefractive layers and elevated ducts on airborne radar and ESM (Electronic Surveillance Measures)
[AD-A155524] N85-32592
Forecasting atmospheric visibility over the summer north Atlantic using the principal discriminant method
[AD-A155537] N85-32593
A numerical and analytical investigation of lee cyclogenesis
[AD-A155607] N85-32594
Hydrographic data from the OPTOMA (Ocean Prediction Through Observations, Modeling and Analysis) program: OPTOMA15, 24 January to 23 February 1985
[AD-A155012] N85-32703
Numerical simulations of the response of intense ocean currents to atmospheric forcing
[AD-A155161] N85-32704
Simulation of the coupled atmospheric and oceanic boundary layer model during MILDEX
[AD-A155166] N85-32705
Coastal erosion along Monterey Bay
[AD-A155610] N85-32707
Review of the psychological issues relating to the effectiveness of structured programming
[AD-A154593] N85-32766
Real-time contour surface display generation
[AD-A155232] N85-32780
Development of computer programs using the method of images to predict the sound field in a wedge overlaying a fast fluid and comparison with laboratory experiments
[AD-A154580] N85-32797
An automated quality assurance surveillance plan for ADP (Automated Data Processing) operations under the Navy's commercial activities program
[AD-A154767] N85-32802
The design and implementation of an object-oriented, production-rule interpreter
[AD-A154769] N85-32803
The formal specification of an abstract machine: Design and implementation
[AD-A155167] N85-32808
A PASCAL interpreter for the functional programming language ELC (Extended lambda calculus)
[AD-A155218] N85-32810
Experience with omega: Implementation of a prototype programming environment: Part 1
[AD-A155438] N85-32811
A microcomputer tutorial on spreadsheets and databases with a simulated budget preparation
[AD-A155516] N85-32813
Survival function of hypo-exponential distributions
[AD-A155518] N85-32814
A simple software environment based on objects and relations
[AD-A155704] N85-32817
Evaluation and implementation of a functional microprogram generator
[AD-A155164] N85-32823
The architectural requirements and integration analysis of a database server for office automation
[AD-A155517] N85-32825
Microcomputer network: Investigation and implementation
[AD-A155631] N85-32826
Propagation of sound in a layered laboratory model
[AD-A155141] N85-32989
Form factor effects on microwave Cerenkov radiation
[AD-A154577] N85-32993
The Human Resource Management Information Network (HRMIN): A cost comparison in accordance with Office of Management and Budget (OMB) Circular no. A-76, 5 April 1979
[AD-A154583] N85-33039

NAVAL RESEARCH LAB., WASHINGTON, D. C.

Mapping with QUASAT (quasar satellite) using short observation times
[AD-A155155] N85-32141
Huffman-coded pulse compression waveforms
[AD-A155322] N85-32243
The plasma erosion opening switch
[AD-A154942] N85-32259
The 2-D simulations of the NRL (Naval Research Laboratory) laser experiment
[AD-A154915] N85-32321
The dynamics of slack marine cables
[AD-A155022] N85-32349
Newton's method as a dynamical system: Global convergence and predictability
[AD-A155170] N85-32564
Measurements of the critical supersaturation of 0.029 to 0.035 micron radius particles at Washington, District of Columbia N85-32676
Fog activation and supersaturation N85-32678
A vectorized nearest-neighbors algorithm of order N using a monotonic logical grid
[AD-A155169] N85-32853
Kalman filter time series analysis of gamma-ray data from NaI(T1) detectors for the ND6620 computer
[AD-A154995] N85-33014
Low frequency instabilities driven by an ion temperature anisotropy
[AD-A154902] N85-33016
Electrostatic ion cyclotron instability due to a nonuniform electric field perpendicular to the external magnetic field
[AD-A155474] N85-33019
Operational window for a plasma erosion opening switch used for voltage multiplication on pulsed power generators
[AD-A155482] N85-33020
Magnetic fields in laser heated plasmas
[DE85-010715] N85-33022

NAVAL SHIP RESEARCH AND DEVELOPMENT CENTER, BETHESDA, MD.

Trailing edge flow and aerodynamic sound. Part 1: Tonal pressure and velocity fluctuations. Part 2: Random pressure and velocity fluctuations
[AD-A154947] N85-32097
An evaluation of four methods of numerical analysis for two-dimensional airfoil flows
[AD-A155202] N85-32098
A variable node finite element method applied to the gas dynamics equations
[AD-A155211] N85-32281
Ductile fracture of dynamically loaded naval structures-compact tension specimen tests and analyses
[AD-A155472] N85-32353

NAVAL SUBMARINE MEDICAL RESEARCH LAB., GROTON, CONN.

The effect of set size on time to recall color coded information
[AD-A155013] N85-32767

NAVAL SURFACE WEAPONS CENTER, DAHLGREN, VA.

A derivation of relativistic effects in satellite tracking
[AD-A154620] N85-32132
Doppler satellite data characteristics
[AD-A154868] N85-32231

NAVAL SURFACE WEAPONS CENTER, WHITE OAK, MD.

Synthesis of energetic materials
[AD-A154887] N85-32210

NETHERLANDS ENERGY RESEARCH FOUNDATION, PETTEN.

Marine aerosols at the Dutch North Sea coast: Size distributions and fractionation of trace elements N85-32664

NEW HAMPSHIRE UNIV., DURHAM.

Radial and latitudinal gradients of anomalous oxygen during 1977 - 1985
[PAPER-SH-4.6-4] N85-33058

NEW MEXICO INST. OF MINING AND TECHNOLOGY, SOCORRO.

Megageomorphology and neotectonics N85-32366
Early evolution of the crust-mantle system N85-33067

NEW YORK STATE COLL. OF AGRICULTURE AND LIFE SCIENCES, ITHACA.

Interaction of opiate and phencyclidine derivatives with the acetylcholine receptor
[AD-A155119] N85-32761

NEW YORK UNIV., NEW YORK.

Influence of chemical form, feeding regimen, and animal species on the gastrointestinal absorption of plutonium
[DE85-010291] N85-32751

NIELSEN ENGINEERING AND RESEARCH, INC., MOUNTAIN VIEW, CALIF.

Notes on unsteady transonic cascade flows
[AD-A154829] N85-32096

NORTH CAROLINA STATE UNIV., RALEIGH.

Transport and formation of summertime cloud condensation nuclei over the Arctic Ocean N85-32686
Aerosol formation by wave action over Ross Sea, Antartica N85-32688

NORTH CAROLINA UNIV., CHAPEL HILL.

Sulfur and carbon cycling in organic-rich marine sediments N85-32729
Microanalysis of dissolved iron and phosphate in pore waters of hypersaline sediment N85-32744

NORTH CAROLINA UNIV., RALEIGH.

Permeation of mixed penetrants through glassy polymer membranes
[AD-A155605] N85-32207

NORTHEAST RADIO OBSERVATORY CORP., WESTFORD, MASS. HAYSTACK OBSERVATORY.

Millstone Hill radar: Capabilities for S/T observations N85-32548

NORTHWESTERN UNIV., EVANSTON, ILL.

Dynamic fracture of concrete and other heterogeneous materials
[AD-A154513] N85-32343

NOTRE DAME UNIV., IND.

Polymer solution-supercritical fluid behavior
[AD-A154514] N85-32192

O

OAK RIDGE GASEOUS DIFFUSION PLANT, TENN.

Liquid-phase compositions from vapor-phase analyses 2: Adaptation of the Prausnitz program to UF6 and some of its potential impurities
[DE85-011521] N85-32819

OAK RIDGE NATIONAL LAB., TENN.

Z-contrast imaging and electron channeling analysis of dopants in semiconductors
[DE85-011410] N85-32269
Two-phase flow visualization in a transparent, atmospheric pressure, boiling water loop
[DE84-016857] N85-32288
Failure mechanisms in metal-sheathed thermocouples
[DE85-011929] N85-32317
Empirical correlation of residual gamma radiation resulting from operation of the Health Physics Research Reactor
[DE85-012075] N85-33008
Magnetics calculations for an ELMO Bumpy Square
[DE85-011438] N85-33021

ODESSA STATE UNIV. (USSR).

Analysis of performance of dynamic thermal diffusion chamber N85-32625

OFFICE NATIONAL D'ETUDES ET DE RECHERCHES AERONAUTIQUES, PARIS (FRANCE).

A 3-D Euler method for internal transonic flows computation with a multi-domain approach N85-32298

OFFICE OF NAVAL RESEARCH, ARLINGTON, VA.

Physical oceanography program science abstracts
[AD-A154637] N85-32701

OFFICE OF NAVAL RESEARCH, LONDON (ENGLAND).

Space research in the United Kingdom: An assessment
[AD-A155334] N85-33038

OHIO STATE UNIV., COLUMBUS.

Experimental and theoretical assessment of a new technique for the non-destructive evaluation of laminated panels
[AD-A155622] N85-32155
Upward continuation of surface gravity anomalies
[AD-A154973] N85-32560
SPLINES. Their equivalence to collocation
[AD-A155250] N85-32565
Structure and physiology of Beggiatoa and Thiothrix N85-32734
Anaerobic reduction of elemental sulfur by Chromatium vinosum and Beggiatoa alba N85-32739
The development and evaluation of point defect models for the growth of passive films on single crystal, polycrystalline, and amorphous metal surfaces
[AD-A154685] N85-33023

OLD DOMINION UNIV., NORFOLK, VA.

An error-dependent model of instrument-scanning behavior in commercial airline pilots
[NASA-CR-3908] N85-32765

OLDENBURG UNIV. (WEST GERMANY).

Cytochromes and iron sulfur proteins in sulfur metabolism of phototrophic bacteria N85-32718
Microbial communities and microprofiles of sulfide and oxygen of alum rock sulfur springs N85-32746

OPEN UNIV., MILTON (ENGLAND).

Carbon and nitrogen in the deep Earth N85-33085

OPHIR CORP., LAKEWOOD, COLO.
Circulation analysis of two snowstorms during the SNOW-TWO program
[AD-A155225] N85-32587
OPTIMETRICS, INC., ANN ARBOR, MICH.
Ship-to-ship propagation: Maritime data analyses
[AD-A155484] N85-32325
OREGON STATE UNIV., CORVALLIS.
The relation between the age of the subconducting slab and the recycling of sediments into the mantle N85-33063
Hydrothermal alteration in the 3.5 b.y. old Onverwacht Group of South Africa N85-33071
The degassing history of the Earth: Noble gas studies of Archaean cherts and zero age glassy submarine basalts N85-33072
The 3.5 b.y. old Onverwacht Group: A remnant of ancient oceanic crust N85-33073
Submarine hydrothermal environments as sites for the origin and evolution of life N85-33074
OREGON UNIV., EUGENE.
Geology and geochemistry of sulfide and sulfate deposition N85-32723
Multiphoton production and detection of atoms
[AD-A155561] N85-33000
ORYX, PARIS (FRANCE).
Large arcuate scars: A geological legacy of the Earth's accretionary past N85-33089

P

PACIFIC NORTHWEST LAB., RICHLAND, WASH.
Modification of the grain size of sputtered copper with additions of oxygen, krypton, silver, or yttrium
[DE85-010975] N85-32189
Biomass thermochemical conversion program
[DE85-011867] N85-32213
VALMET: A valley air pollution model
[DE85-010820] N85-32463
PARIS VII UNIV. (FRANCE).
Variations of particulate sulfur concentrations in a coastal atmospheric environment in connection with the change of air masses origin N85-32692
PARIS XII UNIV., CRETEIL (FRANCE).
Some considerations about the natural atmospheric radioactive aerosol N85-32662
PENNSYLVANIA STATE UNIV., UNIVERSITY PARK.
Recession of graphitic nozzles in rocket motors N85-32144
A multilevel-multigrid method for recirculating flows N85-32271
Network ST radar and related measurements at Pennsylvania State University N85-32544
Antistarshapedness, dispersiveness and mixtures
[AD-A155583] N85-32849
PENNSYLVANIA UNIV., PHILADELPHIA.
Numerical solutions of turbulent models for flow over a flat plate with angle of attack
[DE85-010380] N85-32286
Forced convection on solar collector arrays
[DE85-010381] N85-32287
Summary of the high-efficiency crystalline solar cell research forum N85-32396
Measuring bulk recombination rates and boundary recombination velocities N85-32419
PERFORMANCE MEASUREMENT ASSOCIATES, INC., VIENNA, VA.
The effect of communication-language designs on software specifications
[AD-A155173] N85-32809
PHYSICAL SCIENCES, INC., ANDOVER, MASS.
Theoretical modeling of laser induced optical degradation
[AD-A155302] N85-32323
POLYTECHNIC INST. OF NEW YORK, BROOKLYN.
Acoustic radiation from concentric shells containing an inner fluid
[AD-A155476] N85-32991
POLYTECHNIC INST. OF NEW YORK, FARMINGDALE.
Polymerizable ultraviolet stabilizers N85-32406
PORTLAND STATE UNIV., OREG.
Electrodeposition of chromium and copper in magnetic fields
[AD-A154648] N85-32180
PRINCETON UNIV., N. J.
Bubble dynamics in polymer solutions undergoing shear
[AD-A154575] N85-32193
Some observations on paleogeomorphology N85-32363
PUERTO RICO UNIV., MAYAGUEZ.
An EPR (Electron-Paramagnetic-Resonance) and ENDOR (Electron-Nuclear-Double-Resonance) study of ferroelectric ammonium sulfate
[AD-A155580] N85-33033
PURDUE UNIV., LAFAYETTE, IND.
Multilayer capacitor dielectrics produced from metallo-organic precursors
[AD-A154592] N85-32254
Injection of drag reducing additives into turbulent water flows: Two-component velocity measurements and mixing length model predictions
[AD-A154604] N85-32274
Space imagery and some geomorphological problems of the Guiana Shield, South America N85-32368
MOD silver metallization for photovoltaics N85-32428
A short bibliography of recent developments in selection and ranking procedures
[AD-A155648] N85-32856

R

RADIAN CORP., AUSTIN, TEX.
Emergency modeling of hazardous air pollutants
[AD-A155441] N85-32461
RAND CORP., SANTA MONICA, CALIF.
Investigation of DBMS (Data Base Management Systems) for use in a research environment
[AD-A154862] N85-33042
READING UNIV. (ENGLAND).
Some thoughts on GAIA and the sulfur cycle N85-32727
RESEARCH TRIANGLE INST., RESEARCH TRIANGLE PARK, N.C.
Comprehensive silicon solar-cell computer modeling N85-32421
CARE 3 user friendly interface user's guide
[NASA-CR-172608] N85-32791
RMS TECHNOLOGIES, INC., TREVOSE, PA.
Seat experiments for the full-scale transport aircraft controlled impact demonstration
[AD-A155024] N85-32106
ROCHESTER UNIV., N. Y.
Overlap integrals for atom-metal surface interactions
[AD-A155038] N85-32998
ROCKETDYNE, CANOGA PARK, CALIF.
Basic research in novel inorganic reagents and fluorocarbon chemistry
[AD-A155340] N85-32165
ROCKWELL INTERNATIONAL CORP., DOWNEY, CALIF.
Space Station crew safety alternatives study. Volume 2: Threat development
[NASA-CR-3855] N85-32133
ROCKWELL INTERNATIONAL CORP., THOUSAND OAKS, CALIF.
LSI/VLSI ion implanted planar GaAs IC processing
[AD-A155110] N85-32262
Influence of particle arrangement on sintering
[AD-A155337] N85-32352
ROME AIR DEVELOPMENT CENTER, GRIFFISS AFB, N.Y.
The use of the glistening surface concept in rough surface scattering
[AD-A154922] N85-32234
An analysis of physical optics models for rough surface scattering
[AD-A154960] N85-32235
Compression of spread spectrum signals on an excessively dispersive channel
[AD-A155184] N85-32240
ROME AIR DEVELOPMENT CENTER, HANSCOM AFB, MASS.
Null synthesis with phase and amplitude controls at the subarray outputs
[AD-A155187] N85-32241
ROORKEE UNIV. (INDIA).
Effect of ions on cloud formation and its role in solar terrestrial relationship N85-32697
ROYAL AIRCRAFT ESTABLISHMENT, FARNBOROUGH (ENGLAND).
The effect of abrasive blasting on the fatigue and corrosion of an aluminium-copper alloy
[AD-A154954] N85-32102
Importance and significance of transition temperatures
[AD-A154871] N85-32199
ROYAL NORWEGIAN COUNCIL FOR SCIENTIFIC AND INDUSTRIAL RESEARCH, KJELLER.
The Norwegian seismic array (NORSAR)
[AD-A154751] N85-32555
ROYAL SIGNALS AND RADAR ESTABLISHMENT, MALVERN (ENGLAND).
Aspects of SAR image segmentation
[AD-A154965] N85-32236

S

SAH (C. T.) ASSOCIATES, URBANA, ILL.
Important loss mechanisms in high-efficiency solar cells N85-32424
SANDIA LABS., ALBUQUERQUE, N. MEX.
Burn front velocity as a function of pellet density in iron-potassium perchlorate heat powders
[DE85-011448] N85-32214
Calculation of the propagation constant in a rectangular waveguide containing an inhomogeneous longitudinally magnetized plasma
[DE85-012072] N85-32250
Laser beam interactions with vapor plumes during Nd:YAG laser welding on aluminum
[DE85-009793] N85-32328
Electronic phenomena near semiconductor grain boundaries
[DE85-011543] N85-33035
SANTA BARBARA RESEARCH CENTER, GOLETA, CALIF.
Background equatorial astronomical measurements focal plane assembly (refurbished Hi STAR SOUTH)
[AD-A155215] N85-32313
SASKATCHEWAN UNIV., SASKATOON.
A simple model for testing the effects of gravity-wave-produced vertical oscillations of scattering irregularities on spaced-antenna, horizontal drift measurements N85-32489
Criteria for optimum spacing of spaced antenna, part 3.2A N85-32491
Determination of horizontal and vertical wavelengths of gravity waves in the mesosphere by spaced wind measurements N85-32510
Problems and solutions in analyzing partial-reflection drift data by correlation techniques N85-32529
Aerobic sulfur-oxidizing bacteria: Environmental selection and diversification N85-32712
Microbial colonization and growth on metal sulfides and other mineral surfaces N85-32747
SCHMITT (RAINER), GLASHUTTEN (WEST GERMANY).
Investigations of micro-turbulence in the bottom of the boundary layer
[AD-A155148] N85-32585
SCHOOL OF AEROSPACE MEDICINE, BROOKS AFB, TEX.
Predictive model of electron beam induced flashblindness
[AD-A155260] N85-32763
SCIENCE APPLICATIONS INTERNATIONAL CORP., MCLEAN, VA.
A random layer model for reflection from ocean bottom sediments
[AD-A155019] N85-32988
Understanding coherence losses incurred by bottom-retained signals
[AD-A155559] N85-32992
SCIENCE RESEARCH COUNCIL, CHILTON (ENGLAND).
A note on the proposed UK VHF radar N85-32545
SCIENTIFIC RESEARCH ASSOCIATES, INC., GLASTONBURY, CONN.
Tip vortex computer code SRATIP. User's guide
[NASA-CR-172603] N85-32093
SCRIPPS INSTITUTION OF OCEANOGRAPHY, LA JOLLA, CALIF.
VLF (Very low frequency) workshop held at San Diego California, 24-25 January 1985
[AD-A154652] N85-32224
A transportable, machine oriented library of european sky and terrain radiance distributions with contemporary radiometric and meteorological profiles
[AD-A155254] N85-32590
Constraints on early atmosphere from planetary accretion processes N85-33064
The Aravalli sequence of Rajasthan, India: A Precambrian continental margin? N85-33084
SCRIPPS INSTITUTION OF OCEANOGRAPHY, SAN DIEGO, CALIF.
Possible roles of manganese redox chemistry in the sulfur cycle N85-32731
SOFTECH, INC., FAIRBORN, OHIO.
HLLM software support
[AD-A154828] N85-32805
SOFTECH, INC., WALTHAM, MASS.
Ada (trademark) training curriculum. Advanced Ada topics L305 teacher's guide exercises
[AD-A154621] N85-32798
SOUTH DAKOTA SCHOOL OF MINES AND TECHNOLOGY, RAPID CITY.
Rain volume estimation over areas using satellite and radar data
[NASA-CR-176050] N85-32570

SOUTHWEST RESEARCH INST., SAN ANTONIO, TEX.
Experiments on the influence of active walls on the initial amplitudes and growths of instability waves
[AD-A154630] N85-32275
Measurement and analysis of critical crack tip processes during fatigue crack growth
[NASA-CR-172597] N85-32342
Literature survey of underground construction methods for application to hardened facilities
[AD-A155212] N85-32351
A crew exposure study. Phase II. Volume 2. At sea. Part A
[AD-A155233] N85-32774

SPECTROLAB, INC., SYLMAR, CALIF.
A non-noble front metallization process N85-32430

SPIRE CORP., BEDFORD, MASS.
Excimer laser annealing for fabrication of low-cost solar cells N85-32433
Status of high-efficiency module design and fabrication N85-32446

SPRINGBORN LABS., INC., ENFIELD, CONN.
Encapsulation materials research N85-32407
Encapsulation processing and manufacturing yield analysis N85-32434

SRI INTERNATIONAL CORP., MENLO PARK, CALIF.
NASA space station automation: AI-based technology review
[NASA-CR-176094] N85-32134
NASA space station automation: AI-based technology review. Executive summary
[NASA-CR-176096] N85-32135
Dynamic fracture behavior of structural materials
[AD-A154568] N85-32345
Development of improved dynamic failure models
[AD-A155586] N85-32354
Characteristics and sources of E-region ionization in the continuous aurora
[AD-A155018] N85-32562
USAFSAM review and analysis of radiofrequency radiation bioeffects literature
[AD-A155113] N85-32760

STANFORD LINEAR ACCELERATOR CENTER, CALIF.
Detector problems at the SSC
[DE85-010217] N85-33007

STANFORD RESEARCH INST., MENLO PARK, CALIF.
Speech understanding research
[AD-A155462] N85-32990

STANFORD UNIV., CALIF.
Globally-asynchronous locally-synchronous systems
[AD-A154624] N85-32222
Anisotropy of the permittivity field inferred from aspect-sensitive radar echoes N85-32492
A practical approach to Karmarkar's algorithm
[AD-A155714] N85-32818
Decomposing the joint distribution of several linear combinations of uniform spacings
[AD-A155056] N85-32845

STANFORD UNIV., PALO ALTO, CALIF.
Chemolithotrophy and physiology of bacterial nutrient limitation N85-32730
A simulation study of Sylvester's problem in three dimensions
[AD-A155266] N85-32854

STATE UNIV. OF NEW YORK, ALBANY.
Studies of oxygen- and carbon-related defects in high-efficiency silicon solar cells N85-32420
Ice nucleation of single water droplet by silver iodide: A laboratory observation N85-32630
A review of tectonic aspects of the Limpopo belt and other Archean high-grade gneissic terranes N85-33080

STATE UNIV. OF NEW YORK, BINGHAMTON.
Geomorphic analyses from space imagery N85-32374

STOCKHOLM UNIV. (SWEDEN).
Physical and chemical aerosol characteristics in extremely clean air masses at Cape Grim, Tasmania N85-32655

SUPERWAVE TECHNOLOGY, INC., SANTA CLARA, CALIF.
Microwave-enhanced thin-film deposition N85-32431

SYSTEMS AND APPLIED SCIENCES CORP., MONTEREY, CALIF.
Accuracy and operational use of medium and extended range numerical atmospheric forecasts: A review
[AD-A155027] N85-32579
Medium range atmospheric forecast system: Evaluation report
[AD-A155240] N85-32589
Medium range atmospheric forecast system: Evaluation plan
[AD-A155623] N85-32595

SYSTEMS AND APPLIED SCIENCES CORP., VIENNA, VA.
Automated cell detection as a mesocyclone precursor tool
[AD-A154952] N85-32577
Real-time automated detection of mesocyclones and tornado vortex signatures
[AD-A154968] N85-32578

T

TARTU STATE UNIV. (USSR).
Multi-channel electric aerosol spectrometer N85-32623

TEXAS A&M UNIV., COLLEGE STATION.
A comparison of experimental and theoretical results for rotordynamic coefficients of four annular gas seals
[NASA-CR-176086] N85-32332
Symbolic and interactional perspectives on leadership: An integrative framework
[AD-A155247] N85-32769
The priming effect in task design research
[AD-A154589] N85-32852

TEXAS TECHNOLOGICAL UNIV., LUBBOCK.
Coordinated research program in pulsed power physics
[AD-A154629] N85-32858

TEXAS UNIV., AUSTIN.
A multiplying slot array
[AD-A155570] N85-32245
The moving thermoacoustic array: A theoretical feasibility study
[AD-A154510] N85-32980
The sound field of a moving laser-induced acoustic array (theory)
[AD-A154553] N85-32981

TEXAS UNIV. AT DALLAS, RICHARDSON.
A sampling phasemeter design for pulsed continuous wave signals
[AD-A155237] N85-32264
A retarding ion mass spectrometer for the Dynamics Explorer-1
[NASA-CR-171588] N85-32303

THORN EMI, HAYES (ENGLAND).
The effect of metal overlayers of thermionic dispenser cathodes
[AD-A154795] N85-32995

TOMBERLIN (THOMAS J.), CONSULTANT, MONTREAL (QUEBEC).
Statistical methods for efficient design of community surveys of response to noise: Random coefficients regression models
[NASA-CR-177933] N85-32979

TORONTO UNIV. (ONTARIO).
Micromolecular modeling N85-32405

TOULOUSE UNIV. (FRANCE).
Formation of particles in the air of the humid tropical forests N85-32639
Study of the formation of particles from natural hydrocarbons released by vegetation N85-32640

TRI-CON ASSOCIATES, INC., CAMBRIDGE, MASS.
Fabrication and test of modified quadrupole mass spectrometer
[AD-A155186] N85-32312

TYCHO TECHNOLOGY, INC., BOULDER, COLO.
A high-speed digital signal processor for atmospheric radar, part 7.3A N85-32525

U

UKRAINIAN SCIENTIFIC HYDROMETEOROLOGICAL INST. (USSR).
Photoinduced active sites on ice nucleating aerosol of silver iodide N85-32601
The investigation of natural and artificial ice nuclei by the improved membrane filter method N85-32626

UNION CARBIDE CORP., TONAWANDA, N.Y.
A fluidized-bed reactor for silane pyrolysis N85-32413

UNITED TECHNOLOGIES RESEARCH CENTER, EAST HARTFORD, CONN.
A study of adherent oxide scales
[AD-A155554] N85-32188
Investigation of plasma processes in electronic transition lasers
[AD-A155598] N85-32327

UNIVERSITY COLL., GALWAY (IRELAND).
The nucleation of ice at very low temperatures and pressures N85-32617
The first condensation nucleus conference N85-32637

UNIVERSITY OF EASTERN KENTUCKY, RICHMOND.
Study of proton and neutron activation of metal samples in low Earth orbit
[NASA-CR-171596] N85-32130

UNIVERSITY OF EASTERN WASHINGTON, CHENEY.
Paleoenvironmental investigations at seed cave (Windust cave H-45FR46), Franklin County, Washington
[AD-A154777] N85-32576

UNIVERSITY OF NORTHERN ARIZONA, FLAGSTAFF.
Inactivation of silver iodide by atmospheric nucleation inhibitors N85-32599
Ice active bacteria as condensation nuclei N85-32603

UNIVERSITY OF SOUTH FLORIDA, ST. PETERSBURG.
Carbon and sulfur cycling through geologic time N85-32720

UNIVERSITY OF SOUTHERN ILLINOIS, CARBONDALE.
Regional landform thresholds N85-32362
The role of sulfur in osmoregulation and salinity tolerance in cyanobacteria, algae, and plants N85-32736

UNIVERSITY OF WESTERN KENTUCKY, BOWLING GREEN.
Calibration and use of clutter data for simulation
[AD-A154793] N85-32229

UTAH STATE UNIV., LOGAN.
The Boot Lake MF imaging radar N85-32537

UTAH UNIV., SALT LAKE CITY.
Interaction of solutes with stretched polymers
[AD-A154662] N85-32196
Defects in tetrahedrally coordinated amorphous semiconductors
[AD-A155150] N85-32263
Mechanism of heterogeneous deposition ice nucleation near water-saturation N85-32597
Cloud droplet nucleation and initial growth derived from lidar depolarization studies N85-32635
Doping superlattices in organometallic VPE InP
[AD-A155151] N85-33029

UTRECHT STATE UNIV. (NETHERLANDS).
Cloud condensation on insoluble particles N85-32670

V

VANDERBILT UNIV., NASHVILLE, TENN.
Research on an expert system for database operation of simulation-emulation math models. Volume 1, Phase 1: Results
[NASA-CR-176087] N85-32792
Research on an expert system for database operation of simulation-emulation math models. Volume 2, Phase 1: Results
[NASA-CR-176088] N85-32793

VIRGINIA POLYTECHNIC INST. AND STATE UNIV., BLACKSBURG.
An elliptic calculation procedure for 3-D viscous flow N85-32297
Performance evaluation of flow in turbomachinery blade rows N85-32299
Calculation of 3-D flow without numerical mixing N85-32301

VRIJE UNIVERSITEIT, BRUSSELS (BELGIUM).
An analysis of flow models: From Navier-Stokes to potential flow equations N85-32295
Computation of three-dimensional, inviscid, rotational flows N85-32296

W

WALKER (WILLIAM W., JR.), CONCORD, MASS.
Empirical methods for predicting eutrophication in impoundments. Report 3. Phase 2. Model refinements
[AD-A155483] N85-32462

WALTER REED ARMY INST. OF RESEARCH, WASHINGTON, D.C.
Human performance in continuous/sustained operations and the demands of extended work/rest schedules. An annotated bibliography
[AD-A155619] N85-32771

WASHINGTON UNIV., SEATTLE.
Modeling of the silane FBR system N85-32415
Silicon surface passivation by silicon nitride deposition N85-32423
Airborne measurements of the vertical distribution of Arctic haze N85-32657

WEAPONS SYSTEMS RESEARCH LAB., ADELAIDE (AUSTRALIA).
The determination of dinitrotoluene in single base propellants
[AD-A154672] N85-32209

WEIDLINGER ASSOCIATES, NEW YORK, N.Y.
Acoustic radiation from concentric shells containing an inner fluid
[AD-A155476] N85-32991

WESTINGHOUSE DEFENSE AND ELECTRONIC SYSTEMS CENTER, BALTIMORE, MD.
Stripe filters on multispectral linear arrays
[NASA-CR-175305] N85-32252

WESTINGHOUSE ELECTRIC CORP., PITTSBURGH, PA.
Development of high-efficiency solar cells on silicon web N85-32425
Simultaneous junction formation N85-32426

Laser-assisted solar-cell metallization processing N85-32429
Silicon dendritic web growth N85-32435
Temperature-stress modeling N85-32436
WESTINGHOUSE RESEARCH AND DEVELOPMENT CENTER, PITTSBURGH, PA.
Introduction of structural variations into oxide polymers and their effect on sintering and crystallization
[AD-A155597] N85-32206
WIEN UNIV. (AUSTRIA).
The influence of Brownian coagulation on the size distributions of atmospheric aerosols N85-32643
Variability of rural aerosols under stable weather conditions N85-32663
WILKES COLL., WILKES-BARRE, PA.
Polymer-water interaction studies N85-32411
WISCONSIN UNIV., MADISON.
A numerical study of Taylor-Vortex flow
[AD-A154787] N85-32277
Large-time behavior of viscous surface waves
[AD-A154805] N85-32278
Instability and chaotic behavior in a free-surface flow
[AD-A154879] N85-32279
The optimality of lower confidence limits for the reliability of series systems obtained by the method of key test results or other related techniques
[AD-A154880] N85-32338
Modelling and parameter estimation for distributed vibratory systems
[AD-A154518] N85-32344
On the limiting configuration of interfacial gravity waves
[AD-A154821] N85-32557
Diagnostics of severe convection and subsynoptic scale ageostrophic circulations
[NASA-CR-171581] N85-32571
Scavenging of submicron aerosol particles by snow crystals: Theory and experiments N85-32667
SIGMA - A stochastic-integration global minimization algorithm
[AD-A154878] N85-32806
A note on a theorem of R. Duffin
[AD-A154786] N85-32838
Sobolev-Poincare's inequality and the Neumann problem for u sub t = divergence of the absolute value of the gradient u to the p-2 power x the gradient u
[AD-A154788] N85-32839
On the turning lozange of constant side whose vertices alternate between two fixed circles of a ring
[AD-A154803] N85-32840
The distribution of the number of empty cells in a generalized random allocation scheme
[AD-A154806] N85-32841
Local epi-continuity and local optimization
[AD-A154812] N85-32843
Analysis of unreplicated factorials allowing for possibly faulty observations
[AD-A154813] N85-32848
A second order difference scheme for transient semiconductor device simulation
[AD-A154824] N85-33027
WOODS HOLE OCEANOGRAPHIC INSTITUTION, MASS.
Deep sea mega-geomorphology: Progress and problems N85-32369
Horizontal and vertical structure of velocity, potential vorticity and energy in the gulf stream
[AD-A154753] N85-32702
A review of noble gas geochemistry in relation to early Earth history N85-33081
WYOMING UNIV., LARAMIE.
Concentrations of ice nuclei of different modes of activities N85-32616

Y

YALE UNIV., NEW HAVEN, CONN.
Aerosol analysis and emission spectrometry with free jets
[DE85-010576] N85-32168
On the dependence of the convergence of Gummel's algorithm on the regularity of the solution
[AD-A154628] N85-32832

Z

ZUMBRUNNEN (ALLEN D.), SALT LAKE CITY, UTAH.
High-frequency furnace
[DE85-011210] N85-32291

CONTRACT NUMBER INDEX

Typical Contract Number Index Listing

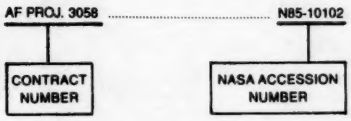

Listings in this index are arranged alphanumerically by contract number. Under each contract number the NASA accession numbers denoting documents that have been produced as a result of research done under that contract are arranged in ascending order. The NASA accession number denotes the number by which the citation is identified.

AF PROJ. 7W05 ..... N85-32579
AF PROJ. 230-3 ..... N85-32198
AF PROJ. 241-9 ..... N85-32198
AF PROJ. 1123 ..... N85-32776
AF PROJ. 2302 ..... N85-32181
AF PROJ. 2305 ..... N85-32234
N85-32241
N85-32262
AF PROJ. 2306 ..... N85-32345
AF PROJ. 2308 ..... N85-32160
AF PROJ. 2311 ..... N85-33097
AF PROJ. 4600 ..... N85-32240
AF PROJ. 4787 ..... N85-32554
AF PROJ. 6690 ..... N85-32558
AF PROJ. 7184 ..... N85-32114
AF PROJ. 7757 ..... N85-32763
AF-AFOSR-0009-83 ..... N85-32343
AF-AFOSR-0032-84 ..... N85-32858
AF-AFOSR-0044-84 ..... N85-32758
AF-AFOSR-0046-82 ..... N85-32998
AF-AFOSR-0081-82 ..... N85-32194
AF-AFOSR-0266-82 ..... N85-32157
AF-AFOSR-0281-83 ..... N85-32344
AF-AFOSR-0326-82 ..... N85-32842
AF-AFOSR-0398-84 ..... N85-32829
ARPA ORDER 1483 ..... N85-32555
ARPA ORDER 2903 ..... N85-32990
ARPA ORDER 4397 ..... N85-32556
ARPA ORDER 4787 ..... N85-32554
ARPA ORDER 338419 ..... N85-32262
DA PROJ. U99-QAXM N85-33003
N85-33004
DA PROJ. 1L1-61102-A-71-A N85-32163
DA PROJ. 1L1-61102-AH-43 ..... N85-32167
DA PROJ. 1L1-61102-AH-45 ..... N85-32151
DA PROJ. 1L1-62120-AH-25 ..... N85-32233
DA PROJ. 1L1-62724-AH-99 ..... N85-32164
N85-32773
DA PROJ. 1T1-61102-BH-57 ..... N85-32574
N85-32995
DA PROJ. 4A1-62731-AT-41 ..... N85-32350
N85-32351
DA PROJ. 231-1 ..... N85-32143
DA PROJ. 667-0 ..... N85-32586
DAAB07-83-C-K514 ..... N85-32798
DAAE07-83-C-R056 ..... N85-32815
DAAG29-78-C-0031 ..... N85-32187
DAAG29-79-C-0155 ..... N85-32836
DAAG29-80-C-0041 ..... N85-32277
N85-32278
N85-32279
N85-32338
N85-32557
N85-32606
N85-32838
N85-32839
N85-32840
N85-32841
N85-32843
N85-32848
N85-33027
DAAG29-81-C-0016 ..... N85-32205
DAAG29-81-C-0027 ..... N85-32180
DAAG29-81-K-0039 ..... N85-32207
DAAG29-81-K-0122 ..... N85-32166
DAAG29-81-K-0123 ..... N85-32354
DAAG29-81-K-0149 ..... N85-33034
DAAG29-81-K-0154 ..... N85-33000
DAAG29-82-C-0006 ..... N85-32591
DAAG29-82-G-0004 ..... N85-33033
DAAG29-82-K-0024 ..... N85-32196
DAAG29-82-K-0033 ..... N85-32187
DAAG29-82-K-0057 ..... N85-33032
DAAG29-82-K-0168 ..... N85-32850
DAAG29-83-C-0006 ..... N85-32206
DAAG29-83-C-0009 ..... N85-32267
DAAG29-83-G-0056 ..... N85-32344
DAAG29-83-K-0018 ..... N85-32324
DAAG29-83-K-0029 ..... N85-32829
DAAG29-84-K-0007 ..... N85-32849
DAAG29-84-K-0058 ..... N85-32836
DAAG29-84-K-0076 ..... N85-32245
DAAK11-80-C-0062 ..... N85-32212
DAAK11-83-C-0049 ..... N85-32761
DAAK21-83-C-0052 ..... N85-32233
DACA88-84-M-0157 ..... N85-32351
DACW39-78-C-0053-REPT-3 ..... N85-32462
DACW68-83-M-5624 ..... N85-32576
DAHC04-75-C-0006 ..... N85-32990
DAJA37-81-C-0740 ..... N85-32806
DAJA45-83-C-0009 ..... N85-32995
DAJA45-83-C-0011 ..... N85-32179
DAJA45-83-C-0023 ..... N85-32574
DAJA45-83-C-0038 ..... N85-32585
DARPA ORDER 3045 ..... N85-32827
DCA100-77-C-0020 ..... N85-32247
DCA100-84-C-0030 ..... N85-32226
DE-AC01-81NE-32084 ..... N85-32270
DE-AC02-76CH-00016 ..... N85-33001
DE-AC02-81-ER-10996 ..... N85-32832
DE-AC03-76SF-00098 ..... N85-32176
N85-32289
DE-AC03-76SF-00515 ..... N85-33007
DE-AC03-81ER-40050 ..... N85-33007
DE-AC04-76DP-00053 ..... N85-32171
DE-AC04-76DP-00613 ..... N85-32315
N85-32318
DE-AC04-76DP-00789 ..... N85-32214
N85-32250
N85-32328
N85-33035
DE-AC04-78-CS-35365 ..... N85-32286
DE-AC04-78CS-35319 ..... N85-32287
DE-AC05-84CR-21400 ..... N85-32288
DE-AC05-84OR-21400 ..... N85-32269
N85-32317
N85-33006
N85-33021
DE-AC05-84OT-21400 ..... N85-32819
DE-AC06-76RL-01830 ..... N85-32189
N85-32213
N85-32463
DE-AI01-76ET-20320 ..... N85-32251
DE-AI01-76ET-20356 ..... N85-32394
DE-AI08-78ET-44802 ..... N85-32316
DE-AM03-76SF00326 ..... N85-32818
DE-AT03-76ER-72018 ..... N85-32818
DE-AT03-82SF-11666 ..... N85-32170
DE-FG01-78ET-11384 ..... N85-32168
DE-FG01-81CS-15077 ..... N85-32291
DNA-IACRO-83-847 ..... N85-33003
DTCG23-80-C-20015 ..... N85-32774
DTFA01-80-Y-10524 ..... N85-32573
DTFA03-81-C-00040 ..... N85-32106
EM-78-C-04-5319 ..... N85-32286
EM-78-C-04-5365 ..... N85-32286
EPA-R-809371-01-0 ..... N85-32667
ESD-84-611 ..... N85-33097
ESTEC-5524/83/NL-PP N85-32826
F59-551 ..... N85-32460
F04701-83-C-0084 ..... N85-32314
N85-32568
F08606-84-C-0002 ..... N85-32555
F19268-82-K-0022 ..... N85-32560
F19628-77-C-0104 ..... N85-33098
F19628-80-C-0042 ..... N85-32242
F19628-81-C-0050 ..... N85-32099
F19628-81-K-0009 ..... N85-32567
F19628-82-C-0023 ..... N85-32577
N85-32578
F19628-82-C-0029 ..... N85-32339
F19628-82-C-0035 ..... N85-33101
F19628-82-C-0060 ..... N85-32590
F19628-82-K-0017 ..... N85-32566
F19628-83-C-0001 ..... N85-32562
F19628-83-C-0062 ..... N85-32313
F19628-83-C-0123 ..... N85-32561
F19628-83-C-0130 ..... N85-32587
F19628-83-K-0027 ..... N85-32565
F19628-84-C-0001 ..... N85-32807
F19628-84-C-0012 ..... N85-32228
F19628-84-C-0037 ..... N85-33099
F19628-84-C-0101 ..... N85-32312
F19628-84-K-0001 ..... N85-32139
F19628-84-K-0002 ..... N85-33100
F19628-84-K-0003 ..... N85-32559
F19628-84-K-0009 ..... N85-33012
F19628-85-C-0002 ..... N85-32306
N85-33025
F29601-82-C-0050 ..... N85-32323
F33615-79-C-1936 ..... N85-32805
F33615-81-C-0005 ..... N85-32757
F33615-81-C-5056 ..... N85-32152
N85-32153
F33615-81-C-5095 ..... N85-33031
F33615-82-C-0501 ..... N85-32984
N85-32986
F33615-82-C-0610 ..... N85-32760
F33615-82-C-2241 ..... N85-32998
F33615-82-K-5009 ..... N85-32155
F33615-83-C-5037 ..... N85-32335
F33615-83-D-4001 ..... N85-32461
F49620-79-C-0038 ..... N85-33018
F49620-80-C-0090 ..... N85-32126
F49620-81-C-0020 ..... N85-32165
F49620-81-C-0082 ..... N85-33024
F49620-81-K-0007 ..... N85-32345
F49620-82-C-0077 ..... N85-32320
F49620-82-C-0090 ..... N85-32140
F49620-83-C-0042 ..... N85-32262
F49620-83-C-0137 ..... N85-32554
F49620-84-C-0049 ..... N85-32556
F49620-84-C-0089 ..... N85-32253
JPL PROJ. 5101-259 ..... N85-32394
MDA903-82-C-0434 ..... N85-32256
MDA903-83-C-0335 ..... N85-32222
MIPR-FY1455-83-N0632 ..... N85-32326
MIPR-FY1455-84-N0631 ..... N85-32326
MIPR-138-84 ..... N85-32128
MIPR-4311-1076 ..... N85-32211
NAGW-685 ..... N85-33044
NAG1-296 ..... N85-32821
NAG1-492 ..... N85-32821
NAG2-251 ..... N85-32095
NAG3-341 ..... N85-32173
N85-32174
N85-32175
N85-32176
NAG3-379 ..... N85-32340
N85-32341
NAG5-386 ..... N85-32570
NASW-3389 ..... N85-33062
N85-33086
NASW-3490 ..... N85-32089
NASW-3676 ..... N85-32709
NASW-3805 ..... N85-32466
NASW-4005 ..... N85-32146
NAS1-14904 ..... N85-32093
NAS1-16000 ..... N85-32172
N85-32177
NAS1-16253 ..... N85-32464
NAS1-16489 ..... N85-32791
NAS1-16978 ..... N85-32979
NAS1-17070 ..... N85-32829
NAS1-17242 ..... N85-32133
NAS1-17571 ..... N85-32215
NAS1-17641 ..... N85-32342

NAS2-11864 ..... N85-32134
N85-32135
NAS3-23687 ..... N85-32119
NAS3-24105 ..... N85-32251
NAS5-23758 ..... N85-33096
NAS5-25622 ..... N85-32252
NAS5-25773 ..... N85-32552
NAS5-27745 ..... N85-32572
NAS5-28441 ..... N85-33057
NAS5-28449 ..... N85-33047
N85-33057
NAS7-918 ..... N85-32394
N85-33051
N85-33052
N85-33053
N85-33056
N85-33058
N85-33059
NAS8-32831 ..... N85-32303
NAS8-33222 ..... N85-32571
NAS8-33716 ..... N85-32332
NAS8-34005 ..... N85-32789
NAS8-35180 ..... N85-32130
NAS8-36038 ..... N85-32790
NAS8-36039 ..... N85-32178
NAS8-36146 ..... N85-32334
NAS8-36285 ..... N85-32792
N85-32793
NAS8-36407 ..... N85-32796
NA82RA-C-0098 ..... N85-32620
NCC2-64 ..... N85-32272
NCC3-30 ..... N85-32330
NGR-05-002-160 ..... N85-33047
N85-33048
N85-33049
N85-33050
N85-33051
N85-33052
N85-33053
N85-33055
N85-33056
N85-33057
N85-33058
N85-33059
N85-33103
NGR-05-003-450 ..... N85-33060
NGR-05-006-160 ..... N85-33046
NGR14-005-181 ..... N85-32520
NGT-23-005-801 ..... N85-32821
NGT-47-003-801 ..... N85-32765
NR PROJ. F59-559 ..... N85-32459
NR PROJ. RR0-2301 ..... N85-32274
NR PROJ. W05-13 ..... N85-32589
NR PROJ. Y08-17 ..... N85-32459
NR PROJ. ZR0-0001 ..... N85-32223
NR PROJ. ZR0-3103 ..... N85-32223
NSF ATM-80-15790 ..... N85-32633
NSF ATM-81-06792 ..... N85-32597
NSF ATM-81-20371 ..... N85-32526
N85-32531
NSF ATM-82-10344 ..... N85-32677
NSF CHE-83-20185 ..... N85-32998
NSF DCR-83-02391 ..... N85-32836
NSF DCR-84-13211 ..... N85-32818
NSF DMR-80-20164 ..... N85-33026
NSF DMR-83-04471 ..... N85-32263
N85-33029
NSF DMR-83-16979 ..... N85-32197
NSF DMS-82-05355 ..... N85-32829
NSF DMS-84-20623 ..... N85-32818
NSF DPP-82-09548 ..... N85-32657
NSF DPP-83-8303964 ..... N85-32605
NSF ECS-83-12142 ..... N85-32818
NSF MCS-80-01960 ..... N85-32557
NSF MCS-80-05387 ..... N85-32842
NSF MCS-81-01639 ..... N85-32278
NSF MCS-81-10556 ..... N85-32838
NSF MCS-82-00406 ..... N85-32557
NSF MCS-82-00632 ..... N85-32843
N85-32848
NSF MEA-82-13925 ..... N85-32197
NSF OCE-82-08746 ..... N85-32702
NSG-7484 ..... N85-32857
NSG-7506 ..... N85-32526
N85-32531
NSG-7576 ..... N85-33078
N00014-75-C-0476 ..... N85-33017
N00014-75-C-0661 ..... N85-32779
N85-33037
N00014-76-C-0100 ..... N85-32749
N00014-76-C-0475 ..... N85-32845
N85-32854
N00014-76-C-0847 ..... N85-32327
N00014-78-C-0246 ..... N85-33010
N00014-78-C-0433 ..... N85-32770
N00014-78-C-0820 ..... N85-32991
N00014-79-C-0385 ..... N85-32193
N00014-79-C-0472 ..... N85-32224
N00014-79-C-0793 ..... N85-32622
N00014-80-C-0048 ..... N85-32837
N00014-80-C-0220 ..... N85-32224
N00014-80-C-0472 ..... N85-32998
N00014-80-C-0490 ..... N85-32264
N00014-80-C-0622 ..... N85-32778
N85-32842
N00014-81-K-0256 ..... N85-32232
N00014-81-K-0650 ..... N85-32195
N85-32346
N00014-81-K-0817 ..... N85-32768
N00014-82-C-0019 ..... N85-32702
N00014-82-C-0199 ..... N85-32275
N00014-82-C-0353 ..... N85-32987
N00014-82-C-0405 ..... N85-32154
N00014-82-C-0499 ..... N85-32809
N00014-82-C-0618 ..... N85-32188
N00014-82-K-0184 ..... N85-32832
N00014-82-K-0265 ..... N85-33023
N00014-82-K-0359 ..... N85-32225
N00014-82-K-0425 ..... N85-32980
N85-32981
N00014-82-K-0523 ..... N85-32159
N00014-83-C-0025 ..... N85-32769
N85-32852
N00014-83-C-0194 ..... N85-32982
N00014-83-C-0303 ..... N85-32988
N85-32992
N00014-83-C-0318 ..... N85-32759
N00014-83-C-0435 ..... N85-32096
N00014-83-C-0444 ..... N85-32800
N00014-83-C-2393 ..... N85-32257
N00014-83-K-0026 ..... N85-32162
N85-32310
N85-33013
N00014-83-K-0083 ..... N85-32200
N00014-83-K-0125 ..... N85-32227
N85-32258
N85-32799
N85-32801
N85-32836
N85-33037
N00014-83-K-0183 ..... N85-32274
N00014-83-K-0321 ..... N85-32254
N00014-83-K-0468 ..... N85-32186
N85-32348
N00014-83-K-0535 ..... N85-32263
N85-33029
N00014-83-K-0613 ..... N85-32192
N00014-83-K-0632 ..... N85-32994
N00014-83-K-2027 ..... N85-33011
N00014-84-C-0112 ..... N85-32770
N00014-84-C-0130 ..... N85-32834
N00014-84-C-0167 ..... N85-32856
N00014-84-C-0233 ..... N85-32844
N00014-84-C-0298 ..... N85-32352
N00014-84-C-0724 ..... N85-32454
N00014-84-C-2034 ..... N85-32229
N00014-84-F-0019 ..... N85-32202
N00014-84-K-0049 ..... N85-32804
N00014-84-K-0286 ..... N85-32216
N00014-84-K-0357 ..... N85-32827
N00014-84-K-0510 ..... N85-32197
N00014-84-K-0545 ..... N85-32161
N85-33026
N00014-84-K-0553 ..... N85-32201
N85-32997
N00014-85-K-0060 ..... N85-32770
N00014-85-K-0343 ..... N85-32818
N00228-82-C-8171 ..... N85-32325
N00228-83-C-3101 ..... N85-32579
N85-32589
N85-32595
PROJ. RR0-1107 ..... N85-32327
PROJ. RR0-1109 ..... N85-32853
PROJ. RR0-1408 ..... N85-32811
N85-32825
PROJ. RR0-3406 ..... N85-32141
RR0-0001 ..... N85-32780
RR0-3302 ..... N85-33019
RR0-4204 ..... N85-32768
RR0-4209 ..... N85-32809
SRI PROJ. PYU-2777 ..... N85-32345
SRI PROJ. 7268 ..... N85-32134
N85-32135
SR0-1403 ..... N85-32281
S12-66001 ..... N85-32098
W-31-109-ENG-38 ..... N85-32292
N85-32751
N85-33002
N85-33006
N85-33009
W-7405-ENG-36 ..... N85-32145
N85-32290
N85-32319
N85-32393
N85-32455
N85-32456
N85-33005
N85-33022
W-7405-ENG-48 ..... N85-32169
N85-32249
N85-32820
N85-32846
N85-33028
N85-33061
ZR0-2303 ..... N85-32353
199-50-42-04-00 ..... N85-32777
199-50-52-06 ..... N85-32708
324-01-00 ..... N85-32215
505-31-01 ..... N85-32831
505-31-01-01-00-21 ..... N85-32830
505-31-04 ..... N85-32156
505-31-53-11 ..... N85-32177
505-31-83-01 ..... N85-32829
505-33-12 ..... N85-32329
505-33-23-02 ..... N85-32342
505-33-33 ..... N85-32150
505-33-43-09 ..... N85-32092
N85-32093
505-33-53-15 ..... N85-32822
505-33-62 ..... N85-32148
N85-32331
505-33-78 ..... N85-32333
505-34-13-30 ..... N85-32791
505-34-31 ..... N85-32122
505-35-13-53 ..... N85-32979
505-36-11 ..... N85-32101
505-40-14 ..... N85-32302
505-42-11 ..... N85-32095
505-43-11 ..... N85-32090
N85-32094
N85-32123
N85-32851
505-43-43-01 ..... N85-32110
N85-32111
505-45-33-07 ..... N85-32765
505-53-23-07 ..... N85-32149
506-53-1A N85-32337
506-53-23-05 ..... N85-32339
506-54-21 ..... N85-32272
533-02-02 ..... N85-32120
533-02-81 ..... N85-32794
533-04-1A N85-32119
533-04-12 ..... N85-32340
N85-32341
534-06-23-03 ..... N85-32151
536-01-11 ..... N85-32795
776-52-61-00 ..... N85-32394
906-54-02 ..... N85-32133

REPORT / ACCESSION NUMBER INDEX

Typical Report / Accession Number Index Listing

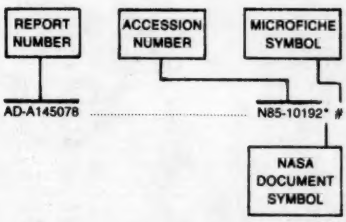

Listings in this index are arranged alphanumerically by report number. The NASA accession number denotes the number by which the citation is identified. An asterisk (*) indicates that the item is a NASA report. A pound sign (#) indicates that the item is available on microfiche.

A-8646 ..... N85-32777* #
A-9363 ..... N85-32708* #

AD-A154508 ..... N85-32253 #
AD-A154510 ..... N85-32980 #
AD-A154512 ..... N85-32756 #
AD-A154513 ..... N85-32343 #
AD-A154514 ..... N85-32192 #
AD-A154517 ..... N85-32387 #
AD-A154518 ..... N85-32344 #
AD-A154520 ..... N85-32157 #
AD-A154521 ..... N85-32158 #
AD-A154533 ..... N85-32208 #
AD-A154552 ..... N85-32124 #
AD-A154553 ..... N85-32981 #
AD-A154566 ..... N85-32749 #
AD-A154568 ..... N85-32345 #
AD-A154575 ..... N85-32193 #
AD-A154577 ..... N85-32993 #
AD-A154578 ..... N85-32127 #
AD-A154580 ..... N85-32797 #
AD-A154583 ..... N85-33039 #
AD-A154584 ..... N85-32388 #
AD-A154587 ..... N85-32982 #
AD-A154589 ..... N85-32852 #
AD-A154592 ..... N85-32254 #
AD-A154593 ..... N85-32766 #
AD-A154594 ..... N85-32273 #
AD-A154596 ..... N85-32220 #
AD-A154597 ..... N85-32255 #
AD-A154600 ..... N85-32700 #
AD-A154604 ..... N85-32274 #
AD-A154617 ..... N85-32221 #
AD-A154619 ..... N85-32994 #
AD-A154620 ..... N85-32132 #
AD-A154621 ..... N85-32798 #
AD-A154624 ..... N85-32222 #
AD-A154628 ..... N85-32832 #
AD-A154629 ..... N85-32858 #
AD-A154630 ..... N85-32275 #
AD-A154633 ..... N85-32223 #
AD-A154635 ..... N85-33040 #
AD-A154637 ..... N85-32701 #
AD-A154642 ..... N85-32179 #
AD-A154644 ..... N85-32304 #
AD-A154647 ..... N85-32194 #
AD-A154648 ..... N85-32180 #
AD-A154650 ..... N85-32125 #
AD-A154652 ..... N85-32224 #
AD-A154654 ..... N85-32225 #
AD-A154656 ..... N85-32195 #
AD-A154662 ..... N85-32196 #
AD-A154669 ..... N85-32553 #
AD-A154670 ..... N85-32833 #
AD-A154672 ..... N85-32209 #
AD-A154676 ..... N85-32142 #
AD-A154677 ..... N85-32226 #
AD-A154678 ..... N85-32834 #
AD-A154679 ..... N85-32256 #
AD-A154681 ..... N85-32257 #
AD-A154682 ..... N85-32128 #
AD-A154684 ..... N85-32346 #
AD-A154685 ..... N85-33023 #
AD-A154694 ..... N85-32305 #
AD-A154698 ..... N85-33024 #
AD-A154700 ..... N85-32112 #
AD-A154703 ..... N85-32347 #
AD-A154704 ..... N85-32197 #
AD-A154705 ..... N85-32799 #
AD-A154706 ..... N85-32091 #
AD-A154708 ..... N85-33010 #
AD-A154709 ..... N85-32800 #
AD-A154710 ..... N85-32554 #
AD-A154711 ..... N85-32320 #
AD-A154714 ..... N85-32574 #
AD-A154715 ..... N85-32459 #
AD-A154716 ..... N85-33036 #
AD-A154722 ..... N85-32181 #
AD-A154723 ..... N85-32227 #
AD-A154724 ..... N85-32228 #
AD-A154726 ..... N85-32778 #
AD-A154735 ..... N85-32575 #
AD-A154736 ..... N85-32306 #
AD-A154742 ..... N85-32801 #
AD-A154745 ..... N85-32258 #
AD-A154747 ..... N85-32159 #
AD-A154750 ..... N85-32216 #
AD-A154751 ..... N85-32555 #
AD-A154753 ..... N85-32702 #
AD-A154755 ..... N85-33011 #
AD-A154757 ..... N85-33041 #
AD-A154758 ..... N85-32757 #
AD-A154759 ..... N85-32276 #
AD-A154760 ..... N85-32556 #
AD-A154761 ..... N85-32835 #
AD-A154762 ..... N85-32160 #
AD-A154763 ..... N85-32773 #
AD-A154767 ..... N85-32802 #
AD-A154768 ..... N85-32307 #
AD-A154769 ..... N85-32803 #
AD-A154771 ..... N85-32836 #
AD-A154773 ..... N85-32779 #
AD-A154776 ..... N85-32804 #
AD-A154777 ..... N85-32576 #
AD-A154780 ..... N85-32308 #
AD-A154781 ..... N85-32389 #
AD-A154783 ..... N85-33025 #
AD-A154784 ..... N85-32837 #
AD-A154785 ..... N85-33037 #
AD-A154786 ..... N85-32838 #
AD-A154787 ..... N85-32277 #
AD-A154788 ..... N85-32839 #
AD-A154793 ..... N85-32229 #
AD-A154795 ..... N85-32995 #
AD-A154796 ..... N85-32758 #
AD-A154798 ..... N85-32230 #
AD-A154799 ..... N85-33026 #
AD-A154803 ..... N85-32840 #
AD-A154805 ..... N85-32278 #
AD-A154806 ..... N85-32841 #
AD-A154809 ..... N85-32842 #
AD-A154811 ..... N85-32198 #
AD-A154812 ..... N85-32843 #
AD-A154813 ..... N85-32848 #
AD-A154818 ..... N85-32963 #
AD-A154820 ..... N85-32984 #
AD-A154821 ..... N85-32557 #
AD-A154824 ..... N85-33027 #
AD-A154827 ..... N85-32996 #
AD-A154828 ..... N85-32805 #
AD-A154829 ..... N85-32096 #
AD-A154862 ..... N85-33042 #
AD-A154864 ..... N85-33012 #
AD-A154868 ..... N85-32231 #
AD-A154870 ..... N85-32348 #
AD-A154871 ..... N85-32199 #
AD-A154875 ..... N85-32108 #
AD-A154876 ..... N85-32161 #
AD-A154878 ..... N85-32806 #
AD-A154879 ..... N85-32279 #
AD-A154880 ..... N85-32338 #
AD-A154886 ..... N85-32232 #
AD-A154887 ..... N85-32210 #
AD-A154893 ..... N85-32985 #
AD-A154897 ..... N85-32200 #
AD-A154902 ..... N85-33016 #
AD-A154904 ..... N85-32558 #
AD-A154905 ..... N85-32233 #
AD-A154907 ..... N85-32807 #
AD-A154912 ..... N85-32390 #
AD-A154913 ..... N85-32109 #
AD-A154914 ..... N85-32113 #
AD-A154915 ..... N85-32321 #
AD-A154918 ..... N85-32152 #
AD-A154922 ..... N85-32234 #
AD-A154937 ..... N85-32139 #
AD-A154942 ..... N85-32259 #
AD-A154947 ..... N85-32097 #
AD-A154949 ..... N85-32114 #
AD-A154950 ..... N85-32162 #
AD-A154952 ..... N85-32577 #
AD-A154954 ..... N85-32182 #
AD-A154958 ..... N85-32986 #
AD-A154959 ..... N85-32987 #
AD-A154960 ..... N85-32235 #
AD-A154961 ..... N85-32309 #
AD-A154962 ..... N85-32559 #
AD-A154965 ..... N85-32236 #
AD-A154966 ..... N85-32391 #
AD-A154967 ..... N85-33097 #
AD-A154968 ..... N85-32578 #
AD-A154973 ..... N85-32560 #
AD-A154975 ..... N85-32237 #
AD-A154981 ..... N85-32126 #
AD-A154986 ..... N85-32310 #
AD-A154987 ..... N85-33013 #
AD-A154988 ..... N85-32561 #
AD-A154989 ..... N85-32392 #
AD-A154995 ..... N85-33014 #
AD-A154999 ..... N85-32201 #
AD-A155012 ..... N85-32703 #
AD-A155013 ..... N85-32767 #
AD-A155018 ..... N85-32562 #
AD-A155019 ..... N85-32988 #
AD-A155020 ..... N85-32202 #
AD-A155022 ..... N85-32349 #
AD-A155023 ..... N85-32997 #
AD-A155024 ..... N85-32106 #
AD-A155027 ..... N85-32579 #
AD-A155028 ..... N85-32163 #
AD-A155029 ..... N85-32844 #
AD-A155031 ..... N85-33028 #
AD-A155034 ..... N85-32580 #
AD-A155035 ..... N85-32859 #
AD-A155038 ..... N85-32998 #
AD-A155042 ..... N85-32335 #
AD-A155043 ..... N85-32260 #
AD-A155050 ..... N85-33043 #
AD-A155056 ..... N85-32845 #
AD-A155059 ..... N85-33015 #
AD-A155065 ..... N85-32153 #
AD-A155069 ..... N85-32999 #
AD-A155070 ..... N85-32563 #
AD-A155092 ..... N85-32759 #
AD-A155100 ..... N85-32581 #
AD-A155101 ..... N85-32238 #
AD-A155102 ..... N85-32203 #
AD-A155103 ..... N85-32239 #
AD-A155106 ..... N85-32164 #
AD-A155107 ..... N85-32115 #
AD-A155109 ..... N85-32261 #
AD-A155110 ..... N85-32262 #
AD-A155113 ..... N85-32760 #
AD-A155117 ..... N85-32140 #
AD-A155119 ..... N85-32761 #
AD-A155137 ..... N85-32582 #
AD-A155138 ..... N85-32583 #
AD-A155139 ..... N85-32584 #
AD-A155140 ..... N85-32183 #
AD-A155141 ..... N85-32989 #
AD-A155142 ..... N85-32184 #
AD-A155147 ..... N85-32116 #
AD-A155148 ..... N85-32585 #
AD-A155150 ..... N85-32263 #
AD-A155151 ..... N85-33029 #
AD-A155155 ..... N85-32141 #
AD-A155161 ..... N85-32704 #

AD-A155163 ..... N85-32280 #
AD-A155164 ..... N85-32823 #
AD-A155166 ..... N85-32705 #
AD-A155167 ..... N85-32808 #
AD-A155169 ..... N85-32853 #
AD-A155170 ..... N85-32564 #
AD-A155171 ..... N85-32350 #
AD-A155173 ..... N85-32809 #
AD-A155184 ..... N85-32240 #
AD-A155185 ..... N85-33003 #
AD-A155186 ..... N85-32312 #
AD-A155187 ..... N85-32241 #
AD-A155195 ..... N85-32762 #
AD-A155196 ..... N85-32117 #
AD-A155202 ..... N85-32098 #
AD-A155204 ..... N85-32242 #
AD-A155206 ..... N85-32565 #
AD-A155211 ..... N85-32281 #
AD-A155212 ..... N85-32351 #
AD-A155214 ..... N85-33098 #
AD-A155215 ..... N85-32313 #
AD-A155216 ..... N85-32185 #
AD-A155218 ..... N85-32810 #
AD-A155221 ..... N85-32586 #
AD-A155222 ..... N85-33030 #
AD-A155223 ..... N85-32454 #
AD-A155225 ..... N85-32587 #
AD-A155227 ..... N85-32099 #
AD-A155229 ..... N85-32143 #
AD-A155230 ..... N85-32588 #
AD-A155231 ..... N85-32768 #
AD-A155232 ..... N85-32780 #
AD-A155233 ..... N85-32774 #
AD-A155237 ..... N85-32264 #
AD-A155238 ..... N85-32186 #
AD-A155240 ..... N85-32589 #
AD-A155242 ..... N85-32775 #
AD-A155247 ..... N85-32769 #
AD-A155248 ..... N85-33017 #
AD-A155250 ..... N85-32566 #
AD-A155251 ..... N85-33099 #
AD-A155254 ..... N85-32590 #
AD-A155256 ..... N85-33100 #
AD-A155257 ..... N85-32567 #
AD-A155259 ..... N85-32282 #
AD-A155260 ..... N85-32763 #
AD-A155264 ..... N85-32265 #
AD-A155266 ..... N85-32854 #
AD-A155293 ..... N85-32118 #
AD-A155294 ..... N85-32322 #
AD-A155300 ..... N85-32283 #
AD-A155302 ..... N85-32323 #
AD-A155306 ..... N85-32568 #
AD-A155322 ..... N85-32243 #
AD-A155326 ..... N85-32776 #
AD-A155330 ..... N85-32154 #
AD-A155334 ..... N85-33038 #
AD-A155337 ..... N85-32352 #
AD-A155338 ..... N85-32314 #
AD-A155340 ..... N85-32165 #
AD-A155344 ..... N85-33018 #
AD-A155434 ..... N85-33101 #
AD-A155435 ..... N85-32460 #
AD-A155438 ..... N85-32811 #
AD-A155441 ..... N85-32461 #
AD-A155443 ..... N85-32324 #
AD-A155450 ..... N85-32812 #
AD-A155452 ..... N85-33031 #
AD-A155462 ..... N85-32990 #
AD-A155465 ..... N85-32824 #
AD-A155466 ..... N85-32855 #
AD-A155471 ..... N85-32266 #
AD-A155472 ..... N85-32353 #
AD-A155474 ..... N85-33019 #
AD-A155475 ..... N85-32591 #
AD-A155476 ..... N85-32991 #
AD-A155477 ..... N85-32121 #
AD-A155479 ..... N85-32267 #
AD-A155481 ..... N85-32336 #
AD-A155482 ..... N85-33020 #
AD-A155483 ..... N85-32462 #
AD-A155484 ..... N85-32325 #
AD-A155486 ..... N85-32706 #
AD-A155489 ..... N85-32100 #
AD-A155516 ..... N85-32813 #
AD-A155517 ..... N85-32825 #
AD-A155518 ..... N85-32814 #
AD-A155524 ..... N85-32592 #
AD-A155525 ..... N85-33102 #
AD-A155528 ..... N85-33032 #
AD-A155530 ..... N85-32187 #
AD-A155536 ..... N85-32244 #
AD-A155537 ..... N85-32593 #
AD-A155554 ..... N85-32188 #
AD-A155555 ..... N85-32204 #
AD-A155558 ..... N85-32326 #
AD-A155559 ..... N85-32992 #
AD-A155560 ..... N85-32205 #
AD-A155561 ..... N85-33000 #
AD-A155564 ..... N85-32770 #
AD-A155569 ..... N85-32268 #
AD-A155570 ..... N85-32245 #
AD-A155580 ..... N85-33033 #
AD-A155583 ..... N85-32849 #
AD-A155584 ..... N85-33034 #
AD-A155586 ..... N85-32354 #
AD-A155589 ..... N85-32166 #
AD-A155597 ..... N85-32206 #
AD-A155598 ..... N85-32327 #
AD-A155599 ..... N85-32815 #
AD-A155600 ..... N85-32816 #
AD-A155603 ..... N85-32850 #
AD-A155605 ..... N85-32207 #
AD-A155607 ..... N85-32594 #
AD-A155608 ..... N85-32246 #
AD-A155609 ..... N85-32284 #
AD-A155610 ..... N85-32707 #
AD-A155612 ..... N85-32355 #
AD-A155619 ..... N85-32771 #
AD-A155622 ..... N85-32155 #
AD-A155623 ..... N85-32595 #
AD-A155628 ..... N85-32356 #
AD-A155630 ..... N85-32167 #
AD-A155631 ..... N85-32826 #
AD-A155642 ..... N85-32285 #
AD-A155645 ..... N85-32764 #
AD-A155646 ..... N85-32750 #
AD-A155647 ..... N85-32247 #
AD-A155648 ..... N85-32856 #
AD-A155668 ..... N85-32827 #
AD-A155704 ..... N85-32817 #
AD-A155714 ..... N85-32818 #
AD-A155737 ..... N85-32211 #
AD-A155739 ..... N85-32248 #
AD-A155740 ..... N85-32212 #

AD-D011718 ..... N85-32311 #

AD-E401350 ..... N85-32211 #
AD-E440281 ..... N85-32356 #

AD-F300613 ..... N85-32118 #
AD-F300613 ..... N85-32265 #
AD-F300613 ..... N85-32282 #
AD-F300613 ..... N85-32283 #
AD-F300613 ..... N85-32322 #
AD-F300613 ..... N85-32763 #
AD-F300613 ..... N85-32854 #
AD-F300614 ..... N85-32323 #
AD-F300619 ..... N85-32212 #
AD-F300619 ..... N85-32248 #
AD-F300620 ..... N85-32167 #
AD-F630641 ..... N85-32259 #
AD-F630645 ..... N85-32116 #
AD-F630645 ..... N85-32183 #
AD-F630645 ..... N85-32184 #
AD-F630645 ..... N85-32582 #
AD-F630645 ..... N85-32583 #
AD-F630645 ..... N85-32584 #
AD-F630645 ..... N85-32585 #
AD-F630645 ..... N85-32989 #
AD-F630659 ..... N85-32209 #
AD-F630659 ..... N85-32553 #
AD-F630659 ..... N85-32833 #

AERONOMICA-ACTA-A-282-1984 ..... N85-33095

AFAMRL-TR-84-017-VOL-3 ..... N85-32984 #
AFAMRL-TR-85-016 ..... N85-32114 #
AFAMRL-TR-85-018 ..... N85-32986 #
AFAMRL-TR-85-028 ..... N85-32126 #

AFESC/ESL-TR-84-55 ..... N85-32461 #

AFGL-AFSG-446 ..... N85-32387 #

AFGL-ERP-887 ..... N85-32558 #
AFGL-ERP-891 ..... N85-32577 #
AFGL-ERP-892 ..... N85-32586 #

AFGL-IP-326 ..... N85-32143 #

AFGL-TR-84-0096 ..... N85-32590 #
AFGL-TR-84-0130 ..... N85-33098 #
AFGL-TR-84-0192 ..... N85-32099 #
AFGL-TR-84-0204 ..... N85-32561 #
AFGL-TR-84-0208 ..... N85-33012 #
AFGL-TR-84-0211 ..... N85-32558 #
AFGL-TR-84-0215 ..... N85-32566 #
AFGL-TR-84-0224 ..... N85-32313 #
AFGL-TR-84-0225 ..... N85-32143 #
AFGL-TR-84-0227 ..... N85-32565 #
AFGL-TR-84-0236 ..... N85-32387 #
AFGL-TR-84-0249 ..... N85-32562 #
AFGL-TR-84-0255 ..... N85-32587 #
AFGL-TR-84-0257 ..... N85-32567 #
AFGL-TR-84-0262 ..... N85-33101 #
AFGL-TR-84-0266 ..... N85-32577 #
AFGL-TR-84-0267 ..... N85-32586 #
AFGL-TR-84-0281 ..... N85-32139 #
AFGL-TR-84-0282 ..... N85-32578 #
AFGL-TR-84-0291 ..... N85-33100 #
AFGL-TR-84-0331 ..... N85-32560 #
AFGL-TR-84-0335 ..... N85-33097 #
AFGL-TR-85-0002 ..... N85-32312 #
AFGL-TR-85-0003 ..... N85-33099 #
AFGL-TR-85-0014 ..... N85-32559 #
AFGL-TR-85-0119 ..... N85-33102 #

AFHRL-TP-85-4 ..... N85-32757 #

AFHRL-TR-84-65 ..... N85-32776 #

AFIT/GA/AA/84D-1 ..... N85-32835 #

AFIT/GAE/AA/84D-17 ..... N85-32305 #
AFIT/GAE/AA/85M-1 ..... N85-32181 #
AFIT/GAE/AA/85M-2 ..... N85-32347 #
AFIT/GAE/AA/85M-6 ..... N85-32112 #

AFIT/GCS/ENG/84D-6-VOL-1 ..... N85-33040 #
AFIT/GCS/ENG/85M-1 ..... N85-32816 #

AFIT/GCS/MA/85J-1 ..... N85-32812 #

AFIT/GE/EE/84D-71 ..... N85-32824 #
AFIT/GE/EE/85M-1 ..... N85-32855 #

AFIT/GE/ENG/85M-2 ..... N85-32121 #
AFIT/GE/ENG/85M-3 ..... N85-32266 #

AFIT/GNE/ENP/85M-11 ..... N85-32833 #
AFIT/GNE/ENP/85M-13 ..... N85-32553 #

AFOSR-85-0377TR ..... N85-32253 #
AFOSR-85-0379TR ..... N85-32157 #
AFOSR-85-0392TR ..... N85-32194 #
AFOSR-85-0395TR ..... N85-32554 #
AFOSR-85-0409TR ..... N85-32128 #
AFOSR-85-0444TR ..... N85-32344 #
AFOSR-85-0447TR ..... N85-32343 #
AFOSR-85-0454TR ..... N85-32758 #
AFOSR-85-0456TR ..... N85-32320 #
AFOSR-85-0457TR ..... N85-32858 #
AFOSR-85-0460TR ..... N85-32345 #
AFOSR-85-0462TR ..... N85-32165 #
AFOSR-85-0466TR ..... N85-32160 #
AFOSR-85-0473TR ..... N85-32140 #
AFOSR-85-0474TR ..... N85-33041 #
AFOSR-85-0486TR ..... N85-32262 #

AFRPL-TR-85-005 ..... N85-33018 #

AFRRI-CR-85-1 ..... N85-33003 #

AFRRI-TR84-8 ..... N85-32999 #

AFTAC-TR-85-4 ..... N85-32142 #

AFWAL-TR-84-2113 ..... N85-32326 #
AFWAL-TR-84-4074 ..... N85-32153 #
AFWAL-TR-84-4119 ..... N85-32198 #
AFWAL-TR-84-4129 ..... N85-32155 #
AFWAL-TR-84-4143 ..... N85-32335 #
AFWAL-TR-84-4189 ..... N85-32152 #
AFWAL-TR-85-1009 ..... N85-32805 #
AFWAL-TR-85-2020 ..... N85-32996 #
AFWAL-TR-85-4031 ..... N85-33031 #

AGARD-LS-140 ..... N85-32293 #

AI/DS-TR-1047-020-1 ..... N85-32800 #

AIAA-85-1876 ..... N85-32120* #
AIAA-85-1891 ..... N85-32122* #
AIAA-85-1980 ..... N85-32794* #

ALO-5319-5 ..... N85-32287 #

AMD-TR-85-4 ..... N85-32762 #

ANL-84-24 ..... N85-33002 #

ANL/NDM-88 ..... N85-33009 #

APRO-84-13 ..... N85-33036 #

AR-4 ..... N85-32345 #

ARAP-536 ..... N85-32837 #

ARL-TR-84-21 ..... N85-32981 #
ARL-TR-85-3 ..... N85-32980 #
ARL-TR-85-5 ..... N85-32264 #

ARL/AERO-PROP-TM-422 ..... N85-32117 #

ARL/AERO-TM-423 ..... N85-32113 #

ARLCB-TR-85011 ..... N85-32356 #

ARLCD-CR-85019 ..... N85-32211 #

ARO-1663.5-GS ..... N85-32128 #
ARO-15104.14-MS ..... N85-32180 #
ARO-15689.9-MS ..... N85-32187 #
ARO-17260.7-PH ..... N85-32205 #
ARO-17753.2-GS ..... N85-32591 #
ARO-17773.15-CH ..... N85-32207 #
ARO-18047.1-CH ..... N85-33000 #
ARO-18112.3-MS ..... N85-33034 #
ARO-18159.3-MS ..... N85-32354 #
ARO-18290.12-CH ..... N85-32166 #
ARO-18399.7-MS ..... N85-32187 #
ARO-18406.12-PH ..... N85-33032 #
ARO-18621.11-CH ..... N85-32196 #
ARO-18688.2-MS ..... N85-32267 #
ARO-19268.4-PH-H ..... N85-33033 #
ARO-19367.26-MA ..... N85-32850 #
ARO-19777.12-PH ..... N85-32324 #
ARO-19804.1-MS ..... N85-32206 #
ARO-20063.3-MA ..... N85-32849 #
ARO-21438.13-EL ..... N85-32245 #

ASA-AF-85-1 ..... N85-32228 #

ASE-4928 ..... N85-33099 #

ASR-2 ..... N85-32119* #

ATR-3 ..... N85-32990 #

AU-AFIT-EN-TR-85-1 ..... N85-32158 #

BBN-5324-VOL-3 ..... N85-32984 #
BBN-5668 ..... N85-32986 #

BDX-613-3222 ..... N85-32318 #
BDX-613-3267 ..... N85-32315 #

BNL-36421 ..... N85-33001 #

BRL-CR-542 ..... N85-32212 #
BRL-CR-543 ..... N85-32323 #

BRL-MR-3440 ..... N85-32167 #

BRL-TR-2645 ..... N85-32283 #

CDTR-85-1 ..... N85-32996 #

CERL-TR-M-85/10 ..... N85-32350 #
CERL-TR-M-85/11 ..... N85-32351 #

CONF-841202-3 ..... N85-32289 #
CONF-850146-6 ..... N85-33007 #
CONF-850282-1 ..... N85-32169 #
CONF-850310-82 ..... N85-33006 #
CONF-850310-90 ..... N85-33021 #
CONF-850388-2 ..... N85-32455 #
CONF-850473-1 ..... N85-32751 #
CONF-850560-1 ..... N85-33001 #
CONF-850610-4 ..... N85-32292 #
CONF-850614-1 ..... N85-32288 #
CONF-850862-2 ..... N85-32846 #
CONF-851048-1 ..... N85-33035 #
CONF-8409229-2 ..... N85-33022 #
CONF-8503100-3 ..... N85-32171 #
CONF-8503129-1 ..... N85-32290 #
CONF-8503131-2 ..... N85-32269 #
CONF-8504124-1 ..... N85-32189 #
CONF-8504128-2-ABST ..... N85-32328 #
CONF-8505102-1 ..... N85-32317 #
CONF-8505136-1 ..... N85-32145 #

CRDC-CR-85004 ..... N85-32761 #

CRDC-TR-84089 ..... N85-32163 #

CRREL-85-5 ..... N85-32700 #
CRREL-85-6 ..... N85-32859 #
CRREL-85-8 ..... N85-33015 #

CSDL-R-1774 ..... N85-32267 #

CWP-028 ..... N85-32804 #

DE84-016857 ..... N85-32288 #
DE85-000784 ..... N85-33002 #
DE85-006195 ..... N85-32292 #
DE85-009602 ..... N85-32290 #
DE85-009607 ..... N85-32145 #
DE85-009624 ..... N85-32455 #
DE85-009793 ..... N85-32328 #
DE85-010014 ..... N85-32318 #
DE85-010217 ..... N85-33007 #
DE85-010291 ..... N85-32751 #
DE85-010333 ..... N85-33005 #
DE85-010380 ..... N85-32286 #
DE85-010381 ..... N85-32287 #
DE85-010504 ..... N85-33006 #
DE85-010576 ..... N85-32168 #
DE85-010715 ..... N85-33022 #
DE85-010767 ..... N85-32319 #
DE85-010807 ..... N85-32171 #
DE85-010820 ..... N85-32463 #
DE85-010928 ..... N85-32846 #
DE85-010936 ..... N85-33028 #
DE85-010975 ..... N85-32189 #
DE85-011210 ..... N85-32291 #
DE85-011410 ..... N85-32269 #
DE85-011438 ..... N85-33021 #
DE85-011448 ..... N85-32214 #
DE85-011521 ..... N85-32819 #
DE85-011543 ..... N85-33035 #
DE85-011685 ..... N85-32316 #
DE85-011767 ..... N85-33061 #
DE85-011813 ..... N85-33001 #
DE85-011852 ..... N85-32169 #
DE85-011862 ..... N85-32820 #
DE85-011867 ..... N85-32213 #
DE85-011890 ..... N85-32393 #
DE85-011894 ..... N85-32456 #
DE85-011929 ..... N85-32317 #
DE85-011978 ..... N85-32270 #
DE85-011979 ..... N85-32289 #
DE85-012053 ..... N85-32315 #
DE85-012072 ..... N85-32250 #
DE85-012075 ..... N85-33008 #
DE85-012095 ..... N85-33009 #
DE85-012288 ..... N85-32170 #
DE85-012818 ..... N85-32249 #

DOC-85HV002 ..... N85-32178* #

DOE/CS-15077/T13 ..... N85-32291 #
DOE/CS-35365/T1 ..... N85-32286 #

DOE/ET-11384/T1 ..... N85-32168 #

DOE/JPL-1012-104 ..... N85-32394* #

DOE/NASA/4105-1 ..... N85-32251* #

DOE/NE-32084/T1 ..... N85-32270 #

DOT/FAA/PM-85/14 ..... N85-32573 #

DPG-TR-85-204 ..... N85-32588 #

DREO-TN-84-33 ..... N85-32208 #
DREO-TN-85-2 ..... N85-32307 #

DRIC-BR-94446 ..... N85-32199 #
DRIC-BR-94938 ..... N85-32182 #
DRIC-BR-95551 ..... N85-32236 #

DTIC/TR-85/4 ..... N85-33043 #

DTNSRDC-83/113 ..... N85-32097 #
DTNSRDC-85/010 ..... N85-32281 #

DTNSRDC/SPD-1139-01 ..... N85-32098 #

DTNSRDC/84/071 ..... N85-32353 #

E-2256 ..... N85-32331* #
E-2523 ..... N85-32330* #
E-2524 ..... N85-32329* #
E-2574 ..... N85-32156* #
E-2591 ..... N85-32337* #
E-2607 ..... N85-32333* #
E-2643 ..... N85-32302* #
E-2661 ..... N85-32148* #

ECAC-CR-83-200 ..... N85-32242 #

EMORY/DC/TR-5 ..... N85-33013 #

EMORY/DC/TR/4 ..... N85-32162 #
EMORY/DC/TR/6 ..... N85-32310 #

ESA-CR(P)-2015 ..... N85-32628 #

ESD-TR-84-042 ..... N85-33025 #
ESD-TR-84-190 ..... N85-32807 #
ESD-TR-84-325 ..... N85-32306 #

ETL-R-068 ..... N85-32109 #
ETL-R-069 ..... N85-32390 #
ETL-R-071 ..... N85-32391 #
ETL-R-073 ..... N85-32392 #

EVT-905 ..... N85-32995 #

FAA-CT-84-10 ..... N85-32106 #
FAA-CT-84-30 ..... N85-32104 #
FAA-CT-85-2 ..... N85-32103 #

FAA-EE-85-1 ..... N85-32983 #
FAA-EE-85-3 ..... N85-32985 #

FCC-4445-4 ..... N85-33023 #

FDRL-85-3 ..... N85-32095* #

FSA-PR-24 ..... N85-32394* #

FTD-ID(RS)T-0020-85 ..... N85-32118 #
FTD-ID(RS)T-0045-85 ..... N85-32091 #
FTD-ID(RS)T-0079-85 ..... N85-32756 #
FTD-ID(RS)T-0162-85 ..... N85-32265 #
FTD-ID(RS)T-1483-84 ..... N85-32575 #
FTD-ID(RS)T-1601-84 ..... N85-33030 #
FTD-ID(RS)T-1626-84 ..... N85-32322 #

F85-227 ..... N85-32789* #
F85-229 ..... N85-32790* #

G-774-1984 ..... N85-32569 #

GA-A-17573 ..... N85-32170 #

GAO/NSIAD-85-37 ..... N85-32261 #

GPO-39-723 ..... N85-32102 #
GPO-40-343 ..... N85-32107 #
GPO-43-064 ..... N85-32458
GPO-43-294 ..... N85-32457 #

GS-CIRC-850-1 ..... N85-32551 #
GS-CIRC-934 ..... N85-32386 #

H-1295 ..... N85-32122* #
H-1300 ..... N85-32794* #
H-1308 ..... N85-32123* #
H-1312 ..... N85-32120* #
H-1313 ..... N85-32851* #

HDL-CR-85-052-1 ..... N85-32233 #

IC/FSD-85-032 ..... N85-32789* #
IC/FSD-85-033 ..... N85-32790* #

ICASE-85-32 ..... N85-32829* #

ICS-TR-139 ..... N85-32770 #

IR-2 ..... N85-32161 #
IR-3 ..... N85-32585 #
IR-5 ..... N85-32760 #

ISBN-92-835-1503-X ..... N85-32293 #
ISBN-963-7701-842 ..... N85-32596 #

JPL-PUB-85-27 ..... N85-32394* #

JPRS-ESA-84-017 ..... N85-32781 #
JPRS-ESA-85-021 ..... N85-32190 #
JPRS-ESA-85-023 ..... N85-32217 #

JPRS-UBB-85-020 ..... N85-32752 #

JPRS-UPM-85-004 ..... N85-32860 #

JR/E-8526 ..... N85-32154 #

JSC-LS-50110 ..... N85-32129*

JSC-18295-PT-1 ..... N85-32137* #

K/OA-5762 ..... N85-32819 #

KLD-TR-159 ..... N85-32554 #

L-15972 ..... N85-32339* #

LA-UR-85-1046 ..... N85-32455 #

LA-UR-85-1094 ..... N85-32290 #
LA-UR-85-1126 ..... N85-32145 #
LA-UR-85-1167 ..... N85-32319 #
LA-UR-85-1251 ..... N85-33022 #

LA-10271-PR ..... N85-33005 #
LA-10335-MS ..... N85-32393 #
LA-10356-SR ..... N85-32456 #

LBL-17773 ..... N85-32289 #

LC-84-600161 ..... N85-32386 #
LC-85-7159 ..... N85-32708* #

LIDS-TH-1470 ..... N85-32827 #

LMSC-F018862 ..... N85-32552* #
LMSC-F035672 ..... N85-32987 #

LPI-TR-85-01 ..... N85-33062* #

MAP-HANDBOOK-14 ..... N85-32466* #

MDC-W5040 ..... N85-32796* #

MECH-84 ..... N85-32197 #

MIT/LCS/TM-264 ..... N85-32801 #
MIT/LCS/TM-265 ..... N85-32836 #
MIT/LCS/TM-270 ..... N85-32799 #
MIT/LCS/TM-272 ..... N85-32778 #
MIT/LCS/TM-273 ..... N85-32842 #

MIT/LCS/TR-330 ..... N85-32227 #
MIT/LCS/TR-331 ..... N85-33037 #
MIT/LCS/TR-332 ..... N85-32779 #
MIT/LCS/TR-333 ..... N85-32258 #

MLM-3238(CP) ..... N85-32171 #

MPL-TM-376 ..... N85-32224 #

MPL-U-11/85 ..... N85-32224 #

MRC-R-900 ..... N85-32556 #

MRC-TSR-2798 ..... N85-32843 #
MRC-TSR-2799 ..... N85-32848 #
MRC-TSR-2800 ..... N85-32557 #
MRC-TSR-2801 ..... N85-33027 #
MRC-TSR-2802 ..... N85-32838 #
MRC-TSR-2803 ..... N85-32338 #
MRC-TSR-2805 ..... N85-32841 #
MRC-TSR-2806 ..... N85-32806 #
MRC-TSR-2807 ..... N85-32279 #
MRC-TSR-2808 ..... N85-32277 #
MRC-TSR-2809 ..... N85-32278 #
MRC-TSR-2811 ..... N85-32839 #
MRC-TSR-2813 ..... N85-32840 #

MRDC41129.9SA ..... N85-32262 #

MRI-R-947 ..... N85-32304 #
MRL-R-951 ..... N85-32276 #

MTI-84TR72 ..... N85-32335 #

MTR-9420 ..... N85-32807 #

NADC-84143-60 ..... N85-32775 #

NAE-AN-26 ..... N85-32125 #

NAS 1.15:77905 ..... N85-32146* #
NAS 1.15:86210 ..... N85-32131* #
NAS 1.15:86229 ..... N85-32465* #
NAS 1.15:86357 ..... N85-32111* #
NAS 1.15:86414 ..... N85-32110* #
NAS 1.15:86433 ..... N85-32151* #
NAS 1.15:86448 ..... N85-32822* #
NAS 1.15:86449 ..... N85-32092* #
NAS 1.15:86512 ..... N35-32147* #
NAS 1.15:86515 ..... N85-32847* #
NAS 1.15:86711 ..... N85-32795* #
NAS 1.15:86714 ..... N85-32090* #
NAS 1.15:86717 ..... N85-32094* #
NAS 1.15:86737 ..... N85-32122* #
NAS 1.15:86739 ..... N85-32794* #
NAS 1.15:86744 ..... N85-32123* #
NAS 1.15:86748 ..... N85-32120* #
NAS 1.15:86749 ..... N85-32851* #
NAS 1.15:86773 ..... N85-32831* #
NAS 1.15:86775 ..... N85-32830* #
NAS 1.15:87035 ..... N85-32337* #
NAS 1.15:87068 ..... N85-32156* #
NAS 1.15:87071 ..... N85-32302* #

NAS 1.15:87078 ..... N85-32333* #
NAS 1.15:87081 ..... N85-32148* #
NAS 1.15:87494 ..... N85-32137* #
NAS 1.15:87495 ..... N85-32129*
NAS 1.15:87570 ..... N85-32710* #
NAS 1.15:87571 ..... N85-32150* #
NAS 1.15:87572 ..... N85-32149* #
NAS 1.21:468 ..... N85-32089* #
NAS 1.21:477 ..... N85-32777* #
NAS 1.21:478 ..... N85-32708* #
NAS 1.21:483 ..... N85-32772* #
NAS 1.21:7011(273) N85-32755*
NAS 1.26:3855 ..... N85-32133* #
NAS 1.26:3908 ..... N85-32765* #
NAS 1.26:3922 ..... N85-32709* #
NAS 1.26:166545 ..... N85-32272* #
NAS 1.26:171581 ..... N85-32571* #
NAS 1.26:171587 ..... N85-32789* #
NAS 1.26:171588 ..... N85-32303* #
NAS 1.26:171589 ..... N85-32178* #
NAS 1.26:171596 ..... N85-32130* #
NAS 1.26:171597 ..... N85-32790* #
NAS 1.26:172449 ..... N85-32172* #
NAS 1.26:172450 ..... N85-32177* #
NAS 1.26:172597 ..... N85-32342* #
NAS 1.26:172601 ..... N85-32464* #
NAS 1.26:172603 ..... N85-32093* #
NAS 1.26:172608 ..... N85-32791* #
NAS 1.26:174925 ..... N85-32119* #
NAS 1.26:174940 ..... N85-32340* #
NAS 1.26:174941 ..... N85-32341* #
NAS 1.26:174950 ..... N85-32251* #
NAS 1.26:175297 ..... N85-33096* #
NAS 1.26:175301 ..... N85-32572* #
NAS 1.26:175305 ..... N85-32252* #
NAS 1.26:175306 ..... N85-32552* #
NAS 1.26:176001 ..... N85-32857* #
NAS 1.26:176037 ..... N85-33062* #
NAS 1.26:176050 ..... N85-32570* #
NAS 1.26:176058 ..... N85-32394* #
NAS 1.26:176060 ..... N85-33044* #
NAS 1.26:176068 ..... N85-33060* #
NAS 1.26:176069 ..... N85-33103* #
NAS 1.26:176070 ..... N85-32174* #
NAS 1.26:176071 ..... N85-32173* #
NAS 1.26:176072 ..... N85-32175* #
NAS 1.26:176073 ..... N85-32334* #
NAS 1.26:176077 ..... N85-32176* #
NAS 1.26:176085 ..... N85-32466* #
NAS 1.26:176086 ..... N85-32332* #
NAS 1.26:176087 ..... N85-32792* #
NAS 1.26:176088 ..... N85-32793* #
NAS 1.26:176089 ..... N85-32796* #
NAS 1.26:176094 ..... N85-32134* #
NAS 1.26:176096 ..... N85-32135* #
NAS 1.26:176097 ..... N85-32136* #
NAS 1.26:176098 ..... N85-32821* #
NAS 1.26:177365 ..... N85-32095* #
NAS 1.26:177932 ..... N85-32215* #
NAS 1.26:177933 ..... N85-32979* #
NAS 1.26:177935 ..... N85-32829* #
NAS 1.55:2312 ..... N85-32357* #
NAS 1.60:2455 ..... N85-32339* #
NAS 1.60:2473 ..... N85-32331* #
NAS 1.60:2488 ..... N85-32329* #
NAS 1.60:2493 ..... N85-32101* #
NAS 1.60:2500 ..... N85-32330* #

NASA-CP-2312 ..... N85-32357* #

NASA-CR-3855 ..... N85-32133* #
NASA-CR-3908 ..... N85-32765* #
NASA-CR-3922 ..... N85-32709* #
NASA-CR-166545 ..... N85-32272* #
NASA-CR-171581 ..... N85-32571* #
NASA-CR-171587 ..... N85-32789* #
NASA-CR-171588 ..... N85-32303* #
NASA-CR-171589 ..... N85-32178* #
NASA-CR-171596 ..... N85-32130* #
NASA-CR-171597 ..... N85-32790* #
NASA-CR-172449 ..... N85-32172* #
NASA-CR-172450 ..... N85-32177* #
NASA-CR-172597 ..... N85-32342* #
NASA-CR-172601 ..... N85-32464* #
NASA-CR-172603 ..... N85-32093* #
NASA-CR-172608 ..... N85-32791* #
NASA-CR-174925 ..... N85-32119* #
NASA-CR-174940 ..... N85-32340* #
NASA-CR-174941 ..... N85-32341* #
NASA-CR-174950 ..... N85-32251* #
NASA-CR-175297 ..... N85-33096* #
NASA-CR-175301 ..... N85-32572* #
NASA-CR-175305 ..... N85-32252* #
NASA-CR-175306 ..... N85-32552* #
NASA-CR-176001 ..... N85-32857* #
NASA-CR-176037 ..... N85-33062* #
NASA-CR-176050 ..... N85-32570* #
NASA-CR-176058 ..... N85-32394* #
NASA-CR-176060 ..... N85-33044* #
NASA-CR-176068 ..... N85-33060* #
NASA-CR-176069 ..... N85-33103* #
NASA-CR-176070 ..... N85-32174* #
NASA-CR-176071 ..... N85-32173* #
NASA-CR-176072 ..... N85-32175* #
NASA-CR-176085 ..... N85-32466* #
NASA-CR-176086 ..... N85-32332* #
NASA-CR-176087 ..... N85-32792* #
NASA-CR-176088 ..... N85-32793* #
NASA-CR-176089 ..... N85-32796* #
NASA-CR-176094 ..... N85-32134* #
NASA-CR-176096 ..... N85-32135* #
NASA-CR-176097 ..... N85-32136* #
NASA-CR-176098 ..... N85-32821* #
NASA-CR-177365 ..... N85-32095* #
NASA-CR-177932 ..... N85-32215* #
NASA-CR-177933 ..... N85-32979* #
NASA-CR-177935 ..... N85-32829* #

NASA-SP-468 ..... N85-32089* #
NASA-SP-477 ..... N85-32777* #
NASA-SP-478 ..... N85-32708* #
NASA-SP-483 ..... N85-32772* #
NASA-SP-7011(273) N85-32755*

NASA-TM-77905 ..... N85-32146* #
NASA-TM-86210 ..... N85-32131* #
NASA-TM-86229 ..... N85-32465* #
NASA-TM-86357 ..... N85-32111* #
NASA-TM-86414 ..... N85-32110* #
NASA-TM-86433 ..... N85-32151* #
NASA-TM-86448 ..... N85-32822* #
NASA-TM-86449 ..... N85-32092* #
NASA-TM-86512 ..... N85-32147* #
NASA-TM-86515 ..... N85-32847* #
NASA-TM-86711 ..... N85-32795* #
NASA-TM-86714 ..... N85-32090* #
NASA-TM-86717 ..... N85-32094* #
NASA-TM-86737 ..... N85-32122* #
NASA-TM-86739 ..... N85-32794* #
NASA-TM-86744 ..... N85-32123* #
NASA-TM-86748 ..... N85-32120* #
NASA-TM-86749 ..... N85-32851* #
NASA-TM-86773 ..... N85-32831* #
NASA-TM-86775 ..... N85-32830* #
NASA-TM-87035 ..... N85-32337* #
NASA-TM-87068 ..... N85-32156* #
NASA-TM-87071 ..... N85-32302* #
NASA-TM-87078 ..... N85-32333* #
NASA-TM-87081 ..... N85-32148* #
NASA-TM-87494 ..... N85-32137* #
NASA-TM-87495 ..... N85-32129*
NASA-TM-87570 ..... N85-32710* #
NASA-TM-87571 ..... N85-32150* #
NASA-TM-87572 ..... N85-32149* #

NASA-TP-2455 ..... N85-32339* #
NASA-TP-2473 ..... N85-32331* #
NASA-TP-2488 ..... N85-32329* #
NASA-TP-2493 ..... N85-32101* #
NASA-TP-2500 ..... N85-32330* #

NATC-TM-85-3-SY ..... N85-32308 #

NATICK/TR-85/035 ..... N85-32773 #
NATICK/TR-85/042 ..... N85-32164 #

NEAR-TR-343 ..... N85-32096 #

NEPRF-CR-85-01 ..... N85-32460 #
NEPRF-CR-85-02 ..... N85-32579 #
NEPRF-CR-85-03 ..... N85-32595 #
NEPRF-CR-85-04 ..... N85-32589 #
NEPRF-CR-85-05 ..... N85-32325 #

NMAB-426 ..... N85-32256 #

NORSAR-CONTRIB-350 ..... N85-32555 #

NOSC/TD-761 ..... N85-32459 #

NOSC/TR-978 ..... N85-32223 #

NPS52-84-013 ..... N85-32780 #
NPS52-85-005 ..... N85-32817 #
NPS52-85-006-PT-1 ..... N85-32811 #
NPS52-85-008 ..... N85-32825 #
NPS61-85-002 ..... N85-32460 #
NPS68-85-016 ..... N85-32703 #
NPS69-85-003 ..... N85-32284 #

NRC-24173 ..... N85-32125 #

NRL-MR-5491 ..... N85-32321 #
NRL-MR-5536 ..... N85-32564 #
NRL-MR-5539 ..... N85-32141 #
NRL-MR-5541 ..... N85-33014 #
NRL-MR-5549 ..... N85-33019 #
NRL-MP-5552 ..... N85-33016 #
NRL-MR-5559 ..... N85-32349 #
NRL-MR-5560 ..... N85-32259 #
NRL-MR-5570 ..... N85-32853 #
NRL-MR-5591 ..... N85-33020 #

NRL-8894 ..... N85-32243 #

NSMRL-1044 ..... N85-32767 #

NSWC/TR-83-55 ..... N85-32132 #
NSWC/TR-83-353 ..... N85-32231 #

NTSB/SS-85/02 ..... N85-32105 #

OMI-116 ..... N85-32325 #

ONR-TR-4 ..... N85-32201 #

ONR-TR3 ..... N85-32997 #

ONRL-R-1-85 ..... N85-33038 #

ORNL-6144 ..... N85-33008 #

OSU-DGSS-360 ..... N85-32560 #

OSU/DGSS-357 ..... N85-32566 #

PAPER-OG-4.2-3 ..... N85-33045* #
PAPER-OG-4.3-8 ..... N85-33046* #
PAPER-OG-7.2-20 ..... N85-33047* #
PAPER-OG-9.2-1 ..... N85-33048* #
PAPER-OG-9.2-2 ..... N85-33049* #
PAPER-OG-9.3-11 ..... N85-33050* #

PAPER-SH-1.5-18 ..... N85-33051* #
PAPER-SH-2.1-4 ..... N85-33052* #
PAPER-SH-2.1-5 ..... N85-33053* #
PAPER-SH-4.1-13 ..... N85-33054* #
PAPER-SH-4.2-9 ..... N85-33055* #
PAPER-SH-4.6-1 ..... N85-33056* #
PAPER-SH-4.6-2 ..... N85-33057* #
PAPER-SH-4.6-4 ..... N85-33058* #
PAPER-SH-4.7-4 ..... N85-33059* #

PB85-182400 ..... N85-32636 #
PB85-182418 ..... N85-32596 #
PB85-917006 ..... N85-32105 #

PMA-85-1 ..... N85-32809 #

PME-FM-85-1 ..... N85-32274 #

PNL-SA-12847 ..... N85-32189 #

PNL-4728-REV-1 ..... N85-32463 #
PNL-5442 ..... N85-32213 #

POLY-M/AE-85-1 ..... N85-32991 #

PPG-861 ..... N85-33017 #

R-3811-10968A ..... N85-32815 #

RADC-TM-84-23 ..... N85-32240 #

RADC-TR-84-159 ..... N85-32234 #
RADC-TR-84-195 ..... N85-32235 #
RADC-TR-84-197 ..... N85-32241 #
RADC-TR-85-60 ..... N85-32228 #
RADC-TR-85-65 ..... N85-32309 #

RAE-TM-MAT/STR-1050 ..... N85-32199 #

RAE-TR-84082 ..... N85-32182 #

RAND/P-7002 ..... N85-33042 #

REPT-1 ..... N85-33026 #
REPT-5 ..... N85-32263 #
REPT-6 ..... N85-33029 #
REPT-85B0381 ..... N85-32131* #
REPT-85B0472 ..... N85-32357* #
REPT-85B0522 ..... N85-32465* #
REPT-100-41 ..... N85-32576 #
REPT-160-6076-4 ..... N85-32193 #
REPT-1984-3 ..... N85-33025 #
REPT-85195 ..... N85-32795* #

REPT-85211 ..... N85-32090* #
REPT-85215 ..... N85-32094* #
REPT-85228 ..... N85-32831* #
REPT-85343 ..... N85-32830* #

RI/RD85-121 ..... N85-32165 #

RR-85-1-ONR ..... N85-32768 #

RSRE-MEMO-3789 ..... N85-32236 #

R84AEB592 ..... N85-32257 #

S-HRG-98-1241 ..... N85-32102 #

SAIC-85/1036 ..... N85-32988 #
SAIC-85/1683 ..... N85-32992 #

SAND-83-1025 ..... N85-32214 #
SAND-84-2667C ..... N85-32328 #
SAND-85-0219 ..... N85-32250 #
SAND-85-10720 ..... N85-33035 #

SBRC-41413 ..... N85-32313 #

SC5410.1AR ..... N85-32352 #

SD-TR-85-01 ..... N85-32314 #
SD-TR-85-13 ..... N85-32568 #

SIO-REF-84-15 ..... N85-32590 #

SR-1 ..... N85-32559 #
SR-1 ..... N85-32561 #
SR-1 ..... N85-32565 #
SR-1 ..... N85-32587 #
SR-1 ..... N85-33012 #
SR-5 ..... N85-32590 #
SR-6 ..... N85-32566 #
SR-6 ..... N85-32578 #
SR-8 ..... N85-32560 #

SRI-ESU-5401 ..... N85-32562 #

SRL-85-05-15 ..... N85-33044* #

SSD84-0053 ..... N85-32133* #

SU-SLAC-PUB-3582 ..... N85-33007 #

SU-SOL-85-5 ..... N85-32818 #

SU-STAN-CS-84-1026 ..... N85-32222 #

SU-TR-356 ..... N85-32845 #
SU-TR-357 ..... N85-32854 #

SWRI-6984 ..... N85-32275 #

T-3309 ..... N85-32101* #
T-6624 ..... N85-32272* #

TACOM-TR-13073 ..... N85-32815 #

TR-ONR-DG-14 ..... N85-32852 #
TR-ONR-DG-15 ..... N85-32769 #

TR-1 ..... N85-32844 #
TR-2 ..... N85-32192 #
TR-2 ..... N85-32994 #
TR-6 ..... N85-32159 #
TR-10 ..... N85-32200 #
TR-29 ..... N85-32991 #
TR-43 ..... N85-32266 #
TR-67 ..... N85-32998 #
TR-85-1 ..... N85-32245 #
TR-85-11 ..... N85-32856 #
TR-714 ..... N85-32306 #
TR-0084A(5472-03)-2 ..... N85-32314 #
TR-0084A(5940-05)-1 ..... N85-32568 #

TRC-SEALS-5-85 ..... N85-32332* #

U-1208-328 ..... N85-32982 #

UCID-20426 ..... N85-32820 #
UCID-20439 ..... N85-32249 #

UCRL-52000-85-4 ..... N85-33061 #
UCRL-53573 ..... N85-33028 #
UCRL-92218 ..... N85-32846 #
UCRL-92602 ..... N85-32169 #

UDR-TR-83-117 ..... N85-32153 #
UDR-TR-84-134 ..... N85-32152 #
UDR-TR-85-10 ..... N85-33031 #

UMASS-ARF-84-004 ..... N85-33012 #

US-PATENT-APPL-SN-737627 ..... N85-32311 #

USAAEFA-83-21 ..... N85-32116 #

USAAVSCOM-TM-85-B-3 ..... N85-32151* #

USAFA-TN-85-4 ..... N85-32115 #

USAFSAM-TR-84-35 ..... N85-32763 #
USAFSAM-TR-85-7 ..... N85-32760 #

USCG-D-5-85 ..... N85-32230 #
USCG-D-11-85-VOL-2-PT-A ..... N85-32774 #

USCG-N-1-85 ..... N85-32108 #

USGS-OFR-85-36 ..... N85-32316 #

UTRC/R85-916564-1 ..... N85-32188 #
UTRC/R85-922617-1 ..... N85-32327 #

WES-INSTRUCTION-K-84-11 ..... N85-32204 #

WES-IR-A-84-2 ..... N85-32388 #

WES-TR-E-81-9-3 ..... N85-32462 #

WES/TR/HL-85-3 ..... N85-32706 #

WHOI-85-16 ..... N85-32702 #

WRAIR-BB-85-1 ..... N85-32771 #

WSRL-0368-TM ..... N85-32209 #

YALEU/DCS/RR-366 ..... N85-32832 #

☆ U.S. GOVERNMENT PRINTING OFFICE: 1985-491-573/20020

FEDERAL DEPOSITORY LIBRARY PROGRAM

The Federal Depository Library Program provides Government publications to designated libraries throughout the United States. The Regional Depository Libraries listed below receive and retain at least one copy of nearly every Federal Government publication, either in printed or microfilm form, for use by the general public. These libraries provide reference services and inter-library loans; however, they are *not* sales outlets. You may wish to ask your local library to contact a Regional Depository to help you locate specific publications, or you may contact the Regional Depository yourself.

ARKANSAS STATE LIBRARY
One Capitol Mall
Little Rock, AR 72201
(501) 371-2326

AUBURN UNIV. AT MONTGOMERY LIBRARY
Documents Department
Montgomery, AL 36193
(205) 279-9110, ext. 253

UNIV. OF ALABAMA LIBRARY
Documents Dept.—Box S
University, AL 35486
(205) 348-7369

DEPT. OF LIBRARY, ARCHIVES AND PUBLIC RECORDS
Third Floor—State Cap.
1700 West Washington
Phoenix, AZ 85007
(602) 255-4121

UNIVERSITY OF ARIZONA LIB.
Government Documents Dept.
Tucson, AZ 85721
(602) 626-5233

CALIFORNIA STATE LIBRARY
Govt. Publications Section
P.O. Box 2037
Sacramento, CA 95809
(916) 322-4572

UNIV. OF COLORADO LIB.
Government Pub. Division
Campus Box 184
Boulder, CO 80309
(303) 492-8834

DENVER PUBLIC LIBRARY
Govt. Pub. Department
1357 Broadway
Denver, CO 80203
(303) 571-2131

CONNECTICUT STATE LIBRARY
Government Documents Unit
231 Capitol Avenue
Hartford, CT 06106
(203) 566-4971

UNIV. OF FLORIDA LIBRARIES
Library West
Documents Department
Gainesville, FL 32611
(904) 392-0367

UNIV. OF GEORGIA LIBRARIES
Government Reference Dept.
Athens, Ga 30602
(404) 542-8951

UNIV. OF HAWAII LIBRARY
Govt. Documents Collection
2550 The Mall
Honolulu, HI 96822
(808) 948-8230

UNIV. OF IDAHO LIBRARY
Documents Section
Moscow, ID 83843
(208) 885-6344

ILLINOIS STATE LIBRARY
Information Services Branch
Centennial Building
Springfield, IL 62706
(217) 782-5185

INDIANA STATE LIBRARY
Serials Documents Section
140 North Senate Avenue
Indianapolis, IN 46204
(317) 232-3686

UNIV. OF IOWA LIBRARIES
Govt. Documents Department
Iowa City, IA 52242
(319) 353-3318

UNIVERSITY OF KANSAS
Doc. Collect—Spencer Lib.
Lawrence, KS 66045
(913) 864-4662

UNIV. OF KENTUCKY LIBRARIES
Govt. Pub. Department
Lexington, KY 40506
(606) 257-3139

LOUISIANA STATE UNIVERSITY
Middleton Library
Govt. Docs. Dept.
Baton Rouge, LA 70803
(504) 388-2570

LOUISIANA TECHNICAL UNIV. LIBRARY
Documents Department
Ruston, LA 71272
(318) 257-4962

UNIVERSITY OF MAINE
Raymond H. Fogler Library
Tri-State Regional Documents Depository
Orono, ME 04469
(207) 581-1680

UNIVERSITY OF MARYLAND
McKeldin Lib.—Doc. Div.
College Park, MD 20742
(301) 454-3034

BOSTON PUBLIC LIBRARY
Government Docs. Dept.
Boston, MA 02117
(617) 536-5400 ext. 226

DETROIT PUBLIC LIBRARY
Sociology Department
5201 Woodward Avenue
Detroit, MI 48202
(313) 833-1409

MICHIGAN STATE LIBRARY
P.O. Box 30007
Lansing, MI 48909
(517) 373-0640

UNIVERSITY OF MINNESOTA
Government Pubs. Division
409 Wilson Library
309 19th Avenue South
Minneapolis, MN 55455
(612) 373-7813

UNIV. OF MISSISSIPPI LIB.
Documents Department
University, MS 38677
(601) 232-5857

UNIV. OF MONTANA
Mansfield Library
Documents Division
Missoula, MT 59812
(406) 243-6700

NEBRASKA LIBRARY COMM.
Federal Documents
1420 P Street
Lincoln, NE 68508
(402) 471-2045
In cooperation with University of Nebraska-Lincoln

UNIVERSITY OF NEVADA LIB.
Govt. Pub. Department
Reno, NV 89557
(702) 784-6579

NEWARK PUBLIC LIBRARY
5 Washington Street
Newark, NJ 07101
(201) 733-7812

UNIVERSITY OF NEW MEXICO
Zimmerman Library
Government Pub. Dept.
Albuquerque, NM 87131
(505) 277-5441

NEW MEXICO STATE LIBRARY
Reference Department
325 Don Gaspar Avenue
Santa Fe, NM 87501
(505) 827-2033, ext. 22

NEW YORK STATE LIBRARY
Empire State Plaza
Albany, NY 12230
(518) 474-5563

UNIVERSITY OF NORTH CAROLINA AT CHAPEL HILL
Wilson Library
BA/SS Documents Division
Chapel Hill, NC 27515
(919) 962-1321

UNIVERSITY OF NORTH DAKOTA
Chester Fritz Library
Documents Department
Grand Forks, ND 58202
(701) 777-2617, ext. 27
(In cooperation with North Dakota State Univ. Library)

STATE LIBRARY OF OHIO
Documents Department
65 South Front Street
Columbus, OH 43215
(614) 462-7051

OKLAHOMA DEPT. OF LIB.
Government Documents
200 NE 18th Street
Oklahoma City, OK 73105
(405) 521-2502

OKLAHOMA STATE UNIV. LIB.
Documents Department
Stillwater, OK 74078
(405) 624-6546

PORTLAND STATE UNIV. LIB.
Documents Department
P.O. Box 1151
Portland, OR 97207
(503) 229-3673

STATE LIBRARY OF PENN.
Government Pub. Section
P.O. Box 1601
Harrisburg, PA 17105
(717) 787-3752

TEXAS STATE LIBRARY
Public Services Department
P.O. Box 12927—Cap. Sta.
Austin, TX 78753
(512) 471-2996

TEXAS TECH UNIV. LIBRARY
Govt. Documents Department
Lubbock, TX 79409
(806) 742-2268

UTAH STATE UNIVERSITY
Merrill Library, U.M.C. 30
Logan, UT 84322
(801) 750-2682

UNIVERSITY OF VIRGINIA
Alderman Lib.—Public Doc.
Charlottesville, VA 22901
(804) 924-3133

WASHINGTON STATE LIBRARY
Documents Section
Olympia, WA 98504
(206) 753-4027

WEST VIRGINIA UNIV. LIB.
Documents Department
Morgantown, WV 26506
(304) 293-3640

MILWAUKEE PUBLIC LIBRARY
814 West Wisconsin Avenue
Milwaukee, WI 53233
(414) 278-3000

ST. HIST LIB. OF WISCONSIN
Government Pub. Section
816 State Street
Madison, WI 53706
(608) 262-4347

WYOMING STATE LIBRARY
Supreme Ct. & Library Bld.
Cheyenne, WY 82002
(307) 777-6344

National Aeronautics and
Space Administration
Code NIT-4
Washington, D.C.
20546

Official Business

Penalty for Private Use, $300

SPECIAL FOURTH-CLASS RATE
POSTAGE & FEES PAID
NASA
WASHINGTON, D.C.
PERMIT No. G 27

NASA

POSTMASTER: If Undeliverable (Section 158
Postal Manual) Do Not Return